

# **ENDOSONOGRAPHY**

FOURTH EDITION

## **Robert H. Hawes, MD**

Medical Director  
Florida Hospital Institute for Minimally Invasive Therapy  
Professor of Internal Medicine  
University of Central Florida College of Medicine  
Orlando, Florida

## **Paul Fockens, MD, PhD**

Professor and Chairman  
Department of Gastroenterology and Hepatology  
Academic Medical Center  
University of Amsterdam  
The Netherlands

## **Shyam Varadarajulu, MD**

Medical Director  
Florida Hospital Center for Interventional Endoscopy  
Professor of Internal Medicine  
University of Central Florida College of Medicine  
Orlando, Florida

ELSEVIER

# ELSEVIER

1600 John F. Kennedy Blvd.  
Ste 1800  
Philadelphia, PA 19103-2899

ENDOSONOGRAPHY, FOURTH EDITION

ISBN: 978-0-323-54723-9

**Copyright © 2019 by Elsevier, Inc. All rights reserved.**

No part of this publication may be reproduced or transmitted in any form or by any means, electronic or mechanical, including photocopying, recording, or any information storage and retrieval system, without permission in writing from the publisher. Details on how to seek permission, further information about the Publisher's permissions policies and our arrangements with organizations such as the Copyright Clearance Center and the Copyright Licensing Agency, can be found at our website: [www.elsevier.com/permissions](http://www.elsevier.com/permissions).

This book and the individual contributions contained in it are protected under copyright by the Publisher (other than as may be noted herein).

## Notices

Knowledge and best practice in this field are constantly changing. As new research and experience broaden our understanding, changes in research methods, professional practices, or medical treatment may become necessary.

Practitioners and researchers must always rely on their own experience and knowledge in evaluating and using any information, methods, compounds, or experiments described herein. In using such information or methods they should be mindful of their own safety and the safety of others, including parties for whom they have a professional responsibility.

With respect to any drug or pharmaceutical products identified, readers are advised to check the most current information provided (i) on procedures featured or (ii) by the manufacturer of each product to be administered, to verify the recommended dose or formula, the method and duration of administration, and contraindications. It is the responsibility of practitioners, relying on their own experience and knowledge of their patients, to make diagnoses, to determine dosages and the best treatment for each individual patient, and to take all appropriate safety precautions.

To the fullest extent of the law, neither the Publisher nor the authors, contributors, or editors, assume any liability for any injury and/or damage to persons or property as a matter of products liability, negligence or otherwise, or from any use or operation of any methods, products, instructions, or ideas contained in the material herein.

Previous editions copyrighted 2015, 2011, and 2006.

**Library of Congress Control Number: 2018940040**

*Content Strategist:* Nancy Anastasi Duffy  
*Content Development Specialist:* Angie Breckon  
*Publishing Services Manager:* Catherine Jackson  
*Senior Project Manager:* Daniel Fitzgerald  
*Designer:* Renee Duenow

Printed in China.

Last digit is the print number: 9 8 7 6 5 4 3 2 1



Working together  
to grow libraries in  
developing countries

[www.elsevier.com](http://www.elsevier.com) • [www.bookaid.org](http://www.bookaid.org)

*For my wife Chris, our son Grant, and our daughter Taylor Hawes Kay,  
her husband Andrew, and our grandson Grayson.*

**RH**

*For Marischka, Matthijs, and Kiki, my dream team also at this 4th edition.*

**PF**

*For Deepa, Archith, Raksha, and worldwide EUS fraternity.*

**SV**

# Contributors

## **Mohammad Al-Haddad, MBBS, MSc, FASGE, FACG, AGAF**

Associate Professor of Medicine  
Division of Gastroenterology and Hepatology  
Indiana University School of Medicine  
Indianapolis, Indiana  
United States

## **Jouke T. Annema, MD, PhD**

Pulmonologist  
Professor of Pulmonary Endoscopy  
Department of Respiratory Medicine  
Academic Medical Center  
University of Amsterdam  
Amsterdam  
The Netherlands

## **Ji Young Bang, MD, MPH**

Center for Interventional Endoscopy  
Florida Hospital  
Orlando, Florida  
United States

## **Omer Basar, MD**

Pancreas Biliary Center  
Gastrointestinal Unit  
Massachusetts General Hospital  
Boston, Massachusetts  
United States

## **William R. Brugge, MD**

Professor of Medicine, HMS  
Director  
Pancreas Biliary Center  
Medicine and Gastrointestinal Unit  
Massachusetts General Hospital  
Boston, Massachusetts  
United States

## **Suresh T. Chari, MD**

Division of Gastroenterology and Hepatology  
Mayo Clinic  
Rochester, Minnesota  
United States

## **Laurence MMJ Crombag, MD**

Pulmonologist  
Department of Respiratory Medicine  
University of Amsterdam  
Amsterdam  
The Netherlands

## **Paul Fockens, MD, PhD**

Professor and Chairman  
Department of Gastroenterology and Hepatology  
Academic Medical Center  
University of Amsterdam  
The Netherlands

## **Larissa L. Fujii-Lau, MD**

Division of Gastroenterology  
Queens Medical Center  
Honolulu, Hawaii  
United States

## **Ferga C. Gleeson, MD, MMedSci**

Professor of Medicine  
Division of Gastroenterology and Hepatology  
Mayo Clinic  
Rochester, Minnesota  
United States

## **Steve Halligan, MB, BS, MD, PhD, FRCP, FRCR, FMedSci**

Professor of Gastrointestinal Radiology  
University College London  
London  
Great Britain

## **Kazuo Hara, MD**

Director  
Department of Gastroenterology  
Aichi Cancer Center Hospital  
Nagoya  
Japan

## **Robert H. Hawes, MD**

Medical Director  
Florida Hospital Institute for Minimally Invasive Therapy  
Professor of Internal Medicine  
University of Central Florida College of Medicine  
Orlando, Florida  
United States

## **Bronte Holt, MBBS (Hons), BMedSci, PhD, FRACP**

Department of Gastroenterology  
St. Vincent's Hospital  
Melbourne  
Australia

**Joo Ha Hwang, MD, PhD**

Professor of Medicine  
Division of Gastroenterology and Hepatology  
Stanford University  
Stanford, California  
United States

**Takao Itoi, MD, PhD, FASGE**

Division of Gastroenterology-Hepatology  
Tokyo Medical University  
Tokyo  
Japan

**Darshana Jhala, MD, B MUS**

Chief of Pathology and Laboratory Medicine Services  
Department of Pathology and Laboratory Services  
Philadelphia VA Medical Center  
Professor of Pathology  
Department of Pathology and Laboratory Medicine  
Hospital of the University of Pennsylvania  
Philadelphia, Pennsylvania  
United States

**Nirag Jhala, MD, MIAC**

Professor of Pathology and Laboratory Medicine  
Director of Anatomic Pathology and Cytology  
Pathology and Laboratory Medicine  
Temple University Hospital  
Medical Director  
Laboratory Services  
North Eastern and Episcopal Hospital  
Temple University Health System  
Philadelphia, Pennsylvania  
United States

**Abdurrahman Kadayifci, MD**

Pancreas Biliary Center  
Medicine and Gastrointestinal Unit  
Massachusetts General Hospital  
Boston, Massachusetts  
United States  
Professor of Medicine  
Unit of Gastroenterology and Endoscopy  
Istanbul Reyap Hospital  
Turkey

**Mouen Khashab, MD**

Director  
Division of Gastroenterology and Hepatology  
John Hopkins Medicine  
Baltimore, Maryland  
United States

**Eun Young (Ann) Kim**

Professor  
Department of Internal Medicine  
Catholic University of Daegu  
Daegu  
Korea

**Wilson T. Kwong, MD, MS**

Assistant Professor  
Gastroenterology  
University of California San Diego  
La Jolla, California  
United States

**Alberto Larghi, MD, PhD**

Digestive Endoscopy Unit  
Catholic University  
Rome  
Italy

**Anne Marie Lennon, MD, PhD, FRCPI, FASGE**

Associate Professor of Medicine and Surgery  
Benjamin Baker Scholar  
Director of the Multidisciplinary Pancreatic Cyst Clinic  
The Johns Hopkins Hospital  
Baltimore, Maryland  
United States

**Michael J. Levy, MD**

Division of Gastroenterology and Hepatology  
Mayo Clinic  
Rochester, Minnesota  
United States

**Girish Mishra, MD, MS, FASGE, FACG, FACP**

Wake Forest School of Medicine  
Winston-Salem, North Carolina  
United States

**Robert Moran, MD, MRCPi**

Advanced Endoscopy Fellow  
The Johns Hopkins Hospital  
Baltimore, Maryland  
United States

**Dongwook Oh, MD**

Division of Gastroenterology  
Department of Internal Medicine  
Eulji University College of Medicine  
Eulji Nowon Hospital  
Seoul  
Korea

**Sarto C. Paquin, MD, FRCPC**

Assistant Professor of Medicine  
Division of Gastroenterology  
Centre Hospitalier de l'Université de Montréal  
Montréal, Quebec  
Canada

**Do Hyun Park, MD, PhD**

Associate Professor  
Division of Gastroenterology  
Department of Internal Medicine  
University of Ulsan College of Medicine  
Asan Medical Center  
Seoul  
South Korea

**Mihai Rimbaş, MD, PhD**

Digestive Endoscopy Unit  
Catholic University  
Rome  
Italy  
Gastroenterology Department  
Colentina Clinical Hospital  
Bucharest  
Romania

**Thomas Rösch, MD**

Department of Interdisciplinary Endoscopy  
University Hospital Hamburg-Eppendorf  
Hamburg  
Germany

**Adrian Săftoiu, MD, PhD, MSc, FASGE**

Visiting Clinical Professor  
Department of Endoscopy  
Copenhagen University Hospital Herlev  
Herlev  
Denmark  
Professor of Diagnostic and Therapeutic Techniques in  
Gastroenterology  
Department of Gastroenterology  
University of Medicine and Pharmacy Craiova  
Craiova  
Romania

**Anand V. Sahai, MD, MSc (Epid), FRCPC**

Professor of Medicine  
Chief  
Division of Gastroenterology  
Centre Hospitalier de l'Université de Montréal  
Montréal, Quebec  
Canada

**Thomas J. Savides, MD**

Professor of Clinical Medicine  
Division of Gastroenterology  
University of California San Diego  
La Jolla, California  
United States

**Thomas Smyrk, MD**

Division of Pathology  
Mayo Clinic  
Rochester, Minnesota  
United States

**Anthony Yuen Bun Teoh, FRCSEd (Gen)**

Associate Professor  
Department of Surgery  
Prince of Wales Hospital  
The Chinese University of Hong Kong  
Hong Kong

**Mark Topazian, MD**

Mayo Clinic  
Rochester, Minnesota  
United States

**Shyam Varadarajulu, MD**

Medical Director  
Florida Hospital Center for Interventional Endoscopy  
Professor of Internal Medicine  
University of Central Florida College of Medicine  
Orlando, Florida  
United States

**Peter Vilmann, MD, DSc, HC, FASGE**

Professor of Endoscopy at Faculty of Health Sciences  
Copenhagen University  
GastroUnit  
Herlev Hospital  
Herlev  
Denmark

**Sachin Wani, MD**

Division of Gastroenterology and Hepatology  
University of Colorado Anschutz Medical Campus  
Aurora, Colorado  
United States

# Preface

It is with great pleasure that we present the fourth edition of *Endosonography*. At the time of the first edition in 2006, endoscopic ultrasonography (EUS) was primarily an imaging technology, and regions outside Japan, Western Europe, and the United States were beginning to acquire the technology and needed training. We strived to produce a resource that combined up-to-date information on the clinical utility of EUS along with videos, which concentrated on the station approach to acquiring appropriate images and image interpretation. The first edition was extremely well received, and we are grateful to Elsevier and the initial set of authors for producing such an outstanding educational resource.

Time marches on, and endoscopy is a constantly evolving discipline. By 2009, there was an explosion of interest in EUS in Asia (especially in China and India), Eastern Europe, and the Middle East. It became apparent that it was time to develop a second edition. The publishing landscape had changed, more and more people (young and old) had “gone digital,” and we needed to analyze the needs of the current generation of EUS trainees. We also wanted this edition to maintain its relevance for a longer time. We added an online component, distributed e-mail updates from the editors, switched from a DVD to putting the videos online, and focused more on linear EUS with FNA (fine-needle aspiration) and EUS-guided interventions. Some of these new features were a success, and some were not. Whereas putting the videos online obviated the need to carry the DVD, our readers’ access to the videos was not seamless.

We introduced the third edition of *Endosonography* at the EUS 2014 symposium in Chennai, India. This edition continued with an online version and added new chapters on tissue acquisition and advanced imaging techniques as well as therapeutics. We provided e-mail updates from the editors in an effort to keep our readers on the cutting edge of EUS. We continued with the “how-to” sections as these are particularly helpful to trainees. Finally, we emphasized the developing discipline of interventional EUS. The third edition remained very popular and continues to garner over 95% of the EUS textbook market worldwide.

With the fourth edition, we continue to refine the content. With the evolution of EUS, some chapters have become less relevant and needed to be shortened and more tightly focused. In general, the relevance of EUS for luminal cancer staging has diminished, the requirements for tissue acquisition have changed, and interventional EUS is evolving and maturing rapidly. The fourth edition is dedicated to evolving in the same directions and to meet these goals. We have refined existing chapters, added new authors, and devoted more attention towards interventions. Most importantly, we have worked very hard to substantially update the videos. Toward this end, we owe a special thanks to Dr. Ji Young Bang who, during a very busy advanced endoscopy training year with us, spent many nights and weekends editing and voicing over countless videos for this fourth edition. While the changes to the fourth edition are intended to keep our readers at the cutting edge of EUS, we are dedicated to maintaining certain content directed toward trainees such as the “how-to” chapters and the videos emphasizing the station approach to image acquisition. Our goal is to provide the very best and most comprehensive textbook on endoscopic ultrasound.

In part to improve access to videos, we developed the EUS app. It is a free download to an iPhone, Android, and iPad. Over 16,000 unique users from 118 countries have downloaded the app, which can now serve as a readily available tool to aid in the mastery of EUS.

We remain steadfastly committed to advancing EUS through education and training. We feel that the fourth edition of *Endosonography* can play an important role in enabling one to achieve excellence in EUS and that a more widespread practice of quality endoscopic ultrasound will ultimately improve patient care around the world. It is our sincere hope that *Endosonography* will play a key role in allowing you to master the discipline of EUS.

Robert H. Hawes  
Paul Fockens  
Shyam Varadarajulu

# Acknowledgments

The first edition of *Endosonography* was introduced in 2006. It gives us great pleasure to now be introducing the fourth edition. We have strived to keep this textbook relevant as EUS has evolved from imaging to tissue acquisition and now to therapeutics. My EUS journey began in 1985 when I was introduced to this technology during my advanced endoscopy training at the Middlesex Hospital in London. With incredible encouragement and support from Glen Lehman, we became early adopters of endoscopic ultrasound at Indiana University and established a clinical EUS program in 1987 and a training program in 1990. Our program attracted young superstars like Mike Kochman, Amitabh Chak, Yang Chen, Tom Savides, and Frank Gress, to whom I am forever grateful for establishing IU as one of the early meccas for learning EUS. In 1994, I moved south, rejoining Peter Cotton to help establish a new Digestive Disease Center at the Medical University of South Carolina. I was very fortunate that Brenda Hoffman had already established an EUS program before I arrived. This began a 17-year relationship with Brenda that saw the MUSC EUS program grow and receive national and international recognition and attracted the best and brightest trainees from around the world to continue the legacy of advanced training in EUS. Manoop Bhutani, Lars Aabakken, Ian Penman, David Williams, Anand Sahai, Mohammad Eloubeidi, Rhys Vaughan, and Mike Wallace are only a few whose EUS careers began at MUSC as advanced EUS fellows. It was during his 2-year advanced fellowship (ERCP and EUS) at MUSC that I met Shyam Varadarajulu. Shyam went on to establish himself as one of the brightest stars in EUS during a 9-year tenure at the University of Alabama at Birmingham. I am now doubly blessed—first, to have Shyam join Paul and me as the third editor for *Endosonography* and, second, to have him as my partner in our Center for Interventional Endoscopy at Florida Hospital Orlando. Our goal and expectation are to continue to play a significant role in advancing EUS around the world. I hope that our latest edition of *Endosonography* will be a useful resource to help readers master the art of EUS. I am incredibly grateful to all the nurses, GI fellows, advanced fellows, and faculty colleagues who have contributed so significantly to teaching EUS. I am truly blessed to have had the opportunity to work with such dedicated and talented people throughout my career. This fourth edition of *Endosonography* is a reflection of a strong commitment by many to advance EUS.

**Robert H. Hawes**

This fourth edition is again dedicated to my EUS partners at the Academic Medical Center of the University of Amsterdam: Jeanin van Hooft, Sheila Krishnadath, Barbara Bastiaansen, Manon van der Vlugt, and Jacques Bergman. Together we offer a very open

EUS service for tertiary care patients, conduct EUS-related research, and train our advanced endoscopy fellows, who increasingly appreciate the value of EUS in combination with ERCP for tertiary pancreaticobiliary care. Through this extensive training EUS has now spread across the country and we are proud to have an excellent EUS network in the Netherlands nowadays. It remains a pleasure to receive many visitors from all over the world who spend anywhere from 2 hours to 2 months at the Academic Medical Center observing EUS procedures. And finally, over the past 20 years we have organized an annual EUS conference in Amsterdam in June, which attracts between 150 and 200 participants, several of whom are avid readers of our textbook. This year's 20th anniversary meeting attracted more than 250 participants and still had the intimate atmosphere where everyone can comment on the cases being presented.

I am grateful to our nursing staff for providing expert support for all our procedures. The nursing team is led by Marjon de Pater, who is irreplaceable in the way she combines high-quality nursing with a good spirit in the team. We are also excellently supported by our anesthesiology team, who provide deep sedation for many of our EUS patients, especially when these procedures are interventional. Finally, I am deeply grateful to my three pillars in life: my wife, Marischka, and my two children, Matthijs and Kiki, one of whom is now an MD and the other one will follow shortly. The future remains bright and I am curious to see where it will take us further.

**Paul Fockens**

I wish to thank my endoscopy partners Robert Hawes, Muhammad Hasan, Udhay Navaneethan, and Ji Young Bang at the Center for Interventional Endoscopy in Florida Hospital for their unstinting support and enthusiasm toward this project. I am indebted to my nurse manager Maria Madrileo and the endoscopy unit staff for their support and infinite patience that enabled us to build not only a successful academic “hybrid” unit but also the largest EUS program in the United States. We currently perform 3600 EUS procedures and conduct 14 randomized trials.

I owe a special thanks to my former colleagues at the University of Alabama at Birmingham (UAB), Mel Wilcox and Shajan Peter, for their perennial encouragement and support of my academic and personal endeavors. The varied pathology and complexity of cases that I saw in Birmingham enabled me to be what I am today. I am particularly grateful to my former UAB nurse manager, Jeannetta Blakely, who spent endless hours helping me design several critical steps in Interventional EUS.

Many visitors from around the world, and particularly from my home country of India, have visited Florida Hospital to learn EUS. Their presence at our center is a source of great inspiration

for me, and I hope to have the pleasure of seeing some of the *Endosonography* readers in our unit in the immediate future.

My special thanks to Rob and Paul for being great mentors and true friends and extending a helping hand when in need. I am also grateful to my numerous professional colleagues who have transcended over the years to become dear personal friends.

My parents and family are my motivation to whom I owe my existence and every success in life—thanks to Mom, Dad, Deepa, Archith, and Raksha.

**Shyam Varadarajulu**

# Principles of Ultrasound

JOO HA HWANG

## KEY POINTS

- Ultrasound is mechanical energy in the form of vibrations that propagate through a medium such as tissue.
- Ultrasound interacts with tissue by undergoing absorption, reflection, refraction, and scattering and produces an image representative of tissue structure.
- Imaging artifacts can be recognized and understood based on a knowledge of the principles of ultrasound.

## Basic Ultrasound Physics

Sound is mechanical energy in the form of vibrations that propagate through a medium such as air, water, or tissue.<sup>1</sup> The frequency of audible sound ranges from 20 to 20,000 Hz (cycles per second). Ultrasound involves a frequency spectrum that is greater than 20,000 Hz. Medical applications use frequencies in the range of 1,000,000 to 50,000,000 Hz (1 to 50 MHz). The propagation of ultrasound results from the displacement and oscillation of molecules from their average position and the subsequent displacement and oscillations of molecules along the direction of propagation of the ultrasound wave.

Ultrasound waves can be described using the common properties of waves. Fig. 1.1 is an illustration of a sinusoidal wave with the pressure amplitude along the  $y$ -axis and the time or distance along the  $x$ -axis. Fig. 1.1 is referred to in the following sections to introduce the basic properties of waves.

## Wavelength, Frequency, and Velocity

The *wavelength* is the distance in the propagating medium that includes one complete cycle (see Fig. 1.1). The wavelength ( $\lambda$ ) is dependent on the frequency ( $f$ ) of the oscillations and the velocity ( $c$ ) of propagation in the medium. The relationship of wavelength, frequency, and velocity is given in Eq. 1.1.

(1.1)

$$c = f\lambda$$

The *frequency* of a wave is the number of oscillations per unit of time. Typically in ultrasound, this is stated in terms of cycles per second or Hertz (1 c/s = 1 Hz). The *period* of a wave ( $\tau$ ) is the inverse of the frequency and represents the time required to complete one cycle. The relationship between frequency and period is given in Eq. 1.2.

(1.2)

$$c = \frac{1}{\tau}$$

The *velocity* of propagation depends on the physical properties of the medium in which the wave is propagating. The primary physical properties governing the velocity of propagation are the density and compressibility of the medium.

## Density, Compressibility, and Bulk Modulus

The *density* ( $\rho$ ) of a medium is the mass per unit volume of that medium ( $\text{kg/m}^3$  in SI units). The *compressibility* ( $K$ ) of a medium is a property that reflects the relationship between the fractional decrease in volume and the pressure applied to a medium. For example, air has high compressibility (a small amount of pressure applied to a volume of air will result in a large fractional decrease in volume), whereas bone has relatively low compressibility (a large amount of pressure applied to a volume of bone will result in a small fractional decrease in volume). Finally, the *bulk modulus* ( $\beta$ ), which is the inverse of the compressibility, is the negative ratio of pressure applied to a medium and the fractional change in volume of the medium and reflects the stiffness of the medium.

The acoustic velocity ( $c$ ) of a medium can be determined once the density ( $\rho$ ) and the compressibility ( $K$ ), or bulk modulus ( $\beta$ ), are known. Eq. 1.3 demonstrates the relationship of the three physical properties.

Density, compressibility, and bulk modulus are not independent of one another. Typically, as density increases, compressibility decreases and bulk modulus increases. However, compressibility and bulk modulus typically vary more rapidly than does density, and they dominate in Eq. 1.3.

(1.3)

$$c = \frac{1}{\sqrt{K\rho}} = \frac{\sqrt{\beta}}{\sqrt{\rho}}$$

The acoustic velocity in different media can be determined by applying the equations to practice. For example, water at 30°C has a density of 996 kg/m<sup>3</sup> and a bulk modulus of 2.27 × 10<sup>9</sup> N/m<sup>2</sup>.<sup>2</sup> Inserting these values into Eq. 1.3 yields an acoustic velocity of 1509 m/s in water. Values for density and bulk modulus have been characterized extensively and can be found in the literature.<sup>2</sup> A summary of relevant tissue properties is given in Table 1.1. The acoustic velocity is not dependent on the frequency of

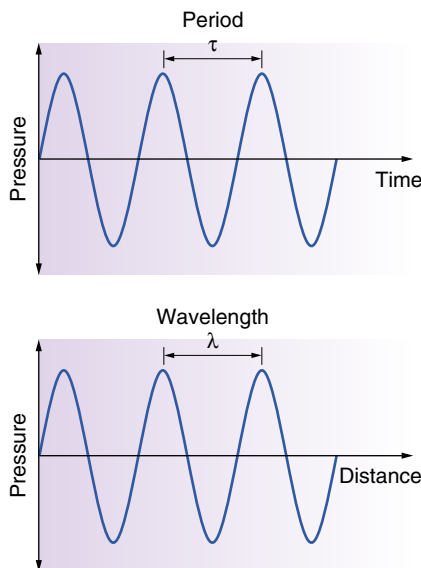


**Fig. 1.1** Sinusoidal wave depicted on the time axis and distance axis. The time to complete one cycle is the period ( $\tau$ ). The distance to complete one cycle is the wavelength ( $\lambda$ ).

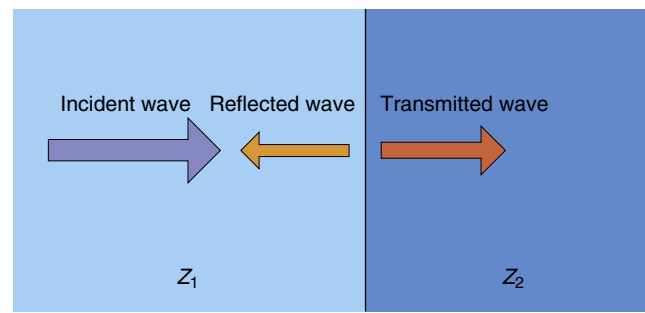


**Fig. 1.2** Reflection of an ultrasound wave at normal incidence to an interface between two media with different acoustic impedances ( $Z$ ).

introduce the concept of *acoustic impedance*. The acoustic impedance ( $Z$ ) of a medium represents the resistance to sound propagating through the medium and is the product of the *density* ( $\rho$ ) and the *velocity* ( $c$ ):

$$(1.4)$$

$$Z = \rho c$$

Sound will continue to propagate through a medium until an interface is reached where the acoustic impedance of the medium in which the sound is propagating differs from the medium that it encounters. At an interface where an acoustic impedance difference is encountered, a proportion of the ultrasound wave will be reflected back toward the transducer and the rest will be transmitted into the second medium. The simplest case of reflection and transmission occurs when the propagating ultrasound wave is perpendicular (90 degrees) to the interface (Fig. 1.2). In this case the percentage of the incident beam that is reflected is as follows:

$$(1.5)$$

$$\% \text{ reflected} = \left( \frac{Z_2 - Z_1}{Z_2 + Z_1} \right)^2 \times 100$$

The percentage of the incident beam that is transmitted is as follows:

$$(1.6)$$

$$\% \text{ transmitted} = 100 - \% \text{ reflected}$$

### Refraction

When the incident beam arrives at the interface at an angle other than 90 degrees, the transmitted beam path diverges from the incident beam path because of refraction (Fig. 1.3). The angle at which the transmitted beam propagates is determined by Snell's law:

$$(1.7)$$

$$\frac{\sin \varphi_1}{\sin \varphi_2} = \frac{c_1}{c_2}$$

The angle of *refraction* is determined by the *acoustic velocities* in the incident ( $c_1$ ) and transmitted ( $c_2$ ) media. There are three possible scenarios for a refracted beam, depending on the relative

**TABLE 1.1 Physical Properties of Tissue**

Tissue or Fluid	Density (kg/m <sup>3</sup> )	Bulk Modulus (×10 <sup>9</sup> N/m <sup>2</sup> )	Acoustic Velocity (m/s)
Water (30°C)	996	2.27	1509
Blood	1050–1075	2.65	1590
Pancreas (pig)	1040–1050	2.63	1591
Liver	1050–1070	2.62	1578
Bone, cortical	1063–2017	28.13	3760

Adapted from Duck FA. *Physical Properties of Tissue*. London: Academic Press; 1990.

the propagating wave (i.e., acoustic waves of different frequencies all propagate with the same acoustic velocity within the same medium).<sup>3</sup>

## Ultrasound Interactions in Tissue

Ultrasound imaging of tissue is achieved by transmitting short pulses of ultrasound energy into tissue and receiving reflected signals. The reflected signals that return to the transducer represent the interactions of a propagating ultrasound wave with tissue. A propagating ultrasound wave can interact with tissue, and the results are *reflection*, *refraction*, *scattering*, and *absorption*.

### Reflection

Specular reflections of ultrasound occur at relative large interfaces (greater than one wavelength) between two media of differing acoustical impedances. At this point, it is important to

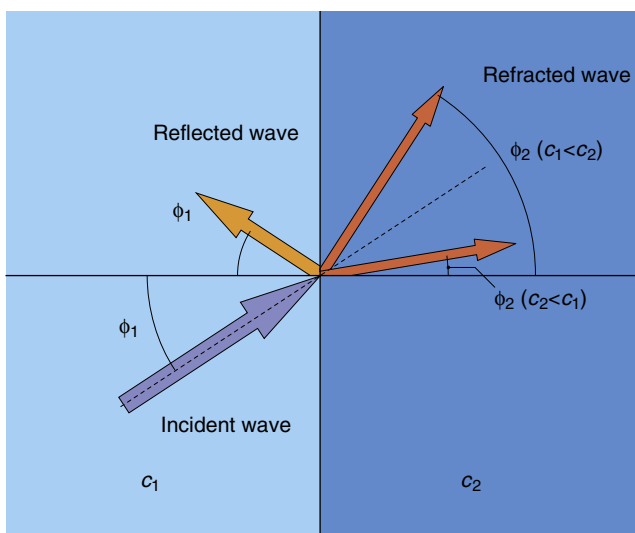


**Fig. 1.3** Refraction and reflection of an incident wave that is not normal to the interface between media with different acoustic velocities ( $c$ ). The angle of reflection is identical to the angle of incidence. The angle of the refracted wave is dependent on the acoustic velocities of the two media and can be determined by applying Snell's law (see text).

speeds of sound between the two media: (1) if  $c_1 > c_2$ , the angle of refraction will be bent toward normal ( $\varphi_1 > \varphi_2$ ); (2) if  $c_1 = c_2$ , the angle of refraction will be identical to the angle of incidence, and the beam will continue to propagate without diverging from its path; (3) if  $c_1 < c_2$ , the angle of refraction will be bent away from normal ( $\varphi_1 < \varphi_2$ ). Refraction of the ultrasound beam can lead to imaging artifacts that are discussed later in the chapter.

### Scattering

Scattering, also termed *nonspecular reflection*, occurs when a propagating ultrasound wave interacts with different components in tissue that are smaller than the wavelength and have different impedance values than the propagating medium.<sup>4</sup> Examples of scatterers in tissue include individual cells, fat globules, and collagen. When an ultrasound wave interacts with a scatterer, only a small portion of the acoustic intensity that reflects off of the scatterer is reflected back to the transducer (Fig. 1.4). In addition, a signal that has undergone scattering by a single scatterer will usually undergo multiple scattering events before returning to the transducer. Scattering occurs in heterogeneous media, such as tissue, and is responsible for the different echotextures of organs such as the liver, pancreas, and spleen. Tissue containing fat or collagen scatters ultrasound to a greater degree than do other tissues, and this is why lipomas and the submucosal layer of the gastrointestinal (GI) tract appear hyperechoic (bright) on ultrasound imaging.<sup>4</sup>

Multiple reflections from nonspecular reflectors within the tissue returning to the transducer result in a characteristic acoustic speckle pattern, or echotexture, for that tissue.<sup>4</sup> Because speckle originates from multiple reflections and does not represent the actual location of a structure, moving the transducer will change the location of the speckle echoes while maintaining a similar speckle pattern. In addition, the noise resulting from acoustic speckle increases with increasing depth as a result of the greater number of signals that have undergone multiple reflections from nonspecular reflectors returning to the transducer.

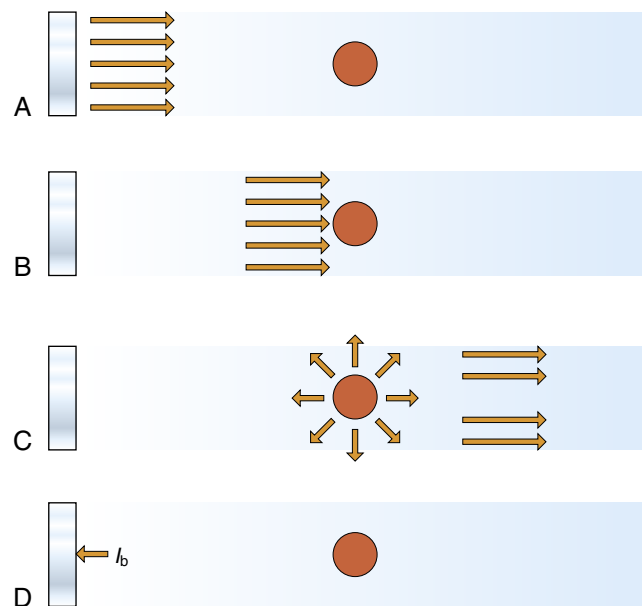


**Fig. 1.4** Schematic representation of single scattering. Scattering occurs from an interface that is smaller than the wavelength of the propagating ultrasound signal. The transducer is responsible for sending and receiving the signal.  $I_b$  is the backscattered intensity that will propagate back to the transducer. (A) The ultrasound signal is transmitted by the transducer and propagates toward the scatterer. (B) The pulse reaches the scatterer. (C) The incident acoustic intensity is scattered in different directions. (D) The backscattered energy received by the transducer is only a small fraction of the incident acoustic intensity that is scattered.

### Absorption

Ultrasound energy that propagates through a medium can be absorbed, resulting in the generation of heat. The *absorption* of ultrasound energy depends on tissue properties and is highly frequency dependent. Higher frequencies cause more tissue vibration and result in greater absorption of the ultrasound energy and more heat generation.

### Ultrasound Intensity

The *intensity* of the ultrasound signal is a parameter that describes the power of the ultrasound signal over a cross-sectional area. As ultrasound waves propagate through tissue, the intensity of the wave becomes attenuated. Attenuation is the result of effects of both scattering and absorption of the ultrasound wave.<sup>1</sup> The *attenuation coefficient* ( $a$ ) is a function of frequency that can be determined experimentally, and it increases with increasing frequency. The frequency of the ultrasound pulse affects both the depth of penetration of the pulse and the obtainable resolution. In general, as the frequency is increased, the depth of penetration decreases, owing to attenuation of the ultrasound intensity, and axial resolution improves, as discussed later in this chapter.

The intensity of the propagating ultrasound energy decreases exponentially as a function of depth and is given by the following equation:

$$(1.8)$$

$$I_x = I_0 e^{-2ax}$$

where  $I_0$  is the initial intensity of the ultrasound pulse and  $I_x$  is the intensity of the ultrasound pulse after it has passed a distance

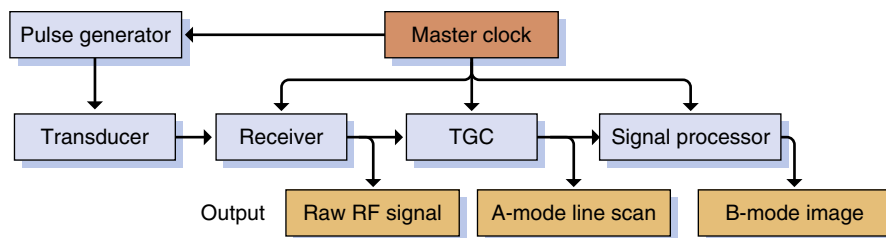


**Fig. 1.5** Ultrasound instrumentation schematic. The overall system is synchronized by a master clock. A pulse generator sends an electrical signal to the transducer, and the result is a transmitted ultrasound pulse. The transducer then receives the backreflected signal resulting from the transmitted pulse. This signal is then passed on to the receiver, which amplifies the entire signal. The output from the receiver is the raw radiofrequency (*RF*) signal. The signal can then undergo time gain compensation (*TGC*), and the subsequent output will be the A-mode line scan. After *TGC*, the signal is further processed, including demodulation and registration, to yield a B-mode image.

$x$  through tissue with an attenuation coefficient  $\alpha$  in Neper/cm ( $Np/cm$ ). As the attenuation coefficient increases with frequency, intensity also decreases exponentially as frequency increases. This equation partially explains the limitation on the depth of imaging because the returning ultrasound pulse from the tissue must be of sufficient intensity to be detected by the ultrasound transducer.

## Basics of Ultrasound Instrumentation

The key component of an ultrasound system is the transducer. A *transducer* is a device that converts one form of energy to another. In the case of ultrasound transducers, electrical energy is converted to mechanical energy, resulting in the transmission of an ultrasound pulse. When an ultrasound signal is then received by the ultrasound transducer, the received mechanical signal is converted back to an electrical signal that is then processed and digitized by the ultrasound processor to yield a real-time image of the tissue being interrogated by the ultrasound transducer (Fig. 1.5).

## Transducers

The active element of an ultrasound transducer, responsible for generating and receiving acoustic signals, is made typically from a piezoelectric ceramic. Piezoelectric ceramics are composed of polar crystals that are aligned in a particular orientation such that when an electric field is applied, the material changes shape.<sup>3</sup> Therefore if an alternating electrical field is applied to the material at a particular frequency, the material will vibrate mechanically at that frequency, similar to an audio speaker. In addition, if the piezoelectric material is deformed by sufficient mechanical pressure (e.g., a reflected ultrasound wave), a detectable voltage will be measured across the material with a magnitude proportional to the applied pressure. The magnitude of the voltage then determines how brightly that signal is represented in B-mode imaging (this is explained in the later section on B-mode imaging).

## Processors

Fig. 1.5 is a block diagram of the components of an ultrasound imaging system. The main components are the ultrasound transducer, processor, and display. Within the processor are electronic components that are responsible for controlling the excitation of the transducer, amplification of the received signal, time gain

compensation (*TGC*), and signal processing resulting in an output signal to the display.

### Transmit/Receive

As described earlier, the ultrasound transducer is responsible for transmitting the ultrasound pulse and receiving reflected pulses. The time interval between the transmission of a pulse and the detection of the reflected pulse gives information about the distance from the interface or nonspecular reflector where the reflection occurred. The distance, or depth, of the interface from the transducer is given by the following equation:

(1.9)

$$D = \frac{v \times t}{2}$$

where  $D$  is the distance from the transducer,  $v$  is the velocity of ultrasound in tissue (assumed to be uniform [1540 m/s] by most ultrasound processors), and  $t$  is the time between the transmitted and received pulses. The product of  $v$  and  $t$  is divided by 2 because the pulse travels twice the distance (to the reflector and back). In addition, the strength of the received signal gives information regarding the impedance mismatch at the interface where the reflection occurred.

### System Gain and Time Gain Compensation

The amplification of the output can be adjusted by the operator in two ways. One is to increase the overall gain of the system, an approach that uniformly increases the amplitude of all echoes received by the transducer. This can improve the detection of weak echoes; however, it generally comes at the expense of overall resolution.

*TGC* is used to compensate for the decreased intensity of echoes that originate from structures further from the transducer. As described earlier, the intensity of the ultrasound signal diminishes exponentially with distance (Eq. 1.8); therefore reflections from interfaces further from the transducer have significantly decreased intensities. The *TGC* function of ultrasound processors allows selective amplification of echoes from deeper structures. Current endoscopic ultrasonography (EUS) processors allow the operator to vary the gain by depth.

### Signal Processor

After *TGC* of the signal has occurred, additional signal processing is performed. The algorithms for signal processing performed differ among ultrasound processors and are closely held

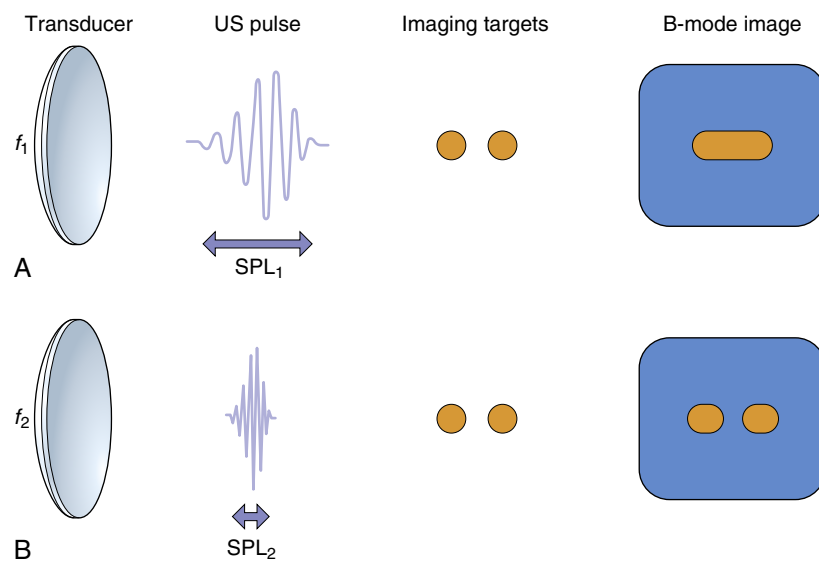


**Fig. 1.6** Concept of axial resolution. Axial resolution is limited by the spatial pulse length ( $SPL$ ). This figure compares the axial resolution of two different ultrasound (US) pulses with different frequencies ( $f_1 < f_2$ ) and identical pulse lengths; therefore  $SPL_1 > SPL_2$ . In (A) the distance between the imaging targets is less than  $SPL_{1/2}$ , thus resulting in a B-mode image that is not able resolve the two discrete targets. In (B) the distance between the imaging targets is greater than  $SPL_{2/2}$ , thus resulting in the ability to resolve the two discrete targets.

proprietary information. In general, some form of demodulation of the radiofrequency (RF) signal is performed to obtain an envelope of the RF signal, which is used to produce a B-mode image. In addition, processing can include threshold suppression to eliminate signals that are below an operator-specified threshold. Leading edge detection, peak detection, and differentiation are additional methods that can be used by processors to improve image quality.<sup>1</sup>

## Imaging Principles

Now that the basic principles of ultrasound physics and instrumentation have been introduced, an overview of imaging principles can be described.

## Resolution

In ultrasound imaging, three different aspects of resolution must be considered: axial, lateral, and elevation or azimuthal resolution.

### Axial Resolution

*Axial resolution* refers to the smallest separation distance between two objects along the beam path that can be detected by the imaging system. Axial resolution is determined by the ultrasound frequency and the spatial pulse length (SPL) of the transmitted ultrasound pulse.<sup>5</sup> The SPL can be determined by the following equation:

(1.10)

$$SPL = \frac{c}{f} \times n$$

where  $c$  is the speed of sound in tissue,  $f$  is the center frequency of the transmitted ultrasound pulse, and  $n$  is the number of cycles

per pulse (typically four to seven cycles). The limit of axial resolution is equal to  $SPL/2$ . This equation demonstrates why using higher frequencies results in greater axial resolution (assuming that pulses have the same number of cycles per pulse). To illustrate this concept, two different ultrasound pulses with qualitatively different center frequencies and SPL are shown in Fig. 1.6. Axial resolution is the most important property in imaging the layered structures of the GI tract wall.

### Lateral Resolution

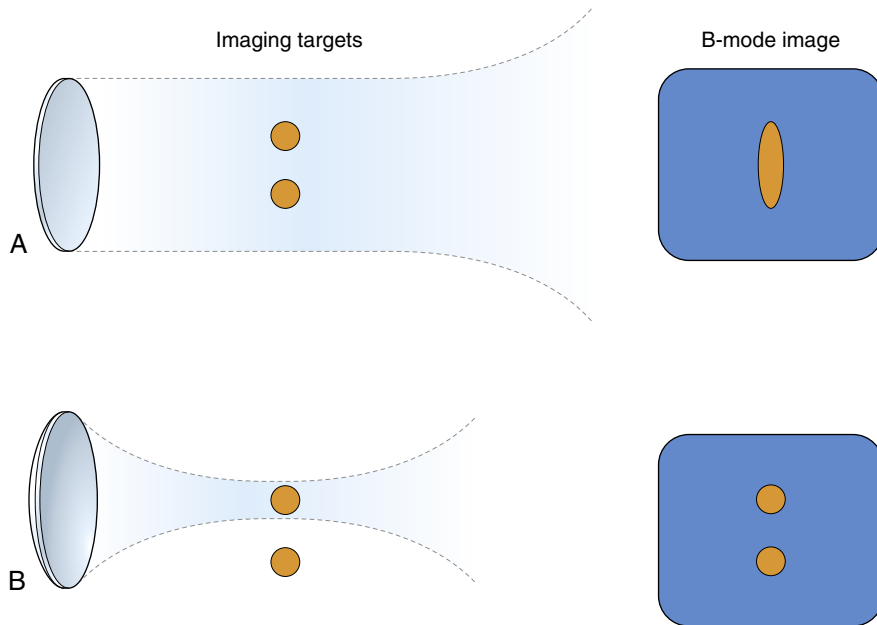
The *lateral resolution* of an imaging system represents the ability to discriminate between two points that are in a plane perpendicular to the ultrasound beam. The beam width of the transducer determines the achievable lateral resolution and is a function of transducer size, shape, frequency, and focusing. Fig. 1.7 illustrates the concept of lateral resolution.

### Elevation Resolution

*Elevation*, or *azimuthal*, *resolution* relates to the fact that, although the image displayed is two dimensional, the actual interrogated plane has a thickness associated with it. The factors governing elevation resolution are similar to those for lateral resolution. In fact, the elevation resolution for a focused, circular disk transducer (as used in the Olympus GF-UM series) is the same as for lateral resolution because of its circular symmetry. For the linear array transducers, the elevation resolution is determined by the beam width characteristics along the plane of imaging.

## A-Mode Scanning

A-mode, or amplitude mode, scanning is obtained by the transmit/receive process described previously with an output yielding an RF line scan of the echoes detected along the axis of a stationary transducer after a pulse of ultrasound has been transmitted. The received signal by the transducer is amplified, yielding the



**• Fig. 1.7** Concept of lateral resolution. Lateral resolution is determined by the ultrasound beam width. This figure compares the lateral resolution of an unfocused transducer (A) and a focused transducer (B) with apertures of the same diameter. The beam width of the unfocused transducer in (A) cannot resolve the two imaging targets; therefore the two targets are displayed as one target on B-mode imaging. The beam width of the focused transducer in (B) is sufficiently narrow to resolve the two imaging targets. If the imaging targets were beyond the focus of the transducer in (B), the broadened beam width would not be able to resolve the two objects, and the B-mode image would be similar to that in (A).

A-mode signal (Fig. 1.8). This form of scanning, rarely used by the clinician, is the basis for all other modes of scanning, including B-mode scanning. In addition, RF signal analysis is an important aspect of research in the area of advanced imaging techniques.

## B-Mode Imaging

B-mode, or brightness mode, scanning results in additional signal processing and movement of the transducer either mechanically or electronically. A B-mode image is created by processing a series of A-mode signals (see Fig. 1.8). For each line in the B-mode image (corresponding to a single A-mode line scan), the digitized RF signal is demodulated, yielding an envelope of the RF signal. The amplitude of the demodulated signal is then used to determine the brightness of the dot corresponding to its location in the B-mode image. As the axis of the transducer output is translated (either mechanically or electronically), additional A-mode signals are obtained and processed, eventually yielding a compound B-mode image (see Fig. 1.8). EUS imaging systems generate a compound B-mode image.

## Doppler

The Doppler effect is used in ultrasound applications to identify objects that are in motion relative to the transducer. In biologic applications the reflective objects in motion are red blood cells. Doppler ultrasound is used in EUS examinations to identify blood flow in vessels. The fundamental basis for the Doppler effect in ultrasound is that an object in motion relative to the source transducer will reflect an ultrasound wave at a different frequency relative to the frequency transmitted by the source transducer; this

is termed the *Doppler shift*. The difference between the transmitted frequency and the shifted frequency is dictated by the velocity ( $v$ ) of the object in motion relative to the transducer. The Doppler shift can be determined by the following equation:

(1.11)

$$f_D = \frac{2vf_t \cos \theta}{c}$$

where  $f_D$  is the Doppler shift frequency, which is the difference between the transmitted and reflected frequencies;  $v$  is the velocity of the object in motion (red blood cells);  $f_t$  is the transmitted frequency;  $\theta$  is the angle at which the object in motion is traveling relative to the direction of the source beam (Fig. 1.9); and  $c$  is the speed of sound in tissue (1540 m/s). This equation illustrates why a Doppler shift is not detected if the transducer is aimed perpendicular (90 degrees) to a blood vessel. At an angle of 90 degrees, Eq. 1.11 demonstrates that  $f_D = 0$ , as  $\cos 90$  degrees = 0. Therefore interrogation of a blood vessel should be at an angle other than 90 degrees, with the greatest Doppler shift detected when the object in motion is moving along the axis of the transmitted ultrasound wave ( $\cos 0$  degrees = 1 and  $\cos 180$  degrees = -1).

The different implementations of Doppler ultrasound include continuous-wave, pulsed-wave, color, and power Doppler.

## Continuous-Wave Doppler

Continuous-wave Doppler represents the simplest configuration of Doppler ultrasound and requires two different transducers: a transmitting and a receiving transducer. The transmitting

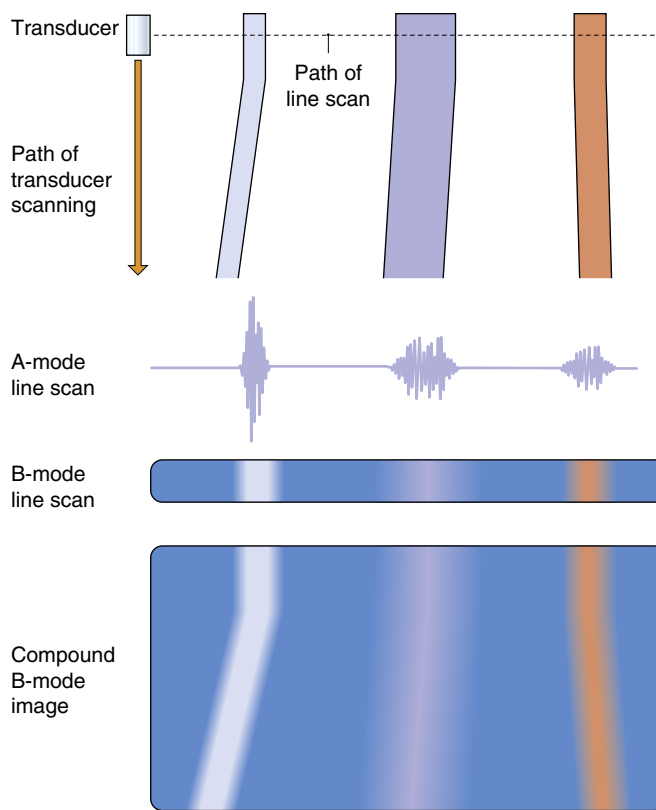


**Fig. 1.8** Conceptual representation of how A-mode line scans, B-mode line scans, and compound B-mode images are obtained. The transducer output is directed into the tissue determining the path of the line scan. An A-mode line scan is obtained after amplification of the received signals by the transducer. The B-mode line scan is obtained after demodulation and additional signal processing of the A-mode signal. The compound B-mode image is produced by obtaining multiple line scans by translating the path of the line scan. This can be accomplished either by mechanically scanning the transducer or by electronically steering a linear array transducer.

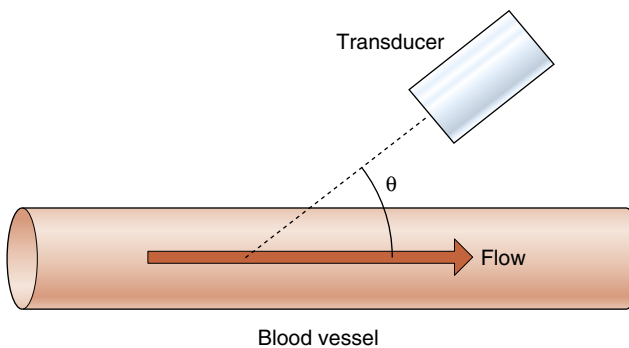


**Fig. 1.9** Conceptual image of Doppler measurements. The angle  $\theta$  determines the strength of the Doppler signal. If  $\theta$  is 90 degrees, then no Doppler signal can be detected.

transducer produces a continuous output of ultrasound at a fixed frequency. The receiving transducer then receives the continuous signal. The transmitted and received signals are added, resulting in a waveform that contains a beat frequency that is equivalent to the Doppler shift frequency. Continuous-wave Doppler does not give any information regarding the depth at which the motion causing the Doppler shift is occurring.

## Pulsed-Wave Doppler

Pulsed-wave Doppler was developed to obtain depth information regarding the location of the motion causing the Doppler shift. In addition, a pulsed-wave Doppler system required only a single transducer to transmit and receive ultrasound signals. The pulse length used for pulsed-wave Doppler is substantially longer than pulses used for imaging. Using electronic gating to time the interval between transmitting and receiving a pulse, this method allows the operator to interrogate a specific location along the axis of the transmitted ultrasound beam for motion. The output from pulsed-wave Doppler is usually in the form of an audible signal. The combination of pulsed-wave Doppler with B-mode imaging, termed *duplex scanning*, allows the operator to interrogate a specific location within a B-mode image.

## Color Doppler

Color Doppler is a method of visually detecting motion or blood flow using a color map that is incorporated into a standard B-mode image. The principles of color Doppler are similar to those of pulsed-wave Doppler. However, a larger region can be interrogated, and detected blood flow is assigned a color, typically blue or red, depending on whether the flow is moving toward or away from the transducer. Frequency shifts are estimated at each point at which motion is detected within an interrogated region, thus yielding information on direction of motion and velocity. Shades of blue or red are used to reflect the relative velocities of the blood flow. All stationary objects are represented on a gray scale, as in B-mode imaging. The benefit of color Doppler is that information on the direction and relative velocity of blood flow can be obtained. Color Doppler is limited by its dependence on the relative angle of the transducer to the blood flow.

## Power Doppler

Power Doppler is the most sensitive Doppler method for detecting blood flow. Again, the basis for power Doppler is similar to that for pulsed-wave and color Doppler. However, in processing the Doppler signal, instead of estimating the frequency shift as in color Doppler, the integral of the power spectrum of the Doppler signal is estimated. This method essentially determines the strength of the Doppler signal and discards any information on velocity or direction of motion. This method is the most sensitive for detecting blood flow and should be used to identify blood vessels when information on direction of flow and velocity is not needed.

## Imaging Artifacts

Image artifacts are findings on ultrasound imaging that do not accurately represent the tissue being interrogated. An understanding of the principles of ultrasound can be used to explain image artifacts. It is important to identify and understand the basis for image artifacts, to interpret ultrasound images correctly. Some common ultrasound imaging artifacts are discussed.

## Reverberation

Reverberations occur when a single transmitted pulse undergoes multiple reflections from a strong reflector over the time of a single line scan. The transmitted pulse first is reflected by the reflector back to the transducer. The reflected pulse then is reflected off the transducer back toward the reflector. This sequence is repeated,

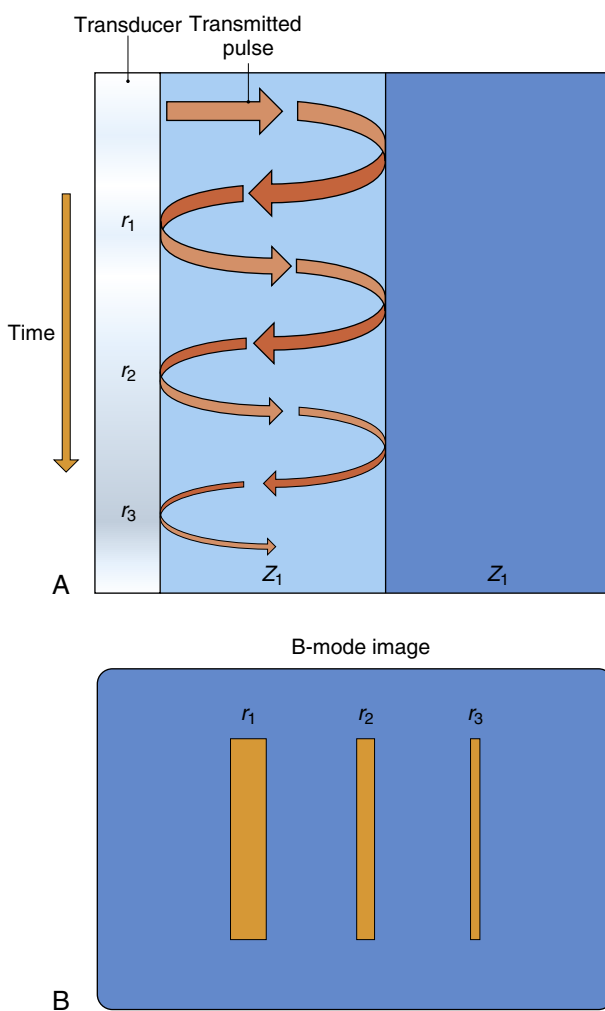


**Fig. 1.10** Reverberation artifacts result from strong reflections of a transmitted pulse from an interface with a large impedance mismatch (e.g., air-water interface). (A) Depiction of how a transmitted signal is reflected by an interface with a large impedance mismatch. The reflected signal is detected by the transducer and is redirected back into the medium. This sequence can be repeated multiple times, depending on the depth of imaging. The reflected signal is progressively attenuated. (B) The corresponding B-mode image from the reverberation depicted in (A). The reflected signals ( $r_1$ ,  $r_2$ , and  $r_3$ ) are spaced equally.

and each time a reflection returns to the transducer a signal is generated, until the signal has been attenuated to the point where it is not detected by the transducer or the line scan has been completed (Fig. 1.10). The duration of the line scan depends on the depth of imaging. A reverberation artifact can be identified by the equal spacing between hyperechoic (bright) bands, with decreasing intensity as the distance from the transducer increases. Reverberation artifact from a mechanical radial scanning ultrasound probe is demonstrated in Fig. 1.11. This particular reverberation artifact is also called the *ring artifact*.<sup>6</sup> The reflections are from the housing of the ultrasound transducer. Reverberation artifacts are also seen with air-water interfaces, such as bubbles (Fig. 1.12).

## Reflection (Mirror Image)

The *reflection, or mirror-image, artifact* occurs when imaging near an air-water interface such as a lumen filled partially with

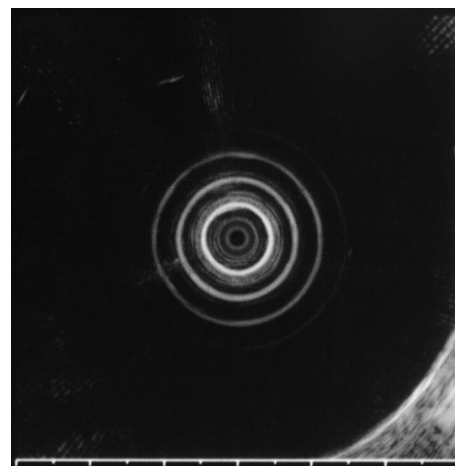


**Fig. 1.11** Endoscopic ultrasonography image of reverberation artifact resulting from multiple reflections from the transducer housing. The concentric rings are equally spaced, with the intensity of the rings decreasing as the distance from the transducer increases.

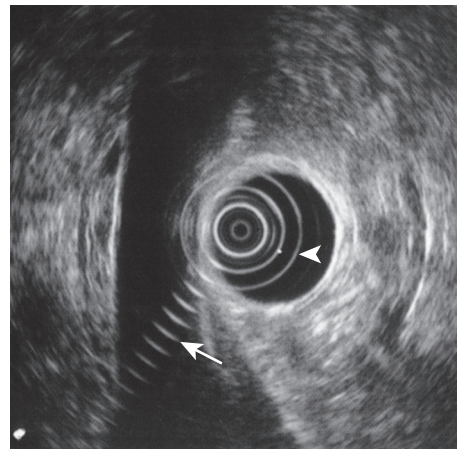


**Fig. 1.12** Endoscopic ultrasonography image of reverberation artifact (arrow) resulting from multiple reflections from an air bubble in the water-filled balloon. The intensity of the artifact does not decrease as rapidly as the reverberation artifact (arrowhead) from the transducer housing. This is because the impedance mismatch of the air-water interface is much greater than the transducer housing interface, with resulting reflected signals of greater intensity.

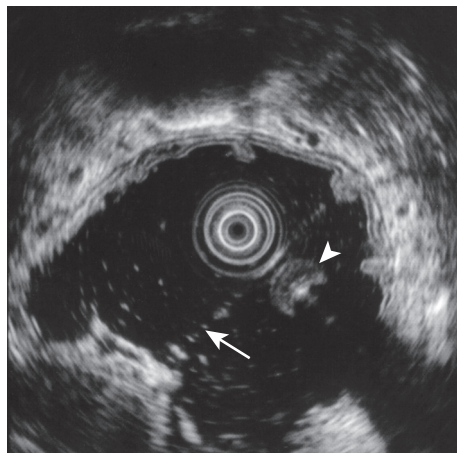
water.<sup>7</sup> In this situation, transmitted ultrasound pulses reflect off the air-water interface (because of the significant impedance mismatch). The result is the creation of multiple reflections that are eventually received by the transducer and lead to production of a mirror image opposite the air-water interface (Figs. 1.13 and 1.14). This artifact is easily identified and can be avoided by removing air and adding more water into the lumen.

## Acoustic Shadowing

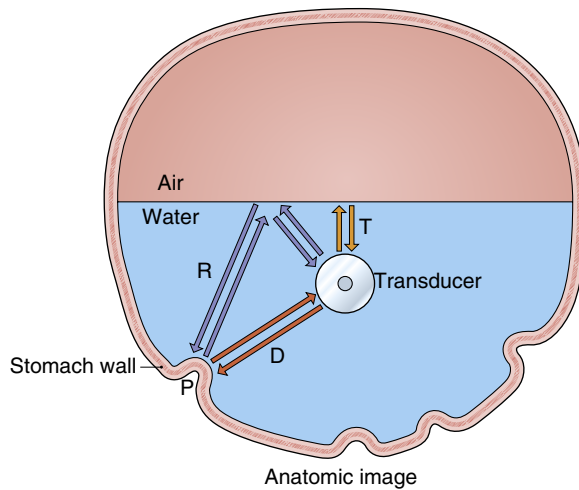
*Acoustic shadowing* is a form of a reflection artifact that occurs when a large impedance mismatch is encountered. When such a mismatch is encountered, a majority of the transmitted pulse is reflected with minimal transmission. This results in a hyperechoic signal at the interface, with no echo signal detected beyond the interface, thus producing a shadow effect. This finding is useful in

diagnosing calcifications in the pancreas (Fig. 1.15) and gallstones in the gallbladder (Fig. 1.16).

Acoustic shadowing can also result from refraction occurring at a boundary between tissues with different acoustic velocities, especially if the boundary is curved (e.g., tumor or cyst). As discussed earlier, refraction of an ultrasound beam occurs when the angle of incidence is not normal to the boundary between tissues with different acoustic velocities, with resulting bending of the ultrasound beam. Because the ultrasound beam



• **Fig. 1.13** Reflection or mirror-image artifact. A mirror image of the transducer (arrowhead) and gastric wall is produced by the reflection of the ultrasound signal from the interface between water and air (arrow) within the gastric lumen.



• **Fig. 1.14** Reflection from an air-water interface produces a mirror-image artifact. Because of the large impedance mismatch between water and air, an ultrasound signal that interacts with an air-water interface is reflected almost completely. The figure on the left is an illustration of an ultrasound probe imaging the gastric wall with an air-water interface. The path denoted by *D* directly images location *P* along the gastric wall. The path denoted by *R* images location *P* because of a reflection from the air-water interface. The path *T* images the transducer because of a reflection from the air-water interface. The figure on the right is an illustration of the resulting ultrasound image. The ultrasound processor registers the location of the image by the direction of the transmitted pulse and the time it receives the reflected signal. The processor accurately registers point *P*, resulting from the reflected signal from path *D*; however, the signal from path *R* is incorrectly registered as point *P'*, with a resulting mirror image appearance. In addition, the reflected signal from path *T* results in shadowing artifact in the mirror image. *EUS*, Endoscopic ultrasonography.

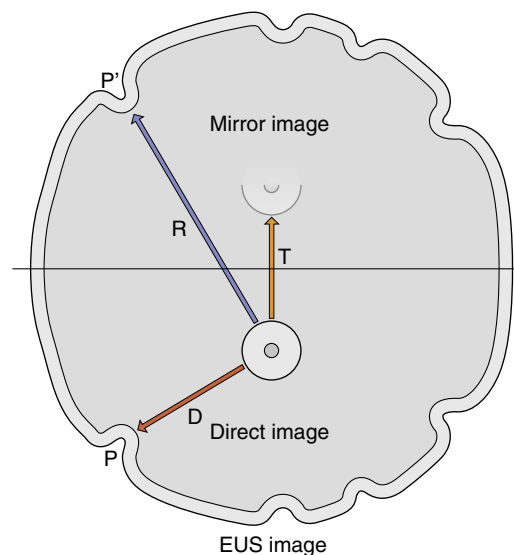
is redirected at this boundary, some regions of the tissue are not interrogated by the ultrasound beam, and the result is an acoustic shadow (Fig. 1.17).<sup>8</sup>

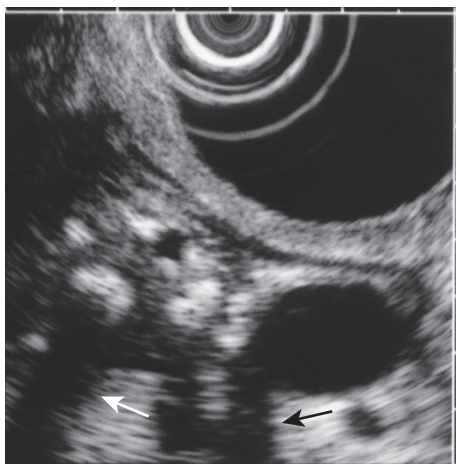
## Through Transmission

*Through transmission* is the enhancement of a structure beyond a fluid-filled structure such as a cyst. The structure beyond a fluid-filled structure demonstrates increased enhancement because the intensity of transmitted ultrasound undergoes less attenuation as it propagates through the cyst and as the reflected signal returns to the transducer. This finding is useful in diagnosing fluid-filled structures such as a cyst or blood vessel (Fig. 1.18).

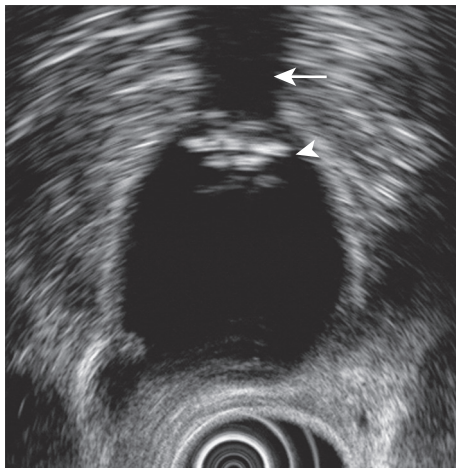
## Tangential Scanning

If the thickness of a structure is being measured, it is important that the ultrasound beam is perpendicular to the structure. If the transducer is at an angle other than 90 degrees to the structure, the thickness will be overestimated.<sup>9</sup> This is particularly important when assessing the thickness of the layers of the GI tract wall and in staging tumors of the GI tract. On radial scanning examination of the GI tract, this artifact can be identified because the thicknesses of the wall layers will not be uniform throughout the image (Fig. 1.19). When staging tumors involving the GI tract wall, tangential imaging can result in overstaging of the tumor. To avoid this artifact, the endoscope tip should be maneuvered to maintain the proper orientation such that the plane of imaging is normal (at 90 degrees) to the structure being imaged.

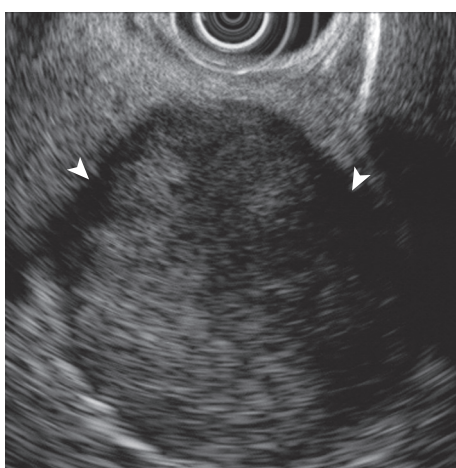




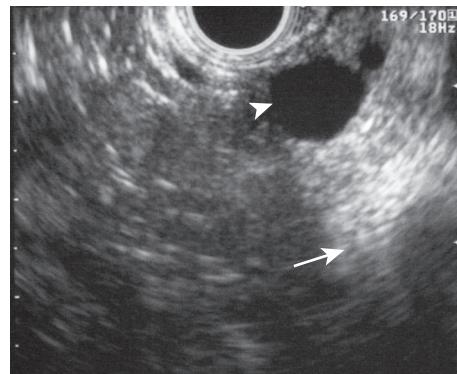
• **Fig. 1.15** Shadowing artifact (arrows) resulting from calcifications in the pancreas.



• **Fig. 1.16** Shadowing artifact (arrow) resulting from gallstones (arrowhead).



• **Fig. 1.17** Acoustic shadowing (arrowheads) resulting from refraction from an interface between normal tissue and tumor.



• **Fig. 1.18** Anechoic cystic lesion (arrowhead) demonstrating enhancement beyond the cyst relative to other structures (white arrow) that are of similar distance from the transducer. This artifact is also called *through transmission*.

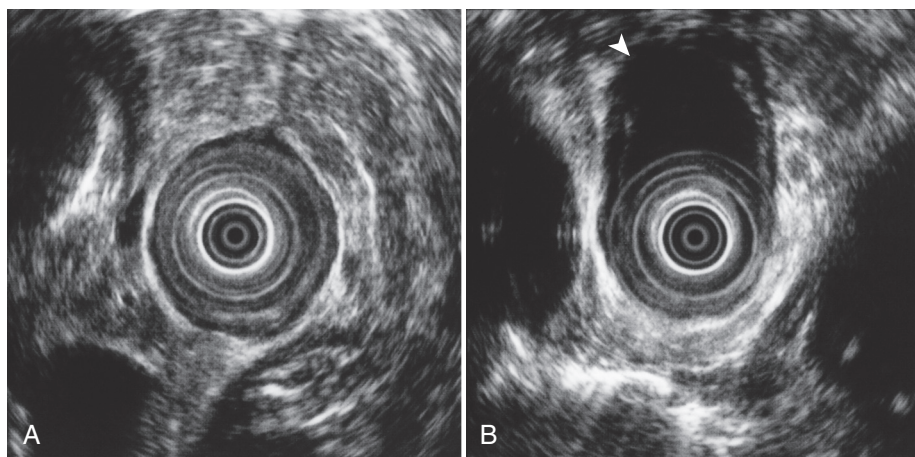
### Side Lobe Artifacts

Side lobes are off-axis secondary projections of the ultrasound beam (Fig. 1.20).<sup>3</sup> The side lobes have reduced intensities compared with the main on-axis projection; however, they can produce image artifacts. Usually, on-axis reflections are greater in intensity than side lobe reflections and thereby obscure any side lobe reflections. However, during imaging of an anechoic structure, the reflected ultrasound energy from a side lobe can be of sufficient intensity to yield a detected signal that is then interpreted by the processor as an on-axis reflection.<sup>10</sup> A side lobe artifact is recognized when the hyperechoic signal does not maintain its position within an anechoic structure such as a cyst or the gallbladder. It may be misinterpreted as sludge in the gallbladder or a mass within a cyst.<sup>6</sup> Fig. 1.21 is an image of a side lobe artifact within the gallbladder. Repositioning of the transducer causes the artifact to disappear.

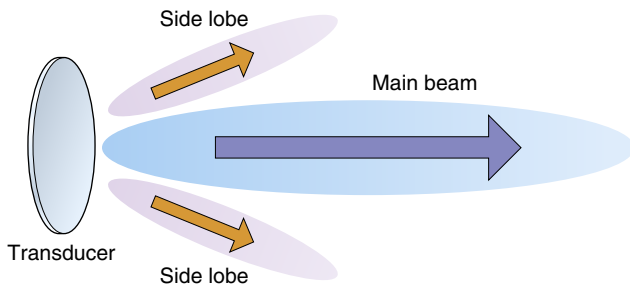
### Endoscopic Ultrasound Elastography

Elastography is an ultrasound-based method for evaluation of tissue “hardness” (i.e., the change in tissue dimensions [strain] arising from an applied force). This concept is closely related to palpation, which physicians have used for centuries to detect pathology associated with higher tissue “stiffness.” There are multiple parameters describing tissue elastic properties, including bulk modulus (see Eq. 1.3, see Table 1.1), which describes the change in volume of the material in response to external stress. As seen from Table 1.1, bulk modulus varies only by no more than 15% among different tissue types. However, palpation elicits different elasticity parameters—Young’s modulus and/or shear modulus, which represent the ratio of tissue displacement (or strain) in a certain direction (longitudinal or transverse) to the applied stress. The elastic moduli of normal soft tissues are known to vary as much as four orders of magnitude and are elevated by the pathologic changes, such as fibrosis, by up to two orders of magnitude, with benign tumors being generally softer than malignant tumors.<sup>11</sup>

In elastography, stress is applied to tissue either externally (e.g., vibration, manual pressure, or balloon inflation in the case of transluminal examination) or internally (e.g., by vascular pulsations and respiratory motion). The resulting strain is measured using ultrasound, as illustrated in Fig. 1.22, showing B-mode images are recorded before and after the application of stress. Each of the B-mode line scans recorded before and after compression

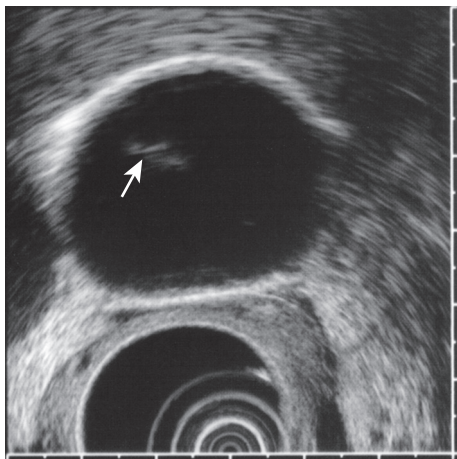


• **Fig. 1.19** Tangential imaging artifact. (A) Normal imaging of a hypertrophic lower esophageal sphincter in a patient with achalasia. (B) Tangential imaging of the same lower esophageal sphincter (note that the balloon was not inflated during acquisition of this image). The gastrointestinal (GI) tract wall layers are distorted and are not uniformly thick circumferentially, a finding suggesting that the transducer is not imaging a normal GI tract wall. As a result, areas of abnormal thickening are noted on imaging and can give the incorrect appearance of a tumor in the GI tract wall (arrowhead).



• **Fig. 1.20** Side lobes represent secondary projections off-axis from the main beam. Side lobes have lower intensities than the main beam, but they can still produce backreflected signals from the tissue of sufficient intensity to be detected by the transducer. However, the transducer assumes that all backreflections originate from the main lobe. Therefore image artifacts can result from side lobe projections.

is then analyzed using cross-correlation techniques to extract the in-depth strain distribution. These strain line scans are then combined into a two-dimensional elastogram, which is superimposed in semitransparent color onto the B-mode image. To indicate tissue softness, the system uses hue color map (on a scale of 1 to 255) where the hardest tissue appears as dark blue and the softest tissue as red. A region of interest (ROI) in which the elasticity information is calculated is selected manually to include the targeted lesion and some of the surrounding tissue. It is worth noting here that the displayed elasticity map is, strictly speaking, not a direct representation of tissue elastic modulus distribution in absolute units, but rather relative tissue displacement distribution within the ROI (because the stress is unknown). Moreover, the diagnosis made based solely on color (blue means malignant) is subject to strong bias and is operator dependent. This approach is called qualitative elastography.<sup>12</sup> Second-generation EUS elastography allows for quantitative analysis of tissue stiffness.<sup>13</sup> Two different areas (A and B) from the ROI are selected for quantitative elastographic analysis, so that area A includes the mass of interest and area B refers to a soft peripancreatic reference area outside the tumor. The parameter B/A (strain ratio) is considered as the measure of the elastographic evaluation.



• **Fig. 1.21** Side lobe artifact identified in the gallbladder (arrow). Repositioning of the transducer results in disappearance of this signal.

## Contrast-Enhanced Harmonic Imaging

Contrast enhancement in ultrasound imaging is based on the backscatter of the ultrasound waves from the ultrasound contrast agents (UCAs) that are administered intravenously. UCAs are usually gas bodies or bubbles of 2- to 6-mm diameter surrounded by a shell and are stable in the circulation and restricted to the inside of the blood vessels until they are eliminated in the expired air. The way UCAs interact with and scatter the incident ultrasound waves with frequency  $f$  depends primarily on the ultrasound pressure amplitude, as illustrated in Fig. 1.23. At low ultrasound pressure levels, the bubble expands and contracts synchronously with the incident pressure wave, and these oscillations are small compared with the bubble radius. The frequency of the scattered ultrasound wave in this case is also  $f$ , and the bubble simply plays the role of an efficient reflector. At larger ultrasound wave amplitudes,

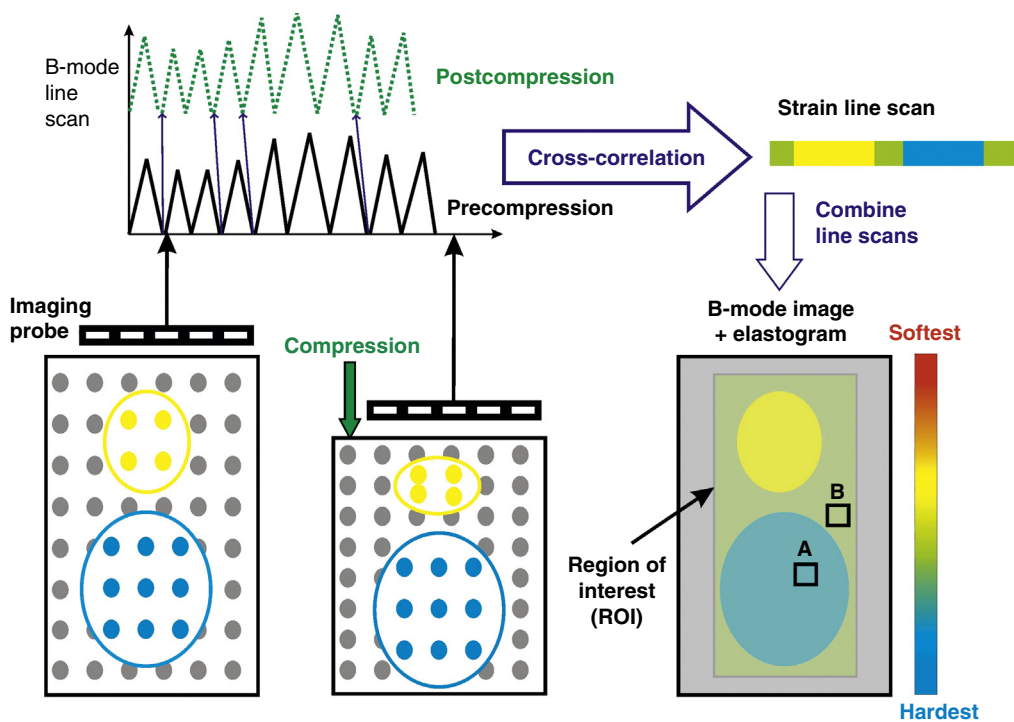


**Fig. 1.22** Conceptual diagram of ultrasound elastography. Two B-mode images are acquired, before and after tissue compression. Tissue displacement within hard inclusions (blue), which are often associated with pathologic changes, is smaller than the displacement of surrounding tissue (gray) or soft inclusions (yellow). B-mode line scans from each of the array elements obtained before and after tissue compression are then compared using cross-correlation techniques to reconstruct the in-depth tissue displacement distribution. The line scans are then combined into a two-dimensional color image representing tissue softness, with a hue diagram range of 1 to 255. This image is only calculated within the region of interest defined by the user to include the lesion of interest and some of the surrounding tissue. Although this qualitative information is often helpful, quantitative measurements of tissue elasticity are more reliable and can be obtained, for example, as follows. Two areas (A and B) are selected on the elastogram, in the lesion of interest and in the fat or connective tissue, and the ratio of the mean strain within these areas is measured.

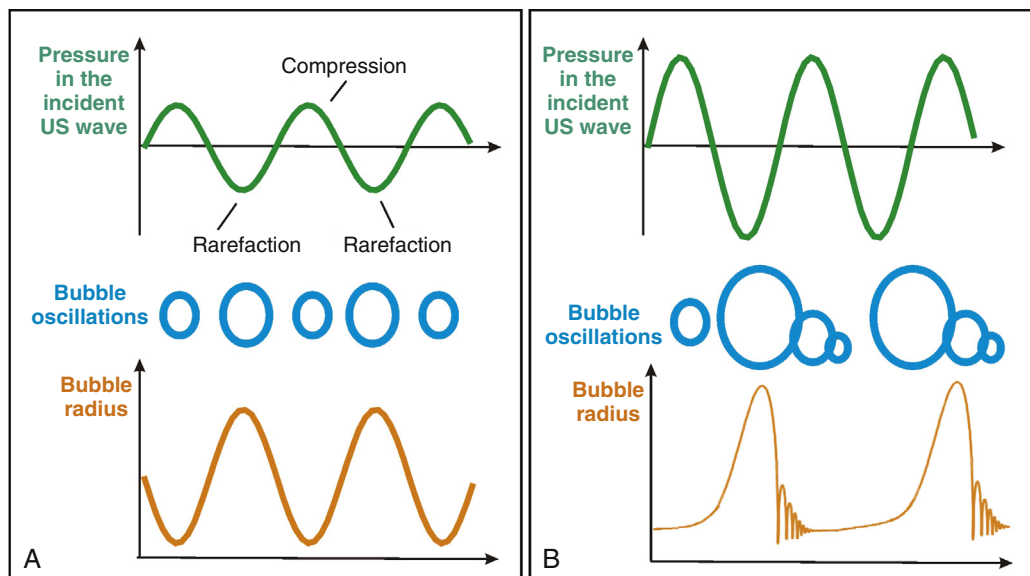


**Fig. 1.23** Scenarios of the response of an ultrasound (US) contrast agent—2- to 6- $\mu\text{m}$  gas bubble covered by a thin shell—to an incident US wave. (A) Low-amplitude US wave. The bubble oscillations are spherically symmetric and small compared with the bubble's initial radius. The compression and expansion of the bubble are synchronized with the compression and rarefaction phases in the ultrasound wave. (B) Higher-amplitude US wave. The bubble oscillations become unstable, with a slow growth phase followed by a rapid collapse and several rebounds. The frequency of bubble collapses is higher than the frequency of the incident US wave.

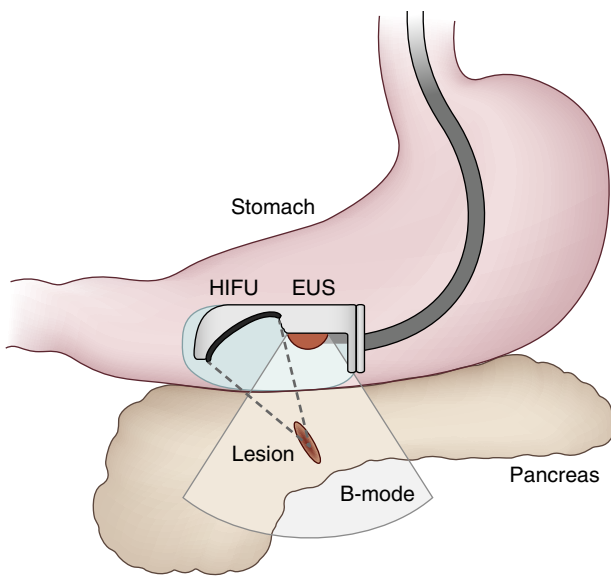


**Fig. 1.24** Illustration depicting an endoscopic ultrasonography–high-intensity focused ultrasound (EUS-HIFU) device in the stomach targeting the pancreas. The device is coupled to the stomach wall by the distended water balloon. The HIFU transducer and the EUS imaging probe are aligned so that the HIFU focus is within the window of B-mode imaging allowing monitoring of lesion formation in real time. (Reproduced with permission from Li T, Khokhlova T, Maloney E, et al. Endoscopic high-intensity focused US: technical aspects and studies in an in vivo porcine model (with video). *Gastrointest Endosc*. 2015;81:1243–1250.)

bubble oscillations become unstable and include periods of slower growth and subsequent rapid collapse. These collapses lead to the generation of secondary ultrasound waves, or harmonics, with a frequency higher than the fundamental frequency by an integer factor multiple:  $2f$ ,  $3f$ , etc. Therefore if the imaging transducer is tuned to transmit at the frequency  $f$  and receive at the frequency  $2f$ , then only the areas containing bubbles (i.e., blood vessels) will be visualized.

The process described previously is commonly referred to as contrast-enhanced harmonic imaging and has been increasingly used in the past years for characterization of microvasculature and perfusion inside the lesion of interest with the aim of improved differential diagnosis, as well as longitudinal monitoring of the effects of chemotherapy and/or antiangiogenic therapy in advanced digestive cancers. The movement of UCAs through the circulation can be monitored by harmonic imaging in real time, which allows measurement of a number of useful quantitative parameters that correlate with the microvascular blood flow such as wash-in and wash-out time, and mean transit time.<sup>13</sup>

## High-Intensity Focused Ultrasound

High-intensity focused ultrasound (HIFU) is an emerging technology that has potential to use ultrasound energy directly for therapeutic purposes, including ablation and enhancing drug delivery.<sup>14–16</sup> HIFU delivers high-intensity ultrasound energy to a target using a focused transducer (Fig. 1.24). Heating and ablation of tissue can then result at the focus depending on the intensity of the ultrasound energy and the duration of exposure. This is analogous to the use of a magnifying glass to focus sunlight to heat objects at the focus of the magnifying glass.

Typically, ablation from a fixed-focus HIFU transducer is the shape of a grain of rice. However, this can be modified by using a multielement ultrasound transducer and electronically steering the focus to create a larger volume of ablation. Heating and ablation of tissue can be performed within the body if there is an acoustic path (i.e., no air or bone) between the ultrasound transducer and the target.

In addition to ablation, HIFU can be used to enhance drug delivery by two different methods. One method involves the simultaneous systemic delivery of temperature-sensitive liposomes loaded with drug.<sup>17</sup> Temperature-sensitive liposomes are loaded with drug and release their payload at specific temperatures, typically in the hyperthermia range of 40°C to 43°C. By targeting the release of drug, higher concentrations of drug can be delivered to a specific target, thereby reducing the overall dose of drug to the patient and limiting the systemic toxicity from the drug. The second method that HIFU can be used to enhance drug delivery is by mechanically disrupting the stroma of a tumor by inciting cavitation within the stroma from high-amplitude ultrasound pulses.<sup>18</sup> This method has been demonstrated to increase drug penetration into animal models of pancreatic cancer that are known to have dense, fibrous stroma, which inhibits drug penetration in pancreatic tumors.

A prototype EUS-HIFU device has been developed and tested in a large animal model (swine).<sup>19</sup> The benefit of an EUS-HIFU device over extracorporeal HIFU systems is the ability to position the HIFU transducer closer to the target. In particular, targets such as tumors in the pancreas and liver are ideal for EUS-HIFU because the acoustic path to the liver and pancreas from an extracorporeal approach is limited due to the ribs and gas within the bowel. Furthermore, by positioning the HIFU transducer closer to the target, less ultrasound energy is required, reducing the risk of causing any damage to intervening structures.

## Summary

The basic principles of ultrasound physics and instrumentation are reviewed in this chapter. In addition, common imaging artifacts are presented and explained by applying the basic principles of ultrasound. These principles should provide an understanding of the capabilities and limitations of ultrasound and how ultrasound images are formed. Understanding these principles will aid the endosonographer in obtaining accurate, high-quality images. Advances in ultrasound technology will broaden the capability of both diagnostic and therapeutic endoscopic ultrasound.

## Key References

1. Hedrick WR, Hykes DL, Starchman DE. *Ultrasound Physics and Instrumentation*. 3rd ed. St. Louis: Mosby; 1995.
2. Duck FA. *Physical Properties of Tissue*. London: Academic Press; 1990.
3. Christensen DA. *Ultrasonic Bioinstrumentation*. New York: John Wiley; 1988.
4. Shung KK, Thieme GA. *Ultrasonic Scattering in Biological Tissues*. Boca Raton, FL: CRC Press; 2000.
6. Hwang JH, Kimmy MB. Basic principles and fundamentals of endoscopic ultrasound imaging. In: Gress FG, Savides TJ, eds. *Endoscopic Ultrasonography*. 3rd ed. West Sussex: Wiley Blackwell; 2016:5–14.

## References

Access the reference list online at [ExpertConsult.com](http://ExpertConsult.com).

## References

1. Hedrick WR, Hykes DL, Starchman DE. *Ultrasound Physics and Instrumentation*. 3rd ed. St. Louis: Mosby; 1995.
2. Duck FA. *Physical Properties of Tissue*. London: Academic Press; 1990.
3. Christensen DA. *Ultrasonic Bioinstrumentation*. New York: John Wiley; 1988.
4. Shung KK, Thieme GA. *Ultrasonic Scattering in Biological Tissues*. Boca Raton, FL: CRC Press; 2000.
5. Harris RA, Follett DH, Halliwell M, Wells PN. Ultimate limits in ultrasonic imaging resolution. *Ultrasound Med Biol*. 1991;17:547–558.
6. Hwang JH, Kimmy MB. Basic principles and fundamentals of endoscopic ultrasound imaging. In: Gress FG, Savides TJ, eds. *Endoscopic Ultrasonography*. 3rd ed. West Sussex: Wiley Blackwell; 2016:5–14.
7. Grech P. Mirror-image artifact with endoscopic ultrasonography and reappraisal of the fluid-air interface. *Gastrointest Endosc*. 1993;39:700–703.
8. Steel R, Poepping TL, Thompson RS, Macaskill C. Origins of the edge shadowing artifact in medical ultrasound imaging. *Ultrasound Med Biol*. 2004;30:1153–1162.
9. Kimmy MB, Martin RW. Fundamentals of endosonography. *Gastrointest Endosc Clin N Am*. 1992;2:557–573.
10. Laing FC, Kurtz AB. The importance of ultrasonic side-lobe artifacts. *Radiology*. 1982;145:763–768.
11. Greenleaf JF, Fatemi M, Insana M. Selected methods for imaging elastic properties of biological tissues. *Annu Rev Biomed Eng*. 2003;5:57–78.
12. Iglesias-Garcia J, Dominguez-Munoz JE. Endoscopic ultrasound image enhancement elastography. *Clin N Am*. 2012;22:333–348.
13. Gheonea D-I, Saftoiu A. Beyond conventional endoscopic ultrasound: elastography, contrast enhancement and hybrid techniques. *Curr Opin Gastroenterol*. 2011;27:423–429.
14. Dubinsky TJ, Cuevas C, Dighe MK, et al. High-intensity focused ultrasound: current and potential oncologic applications. *AJR Am J Roentgenol*. 2008;190:191–199.
15. Jang HJ, Lee JY, Lee DH, et al. Current and future applications of high-intensity focused ultrasound (HIFU) for pancreas cancer. *Gut Liver*. 2010;4:S57–S61.
16. Maloney E, Hwang JH. Emerging HIFU applications in cancer therapy. *Int J Hyperthermia*. 2015;31:302–309.
17. Chen H, Hwang JH. Ultrasound-targeted microbubble destruction for chemotherapeutic drug delivery to solid tumors. *J Ther Ultrasound*. 2013;1:10.
18. Li T, Wang YN, Khokhlova TD, et al. Pulsed high intensity focused ultrasound (pHIFU) enhances delivery of doxorubicin in a preclinical model of pancreatic cancer. *Cancer Res*. 2015;75:3738–3746.
19. Li T, Khokhlova T, Maloney E, et al. Endoscopic high-intensity focused US: technical aspects and studies in an in vivo porcine model (with video). *Gastrointest Endosc*. 2015;81:1243–1250.

# 2

# Equipment

GIRISH MISHRA

## KEY POINTS

- A comprehensive endoscopic ultrasound (EUS) service requires the full gamut of echoendoscopes (radial and linear) and probes (miniprobe and rectal) available
- There has been tremendous advancement in needle designs and options with the advent of fine-needle biopsies
- Needle-based probes allow for microscopic biopsies and nonsurgical treatment of cystic lesions and neuroendocrine tumors
- Direct deployment of lumen-apposing stents under EUS guidance has heralded a new era of endoscopic therapy for pseudocysts, biliary drainage, and luminal access

## Introduction

The fundamental designs of the echoendoscopes have not changed drastically since 2010. Differing feel of the scope, tip articulation, and the corresponding ultrasound image inherently distinguish the main scopes available. Current echoendoscopes have overcome the technical challenges from their predecessors that were saddled with limitations in maneuverability and endoscopic views. The console of each processor is designed slightly differently, yet they all achieve a common end result—detailed ultrasound images at varying frequencies. Knowledge of basic ultrasound terminology and physics is imperative regardless of the processor and scope manufacturing. However, since 2015, the burgeoning field of tissue acquisition via different needle designs, including the capabilities for core biopsies, has heralded a “dawn of a new era.” In fact, many have coined the phrase “optical biopsy” to describe imaging obtained from a needle-based probe via EUS. A corollary to the needle-based diagnostic capabilities is the emerging therapeutic options available with needle-based radiofrequency ablation (RFA) for cysts and small neuroendocrine tumors. Finally, this chapter will summarize the excitement surrounding tissue-apposing luminal stents for pseudocyst drainage, biliary drainage, and creating hepaticogastrostomy—all solely through the EUS scope.

## Equipment

Although the advent of EUS technology witnessed intense competition between our industry colleagues to bring forward differing scope designs focusing on radial and linear technology, the most recent additions to the EUS armamentarium have involved

accessories such as refinements in needle technology and the ability to acquire core biopsy material. Taking a cue from endosonographers who have repeatedly thought “outside of the box,” manufacturers have partnered to develop needle-based probes that may allow “optical biopsies,” obviating the need for obtaining any tissue at all. Balancing exquisite diagnostic capabilities with therapeutic aplomb has always remained at the heart of endoscopy. Historical perspective from the evolution of diagnostic endoscopic retrograde cholangiopancreatography (ERCP) to therapeutic has provided a template for its sister technology—EUS. Not surprising, the past several years have served notice as to the direction of EUS—therapeutic applications with its requisite accessories have garnered the attention, fascination, and economic energy of endosonographers and industry.

## Radial Scopes

All three manufacturers (Olympus, Center Valley, Pennsylvania; Pentax, Montvale, New Jersey; and Fujifilm, Wayne, New Jersey) offer forward-viewing gastrosopes with 360-degree, electronic, radial-array ultrasound transducers that generate high-resolution ultrasound images. The scope designs and processor capabilities are outlined in [Table 2.1](#). Current-generation electronic radial echoendoscopes use high-resolution videochip technology for high-resolution imaging. Virtually all current-generation radial scopes are electronic, in which the piezoelectric crystals are arranged in a band around the shaft of the endoscope perpendicular to the long axis of instrument, generating a 360-degree cross-sectional image. There are subtle differences in the scope designs of these three instruments. The suction channel and optical sensor is displaced proximal to the transducer in the Olympus design ([Fig. 2.1A](#)). The suction channel and the optical sensor are placed at the distal tip of the Pentax echoendoscope (see [Fig. 2.1B](#)). Fujifilm’s echoendoscope has a similar suction and optical sensor design while being equipped with the ultrasmall Super CCD (charged-couple device) Chip images (see [Fig. 2.1C](#)). All three scope designs incorporate a water-filled balloon around the transducer to achieve acoustic coupling. At the inception of EUS technology, most endosonographers used a radial echoendoscope first, followed by a linear, when a fine-needle aspiration (FNA) was deemed necessary. With time, this practice has become mostly obsolete such that most endosonographers now proceed directly with the linear echoendoscope in virtually every case. The exceptions to this *modus operandi* would be for primary staging of esophageal, gastric, or rectal cancer and for further visualization and characterization of submucosal lesions.

**TABLE 2.1** Echoendoscopes, Processors, and Specifications

Manufacturer	Model	Frequency (MHz)	Field of View	Scanning Angle (Degree) Type of Scan	Insertion Tube OD (mm) Channel ID (mm)	Compatible Processors
Olympus	GF-UE160-AL5	5, 6, 7.5, 10	100 degree (55 degree forward oblique)	360 Elect Radial	11.8/2.2	EU-ME1/2 Premier Plus, SSD-a5/10, ProSound F75
	GF-UC140P-AL5	5, 6, 7.5, 10	100 degree (55 degree forward oblique)	180 Curvilinear	11.8/2.8	EU-ME1/2 Premier Plus, SSD-a5/10, ProSound F75
	GF-UCT140-AL5	5, 6, 7.5, 10	100 degree (55 degree forward oblique)	180 Curvilinear	12.6/3.7	EU-ME1/2 Premier Plus, SSD-a5/10, ProSound F75
	GF-UCT180	5, 6, 7.5, 10	100 degree (55 degree forward oblique)	180 Curvilinear	12.6/3.7	EU-ME1/2 Premier Plus, SSD-a5/10, ProSound F75
	TGF-UC180J	5, 7.5, 10, 12	120 degree (forward viewing)	90 Curvilinear	12.6/3.7	EU-ME1/2 Premier Plus, SSD-a5/10, ProSound F75
Pentax	EG-3670URK	5, 6, 7.5, 9, 10	140 degree (forward viewing)	360 Elect Radial	12.1/2.4	Hitachi HI VISION Preirus, Hitachi Noblus
	EG-3870UTK	5, 6, 7.5, 9, 10	120 degree (forward oblique)	120 Curvilinear	12.8/3.8	Hitachi HI VISION Preirus, Hitachi Noblus
	EG-3270UK	5, 6, 7.5, 9, 10	120 degree (forward oblique)	120 Curvilinear	10.8/2.8	Hitachi HI VISION Preirus, Hitachi Noblus
Fujifilm	EG-530UR2	5, 7.5, 10, 12	140 degree (forward viewing)	360 Elect Radial	11.4/2.2	EPX-4440HD, EPX-4400HD, EPX-4400, SU-1
	EG-530UT2	5, 7.5, 10, 12	140 degree (forward oblique)	124 Curvilinear	13.9/3.8	EPX-4440HD, EPX-4400HD, EPX-4400, SU-1

ID, Inner diameter; OD, outer diameter.

## Linear Scopes

The same three manufacturers (Olympus, Pentax, and Fujifilm) offer linear echoendoscopes with slight differences in the “feel” of the echoendoscope, tip maneuverability, and the shape of the transducers, all of which impact the ultrasound image produced (see Table 2.1). For most endosonographers, these scopes represent the “workhorse” scopes in that they offer both diagnostic and therapeutic capabilities. The choice of scope is a matter of personal preference, but technically there are distinct differences in the scope design and the ensuing images (Fig. 2.2). In general, the Olympus transducer has a more contoured, rounded tip, allowing for increased imaging of tissue anterior to the echoendoscope. Pentax linear echoendoscopes incorporate a Hi-Compound feature, which combines frequency and spatial compounding, allowing an image to be scanned from multiple angles. Fujifilm echoendoscopes combine easier maneuverability with similar therapeutic options; at present, there is only one linear echoendoscope option with a unique processor platform. An elevator is present on each of these scopes, allowing the operator

to vary the angle at which the needle enters the tissue. Even without using the elevator, the angle of the needle puncture into the tissue/lesion differs. The therapeutic linear scopes (often designated with a “T”) have a larger working channel (3.8 mm with Fujifilm and Pentax), allowing for therapeutic interventions such as stent deployment for pseudocyst drainage and biliary decompression.

Pentax Medical has developed a newer slim linear echoendoscope (EG-3270UK), which has a smaller 2.8-mm instrument channel design and a new elevator design to allow for more needle control (Fig. 2.3). The insertion tube is smaller in caliber as well (10.8 mm). This device recently received US Food and Drug Administration (FDA) approval for its use in the United States.

Olympus has introduced a forward-viewing, curved linear array (TGF-UC 180J) with a zero-degree working channel designed to perform interventional procedures (Fig. 2.4). Features of this scope design include a short distal tip, straight working channel, extensive angulation, and an auxiliary water channel, obviating the need for a balloon.



**• Fig. 2.1** (A) GF-UE160-AL5 is a 360-degree radial array scanning endoscope. (B) Pentax EG-3670URK is a 360-degree radial array scanning endoscope. (C) Fujifilm EG-530UR2 Ultrasonic Radial Scanning Endoscope is a 360-degree radial array scanning endoscope. ([A] Image courtesy of Olympus America, Center Valley, Pennsylvania; [B] Image courtesy of Pentax Medical, Montvale, New Jersey; [C] Image courtesy of Fujifilm, Wayne, New Jersey.)

## Processors

Each echoendoscope requires a distinct and unique ultrasound processor for imaging; the cost implications and the hindrance that this imposes is implicit. Table 2.1 summarizes the compatible processors with each scope. There are unique features and enhancements to the designs of the processors that worth highlighting. Fujifilm promotes its second-generation scopes that use small Super CCD chip technology which offer bright, vivid, high-resolution endoscopic images with the integration of ZONE Sonography and Sound Speed Correction technologies to deliver ultrasound images. The new compact Sonart Su-1 processor can be used for both its radial and linear echoendoscopes (Fig. 2.5). Fundamental imaging is obtained at 5, 7.5, 10, and 12 MHz with tissue harmonic imaging at 8 and 10 MHz. Compound harmonic imaging, sound speed imaging and elastography are added features.

Pentax uses a Hitachi Ultrasound platform with fundamental imaging frequencies at 5, 6, 7.5, 9, and 10 MHz. Noblus serves as their compact processor, touted to be no larger than a laptop

(Fig. 2.6A). The HI VISION Preirus ultrasound platform combines Hi-Compound imaging with Hi-Resolution (see Fig. 2.6B). These technologies report enhanced organ boundary visualization and reduced angle-dependent artifacts.

Olympus offers two distinct ultrasound platforms, the Hitachi-Aloka ProSound F75 and EU-ME2 (and Premier Plus) (Fig. 2.7A and B). The ProSound distinguishes itself by offering a sleek, ergonomically engineered console and screen that can be adjusted horizontally and vertically per the endosonographer's wishes. Imaging frequencies are at 5, 6, 7.5, and 10 MHz with the ProSound and up to 12 MHz with the EU-ME2 and Premier Plus. A contrast echo feature with this device enables the display of microvascularization of blood vessels to the capillary level. Of the many enhanced ultrasound physics capabilities, the eFlow feature that enables increased sensitivity to flow at low velocities and in small vessels is attractive and useful, particularly when assessing for the ideal path of needle puncture. The EU-ME2 Premier Plus represents the world's only ultrasound processor for endoscopic and bronchoscopic applications. The versatility and universal



• **Fig. 2.2** (A) Olympus GF-UCT curved linear array. (B) Pentax EG-3870UTK curved linear array. (C) Fujifilm EG-530UT2 Ultrasonic Convex Scanning Endoscope. ([A] Image courtesy of Olympus America, Center Valley, Pennsylvania; [B] Image courtesy of Pentax Medical, Montvale, New Jersey; [C] Image courtesy of Fujifilm, Wayne, New Jersey.)



• **Fig. 2.3** Pentax EG-3270UK slim curved linear array. (Image courtesy of Pentax Medical, Mississauga, Ontario, Canada.)



• **Fig. 2.4** TGF-UC180J forward-viewing curved linear array for interventional procedures with a zero degree working channel. (Image courtesy of Olympus America, Center Valley, Pennsylvania.)

capabilities are attractive if the same processor needs to be shared between pulmonologists and gastroenterologists performing endobronchial and endoscopic ultrasound respectively. In addition, this processor is backward compatible, meaning that the processor can be used with older/current Olympus EUS scopes while being forward compatible as newer (future/forward) EUS scopes are introduced. This processor provides image quality equal to a larger radiology processor while maintaining its compact design.

## Endoscopic Ultrasound With Elastography

Unfortunately, despite advances in needle design and increased endosonographer experience, EUS FNA yields false-negative results in 20% to 40% of pancreatic malignancy cases deemed technically challenging or with concomitant chronic pancreatitis. The development of EUS elastography (EUS-E) aims to differentiate benign from malignant solid pancreatic masses without the need

for biopsy. EUS-E works by applying a compressive force to a mass during real-time EUS to assess the relative stiffness of a lesion compared with the adjacent normal tissue, with tumors or inflammatory lesions appearing less compressible. The degree of tissue strain from compression produces a color-coded elastography image that is then superimposed on conventional B-mode imaging, such that red reflects soft tissue, blue represents hard tissue, and tissue with intermediate stiffness appears yellow/green (Fig. 2.8). All three processors discussed previously have elastography capabilities. Elastography can be added to the Olympus Aloka ProSound platform with an added cost. The Pentax HiVision Preirus offers the most robust, refined, and sophisticated elastography capabilities.

## Miniprobes

At present, only Olympus manufactures catheter probes that are approved internationally and FDA cleared for use in the United States. Fujifilm also manufactures probes, which are available internationally. An array of ultrasound probes with varying frequencies (12 to 30 MHz) is available (Table 2.2). We rely exclusively on the 12 MHz and 20 MHz (UM-2R and UM-3R) in our clinical practice (Fig. 2.9). These small-caliber miniprobes measure 2.0 to 2.5 mm and can be advanced through the working channel of any standard diagnostic or therapeutic upper endoscope or colonoscope whose working channel is >2.8 mm. A balloon sheath may be used to enhance acoustic coupling; a two-channel endoscope allows for simultaneous ultrasound images with the ability to instill water or suction through the second channel. Such needs are obviated in the colon by instilling water in the lumen. The ultrasound image is mechanical and radial and offers a 360-degree view. An additional motor drive unit is required that attaches to



• **Fig. 2.5** Fujifilm SU-1 Ultrasonic Processor for both radial and linear echoendoscopes. (Image courtesy of Fujifilm, Wayne, New Jersey.)

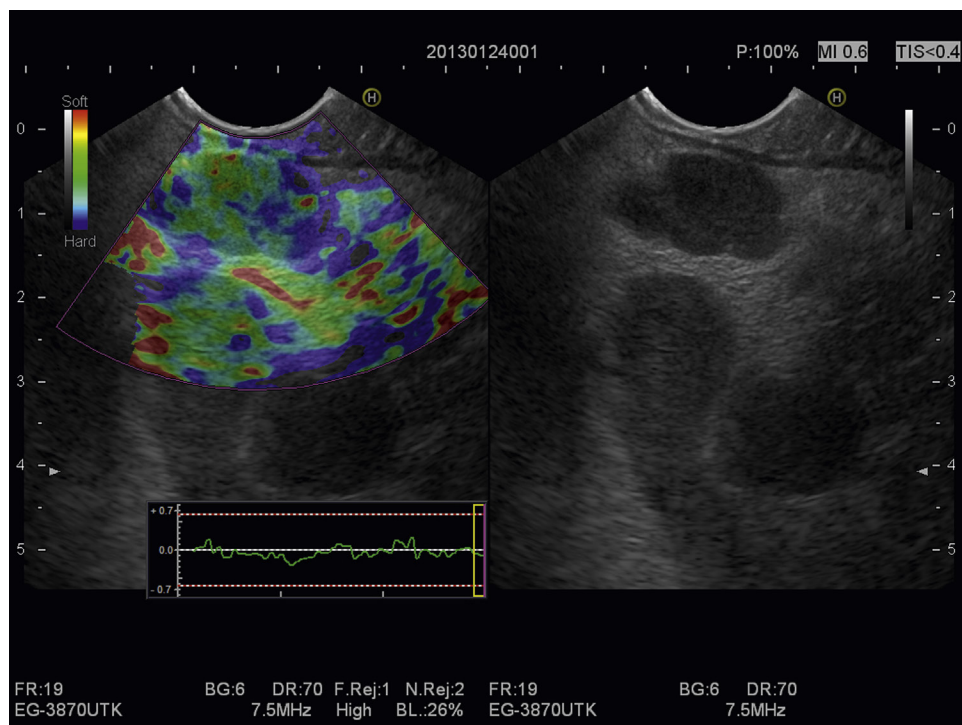


• **Fig. 2.6** (A) Noblus processor. (B) HI VISION Preirus ultrasound processor. (Images courtesy of Pentax Medical, Montvale, New Jersey.)





• **Fig. 2.7** (A) Hitachi-Aloka ProSound F75 ultrasound processor. (B) EU-ME2 and Premier Plus ultrasound processors. (Image courtesy of Olympus America, Center Valley, Pennsylvania.)



• **Fig. 2.8** Sonoelastography images using real-time Doppler technology to provide information about the relative stiffness of suspicious tissue. Hard tissue (malignant) is depicted as blue. (Image courtesy of Pentax Medical, Montvale, New Jersey.)

**TABLE 2.2** Miniprobes

Manufacturer	Model	Compatible Probe Drive Units	Frequency (MHz)	Working Length (cm)	Minimum Working Channel (mm)
Olympus aFujifilm	UM-2R-3	MAJ-1720	12	205	2.8
	UM-3R-3	SP-702	20	205	2.8
	UM-G20-29R-3	Suitable for DBE	20	205	3.2
	UM-DP12-25R		12	205	2.8
	UM-DP20-25R		20	205	2.8
	UM-DG20-31R		20	205	3.7
	P2625-M		25	220	2.6
	P2620-M		20	220	2.6
	P2615-M		15	220	2.6
	P2612-M		12	220	2.6
	P2620-L		20	270	2.8
	P2615-L		15	270	2.8
	P2612-L		12	270	2.8

<sup>a</sup>Not available in the United States.

DBE, Double balloon enteroscope.



• **Fig. 2.9** Olympus UM-2R-3 12-MHz ultrasound probe. (Image courtesy of Olympus America, Center Valley, Pennsylvania.)

the catheter probe and an ultrasound processor. The clinical utility of these high-frequency probes is to better image small, superficial lesions often <1.0 cm in size in the esophagus, stomach, or other areas in the gastrointestinal track. These probes are ideal for further interrogating small intramural or subepithelial lesions that might become “squashed” and hence difficult to study with the standard echoendoscopes. A colonoscopy with a miniprobe has allowed us to better characterize sometimes subtle and difficult to characterize lesions in the terminal ileum and locations in the colon not accessible by our standard radial echoendoscopes. This information has been profoundly reassuring for our patients and referring physicians.

These probes can be somewhat technically challenging to use. The motor unit should never be turned unless the distal tip of probe is clearly visualized outside of the endoscope. The probe needs to be in proximity of the lesion being interrogated, with fine adjustments to achieve the proper angle needed for ideal images. The listed number of uses (50 to 100) for the catheter probes is directly proportional to the care and handling. These ultrasound probes should never be coiled; we house them in a long cylindrical tube against a wall. A wire-guided version can be advanced into the biliary or pancreatic ductal systems via ERCP to obtain intraductal ultrasound.

## Rectal Probes

Olympus manufactures two 360-degree mechanical radial scanning rectal probes (RU-75M-R1 and RU-12M-R1) that offer

depth comparable to its conventional radial echoendoscopes at 7.5 and 12 MHz, respectively. The rigid, yet light and slim insertion probe at 12-mm outer diameter allows for excellent imaging of the anal sphincter muscles when evaluating for fecal incontinence. Rectal tumors and polyps can be further assessed; however, these probes lack an endoscope.

## Accessories

The past decade has witnessed a relatively stable influx of new scope and processor design. However, there has been a precipitous rise in the refinements in needle design and emergence of newer accessories for obtaining core biopsies. Specific needles designed for celiac plexus neurolysis, and fiducial placement further highlight the expanding field and market for EUS therapeutics. Exciting developments in needle-based probes and RFA devices over the past few years offer adjunct devices to help diagnose and treat pancreatic lesions. Finally, platforms for direct EUS-guided pseudocyst, biliary, and gallbladder drainage devices offer therapeutic options that were brushed off as wishful thinking just a few years ago.

## Fine-Needle Aspiration Needles

The expansion of FNA needle manufacturers attests to this rapidly expanding market. Virtually all needle designs incorporate proprietary nuances to the needle tip, stylet compositions, and configuration, along with differing sheath materials, length, and attachment to the FNA channel. The unique handle designs and feel also distinguish the different needles. Numerous single-use needle devices are available in 19-, 22-, and 25-G. **Table 2.3** summarizes the currently available FNA needles and highlights some of the subtle differences—proprietary modifications in the needles such as laser etching, mechanical dimpling, or sandblasting of the leading tip enhances echogenicity for ultrasound visualization. Needle and sheath composition may consist of aluminum, stainless steel, chromium-cobalt, and nitinol. **Fig. 2.10** depicts the majority of the FNA needles available on the market. The Beacon needle (Medtronic, Sunnyvale, California) differs from others because the needle is advanced within a delivery sheath that is capable of

**TABLE 2.3** Fine-Needle Aspiration

Company	Product Name(s)	Sizes	Needle Design	Design Features and Intended Benefits
Cook Medical	EchoTip Ultra	19 Ga 22 Ga 25 Ga	Lancet	<ul style="list-style-type: none"> <li>• Echogenic needle for better targeting and visibility</li> <li>• Naturally contoured handle</li> <li>• Sheath adjuster allows for compatibility with multiple echoendoscopes</li> <li>• Coiled sheath facilitates greater needle flexibility (ECHO-3-22 only)</li> </ul>
Boston Scientific	Expect Expect Slimline	19 Ga 19 Ga Flexible (Nitinol) 22 Ga 25 Ga	Lancet	<ul style="list-style-type: none"> <li>• Sharp needle grind for precise targeting and sampling with echogenic tip</li> <li>• Cobalt-chromium construction—provides benefits over stainless steel alloys including greater hardness and tensile properties to deliver superior needle penetration</li> <li>• Increased resistance to needle damage</li> <li>• Stylet cap with integrated clip</li> </ul>
Olympus	EZ Shot 3 Plus	19 Ga + 19 Ga (sidehole) 22 Ga + (sidehole) 25 Ga	Menghini	<ul style="list-style-type: none"> <li>• Requires less force to pass into torqued endoscope</li> <li>• Sharper Menghini tip allows for smooth puncture, even from oblique angles</li> <li>• Needle remains straight during fanning or after multiple passes</li> <li>• Multilayered metal coil sheath allows greater force transmission</li> </ul>
Medtronic	Beacon EUS Delivery System	19-Ga (nitinol) 22-Ga 25-Ga (Both stainless steel)	Lancet	<ul style="list-style-type: none"> <li>• Engineered to improve clinical workflow by facilitating the passage of multiple needles through a single delivery system without removing the delivery system</li> <li>• Only FDA-cleared EUS safety needle with automated safety shield</li> <li>• Four cutting edges to help improve tissue yield for cytology</li> </ul>
Medi-Globe GmbH	SonoTip Pro Control	19 Ga 22 Ga 25 Ga	Standard cut with back cut without special facet	<ul style="list-style-type: none"> <li>• Twist-Lock Technology (TLT) for needle length and sheath length adjustment</li> <li>• Super-beveled needle features a large needle opening for an atraumatic puncture and optimal clean yield of cytologic specimen</li> <li>• Optimized lighter stylet for faster stylet insertion time and easier coiling</li> <li>• Specially treated needle for needle visibility</li> </ul>
Con-Med	ClearView	19 Ga 22 Ga 25 Ga (round, extended bevel, or extended bevel with sheath stabilizer)	Lancet	<ul style="list-style-type: none"> <li>• TLT allowing single hand operation to lock and unlock needle and sheath position</li> <li>• Laser-etched needle for clear visibility with ultrasound</li> <li>• Nitinol stylet with locking cap</li> <li>• Enhanced Luer-Lok design</li> </ul>

EUS, Endoscopic ultrasound.

accommodating different needle gauges during the same procedure. The same needle or a different gauge needle can be reinserted through the delivery sheath to perform multiple passes.

### Fine-Needle Biopsy Needles

Unfortunately, despite advancement in needle designs, multiple needle passes are often required to obtain an adequate sample for analysis, and the diagnostic accuracy of tissue has been found to be suboptimal without an on-site cytopathologist. In addition,

our oncology colleagues often lament that in the current era of precision medicine, a core tissue sample is vital—achieving only a cytologic diagnosis is not sufficient for diagnosing well-differentiated pancreatic adenocarcinomas, metastatic lesions, and lymphomas because their tissue morphology is necessary for precise histologic evaluation for optimal treatment planning. Fine-needle biopsy (FNB) has now become additive but sometimes compulsory at centers lacking on-site cytology capabilities. Table 2.4 summarizes the current FNB, and Fig. 2.11 illustrates these different FNB options. From an engineering standpoint,



• **Fig. 2.10** (A) EchoTip Ultra fine-needle aspiration (FNA) needles with differing sheath designs. (B) Expect and Expect Slimline FNA needle with differing contoured handle design. (C) EZ Shot 3 Plus FNA needle designed for greater needle force. (D) Beacon endoscopic ultrasound delivery system. (E) SonoTip Pro Control FNA needle. (F) ClearView FNA needle. ([A] Permission for use granted by Cook Medical, Bloomington, Indiana; [B] Permission for use granted by Boston Scientific, Marlborough, Massachusetts; [C] Permission for use granted by Olympus America, Center Valley, Pennsylvania; [D] All rights reserved. Used with permission of Medtronic; [F] Image courtesy of Medi-Globe GmbH, Achenmühle, Germany.)

**TABLE 2.4** Fine-Needle Biopsy

Company	Product Name	Sizes and Design	Design Features and Intended Benefits
Cook Medical	EchoTip ProCore	19-C (Lancet) 20-C (Menghini) 22-C (Lancet) 25-C (Lancet)	<ul style="list-style-type: none"> <li>Core trap technology designed for receiving sample into the needle</li> <li>Nitinol ReCoil stylet provides secure management minimizing contamination risk</li> <li>Coiled sheath facilitates stainless steel needle flexibility</li> </ul>
Boston Scientific	Acquire	19-Ga 22-Ga (All Franseen) 25-Ga	<ul style="list-style-type: none"> <li>Three symmetrical cutting surfaces with fully formed heels are designed to maximize tissue capture and minimize fragmentation</li> <li>Cobalt-chromium needle offers greater tensile properties for better needle penetration, less kinking, less deformation after multiple passes</li> <li>Controlzone and Lubricomp polymer are two ergonomically defined areas designed to optimize control during actuation</li> </ul>
Medtronic	SharkCore	19-Ga 22-Ga 25-Ga	<ul style="list-style-type: none"> <li>Six distal cutting edges are specifically designed to acquire cohesive units with intact cell architecture</li> <li>By minimizing tissue stacking and fracturing, the needle can potentially provide better core samples</li> </ul>
US Endoscopy	Moray	Micro Forceps	<ul style="list-style-type: none"> <li>Serrated jaws that effectively grab tissue</li> <li>0.8-mm stainless steel spring sheath that is compatible with most 19-G FNA needles</li> <li>Designed to take tissue sample from the wall of pancreatic cystic lesions which can be challenging</li> </ul>

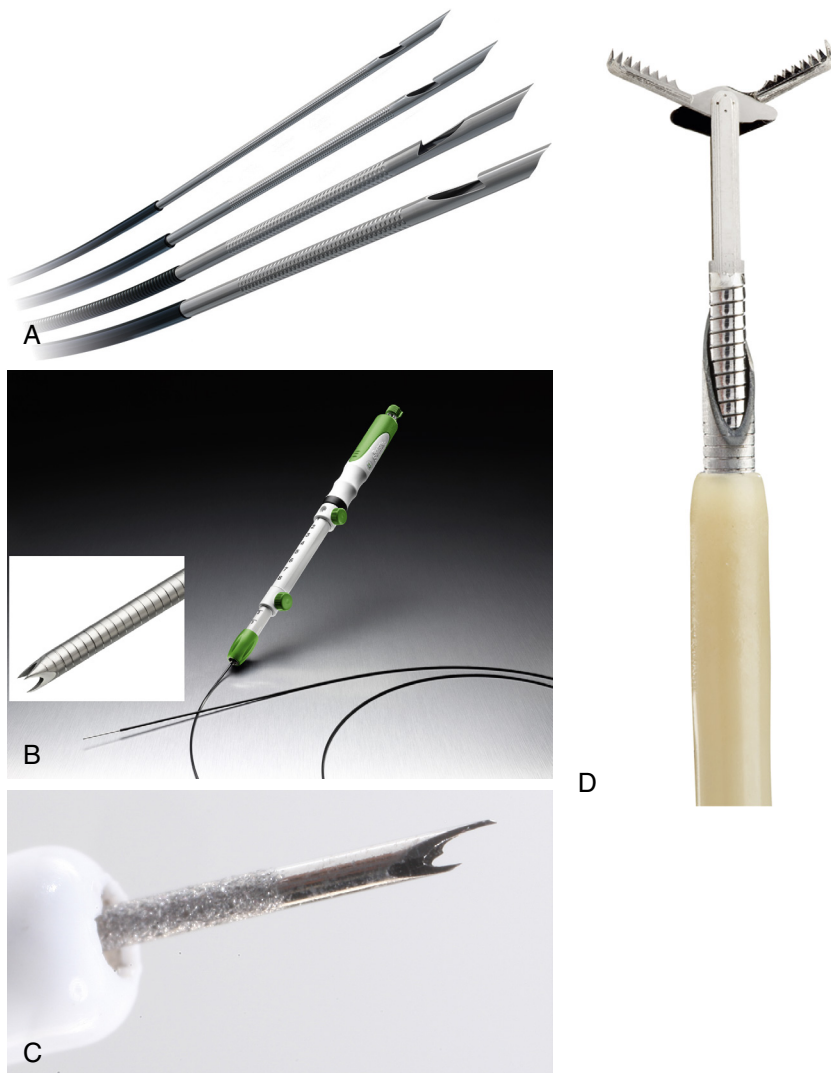
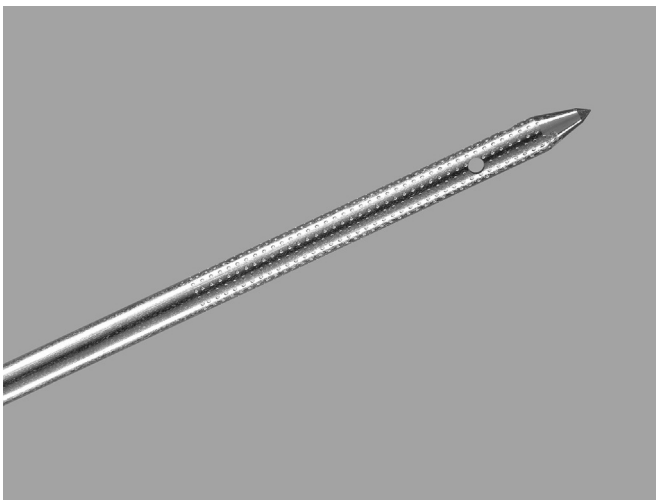


**Fig. 2.11** (A) EchoTip ProCore fine-needle biopsy. (B) Acquire fine-needle biopsy with a close-up. (C) SharkCore fine-needle biopsy. (D) Moray microforceps inserted through a 19-gauge fine-needle aspiration needle. ([A] Permission for use granted by Cook Medical, Bloomington, Indiana; [B] Permission for use granted by Boston Scientific, Marlborough, Massachusetts; [C] All rights reserved. Used with permission of Medtronic; [D] Image courtesy of US Endoscopy, Mentor, Ohio.)



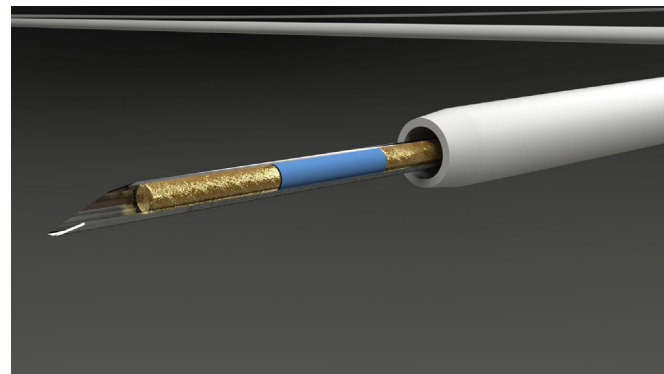
• **Fig. 2.12** EchoTipUltra celiac plexus neurolysis needle ECHO-20-CPN. (Permission for use granted by Cook Medical, Bloomington, Indiana.)

concepts such as reverse bevel needle design, three symmetric cutting surfaces, six distal cutting edges, and a forceps through a standard 19-gauge needle have all been used. The Moray (US Endoscopy, Mentor, Ohio) microforceps needle is designed exclusively to obtain tissue from pancreatic cysts and can be advanced through the lumen of a 19-gauge needle—the initial performance appears promising.

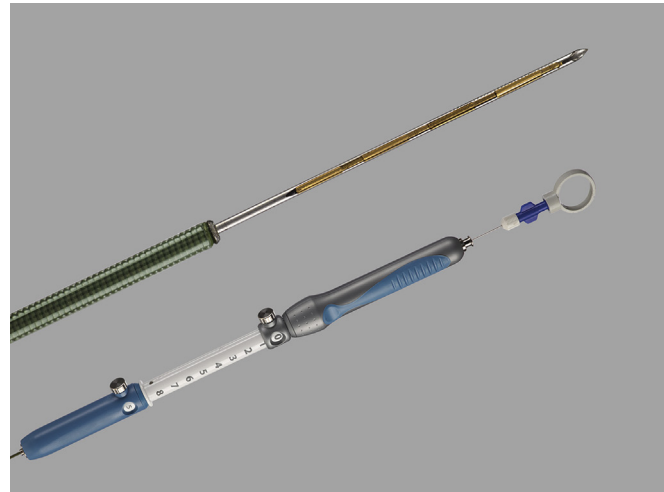
Needles have been developed to inject or deliver contents rather than for tissue acquisition. EchoTipUltra Celiac Plexus Neurolysis Needle (Fig. 2.12, Cook Medical, Bloomington, Indiana) is a 20-gauge, cone-shaped tip needle with side holes specifically designed for delivering neurolysis agents radially by spray into the plexus.

### Endoscopic Ultrasound-Guided Fiducial Placement

Stereotactic body radiotherapy (SBRT) was developed as a means to better target locally invasive disease and minimize irradiation of adjacent organs. SBRT achieves this via implantation of inactive radiographic markers into the target lesion. These markers (cylindrical gold seeds) serve as reference points for pinpointing and tracking the tumor during SBRT. Traditionally, fiducial placement has been attempted either intraoperatively or percutaneously by interventional radiology under computed tomography (CT) guidance. In the past few years, EUS has been increasingly used for fiducial placement in patients with inoperable pancreatic cancer, with two distinct needles in the market specifically designed for fiducial placement. Both needle designs obviate the need for manually loading the gold markers. Beacon fine-needle fiducial (FNF) needle (available in 22- and 19-gauge) is preloaded with two solid gold fiducial markers and enables easy target visualization (Fig. 2.13). Each fiducial marker features a knurled (ridged) exterior design that helps to reduce migration. The markers generate a clear echogenic signature that can be clearly visualized across imaging modalities. EchoTipUltra Fiducial Needle (Fig. 2.14, CookMedical) allows the placement of four solid gold fiducials preloaded in the distal tip. A coiled sheath facilitates placement in technically challenging areas, and the stylet ring facilitates marker placement.



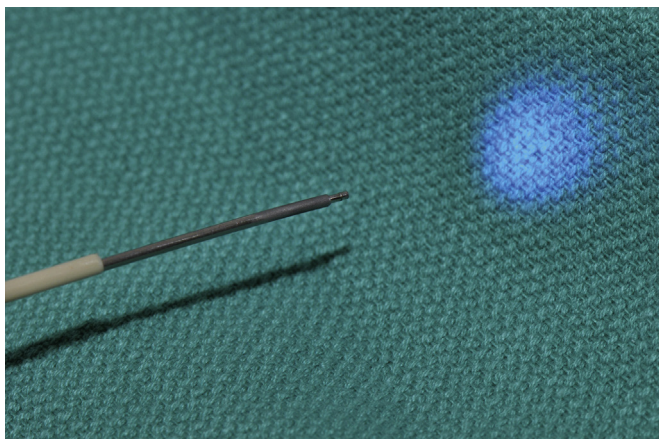
• **Fig. 2.13** Beacon FNF fiducial needle. (All rights reserved. Used with permission of Medtronic.)



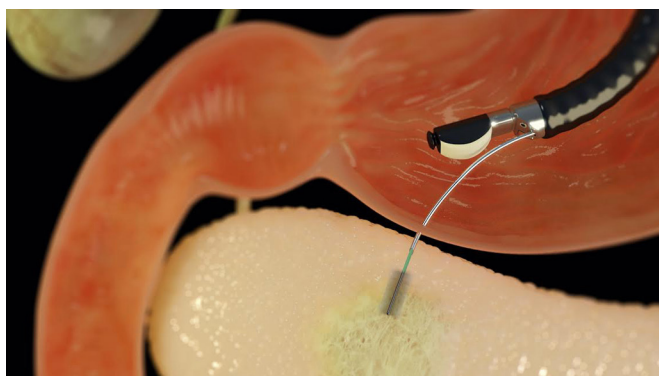
• **Fig. 2.14** EchoTipUltra fiducial needle ECHO-22-F. (Permission for use granted by Cook Medical, Bloomington, Indiana.)

### Confocal Laser Endomicroscopy

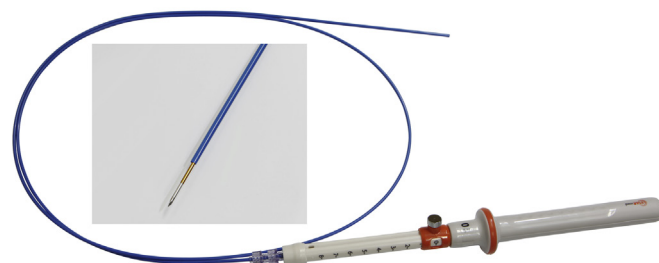
Confocal laser endomicroscopy (CLE) is an exciting, novel technology that allows for high-resolution imaging of the biliary tree and pancreatic lesions. CLE allows real-time imaging of the gastrointestinal (GI) tract at approximately 10,000-fold magnification such that the endoscopic images resemble light microscopy with resolution of approximately 1  $\mu\text{m}$ . Fluorescent light is then reflected from the selected tissue through the aperture, which excludes any light reflected at angles that do not refocus into the lens. In essence, this adjunct to EUS acts as an “optical biopsy” by providing real-time tissue histopathology. Currently, two primary modalities of CLE are available: endoscope-based confocal laser endomicroscopy (eCLE) created by Pentax and Optiscan (Pentax and Optiscan, Notting Hill, Victoria, Australia), which incorporates the confocal scanner into the distal tip of conventional endoscopes, and a probe-based confocal laser endomicroscopy (pCLE), which is miniaturized to 250 to 300  $\mu\text{m}$ , allowing it to be introduced through endoscopic accessory channels (Cellvizio, Mauna Kea Technologies, Paris, France). The most recent development in CLE has been a miniprobe with increased flexibility to allow introduction through either a 19-gauge or 22-gauge FNA needle, referred to as needle-based CLE (nCLE) (Fig. 2.15).



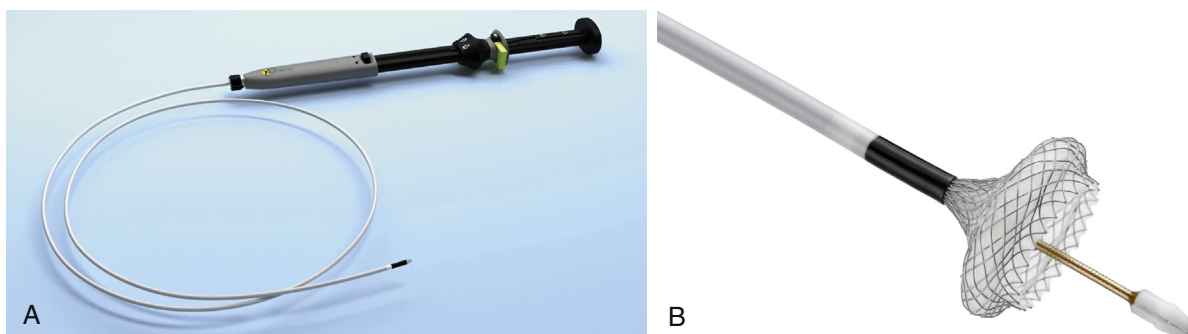
• **Fig. 2.15** Needle-based confocal laser endomicroscopy. Cellvizio, Mauna Kea Technologies, Paris, France. (Image courtesy of Dr. Michael Wallace.)



• **Fig. 2.16** Habib radiofrequency catheter through endoscopic ultrasound elastography fine-needle aspiration needle. (Image courtesy of EMCision UK, London, UK.)



• **Fig. 2.17** Endoscopic ultrasound-guided radiofrequency ablation electrode with insert showing close-up. (Image courtesy of TaeWoong Medical, Gyeonggi-do, Korea.)



• **Fig. 2.18** (A) Axios transenteric deliver system. (B) Axios stent. (Permission for use granted by Boston Scientific, Marlborough, Massachusetts.)

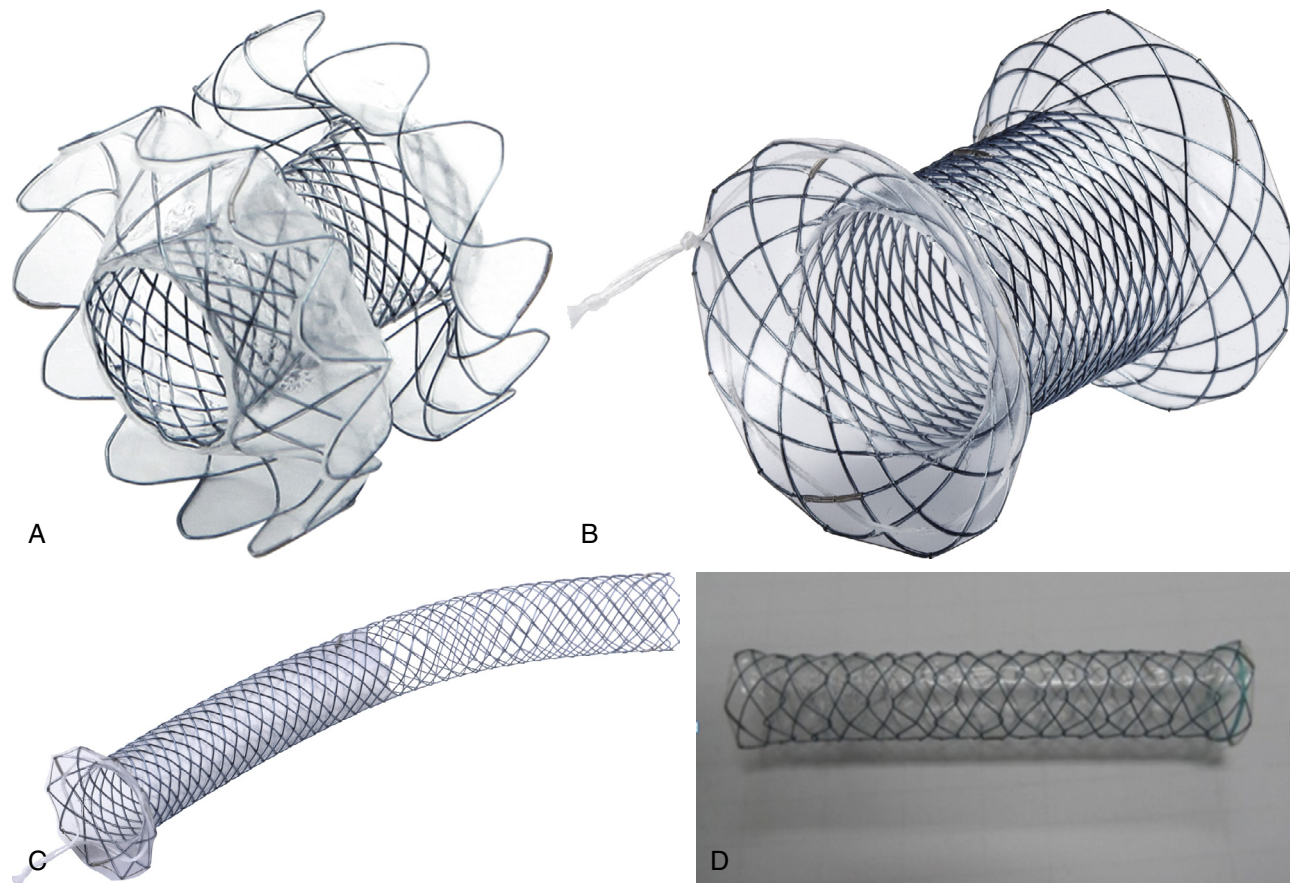
nCLE may serve as an adjunct to EUS to increase the diagnostic accuracy of neoplastic pancreatic cysts.

## Radiofrequency Ablation

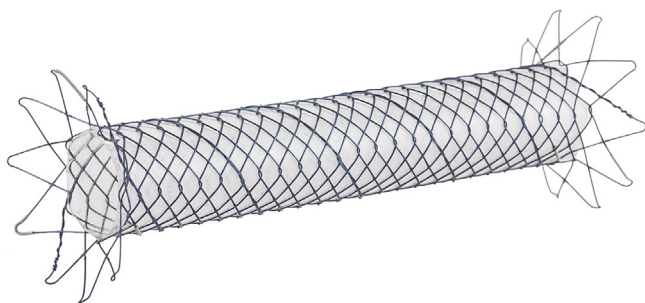
RFA has been studied and applied to esophageal, rectal, and liver malignancies. To date, the conventional approaches have been either percutaneous or intraoperative. By delivering heat at the site of contact, RFA induces local coagulative tumor necrosis. The Habib (EndoHPB, EMCision UK, London, UK) EUS RFA is a novel monopolar catheter used to cauterize and coagulate tissue with early experience in pancreatic cysts and neuroendocrine tumors (Fig. 2.16). This device can access deep parenchymal lesions in abdominal organs through an echoendoscope and FNA needle. The Habib EUS RFA is a 1 Fr wire (0.33 mm, 0.013 in.) which has a working length of 220 cm and is compatible with scopes that have a working channel of 2.4 mm or greater, and less than 200 cm in length. RF power is applied to the electrode at the end of wire to cauterize or coagulate tissue using commonly available RF generators. TaeWoong Medical (Gyeonggi-do, Korea) has recently developed an EUS-guided RFA electrode designed to ablate locally advanced unresectable pancreatic cancer, neuroendocrine tumors, and cystic neoplasms (Fig. 2.17). This monopolar device is echogenic and contains an inner cooling system that makes it possible to ablate a large volume of tumor without tissue charring. The VIVA Combo generator is recommended with this RFA needle, which comes in either an 18 or 19 gauge.

## Endoscopic Ultrasound-Guided Lumen-Apposing Stents

In its infancy, interventional EUS was handicapped by a lack of EUS-specific accessories, namely stents that could be inserted directly through the EUS scope. After years of improvising and combining ERCP for stent insertion into pseudocysts and other desired adjacent structures such as ducts, several stents are now available to achieve EUS-directed stent placement into pseudocysts, bile ducts, and the gallbladder. The AXIOS Stent (Boston Scientific) is a lumen-apposing metal stent that is placed under EUS guidance (Fig. 2.18). TaeWoong Medical (Gyeonggi-Do, Korea) has added several self-expandable stents for EUS-guided drainage (Fig. 2.19). Finally, Standard Sci-Tech (Seoul, Korea) has introduced a specific stent for EUS-guided gallbladder drainage (Fig. 2.20). All of the lumen-apposing stents are summarized in Table 2.5.



• **Fig. 2.19** (A) Spaxus stent. (B) Nagi. (C) Giobor. (D) Supremo. (Image courtesy of TaeWoong Medical, Geyonggi-do, Korea.)



• **Fig. 2.20** Bonastent. (Image courtesy of Standard Sci-Tech, Seoul, Korea.)

**TABLE  
2.5****Endoscopic Ultrasound-Guided Drainage and Stents**

Company	Stent Name	Indication	Design Features
Boston Scientific	Axios	Endoscopic device to deliver a transenteric stent between the GI tract and a pseudocyst	<ul style="list-style-type: none"> <li>Proprietary one-step combined diathermic ring and cut-wired provides access into target tissue</li> <li>MRI conditional, fully covered self-expanding metal stent preloaded in the delivery catheter</li> <li>Perpendicular flanges secure tissue layers and help to prevent migration</li> <li>Large diameter lumen (10–15 mm) apposition stent enables rapid, effective drainage allowing passage of the endoscope through the stent for cystoscopy, irrigation, and débridement</li> </ul>
TaeWoong Medical	Spaxus Nagi Giobor Supremo (Only approved in Japan)	Drainage of pancreatic pseudocyst or gallbladder Pancreatic pseudocyst drainage Biliary drainage, specifically for EUS-guided hepaticogastrostomy Biliary drainage	<ul style="list-style-type: none"> <li>Lumen-apposing design to prevent migration</li> <li>Fully silicone-coated to prevent leakage and in-growth</li> <li>Flexible design accommodates apposition regardless of wall thickness</li> <li>Variable diameter (8, 10, 16 mm) with 20-mm length stent</li> <li>Wide and smooth flare edges to prevent migration and stent related luminal damage</li> <li>Variable diameters (10, 12, 14, and 16 mm) and length from 1 to 3 cm</li> <li>9 and 10 Fr delivery systems</li> <li>Half covered and half uncovered design for placement between the stomach and hepatic duct</li> <li>Covered part: bridge from stomach to hepatic duct to prevent leakage</li> <li>Uncovered part: into hepatic duct to prevent stent migration and blocking side branch</li> <li>Silicone covered and both flare designed with one string</li> </ul>
Standard Sci-Tech	Bonastent	Gallbladder drainage	<ul style="list-style-type: none"> <li>Two big flanges at both ends to prevent stent migration</li> <li>The thinnest delivery system (8 Fr diameter) for easy maneuverability in gallbladder drainage</li> <li>Variable stent diameters (10 mm, 16 mm) and length (30 mm, 100 mm)</li> <li>Proven long-term clinical effectiveness and safety</li> </ul>

EUS, Endoscopic ultrasound elastography; MRI, magnetic resonance image.

The opportunities and inherent excitement afforded by the ever-expanding field of interventional endosonography has only been possible over the past several years, due to the combined efforts of endosonographers who have accepted no boundaries and our industry colleagues who have partnered and invested

in realizing these dreams knowing very well that the return on investment would undoubtedly be delayed. Distilling the gamut of echoendoscopes, processors, and accessories into these several pages is a grave injustice to the breadth of equipment now available.

# 3

## Training and Simulators

SACHIN WANI

### KEY POINTS

- EUS is an advanced endoscopic procedure that is operator dependent, and training in a structured program is required for the development of cognitive, technical, and integrative skills beyond those required for standard endoscopic procedures.
- The consensus opinion on the ideal format for EUS training is through a structured, hands-on experience with patients in a supervised setting. Self-education, reliance on animal models, computer-based courses, or short training courses as the sole method of training is discouraged.
- Trainees need to be aware of the key end points for technical, cognitive, and integrative aspects of EUS. The training center and environment plays a critical role in the overall training process.
- EUS has traditionally been taught by apprenticeship, and competence in EUS has been assessed by the trainers' subjective assessment of overall competence and/or meeting an arbitrary volume for procedures completed.
- Guidelines for assessing competency are primarily based on expert opinion and consensus.
- Recent data clearly demonstrate substantial variability in EUS learning curves among trainees, and a specific volume threshold during training does not ensure competence.
- Given that methods for assessing competence during endoscopic training are in transition and given an increasing focus on competency-based medical education (CBME), emphasis needs to be shifted away from the number of procedures performed to well-defined and validated competency thresholds.
- The use of a validated structured assessment tool such as TEESAT is critical to standardize evaluation of competence in EUS.
- Because quality measurement is the "new normal" in gastroenterology, the importance of measuring and monitoring quality in EUS needs to be instilled early during training.

### Introduction

Since its introduction, endoscopic ultrasound (EUS) has evolved as a vital endoscopic procedure for the diagnosis and staging of pancreaticobiliary and luminal gastrointestinal (GI) malignancies. EUS-guided fine-needle aspiration (EUS FNA) and EUS-guided fine-needle biopsy (FNB) are standard practice

for EUS-guided tissue acquisition (EUS TA) for diagnostic purposes from pancreatic masses, lymph nodes, mediastinal and subepithelial lesions, and other lesions within the region of the upper and lower GI tract.<sup>1,2</sup> The diagnosis, staging, and treatment of GI cancers have evolved into a multidisciplinary approach often using EUS as a central tool for both diagnosis and staging.<sup>3,4</sup> EUS is the most sensitive imaging modality for the detection of pancreatic masses and is particularly useful when results of other cross-sectional imaging modalities are inconclusive.<sup>5,6</sup> In addition, the accuracy of EUS FNA has been evaluated in several studies in patients with pancreatic cancer and other GI malignancies.<sup>7,8</sup> Recently, the role of EUS has expanded from a diagnostic modality to one that is capable of guiding therapeutic interventions (interventional EUS). Numerous advances have been made in the field of interventional EUS, and some of these applications include drainage of pancreatic fluid collections, biliary and pancreatic access and drainage, angiotherapy for varices, treatment of premalignant and malignant conditions including pancreatic cystic lesions, fiducial marker placement, and celiac plexus neurolysis and block, and anastomosis creation.<sup>9</sup>

The clinical effectiveness of EUS and EUS TA depends on the judicious use of these techniques and competency of the performing endosonographer. The increasing sophistication of this technique, higher-risk profiles for some of the EUS-guided interventions, and the need for additional interventions or repeat procedures following a failed or nondiagnostic EUS underscore the importance of adequate training.<sup>10,11</sup> As the applications for EUS have become increasingly recognized, the demand for well-trained endosonographers has increased and the limited availability of EUS is largely due to a lack of skilled endosonographers. It is clear that EUS is operator dependent and that additional training is required for the development of technical, cognitive, and integrative skills beyond those required for standard endoscopic procedures.<sup>11</sup> Several guidelines have been published for EUS training, based primarily on expert opinion and limited published data.<sup>12–14</sup> This chapter highlights the current status of training in EUS and the methods of EUS training and recommendations for training programs. It will also review the current state of competency assessment during EUS training and discuss the shifting paradigm from procedure volume as a surrogate of competency to validated competency thresholds. The current guidelines in training, credentialing, and privileging will be reviewed, and, finally, the importance of quality metrics in EUS during training will be highlighted.

## Training in Endoscopic Ultrasound

Training in endoscopy entails both cognitive and technical elements that are required to safely and proficiently perform these procedures. Over the past decade, training in EUS has evolved from a self-directed training model to a formal and supervised training model. The consensus opinion on the ideal format for EUS training is through a structured, hands-on experience with patients in a supervised setting.<sup>12–14</sup> The duration of training can vary; however, self-education, reliance on animal models or computer-based courses, or short training courses as the sole method of training are discouraged. A core curriculum for training in EUS has been established by the American Society for Gastrointestinal Endoscopy (ASGE).<sup>15</sup> Prior to embarking on learning EUS, trainees are required to master standard upper endoscopy and colonoscopy. Trainees are expected to have completed at least 18 months of standard GI training and should have expertise in basic endoscopy, including thorough visualization of the GI tract, minimizing patient discomfort, proper identification of normal and abnormal findings, and proficiency in basic therapeutic techniques. Although some trainees may be exposed to EUS during their standard GI training, procedural exposure should not be equated with procedural competence.

EUS training should focus on the cognitive and technical aspects of the procedure. Understanding procedural indications, contraindications, risks and limitations, in addition to learning how to interpret EUS findings (normal and abnormal) and incorporating them into management algorithms, is an integral part of this process. Cognitive education is also achieved through reading, reviewing videos and atlases, and attending lectures and conferences, combined with supervised hands-on experience under the mentorship of expert endoscopists.<sup>16</sup> The training process usually begins by observing a primary endoscopist perform EUS and becoming acquainted with the unique endoscopic and EUS view of the echoendoscope. The trainee should have the understanding of how relevant equipment works, including the processors, and ultimately gain proficiency in the use of radial array and curvilinear array echoendoscopes. As with general endoscopy, one of the initial challenges is intubating the esophagus. Trainees are expected to safely intubate and traverse the esophagus, the gastroesophageal junction, intubate, and traverse the duodenal sweep. Trainees should be proficient in evaluating structures visualized at various stations during EUS (Table 3.1). Trainees should be adept at TNM staging (tumor, node, and metastasis). Proficiency in EUS TA using EUS FNA and EUS FNB needles is expected at the end of training. Trainees are also expected to understand the advantages and limitations of different EUS TA techniques.<sup>17</sup> Understanding the basics of specimen handling and the role of on-site cytopathology evaluation is critical.<sup>5,17</sup> Trainees should maintain a procedure log of only those procedures during which they had hands-on training. This log should include the indication and the end points achieved by the trainee. This will not only be helpful for credentialing purposes but also allows for competency assessment. The key end points of training in EUS are highlighted in Table 3.1.

In addition, EUS training should take place at a center fitted with all the basic equipment necessary to perform EUS and where an adequate number of experienced trainers are present who have a track record of adequate case volume and effective endoscopic teaching. An ideal environment also provides interaction with a multidisciplinary team that includes surgeons, oncologists, radiation oncologists, cytopathologists, and radiologists.

Training programs should educate trainees on preparing a comprehensive written report of important normal and abnormal findings, and communication of findings and results to referring physicians, patients, and family members. The trained endosonographer should be able to deliver bad news in a clear and comprehensive manner. A recent survey study showed that the comfort level for disclosing a pancreatic cancer diagnosis after EUS was higher among experienced (>5 years in practice) and high-volume endosonographers. Although the vast majority of endosonographers felt obligated to share the diagnosis of cancer, the lack of proper training and time were limiting factors.<sup>18</sup> This highlights the need for formal communication skills training during GI fellowship training. Unfortunately, the majority of EUS programs across the United States have limited, if any, extramural funding and may require additional clinical responsibilities to help support the trainee's salary. While understanding the financial limitations of most institutions, training programs should strive to limit the clinical responsibilities unrelated to EUS when developing their core curriculum. Ideally, programs should provide protected research time and encourage academic pursuits such as designing research protocols, preparing manuscripts, writing grant proposals, and attending EUS courses. Creating an environment emphasizing endoscopic research and clinical investigation should be a fundamental goal for each training program. Exposure to endoscopy unit management including scheduling, staffing, equipment maintenance, and management skills is also a valuable asset to any

**TABLE 3.1 Suggested End Points for Endoscopic Ultrasound Training**

### Technical Aspects

1. Esophageal intubation
2. Intubating the pylorus and traversing the duodenal sweep
3. Visualization of relevant structures at the following stations:
  - a. Aortopulmonary window and subcarina
  - b. Body and tail of pancreas
  - c. Head and neck of pancreas
  - d. Uncinate process of pancreas
  - e. Ampulla
  - f. Common bile duct, common hepatic duct, and gallbladder
  - g. Portosplenic confluence
  - h. Celiac axis
  - i. Left lobe of liver
4. EUS-guided tissue acquisition (EUS FNA and EUS FNB)
5. EUS-guided celiac plexus neurolysis and block
6. Recognition and management of adverse events (bleeding, perforation, pancreatitis, infections, cardiopulmonary events, hospitalization, and mortality)

### Cognitive Aspects

1. Clear understanding of informed consent and procedure indications, contraindications and alternatives
2. Identify lesion of interest or appropriately ruled out
3. Appropriate TNM staging
4. Appropriate characterization of subepithelial lesions
5. Provide appropriate differential diagnosis
6. Formulate appropriate management plan (including surveillance, EUS-guided tissue acquisition, and referral to surgery)
7. Clear understanding of use of antibiotics and knowledge of anticoagulants

EUS FNA, Endoscopic ultrasound-guided fine-needle aspiration; EUS FNB, endoscopic ultrasound-guided fine-needle biopsy; TNM, tumor, node, metastasis.

training program. Many trainees in EUS may pursue future academic positions, and these are invaluable skills to acquire early in an academic career. Although a common goal for most training programs is the development of future academic endosonographers, some trainees may express different career interests that conflict with the goals of the training program. Understanding and recognizing the program's expectations and trainee's career interests is crucial to an enjoyable and successful training experience.

## Current Status of Endoscopic Ultrasound Training

In the United States, training in EUS has shifted to dedicated advanced endoscopy fellowships, occurring in a fourth year of training after a standard GI fellowship.<sup>19</sup> The number of advanced endoscopy fellowship programs (typically a 1-year training program of combined training in EUS and ERCP) has increased dramatically. A total of 62 programs offering EUS training were listed in the 2016–17 Advanced Endoscopy Fellowship match program through the ASGE (<http://www.asgematch.com>), some of which train more than one trainee per year. These programs are typically offered to physicians who have completed formal GI fellowship training. The number of programs listed may be an underestimate because there are programs and applicants that do not participate in the match. It should be noted that these programs are not recognized by the Accreditation Council for Graduate Medical Education (ACGME). Due to the lack of a fixed mandatory curriculum, there are limited data on the composition and outcomes of EUS training among advanced endoscopy trainees completing these programs. Results from a recent prospective multicenter study evaluating competence among advanced endoscopy trainees showed that the median number of EUS exams performed per trainee was 300 (range: 155 to 650). In terms of indications, suspected pancreatic mass accounted for 24.5% of the graded procedures, and pancreatic cyst (17.8%), subepithelial lesion (7%), and luminal malignancy (6.9%) represented the other major indications. The majority of the graded EUS exams were performed using the linear echoendoscope (67.5%) and in the ambulatory setting (82.6%). At the end of training, nearly all trainees felt comfortable with independently performing EUS, EUS FNA, EUS-guided celiac plexus block and neurolysis, and EUS-guided pseudocyst drainage. However, 50% of trainees were not comfortable placing fiducials and performing interventional EUS

procedures such as biliary and pancreatic drainage. Nearly half of the trainees planned to practice at an academic center and expected a majority of their practice to be in advanced endoscopy.<sup>20</sup>

## Guidelines for Competency Assessment

Advanced endoscopy has traditionally been taught by apprenticeship wherein a trainee is expected to develop skill and expertise with hands-on experience. Competence in EUS has been historically assessed by the trainers' subjective assessment of overall competence and/or meeting an arbitrary volume for procedures completed.<sup>21</sup> Several guidelines for assessment of competency in EUS have been published by GI societies (Table 3.2).<sup>12–14,22</sup> These guidelines are primarily based on expert opinion and consensus and continue to use an absolute procedure volume to determine competence in EUS, with thresholds varying between guidelines. There are limited data regarding competency assessment for the performance of therapeutic maneuvers such as celiac plexus neurolysis/block, placement of fiducials, cyst drainage, and biliary or pancreatic access. These current guidelines lack validation with regard to competence and feasibility of training. In addition, they do not account for the fact that trainees differ considerably in the rates at which they learn and develop endoscopic skills. Available data and expert opinion suggest that the majority of trainees are not competent at the previously defined thresholds and require double the number of proposed procedures to achieve competence in EUS. Thus the number of procedures completed during training alone does not ensure competence and is a suboptimal marker for competence in EUS.

## Learning Curves and Competence in Endoscopic Ultrasound

Competency is defined as the minimum level of skill, knowledge, and/or expertise acquired through training and experience, required to safely and proficiently perform a task or procedure.<sup>12</sup> There have been few published reports regarding learning curves in EUS.<sup>10,11,23–31</sup> Recognizing this goal and understanding the limitations of a 3-year curriculum has been the major impetus for establishing fourth-year fellowships in EUS.

Recent studies have focused on comprehensive evaluation of EUS competence during advanced endoscopy training.<sup>10,11</sup> A pilot study conducted at three tertiary care referral centers prospectively

**TABLE 3.2**

**Guidelines for Assessment of Endoscopic Ultrasound Competency**

	ASGE (United States)	FOCUS (Canadian)	ESGE (Europe)	BSG (United Kingdom)
Year of publication	2017	2016	2012	2011
Total number of cases	225	250	NR	250
Pancreaticobiliary indication	NR	100	NR	150 (75 pancreatic cancer)
Luminal indication (mucosal)	NR	25 rectal EUS	NR	80 (10 rectal EUS)
Subepithelial lesion	NR	NR	NR	20
EUS FNA	NR	50 (10 CPB, CPN)	50 (30 pancreatic)	75 (45 pancreatic)

ASGE, American Society for Gastrointestinal Endoscopy; BSG, British Society of Gastroenterology; CPB, celiac plexus block; CPN, celiac plexus neurolysis; ESGE, European Society of Gastrointestinal Endoscopy; EUS FNA, Endoscopic ultrasound-guided fine-needle aspiration; FOCUS, Forum on Canadian Endoscopic Ultrasound; NR, not reported.

defined learning curves in EUS among five advanced endoscopy trainees. In this study, trainees were graded at intervals of 10 EUS exams using a standardized evaluation tool (discussed later) and cumulative sum analysis (CUSUM). Two trainees crossed the threshold for competence at case numbers 255 and 295, and the others demonstrated the need for ongoing supervision. This study highlighted the substantial variability in achieving competence and a consistent need for more supervision in all trainees.<sup>10</sup> This study was followed by a larger multicenter validation study which included 17 advanced endoscopy trainees at 15 centers. Learning curves using CUSUM confirmed the significant variation, and only two trainees crossed the threshold for competence (at cases 225 and 245) (Fig. 3.1). The authors concluded that a specific number of cases performed during training does not ensure competence in EUS and that 225 cases should be considered as the minimum caseload for training because no trainee in this study achieved competence prior to this point.<sup>11</sup>

One retrospective study showed that endosonographers with a formal supervised training experience in pancreaticobiliary EUS achieved a significantly higher sensitivity when using EUS FNA for the diagnosis of pancreatic malignancy as compared with those without formal FNA training.<sup>26</sup> A crucial component to any EUS training program is focused on GI tumor staging. Studies in endosonographic staging of esophageal cancer suggested that at least 75 to 100 procedures were required before an acceptable level of accuracy was achieved.<sup>24,25</sup> Ideally, the accuracy of EUS staging should be compared with a “gold standard,” such as surgical histopathology; however, surgical specimens are not always readily available and patients may have received preoperative radiation and chemotherapy that may affect staging. In these circumstances, staging by a trainee is compared with that of a skilled and competent endosonographer.

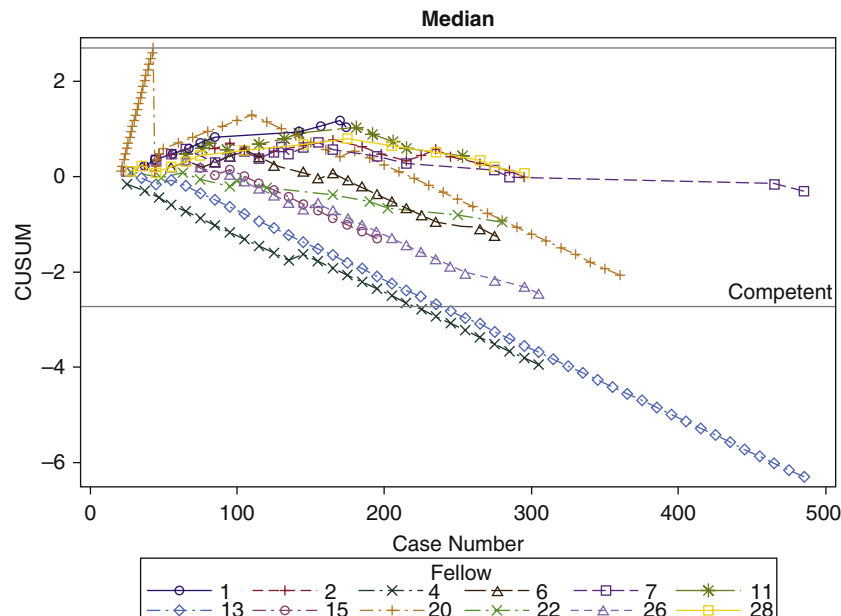
There are limited data on learning curves in EUS TA, and it is unclear when EUS FNA should be initiated during the training

process (after the completion of a prerequisite number of EUS exams or at the initiation of training). A single center study suggested that when initiated at the onset of EUS training, attending-supervised, trainee-directed EUS FNA is safe and has comparable performance characteristics to trainer EUS FNA.<sup>28</sup> The learning curves for EUS FNA for solid pancreatic lesions have been described with increasing sensitivity for the cytopathologic diagnosis of cancer with a decreasing number of passes needed to obtain adequate results.<sup>32–34</sup>

Similarly, there are limited data on learning curves and criteria for competence in interventional EUS. These procedures are technically more challenging compared with diagnostic EUS (with or without EUS TA) and routine ERCP procedures. Endoscopists who desire proficiency in interventional EUS need to be highly skilled in EUS TA and ERCP techniques. Trainees need to understand that they may not gain proficiency in many interventional EUS procedures during their advanced endoscopy fellowship and will ultimately acquire these skills and competence in clinical practice under the guidance of a senior partner/mentor. Experts suggest the following prerequisites for interventional EUS: high volume of EUS and ERCP cases (>200 to 300 EUS and ERCPs/year), high success rate for standard ERCP, and practice at a center with pancreaticobiliary surgery and interventional radiology backup.<sup>9</sup> Other experts recommend completion of at least greater than 10 EUS-guided pseudocyst drainage procedures before attempting EUS-guided pancreaticobiliary drainage and beginning with easier EUS-guided biliary techniques (EUS-guided rendezvous).<sup>35</sup>

## Towards Competency-Based Medical Education

The current status of EUS training is limited by the lack of a clear definition of competence and the ongoing use of volume-based thresholds as a surrogate marker for endoscopic skill



• Fig. 3.1 Overall graphical representation of the learning curves among all trainees by using cumulative sum analysis (CUSUM). Crossing the lower limit threshold indicated the performance was within preset acceptable failure rate and competency was achieved. (Reproduced with permission from Wani S, Hall M, Keswani RN, et al. Variation in aptitude of trainees in endoscopic ultrasonography, based on cumulative sum analysis. *Clin Gastroenterol Hepatol*. 2015;13:1318–1325.e2.)

level and competence. As described previously, the currently set volume thresholds are based on limited data and the overall assessment by trainers remains highly subjective. There is an increasing emphasis on standardizing competency assessment and demonstrating readiness for independent practice as medical training in the United States transitions from an apprenticeship model to competency-based medical education (CBME). CBME is an “outcomes-based approach to the design, implementation, assessment and evaluation of a medical education program using an organizing framework of competencies”—a concept that is quickly moving from theory to reality for subspecialty fellowship training.<sup>36,37</sup> The ACGME has replaced its reporting system with the Next Accreditation System (NAS), which is a continuous assessment reporting system focused on ensuring that specific milestones are reached throughout training, that competence is achieved by all trainees, and that these assessments are documented by training programs. Thus it is incumbent upon endoscopy training programs and program directors to evolve with the new ACGME/NAS requirements and assess and document competence among all trainees.<sup>38–40</sup> In a nationwide survey of trainees and program directors of ACGME-accredited gastroenterology fellowship programs in the United States, 23% of the 94 participating programs lacked a formal endoscopy curriculum. Program directors reported procedural volume and attending written evaluations as the primary measures of competence at the majority of these programs. Less than one-third of programs used skill assessment tools or specific quality metrics for the evaluation of competency.<sup>21</sup>

Objective measures of competence in GI endoscopy including EUS can be separated into three domains: cognitive (e.g., clinical knowledge/understanding of disease; understanding of procedure/risks/benefits/alternatives), technical/psychomotor skills (e.g., endoscope control, EUS TA skill), and integrative/nontechnical skills (e.g., communication, teamwork).<sup>41</sup> Competence assessments are critical to determine if trainees have mastered these objective measures and demonstrate readiness for independent practice. There are two types of assessments that can be used: (1) formative assessment—used to monitor learner progress and provide trainees with benchmarks for their learning and feedback for further improvement, and (2) summative assessment—performed at the end of training to determine if thresholds and objectives have been reached.<sup>41</sup> The latter is frequently used for credentialing and certification but clearly has no role during the actual training process.

In an effort to standardize the evaluation of the cognitive, technical, and integrative aspects of EUS and more clearly define endoscopic competence, the use of a validated structured assessment tool is critical. An ideal assessment tool needs to be reliable (consistent and reproducible), valid (measure what they are supposed to measure), impactful on education, and acceptable to all stakeholders.<sup>42</sup> The EUS and ERCP Skills Assessment Tool (TEESAT) has been used in published and ongoing studies evaluating advanced endoscopy training in the United States.<sup>10,11,40,43</sup> With regard to EUS, this tool allows for documentation of the indication for the procedure and the type of echoendoscope used, followed by the grading of trainees in technical and cognitive end points, using a four-point scoring system with well-defined anchors (Fig. 3.2). Recently, we have described a novel and comprehensive data collection and reporting system that allows for the generation of learning curves on-demand and the creation of a centralized database that enables

program directors, trainers, and trainees to identify specific skill deficiencies in training and facilitate tailored and individualized remediation. This process allows for efficient data collection, interfacing, and analysis and the comparison of performance with peers nationwide (benchmarking).<sup>40,43</sup> Results from a large prospective multicenter study evaluating learning curves and competence in EUS and ERCP among 22 advanced endoscopy trainees using this comprehensive data collection and reporting system and a validated assessment tool (TEESAT) confirmed the substantial variability in achieving competence in EUS among trainees. Overall technical and cognitive competence in EUS was achieved by 82% and 76% of trainees at the end of their training.<sup>43</sup>

It is hoped that this work will facilitate advanced endoscopy training programs to evolve with the ACGME/NAS reporting requirements and establish reliable and generalizable learning curves (milestones) and competency benchmarks that national GI societies and training programs can use to develop credentialing guidelines. For CBME to be implemented in medical subspecialty training, a paradigm shift in the evaluation of endoscopic training and in the definition of competence will be required. It is clear that procedural volume thresholds can be no longer be used as measures of competence given the significant variability in trainee learning curves and procedural volumes at the training institutions. Ensuring that trainees are capable of safely and proficiently performing EUS independently at the conclusion of training will require ongoing objective evaluations during the course of training to ensure that preset thresholds of technical, cognitive, and integrative milestones are met.

## Credentialing, Recredentialing, and Renewal of Privileges in Endoscopic Ultrasound

Credentialing is the process of assessing and validating the qualifications of a licensed independent practitioner to provide patient care.<sup>12</sup> Determining qualifications for credentialing is based upon an assessment of the individual's current medical license, knowledge base, training and/or experience, current competence, and ability to independently perform the procedure or patient care requested. The ASGE has provided guidelines for credentialing and granting hospital privileges to perform routine GI endoscopy including EUS.<sup>12</sup> Credentialing for EUS should be determined separately from other endoscopic procedures such as sigmoidoscopy, colonoscopy, esophagogastroduodenoscopy, ERCP, or any other endoscopic procedure. Determining competency and qualifications for credentialing can be somewhat challenging because trained individuals possess varying degrees of skill in EUS, along with recognized limitations. Nevertheless, providing a minimum number of procedures (225 procedures for EUS) necessary prior to assessing competency creates objective criteria for assessment in the credentialing process. As with credentialing in general GI endoscopy, competency is ultimately assessed by the training director or other independent proctor. EUS is performed in a variety of anatomic locations for various indications.<sup>44,45</sup> Privileging in one or more of these areas may be considered separately, but training must be considered adequate in the areas for which privileging is requested.

Over the course of time, physicians who have received appropriate privileges to perform EUS may change the scope of their clinical practice and subsequently reduce the frequency

## The EUS and ERCP Skills Assessment Tool (TEESAT)

Date of Procedure: \_\_\_\_\_

Procedure Number: \_\_\_\_\_

**EUS**

Assigned Code: \_\_\_\_\_

**Indication for EUS (mark all that apply):** Radial  Linear

- |                                       |   |  |  |
|---------------------------------------|---|--|--|
| <input type="checkbox"/> Panc Mass    | <input type="checkbox"/> Biliary dilation | <input type="checkbox"/> Abdominal/Mediastinal lymphadenopathy | <input type="checkbox"/> Possible subepithelial lesion |
| <input type="checkbox"/> Panc Cyst    | <input type="checkbox"/> PD Dilation      | <input type="checkbox"/> Luminal GI cancer                     | <input type="checkbox"/> Mediastinal mass              |
| <input type="checkbox"/> Other: _____ |   |  |  |

**EUS: Technical Aspects:**

1(superior) =achieves independently 2(advanced) =achieves with minimal verbal instruction

3(intermediate) = achieves with multiple verbal instruction or hands on assistance

4 (novice) =unable to complete requiring trainer to take over

N/T= not attempted for reasons other than trainee skill N/A= not applicable

Intubation	1	2	3	4	N/T	N/A
AP window	1	2	3	4	N/T	N/A
Body of pancreas	1	2	3	4	N/T	N/A
Tail of pancreas	1	2	3	4	N/T	N/A
Head/neck of pancreas	1	2	3	4	N/T	N/A
Uncinate	1	2	3	4	N/T	N/A
Ampulla	1	2	3	4	N/T	N/A
Gallbladder	1	2	3	4	N/T	N/A
CBD/CHD	1	2	3	4	N/T	N/A
Portosplenic confluence	1	2	3	4	N/T	N/A
Celiac axis	1	2	3	4	N/T	N/A
Achieve FNA	1	2	3	4	N/T	N/A
Achieve celiac plexus block/ neurolysis	1	2	3	4	N/T	N/A

**EUS: Cognitive Aspects**

Identify lesion of interest or appropriately ruled out	1	2	3	4	N/T	N/A
Appropriate TNM stage	1	2	3	4	N/T	N/A
Characterize subepithelial lesion (wall layers)	1	2	3	4	N/T	N/A
Appropriate differential diagnosis	1	2	3	4	N/T	N/A
Appropriate management plan (FNA, refer to surgery, surveillance or no surveillance)	1	2	3	4	N/T	N/A

- **Fig. 3.2** Standardized grading tool to assess competence in endoscopic ultrasound (EUS). (The EUS and ERCP Competency Assessment Tool.)

## The EUS and ERCP Skills Assessment Tool (TEESAT)

Date of Procedure: \_\_\_\_\_

Procedure Number: \_\_\_\_\_

**Overall Assessment:**

Global Overall Assessment (subjective)				
1	2	3	4	5
Below average for level of training requiring frequent assistance	Average level of training requiring appropriate level of supervision or assistance			Superior for level of training, ready for independent practice

**Immediate Post-Procedure Complications:**Procedure done in ambulatory setting?     Yes     NoPatient admitted post-procedure?     Yes     No**If yes,**

- Pain requiring hospitalization
- Pancreatitis
  - Mild
  - Moderate
  - Severe
- Bleeding
  - Immediate
  - Delayed
- Perforation
- Cardiopulmonary complications
- Mortality
- Other: \_\_\_\_\_

• Fig. 3.2, Cont'd

of performing one or more EUS procedures. It has been suggested that ongoing experience in advanced endoscopy is necessary to retain the technical skills required to safely and adequately perform these technically challenging procedures. The goal of recredentialing is to ensure continued clinical competence while promoting continuous quality improvement and maintaining patient safety. If ongoing experience is not maintained at some objective level, the quality of care provided to the patient may diminish, potentially leading to adverse events. The ASGE has provided useful guidelines for renewing endoscopic privileges and assuring continued clinical competence in EUS.<sup>12</sup> However, it is the responsibility of each institution to develop and maintain individual guidelines for granting and renewing privileges. The threshold number of procedures necessary for recredentialing may vary between institutions; however, this threshold must be commensurate with the technical

and cognitive skills required for advanced procedures such as EUS. Individual institutions must establish a frequency for the renewal process, along with contingency plans when minimal competence cannot be assured. The Joint Commission has mandated that renewal of clinical endoscopic privileges be made for a period of no more than 2 years. Endosonographers seeking renewal of privileges must document an adequate case-load over a set period of time to maintain the necessary skills required for EUS. This documentation may include procedure log books or patient records and should focus on objective measures such as number of cases, success rates, and adverse events. Ongoing quality improvement efforts may be assessed as part of the recredentialing process and may include measurement of specific quality metrics set forth in published guidelines.<sup>1,2</sup> Continued cognitive training through participation in educational activities and/or quality improvement activities should

also be a prerequisite for the renewal of privileges. Individual institutions should have a mechanism in place for addressing instances when minimal competency cannot be assured and decredentialing may be required when endosonographers fail to meet accepted national and institutional requirements for competency.<sup>12</sup>

## Endoscopic Ultrasound Training Using Simulators

Considerable technological advances have been made in the development of endoscopic simulators over the past decade. Endoscopic simulator modalities in flexible endoscopy include live animals, ex vivo organs, computer simulation, and mechanical models. Several studies have evaluated the role of simulator-based training in endoscopic training and limited to upper endoscopy, sigmoidoscopy, colonoscopy, and ERCP.<sup>30</sup> Authors of a recent systematic review in training and competence assessment in GI endoscopy proposed the implementation of simulator training in GI endoscopic training curricula for the previously listed procedures given the potential for speeding up the early learning curve.<sup>30</sup> Only a few reports on simulator-based training in EUS were identified with no validation studies reported, and hence no recommendations were made based on limited evidence.

A variety of simulators are currently available, ranging from animal-based simulators (Erlangen Endo-Trainer; Erlangen, Germany) to the computer-based simulators manufactured by CAE Healthcare (Endo VR Simulator; Montreal, Quebec, Canada) and Simbionix Corp. (GI-Mentor II; Cleveland, Ohio). Simbionix Corp. developed the first computer-based EUS simulator providing a platform for hands-on training and practice of EUS procedures.<sup>46,47</sup> The computer-based simulator generates ultrasound images in real time from three-dimensional anatomic models constructed from computed tomography (CT) and magnetic resonance imaging (MRI) images from real patients. The trainee inserts a customized echoendoscope into the specially designed GI-Mentor mannequin and simultaneously receives visual feedback from the monitor, along with tactile sensation from scope maneuvering during the procedure. A highly sensitive tracking system translates position and direction of the camera into realistic computer-generated images. The EUS module allows the trainee to switch from endoscopic to ultrasound images in real time and also provides training in both radial and linear ultrasound probes. Split-screen capability provides ultrasound images alongside of three-dimensional anatomic maps, further assisting in the interpretation and understanding of generated EUS images. The module also allows trainees to practice keyboard functions, such as labeling of organs, magnifying images, changing frequencies, and measuring with calipers. Following completion of the examination, the computer software permits performance evaluation by reviewing all saved images (up to 50 frozen images per procedure) and indicating anatomy and landmarks that were improperly identified by the user. Although the Simbionix GI-Mentor II EUS training module presents an exciting approach to training in EUS, there are currently no published validation studies or clinical trials assessing EUS simulators. A small study was published on learning EUS using the new Erlangen Active Simulator for Interventional Endoscopy (EASIE-R) (ENDOSIM, LLC, Nahant, Massachusetts). A single study demonstrated a learning effect by repeated exercise and improvement in performance

was noted during EUS procedures in a live porcine model.<sup>48</sup> Training models have been used to teach interventional EUS, including live porcine models.<sup>9</sup> An ex vivo model for training in EUS-guided biliary drainage procedures has been described. This model includes a three-dimensional printer-constructed polycarbonate model of the biliary tree surrounded by porcine liver tissue.<sup>9,49</sup> Similarly, an ex vivo model for training in EUS-guided drainage of pancreatic cysts and fluid collections has been described.<sup>50</sup>

Several issues need to be addressed before simulator use can be fully integrated into EUS training programs in an effective and efficient manner. Although simulators represent useful educational tools, prospective studies (ideally randomized controlled trials) to determine the validity of simulators for EUS training are needed demonstrating a decrease in the number of clinical procedures needed to achieve technical and cognitive competency. Validated simulator-based assessment tools that closely reproduce the key components of the endoscopic procedure are required.<sup>51</sup> The ASGE Preservation and Incorporation of Valuable Endoscopic Innovations statement addressed two main relevant questions that need to be answered before widespread adoption of simulators can be recommended in endoscopic training.<sup>52</sup> The thresholds recommended were as follows: (1) for an endoscopy simulator to be integrated into the standard instruction for a procedure, it must demonstrate a 25% or greater reduction in the median number of clinical cases required for the trainees to achieve the minimal competence parameters for that procedure and (2) simulator-based assessment tools must be procedure specific and predictive of independently defined minimal competence parameters from real procedures with a kappa value of at least 0.70 for high-stakes assessment.

## Quality Metrics in Endoscopic Ultrasound

Given the currently changing healthcare landscape, especially in the United States, the importance of measuring and monitoring quality in EUS needs to be instilled early during training. With the endorsement of several gastroenterology quality measures by the National Quality Forum, quality measurement is the “new normal” in gastroenterology.<sup>53</sup> Unfortunately, available data suggest that trainees have limited knowledge of quality measures.<sup>54</sup> It is critical that training programs promote a culture of continuous quality improvement among trainees and adopt formal approaches to educate trainees on defining and measuring the quality of care. Quality measures for EUS were outlined by the ASGE/American College of Gastroenterology (ACG) Task Force on Quality in Endoscopy (Table 3.3).<sup>1,2</sup> The priority quality measures for EUS include: (1) frequency with which all GI cancers are staged with the American Joint Committee on Cancer (AJCC)/Union for International Cancer Control (UICC) TNM staging system, (2) diagnostic rates and sensitivity for malignancy in patients undergoing EUS-guided FNA of pancreatic masses, and (3) the incidence of adverse events after EUS-guided FNA (acute pancreatitis, bleeding, perforation, and infection).

## Future Directions

Data regarding EUS performance among trainees during their initial few years of clinical practice are limited. Additional studies are needed to assess the performance of trainees at the onset of independent practice to better characterize the adequacy of

**TABLE  
3.3****Summary of Proposed Quality Indicators for Endoscopic Ultrasound<sup>a</sup>**

Quality Indicator	Type of Measure	Performance Target (%)
<b>Preprocedure</b>		
1. Frequency with which EUS is performed for an indication that is included in a published standard list of appropriate indications and the indication is documented	Process	>80
2. Frequency with which consent is obtained, including specific discussions of risks associated with EUS, and fully documented	Process	>98
3. Frequency with which appropriate antibiotics are administered in the setting of FNA of cystic lesions	Process	N/A
4. Frequency with which EUS exams are performed by trained endosonographers	Process	>98
<b>Intraprocedure</b>		
5. Frequency with which the appearance of relevant structures, specific to the indication for the EUS, is documented	Process	>98
6a. <b>Frequency with which all gastrointestinal cancers are staged with the AJCC/UICC TNM staging system (priority indicator)</b>	Process	>98
6b. Frequency with which pancreatic mass measurements are documented along with evaluation for vascular involvement, lymphadenopathy, and distant metastases.	Process	>98
6c. Frequency with which EUS wall layers involved by subepithelial masses are documented	Process	>98
7a. Percentage of patients with distant metastasis, ascites, and lymphadenopathy undergoing EUS FNA who have tissue sampling of both the primary tumor diagnosis and lesions outside of the primary field when this would alter patient management	Process	>98
7b. Diagnostic rate of adequate sample in all solid lesions undergoing EUS FNA (adequate sample is defined by the presence of cells/tissue from the representative lesion in question)	Outcome	≥85
7c. <b>Diagnostic rates and sensitivity for malignancy in patients undergoing EUS FNA of pancreatic masses (priority indicator)</b>	Outcome	Diagnostic rate: ≥70 Sensitivity: ≥85
<b>Postprocedure</b>		
8. Frequency with which the incidence of adverse events after EUS FNA (acute pancreatitis, bleeding, perforation, and infection) is documented	Process	>98
9. <b>Incidence of adverse events after EUS FNA (acute pancreatitis, bleeding, perforation, and infection) (priority indicator)</b>	Outcome	Acute pancreatitis: <2% Perforation: <0.5% Clinically significant bleeding: <1%

<sup>a</sup>This list of potential quality indicators was meant to be a comprehensive listing of measurable end points. It is not the intention of the task force that all end points be measured in every practice setting. In most cases, validation may be required before a given end point may be universally adopted.

AJCC, American Joint Committee on Cancer; EUS FNA, Endoscopic ultrasound-guided fine-needle aspiration; N/A, not available; TNM, tumor, node, metastasis; UICC, Union for International Cancer Control. Adapted from Wani S, Wallace MB, Cohen J, et al. Quality indicators for EUS. *Am J Gastroenterol*. 2015;110:102–113; and Wani S, Wallace MB, Cohen J, et al. Quality indicators for EUS. *Gastrointest Endosc*. 2015;81:67–80.

their training. Such data would shed light on the modifications required to current training programs to help ensure that trainees achieve competence at the time of completion of formal training. Confirming the durability of a trainee's endoscopic proficiency once in independent clinical practice and the achievement of relevant quality metrics thresholds in EUS (the definitive end point in competency assessment) needs to be a priority for future studies.<sup>1,2</sup> As the majority of EUS exams in training are performed for diagnostic and TA purposes, strategies to increase trainee exposure to advanced and interventional EUS are warranted. Competency criteria for interventional EUS procedures need to be defined. Future studies need to determine the validity of simulators for EUS training and if they result in a decrease in the number of clinical procedures needed to achieve technical and cognitive competence. Finally, systems that allow tracking outcomes in EUS are required.

## Conclusions

Training in EUS has evolved from a self-directed training model to a formal and supervised training model, typically occurring under the auspices of an advanced endoscopy fellowship. EUS has traditionally been taught by apprenticeship, and competence in EUS has been assessed by the trainers' subjective assessment of overall competence and/or meeting an arbitrary volume for procedures completed. Recent data clearly demonstrate substantial variability in EUS learning curves among trainees and a specific volume threshold during training does not ensure competence. Given that methods for assessing competence during endoscopic training are in transition and given an increasing focus on CBME, emphasis needs to be shifted away from the number of procedures performed to well-defined and validated competency thresholds. In an effort to standardize the evaluation of cognitive, technical,

and integrative aspects of EUS and clearly define competence, the use of a validated structured assessment tool such as TEESAT is critical. Because quality measurement is the “new normal,” the importance of measuring and monitoring quality in EUS needs to be instilled early during training. Finally, ensuring that all trainees achieve these thresholds and attain the skills necessary for safe and effective independent practice will ultimately improve the quality of patient care.

## Key References

1. Wani S, Wallace MB, Cohen J, et al. Quality indicators for EUS. *Am J Gastroenterol.* 2015;110:102–113.
9. Committee AT, Maple JT, Pannala R, et al. Interventional EUS (with videos). *Gastrointest Endosc.* 2017;85:465–481.
10. Wani S, Cote GA, Keswani R, et al. Learning curves for EUS by using cumulative sum analysis: implications for American Society for Gastrointestinal Endoscopy recommendations for training. *Gastrointest Endosc.* 2013;77:558–565.
11. Wani S, Hall M, Keswani RN, et al. Variation in aptitude of trainees in endoscopic ultrasonography, based on cumulative sum analysis. *Clin Gastroenterol Hepatol.* 2015;13:1318–1325.e2.
12. Committee ASoP, Faulk AL, Lightdale JR, et al. Guidelines for privileging, credentialing, and proctoring to perform GI endoscopy. *Gastrointest Endosc.* 2017;85:273–281.

## References

Access the reference list online at [ExpertConsult.com](http://ExpertConsult.com).

## References

1. Wani S, Wallace MB, Cohen J, et al. Quality indicators for EUS. *Am J Gastroenterol.* 2015;110:102–113.
2. Wani S, Wallace MB, Cohen J, et al. Quality indicators for EUS. *Gastrointest Endosc.* 2015;81:67–80.
3. Boniface MM, Wani SB, Schefter TE, et al. Multidisciplinary management for esophageal and gastric cancer. *Cancer Manag Res.* 2016;8:39–44.
4. Meguid C, Schulick RD, Schefter TE, et al. The multidisciplinary approach to GI cancer results in change of diagnosis and management of patients. Multidisciplinary care impacts diagnosis and management of patients. *Ann Surg Oncol.* 2016;23:3986–3990.
5. Wani S, Mullady D, Early DS, et al. The clinical impact of immediate on-site cytopathology evaluation during endoscopic ultrasound-guided fine needle aspiration of pancreatic masses: a prospective multicenter randomized controlled trial. *Am J Gastroenterol.* 2015;110:1429–1439.
6. DeWitt J, Devereaux B, Chriswell M, et al. Comparison of endoscopic ultrasonography and multidetector computed tomography for detecting and staging pancreatic cancer. *Ann Intern Med.* 2004;141:753–763.
7. Hewitt MJ, McPhail MJ, Possamai L, et al. EUS-guided FNA for diagnosis of solid pancreatic neoplasms: a meta-analysis. *Gastrointest Endosc.* 2012;75:319–331.
8. Madhoun MF, Wani SB, Rastogi A, et al. The diagnostic accuracy of 22-gauge and 25-gauge needles in endoscopic ultrasound-guided fine needle aspiration of solid pancreatic lesions: a meta-analysis. *Endoscopy.* 2013;45:86–92.
9. Committee AT, Maple JT, Pannala R, et al. Interventional EUS (with videos). *Gastrointest Endosc.* 2017;85:465–481.
10. Wani S, Cote GA, Keswani R, et al. Learning curves for EUS by using cumulative sum analysis: implications for American Society for Gastrointestinal Endoscopy recommendations for training. *Gastrointest Endosc.* 2013;77:558–565.
11. Wani S, Hall M, Keswani RN, et al. Variation in aptitude of trainees in endoscopic ultrasonography, based on cumulative sum analysis. *Clin Gastroenterol Hepatol.* 2015;13:1318–1325.e2.
12. Committee ASOP, Faulk AL, Lightdale JR, et al. Guidelines for privileging, credentialing, and proctoring to perform GI endoscopy. *Gastrointest Endosc.* 2017;85:273–281.
13. Polkowski M, Larghi A, Weynand B, et al. Learning, techniques, and complications of endoscopic ultrasound (EUS)-guided sampling in gastroenterology: European Society of Gastrointestinal Endoscopy (ESGE) Technical Guideline. *Endoscopy.* 2012;44:190–206.
14. Arya N, Sahai AV, Paquin SC. Credentialing for endoscopic ultrasound: a proposal for Canadian guidelines. *Endosc Ultrasound.* 2016;5:4–7.
15. Committee AT, DiMaio CJ, Mishra G, et al. EUS core curriculum. *Gastrointest Endosc.* 2012;76:476–481.
16. Committee AT, Adler DG, Bakis G, et al. Principles of training in GI endoscopy. *Gastrointest Endosc.* 2012;75:231–235.
17. Wani S, Muthusamy VR, Komanduri S. EUS-guided tissue acquisition: an evidence-based approach (with videos). *Gastrointest Endosc.* 2014;80:939–959. e7.
18. Komanduri S, Quinton S, Srivastava A, et al. Endosonographers' approach to delivering a diagnosis of pancreatic cancer: obligated but undertrained. *Endosc Int Open.* 2016;4:E242–E248.
19. Elta GH, Jorgensen J, Coyle WJ. Training in interventional endoscopy: current and future state. *Gastroenterology.* 2015;148:488–490.
20. Wilson R, Keswani R, Hall M, et al. Composition and trainee perception of EUS training in advanced endoscopy training programs (AETPs) in the US: results from a prospective multicenter study evaluating competence among advanced endoscopy trainees (AETs). *Gastroenterology.* 2016;150:S38–S39.
21. Patel SG, Keswani R, Elta G, et al. Status of competency-based medical education in endoscopy training: a nationwide survey of US ACGME-accredited gastroenterology training programs. *Am J Gastroenterol.* 2015;110:956–962.
22. Meenan J, Harris K, Oppong K, et al. Service provision and training for endoscopic ultrasound in the UK. *Frontline Gastroenterology.* 2011;2:188–194.
23. Hoffman B, Wallace MB, Eloubeidi MA, et al. How many supervised procedures does it take to become competent in EUS? Results of a multicenter three year study. *Gastrointest Endosc.* 2000;51:AB139.
24. Fockens P, Van den Brande JH, van Dullemen HM, et al. Endosonographic T-staging of esophageal carcinoma: a learning curve. *Gastrointest Endosc.* 1996;44:58–62.
25. Schlick T, Heintz A, Junginger T. The examiner's learning effect and its influence on the quality of endoscopic ultrasonography in carcinoma of the esophagus and gastric cardia. *Surg Endosc.* 1999;13:894–898.
26. Nayar M, Joy D, Wadehra V, et al. Effect of dedicated and supervised training on achieving competence in EUS-FNA of solid pancreatic lesions. *Scand J Gastroenterol.* 2011;46:997–1003.
27. Fritscher-Ravens A, Cuming T, Dhar S, et al. Endoscopic ultrasound-guided fine needle aspiration training: evaluation of a new porcine lymphadenopathy model for in vivo hands-on teaching and training, and review of the literature. *Endoscopy.* 2013;45:114–120.
28. Cote GA, Hovis CE, Kohlmeier C, et al. Training in EUS-guided fine needle aspiration: safety and diagnostic yield of attending supervised, trainee-directed FNA from the onset of training. *Diagn Ther Endosc.* 2011;2011:378540.
29. Konge L, Vilimann P, Clementsen P, et al. Reliable and valid assessment of competence in endoscopic ultrasonography and fine-needle aspiration for mediastinal staging of non-small cell lung cancer. *Endoscopy.* 2012;44:928–933.
30. Ekkelenkamp VE, Koch AD, de Man RA, et al. Training and competence assessment in GI endoscopy: a systematic review. *Gut.* 2016;65:607–615.
31. James PD, Antonova L, Martel M, et al. Measures of trainee performance in advanced endoscopy: a systematic review. *Best Pract Res Clin Gastroenterol.* 2016;30:421–452.
32. Eloubeidi MA, Tamhane A. EUS-guided FNA of solid pancreatic masses: a learning curve with 300 consecutive procedures. *Gastrointest Endosc.* 2005;61:700–708.
33. Mertz H, Gautam S. The learning curve for EUS-guided FNA of pancreatic cancer. *Gastrointest Endosc.* 2004;59:33–37.
34. Harewood GC, Wiersema LM, Halling AC, et al. Influence of EUS training and pathology interpretation on accuracy of EUS-guided fine needle aspiration of pancreatic masses. *Gastrointest Endosc.* 2002;55:669–673.
35. Kahaleh M. Training the next generation of advanced endoscopists in EUS-guided biliary and pancreatic drainage: learning from master endoscopists. *Gastrointest Endosc.* 2013;78:638–641.
36. Frank JR, Mungroo R, Ahmad Y, et al. Toward a definition of competency-based education in medicine: a systematic review of published definitions. *Med Teach.* 2010;32:631–637.
37. Frank JR, Snell LS, Cate OT, et al. Competency-based medical education: theory to practice. *Med Teach.* 2010;32:638–645.
38. Keswani RN, Wani S. Competency in upper endoscopy: the “End of the Road” is just the beginning? *Gastroenterology.* 2016;151:763–765.
39. Rex DK, Schoenfeld PS, Cohen J, et al. Quality indicators for colonoscopy. *Am J Gastroenterol.* 2015;110:72–90.
40. Wani S, Hall M, Wang AY, et al. Variation in learning curves and competence for ERCP among advanced endoscopy trainees by using cumulative sum analysis. *Gastrointest Endosc.* 2016;83:711–719.e11.

41. Epstein RM. Assessment in medical education. *N Engl J Med.* 2007;356:387–396.
42. van der Vleuten CP, Schuwirth LW. Assessing professional competence: from methods to programmes. *Med Educ.* 2005;39:309–317.
43. Wani S, Keswani R, Hall M, et al. A prospective multicenter study evaluating learning curves and competence in EUS and ERCP among advanced endoscopy trainees: the Rapid Assessment of Trainee Endoscopy Skills (RATES) Study. *Gastrointest Endosc.* 2016;83:AB113.
44. Committee ASOP, Early DS, Ben-Menachem T, et al. Appropriate use of GI endoscopy. *Gastrointest Endosc.* 2012;75:1127–1131.
45. Dumonceau JM, Polkowski M, Larghi A, et al. Indications, results, and clinical impact of endoscopic ultrasound (EUS)-guided sampling in gastroenterology: European Society of Gastrointestinal Endoscopy (ESGE) Clinical Guideline. *Endoscopy.* 2011;43:897–912.
46. Gerson LB. Evidence-based assessment of endoscopic simulators for training. *Gastrointest Endosc Clin N Am.* 2006;16:489–509, vii–viii.
47. Desilets DJ, Banerjee S, Barth BA, et al. Endoscopic simulators. *Gastrointest Endosc.* 2011;73:861–867.
48. Barther M, Gasmi M, Boustiere C, et al. EUS training in a live pig model: does it improve echo endoscope hands-on and trainee competence? *Endoscopy.* 2007;39:535–539.
49. Dhir V, Itoi T, Fockens P, et al. Novel ex vivo model for hands-on teaching of and training in EUS-guided biliary drainage: creation of “Mumbai EUS” stereolithography/3D printing bile duct prototype (with videos). *Gastrointest Endosc.* 2015;81:440–446.
50. Baron TH, DeSimio TM. New ex-vivo porcine model for endoscopic ultrasound-guided training in transmural puncture and drainage of pancreatic cysts and fluid collections (with videos). *Endosc Ultrasound.* 2015;4:34–39.
51. Cohen J, Thompson CC. The next generation of endoscopic simulation. *Am J Gastroenterol.* 2013;108:1036–1039.
52. Cohen J, Bosworth BP, Chak A, et al. Preservation and Incorporation of Valuable Endoscopic Innovations (PIVI) on the use of endoscopy simulators for training and assessing skill. *Gastrointest Endosc.* 2012;76:471–475.
53. Saini SD, Waljee AK, Schoenfeld P, et al. The increasing importance of quality measures for trainees. *Gastroenterology.* 2014;147:725–729.
54. Thompson JS, Lebwohl B, Syngal S, et al. Knowledge of quality performance measures associated with endoscopy among gastroenterology trainees and the impact of a web-based intervention. *Gastrointest Endosc.* 2012;76:100–106.e1–e4.

# 4

# Indications, Preparation, and Adverse Effects

MARK TOPAZIAN

## KEY POINTS

- The primary indications for endoscopic ultrasound (EUS) are cancer diagnosis and staging, assessment (usually combined with EUS fine-needle aspiration [FNA]) of lymph nodes, and evaluation of pancreatic disease and subepithelial lesions of the gastrointestinal tract. Typically EUS is indicated when there is potential additive value after noninvasive imaging has been performed.
- Prophylactic antibiotics are recommended for EUS FNA of cystic lesions.
- Guidelines recommend discontinuation of antithrombotic drugs prior to EUS FNA. However, it may be reasonable to continue these drugs when the risk of thrombosis or thromboembolism is high and the perceived bleeding risk of EUS FNA is low. In such cases, use of a small-caliber FNA needle and real-time on-site cytopathology may be useful.
- The risk of perforation may be higher with EUS than for standard endoscopy. Caution should be exercised when intubating the patient, traversing stenotic tumors, and passing the instrument beyond the apex of the duodenal bulb, because these are all situations in which the long, rigid tip increases the difficulty of passing the instrument.
- This chapter summarizes general indications for EUS, discusses patient evaluation and preparation for EUS procedures, and reviews the risks and adverse effects of EUS, EUS-guided tissue acquisition, and selected EUS-guided therapeutic interventions.

## Indications

Since the introduction of EUS in 1980, its clinical role has continued to expand. EUS should be performed when it has the potential to affect patient management, such as when establishing a diagnosis, obtaining locoregional tumor staging, or enabling therapeutic intervention. This overview of indications and risks is supplemented by the detailed discussions of specific indications that can be found in relevant chapters throughout this book.

## Diagnostic Imaging

Endosonographic findings can be diagnostic for certain lesions, including gut duplication cysts, lipomas, bile duct stones, and

some branch duct intraductal papillary mucinous neoplasias. However, in other situations, EUS imaging alone does not provide a confident diagnosis, and EUS-guided FNA or core biopsy (FNB) is indicated to facilitate cytologic or histologic diagnosis. Follow-up imaging may be indicated when EUS demonstrates a benign-appearing lesion, to identify interval growth or other signs suggestive of malignancy.

## Tumor Staging

Initial evaluation of patients with gastrointestinal (GI) cancers includes assessment of operative risk and determination of tumor stage. Accurate staging determines prognosis and guides treatment decisions. Staging usually begins with noninvasive imaging such as computed tomography (CT), magnetic resonance imaging (MRI), or positron emission tomography (PET), which are generally superior to EUS for excluding distant metastases. EUS is often performed for tumor (T) and nodal (N) staging because it provides an accuracy of approximately 85% for locoregional staging of GI luminal cancers.<sup>1–5</sup> Factors such as the number of malignant lymph nodes present may have both staging and prognostic relevance,<sup>6</sup> and findings of EUS and CT or MR are complementary in some situations, for instance staging of vascular involvement by pancreatic cancer.<sup>7</sup> Prior radiation therapy substantially decreases the T-staging accuracy of EUS.<sup>8</sup>

EUS provides important nodal staging information in patients with lung, esophageal, and rectal cancer. The typical EUS characteristics of malignant lymph nodes are hypoechoogenicity, round shape, smooth border, and size greater than 1 cm in the short axis; however, these features are at best 75% accurate for predicting malignancy in lymph nodes when compared with EUS FNA results or surgical histology.<sup>9</sup> Overlap in appearance between benign and malignant lymph nodes makes nodal staging problematic by EUS, and the aforementioned criteria are less useful in lung cancer, rectal cancer, and cholangiocarcinoma.<sup>3,10,11</sup> Overstaging may result from enlarged reactive lymph nodes that are deemed malignant on the basis of their EUS appearance alone. The addition of FNA improves nodal staging accuracy, but it also introduces the possibility of false-positive results, particularly when luminal cancer or Barrett esophagus is present.<sup>12</sup> When aspirating lymph nodes, one should avoid traversing the primary tumor to minimize the risk of a false-positive cytologic finding and tumor seeding.

EUS has a limited role in establishing the presence or absence of distant metastasis (M stage). Sometimes a suspicious lesion (such as a left adrenal mass in a patient with lung cancer) is best approached for tissue sampling via EUS, or a previously unsuspected metastasis is diagnosed during EUS performed for local staging (e.g., a left lobe liver lesion in a patient with pancreatic cancer). EUS FNA appears reasonably safe when sampling the liver and adrenal glands.<sup>13–15</sup>

EUS has been compared with PET in staging of esophageal cancer. PET has the ability to identify distant metastatic disease more accurately than EUS and CT, upstaging patients who were previously considered to have localized disease and excluding the possibility of curative R0 surgical resection. However, PET has limited accuracy in staging local and regional disease, and EUS remains superior to PET or CT for this indication. It appears that PET and EUS are complementary for optimal staging.<sup>16,17</sup>

In patients with a pancreatic mass that is visible on CT, EUS and CT provide comparable accuracy with regard to vascular invasion and nodal involvement.<sup>2</sup> However, EUS retains a key role in the evaluation of suspected pancreatic cancer for two reasons: EUS can detect abnormalities missed by CT and provides a preferred means of obtaining tissue specimens during the examination. EUS can also identify small metastatic lesions that were not identified on CT, including left lobe liver metastases, perivascular cuffing by tumor, and malignant involvement of celiac ganglia.<sup>18–20</sup> The ability to obtain tissue specimens from these sites or from the primary pancreatic mass is important both for diagnosis and staging. Pancreatic mass lesions may be adenocarcinoma, other neoplasms such as neuroendocrine tumors or metastases, or benign conditions such as autoimmune pancreatitis, and these lesions cannot always be differentiated by clinical findings, imaging, and laboratory tests; EUS FNA and FNB allow efficient diagnosis in many such cases. Because EUS is superior to CT for detection of small pancreatic cancers, it should be performed if clinical or CT findings raise the question of a pancreatic tumor not visualized by CT.

EUS has a role in staging non–small cell lung cancer (NSCLC) because CT and PET have poor accuracy for the detection of mediastinal lymph node metastases. Lung cancer patients without suspicious mediastinal adenopathy on CT have up to a 35% prevalence of malignant mediastinal adenopathy.<sup>21</sup> To limit false-positive and false-negative diagnoses of nodal stage, lymph node tissue sampling is advocated when it will change the management strategy (typically when a visualized lymph node is contralateral to the primary tumor). Sampling of all relevant nodal stations traditionally required surgical mediastinoscopy; however, a combination of EUS and endobronchial ultrasound (EBUS) for staging in NSCLC has a negative predictive value of 97% in the evaluation of mediastinal lymph nodes.<sup>22</sup> EUS and EBUS are complementary, because neither test visualizes all relevant mediastinal lymph node stations. EUS also allows evaluation of the left adrenal gland for previously undetected distant metastases.

## Tissue Acquisition

The development of linear EUS technology in the early 1990s allowed for EUS FNA and FNB of lesions within and extrinsic to the GI tract wall. Common indications for FNA include pancreatic mass lesions, nodal staging of esophageal, pancreatic, bile duct, and rectal cancers. EUS FNA is often the least invasive and most successful means of obtaining tissue specimens. Molecular characterization of tissue acquired during EUS is increasingly relevant to clinical care because it may predict prognosis and guide individualized patient management.<sup>23</sup>

Less invasive approaches for establishing a tissue diagnosis include transabdominal ultrasound or CT-guided biopsy. These methods are well established and more cost-effective than EUS in certain scenarios (e.g., in patients with a pancreatic mass and suspicious liver lesions that can be targeted for percutaneous biopsy). However, these methods may be limited by their poor sensitivity in the diagnosis of small lesions or by concern for potential tumor seeding of the biopsy needle tract. EUS may be favored in these situations, as well as when EUS is indicated for other reasons, such as locoregional staging or celiac plexus/ganglia neurolysis. Although the diagnostic accuracy of EUS FNA for liver and nodal metastases is generally greater than 85%, this method is less accurate in other settings, including diagnosis of pancreatic cystic lesions, stromal tumors, previously radiated lesions, and autoimmune pancreatitis. EUS FNB safely improves the diagnostic accuracy of EUS in selected settings.<sup>24</sup>

## Therapy

EUS facilitates access to target structures for therapeutic intervention. The EUS needle is essentially a conduit that allows for the passage of guidewires or placement of materials with therapeutic intent. The first such therapies to be developed were EUS-guided celiac plexus/ganglia neurolysis or block<sup>25,26</sup> and EUS-guided pseudocyst drainage.<sup>27</sup> EUS is also used to facilitate drainage of otherwise inaccessible biliary and pancreatic ducts,<sup>28</sup> angiotherapy for GI bleeding,<sup>29</sup> placement of fiducials to guide radiation therapy,<sup>30</sup> recovery of migrated stents, and transduodenal gallbladder drainage.<sup>31</sup> EUS fine-needle injection (EUS FNI) is a developing means of delivering therapeutic agents into solid cancers and cystic neoplasms. The safety, efficacy, and clinical role of these procedures are discussed in more detail in other chapters.

## Contraindications

Absolute contraindications to EUS are few and include unacceptable sedation risks. Coagulopathy (international normalized ratio [INR] >1.5) and thrombocytopenia (platelets <50,000) are relative contraindications to EUS FNA, which should be deferred if possible while coagulopathy or thrombocytopenia are corrected. Other relative contraindications include newly diagnosed cancer in a patient who has not undergone appropriate initial evaluation, altered anatomy prohibiting access via EUS, and the presence of intervening vital structures in the planned needle path for EUS FNA.

## Patient Preparation

### General Measures

EUS is performed in both outpatient and hospital settings, and open-access referrals are increasingly allowed. The setting and extent of the preprocedure evaluation can vary as a result. Initial evaluation should include a history, physical examination, and review of relevant medical records and imaging studies to determine the need, risks, benefits, alternatives, and timing of EUS and to document acquisition of informed consent (Box 4.1). Because emergency EUS is uncommon, involved parties should generally have the necessary time for adequate evaluation and discussion of patient and family concerns. A professional and unhurried

**• BOX 4.1 Factors That May Affect the Performance of Endoscopic Ultrasound**

- Severity and urgency of EUS examination
- Prior endoscopic examinations (findings and complications)
- Results of other imaging studies (including image review)
- Prior tissue sampling results
- Administration of chemoradiation (and timing relative to EUS)
- Comorbid illnesses:
  - Cardiopulmonary disease
  - Diabetes
  - Hypertension
  - Hepatic disease
  - Hematologic disease
  - Bleeding diathesis
- Surgical history (including altered GI tract anatomy)
- Medications:
  - Antihypertensives
  - Antithrombotics
  - Antiepileptics
  - Aspirin and other nonsteroidal antiinflammatory agents
  - Cardiac medications
  - Hypoglycemic agents
  - MAO inhibitors
  - Oral birth control pills
  - Pulmonary medications
- Psychiatric disease
- Drug allergies
- Ability to give informed consent
- Available transportation

EUS, Endoscopic ultrasound; GI, gastrointestinal; MAO, monoamine oxidase.

demeanor facilitates open communication and helps patients and their families to prepare for the exam.

When scheduling the procedure, outpatients should be instructed on their preparation responsibilities, the use of other medications, and the need to avoid alcohol and other sedatives. Patients should know that they will receive sedation or anesthesia, with resulting restrictions on postprocedure activities and the need for transportation assistance. Patients are informed of the potential signs and symptoms of adverse outcomes, as well as contact persons and phone numbers to call in the event they experience problems after their endoscopy. These instructions are reviewed after the procedure, with the patient and their accompanying adult.

Deeper sedation may be required for EUS than for routine endoscopic procedures because of the longer examination time and the need to minimize movement of the patient. As for all patient-sedated endoscopic procedures, careful monitoring is required throughout the procedure and recovery period. Administration of supplemental oxygen to all patients receiving sedation is recommended. Although conscious sedation or monitored anesthesia care (MAC) is routinely given for upper gastrointestinal (UGI) EUS, it is optional for rectal EUS.

UGI EUS is ideally performed following an overnight fast. At a minimum, patients should avoid solid foods for 6 hours and clear liquids (except sips of water to ingest medications) for 2 hours before the procedure. When there is concern for incomplete gastric emptying as a result of dysmotility or obstruction, a more prolonged clear liquid diet and airway protection during the exam may be advised. Retained gastric contents increase the risk of aspiration, produce imaging artifacts, and impair the overall examination quality.

Although some endosonographers perform rectal EUS after administering enemas alone, a full colon preparation is preferred, to optimize image quality and potentially reduce infectious complications associated with FNA.

## Laboratory Studies

Surgical series have consistently demonstrated a lack of utility of routine preoperative studies such as complete blood count, blood cross matching, routine chemistry studies, coagulation parameters, urinalysis, chest radiograph, and electrocardiogram for patients without evidence of relevant underlying disorders.<sup>32</sup> Routine preoperative testing in healthy patients rarely identifies abnormal findings and does not predict or correlate with patient outcomes. Therefore routine screening in asymptomatic patients is discouraged. Instead, endoscopists are advised to order preprocedure testing selectively, based on clinical suspicion arising from the initial evaluation, including a history of bleeding diathesis. This more focused approach greatly enhances the yield of preoperative testing without compromising patient outcomes.<sup>33</sup>

An exception may be women of childbearing age in whom pregnancy is possible. Although pregnancy is not a contraindication to endoscopic procedures or conscious sedation, it may be important to know whether a woman is pregnant (e.g., to determine whether airway protection is required and prior to use of fluoroscopy). When possible, it is advisable to avoid or delay EUS until after delivery. When EUS cannot be delayed, appropriate measures should be undertaken to lessen the risk to the unborn child.

## Medications

### Daily Medications

Patients are instructed to continue their cardiac, antihypertensive, pulmonary, antiepileptic, psychiatric, and contraceptive medications. These medications are ingested with sips of water early on the day of the procedure. Diabetic patients are advised to take half of their morning insulin dose at the usual time and the remaining dose with a postprocedure meal. Oral hypoglycemic agents are withheld the morning of the procedure and until resumption of a normal diet.

### Antithrombotic Drugs

Suggested management of antithrombotic agents in patients undergoing EUS FNA or EUS-guided therapy is shown in Table 4.1. These guidelines are based on recent consensus statements published by the American Society for Gastrointestinal Endoscopy (ASGE) and the British Society of Gastroenterology (BSG), which provide guidance on the management of antithrombotic drugs before and after endoscopy.<sup>34,35</sup> Management of antithrombotic drugs before and after endoscopy should be individualized based on patient and procedural factors and determined in consultation with the patient and their other physicians.

Periprocedural management of antithrombotic drugs requires an assessment of both the likelihood of procedurally induced bleeding and the patient's underlying risk of thromboembolism. Endoscopic procedures may be categorized as having either a high risk or a low risk of inducing bleeding. EUS without FNA is regarded as a low-risk procedure similar to diagnostic upper GI endoscopy or colonoscopy. In general, because EUS is a low-risk procedure, antithrombotic therapy does not need to be interrupted in patients undergoing diagnostic EUS without FNA so long as anticoagulation is not supratherapeutic.

**TABLE  
4.1****Antithrombotic Drug Management Prior to Endoscopic Ultrasound**

Drug	Procedure	Management	Interval Between Last Dose and Procedure	Comments
Warfarin	EUS	Continue		Ensure that INR is not supratherapeutic
Warfarin	EUS FNA, EUS-guided therapy	Discontinue <sup>a</sup>	3–7 days (usually 5), INR should be $\leq 1.5$ for procedure	Consider bridging therapy with heparin <sup>b</sup> ; usually safe to resume warfarin on the same or next day
Dabigatran, rivaroxaban, apixaban, edoxaban	EUS	Continue		
Dabigatran	EUS FNA, EUS-guided therapy	Discontinue <sup>a</sup>	2–3 days if GFR is $\geq 50$ mL/min, 3–4 days if GFR is 30–49 mL/min	Bridging therapy not recommended; resume drug when bleeding risk is low
Rivaroxaban, apixaban, edoxaban	EUS FNA, EUS-guided therapy	Discontinue <sup>a</sup>	2 days if GFR is $\geq 60$ mL/min, 3 days if GFR is 30–59 mL/min, 4 days if GFR is $< 30$ mL/min	Bridging therapy not recommended; resume drug when bleeding risk is low
Heparin	EUS	Continue		
Heparin	EUS FNA, EUS-guided therapy	Discontinue <sup>a</sup>	4–6 hours for unfractionated heparin	Skip one dose if using low molecular weight heparin
Aspirin	All EUS procedures	Continue	N/A	Low-dose aspirin does not substantially increase the risk of endoscopic procedures
Aspirin with dipyridamole	EUS	Continue		
Aspirin with dipyridamole	EUS FNA, EUS-guided therapy	Discontinue <sup>a</sup>	2–7 days	Consider continuing aspirin monotherapy
P2Y <sub>12</sub> receptor antagonists (clopidogrel, prasugrel, ticlopidine, ticagrelor, cangrelor)	EUS	Continue		
P2Y <sub>12</sub> receptor antagonists (clopidogrel, prasugrel, ticlopidine, ticagrelor, cangrelor)	EUS FNA, EUS-guided therapy	Coronary stent in place: discuss with cardiologist No coronary stent: Discontinue, <sup>a</sup> consider substituting aspirin	5 days (clopidogrel or ticagrelor), 7 days (prasugrel), 10–14 days (ticlopidine)	High risk of stent thrombosis for at least 12 months after insertion of drug-eluting coronary stent or at least 1 month after insertion of bare metal coronary stent

<sup>a</sup>May be appropriate to continue the antithrombotic drug in situations where the risk of thromboembolism is high (see Table 4.2), the perceived bleeding risk is relatively low, or endoscopic control of bleeding could be readily accomplished. See chapter text.

<sup>b</sup>Bridging therapy with low molecular weight heparin should be considered for patients discontinuing warfarin who are at high risk for thromboembolism, including those with (1) atrial fibrillation with a CHA<sub>2</sub>DS<sub>2</sub>-VASC score  $\geq 2$ , (2) mechanical mitral valve; (3) mechanical aortic valve with other thromboembolic risk factors or older-generation mechanical aortic valve; (4) venous thromboembolism within the past 3 months, (5) known severe thrombophilia (protein C or S, or antithrombin deficiency, antiphospholipid antibodies). CHA<sub>2</sub>DS<sub>2</sub>-VASC score: Congestive heart failure [1 point], Hypertension [1 point], Age  $\geq 75$  years [2 points], Diabetes mellitus [1 point], Stroke [2 points], Vascular disease [1 point], Age 65 to 74 years [1 point], Sex category, that is, female sex [1 point].

EUS, Endoscopic ultrasound; EUS FNA, endoscopic ultrasound-guided fine-needle aspiration; GFR, glomerular filtration rate; INR, international normalized ratio.

Adapted from Acosta RD, Abraham NS, Chandrasekhar V, et al. The management of antithrombotic agents for patients undergoing GI endoscopy. *Gastrointest Endosc*. 2016;83:3–16; and Veitch AM, Vanbiervliet G, Gershlick AH, et al. Endoscopy in patients on antiplatelet or anticoagulant therapy, including direct oral anticoagulants: British Society of Gastroenterology (BSG) and European Society of Gastrointestinal Endoscopy (ESGE) guidelines. *Gut*. 2016;65:374–389.

Guidelines classify EUS FNA as a high-risk procedure for inducing bleeding. The incidence of bleeding after EUS FNA in patients on various antithrombotic drugs is largely unknown. Hemorrhage has been reported after FNA in two of six patients receiving low molecular weight heparin<sup>36</sup> and in none of 10 patients receiving clopidogrel.<sup>37</sup> Although EUS FNA probably has a lower overall risk of clinically significant bleeding than other high-risk procedures such as endoscopic polypectomy or sphincterotomy, it is still considered a

high-risk procedure because when bleeding results it may be inaccessible or uncontrollable by endoscopic means. Although there is limited experience with EUS FNB in patients on therapeutic doses of antithrombotic drugs, the risk of hemorrhage is likely to be somewhat higher with FNB than FNA and probably varies with the FNB needle design, as well as anatomic and patient factors. Some EUS-guided therapeutic interventions also have a risk of bleeding that exceeds that of EUS FNA alone.

**TABLE  
4.2****Risk of Thromboembolic Events in Patients Interrupting Anticoagulant Therapy**

Indication for Anticoagulation	Risk of Thromboembolism		
	Low	Medium	High
Mechanical Heart Valve	Bileaflet aortic valve prosthesis with no other risk factors for stroke	Bileaflet aortic valve with 1 or more of the following: AF, prior CVA or TIA, hypertension, diabetes, CHF, age $\geq$ 75 years	Any mitral valve prosthesis; any caged-ball or tilting disc aortic valve prosthesis; recent (within 6 months) CVA or TIA
Venous Thromboembolism	VTE > 12 months previous and no other risk factors	VTE within the past 3–12 months; nonsevere thrombophilia (heterozygous factor V Leiden or prothrombin gene mutation), recurrent VTE, active cancer	Recent (within 3 months) VTE; severe thrombophilia (protein C or S, or antithrombin deficiency, antiphospholipid antibodies)

*AF*, Atrial fibrillation; *CHF*, congestive heart failure; *CVA*, cerebrovascular accident; *TIA*, transient ischemic attack; *VTE*, venous thromboembolism.

Adapted from Acosta RD, Abraham NS, Chandrasekhara V, et al. The management of antithrombotic agents for patients undergoing GI endoscopy. *Gastrointest Endosc*. 2016;83:3–16.

The guidelines shown in Table 4.1 must be thoughtfully applied to individual patient situations. Although EUS FNA is categorized as a higher risk procedure, there are few empirical data to support this categorization, and discontinuation of anti-thrombotic therapy may have devastating results, particularly in patients who are at high risk for thromboembolic events such as those with recently placed coronary stents and some patients with mechanical heart valves or history of venous thromboembolism (Table 4.2). Continuation of antithrombotic drugs in patients undergoing EUS FNA or selected EUS-guided therapies may be justified in some circumstances. In such patients, bloody aspirates may be obtained during EUS FNA, impairing cytologic analysis. This possibility should be considered when choosing the degree of negative pressure to apply during FNA and the duration of FNA passes. In patients taking antithrombotics, it may be prudent to use a smaller caliber (22 or 25 gauge) FNA needle and to use real-time on-site cytopathology evaluation to limit the number of FNA passes required.

### Resuming Antithrombotic Therapy

Antithrombotic drugs may be resumed once the bleeding risk is low. Available evidence suggests that most FNA-related bleeding is immediate, and delayed bleeding is rare. It is our practice to resume antithrombotic drugs 4 to 6 hours after FNA unless bleeding complications occurred, in which case additional delay may be prudent.

Patients resuming warfarin therapy will not be fully anticoagulated for several days, and bridging therapy may be warranted (see Table 4.1). Those receiving direct oral anticoagulants do not need bridging therapy because they will be fully anticoagulated within several hours of their first oral dose.

### Prophylactic Antibiotics

Bacteremia develops after 4% to 25% of routine endoscopic procedures, including diagnostic EUS; however, clinically significant infections are rare after diagnostic endoscopy.<sup>38</sup> Bacteremia is reported after EUS FNA of cystic or solid lesions along the upper GI tract in 4% to 6% of patients and after EUS FNA of solid lesions along the lower GI tract in 2%.<sup>39–43</sup> The highest rates of bacteremia and/or postprocedure infection are reported following esophageal sclerotherapy, esophageal stricture dilation,

endoscopic placement of feeding tubes, ERCP in patients with biliary obstruction, endoscopic drainage of pancreatic fluid collections, and EUS-guided biliary drainage procedures.<sup>44</sup>

Prophylactic antibiotics are recommended prior to EUS and EUS FNA in certain situations (Table 4.3). Patients with cirrhosis and acute GI bleeding should receive antibiotics to lower the risk of bacterial peritonitis, as well as patients receiving peritoneal dialysis undergoing lower GI endoscopic procedures. The American Heart Association (AHA) does not recommend antibiotic prophylaxis solely to prevent infective endocarditis in patients undergoing GI endoscopy.<sup>45</sup> However, in patients at high risk of infective endocarditis who are receiving antibiotics to treat a known or suspected infection such as cholangitis or infected pancreatic fluid collection, the AHA recommends including an agent active against enterococcus in the antibiotic regimen. This is because enterococcus is the intestinal microorganism most likely to cause infectious endocarditis. Patients with severe neutropenia (absolute neutrophil count <500 cells/ $\mu$ L) may also benefit from antibiotic prophylaxis prior to endoscopy.<sup>38</sup>

Prophylactic antibiotics are not recommended prior to EUS FNA of solid lesions along the upper or lower GI tracts because the risk of infection appears to be low (<1%).<sup>46</sup> However antibiotics are recommended prior to EUS FNA of cystic lesions along the upper or lower GI tract, and many endosonographers administer penicillin or quinolone antibiotics prior to cyst aspiration and for 3 to 5 days afterward. Widespread use of prophylactic antibiotics for cystic lesions was adopted following the report of a 14% risk of pancreatic cyst infection following EUS FNA,<sup>47</sup> and, although subsequent studies have not demonstrated a convincing benefit of prophylactic antibiotics in EUS FNA of pancreatic cysts,<sup>48,49</sup> therapy is still recommended. It appears that FNA of mediastinal cystic lesions may carry a relatively high risk of infection,<sup>50</sup> and infection of mediastinal cysts, as well as fungal mediastinitis, have been reported despite use of prophylaxis.

Prophylactic antibiotics are typically administered to patients undergoing most types of EUS-guided therapeutic intervention, including EUS-guided celiac plexus block, drainage of pancreatic fluid collections, and EUS-guided ductal access procedures.

**TABLE 4.3** Antibiotic Prophylaxis for Endoscopic Ultrasound

Patient Condition	Procedure Contemplated	Goal of Prophylaxis	Periprocedural Antibiotic Prophylaxis
Lesion requiring EUS exam	Diagnostic EUS without FNA	Prevention of infection	Not recommended <sup>a</sup>
Solid lesion along upper GI tract	EUS FNA	Prevention of local infection	Not recommended <sup>a</sup>
Solid lesion along lower GI tract	EUS FNA	Prevention of local infection	Not recommended <sup>a</sup>
Cystic lesions along GI tract (including mediastinum)	EUS FNA	Prevention of cyst infection	Recommended
Sterile pancreatic fluid collection	Transmural drainage	Prevention of local infection	Recommended
Obstructed biliary or pancreatic ducts	EUS-guided biliary or pancreatic duct drainage	Prevention of local infection or cholangitis	Recommended; may continue antibiotics after the procedure
Abdominal pain	EUS-guided celiac plexus block	Prevention of local infection	Recommended
Cirrhosis with acute GI bleeding	Any endoscopic procedure	Prevention of infectious complications and reduction of mortality	Recommended, upon hospital admission <sup>b</sup>
Continuous peritoneal dialysis	Lower GI tract endoscopy	Prevention of bacterial peritonitis	Recommended
Severe neutropenia (<500 cells/ $\mu$ L)	Any endoscopic procedure	Prevention of local and systemic infection	Insufficient data, consider prophylaxis
All cardiac conditions	Any endoscopic procedure	Prevention of infective endocarditis	Not recommended <sup>c</sup>
Synthetic vascular graft and other nonvalvular cardiovascular devices	Any endoscopic procedure	Prevention of graft and device infection	Not recommended <sup>c</sup>
Prosthetic joints	Any endoscopic procedure	Prevention of septic arthritis	Not recommended <sup>c</sup>

<sup>a</sup>Low rates of bacteremia and local infection, but see other patient conditions listed in this table.  
<sup>b</sup>Risk for bacterial infection associated with cirrhosis and GI bleeding is well established; ceftriaxone or a quinolone antibiotic recommended.  
<sup>c</sup>Very low risk of infection.

EUS, Endoscopic ultrasound; EUS FNA, endoscopic ultrasound-guided fine-needle aspiration; GI, gastrointestinal.

Adapted from Khashab MA, Chithadi KV, Acosta RD, et al. Antibiotic prophylaxis for GI endoscopy. *Gastrointest Endosc*. 2015;81:81–89.

## Risks and Adverse Effects

EUS shares the risks and adverse effects of other endoscopic procedures, including cardiovascular events, unwanted effects of conscious sedation, and allergic reactions to medications. This discussion focuses on adverse effects specifically associated with EUS, EUS FNA or FNB, and EUS-guided therapeutic interventions.

### Perforation

The incidence of GI perforation during EUS ranged from 0% to 0.4% in prospective series enrolling more than 300 patients.<sup>47,51</sup> Although available data are limited, perforation is probably more common with UGI EUS than with EGD.<sup>52</sup> The increased risk is partly accounted for by echoendoscope design, which combines oblique or side-viewing optics with a relatively long rigid tip that extends well beyond the optical lens. The tip of the endoscope may cause luminal perforation during advancement, particularly in areas of angulation (oropharynx or apex of duodenal bulb), stenosis (esophageal cancer), or a blind lumen (pharyngeal or esophageal diverticula). The risk may be increased early in an endosonographer's experience<sup>53</sup> or when experienced endosonographers use new equipment with different tip design, length, and deflection characteristics.

Intubation of the esophagus with the echoendoscope remains a partially blind maneuver. In one prospective study, 4894 patients underwent UGI tract EUS, and only three patients experienced cervical esophageal perforations.<sup>54</sup> Understanding the possible risk factors (age >65 years, history of swallowing difficulties, known cervical osteophytes, kyphosis of the spine, or hyperextension of the neck) may help to identify high-risk patients.

Approximately 15% to 40% of patients with esophageal cancer have a nontraversable obstructing esophageal tumor. Some investigators discourage routine dilation of obstructing tumors given the risk and tendency for advanced disease (85% to 90% likelihood of T3 or T4 disease) in this setting, whereas others report that distant lymphadenopathy is diagnosed in 10% to 40% of patients requiring dilation.<sup>55,56</sup>

Although initial studies reported perforation rates as high as 24% with esophageal dilation followed by immediate EUS, more recent studies found this practice safe.<sup>55,56</sup> There are several likely explanations for the apparent improvement in safety over time. Radial echoendoscopes introduced in the mid-1990s were of smaller diameter than older devices, so dilation was usually performed to 14 or 15 mm rather than 16 to 18 mm, as in earlier studies. In addition, greater awareness of this potential complication has probably led to less aggressive dilation practices.

For patients with circumferential stenosis, judicious stepwise dilation is undertaken to a maximum of 15 mm. Two large studies reporting on the safety of dilation followed the “rule of three”; (three stepwise 1-mm increases in dilator diameter above the diameter at which resistance was first encountered) and did not use “unacceptable force” to dilate.<sup>55,56</sup> Dilation allowed immediate passage of an echoendoscope beyond the tumor in 75% to 85% of cases. Extreme caution is necessary when semicircumferential infiltration is present because the normal (and hence thinner) esophageal wall may be at increased risk of tearing in this setting.

Miniprobes passed through a stenotic malignant esophageal tumor may improve the accuracy of T and N staging, but the limited depth of penetration does not allow a complete examination, particularly with regard to celiac axis nodes. Another alternative is use of the EBUS device passed into the esophagus. The EBUS scope is approximately 6.9 mm in diameter, can provide staging information, and has the ability to sample celiac nodes and liver lesions through FNA.<sup>57</sup>

## Bleeding

The risk of bleeding with EUS is mainly related to the performance of FNA. The incidence of clinically significant bleeding with FNA was 0% to 0.4% in two prospective studies enrolling more than 300 patients, and it was 1.3% in a retrospective study.<sup>58</sup> FNA of pancreatic cystic lesions has been associated with a 6% rate of self-limited bleeding into the cyst.<sup>59</sup>

A small amount of luminal bleeding is often seen endoscopically at FNA puncture sites, but it is generally without sequelae. Bleeding may also occur in the gut wall, adjacent tissue, or target structure undergoing aspiration. Such bleeding may be detected sonographically as a hypoechoic expansion of soft tissue or an enlargement of a lymph node or mass.<sup>58</sup> Alternatively, echogenic material may be seen filling a previously anechoic cyst or duct lumen or collecting in ascites. As blood clots, it increases in echogenicity and may thus become less apparent. When there is bleeding into a large potential space (such as the peritoneal cavity), the extent of blood loss may be difficult to assess because of pooling of blood outside the range of EUS imaging.

EUS-induced extraluminal bleeding is seldom associated with clinically important sequelae such as need for transfusion, angiography, or surgical intervention. Because most endosonographers avoid sonographically visible vessels when selecting a needle path for FNA, bleeding usually occurs from small vessels. Because the bleeding site is often extraluminal, methods of endoscopic hemostasis are usually not applicable. When bleeding occurs, it is often possible to apply transmitted pressure to the bleeding site by deflecting the tip of the echoendoscope against the gut wall. Arterial bleeding might be treated with injection of dilute epinephrine under EUS guidance, although the risk of inducing ischemia with this maneuver is undetermined. The efficacy of these interventions is not well studied.

## Infection

Infectious complications are uncommon after EUS FNA and may include those associated with the endoscopy itself (such as aspiration pneumonia) or with FNA (such as abscess or cholangitis).

Although infection appears to be rare after EUS FNA of solid lesions,<sup>60</sup> it may develop following aspiration of cystic lesions in the pancreas, mediastinum, and elsewhere.<sup>1</sup> Prophylactic

antibiotics are recommended prior to aspiration of pancreatic cystic lesions, although recent retrospective studies have not shown a clear benefit to prophylaxis.<sup>48,49</sup> Mediastinitis and sepsis have been reported after EUS FNA of mediastinal cysts, and prophylactic antibiotics seem warranted in this setting, although infection may occur even though prophylaxis has been given.<sup>50</sup> Technical issues may affect the risk of cyst infection, including the number of needle passes, the complexity of the cystic lesion, and the ability to aspirate all fluid from the cyst.

## Pancreatitis

Pancreatitis occurs in up to 2% of patients after EUS FNA of solid and cystic pancreatic lesions.<sup>46,61–63</sup> The largest studies of EUS FNA of solid pancreatic lesions report an incidence of pancreatitis of 0.3% to 0.6%.<sup>46,61,62</sup> Pancreatitis occurring after EUS FNA is generally mild, but severe pancreatitis and fatal complications have been reported.<sup>44</sup>

Limiting the number of needle passes, minimizing the amount of “normal” pancreatic parenchyma that must be traversed, and avoiding the pancreatic duct during EUS FNA procedures may ameliorate the risk of pancreatitis. However, in one small series, 12 patients with dilated pancreatic ducts underwent intentional EUS-guided aspiration of the duct without complications.<sup>64</sup> Cytologic yield on aspirated pancreatic duct fluid was 75%.

## Other Adverse Effects of EUS and EUS FNA

There is a risk of tumor seeding along the needle track when performing EUS FNA. Although there are only a few case reports documenting this occurrence, the true incidence is unknown because track seeding may go undetected. In one study of patients with cholangiocarcinoma undergoing surgery, peritoneal metastases were present in 83% of those who had undergone previous transperitoneal FNA of their tumor, versus 8% of those who had not.<sup>65</sup> This suggests that transperitoneal FNA of cholangiocarcinoma should be avoided when curative therapies (such as liver transplantation) are an option. The issue of needle track seeding risk is of minimal concern for pancreatic head lesions sampled from the duodenum because the needle tract lies within the field of resection during pancreaticoduodenectomy.

Bile peritonitis may result from traversal of the bile duct or gallbladder,<sup>66</sup> especially in the presence of an obstructed biliary system. Patients may require cholecystectomy after aspiration of bile across a normal gallbladder wall, but FNA of masses in the gallbladder wall seemed to be safe in small series.<sup>67,68</sup> If biliary puncture occurs, antibiotics should be administered, and biliary drainage should be established in those with biliary obstruction.

A final adverse effect of diagnostic EUS is missed or mis-staged lesions. Although this error does no immediate, periprocedural harm to the patient, the long-term consequences have not been fully studied. Careful review of the patient’s history and imaging studies, as well as formal training in EUS, may decrease the amount of missed lesions encountered in general practice.

## Therapeutic Endoscopic Ultrasound

EUS-guided therapeutic interventions entail additional risks beyond those described previously. Celiac plexus block or neurolysis may be complicated by abscess, transverse myelitis with lower extremity paralysis,<sup>69</sup> or death due to thrombosis or necrosis of the celiac artery and aorta.<sup>70</sup> EUS-guided drainage of pancreatic fluid

collections has been associated with bleeding, visceral perforation, stent migration, and infection. Bleeding may be less common when a lumen-apposing metal stent (LAMS) is placed across the drainage site. However, LAMS have also been reported to cause late hemorrhage due to erosion into adjacent vessels after resolution of the drained fluid collection. Although the true incidence of this complication is unclear, removal or replacement of a LAMS with plastic pigtail stents after complete necrosectomy and before resolution of the collection has been advocated.<sup>71</sup> EUS-guided biliary drainage procedures have been associated with adverse event rates exceeding 20%, including bile peritonitis, hemorrhage, pneumoperitoneum, sepsis, and perforation. In one study, use of a needle knife to establish the transmural biliary drainage tract was associated with a higher risk of adverse events.<sup>72</sup> Portal vein thrombosis has been reported in patients who underwent pancreatic cyst ethanol lavage and paclitaxel injection.<sup>73</sup>

## Key References

1. Crabtree TD, Yacoub WN, Puri V, et al. Endoscopic ultrasound for early stage esophageal adenocarcinoma: implications for staging and survival. *Ann Thorac Surg.* 2011;91:1509–1515; discussion 1515–1516.
38. Khashab MA, Chithadi KV, Acosta RD, et al. Antibiotic prophylaxis for GI endoscopy. *Gastrointest Endosc.* 2015;81:81–89.
44. Wang K, Zhu J, Xing L, et al. Assessment of efficacy and safety of EUS-guided biliary drainage: a systematic review. *Gastrointest Endosc.* 2016;83:1218–1227.
55. Pfau PR, Ginsberg GG, Lew RJ, et al. Esophageal dilation for endoscopic evaluation of malignant esophageal strictures is safe and effective. *Am J Gastroenterol.* 2000;95:2813–2815.
56. Wallace MB, Hawes RH, Sahai AV, et al. Dilation of malignant esophageal stenosis to allow EUS guided fine-needle aspiration: safety and effect on patient management. *Gastrointest Endosc.* 2000;51:309–313.

## References

Access the reference list online at [ExpertConsult.com](http://ExpertConsult.com).

## References

1. Crabtree TD, Yacoub WN, Puri V, et al. Endoscopic ultrasound for early stage esophageal adenocarcinoma: implications for staging and survival. *Ann Thorac Surg.* 2011;91:1509–1515; discussion 1515–1516.
2. Dewitt J, Devereaux BM, Lehman GA, et al. Comparison of endoscopic ultrasound and computed tomography for the preoperative evaluation of pancreatic cancer: a systematic review. *Clin Gastroenterol Hepatol.* 2006;4:717–725; quiz 664.
3. Gleeson FC, Rajan E, Levy MJ, et al. EUS-guided FNA of regional lymph nodes in patients with unresectable hilar cholangiocarcinoma. *Gastrointest Endosc.* 2008;67:438–443.
4. Talebian M, von Bartheld MB, Braun J, et al. EUS-FNA in the preoperative staging of non-small cell lung cancer. *Lung Cancer.* 2010;69:60–65.
5. Zeppa P, Barra E, Napolitano V, et al. Impact of endoscopic ultrasound-guided fine needle aspiration (EUS-FNA) in lymph nodal and mediastinal lesions: a multicenter experience. *Diagn Cytopathol.* 2011;39:723–729.
6. Chen J, Xu R, Hunt GC, et al. Influence of the number of malignant regional lymph nodes detected by endoscopic ultrasonography on survival stratification in esophageal adenocarcinoma. *Clin Gastroenterol Hepatol.* 2006;4:573–579.
7. Glazer ES, Rashid OM, Klapman JB, et al. Endoscopic ultrasonography complements computed tomography in predicting portal or superior mesenteric vein resection in patients with borderline resectable pancreatic carcinoma. *Pancreatology.* 2017;17:130–134.
8. Zhao YL, Cao DM, Zhou QC, et al. Accuracy of endorectal endoscopic ultrasound (EUS) for locally advanced rectal cancer (LARC) restaging after neoadjuvant chemoradiotherapy (NAT): a meta-analysis. *Hepatogastroenterology.* 2014;61:978–983.
9. de Melo Jr SW, Panjala C, Crespo S, et al. Interobserver agreement on the endosonographic features of lymph nodes in aerodigestive malignancies. *Dig Dis Sci.* 2011;56:3204–3208.
10. Gleeson FC, Clain JE, Rajan E, et al. EUS-FNA assessment of extramesenteric lymph node status in primary rectal cancer. *Gastrointest Endosc.* 2011;74:897–905.
11. Gill KR, Ghabril MS, Jamil LH, et al. Endosonographic features predictive of malignancy in mediastinal lymph nodes in patients with lung cancer. *Gastrointest Endosc.* 2010;72:265–271.
12. Gleeson FC, Kipp BR, Caudill JL, et al. False positive endoscopic ultrasound fine needle aspiration cytology: incidence and risk factors. *Gut.* 2010;59:586–593.
13. Jhala NC, Jhala D, Eloubeidi MA, et al. Endoscopic ultrasound-guided fine-needle aspiration biopsy of the adrenal glands: analysis of 24 patients. *Cancer.* 2004;102:308–314.
14. Pineda JJ, Diehl DL, Miao CL, et al. EUS-guided liver biopsy provides diagnostic samples comparable with those via the percutaneous or transjugular route. *Gastrointest Endosc.* 2016;83:360–365.
15. Puri R, Thandassery RB, Choudhary NS, et al. Endoscopic ultrasound-guided fine-needle aspiration of the adrenal glands: analysis of 21 patients. *Clin Endosc.* 2015;48:165–170.
16. McDonough PB, Jones DR, Shen KR, et al. Does FDG-PET add information to EUS and CT in the initial management of esophageal cancer? A prospective single center study. *Am J Gastroenterol.* 2008;103:570–574.
17. Stigt JA, Oostdijk AH, Timmer PR, et al. Comparison of EUS-guided fine needle aspiration and integrated PET-CT in restaging after treatment for locally advanced non-small cell lung cancer. *Lung Cancer.* 2009;66:198–204.
18. Levy MJ, Gleeson FC, Zhang L. Endoscopic ultrasound fine-needle aspiration detection of extravascular migratory metastasis from a remotely located pancreatic cancer. *Clin Gastroenterol Hepatol.* 2009;7:246–248.
19. Levy MJ, Topazian M, Keeney G, et al. Preoperative diagnosis of extrapancreatic neural invasion in pancreatic cancer. *Clin Gastroenterol Hepatol.* 2006;4:1479–1482.
20. Singh P, Mukhopadhyay P, Bhatt B, et al. Endoscopic ultrasound versus CT scan for detection of the metastases to the liver: results of a prospective comparative study. *J Clin Gastroenterol.* 2009;43:367–373.
21. Micames CG, McCrory DC, Pavie DA, et al. Endoscopic ultrasound-guided fine-needle aspiration for non-small cell lung cancer staging: a systematic review and metaanalysis. *Chest.* 2007;131:539–548.
22. Wallace MB, Woodward TA, Raimondo M. Endoscopic ultrasound and staging of non-small cell lung cancer. *Gastrointest Endosc Clin N Am.* 2005;15:157–167, x.
23. Diaz Del Arco C, Esteban Lopez-Jamar JM, Ortega Medina L, et al. Fine-needle aspiration biopsy of pancreatic neuroendocrine tumors: correlation between Ki-67 index in cytological samples and clinical behavior. *Diagn Cytopathol.* 2017;45:29–35.
24. Levy MJ, Reddy RP, Wiersema MJ, et al. EUS-guided trucut biopsy in establishing autoimmune pancreatitis as the cause of obstructive jaundice. *Gastrointest Endosc.* 2005;61:467–473.
25. Gress F, Schmitt C, Sherman S, et al. Endoscopic ultrasound-guided celiac plexus block for managing abdominal pain associated with chronic pancreatitis: a prospective single center experience. *Am J Gastroenterol.* 2001;96:409–416.
26. Schmulewitz N, Hawes R. EUS-guided celiac plexus neurolysis—technique and indication. *Endoscopy.* 2003;35:S49–S53.
27. Seifert H, Dietrich C, Schmitt T, et al. Endoscopic ultrasound-guided one-step transmural drainage of cystic abdominal lesions with a large-channel echo endoscope. *Endoscopy.* 2000;32:255–259.
28. Chen YI, Levy MJ, Moreels TG, et al. An international multicenter study comparing EUS-guided pancreatic duct drainage with enteroscopy-assisted endoscopic retrograde pancreatography after Whipple surgery. *Gastrointest Endosc.* 2017;85:170–177.
29. Levy MJ, Wong Kee Song LM, Farnell MB, et al. Endoscopic ultrasound (EUS)-guided angiotherapy of refractory gastrointestinal bleeding. *Am J Gastroenterol.* 2008;103:352–359.
30. Chavalitdhamrong D, DiMaio CJ, Siersema PD, et al. Technical advances in endoscopic ultrasound-guided fiducial placement for the treatment of pancreatic cancer. *Endosc Int Open.* 2015;3:E373–E377.
31. Choi JH, Kim HW, Lee JC, et al. Percutaneous transhepatic versus EUS-guided gallbladder drainage for malignant cystic duct obstruction. *Gastrointest Endosc.* 2017;85:357–364.
32. Benarroch-Gampel J, Sheffield KM, Duncan CB, et al. Preoperative laboratory testing in patients undergoing elective, low-risk ambulatory surgery. *Ann Surg.* 2012;256:518–528.
33. Levy MJ, Anderson MA, Baron TH, et al. Position statement on routine laboratory testing before endoscopic procedures. *Gastrointest Endosc.* 2008;68:827–832.
34. Acosta RD, Abraham NS, Chandrasekhara V, et al. The management of antithrombotic agents for patients undergoing GI endoscopy. *Gastrointest Endosc.* 2016;83:3–16.
35. Veitch AM, Vanbiervliet G, Gershlick AH, et al. Endoscopy in patients on antiplatelet or anticoagulant therapy, including direct oral anticoagulants: british society of gastroenterology (BSG) and european society of gastrointestinal endoscopy (ESGE) guidelines. *Gut.* 2016;65:374–389.
36. Kien-Fong Vu C, Chang F, Doig L, et al. A prospective control study of the safety and cellular yield of EUS-guided FNA or Trucut biopsy in patients taking aspirin, nonsteroidal anti-inflammatory drugs, or prophylactic low molecular weight heparin. *Gastrointest Endosc.* 2006;63:808–813.
37. Trindade AJ, Hirten R, Slattery E, et al. Endoscopic ultrasound-guided fine-needle aspiration of solid lesions on clopidogrel may not be a high-risk procedure for bleeding: a case series. *Dig Endosc.* 2016;28:216–219.

38. Khashab MA, Chithadi KV, Acosta RD, et al. Antibiotic prophylaxis for GI endoscopy. *Gastrointest Endosc.* 2015;81:81–89.
39. Barawi M, Gottlieb K, Cunha B, et al. A prospective evaluation of the incidence of bacteremia associated with EUS-guided fine-needle aspiration. *Gastrointest Endosc.* 2001;53:189–192.
40. Early DS, Acosta RD, Chandrasekhara V, et al. Adverse events associated with EUS and EUS with FNA. *Gastrointest Endosc.* 2013;77:839–843.
41. Janssen J, Konig K, Knop-Hammad V, et al. Frequency of bacteremia after linear EUS of the upper GI tract with and without FNA. *Gastrointest Endosc.* 2004;59:339–344.
42. Levy MJ, Norton ID, Clain JE, et al. Prospective study of bacteremia and complications with EUS FNA of rectal and perirectal lesions. *Clin Gastroenterol Hepatol.* 2007;5:684–689.
43. Levy MJ, Norton ID, Wiersema MJ, et al. Prospective risk assessment of bacteremia and other infectious complications in patients undergoing EUS-guided FNA. *Gastrointest Endosc.* 2003;57:672–678.
44. Wang K, Zhu J, Xing L, et al. Assessment of efficacy and safety of EUS-guided biliary drainage: a systematic review. *Gastrointest Endosc.* 2016;83:1218–1227.
45. Wilson W, Taubert KA, Gewitz M, et al. Prevention of infective endocarditis: guidelines from the American Heart Association: a guideline from the American Heart Association Rheumatic Fever, Endocarditis, and Kawasaki Disease Committee, Council on Cardiovascular Disease in the Young, and the Council on Clinical Cardiology, Council on Cardiovascular Surgery and Anesthesia, and the Quality of Care and Outcomes Research Interdisciplinary Working Group. *Circulation.* 2007;116:1736–1754.
46. Eloubeidi MA, Tamhane A, Varadarajulu S, et al. Frequency of major complications after EUS-guided FNA of solid pancreatic masses: a prospective evaluation. *Gastrointest Endosc.* 2006;63:622–629.
47. Wiersema MJ, Vilimann P, Giovannini M, et al. Endosonography-guided fine-needle aspiration biopsy: diagnostic accuracy and complication assessment. *Gastroenterology.* 1997;112:1087–1095.
48. Guarner-Argente C, Shah P, Buchner A, et al. Use of antimicrobials for EUS-guided FNA of pancreatic cysts: a retrospective, comparative analysis. *Gastrointest Endosc.* 2011;74:81–86.
49. Lee LS, Saltzman JR, Bounds BC, et al. EUS-guided fine needle aspiration of pancreatic cysts: a retrospective analysis of complications and their predictors. *Clin Gastroenterol Hepatol.* 2005;3:231–236.
50. Diehl DL, Cheruvattath R, Facktor MA, et al. Infection after endoscopic ultrasound-guided aspiration of mediastinal cysts. *Interact Cardiovasc Thorac Surg.* 2010;10:338–340.
51. O'Toole D, Palazzo L, Arotcarena R, et al. Assessment of complications of EUS-guided fine-needle aspiration. *Gastrointest Endosc.* 2001;53:470–474.
52. Cotton PB, Eisen GM, Aabakken L, et al. A lexicon for endoscopic adverse events: report of an ASGE workshop. *Gastrointest Endosc.* 2010;71:446–454.
53. Das A, Sivak Jr MV, Chak A. Cervical esophageal perforation during EUS: a national survey. *Gastrointest Endosc.* 2001;53:599–602.
54. Eloubeidi MA, Tamhane A, Lopes TL, et al. Cervical esophageal perforations at the time of endoscopic ultrasound: a prospective evaluation of frequency, outcomes, and patient management. *Am J Gastroenterol.* 2009;104:53–56.
55. Pfau PR, Ginsberg GG, Lew RJ, et al. Esophageal dilation for endosonographic evaluation of malignant esophageal strictures is safe and effective. *Am J Gastroenterol.* 2000;95:2813–2815.
56. Wallace MB, Hawes RH, Sahai AV, et al. Dilation of malignant esophageal stenosis to allow EUS guided fine-needle aspiration: safety and effect on patient management. *Gastrointest Endosc.* 2000;51:309–313.
57. Liberman M, Hanna N, Duranteau A, et al. Endobronchial ultrasonography added to endoscopic ultrasonography improves staging in esophageal cancer. *Ann Thorac Surg.* 2013;96:232–236; discussion 236–238.
58. Affi A, Vazquez-Sequeiros E, Norton ID, et al. Acute extraluminal hemorrhage associated with EUS-guided fine needle aspiration: frequency and clinical significance. *Gastrointest Endosc.* 2001;53:221–225.
59. Varadarajulu S, Eloubeidi MA. Frequency and significance of acute intracystic hemorrhage during EUS-FNA of cystic lesions of the pancreas. *Gastrointest Endosc.* 2004;60:631–635.
60. Williams DB, Sahai AV, Aabakken L, et al. Endoscopic ultrasound guided fine needle aspiration biopsy: a large single centre experience. *Gut.* 1999;44:720–726.
61. Eloubeidi MA, Chen VK, Eltoum IA, et al. Endoscopic ultrasound-guided fine needle aspiration biopsy of patients with suspected pancreatic cancer: diagnostic accuracy and acute and 30-day complications. *Am J Gastroenterol.* 2003;98:2663–2668.
62. Eloubeidi MA, Gress FG, Savides TJ, et al. Acute pancreatitis after EUS-guided FNA of solid pancreatic masses: a pooled analysis from EUS centers in the United States. *Gastrointest Endosc.* 2004;60:385–389.
63. Gress F, Michael H, Gelrud D, et al. EUS-guided fine-needle aspiration of the pancreas: evaluation of pancreatitis as a complication. *Gastrointest Endosc.* 2002;56:864–867.
64. Lai R, Stanley MW, Bardales R, et al. Endoscopic ultrasound-guided pancreatic duct aspiration: diagnostic yield and safety. *Endoscopy.* 2002;34:715–720.
65. Heimbach JK, Sanchez W, Rosen CB, et al. Trans-peritoneal fine needle aspiration biopsy of hilar cholangiocarcinoma is associated with disease dissemination. *HPB (Oxford).* 2011;13:356–360.
66. Jacobson BC, Waxman I, Parmar K, et al. Endoscopic ultrasound-guided gallbladder bile aspiration in idiopathic pancreatitis carries a significant risk of bile peritonitis. *Pancreatology.* 2002;2:26–29.
67. Jacobson BC, Pitman MB, Brugge WR. EUS-guided FNA for the diagnosis of gallbladder masses. *Gastrointest Endosc.* 2003;57:251–254.
68. Meara RS, Jhalia D, Eloubeidi MA, et al. Endoscopic ultrasound-guided FNA biopsy of bile duct and gallbladder: analysis of 53 cases. *Cytopathology.* 2006;17:42–49.
69. Fujii L, Clain JE, Morris JM, et al. Anterior spinal cord infarction with permanent paralysis following endoscopic ultrasound celiac plexus neurolysis. *Endoscopy.* 2012;44(suppl 2 UCTN):E265–E266.
70. Loeve US, Mortensen MB. Lethal necrosis and perforation of the stomach and the aorta after multiple EUS-guided celiac plexus neurolysis procedures in a patient with chronic pancreatitis. *Gastrointest Endosc.* 2013;77:151–152.
71. Bang JY, Hasan M, Navaneethan U, et al. Lumen-apposing metal stents (LAMS) for pancreatic fluid collection (PFC) drainage: may not be business as usual. *Gut.* 2017;66:2054–2056.
72. Park DH, Jang JW, Lee SS, et al. EUS-guided biliary drainage with transluminal stenting after failed ERCP: predictors of adverse events and long-term results. *Gastrointest Endosc.* 2011;74:1276–1284.
73. Oh HC, Seo DW, Kim SC. Portal vein thrombosis after EUS-guided pancreatic cyst ablation. *Dig Dis Sci.* 2012;57:1965–1967.

# 5

# New Techniques in EUS: Real-Time Elastography, Contrast-Enhanced EUS, and Fusion Imaging

ADRIAN SĂFTOIU AND PETER VILMANN

## KEY POINTS

- Endoscopic ultrasound (EUS) has improved considerably in the past years through development of real-time EUS elastography, contrast-enhanced EUS and fusion EUS imaging.
- Real-time EUS elastography provides qualitative and semi-quantitative data about tissue stiffness, possibly allowing differentiation of benign and malignant tumors.
- Contrast-enhanced harmonic EUS using specific software (with low mechanical index capabilities) is already established as a procedure useful for the differential diagnosis of focal pancreatic masses.
- Fusion EUS imaging represents a combination of EUS and computed tomography/magnetic resonance imaging (CT/ MRI), which is still under development, with the aim of decreasing the difficult learning curve of EUS, but also increasing diagnostic confidence and better orientation of multiple target lesions.

Endoscopic ultrasound (EUS) represents a high-resolution imaging technique used mainly for the diagnosis and staging of digestive cancers situated in the vicinity of the gastrointestinal (GI) tract. The method is increasingly used in medical centers around the world due to a significant clinical impact, especially after the addition of EUS-guided fine-needle aspiration (EUS FNA), which is able to confirm a tissue diagnosis of malignancy. Due to the increased resolution of EUS technology, even as compared to other cross-sectional imaging methods (such as computed tomography [CT] or magnetic resonance imaging [MRI]), several other methods were further developed to extend its capabilities, including real-time EUS elastography, contrast-enhanced EUS, and fusion imaging.<sup>1,2</sup>

## Real-Time Endoscopic Ultrasound Elastography

Elasticity imaging has been reported useful for the characterization and differentiation of benign and malignant tissues due to

the inherent differences in the hardness of tissues. Thus, malignant tumors are usually stiffer as compared with benign masses, whereas the strain information induced by small tissue deformations can be computed and displayed in real time. Initial clinical applications included breast<sup>3–6</sup> and prostate cancer,<sup>6–10</sup> as well as lymph nodes,<sup>11–15</sup> thyroid masses,<sup>16–19</sup> or focal liver lesions.<sup>20</sup> Recently, real-time elastography was extensively used to characterize liver fibrosis in chronic liver diseases, including chronic hepatitis B or C, and also liver cirrhosis.<sup>21–24</sup> The technique has the distinct advantage that it can be used with various ultrasound transducers, thus extending the method to virtually all organs. The method has been successfully applied with intraoperative<sup>25,26</sup> or intracavitary<sup>27</sup> transducers, as well as EUS probes.

## Technical Details

Real-time sonoelastography represents a certain technical improvement over gray-scale ultrasound, allowing the estimation of tissue strain, during slight compressions induced by transducer or small heart/vessel movements.<sup>28</sup> The method works in real time in a similar manner as color Doppler, the strain information being visually converted into a hue color scale and displayed as a transparent overlay imposed on the gray-scale ultrasound information.<sup>29,30</sup> The principle of real-time elastography consists of measurement of tissue displacement induced by small compressions, which are inducing strain that is usually smaller in harder tissues as compared to soft tissues (Fig. 5.1). A complex algorithm called combined autocorrelation method allows the calculation of axial strain along the direction of ultrasound waves, which also corresponds to the direction of compressions.<sup>28</sup> Consequently, soft tissues are easy to compress being displayed in low-hue values approaching green, whereas hard tissues are difficult to strain, thus being displayed in high-hue values approaching blue. The information can be further quantified by taking into consideration a numerical hue scale from 0 to 255. Both the basic principles, as well as the clinical applications for the usage of ultrasound elastography, are carefully reviewed in two comprehensive guidelines and recommendations issued by the European Federation Societies in Ultrasound in Medicine and Biology (EFSUMB).<sup>31,32</sup>

EUS elastography equipment includes a state-of-the-art ultrasound system with real-time sonoelastography capabilities, coupled with conventional endoscopic radial or linear EUS transducers. The usual setting includes a two-panel EUS image, with the conventional gray-scale (B-mode) image on the right panel and the transparent overlay elastography image on the left side (Fig. 5.2). The elastography region of interest is trapezoidal in shape and can be freely selected to encompass at least half of the examined targeted lesion, as well as the surrounding tissues. Tissue elasticity values are represented in a hue color scale, with values from 0 to 255. Consequently, the color information can be semi-quantified as average values, whereas all the necessary statistical data (average strain histograms and standard deviation) can be easily calculated by using the latest versions of software (Figs. 5.3 to 5.5). The system also includes the possibility of calculation of strain ratio (i.e., an estimation of the modulus ratio between two user-defined areas of interest), thus representing a semi-quantitative evaluation of strain differences between the areas.<sup>33</sup> However, it should be taken into consideration that changing the reference area to a deeper position significantly influences strain ratio measurements,

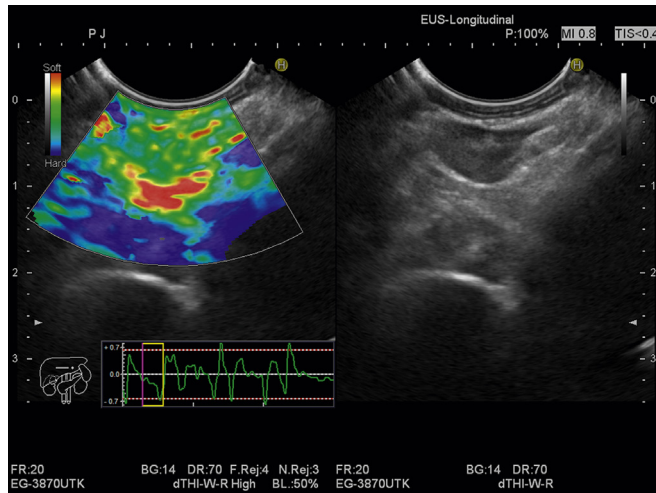


**Fig. 5.1** Benign mediastinal lymph node. Endoscopic ultrasound elastography showing a relatively homogeneous mixture of green and yellow, indicating a relatively soft structure as compared to the surrounding tissues (left).

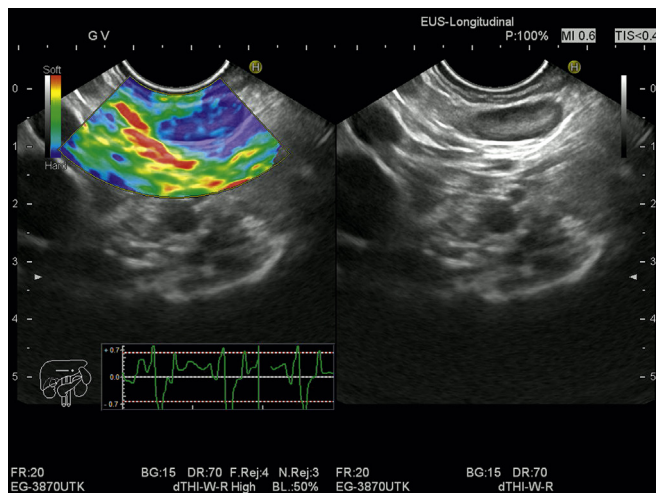


**Fig. 5.2** Malignant mediastinal lymph node. Endoscopic ultrasound elastography showing a relatively homogeneous mixture of blue, indicating a relatively hard structure as compared to the surrounding tissues (left).

which are otherwise independent of the size and other parameters (for example, the elastography dynamic range). It is not yet clear if the usage of strain ratios or strain histograms should be the preferred method, while further studies will be necessary to show the differences between various methodologies.<sup>34</sup>

## Clinical Applications

Real-time EUS elastography was initially reported to be useful in a pilot study, which included a low number of patients with focal pancreatic masses ( $n = 24$ ) and lymph nodes ( $n = 25$ ).<sup>35</sup> A high sensitivity of 100% but a low specificity of 67% and 50% for pancreatic masses and lymph nodes, respectively, determined criticism of the study methodology, including qualitative pattern evaluation and establishment of diagnostic criteria in the same group of

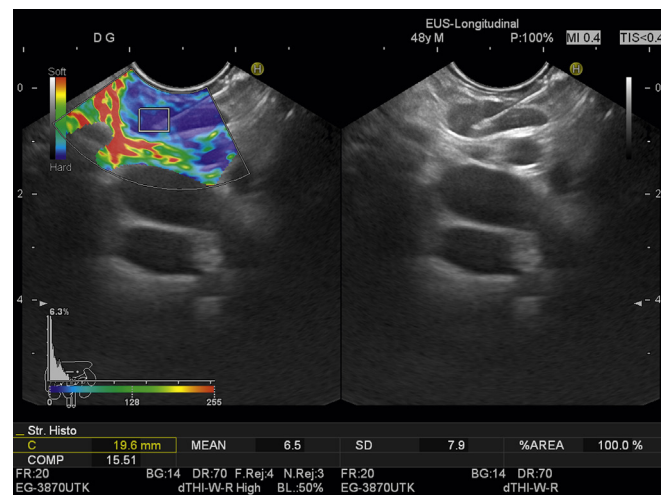


**Fig. 5.3** Malignant mediastinal lymph node. Endoscopic ultrasound elastography with EUS-guided FNA showing a relatively hard (blue) homogeneous lymph node (left). A smaller rectangular region of interest is selected at the level of the lymph node and a hue histogram can be displayed, showing low mean elasticity (strain) values.

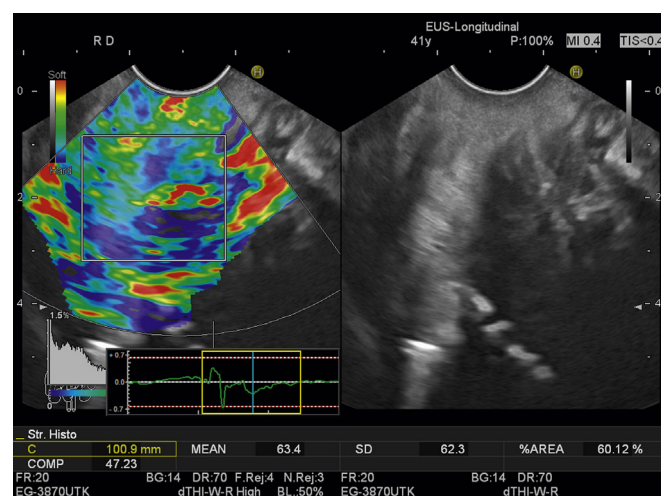


**Fig. 5.4** Chronic pseudotumoral pancreatitis. Endoscopic ultrasound elastography showing a relatively heterogeneous mixture of blue, green, and red, indicating a relatively intermediate elasticity structure as compared to the surrounding tissues (left). Hue histogram analysis can be also performed to obtain semiquantitative data on the elasticity of the focal mass (mean 63.4, SD 62.3).

patients. The study was, however, continued with a multicenter trial that analyzed 222 patients with focal pancreatic masses ( $n = 121$ ) and lymph nodes ( $n = 101$ ), accompanied by interobserver variability data that indicated good values of the  $\kappa$  coefficient of 0.785 for pancreatic masses and 0.657 for lymph nodes.<sup>36</sup> EUS elastography was proven to have higher sensitivity and specificity values as compared with conventional gray-scale EUS images of 92.3% and 80.0% for the differential diagnosis of focal pancreatic masses and of 91.8% and 82.5% for the differential diagnosis of lymph nodes. Based on the published data, EUS elastography was thus suggested to be superior as compared with conventional B-mode (gray-scale) imaging that might be utilized in patients with pancreatic masses and negative EUS FNA and also to increase the yield of EUS FNA for patients with multiple lymph nodes.<sup>37</sup> Moreover, several prospective studies using qualitative or quantitative criteria were subsequently published and supported the value of real-time EUS elastography in larger patient subgroups and multicenter trial designs (Tables 5.1 and 5.2).

### Lymph Nodes

An initial feasibility study that aimed to establish the value of EUS elastography for the differential diagnosis of lymph nodes was based on qualitative pattern analysis of 42 cervical, mediastinal, or abdominal lymph nodes, taking into consideration five characteristic patterns previously described for breast lesions, which allowed the establishment of a provisional diagnosis of benign (see Fig. 5.1, Video 5.1) or malignant (Fig. 5.2, Video 5.2) lymph nodes.<sup>38</sup> Sensitivity, specificity, and accuracy for the qualitative pattern analysis were 91.7%, 94.4%, and 92.86%, respectively, with an area under receiver operating characteristic (AUROC) curve of 0.949. Several limitations of the method were acknowledged, including selection bias of the best EUS images, chosen arbitrarily by the examiner from a longer EUS elastography video. Similar results were obtained by another group that analyzed 66 mediastinal lymph nodes based on the same qualitative analysis of color patterns.<sup>39</sup> The accuracy was variable for three examiners, between 81.8% and 87.9% for benign lymph nodes and between 84.6% and 86.4% for malignant lymph nodes, with an excellent interobserver analysis ( $\kappa = 0.84$ ).

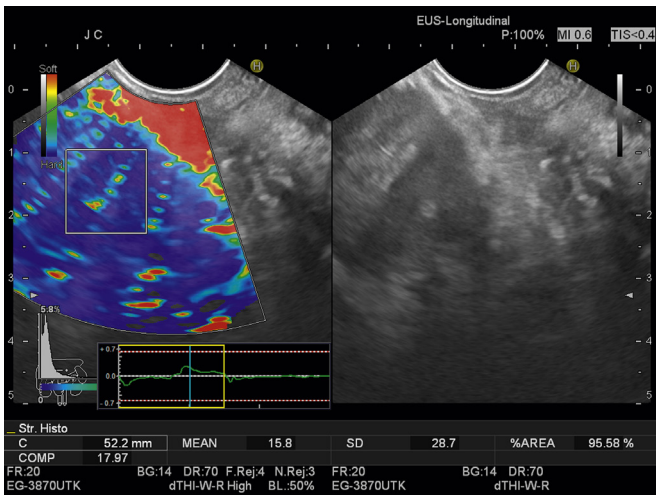


**Fig. 5.5** Pancreatic adenocarcinoma. Endoscopic ultrasound elastography showing a relatively homogeneous hard (blue) mass, indicating a relatively hard elasticity structure as compared to the surrounding tissues (left). Hue histogram analysis can be also performed to obtain semiquantitative data on the elasticity of the focal mass (mean 15.8, SD 28.7).

A recent qualitative study also analyzed the role of elastography for prediction of lymph node malignancy. Thus, consideration of different scores for the differential diagnosis indicated a sensitivity of 79.3% and specificity of 100%.<sup>40</sup> For the patients with esophageal cancer only, the sensitivity and specificity of EUS elastography were 91.2% and 94.5%, respectively, significantly higher than the values of conventional B-mode EUS examinations.<sup>41</sup>

Another prospective study was designed to test the accuracy of computer-enhanced dynamic analysis of EUS elastography movies for the differential diagnosis between benign and malignant lymph nodes.<sup>42</sup> A total number of 78 lymph nodes were included, and average hue histograms were calculated for each EUS elastography video in order to better describe the elasticity of each lymph node according to calculations based on the hue scale of the ultrasound system. The ROC analysis for the average hue histogram values inside lymph nodes yielded an AUROC of 0.928 for the differential diagnosis, with a sensitivity, specificity, and accuracy of 85.4%, 91.9%, and 88.5%, respectively, based on a cutoff level situated in the middle of the green-blue rainbow scale. The study also reported a high positive predictive value (PPV) of 92.1% and a high negative predictive value (NPV) of 85%, implying that the most probable malignant lymph nodes could be targeted by EUS FNA (see Fig. 5.3), whereas EUS FNA could be avoided in the lymph nodes that are considered most probably benign.

Another group looked at the intraobserver and interobserver agreement of EUS elastography, including the values of strain ratios, for the differential diagnosis of benign and malignant lymph nodes.<sup>43</sup> Both elastography and elastography strain ratio evaluations of lymph nodes were feasible and had a good interobserver agreement of 0.58 and 0.59 (based on a cutoff of 3.81 for the strain ratio), respectively. The same group further looked at EUS elastography and elastography strain ratios based on histology results after marking of lymph nodes with EUS FNA.<sup>37</sup>

**TABLE 5.1** Sensitivity and Specificity of Endoscopic Ultrasound Elastography for the Differential Diagnoses of Lymph Nodes

Reference	Number of Lymph Nodes	Sensitivity (%)	Specificity (%)
Giovannini and coworkers <sup>35</sup>	25	100	50
Săftoiu and coworkers <sup>38</sup>	42	91.7	94.4
Janssen and coworkers <sup>39</sup>	66	87.9	86.4
Săftoiu and coworkers <sup>42</sup>	78	85.4	91.9
Giovannini and coworkers <sup>36</sup>	101	91.8	82.5
Larsen and coworkers <sup>37</sup>	56	55	82
Okasha and coworkers <sup>40</sup>	88	79.3	100
Sazuka and coworkers <sup>41</sup>	115	91.2	94.5

**TABLE 5.2** Sensitivity and Specificity of Endoscopic Ultrasound Elastography for the Differential Diagnoses of Focal Pancreatic Masses

Reference	Number of Patients	Sensitivity (%)	Specificity (%)
Giovannini and coworkers <sup>35</sup>	24	100	67
Hirche and coworkers <sup>46</sup>	70	41	53
Săftoiu and coworkers <sup>47</sup>	43	93.8	63.6
Giovannini and coworkers <sup>36</sup>	121	92.3	80.0
Iglesias-Garcia and coworkers <sup>48</sup>	130	100	85.5
Iglesias-Garcia and coworkers <sup>49</sup>	86	100	92.9
Săftoiu and coworkers <sup>52</sup>	54	84.8	76.2
Schrader and coworkers <sup>51</sup>	86	100	100
Săftoiu and coworkers <sup>52</sup>	258	93.4	66.0
Dawwas and coworkers <sup>53</sup>	111	100	16.7
Kongkam and coworkers <sup>54</sup>	38	86.2	66.7
Kim and coworkers <sup>55</sup>	157	95.6	96.3

The sensitivity of EUS was higher than elastography, whereas the specificity was lower as compared to elastography and strain ratios.

A recent meta-analysis that included 368 patients with 431 lymph nodes was also published, indicating a pooled sensitivity of EUS elastography of 88% with a specificity of 85% for the differential diagnosis of benign and malignant lymph nodes.<sup>44</sup> After subgroup analysis with exclusion of outliers, the sensitivity and specificity were 85% and 91%, respectively, leading the authors to conclude that EUS elastography is a valuable noninvasive method used to differentiate benign and malignant lymph nodes.

### Pancreatic Masses

Similar qualitative pattern analysis was used for the visualization and differentiation of pancreatic lesions in a prospective study that included 73 patients: 20 with normal pancreas, 20 with chronic pancreatitis, and 33 with focal pancreatic lesions.<sup>45</sup> Although EUS elastography videos were considered reproducible and could be easily obtained in all the patients included, there was no visible difference between chronic pancreatitis and pancreatic adenocarcinoma. Another study included 70 patients with focal pancreatic masses assessed by qualitative EUS elastography.<sup>46</sup> Again, only 56% of the patients with solid pancreatic lesions had reproducible

elastographic tracings, probably because of an incomplete delineation of large lesions (>35 mm in diameter) or due to the large distance from transducer.

Semi-quantitative analysis based on average hue histograms of the EUS elastography videos showed that the method can be reliably used for the differentiation of normal pancreas, chronic pancreatitis (see Fig. 5.4, Video 5.3), and pancreatic cancer (see Fig. 5.5, Video 5.4).<sup>47</sup> A subgroup analysis performed for the patients with focal pancreatic masses (pseudotumoral chronic pancreatitis and pancreatic cancer) yielded an AUROC of 0.847, with good sensitivity, specificity, and accuracy rates of 93.8%, 63.6%, and 86.1%, respectively. The PPV and NPV were 88.2% and 77.8%, respectively. To increase the accuracy, an artificial neural network (ANN) model was further applied and showed a good testing performance of 90% on average, with a very good stability of the ANN model and an AUROC of 0.965, indicating also a very good classification performance. EUS elastography thus offers complementary information added to the conventional gray-scale information.

Several other studies using various methodologies also tested the value of real-time EUS elastography in the clinical practice. A large, single-center study involving 130 patients used qualitative pattern analysis with four patterns (homogeneous or heterogeneous, predominantly green or blue patterns) to yield a sensitivity, specificity, and accuracy of 100%, 85.5%, and 94%, respectively.<sup>48</sup> Due to the large subjectivity of the method, the same group published a further study with semi-quantitative EUS elastography based on strain ratio, calculated as a quotient between two regions of interest (ROIs): the representative reference area and the focal mass.<sup>49</sup> Based on a total number of 86 consecutive patients with solid focal pancreatic masses, the method was found to be useful with an AUROC of 0.983 and very high sensitivity and specificity of 100% and 92.9%, respectively. Strain ratio measurements were recently used by another group in 109 patients with pancreatic lesions (normal pancreas, chronic pancreatitis, pancreatic cancer, and neuroendocrine tumors).<sup>50</sup> A separate analysis for the red, green, and blue channels achieved a better separation between the groups with normal pancreas and malignant pancreatic lesions, with a high sensitivity and specificity of 100%. Based on quantitative morphometry for pancreatic fibrosis, another group tried to correlate it with pancreatic stiffness but found no relationship.<sup>51</sup> Although important, this study lacked a group of patients with chronic pancreatitis and thus lacked the most significant and difficult cases for differential diagnosis. A combination of contrast-enhanced power Doppler and real-time EUS elastography also yielded good results for the differentiation of focal pancreatic masses, even though the sensitivity, specificity, and accuracy of elastography had lower values of 84.8%, 76.2%, and 81.5%, respectively, as compared to the combined approach.<sup>52</sup> A recent prospective study included 111 semi-quantitative EUS elastography procedures based on strain ratio measurements performed in 104 patients with solid pancreatic masses with the final diagnosis confirmed by pancreatic cytology or histology.<sup>53</sup> The reported areas under the ROC curves for detection of pancreatic malignancy were 0.69 and 0.72 for strain ratio and mass elasticity, respectively, with an overall accuracy of 86.5% and 83.8% (based on cutoffs of 4.65 for strain ratio [SR] and 0.27% for mass elasticity), respectively. In concordance with previous studies, the authors suggested that the modest diagnostic role indicates that EUS elastography could supplement EUS FNA and does not replace tissue sampling. Indeed, a recent study showed that negative results of the combination of EUS FNA and EUS elastography are more reliable to

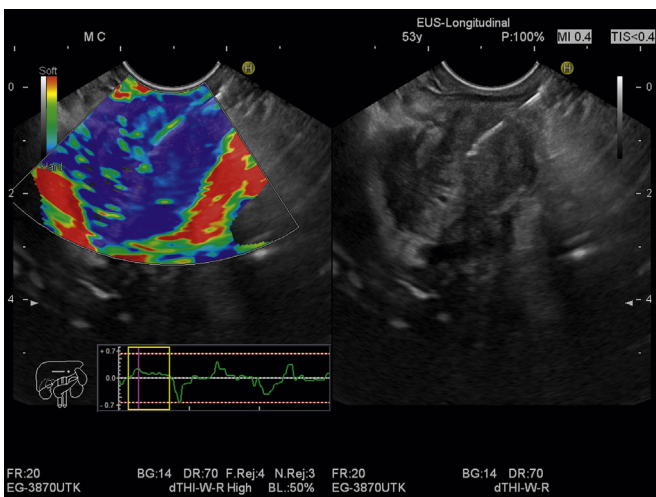


**Fig. 5.6** Pancreatic adenocarcinoma. Endoscopic ultrasound elastography with EUS-guided FNA, showing the same appearance of a relatively homogeneous hard (blue) focal pancreatic mass as compared to the surrounding tissues (left).

exclude malignancy in focal pancreatic masses.<sup>54</sup> Another option is to use two separate cutoffs for the reliable diagnosis of chronic pancreatitis and pancreatic cancer, although there will be a gray zone in between the cutoffs, where diagnosis should still depend on other imaging tests or EUS FNA.<sup>55</sup>

Although EUS elastography brings significant complementary information when added to conventional EUS imaging, the methodology is not yet firmly established, and the choice of either qualitative or semi-quantitative methods of evaluation for EUS elastography images or movies is not yet clear.<sup>34</sup> This explains the significant heterogeneity between the published studies (see Table 5.2) and also the variability of the results encountered for sensitivity, specificity, and accuracy. Nevertheless, a large European, prospective, multicenter trial was performed by the European EUS elastography study group comprising 13 centers and 258 patients.<sup>56,57</sup> Both a qualitative evaluation by two doctors and also a semi-quantitative evaluation by average hue histograms of three separate videos were performed blindly in order to test intraobserver and interobserver variability. For interobserver analysis, qualitative diagnosis of the recorded videos revealed a  $\kappa$  value of 0.72, whereas for intraobserver analysis the single measure intraclass coefficient ranged between 0.86 and 0.94. Based on a cutoff of 175 for the average hue histograms, the sensitivity, specificity, and accuracy were 94.4%, 66.0%, and 85.4%, respectively, with a corresponding AUROC of 0.894. The PPV was 92.5%, whereas the NPV was 68.9%, implying that EUS elastography could be used in cases with a strong suspicion of pancreatic cancer and negative EUS FNA (which represent up to 25% of focal pancreatic masses). Thus the patients with negative EUS FNA and high-hue histogram values ( $>185$ ) might be referred to repeat EUS FNA (Fig. 5.6) or even directly to surgery, whereas those with negative EUS FNA and lower high-hue histogram values ( $<170$ ) could be followed-up.

Four meta-analyses have been published concerning the value of EUS elastography for the differential diagnosis of benign and malignant focal pancreatic masses.<sup>58–61</sup> Besides the fact that the meta-analyses are based on the same original studies included, they all found a high pooled sensitivity (85% to 99%) and lower pooled specificity (64% to 76%). Different values of the AUROC curve (0.8695 to 0.9624) were dependent on the qualitative or semi-quantitative analysis (based on strain ratios or

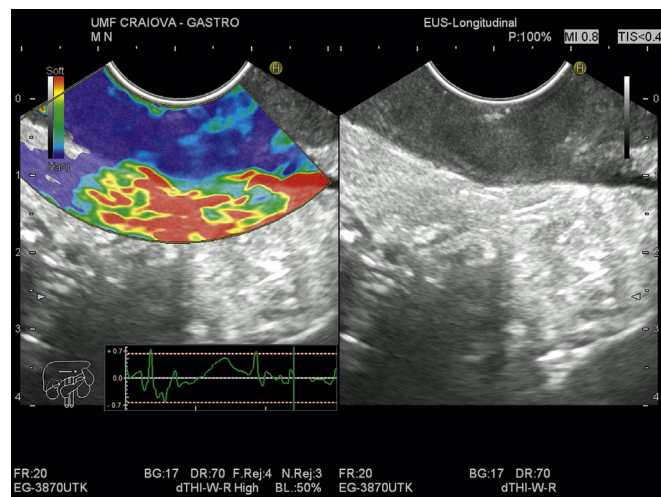


**Fig. 5.7** Gastric adenocarcinoma. Endoscopic ultrasound elastography at the level of the enlarged and invaded gastric wall showing a relatively homogeneous hard (blue) mass, indicating a relatively hard elasticity structure as compared to the surrounding tissues (left).

strain histograms), although there was no significant difference between methods. Consequently, all authors concluded that EUS elastography might bring additional information to EUS FNA for the differential diagnosis of focal pancreatic masses, without being able to exclude EUS FNA for the confirmation of malignancy.

A few recent studies also looked at the utility of EUS elastography for the evaluation of chronic pancreatitis. Thus, there is a linear correlation between the number of EUS criteria of chronic pancreatitis and the strain ratio calculated through EUS elastography, leading to an overall accuracy for the diagnosis of chronic pancreatitis of 91.1%.<sup>62</sup> A similar value was reported for strain histograms obtained with EUS elastography of the pancreatic body, with values over 50 having a high accuracy of 99.3% for the differentiation between chronic pancreatitis and healthy pancreatic tissue in people aged over 60.<sup>63</sup> Moreover, a direct relationship has been shown between the probability of pancreatic exocrine insufficiency (measured by [13] C-mixed triglyceride breath test) and strain ratio based on EUS elastography, reaching 92.8% for strain ratio values higher than 5.5.<sup>64</sup>

### Other Applications

The feasibility of EUS elastography for the characterization of focal liver lesions was reported in only a few papers and case presentations.<sup>65–70</sup> The left liver lobe and part of the right liver lobe can be examined by EUS during staging of other GI tract tumors, with malignant liver masses (especially metastasis) showing a consistent “hard” pattern surrounded by “soft” tissue.

Other indications were proposed for EUS elastography because most of the solid tumors have a “hard” appearance, including esophageal tumors, gastric tumors (Fig. 5.7),<sup>71</sup> gastrointestinal stromal tumors (GISTs) (Fig. 5.8),<sup>72</sup> or adrenal tumors. However, the clinical utility of these findings remains to be established in further studies.

### Future Techniques

Three-dimensional EUS elastography is a feasible technique, implementing either freehand or automatic reconstruction techniques, through use of the usual transducers or high-quality

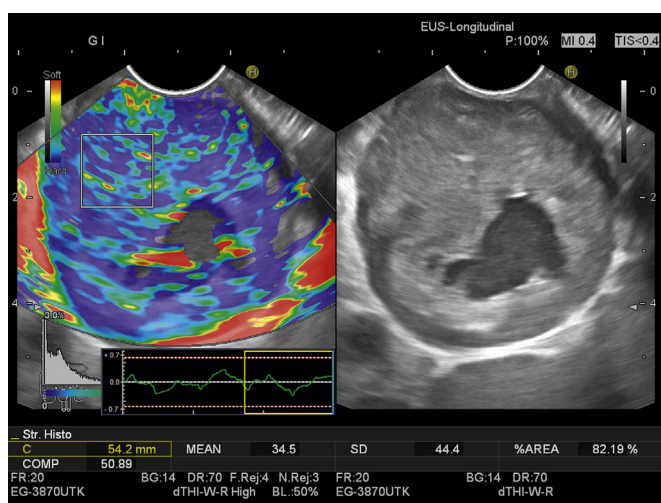


**Fig. 5.8** Malignant gastrointestinal stromal tumor. Endoscopic ultrasound elastography showing a relatively heterogeneous hard (predominantly blue) mass, indicating a relatively hard elasticity structure as compared to the surrounding tissues (left). Areas of necrosis are not displayed by the elastography software.

transducer arrays.<sup>73</sup> The technology is already available in real-time for transabdominal ultrasound (four-dimensional real-time elastography) by using dedicated transducers, thus raising the hope that it will soon be available for EUS, as well. A significant advantage might be conferred during the follow-up of radiofrequency ablation (RFA) lesions, which are extremely difficult to visualize through conventional ultrasound methods.

## Contrast-Enhanced Endoscopic Ultrasound Elastography

This technique was initially established using the usual Doppler techniques (color or power Doppler flow imaging) in combination with administration of second-generation microbubble ultrasound contrast agents (UCAs) as Doppler signal enhancers. Due to recent advances in EUS systems, second-generation intravenous UCAs can now be used in association with low mechanical index (MI) techniques in order to improve visualization of tissue perfusion and to differentiate benign from malignant focal lesions, as well as to guide therapeutic procedures.<sup>74,75</sup> Contrast-enhanced EUS (CE-EUS) has become an established indication for the discrimination of focal pancreatic masses (especially hypoenhancing pancreatic adenocarcinomas as compared to other isoenhancing or hyperenhancing lesions, including mass-forming chronic pancreatitis or neuroendocrine tumors) and possibly for the discrimination of pseudocysts from pancreatic cystic tumors. Furthermore, dynamic quantification of microvascularization and tissue perfusion can be easily performed based on various software programs embedded in the ultrasound systems or available for off-line use with visualization of time-intensity curves (TIC analysis) and calculation of various quantitative variables.<sup>76</sup>

## Technical Details

CE-EUS examinations should be performed in association with a careful evaluation of the lesions through conventional grayscale examinations. There are several techniques used for EUS

examinations based on second-generation microbubble UCAs. Initially, these consisted of Doppler signal enhancement during color Doppler and/or power Doppler, although the usage of these high-MI methods was hampered by the presence of both flash (induced by tissue motion) and blooming (induced by signal saturation) artifacts. Recently, the same specific contrast harmonic imaging techniques used in transabdominal ultrasound (US) have been developed for usage with both radial and linear EUS transducers.<sup>77</sup> Contrast-specific EUS modes are based on separation of linear ultrasound signals induced by the tissues and utilization of the nonlinear response produced by the microbubbles, thus obtaining a better signal (contrast to noise ratio).<sup>78,79</sup>

The most commonly used agent in Europe contains phospholipid-stabilized microbubbles of sulfur hexafluoride (SonoVue), which are injected into a large peripheral vein and able to pass through the lung circulation without being destroyed. This agent is classified as a blood pool agent and is restricted in the intravascular compartment until it is eliminated through expired air. Dosage for EUS examinations should be higher than transabdominal US due to the high frequency of EUS transducers, being usually 4.8 mL of SonoVue.<sup>79</sup> For the pancreas and other GI tract organs (except the liver, which has a dual blood supply), there is an initial early arterial phase (usually 10 to 30 seconds after contrast injection), followed by a late venous phase usually lasting from approximately 30 to 120 seconds.<sup>80</sup>

Further details of the examination techniques are outside the scope of this chapter and are described in detail elsewhere.<sup>72–80</sup> Thus, the examination uses a low MI (usually below 0.3), defined as a standard measure of the acoustic power, that is, the amplitude of an ultrasound wave at peak negative pressure (PNP) estimated in situ, divided by the square root of the center frequency (Fc) of the ultrasound wave. Examinations are based on nondestructive low-MI nonlinear imaging techniques, whereas the MI can be set up to values between 0.08 and 0.12. Relatively higher values are used by most studies (usually between 0.1 and 0.2), but some microbubbles will be destroyed, although the enhancement will be better delineated. The usual method of low-MI ultrasound examination is called dynamic contrast harmonic imaging (dCHI) and uses a wideband pulse inversion technique, including two pulses with inverted phase and received information with addition of the frequency spectrum of the pulses, thus eliminating the linear information from the tissues and showing the harmonic information produced by the microbubbles.

## Clinical Applications

Initial feasibility studies proved the value of CE-EUS, using a technique that is quite similar to contrast-enhanced transabdominal ultrasound. The first pilot study used a linear EUS prototype and low MI (0.09 to 0.25) in conjunction with a second-generation microbubble contrast agent (SonoVue or Sonazoid), allowing the delineation of the arterial and venous phase of the pancreas.<sup>81</sup> The same results were obtained by using a different radial EUS prototype system, showing the real-time continuous images of finely branching vessels of the pancreas, with a slightly higher MI (0.4) and the same second-generation contrast agent (SonoVue).<sup>82</sup>

This opened up the clinical usage of CE-EUS, although some of the contrast agents are still considered off-label indications. Thus, SonoVue is registered in the European Union for liver, breast, and vascular applications, but pancreatic imaging is not mentioned



**Fig. 5.9** Pseudotumoral chronic pancreatitis. Contrast-enhanced color Doppler showing multiple Doppler signals inside the hypervasculat pancreatic mass (*left*), some with arterial-type signal inside proven by pulsed Doppler (*right*).

specifically. Consequently, as mentioned in the current EFSUMB guidelines, an informed consent should be obtained from the patient for the usage of second-generation contrast agents during CE-EUS with examinations of pancreas and GI tract; the examination and safety of the patient are within the responsibility of the examining doctor.<sup>76</sup> A recent (2016) FDA approval has been obtained for LUMASON (sulfur hexafluoride lipid-type A microspheres, known globally as SonoVue) examinations of the liver (and also pediatric examinations), thus paving the way for CE-EUS procedures, as well. However, a specific institutional review board (IRB) approval should be obtained for individual studies.

### Pancreatic Diseases

There are several reports in the literature concerning the usage of CE-EUS for detection, characterization, and assessment of staging and resectability of focal pancreatic masses, using the technique as a one-stop shop for complete analysis of the tumors.<sup>1,2</sup> This is based on the proven hypovascular nature of pancreatic adenocarcinomas in more than 90% of cases, a feature that was reliably and consistently shown by contrast-enhanced CT or angiography. However, none of the cross-sectional techniques (including dynamic contrast-enhanced CT or MR imaging) reaches the high resolution of EUS examinations, which usually allow a confirmation of the final cytologic or micro-histologic diagnosis through EUS FNA.

Initial studies used color Doppler or power Doppler with the addition of the second-generation contrast agent and usage of conventional software, with high-MI values that usually destroy the microbubbles quickly.<sup>83–89</sup> Also, there are certain artifacts (flash or blooming artifacts), usually induced by movement or saturation of the transducer. An initial feasibility study of power Doppler EUS-assessed perfusion by contrast-enhanced power Doppler EUS in 23 patients with inflammatory pseudotumor (Fig. 5.9, Video 5.5) and pancreatic carcinoma (Fig. 5.10, Video 5.6), with a sensitivity and specificity of 94% and 100%, respectively.<sup>83</sup> These results were further confirmed by other authors using the same qualitative approach (Table 5.3). Another study showed the same hypovascular pattern encountered in most of the pancreatic adenocarcinomas, whereas an isovascular or hypervascular pattern was displayed in all other masses (neuroendocrine tumors, serous microcystic adenomas, and even one teratoma). Considering



**Fig. 5.10** Pancreatic adenocarcinoma. Contrast-enhanced power Doppler showing multiple power Doppler signals (collaterals) surrounding the hypovascular pancreatic mass.

hypovascularity as a sign of malignancy in pancreatic tumors led to a sensitivity of 92% and a specificity of 100%.<sup>84</sup> The method is useful in small pancreatic carcinomas (less than 2 cm), with a sensitivity of 83.3%, significantly higher than the sensitivity of contrast-enhanced CT, which was only 50%.<sup>85</sup>

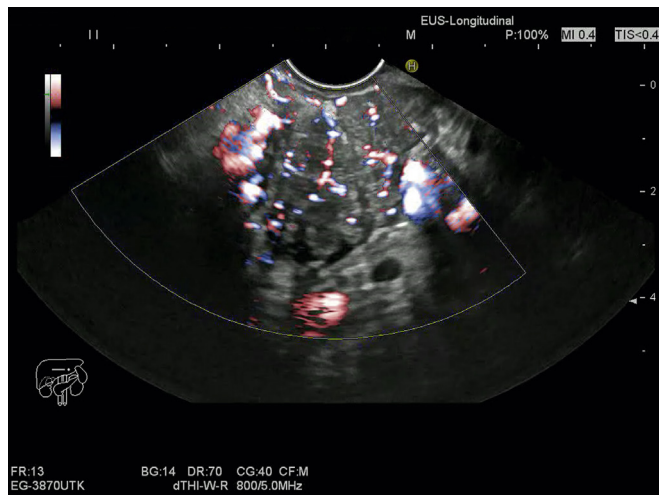
Furthermore, the vascularity index (i.e., the percentage of positive Doppler areas reported to the total area of the focal mass) obtained during the late phase of contrast enhancement, after disappearance of the initial blooming effect induced by contrast injection, is useful for the differential diagnosis of pancreatic adenocarcinoma and pseudotumoral chronic pancreatitis.<sup>86,87</sup> These kinds of quantitative techniques seem more appropriate, despite the artifacts induced by contrast enhancement during color and power Doppler EUS. Vascularity index can also be used in combination with the pulsed Doppler sampling of various vessels inside the pancreatic masses, including calculation of resistivity index (RI) and pulsatility index (PI), with values of the RI over 0.7 being indicative of a malignant lesion.

Moreover, most of the intratumoral vessels in pancreatic adenocarcinomas are arterioles, whereas inflammatory chronic pancreatitis masses have both arterioles and venules, both detectable by pulsed Doppler sampling used during CE-EUS. Using this approach for differentiation between inflammatory masses and pancreatic carcinoma, the sensitivity was improved, reaching 91.1% with an excellent specificity of 93.3%.<sup>86</sup> Lower values were obtained in a subsequent study that used a cutoff value of 20% for the vascularity index, yielding a sensitivity of 90.9% and a specificity of 71.4%.<sup>87</sup> However, contrast-enhanced power Doppler has been combined in the same study with real-time EUS elastography, yielding a sensitivity of 75.8% and a specificity of 95.2% for the differential diagnosis of focal pancreatic masses. The differential diagnosis is complicated by the fact that around 10% of the patients with pancreatic adenocarcinomas have hypervascular tumors, either due to a neuroendocrine differentiation or to the poor differentiation and advanced stage of the tumor. Neuroendocrine tumors can be characterized as hypervascular lesions (Fig. 5.11, Video 5.7), easily visualized by CE-EUS, which has a higher sensitivity of 95.1% in comparison with CT or US and is very useful for the assessment of necrotic or hemorrhagic areas inside the tumors.<sup>88</sup> Autoimmune pancreatitis can be differentiated from pancreatic adenocarcinoma, as both focal and diffuse forms show hyperenhancement during CE-EUS.<sup>89</sup>

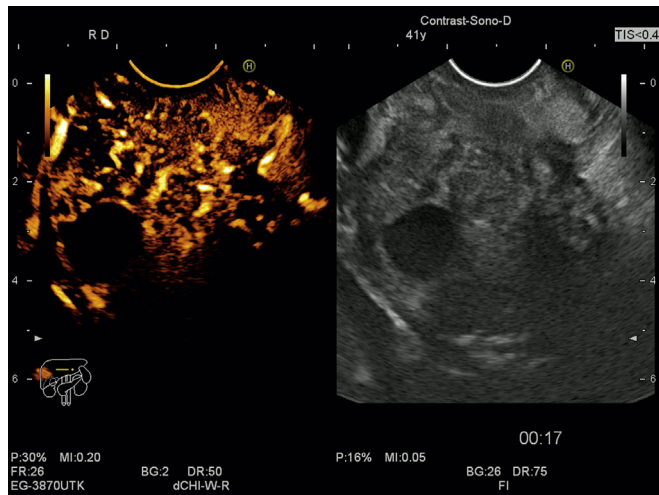
**TABLE 5.3** Sensitivity and Specificity of Contrast-Enhanced Endoscopic Ultrasound for the Differential Diagnoses of Focal Pancreatic Masses

Reference	Number of Patients	Sensitivity (%)	Specificity (%)
<b>High Mechanical Index</b>			
Becker and coworkers <sup>83</sup>	23	94	100
Hocke and coworkers <sup>86</sup>	86	91.1	93.3
Dietrich and coworkers <sup>84</sup>	93	92	100
Sakamoto and coworkers <sup>85</sup>	156	83.3	100
Săftoiu and coworkers <sup>87</sup>	54	90.9	71.4
<b>Low Mechanical Index</b>			
Fusaroli and coworkers <sup>90</sup>	90	96	98
Napoleon and coworkers <sup>91</sup>	35	89	88
Seicean and coworkers <sup>92</sup>	30	80	91.7
Romagnuolo and coworkers <sup>93</sup>	24	100	72.7
Matsubara and coworkers <sup>94</sup>	91	95.8	92.6
Gheonea and coworkers <sup>95</sup>	51	93.8	89.5
Gincul and coworkers <sup>100</sup>	100	96	94
Park and coworkers <sup>101</sup>	90	92	68
Săftoiu and coworkers <sup>102</sup>	167	87.5	92.7
Yamashita and coworkers <sup>104</sup>	147	94	71
Dietrich and coworkers <sup>103</sup>	219	67	86

Low-MI (harmonic) CE-EUS seems to be more advantageous, although the currently published data is still limited (see Table 5.3). The technique, which is significantly superior to transabdominal US techniques, allows the assessment of microvessel architecture when hampered by the presence of bowel air or obesity, which induce significant artifacts and impede a good visualization of the pancreas.<sup>76</sup> After the initial pilot studies<sup>90,91</sup> and the appearance of commercial EUS systems with low-MI (harmonic) CE-EUS availability, several articles described the technique and the results in focal pancreatic masses, including pseudotumoral chronic pancreatitis (Fig. 5.12, Video 5.8), pancreatic adenocarcinoma (Fig. 5.13, Video 5.9), and neuroendocrine tumors (Fig. 5.14,



• **Fig. 5.11** Malignant neuroendocrine tumor. Contrast-enhanced power Doppler showing multiple power Doppler signals inside the hypervascular pancreatic mass.



• **Fig. 5.12** Pseudotumoral chronic pancreatitis. Low mechanical index contrast-enhanced endoscopic ultrasound showing intense uptake of the contrast in the arterial phase, with a small (avascular) pseudocyst at the level of the pancreatic mass (*left*).

**Video 5.10.** The initial studies varied in methodology (e.g., with variable MI settings from 0.08 to 0.4, as well as various qualitative or quantitative methods for signal processing). In the presence of hypoenhancing masses, the sensitivity and specificity reached 96% and 98%, respectively, for the diagnosis of pancreatic adenocarcinoma, and CE-EUS allowed the detection of small lesions that could not be visualized during conventional EUS due to the presence of biliary stents or chronic pancreatitis.<sup>90</sup> The sensitivity and specificity had lower values in another study that analyzed qualitatively the pancreatic microcirculation in 35 patients, being 89% and 88%, respectively.<sup>91</sup> Although these values were not improved by quantitative analysis, a more objective way for reporting the results of the CE-EUS procedures might be based on histograms and index of contrast uptake, methods that yielded a sensitivity and specificity of 80% and 91.7%, respectively.<sup>92</sup> A small study also tested the feasibility of another second-generation perflutren lipid microsphere contrast agent with good sensitivity and specificity of 100% and 72.7%, respectively, although it was based on a limited number of patients.<sup>93</sup> Recently, another group described

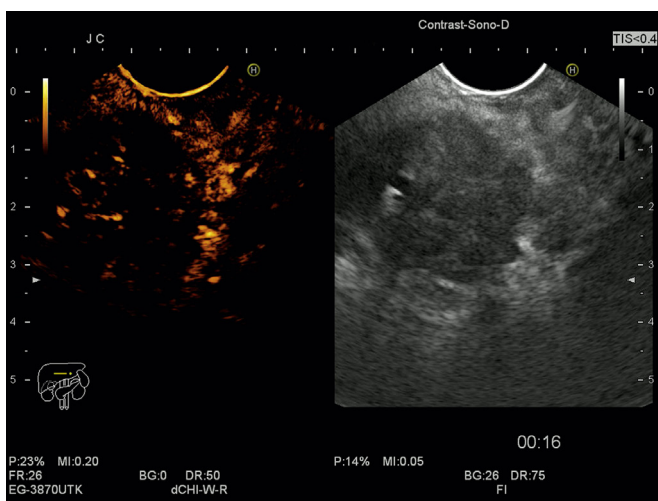


**Fig. 5.13** Pancreatic adenocarcinoma. Low mechanical index contrast-enhanced endoscopic ultrasound showing discrete uptake of the contrast in the arterial phase at the level of the hypovascular pancreatic mass, in comparison with the neighboring pancreatic parenchyma (left).

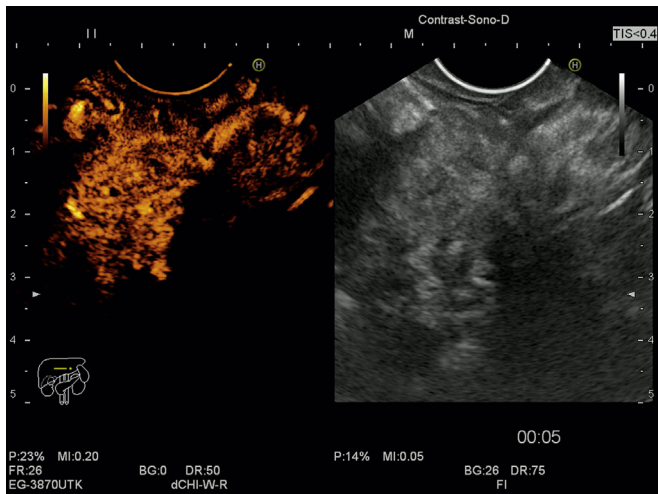


**Fig. 5.14** Malignant neuroendocrine tumor. Low mechanical index contrast-enhanced endoscopic ultrasound showing intense uptake of the contrast in the arterial phase, at the level of the focal pancreatic mass (left).

a dynamic quantitative analysis of CE-EUS for the diagnosis of pancreatic diseases, reaching high values of sensitivity and specificity of 95.8% and 92.6%, respectively, through the use of TIC analysis based on 91 patients with focal pancreatic masses, including 48 patients with pancreatic adenocarcinoma, 14 patients with autoimmune pancreatitis, 13 patients with mass-forming pancreatitis, and 16 patients with pancreatic neuroendocrine tumors.<sup>94</sup> This was also reported by a study published by our group based on quantitative low-MI CE-EUS used for the differential diagnosis of chronic pseudotumoral pancreatitis and pancreatic cancer, which showed a sensitivity and specificity of 93.75% and 89.47%, respectively.

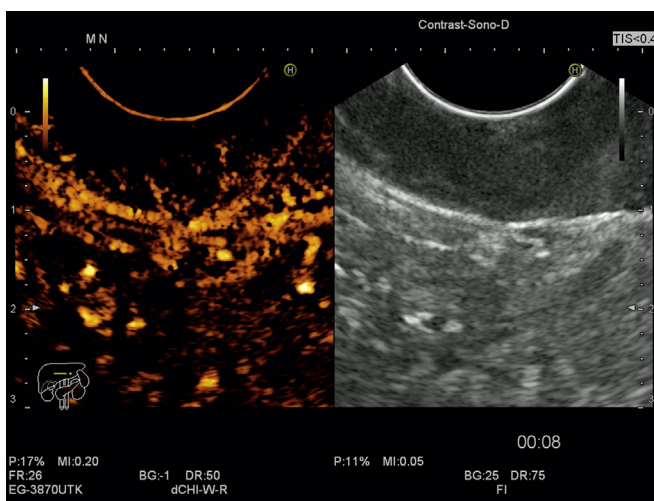
There has been a significant improvement in the software options needed for quantification of perfusion inside focal masses based on TIC analysis with wash-in and wash-out times after bolus injection of contrast performed through curve fitting by computer-enhanced algorithms.<sup>76</sup> Several parameters proportional to the tissue blood flow can be determined (like the peak intensity, area under the curve, time to peak intensity, slope of

the wash-in, and mean transit time), which might considerably improve the characterization and follow-up of the patients.<sup>96</sup> Moreover, new software, which is independent of the ultrasound system and user variables, has automatic motion compensation, allowing for a more standardized quantification process through linearization of the Digital Imaging and Communications in Medicine (DICOM) clips during off-line analysis of the CE-EUS video clips.<sup>97</sup>

Based on initial studies, a meta-analysis including 12 studies and 1139 patients showed clearly that pooled sensitivity of CE-EUS for the differential diagnosis of pancreatic adenocarcinomas was 0.94, with a specificity of 0.89.<sup>98</sup> Furthermore, the AUROC curve was 0.9732. Both studies based on enhanced color/power Doppler and harmonic EUS consistently showed that visualization of a hypoenhanced pancreatic lesion was an accurate predictor of pancreatic adenocarcinoma. Another recent meta-analysis included both studies using contrast-enhanced ultrasound (23 studies) and contrast-enhanced endoscopic ultrasound (4 studies), indicating a pooled sensitivity of 0.89 and specificity of 0.84.<sup>99</sup>

A prospective multicentric trial using qualitative CEH-EUS evaluation of solid pancreatic masses yielded high values of the sensitivity and specificity of 96% and 94%, for the differential diagnosis of focal pancreatic masses, with all negative EUS FNA cases classified correctly by CEH-EUS.<sup>100</sup> Besides showing hypovascularity in both the arterial and venous phases, the method thus seems to be useful for evaluation of patients with negative or insufficient EUS FNA samples.<sup>100,101</sup> A larger prospective multicentric study has confirmed the results of the initial studies, by including 167 consecutive patients with chronic pancreatitis or pancreatic cancer. The authors used dynamic contrast-enhanced harmonic EUS based on TIC analysis and found an 87.5% and 92.7% sensitivity and specificity, respectively. The most useful parameter for the differential diagnosis was the peak enhancement. Moreover, the use of automated ANN analysis further improved the sensitivity and specificity to 94.6% and 94.4%.<sup>102</sup> This has been proven also in small pancreatic solid lesions (less than 15 mm), where contrast-enhanced ultrasound or EUS allowed the differential diagnosis of pancreatic ductal adenocarcinoma.<sup>103</sup>

Furthermore, there is a clear correlation between the hypovascularity depicted by early arterial phase contrast-enhanced imaging, which correlates with the degree of fibrosis and necrosis, as well as the lower number of vessels.<sup>104</sup> This led to the concept of targeting of the EUS FNA based on contrast-enhanced examinations.<sup>105</sup> Thus, the percentage of adequate biopsies in the contrast-harmonic EUS group was shown to be higher as compared with the EUS group.<sup>106</sup> Another approach has been used with an initial EUS FNA, followed by contrast-enhanced harmonic EUS and a second contrast-guided EUS FNA. This led to an increase in accuracy of EUS FNA from 78.4% to 94%, indicating that qualitative assessment of the contrast uptake within the lesion could be useful for the patients with false negative EUS FNA.<sup>107</sup> A retrospective study also showed that contrast-enhanced harmonic EUS FNA decreases the number of passes required to establish diagnosis, with a sufficient sample obtained in one needle pass in 60% of cases, as compared to 25% for the conventional EUS FNA.<sup>108</sup> Moreover, the sequential usage of EUS elastography followed by contrast-enhanced EUS is extremely useful for the patients with negative EUS FNA, as it allows the selection of either benign or malignant focal pancreatic masses with 100% specificity, visualized as soft hypervascular masses or hard hypovascular masses.<sup>109</sup>

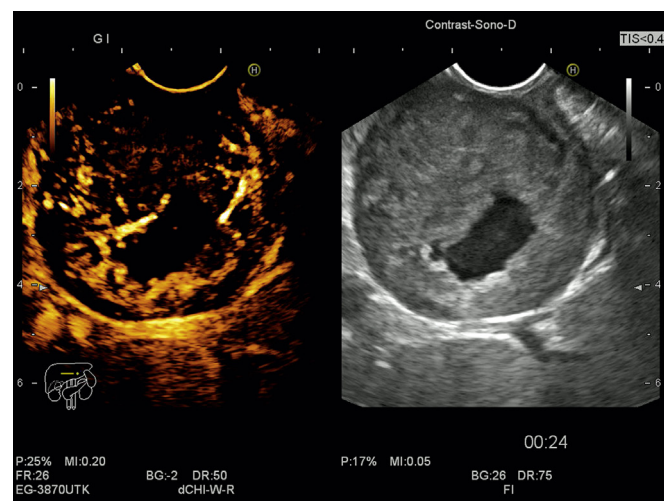


• **Fig. 5.15** Gastric adenocarcinoma. Low mechanical index contrast-enhanced endoscopic ultrasound showing uptake of the contrast in the arterial phase, at the periphery of the gastric tumor (*left*).

Contrast-enhanced EUS has been used recently for cystic pancreatic masses, for evaluation of mural nodules, but also for the differential diagnosis between benign and malignant pancreatic cystic lesions. Thus, the difference between clots and mural nodules is based on the visualization of blood flow inside, leading to a classification of several types (low papillary nodule, polypoid nodule, papillary nodule, and invasive nodule). Presence of type 3 and 4 mural nodules was associated with malignant intraductal papillary mucinous neoplasms (IPMN), with a sensitivity and specificity of 60% and 92.9%, respectively.<sup>110</sup> A small study also confirmed that clots have no vascularity, and mural nodules have vascularity depicted by contrast-enhanced EUS, with a sensitivity and specificity of 100% and 80%.<sup>111</sup> Evaluation by CEH-EUS is useful for the differential diagnosis of benign and malignant branch-duct IPMN, by measuring the height of mural nodules, with a significantly improved accuracy, reaching 98%.<sup>112</sup> Quantification based on TIC analysis showed a higher relative intensity at the level of mural nodules as compared with pancreatic parenchyma, for nodules with high grade dysplasia/invasive carcinoma, with a linear correlation between the contrast intensity and microvessel density.<sup>113</sup> Although more studies will be necessary to clarify the role of contrast-enhanced EUS for the differential diagnosis of cystic pancreatic lesions, the technique is clearly valuable for guiding EUS FNA in hyperenhanced areas as opposed to nonenhanced areas composed of debris or mucus.<sup>114</sup>

### Other Applications

Although EUS is useful for staging of GI tract cancer (esophageal, gastric, and colorectal), the usage of CE-EUS is not yet established clinically for these patients. Initial studies proved that CE-EUS improves the overall accuracy for assessment of depth of invasion of GI tract cancer,<sup>115</sup> as well as a better visualization of the microvasculature and follow-up during treatment (Fig. 5.15, Video 5.11). A recent study of gastric adenocarcinoma patients assessed the correlations between contrast-enhanced power Doppler EUS and the values of angiogenesis markers, showing that postcontrast values of vascularity index were correlated with intratumoral microvascular density assessed by CD34 immunohistochemical analysis, as well as with the values of vascular endothelial growth factor (VEGF) assessed by real-time polymerase chain reaction (RT-PCR).<sup>116</sup>



• **Fig. 5.16** Gastrointestinal stromal tumor. Low mechanical index contrast-enhanced endoscopic ultrasound showing increased uptake of the contrast in the arterial phase, with a central zone of necrosis (*left*).

A small study indicated that CE-EUS can be used to differentiate GISTS from other benign tumors (lipoma or leiomyoma) based on the hyperenhanced appearance of GISTS.<sup>117</sup> Contrast-enhanced EUS has recently been used for the assessment of tumor vascularity in order to predict the preoperative malignancy risk of GISTS through identification of irregular vessels (Fig. 5.16, Video 5.12).<sup>118</sup> The sensitivity, specificity, and accuracy for identification of irregular vessels and thus prediction of malignancy was 100%, 63%, and 83%, respectively, being comparable to EUS-guided FNA, which had similar figures of 63%, 92%, and 81%, respectively. Another study also confirmed the correlation between the presence of intratumoral vessels visualized by CE-EUS and higher degrees of angiogenesis identified through immunohistochemical analysis of VEGF.<sup>119</sup> A multicentric trial including 62 subepithelial lesions, comprising GISTS and leiomyomas, showed that hyperenhancement during the arterial phase of contrast-enhanced EUS has a sensitivity and specificity of 98% and 100% for the diagnosis of GIST, with necrotic avascular areas depicted in 88% of the GIST patients, as opposed to leiomyoma.<sup>120</sup>

Microvascularity of intraabdominal lesions can be easily depicted by CE-EUS, the method being useful for differentiation of benign and malignant lesions.<sup>121</sup> This has been tested in 43 patients with indeterminate abdominal lesions, reaching a high interobserver agreement of 0.953. The sensitivity, specificity, and accuracy for the differential diagnosis of benign and malignant lesions were very high, being equal to 96.3%, 100%, and 97.6%, respectively. The combination of color Doppler and CEH-EUS can be safely used in visceral vascular diseases for evaluation of the splanchnic vessels.<sup>122</sup>

### Future Techniques

Three-dimensional EUS has been described previously in order to better assess the relationship between tumors and neighboring structures,<sup>73</sup> whereas the technology allowed freehand reconstruction during contrast-enhanced power Doppler EUS. More recently, low-MI contrast-enhanced harmonic three-dimensional EUS was proven to be feasible, showing a good characterization of vascularity and outer borders on tumor lesions.<sup>123</sup> However, automatic acquisition and real-time four-dimensional techniques

with quantification software would be necessary to better define the clinical impact of this exciting technique.

Contrast-enhanced transabdominal ultrasound has been proposed for longitudinal monitoring of antiangiogenic treatment effects, especially in association with the use of specific quantification software that allows perfusion assessment.<sup>75</sup> Current recommendations endorse the use of dynamic CEUS for the assessment of response to biologic therapy in some hypervascular tumors (e.g., hepatocellular carcinoma, metastatic GIST, or metastatic renal cell carcinoma), provided that appropriate software for contrast signal quantification is available.<sup>76</sup> Contrast-enhanced harmonic EUS has been recently used for the evaluation of response to chemotherapy in advanced gastric cancer patients, showing both the change in size and vascularity, with clear implications for prognosis evaluations.<sup>124</sup> A similar methodology has been used for advanced pancreatic cancer patients undergoing chemotherapy, showing that both progression-free survival and overall survival were significantly longer for the patients with visible vessels during CE-EUS.<sup>125</sup>

By using specific ligands conjugated to the surface of microbubble UCAs, targeted contrast agents can be directed *in vivo* toward specific endothelial cell surface receptors.<sup>126</sup> One of the most-used targeted UCA is linked with monoclonal antibodies directed toward VEGF receptor 2 (VEGFR2), allowing quantification of VEGFR2 expression inside tumor vessels and monitoring of treatment response.<sup>127</sup> This kind of microbubble carrier can also be used for targeted treatment through incorporation of chemotherapeutic or gene vectors delivered at cellular levels based on the enhanced uptake in the presence of contrast-enhanced ultrasound, a mechanism called sonoporation.<sup>128</sup> However, none of these agents is currently available for clinical use in human patients; all of them are awaiting clinical translation.

## Fusion Imaging

Fusion imaging based on ultrasound represents a combination of ultrasound with CT/MR based on electromagnetic positioning tracking of the ultrasound transducer and coregistration with the corresponding CT/MR image obtained based on the three-dimensional cube data set obtained previously.<sup>129</sup> Various applications have been described, including transabdominal ultrasound (TUS),<sup>130</sup> EUS,<sup>131</sup> laparoscopic ultrasound (LUS),<sup>132</sup> and natural orifice transluminal endoscopic surgery (NOTES)

procedures,<sup>133</sup> with the aim of improving lesion targeting and increasing the endoscopist's confidence and performance during interventional procedures. The procedure has also been tested in patients, showing an easier image interpretation based on multiple imaging modalities, better lesion targeting during FNA or other interventional procedures, as well as possible shortening of the learning curve.<sup>134</sup> A recent review described in detail the current techniques of fusion imaging based on ultrasound and EUS, with several applications in the field of enhanced diagnosis, staging, and follow-up of oncologic patients.<sup>135</sup> A novel EUS fusion imaging system has been tested in a clinical set-up, based on real-time coregistration of EUS and CT images, using electromagnetic sensors placed inside the biopsy channel of the endoscope for coregistration of the images.<sup>136</sup> Although the system needs further testing and improvement of the software, it could represent a novel approach for complex evaluations of oncological patients. Based on the advancement of current imaging systems, other techniques could be easily fused, like elastography and low-MI contrast-enhanced EUS with CT/MR, or positron emission tomography (PET)-CT/MR images.

## Key References

103. Dietrich CF, Sahai AV, D'Onofrio M, et al. Differential diagnosis of small solid pancreatic lesions. *Gastrointest Endosc.* 2016;84(6): 933–940.
105. Seicean A, Jinga M. Harmonic contrast-enhanced endoscopic ultrasound fine-needle aspiration: fact or fiction? *Endosc Ultrasound.* 2017;6(1):31–36.
109. Iordache S, Costache MI, Popescu CF, et al. Clinical impact of EUS elastography followed by contrast-enhanced EUS in patients with focal pancreatic masses and negative EUS-guided FNA. *Med Ultrason.* 2016;18(1):18–24.
114. Fusaroli P, Serrani M, De Giorgio R, et al. Contrast harmonic-endoscopic ultrasound is useful to identify neoplastic features of pancreatic cysts (with videos). *Pancreas.* 2016;45(2):265–268.
120. Ignee A, Jenssen C, Hocke M, et al. Contrast-enhanced (endoscopic) ultrasound and endoscopic ultrasound elastography in gastrointestinal stromal tumors. *Endosc Ultrasound.* 2017;6(1):55–60.

## References

Access the reference list online at [ExpertConsult.com](http://ExpertConsult.com).

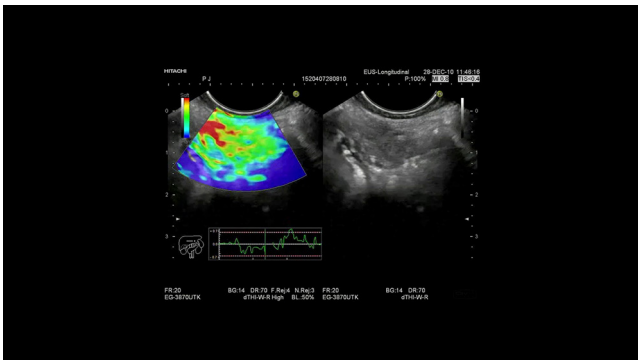
## References

1. Săftoiu A. State-of-the-art imaging techniques in endoscopic ultrasound. *World J Gastroenterol.* 2011;17:691–696.
2. Gheonea DI, Săftoiu A. Beyond conventional endoscopic ultrasound: elastography, contrast enhancement and hybrid techniques. *Curr Opin Gastroenterol.* 2011;27:423–429.
3. Céspedes I, Ophir J, Ponnekanti H, Maklad N. Elastography: elasticity imaging using ultrasound with application to muscle and breast in vivo. *Ultrason Imaging.* 1993;15:73–88.
4. Hiltawsky KM, Krüger M, Starke C, et al. Freehand ultrasound elastography of breast lesions: clinical results. *Ultrasound Med Biol.* 2001;27(11):1461–1469.
5. Itoh A, Ueno E, Tohno E, et al. Breast disease: clinical application of US elastography for diagnosis. *Radiology.* 2006;239:341–350.
6. Ginat DT, Destounis SV, Barr RG, et al. US elastography of breast and prostate lesions. *Radiographics.* 2009;29:2007–2016.
7. Cochlin DL, Ganatra RH, Griffiths DF. Elastography in the detection of prostatic cancer. *Clin Radiol.* 2002;57:1014–1020.
8. König K, Scheipers U, Pesavento A, et al. Initial experiences with real-time elastography guided biopsies of the prostate. *J Urol.* 2005;174:115–117.
9. Pallwein L, Aigner F, Faschingbauer R, et al. Prostate cancer diagnosis: value of real-time elastography. *Abdom Imaging.* 2008;33:729–735.
10. Kapoor A, Kapoor A, Mahajan G, Sidhu BS. Real-time elastography in the detection of prostate cancer in patients with raised PSA level. *Ultrasound Med Biol.* 2011;37:1374–1381.
11. Alam F, Naito K, Horiguchi J, et al. Accuracy of sonographic elastography in the differential diagnosis of enlarged cervical lymph nodes: comparison with conventional B-mode sonography. *AJR Am J Roentgenol.* 2008;191:604–610.
12. Tan R, Xiao Y, He Q. Ultrasound elastography: its potential role in assessment of cervical lymphadenopathy. *Acad Radiol.* 2010;17:849–855.
13. Bhatia KS, Cho CC, Yuen YH, et al. Real-time qualitative ultrasound elastography of cervical lymph nodes in routine clinical practice: interobserver agreement and correlation with malignancy. *Ultrasound Med Biol.* 2010;36:1990–1997.
14. Choi JJ, Kang BJ, Kim SH, et al. Role of sonographic elastography in the differential diagnosis of axillary lymph nodes in breast cancer. *J Ultrasound Med.* 2011;30:429–436.
15. Taylor K, O'Keeffe S, Britton PD, et al. Ultrasound elastography as an adjuvant to conventional ultrasound in the preoperative assessment of axillary lymph nodes in suspected breast cancer: a pilot study. *Clin Radiol.* 2011;66(11):1064–1071.
16. Park SH, Kim SJ, Kim EK, et al. Interobserver agreement in assessing the sonographic and elastographic features of malignant thyroid nodules. *AJR Am J Roentgenol.* 2009;193(5):W416–W423.
17. Bojunga J, Herrmann E, Meyer G, et al. Real-time elastography for the differentiation of benign and malignant thyroid nodules: a meta-analysis. *Thyroid.* 2010;20:1145–1150.
18. Ding J, Cheng HD, Huang J, et al. An improved quantitative measurement for thyroid cancer detection based on elastography. *Eur J Radiol.* 2011;81(4):800–805.
19. Xing P, Wu L, Zhang C, et al. Differentiation of benign from malignant thyroid lesions: calculation of the strain ratio on thyroid sonoelastography. *J Ultrasound Med.* 2011;30:663–669.
20. Kapoor A, Kapoor A, Mahajan G, et al. Real-time elastography in differentiating metastatic from nonmetastatic liver nodules. *Ultrasound Med Biol.* 2011;37:207–213.
21. Gheonea DI, Săftoiu A, Ciurea T, et al. Real-time sono-elastography in the diagnosis of diffuse liver diseases. *World J Gastroenterol.* 2010;16:1720–1726.
22. Wang J, Guo L, Shi X, et al. Real-time elastography with a novel quantitative technology for assessment of liver fibrosis in chronic hepatitis B. *Eur J Radiol.* 2012;81:e31–e36.
23. Koizumi Y, Hirooka M, Kisaka Y, et al. Liver fibrosis in patients with chronic hepatitis C: noninvasive diagnosis by means of real-time tissue elastography—establishment of the method for measurement. *Radiology.* 2011;258:610–617.
24. Hirooka M, Koizumi Y, Hiasa Y, et al. Hepatic elasticity in patients with ascites: evaluation with real-time tissue elastography. *AJR Am J Roentgenol.* 2011;196:W766–W771.
25. Inoue Y, Takahashi M, Arita J, et al. Intra-operative freehand real-time elastography for small focal liver lesions: “visual palpation” for non-palpable tumors. *Surgery.* 2010;148:1000–1011.
26. Kato K, Sugimoto H, Kanazumi N, et al. Intra-operative application of real-time tissue elastography for the diagnosis of liver tumours. *Liver Int.* 2008;28(9):1264–1271.
27. Waage JE, Havre RF, Odegaard S, et al. Endorectal elastography in the evaluation of rectal tumours. *Colorectal Dis.* 2010;13(10):1130–1137.
28. Frey H. [Realtime elastography. A new ultrasound procedure for the reconstruction of tissue elasticity]. *Radiologe.* 2003;43: 850–855.
29. Săftoiu A, Vilman P. Endoscopic ultrasound elastography—a new imaging technique for the visualization of tissue elasticity distribution. *Journal Gastrointest Liv Dis.* 2006;15:161–165.
30. Dietrich CF, Săftoiu A, Janssen C. Real time elastography endoscopic ultrasound (RTE-EUS), a comprehensive review. *Eur J Radiol.* 2014;83(3):405–414.
31. Bamber J, Cosgrove D, Dietrich CF, et al. EFSUMB guidelines and recommendations on the clinical use of ultrasound elastography. Part 1: basic principles and technology. *Ultraschall Med.* 2013;34:169–184.
32. Cosgrove D, Piscaglia F, Bamber J, et al. EFSUMB guidelines and recommendations on the clinical use of ultrasound elastography. Part 2: clinical applications. *Ultraschall Med.* 2013;34:238–253.
33. Havre RF, Waage JR, Gilja OH, et al. Real-time elastography: strain ratio measurements are influenced by the position of the reference area. *Ultraschall Med.* 2011. [Epub ahead of print].
34. Săftoiu A, Vilman P. Differential diagnosis of focal pancreatic masses by semiquantitative EUS elastography: between strain ratios and strain histograms. *Gastrointest Endosc.* 2013;78: 188–189.
35. Giovannini M, Hookey LC, Bories E, et al. Endoscopic ultrasound elastography: the first step towards virtual biopsy? Preliminary results in 49 patients. *Endoscopy.* 2006;38:344–348.
36. Giovannini M, Thomas B, Erwan B, et al. Endoscopic ultrasound elastography for evaluation of lymph nodes and pancreatic masses: a multicenter study. *World J Gastroenterol.* 2009;15:1587–1593.
37. Larsen MH, Fristrup C, Hansen TP, et al. Endoscopic ultrasound, endoscopic sonoelastography, and strain ratio evaluation of lymph nodes with histology as gold standard. *Endoscopy.* 2012;44:759–766.
38. Săftoiu A, Vilman P, Hassan H, Gorunescu F. Analysis of endoscopic ultrasound elastography used for characterisation and differentiation of benign and malignant lymph nodes. *Ultraschall Med.* 2006;27:535–542.
39. Janssen J, Dietrich CF, Will U, Greiner L. Endosonographic elastography in the diagnosis of mediastinal lymph nodes. *Endoscopy.* 2007;39:952–957.
40. Okasha HH, Mansour M, Attia KA, et al. Role of high resolution ultrasound/endosonography and elastography in predicting lymph node malignancy. *Endosc Ultrasound.* 2014;3(1):58–62.
41. Sazuka T, Akai T, Uesato M, et al. Assessment for diagnosis of lymph node metastasis in esophageal cancer using endoscopic ultrasound elastography. *Esophagus.* 2016;13:254–263.
42. Săftoiu A, Vilman P, Ciurea T, et al. Dynamic analysis of EUS used for the differentiation of benign and malignant lymph nodes. *Gastrointest Endosc.* 2007;66:291–300.

43. Larsen MH, Fistrup CW, Mortensen MB. Intra- and interobserver agreement of endoscopic sonoelastography in the evaluation of lymph nodes. *Ultraschall Med.* 2011;32(suppl 2):E45–E50.
44. Xu W, Shi J, Zeng X, et al. EUS elastography for the differentiation of benign and malignant lymph nodes: a meta-analysis. *Gastrointest Endosc.* 2011;74(5):1001–1009.
45. Janssen J, Schröder E, Greiner L. EUS elastography of the pancreas: feasibility and pattern description of the normal pancreas, chronic pancreatitis, and focal pancreatic lesions. *Gastrointest Endosc.* 2007;65:971–978.
46. Hirche TO, Ignee A, Barreiros AP, et al. Indications and limitations of endoscopic ultrasound elastography for evaluation of focal pancreatic lesions. *Endoscopy.* 2008;40:910–917.
47. Säfioiu A, Vilman P, Gorunescu F, et al. Neural network analysis of dynamic sequences of EUS elastography used for the differential diagnosis of chronic pancreatitis and pancreatic cancer. *Gastrointest Endosc.* 2008;68:1086–1094.
48. Iglesias-Garcia J, Larino-Noia J, Abdulkader I, et al. EUS elastography for the characterization of solid pancreatic masses. *Gastrointest Endosc.* 2009;70:1101–1108.
49. Iglesias-Garcia J, Larino-Noia J, Abdulkader I, et al. Quantitative endoscopic ultrasound elastography: an accurate method for the differentiation of solid pancreatic masses. *Gastroenterology.* 2010;139:1172–1180.
50. Itokawa F, Itoi T, Sofuni A, et al. EUS elastography combined with the strain ratio of tissue elasticity for diagnosis of solid pancreatic masses. *J Gastroenterol.* 2011;46:843–853.
51. Schrader H, Wiese M, Ellrichmann M, et al. Diagnostic value of quantitative EUS elastography for malignant pancreatic tumors: relationship with pancreatic fibrosis. *Ultraschall Med.* 2011;33(7):E196–E201.
52. Säfioiu A, Lordache SA, Gheonea DI, et al. Combined contrast-enhanced power Doppler and real-time sonoelastography performed during EUS, used in the differential diagnosis of focal pancreatic masses (with videos). *Gastrointest Endosc.* 2010;72:739–747.
53. Dawwas MF, Taha H, Leeds JS, et al. Diagnostic accuracy of quantitative EUS elastography for discriminating malignant from benign solid pancreatic masses: a prospective, single-center study. *Gastrointest Endosc.* 2012;76:953–961.
54. Kongkam P, Lakananurak N, Navicharern P, et al. Combination of EUS-FNA and elastography (strain ratio) to exclude malignant solid pancreatic lesions: a prospective single-blinded study. *J Gastroenterol Hepatol.* 2015;30(11):1683–1689.
55. Kim SY, Cho JH, Kim YJ, et al. Diagnostic efficacy of quantitative endoscopic ultrasound elastography for differentiating pancreatic disease. *J Gastroenterol Hepatol.* 2017;32:1115–1122.
56. Säfioiu A, Vilman P, Gorunescu F, et al. Accuracy of endoscopic ultrasound elastography used for differential diagnosis of focal pancreatic masses: a multicenter study. *Endoscopy.* 2011;43:596–603.
57. Säfioiu A, Vilman P, Gorunescu F, et al. European EUS Elastography Multicentric Study Group. Efficacy of an artificial neural network-based approach to endoscopic ultrasound elastography in diagnosis of focal pancreatic masses. *Clin Gastroenterol Hepatol.* 2012;10(1):84–90.e1.
58. Pei Q, Zou X, Zhang X, et al. Diagnostic value of EUS elastography in differentiation of benign and malignant solid pancreatic masses: a meta-analysis. *Pancreatology.* 2012;12:402–E408.
59. Xu W, Shi J, Li X, et al. Endoscopic ultrasound elastography for differentiation of benign and malignant pancreatic masses: a systematic review and meta-analysis. *Eur J Gastroenterol Hepatol.* 2013;25:218–224.
60. Hu DM, Gong TT, Zhu Q. Endoscopic ultrasound elastography for differential diagnosis of pancreatic masses: a meta-analysis. *Dig Dis Sci.* 2013;58:1125–1131.
61. Ying L, Lin X, Xie ZL, et al. Clinical utility of endoscopic ultrasound elastography for identification of malignant pancreatic masses: a meta-analysis. *J Gastroenterol Hepatol.* 2013;28:1434–1443.
62. Iglesias-Garcia J, Domínguez-Muñoz JE, Castiñeira-Alvariño M, et al. Quantitative elastography associated with endoscopic ultrasound for the diagnosis of chronic pancreatitis. *Endoscopy.* 2013;45(10):781–788.
63. Janssen J, Papavassiliou I. Effect of aging and diffuse chronic pancreatitis on pancreas elasticity evaluated using semiquantitative EUS elastography. *Ultraschall Med.* 2014;35(3):253–258.
64. Dominguez-Muñoz JE, Iglesias-Garcia J, Castiñeira Alvariño M, et al. EUS elastography to predict pancreatic exocrine insufficiency in patients with chronic pancreatitis. *Gastrointest Endosc.* 2015;81(1):136–142.
65. Rustemovic N, Hristic I, Opacic M, et al. EUS elastography in the diagnosis of focal liver lesions. *Gastrointest Endosc.* 2007;66:823–824.
66. Iglesias Garcia J, Larino Noia J, Souto R, et al. Endoscopic ultrasound (EUS) elastography of the liver. *Rev Esp Enferm Dig.* 2009;101:717–719.
67. Gheorghe L, Gheorghe C, Cotruta B, Carabela A. CT aspects of gastrointestinal stromal tumors: adding EUS and EUS elastography to the diagnostic tools. *J Gastrointest Liver Dis.* 2007;16:346–347.
68. Kato K, Sugimoto H, Kanazumi N, et al. Intra-operative application of real-time tissue elastography for the diagnosis of liver tumours. *Liver Int.* 2008;28:1264–1271.
69. Gheorghe L, Jacob S, Jacob R, et al. Real time elastography—a non-invasive diagnostic method of small hepatocellular carcinoma in cirrhosis. *J Gastrointest Liver Dis.* 2009;18:439–446.
70. Kapoor A, Kapoor A, Mahajan G, et al. Real-time elastography in differentiating metastatic from nonmetastatic liver nodules. *Ultrasound Med Biol.* 2011;37:207–213.
71. Carrara S, Doglioni C, Arcidiacono PG, Testoni PA. Gastric metastasis from ovarian carcinoma diagnosed by EUS-FNA biopsy and elastography. *Gastrointest Endosc.* 2011;74:223–225.
72. Gheorghe L, Gheorghe C, Cotruta B, Carabela A. CT aspects of gastrointestinal stromal tumors: adding EUS and EUS elastography to the diagnostic tools. *J Gastrointest Liver Dis.* 2007;16:346–347.
73. Säfioiu A, Gheonea DI. Tridimensional (3D) endoscopic ultrasound—a pictorial review. *J Gastrointest Liver Dis.* 2009;18:501–505.
74. Reddy NK, Ionciuc AM, Säfioiu A, et al. Contrast-enhanced endoscopic ultrasonography. *World J Gastroenterol.* 2011;17:42–48.
75. Säfioiu A, Dietrich CF, Vilman P. Contrast-enhanced harmonic endoscopic ultrasound. *Endoscopy.* 2012;44:612–617.
76. Piscaglia F, Nolsoe C, Dietrich CF, et al. The EFSUMB guidelines and recommendations on the clinical practice of contrast-enhanced ultrasound (CEUS): update 2011 on non-hepatic applications. *Ultraschall Med.* 2012;33:33–59.
77. Greis C, Dietrich CF. Ultrasound contrast agents and contrast enhanced sonography. In: Dietrich CF, ed. *Endoscopic Ultrasound, an Introductory Manual and Atlas.* 2nd ed. Thieme Verlag; 2011.
78. Dietrich CF. Contrast-enhanced low mechanical index endoscopic ultrasound (CELMI-EUS). *Endoscopy.* 2009;41(suppl 2):E43–E44.
79. Sanchez MVA, Varadarajulu S, Napoleon B. EUS contrast agents: what is available, how do they work, and are they effective? *Gastrointest Endosc.* 2009;69:S71–S77.
80. Clouston M, Cosgrove D, Albrecht T, et al. Guidelines and good clinical practice recommendations for contrast enhanced ultrasound (CEUS)—update 2008. *Ultraschall Med.* 2008;29:28–44.
81. Dietrich CF, Ignee A, Frey H. Contrast-enhanced endoscopic ultrasound with low mechanical index: a new technique. *Z Gastroenterol.* 2005;43:1219–1223.

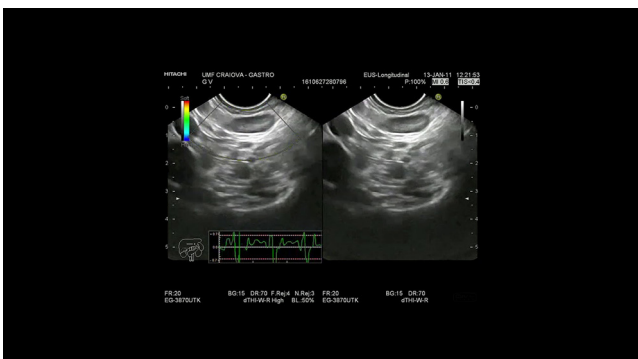
82. Kitano M, Takagi T, Sakamoto H, et al. Dynamic imaging of pancreatic tumors by contrast-enhanced harmonic EUS with long-lasting contrast. *Gastrointest Endosc.* 2009;67:141–150.
83. Becker D, Strobel D, Bernatik T, Hahn EG. Echo-enhanced color- and power-Doppler EUS for the discrimination between focal pancreatitis and pancreatic carcinoma. *Gastrointest Endosc.* 2001;53:784–789.
84. Dietrich CF, Ignee A, Braden B, et al. Improved differentiation of pancreatic tumors using contrast-enhanced endoscopic ultrasound. *Clin Gastroenterol Hepatol.* 2008;6:590–597, e1.
85. Sakamoto H, Kitano M, Suetomi Y, et al. Utility of contrast-enhanced endoscopic ultrasonography for diagnosis of small pancreatic carcinomas. *Ultrasound Med Biol.* 2008;34:525–532.
86. Hocke M, Schulze E, Gottschalk P, et al. Contrast-enhanced endoscopic ultrasound in discrimination between focal pancreatitis and pancreatic cancer. *World J Gastroenterol.* 2006;12:246–250.
87. Săftoiu A, Iordache SA, Gheonea DI, et al. Combined contrast-enhanced power Doppler and real-time sonoelastography performed during EUS, used in the differential diagnosis of focal pancreatic masses (with videos). *Gastrointest Endosc.* 2010;72:739–747.
88. Ishikawa T, Itoh A, Kawashima H, et al. Usefulness of EUS combined with contrast-enhancement in the differential diagnosis of malignant versus benign and preoperative localization of pancreatic endocrine tumors. *Gastrointest Endosc.* 2010;71:951–959.
89. Hocke M, Ignee A, Dietrich CF. Contrast-enhanced endoscopic ultrasound in the diagnosis of autoimmune pancreatitis. *Endoscopy.* 2011;43(2):163–165.
90. Fusaroli P, Spada A, Mancino MG, Caletti G. Contrast harmonic echo-endoscopic ultrasound improves accuracy in diagnosis of solid pancreatic masses. *Clin Gastroenterol Hepatol.* 2010;8:629–634.
91. Napoleon B, Alvarez-Sanchez MV, Gincoul R, et al. Contrast-enhanced harmonic endoscopic ultrasound in solid lesions of the pancreas: results of a pilot study. *Endoscopy.* 2010;42:564–570.
92. Seicean A, Badea R, Stan-Iuga R, et al. Quantitative contrast-enhanced harmonic endoscopic ultrasonography for the discrimination of solid pancreatic masses. *Ultraschall Med.* 2010;31:571–576.
93. Romagnuolo J, Hoffman B, Vela S, et al. Accuracy of contrast-enhanced harmonic EUS with a second-generation perflutren lipid microsphere contrast agent (with video). *Gastrointest Endosc.* 2011;73:52–63.
94. Matsubara H, Itoh A, Kawashima H, et al. Dynamic quantitative evaluation of contrast-enhanced endoscopic ultrasonography in the diagnosis of pancreatic diseases. *Pancreas.* 2011;40:1073–1079.
95. Gheonea DI, Streba CT, Ciurea T, Săftoiu A. Quantitative low mechanical index contrast-enhanced endoscopic ultrasound for the differential diagnosis of chronic pseudotumoral pancreatitis and pancreatic cancer. *BMC Gastroenterol.* 2013;13:2.
96. Gauthier TP, Averkiou MA, Leen EL. Perfusion quantification using dynamic contrast-enhanced ultrasound: the impact of dynamic range and gain on time-intensity curves. *Ultrasonics.* 2011;51:102–106.
97. Peronneau P, Lassau N, Leguerney I, et al. Contrast ultrasonography: necessity of linear data processing for the quantification of tumor vascularization. *Ultraschall Med.* 2010;31:370–378.
98. Gong TT, Hu DM, Zhu Q. Contrast-enhanced EUS for differential diagnosis of pancreatic mass lesions: a meta-analysis. *Gastrointest Endosc.* 2012;76:301–309.
99. D’Onofrio M, Biagioli E, Gerardi C, et al. Diagnostic performance of contrast-enhanced ultrasound (CEUS) and contrast-enhanced endoscopic ultrasound (ECEUS) for the differentiation of pancreatic lesions: a systematic review and meta-analysis. *Ultraschall Med.* 2014;35(6):515–521.
100. Gincul R, Palazzo M, Pujol B, et al. Contrast-harmonic endoscopic ultrasound for the diagnosis of pancreatic adenocarcinoma: a prospective multicenter trial. *Endoscopy.* 2014;46(5):373–379.
101. Park JS, Kim HK, Bang BW, et al. Effectiveness of contrast-enhanced harmonic endoscopic ultrasound for the evaluation of solid pancreatic masses. *World J Gastroenterol.* 2014;20(2):518–524.
102. Săftoiu A, Vilmann P, Dietrich CF, et al. Quantitative contrast-enhanced harmonic EUS in differential diagnosis of focal pancreatic masses (with videos). *Gastrointest Endosc.* 2015;82(1):59–69.
103. Dietrich CF, Sahai AV, D’Onofrio M, et al. Differential diagnosis of small solid pancreatic lesions. *Gastrointest Endosc.* 2016;84(6):933–940.
104. Yamashita Y, Kato J, Ueda K, et al. Contrast-enhanced endoscopic ultrasonography for pancreatic tumors. *Biomed Res Int.* 2015;2015:491782.
105. Seicean A, Jinga M. Harmonic contrast-enhanced endoscopic ultrasound fine-needle aspiration: fact or fiction? *Endosc Ultrasound.* 2017;6(1):31–36.
106. Hou X, Jin Z, Xu C, et al. Contrast-enhanced harmonic endoscopic ultrasound-guided fine-needle aspiration in the diagnosis of solid pancreatic lesions: a retrospective study. *PLoS One.* 2015;10(3). e0121236.
107. Seicean A, Badea R, Moldovan-Pop A, et al. Harmonic contrast-enhanced endoscopic ultrasonography for the guidance of fine-needle aspiration in solid pancreatic masses. *Ultraschall Med.* 2017;38:174–182.
108. Sugimoto M, Takagi T, Hikichi T, et al. Conventional versus contrast-enhanced harmonic endoscopic ultrasonography-guided fine-needle aspiration for diagnosis of solid pancreatic lesions: a prospective randomized trial. *Pancreatology.* 2015;15(5):538–541.
109. Iordache S, Costache MI, Popescu CF, et al. Clinical impact of EUS elastography followed by contrast-enhanced EUS in patients with focal pancreatic masses and negative EUS-guided FNA. *Med Ultrason.* 2016;18(1):18–24.
110. Ohno E, Hirooka Y, Itoh A, et al. Intraductal papillary mucinous neoplasms of the pancreas: differentiation of malignant and benign tumors by endoscopic ultrasound findings of mural nodules. *Ann Surg.* 2009;249(4):628–634.
111. Yamashita Y, Ueda K, Itonaga M, et al. Usefulness of contrast-enhanced endoscopic sonography for discriminating mural nodules from mucous clots in intraductal papillary mucinous neoplasms: a single-center prospective study. *J Ultrasound Med.* 2013;32(1):61–68.
112. Harima H, Kaino S, Shinoda S, et al. Differential diagnosis of benign and malignant branch duct intraductal papillary mucinous neoplasm using contrast-enhanced endoscopic ultrasonography. *World J Gastroenterol.* 2015;21(20):6252–6260.
113. Yamamoto N, Kato H, Tomoda T, et al. Contrast-enhanced harmonic endoscopic ultrasonography with time-intensity curve analysis for intraductal papillary mucinous neoplasms of the pancreas. *Endoscopy.* 2016;48(1):26–34.
114. Fusaroli P, Serrani M, De Giorgio R, et al. Contrast harmonic-endoscopic ultrasound is useful to identify neoplastic features of pancreatic cysts (with videos). *Pancreas.* 2016;45(2):265–268.
115. Nomura N, Goto H, Niwa Y, et al. Usefulness of contrast-enhanced EUS in the diagnosis of upper GI tract diseases. *Gastrointest Endosc.* 1999;50:555–560.
116. Iordache S, Filip MM, Georgescu CV, et al. Contrast-enhanced power Doppler endosonography and pathological assessment of vascularization in advanced gastric carcinomas—a feasibility study. *Med Ultrason.* 2012;14:101–107.
117. Kannengiesser K, Mahlke R, Petersen F, et al. Contrast-enhanced harmonic endoscopic ultrasound is able to discriminate benign submucosal lesions from gastrointestinal stromal tumors. *Scand J Gastroenterol.* 2012;47:1515–1520.

118. Sakamoto H, Kitano M, Matsui S, et al. Estimation of malignant potential of GI stromal tumors by contrast-enhanced harmonic EUS (with videos). *Gastrointest Endosc.* 2011;73: 227–237.
119. Yamashita Y, Kato J, Ueda K, et al. Contrast-enhanced endoscopic ultrasonography can predict a higher malignant potential of gastrointestinal stromal tumors by visualizing large newly formed vessels. *J Clin Ultrasound.* 2015;43(2):89–97.
120. Ignee A, Janssen C, Hocke M, et al. Contrast-enhanced (endoscopic) ultrasound and endoscopic ultrasound elastography in gastrointestinal stromal tumors. *Endosc Ultrasound.* 2017;6(1):55–60.
121. Xia Y, Kitano M, Kudo M, et al. Characterization of intra-abdominal lesions of undetermined origin by contrast-enhanced harmonic EUS (with videos). *Gastrointest Endosc.* 2010;72: 637–642.
122. Paik WH, Choi JH, Seo DW, et al. Clinical usefulness with the combination of color Doppler and contrast-enhanced harmonic EUS for the assessment of visceral vascular diseases. *J Clin Gastroenterol.* 2014;48(10):845–850.
123. Hocke M, Dietrich CF. New technology—combined use of 3D contrast enhanced endoscopic ultrasound techniques. *Ultraschall Med.* 2011;32:317–318.
124. Matsui S, Kudo M, Kitano M, Asakuma Y. Evaluation of the response to chemotherapy in advanced gastric cancer by contrast-enhanced harmonic EUS. *Hepatogastroenterology.* 2015;62(139):595–598.
125. Yamashita Y, Ueda K, Itonaga M, et al. Tumor vessel depiction with contrast-enhanced endoscopic ultrasonography predicts efficacy of chemotherapy in pancreatic cancer. *Pancreas.* 2013;42(6):990–995.
126. Kruskal JB. Can contrast-enhanced US with targeted microbubbles monitor the response to antiangiogenic therapies? *Radiology.* 2008;246:339–340.
127. Willmann JK, Paulmurugan R, Chen K, et al. US imaging of tumor angiogenesis with microbubbles targeted to vascular endothelial growth factor receptor type 2 in mice. *Radiology.* 2008;246:508–518.
128. Postema M, Gilja OH. Ultrasound-directed drug delivery. *Curr Pharm Biotechnol.* 2007;8:355–361.
129. Estépar RS, Stylopoulos N, Ellis R, et al. Towards scarless surgery: an endoscopic ultrasound navigation system for transgastric access procedures. *Comput Aided Surg.* 2007;12:311–324.
130. Ewertsen C, Henriksen BM, Torp-Pedersen S, Bachmann Nielsen M. Characterization by biopsy or CEUS of liver lesions guided by image fusion between ultrasonography and CT, PET/CT or MRI. *Ultraschall Med.* 2011;32:191–197.
131. Vosburgh KG, Stylopoulos N, Estépar RS, et al. EUS with CT improves efficiency and structure identification over conventional EUS. *Gastrointest Endosc.* 2007;65:866–870.
132. Estépar RS, Westin CF, Vosburgh KG. Towards real time 2D to 3D registration for ultrasound-guided endoscopic and laparoscopic procedures. *Int J Comput Assist Radiol Surg.* 2009;4:549–560.
133. Fernández-Esparrach G, Estépar SR, Guarner-Argente C, et al. The role of a computed tomography-based image registered navigation system for natural orifice transluminal endoscopic surgery: a comparative study in a porcine model. *Endoscopy.* 2010;42:1096–1103.
134. Obstein KL, Estépar RS, Jayender J, et al. Image registered gastroscopic ultrasound (IRGUS) in human subjects: a pilot study to assess feasibility. *Endoscopy.* 2011;43:394–399.
135. Ewertsen C, Säfoui A, Gruionu LG, et al. Real-time image fusion involving diagnostic ultrasound. *AJR Am J Roentgenol.* 2013;200(3):W249–W255.
136. Gruionu LG, Saftoui A, Gruionu G. A novel fusion imaging system for endoscopic ultrasound. *Endosc Ultrasound.* 2016;5(1):35–42.



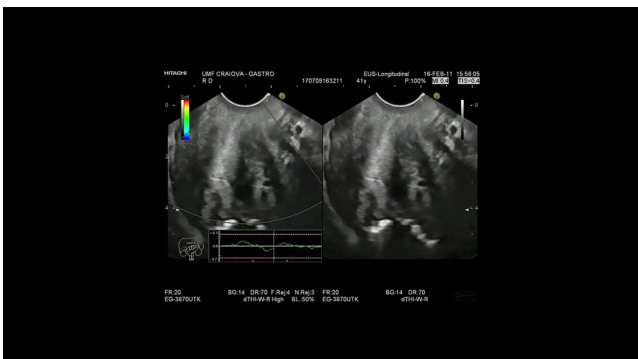
### Video 5.1 Benign Mediastinal Lymph Node

Endoscopic ultrasound elastography showing a relatively homogeneous mixture of green and yellow, indicating a relatively soft structure as compared to the surrounding tissues (left).



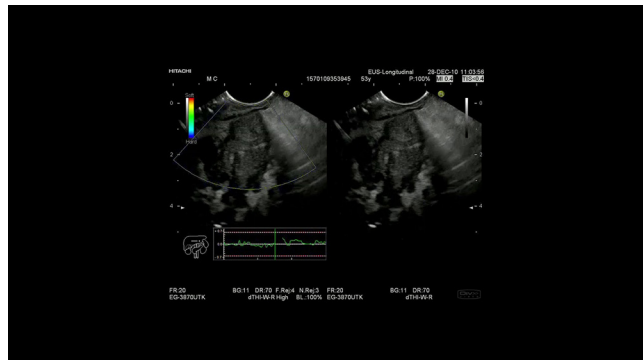
### Video 5.2 Malignant Mediastinal Lymph Node

Endoscopic ultrasound elastography showing a relatively homogeneous mixture of blue, indicating a relatively hard structure as compared to the surrounding tissues (left).



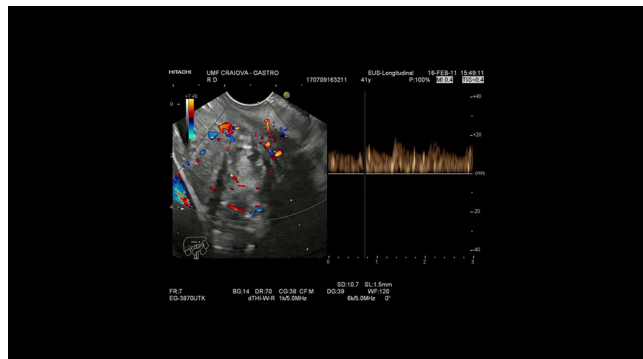
### Video 5.3 Chronic Pseudotumoral Pancreatitis

Endoscopic ultrasound elastography showing a relatively heterogeneous mixture of blue, green, and red, indicating a relatively intermediate elasticity structure as compared to the surrounding tissues (left). Hue histogram analysis can be also performed to obtain semiquantitative data on the elasticity of the focal mass (mean 63.4, SD 62.3).



### Video 5.4 Pancreatic Adenocarcinoma

Endoscopic ultrasound elastography showing a relatively homogeneous hard (blue) mass, indicating a relatively hard elasticity structure as compared to the surrounding tissues (left). Hue histogram analysis can also be performed to obtain semiquantitative data on the elasticity of the focal mass (mean 15.8, SD 28.7).



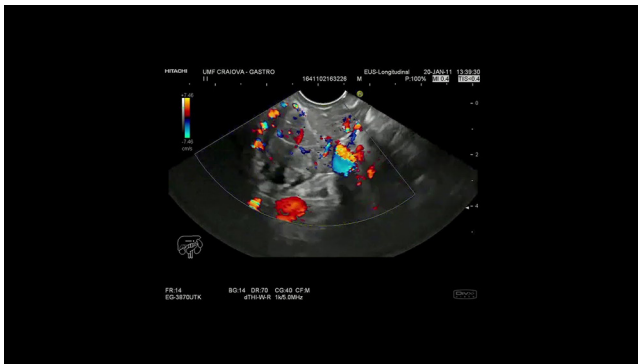
### Video 5.5 Pseudotumoral Chronic Pancreatitis

Contrast-enhanced color Doppler showing multiple Doppler signals inside the hypervascular pancreatic mass (left), some with arterial-type signal inside proven by pulsed Doppler (right).



### Video 5.6 Pancreatic Adenocarcinoma

Contrast-enhanced power Doppler showing multiple power Doppler signals (collaterals) surrounding the hypovascular pancreatic mass.



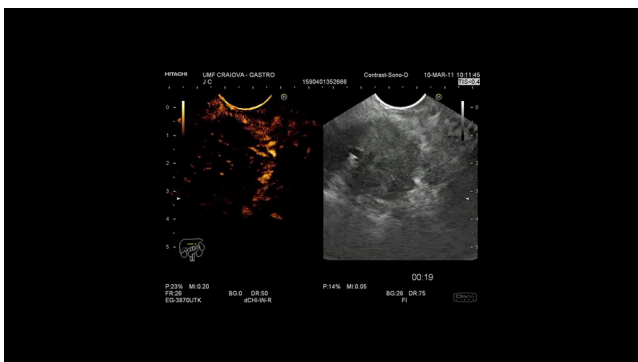
### Video 5.7 Malignant Neuroendocrine Tumor

Contrast-enhanced power Doppler showing multiple power Doppler signals inside the hypervascular pancreatic mass. (Based on Gheonea DI, Streba CT, Ciurea T, Săftoiu A. Quantitative low mechanical index contrast-enhanced endoscopic ultrasound for the differential diagnosis of chronic pseudotumoral pancreatitis and pancreatic cancer. *BMC Gastroenterol.* 2013;13:2.)



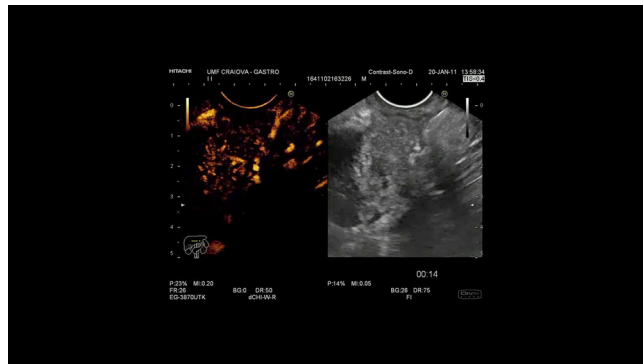
### Video 5.8 Pseudotumoral Chronic Pancreatitis

Low mechanical index contrast-enhanced EUS showing intense uptake of the contrast in the arterial phase, with a small (avascular) pseudocyst at the level of the pancreatic mass (left).



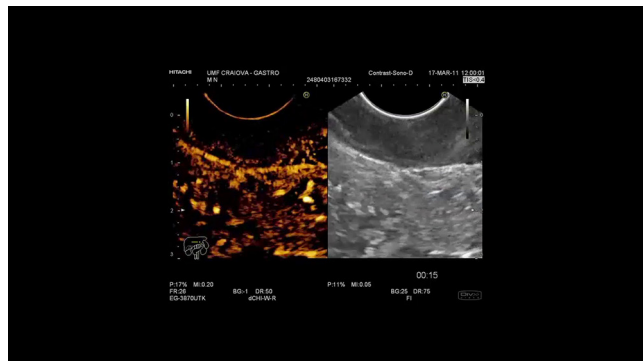
### Video 5.9 Pancreatic Adenocarcinoma

Low mechanical index contrast-enhanced endoscopic ultrasound showing discrete uptake of the contrast in the arterial phase at the level of the hypovascular pancreatic mass, in comparison with the neighboring pancreatic parenchyma (left).



### Video 5.10 Malignant Neuroendocrine Tumor

Low mechanical index contrast-enhanced endoscopic ultrasound showing intense uptake of the contrast in the arterial phase, at the level of the focal pancreatic mass (left).



### Video 5.11 Gastric Adenocarcinoma

Low mechanical index contrast-enhanced endoscopic ultrasound showing uptake of the contrast in the arterial phase, at the periphery of the gastric tumor (left).



### Video 5.12 Gastrointestinal Stromal Tumor

Low mechanical index contrast-enhanced endoscopic ultrasound showing increased uptake of the contrast in the arterial phase, with a central zone of necrosis (left).

# 6

# How to Perform Endoscopic Ultrasonography in the Esophagus and Mediastinum

ROBERT H. HAWES, SHYAM VARADARAJULU, AND PAUL FOCKENS

## Esophagus

Obtaining high-quality images of the esophageal wall is one of the more difficult tasks that an endosonographer will encounter. One has to deal with the “catch 22” that pits adequate coupling of the ultrasound signal to the esophageal wall against wall compression. This situation can lead to inaccurate assessment of invasion depth in patients with early esophageal cancer or to missing lesions completely in the case of varices. Numerous techniques can be used to overcome these conflicting goals.

In the case of a relatively advanced mass in the esophagus, minimal or no balloon inflation is sufficient to couple the ultrasound signal to the esophageal wall without causing compression that adversely affects staging accuracy. In this circumstance, the electronic radial instrument has an advantage over the mechanical radial device because of the absence of ringdown artifact and the superior near-field resolution of electronic array technology. Periesophageal structures (e.g., lymph nodes) are not affected by the amount of balloon inflation.

When compression of the esophageal wall needs to be avoided, several different techniques can be used. The simplest is to instill water into the gut lumen by pressing the air/water button to its first position. This maneuver sprays water across the endoscopic image lens. Remarkably, this does a very good job of filling the lumen with water while reducing the risk of aspiration. This technique can be used with the standard radial echoendoscope or when using a high-frequency catheter probe in conjunction with a single- or dual-channel forward-viewing endoscope. The images generated are often fleeting because of peristalsis and variability in water filling. As a result, the cine function on the console becomes important in that it allows one to freeze the image and then scroll through the stored images to save the best one. High-resolution esophageal images can be obtained only when the esophagus is in its relaxed state, and this occurs only periodically. Agents normally used to paralyze the stomach, duodenum, and colon have little to no effect on esophageal contractions.

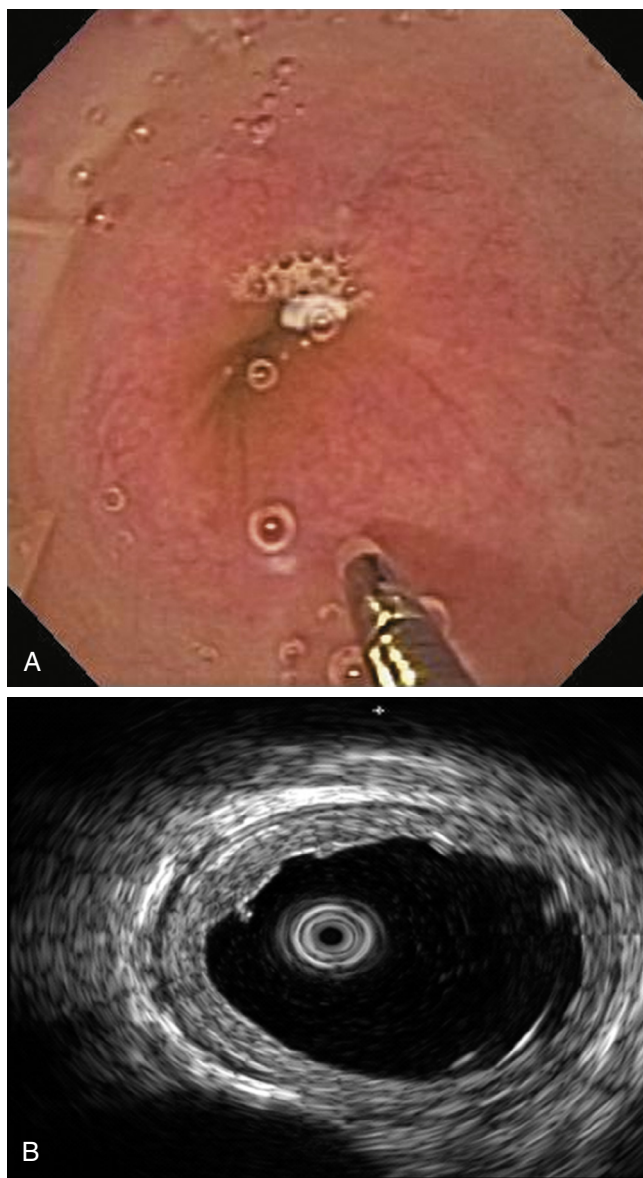
A second method that can be used with a radial scanning echoendoscope is to instill water through the biopsy channel. If this technique is used, it is recommended that water be slowly

siphoned into the esophagus rather than actively pumped or vigorously instilled by syringe. There is a very real risk of aspiration if high volumes are instilled over a short time, especially when topical pharyngeal anesthesia has also been applied.

Until the advent of the electronic radial echoendoscope, the device of choice for high-quality images of the esophageal wall was a high-frequency ultrasound probe. However, the newer electronic radial echoendoscopes have excellent near-field resolution and provide superb images without the need for significant balloon inflation. Nonetheless, if one wishes to stage early (T1m,sm) esophageal cancer (to determine the presence or absence of penetration through the muscularis mucosa), high-frequency catheter probes (20 to 30 MHz) would still be considered the instruments of choice.

When catheter probes are used for esophageal imaging, several techniques can be used. One method is to use a bare catheter and instill water through the air/water channel. A second method is to use an ultrasound catheter with an attachable balloon. This technique still risks compression of the esophageal wall layers with inflation of the balloon. However, because the focal length of the catheter is very short, only a small amount of balloon inflation is necessary, thereby minimizing this risk.

Another technique that has been described is to affix a transparent, low-compliance condom onto the end of a double-channel endoscope (Fig. 6.1). The condom is taped onto the end of the endoscope such that approximately 2 to 3 cm of the condom protrude beyond the tip of the endoscope. This redundant portion of the condom is folded across the imaging lens as the endoscope is passed into the esophagus. During the intubation process, it is extremely important to avoid instilling air (a common habit) because this will inflate the condom and could compromise the patient’s airway. After entering the esophagus, the instrument is passed into the stomach lumen, and air is “bled” from the condom tip (instill water-aspirate; reinstate; reaspire and repeat until all the air is gone). Once the condom has been bled, the endoscope is withdrawn to the level of the lesion, and the condom is filled with water. Because of the low compliance of the condom, it tends to elongate rather than compress the wall layers. The ultrasound catheter is then advanced into the lumen of the condom,

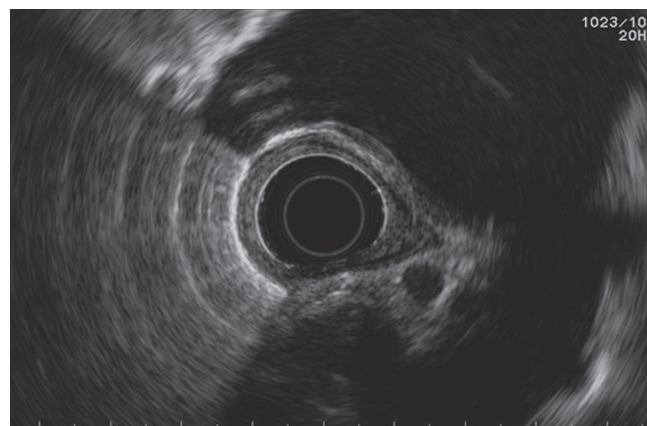


• **Fig. 6.1** Endoscopic view of the esophageal lumen. (A) View with a water-filled condom. (B) The esophageal wall layers as visualized with a high-frequency catheter probe using the condom technique.

and imaging proceeds (Video 6.1). With this technique, the coupling of the ultrasound waves to the esophageal wall is virtually perfect. With the transparent condom, the lesion can be viewed endoscopically in real time, thus assuring that the catheter probe is positioned correctly. Because the water is completely contained within the condom, there is no risk of aspiration.

Whichever technique is used, the risk of aspiration should be minimized while good coupling of the ultrasound waves to the esophageal wall is achieved without inducing compression. These techniques are used for patients with early esophageal cancer, with Barrett esophagus with or without nodules, and with small submucosal lesions.

The other major problem with esophageal endoscopic ultrasonography (EUS) is tangential imaging. The esophagus is often perceived as a straight tube, but in most cases it has some tortuosity. The imaging section of an echoendoscope, as well as a catheter probe, is straight and rigid. Imaging a tortuous tube with



• **Fig. 6.2** Muscularis layer of the esophageal wall. The muscularis layer of the esophageal wall appears blurred and focally thickened secondary to tangential imaging.

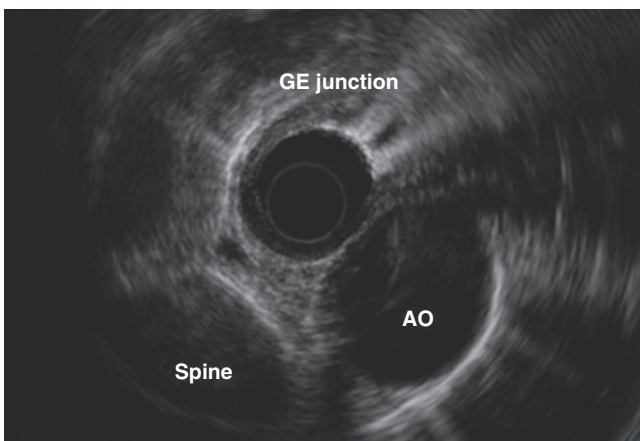
a straight instrument creates tangential imaging. The endosonographer must be trained to recognize tangential imaging and must be aware of the maneuvers that will correct it. The consequence of unrecognized tangential imaging is overstaging malignant lesions or missing the layer of origin of a submucosal lesion. Tangential imaging is characterized by focal thickening of the esophageal wall associated with blurring and triangulation of the deep border of the esophageal wall (Fig. 6.2). If one recognizes tangential imaging, the corrective action is usually to use all four directional dials (*do not torque the scope shaft*) to move the transducer in the direction where tangential imaging is seen. When the deep edge of the muscularis propria layer becomes smooth and the layer is seen sharply, tangential imaging has been corrected.

## Mediastinum

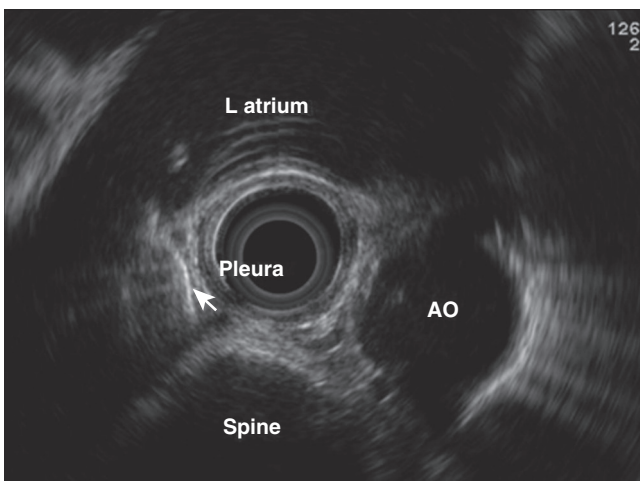
### Radial Echoendoscope

Examination of the mediastinum with a radial echoendoscope is relatively straightforward. The learning curve should be short (compared with EUS of the pancreas) because the EUS images correlate with a thoracic computed tomography (CT) scan. It is recommended that a systemic approach be applied to all EUS examinations and that images be presented with a standard orientation. This approach holds true for mediastinal imaging. To begin the mediastinal study, the echoendoscope tip is placed in the distal esophagus near the gastroesophageal junction. The aorta is a round, anechoic structure that is a constant anatomic finding throughout the examination until withdrawal proximal to the aortic arch. It is recommended that the endoscopic ultrasound image be presented on the monitor in an orientation that exactly matches a CT slice. To accomplish this, the aorta should be rotated (using the rotation function on the instrument panel, *not* by torquing the scope shaft) to the 5-o'clock position. This will present the spine at 7 o'clock (Fig. 6.3), and the heart and respiratory tree will emerge in the 12-o'clock position.

With the transducer placed in the distal esophagus and the aorta located in the 5-o'clock position, the examination begins (Video 6.2). The balloon should be inflated sufficiently to displace any intraluminal air, and the transducer itself should be placed approximately in the center of the balloon (again using right/left and up/down dials and *not* by torquing the scope shaft). With this starting position, the echoendoscope is then slowly withdrawn.



• **Fig. 6.3** Endoscopic ultrasonography image when the radial echoendoscope is positioned at the gastroesophageal (GE) junction. The aorta (AO) is located at the 5-o'clock position, and the spine is at 7 o'clock.



• **Fig. 6.4** View of the left atrium. On gradual withdrawal of the radial echoendoscope from the gastroesophageal junction, the left atrium (L atrium) appears as a pulsating structure in the upper half of the EUS screen. AO, Aorta; arrow, pleura.

The anatomy around the distal esophagus is not complex, and as the examination begins, the aorta, spine, and portions of the left and right lung are the only anatomic structures that can be identified. The lungs are seen only as a very bright white line. The area of the mediastinum surrounding the distal esophagus corresponds to area 8 of the American Thoracic Society (ATS) areas.<sup>1</sup>

As the instrument is slowly withdrawn, usually approximately 35 cm from the incisors, an anechoic structure begins to emerge at approximately the 12-o'clock position (it could emerge anywhere from 10 to 2 o'clock). This structure is the left atrium (Fig. 6.4). As the echoendoscope is withdrawn further, the left atrium gradually disappears. The subcarinal space is located from 10 to 12 o'clock and extends from where the left atrium disappears to where the left and right main stem bronchi come together to form the trachea (Fig. 6.5).

The subcarinal space may be 3 to 4 cm in length and is designated area 7 by the ATS. The subcarina should be examined by withdrawing the echoendoscope in 1-cm increments while observing the 10- to 2-o'clock area for lymph nodes. Lymph nodes are typically well-circumscribed, relatively echo-poor structures that may be triangular, elongated, or round and located adjacent

to the esophagus (see Fig. 6.5C). The inner echo architecture can vary from being almost anechoic to having a very bright central echo. On withdrawal of the endoscope, after the disappearance of the left atrium, eventually the right or left main stem bronchus emerges. Obviously, the left main stem bronchus is present on the same side of the screen as the aorta. Air-filled structures on EUS show up as very bright "ribs" on the monitor (see Fig. 6.5B).

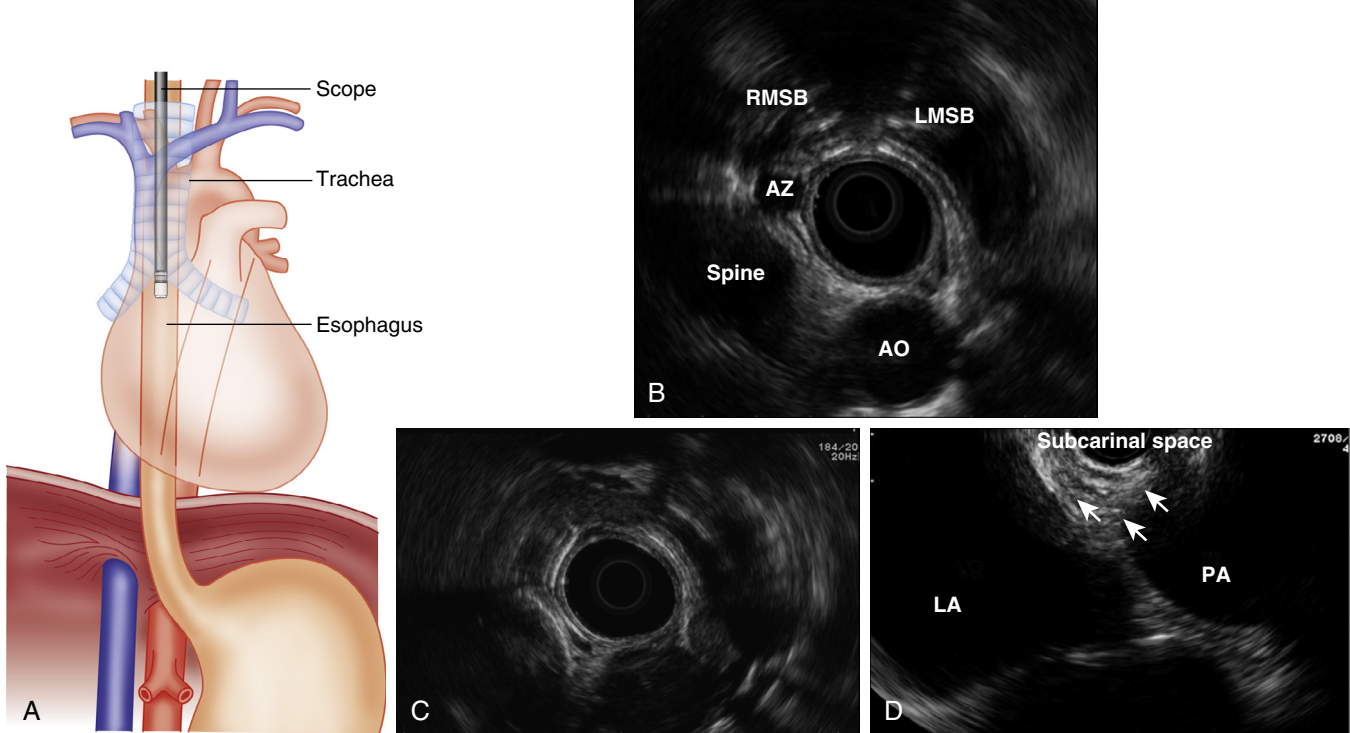
On further withdrawal of the endoscope, three distinctive findings are seen over the span of 2 to 3 cm: the trachea, the elongated azygous vein, and the aortic arch (Fig. 6.6). First, the left and right main stem bronchi come together to form the trachea, which is represented as a typical air-filled structure (echogenic ribs) at the 12-o'clock position. The second anatomic landmark is the azygous vein, up to now seen as a round, anechoic structure near the spine, or occasionally between the spine and the aorta, that elongates and moves anteriorly to join the superior vena cava. The third anatomic landmark is the elongation of the aorta, representing the aortic arch.

The area at 3 o'clock, just distal to the arch of the aorta, is the aortopulmonary window (area 4L/5) (Fig. 6.7). After the aortic arch, further withdrawal of the endoscope demonstrates the great vessels coming off the aortic arch. However, other than the trachea and the spine, this area is devoid of any significant anatomic landmarks. Nonetheless, this area is extremely important to image to look for periesophageal and paratracheal lymph nodes (area 2). Any confirmed metastatic lymph node found above the aortic arch in association with upper gastrointestinal cancer essentially represents unresectable disease.

### Linear Array Echoendoscope

Examination of the mediastinum with the linear array echoendoscope is more time consuming and tedious when compared with examination with the radial instrument. Because of the narrow field of view, it is critical to adopt a systematic approach to the examination. When examining the area around the distal esophagus (area 8), the starting point is the aorta, which appears as a linear, anechoic structure that essentially fills the field of view. From here, it is necessary to rotate the echoendoscope purposefully 180 degrees in a clockwise fashion, return to the neutral position (aorta), and then rotate 180 degrees in a counterclockwise direction. This needs to be done initially and then repeated after withdrawing 1 to 2 cm. Effective rotating (torquing) of the linear echoendoscope is a fundamental skill required to perform linear EUS competently. A simple method to determine whether the torquing technique is correct is to watch the distance numbers on the scope shaft. If they rotate around the axis of the scope 1 to 1 during torquing, the maneuver is being performed correctly (Video 6.3).

The two most important areas in the mediastinum in which to look for lymph nodes are the subcarinal space (area 7) and the aortopulmonary window (area 4L/5). One should take a systematic approach to locate and image both areas with the linear echoendoscope. There are two ways to locate the subcarinal space. The first is to begin the examination in the distal esophagus (at 35 to 40 cm on the scope shaft). The instrument should be rotated in a clockwise or counterclockwise direction until the aorta is found. After the aorta has been located, the instrument should be torqued 180 degrees (clockwise or counterclockwise, whichever is more comfortable) and then slowly withdrawn. The aorta is positioned posteriorly, and this maneuver orients the image anteriorly.

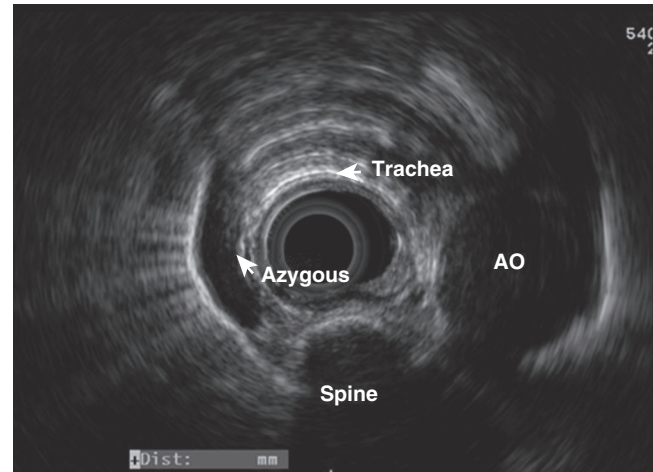


**• Fig. 6.5** Subcarinal region. (A) The position of the scope when visualizing the subcarinal region. At this site, on radial imaging, (B) the right and the left main stem bronchi (RMSB and LMSB, respectively) come together to form the trachea, and (C) the characteristic draping lymph nodes are seen in this station. (D) On linear imaging, two structures characterize the subcarinal space (*arrows*): the one on the left is the left atrium (LA), and the one on the right is the pulmonary artery (PA). AO, Aorta; AZ, azygous vein.

As the instrument is withdrawn, usually approximately 35 cm from the incisors, a large anechoic structure is seen, and this represents the left atrium. The instrument should then be subtly torqued either clockwise or counterclockwise until the left atrium is centered. The instrument is then further withdrawn until the left atrium is situated on the left side of the ultrasound image. When this has been achieved, a slight tip deflection upward will bring a round, anechoic structure into view on the right side of the screen; this represents the pulmonary artery. The area between the left atrium and the pulmonary artery represents the subcarinal space (see Fig. 6.5D). Full interrogation of the subcarinal space then requires careful clockwise and counterclockwise torquing.

The second way to find the subcarinal space is to locate the aorta in the middle of the esophagus. With the aorta occupying the screen, the echoendoscope is slowly withdrawn until the aorta disappears; this represents the aortic arch. At this point, 180 degrees of clockwise torque are applied. This maneuver orients the image anteriorly, and one encounters the typical echogenic ribs, which represent the trachea. After the trachea has been located, the scope is advanced 1 to 2 cm. When the trachea disappears, this represents the bifurcation into the left and right main stem bronchi. Thus one is now viewing the subcarinal space. Just as with the first maneuver, the left atrium is seen on the left side of the screen, and the pulmonary artery is on the right.

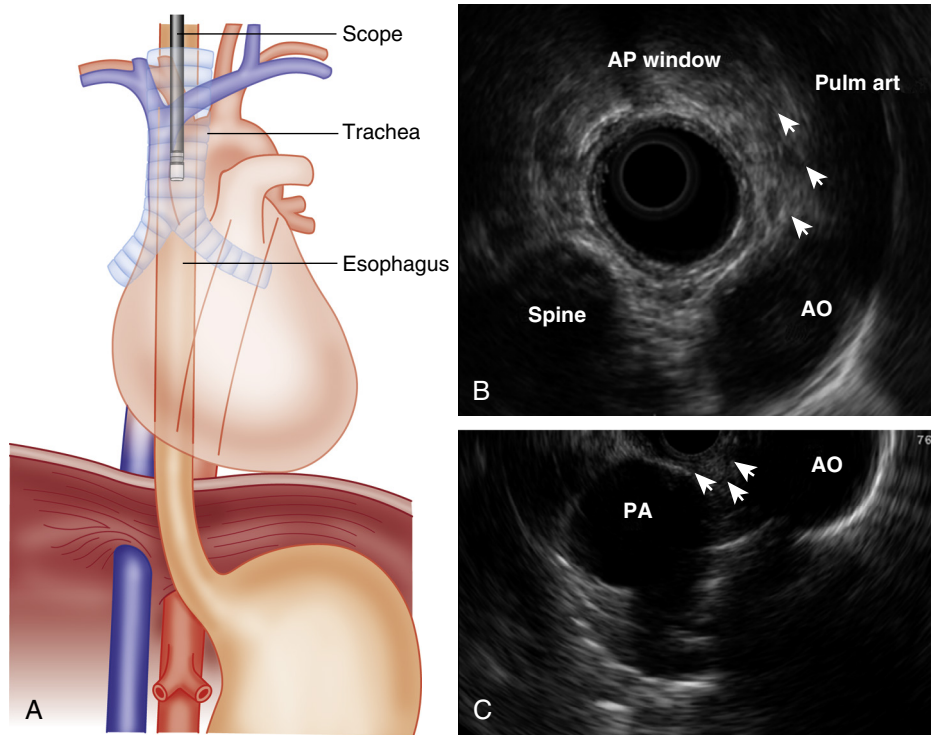
The other important anatomic station in the mediastinum is the aortopulmonary window (area 4L/5). This is essentially the area underneath the arch of the aorta. This area can be found most easily by locating the aorta in the middle of the esophagus and then withdrawing the instrument until the aorta disappears. From this position, one advances the scope by 1 to 2 cm, at a level underneath the aortic arch. The scope is rotated 60 degrees in a



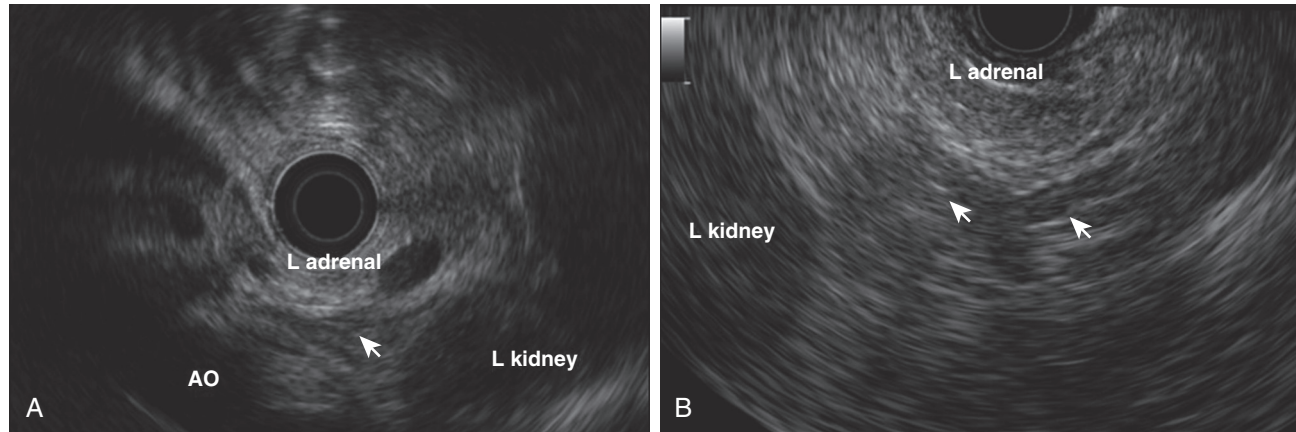
**• Fig. 6.6** Trachea, azygous vein, and aortic arch (AO). On upward withdrawal of the radial echoendoscope 2 to 3 cm from the subcarina, the trachea, azygous vein, and the aortic arch are seen.

clockwise direction and comes slightly “up” on the up/down dial. With the linear echoendoscope, the aortopulmonary window is seen as the space between the aorta (round, anechoic structure on the right side of the screen) and the pulmonary artery (round, anechoic structure on the left side of the screen; see Fig. 6.7C).

Above the area of the aortic arch, the left and right paratracheal area can be examined by torquing the scope clockwise and counterclockwise off the trachea every 2 cm (area 2). This is a critical area to examine in patients with distal esophageal cancer because malignant lymph nodes in this area represent metastatic disease.



**• Fig. 6.7** Aortopulmonary window. (A) The position of the echoendoscope for visualizing the aortopulmonary (AP) window. (B) On radial imaging, at 3 o'clock, the pulmonary artery (PA) is seen superior to the arch of the aorta (AO). (C) On linear imaging, the anechoic structure on the left of the screen is the PA, and the anechoic structure on the right is the AO, with arrows pointing to the left paratracheal space.



**• Fig. 6.8** Left adrenal gland. The left adrenal gland (arrows) with the typical “seagull” appearance as seen using (A) radial and (B) linear echoendoscopes. AO, Aorta; L, left.

Another alternative technique to examine the mediastinum using the linear array echoendoscope is to identify the aorta at the gastroesophageal junction. The echoendoscope is then torqued 360 degrees in a clockwise or counterclockwise direction to identify the aorta once more and then withdrawn 3 cm into the esophagus. This 360-degree torquing maneuver is continued proximally at 3-cm intervals until the upper esophageal sphincter is reached. This technique enables access to all the posterior mediastinal stations for lymph node sampling (Video 6.4).

### How to Examine the Adrenal Glands

The left adrenal gland is an important landmark in lung cancer staging. This gland can be identified in more than 95% of EUS examinations by using either of the two techniques described here.

It is easier to locate the adrenal gland with the linear scope as compared with the radial instrument. However, the technique for locating the adrenal gland is the same. The most straightforward approach involves locating the aorta at the gastroesophageal junction and then advancing the scope to the point where the celiac artery takes off. The scope is advanced along the celiac artery, and then slight clockwise torque is applied to the echoendoscope. The left adrenal gland is seen as a structure with a central “body” and two “wings” (Video 6.5). It is often described as resembling a seagull in flight. An echogenic line frequently runs in the middle of the wings (Fig. 6.8).

In the second technique the echoendoscope is advanced into the proximal stomach, and the abdominal aorta is identified just below the gastroesophageal junction. The splenic vein is then identified by advancing the transducer forward with a clockwise

rotation. The splenic hilum is found by following the splenic vein laterally. The left kidney is then imaged by advancing the scope from the splenic hilum. The left kidney is seen in cross section with a central echo-rich area representing the renal pelvis and caliceal system and a surrounding homogeneous echo-poor area representing the cortex. The left adrenal gland is found just below the splenic vein, between the left kidney and the abdominal aorta.

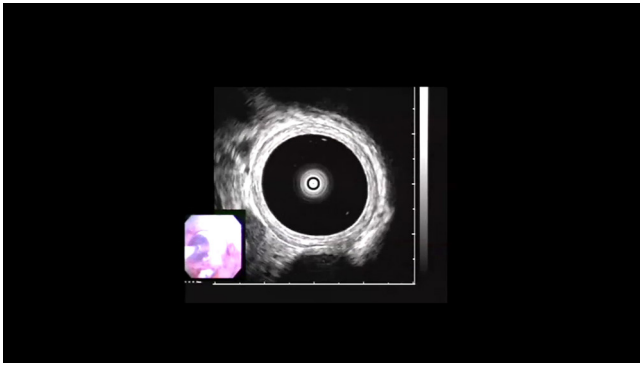
The right adrenal gland generally cannot be well visualized by EUS because it is located farther away from the stomach and is superior to the duodenal sweep. In 20% of cases, it can be seen with the transducer deep into the duodenal lumen beyond the ampulla and with morphologic characteristics similar to those of the left adrenal gland. Even when detected by EUS, the right adrenal gland usually is located deep or adjacent to the inferior vena cava, thereby making EUS-guided fine-needle aspiration difficult but not impossible.

## Summary

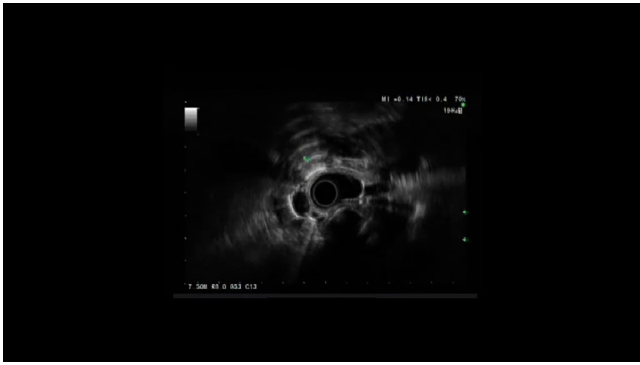
Evaluation of the mediastinum by EUS is relatively straightforward. Images obtained by the radial scanning instrument correlate very precisely with images of a CT scan. Linear images are more difficult to interpret, and successful examination of the mediastinum using a linear array echoendoscope requires a systematic approach.

## Key Reference

1. Mountain CF, Dresler CM. Regional lymph node classification for lung cancer staging. *Chest*. 1997;111:1718–1723.



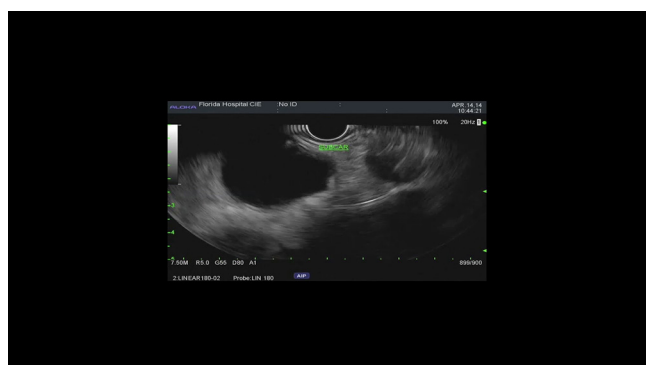
**Video 6.1** Examination of the Esophagus Using a High-Frequency Catheter Probe Passed Via a Dual-Channel Gastroscope Using the Condom Technique (With Narration)



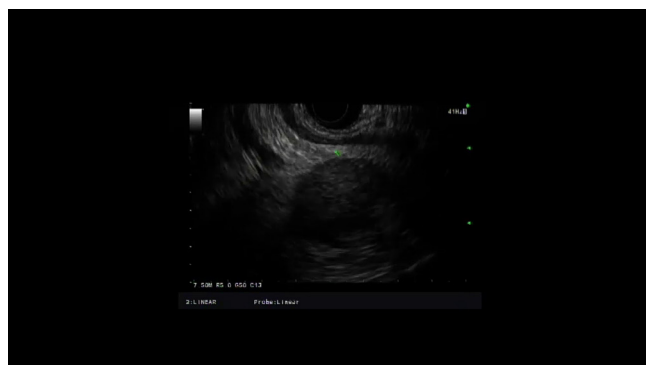
**Video 6.2** Examination of the Mediastinum Using a Radial Echoendoscope (With Narration)



**Video 6.3** Examination of the Mediastinum Using a Curvilinear Array Echoendoscope (With Narration)



**Video 6.4** The 360-Degree Torquing Technique for Evaluation of the Posterior Mediastinum Using a Curvilinear Array Echoendoscope (With Narration)



**Video 6.5** Evaluation of the Left Adrenal Gland Using a Linear Array Echoendoscope (With Narration)

# EUS and EBUS in Non-Small Cell Lung Cancer

LAURENCE MMJ CROMBAG AND JOUKE T. ANNEMA

## KEY POINTS

- Endoscopic ultrasonography (EUS)-guided fine-needle aspiration (EUS FNA) and endobronchial ultrasound-guided transbronchial needle aspiration (EBUS-TBNA) are the techniques of choice in case mediastinal nodal sampling is indicated for the diagnosis and staging of lung cancer.
- Combined endosonographic nodal staging (EUS and EBUS) improves nodal staging versus either procedure alone.
- Incorporation of endosonography in the staging algorithm for non-small cell lung cancer improves locoregional staging, reduces both the number of mediastinoscopies and unnecessary thoracotomies, and is cost-effective.
- EUS performed with the EBUS scope (EUS-B) seems similar to conventional EUS for mediastinal nodal staging.
- EUS and EBUS can diagnose intrapulmonary tumors, in case they are located adjacent to the esophagus and major airways, respectively.

## Introduction

Transesophageal endoscopic ultrasonography (EUS)-guided fine-needle aspiration (FNA) and endobronchial ultrasound (EBUS)-guided transbronchial needle aspiration (TBNA) are minimally invasive techniques for the diagnosis and staging of lung cancer. The worldwide incidence of lung cancer exceeds 1 million, and one-third of these patients present with mediastinal metastases. The stage of disease determines prognosis and treatment. In case the lung malignancy is confined to the lung and hilar lymph nodes (stage I or II, [N0/N1 disease]), surgery or stereotactic radiotherapy (SABR) with curative intent is the treatment of choice.<sup>1</sup> However, when mediastinal lymph nodes are involved (stage III, [N2/N3 disease]), combined chemoradiotherapy is usually indicated.<sup>2</sup> Patients presenting with distant metastases (stage IV) will be treated with chemotherapy or targeted therapies. Therefore accurate mediastinal staging is crucial for optimal staging and treatment planning. Computed tomography (CT) of the chest and positron emission tomography (PET) are commonly used techniques in the initial characterization of lung tumors and for the search for metastases, but these tests are insufficient for accurate mediastinal staging.<sup>3,4</sup> Additional tissue

confirmation is recommended in patients with enlarged (short axis >10 mm) and/or fluorodeoxyglucose (FDG) avid intrathoracic lymph nodes and in patients with a normal mediastinum who have an increased risk of mediastinal involvement (centrally located tumor or a primary tumor size >3 cm).<sup>4–6</sup> Starting mediastinal nodal tissue sampling by endosonography has been proven to be superior over initial surgical staging,<sup>7</sup> and therefore guidelines recommend endosonography as the technique of choice when mediastinal staging is indicated.<sup>4,6,8</sup> In this chapter the role of EUS FNA and EBUS TBNA for the diagnosis and staging of lung cancer will be evaluated. How to perform EBUS and EUS in the mediastinum will be explained with an emphasis on mediastinal nodal anatomy.

The indications for both methods are addressed (Table 7.1), as well as the concept of combined (esophageal and endobronchial) echoendoscopic staging of the mediastinum. In particular, the single scope, single operator staging approach: performing EBUS and EUS with only an EBUS scope (EUS-B) by introducing the EUS-B in the esophagus following an EBUS examination will be discussed. The position of endosonography in lung cancer staging algorithms will be addressed. In addition, tips and tricks regarding training and setting up an EBUS/EUS service will be provided.

## Endoscopic Ultrasonography-Guided Fine-Needle Aspiration for the Diagnosis and Staging of Lung Cancer

### Procedure

Conventional mediastinal EUS is performed with gastrointestinal (GI) linear echoendoscopes with the patient in a left lateral position using midazolam or propofol sedation as previously described (see Chapter 6). In addition to a mediastinal nodal evaluation, the left adrenal gland (LAG) (a predilection site of distant metastases) and primary lung tumors (in case located adjacent to the esophagus) can be evaluated. A systematic investigation is advised. Lymph nodes and abnormalities are related to specific (vascular) landmarks such as aorta, pulmonary artery, left atrium, and the liver (Fig. 7.1 EUS for lung cancer staging).

## Intrapulmonary Tumors (T) and Endoscopic Ultrasonography

Intrapulmonary tumors that are located adjacent to or near the esophagus can be visualized by EUS (Fig. 7.2).<sup>9</sup> After the primary tumor has been identified, real-time EUS-guided biopsy of the intrapulmonary lesion is possible (see Fig. 7.2). A meta-analysis

**TABLE 7.1** Indications for Endosonography for the Diagnosis and Staging of Lung Cancer

Mediastinal Lymph Nodes	EUS (B) FNA	EBUS TBNA
Paratracheal to the left	++	++
Paratracheal to the right	-	++
Aortopulmonary window	+	-
Subcarinal	++	++
Lower mediastinum	++	-
Hilar	-	++
Mediastinal restaging	+	+
FDG PET uptake in lymph node within reach	++	++
Lung tumor located adjacent to the esophagus	++	-
Lung tumor located adjacent to the trachea or main bronchi	-	++
Suspected left adrenal metastasis	++	-

++, Strong evidence; +, moderate evidence; -, no evidence; EBUS, endobronchial ultrasound; EUS, endoscopic ultrasonography; FDG, fluorodeoxyglucose; FNA, fine-needle aspiration; PET, positron emission tomography; TBNA, transbronchial needle aspiration.

showed that the average sensitivity of EUS FNA for diagnosing malignant intrapulmonary tumor is 92%.<sup>10</sup> The risk of a pneumothorax is almost negligible.

After the primary tumor has been identified, mediastinal tumor invasion (T4), (defined as invasion in the mediastinum, centrally located large vessels, or vertebrae), can be assessed (Figs. 7.3 and 7.4). CT has limited sensitivity and specificity (<75%) for mediastinal invasion,<sup>11</sup> and PET has no value in detecting T4 tumors because of its limited anatomic resolution.<sup>12</sup> A large study evaluated the diagnostic value of EUS in the assessment of mediastinal/vascular tumor invasion (T4) in non–small cell lung cancer (NSCLC) patients whom additionally underwent surgical-pathologic staging. The sensitivity, specificity, negative predictive value (NPV), and positive predictive value (PPV) of EUS for diagnosing mediastinal/great vessel invasion were 42%, 95%, 83%, and 73%, respectively. The sensitivity, specificity, NPV, and PPV of chest CT for assessing T4 status were 76%, 61%, 88%, and 41%, respectively. Importantly, the combination of EUS and CT had an excellent specificity and PPV and NPV.<sup>13</sup>

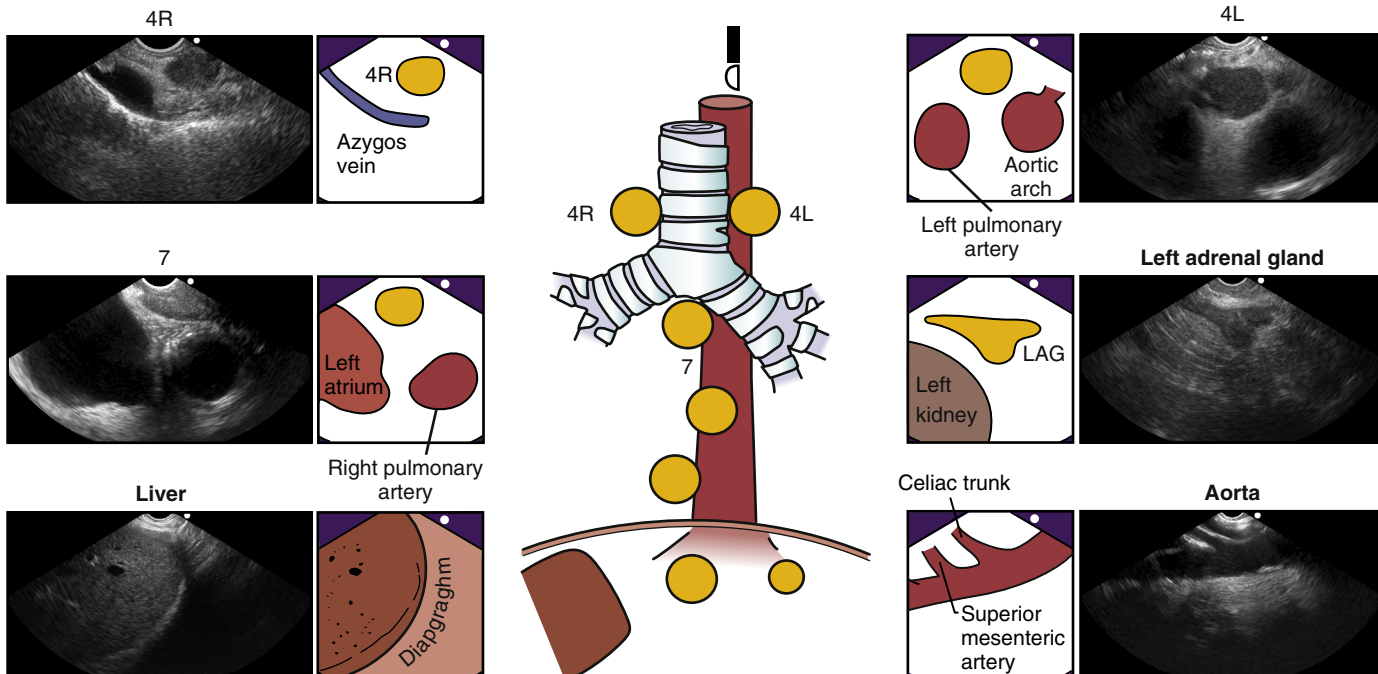
In conclusion, intrapulmonary tumors can be visualized and sampled safely by EUS FNA provided the tumors are located adjacent to the esophagus. In addition to establishing a tissue diagnosis, EUS can detect mediastinal tumor invasion, especially of vascular structures.

## Mediastinal Nodal (N) Staging and Endoscopic Ultrasonography

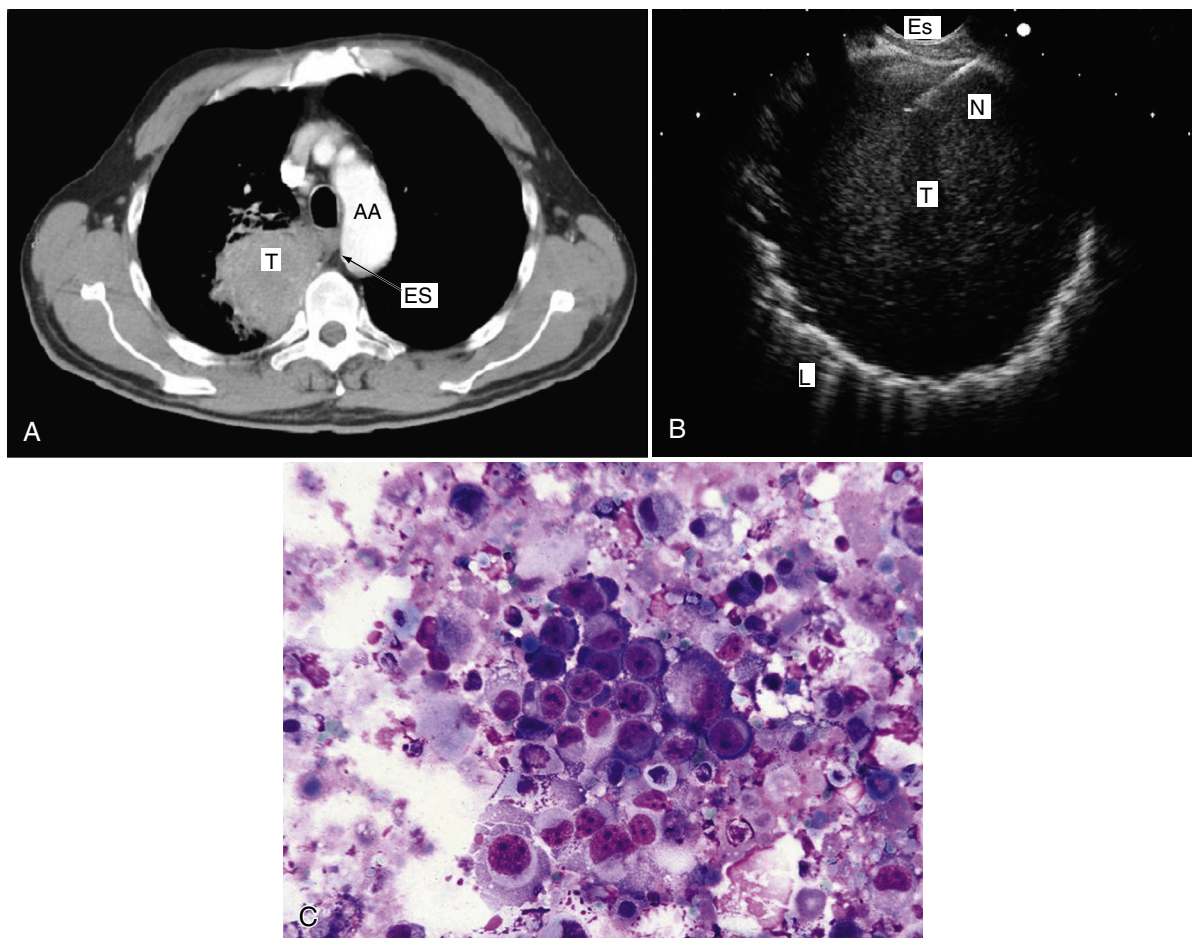
Evaluation of the mediastinum by EUS should be performed in a standardized fashion (see Chapter 6) to examine all mediastinal lymph node stations that can be detected from the esophagus (see Fig. 7.1). We strongly favor this approach above the so-called hit-and-run approach, in which only a single PET avid or enlarged node is targeted. The EUS Assessment Tool (EUSAT) can be

## EUS 6 Landmarks

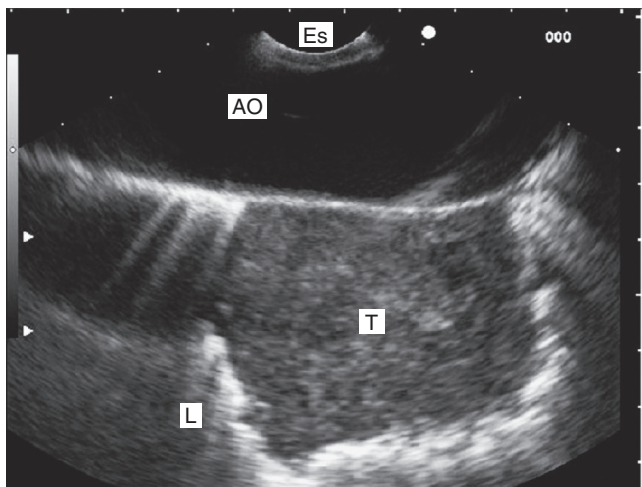
Search for the landmarks in this order:  
Liver → Abdominal aorta → Left adrenal gland → 7 → 4L → 4R



• **Fig. 7.1** The six endoscopic ultrasonography landmarks. LAG, Left adrenal gland. (Courtesy of P. Clementsen, MD, PhD.)



**• Fig. 7.2** A 53-year-old smoker with suspected lung cancer in whom bronchoscopy did not establish a diagnosis. (A) Computed tomography of the chest demonstrating an intrapulmonary tumor (*T*) in the right upper lobe located adjacent to the esophagus (*Es*). (B) Corresponding endoscopic ultrasonography fine-needle aspiration image. Notice the needle (*N*) located in the tumor (*T*). (C) Cytology of fine-needle aspirate demonstrating a squamous cell carcinoma. AA, Aortic arch; *Es*, esophagus; *L*, compromised lung tissue.



**• Fig. 7.3** Left upper lobe tumor (*T*) located adjacent to the aorta (*AO*). There are no signs of tumor invasion in the aorta (T4). *Es*, Esophagus; *L*, compromised lung tissue.

helpful for a structural assessment.<sup>14</sup> This assessment tool scores performance on the following domains: scope introduction, nodal anatomy, and safe needle handling and tissue sampling. Lymph nodes should be described in relation to the anatomic (vascular)

landmarks and given a number according to the tumor, node, metastasis (TNM) classification.<sup>15</sup> After an initial orientation, enlarged (short axis >10 mm) or sonographically suspicious nodes should be sampled for biopsy, starting with contralateral (N3) nodes before ipsilateral (N2) lymph nodes in order to prevent upstaging.

### Diagnostic Reach of Endoscopic Ultrasonography

Lymph nodes that lie adjacent to the esophagus or centrally located vessels can be visualized by EUS. These lymph nodes are located in the following regions: low paratracheal on the left (station 4 left; [Fig. 7.5](#)), aortopulmonary window (station 4 left and 5; [Fig. 7.6](#)), para-aortal (station 6; [Fig. 7.7](#)), subcarinal (station 7; [Figs. 7.8 and 7.9](#)), lower paraesophageal (station 8), and pulmonary ligamentum (station 9; [Fig. 7.10](#)). Lymph nodes located in the aortopulmonary window can be detected by EUS but sampled only in selected cases due to the interposition of the pulmonary artery. Para-aortal nodes are located on the other side of the aorta and can be well visualized by EUS (see [Fig. 7.7](#)). In carefully selected cases, these lymph nodes can be aspirated either transaortally<sup>16</sup> or by a long approach (7 to 8 cm) from the proximal esophagus to obtain a tissue

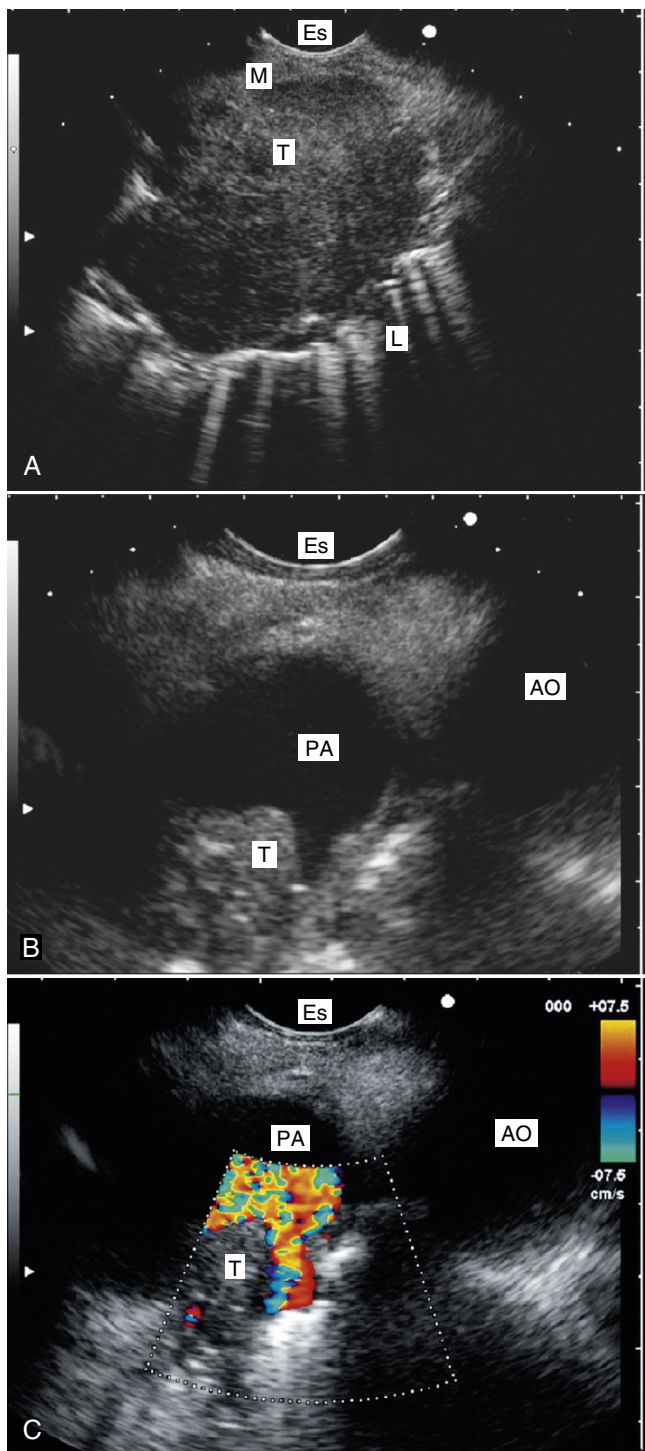


**Fig. 7.4** Large cell carcinoma. (A) Centrally located large cell carcinoma (*T*) invading the mediastinum (*M*). (B and C) Centrally located left-sided tumor (*T*) invading the pulmonary artery (*PA*), with (C) and without (B) color Doppler. *AO*, Aorta; *Es*, esophagus; *L*, compromised lung tissue.

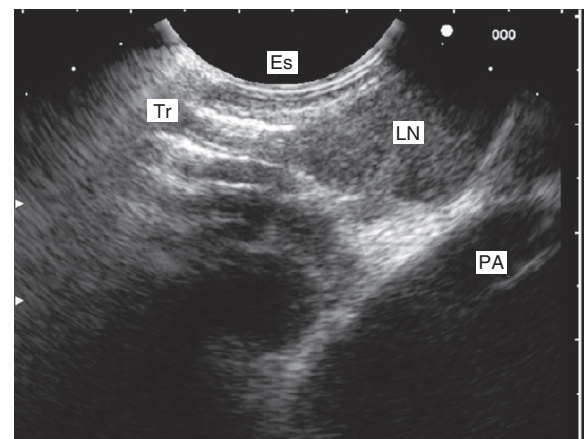


**Fig. 7.5** Lower paratracheal lymph node (*LN*) on the left (station 4L) located between the esophagus (*Es*), trachea (*Tr*), and pulmonary artery (*PA*).

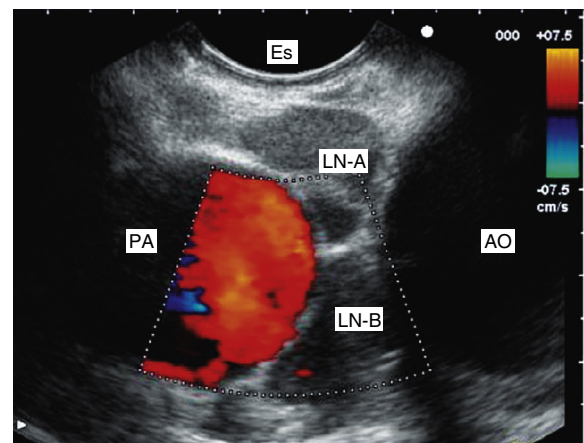


**Fig. 7.6** Left paratracheal lymph node (station 4L, *LN-A*) located between the aorta (*AO*), pulmonary artery (*PA*), and esophagus (*Es*) and the aortopulmonary node (station 5, *LN-B*).

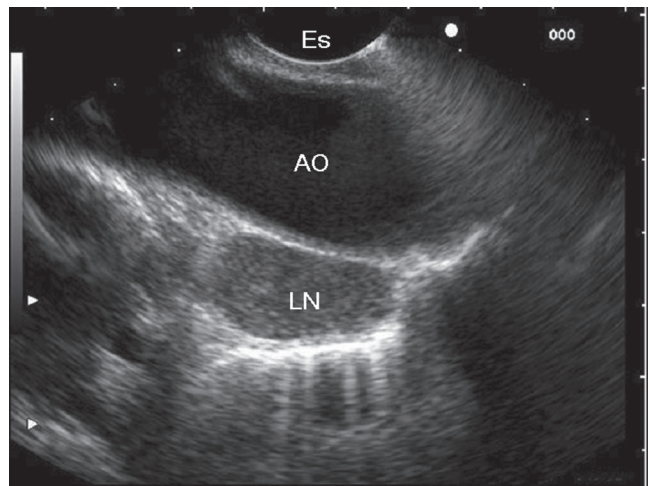


**Fig. 7.7** Lymph node (*LN*) located adjacent to the aortic arch (*AO*) (station 6). *Es*, Esophagus.

diagnosis.<sup>17</sup> Otherwise this region can be reached only by surgical methods such as mediastinotomy or video-assisted thoracoscopy (VATS). EUS has limitations in its diagnostic reach because air in the trachea and main bronchi inhibits visualization of the upper paratracheal lymph node (station 2R) and the lower paratracheal station on the right (station 4R) in most cases.

### Endoscopic Ultrasonography Versus Endoscopic Ultrasonography–Fine-Needle Aspiration

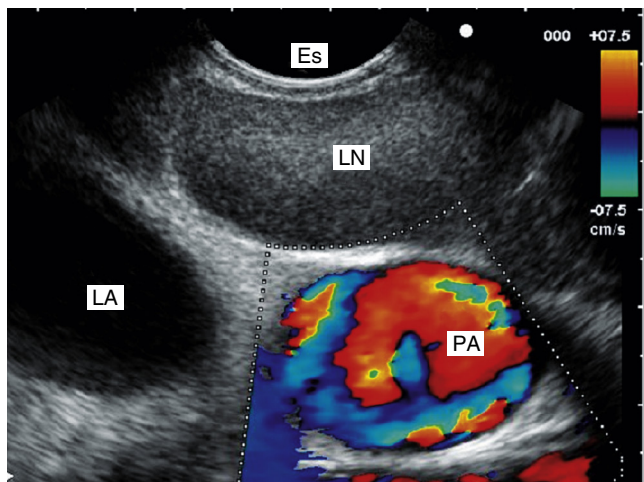
Several ultrasonographic features of mediastinal lymph nodes, such as size (short axis >10 mm), round shape, heterogeneous echogenicity, sharp distinctive margin, and coagulation necrosis sign are associated with malignant involvement.<sup>18–21</sup> However, EUS in combination with FNA is more accurate than

EUS imaging alone.<sup>22,23</sup> Therefore FNA is always required before a lymph node can be designated as malignant (Figs. 7.11 and 7.12 and Video 7.1).<sup>24</sup> For this reason, curved linear, not radial, ultrasound probes are required for mediastinal staging of NSCLC. Of the different needle sizes (19, 22, and 25 gauge) available for nodal staging, the 22 gauge is regarded as the standard size. Elastography is a technical application that depicts the mechanical properties of tissue during endosonography. An accuracy of 85% for differentiating benign from malignant mediastinal nodes has been reported.<sup>25</sup> The results are good for a noninvasive technique but remain inferior to the success rate of EUS-guided FNA.<sup>22,23</sup> The value of elastography is investigational, and this technique may be helpful in selecting target lymph nodes for biopsy.

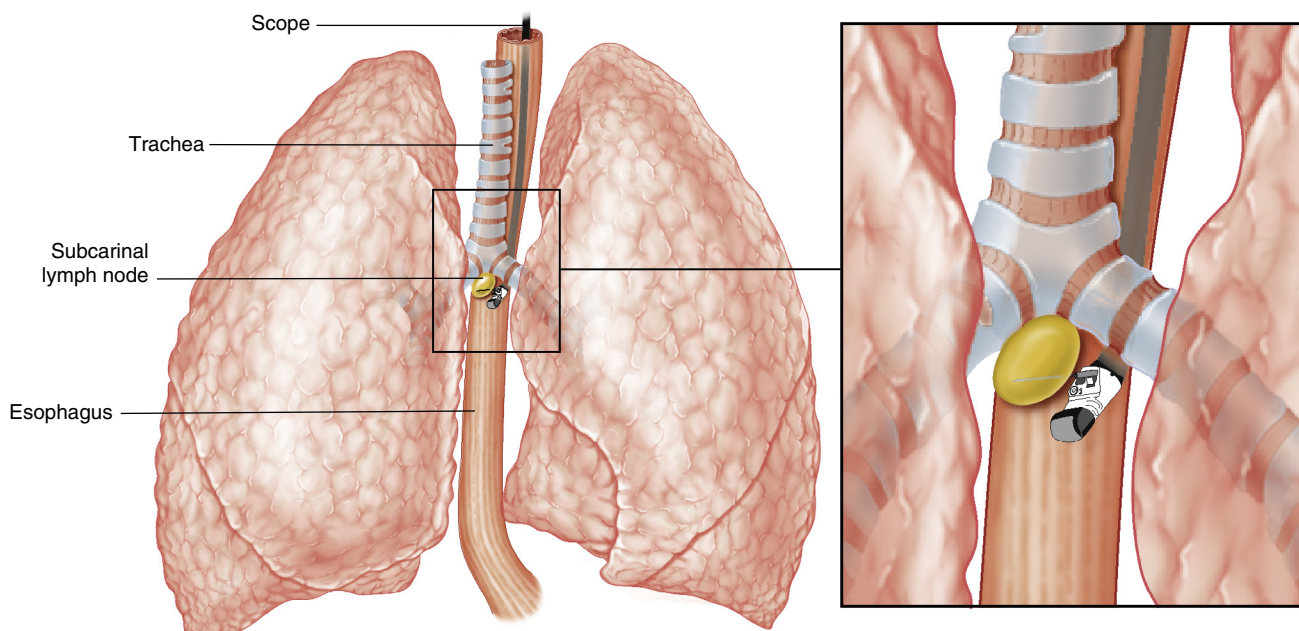
The advised number of biopsies per lymph node range from three to five passes to obtain an optimal yield.<sup>26,27</sup> The optimal sampling technique (suction/stylet use) is still under discussion. No benefit in diagnostic yield has been correlated with the position of the needle in the lymph node (central vs. peripheral) nor the application of suction.<sup>27</sup> In addition to conventional cytology evaluation, cell blocks can be made of EUS fine-needle aspirates on which immunohistochemistry and molecular analysis can be performed. EUS FNA of mediastinal lymph nodes is safe, and complications such as a mediastinitis are rare.<sup>28</sup>

### Accuracy of Mediastinal Staging (N) by Endoscopic Ultrasonography

In a meta-analysis of 18 studies of EUS FNA for the mediastinal staging of lung cancer, sensitivity was 83% (95% confidence interval [CI], 78% to 87%) and specificity was 97% (95% CI, 96% to 98%).<sup>29</sup> In those patients with enlarged lymph nodes on CT, sensitivity was 90% (95% CI, 84% to 94%). Although PPVs were reported in most studies, tumor-positive findings were verified by surgical-pathologic staging in only one study.<sup>30</sup> Although

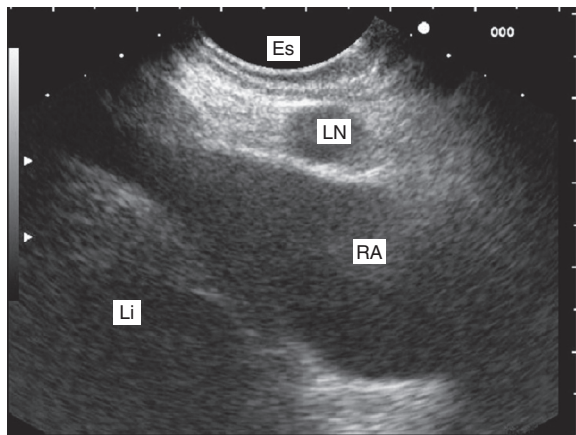


• Fig. 7.8 Subcarinal lymph node (*LN*) located between the esophagus (*Es*), pulmonary artery (*PA*), with color Doppler signal, and left atrium (*LA*).



• Fig. 7.9 Diagram showing transesophageal ultrasound-guided fine-needle aspiration of a subcarinal lymph node.

false-positive EUS FNA findings have seldom been reported, they are possible when the primary tumor is located immediately adjacent to a lymph node, a situation in which the EUS images can be misinterpreted.<sup>30</sup> Most studies are performed in selected patients with enlarged (>1 cm) mediastinal lymph nodes at CT, and therefore the results apply only to patients in that category. Few studies have focused specifically on small (short axis ≤10 mm) nodes;

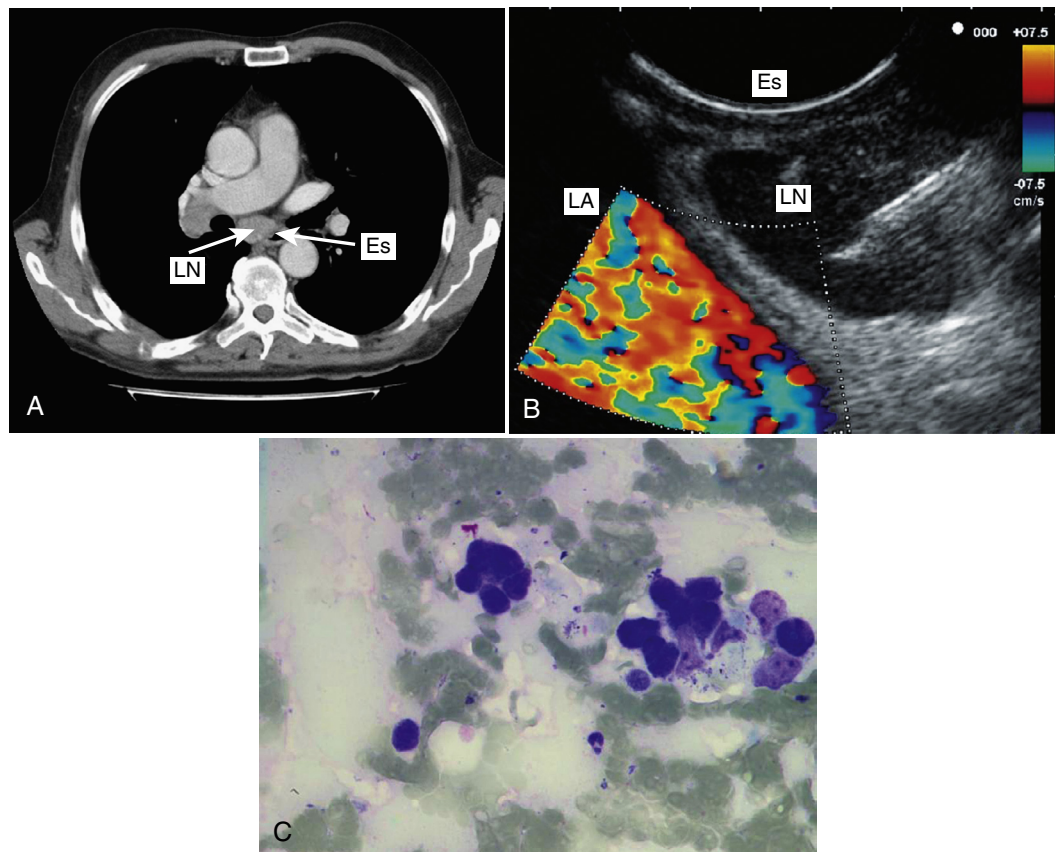


• **Fig. 7.10** Lymph node (*LN*) located in the pulmonary ligamentum (station 9). *Es*, Esophagus; *Li*, liver; *RA*, right atrium.

sensitivity has varied between 35% and 93%.<sup>31,32</sup> The pooled sensitivity in a meta-analysis for this subgroup was 58% (95% CI, 39% to 75%).<sup>29</sup>

### Distant Metastases (M1) and Endoscopic Ultrasonography

Of the common locations of distant lung cancer metastases, lesions located in the left liver lobe and (left) adrenal gland can be identified (Figs. 7.13 and 7.14) and sampled by EUS-B (Video 7.2). In patients with a LAG suspected for distant metastasis on imaging, pathologic confirmation by EUS FNA is advised<sup>6</sup> because benign LAG enlargement is common, also in a lung cancer setting. Traditionally, adrenal masses have been sampled by percutaneous biopsy. This technique has a sensitivity and NPV for adrenal biopsy of 73% and 60%, respectively, and has a considerable risk of complications.<sup>33,34</sup> In lung cancer patients with a suspected LAG on imaging, the sensitivity of EUS FNA for LAG metastasis is at least 86%.<sup>35</sup> Although technically more demanding, EUS-B has similar outcomes in comparison to conventional EUS for LAG analysis (87% vs. 83%).<sup>36</sup> Patients with disseminated lung cancer often present with liver metastases. The standard procedure for the detection of liver metastases is transabdominal ultrasonography. Investigators have reported that liver metastases can be assessed by EUS FNA using a transgastric approach.<sup>37,38</sup>



• **Fig. 7.11** A 54-year-old man with proven non–small cell lung cancer who was fit for surgical resection. (A) Computed tomography of the chest demonstrating a centrally located non–small cell lung carcinoma of the right lung and an enlarged subcarinal lymph node (*LN*). (B) Real-time endoscopic ultrasonography-guided aspiration of the subcarinal lymph node (*LN*) located between the esophagus (*Es*) and the left atrium (*LA*). (C) Cytologic appearance of a lymph node metastasis.

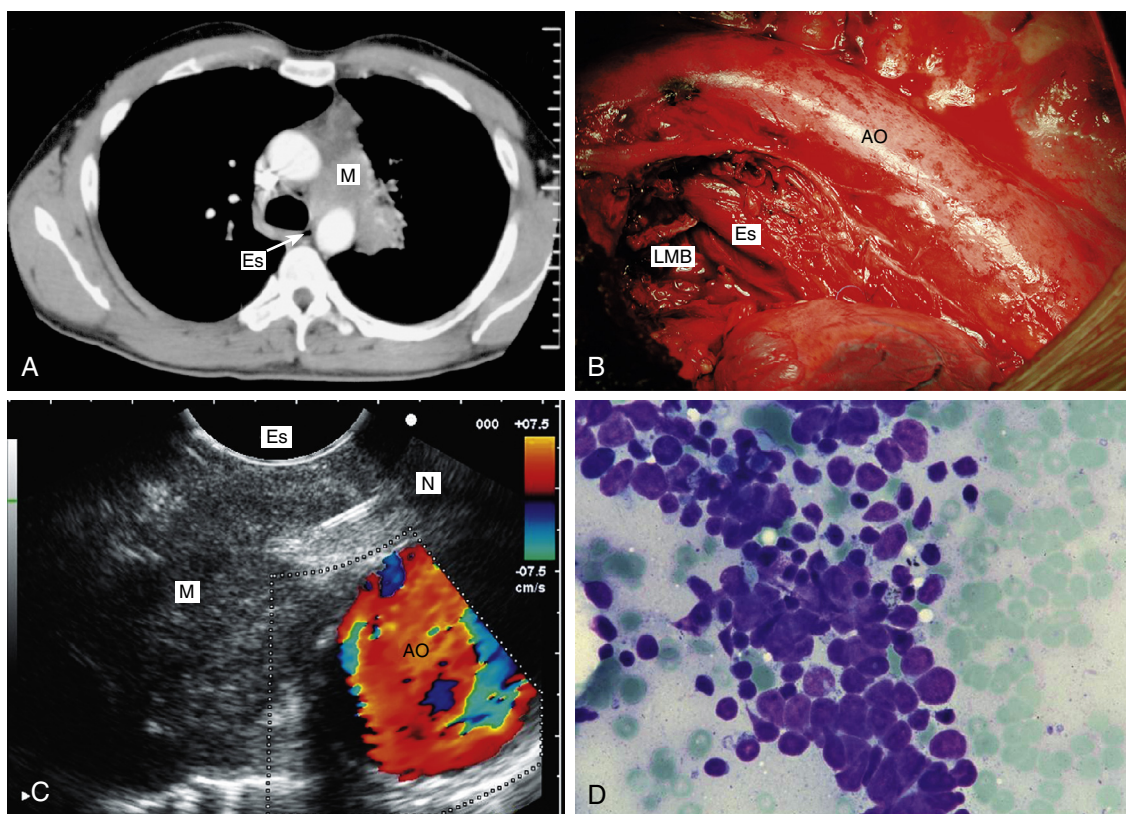


**Fig. 7.12** A 66-year-old man, heavy smoker with suspected lung cancer, in whom bronchoscopy was nondiagnostic. (A) Computed tomography of the chest demonstrating a mass (*M*) in the aortopulmonary window. (B) In another patient just after left-sided pneumonectomy, the close relationship is seen between the esophagus (*Es*) and the aortopulmonary window. (C) Corresponding EUS image with fine-needle aspiration of the mass (*M*) located between the esophagus (*Es*) and the aorta (*AO*) (with color Doppler). *LMB*, Left main bronchus; *N*, needle. (D) Cytologic appearance of small cell carcinoma.

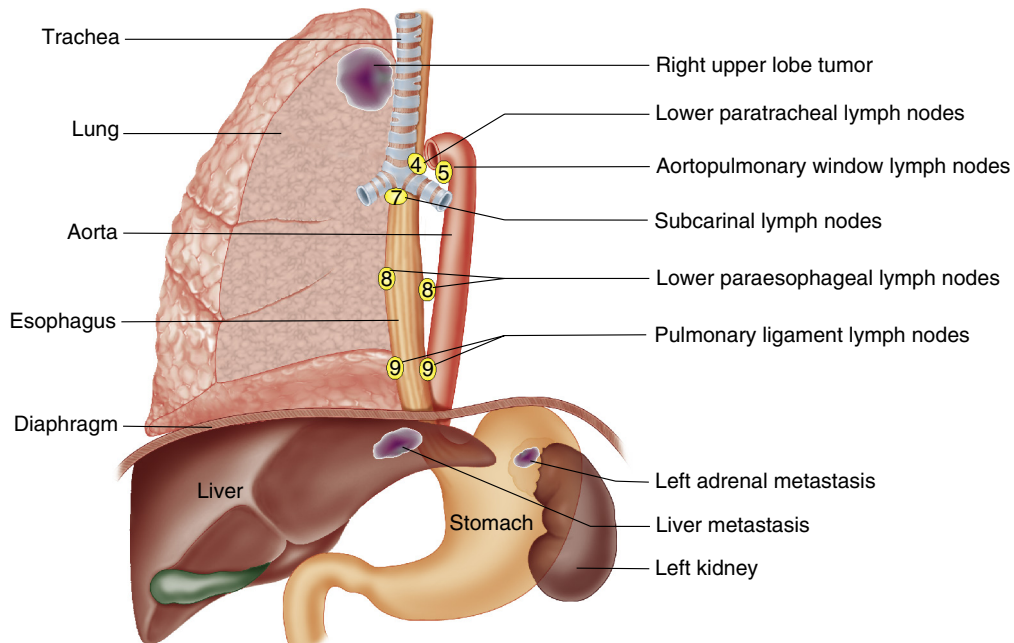
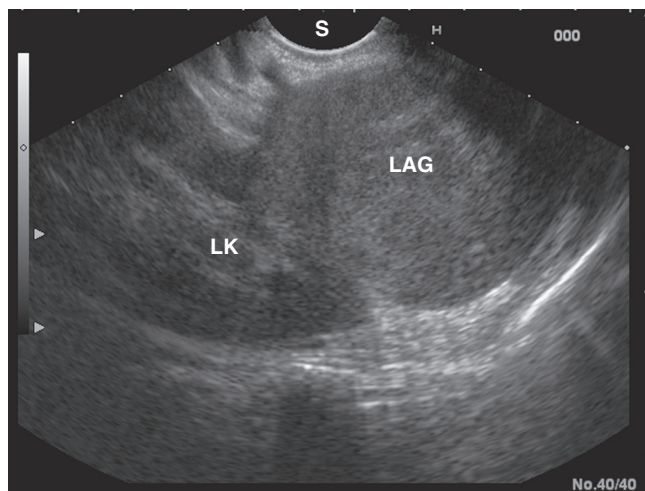
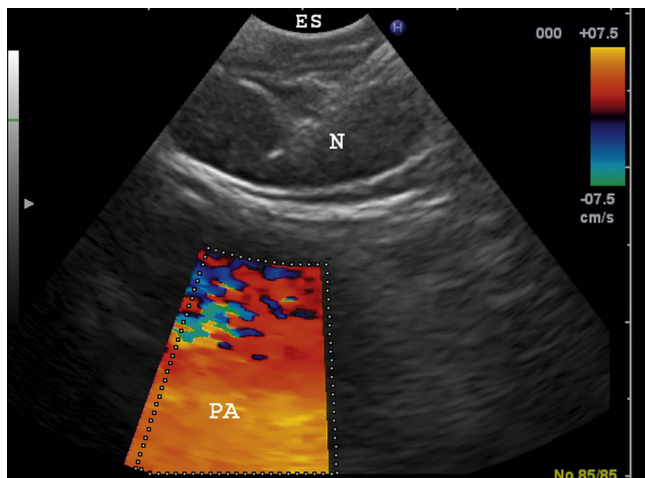


**Fig. 7.13** Endoscopic ultrasonography (EUS) fine-needle aspiration (FNA) in non-small cell lung cancer. EUS FNA in non-small cell lung cancer can sample intrapulmonary tumors and detect mediastinal tumor invasion (T4), assess mediastinal lymph nodes, and identify distant metastases located in the left liver lobe and left adrenal gland.



• **Fig. 7.14** Transgastric endoscopic ultrasonography image of the left kidney (LK) and metastatic involvement of the left adrenal gland (LAG). S, Stomach.



• **Fig. 7.15** Endoscopic ultrasonography (EUS) fine-needle aspiration of a subcarinal lymph node (station 7) with an endobronchial ultrasound scope. Notice the smaller ultrasound range in comparison with an investigation with a conventional EUS scope (see Fig. 7.7). ES, Esophagus; N, needle; PA, pulmonary artery.

## Endoscopic Ultrasound Using the Endobronchial Ultrasound Scope

EUS can also be performed with an EUS-B. Typically, this is done following an endobronchial (EBUS) procedure in the same setting by the same operator, with patient in supine position.<sup>39,40</sup> After the endobronchial procedure the EUS-B is retracted from the airways above the vocal cords and subsequently gently introduced into the esophagus. As during a conventional EUS procedure, a systematic evaluation of the lymph nodes adjacent to the esophagus, liver, and LAG can be performed (Video 7.4) using the EUSAT.<sup>14</sup> Even though the conventional EUS scope is more stable as a result of the increased tube diameter and has a wider scanning angle (field of view 120 to 180 degrees compared with 60 degrees of the EBUS), there seems to be no difference in yield between conventional EUS and EUS-B for mediastinal nodal staging (Fig. 7.15).<sup>41</sup> In addition, the LAG can be detected and sampled with the EUS-B.<sup>36,42</sup> By using only the EUS-B, complete mediastinal, hilar, and LAG staging can be performed in a single endoscopy procedure with one operator. This single scope single operator staging strategy is likely to reduce patient burden and seems to be cost-effective.

## Endobronchial Ultrasound-Guided Transbronchial Needle Aspiration for the Diagnosis and Staging of Lung Cancer

EBUS enables visualization of intrapulmonary lesions, mediastinal and hilar lymph nodes, and mediastinal masses located adjacent to the main airways (Fig. 7.16). Similar to EUS in gastroenterology, EBUS development started with radial probes. With radial EBUS, lesions can be detected but not (yet) sampled under real-time ultrasound control. Radial EBUS is mainly used for the detection of peripheral lung lesions that can subsequently be sampled using fluoroscopy or guide sheets. Linear EBUS, commercially available since 2004, enables real-time controlled sampling of mediastinal or hilar nodes and centrally located lung tumors, similar to EUS FNA. In this chapter, only linear EBUS applications for the diagnosis and staging of lung cancer are discussed.

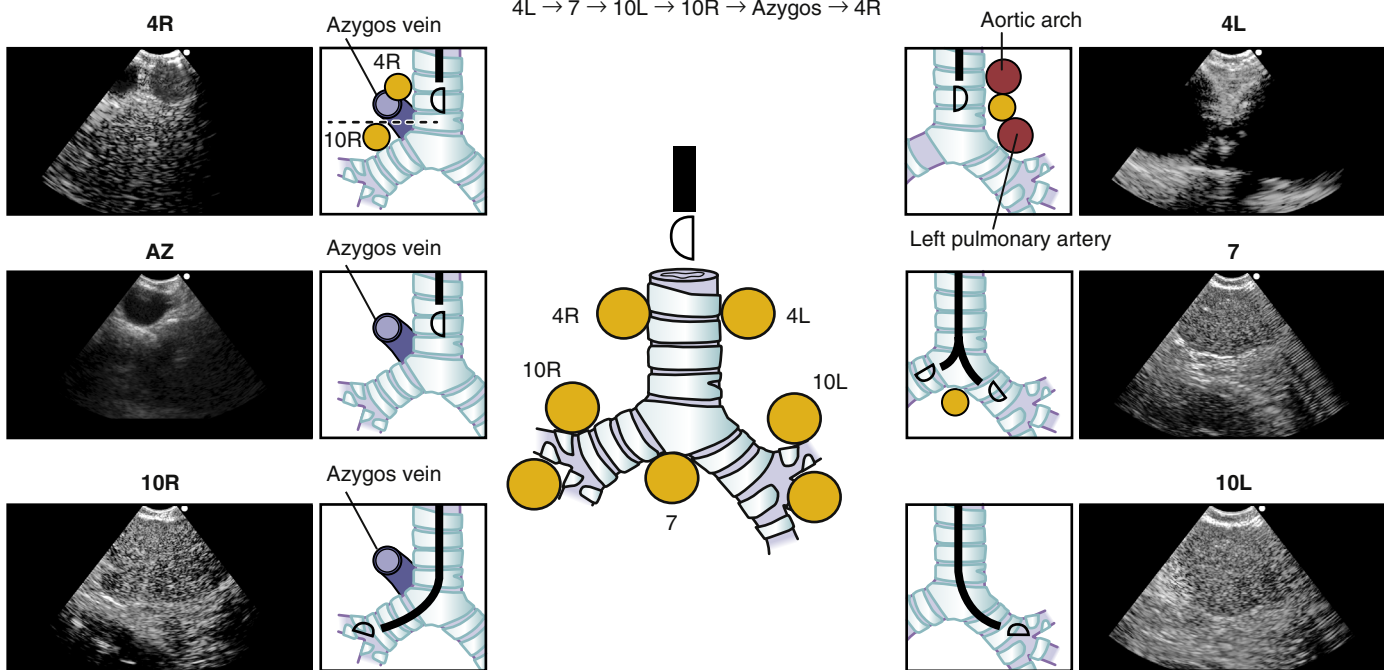
### Endobronchial Ultrasound Procedure

Linear EBUS scopes (Olympus XBF UC 160 F, Fujinon EB-530 US, Pentax EB 1970 UK; Fig. 7.17) are modified bronchoscopes with an electronic linear ultrasound transducer (scanning range, 5 to 12 MHz) integrated in the distal end of the scope. A light source is also available and is positioned at a 10- to 30-degree angle. EBUS investigations are commonly performed with the patient under conscious sedation using low-dose midazolam or propofol sedation. The examination takes approximately 15 to 20 minutes. Before endoscopy, the pharynx is sprayed with lidocaine, and often codeine is administered to suppress the cough reflex. Patients are investigated lying in a supine position, and the scope is introduced orally into the trachea. During an EBUS investigation, both white optical light and transbronchial ultrasound images are available. With the endobronchial view, the position of the EBUS scope in the tracheobronchial tree is evident (Fig. 7.18). When the ultrasound transducer is directed toward the airway mucosa, lymph nodes adjacent to the airway wall can be visualized (Fig. 7.19). Optionally, a water-filled balloon can be attached to the ultrasound head to increase contact. During visualization of the lymph nodes, the endoscopic view is often limited because of the close proximity of the optical source to the airway wall (see Fig. 7.19). After positioning a sheet that protects the working channel of the scope from the needle, lymph nodes can be aspirated in a real-time controlled fashion (see Fig. 7.19 and Video 7.5). There is no evidence of any benefit derived from applying suction to EBUS-guided biopsies for adequacy, diagnosis, or quality between these sample techniques.<sup>43</sup> Three needle passes are advised for an optimal yield.<sup>44</sup> Twenty-two-gauge needles are standard—19- and 25-gauge needles are also available. EBUS-related complications are very rare.<sup>45</sup>

### Diagnosing Intrapulmonary Tumors (T) by Endobronchial Ultrasound

In patients with a centrally located lung tumor after a nondiagnostic bronchoscopy, a CT-guided lung biopsy is often unattractive, given the close proximity of the tumor to centrally located vessels that pose an increased risk of pneumothorax and hemoptysis. Intrapulmonary tumors that are located immediately adjacent to the trachea or the main bronchi can be visualized (Fig. 7.20) and sampled by EBUS TBNA. In these patients, EBUS has a high diagnostic accuracy<sup>46,47</sup> and the risk of a pneumothorax is neglectable.

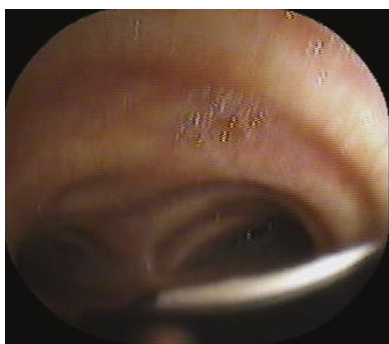
## EBUS 6 Landmarks



• Fig. 7.16 The six endobronchial ultrasound landmarks. (Courtesy of P. Clementsen, MD, PhD.)



• Fig. 7.17 Convex endobronchial ultrasound Pentax EB 1970 UK scope.

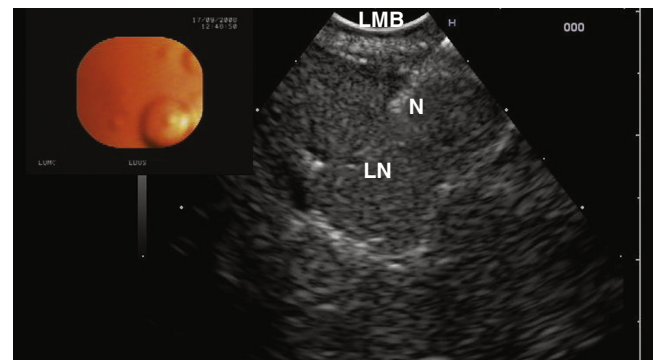


• Fig. 7.18 Optical image during endobronchial ultrasound demonstrating the position of the endoscope in the distal trachea. The main carina and ostia of the left and right main bronchi can be seen. Notice the white line at the bottom end of the image representing the ultrasound head of the scope.

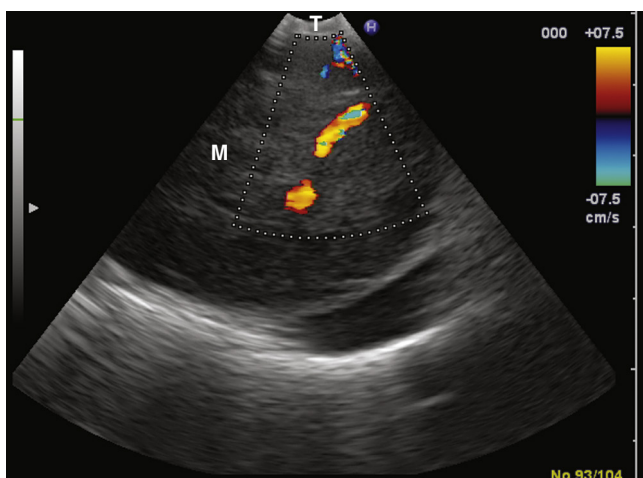
## Nodal Staging (N) by Endobronchial Ultrasound

Mediastinal nodal sampling is the major indication for EBUS TBNA (Video 7.3). Mediastinal lymph nodes that can be reached are located adjacent to the trachea (above the level of the aortic arch, stations 2L and 2R; below the aortic arch, stations 4L and 4R; Figs. 7.21 and 7.22) or main bronchi (station 7, which can be reached from both the left and right main bronchi). With the experimental elastography technique, the stiffness of a node can be assessed (Fig. 7.23). Whether elastography influences the biopsy procedure or diagnostic yield is under investigation. It is of critical importance that the lymph nodes identified by EBUS are given the appropriate number according to the revised eighth edition of the TNM classification to prevent understaging or overstaging.<sup>15</sup>

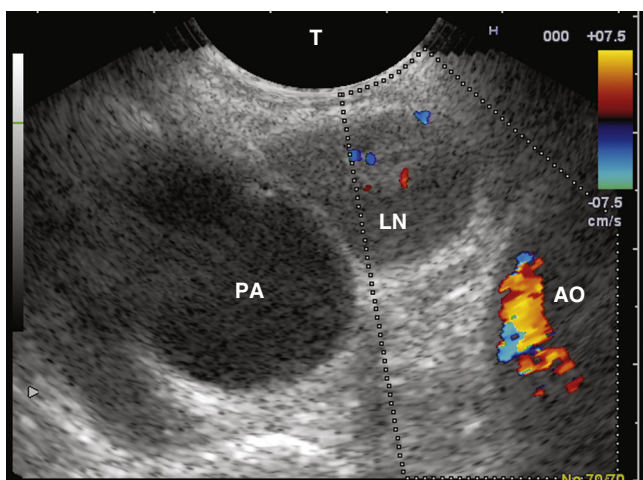
A systematic nodal examination (see Video 7.5) is to be preferred over a so-called hit and run approach in which



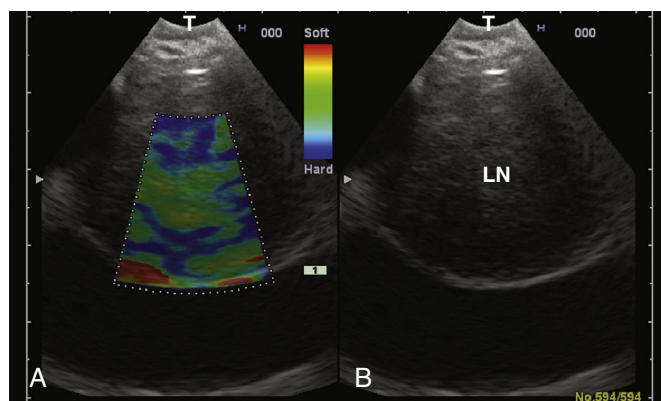
• Fig. 7.19 Real-time endobronchial ultrasound transbronchial needle aspiration of a subcarinal lymph node (station 7). Notice that when contact between the ultrasound transducer and the airway mucosa is made, the optical image disappears (left upper corner). LMB, Position of the endoscope in the left main bronchus; LN, lymph node; N, needle.



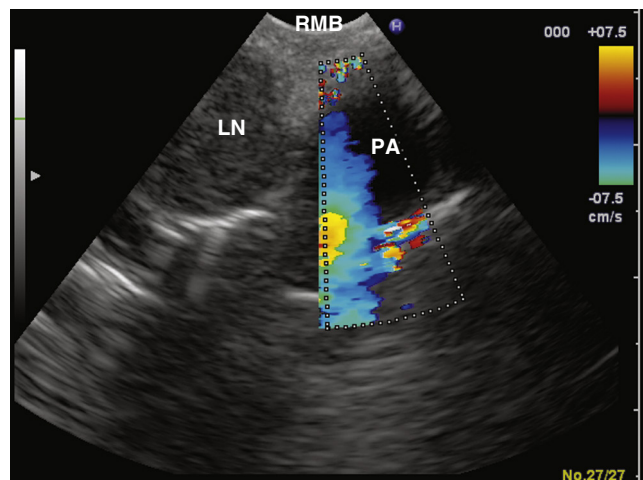
• **Fig. 7.20** Adenocarcinoma (*M*) of the right upper lobe detected by endobronchial ultrasound from the trachea (*T*). Note the vessel running through the intrapulmonary tumor.



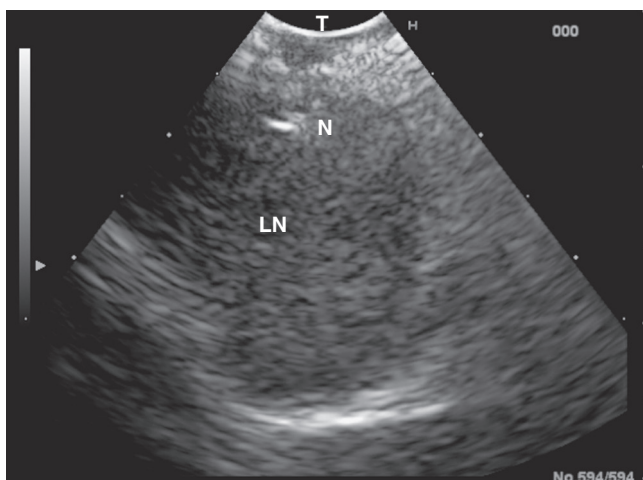
• **Fig. 7.21** Endobronchial ultrasound (EBUS) image of a left paratracheal lymph node (*LN*) (station 4L) detected by EBUS from the trachea (*T*). *AO*, Aorta; *PA*, pulmonary artery.



• **Fig. 7.23** Enlarged right-sided lower paratracheal node. Endobronchial ultrasound image (B) of an enlarged right-sided lower paratracheal node (station 4R). The blue color at elastography (A) shows the increased stiffness of the nodal tissue.



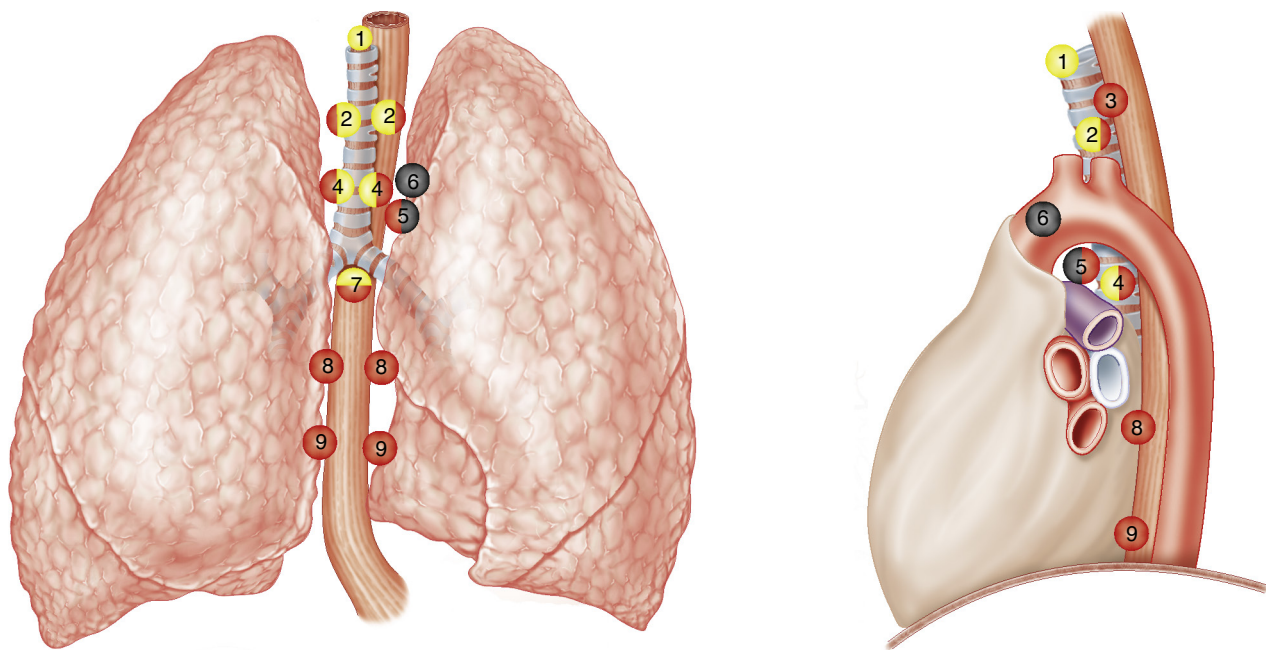
• **Fig. 7.24** Endobronchial ultrasound image of intrapulmonary node (*LN*) on the right detected from the right upper lobe carina (station 11R). The Doppler signal demonstrates a branch from the pulmonary artery (*PA*). *RMB*, Position of the scope in the right main bronchus.



• **Fig. 7.22** Endobronchial ultrasound transbronchial needle aspiration image of a paratracheal node (*LN*) on the right (station 4R). *N*, Needle; *T*, position of the scope in the trachea.

selectively the FDG avid or enlarged is sampled. The EBUS Assessment Tool (EBUSAT) can be helpful for a structural assessment.<sup>48</sup> This assessment tool scores performance on nodal anatomy and technical skills such as scope introduction, needle handling, and tissue sampling. Meta-analyses on EBUS for mediastinal staging show a sensitivity in detecting mediastinal nodal metastases (N2/N3 disease) ranging from 72% to 93%.<sup>4,49–51</sup> The range is probably caused by variability in patient and study characteristics (e.g., prevalence of mediastinal metastases).

EBUS is also the technique of choice for sampling lymph nodes located in the hilum of the lung (out of reach of the surgeon/mastostomy) and has a sensitivity of 91% in case the patient has either enlarged or FDG PET-active hilar nodes (Fig. 7.24; Video 7.6).<sup>52</sup> EBUS TBNA is commonly used as both a diagnostic and staging modality. This requires obtaining sufficient material not only for identification of malignant cells but also for subtyping and molecular testing.<sup>53</sup>



• Fig. 7.25 Mediastinal staging techniques and their diagnostic reach. Black ball, Within reach of mediastinotomy or video-assisted thoracoscopy; red ball, within reach of endoscopic ultrasonography; yellow ball, within reach of endobronchial ultrasound and mediastinoscopy.

## Combined Nodal Staging (Endobronchial Ultrasound + Endobronchial Ultrasound Scope)

EUS and EBUS are complementary techniques in their diagnostic reach (Fig. 7.25). In combination, EUS FNA and EBUS TBNA can reach most mediastinal and hilar nodal stations.<sup>54–57</sup> EBUS has access to the paratracheal zones (stations 2R, 4R, 2L, 4L), and EUS reaches the lower mediastinum (stations 8 and 9; see Fig. 7.1). The subcarinal area (station 7) and the left paratracheal station 4L can be reached by both methods. Complete echoendoscopic staging of the mediastinum can be performed with a single EUS-B.<sup>39,58</sup>

A systematic review of the added value and diagnostic accuracy of the combined use of EBUS and EUS-B in detecting mediastinal nodal metastases (N2/N3 disease) showed that the combined use of EBUS and EUS-B leads to a significant increase in sensitivity and detection rate compared with either test alone.<sup>51</sup> Performing EUS-B after EBUS increases sensitivity for detecting mediastinal nodal metastases by 12% and by performing an EBUS procedure after an EUS-B procedure sensitivity increased by 22%.<sup>51</sup> Therefore the most recent lung cancer staging guideline (2016) “Combined endobronchial and esophageal endosonography for the diagnosis and staging of lung cancer,” endorsed by the European Society of Gastrointestinal Endoscopy (ESGE), the European Respiratory Society (ERS), and the European Society of Thoracic Surgeons (ESTS), recommends the combination EBUS TBNA and EUS-B FNA over either test alone.<sup>6</sup>

## Endobronchial Ultrasound Versus Endoscopic Ultrasonography Versus Surgical Staging

All available biopsy techniques have a different diagnostic reach, and, unfortunately, none can sample all mediastinal N2/N3 lymph node stations. For the various sampling techniques,

sensitivity and specificity are regularly based on the specific area that can be reached by the technique under investigation and not on the mediastinum as a whole. EUS and EBUS have a complimentary diagnostic reach (see Fig. 7.25) and an overlap in left paratracheal (4L) and subcarinal region (7). When EUS and EBUS are combined, virtually all mediastinal nodal stations can be investigated. The strength of endosonography is the minimally invasive confirmation of mediastinal lymph node metastases or mediastinal tumor invasion. In case both EBUS and EUS can reach the target nodes, EUS FNA has the advantage of comparable tolerance with fewer doses of anesthetics and sedatives, a shorter procedure time, and fewer oxygen desaturations during the procedure compared with EBUS TBNA.<sup>59</sup>

Surgical staging, mediastinoscopy, and VATS are more invasive in comparison with endosonography, yet has the advantage of taking large biopsies. Mediastinoscopy has a similar diagnostic range as EBUS: upper and lower paratracheal (stations 2L, 4L, 2R, 4R) and subcarinal (station 7) nodes and has a sensitivity of 79% for mediastinal nodal metastases.<sup>7</sup> VATS has been shown to be more accurate than EUS FNA for lymph nodes located in stations 5 and 6 (Table 7.2).<sup>60</sup>

## Position of Endoscopic Ultrasonography and Endobronchial Ultrasound in Lung Cancer Staging Algorithms

Guidelines recommend needle-based techniques as initial, invasive, nodal staging modality in lung cancer patients.<sup>4,6,8</sup> In case the clinical suspicion of mediastinal involvement remains high after a negative result using a needle-based technique, surgical staging should be considered.<sup>4,6</sup> Factors associated with higher

**TABLE 7.2 RCTs Comparing Operating Characteristics of Endosonography Versus Mediastinoscopy and Surgical Staging in Mediastinal Staging of Lung Cancer**

RCT	No. of Patients	Sensitivity Endosonography (EUS and/ or EBUS) for Mediastinal Metastasis	Sensitivity of MS/Surgical Staging	NPV Endosonography	NPV Surgical Staging	Complication Rate Endosonography	Complication Rate Surgical Staging
Tournoy et al., 2008 <sup>69</sup>	40	93% (95% CI: 66%–99%)	73% (95% CI: 39%–93%)	83% (95% CI 35%–99%)	73% (95% CI 39%–93%)	0%	5%
Annema et al., 2010 <sup>7</sup>	241	85% (95% CI: 74%–92%)	79% (95% CI: 66%–88%)	85% (95% CI, 75%–92%)	86% (95% CI, 76%–92%)	1%	6%

CI, Confidence interval; EBUS, endobronchial ultrasound; EUS, endoscopic ultrasonography; MS, mediastinoscopy; NPV, negative predictive value; RCT, randomized controlled/clinical trial.

risk of mediastinal lymph node involvement (EBUS lymph node characteristics, FDG avidity, etc.) should be taken into account for this decision.<sup>61</sup> It has been reported that a surgical staging procedure after a negative endosonography is beneficial for patients with an abnormal mediastinum, and not a normal mediastinum.<sup>62</sup> Under which circumstances confirmatory surgical staging after a negative endosonography can be omitted is subject of investigation.

Implementation of endosonography in local lung cancer staging protocols obviously depends on the availability and expertise of EUS and EBUS and its practitioners, the presence of imaging modalities such as integrated CT PET, and surgical expertise. EUS and EBUS are positioned early in diagnostic and staging algorithms for NSCLC, especially in those patients with a high pretest probability of mediastinal disease.

In hospitals that have access to both endosonography and integrated CT PET scanning, the following strategy is proposed for patients with (suspected) lung cancer who are candidates for surgical resection: PET CT followed by bronchoscopy, combined with EBUS (and EUS-B) in patients with centrally located tumors or enlarged (>1 cm) or PET-positive mediastinal lymph nodes. Confirmatory surgical staging by mediastinoscopy is advised in case EUS or EBUS do not provide proof of mediastinal metastasis or tumor invasion. Ideally, conventional bronchoscopy and EBUS/EUS(B) are performed in a single session under optimal sedation with on-site cytologic evaluation (Fig. 7.26).

In patients with a peripherally located tumor without enlarged or FDG-positive mediastinal lymph nodes, thoracotomy can be performed directly following bronchoscopy because the probability of mediastinal metastases is very low.<sup>63</sup>

In centers without access to PET, it is recommended to perform EBUS and/or EUS based on CT scan of the chest.

## Training and Competency

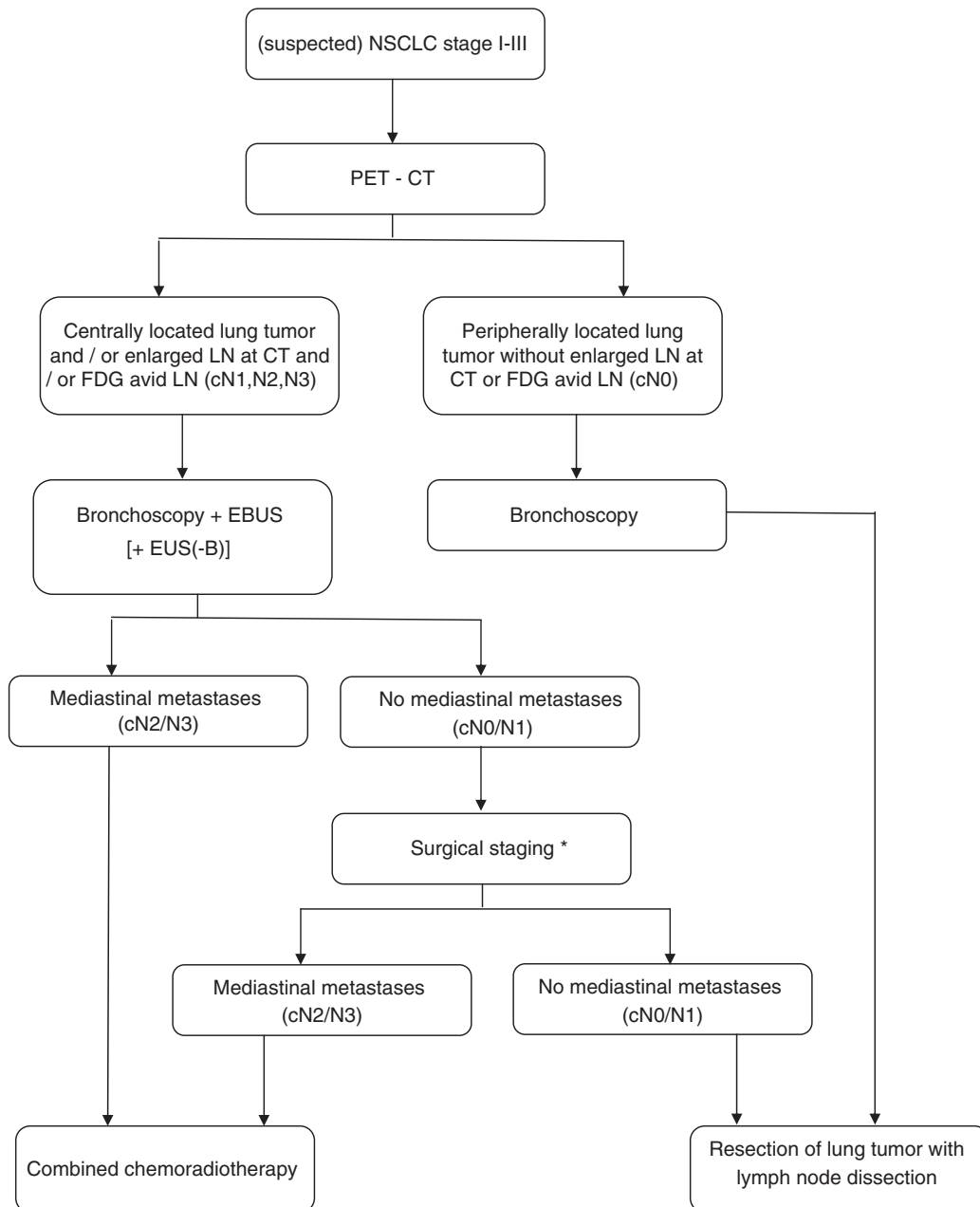
The quality and safety of endosonography is dependent on the skills and experience of the operator and the endoscopy team. Good cooperation with (cyto)pathologists is key for optimal results. Diagnostic yield improves with practice, and the number of complications is associated with operator experience.<sup>64</sup>

In a randomized controlled trial, virtual reality simulator EBUS training was shown to be more effective than traditional apprenticeship EBUS training.<sup>48</sup> Therefore it is recommended that new trainees in endosonography follow a structured training curriculum including theory and simulation-based training followed by supervised practice on patients. Ideally competency assessment using validated tools should be part of such programs.<sup>6</sup> The ERS has developed a structured training program to train qualified doctors to be able to independently and competently perform EBUS. This is a three-part training program (I: theory; II: clinical and simulation training; III: supervised training) that will ensure that participants have all the necessary knowledge and skills required to obtain ERS certification in EBUS.<sup>65</sup>

The fact that gastroenterologists are not generally familiar with lung cancer staging, and chest physicians are not used to performing EUS-B, may be a barrier for implementation of the combined EBUS EUS-B strategy. However, it has been shown that with a dedicated training and EUS implementation strategy, chest physicians can obtain similar results as achieved by experts.<sup>66</sup> Although the safety record of endosonography is impressive, monitoring for complications during these interventional techniques is recommended. A quality indicator for any endosonography service is the false-negative rate. This should be evaluated on a regular basis.

## Future Perspectives

Linear EBUS/EUS is regarded as one of the most important innovations since the invention of flexible bronchoscopy 50 years ago. In a little more than a decade, endosonography has been positioned as the first line diagnostic tissue staging procedure for lung cancer. Investments in equipment, needles, training, and cytopathologic expertise are requirements for a successful endosonography service. Training and (simulation-based) learning will be important. Future studies will shed further light on optimal needle handling and tissue processing. The development of “smart” needles, including needle-based confocal laser endomicroscopy (nCLE), might be beneficial to reduce the false-negative rate.<sup>67,68</sup> The current challenge will be to implement EBUS/EUS-B on a global scale.



\*When motivated confirmatory surgical staging can be omitted in selected cases (see also text)

- **Fig. 7.26** Proposed role of endoscopic ultrasonography (EUS) fine-needle aspiration and endobronchial ultrasound (EBUS) transbronchial needle aspiration in the mediastinal staging of non-small cell lung cancer (NSCLC) (with availability of positron emission tomography [PET]). CT, Computed tomography; FDG, fluorodeoxyglucose; LN, lymph node.

## Key References

4. Silvestri GA, Gonzalez AV, Jantz MA, et al. Methods for staging non-small cell lung cancer: diagnosis and management of lung cancer. 3rd ed: American College of Chest Physicians evidence-based clinical practice guidelines. *Chest*. 2013;143:e211S–e250S.
6. Vilman P, Clementsen PF, Colella S, et al. Combined endobronchial and esophageal endosonography for the diagnosis and staging of lung cancer: European Society of Gastrointestinal Endoscopy (ESGE) guideline, in cooperation with the European Respiratory Society (ERS) and the European Society of Thoracic Surgeons (ESTS). *Endoscopy*. 2015;47:c1.
7. Annema JT, van Meerbeeck JP, Rintoul RC, et al. Mediastinoscopy vs endosonography for mediastinal nodal staging of lung cancer: a randomized trial. *JAMA*. 2010;304:2245–2252.
36. Crombag LMMJ. EUS-B-FNA vs conventional EUS-FNA for left adrenal gland analysis in lung cancer patients. In: Artur Szlubowski JAS, Schuurbiers O, Korevaar DA, Bonta PI, Annema JT, eds. *Lung Cancer*. 2017.
51. Korevaar DA, Crombag LM, Cohen JF, et al. Added value of combined endobronchial and oesophageal endosonography for mediastinal nodal staging in lung cancer: a systematic review and meta-analysis. *Lancet Respir Med*. 2016;4:960–968.

## References

Access the reference list online at [ExpertConsult.com](#).

## References

1. Howington JA, Blum MG, Chang AC, et al. Treatment of stage I and II non-small cell lung cancer: diagnosis and management of lung cancer, 3rd ed: American College of Chest Physicians evidence-based clinical practice guidelines. *Chest*. 2013;143:e278S–e313S.
2. Rarnath N, Dilling TJ, Harris LJ, et al. Treatment of stage III non-small cell lung cancer: diagnosis and management of lung cancer, 3rd ed: American College of Chest Physicians evidence-based clinical practice guidelines. *Chest*. 2013;143:e314S–e340S.
3. Schmidt-Hansen M, Baldwin DR, Hasler E, et al. PET-CT for assessing mediastinal lymph node involvement in patients with suspected resectable non-small cell lung cancer. *Cochrane Database Syst Rev*. 2014;Cd009519.
4. Silvestri GA, Gonzalez AV, Jantz MA, et al. Methods for staging non-small cell lung cancer: diagnosis and management of lung cancer, 3rd ed: American College of Chest Physicians evidence-based clinical practice guidelines. *Chest*. 2013;143:e211S–e250S.
5. De LP, Dooms C, Kuzdzal J, et al. Revised ESTS guidelines for preoperative mediastinal lymph node staging for non-small-cell lung cancer. *Eur J Cardiothorac Surg*. 2014;45:787–798.
6. Vilman P, Clementsen PF, Colella S, et al. Combined endobronchial and esophageal endosonography for the diagnosis and staging of lung cancer: European Society of Gastrointestinal Endoscopy (ESGE) guideline, in cooperation with the European Respiratory Society (ERS) and the European Society of Thoracic Surgeons (ESTS). *Endoscopy*. 2015;47:c1.
7. Annema JT, van Meerbeeck JP, Rintoul RC, et al. Mediastinoscopy vs endosonography for mediastinal nodal staging of lung cancer: a randomized trial. *JAMA*. 2010;304:2245–2252.
8. Vansteenkiste J, De RD, Eberhardt WE, et al. Early and locally advanced non-small-cell lung cancer (NSCLC): ESMO Clinical Practice Guidelines for diagnosis, treatment and follow-up. *Ann Oncol*. 2013;24(suppl 6):vi89–vi98.
9. Annema JT, Veselic M, Rabe KF. EUS-guided FNA of centrally located lung tumours following a non-diagnostic bronchoscopy. *Lung Cancer*. 2005;48:357–361; discussion 63–64.
10. Korevaar DA, Colella S, Spijker R, et al. Esophageal endosonography for the diagnosis of intrapulmonary tumors: a systematic review and meta-analysis. *Respiration*. 2017;93:126–137.
11. Venuta F, Rendina EA, Ciriaci P, et al. Computed tomography for preoperative assessment of T3 and T4 bronchogenic carcinoma. *Eur J Cardiothorac Surg*. 1992;6:238–241.
12. Pieterman RM, van Putten JW, Meuzelaar JJ, et al. Preoperative staging of non-small-cell lung cancer with positron-emission tomography. *N Engl J Med*. 2000;343:254–261.
13. Kuijvenhoven JC, Crombag L, Breen DP, et al. Esophageal ultrasound (EUS) assessment of T4 status in NSCLC patients. *Lung Cancer*. 2017;114:50–55.
14. Konge L, Vilman P, Clementsen P, et al. Reliable and valid assessment of competence in endoscopic ultrasonography and fine-needle aspiration for mediastinal staging of non-small cell lung cancer. *Endoscopy*. 2012;44:928–933.
15. Goldstraw P, Chansky K, Crowley J, et al. The IASLC lung cancer staging project: proposals for revision of the TNM stage groupings in the Forthcoming (Eighth) Edition of the TNM classification for lung cancer. *J Thorac Oncol*. 2016;11:39–51.
16. von Bartheld MB, Rabe KF, Annema JT. Transaortic EUS-guided FNA in the diagnosis of lung tumors and lymph nodes. *Gastrointest Endosc*. 2009;69:345–349.
17. Liberman M, Duranteau A, Grunenwald E, et al. New technique performed by using EUS access for biopsy of para-aortic (station 6) mediastinal lymph nodes without traversing the aorta (with video). *Gastrointest Endosc*. 2011;73:1048–1051.
18. Catalano MF, Sivak Jr MV, Rice T, et al. Endosonographic features predictive of lymph node metastasis. *Gastrointest Endosc*. 1994;40:442–446.
19. Fujiwara T, Yasufuku K, Nakajima T, et al. The utility of sonographic features during endobronchial ultrasound-guided transbronchial needle aspiration for lymph node staging in patients with lung cancer: a standard endobronchial ultrasound image classification system. *Chest*. 2010;138:641–647.
20. Gill KR, Ghahreman MS, Jamil LH, et al. Endosonographic features predictive of malignancy in mediastinal lymph nodes in patients with lung cancer. *Gastrointest Endosc*. 2010;72:265–271.
21. Memoli JS, El-Bayoumi E, Pastis NJ, et al. Using endobronchial ultrasound features to predict lymph node metastasis in patients with lung cancer. *Chest*. 2011;140:1550–1556.
22. Saftoiu A, Vilman P, Ciurea T, et al. Dynamic analysis of EUS used for the differentiation of benign and malignant lymph nodes. *Gastrointest Endosc*. 2007;66:291–300.
23. Toloza EM, Harpole L, Dettberbeck F, McCrory DC. Invasive staging of non-small cell lung cancer: a review of the current evidence. *Chest*. 2003;123:157s–166s.
24. Schmulewitz N, Wildi SM, Varadarajulu S, et al. Accuracy of EUS criteria and primary tumor site for identification of mediastinal lymph node metastasis from non-small-cell lung cancer. *Gastrointest Endosc*. 2004;59:205–212.
25. Janssen J, Dietrich CF, Will U, Greiner L. Endosonographic elastography in the diagnosis of mediastinal lymph nodes. *Endoscopy*. 2007;39:952–957.
26. LeBlanc JK, Ciaccia D, Al-Assi MT, et al. Optimal number of EUS-guided fine needle passes needed to obtain a correct diagnosis. *Gastrointest Endosc*. 2004;59:475–481.
27. Wallace MB, Kennedy T, Durkalski V, et al. Randomized controlled trial of EUS-guided fine needle aspiration techniques for the detection of malignant lymphadenopathy. *Gastrointest Endosc*. 2001;54:441–447.
28. Aerts JG, Kloover J, Los J, et al. EUS-FNA of enlarged necrotic lymph nodes may cause infectious mediastinitis. *J Thorac Oncol*. 2008;3:1191–1193.
29. Micames CG, McCrory DC, Pavay DA, et al. Endoscopic ultrasound-guided fine-needle aspiration for non-small cell lung cancer staging: a systematic review and metaanalysis. *Chest*. 2007;131:539–548.
30. Annema JT, Versteegh MI, Veselic M, et al. Endoscopic ultrasound added to mediastinoscopy for preoperative staging of patients with lung cancer. *JAMA*. 2005;294:931–936.
31. LeBlanc JK, Devereaux BM, Imperiale TF, et al. Endoscopic ultrasound in non-small cell lung cancer and negative mediastinum on computed tomography. *Am J Respir Crit Care Med*. 2005;171:177–182.
32. Wallace MB, Ravenel J, Block MI, et al. Endoscopic ultrasound in lung cancer patients with a normal mediastinum on computed tomography. *Ann Thorac Surg*. 2004;77:1763–1768.
33. Mody MK, Kazerooni EA, Korobkin M. Percutaneous CT-guided biopsy of adrenal masses: immediate and delayed complications. *J Comput Assist Tomogr*. 1995;19:434–439.
34. Osman Y, El-Mekresh M, Gomha AM, et al. Percutaneous adrenal biopsy for indeterminate adrenal lesion: complications and diagnostic accuracy. *Urol Int*. 2010;84:315–318.
35. Schuurbiers OC, Tournoy KG, Schoppers HJ, et al. EUS-FNA for the detection of left adrenal metastasis in patients with lung cancer. *Lung Cancer*. 2011;73:310–315.
36. Crombag LMMJ. EUS-B-FNA vs conventional EUS-FNA for left adrenal gland analysis in lung cancer patients. In: Artur Szlubowski JAS, Schuurbiers O, Korevaar DA, Bonta PI, Annema JT, eds. *Lung Cancer*; 2017.
37. Hollerbach S, Willert J, Topalidis T, et al. Endoscopic ultrasound-guided fine-needle aspiration biopsy of liver lesions: histological and cytological assessment. *Endoscopy*. 2003;35:743–749.

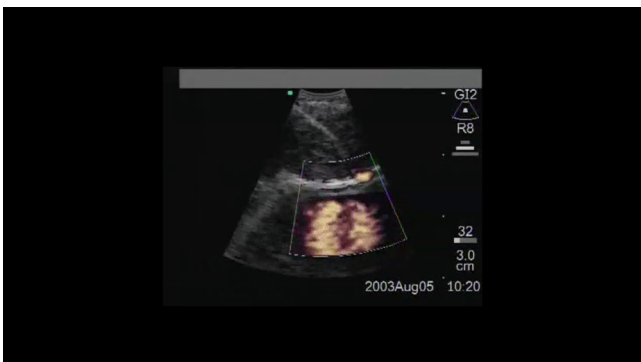
38. Prasad P, Schmulewitz N, Patel A, et al. Detection of occult liver metastases during EUS for staging of malignancies. *Gastrointest Endosc.* 2004;59:49–53.
39. Herth FJ, Krasnik M, Kahn N, et al. Combined endoscopic-endobronchial ultrasound-guided fine-needle aspiration of mediastinal lymph nodes through a single bronchoscope in 150 patients with suspected lung cancer. *Chest.* 2010;138:790–794.
40. Kang HJ, Hwangbo B, Lee GK, et al. EBUS-centred versus EUS-centred mediastinal staging in lung cancer: a randomised controlled trial. *Thorax.* 2014;69:261–268.
41. Szlubowski A, Soja J, Kocon P, et al. A comparison of the combined ultrasound of the mediastinum by use of a single ultrasound bronchoscope versus ultrasound bronchoscope plus ultrasound gastroscope in lung cancer staging: a prospective trial. *Interact Cardiovasc Thorac Surg.* 2012;15:442–446; discussion 6.
42. Crombag LM, Annema JT. Left adrenal gland analysis in lung cancer patients using the endobronchial ultrasound scope: a feasibility trial. *Respiration.* 2016;91:235–240.
43. Casal RF, Staerkel GA, Ost D, et al. Randomized clinical trial of endobronchial ultrasound needle biopsy with and without aspiration. *Chest.* 2012;142:568–573.
44. Lee HS, Lee GK, Lee HS, et al. Real-time endobronchial ultrasound-guided transbronchial needle aspiration in mediastinal staging of non-small cell lung cancer: how many aspirations per target lymph node station? *Chest.* 2008;134:368–374.
45. von Bartheld MB, van BA, Annema JT. Complication rate of endosonography (endobronchial and endoscopic ultrasound): a systematic review. *Respiration.* 2014;87:343–351.
46. Nakajima T, Yasufuku K, Fujiwara T, et al. Endobronchial ultrasound-guided transbronchial needle aspiration for the diagnosis of intrapulmonary lesions. *J Thorac Oncol.* 2008;3:985–988.
47. Tournoy KG, Rintoul RC, van Meerbeeck JP, et al. EBUS-TBNA for the diagnosis of central parenchymal lung lesions not visible at routine bronchoscopy. *Lung Cancer.* 2009;63:45–49.
48. Konge L, Clementsen PF, Ringsted C, et al. Simulator training for endobronchial ultrasound: a randomised controlled trial. *Eur Respir J.* 2015;46:1140–1149.
49. Adams K, Shah PL, Edmonds L, Lim E. Test performance of endobronchial ultrasound and transbronchial needle aspiration biopsy for mediastinal staging in patients with lung cancer: systematic review and meta-analysis. *Thorax.* 2009;64:757–762.
50. Gu P, Zhao YZ, Jiang LY, et al. Endobronchial ultrasound-guided transbronchial needle aspiration for staging of lung cancer: a systematic review and meta-analysis. *Eur J Cancer.* 2009;45:1389–1396.
51. Korevaar DA, Crombag LM, Cohen JF, et al. Added value of combined endobronchial and oesophageal endosonography for mediastinal nodal staging in lung cancer: a systematic review and meta-analysis. *Lancet Respir Med.* 2016;4:960–968.
52. Ernst A, Eberhardt R, Krasnik M, Herth FJ. Efficacy of endobronchial ultrasound-guided transbronchial needle aspiration of hilar lymph nodes for diagnosing and staging cancer. *J Thorac Oncol.* 2009;4:947–950.
53. van der Heijden EH, Casal RF, Trisolini R, et al. Guideline for the acquisition and preparation of conventional and endobronchial ultrasound-guided transbronchial needle aspiration specimens for the diagnosis and molecular testing of patients with known or suspected lung cancer. *Respiration.* 2014;88:500–517.
54. Rintoul RC, Skwarski KM, Murchison JT, et al. Endobronchial and endoscopic ultrasound-guided real-time fine-needle aspiration for mediastinal staging. *Eur Respir J.* 2005;25:416–421.
55. Szlubowski A, Zielinski M, Soja J, et al. A combined approach of endobronchial and endoscopic ultrasound-guided needle aspiration in the radiologically normal mediastinum in non-small-cell lung cancer staging—a prospective trial. *Eur J Cardiothorac Surg.* 2010;37:1175–1179.
56. Vilmann P, Krasnik M, Larsen SS, et al. Transesophageal endoscopic ultrasound-guided fine-needle aspiration (EUS-FNA) and endobronchial ultrasound-guided transbronchial needle aspiration (EBUS-TBNA) biopsy: a combined approach in the evaluation of mediastinal lesions. *Endoscopy.* 2005;37:833–839.
57. Wallace MB, Pascual JM, Raimondo M, et al. Minimally invasive endoscopic staging of suspected lung cancer. *JAMA.* 2008;299:540–546.
58. Hwangbo B, Lee GK, Lee HS, et al. Transbronchial and transesophageal fine-needle aspiration using an ultrasound bronchoscope in mediastinal staging of potentially operable lung cancer. *Chest.* 2010;138:795–802.
59. Oki M, Saka H, Ando M, et al. Transbronchial vs transesophageal needle aspiration using an ultrasound bronchoscope for the diagnosis of mediastinal lesions: a randomized study. *Chest.* 2015;147:1259–1266.
60. Cerfolio RJ, Bryant AS, Eloubeidi MA. Accessing the aortopulmonary window (#5) and the paraaortic (#6) lymph nodes in patients with non-small cell lung cancer. *Ann Thorac Surg.* 2007;84:940–945.
61. Kinsey CM, Arenberg DA. Endobronchial ultrasound-guided transbronchial needle aspiration for non-small cell lung cancer staging. *Am J Respir Crit Care Med.* 2014;189:640–649.
62. Tournoy KG, Keller SM, Annema JT. Mediastinal staging of lung cancer: novel concepts. *Lancet Oncol.* 2012;13:e221–e229.
63. De Wever W, Stroobants S, Coolen J, Verschakelen JA. Integrated PET/CT in the staging of nonsmall cell lung cancer: technical aspects and clinical integration. *Eur Respir J.* 2009;33:201–212.
64. Stather DR, Maceachern P, Chee A, et al. Trainee impact on advanced diagnostic bronchoscopy: an analysis of 607 consecutive procedures in an interventional pulmonary practice. *Respiriology (Carlton, Vic).* 2013;18:179–184.
65. Farr A, Clementsen P, Herth F, et al. Endobronchial ultrasound: launch of an ERS structured training programme. *Breathe (Sheffield, England).* 2016;12:217–220.
66. Annema JT, Bohoslavsky R, Burgers S, et al. Implementation of endoscopic ultrasound for lung cancer staging. *Gastrointest Endosc.* 2010;71:64–70, e1.
67. Wijmans L, de Bruin DM, Meijer SL, Annema JT. Real-time optical biopsy of lung cancer. *Am J Respir Crit Care Med.* 2016;194:e10–e11.
68. Wijmans L, d'Hooghe JN, Bonta PI, Annema JT. Optical coherence tomography and confocal laser endomicroscopy in pulmonary diseases. *Curr Opin Pulm Med.* 2017;23:275–283.
69. Tournoy KG, De Ryck F, Vanwalleghem LR, et al. Endoscopic ultrasound reduces surgical mediastinal staging in lung cancer: a randomized trial. *Am J Respir Crit Care Med.* 2008;177:531–535.



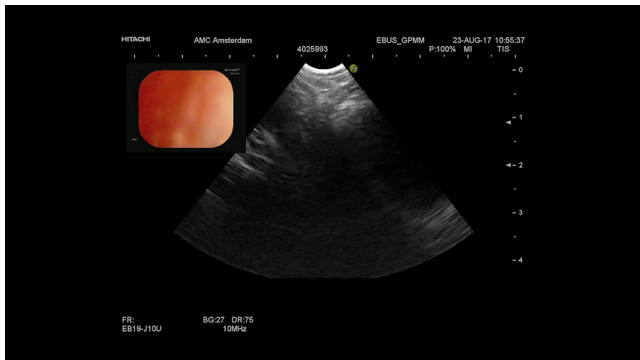
**Video 7.1** Endoscopic Ultrasonography-Guided Fine-Needle Aspiration of the Subcarinal Lymph Node in a Patient With Non-Small Cell Lung Cancer



**Video 7.2** Endoscopic Ultrasonography-Guided Fine-Needle Aspiration of the Left Adrenal Gland in a Patient With Metastatic Non-Small Cell Lung Cancer

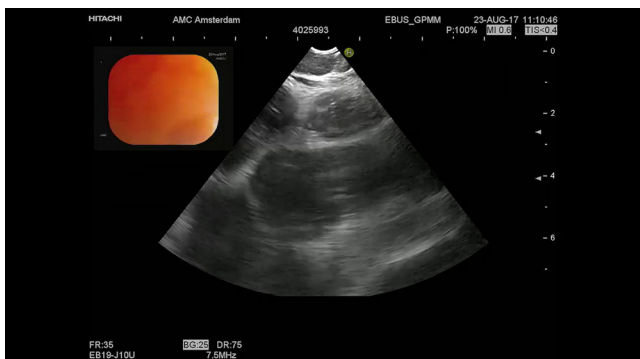


**Video 7.3** Endobronchial Ultrasound-Guided Transbronchial Needle Aspiration of an Enlarged Subcarinal Lymph Node in a Patient With Non-Small Cell Lung Cancer



**Video 7.4** Systematic Endobronchial Ultrasound Evaluation in a Sarcoidosis Stage 1 Patient, Demonstrating Lymph Nodes 4L (Paratracheal Left), 5 (Subaortic), 7 (Subcarinal), 11L (Hilar Left), and 11R (Hilar Right), Azygos Vein (Draining Into Superior Vena Cava) and Lymph Node 4R (Paratracheal Right)

The left upper panel shows the position of the transducer in the trachea and bronchial tree.



**Video 7.5** Systematic EUS-B (Endoscopic Ultrasonography With the Endobronchial Ultrasound Scope) Evaluation of the Mediastinum in a Patient With Sarcoidosis Stage 1, Demonstrating the Following Anatomic Landmarks: Liver, Left Atrium, Aortic Valve, Pulmonary Trunk, and Aortic Arch, and the Following Mediastinal Lymph Nodes: Station 7 (Subcarinal—Between Left Atrium and Pulmonary Trunk), Station 4L (Paratracheal Left—Between Aortic Arch and Left Sided Pulmonary Artery), and Station 6 (Para-Aortic—on the Far Side of the Aortic Arch)



**Video 7.6** Endobronchial Ultrasound-Guided Transbronchial Needle Aspiration on an Enlarged Right-Sided Hilar Node (Station 11R) in a Patient With an Adenocarcinoma of the Right Upper Lobe

Note the ultrasound transducer in the right lower corner and the sheath (protecting the working channel of the scope) in the right upper corner. Transbronchial needle aspiration is performed using a 25-gauge needle.

# Endoscopic Ultrasound in Esophageal and Gastric Cancer

BRONTE HOLT

## KEY POINTS

- Both radial or linear echoendoscopes can be used for evaluation and staging of esophageal and gastric cancer.
- The role of EUS is limited in patients with early-stage esophageal and gastric cancer except for ruling out nodal involvement.
- EUS-guided fine-needle aspiration of local and regional lymph nodes is important in determining whether patients with T1 or T2 disease receive neoadjuvant chemoradiotherapy or proceed directly to surgery.
- Confirmation of metastatic disease by EUS-guided fine-needle aspiration can determine whether treatment is of curative or palliative intent.
- The inability to advance a gastroscope past a malignant esophageal mass corresponds to locally advanced disease (stage T3 or greater).
- EUS enables the detection of low volume ascites (missed by computed tomography) in gastric cancer that may correspond to peritoneal involvement.
- EUS accurately assesses disease stage in gastric MALT and more importantly can predict clinical response to treatment.
- EUS-guided fine-needle biopsy enables definitive histologic diagnosis in linitis plastica and in patients with thickened gastric folds that can be otherwise missed on standard endoscopic biopsies.

## Esophageal Cancer

### Background

The global burden of esophageal cancer is high, with it ranked as the fifth and eighth most common cause of cancer-related deaths in men and women, respectively, worldwide.<sup>1</sup> In 2012 an estimated 455,800 new cases were diagnosed and the disease resulted in 400,200 deaths.<sup>2</sup> At the time of presentation, almost half of patients have locally advanced or metastatic disease. Because of this rapid spread and late presentation, the 5-year survival is poor, measuring 18.4% overall.<sup>3</sup> Although squamous cell carcinoma (SCC) is the most common type of esophageal cancer worldwide, in Western countries the incidence of SCC has decreased and adenocarcinoma has increased over the past few decades.<sup>4,5</sup>

### Esophageal Cancer Staging

Esophageal cancer staging is defined by the American Joint Committee on Cancer (AJCC) Staging System that establishes tumor-node-metastasis (TNM) subclassifications based on the depth of invasion of the primary tumor (T), lymph node involvement (N), and extent of metastatic disease (M). The 8th edition of the AJCC Cancer staging manual was published in 2017 (Table 8.1)<sup>6</sup> and will be in clinical use in 2018.<sup>7</sup> The TNM components for staging esophageal adenocarcinoma and SCC are the same; however, the AJCC anatomic stage groups differ depending on histologic type because of differing mortality rates between adenocarcinoma and SCC stages.

The esophageal wall has four main layers: the mucosa, submucosa, muscularis propria, and adventitia. The mucosal layer includes the epithelium, lamina propria, and muscularis mucosae and is separated from the submucosa by a basement membrane. T1a cancers are confined within the mucosa and are often called intramucosal cancers; they can invade the lamina propria, as deeply as the muscularis mucosae. T2 tumors invade the muscularis propria and T3 the adventitia, and T4 denotes invasion of adjacent structures. Management is dependent on tumor stage, and accurate preoperative determination of disease stage is therefore essential to select the appropriate treatment for each patient, including endoscopic resection (ER), surgery, chemotherapy, radiation, or palliative care.

### Management Pathways in Esophageal Cancer

Tumors limited to the mucosa or submucosa (T1) have a high rate of cure from endoscopic or surgical resection.<sup>8</sup> Outcomes of Tis high grade dysplasia (HGD) and T1a tumors are similar, and ER for staging and therapy has demonstrated efficacy.<sup>9</sup> The goal of endoscopic therapy is the complete removal or eradication of early stage disease. Lesions that are limited to the mucosa (Tis), lamina propria, or muscularis mucosae (T1a) can be removed by ER, with a low risk of lymph node metastases (0% to 3%).<sup>10-14</sup> In patients with T1b disease, the optimal treatment strategy depends on histopathologic characteristics of the ER specimen and the patient's clinical status. ER may be a valid alternative to surgery and is recommended in patients who are borderline fit for surgery and if the ER specimen has submucosal invasion less than 500 µm, tumor differentiation grade "well" or "moderate", no lymphovascular invasion, and no tumor infiltration in the deep resection margin.<sup>15,16</sup> These tumors are considered "low-risk" T1b cancers, with

**TABLE 8.1****The American Joint Commission on Cancer TNM Classification for Esophageal Cancer, 8th Edition****Anatomic Stage/Prognostic Groups, Adenocarcinoma**

Stage 0	Tis	N0	M0
Stage I	T1	N0	M0
Stage IIA	T1	N1	M0
Stage IIB	T2	N0	M0
Stage III	T2	N1	M0
Stage III	T3	N0 or N1	M0
Stage III	T4a	N0 or N1	M0
Stage IVA	T1-4a	N2	M0
Stage IVA	T4b	N0, N1, or N2	M0
Stage IVA	Any T	N3	M0
Stage IVB	Any T	Any N	M1

**Anatomic Stage/Prognostic Groups, Squamous Cell Carcinoma**

Stage 0	Tis	N0	M0
Stage I	T1	N0 or N1	M0
Stage II	T2	N0 or N1	M0
Stage II	T3	N0	M0
Stage III	T3	N1	M0
Stage III	T1, T2, or T3	N2	M0
Stage IVA	T4	N0, N1, or N2	M0
Stage IVA	Any T	N3	M0
Stage IVB	Any T	Any N	M1

**Primary Tumor (T)**

TX	Primary tumor cannot be assessed
T0	No evidence of primary tumor
Tis	High-grade dysplasia, defined as malignant cells confined to the epithelium by the basement membrane
T1	Tumor invades lamina propria, muscularis mucosa, or submucosa
T1a	Tumor invades lamina propria or muscularis mucosa
T1b	Tumor invades submucosa
T2	Tumor invades muscularis propria
T3	Tumor invades adventitia
T4	Tumor invades adjacent structures
T4a	Tumor invades pleura, pericardium, azygos vein, diaphragm, or peritoneum
T4b	Tumor invades adjacent structures such as the aorta, vertebral body, or airway

**Regional Lymph Nodes (N)**

NX	Regional lymph nodes cannot be assessed
N0	No regional lymph node metastasis
N1	Metastasis in 1–2 regional lymph nodes
N2	Metastasis in 3–6 regional lymph nodes
N3	Metastasis in seven or more regional lymph nodes

**Distant Metastasis (M)**

M0	No distant metastasis
M1	Distant metastasis

Amin MB, Edge SB, Greene FL, et al., eds. *AJCC Cancer Staging Manual*. 8th ed. New York: Springer; 2017.

a risk of lymph node metastasis of less than 2%.<sup>17,18</sup> However, discussion about comparative risk of esophagectomy versus potential for concurrent nodal disease should be undertaken, especially in cases with larger tumors or deeper invasion.<sup>19</sup>

The most important risk factor predicting lymph node metastasis in both early adenocarcinoma and SCC is the depth of infiltration of the lesion.<sup>20,21</sup> Survival is significantly worse once the esophageal cancer breaches the submucosa<sup>22</sup> and there is lymphovascular invasion.<sup>23</sup> This is largely related to early lymph node metastases, seen in up to 35% of T1b tumors and 78% to 85% of T3 tumors.<sup>24,25</sup> The lymphatic drainage of the esophagus is unique in the gastrointestinal (GI) tract, with a freely anastomosing

network in the mucosa and submucosa, intermittently piercing the muscularis propria to drain into regional lymph nodes or directly into the thoracic duct. The upper third of the esophagus drains into the paratracheal and internal jugular nodes, the middle third into the mediastinal node, and the lower third into nodes situated around the aorta and celiac axis. This intricate lymphatic system allows bidirectional tumor spread via the thoracic duct to involve the regional and systemic lymph nodes in the abdomen and mediastinum and development of “skip metastases.”<sup>26–29</sup>

Patients with locally advanced disease which is potentially surgically resectable are usually offered neoadjuvant chemoradiotherapy to improve survival outcomes.<sup>30–33</sup> Chemoradiotherapy

followed by surgery is considered a standard treatment option for patients with stages II, III, and IVa disease.<sup>34</sup> Neoadjuvant chemoradiotherapy rather than chemotherapy is generally used because it confers superior pathologic response and may improve outcomes.<sup>35</sup> For early stage tumors the role of preoperative chemoradiotherapy remains controversial. A randomized controlled trial of 195 patients with early stage cancer (stage I or II) randomized to neoadjuvant chemoradiotherapy followed by surgery or to surgery alone showed no survival advantage with neoadjuvant therapy.<sup>36</sup>

For patients who are either medically inoperable or have unresectable tumors, the efficacy of definitive chemoradiotherapy has been established.<sup>37,38</sup> For patients with esophageal SCC, definitive chemoradiotherapy may offer equivalent outcomes compared with preoperative chemoradiotherapy followed by surgical resection.<sup>39,40</sup>

Stage-dependent treatment protocols require the most complete and accurate staging possible, not only to select patients for surgery with or without neoadjuvant chemoradiotherapy, but also to minimize the rate of unnecessary surgery in metastatic disease.

## Staging of Newly Diagnosed Esophageal Cancer

The preoperative evaluation of esophageal adenocarcinoma involves a careful endoscopic assessment, with or without the addition of computed tomography (CT), and positron emission tomography (PET)/CT with fluorodeoxyglucose (FDG), and endoscopic ultrasonography (EUS). These modalities have a limited role in the initial work-up of superficial esophageal cancers (Tis and T1) because ER is the best method for determining depth of invasion (T staging) and EUS is less accurate for early stage lesions (T1 or T2) compared with more advanced tumors.<sup>22,41–43</sup> In contrast, in advanced esophageal cancers, a multimodality approach to preoperative staging cancer is required to determine a treatment plan<sup>44</sup> and this may reduce the number of unnecessary surgeries performed and potentially improve survival.<sup>45</sup>

Following initial diagnosis using upper endoscopy and tissue biopsy, the National Comprehensive Cancer Network (NCCN) guidelines<sup>46</sup> recommend CT of the chest, abdomen, and pelvis with oral and intravenous contrast as the first staging study (Table 8.2). The prime strength of CT and PET scanning in preoperative staging is the detection of distant metastases that identify patients who are not surgical candidates.<sup>47,48</sup> CT is limited in defining the local extent and nodal involvement of esophageal cancer but is very useful in identifying patients with metastatic disease. These patients require histologic confirmation of metastatic disease, after which further investigations to evaluate the T and N status are generally not required. If CT is negative or equivocal for metastatic disease, FDG PET/CT is often used because it detects previously unsuspected metastatic disease in 15% to 20% of patients<sup>49–51</sup> and assesses malignant involvement of any lymphadenopathy detected on CT.<sup>52</sup>

In a prospective study of EUS, CT, and PET in 42 patients with esophageal cancer, accuracy for distant nodal metastasis was significantly higher for FDG PET than the combined use of CT and EUS (86% vs. 62%,  $P = .0094$ ).<sup>53</sup> However, PET was not as accurate as the combination of EUS and CT for locoregional lymph node staging. A retrospective study of 148 patients who had EUS and FDG PET for esophageal cancer staging found PET was not as accurate as EUS-guided fine-needle aspiration (FNA) and PET identified distant metastases only in those patients with incomplete EUS or who had nodal disease detected by EUS.<sup>54</sup> PET CT has a higher accuracy

**TABLE 8.2 Work-Up of Esophageal and Esophagogastric Junction Cancers**

- Upper GI endoscopy and biopsy
- Chest/abdominal CT with oral and IV contrast
- Pelvic CT with contrast as clinically indicated
- PET/CT evaluation if no evidence of M1 disease
- Complete blood count and comprehensive chemistry profile
- EUS if no evidence of M1 disease
- ER is essential for the accurate staging of early-stage cancers (T1a or T1b)
- Biopsy of metastatic disease as clinically indicated
- HER2 testing if metastatic adenocarcinoma is documented/suspected
- Bronchoscopy, if tumor is at or above the carina with no evidence of M1 disease
- Assign Siewert category
- Nutritional assessment and counseling
- Smoking cessation advice, counseling, and pharmacotherapy as indicated
- Screen for family history

CT, Computed tomography; ER, endoscopic resection; EUS, endoscopic ultrasound; GI, gastrointestinal; IV, intravenous; PET, positron emission tomography.

National Comprehensive Cancer Network Guidelines V 1.2017, Esophageal and Esophagogastric Junction Cancers.

than CT alone for distant and locoregional metastases but is inferior to EUS for locoregional staging.<sup>55–57</sup> In a systematic review, FDG PET had a pooled sensitivity and specificity for the detection of locoregional metastases of 0.51 (95% confidence interval [CI], 0.34 to 0.69) and 0.84 (95% CI, 0.76 to 0.91), respectively. For distant metastases, pooled sensitivity and specificity was 0.67 (95% CI, 0.58 to 0.76) and 0.97 (95% CI, 0.90 to 1.0), respectively.<sup>53</sup>

If CT and FDG PET/CT do not demonstrate distant disease, EUS staging should be performed to establish the extent of locoregional disease prior to initiation of treatment.<sup>35,58,59</sup> EUS is recognized as the most accurate imaging method for initial locoregional staging in esophageal cancer.<sup>60–65</sup> Sihvo and coworkers found EUS to be more accurate in detecting locoregional lymph node metastases than PET and CT (72%, 60%, and 58%, respectively).<sup>66</sup> The addition of EUS to CT and PET increased the nodal staging accuracy from 70% to 91% ( $P = .008$ ). A study by Pfau and coworkers evaluating EUS, CT, and PET in staging esophageal cancer found that EUS changed management by guiding the need for neoadjuvant therapy in 34.8% of patients.<sup>67</sup> The major impact on treatment plans of EUS was in patients with locally advanced disease: EUS identified a significantly greater number of patients (58.9%) with locoregional nodes than either CT (26.8%,  $P = .0006$ ) or PET (37.5%,  $P = .02$ ). In a retrospective study of 29 patients with no metastatic disease on CT and PET scan who underwent EUS, pathology confirmed nodal involvement was correctly identified by CT in 6 of 11 patients (54.5%), by PET in 4 of 11 patients (36.4%), and by EUS in 10 of 11 patients (90.9%).<sup>63</sup> Overall accuracy for N staging was 69% for CT, 56% for PET, and 81% for EUS. The sensitivity, specificity, positive predictive value (PPV), negative predictive value (NPV), and overall accuracy of EUS for detection of locoregional lymph node metastasis were 91%, 60%, 83%, 75%, and 81%, respectively.

PET scan, CT, and EUS were performed in a prospective study of 75 patients with newly diagnosed esophageal cancer, with tissue

confirmation or FNA used as the “gold standard” of disease.<sup>69</sup> Accurate T stage by CT and PET was seen in 42% of cases and by EUS in 71% ( $P = .14$ ). CT, EUS, and PET had a similar performance in nodal staging: the sensitivity and specificity of N staging for CT was 84% and 67%, for EUS was 86% and 67%, and for PET was 82% and 60% ( $P = .38$ ), respectively. The sensitivity and specificity for distant metastasis were 81% and 82% for CT, 73% and 86% for EUS, and 81% and 91% for PET ( $P = .25$ ), respectively. Another prospective study showed that the addition of FDG PET to EUS and CT did not change management if a complete EUS examination had been performed, but it did offer some benefit in patients with incomplete EUS due to stenosing tumors.<sup>70</sup>

## Endoscopic Ultrasound Examination Technique

### Scope Selection

Esophageal cancers can be examined using a radial or curvilinear array echoendoscope or a high-frequency probe (HFP). The operating characteristics of these scopes are described elsewhere in this book. Choice of scope depends on operator expertise and preference, whether FNA will be performed if a suspicious lymph node or metastatic deposit is seen, and whether a malignant stricture is present. The advantage of the radial scope relates to the 360-degree ultrasound field of view in the transverse plane perpendicular to the long axis of the echoendoscope. Maintaining the scope within the center of the GI lumen and orienting the spine to the 6-o'clock position allows relatively rapid imaging and staging and limits the risk of tangential imaging during T staging. The major drawback of the radial scope is the lack of FNA capability, which can be performed with the curvilinear scope.

The narrower field of view of the curvilinear scope makes staging a more dynamic process to ensure the tumor is imaged “en face” so the wall layers are not viewed tangentially, and all nodal stations and sites of potential metastatic spread are evaluated. Similar TNM staging accuracy can be achieved with both scopes<sup>71</sup>; however, given the benefit of cytologic confirmation of nodal or metastatic spread the curvilinear scope is increasingly used.

Miniprobe ultrasound uses higher-frequency ultrasound (20 to 30 MHz). The probe can be passed through the upper endoscope working channel and applied under direct endoscopic visualization on the lesion of interest. HFPs provide a more detailed visualization of the esophageal wall, allowing one to delineate nine layers in the esophageal wall. The first and second layers correspond to the superficial mucosa (hyperechoic and hypoechoic, respectively), the third layer is the lamina propria (hyperechoic), the fourth layer is the muscularis mucosa (hypoechoic), the fifth layer is the submucosa (hyperechoic), the sixth, seventh, and eighth layers (hypoechoic, hyperechoic, and hypoechoic) are the inner circular muscle, intermuscular connective tissue, and outer longitudinal muscle of the muscularis propria, respectively, and the ninth layer is adventitia (hyperechoic). The strength of HFPs is most suited to T staging because it produces high-resolution images close to the probe. However, the depth of penetration decreases significantly 5 to 6 cm from the probe and the utility of HFPs for nodal and metastases detection is limited.

### Patient Preparation

The diagnosis of esophageal cancer has generally been made prior to referral for EUS, and preceding investigations such as endoscopy reports, histology, and cross-sectional imaging are first reviewed. An upper endoscopy is performed directly

before the EUS to document the tumor location, length, and configuration; relationship to the upper and lower esophageal sphincters and gastric cardia; and degree of luminal stenosis and to remove any food or liquid from above the lesion to reduce the risk of aspiration. Barrett-associated neoplasia and squamous cell neoplasia can be multifocal, and the remainder of the esophagus requires careful endoscopic assessment. This can be enhanced with the use of high-definition white light and narrow band imaging with dual focus technology, with or without chromoendoscopy.<sup>72,73</sup>

### Obstructing Tumors

The diagnostic benefit of EUS examination in patients with stenotic esophageal tumors is limited. Complete staging EUS examination may be hampered by the presence of malignant stenosis obstructing passage of the scope. The esophagus may be dilated to allow scope passage and imaging through the length of the stricture and beyond. To pass the linear or radial scope, the stricture needs to be dilated to a diameter of 13 to 15 mm. Dilating a tight stricture to this diameter during one endoscopy session carries a significant risk of perforation of up to 24%.<sup>74</sup> Stepwise dilation over more than one endoscopy may reduce this risk<sup>75</sup>; however, performing multiple procedures to achieve complete EUS staging may be challenging for patients and endoscopy centers to facilitate. The very presence of a stricture that impedes passage of a diagnostic gastroscope may indicate advanced disease, which may require neoadjuvant or definitive chemotherapy, radiotherapy, or a combination of both (Fig. 8.1). In a recent multicenter retrospective cohort study of 100 patients with newly diagnosed nonmetastatic esophageal cancer referred for staging EUS, the diagnostic gastroscope could not pass through the malignant stricture in 46 patients. This had 100% correlation with locally advanced (T3 or T4) disease on EUS.<sup>76</sup>

### TNM Staging

The echoendoscope examination generally begins after an upper endoscopy. Initial passage of the echoendoscope is done slowly and carefully and largely “by feel” as it passes through the tumor rather than under direct vision. The sequence of staging generally is to examine for metastatic disease, then nodal involvement, followed by tumoral staging. This allows for early identification of disease that may upstage the tumor.

EUS is considered the modality of choice for accurate local staging, with a pooled sensitivity of 81% to 90% and 84.7% to 96.7% for T and N staging, respectively.<sup>57</sup> In Barrett esophagus with high-grade dysplasia and early adenocarcinoma the pooled sensitivity and specificity of EUS for N staging is 71% (95% CI, 49% to 87%) and 94% (95% CI, 89% to 97%), respectively, with a pooled NPV of 96% (95% CI, 93% to 99%).<sup>77</sup> A summary of studies reporting the accuracy of EUS for T and N staging and for EUS compared with other staging modalities are shown in Tables 8.3 and 8.4, respectively.

**T Stage.** T staging can be assisted by techniques to improve acoustic coupling and identification of the wall layers. These include using a balloon on the tip of the echoendoscope or low-volume water insufflation of the esophagus once the scope is in position over the tumor. Care must be taken to minimize the risk of aspiration with the latter technique, including using a small volume of water, raising the head of the bed, and regularly suctioning the stomach. It is important to avoid tangential imaging because it might lead to overstaging of the tumor.

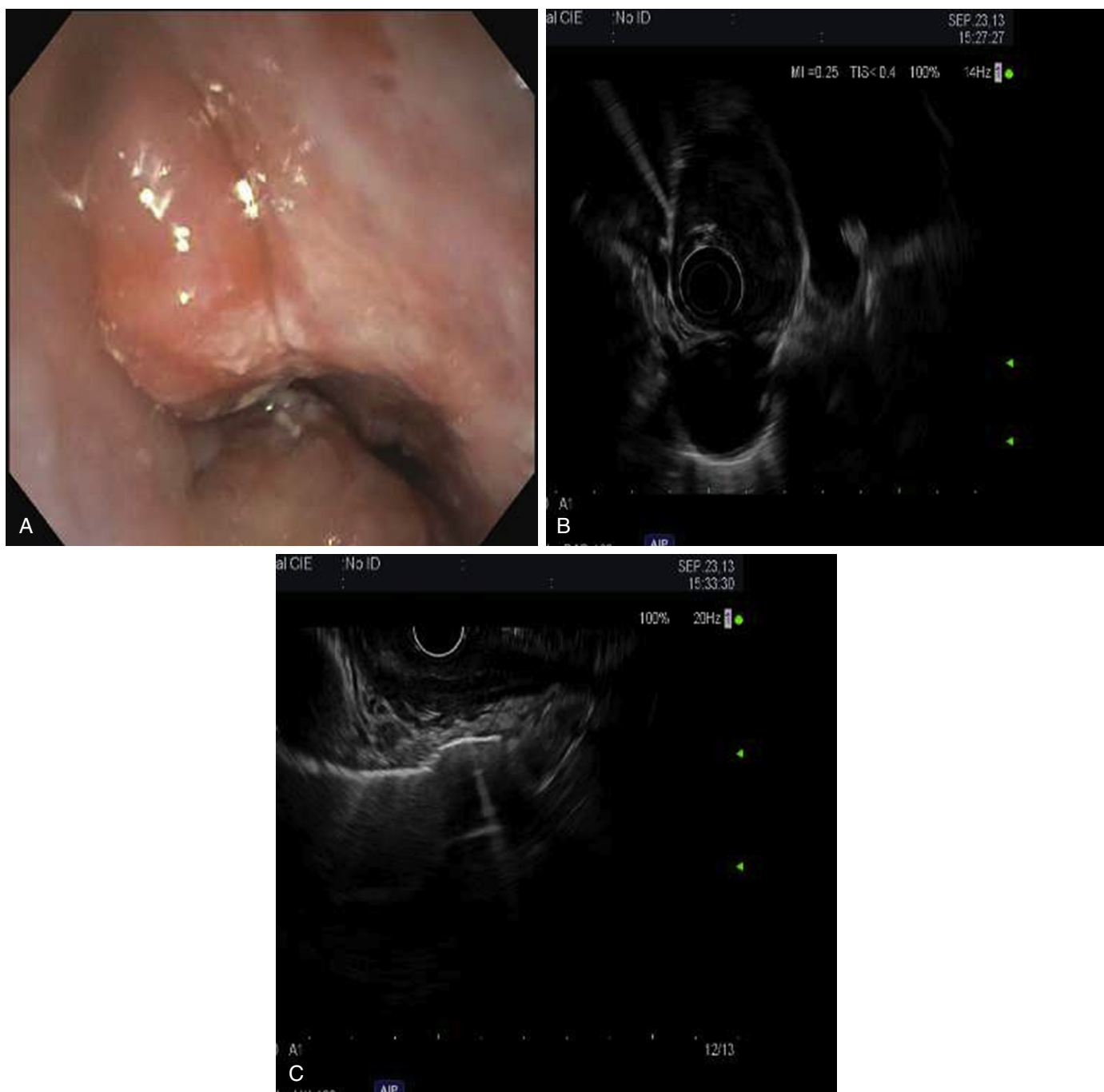


**Fig. 8.1** (A) On gastroscopy a tight stricture is seen at the distal esophagus due to adenocarcinoma. (B) On radial imaging the tumor invades the muscularis layer consistent with T3 disease (T3N0). (C) On “wedging” the linear echoendoscope transducer at the tumor site, additional disease burden such as nodal involvement could be recognized in the same patient (T3N1).

The esophageal wall has five layers (Table 8.5) on imaging with the curvilinear and radial EUS scope using frequencies of 5 to 10 MHz (Fig. 8.2). The first hyperechoic layer corresponds to the superficial mucosa, the second hypoechoic layer to deep mucosa, the third hyperechoic layer to submucosa, the fourth hypoechoic layer to muscularis propria, and the fifth hyper-echoic layer to adventitia. Tumors appear as a hypoechoic expansion, and the degree of infiltration of the tumor through the esophageal wall layers determines the tumor stage. Expansion of layers 1 to 3 corresponds with infiltration of the superficial

and deep mucosa and submucosal layers, which is T1 disease. Expansion of layers 1 to 4 correlates with penetration into the muscularis propria, which is T2 disease. Expansion beyond the smooth outer border of the muscularis propria correlates with invasion of the adventitia, corresponding to T3 disease. Loss of a bright tissue plane between the area of tumor and surrounding structures such as the pleura, diaphragm, and pericardium correlates with T4a disease, whereas invasion of surrounding structures such as the trachea, aorta, lungs, or heart correlates with T4b disease (Fig. 8.3).

**TABLE  
8.3****Accuracy of Endoscopic Ultrasound in Staging Esophageal Cancers**

Study	Design	Number of Patients	Accuracy (%)	
			T Stage	N Stage
Nesje (2000) <sup>a</sup>	Prospective	54	70	90
Heidemann (2000) <sup>b</sup>	Consecutive	68	79	79
Vazquez-Sequeiros (2001) <sup>c</sup>	Consecutive	64	Unspecified	70
Kienle (2002) <sup>d</sup>	Prospective	117	69	79
Chang (2003) <sup>e</sup>	Prospective	60	83	89
Wu (2003) <sup>f</sup>	Prospective	31	84	71
Vazquez-Sequeiros and coworkers <sup>g</sup>	Prospective	125	86	87
DeWitt and coworkers <sup>h</sup>	Prospective	102	72	75
Lowe and coworkers <sup>i</sup>	Prospective	75	71	81
Zhang (2005) <sup>j</sup>	Retrospective	34	79	74
Moorjani (2007) <sup>k</sup>	Prospective	50	64	72
Shimpi (2007) <sup>l</sup>	Prospective	42	76	89
Kutup and coworkers <sup>m</sup>	Prospective	214	66	64
Sandha and coworkers <sup>n</sup>	Prospective	16	80	81
Mennigen (2008) <sup>o</sup>	Prospective	97	73	74
Omloo (2008) <sup>p</sup>	Prospective	125	76	70
Takizawa (2009) <sup>q</sup>	Prospective	159	Unspecified	64
Smith (2010) <sup>r</sup>	Retrospective	95	72	76

<sup>a</sup>Nesje LB, Svanes K, Viste A, et al. Comparison of a linear miniature ultrasound probe and a radial-scanning echoendoscope in TN staging of esophageal cancer. *Scand J Gastroenterol*. 2000;35:997–1002.

<sup>b</sup>Heidemann J, Schilling MK, Schmassmann A, et al. Accuracy of endoscopic ultrasonography in preoperative staging of esophageal carcinoma. *Dig Surg*. 2000;17:219–224.

<sup>c</sup>Vazquez-Sequeiros E, Norton ID, Clain JE, et al. Impact of EUS-guided fine-needle aspiration on lymph node staging in patients with esophageal carcinoma. *Gastrointest Endosc*. 2001;53:751–757.

<sup>d</sup>Kienle P, Buhl K, Kuntz C, et al. Prospective comparison of endoscopy, endosonography and computed tomography for staging of tumours of the oesophagus and gastric cardia. *Digestion*. 2002;66:230–236.

<sup>e</sup>Chang KJ, Soetikno RM, Bastidas D, et al. Impact of endoscopic ultrasound combined with fine-needle aspiration biopsy in the management of esophageal cancer. *Endoscopy*. 2003;35:962–966.

<sup>f</sup>Wu LF, Wang BZ, Feng JL, et al. Preoperative TN staging of esophageal cancer: comparison of miniprobe ultrasonography, spiral CT and MRI. *World J Gastroenterol*. 2003;9:219–224.

<sup>g</sup>Zhang X, Watson DI, Lally C, Bessell JR. Endoscopic ultrasound for preoperative staging of esophageal carcinoma. *Surg Endosc*. 2005;19(12):1618–1621.

<sup>h</sup>Moorjani N, Junemann-Ramirez M, Judd O, et al. Endoscopic ultrasound in esophageal carcinoma: comparison with multislice computed tomography and importance in the clinical decision making process. *Minerva Chir*. 2007;62:217–223.

<sup>i</sup>Shimpi RA, George J, Jowell P, Gress FG. Staging of esophageal cancer by EUS: staging accuracy revisited. *Gastrointest Endosc*. 2007;66:475–482.

<sup>j</sup>Mennigen R, Tuebergen D, Koehler G, et al. Endoscopic ultrasound with conventional probe and miniprobe in preoperative staging of esophageal cancer. *J Gastrointest Surg*. 2008;12: 256–262.

<sup>k</sup>Omloo JM, Sloof GW, Boellaard R, et al. Importance of fluorodeoxyglucose-positron emission tomography (FDG-PET) and endoscopic ultrasonography parameters in predicting survival following surgery for esophageal cancer. *Endoscopy*. 2008;40:464–471.

<sup>l</sup>Takizawa K, Matsuda T, Kozu T, et al. Lymph node staging in esophageal squamous cell carcinoma: a comparative study of endoscopic ultrasonography versus computed tomography. *J Gastroenterol Hepatol*. 2009;24:1687–1691.

<sup>m</sup>Smith BR, Chang KJ, Lee JG, Nguyen NT. Staging accuracy of endoscopic ultrasound based on pathologic analysis after minimally invasive esophagectomy. *Am Surg*. 2010;76(11):1228–1231.

**N Stage.** The survival of patients with esophageal carcinoma depends largely on the presence or absence of lymph node involvement at the time of diagnosis.<sup>78,79</sup> In patients who have surgery, stage for stage, survival is worse if a lesser lymphadenectomy is done. This survival difference is likely due to the result of stage migration because the probability of identifying positive lymph nodes is directly correlated to the adequacy of the lymphadenectomy.<sup>80</sup>

EUS has an important role in identifying malignant lymph nodes, to help plan a treatment pathway, and for predicting

the prognosis.<sup>81</sup> Several nodal characteristics are associated with malignant involvement: size greater than 5 to 10 mm, round shape, sharp boarders, and hypoechoic (dark) pattern.<sup>82</sup> The accuracy of this diagnosis correlates with the number of EUS criteria present.<sup>83</sup> The presence of all four features has a sensitivity of 89% and specificity of 92% for lymph node metastasis.<sup>57,84</sup>

Modified lymph node criteria were proposed by Vazquez-Sequeiros and coworkers, with the addition of three EUS features: lymph node in the celiac region, ≥5 nodes identified, and

**TABLE 8.4****Accuracy of Imaging Modalities in Staging Esophageal Cancer**

Study	Number of Patients	Stage	EUS (%)	CT (%)	MRI (%)	PET (%)
Kienle (2002) <sup>a</sup>	117	T	69	33		
		N	79	67		
Wu (2003) <sup>b</sup>	31	T	84	68	60	
		N	71	78	64	
Sihvo and coworkers <sup>66</sup>	55	N	72	58		60
Vazquez-Sequeiros and coworkers <sup>90</sup>	125	T	86	72		
		N	87	51		
Lowe and coworkers <sup>69</sup>	69	T	71	42		42
		N	81	80		76
Sandha and coworkers <sup>63</sup>	16	T	80			
		N	81	69		56
Omloo (2008) <sup>c</sup>	125	T	76	97		
		N	70	61		
Keswani and coworkers <sup>54</sup>	245	N	86			44

*CT*, Computed tomography; *EUS*, endoscopic ultrasound; *MRI*, magnetic resonance imaging; *PET*, positron emission tomography.

<sup>a</sup>Kienle P, Buhl K, Kuntz C, et al. Prospective comparison of endoscopy, endosonography and computed tomography for staging of tumours of the oesophagus and gastric cardia. *Digestion*. 2002;66:230–236.

<sup>b</sup>Wu LF, Wang BZ, Feng JL, et al. Preoperative TN staging of esophageal cancer: comparison of miniprobe ultrasonography, spiral CT and MRI. *World J Gastroenterol*. 2003;9:219–224.

<sup>c</sup>Omloo JM, Sloof GW, Boellaard R, et al. Importance of fluorodeoxyglucose-positron emission tomography (FDG-PET) and endoscopic ultrasonography parameters in predicting survival following surgery for esophageal cancer. *Endoscopy*. 2008;40:464–471.

**TABLE 8.5****Esophageal Wall Layers With the Radial and Curvilinear Echoendoscope**

EUS Layer	Esophageal Wall Layer	Echogenicity
1	Interface between lumen and mucosa	Hyperechoic
2	Deep mucosa including muscularis mucosa	Hypoechoic
3	Submucosa	Hyperechoic
4	Muscularis propria	Hypoechoic
5	Adventitia interface	Hyperechoic

*EUS*, Endoscopic ultrasound.

T3-T4 disease.<sup>85</sup> The modified EUS criteria were more accurate than standard criteria, with 86% accuracy achieved when ≥3 of the 7 modified EUS criteria were used. Multivariable logistic regression analysis found that the EUS lymph node criteria of size ≥5 mm, rounded shape, ≥5 lymph nodes identified, and tumor stage T3-T4 best predicted malignant nodal involvement.

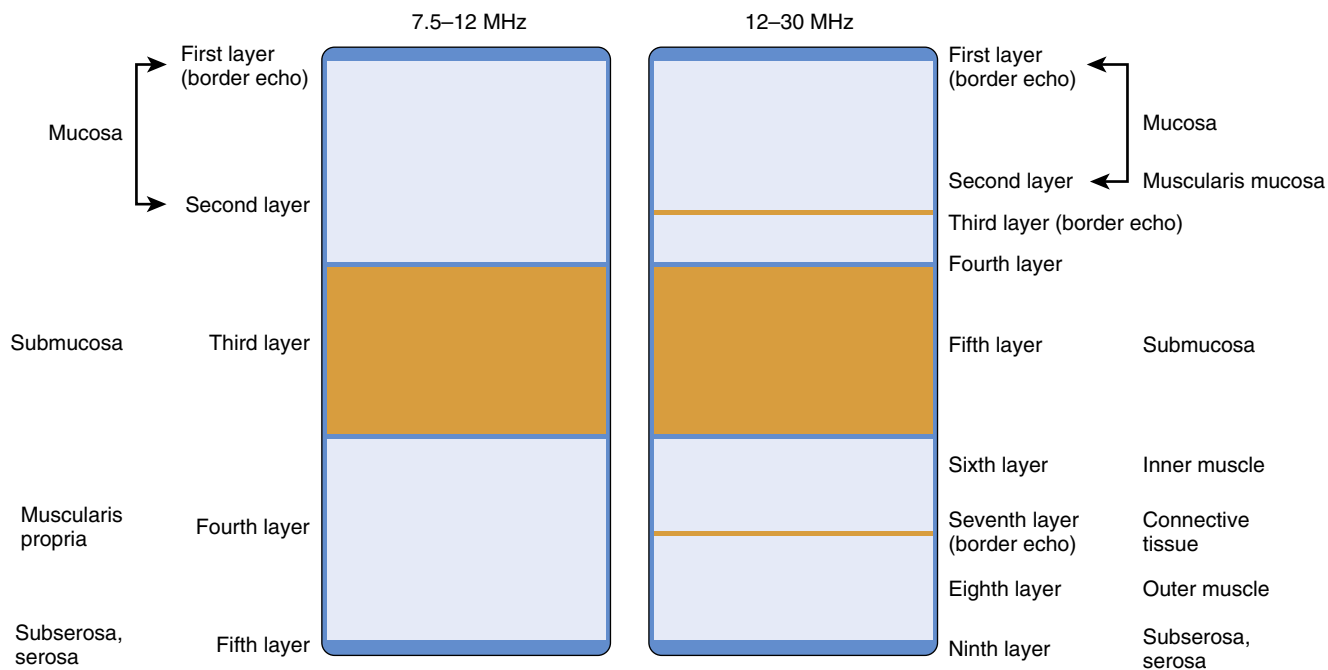
Malignant involvement is also confirmed by FNA for cytology assessment.<sup>54</sup> FNA of suspicious lymph nodes should be performed without traversing the primary tumor or major blood vessels because this can lead to false-positive results, bleeding, and potentially risk tumor seeding. Furthermore, FNA should only be performed if it will impact treatment decisions.

EUS alone is insufficient for lymph node staging because metastatic lymph nodes may be beyond the depth of ultrasound penetration, past a stricturing tumor, or involve distal lymph nodal groups without regional lymph node disease.<sup>51,86</sup> A combination of EUS, CT, and FDG PET/CT is often used to minimize the risk of understaging. EUS detects more locoregional node involvement than CT or PET<sup>65</sup> and has a specificity of 70% (95% CI, 65% to 75%) and a sensitivity of 80% (95% CI, 75% to 84%).<sup>50</sup> The combination of EUS FNA with CT further improves the diagnostic accuracy of local lymph node involvement.<sup>87</sup>

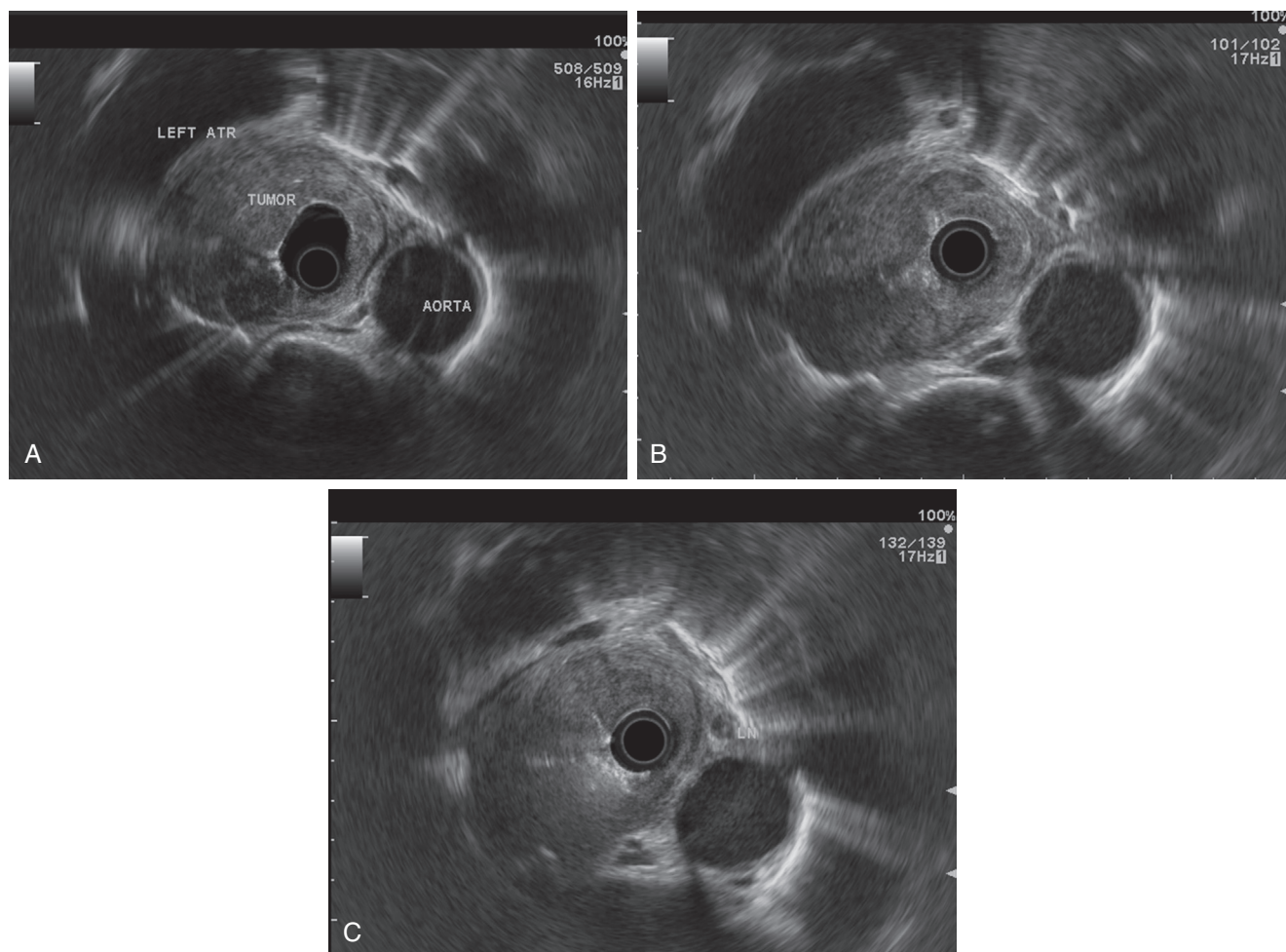
**M Stage.** Imaging begins in the duodenum and antrum of the stomach to examine the liver and portal and peripancreatic lymph nodes. The area surrounding the fundus and cardia of the stomach are scanned to look for perigastric, peripancreatic, and celiac axis lymphadenopathy. Other sites of metastases include the left adrenal gland and peritoneum, which is suggested by free peritoneal fluid (ascites). Metastases to the left liver lobe (median size, 5 mm) or collections of malignant pleural fluid unsuspected at CT were diagnosed by EUS FNA in 3% to 5% of patients in a prospective and a retrospective study that together included a total of 207 patients.<sup>88,89</sup>

### Role of Fine-Needle Aspiration in Staging

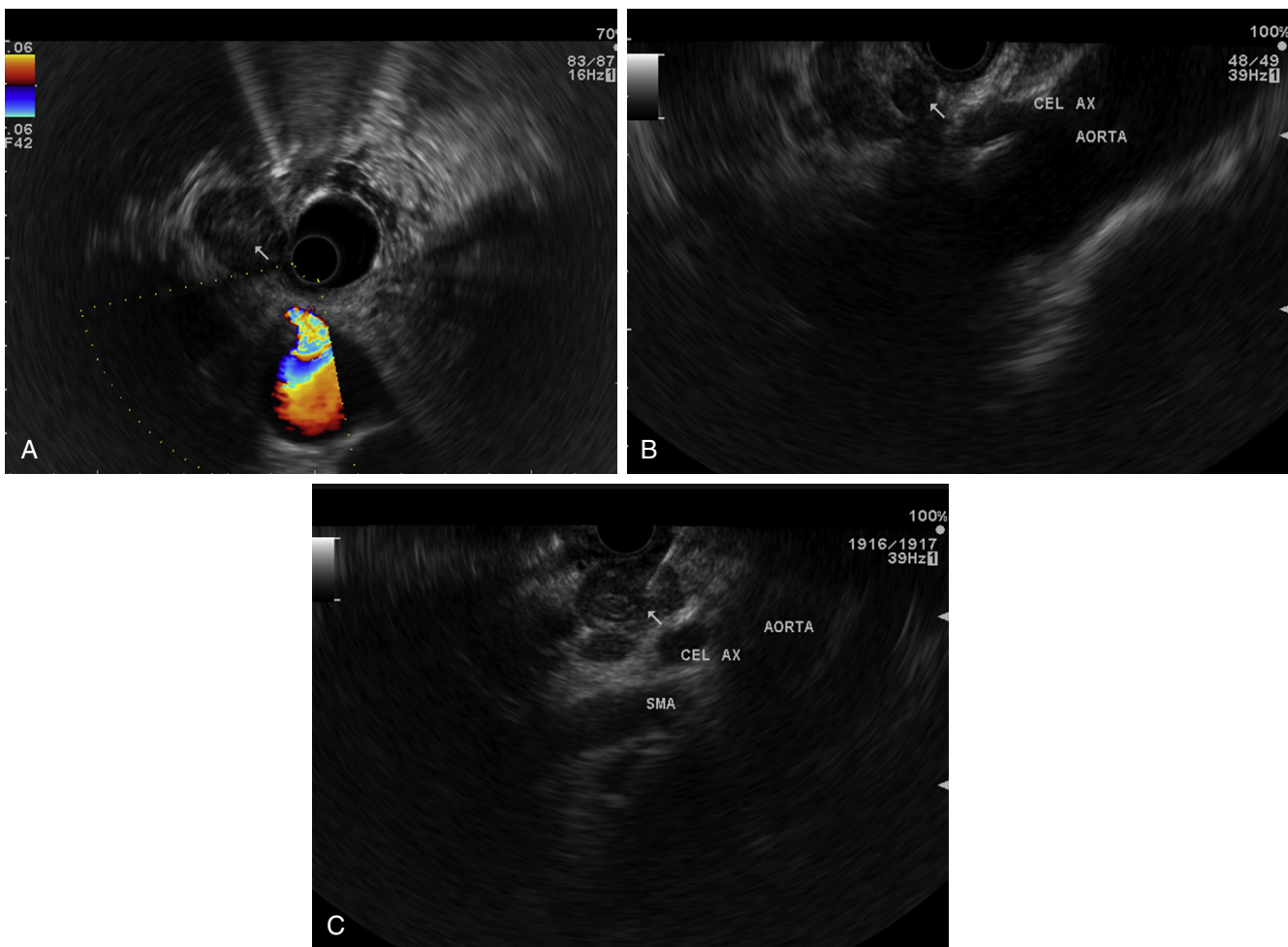
Tissue confirmation of nodal involvement or metastatic disease is important for selecting appropriate treatment pathways (Fig. 8.4). The presence of nodal involvement in T1-T2 disease determines whether patients receive neoadjuvant chemoradiotherapy or proceed directly to surgery, and confirmation of metastatic disease may determine whether treatment will be of curative or palliative intent.<sup>44</sup>



• **Fig. 8.2** Schematic representation of the normal esophageal and gastric wall as examined using a radial echoendoscope and a high-frequency miniprobe.



• **Fig. 8.3** A bulky esophageal tumor was identified, with pleural (A) and left atrium (B) invasion and a peritumoral lymph node (C). This was consistent with T4bN1 disease.



**• Fig. 8.4** (A) Celiac lymph node identified in a patient with esophageal cancer using a radial echoendoscope. (B and C) Linear echoendoscope passed to perform fine-needle aspiration for cytology confirmation.

The addition of FNA to EUS improves identification of malignant lymph nodes compared with EUS alone. In a prospective blinded comparison study in 125 patients, EUS, EUS FNA, and helical CT results were compared with the pathologic evaluation of resected lymph nodes.<sup>90</sup> The accuracy of EUS FNA for lymph node staging (87%) was higher than that of EUS alone (74%,  $P = .01$ ) or helical CT (51%,  $P < .001$ ). Furthermore, EUS FNA significantly modified tumor stage determined by helical CT in 38% of patients, usually towards a higher stage. Clinical treatment plan is also impacted by performing FNA on suspicious lymph nodes. In a prospective cohort study of 109 patients referred for EUS, FNA was performed in 13% and the cytology results impacted management plan in all patients.<sup>86</sup>

## Early Esophageal Cancer

Esophageal cancer is termed “early” if it involves the mucosal (T1a) or submucosal (T1b) layers and does not invade the muscularis propria (T2 disease). Three distinct layers are described in the esophageal mucosa: the epithelium (m1), the lamina propria (m2), and the muscularis mucosae (m3). In Barrett esophagus, because of the existence of a newly formed muscularis mucosae beneath the Barrett epithelium, the mucosal layer is divided into four layers.<sup>91</sup> In the operative specimen the submucosa is divided

into three sections of equivalent thickness and termed sm1, sm2, and sm3. The muscularis propria is not present in an ER specimen; therefore submucosal invasion is described using a micrometric scale starting from the muscularis mucosae.

Cancer invading only the superficial mucosal levels (m1 and m2) can be treated by ER,<sup>14,92</sup> and invasion into deep submucosa levels (sm2 and sm3) usually requires surgery. Middle level invasion (m3 and superficial submucosa) requires balancing of clinical factors with patient performance status and operative risks, and ER may be suitable for select patients with “low risk” submucosal invasion.<sup>18</sup> The critical depth assessment of early esophageal neoplasia is to distinguish T1a from T1b lesions.

The risk of nodal involvement in early adenocarcinoma confined to the mucosa (T1a) ranges between 0% and 3%, and when the lesion extends into the submucosal layer (T1b) this risk is up to 30%.<sup>13,26,93,94</sup> Early adenocarcinoma behaves less aggressively than SCC, for which the risk of lymph node metastasis starts to increase with invasion of the muscularis mucosae (m3),<sup>95</sup> and surgery is generally recommended if any submucosal invasion is seen.<sup>96,97</sup>

The main role for EUS in staging early esophageal cancer is to exclude suspicious lymph nodes in “high-risk” lesions with conventional EUS followed by FNA, if necessary (Fig. 8.5). Its utility in staging prior to endoscopic or surgical treatment in early neoplasia



**Fig. 8.5** Esophageal tumor invasion of the submucosa is seen, with an adjacent enlarged, rounded and hypoechoic lymph node (T1N1).

is debatable.<sup>98,99</sup> Isolated thickening of the mucosal layer alone may be difficult to see on EUS, resulting in loss of sensitivity of EUS for superficial disease. Similarly, standard EUS scopes (frequency 7.5 to 12 MHz) have a higher penetration, which is important for lymph node staging, but a lower resolution which limits its ability to accurately distinguish tumor penetration through the muscularis mucosa, or superficial from deep penetration of the submucosa.<sup>100,101</sup> The main risk is overstaging in early disease. In a single center retrospective review of 109 patients with Barrett neoplasia, EUS classified lesions as suspicious for invasion in 19 patients; 84% of them had no evidence of invasion in final pathology.<sup>102</sup>

### High-Frequency Probes

In a prospective randomized crossover study comparing the accuracy of HFPs and conventional radial EUS in distinguishing between mucosal and submucosal adenocarcinoma arising within Barrett mucosa, the accuracy of HFPs was significantly higher than radial EUS; however, the overall accuracy of T staging was low with both methods: HFPs 64% and conventional radial EUS 49%.<sup>40</sup> Another study found that HFPs had only a limited accuracy in the detection of submucosal invasion: overall accuracy, sensitivity, and specificity to differentiate T1a from T1b tumors was 73.5%, 62%, and 76.5%, respectively.<sup>103</sup> Staging was incorrect in 26.5% (overstaging 18.6%, understaging 7.8%), and nearly 70% of the tumors which were assessed as submucosal had cancer limited to the mucosa on the final resection specimen. In another study, the overall sensitivity of HFPs for submucosal infiltration was only 48%, which decreased to 14.3% for tumors at the gastroesophageal junction.<sup>104</sup> The low sensitivity was largely due to difficulty in identifying tumors with early submucosal invasion, whereas tumors involving the deeper submucosal layers were correctly diagnosed in most of the cases.

### Endoscopic Evaluation

The macroscopic type of early neoplasia classified per the Paris classification (Table 8.6)<sup>13</sup> helps to predict the depth of tumor invasion, thereby the risk of lymph node metastases and whether endoscopic therapy should be performed.<sup>13,102,105,106</sup> Endoscopic staging of early esophageal cancer using a high-resolution endoscope has a similar diagnostic accuracy as EUS using an HFP (82.9% vs. 79.6%).<sup>102,104</sup> The Paris classification system categorizes superficial neoplastic lesions as type 0 and is divided into the following groups: polypoid or protruding (type 0-I), nonpolypoid and nonexcavated (type 0-II), and nonpolypoid with a frank ulcer (type III).

**TABLE 8.6** **Paris Endoscopic Classification of Superficial Neoplastic Lesions**

Type 0 Neoplastic Lesions of The Digestive Tract		
Polypoid	Protruded, pedunculated	0-Ip
	Protruded, sessile	0-Is
Nonpolypoid	Slightly elevated	0-IIa
	Flat	0-IIb
Excavated (ulcer)	Slightly depressed	0-IIc
	Excavated (ulcer)	0-III

Adapted from The Paris endoscopic classification of superficial neoplastic lesions: esophagus, stomach, and colon. *Gastrointest Endosc*. 2003;58(suppl): S3–S43.

Type 0-I is further segmented into pedunculated (0-Ip) and sessile (0-Is) groups, and type 0-II into three variants: slightly elevated (0-IIa), completely flat (0-IIb), and slightly depressed without an ulcer (0-IIc). Mixed types consist of two or more distinct types of morphology, such as a slightly elevated lesion containing a depression, which is classified as 0-IIa+IIc. Approximately 85% of early superficial neoplastic lesions in Barrett esophagus are Paris type 0-II lesions. Neoplastic lesions in Barrett mucosa with Paris type 0-IIb morphology (slightly raised, flat) rarely contain submucosal invasion, with neoplasia limited to the mucosal layer in 96% of cases.<sup>103</sup> This is in comparison to Paris Type 0-I and 0-IIa + c lesions, which have a higher risk of containing submucosal invasion.

Given the limitations of cross-sectional imaging and EUS in staging superficial esophageal cancer, ER has become a useful diagnostic tool and should be considered the therapy of choice for dysplasia associated with visible lesions and T1a adenocarcinoma. For small, nodular lesions ≤2 cm, ER provides a more accurate depth of invasion than EUS.<sup>99</sup> A decision to proceed to further therapy, such as surgical resection or ablation, or to consider the ER completely therapeutic depends on the pathology of the resection specimen. It is unclear whether superficial T1b cancer (invading the superficial submucosa <500 μm) can be confidently treated by ER. Although series suggest this carries a low risk of lymph node metastases,<sup>8,16,18</sup> not all the literature supports this.<sup>98,107</sup> In patients who are a high surgical risk, ER can be considered as an alternative to surgery for treatment of “good prognosis” T1b adenocarcinomas, which include submucosal invasion less than 500 μm, clear deep resection margins on the ER specimen (R0), graded as well differentiated, and with no lymphovascular invasion.<sup>15,16</sup>

EUS ± FNA should be considered when the endoscopist cannot exclude advanced stage based on the endoscopic appearance of nodular or ulcerated lesions and in patients with T1b (sm1) disease on staging ER in whom endoscopic therapy is being considered, to evaluate and exclude lymph node involvement.<sup>108</sup>

### Restaging After Neoadjuvant Therapy

Neoadjuvant therapy is recommended for most patients with locally advanced disease.<sup>44</sup> The objectives of neoadjuvant therapy are to decrease the tumor burden which may enable more patients to undergo potentially curative surgical resection, and diminish the risk of recurrence. Patients need to be restaged after completing neoadjuvant therapy to determine whether they are suitable for

resection or should be referred for palliative management. Endoscopic biopsies performed after chemotherapy or radiotherapy may miss residual disease,<sup>109</sup> and endoscopic evaluation requires careful examination for mucosal surface changes, with multiple biopsies taken of any visualized abnormalities and strictures.

Although EUS has clear benefits in the initial staging of esophageal cancer, it is not as reliable for restaging after neoadjuvant therapy.<sup>110</sup> This is due to the local inflammatory and fibrotic responses to chemotherapy and radiation, which cause hypoechoic wall thickening on EUS. This can lead to overestimation of the depth of tumoral invasion and potentially exclude suitable patients from surgical resection.

EUS FNA has lower accuracy than integrated FDG PET/CT for lymph node restaging after neoadjuvant therapy but has similar accuracy in distinguishing between T1-3 and T4 disease. In a prospective trial of 48 consecutive patients who had undergone neoadjuvant chemoradiotherapy, the accuracy for nodal disease was 78%, 78%, and 93% for CT scan, EUS FNA, and FDG PET/CT, respectively ( $P = .04$ ).<sup>111</sup> The accuracy of each test for distinguishing pathologic T4 from T1-T3 disease was 76%, 80%, and 80% for CT scan, EUS FNA, and FDG PET/CT, respectively. Fifteen (31%) patients were complete responders, and FDG PET/CT accurately predicted complete response in 89% compared with 67% for EUS FNA ( $P = .045$ ) and 71% for CT ( $P = .05$ ). It is unclear whether EUS FNA should be performed for cytologic confirmation if suspicious lymph nodes or areas of wall thickening are seen on FDG PET/CT or CT.

Imaging characteristics may predict the likelihood of a pathologic response following neoadjuvant chemoradiotherapy. In a retrospective study of 103 patients, reduced EUS mass size (0.7 vs. 1.7 cm,  $P = .01$ ), reduction in esophageal wall thickness on CT (13.3 vs. 15.3 mm,  $P = .04$ ), and lower PET standardized uptake value (SUV) (3.1 vs 5.8,  $P = .01$ ) correlated with pathologic response, which was defined as  $\leq 10\%$  viable cells.<sup>112</sup>

## Influence of Endoscopic Ultrasound on Patient Management

The use of EUS in staging esophageal cancer changes patient management in up to 38% of cases. The change in management is most commonly by increasing the tumor stage, by detecting malignant lymph nodes or metastatic disease.<sup>86-88,113-115</sup>

EUS FNA was used in a prospective study to select the surgical approach in patients with resectable distal esophageal cancer and mediastinal lymph nodes visualized on EUS: EUS FNA changed the management in 23% of 48 patients, by allocating patients with positive lymph nodes to transthoracic esophagectomy, and those without lymph node involvement to transhiatal resection, which has limited ability to resect lymph nodes.<sup>116</sup>

## Cost-Effectiveness of Endoscopic Ultrasound in Esophageal Cancer

EUS has been shown to be economical in multiple studies. EUS staging prior to treatment saves an average of \$US 3443 per patient, by identification of stage I and stage IV tumors, which prevented unnecessary neoadjuvant chemoradiotherapy or surgery, respectively.<sup>117</sup> In a study looking at whether initial CT or EUS costs less to diagnose advanced esophageal cancer, CT was the initial staging test of choice in most settings, but in a referral center EUS found advanced disease (T4 and/or M1) more frequently than CT (44% vs 13%,  $P < .0001$ ) and was the least costly strategy.<sup>118</sup> Another study found that in patients without metastatic disease, EUS was

the most cost-effective staging modality, at \$US 13,811, versus CT-guided FNA at \$US 14,350, and surgery at \$US 13,992.<sup>119</sup> Another cost-saving method is selective rather than routine use of FNA for suspicious lymph nodes during EUS.<sup>83</sup>

## Impact of Endoscopic Ultrasound on Survival

A randomized trial of 223 patients with nonmetastatic gastroesophageal cancer was performed to assess whether the addition of EUS to usual staging tests changes treatment.<sup>120</sup> EUS significantly improved participant survival, with a hazard ratio of 0.706 (95% CI from 0.501 to 0.996) and an increase of 121 days in estimated median survival: from 1.63 years in the group that had standard work-up to 1.96 years in the group that included EUS. Quality-adjusted survival was significantly higher (66 days), and there was a substantial, although nonsignificant, net saving of £2,800 per trial participant. Combining these survival and economic findings, there was a 96.6% probability of being cost-effective by National Institute for Health and Care Excellence (NICE) criteria. The use of EUS also increased the proportion of tumors completely resected from 80% (44 of 55) to 91% (48 of 53) ( $P = \text{NS}$ ). Two retrospective studies examined the effect of EUS staging on patient survival. The first study reported significantly better survival and reduced recurrence rate, due to improved selection of patients for surgery and neoadjuvant treatment.<sup>121</sup> The second study found no survival advantage from EUS staging, but it reported only on patients suitable for surgery.<sup>43</sup>

## Learning Curve and Procedural Volume

Accuracy of tumoral staging by EUS is dependent in part on the learning curve of the endosonographer, with a study suggesting that at least 100 examinations are required to provide accurate T staging in patients with esophageal cancer.<sup>122</sup> In addition, the location where the EUS is performed may affect preoperative staging. A comparison study of outcomes in a low- and high-EUS volume hospital showed higher sensitivity and specificity of staging in a high-volume compared with low-volume center.<sup>123</sup>

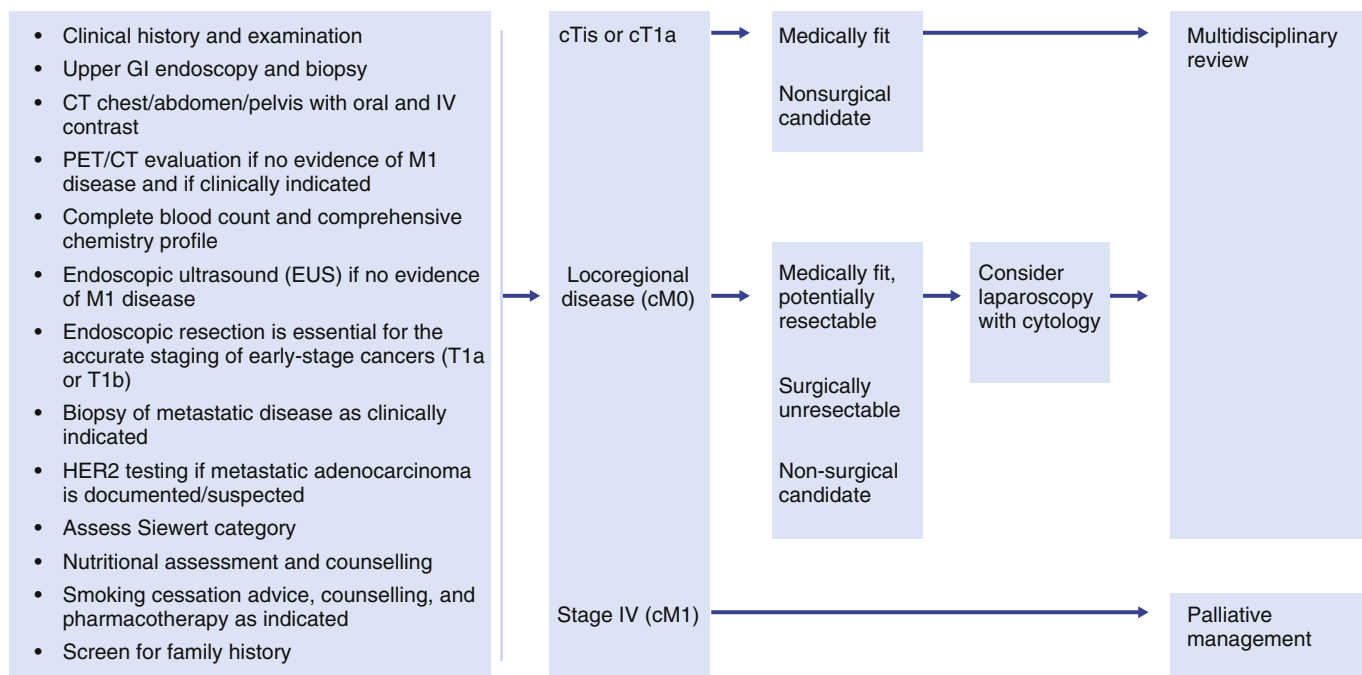
## Summary

EUS is an important part of the initial staging algorithm in patients with newly diagnosed esophageal cancer and no metastatic disease on CT scan, with or without FDG PET/CT, because it improves locoregional staging and can detect occult metastatic disease in a small but important proportion of patients. The accuracy of identifying malignant lymph nodes or metastatic disease is increased with the addition of FNA. The inclusion of EUS in staging protocols has demonstrated capacity to alter patient management and significantly improve patient survival and is cost effective. EUS has a limited role in early esophageal cancer, with greatest benefit likely seen in patients with submucosal disease (T1b) in whom endoscopic therapy is being considered, to exclude nodal or metastatic disease. EUS is also not routinely used for restaging after neoadjuvant therapy, due to its relatively low accuracy and tendency to overstage disease.

## Gastric Cancer

### Background

In 2017 the American Cancer Society estimates 28,000 new diagnoses and 10,960 deaths due to gastric cancer will occur in



• **Fig. 8.6** National Comprehensive Cancer Network Guidelines for the work-up of gastric cancer. CT, Computed tomography; GI, gastrointestinal; PET, positron emission tomography. (Adapted from the National Comprehensive Cancer Network Guidelines V 1.2017, Gastric Cancer.)

the United States.<sup>124</sup> Globally, gastric cancer is the fourth most common cancer and the second most common cause of cancer-related death.<sup>125</sup> There have been significant improvements in survival rates in the United States over the past 40 years; however, the 5-year relative survival rate remains low at 30%.<sup>3,126</sup> Potential targets for disease prevention include *Helicobacter pylori* infection, diet, smoking and alcohol use,<sup>127</sup> and early neoplasia detection through population screening in high-incidence countries.<sup>128</sup>

### Role of Endoscopic Ultrasound

Noninvasive imaging studies such as CT are widely available, but they lack accuracy for assessing the depth of tumor invasion or lymph node involvement.<sup>129,130</sup> EUS is the most reliable nonsurgical method available for evaluating the depth of invasion of primary gastric cancers,<sup>131,132</sup> is relatively low risk, and provides a more accurate prediction of T and N stage than CT imaging.<sup>133–135</sup> Moreover, EUS-guided FNA of both regional and distant lymph nodes adds to the accuracy of nodal staging.<sup>136,137</sup> Small metastatic deposits in the left lobe of the liver or low-volume malignant ascites can be diagnosed by EUS FNA, obviating the need for staging laparoscopy by establishing nonoperative diagnosis. EUS does not add to patient management in patients with metastatic gastric cancer identified by CT, and the role of EUS in restaging after chemotherapy or radiation therapy is unclear.

### Gastric Cancer Work-Up (Fig. 8.6)

Most gastric cancers are diagnosed on endoscopy, with multiple biopsies taken for histology and the cancer location in the stomach, and the relationship to the esophagogastric junction (EGJ)

for proximal tumors documented. In addition, endoscopic examination enables identification of complications such as luminal obstruction or bleeding. Endoscopic mucosal resection (EMR) or endoscopic submucosal dissection (ESD) of superficial lesions can be performed to provide a larger specimen for histology assessment of the degree of differentiation, presence of lymphovascular invasion, and the depth of infiltration.<sup>138</sup> EMR and ESD provide both accurate T staging for early cancers and have the potential to be therapeutic, as is discussed later.

A CT of the chest, abdomen, and pelvis with oral and intravenous contrast is performed to determine the extent of disease, followed by an EUS if no metastatic disease is seen on CT. In patients being considered for surgical resection without neoadjuvant therapy, laparoscopy to detect radiologically occult metastatic disease in patients with T3 or node-positive disease can be considered. In patients planned for neoadjuvant therapy, laparoscopy with peritoneal washings should be considered.<sup>139,140</sup>

### Gastric Cancer Staging

Gastric cancer staging is defined by the AJCC Staging System and is shown in Table 8.7.<sup>6</sup> The 8th edition includes changes to the definition of the anatomic boundary between esophagus and stomach, a subdivision of N3 disease according to the number of involved nodes, reclassification of T4aN2 and T4bN0 tumors as stage IIIA disease, and separate prognostic stage groups for clinical and pathologic staging, including pathologic staging after neoadjuvant therapy.

The radial echoendoscope is generally preferred for gastric cancer staging because of its ease of manipulation and its ability to evaluate the relationship between the lesion and adjacent organs. The ultrasonic miniprobe is useful for small lesions because these

**TABLE  
8.7****TNM Staging for Gastric Cancer, American Joint Committee on Cancer Staging System, 8th Edition****Anatomic Stage/Prognostic Groups**

Stage 0	Tis	N0	M0
Stage I	T1 or T2	N0	M0
Stage IIA	T1 or T2	N1, N2, or N3	M0
Stage IIB	T3 or T4a	N0	M0
Stage III	T3 or T4a	N1, N2, or N3	M0
Stage IVA	T4b	Any N	M0
Stage IVB	Any T	Any N	M1

**Primary Tumor (T)**

TX	Primary tumor cannot be assessed
T0	No evidence of primary tumor
Tis	Carcinoma in situ: intraepithelial tumor without invasion of the lamina propria
T1	Tumor invades lamina propria, muscularis mucosa, or submucosa
T1a	Tumor invades lamina propria or muscularis mucosa
T1b	Tumor invades submucosa
T2	Tumor invades muscularis propria
T3	Tumor penetrates subserosal connective tissue without invasion of visceral peritoneum or adjacent structures
T4	Tumor invades serosa (visceral peritoneum) or adjacent structures
T4a	Tumor invades serosa (visceral peritoneum)
T4b	Tumor invades adjacent structures

**Regional Lymph Nodes (N)**

NX	Regional lymph node(s) cannot be assessed
N0	No regional lymph node metastasis
N1	Metastasis in 1–2 regional lymph nodes
N2	Metastasis in 3–6 regional lymph nodes
N3	Metastasis in seven or more regional lymph nodes
N3a	Metastasis in 7–15 regional lymph nodes
N3b	Metastasis in 16 or more regional lymph nodes

**Distant Metastasis (M)**

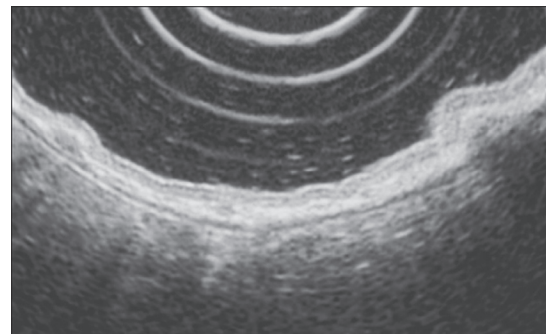
M0	No distant metastasis
M1	Distant metastasis

From Amin MB, Edge SB, Greene FL, et al., eds. *AJCC Cancer Staging Manual*. 8th ed. New York: Springer; 2017.

lesions can be viewed simultaneously by endoscopy and endo-sonography (Fig. 8.7). In patients with suspected nodal disease in which cytology confirmation is required, a curvilinear echoendoscope is used. EUS assesses the depth of tumor invasion (T stage), the presence of abnormal or enlarged lymph nodes (N stage), and metastatic lesions in surrounding organs or ascites<sup>141</sup> and can help treatment planning in patients who are being considered for ER (EMR or ESD).<sup>142</sup>

**T Staging**

The patient is positioned with the lesion in the dependent positon. Water is instilled into the stomach to submerge the lesion and air is aspirated to optimize acoustic coupling and allow evaluation of the lesion without contact, avoiding compression of tissue planes and inaccurate T staging. The EUS transducer is maintained perpendicular to the lesion to avoid tangential imaging. Five distinct layers of the gastric wall are seen with the radial and linear echoendoscope—three hyperechoic and two hypoechoic—visible as alternating bright and dark layers. The first two echo layers correspond histologically to the mucosa, the third corresponds to the submucosa, the fourth to the muscularis propria, and the fifth to the serosa. Gastric cancer appears as a hypoechoic expansion of the gastric wall layers, with gradual loss of the layered pattern of the normal stomach wall corresponding with greater depths of tumor



• **Fig. 8.7** The nine-layer esophageal and gastric wall, examined using a 20-MHz high-frequency endoscopic ultrasonography miniprobe.

penetration, correlating with higher T stage (Fig. 8.8). Expansion of layers 1 to 3 corresponds with infiltration into the submucosa (T1); expansion of layers 1 to 4 correlates infiltration of the muscularis propria (T2); and expansion beyond the muscularis propria resulting in an irregular outer border indicates subserosal invasion (T3 disease). T4a disease is recognized by loss of the bright serosa layer, and extension of the mass into surrounding organs such as the liver, pancreas, and spleen indicates T4b disease.

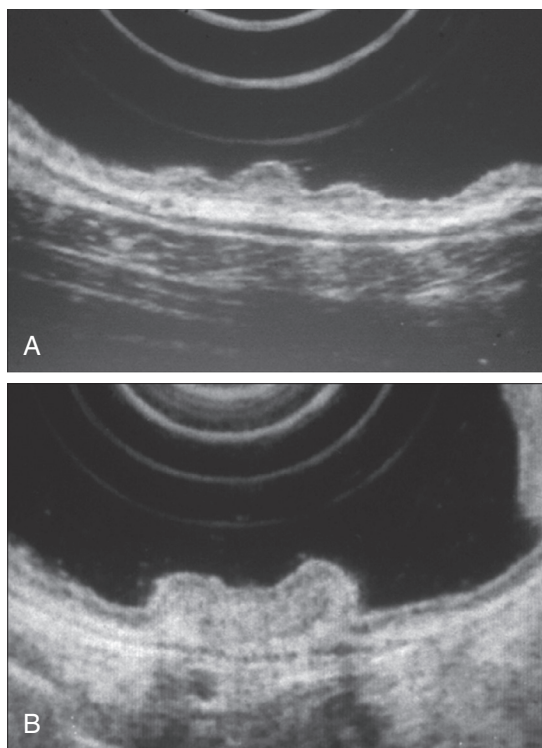


**Fig. 8.8** Early stage gastric cancer. (A) Early stage gastric cancer confined to the mucosal layer. (B) Early stage gastric cancer extending to the submucosal layer.

### N Staging

Perigastric and regional lymph node stations are surveyed and suspicious features documented (hypoechoic, sharp borders, round shape, size >10 mm). FNA can be performed for cytologic confirmation if it will impact the treatment plan and can be performed without passing the needle through the primary tumor.

### M Staging

The echoendoscope is advanced to the gastric antrum, and surrounding structures (left lobe of liver, peritoneum, pleural layers of the lung, and mediastinum) are carefully examined on slow withdrawal. Metastatic lesions, malignant ascites, pleural effusion, or metastasis in distant nodes can be missed on staging CT, and their detection by EUS with or without FNA can change patient management (Fig. 8.9).<sup>143–145</sup>

### Management Pathways in Gastric Cancer

Superficial cancers have a very low risk of lymph node or distant metastases,<sup>146</sup> and endoscopic evaluation with magnification and with contrast or digital chromoendoscopy have a high accuracy for predicting the depth of invasion.<sup>147,148</sup> Submucosal involvement usually obligates surgery due to a nearly 20% risk of nodal metastasis.<sup>149</sup> Precise endoscopic evaluation of these lesions is recommended to assess endoscopic resectability, with EUS reserved only for selected cases. CT is generally not necessary because the risk of metastatic disease is very low in a lesion in which ER is feasible.<sup>141,150,151</sup> Comparisons between EMR with ESD for the treatment of early gastric cancer,<sup>152–154</sup> show ESD obtains a higher rate of en bloc resection (92% vs. 52%; odds ratio [OR] 9.69, 95% CI 7.74 to 12.13),



**Fig. 8.9** Hepatic metastasis of gastric cancer. Endoscopic ultrasonography-guided fine-needle aspiration of a metastatic deposit in the left lobe of the liver.

histologically complete resection (82% vs. 42%; OR 5.66, 95% CI 2.92 to 10.96), and lower recurrence (1% vs. 6%; OR 0.10, 95% CI 0.06 to 0.18). However, ESD has a longer procedural time (mean, 59.4 min longer; 95% CI 16.8 to 102) and a higher risk of perforation (4% vs. 1%; OR 4.67, 95% CI 2.77 to 7.87) (Table 8.8). European Society Gastrointestinal Endoscopy (ESGE) guidelines suggest that ESD should be considered in any gastric lesion with very low possibility of lymph node metastasis.<sup>155</sup>

According to the Japanese guidelines for gastric cancer<sup>132</sup> and expanded National Cancer Centre criteria,<sup>156</sup> ESD should be performed for:

- Gastric dysplasia of any size;
- Intramucosal differentiated-type adenocarcinoma, without ulceration (size ≤2 cm absolute indication, >2 cm expanded indication);
- Intramucosal differentiated-type adenocarcinoma, with ulcer, size ≤3 cm (expanded indication);
- Intramucosal undifferentiated-type adenocarcinoma, size ≤2 cm (expanded indication);
- Differentiated-type adenocarcinoma with superficial submucosal invasion (sm1, ≤500 μm), and size ≤3 cm (expanded indication).

Surgery is recommended when histologic evaluation of the ESD specimen shows lymphovascular invasion, submucosal infiltration greater than 500 μm, positive vertical margins, or ulcerated features in tumors greater than 30 mm or with submucosal invasion.<sup>150</sup>

Patients with mucosal disease and lymph node metastases (T1N1 or higher) or T2 disease without distant metastases are considered for neoadjuvant therapy and surgery.<sup>157,158</sup> Patients without metastatic disease after preoperative treatment have surgical resection, which is generally followed by adjuvant chemotherapy or chemoradiotherapy.<sup>159</sup> Patients with distant metastatic disease, invasion of major vasculature, or distant lymph nodes are typically unresectable, and treatment is based on symptom palliation and possible survival benefit.

### Accuracy of Endoscopic Ultrasound for Staging Gastric Cancer

After endoscopy, EUS is the most important diagnostic procedure for local staging in patients with gastric cancer (Table 8.9). EUS is regarded as the modality of choice for local staging, with an

**TABLE 8.8****Outcomes of Endoscopic Submucosal Dissection for Gastric Superficial Lesions (Meta-Analyses)**

Author (Year)	Number of Lesions	En Bloc Resection Rate Lesions, n/N (%)	Complete R0 Resection Rate Lesions, n/N (%)	Curative Resection Rate Lesions, n/N (%)	Local Recurrence Rate Lesions, n/N (%)	Procedure-Related Bleeding Lesions, n/N (%)	Procedure-Related Perforation Lesions, n/N (%)	Range of Mean Operation Time, min
Park and coworkers <sup>153</sup> (2011)	1734	1055/1150 (92%)	1287/1401 (92%)	774/973 (80%)	13/1592 (<1%)	116/1642 (7%)	80/1762 (5%)	33–84
Lian and coworkers <sup>152</sup> (2012)	1495	1328/1437 (92%)	1227/1495 (82%)		11/1438 (<1%)	82/876 (9%)	62/1438 (4%)	34–116
Facciorusso and coworkers <sup>154</sup> (2014)	1916	1328/1437 (92%)	1227/1495 (82%)		12/1859 (<1%)	62/1438 (4%)	62/1438 (4%)	34–116

**TABLE 8.9****Accuracy of Endoscopic Ultrasound in Gastric Cancer T Staging**

Author (Year)	Frequency (MHz)	Patients (n)	T Stage Accuracy (%)
Tseng (2000) <sup>a</sup>	7.5–12	74	85
Willis (2000) <sup>b</sup>	7.5–12	116	78
Habermann and coworkers <sup>161</sup> (2004)	7.5–12	51	86
Tsendsuren (2006) <sup>c</sup>	5–7.5	41	69
Ganpathi and coworkers <sup>134</sup> (2006)	7.5–20	126	80
Bentrem and coworkers <sup>141</sup> (2007)	7.5–12	225	57
Lok (2008) <sup>d</sup>	5–20	123	64
Repiso (2010) <sup>e</sup>	7.5–20	46	70

<sup>a</sup>Tseng L, Mo L, Tio T, et al. Video-endoscopic ultrasonography in staging gastric carcinoma. *Hepatogastroenterology*. 2000;47:897–900.

<sup>b</sup>Willis S, Truong S, Gribnitz S, et al. Endoscopic ultrasonography in the preoperative staging of gastric cancer: accuracy and impact on surgical therapy. *Surg Endosc*. 2000;14:951–954.

<sup>c</sup>Tsendsuren T, Jun S, Mian X. Usefulness of endoscopic ultrasonography in preoperative TNM staging of gastric cancer. *World J Gastroenterol*. 2006;12:43–47.

<sup>d</sup>Lok K, Lee C, Yiu H, et al. Current utilization and performance status of endoscopic ultrasound in a community hospital. *J Dig Dis*. 2008;9:41–47.

<sup>e</sup>Repiso A, Gomez-Rodriguez R, Lopez-Pardo R, et al. Usefulness of endoscopic ultrasonography in preoperative gastric cancer staging: diagnostic yield and therapeutic impact. *Rev Esp Enferm Dig*. 2010;102:413–420.

accuracy ranging from 65% to 92.1% for T stage<sup>160</sup> and from 66% to 90% for N stage.<sup>161,162</sup> In a recent meta-analysis of the diagnostic accuracy of EUS for the preoperative locoregional staging of primary gastric cancer, 66 studies published between 1988 and 2012, using histology as the reference and involving 7747 patients, were identified.<sup>163</sup> The pooled accuracy of EUS in discriminating between T1-T2 (superficial) versus T3-T4 (advanced) gastric cancer was 88%; in discriminating between T1 (early gastric cancer) versus T2 (muscle-infiltrating) gastric cancer was 86.5%; and between T1a versus T1b gastric cancer was 83.4%. The pooled accuracy of EUS in determining nodal stage (positive vs. negative) was 75%. The results are summarized in Table 8.10. Another meta-analysis showed that the pooled accuracy for T stage was 75% with a moderate Kappa value (0.52). EUS was most accurate for T3 cancers (85%), followed by T4

(79%), T1 (77%), and T2 (65%) cancers. The pooled accuracy, sensitivity, and specificity of EUS for N staging (N0 vs. N+) was 64%, 74%, and 80%, respectively.<sup>164</sup>

EUS has a limited role in staging the depth of invasion in superficial gastric cancers, with a T stage accuracy of 41.4% to 87% (Table 8.11). A meta-analysis by Pei and coworkers identified that EUS had a pooled sensitivity and specificity of staging mucosal disease of 76% (95% CI: 74% to 78%) and 72% (95% CI: 69% to 75%), respectively. The pooled sensitivity and specificity of EUS in detecting submucosal invasion was 62% (95% CI: 59% to 66%) and 78% (95% CI: 76% to 80%), respectively.<sup>165</sup>

### M Staging

EUS has a limited role in the detection of metastatic disease, such as ascites and peritoneal and liver metastases, with an overall

**TABLE 8.10 Diagnostic Performance of Endoscopic Ultrasound in Assessing Disease Stage in Gastric Cancer**

Hypothetical Cohort of 1000 Patients With Gastric Cancer						
Stage Groups	Sensitivity	Specificity	Positive Likelihood Ratio	Negative Likelihood Ratio	Diagnostic Odds Ratio	Clinical Application
T1-2 (superficial) vs. T3-4 (advanced)	0.86 95% CI: 0.81–0.90	0.90 95% CI: 0.87–0.93	8.9 95% CI: 6.8–11.6	0.16 95% CI: 0.12–0.22	56 95% CI: 37–85	EUS might be more reliable in correctly identifying T3-T4 cases compared with T1-T2 cases
T1 (early gastric cancer) vs. T2 (muscle-infiltrating)	0.85 95% CI: 0.78–0.91	0.90 95% CI: 0.85–0.93	8.5 95% CI: 5.9–12.3	0.17 95% CI: 0.12–0.24	50 95% CI: 32–79	Increases the probability of being classified as T1 from 70% (average prevalence of T1 cases) to 94% when positive; lowers the same probability to 26% when negative. EUS accuracy is not optimal either for disease depth confirmation or exclusion.
T1a vs. T1b	0.87 95% CI: 0.81–0.92	0.75 95% CI: 0.62–0.84	3.4 95% CI: 2.3–5.0	0.17 95% CI: 0.12–0.24	20 95% CI: 12–33	Increases the probability of being classified as T1 from 70% (average prevalence of T1a cases) to 88% when positive; lowers the same probability to 30% when negative. EUS accuracy is not optimal either for disease depth confirmation or exclusion.
N0 vs. N+	0.83 95% CI: 0.79–0.87	0.67 95% CI: 0.61–0.72	2.5 95% CI: 2.1–2.9	0.25 95% CI: 0.20–0.31	10 95% CI: 7–13	Increases the probability of being classified as N+ from 50% (average prevalence of N+ cases) to 62% when positive; lowers the same probability to 14% when negative. EUS accuracy is not optimal either for lymph node metastatic involvement confirmation or exclusion.

Adapted from Mocellin S, Pasquali S. Diagnostic accuracy of endoscopic ultrasonography (EUS) for the preoperative locoregional staging of primary gastric cancer. *Cochrane Database of Syst Rev*. 2015(2):CD009944.

**TABLE  
8.11****Accuracy of Endoscopic Ultrasound for T Staging in Early Gastric Cancer**

Author (Year)	Study Design	Number of Lesions	T Stage Accuracy (%)
Yanai (1999) <sup>a</sup>	Prospective	52	71
Hizawa (2002) <sup>b</sup>	Retrospective	234	78
Kim and coworkers <sup>172</sup> (2007)	Retrospective	206	58.3–64.4
Choi and coworkers <sup>147</sup> (2010)	Prospective	955	67
Kim (2010) <sup>c</sup>	Prospective	176	80.7
Choi (2010) <sup>d</sup>	Prospective	388	78.9
Okada and coworkers <sup>142</sup> (2011)		542	43.5–87.5
Tsuzuki (2011) <sup>e</sup>	Retrospective	105	86
Park (2011) <sup>f</sup>	Retrospective	152	41.4
Yamamoto (2012) <sup>g</sup>	Retrospective	75	82.7
Kim (2014) <sup>h</sup>	Retrospective	393	71.5
Lee (2016) <sup>i</sup>	Retrospective	393	71.5

<sup>a</sup>Yanai H, Noguchi T, Mizumachi S, et al. A blind comparison of the effectiveness of endoscopic ultrasonography and endoscopy in staging early gastric cancer. *Gut*. 1999;44:361–365.

<sup>b</sup>Hizawa K, Iwai K, Esaki M, et al. Is endoscopic ultrasonography indispensable in assessing the appropriateness of endoscopic resection for gastric cancer? *Endoscopy*. 2002;34:973–978.

<sup>c</sup>Kim GH, Park do Y, Kida M, et al. Accuracy of high-frequency catheter-based endoscopic ultrasonography according to the indications for endoscopic treatment of early gastric cancer. *J Gastroenterol Hepatol*. 2010;25:506–511.

<sup>d</sup>Choi J, Kim SG, Im JP, et al. Is endoscopic ultrasonography indispensable in patients with early gastric cancer prior to endoscopic resection? *Surg Endosc*. 2010;24:3177–3185.

<sup>e</sup>Tsuzuki T, Okada H, Kawahara Y, et al. Usefulness and problems of endoscopic ultrasonography in prediction of the depth of tumor invasion in early gastric cancer. *Acta Med Okayama*. 2011;65: 105–112.

<sup>f</sup>Park JM, Ahn CW, Yi X, et al. Efficacy of endoscopic ultrasonography for prediction of tumor depth in gastric cancer. *J Gastric Cancer*. 2011;11:109–115.

<sup>g</sup>Yamamoto S, Nishida T, Kato M, et al. Evaluation of endoscopic ultrasound image quality is necessary in endosonographic assessment of early gastric cancer invasion depth. *Gastroenterol Res Pract*. 2012;194530.

<sup>h</sup>Kim SJ, Choi CW, Kang DH, et al. Efficacy of endoscopic ultrasonography compared to conventional endoscopy in decision making of early gastric cancer treatment. *Gastrointest Endosc*. 2014;79(suppl 5):AB404.

<sup>i</sup>Lee JY, Choi IJ, Kim CG, et al. Therapeutic decision-making using endoscopic ultrasonography in endoscopic treatment of early gastric cancer. *Gut Liver*. 2016;10:42–50.

pooled sensitivity of 73.2%.<sup>166</sup> In a study involving 234 patients, 42% had positive EUS-guided FNA when targeting distant metastases based on echo features and location.<sup>167</sup> Most sampled lesions were mediastinal nodes. EUS-guided FNA changed the subsequent management by precluding surgery in 15% of these patients. Endosonographic detection and FNA of ascites or pleural effusion also improves tumor staging,<sup>168</sup> and EUS has greater sensitivity (87.1%) than combined ultrasound with CT (16.1%) and laparoscopy or laparotomy (40.9%) at predicting peritoneal metastases.<sup>169</sup>

### Limitations of Endoscopic Ultrasound in Staging

- Interpretation of EUS findings: On blinded review of 33 videotaped EUS studies to stage gastric cancer, T stage accuracy was higher in endoscopists who were aware of the clinical history compared with those who were not (66.7% vs. 45.5%).<sup>170</sup>
- Interobserver variability in interpreting EUS findings.<sup>171</sup>
- Tumor size and histologic type: increased likelihood of inaccurate T staging with undifferentiated histologic type (more likely to be understaged) and larger tumor size (more likely to be overstaged).<sup>172</sup>
- Tumor location (cardia, fundus, the lesser curve at the incisura, pyloric channel), vascular pulsation, breathing motion, air bubbles, and mucus can reduce staging accuracy.

- Microscopic invasion is the most frequent cause of understaging, and overstaging can be caused by peritumoral fibrosis, ulceration, and inflammation.<sup>173</sup>
- Difficulty in differentiating malignant from benign inflammatory lymph nodes.
- Inability to visualize distant lymph nodes and metastases

### Comparison of Endoscopic Ultrasound With Other Imaging Modalities

Multidetector CT (MDCT) is the most common radiologic method used to stage gastric cancer and has greatest utility in assessing for distant metastases. It is complementary to EUS for gastric cancer staging. Accuracy of CT for locoregional staging is 65% to 85%.<sup>174–178</sup> The T stage accuracy is 69% to 89%,<sup>171,172,179</sup> and N stage accuracy is 69% to 92%.<sup>180,181</sup> A meta-analysis showed the sensitivity and specificity of CT for the identification of lymph node status were 77% and 78%, respectively.<sup>182</sup> The NPV of CT in identifying patients suitable for primary gastrectomy and requiring diagnostic laparoscopy is quite low, particularly for excluding lymph node metastases. A recent retrospective cohort study of 2414 patients with gastric cancer diagnosed at 116 institutions compared preoperative abdominal CT reports with the surgical and pathologic reports<sup>183</sup>; 570 patients

had gastrectomy performed, of whom the CT reported no local invasion in 536 patients and local invasion was confirmed at surgery in 70 patients. The NPV of CT in detecting local invasion was 86.9% and for detecting lymph node metastases was 43.4%. In patients with a negative preoperative CT who had abdominal exploration, the NPV was 52.3%. The diagnostic accuracy of magnetic resonance imaging (MRI) and PET is similar to CT.<sup>177,184,185</sup> MRI studies report an accuracy ranging from 73.5% to 87.5 % for T stage and from 55.2% to 65 % for N stage.<sup>186,187</sup>

The diagnostic accuracy of EUS and MDCT for locoregional staging are similar.<sup>162</sup> A prospective comparison study of 52 patients with gastric cancer showed EUS has significantly higher sensitivity for T and N staging than MDCT and MRI; however, MDCT has greater specificity than both EUS and MRI.<sup>188</sup> A systematic review showed the diagnostic accuracy of T staging with EUS, CT, and MRI was between 65% and 92.1%, 77.1% and 88.9%, and 71.4% and 82.6%, respectively. Sensitivity for assessing T4 (serosal) involvement for EUS, CT, and MRI varied between 77.8% and 100%, 82.8% and 100%, and 89.5% and 93.1%, respectively. Specificity for assessing T4 (serosal) involvement for EUS, CT, and MRI varied between 67.9% and 100%, 80% and 96.8%, and 91.4% and 100%, respectively.<sup>160</sup> Another study showed lymph node staging with EUS has a sensitivity and specificity of 71% and 49%, respectively; MDCT has a sensitivity and specificity of 80% and 78%, respectively; and MRI has a sensitivity and specificity of 68% and 75%, respectively.<sup>189</sup>

CT is the primary modality for assessing distant metastases. A systematic review compared the ability of different imaging modalities to detect distant metastases. The pooled sensitivity and specificity for detecting peritoneal metastases was 34% and 96% for EUS, 33% and 99% for CT, 28% and 97% for <sup>18</sup>FDG PET, and 9% and 99% for conventional ultrasound, respectively.<sup>190</sup>

## Patient Selection for Staging Laparoscopy

Laparoscopy is recommended as a staging procedure for patients with apparent localized gastric cancer on CT and EUS.<sup>191,192</sup> In a prospective study of 94 patients with localized gastric cancer who underwent staging EUS followed by laparoscopy, metastatic disease was noted in 4% of patients with T1 or T2, N0 disease as compared with 25% of patients with T3 or T4 or N+ disease.<sup>193</sup> The NPV for metastatic disease in patients staged T1 or T2, N0 by EUS was 96%. This finding suggests that staging laparoscopy could be used selectively in those with T3 or T4 or N+ disease as staged by EUS.

## Predictor of Survival After Neoadjuvant Chemotherapy

EUS has limited role in restaging after neoadjuvant chemotherapy. In a retrospective cohort study of 145 patients who had curative-intent surgery, both EUS staging and surgical histology was available in 69 patients.<sup>194</sup> The accuracy of EUS in T stage and N stage evaluation was 44.9% and 56.5%, respectively. In a prospective study of 40 patients with locally advanced gastric cancer, patients had a CT and EUS before and after neoadjuvant chemotherapy, followed by surgical resection.<sup>195</sup> After chemotherapy, the T stage accuracy of CT and EUS was 57% and 47%, respectively. The accuracy of N staging for CT and EUS was 37% and 39%, respectively. Patients downstaged by EUS had a higher 3-year overall survival rate than patients who were not downstaged (69% vs. 41%). The 2-year recurrence-free survival rate was also

higher in patients who were downstaged by EUS than those who were not (77% vs. 47%). Conversely, no difference in survival or recurrence-free survival rates were seen in patients who were downstaged on CT.

## Gastric Cancer: Examination Checklist

- Primary tumor: depth of penetration
- Regional lymph nodes: paracardial, perigastric, peripyloric, celiac, left gastric artery, hepatoduodenal artery, hepatic artery, splenic artery, splenic hilum.
- Metastatic lymph nodes: pancreatoduodenal, retropancreatic, peripancreatic, superior mesenteric, paraaortic, retroperitoneal
- Left lobe of the liver: metastatic deposits
- Peritoneum: low-volume malignant ascites
- Pleural lining: malignant effusion
- Mediastinal lymph nodes: metastatic spread

## Primary Gastric Non-Hodgkin Lymphoma

The stomach is the most common extranodal site of non-Hodgkin lymphoma (NHL) and accounts for 70% of all gastrointestinal lymphomas.<sup>196,197</sup> Primary NHL and disseminated nodal disease can both occur in the stomach. Most primary gastric lymphomas are either the extranodal marginal zone B-cell lymphoma of mucosa-associated lymphoid tissue (MALT) type or diffuse large B-cell lymphoma (DLBCL). Other rare types include mantle cell lymphoma, follicular lymphomas, and peripheral T-cell lymphoma. EUS is the most accurate modality for local staging of gastric lymphoma.<sup>198–202</sup> Secondary gastric NHL reflects disseminated disease that requires extensive diagnostic and systemic treatment strategies.

## Diffuse Large B-Cell Lymphoma

DLBCL most commonly presents with advanced disease, with systemic symptoms such as abdominal pain, gastric outlet obstruction, bleeding, or perforation.<sup>203</sup> DLBCL appears as large and often multiple ulcers or a protruding exophytic mass on endoscopy. Histology reveals confluent sheets or clusters of large cells that resemble centroblasts or immunoblasts.<sup>204</sup> DLBCL are cytogenetically, biologically, and clinically different from MALT lymphoma and have a worse prognosis. Although EUS may help to determine the depth of tumor penetration into the gastric wall, local staging alone has a lesser impact, given the extent of disease and the multimodality treatment involved in the care of these patients.

## Mucosa-Associated Lymphoid Tissue Lymphoma

MALT lymphoma is a low-grade disease that can occur anywhere in the gastrointestinal tract, but it is most commonly found in the stomach and accounts for approximately 35% of primary gastric lymphomas (Video 8.1).<sup>205,206</sup> MALT lymphoma is often associated with *H. pylori*,<sup>207</sup> and disease regression can occur following eradication therapy.<sup>208</sup>

Most patients with early stage MALT lymphoma are asymptomatic or present with nonspecific symptoms such as epigastric pain or discomfort, anorexia, weight loss, nausea or vomiting, occult gastrointestinal bleeding, and early satiety.<sup>209</sup> The diagnosis is usually established by upper endoscopy findings of

mucosal erythema, a mass or polypoid lesion with or without ulceration, benign-appearing gastric ulcer and nodularity, or thickened gastric folds and biopsy for pathologic confirmation. Standard biopsies may be negative, so multiple biopsy specimens should be obtained from the stomach, the duodenum, and the gastroesophageal junction, from both normal- and abnormal-appearing gastric mucosa, using large biopsy specimens where possible. Gastric lymphoma can infiltrate the submucosa with normal overlying mucosa, and snare biopsies, biopsies-within-biopsies (“tunnel biopsies”), and needle aspiration can increase diagnostic yield.<sup>210</sup> Following endoscopic diagnosis, work-up includes EUS for tumor local staging and CT of the chest, abdomen, and pelvis.

In general, patients with early stage (mucosal or submucosal disease without lymph node involvement) *H. pylori*-positive lymphoma are initially treated by *H. pylori* eradication. Patients without *H. pylori* infection and tumors with the t(11;18) translocation are typically treated with local radiation. Patients with more advanced-stage (>T2, N+) disease are treated with *H. pylori* eradication therapy if they are *H. pylori* positive and then are either observed until the development of symptoms or given more aggressive chemotherapy or immunotherapy. Gastric resection is reserved for patients with complications such as perforation or obstruction.<sup>211,212</sup>

## Role of Endoscopic Ultrasound in MALT Lymphoma

The role of EUS in the management of MALT lymphoma can be categorized as follows:

- Local staging of disease: Evaluates the depth of gastric wall involvement and the presence of perigastric lymphadenopathy. Suspicious lymph nodes are sampled by FNA for histology and flow cytometry.<sup>213</sup>
- Tissue diagnosis: EUS-guided FNA or core tissue sampling of the deeper wall layers can be performed in patients with negative endoscopic biopsies.<sup>214</sup>
- Predicting response to therapy: There is a direct relationship between tumor grading by EUS and response to therapy.<sup>215</sup> Patients with mucosal and submucosal disease have better clinical outcomes compared with patients with deeper wall layer involvement.
- Posttreatment follow-up: EUS may show restoration of normal gastric wall layers or significant reduction in thickness of the wall layers following successful treatment.<sup>216</sup> Patients with persistently thick gastric wall layers are more likely to have residual disease, even when endoscopic biopsy is negative.

## Staging

NHLs are staged using the World Health Organization classification<sup>217</sup> and Lugano Classification.<sup>218</sup> The Lugano Classification stages primary nodal lymphomas as limited (Stages I and II) or advanced (Stages III and IV) disease, based primarily on nodal involvement on one or both sides of the diaphragm. EUS assessment of the depth of lymphoma infiltration is based on the TNM classification for gastric cancer.

## Accuracy of Endoscopic Ultrasound in Staging MALT Lymphoma

EUS features that differentiate MALT from cancer include: (1) infiltrative gastric cancer typically grows vertically (transmural)

through the gastric wall and lymphoma grows horizontally; (2) gastric wall thickening is typically more diffuse and homogeneous in lymphoma than in gastric cancer; (3) lymphoma rarely results in luminal narrowing and obstruction, most commonly involves the distal half of the stomach, and is often multifocal within the stomach; (4) at an early stage, lymphomas can manifest with thickening of the second layer alone or separately in the second and third layers with preservation of layer architecture; in advanced stages, lymphomas show diffuse thickening with fusion of wall layers; and (5) diffuse and superficial infiltration is more often indicative of a low-grade MALT lymphoma, whereas the presence of masses is more frequently associated with aggressive high-grade lymphomas.<sup>219</sup>

EUS is the most accurate imaging modality for the evaluation and staging of gastric lymphomas. In a prospective multicenter study the accuracy of EUS T staging was 59%.<sup>220</sup> Another study reported the sensitivity and specificity of EUS for T staging was 89% and 97%, respectively.<sup>221</sup> EUS accuracy of lymph node detection is 71%<sup>197</sup> and is increased by FNA of suspicious lymph nodes.<sup>222</sup> The overall sensitivity, specificity, and accuracy of EUS-guided FNA for the diagnosis of lymphoma was 74%, 93%, and 81%, respectively, when combined with flow cytometry and immunohistochemistry.<sup>223</sup>

## Role of Endoscopic Ultrasound in Predicting Response to Therapy and in Follow-Up

EUS can predict response to therapy in patients with localized disease.<sup>197,224</sup> In a pilot study of 22 patients, complete remission was achieved in 12 of 14 patients with lymphoma limited to the second or third layer (mucosa or submucosa) at EUS, compared with none of 10 patients with deeper gastric wall involvement.<sup>225</sup> Thus EUS may help to differentiate which patients are suitable for antibiotic therapy alone and who should be referred for additional oncologic treatment. Predictive factors for regression of MALT lymphoma following *H. pylori* treatment include disease localized to the mucosa and no nodal involvement or high-grade component.<sup>226–228</sup> EUS is more accurate at predicting response rate than endoscopic features or histologic grade.<sup>229</sup>

EUS can assess for residual disease and predict which patients will achieve remission with *H. pylori* eradication alone.<sup>197</sup> Early stage lesions (T1) may regress following *H. pylori* therapy alone, and more advanced lesions (T2 to T4) may require more aggressive treatment protocols, including combination chemotherapy, radiation therapy, and surgery. Assessment of response to therapy requires long-term follow-up with upper endoscopy and biopsies in combination with EUS. When biopsy results remain positive for lymphoma but EUS shows no structural wall changes, it may be appropriate to “wait and watch” because *H. pylori* therapy may take up to 18 months to produce complete remission.<sup>230</sup> In addition, recurrent wall thickening or disruption may indicate recurrent disease in patients previously thought to be in remission. Patients with a persistently thickened gastric wall on EUS despite adequate antibiotic therapy should be considered for other treatment modalities, even if endoscopic biopsy is negative, because the likelihood of persistent or recurrent lymphoma is high.

The surveillance interval for EUS has not been well defined. Furthermore, one of the main EUS features used to define remission is normalization of the gastric wall thickness to ≤4 mm with preserved five-layer structure and the absence of suspicious lymph nodes. In a study of 33 patients with primary gastric lymphoma

followed up for a median of 15 months, EUS detected histologic relapse in only one of five patients; 82% of patients achieved histologic remission, whereas EUS remission was noted in only 64%.<sup>231</sup>

Another study found that reduction in wall thickness after *H. pylori* eradication predicted a complete response: 40% at 12 months and 84% at the end of 24 months.<sup>232</sup> Half of the study patients had persistent EUS changes in the absence of endoscopic lesions. This may be due to overstaging of residual disease, persistent lymphoma limited to the submucosa or deeper layers, or a limitation of histology in identifying residual lymphoma. A persistently abnormal EUS with negative histology may not be clinically relevant for all patients with MALT after treatment<sup>233</sup> and often resolves on prolonged follow-up and correlates with histologic remission, unlike that seen in “high-grade” gastric lymphomas.<sup>234</sup>

### Limitations of Staging Endoscopic Ultrasound

Interobserver agreement in assessing MALT lymphoma staging by EUS was assessed in a multicenter study involving 96 patients.<sup>235</sup> Overall, interobserver agreement for T stage was fair, before and after treatment ( $\kappa = 0.38$  and  $\kappa = 0.37$ , respectively). Interobserver agreement for N stage was substantial before treatment but only fair after treatment ( $\kappa = 0.63$  and  $\kappa = 0.34$ , respectively). Interobserver agreement correlated with the operator level of experience.

### Evaluation of Thickened Gastric Folds

The normal five-layered gastric wall is between 0.8 and 3.6 mm on EUS and is considered thickened when it exceeds 4 mm.<sup>236</sup> There are multiple possible causes of thickened gastric folds observed at endoscopy (Table 8.12), and those commonly encountered in clinical practice are linitis plastica, Ménétrier disease, and lymphoma.

### Linitis Plastica

Linitis plastica is also known as scirrhous-type gastric cancer and is characterized endoscopically by thickened gastric folds and poor stomach distension on insufflation (Video 8.2). Histopathologically, linitis plastica is characterized by the diffuse growth of

**TABLE 8.12 Differential Diagnosis for Thickened Gastric Folds Noted at Endoscopy**

Category	Disorder
Malignant diseases	Adenocarcinoma, linitis plastica, lymphoma, metastases
Infections	Secondary syphilis, tuberculosis, cytomegalovirus infection, herpes simplex virus infection, histoplasmosis, cryptococcosis, aspergillosis, <i>H. pylori</i> infection, anisakiasis
Infiltrative disorders	Crohn disease, sarcoidosis, amyloidosis, gastritis diseases (eosinophilic, granulomatous, and lymphocytic)
Vascular disorders	Portal hypertensive gastropathy, gastric varices
Other diseases	Ménétrier disease, Zollinger-Ellison syndrome, hyperrugosity, gastritis cystica profunda

malignant cells with signet ring features and is usually associated with marked submucosal fibrosis and gastric wall thickening.<sup>237</sup> The diagnosis is often challenging because of the lack of a distinct, protruding lesion and the difficulty in obtaining deeper diagnostic tissue from standard biopsy forceps; these are negative in up to 30% of cases, particularly in the absence of visible mucosal lesions. On EUS, linitis plastica is characterized by diffuse thickening of all gastric wall layers,<sup>238</sup> as well as thickening primarily confined to the second, third, and fourth layers of the gastric wall.<sup>239</sup> Thickening of the fourth layer (muscularis propria) is rarely benign, and should raise the concern of linitis plastica in the setting of large gastric folds. If EUS-guided FNA is performed following negative endoscopic biopsies, cytology shows malignant epithelial cells containing eccentric nuclei with foamy cytoplasm (resembling degenerated histiocytes) and rare cells with intracytoplasmic vacuoles and crescent-shaped, hyperchromatic nuclei, characteristic of signet ring cells.<sup>240</sup>

### Ménétrier Disease

Ménétrier disease is characterized by epithelial hyperplasia involving the surface and foveolar mucous cells. The pathogenesis of Ménétrier disease is incompletely understood but may involve transforming growth factor-alpha (TGF- $\alpha$ ). TGF- $\alpha$  increases gastric mucus production and inhibits acid secretion,<sup>241</sup> and levels are usually elevated in the gastric mucous cells in patients with Ménétrier disease. Patients typically present with epigastric pain, asthenia, anorexia, weight loss, edema, and vomiting. The enlarged folds are usually confined to the body and fundus of the stomach. The folds are frequently symmetrically enlarged, although asymmetrical enlargement with a polypoid appearance can occur. Snare resection or full-thickness biopsy is usually required for diagnosis, which is established by the demonstration of extreme foveolar hyperplasia with glandular atrophy.<sup>242,243</sup> At EUS, Ménétrier disease displays a more localized thickening, which is hyperechoic rather than hypoechoic, predominantly involving the second gastric layer.<sup>244</sup>

### Large Gastric Folds

The layer of gastric wall thickening on EUS, as well as EUS sampling can help to diagnose the cause of large gastric folds. In a study of 21 patients with gastric wall thickening, EUS Tru-Cut biopsy had a sensitivity, specificity, and positive and negative predictive values of 85%, 100%, 100%, and 74%, respectively, for the diagnosis of malignancy.<sup>245</sup>

The role of EUS in evaluating large gastric folds was assessed in a study of 28 patients, most of whom had endoscopic biopsies inconclusive for malignancy.<sup>246</sup> Biopsies were not performed in four patients because EUS demonstrated gastric varices. Three patients with normal biopsies had wall thickening involving layers 3 and 4 on EUS and were diagnosed with primary gastric carcinoma at laparotomy. In the remaining 21 patients, large-forceps endoscopic biopsy revealed acute or chronic inflammation in 16 (67%), malignancy in 4 (17%), and Ménétrier disease in 1 (4%). Malignancy did not develop in any of the patients, with gastric wall thickening limited to layer two during a mean follow-up of 35 months. The investigators concluded that endoscopic biopsies are diagnostic when EUS abnormalities involve the mucosal layer alone. Abnormalities involving the muscularis propria in the absence of ulceration strongly suggest malignancy and should be

investigated further if endoscopic biopsies are negative. EUS can also be used to diagnose gastric varices, where biopsies should be avoided.

In a prospective study of 61 patients, Gines and colleagues reported that submucosal thickening with or without muscularis propria thickening was the single most important predictor of malignancy, with a 95% probability; this compared with a 5% probability of malignancy when only superficial layers were involved.<sup>247</sup> In another study that analyzed the EUS features in 35 patients with giant gastric folds, Ménétrier disease was suspected when the second layer alone was thickened, and anisakiasis was considered when the third layer alone was thickened. Linitis plastica typically had an abnormally enlarged third and fourth layer. Although the second and third layers could be thickened in healthy subjects with simple hyperrugosity, these layers could also be thickened in patients with gastric lymphoma. Fourth-layer thickening was seen only in malignant conditions.

Gastritis cystic profunda is a rare cause of thickened gastric folds in which multiple small cysts are seen in the mucosa and submucosa of the stomach.<sup>248</sup> The diagnosis is usually established by findings at EUS and mucosectomy. EUS should be used in conjunction with endoscopic biopsy and can assist in determining the best site for biopsy to reduce false-negative results.

## Endoscopic Ultrasound-Based Work-Up

When the EUS pattern is normal and endoscopic findings are inconclusive, multiple standard endoscopic biopsies should be performed and large-forceps biopsy or snare biopsy considered. When abnormalities involve layer 2 (mucosa), endoscopic

biopsies are diagnostic. When abnormalities involve layers 2 and 3 (mucosa, submucosa), large-forceps biopsy is appropriate. When abnormalities involve layer 4 (muscularis propria), malignancy should be strongly suspected even if results of standard biopsies are negative, and EUS-guided FNA or core biopsy should be performed.

## Key References

13. The Paris endoscopic classification of superficial neoplastic lesions: esophagus, stomach, and colon. *Gastrointest Endosc.* 2003;58(suppl): S3–S43.
44. Boniface MM, Wani SB, Scheftel TE, et al. Multidisciplinary management for esophageal and gastric cancer. *Cancer Manag Res.* 2016;8:39–44.
57. Crabtree TD, Yacoub WN, Puri V, et al. Endoscopic ultrasound for early stage esophageal adenocarcinoma: implications for staging and survival. *Ann Thorac Surg.* 2011;91:1509–1515.
102. Fernández-Sordo JO, Konda VJA, Chennat J, et al. Is endoscopic ultrasound (EUS) necessary in the pre-therapeutic assessment of Barrett's esophagus with early neoplasia. *J Gastrointest Oncol.* 2012;3(4):314–321.
197. Koch P, del Valle F, Berdel W, et al. Primary gastrointestinal non-Hodgkin's lymphoma: I. Anatomic and histologic distribution, clinical features, and survival data of 371 patients registered in the German multicenter study GIT NHL 01/92. *J Clin Oncol.* 2001;19:3861–3873.

## References

Access the reference list online at [ExpertConsult.com](http://ExpertConsult.com).

## References

1. Jemal A, Bray F, Center MM, et al. Global cancer statistics. *CA Cancer J Clin.* 2011;61(2):69–90.
2. American Cancer Society. *Global Cancer Facts & Figures*. 3rd ed. Atlanta: American Cancer Society; 2015.
3. Howlader N, Noone AM, Krapcho M, et al (eds). *SEER Cancer Statistics Review, 1975–2013*. Bethesda, MD: National Cancer Institute, [http://seer.cancer.gov/csr/1975\\_2013/](http://seer.cancer.gov/csr/1975_2013/), based on November 2015 SEER data submission, posted to the SEER web site; April 2016.
4. Edgren G, Adami HO, Weiderpass E, et al. A global assessment of the oesophageal adenocarcinoma epidemic. *Gut.* 2013;62(10): 1406–1414.
5. Hur C, Miller M, Kong CY, et al. Trends in esophageal adenocarcinoma incidence and mortality. *Cancer.* 2013;119(6): 1149–1158.
6. Amin MB, Edge SB, Greene FL, et al, eds. *AJCC Cancer Staging Manual*. 8th ed. New York: Springer; 2017.
7. American Joint Committee on Cancer, accessed <https://cancerstaging.org/About/news/Pages/Implementation-of-AJCC-8th-Edition-Cancer-Staging-System.aspx>, accessed April 2017.
8. Westerterp M, Koppert LB, Buskens CJ, et al. Outcome of surgical treatment for early adenocarcinoma of the esophagus or gastro-esophageal junction. *Virchows Arch.* 2005;446:497–504.
9. Manner H, Pech O, Heldmann Y, et al. Efficacy, safety, and long-term results of endoscopic treatment for early stage adenocarcinoma of the esophagus with low-risk sm1 invasion. *Clin Gastro Hepatol.* 2013;11:630–635.
10. Nentwich MF, von Loga K, Reeh M, et al. Depth of submucosal tumor infiltration and its relevance in lymphatic metastasis formation for T1b squamous cell and adenocarcinomas of the esophagus. *J Gastrointest Surg.* 2014;18:242–249.
11. Leggett CL, Lewis JT, Wu TT, et al. Clinical and histological determinants of mortality for patients with Barrett's esophagus-related T1 esophageal adenocarcinoma. *Clin Gastroenterol Hepatol.* 2014;13(4):658–664.
12. Lee L, Ronellenfitsch U, Hofstetter WL, et al. Predicting lymph node metastases in early esophageal adenocarcinoma using a simple scoring system. *J Am Coll Surg.* 2013;217:191–199.
13. The Paris endoscopic classification of superficial neoplastic lesions: esophagus, stomach, and colon. *Gastrointest Endosc.* 2003;58(suppl):S3–S43.
14. Pech O, May A, Manner H, et al. Long-term efficacy and safety of endoscopic resection for patients with mucosal adenocarcinoma of the esophagus. *Gastroenterology.* 2014;146: 652–660.
15. Weusten B, Bisschops R, Coron E, et al. Endoscopic management of Barrett's esophagus: european society of gastrointestinal endoscopy (ESGE) position statement. *Endoscopy.* 2017;49: e1–e4.
16. Alvarez Herrero L, Pouw RE, van Vilsteren FG, et al. Risk of lymph node metastasis associated with deeper invasion by early adenocarcinoma of the esophagus and cardia: study based on endoscopic resection specimens. *Endoscopy.* 2010;42: 1030–1036.
17. Manner H, Pech O, Heldmann Y, et al. The frequency of lymph node metastasis in early-stage adenocarcinoma of the esophagus with incipient submucosal invasion (pT1b sm1) depending on histological risk patterns. *Surg Endosc.* 2015;29:1888–1896.
18. Manner H, May A, Pech O, et al. Early Barrett's carcinoma with "low-risk" submucosal invasion: long-term results of endoscopic resection with a curative intent. *Am J Gastroenterol.* 2008;103:2589–2597.
19. Dubecz A, Kern M, Solymosi N, et al. Predictors of lymph node metastasis in surgically resected T1 Esophageal Cancer. *Ann Thorac Surg.* 2015;99:1879–1886.
20. Buskens CJ, Westerterp M, Lagarde SM, et al. Prediction of appropriateness of local endoscopic treatment for high-grade dysplasia and early adenocarcinoma by EUS and histopathologic features. *Gastrointest Endosc.* 2004;60:703–710.
21. Pennathur A, Farkas A, Krasinskas AM, et al. Esophagectomy for T1 esophageal cancer: outcomes in 100 patients and implications for endoscopic therapy. *Ann Thorac Surg.* 2009;87:1048–1054.
22. Rice TW, Mason DP, Murthy SC, et al. T2N0M0 esophageal cancer. *J Thorac Cardiovasc Surg.* 2007;133:317–324.
23. Raja S, Rice TW, Goldblum JR, et al. Esophageal submucosa: the watershed for esophageal cancer. *J Thorac Cardiovasc Surg.* 2011;142:1403–1411.
24. Hagen JA, DeMeester SR, Peters JH, et al. Curative resection for esophageal adenocarcinoma: analysis of 100 en bloc esophagectomies. *Ann Surg.* 2001;234:520–530.
25. Lerut T, Nafteux P, Moons J, et al. Three-field lymphadenectomy for carcinoma of the esophagus and gastroesophageal junction in 174 Ro resections: impact on staging, disease-free survival, and outcome. A plea for adaptation of TNM classification in upper-half esophageal carcinoma. *Ann Surg.* 2004;240:962–974.
26. Nigro JJ, Hagen JA, DeMeester TR, et al. Prevalence and location of nodal metastases in distal esophageal adenocarcinoma confined to the wall: implications for therapy. *J Thorac Cardiovasc Surg.* 1999;117:16–23.
27. Schroder W, Monig SP, Baldus SE, et al. Frequency of nodal metastases to the upper mediastinum in Barrett's cancer. *Ann Surg Oncol.* 2002;9:807–811.
28. Lagarde SM, ten Kate Fiebo JW, Reitsma Johannes B, et al. Prognostic factors in adenocarcinoma of the esophagus or gastroesophageal junction. *J Clin Oncol.* 2006;24:4347–4355.
29. D'Journo XB, Doddoli C, Michelet P, et al. Transthoracic esophagectomy for adenocarcinoma of the oesophagus: standard versus extended two field mediastinal lymphadenectomy? *Eur J Cardiothorac Surg.* 2005;27:697–704.
30. Kidane B, Coughlin S, Vogt K, Malthaner R. Preoperative chemotherapy for resectable thoracic esophageal cancer. *Cochrane Database Syst Rev.* 2015;(5):CD001556.
31. Fiorica F, Di Bona D, Schepis F, et al. Preoperative chemoradiotherapy for oesophageal cancer: a systematic review and meta-analysis. *Gut.* 2004;53(7):925–930.
32. Bancewicz J, Clark PI, Smith DB, et al. Surgical resection with or without preoperative chemotherapy in oesophageal cancer: a randomised controlled trial. *Lancet.* 2002;359:1727–1733.
33. Walsh TN, Noonan N, Hollywood D, et al. A comparison of multimodal therapy and surgery for esophageal adenocarcinoma. *N Engl J Med.* 1996;335(7):462–467.
34. van Hagen P, Hulshof MC, van Lanschot JJ, et al. Preoperative chemoradiotherapy for esophageal or junctional cancer. *N Engl J Med.* 2012;366(22):2074–2084.
35. Stahl M, Budach W, Meyer H-J, et al. Esophageal cancer: clinical practice guidelines for diagnosis, treatment and follow-up. *Ann Oncol.* 2010;21(suppl 5):v46–v49.
36. Mariette C, Dahan L, Mornex F, et al. Surgery alone versus chemoradiotherapy followed by surgery for stage I and II esophageal cancer: final analysis of randomized controlled phase III trial FFCD 9901. *J Clin Oncol.* 2014;32(23):2416–2422.
37. Cooper JS, Guo MD, Herskovic A, et al. Chemoradiotherapy of locally advanced esophageal cancer: long-term follow-up of a prospective randomized trial (RTOG 85-01). Radiation Therapy Oncology Group. *JAMA.* 1999;281(17):1623–1627.
38. Minsky BD, Pajak TF, Ginsberg RJ, et al. INT 0123 (Radiation Therapy Oncology Group 94-05) phase III trial of combined-modality therapy for esophageal cancer: high-dose versus standard-dose radiation therapy. *J Clin Oncol.* 2002;20(5):1167–1174.

39. Stahl M, Stuschke M, Lehmann N, et al. Chemoradiation with and without surgery in patients with locally advanced squamous cell carcinoma of the esophagus. *J Clin Oncol.* 2005;23(10):2310–2317.
40. Bedenne L, Michel P, Bouche O, et al. Chemoradiation followed by surgery compared with chemoradiation alone in squamous cancer of the esophagus: FFCD 9102. *J Clin Oncol.* 2007;25(1):1160–1168.
41. Kutup A, Link BC, Schurr PG, et al. Quality control of endoscopic ultrasound in preoperative staging of esophageal cancer. *Endoscopy.* 2007;39:715–719.
42. Pech O, Gunter E, Dusemund F, Ell C. Value of high-frequency miniprobes and conventional radial endoscopic ultrasound in the staging of early Barrett's carcinoma. *Endoscopy.* 2010;42:98–103.
43. DeWitt J, Kesler K, Brooks JA, et al. Endoscopic ultrasound for esophageal and gastroesophageal junction cancer: impact of increased use of primary neoadjuvant therapy on preoperative locoregional staging accuracy. *Dis Esophagus.* 2005;18:21–27.
44. Boniface MM, Wani SB, Scheftel TE, et al. Multidisciplinary management for esophageal and gastric cancer. *Cancer Manag Res.* 2016;8:39–44.
45. van Westreenen HL, Heeren PA, van Dullemen HN, et al. Positron emission tomography with F-18-fluorodeoxyglucose in a combined staging strategy of esophageal cancer prevents unnecessary surgical explorations. *J Gastrointest Surg.* 2005;9:54–61.
46. National comprehensive cancer network (NCCN) clinical practice guidelines in oncology: esophageal and esophagogastric junction cancers. Version 1.2017. Accessed April 2017: [https://www.nccn.org/professionals/physician\\_gls/pdf/esophageal.pdf](https://www.nccn.org/professionals/physician_gls/pdf/esophageal.pdf).
47. Akdamar M, Eloubeidi MA. A prospective comparison of computerized tomography (CT), 18 fluorodeoxyglucose positron emission tomography (FDG-PET) and endoscopic ultrasonography (EUS) in the preoperative evaluation of potentially operable esophageal cancer (ECA) patients. *Am J Gastroenterol.* 2005;98:s5.
48. van Westreenen HL, Heeren PA, Jager PL, et al. Pitfalls of positive findings in staging esophageal cancer with F-18-fluorodeoxyglucose positron emission tomography. *Ann Surg Oncol.* 2003;10(9):1100–1105.
49. Downey RJ, Akhurst T, Ilson D, et al. Whole body 18FDG-PET and the response of esophageal cancer to induction therapy: results of a prospective trial. *J Clin Oncol.* 2003;21:428–432.
50. Luketich JD, Schauer PR, Meltzer CC, et al. Role of positron emission tomography in staging esophageal cancer. *Ann Thorac Surg.* 1997;64:765–769.
51. Liberale G, Van Laethem JL, Gay F, et al. The role of PET scan in the preoperative management of oesophageal cancer. *Eur J Surg Oncol.* 2004;30:942–947.
52. Van Vliet EP, Heijnenbrok-Kal MH, Hunink MG, et al. Staging investigations for oesophageal cancer: a meta-analysis. *Br J Cancer.* 2008;98(3):547–557.
53. Lerut T, Flamen P, Ectors N, et al. Histopathologic validation of lymph node staging with FDG-PET scan in cancer of the esophagus and gastroesophageal junction: a prospective study based on primary surgery with extensive lymphadenectomy. *Ann Surg.* 2000;232:743–752.
54. Keswani RN, Early DS, Edmundowicz SA, et al. Routine positron emission tomography does not alter nodal staging in patients undergoing EUS-guided FNA for esophageal cancer. *Gastrointest Endosc.* 2009;69:1210–1217.
55. van Westreenen HL, Westerterp M, Bossuyt PM, et al. Systematic review of the staging performance of 18F-fluorodeoxyglucose positron emission tomography in esophageal cancer. *J Clin Oncol.* 2004;22:3805–3812.
56. Westerterp M, Van Westreenen HL, Sloof GW, et al. Role of positron emission tomography in the (re-)staging of oesophageal cancer. *Scand J Gastroenterol Suppl.* 2006;41:116–122.
57. Crabtree TD, Yacoub WN, Puri V, et al. Endoscopic ultrasound for early stage esophageal adenocarcinoma: implications for staging and survival. *Ann Thorac Surg.* 2011;91:1509–1515.
58. Ajani JA, D'Amico JA, Almhanna K, et al. Esophageal and esophagogastric junction cancers, version 1.2015. *J Natl Compr Canc Netw.* 2015;13:194–227.
59. Puli SR, Reddy JB, Bechtold ML, et al. Staging accuracy of esophageal cancer by endoscopic ultrasound: a meta-analysis and systematic review. *World J Gastroenterol.* 2008;14:1479–1490.
60. Polkowski M. Endosonographic staging of upper intestinal malignancy. *Best Pract Res Clin Gastroenterol.* 2009;23:649–661.
61. Kelly S, Harris KM, Berry E, et al. A systematic review of the staging performance of endoscopic ultrasound in gastro-oesophageal carcinoma. *Gut.* 2001;49:534–539.
62. Pech O, May A, Gunter E, et al. The impact of endoscopic ultrasound and computed tomography on the TNM staging of early cancer in Barrett's esophagus. *Am J Gastroenterol.* 2006;101:2223–2229.
63. Sandha GS, Severin D, Postema E, et al. Is positron emission tomography useful in locoregional staging of esophageal cancer? Results of a multidisciplinary initiative comparing CT, positron emission tomography and EUS. *Gastrointest Endosc.* 2008;67:402–409.
64. Rice TW. Clinical staging of esophageal carcinoma. CT, EUS, and PET. *Chest Surg Clin N Am.* 2000;10:471–485.
65. Choi J, Kim SG, Kim JS, et al. Comparison of endoscopic ultrasonography (EUS), positron emission tomography (PET), and computed tomography (CT) in the preoperative locoregional staging of resectable esophageal cancer. *Surg Endosc.* 2010;24:1380–1386.
66. Sihvo EI, Rasanen JV, Knuuti MJ, et al. Adenocarcinoma of the esophagus and the esophagogastric junction: positron emission tomography improves staging and prediction of survival in distant but not locoregional disease. *J Gastrointest Surg.* 2004;8:988–996.
67. Pfau PR, Perlman SB, Stanko P, et al. The role and clinical value of EUS in a multimodality esophageal carcinoma staging program with CT and positron emission tomography. *Gastrointest Endosc.* 2007;65(3):377–384.
68. Deleted in review.
69. Lowe VJ, Booya F, Fletcher JG, et al. Comparison of positron emission tomography, computed tomography, and endoscopic ultrasound in the initial staging of patients with esophageal cancer. *Mol Imaging Biol.* 2005;7:422–430.
70. McDonough PB, Jones DR, Shen KR, et al. Does FDG-PET add information to EUS and CT in the initial management of esophageal cancer? A prospective single center study. *Am J Gastroenterol.* 2008;103:570–574.
71. Siemsen M, Svendsen LB, Knigge U, et al. A prospective randomized comparison of curved array and radial echoendoscopy in patients with esophageal cancer. *Gastrointest Endosc.* 2003;58:671–676.
72. Takahashi M, Shimizu Y, Ono M, et al. Endoscopic diagnosis of early neoplasia of the esophagus with narrow band imaging: correlations among background coloration and iodine staining findings. *J Gastroenterol Hepatol.* 2014;29:762–768.
73. Chedgy FJQ, Subramaniam S, Kandiah K, et al. Acetic acid chromoendoscopy: improving neoplasia detection in Barrett's esophagus. *World J Gastroenterol.* 2016;22(25):5753–5760.
74. Van Dam J, Rice TW, Catalano MF, et al. High-grade malignant stricture is predictive of esophageal tumor stage. Risks of endosonographic evaluation. *Cancer.* 1993;71:2910–2917.
75. Pfau PR, Ginsberg GG, Lew RJ, et al. Esophageal dilation for endosonographic evaluation of malignant esophageal strictures is safe and effective. *Am J Gastroenterol.* 2000;95:2813–2815.

76. Bang JY, Ramesh J, Hasan M, et al. Endoscopic ultrasonography is no required for staging malignant esophageal strictures that preclude the passage of a diagnostic gastroscope. *Dig Endosc.* 2016;28:650–656.
77. Qumseya BJ, Brown J, Abraham M, et al. Diagnostic performance of EUS in predicting advanced cancer among patients with Barrett's esophagus and high-grade dysplasia/early adenocarcinoma: systematic review and meta-analysis. *Gastrointest Endosc.* 2015;81:865–874.
78. Lerut TE, de Leyn P, Coosemans W, et al. Advanced esophageal carcinoma. *World J Surg.* 1994;18:379–387.
79. Waterman TA, Hagen JA, Peters JH, et al. The prognostic importance of immunohistochemically detected node metastases in resected esophageal adenocarcinoma. *Ann Thorac Surg.* 2004;78:1161–1169.
80. Rizk N, Venkatraman E, Park B, et al. The prognostic importance of the number of involved lymph nodes in esophageal cancer: Implications for revisions of the American Joint Committee on Cancer staging system. *J Thorac Cardiovasc Surg.* 2006;132:1374–1381.
81. Natsugoe S, Yoshinaka H, Shimada M, et al. Number of lymph node metastases determined by presurgical ultrasound and endoscopic ultrasound is related to prognosis in patients with esophageal carcinoma. *Ann Surg.* 2001;234(5):613–618.
82. Catalano MF, Sivak MVJ, Rice T, et al. Endosonographic features predictive of lymph node metastasis. *Gastrointest Endosc.* 1994;40:442–446.
83. Chen VK, Eloubeidi MA. Endoscopic ultrasound-guided fine needle aspiration is superior to lymph node echofeatures: a prospective evaluation of mediastinal and peri-intestinal lymphadenopathy. *Am J Gastroenterol.* 2004;99:628–633.
84. Bhutani MS, Hawes RH, Ho man BJ. A comparison of the accuracy of echo features during endoscopic ultrasound (EUS) and EUS-guided needle aspiration for diagnosis of malignant lymph node invasion. *Gastrointest Endosc.* 1997;45:474–479.
85. Vazquez-Sequeiros E, Levy MJ, Clain JE, et al. Routine vs. selective EUS-guided FNA approach for preoperative nodal staging of esophageal cancer. *Gastrointest Endosc.* 2006;63(2):204–211.
86. Prenzel KL, Bollscheiler E, Schröder W, et al. Prognostic relevance of skip metastases in esophageal cancer. *Ann Thorac Surg.* 2010;90(5):1662–1667.
87. Sgourakis G, Gockel I, Lyros O, et al. Detection of lymph node metastases in esophageal cancer. *Expert Rev Anticancer Ther.* 2011;11(4):601–612.
88. Mortensen MB, Pless T, Durup J, et al. Clinical impact of endoscopic ultrasound-guided fine needle aspiration biopsy in patients with upper gastrointestinal tract malignancies. A prospective study. *Endoscopy.* 2001;33:478–483.
89. McGrath K, Brody D, Luketich J, et al. Detection of unsuspected left hepatic lobe metastases during EUS staging of cancer of the esophagus and cardia. *Am J Gastroenterol.* 2006;101:1742–1746.
90. Vazquez-Sequeiros E, Wiersema MJ, Clain JE, et al. Impact of lymph node staging on therapy of esophageal carcinoma. *Gastroenterology.* 2003;125:1626–1635.
91. Takubo K, Sasajima K, Yamashita K, et al. Double muscularis mucosae in Barrett's esophagus. *Hum Pathol.* 1991;22:1158–1161.
92. Pimentel-Nunes P, Dinis-Ribeiro M, Ponchon T, et al. Endoscopic submucosal dissection: european society of gastrointestinal endoscopy (ESGE) guideline. *Endoscopy.* 2015;47:829–854.
93. Rice TW, Zuccaro Jr G, Adelstein DJ, et al. Esophageal carcinoma: depth of tumor invasion is predictive of regional lymph node status. *Ann Thorac Surg.* 1998;65:787–792.
94. Stein HJ, Feith M, Mueller J, et al. Limited resection for early adenocarcinoma in Barrett's esophagus. *Ann Surg.* 2000;232:733–742.
95. Pech O, Gunter E, Ell C. Endosonography of high-grade intraepithelial neoplasia/early cancer. *Best Pract Res Clin Gastroenterol.* 2009;23:639–647.
96. Watanabe H, Komukai S, Ajioka Y, et al. Histopathology of m3 and sm1 invasive squamous cell carcinoma of the esophagus with special reference to endoscopic resection. *Stomach and Intestine.* 1998;33:1001–1009.
97. Kashimura H, Watanabe H, Yoichi Ajioka Y, et al. The risk factors for nodal micrometastasis of submucosal invasive gastric carcinoma with special reference to assessment of the indication for endoscopic treatment. *Gastric Cancer.* 1999;2:33–39.
98. Pouw RE, Heldoorn N, Herrero LA, et al. Do we still need EUS in the workup of patients with early esophageal neoplasia? A retrospective analysis of 131 cases. *Gastrointest Endosc.* 2011;73:662–668.
99. Young PE, Gentry AB, Acosta RD, et al. Endoscopic ultrasound does not accurately stage early adenocarcinoma or high-grade dysplasia of the esophagus. *Clin Gastroenterol Hepatol.* 2010;8:1037–1041.
100. Barbour AP, Jones M, Brown I, et al. Risk stratification for early esophageal adenocarcinoma: analysis of lymphatic spread and prognostic factors. *Ann Surg Oncol.* 2010;17:2494–2502.
101. Thosani N, Singh H, Kapadia A, et al. Diagnostic accuracy of EUS in differentiating mucosal versus submucosal invasion of superficial esophageal cancers: a systematic review and meta-analysis. *Gastrointest Endosc.* 2012;75:242–253.
102. Fernández-Sordo JO, Konda VJA, Chennat J, et al. Is endoscopic ultrasound (EUS) necessary in the pre-therapeutic assessment of Barrett's esophagus with early neoplasia. *J Gastrointest Oncol.* 2012;3(4):314–321.
103. Chemaly M, Scalzone O, Durivage G, et al. Miniprobe EUS in the pretherapeutic assessment of early esophageal neoplasia. *Endoscopy.* 2008;40(1):2–6.
104. May A, Guenter E, Roth F, et al. Accuracy of staging in oesophageal cancer using high resolution endoscopy and high resolution endosonography: a comparative, prospective, and blinded trial. *Gut.* 2004;53:634–640.
105. Pech O, Gossner L, Manner H, et al. Prospective evaluation of the macroscopic types and location of early Barrett's neoplasia in 380 lesions. *Endoscopy.* 2007;39:588–593.
106. Peters FP, Brakenhoff KP, Curvers WL, et al. Histologic evaluation of resection specimens obtained at 293 endoscopic resections in Barrett's esophagus. *Gastrointest Endosc.* 2008;67:604–609.
107. Dunbar KB, Spechler SJ. The risk of lymph-node metastases in patients with high-grade dysplasia or intramucosal carcinoma in Barrett's esophagus: a systematic review. *Am J Gastroenterol.* 2012;107:850–862.
108. Fitzgerald RC, di Pietro M, Ragunath K, et al. British Society of Gastroenterology guidelines on the diagnosis and management of Barrett's oesophagus. *Gut.* 2014;63:7–42.
109. Sarkaria IS, Rizk NP, Bains MS, et al. Post-treatment endoscopic biopsy is a poor-predictor of pathologic response in patients undergoing chemoradiation therapy for esophageal cancer. *Ann Surg.* 2009;249:764–767.
110. Ribeiro A, Franceschi D, Parra J, et al. Endoscopic ultrasound restaging after neoadjuvant chemotherapy in esophageal cancer. *Am J Gastroenterol.* 2006;101(6):1216–1221.
111. Cerfolio RJ, Bryant AS, Ohja B, et al. The accuracy of endoscopic ultra-sonography with fine-needle aspiration, integrated positron emission tomography with computed tomography, and computed tomography in restaging patients with esophageal cancer after neoadjuvant chemoradiotherapy. *J Thorac Cardiovasc Surg.* 2005;129:1232–1241.
112. Swisher SG, Maish M, Erasmus JJ, et al. Utility of PET, CT, and EUS to identify pathologic responders in esophageal cancer. *Ann Thorac Surg.* 2004;78(4):1152–1160.

113. Chong AK, Caddy GR, Desmond PV, Chen RY. Prospective study of the clinical impact of EUS. *Gastrointest Endosc.* 2005;62:399–405.
114. Mortensen MB, Edwin B, Hünerbein M, et al. Impact of endoscopic ultrasonography (EUS) on surgical decision-making in upper gastrointestinal tract cancer: an international ulticentre study. *Surg Endosc.* 2007;21:431–438.
115. Giovannini M, Monges G, Seitz JF, et al. Distant lymph node metastases in esophageal cancer: impact of endoscopic ultrasound-guided biopsy. *Endoscopy.* 1999;31:536–540.
116. Marsman WA, Brink MA, Bergman JJ, et al. Potential impact of EUS-FNA staging of proximal lymph nodes in patients with distal esophageal carcinoma. *Endoscopy.* 2006;38:825–829.
117. Shumaker DA, de Garmo P, Faigel DO. Potential impact of preoperative EUS on esophageal cancer management and cost. *Gastrointest Endosc.* 2002;56:391–396.
118. Hadzijahic N, Wallace MB, Hawes RH, et al. CT or EUS for the initial staging of esophageal cancer? A cost minimization analysis. *Gastrointest Endosc.* 2000;52:715–720.
119. Harewood GC, Wiersema MJ. A cost analysis of endoscopic ultrasound in the evaluation of esophageal cancer. *Am J Gastroenterol.* 2002;97:452–458.
120. Russell IT, Edwards RT, Gliddon AE, et al. Cancer of oesophagus or gastricus—new assessment of technology of endosonography (COGNATE): report of pragmatic randomised trial. *Health Technol Assess.* 2013;17(39).
121. Harewood GC, Kumar KS. Assessment of clinical impact of endoscopic ultrasound on esophageal cancer. *J Gastroenterol Hepatol.* 2004;19(4):433–439.
122. Fockens P, van den Brande JH, van Dullemen MH, et al. Endosonographic T-staging of esophageal carcinoma: a learning curve. *Gastrointest Endosc.* 1996;44:58–62.
123. van Vliet EP, Eijkemans MJ, Poley JW, et al. Staging of esophageal carcinoma in a low-volume EUS center compared with reported results from high-volume centers. *Gastrointest Endosc.* 2006;63(7):938–947.
124. Siegel RL, Miller KD, Jemal A. Cancer statistics. *CA Cancer J Clin.* 2017;67:7–30.
125. Ferlay J, Soerjomataram, Dikshit R, et al. Cancer incidence and mortality worldwide: sources, methods and major patterns in GLOBOCAN 2012. *Int J Cancer.* 2015;136:E359–E386.
126. Siegel RL, Miller KD, Jemal A. Cancer statistics, 2015. *CA Cancer J Clin.* 2015;65(1):5–29.
127. Den Hoed CM, Kuipers EJ. Gastric cancer: how can we reduce the incidence of this disease? *Curr Gastroenterol Rep.* 2016;18:34.
128. Hamashima C, Shabana M, Okada K, et al. Mortality reduction from gastric cancer by endoscopic and radiographic screening. *Cancer Sci.* 2015;106:1744–1749.
129. Botet J, Lightdale C, Zauber A, et al. Preoperative staging of gastric cancer: comparison of endoscopic US and dynamic CT. *Radiology.* 1991;181:426–432.
130. Sussman S, Halvorsen RJ, Illescas F, et al. Gastric adenocarcinoma: CT versus surgical staging. *Radiology.* 1988;167:335–340.
131. Power D, Schattner M, Gerdes H, et al. Endoscopic ultrasound can improve the selection for laparoscopy in patients with localized gastric cancer. *J Am Coll Surg.* 2009;208:173–178.
132. Mourid R, Yoshida S, Tanaka S, et al. Usefulness of endoscopic ultrasonography in determining the depth of invasion and indication for endoscopic treatment of early gastric cancer. *J Clin Gastroenterol.* 2009;43:318–322.
133. Blackshaw G, Lewis W, Hopper A, et al. Prospective comparison of endosonography, computed tomography, and histopathological stage of junctional oesophagogastric cancer. *Clin Radiol.* 2008;63:1092–1098.
134. Ganpathi I, So J, Ho K. Endoscopic ultrasonography for gastric cancer: does it influence treatment? *Surg Endosc.* 2006;20:559–562.
135. Polkowski M, Palucki J, Wronska E, et al. Endosonography versus helical computed tomography for locoregional staging of gastric cancer. *Endoscopy.* 2004;36:617–623.
136. Sultan J, Robinson S, Hayes N, et al. Endoscopic ultrasonography-detected low-volume ascites as a predictor of inoperability for oesophagogastric cancer. *Br J Surg.* 2008;95:1127–1130.
137. Singh P, Mukhopadhyay P, Bhatt B, et al. Endoscopic ultrasound versus CT scan for detection of the metastases to the liver: results of a prospective comparative study. *J Clin Gastroenterol.* 2009;43:367–373.
138. Japanese Gastric Cancer Association. Japanese gastric cancer treatment guidelines 2010 (ver. 3). *Gastric Cancer.* 2011;14:113–123.
139. Sarella AI, Lefkowitz R, Brennan MF, Karpeh MS. Selection of patients with gastric adenocarcinoma for laparoscopic staging. *Am J Surg.* 2006;191:134–138.
140. Mezhir JJ, Shah MA, Jacks LM, et al. Positive peritoneal cytology in patients with gastric cancer: natural history and outcome of 291 patients. *Ann Surg Oncol.* 2010;17:3173–3180.
141. Bentrem D, Gerdes H, Tang L, et al. Clinical correlation of endoscopic ultrasonography with pathologic stage and outcome in patients undergoing curative resection for gastric cancer. *Ann Surg Oncol.* 2007;14(6):1853–1859.
142. Okada K, Fujisaki J, Kasuga A, et al. Endoscopic ultrasonography is valuable for identifying early gastric cancers meeting expanded-indication criteria for endoscopic submucosal dissection. *Surg Endosc.* 2011;25(3):841–848.
143. Wang J, Hsieh J, Huang Y, et al. Endoscopic ultrasonography for preoperative locoregional staging and assessment of resectability in gastric cancer. *Clin Imaging.* 1998;22:355–359.
144. Prasad P, Schmulewitz N, Patel A, et al. Detection of occult liver metastases during EUS for staging of malignancies. *Gastrointest Endosc.* 2004;59:49–53.
145. Yoshida S, Tanaka S, Kuniihiro K, et al. Diagnostic ability of high-frequency ultrasound probe sonography in staging early gastric cancer, especially for submucosal invasion. *Abdom Imaging.* 2005;30:518–523.
146. Gotoda T, Yanagisawa A, Sasako M, et al. Incidence of lymph node metastasis from early gastric cancer: estimation with a large number of cases at two large centers. *Gastric Cancer.* 2000;3:219–225.
147. Choi J, Kim SG, Im JP, et al. Comparison of endoscopic ultrasonography and conventional endoscopy for prediction of depth of tumor invasion in early gastric cancer. *Endoscopy.* 2010;42:705–713.
148. Choi J, Kim SG, Im JP, et al. Endoscopic prediction of tumor invasion depth in early gastric cancer. *Gastrointest Endosc.* 2011;73:917–927.
149. Hölscher A, Drebber U, Möning S, et al. Early gastric cancer: lymph node metastasis starts with deep mucosal infiltration. *Ann Surg.* 2009;250:791–797.
150. Folli S, Morgagni P, Roviello F, et al. Risk factors for lymph node metastases and their prognostic significance in early gastric cancer (EGC) for the Italian research group for gastric cancer (IRGGC). *Jpn J Clin Oncol.* 2001;31:495–499.
151. Son SY, Park JY, Ryu KW, et al. The risk factors for lymph node metastasis in early gastric cancer patients who underwent endoscopic resection: is the minimal lymph node dissection applicable? A retrospective study. *Surg Endosc.* 2013;27:3247–3253.
152. Lian J, Chen S, Zhang Y, et al. A meta-analysis of endoscopic submucosal dissection and EMR for early gastric cancer. *Gastrointest Endosc.* 2012;76:763–770.
153. Park YM, Cho E, Kang HY, et al. The effectiveness and safety of endoscopic submucosal dissection compared with endoscopic mucosal resection for early gastric cancer: a systematic review and metaanalysis. *Surg Endosc.* 2011;25:2666–2677.
154. Facciorusso A, Antonino M, Di Maso M, et al. Endoscopic submucosal dissection vs endoscopic mucosal resection for early gastric cancer: a meta-analysis. *World J Gastrointest Endosc.* 2014;6:555–563.

155. Pimentel-Nunes P, Dinis-Ribeiro M, Ponchon T, et al. Endoscopic submucosal dissection: european society of gastrointestinal endoscopy (ESGE) guideline. *Endoscopy*. 2015;47:829–854.
156. Gotoda T, Iwasaki M, Kusano C, et al. Endoscopic resection of early gastric cancer treated by guideline and expanded National Cancer Centre criteria. *Br J Surg*. 2010;97:868–871.
157. Min YW, Min BH, Lee JH, Kim JJ. Endoscopic treatment for early gastric cancer. *World J Gastroenterol*. 2014;20(16):4566–4573.
158. Cunningham D, Allum W, Stenning S, et al. Perioperative chemotherapy versus surgery alone for resectable gastroesophageal cancer. *N Engl J Med*. 2006;355:11–20.
159. Macdonald J, Smalley S, Benedetti J, et al. Chemoradiotherapy after surgery compared with surgery alone for adenocarcinoma of the stomach or gastroesophageal junction. *N Engl J Med*. 2001;345:725–730.
160. Kwee R, Kwee T. Imaging in local staging of gastric cancer: a systematic review. *J Clin Oncol*. 2007;25:2107–2116.
161. Habermann C, Weiss F, Riecken R, et al. Preoperative staging of gastric adenocarcinoma: comparison of helical CT and endoscopic US. *Radiology*. 2004;230:465–471.
162. Hwang SW, Lee DH, Lee SH, et al. Preoperative staging of gastric cancer by endoscopic ultrasonography and multidetector-row computed tomography. *J Gastroenterol Hepatol*. 2010;25:512–518.
163. Mocellin S, Pasquali S. Diagnostic accuracy of endoscopic ultrasonography (EUS) for the preoperative locoregional staging of primary gastric cancer. *Cochrane Database Syst Rev*. 2015;(2):CD009944.
164. Cardoso R, Coburn N, Seeveratnam R, et al. A systematic review and meta-analysis of the utility of EUS for preoperative staging for gastric cancer. *Gastric Cancer*. 2012;15(suppl 1):S19–S26.
165. Pei Q, Wang L, Pan J, et al. Endoscopic ultrasonography for staging depth of invasion in early gastric cancer: a meta-analysis. *J Gastroenterol Hepatol*. 2015;30:1566–1573.
166. Puli S, Batapati Krishna Reddy J, Bechtold M, et al. How good is endoscopic ultrasound for TNM staging of gastric cancers? A meta-analysis and systematic review. *World J Gastroenterol*. 2008;14:4011–4019.
167. Hassan H, Vilmann P, Sharma V. Impact of EUS-guided FNA on management of gastric carcinoma. *Gastrointest Endosc*. 2010;71:500–504.
168. Chang K, Albers C, Nguyen P. Endoscopic ultrasound-guided fine needle aspiration of pleural and ascitic fluid. *Am J Gastroenterol*. 1995;90:148–150.
169. Lee Y, Ng E, Hung L, et al. Accuracy of endoscopic ultrasonography in diagnosing ascites and predicting peritoneal metastases in gastric cancer patients. *Gut*. 2005;54:1541–1545.
170. Meining A, Dittler H, Wolf A, et al. You get what you expect? A critical appraisal of imaging methodology in endosonographic cancer staging. *Gut*. 2002;50:599–603.
171. Meining A, Rösch T, Wolf A, et al. High interobserver variability in endosonographic staging of upper gastrointestinal cancers. *Z Gastroenterol*. 2003;41:391–394.
172. Kim J, Song K, Youn Y, et al. Clinicopathologic factors influence accurate endosonographic assessment for early gastric cancer. *Gastrointest Endosc*. 2007;66:901–908.
173. Meyer L, Meyer F, Schmidt U, et al. Endoscopic ultrasonography (EUS) in preoperative staging of gastric cancer—demand and reality. *Pol Przegl Chir*. 2012;84:152–157.
174. Hur J, Park MS, Lee JH, et al. Diagnostic accuracy of multidetector row computed tomography in T- and N staging of gastric cancer with histopathologic correlation. *J Comp Assist Tomogr*. 2006;30(3):372–377.
175. Kawaguchi T, Ichikawa D, Komatsu S, et al. Clinical evaluation of JCGC and TNM staging on multidetector-row computed tomography in preoperative nodal staging of gastric cancer. *Hepatogastroenterology*. 2011;58(3):838–841.
176. Kim AY, Kim HJ, Ha HK. Gastric cancer by multidetector row CT: preoperative staging. *Abdom Imaging*. 2005;30(4):465–472.
177. Kumano S, Murakami T, Kim T, et al. T staging of gastric cancer: role of multi-detector row CT. *Radiology*. 2005;237(3):961–966.
178. Stell DA, Carter CR, Stewart I, Anderson JR. Prospective comparison of laparoscopy, ultrasonography and computed tomography in the staging of gastric cancer. *Br J Surg*. 1996;83(9):1260–1262.
179. Chen CY, Wu DC, Kang WY, Hsu JS. Staging of gastric cancer with 16-channel MDCT. *Abdom Imaging*. 2006;31(5):514–520.
180. Chen CY, Hsu JS, Wu DC, et al. Gastric cancer: preoperative local staging with 3D multi-detector row CT—correlation with surgical and histopathologic results. *Radiology*. 2007;242:472–482.
181. Yang DM, Kim HC, Jin W, et al. 64 Multidetector-row computed tomography for preoperative evaluation of gastric cancer: histological correlation. *J Comp Assist Tomogr*. 2007;31(1):98–103.
182. Seeveratnam R, Cardoso R, McGregor C, et al. How useful is preoperative imaging for tumor, node, metastasis (TNM) staging of gastric cancer? A meta-analysis. *Gastric Cancer*. 2012;15(suppl 1):S3–S18.
183. Kagedan DJ, Frankul F, El-Sedfy A, et al. Negative predictive value of preoperative computed tomography in determining pathologic local invasion, nodal disease, and abdominal metastases in gastric cancer. *Curr Oncol*. 2016;23(4):273–279.
184. Ha TK, Choi YY, Song SY, Kwon SJ. F18-fluorodeoxyglucose positron emission tomography and computed tomography is not accurate in preoperative staging of gastric cancer. *J Korean Surg Soc*. 2011;81(2):104–110.
185. Kim EY, Lee WJ, Choi D, et al. The value of PET/CT for preoperative staging of advanced gastric cancer: comparison with contrast-enhanced CT. *Eur J Radiol*. 2011;79(2):183–188.
186. Kang BC, Kim JH, Lee DY, et al. Value of the dynamic and delayed MR sequence with Gd-DTPA in the T-staging of stomach cancer: correlation with the histopathology. *Abdom Imaging*. 2000;25(1):14–24.
187. Sohn KM, Lee JM, Lee SY, et al. Comparing MR imaging and CT in the staging of gastric carcinoma. *AJR Am J Roentgenol*. 2000;174(6):1551–1557.
188. Giganti F, Orsenigo E, Arcidiacono PG, et al. Preoperative locoregional staging of gastric cancer: is there a place for magnetic resonance imaging? Prospective comparison with EUS and multidetector computed tomography. *Gastric Cancer*. 2016;19(1):216–225.
189. Kwee R, Kwee T. Imaging in assessing lymph node status in gastric cancer. *Gastric Cancer*. 2009;12:6–22.
190. Wang Z, Chen JQ. Imaging in assessing hepatic and peritoneal metastases of gastric cancer: a systematic review. *BMC Gastroenterol*. 2011;11:19.
191. Kayaalp C, Arda K, Orug T, Ozçay N. Value of computed tomography in addition to ultrasound for preoperative staging of gastric cancer. *Eur J Surg Oncol*. 2002;28:540–543.
192. Burke E, Karpeh M, Conlon K, Brennan M. Laparoscopy in the management of gastric adenocarcinoma. *Ann Surg*. 1997;225:262–267.
193. Power D, Schattner M, Gerdes H, et al. Endoscopic ultrasound can improve the selection for laparoscopy in patients with localized gastric cancer. *J Am Coll Surg*. 2009;208:173–178.
194. Serrano OK, Huang K, Ng N, et al. Correlation between preoperative endoscopic ultrasound and surgical pathology staging of gastric adenocarcinoma: a single institution retrospective review. *J Surg Oncol*. 2016;113(1):42–45.
195. Park S, Lee J, Kim C, et al. Endoscopic ultrasound and computed tomography in restaging and predicting prognosis after neoadjuvant chemotherapy in patients with locally advanced gastric cancer. *Cancer*. 2008;112:2368–2376.

196. Papaxoinis G, Papageorgiou S, Rontogianni D, et al. Primary gastrointestinal non-Hodgkin's lymphoma: a clinicopathologic study of 128 cases in Greece. A Hellenic Cooperative Oncology Group study (HeCOG). *Leuk Lymphoma*. 2006;47:2140–2146.
197. Koch P, del Valle F, Berdel W, et al. Primary gastrointestinal non-Hodgkin's lymphoma: I. Anatomic and histologic distribution, clinical features, and survival data of 371 patients registered in the German multicenter study GIT NHL 01/92. *J Clin Oncol*. 2001;19:3861–3873.
198. Suekane H, Iida M, Yao T, et al. Endoscopic ultrasonography in primary gastric lymphoma: correlation with endoscopic and histologic findings. *Gastrointest Endosc*. 1993;39:139–145.
199. Palazzo L, Roseau G, Ruscone-Fournestraux A, et al. Endoscopic ultrasonography in the local staging of primary gastric lymphoma. *Endoscopy*. 1993;25:502–508.
200. Van Dam J. The role of endoscopic ultrasonography in monitoring treatment: response to chemotherapy in lymphoma. *Endoscopy*. 1994;26:772–773.
201. Hordijk M. Restaging after radiotherapy and chemotherapy: value of endoscopic ultrasonography. *Gastrointest Endosc Clin N Am*. 1995;5:601–608.
202. Caletti G, Fusaroli P, Togliani T, et al. Endosonography in gastric lymphoma and large gastric folds. *Eur J Ultrasound*. 2000;11:31–40.
203. Zullo A, Hassan C, Andriani A, et al. Primary low-grade and high-grade gastric MALT-lymphoma presentation. *J Clin Gastroenterol*. 2010;44(5):340–344.
204. De Paepe P, Achter R, Verhoef G, et al. Large cleaved and immunoblastic lymphoma may represent two distinct clinicopathologic entities within the group of diffuse large B-cell lymphomas. *J Clin Oncol*. 2005;23:7060–7068.
205. Radaszkiewicz T, Dragosics B, Bauer P. Gastrointestinal malignant lymphomas of the mucosa-associated lymphoid tissue: factors relevant to prognosis. *Gastroenterology*. 1992;102:1628–1638.
206. Cogliatti S, Schmid U, Schumacher U, et al. Primary B-cell gastric lymphoma: a clinicopathological study of 145 patients. *Gastroenterology*. 1991;101:1159–1170.
207. Parsonnet J, Hansen S, Rodriguez L, et al. Helicobacter pylori infection and gastric lymphoma. *N Engl J Med*. 1994;330:1267–1271.
208. Fischbach W, Goebeler-Kolve ME, Greiner A. Diagnostic accuracy of EUS in the local staging of primary gastric lymphoma: results of a prospective, multicenter study comparing EUS with histopathologic stage. *Gastrointest Endosc*. 2002;56:696–700.
209. Caletti G, Ferrari A, Brocchi E, Barbara L. Accuracy of endoscopic ultrasonography in the diagnosis and staging of gastric cancer and lymphoma. *Surgery*. 1993;113:14–27.
210. Yasuda I, Tsurumi H, Omar S, et al. Endoscopic ultrasound-guided fine-needle aspiration biopsy for lymphadenopathy of unknown origin. *Endoscopy*. 2006;38:919–924.
211. Wiersema M, Gatzimos K, Nisi R, Wiersema L. Staging of non-Hodgkin's gastric lymphoma with endosonography-guided fine-needle aspiration biopsy and flow cytometry. *Gastrointest Endosc*. 1996;44:734–736.
212. Ikoma N, Badgwell BD, Mansfield PF. Multimodality treatment of gastric lymphoma. *Surg Clin North Am*. 2017;97(2):405–420.
213. Kuldau JG, Holman PR, Savides TJ. Diagnosis and management of gastrointestinal lymphoma. In: Faigel DO, Kochman ML, eds. *Endoscopic Oncology: Gastrointestinal Endoscopy and Cancer Management*. 1st ed. Toronto, NJ: Humana Press; 2006:139–149. [Chapter 13].
214. Wiersema M, Gatzimos K, Nisi R, Wiersema L. Staging of non-Hodgkin's gastric lymphoma with endosonography-guided fine-needle aspiration biopsy and flow cytometry. *Gastrointest Endosc*. 1996;44:734–736.
215. Caletti G, Ferrari A, Bocus P, et al. Endoscopic ultrasonography in gastric lymphoma. *Schweiz Med Wochenschr*. 1996;126:819–825.
216. Yeh H, Chen G, Chang W, et al. Long-term follow up of gastric low-grade mucosa-associated lymphoid tissue lymphoma by endosonography emphasizing the application of a miniature ultrasound probe. *J Gastroenterol Hepatol*. 2003;18:162–167.
217. Swerdlow SH, Campo E, Pileri SA, et al. The 2016 revision of the World Health Organization classification of lymphoid neoplasms. *Blood*. 2016;127:2375–2390.
218. Cheson BD, Fisher RI, Barrington SF, et al. Recommendations for initial evaluation, staging and response assessment of Hodgkin and non-Hodgkin lymphoma—the lugano classification. *J Clin Oncol*. 2014;32(27):3059–3067.
219. Taal B, Boot H, van Heerde P, et al. Primary non-Hodgkin lymphoma of the stomach: endoscopic pattern and prognosis in low versus high grade malignancy in relation to the MALT concept. *Gut*. 1996;39:556–561.
220. Fischbach W, Goebeler-Kolve ME, Greiner A. Diagnostic accuracy of EUS in the local staging of primary gastric lymphoma: results of a prospective, multicenter study comparing EUS with histopathologic stage. *Gastrointest Endosc*. 2002;56:696–700.
221. Caletti G, Ferrari A, Brocchi E, Barbara L. Accuracy of endoscopic ultrasonography in the diagnosis and staging of gastric cancer and lymphoma. *Surgery*. 1993;113:14–27.
222. Wiersema M, Gatzimos K, Nisi R, Wiersema L. Staging of non-Hodgkin's gastric lymphoma with endosonography-guided fine-needle aspiration biopsy and flow cytometry. *Gastrointest Endosc*. 1996;44:734–736.
223. Pavlick A, Gerdes H, Portlock C. Endoscopic ultrasound in the evaluation of gastric small lymphocytic mucosa-associated lymphoid tumors. *J Clin Oncol*. 1997;15:1761–1766.
224. Sackmann M, Morgner A, Rudolph B, et al. Regression of gastric MALT lymphoma after eradication of Helicobacter pylori is predicted by endosonographic staging. MALT Lymphoma Study Group. *Gastroenterology*. 1997;113:1087–1090.
225. Ruskoné-Fournestraux A, Lavergne A, Aegeuter P, et al. Predictive factors for regression of gastric MALT lymphoma after anti-Helicobacter pylori treatment. *Gut*. 2001;48:297–303.
226. Nakamura S, Matsumoto T, Suekane H, et al. Predictive value of endoscopic ultrasonography for regression of gastric low grade and high grade MALT lymphomas after eradication of Helicobacter pylori. *Gut*. 2001;48:454–460.
227. Caletti G, Zinzani P, Fusaroli P, et al. The importance of endoscopic ultrasonography in the management of low-grade gastric mucosa-associated lymphoid tissue lymphoma. *Aliment Pharmacol Ther*. 2002;16:1715–1722.
228. Levy M, Copie-Bergman C, Traulle C, et al. Conservative treatment of primary gastric low-grade B-cell lymphoma of mucosa-associated lymphoid tissue: predictive factors of response and outcome. *Am J Gastroenterol*. 2002;97:292–297.
229. Zucca E, Cavalli F. Are antibiotics the treatment of choice for gastric lymphoma? *Curr Hematol Rep*. 2004;3:11–16.
230. Püspök A, Raderer M, Chott A, et al. Endoscopic ultrasound in the follow up and response assessment of patients with primary gastric lymphoma. *Gut*. 2002;51:691–694.
231. Yeh H, Chen G, Chang W, et al. Long-term follow up of gastric low-grade mucosa-associated lymphoid tissue lymphoma by endosonography emphasizing the application of a miniature ultrasound probe. *J Gastroenterol Hepatol*. 2003;18:162–167.
232. Di Raimondo F, Caruso L, Bonanno G, et al. Is endoscopic ultrasound clinically useful for follow-up of gastric lymphoma? *Ann Oncol*. 2007;18:351–356.

234. Vetro C, Romano A, Chiarenza A, et al. Endoscopic ultrasonography in gastric lymphomas: appraisal on reliability in long-term follow-up. *Hematol Oncol*. 2012;30:180–185.
235. Fusaroli P, Buscarini E, Peyre S, et al. Interobserver agreement in staging gastric malt lymphoma by EUS. *Gastrointest Endosc*. 2002;55:662–668.
236. Kimmey M, Martin R, Haggitt R, et al. Histologic correlates of gastrointestinal ultrasound images. *Gastroenterology*. 1989;96:433–441.
237. Feng J, Al-Abbad M, Kodali U, Dhar R. Cytologic diagnosis of gastric linitis plastica by endoscopic ultrasound guided fine-needle aspiration. *Diagn Cytopathol*. 2006;34:177–179.
238. Levine M, Kong V, Rubesin S, et al. Scirrhous carcinoma of the stomach: radiologic and endoscopic diagnosis. *Radiology*. 1990;175:151–154.
239. Fujishima H, Misawa T, Chijiwa Y, et al. Scirrhous carcinoma of the stomach versus hypertrophic gastritis: findings at endoscopic US. *Radiology*. 1991;181:197–200.
240. Feng J, Al-Abbad M, Kodali U, Dhar R. Cytologic diagnosis of gastric linitis plastica by endoscopic ultrasound guided fine-needle aspiration. *Diagn Cytopathol*. 2006;34:177–179.
241. Dempsey P, Goldenring J, Soroka C, et al. Possible role of transforming growth factor alpha in the pathogenesis of Ménétrier's disease: supportive evidence from humans and transgenic mice. *Gastroenterology*. 1992;103:1950–1963.
242. Wolfsen H, Carpenter H, Talley N. Menetrier's disease: a form of hypertrophic gastropathy or gastritis? *Gastroenterology*. 1993;104:1310–1319.
243. Sundt TR, Compton C, Malt R. Ménétrier's disease. A trivalent gastropathy. *Ann Surg*. 1988;208:694–701.
244. Hizawa K, Kawasaki M, Yao T, et al. Endoscopic ultrasound features of protein-losing gastropathy with hypertrophic gastric folds. *Endoscopy*. 2000;32:394–397.
245. Thomas T, Kaye PV, Ragunath K, Aithal GP. Endoscopic-ultrasound-guided mural trucut biopsy in the investigation of unexplained thickening of esophagogastric wall. *Endoscopy*. 2009;41:335–339.
246. Mendis R, Gerdes H, Lightdale C, Botet J. Large gastric folds: a diagnostic approach using endoscopic ultrasonography. *Gastrointest Endosc*. 1994;40:437–441.
247. Gines A, Pellise M, Fernandez-Esparrach G, et al. Endoscopic ultrasonography in patients with large gastric folds at endoscopy and biopsies negative for malignancy: predictors of malignant disease and clinical impact. *Am J Gastroenterol*. 2006;101:64–69.
248. Okada M, Iizuka Y, Oh K, et al. Gastritis cystica profunda presenting as giant gastric mucosal folds: the role of endoscopic ultrasonography and mucosectomy in the diagnostic work-up. *Gastrointest Endosc*. 1994;40:640–644.



**Video 8.1** A Mass in the Gastric Fundus Was Identified on Gastroscopy

Multiple biopsies were taken, and endoscopic ultrasonography (EUS) performed. EUS demonstrated a T1N0 lesion. Histology confirmed a mucosa-associated lymphoid tissue lymphoma.



**Video 8.2** The Gastric Mucosa Was Friable, and the Stomach Distracted Poorly on Insufflation

No raised or ulcerative mass was seen. On endoscopic ultrasonography, there was diffuse loss of the normal gastric wall layers and thickening of the gastric wall. The tumor extended through the serosa and a perigastric lymph node was identified. This was consistent with linitis plastica, staged as uT3N1.

# 9

# Endoscopic Ultrasonography in the Evaluation of Posterior Mediastinal Lesions

WILSON T. KWONG AND THOMAS J. SAVIDES

## KEY POINTS

- Criteria exist to differentiate benign from malignant mediastinal lymph nodes, but used alone these criteria are not sufficiently accurate. Endoscopic ultrasonography-guided fine-needle aspiration (EUS FNA) is required to make sound clinical decisions.
- The overall accuracy for the diagnosis of posterior mediastinal malignancies with transesophageal EUS FNA is greater than 90%.
- The diagnosis of lymphoma in the posterior mediastinum is made by cytology and flow cytometry studies on EUS FNA and core biopsy specimens.
- EUS FNA can be valuable in helping to establish a diagnosis of granulomatous disease involving the mediastinum (sarcoidosis, histoplasmosis, tuberculosis).
- Most mediastinal cysts are benign, and because the risk of infection is high, EUS FNA should not be performed. If a high suspicion of malignancy exists, the cyst should undergo one puncture and be fully drained, and antibiotics should be administered.

Transesophageal endoscopic ultrasonography (EUS) with fine-needle aspiration (FNA) offers minimally invasive access for the evaluation and biopsy of posterior mediastinal lesions.<sup>1</sup> Usually these lesions are first detected with computed tomography (CT), but occasionally lesions are incidentally detected during passage of the echoendoscope through the esophagus on the way to image gastrointestinal or pancreatic disease. Transesophageal EUS is well suited to image the posterior mediastinum but is unable to access or visualize much of the anterior mediastinum. The cardiac structures in the middle mediastinum are well visualized and there are a few reports of EUS FNA of atrial and pericardial lesions. This chapter focuses on EUS diagnosis of posterior mediastinal masses, lymph nodes, and cysts. The role of EUS FNA in lung cancer staging is discussed in Chapter 7.

## Endoscopic Ultrasonography Evaluation of Enlarged Posterior Mediastinal Lymph Nodes

### Endoscopic Ultrasonography Appearance of Benign Posterior Mediastinal Lymph Nodes

Mediastinal lymph nodes are commonly encountered during EUS for nonthoracic indications. The most common EUS feature of these benign lymph nodes is a triangular or crescent shape, with possibly an echogenic center (Fig. 9.1). The echogenic center represents the hilum of the lymph node. Intranodal blood vessels also suggest benign lymph nodes.<sup>2,3</sup>

The prevalence of posterior mediastinal adenopathy varies with geographic region of the world, depending on the risk of endemic pulmonary infections. A prospective study from England and Sweden revealed that 62% of patients had posterior mediastinal lymph nodes, with a mean of 1.4 lymph nodes per patient. Nearly all of these lymph nodes had a short-axis diameter of 5 mm or less.<sup>4</sup>

### Endoscopic Ultrasonography Appearance of Malignant Posterior Mediastinal Lymph Nodes

EUS findings associated with malignant lymph nodes include round shape, short-axis diameter greater than 10 mm, hypoechoic echotexture, and well-demarcated borders (Fig. 9.2, Video 9.1).<sup>5</sup> If all four features are present in a lymph node, the chance of malignancy may be as low as 50% with a 60% accuracy.<sup>5</sup> For this reason, tissue sampling is important to obtain diagnostic cytopathologic material of enlarged mediastinal lymph nodes.

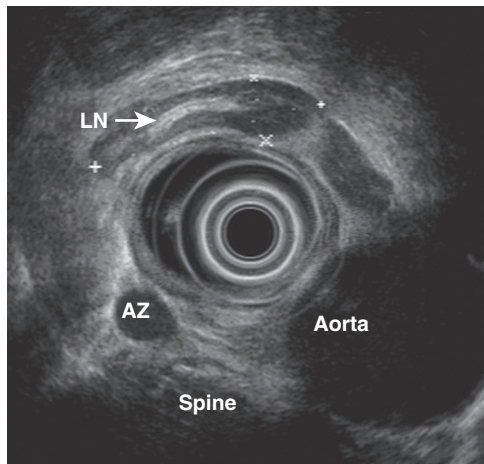
Elastography has been reported in the evaluation of mediastinal lymph nodes and masses.<sup>6</sup> However, the sensitivity and specificity (in the range of 80% to 90%) of this technique are lower than those of transesophageal or transbronchial EUS-guided FNA (>90% range). Therefore elastography needs further assessment and improvement before widespread use of this method can be recommended.

## Transesophageal Endoscopic Ultrasonography Fine-Needle Aspiration of Mediastinal Lymph Nodes

Table 9.1 shows the types of pathologic lesions that can be diagnosed with transesophageal EUS FNA cytology.

## Technique for Endoscopic Ultrasonography Fine-Needle Aspiration of Posterior Mediastinal Lesions

Cross-sectional imaging studies including CT, magnetic resonance imaging (MRI), and positron emission tomography (PET) exams of the chest and abdomen should be reviewed to identify the location of the lesion of interest and its relative location to surrounding structures. This will determine whether a lesion is accessible by transesophageal EUS FNA and assist in locating the lesion with the linear array echoendoscope. If the EUS is performed to evaluate enlarged mediastinal or periesophageal lymph nodes, it is advisable to perform an esophagogastroduodenoscopy (EGD) with a forward-viewing scope first to assess for any esophageal or gastric pathology that may explain the lymphadenopathy. Identification of a luminal mass amenable to biopsy may preclude the need for EUS FNA. The linear echoendoscope is passed into the esophagus



• **Fig. 9.1** Benign mediastinal lymph node. Note the triangular appearance with a central hyperechoic stripe. AZ, Azygous vein; LN, lymph node.



• **Fig. 9.2** Endoscopic ultrasonography-guided fine-needle aspiration of a malignant mediastinal lymph node.

and stomach, and then ultrasound imaging is performed as the scope is withdrawn with sweeping motions in a clockwise and counterclockwise fashion to obtain a 360-degree view with the linear echoendoscope. The liver, celiac axis, left adrenal gland, and posterior mediastinum are evaluated for other lymphadenopathy in other lymph node regions, ascites, liver masses, and for other clues as to an advanced malignancy or lymphoma.

During the EUS evaluation of enlarged mediastinal lymph nodes, there are usually several identified. These may be discrete, separate lymph nodes, which is often the case in malignancy, or a conglomeration of matted lymph nodes which can be seen in granulomatous disease. The location of each lesion is documented in terms of the distance in centimeters of the transducer tip from the incisors and the anatomic site (e.g., subcarinal, left paraesophageal, right paratracheal, aortopulmonary window) to assist in future identification and comparison on future examinations. For each lesion, the short-axis and long-axis dimensions are measured, and the degree of demarcation is described (well demarcated or poorly demarcated). The shape is described in terms of round, oval, triangular, draping, or matted. The echogenicity is described in terms of hypoechoic, hyperechoic, heterogeneous, or anechoic.

Transesophageal EUS FNA is generally performed using a linear array echoendoscope and usually a 22- or 25-gauge aspiration or core biopsy needle. Given the esophageal location of mediastinal FNA, the scope is generally straight which allows for easier movement and maneuverability of the needle compared to transduodenal FNA where the scope is more angulated. If there is more than one possible lesion to sample for biopsy, the lesion that is most likely to be malignant (i.e., rounder, larger, more hypoechoic, more demarcated; Fig. 9.3) is chosen as the target.<sup>7</sup> However, the presence of intervening blood vessels and distance from the esophagus should also be taken into account as this may make FNA of certain lymph nodes easier and safer. The Doppler imaging function should be utilized to examine the FNA needle trajectory to ensure there are no significant vessels that may complicate FNA. Needle passage through an adjacent blood vessel can usually be avoided by displacing the esophagus with the scope tip to create a different needle path. However, there have been case reports where transaortic EUS FNA puncture with 22- and 25-gauge needles was successfully and safely used for biopsy of

**TABLE 9.1** Posterior Mediastinal Lesions That Can Be Diagnosed With Endoscopic Ultrasonography-Guided Fine-Needle Aspiration

Malignant	Benign
Lung cancer	Reactive
Primary or metastatic	Granulomatous disease
NSCLC	Histoplasmosis
Small-cell	Sarcoid
Mesothelioma	Tuberculosis
Lymphoma	Duplication cyst
Metastatic from nonlung primary	Leiomyoma
GIST	Mediastinitis/abscess
Spindle cell neoplasm	Pleural effusion

*GIST*, Gastrointestinal stromal tumor; *NSCLC*, Non–small-cell lung cancer.

mediastinal lesions where the aorta was between the lesion and the esophagus.<sup>8–10</sup> Once the lesion has been brought into view, the needle is passed through the esophageal wall and into the lymph node under constant ultrasound visualization. The internal stylet (optional) is then removed, intermittent suction may be applied, and the needle is moved back and forth within the lesion to sample the edges as well as the center of the lesion (Video 9.2).

The needle is then pulled out of the scope, the stylet is slowly reintroduced into the needle, and the aspirated material is slowly expressed either onto a microscope slide and/or into medium for cell block pathology or flow cytometry. The availability of immediate cytologic evaluation may increase the diagnostic yield and allow for fewer passes.<sup>11,12</sup> If immediate cytologic evaluation raises the possibility of lymphoma or lymphoma is suspected based on

clinical history, additional passes should be obtained for flow cytometry and fine-needle core biopsies should be considered. Several core needles are now available which are capable of obtaining larger samples of tissue for histopathology; these can provide tissue architecture which is usually necessary to differentiate the various subtypes of lymphoma. If immediate cytologic evaluation suggests infection, additional passes may be made for microbiologic studies. A final diagnosis is provided only after the cytopathologist has evaluated all processed specimen slides and cell block material. In general, diagnostic material from posterior mediastinal lesions can be obtained within two to five EUS FNA cytology passes, and one to two core biopsy passes.<sup>13–16</sup>

## Endobronchial Ultrasound

Endobronchial ultrasound (EBUS)-guided FNA has become increasingly available, especially as performed by interventional pulmonologists and thoracic surgeons.<sup>17,18</sup> EBUS provides unique access to lymph nodes and masses adjacent to the trachea, as well as the subcarinal and perihilar areas. The combination of transesophageal and transbronchial EUS provides nearly complete mediastinal evaluation<sup>19–21</sup> and avoids risks of mediastinoscopy or other more invasive surgeries to obtain a tissue diagnosis.

## Accuracy of Endoscopic Ultrasonography Fine-Needle Aspiration for Diagnosing Posterior Mediastinal Lesions

The overall accuracy rate for diagnosing posterior mediastinal malignancy with transesophageal EUS FNA cytology is approximately 93%.<sup>7</sup> A meta-analysis of 76 studies ( $n = 9310$  patients) found a pooled sensitivity of 88% and specificity of 96%.<sup>22</sup> Table 9.2 shows a summary of the accuracy rates for EUS FNA for diagnosing malignancy in posterior mediastinal lesions.



**Fig. 9.3** Appearance of a malignant mediastinal lymph node—note the hypoechoic, round, well-defined appearance and size greater than 10 mm.

**TABLE 9.2** Summary of Studies Evaluating the Operating Characteristics of Endoscopic Ultrasonography-Guided Fine-Needle Aspiration for Diagnosing Malignant Posterior Mediastinal Lesions

Authors (Year)	<i>n</i>	Sensitivity (%)	Specificity (%)	Accuracy (%)	PPV (%)	NPV (%)
Giovannini and coworkers <sup>103</sup> (1995)	24	81	100	83	—	—
Silvestri and coworkers <sup>104</sup> (1996)	27	89	100	—	—	—
Gress and coworkers <sup>105</sup> (1997)	52	95	81	96	—	—
Hünerbein and coworkers <sup>106</sup> (1998)	23	89	83	87	—	—
Serna and coworkers <sup>107</sup> (1998)	21	86	100	—	—	—
Vazquez-Sequeiros and coworkers <sup>108</sup> (2001)	82	96	100	98	94	100
Fritscher-Ravens and coworkers <sup>58</sup> (2000)	153	92	100	95	—	—
Wallace and coworkers <sup>15</sup> (2001)	121	87	100	—	—	—
Devereaux and coworkers <sup>91</sup> (2002)	49	—	—	94	—	—
Larsen and coworkers <sup>109</sup> (2002)	79	92	100	94	100	80
Hernandez and coworkers <sup>110</sup> (2004)	59	—	—	84	—	—
Savides and coworkers <sup>72</sup> (2004)	59	96%	100	98	100	97
Eloubeidi and coworkers <sup>111</sup> (2005)	104	93%	100	97	100	97
Overall	91	97	100	97	99	94

NPV, Negative predictive value; PPV, positive predictive value.

Several studies showed that the diagnostic accuracy of malignant posterior mediastinal lymph nodes increases with the use of EUS FNA cytology over simple EUS appearance alone.<sup>22–24</sup>

## Risks of Endoscopic Ultrasonography Fine-Needle Aspiration of Posterior Mediastinal Lesions

EUS FNA of posterior mediastinal lesions is safe, with few complications reported in the thousands of patients described in retrospective and prospective trials. A pooled review of prospective studies revealed a 0.43% risk of complications with mediastinal EUS FNA, mostly pain, bleeding, and perforation.<sup>25</sup> However, several cases of mediastinitis have also been reported after transesophageal EUS FNA.<sup>26–37</sup> A case of mediastinitis with osteomyelitis has also been reported in the setting of FNA.<sup>32</sup> Although most of these cases have involved mediastinal cysts, some patients with solid lesions (nodes or masses) have also developed post-EUS FNA mediastinitis.

There is a single case of esophageal wall seeding with tumor after EUS FNA of a posterior mediastinal malignant node from a primary gastric cancer.<sup>38</sup> This occurred in the setting of several passes using a large 19-G needle, which may have contributed to the seeding. A case of esophagomediastinal fistula formation after EUS FNA of a posterior mediastinal lymph node resulting from tuberculosis has also been reported.<sup>39</sup> Two cases of esophageal wall rupture in the setting of FNA requiring thoracotomy have been reported.<sup>40</sup> Despite rare reports of severe complications, EUS FNA and EBUS FNA of mediastinal lesions appear to be very safe. Two large, retrospective studies with 16,181 and 16,750 EUS and EBUS procedures with mediastinal FNA demonstrated a mortality of 0 to 0.04% and an adverse event rate of 0.22%.<sup>41,42</sup>

## Endoscopic Ultrasonography Fine-Needle Aspiration Compared With Other Modalities for Evaluation and Biopsy of Posterior Mediastinal Lymph Nodes or Masses

The noninvasive imaging modalities commonly used to evaluate enlarged mediastinal lymph nodes are CT scan and PET scan. These modalities have mostly been compared with EUS FNA in the setting of suspected lung cancer. Both EUS alone and EUS FNA have been shown to be more accurate than CT alone (using short-axis lymph node diameter >10 mm) for diagnosing malignant posterior mediastinal lymph nodes.<sup>43</sup>

PET scanning detects increased uptake of the glucose analog <sup>18</sup>F-2-deoxy-D-glucose. Increased uptake can occur both in malignancy and in inflammatory conditions. A meta-analysis comparing CT with PET scan for evaluation of mediastinal adenopathy in patients with lung cancer revealed that when the CT scan showed enlarged lymph nodes, the sensitivity of PET was 100%, but the specificity was only 78%, in contrast to no CT findings of lymph node enlargement (sensitivity of 82% and specificity of 93%).<sup>44</sup> The low specificity of PET scan implies that 22% of patients with PET-positive enlarged mediastinal lymph nodes actually do not have malignancy (false-positive PET scan). Therefore these PET-positive lymph nodes should undergo tissue biopsy if it is critical to be certain about the diagnosis of malignancy in the nodes. Several studies confirmed the poor specificity of PET compared with transesophageal EUS FNA.<sup>45,46</sup> One large study found that the EUS FNA positive predictive value of malignancy

was 100% compared with 40% for PET.<sup>24</sup> A recent study comparing EUS FNA to PET CT demonstrated superior performance of EUS FNA in the evaluation of mediastinal and upper abdominal lymphadenopathy.<sup>46</sup> The sensitivity, specificity, positive predictive value, negative predictive value, and overall accuracy of EUS FNA were 91.3%, 100%, 100%, 92.5%, and 95.8%, respectively. The same values for PET CT were 75%, 25%, 50%, 50%, and 50%, respectively. The combination of PET and EUS FNA improves the specificity and overall accuracy as compared with PET alone.<sup>47,48</sup>

The other modalities for obtaining tissue samples from posterior mediastinal lesions are percutaneous CT-guided transthoracic FNA, bronchoscopy with transbronchial biopsy, EBUS with transbronchial FNA, and mediastinoscopy with biopsy. Percutaneous transthoracic FNA is generally not used for biopsy of posterior mediastinal lesions because of the risk of pneumothorax or puncture of a major vessel. The diagnostic yield of transbronchial FNA without EBUS is lower than that of EUS FNA, whereas EBUS has a similar diagnostic yield in the biopsying of adenopathy locations visualized by both transesophageal EUS and EBUS.<sup>20</sup> Mediastinoscopy is associated with greater difficulty (and potentially increased risk) in accessing the lymph nodes in stations that are the most easily visualized and biopsied with transesophageal EUS FNA (subcarina, posterior aortopulmonic window, and periesophageal stations). Therefore the less invasive EUS FNA and EBUS FNA are increasingly replacing mediastinoscopy at most referral centers.

## Differential Diagnosis of Enlarged Posterior Mediastinal Lymph Nodes

Enlarged mediastinal lymph nodes are usually defined by CT findings of lymph nodes 10 mm diameter or larger. In the setting of a peripheral lung mass and mediastinal lymph nodes, the main concern is primary lung cancer with metastatic disease. The finding of numerous posterior mediastinal and hilar lymph nodes raises the question of whether the diagnosis is benign (sarcoid, histoplasmosis, tuberculosis, reactive) or malignant (especially lymphoma). Often the clinical history suggests the origin.

## Malignant Posterior Mediastinal Lymph Nodes

The rate of diagnosis of malignancy with EUS FNA of posterior mediastinal nodes in patients without a known diagnosis of cancer varies depending on prior pulmonary evaluation and local referral patterns; however, it is approximately 50%, and most cancers are of pulmonary origin.<sup>23,49</sup> Table 9.2 shows the reported operating characteristics of EUS FNA for diagnosing malignancy in posterior mediastinal adenopathy. The overall sensitivity, specificity, and accuracy are greater than 90%.

### Metastatic Disease From Thoracic Tumors

#### Lung Cancer

Most thoracic tumors originate as primary lung cancer. This disease is generally divided into small-cell and non-small-cell lung cancer (NSCLC) pathologic types, and 80% of lung cancer is NSCLC. EUS FNA cytology can diagnose and stage metastatic lung cancer to mediastinal lymph nodes from both small-cell carcinoma and NSCLC.<sup>7</sup> In addition to lymph nodes, lung cancer

can present as a mediastinal mass due to metastatic spread. Further discussion of EUS FNA for lung cancer staging is discussed in detail in Chapter 7.

### Mesothelioma

Mesothelioma is a much rarer pleura-based tumor of the thoracic cavity associated with asbestos exposure and can present with pleural-based tumors and effusions (Fig. 9.4). EUS FNA can diagnose mesothelioma metastases in posterior mediastinal lymph nodes.<sup>50–52</sup> The combination of transbronchial EBUS FNA and transesophageal EUS FNA may increase the sensitivity of diagnosed metastatic mesothelioma, especially because mesothelioma can also metastasize or directly extend below the diaphragm into the abdominal cavity, where EUS FNA can detect metastases.<sup>53</sup>

### Metastatic Disease From Extrathoracic Malignancy

Various tumors result in metastases to the posterior mediastinum, and they appear as either a lymph node or a mass (Fig. 9.5). Metastatic lymph nodes from breast, colon, renal, testicular, laryngeal, pancreas, and esophageal cancers have been diagnosed by trans-thoracic EUS FNA.<sup>54–56</sup>



• Fig. 9.4 Pleural based masses and pleural effusion in mesothelioma.



• Fig. 9.5 Mediastinal mass from metastatic lung adenocarcinoma.

### Lymphoma

EUS FNA and fine-needle biopsy (FNB) can diagnose lymphoma in posterior mediastinal lymph nodes by obtaining material that can be evaluated with cytology, histopathology, flow cytometry, and immunohistochemistry. In one study, the sensitivity of lymphoma diagnosis increased from 44% to 86% with the addition of flow cytometry and immunocytochemistry.<sup>57</sup> Nodal architecture is often necessary to distinguish lymphoma subtypes and it is therefore recommended that a core biopsy needle be utilized when lymphoma is suspected, either based on initial cytology results or clinical picture to avoid a repeat EUS procedure for tissue diagnosis.

### Benign Posterior Mediastinal Lymph Nodes

#### Reactive Lymph Nodes

Reactive lymph nodes are usually the result of previous pulmonary infections. Cytologically, they appear as a mixture of lymphoid elements, with reactive and hyperplastic features.

#### Granulomatous Lymph Nodes

EUS FNA cytology is able to demonstrate granulomatous disease in lymph nodes. The cytologic appearance is that of histiocytes in a swirling pattern. The differential diagnosis usually includes sarcoid, histoplasmosis, tuberculosis, and coccidiomycosis. The presence or absence of caseating granulomas does not necessarily help with the diagnosis because caseation can be seen in all of these disorders. Sending EUS FNA cytology material for fungal stains and culture, acid-fast bacillus stain, and mycobacterial culture can help to determine whether the cause is infectious. Lymphoma is also rarely associated with granulomas.

#### Sarcoid

Sarcoid is a multisystemic granulomatous disease of unknown origin. It typically involves mediastinal lymph nodes. The final diagnosis is made by using clinical criteria and by excluding other causes of granulomatous disease. No pathognomonic laboratory or pathologic finding exists for this disease. Elevated serum angiotensin-converting enzyme levels may suggest this diagnosis. The diagnosis of noncaseating granulomas in a mediastinal lymph node supports the diagnosis of sarcoid.

The usual endosonographic appearance of posterior mediastinal sarcoid is the presence of numerous enlarged lymph nodes (Fig. 9.6). EUS FNA can obtain granulomatous material to support the diagnosis of sarcoid with a high degree of accuracy (Table 9.3).<sup>58–61</sup> One retrospective study found the sensitivity and specificity of EUS FNA for diagnosing granulomas in suspected sarcoid to be 89% and 96%, respectively.<sup>62</sup> Another study found that EUS FNA demonstrated noncaseating granulomas in 41 of 50 patients (82%) with a final clinical diagnosis of sarcoidosis.<sup>59</sup> A study of patients with bilateral hilar lymphadenopathy, in whom EUS FNA was performed with a 19-G needle and whose material was sent for both cytologic and histopathologic examination, found that 94% of the histopathology specimens had noncaseating granulomas, compared with 79% of the cytology specimens ( $P = .04$ ).<sup>34</sup> Studies suggest that sarcoid lymph nodes aspirated via the transesophageal route may be at increased risk for mediastinitis (albeit rare) compared to EBUS FNA.<sup>36,37</sup> EBUS FNA has been shown to be superior to blind transbronchial FNA in the diagnosis of sarcoid.<sup>63,64</sup>



• Fig. 9.6 Multiple mediastinal lymph nodes in sarcoidosis.

**TABLE 9.3 Diagnostic Accuracy of Endoscopic Ultrasonography-Guided Fine-Needle Aspiration for Sarcoidosis**

Authors (Year)	n	Sensitivity (%)	Specificity (%)
Fritscher-Ravens and coworkers <sup>58</sup> (2000)	19	100	94
Wildi and coworkers <sup>62</sup> (2004)	28	89	96
Annema and coworkers <sup>59</sup> (2005)	50	82	—
Overall	97	90	95

## Histoplasmosis

Histoplasmosis is caused by infection with *Histoplasma capsulatum*. Within the United States, infection is most common in the midwestern states located in the Ohio and Mississippi River valleys. The diagnosis is typically made by histopathology, serologic testing, or antigen testing. Histoplasmosis usually is suspected either because of pulmonary symptoms or because of incidentally found mediastinal adenopathy on CT scan.

EUS FNA can diagnose granulomas in patients with suspected histoplasmosis.<sup>65</sup> Histoplasmosis should be suspected in patients with enlarged posterior mediastinal lymph nodes and granulomas on EUS FNA, particularly if these patients have spent time in areas endemic for *Histoplasma* infection. Histoplasmosis can also cause dysphagia resulting from compression of the esophagus by enlarged, fibrosing lymph nodes. The EUS appearance of mediastinal histoplasmosis that causes dysphagia includes the finding of a large mass of matted together, calcified lymph nodes that are adherent to a focally thickened esophageal wall.

## Tuberculosis

*Mycobacterium tuberculosis* can cause enlarged mediastinal lymph nodes, as well as a lymph node tuberculoma mass (Fig. 9.7). EUS findings suggestive of tuberculosis in mediastinal lymph nodes include patchy anechoic/hypoechoic areas or hyperechoic foci.<sup>66</sup> EUS FNA can obtain material for *M. tuberculosis* culture.<sup>67,68</sup> Patients with granulomas identified on EUS FNA should have material submitted for mycobacterial culture. The addition of



• Fig. 9.7 Posterior mediastinal tuberculoma.

**TABLE 9.4 Diagnostic Accuracy of Endoscopic Ultrasonography-Guided Fine-Needle Aspiration for Tuberculosis**

Authors (Year)	n	Sensitivity (%)	Specificity (%)	Accuracy (%)	PPV (%)	NPV (%)
Dhir and coworkers <sup>112</sup> (2011)	66	97	100	—	100	97
Puri and coworkers <sup>113</sup> (2012)	32	84	—	—	—	—
Puri and coworkers <sup>114</sup> (2010)	60	71	100	93	100	—
Fritscher-Ravens and coworkers <sup>115</sup> (2011)	28	86	100	—	100	91
Song and coworkers <sup>116</sup> (2010)	24	83	—	90	—	—
Overall	210	85	100	92	100	95

NPV, Negative predictive value; PPV, positive predictive value.

polymerase chain reaction testing for *M. tuberculosis* in samples obtained by EUS FNA may help increase the diagnostic yield compared with cytologic study and culture in patients suspected to have tuberculosis. The accuracy of EUS FNA in the diagnosis of tuberculosis is provided in Table 9.4.

## Other Infections

EUS FNA has also been reported to diagnosis infection with *Coccidioides immitis*, *Mycobacterium kansasii*, *Aspergillosis*, and *Nocardia*.<sup>69–71</sup>

## Impact of Endoscopic Ultrasonography Fine-Needle Aspiration of Mediastinal Lymph Nodes on Subsequent Thoracic Surgery Rates

One study found that among 59 patients with mediastinal adenopathy who were referred for surgical mediastinoscopy but



• Fig 9.8 Matted lymph nodes forming a conglomerate mass.

instead underwent EUS FNA first, only 22% of them eventually needed thoracic surgery.<sup>23</sup> Based on initial CT scan findings, 42% of the patients who had a lung mass and mediastinal lymph nodes underwent surgery, compared with only 6% of patients with only mediastinal lymph nodes without an associated lung mass. The reason for this difference was that patients with lung masses and negative lymph nodes underwent surgical resection of the primary cancer, whereas those with only mediastinal adenopathy did not undergo surgery because either they had benign disease (i.e., sarcoid or reactive lymph nodes) or unresectable disease (i.e., lymphoma). Only 4% of patients with a positive EUS FNA result underwent subsequent surgery. These results are similar to those of other studies in which 38% to 41% of patients who underwent EUS FNA subsequently underwent thoracic surgery.<sup>72,73</sup>

## Mediastinal Masses

The distinction between a posterior mediastinal mass and a lymph node can be difficult because some lymph nodes are very large, whereas some masses are extremely small. Additionally, numerous lymph nodes matted together can form a conglomerate mass (Fig. 9.8). Usually, a mass is larger than an enlarged lymph node (i.e., several centimeters in diameter), but no standardized terminology exists. Generally, when the term *mass* is used, there is only a single lesion, or one lesion that is significantly larger than adjacent lymph nodes. For the purpose of this section, only discrete, non-lymph node masses are discussed.

The differential diagnosis of a posterior mediastinal mass includes primary lung cancer (Video 9.3) extending into the posterior mediastinum, metastatic cancer (either primary lung cancer or nonthoracic cancer), neurogenic tumor, cyst, thymoma (Video 9.4), and infection. Transesophageal EUS FNA can easily sample posterior mediastinal masses for biopsy.

## Malignant Posterior Mediastinal Masses

Just as with mediastinal lymph nodes, approximately 50% of mediastinal masses that undergo EUS FNA are malignant.<sup>54,74,75</sup> Primary lung cancer masses that abut the esophagus can easily and safely undergo biopsy with transesophageal EUS FNA.<sup>76,77</sup> Mediastinal metastases from primary cancer of the lung, breast, colon



• Fig 9.9 Esophageal leiomyoma—the lesion arises from the fourth layer of the esophageal wall and grows extraluminally.

(Video 9.5), kidney, testicle, cervix, larynx, and esophagus have been diagnosed with transesophageal EUS FNA.<sup>54,76</sup> EUS FNA has also been reported to diagnose cases of primary mediastinal plasmacytoma and mediastinal granular cell tumor.<sup>78,79</sup>

## Neurogenic Tumors

Primary neoplasms of the posterior mediastinum are rare. Neurogenic tumors account for approximately 75% of these primary posterior mediastinal neoplasms.<sup>80</sup> Neurogenic tumors may arise from peripheral nerves (schwannoma, neurilemoma, neurofibroma, nerve-sheath tumors), sympathetic ganglia (ganglioneuroma, ganglioneuroblastoma, neuroblastoma), or parasympathetic ganglia (paraganglioma).<sup>44</sup> These are usually benign tumors, but approximately 10% to 20% may be malignant.<sup>81,82</sup> EUS FNA cytologic examination can diagnose mediastinal schwannoma.<sup>83,84</sup>

## Leiomyoma and Gastrointestinal Stromal Tumors

Gastrointestinal spindle cell tumors can arise from the muscularis propria of the esophagus and extend predominantly into the posterior mediastinum, rather than into the esophageal lumen (Fig. 9.9). These tumors can have a CT and endoscopic appearance that more closely resembles that of a posterior mediastinal mass than an esophageal wall mass.<sup>85–87</sup> Esophageal spindle cell neoplasms are usually c-kit-negative leiomyomas, although occasionally they can be c-kit-positive gastrointestinal stromal tumors (GISTs).<sup>85,86</sup> These tumors have an EUS appearance of a hypoechoic mass with some internal signal and occasional acoustic enhancement, which sometimes makes them difficult to distinguish from cysts.<sup>86</sup> Because GISTs are highly metabolically active, they can often be diagnosed and followed with PET scans.<sup>88</sup> Although leiomyomas generally are PET-negative tumors, there have been reports of PET-positive esophageal or posterior mediastinal leiomyomas.<sup>87</sup> EUS FNA can be used to diagnose both posterior mediastinal leiomyomas and GISTs and can be considered when the distinction between a cyst and a GIST is uncertain.

## Mesothelioma

Mesothelioma is a rare malignant tumor associated with asbestos exposure. This tumor is usually recognized as pleural thickening on CT, but sometimes the initial appearance is that of a

mediastinal mass. The presence of metastatic lymphadenopathy is considered in the decision regarding surgical resection. EUS FNA has been used to diagnose mesothelioma in both mediastinal masses and lymph nodes.<sup>89,90</sup>

## Benign Posterior Mediastinal Masses

Benign causes of mediastinal “masses” that can be diagnosed with EUS FNA include histoplasmosis, sarcoidosis, leiomyoma, duplication cysts, and teratomas.<sup>91</sup> Tuberculosis can also appear as a tuberculoma mass (see Fig. 9.7). A case of lymphangiomyoma, a rare malformation of the lymphatic system, has been reported as a posterior mediastinal mass detected with EUS.<sup>92</sup>

### Mediastinal Cysts

Congenital foregut cysts are the most common benign mediastinal cysts, and they account for 10% to 15% of mediastinal masses.<sup>93</sup> These cysts probably arise as a result of aberrant development of the primitive foregut. These foregut cysts may be categorized on the basis of the embryonic origin into bronchogenic or neuroenteric (esophageal duplication cysts and neuroenteric cysts). Esophageal duplication cysts are adherent to the esophagus, whereas those away from the esophageal wall are suggestive of bronchogenic cysts. Because it is usually difficult to determine whether the cyst is bronchogenic or esophageal in origin, the term *duplication cyst* is often used to describe the lesion. The pathologic evaluation of duplication cysts reveals them to be typically lined by columnar epithelium.

Most patients with posterior mediastinal cysts are asymptomatic, and the cysts are discovered incidentally during other imaging studies. When symptoms occur, they can include chest pain, cough, dyspnea, and dysphagia. CT scan findings include well-defined, homogeneous lesions ranging in size from 2 to 10 cm. These cysts are nonenhancing with intravenous contrast. They can sometimes be mistaken for a mass based on CT findings. Surgical resection may be indicated in symptomatic patients. Because the risk of malignancy is so rare, incidentally found lesions can usually be followed clinically.

The EUS appearance of a mediastinal cyst (Video 9.6) is usually a round or tubular anechoic structure with acoustic enhancement (Fig. 9.10) which can help distinguish a cyst from a solid lesion which should not exhibit acoustic enhancement (see Fig. 9.9). Additionally, the cyst wall may exhibit a visible wall layer

pattern which can also help distinguish it from a leiomyoma or GIST. Some cysts appear to be mass lesions because of a more hypoechoic (rather than anechoic) echotexture and minimal acoustic enhancement. Because it can be difficult to distinguish mediastinal cysts from esophageal leiomyomas or GISTS, these lesions sometimes undergo EUS FNA. These masslike cysts usually consist of thick, gelatinous cyst material.<sup>28,30</sup>

Mediastinal cysts can easily be aspirated with EUS FNA, but this is usually performed only when the EUS appearance is not compatible with a cyst and the lesion appears to be a possible mass.<sup>26,30,94</sup> Cytologic examination may reveal benign amorphous debris, degenerated cells, macrophages, needlelike crystals, mucinous material, or detached ciliary tufts.<sup>92</sup>

The risk of aspirating cystic mediastinal lesions was demonstrated by several reports of patients who developed mediastinitis after undergoing EUS FNA.<sup>27,28,30</sup> These patients required treatment with antibiotics, surgery, or endoscopic cyst drainage. None of the patients with reported bacterial mediastinitis after EUS FNA had received preprocedure or intraprocedure antibiotics. This situation raises the possibility that mediastinitis after EUS FNA of cysts may be prevented or minimized by the use of preprocedure or intraprocedure antibiotics. One series in which 22 patients underwent EUS FNA of posterior mediastinal cysts with 22-G needles and received intravenous ciprofloxacin followed by 5 days of oral ciprofloxacin reported no cases of mediastinitis.<sup>95</sup> This finding suggests that periprocedure antibiotics may prevent infection or mediastinitis when FNA of a cyst is performed.<sup>95</sup>

Despite the use of preprocedure antibiotics, in one reported case, EUS FNA of a duplication cyst resulted in *Candida albicans* infection of the cyst.<sup>26</sup> A 5-cm paratracheal cyst was aspirated, and gelatinous material was obtained. The patient subsequently underwent surgical resection, and culture grew *C. albicans*, which was not present on the original EUS FNA. This organism was believed to have been introduced at the time of EUS FNA. The patient, who had been administered prophylactic antibiotics, did not develop mediastinitis. However, this finding again emphasizes the possible infectious risks in mediastinal cysts even with prophylactic antibiotics.

Because of these reports of mediastinitis after aspirating posterior mediastinal duplication cysts, and given the benign nature of these cysts, any obvious posterior mediastinal duplication cyst should not be aspirated with EUS FNA. If there is a question that the lesion may be a cyst versus a malignant tumor, then the safest next diagnostic test may be thoracic magnetic resonance imaging or CT or PET scan to confirm the presence of a cyst and to exclude malignancy.<sup>30</sup> If EUS FNA is performed, a smaller gauge (i.e., 25-G) needle ideally should be used to minimize introduction of infection into the cyst. If the lesion turns out to be a cyst (i.e., mucinous fluid), then the cyst should be completely drained if possible, and prophylactic antibiotics should be administered. A typical approach is to administer intravenous antibiotics during the procedure and oral antibiotics for the next 3 to 5 days afterward to minimize any risk of mediastinitis.<sup>95</sup>

### Drainage of Mediastinal Pseudocysts and Abscesses

Pseudocysts can rarely extend into the mediastinum and should be considered in those with a cystic lesion in the mediastinum and a history of acute or chronic pancreatitis. Case reports have reported successful management with conservative measures as well as transpillary and transmural drainage.<sup>96–98</sup> Acute mediastinitis and mediastinal abscesses occur most commonly after thoracic surgery or esophageal perforation. Patients generally have symptoms of sepsis. CT scan may show mediastinal fluid collections.



• Fig. 9.10 Mediastinal duplication cyst. Note the acoustic enhancement of the ultrasound signal.

In a series of 18 critically ill patients with clinical mediastinitis (mostly after thoracic surgery) who underwent EUS FNA, the EUS appearance of the abscesses were 2 to 4 cm, inhomogeneous, well-demarcated hyperechoic areas. Some lesions had hyperechoic 2- to 3-mm spots with shadowing that were thought to represent air. EUS FNA revealed purulent material and bacterial organisms on microbiology culture. No apparent complications resulted from performing EUS FNA in the mediastinal abscesses. EUS FNA has also been reported to diagnose candidal mediastinitis.<sup>99</sup> There are reports of a mediastinal abscess drainage by EUS FNA aspiration, followed by placement of a transesophageal pigtail stent,<sup>100</sup> and more recently lumen apposing metal stents.<sup>101</sup> The limited number of case reports of transesophageal EUS-guided drainage of mediastinal pseudocysts and abscesses appear to demonstrate good efficacy and safety.

## Pleural Effusions

EUS FNA can also sample pleural effusions that abut the esophagus. This is important in the staging of non–small-cell lung cancer as it upstages the patient to stage IV disease if positive for malignancy.<sup>102</sup>

## Summary

EUS is a very safe and effective means of visualizing and characterizing posterior mediastinal lesions. EUS FNA allows the ability to

biopsy posterior mediastinal lesions accurately and safely to determine malignancy. Because of the high rate of reported infectious complications after EUS FNA of mediastinal cysts, biopsy should be avoided if a cyst is suspected.

## Key References

5. Jamil LH, Kashani A, Scimeca D, et al. Can endoscopic ultrasound distinguish between mediastinal benign lymph nodes and those involved by sarcoidosis, lymphoma, or metastasis? *Dig Dis Sci.* 2014;59(9):2191–2198.
7. Wallace MB, Fritscher-Ravens A, Savides TJ. Endoscopic ultrasound for the staging of non–small-cell lung cancer. *Endoscopy.* 2003;35(7):606–610.
23. Vazquez-Sequeiros E, Wiersema MJ, Clain J, et al. Impact of lymph node staging on therapy of esophageal carcinoma. *Gastroenterology.* 2003;125(6):1626–1635.
30. Westerterp M, van den Berg JG, van Lanschot JJ, Fockens P. Intramural bronchogenic cysts mimicking solid tumors. *Endoscopy.* 2004;36(12):1119–1122.
95. Fazel A, Moezardalan K, Varadarajulu S, et al. The utility and the safety of EUS-guided FNA in the evaluation of duplication cysts. *Gastrointest Endosc.* 2005;62(4):575–580.

## References

Access the reference list online at [ExpertConsult.com](http://ExpertConsult.com).

## References

1. Jue TL, Sharaf RN, Appalaneni V, et al. Role of EUS for the evaluation of mediastinal adenopathy. *Gastrointest Endosc.* 2011;74(2):239–245.
2. Sawhney MS, Debold SM, Kratzke RA, et al. Central intranodal blood vessel: a new EUS sign described in mediastinal lymph nodes. *Gastrointest Endosc.* 2007;65(4):602–608.
3. Hall JD, Kahaleh M, White GE, et al. Presence of lymph node vascularity: a new EUS criterion for benign nodes? *Dig Dis Sci.* 2009;54(1):118–121.
4. Kalaitzakis E, Sadik R, Doig L, Meenan J. Defining the lymph node burden in a northern european population without malignancy: the potential effect of geography in determining a need for FNA? *Dis Esophagus.* 2009;22(5):409–417.
5. Jamil LH, Kashani A, Scimeca D, et al. Can endoscopic ultrasound distinguish between mediastinal benign lymph nodes and those involved by sarcoidosis, lymphoma, or metastasis? *Dig Dis Sci.* 2014;59(9):2191–2198.
6. Janssen J, Dietrich CF, Will U, Greiner L. Endosonographic elastography in the diagnosis of mediastinal lymph nodes. *Endoscopy.* 2007;39(11):952–957.
7. Wallace MB, Fritscher-Ravens A, Savides TJ. Endoscopic ultrasound for the staging of non-small-cell lung cancer. *Endoscopy.* 2003;35(7):606–610.
8. Wallace MB, Woodward TA, Raimondo M, et al. Transaortic fine-needle aspiration of centrally located lung cancer under endoscopic ultrasound guidance: the final frontier. *Ann Thorac Surg.* 2007;84(3):1019–1021.
9. von Bartheld MB, Rabe KF, Annema JT. Transaortic EUS-guided FNA in the diagnosis of lung tumors and lymph nodes. *Gastrointest Endosc.* 2009;69(2):345–349.
10. Kazakov J, Hegde P, Tahiri M, et al. Endobronchial and endoscopic ultrasound-guided transvascular biopsy of mediastinal, hilar, and lung lesions. *Ann Thorac Surg.* 2017;103:951–955.
11. Klapman JB, Logrono R, Dye CE, Waxman I. Clinical impact of on-site cytopathology interpretation on endoscopic ultrasound-guided fine needle aspiration. *Am J Gastroenterol.* 2003;98(6):1289–1294.
12. Tournoy KG, Praet MM, Van MG, Van Meerbeeck JP. Esophageal endoscopic ultrasound with fine-needle aspiration with an on-site cytopathologist: high accuracy for the diagnosis of mediastinal lymphadenopathy. *Chest.* 2005;128(4):3004–3009.
13. Emery SC, Savides TJ, Behling CA. Utility of immediate evaluation of endoscopic ultrasound-guided transesophageal fine needle aspiration of mediastinal lymph nodes. *Acta Cytol.* 2004;48(5):630–634.
14. LeBlanc JK, Ciaccia D, Al-Assi MT, et al. Optimal number of EUS-guided fine needle passes needed to obtain a correct diagnosis. *Gastrointest Endosc.* 2004;59(4):475–481.
15. Wallace MB, Kennedy T, Durkalski V, et al. Randomized controlled trial of EUS-guided fine needle aspiration techniques for the detection of malignant lymphadenopathy. *Gastrointest Endosc.* 2001;54(4):441–447.
16. Erickson RA, Sayage-Rabie L, Beissner RS. Factors predicting the number of EUS-guided fine-needle passes for diagnosis of pancreatic malignancies. *Gastrointest Endosc.* 2000;51(2):184–190.
17. Herth FJ, Eberhardt R, Vilimann P, et al. Real-time endobronchial ultrasound guided transbronchial needle aspiration for sampling mediastinal lymph nodes. *Thorax.* 2006;61(9):795–798.
18. Gilbert S, Wilson DO, Christie NA, et al. Endobronchial ultrasound as a diagnostic tool in patients with mediastinal lymphadenopathy. *Ann Thorac Surg.* 2009;88(3):896–900, discussion 901–902.
19. Khoo KL, Ho KY, Nilsson B, Lim TK. EUS-guided FNA immediately after unrevealing transbronchial needle aspiration in the evaluation of mediastinal lymphadenopathy: a prospective study. *Gastrointest Endosc.* 2006;63(2):215–220.
20. Wallace MB, Pascual JM, Raimondo M, et al. Minimally invasive endoscopic staging of suspected lung cancer. *JAMA.* 2008;299(5):540–546.
21. Zhang R, Ying K, Shi L, et al. Combined endobronchial and endoscopic ultrasound-guided fine needle aspiration for mediastinal lymph node staging of lung cancer: a meta-analysis. *Eur J Cancer.* 2013;49(8):1860–1867.
22. Puli SR, Batapati Krishna Reddy J, Bechtold ML, et al. Endoscopic ultrasound: its accuracy in evaluating mediastinal lymphadenopathy? A meta-analysis and systematic review. *World J Gastroenterol.* 2008;14(19):3028–3037.
23. Vazquez-Sequeiros E, Wiersema MJ, Clain J, et al. Impact of lymph node staging on therapy of esophageal carcinoma. *Gastroenterology.* 2003;125(6):1626–1635.
24. Chen VK, Eloubeidi MA. Endoscopic ultrasound-guided fine needle aspiration is superior to lymph node echofeatures: a prospective evaluation of mediastinal and peri-intestinal lymphadenopathy. *Am J Gastroenterol.* 2004;99(4):628–633.
25. Wang KX, Ben QW, Jin ZD, et al. Assessment of morbidity and mortality associated with EUS-guided FNA: a systematic review. *Gastrointest Endosc.* 2011;73(2):283–290.
26. Ryan AG, Zamvar V, Roberts SA. Iatrogenic candidal infection of a mediastinal foregut cyst following endoscopic ultrasound-guided fine-needle aspiration. *Endoscopy.* 2002;34(10):838–839.
27. Annema JT, Veselic M, Versteegh MI, Rabe KF. Mediastinitis caused by EUS-FNA of a bronchogenic cyst. *Endoscopy.* 2003;35(9):791–793.
28. Wildi SM, Hoda RS, Fickling W, et al. Diagnosis of benign cysts of the mediastinum: the role and risks of EUS and FNA. *Gastrointest Endosc.* 2003;58(3):362–368.
29. Varadarajulu S, Fraig M, Schmulewitz N, et al. Comparison of EUS-guided 19-gauge trucut needle biopsy with EUS-guided fine-needle aspiration. *Endoscopy.* 2004;36(5):397–401.
30. Westerterp M, van den Berg JG, van Lanschot JJ, Fockens P. Intramural bronchogenic cysts mimicking solid tumors. *Endoscopy.* 2004;36(12):1119–1122.
31. Pai KR, Page RD. Mediastinitis after EUS-guided FNA biopsy of a posterior mediastinal metastatic teratoma. *Gastrointest Endosc.* 2005;62(6):980–981.
32. Savides TJ, Margolis D, Richman KM, Singh V. *Gemella morbillorum* mediastinitis and osteomyelitis following transesophageal endoscopic ultrasound-guided fine-needle aspiration of a posterior mediastinal lymph node. *Endoscopy.* 2007;39(suppl 1):E123–E124.
33. Aerts JG, Kloover J, Los J, et al. EUS-FNA of enlarged necrotic lymph nodes may cause infectious mediastinitis. *J Thorac Oncol.* 2008;3(10):1191–1193.
34. Iwashita T, Yasuda I, Doi S, et al. The yield of endoscopic ultrasound-guided fine needle aspiration for histological diagnosis in patients suspected of stage I sarcoidosis. *Endoscopy.* 2008;40(5):400–405.
35. Diehl DL, Cheruvattath R, Facktor MA, Go BD. Infection after endoscopic ultrasound-guided aspiration of mediastinal cysts. *Interact Cardiovasc Thorac Surg.* 2010;10(2):338–340.
36. von Bartheld M, van der Heijden E, Annema J. Mediastinal abscess formation after EUS-guided FNA: are patients with sarcoidosis at increased risk? *Gastrointest Endosc.* 2012;75(5):1104–1107.
37. Allen BD, Penman I. Mediastinal abscess formation after EUS-guided FNA in patients with sarcoidosis. *Gastrointest Endosc.* 2012;76(5):1078–1079, author reply 1079.
38. Doi S, Yasuda I, Iwashita T, et al. Needle tract implantation on the esophageal wall after EUS-guided FNA of metastatic mediastinal lymphadenopathy. *Gastrointest Endosc.* 2008;67(6):988–990.
39. von Bartheld MB, van Kralingen KW, Veenendaal RA, et al. Mediastinal-esophageal fistulae after EUS-FNA of tuberculosis of the mediastinum. *Gastrointest Endosc.* 2010;71(1):210–212.
40. Ceuterick V, Decaluwe H, Coosemans W, et al. Esophageal wall rupture after EUS-FNA for mediastinal staging: report of two cases. *Acta Chir Belg.* 2016;116(1):48–50.

41. von Bartheld MB, Annema JT. Endosonography-related mortality and morbidity for pulmonary indications: a nationwide survey in the Netherlands. *Gastrointest Endosc.* 2015;82(6):1009–1015.
42. von Bartheld MB, van Breda A, Annema JT. Complication rate of endosonography (endobronchial and endoscopic ultrasound): a systematic review. *Respiration.* 2014;87(4):343–351.
43. Fritscher-Ravens A, Bohuslavizki KH, Brandt L, et al. Mediastinal lymph node involvement in potentially resectable lung cancer: comparison of CT, positron emission tomography, and endoscopic ultrasonography with and without fine-needle aspiration. *Chest.* 2003;123(2):442–451.
44. Gould MK, Kuschner WG, Rydzak CE, et al. Test performance of positron emission tomography and computed tomography for mediastinal staging in patients with non-small-cell lung cancer: a meta-analysis. *Ann Intern Med.* 2003;139(11):879–892.
45. Fritscher-Ravens A, Davidson BL, Hauber HP, et al. Endoscopic ultrasound, positron emission tomography, and computerized tomography for lung cancer. *Am J Respir Crit Care Med.* 2003;168(11):1293–1297.
46. Redondo-Cerezo E, Martínez-Cara JG, Esquivias J, et al. Endoscopic ultrasonography-fine needle aspiration versus PET-CT in undiagnosed mediastinal and upper abdominal lymphadenopathy: a comparative clinical study. *Eur J Gastroenterol Hepatol.* 2015;27(4):455–459.
47. Kalade AV, Eddie Lau WF, Conron M, et al. Endoscopic ultrasound-guided fine-needle aspiration when combined with positron emission tomography improves specificity and overall diagnostic accuracy in unexplained mediastinal lymphadenopathy and staging of non-small-cell lung cancer. *Intern Med J.* 2008;38(11):837–844.
48. Bataille L, Lonneux M, Weynand B, et al. EUS-FNA and FDG-PET are complementary procedures in the diagnosis of enlarged mediastinal lymph nodes. *Acta Gastroenterol Belg.* 2008;71(2):219–229.
49. Catalano MF, Nayar R, Gress F, et al. EUS-guided fine needle aspiration in mediastinal lymphadenopathy of unknown etiology. *Gastrointest Endosc.* 2002;55(7):863–869.
50. Kahi CJ, Dewitt JM, Lykens M, et al. Diagnosis of a malignant mesothelioma by EUS-guided FNA of a mediastinal lymph node. *Gastrointest Endosc.* 2004;60(5):859–861.
51. Bean SM, Eloubeidi MA, Cerfolio R, et al. Endoscopic ultrasound-guided fine needle aspiration is useful for nodal staging in patients with pleural mesothelioma. *Diagn Cytopathol.* 2008;36(1):32–37.
52. Tournoy KG, Burgers SA, Annema JT, et al. Transesophageal endoscopic ultrasound with fine needle aspiration in the preoperative staging of malignant pleural mesothelioma. *Clin Cancer Res.* 2008;14(19):6259–6263.
53. Rice DC, Steliga MA, Stewart J, et al. Endoscopic ultrasound-guided fine needle aspiration for staging of malignant pleural mesothelioma. *Ann Thorac Surg.* 2009;88(3):862–868, discussion 868–869.
54. Dewitt J, Ghorai S, Kahi C, et al. EUS-FNA of recurrent post-operative extraluminal and metastatic malignancy. *Gastrointest Endosc.* 2003;58(4):542–548.
55. Kramer H, Koeter GH, Sleijfer DT, et al. Endoscopic ultrasound-guided fine-needle aspiration in patients with mediastinal abnormalities and previous extrathoracic malignancy. *Eur J Cancer.* 2004;40(4):559–562.
56. Hahn M, Faigel DO. Frequency of mediastinal lymph node metastases in patients undergoing EUS evaluation of pancreaticobiliary masses. *Gastrointest Endosc.* 2001;54(3):331–335.
57. Ribeiro A, Vazquez-Sequeiros E, Wiersma LM, et al. EUS-guided fine-needle aspiration combined with flow cytometry and immunocytochemistry in the diagnosis of lymphoma. *Gastrointest Endosc.* 2001;53(4):485–491.
58. Fritscher-Ravens A, Sriram PV, Topalidis T, et al. Diagnosing sarcoidosis using endosonography-guided fine-needle aspiration. *Chest.* 2000;118(4):928–935.
59. Annema JT, Veselic M, Rabe KF. Endoscopic ultrasound-guided fine-needle aspiration for the diagnosis of sarcoidosis. *Eur Respir J.* 2005;25(3):405–409.
60. Michael H, Ho S, Pollack B, et al. Diagnosis of intra-abdominal and mediastinal sarcoidosis with EUS-guided FNA. *Gastrointest Endosc.* 2008;67(1):28–34.
61. Cooke JR, Behling CA, Perricone A, Savides TJ. Using transesophageal endoscopic ultrasound-guided fine needle aspiration to diagnose sarcoidosis in patients with mediastinal lymphadenopathy. *Clin Pulm Med.* 2008;15(1):13–17.
62. Wildi SM, Judson MA, Fraig M, et al. Is endosonography guided fine needle aspiration (EUS-FNA) for sarcoidosis as good as we think? *Thorax.* 2004;59(9):794–799.
63. Tremblay A, Stather DR, Maceachern P, et al. A randomized controlled trial of standard versus endobronchial ultrasonography-guided transbronchial needle aspiration in patients with suspected sarcoidosis. *Chest.* 2009;136(2):340–346.
64. Tournoy KG, Bolly A, Aerts JG, et al. The value of endoscopic ultrasound after bronchoscopy to diagnose thoracic sarcoidosis. *Eur Respir J.* 2010;35(6):1329–1335.
65. Gailey MP, Klutts JS, Jensen CS. Fine-needle aspiration of histoplasmosis in the era of endoscopic ultrasound and endobronchial ultrasound: cytomorphologic features and correlation with clinical laboratory testing. *Cancer Cytopathol.* 2013;121(9):508–517.
66. Rana SS, Bhasin DK, Srinivasan R, Singh K. Endoscopic ultrasound (EUS) features of mediastinal tubercular lymphadenopathy. *Hepatogastroenterology.* 2011;58(107-108):819–823.
67. Kramer H, Nieuwenhuis JA, Groen HJ, Wempe JB. Pulmonary tuberculosis diagnosed by esophageal endoscopic ultrasound with fine-needle aspiration. *Int J Tuberc Lung Dis.* 2004;8(2):272–273.
68. Fritscher-Ravens A, Schirrow L, Pothmann W, et al. Critical care transesophageal endosonography and guided fine-needle aspiration for diagnosis and management of posterior mediastinitis. *Crit Care Med.* 2003;31(1):126–132.
69. Chaya CT, Schnadig V, Gupta P, et al. Endoscopic ultrasound-guided fine-needle aspiration for diagnosis of an infectious mediastinal mass and/or lymphadenopathy. *Endoscopy.* 2006;38(suppl 2):E99–E101.
70. Naidu VG, Tammineni AK, Biscopink RJ, et al. *Coccidioides immitis* and *Mycobacterium tuberculosis* diagnosed by endoscopic ultrasound. *J S C Med Assoc.* 2009;105(1):4–7.
71. Rodrigues-Pinto E, Lopes S, Principe F, et al. Pulmonary aspergillosis diagnosed by endoscopic ultrasound fine-needle aspiration. *Endosc Ultrasound.* 2016;5(1):58–60.
72. Savides TJ, Perricone A. Impact of EUS-guided FNA of enlarged mediastinal lymph nodes on subsequent thoracic surgery rates. *Gastrointest Endosc.* 2004;60(3):340–346.
73. Srinivasan R, Bhutani MS, Thosani N, et al. Clinical impact of EUS-FNA of mediastinal lymph nodes in patients with known or suspected lung cancer or mediastinal lymph nodes of unknown etiology. *J Gastrointest Liver Dis.* 2012;21(2):145–152.
74. Catalano MF, Rosenblatt ML, Chak A, et al. Endoscopic ultrasound-guided fine needle aspiration in the diagnosis of mediastinal masses of unknown origin. *Am J Gastroenterol.* 2002;97(10):2559–2565.
75. Panelli F, Erickson RA, Prasad VM. Evaluation of mediastinal masses by endoscopic ultrasound and endoscopic ultrasound-guided fine needle aspiration. *Am J Gastroenterol.* 2001;96(2):401–408.
76. Varadarajulu S, Hoffman BJ, Hawes RH, Eloubeidi MA. EUS-guided FNA of lung masses adjacent to or abutting the esophagus after unrevealing CT-guided biopsy or bronchoscopy. *Gastrointest Endosc.* 2004;60(2):293–297.

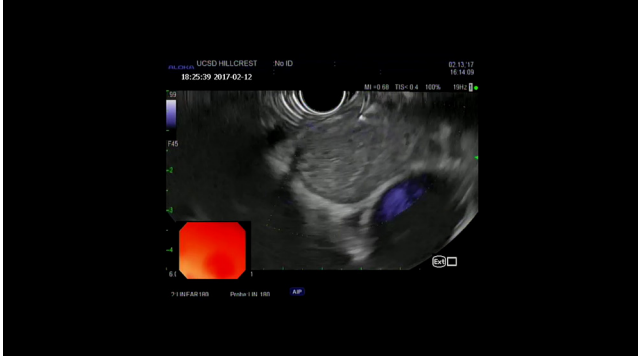
77. Vazquez-Sequeiros E, Levy MJ, Van Domselaar M, et al. Diagnostic yield and safety of endoscopic ultrasound guided fine needle aspiration of central mediastinal lung masses. *Diagn Ther Endosc.* 2013;2013:150492.
78. Mallo R, Gottlieb K, Waggoner D, Wittenkeller J. Mediastinal plasmacytoma detected by echocardiography and biopsied with EUS-FNA. *Echocardiography.* 2008;25(9):997–998.
79. Bean SM, Eloubeidi MA, Eltoum IA, et al. Preoperative diagnosis of a mediastinal granular cell tumor by EUS-FNA: a case report and review of the literature. *Cytojournal.* 2005;2(1):8.
80. Macchiarini P, Ostertag H. Uncommon primary mediastinal tumours. *Lancet Oncol.* 2004;5(2):107–118.
81. Okubo Y, Yokose T, Motohashi O, et al. Duodenal rare neuroendocrine tumor: clinicopathological characteristics of patients with gangliocytic paraganglioma. *Gastroenterol Res Pract.* 2016; 2016:5257312.
82. Sharma SS, Jhajharia A, Maharshi S, et al. Mediastinal paraganglioma: specific endoscopic ultrasound features. *Endosc Ultrasound.* 2013;2(2):105–106.
83. McGrath KM, Ballo MS, Jowell PS. Schwannoma of the mediastinum diagnosed by EUS-guided fine needle aspiration. *Gastrointest Endosc.* 2001;53(3):362–365.
84. Pakseresht K, Reddymasu SC, Oropeza-Vail MM, et al. Mediastinal schwannoma diagnosed by endoscopic ultrasonography-guided fine needle aspiration cytology. *Case Rep Gastroenterol.* 2011;5(2):411–415.
85. Lee JR, Anstadt MP, Khwaja S, Green LK. Gastrointestinal stromal tumor of the posterior mediastinum. *Eur J Cardiothorac Surg.* 2002;22(6):1014–1016.
86. Portale G, Zaninotto G, Costantini M, et al. Esophageal GIST: case report of surgical enucleation and update on current diagnostic and therapeutic options. *Int J Surg Pathol.* 2007;15(4):393–396.
87. Miyoshi K, Naito M, Ueno T, et al. Abnormal fluorine-18-fluorodeoxyglucose uptake in benign esophageal leiomyoma. *Gen Thorac Cardiovasc Surg.* 2009;57(11):629–632.
88. Van den Abbeele AD. The lessons of GIST—PET and PET/CT: a new paradigm for imaging. *Oncologist.* 2008;13(suppl 2):8–13.
89. Bakdounes K, Jhala N, Jhala D. Diagnostic usefulness and challenges in the diagnosis of mesothelioma by endoscopic ultrasound guided fine needle aspiration. *Diagn Cytopathol.* 2008;36(7):503–507.
90. Balderramo DC, Pellise M, Colomo L, et al. Diagnosis of pleural malignant mesothelioma by EUS-guided FNA (with video). *Gastrointest Endosc.* 2008;68(6):1191–1192, discussion 1192–1193.
91. Devereaux BM, Leblanc JK, Yousif E, et al. Clinical utility of EUS-guided fine-needle aspiration of mediastinal masses in the absence of known pulmonary malignancy. *Gastrointest Endosc.* 2002;56(3):397–401.
92. Tang SJ, Sreenarasimhaiah J, Tang L, et al. Endoscopic injection sclerotherapy with doxycycline for mediastinal and esophageal lymphangiomyoma. *Gastrointest Endosc.* 2007; 66(6):1196–1200.
93. Wiechowska-Kozlowska A, Wunsch E, Majewski M, et al. Esophageal duplication cysts: endosonographic findings in asymptomatic patients. *World J Gastroenterol.* 2012;18(11):1270–1272.
94. Eloubeidi MA, Cohn M, Cerfolio RJ, et al. Endoscopic ultrasound-guided fine-needle aspiration in the diagnosis of foregut duplication cysts: the value of demonstrating detached ciliary tufts in cyst fluid. *Cancer.* 2004;102(4):253–258.
95. Fazel A, Mozzardalan K, Varadarajulu S, et al. The utility and the safety of EUS-guided FNA in the evaluation of duplication cysts. *Gastrointest Endosc.* 2005;62(4):575–580.
96. Rana SS, Bhasin DK, Rao C, et al. Esophageal stricture following successful resolution of a mediastinal pseudocyst by endoscopic transpapillary drainage. *Endoscopy.* 2012;44 (Suppl 2) UCTN:E121-2.
97. Gornals JB, Loras C, Mast R, et al. Endoscopic ultrasound-guided transesophageal drainage of a mediastinal pancreatic pseudocyst using a novel lumen-apposing metal stent. *Endoscopy.* 2012;44 (Suppl 2) UCTN:E211-2.
98. Sugimoto S, Yamagishi Y, Higuchi H, Kanai T. Endoscopic ultrasound-guided drainage for a mediastinal pancreatic pseudocyst. *Intern Med.* 2014;53(22):2651–2652.
99. Prasad VM, Erickson R, Contreras ED, Panelli F. Spontaneous candida mediastinitis diagnosed by endoscopic ultrasound-guided, fine-needle aspiration. *Am J Gastroenterol.* 2000;95(4):1072–1075.
100. Kahaleh M, Yoshida C, Kane L, Yeaton P. EUS drainage of a mediastinal abscess. *Gastrointest Endosc.* 2004;60(1): 158–160.
101. Consiglieri CF, Escobar I, Gornals JB. EUS-guided transesophageal drainage of a mediastinal abscess using a diabolo-shaped lumen-apposing metal stent. *Gastrointest Endosc.* 2015;81(1):221–222.
102. Lococo F, Cesario A, Attili F, et al. Transoesophageal endoscopic ultrasound-guided fine-needle aspiration of pleural effusion for the staging of non-small-cell lung cancer. *Interact Cardiovasc Thorac Surg.* 2013;17:237–241.
103. Giovannini M, Seitz JF, Monges G, et al. Fine-needle aspiration cytology guided by endoscopic ultrasonography: results in 141 patients. *Endoscopy.* 1995;27(2):171–177.
104. Silvestri GA, Hoffman BJ, Bhutani MS, et al. Endoscopic ultrasound with fine-needle aspiration in the diagnosis and staging of lung cancer. *Ann Thorac Surg.* 1996;61(5):1441–1445.
105. Gress FG, Hawes RH, Savides TJ, et al. Endoscopic ultrasound-guided fine-needle aspiration biopsy using linear array and radial scanning endosonography. *Gastrointest Endosc.* 1997;45(3):243–250.
106. Hünerbein M, Dohmoto M, Haensch W, et al. Endosonography-guided biopsy of mediastinal and pancreatic tumors. *Endoscopy.* 1998;30(1):32–36.
107. Serna DL, Aryan HE, Chang KJ, et al. An early comparison between endoscopic ultrasound-guided fine-needle aspiration and mediastinoscopy for diagnosis of mediastinal malignancy. *Am Surg.* 1998;64(10):1014–1018.
108. Vazquez-Sequeiros E, Norton ID, Clain JE, et al. Impact of EUS-guided fine-needle aspiration on lymph node staging in patients with esophageal carcinoma. *Gastrointest Endosc.* 2001;53(7):751–757.
109. Larsen SS, Krasnik M, Vilmann P, et al. Endoscopic ultrasound guided biopsy of mediastinal lesions has a major impact on patient management. *Thorax.* 2002;57(2):98–103.
110. Hernandez LV, Mishra G, George S, et al. A descriptive analysis of EUS-FNA for mediastinal lymphadenopathy: an emphasis on clinical impact and false negative results. *Am J Gastroenterol.* 2004;99(2):249–254.
111. Eloubeidi MA, Cerfolio RJ, Chen VK, et al. Endoscopic ultrasound-guided fine needle aspiration of mediastinal lymph node in patients with suspected lung cancer after positron emission tomography and computed tomography scans. *Ann Thorac Surg.* 2005;79(1):263–268.
112. Dhir V, Mathew P, Bhandari S, et al. Endosonography-guided fine needle aspiration cytology of intra-abdominal lymph nodes with unknown primary in a tuberculosis endemic region. *J Gastroenterol Hepatol.* 2011;26(12):1721–1724.
113. Puri R, Khaliq A, Kumar M, et al. Esophageal tuberculosis: role of endoscopic ultrasound in diagnosis. *Dis Esophagus.* 2012;25(2):102–106.
114. Puri R, Vilman P, Sud R, et al. Endoscopic ultrasound-guided fine-needle aspiration cytology in the evaluation of suspected tuberculosis in patients with isolated mediastinal lymphadenopathy. *Endoscopy.* 2010;42(6):462–467.
115. Fritscher-Ravens A, Ghanbari A, Topalidis T, et al. Granulomatous mediastinal adenopathy: can endoscopic ultrasound-guided fine-needle aspiration differentiate between tuberculosis and sarcoidosis? *Endoscopy.* 2011;43(11):955–961.
116. Song HJ, Park YS, Seo DW, et al. Diagnosis of mediastinal tuberculosis by using EUS-guided needle sampling in a geographic region with an intermediate tuberculosis burden. *Gastrointest Endosc.* 2010;71(7):1307–1313.



**Video 9.1** Endosonographic Features of a Malignant Lymph Node in the Posterior Mediastinum



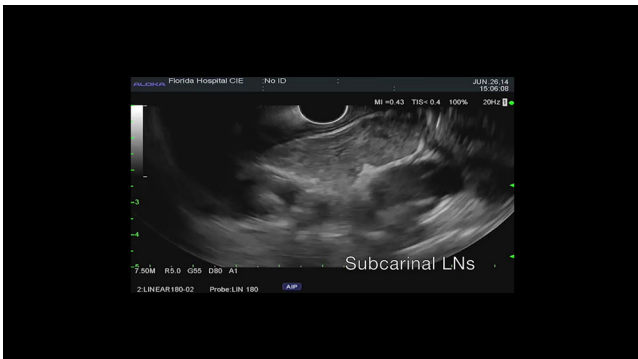
**Video 9.4** Endoscopic Ultrasound-Guided Fine-Needle Aspiration of a Posterior Mediastinal Mass Proven to Be a Recurrent Thymoma



**Video 9.2** Technique of Transesophageal Endoscopic Ultrasonography-Guided Fine-Needle Aspiration



**Video 9.5** Endoscopic Ultrasonography-Guided Fine-Needle Aspiration of a Posterior Mediastinal Mass Proven to Be a Metastatic Colon Cancer



**Video 9.3** Endoscopic Ultrasonography-Guided Fine-Needle Aspiration of a Posterior Mediastinal Mass Proven to Be Adenocarcinoma of the Lung



**Video 9.6** Diagnosis of Duplication Cyst by Endoscopic Ultrasonography and Tissue Sampling

# 10

## How to Perform Endoscopic Ultrasonography in the Stomach

ROBERT H. HAWES, SHYAM VARADARAJULU, AND PAUL FOCKENS

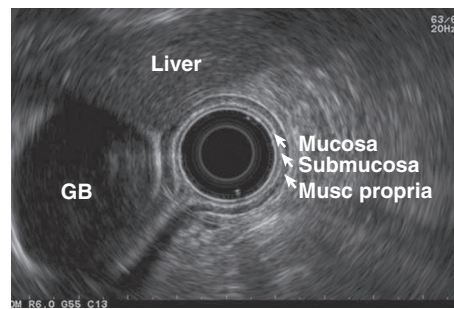
The two basic techniques for examining the stomach are the balloon inflation procedure and the water-filled stomach method. Both methods can be employed with either the linear or radial echoendoscope, but examination with the radial scope is easier and more efficient because of the larger viewing field. The balloon inflation method is preferred for rapid screening of submucosal lesions and the examination of perigastric structures (Fig. 10.1). The water-filled method is best for examining the gastric wall layers and the careful and accurate evaluation of specific lesions (Fig. 10.2). With the balloon inflation technique, the tip of the echoendoscope is advanced to the immediate prepyloric antrum. The balloon is fully inflated and continuous suction is applied to remove air from the gastric lumen. When the gastric wall is completely collapsed around the balloon, the balloon is centered as well as possible, and slow withdrawal is performed (Video 10.1).

When one is learning endoscopic ultrasonography (EUS), it is critical that images are displayed in a standard orientation. In the case of gastric imaging, the liver is easily recognized and should be electronically rotated until it is positioned in the 9- to 12-o'clock space. This orientation will cause the pancreas to emerge at the 6-o'clock position on withdrawal, and the spleen and left kidney will appear between 12 and 4 o'clock. The examiner's eyes should then be fixed on both the gastric wall and the perigastric structures. If a lesion or abnormality is recognized, specific maneuvers can be applied to obtain detailed imaging.

With the water-filled method, the stomach is collapsed (removing all air), and 200 to 400 mL of fluid is instilled into the gastric lumen (see Fig. 10.2 and Video 10.2). High-quality imaging of the gastric wall requires attention to detail on two points: (1) the transducer must be positioned at a perpendicular angle to the gastric wall or a specific lesion (Video 10.3) and (2) the tip of the echoendoscope must be positioned within the focal zone of the transducer (see Chapter 1). This second point is absolutely critical when using the mechanical radial echoendoscope but is less important with electronic radial instruments. To obtain superfine images with the water-filled method, one should consider using an agent to paralyze peristalsis and instill water into the gastric lumen in a way that minimizes the production of microbubbles (slow infusion versus a water jet technique).

The difficulty or impossibility of obtaining perpendicular images in some areas presents a significant challenge in gastric EUS. An example is the gastric antrum. It may be impossible to adjust the tip deflection in a way that positions the transducer

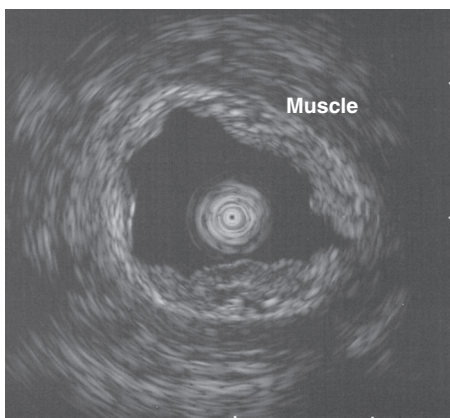
perpendicular to the antral wall while at the same time not pressing the transducer against the wall. The consequence of an inability to achieve optimal orientation between the transducer and the surface of the stomach is tangential imaging. If the ultrasound waves pass tangentially across the gastric wall, the layers will appear abnormally thick. This appearance can lead to overstaging of early gastric cancer or inaccurate determination of the layer of origin in submucosal masses. With large bulky tumors, where one is trying to differentiate stage T3 from stage T4, this is less of an issue than with very superficial lesions in which one is trying to determine whether endoscopic mucosal resection (EMR) is appropriate. In the antrum, it is sometimes easier to use a dual-channel endoscope and a high-frequency catheter probe to achieve good



• **Fig. 10.1** Balloon inflation method. Gastric wall layers as imaged using a radial echoendoscope. GB, Gallbladder.



• **Fig. 10.2** Water-filled method. With the radial echoendoscope positioned in the gastric lumen and the stomach filled with water, the individual layers of the gastric wall can be well visualized.



• **Fig. 10.3** Imaging in the gastric antrum. Gastric wall layers as visualized using a high-frequency catheter probe with the water-filled technique.

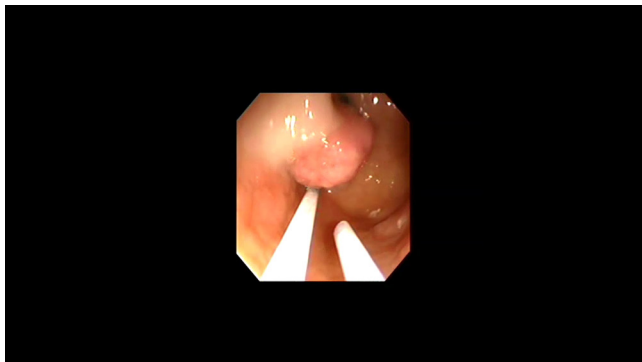
positioning (Video 10.4 and [Fig. 10.3](#)). However, if the lesion is large, the depth of penetration of the catheter probe will be insufficient for accurate staging.

## Summary

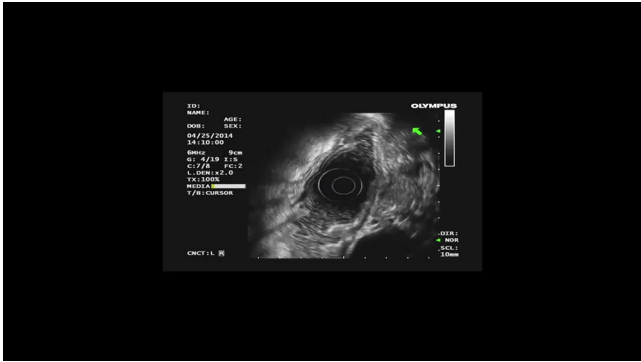
Two techniques are described for gastric imaging using standard echoendoscopes. Attention to proper technique is critical to accurate imaging. Evaluation of large lesions ( $>2$  cm), global imaging of the stomach, and assessment of the perigastric space are best accomplished with standard echoendoscopes. Imaging of small lesions, where it is advantageous to obtain simultaneous endoscopic and ultrasound images, is best accomplished with catheter probes in conjunction with dual-channel endoscopes.



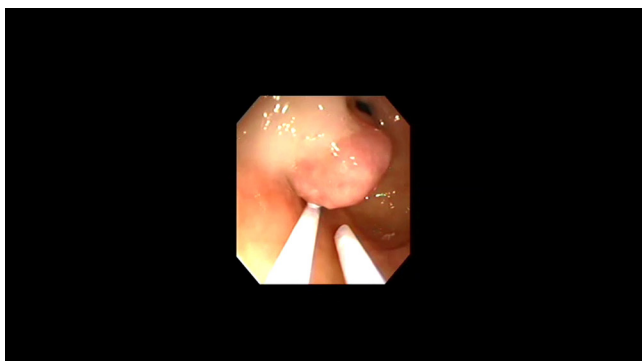
**Video 10.1** Video Demonstrating the Balloon-Inflation Method for Examining the Stomach Using a Radial Echoendoscope



**Video 10.3** Radial Endoscopic Ultrasonography, Performed After Instillation of Water, Reveals a T1 Gastric Cancer Confined to the Mucosal Layer



**Video 10.2** Video Demonstrating the Water-Filled Method for Examining the Stomach Using a Radial Echoendoscope



**Video 10.4** Endoscopic Ultrasonography Examination Performed Using a 20-MHz High-Frequency Miniprobe (Water-Filled Method) Revealing a T1 Gastric Cancer Confined to the Mucosal Region

# Subepithelial Lesions

EUN YOUNG (ANN) KIM

## KEY POINTS

- Endoscopic ultrasonography (EUS) can accurately differentiate a mural lesion from extrinsic compression against the gut wall.
- Determination of the cause of an intramural lesion is based on its layer of origin and internal echo characteristics.
- The finding of an intact submucosal layer running deep below a mural lesion indicates that the lesion can be removed safely by endoscopic mucosal resection.
- Carcinoid tumors can usually be diagnosed with standard mucosal biopsies because these tumors emanate from the deep mucosal layer.
- Gastrointestinal stromal tumors can be differentiated from leiomyomas by immunohistochemical staining for CD117 (c-kit proto-oncogene protein product).

The term *submucosal lesion* is used by endoscopists to describe any bulge covered with normal mucosa, usually found incidentally during gastrointestinal (GI) endoscopy or barium contrast radiography. This lesion could be either an intramural mass or an impression caused by extramural structures. Recently the term “*subepithelial lesion (SEL)*” has been used more frequently than “*submucosal lesion*” because intramural lesions may arise from any layer of the GI wall underneath the epithelium. In the past, the prevalence of suspected gastric submucosal lesions at routine endoscopy was reported to be as low as 0.36%.<sup>1</sup> More recently, however, the detection rate has notably increased, especially with regard to small lesions. Advances in technology and the close attention paid to these lesions may be responsible for this augmentation.

To characterize the cause of protrusion, some noninvasive imaging methods, such as transabdominal ultrasonography (USG), computed tomography (CT), and magnetic resonance imaging (MRI), have been used, but they are often insufficient. With endoscopic ultrasonography (EUS), however, the clinician can visualize the structure of gut wall layers clearly. Thus, EUS can not only differentiate SELs from extramural structures but also identify the layers of origin and endosonographic characteristics of intraluminal lesions.<sup>2–7</sup> EUS is now accepted as the modality of choice for visualizing SELs with high precision.

The differential diagnosis of SELs includes a wide variety of benign and malignant subepithelial neoplasms as well as non-neoplastic lesions (Video 11.1). To evaluate SELs, the transition zone (the area where the tumor arises from normal gut

wall layers) should be examined carefully to determine the layer of origin. Next, the size and echo pattern of the tumor—such as the smoothness of the border, internal features, echogenicity, and vascularity—should be observed. In addition, the relationship with other adjacent organs and the presence of adenopathy nearby provide valuable information. From the information gathered, an educated guess on the SEL for the differential diagnosis can be made with reasonable accuracy (Table 11.1).<sup>7</sup> The reported accuracy of EUS in predicting the pathologic diagnosis of SELs has shown a wide range, from 45.5% to 82.9% (Table 11.2).<sup>8–14</sup> If tissue was obtained from EUS-guided fine-needle aspiration (EUS FNA), the diagnostic accuracy increased markedly, ranging from 63% to 98%.<sup>15,16</sup> Detailed description comes later in this chapter.

Diagnostic information on the SELs, including the origin of the wall layer provided by EUS, also helps in deciding whether a lesion should be removed or followed *in situ*.<sup>17,18</sup> Lesions confined to the mucosal or submucosal layers can be safely removed endoscopically. Surgical resection, if needed, is generally recommended for lesions located in the muscularis propria, although advances in endoscopic techniques such as endoscopic submucosal dissection (ESD) have made it possible for these lesions to be removed by experienced clinicians with minimal risk to the patient.<sup>19,20</sup> EUS can be used for following up after resection.<sup>21</sup>

## Comparison of Accuracy Between Endoscopic Ultrasonography and Other Imaging Modalities

Differentiation of SELs is one of the main indications for EUS. Compared with endoscopy, barium contrast radiography, USG, CT, and MRI, EUS has a higher accuracy in detecting and assessing the size and location of SELs.<sup>22</sup> When viewed endoscopically, the surface of a SEL is usually smooth and has a color similar to that of the surrounding mucosa, without ulceration or erosion. Sometimes these lesions show a slight color change and certain morphologic characteristics, but it is often impossible to differentiate them by endoscopy alone. USG provides diagnostic information only for very large SELs. In a study of patients with endosonographically diagnosed gastric SELs, 82.5% of tumors were visualized and measured by USG after the stomach was filled with water.<sup>23</sup> Like CT and MRI, USG can also provide useful information on perigastric structures. CT may be used to evaluate a SEL especially when it is malignant and metastasis is suspected. However, a study pointed out that large submucosal tumors previously identified by EUS were visualized in only two-thirds of cases by preoperative CT.<sup>22</sup> Reported mean sizes of possibly malignant

**TABLE 11.1****Endoscopic Ultrasound Characteristics of Various Subepithelial Lesions**

Cause	EUS Layers <sup>a</sup>	EUS Appearance
Gastrointestinal stromal tumor	Fourth (rarely second)	Hypoechoic (irregular borders, echogenic foci with mixed echogenicity; anechoic areas suggest malignancy)
Leiomyoma	Fourth, second	Hypoechoic
Aberrant pancreas	Second, third, and/or fourth	Hypoechoic or mixed echogenicity (anechoic ductal structure may be present)
Lipoma	Third	Hyperechoic
Carcinoid	Second and/or third	Mildly hypoechoic, homogeneous
Granular cell tumor	Second or third	Homogeneous hypoechoic mass with smooth borders
Cyst	Third	Anechoic, round or oval (three- or five-layer walls suggest duplication cyst)
Varices	Third	Anechoic, tubular, serpiginous
Inflammatory fibroid polyp	Second and/or third	Hypoechoic, homogeneous, or mixed echogenicity, indistinct margin
Glomus tumor	Third or fourth	Hypoechoic, smooth margin, internal heterogeneous echo mixed with high echoic spots
Lymphoma	Second, third, and/or fourth	Hypoechoic
Metastatic deposits	Any or all	Hypoechoic, heterogeneous

<sup>a</sup>First layer, interface of luminal fluid and mucosa; second layer, deep mucosa; third layer, submucosa; fourth layer, muscularis propria; fifth layer, serosa or adventitia.

EUS, Endoscopic ultrasound.

**TABLE 11.2****Diagnostic Accuracy of Endoscopic Ultrasound for Gastrointestinal Subepithelial Lesions**

Authors (Year)	Number of Patients	Accuracy (%)
Lim and coworkers <sup>8</sup> (2016)	99	66.7
Reddymasu and coworkers <sup>9</sup> (2012)	37	49
Karaca and coworkers <sup>10</sup> (2010)	22	45.5
Ji and coworkers <sup>11</sup> (2008)	76	82.9
Kwon and coworkers <sup>12</sup> (2005)	58	79.3
Kojima and coworkers <sup>13</sup> (1999)	54	74
Matsui and coworkers <sup>14</sup> (1998)	15	60

SELs detected and not detected by CT were 27.4 mm and 11 mm, respectively.<sup>24</sup> Currently high-quality images are available through multidetector computed tomography (MDCT). The diagnostic accuracy of MDCT is expected to be improved to even higher levels because MDCT can offer images from multiplanar and three-dimensional reconstructions. Overall accuracy of MDCT in the detection and classification of SELs from a recent study was 85.3% and 78.8%, respectively.<sup>25</sup>

In addition to detection, only EUS can establish the precise location of the lesion within the GI wall layer and provide information on the sonographic characteristics of the SEL. The narrow differential diagnosis of SELs afforded by the use of EUS improves decision making. Based on EUS, the clinician can decide between observation with reexamination in patients with suspected benign lesions or resection when the lesion is likely to be malignant.

In the differentiation between SELs and extraluminal compression, EUS also demonstrates higher accuracy than endoscopy, USG, and CT. In a multicenter study, endoscopy was able to differentiate SELs from extraluminal compressions with sensitivity and specificity of 87% and 29%, respectively.<sup>26</sup> In another study, ultrasonography and CT established the diagnosis in only 16% of cases, compared with 100% for EUS.<sup>27</sup> Another comparison of ultrasonography, CT, and EUS reported an accuracy of 22%, 28%, and 100%, respectively, in differentiating SELs from extraluminal compression.<sup>28</sup> One study suggested that if the size of a SEL is greater than 10 mm, MDCT may depict and differentiate it from extraluminal compression.<sup>29</sup>

## Extramural Lesions

### EXAMINATION CHECKLIST

Check the integrity of the five wall layers between the lesion and the gut lumen.

Because EUS is able to visualize the gut wall layers in detail, it can readily differentiate the intramural and extramural nature of subepithelial masslike lesions. When EUS demonstrates the integrity of all gut wall layers between the gut lumen and the lesion, it is safe to say that the lesion is an impression caused by an extramural structure.

Although the extramural structures that compress the gut wall are on occasion pathologic masses, such findings are more likely to represent adjacent normal structures (Table 11.3).<sup>26–28,30</sup> A study revealed that when EUS evaluation was done for patients with suspected extraluminal compression or SELs during endoscopy, 66.4% were proven to be extraluminal compression. It is worth noting that only 11% were due to pathologic lesions, and others were related to adjacent normal organs or vessels.<sup>31</sup>

**TABLE 11.3 Causes of Extraluminal Compression Mimicking Subepithelial Lesion**

Normal Organ	Pathologic Condition
Liver	Pancreatic cystic tumor
Spleen	Pancreatic pseudocyst
Blood vessel	Hepatic cyst
Gallbladder	Vascular anomaly including aneurysm
Pancreas	Lymphoma
Bowel loop	Colonic tumor
Vertebra	Mediastinal tumor or lymphadenopathy
Kidney	Lung cancer

A normal spleen usually makes an impression in the gastric fundus and upper body (Fig. 11.1), and the gallbladder compresses the gastric antrum. Transient gastric impression is often caused by bowel loops. Other causes of gastric impression include vessels in the splenic hilum, the pancreatic tail, and the left lobe of the liver. Abnormal structures such as pancreatic pseudocysts, splenic artery aneurysms, aortic aneurysms, cystic tumors of the pancreas or liver, colonic tumors, and lymphomas may also produce endoscopically visible impressions on the gastric wall. Adjacent structures, such as the aortic arch and vertebrae, can also press on the esophagus. Other potential causes of esophageal impression are vascular anomalies, such as a right descending aortic arch, anomalous branches of the aortic arch, aneurysm, and left atrial dilation. Enlarged mediastinal lymph nodes or mediastinal tumors, lung cancer, and lymphomas are also known to compress the esophagus.

When using EUS, the suspected area of gastric impression should be observed by the two-step method. First, at a low frequency of 7.5 MHz, the examiner should survey the gross relationship between the extramural structure and the gut wall. Then, at a higher frequency of 12 MHz, the outer hyperechoic serosal layer should be observed carefully to determine whether it is intact or disrupted. This method allows reliable differentiation between gastric wall impression and gastric wall infiltration caused by an extragastric tumor. For the examination of small lesions, a high-frequency catheter ultrasound probe is technically easier to use than a conventional echoendoscope. In the esophagus, the endosonographer may encounter difficulties in this evaluation owing to interference from the air-filled bronchial system.

## Evaluation of Subepithelial Lesions

### EXAMINATION CHECKLIST

- Carefully examine the transition zone between the normal gut wall and the lesion to determine the layer of origin.
- Measure the size of the lesion and observe the echo pattern (e.g., echogenicity, internal features, vascularity, and smoothness of the border).
- Check the presence of adjacent lymphadenopathy.
- Small lesions measuring less than 1 to 2 cm may be better imaged using high-frequency catheter ultrasound probes.
- For better imaging of the wall layers and the evaluation of SELs, it may be necessary to instill water or jelly into the luminal tract to obtain better acoustic coupling. Aspiration precautions should be taken under these circumstances.

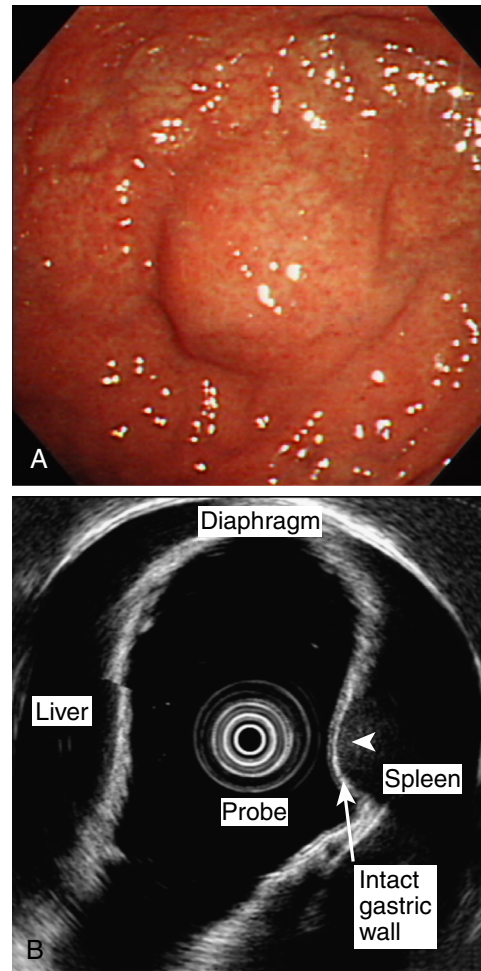


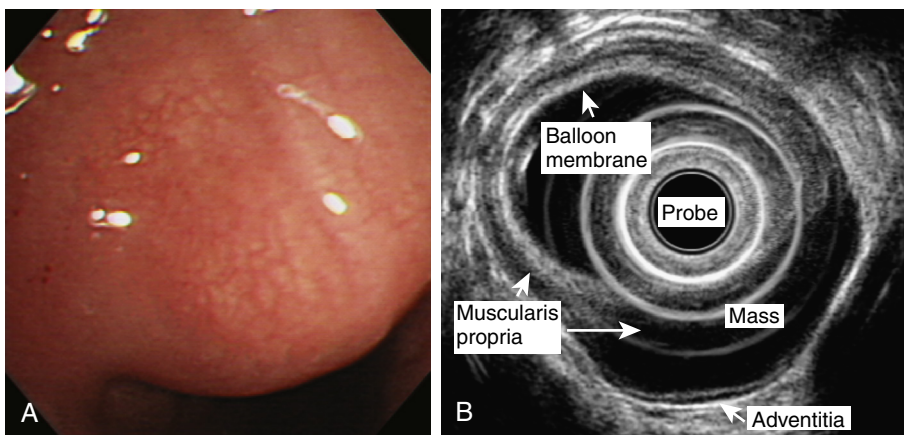
**Fig. 11.1** Extraluminal compression. (A) Endoscopic image of gastric wall compression by normal spleen. An ill-defined elevated area is seen at the gastric fundus. (B) Endosonographic view of spleen (arrowhead) compressing the gastric wall (arrow).

## Gastrointestinal Stromal Tumor

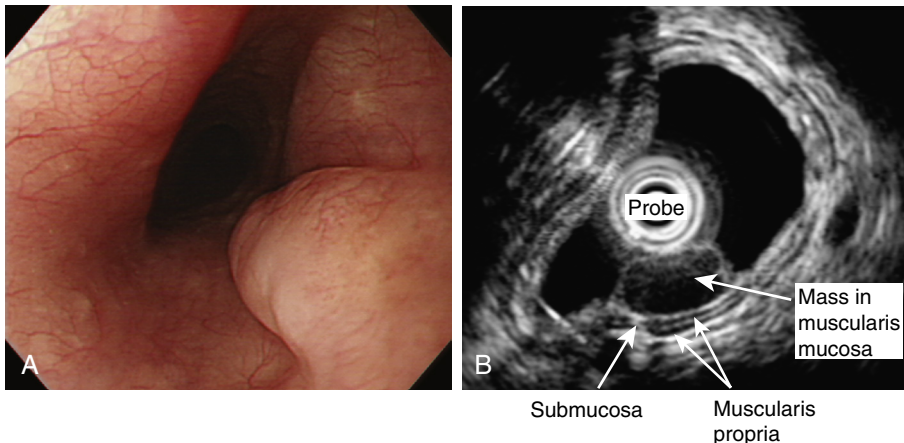
### DIAGNOSTIC CHECKLIST

- Origin in second or fourth gastric wall layer.
- Generally a well-circumscribed, hypoechoic, relatively homogeneous mass.
- If malignant, noticeable characteristics include large size, features of heterogeneous echo texture with hyperechoic foci and/or anechoic necrotic zones, irregular extraluminal border, and adjacent malignant-looking lymphadenopathy.

Gastrointestinal stromal tumors (GISTs) are among the most common mesenchymal tumors in the GI tract; they are also the most commonly identified intramural SELs in the upper GI tract. Previously these tumors were classified as GI smooth muscle tumors, such as leiomyomas and leiomyosarcomas, owing to histologic findings of circular palisades of spindle cells with prominent nuclei and an apparent origin in the muscularis propria layer of the gut wall. However, with the development of newer molecular markers and an improved understanding of the biologic behavior of these tumors, GISTs are now classified as a distinct but heterogeneous group of mesenchymal tumors with varying



**• Fig. 11.2** Esophageal benign gastrointestinal stromal tumor (GIST). (A) Endoscopic finding of a histologically proven benign esophageal GIST. (B) Radial scanning endoscopic ultrasound image showing a homogeneous, hypoechoic mass arising from the fourth sonographic layer, corresponding to the muscularis propria.



**• Fig. 11.3** Esophageal leiomyoma. (A) Endoscopic image shows an elongated submucosal lesion visible in the midesophagus. (B) Endosonographic view using a 20-MHz catheter probe. The lesion is homogeneous, hypoechoic, and associated with the muscularis mucosa.

differentiation. Interstitial cells of Cajal, also known as pacemaker cells of the GI tract, are now believed to be the precursor of GISTs that typically express the c-kit proto-oncogene, a transmembrane tyrosine kinase receptor. With immunohistochemical staining techniques, most GISTs stain positive for CD117, an epitope of kit protein and, sometimes, CD34 but negative for desmin. Leiomyomas express smooth muscle actin and desmin, and schwannomas produce S-100 protein and neuron-specific enolase.<sup>32</sup>

According to the more recent classification, approximately 80% of GI mesenchymal tumors are GISTs, and approximately 10% to 30% of GISTs are malignant.<sup>33</sup> Leiomyomas are the most common mesenchymal tumors in the esophagus, but they rarely occur in the stomach and small bowel. In contrast, GISTs are rare in the esophagus and are more common in the stomach (60% to 70%) and small bowel (20% to 25%).<sup>34</sup>

The most common symptoms associated with GISTs are vague abdominal discomfort and pain, but most lesions are small (<2 cm) and asymptomatic. Larger lesions (>2 cm) may be ulcerated on top of the mass, and patients may present with bleeding or anemia. Occasionally, GISTs cause intestinal obstruction.

In defining the prognosis of patients with GISTs, it has been recommended that a “grading as to the risk of aggressive

behavior” be used instead of the term *benign*. This means that no GIST can be definitively labeled as benign; all are considered to have some malignant potential. Pathologists classify GISTs as “very low risk,” “low risk,” “intermediate risk,” and “high risk,” according to the size of the mass and the mitotic count of the resected specimen.<sup>35</sup>

Endosonographically, a GIST is typically a well-circumscribed, hypoechoic, relatively homogeneous mass that can arise from either the second hypoechoic layer (muscularis mucosa) or more frequently the fourth hypoechoic layer (muscularis propria) (Fig. 11.2). In contrast, leiomyomas (Fig. 11.3) showing homogeneous hypoechoic patterns arise from the muscularis mucosa more frequently than do GISTs. Gastric schwannomas are rare mesenchymal tumors also appearing as hypoechoic lesions originating from fourth hypoechoic layer, but they frequently show a heterogeneous pattern with decreased echogenicity compared with the normal proper muscle layer.<sup>36</sup>

The images of GISTs, leiomyomas, and schwannomas are seen as relatively homogeneous hypoechoic masses under EUS and cannot be differentiated unless special immunohistochemical tissue staining is performed. One study suggested that GISTs have a marginal hypoechoic halo and relatively higher echogenicity

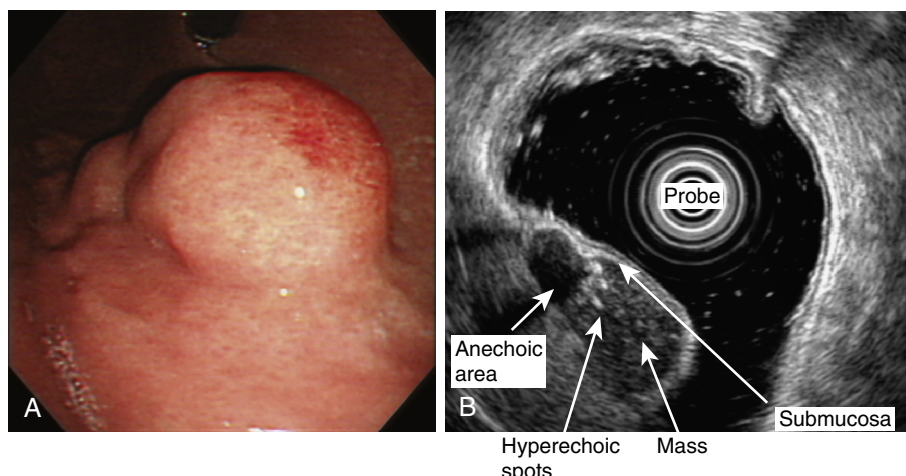


**Fig. 11.4** Malignant gastrointestinal stromal tumor (GIST) of the stomach. (A) Endoscopy shows a submucosal mass in the body of the stomach. (B) Radial scanning endoscopic ultrasound image of histologically proven malignant GIST showing hyperechoic spots and an anechoic area. The mass is contiguous with the fourth sonographic layer.

compared with the adjacent muscular layer.<sup>37</sup> Another study added inhomogeneity and hyperechoic spots to the foregoing features, and the presence of at least two of these four features predicted GISTs with 89.1% sensitivity and 85.7% specificity.<sup>38</sup>

Several studies have attempted to predict the potential malignancy of GISTs based on the EUS characteristics of the lesion, but none has obtained completely satisfying results. In addition to size and mucosal ulcer, other EUS characteristics were considered as possible predictive factors, but size was the only consistently definitive predictive factor.<sup>38–41</sup> EUS features mentioned by the authors were distorted shape, lobulation, irregular border, increased echogenicity in comparison with the surrounding muscle echo, inhomogeneity, hyperechoic spots, anechoic area, marginal halo, and extraluminal growth pattern. In one study, an internal hypoechoic feature was suggested as a predictive marker of tumor progression.<sup>40</sup> When malignant changes occur, GISTs commonly show a heterogeneous echo texture with hyperechoic deposits or anechoic necrotic zones inside large tumors (Fig. 11.4). In one report, EUS findings of tumor size greater than 4 cm, an irregular extraluminal border, echogenic foci, and anechoic spaces were strong indicators of malignancy.<sup>42</sup> Sensitivity ranged between 80% and 100% in detecting malignancy when at least two of four features were present.<sup>42</sup> Another study found a correlation with malignancy when irregular extraluminal margins, cystic spaces, and lymph nodes were seen. The presence of two of these three features had a positive predictive value of 100% for malignant or borderline-malignant tumors.<sup>43</sup> Nonetheless, a lack of defined risk factors could not exclude a malignant potential. A multicenter study reported that malignancy or indeterminate GIST status correlated with the presence of ulceration, tumor size larger than 3 cm, irregular margins, and gastric location but not with hyperechoic or hypoechoic internal foci.<sup>44</sup>

Recently, contrast-enhanced harmonic EUS (CEH EUS) has been introduced. CEH EUS can demonstrate the perfusion characteristics of SELs, and it is helpful for establishing a differential diagnosis. The image of GIST is hyperenhanced after infusion of ultrasound contrast; in consequence, the CEH EUS signal intensity of GISTs is higher than that of other benign lesions.<sup>45</sup> It is suggested that hyperenhancement and avascular areas in the center of the lesion<sup>46</sup> are shown in GISTs but not in leiomyomas (Fig. 11.5). In addition,

prediction of a malignant GIST was possible with CEH EUS by identifying irregular intratumoral vessels with 83% accuracy.<sup>47</sup>

Use of EUS elastography for the differential diagnosis of gastric SELs has recently been suggested. It might be especially helpful for differentiating GISTs from other SELs because GISTs may be harder than other SELs.<sup>48</sup>

EUS FNA and EUS-guided fine-needle tissue-core biopsy (EUS FNB) can be performed for immunohistochemical examination to achieve better diagnostic accuracy of GISTs (Table 11.4).<sup>50–58</sup> A major drawback of EUS FNA is its inability to differentiate with absolute certainty benign from malignant GISTs. However, staining for ki-67 (MIB-1), a marker of cell proliferation, may enable the discrimination of benign from malignant GISTs with EUS FNA.<sup>57,58</sup> The role of EUS FNA is further described later in this chapter.

Because small (<1 cm) asymptomatic mesenchymal tumors are rarely malignant, a policy of close follow-up with EUS may be justified, although an optimal surveillance strategy has not yet been established. Excision is advised when growth of the lesion, a change in the echo pattern, or necrosis is noted during yearly follow-up with EUS. Surgical treatment is indicated for lesions greater than 3 cm in diameter with features suggestive of malignancy. For lesions between 1 and 3 cm, EUS FNA can be recommended, or ESD can be chosen as a definite diagnostic and therapeutic tool with some risk of bleeding and perforation (2% to 3% in specialized centers). When the lesion is confirmed to be a GIST, the risk of malignant transformation needs to be discussed with the patient; more careful follow-up or early resection should be considered.

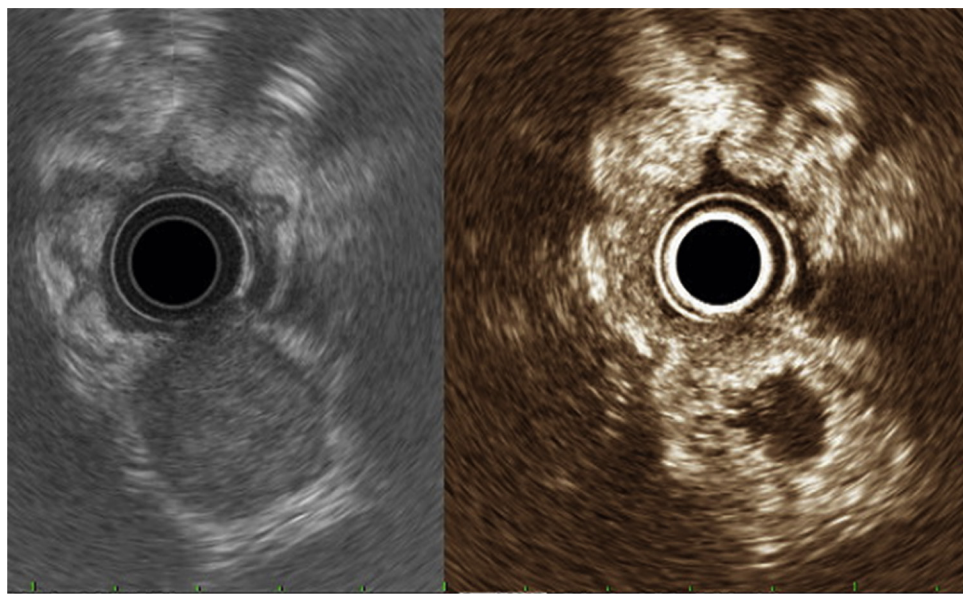
## Aberrant Pancreas

### DIAGNOSTIC CHECKLIST

Origin in the second, third, and/or fourth layers.

Hypoechoic or mixed echogenicity with internal anechoic ductal structure.

The term *aberrant pancreas* is used to describe ectopic pancreatic tissue lying outside its normal location with no anatomic or vascular connection to the pancreas proper. These lesions are also termed



• Fig. 11.5 Contrast-enhanced harmonic imaging of a gastrointestinal stromal tumor. After contrast injection, the exophytic mass shows hypervascularization with a central avascular area.

**TABLE 11.4 Diagnostic Accuracy of Endoscopic Ultrasound-Guided Tissue Acquisition for Gastrointestinal Stromal Tumors**

Authors (Year)	Number of Patients	Accuracy (%)	Diagnostic Method
El Chafic and coworkers <sup>49</sup> (2017)	91	57	EUS FNA <sup>a</sup>
	15	87	EUS FNB <sup>a</sup>
DeWitt and coworkers <sup>50</sup> (2011)	38	76	EUS FNA <sup>b</sup>
		79	EUS TCB <sup>b</sup>
Watson and coworkers <sup>51</sup> (2011)	65	80	EUS FNA <sup>a</sup>
		70	EUS FNA <sup>b</sup>
Fernandez-Esparrach and coworkers <sup>52</sup> (2010)	40	60	EUS TCB <sup>b</sup>
Sepe and coworkers <sup>53</sup> (2009)	37	78	EUS FNA <sup>a</sup>
Chatzipantelis and coworkers <sup>54</sup> (2008)	17	100	EUS FNA <sup>a</sup>
Akahoshi and coworkers <sup>55</sup> (2007)	29	97	EUS FNA <sup>a</sup>
Mochizuki and coworkers <sup>56</sup> (2006)	18	83	EUS FNA <sup>a</sup>
Okubo and coworkers <sup>57</sup> (2004)	14	79	EUS FNA <sup>c</sup>
Ando and coworkers <sup>58</sup> (2002)	23	91	EUS FNA <sup>d</sup>

<sup>a</sup>For diagnosis of GISTs.

<sup>b</sup>For diagnosis of gastrointestinal mesenchymal tumors.

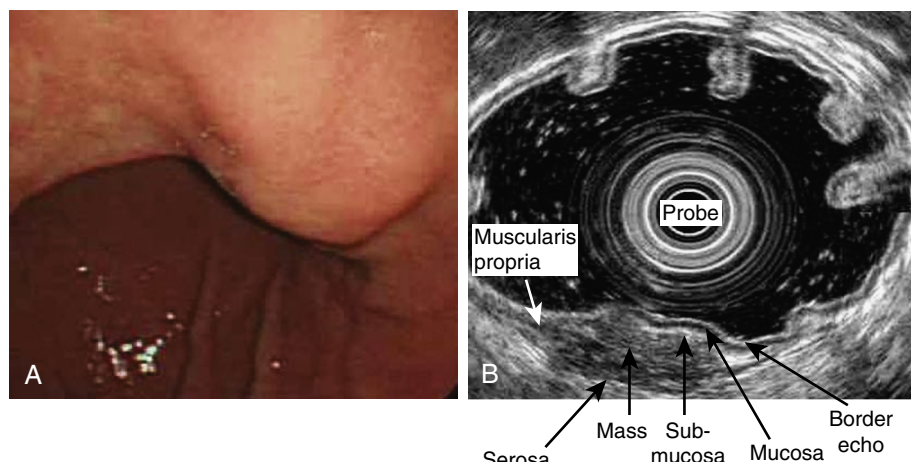
<sup>c</sup>For differentiating between low-grade and high-grade malignancy of GISTs.

<sup>d</sup>For differentiating between benign and malignant GISTs.

EUS, Endoscopic ultrasonography; FNA, fine-needle aspiration; FNB, fine-needle biopsy; GIST, gastrointestinal stromal tumor; TCB, fine-needle biopsy using a Tru-Cut needle.

*ectopic pancreas, pancreatic rest, and heterotopic pancreas.* They are typically discovered incidentally during endoscopy, surgery, or autopsy. Aberrant pancreas is encountered in approximately 1 of every 500 operations performed in the upper abdomen; the incidence in autopsy series has been estimated to be between 0.6% and 13.7%.<sup>59</sup> Aberrant pancreas is usually located in the stomach

wall (frequently along the greater curvature of the antrum), duodenum, small intestine, or anywhere in the GI tract. Patients with aberrant pancreas are usually asymptomatic, but rare complications such as pancreatitis, cyst formation, ulceration, bleeding, gastric outlet obstruction, obstructive jaundice, and malignancy can occur.<sup>60</sup>



• **Fig. 11.6** Aberrant pancreas. (A) Endoscopic image of an indistinct submucosal lesion. (B) Corresponding endoscopic ultrasound image showing an ill-defined, slightly hypoechoic inhomogeneous mass involving the third and fourth gastric layers.

On endoscopy, an aberrant pancreas appears as a submucosal nodule, usually small, with a characteristic central umbilication that corresponds to a draining duct. The characteristic EUS features of aberrant pancreas are heterogeneous lesions, mainly hypoechoic or intermediate echogenic masses accompanied by scattered small hyperechoic areas, with indistinct margins within the gut wall (Fig. 11.6). Generally an anechoic area and fourth layer thickening accompany the lesions. Anechoic cystic or tubular structures within the lesion correlate with ductal structures. They commonly arise from the third and fourth layers.<sup>61</sup> However, lesions may develop in any location from the deep mucosal to the serosal layer.

The management of aberrant pancreas remains controversial. It should be guided by symptoms and the possibility of malignancy. Asymptomatic lesions do not necessarily require resection and can be followed expectantly. If needed, endoscopic removal is useful for both accurate diagnosis and treatment, although surgical resection is preferred to endoscopic resection when the muscularis propria is involved.

## Lipoma

### DIAGNOSTIC CHECKLIST

Origin in the third layer.  
Hyperechoic, homogeneous lesion with regular margins.

Lipomas are benign tumors composed of mature lipocytes. They are found incidentally in any part of the GI tract and more frequently in the lower tract. Lipomas are rarely symptomatic, but they may result in hemorrhage, abdominal pain, and intestinal obstruction.<sup>62</sup>

Endoscopically, most lipomas are solitary, with a smooth bulge and a yellow hue. They are soft and indented when pressed with biopsy forceps ("pillow" or "cushion" sign). On endosonography, lipomas characteristically appear as intensely hyperechoic, homogeneous lesions with clean regular margins arising from the third layer of the GI tract, which corresponds to the submucosa (Fig. 11.7).<sup>63,64</sup> The endoscopic and endosonographic characteristics make it possible

to diagnose lipomas in most cases. Once lipoma has been confirmed, follow-up EUS is not recommended. The incidentally found lipoma does not require treatment, but local excision is advised for symptomatic lipomas associated with bleeding or obstruction. Resection is also recommended when it is impossible to distinguish between a lipoma and a malignant neoplasm, such as a liposarcoma, even though this lesion is rare in the GI tract.<sup>65</sup>

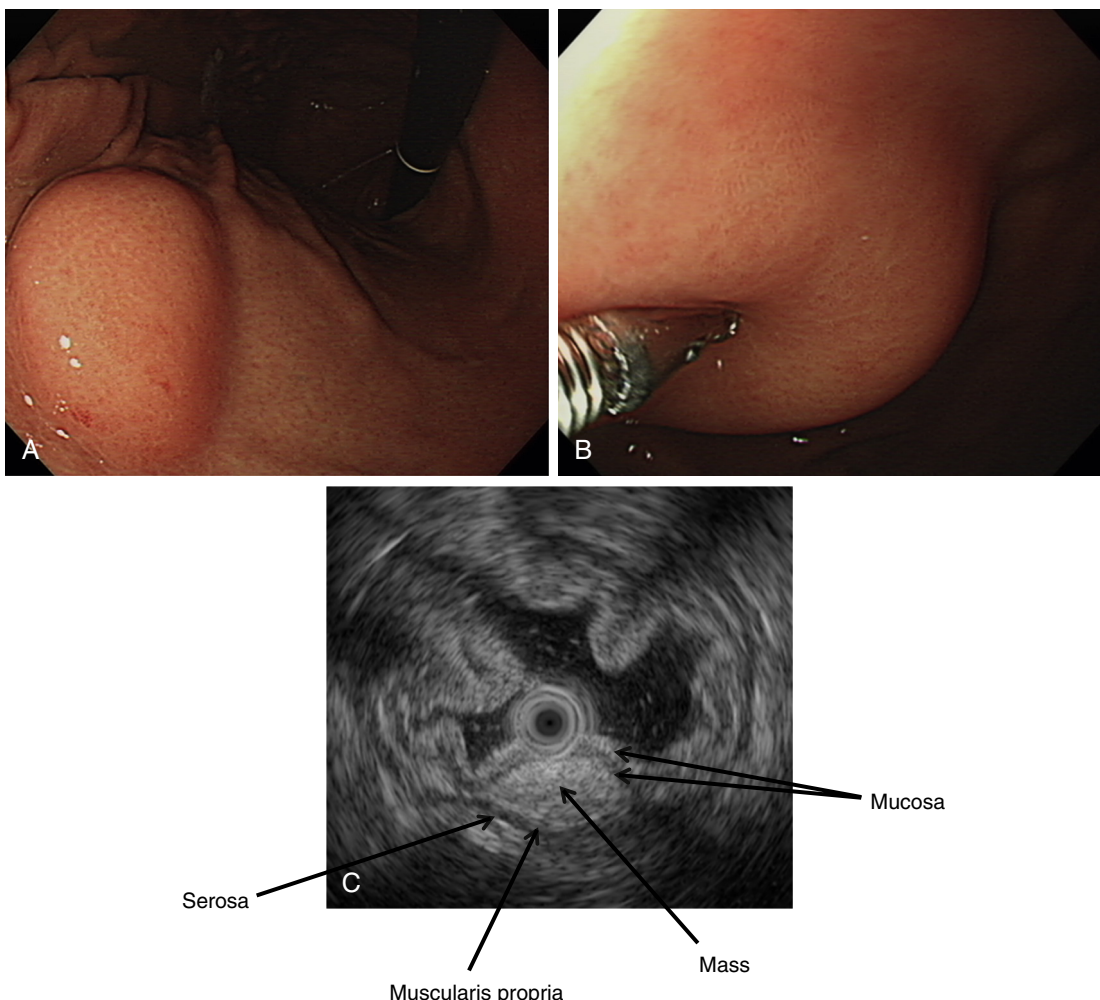
## Carcinoid Tumor

### DIAGNOSTIC CHECKLIST

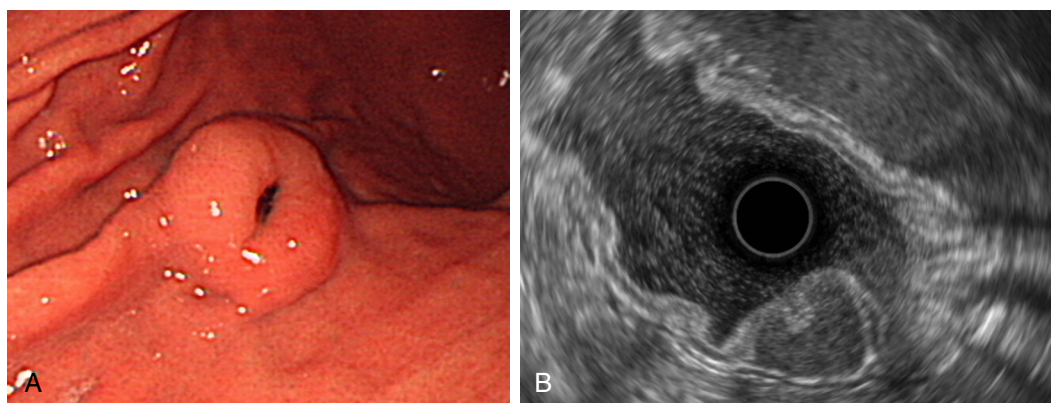
Origin in the second layer.  
Homogeneous, well-demarcated, and mildly hypoechoic or isoechoic lesion.

Carcinoid tumors are slow-growing neuroendocrine tumors with malignant potential. They may arise at various sites, most commonly the GI tract and lung. GI carcinoid tumors are generally discovered incidentally during endoscopy, surgery, or autopsy originating from the appendix, rectum, stomach, or small intestine. Rectal carcinoids are common and represent approximately 20% of all GI carcinoid lesions. Carcinoid tumors are usually asymptomatic, but rare complications include hemorrhage, abdominal pain, intestinal obstruction, and the endocrine carcinoid syndrome, which results from secretion of functionally active substances.

Endoscopically, carcinoid tumors are small, round, sessile, or polypoid lesions with a smooth surface and a yellow hue. They usually have normal overlying mucosa and seldom ulcerate. Gastric and ileal carcinoids are commonly multiple, whereas those arising elsewhere are typically solitary. The endosonographic appearance of carcinoids is usually that of a homogeneous, well-demarcated, and mildly hypoechoic or isoechoic mass (Fig. 11.8). These lesions arise from the second layer of the GI tract and may invade beyond the third submucosal layer.<sup>66</sup> Deep mucosal biopsy is normally diagnostic. EUS accurately defines the size and extent of masses and can guide management. When the lesion is smaller than 2 cm, does not invade further than the third layer, and no adenopathy is noted, endoscopic resection is possible.<sup>13,67,68</sup>



• **Fig. 11.7** Gastric lipoma. (A) Endoscopic view of a round elevated lesion covered with normal mucosa. (B) Cushion sign. The mass is soft and shows indentation when pressed with biopsy forceps. (C) Endosonography reveals a homogeneous, hyperechoic mass with smooth borders within the third gastric wall layer.



• **Fig. 11.8** Gastric carcinoid tumor. (A) Endoscopic image of a round, umbilicated, submucosal lesion in the gastric body. (B) Endosonographic view of a homogeneous, hypoechoic, umbilicated mass within the second sonographic layer.

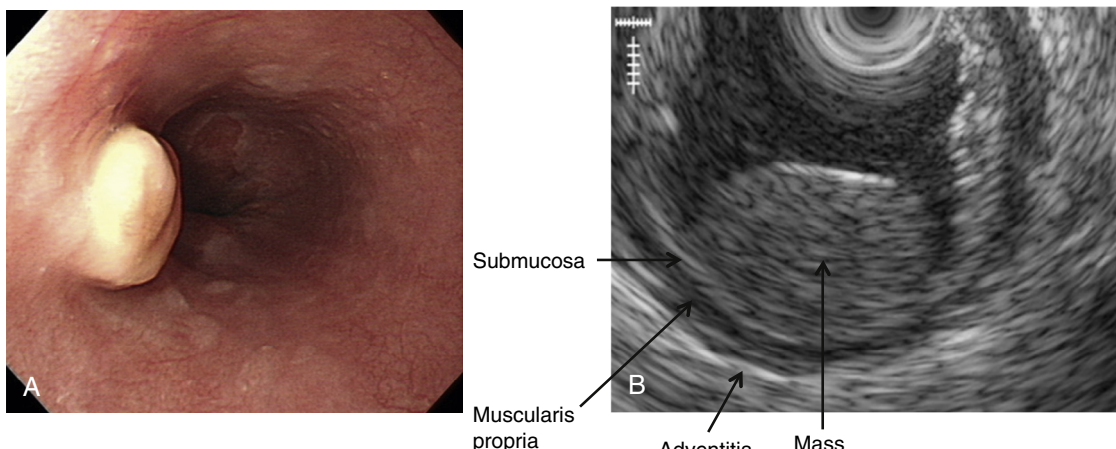


**Fig. 11.9** Granular cell tumor of the esophagus. (A) Small, round, molar tooth-like polypoid lesion in the esophagus. (B) Endosonographic image shows a homogeneous, hypoechoic lesion with smooth margins within the second layer.

## Granular Cell Tumor

### DIAGNOSTIC CHECKLIST

Origin in the second or third layer.  
Hypoechoic, homogeneous lesion with smooth margins.

Granular cell tumors (GCTs) are rare lesions of neural derivation, as supported by immunophenotypic and ultrastructural evidence. The granularity of the tumor cells results from the accumulation of secondary lysosomes in the cytoplasm. Visceral involvement is encountered as mucosal or submucosal nodules anywhere in the GI tract, larynx, bronchi, gallbladder, and biliary tract. Approximately 2.7% to 8.1% of GCTs involve the digestive tract, and these tumors are multiple in approximately 5% to 12% of patients. GCTs are usually found incidentally during endoscopy or colonoscopy and are located mostly in the esophagus; other locations include the stomach (10%) and rarely the colon or rectum.<sup>69</sup> GCTs are generally considered benign, but in 2% to 3% of cases they are malignant.<sup>70</sup>

The endoscopic appearance of GCTs is that of small, isolated nodules or polyps resembling molar teeth, with normal overlying mucosa having a yellow hue. Most GCTs are small (<4 cm), but larger size is associated with malignant potential. At EUS, GCTs appear as hypoechoic, homogeneous lesions with smooth margins originating from the second or third layer of the GI tract (Fig. 11.9).<sup>71</sup> One study using EUS examined 15 patients with 21 GCTs and found that tumor size was less than 2 cm in 95% of cases. In all patients, echo patterns were hypoechoic and solid. The tumors arose in the inner layers in 95% of cases (second layer, 15; third layer, 5).<sup>72</sup> The EUS pattern of leiomyoma originating from the muscularis mucosal layer can be similar to GCT. A study attempted to differentiate GCT from leiomyoma by using EUS characteristics. The authors suggested two differential EUS features: (1) although both lesions were hypoechoic, GCTs demonstrated slightly higher echogenicity compared to the surrounding normal muscle layer, and (2) the margins of GCTs were less well defined than those of leiomyomas.<sup>73</sup>

For asymptomatic GCTs that are not excised, surveillance EUS every 1 to 2 years is recommended to monitor changes in size. Local endoscopic snare excision can be performed for small tumors limited to the mucosa.

## Cysts—Including Duplication Cyst

### DIAGNOSTIC CHECKLIST

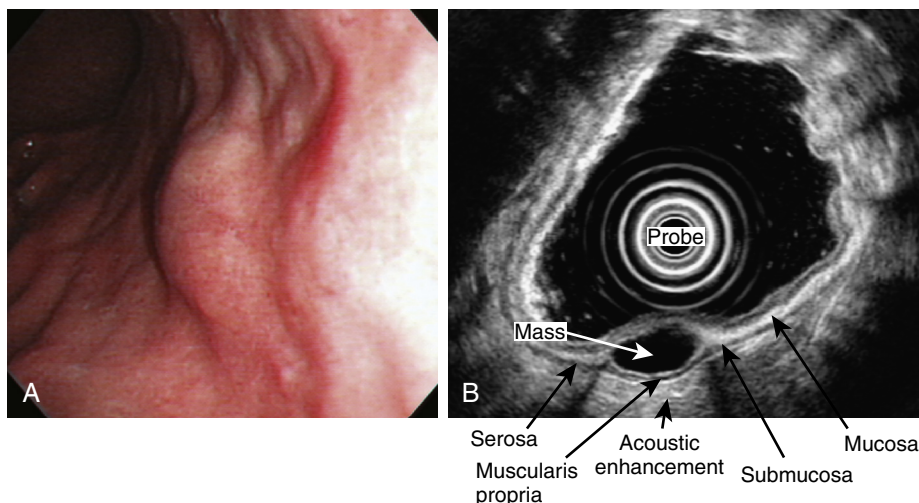
Origin in the third layer.  
Anechoic, round, or oval lesion showing posterior acoustic enhancement (if the lesion has three- or five-layered walls, this suggests a duplication cyst).  
Antibiotics are indicated for EUS FNA of a bronchogenic cyst.

Endosonographically, cysts in the GI tract appear as anechoic structures, but some may be seen as hypoechoic lesions containing echogenic foci.

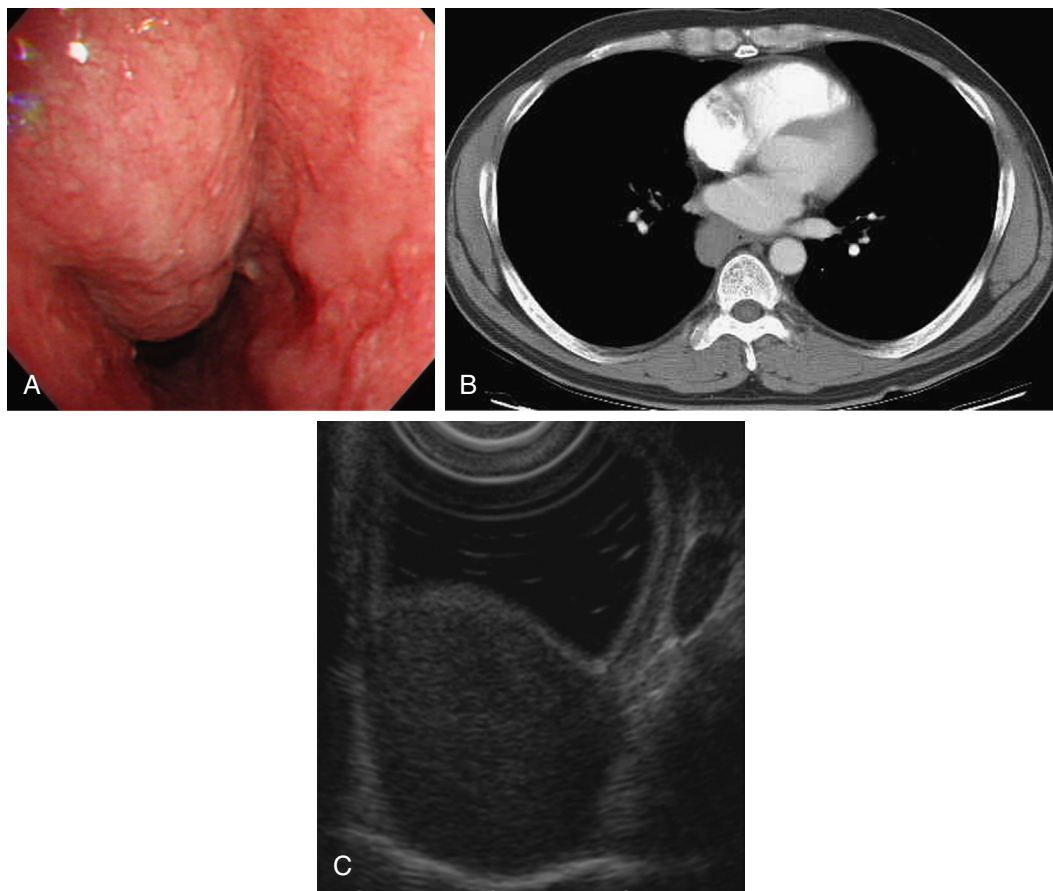
Cystic submucosal tumors may be classified into three EUS types: simple cystic, multicystic, and solid cystic tumors.<sup>74</sup> The simple cystic type is more frequent in occurrence and, rarely, Brunner gland hamartomas or heterotopic gastric mucosa can resemble a simple cyst. The multicystic type is common in lymphangiomas, gastric cystic malformations, hemangiomas, and Brunner gland hamartomas. The solid cystic type includes duplication cysts, heterotopic gastric mucosa, aberrant pancreas, myogenic tumors with advanced cystic degeneration, and gastric tuberculomas.

Gastric cyst is a rare clinical entity and is usually asymptomatic. It may result from a resolved inflammatory process. Endosonographically, the cysts appear in the submucosal layer of the gastric wall as sharply demarcated, anechoic, rounded, or ovoid structures with dorsal acoustic accentuation (Fig. 11.10). The inflammatory cyst always shows a single hyperechoic wall layer.

In adults, foregut cysts are usually asymptomatic and are discovered incidentally during radiographic or endoscopic examination. Foregut cysts are categorized on the basis of their anomalous embryonic origin into bronchogenic and neuroenteric cysts. Bronchogenic cysts represent 50% to 60% of all mediastinal cysts<sup>75</sup>; they can be diagnosed easily with EUS as anechoic masses without wall layers (Fig. 11.11). But some lesions may be seen as hypoechoic or



• **Fig. 11.10** Gastric cyst. (A) Endoscopic view of a smooth bulge in the body of the stomach. (B) Endoscopic ultrasound revealed a sharply demarcated, anechoic, ovoid structure within the third gastric wall layer.

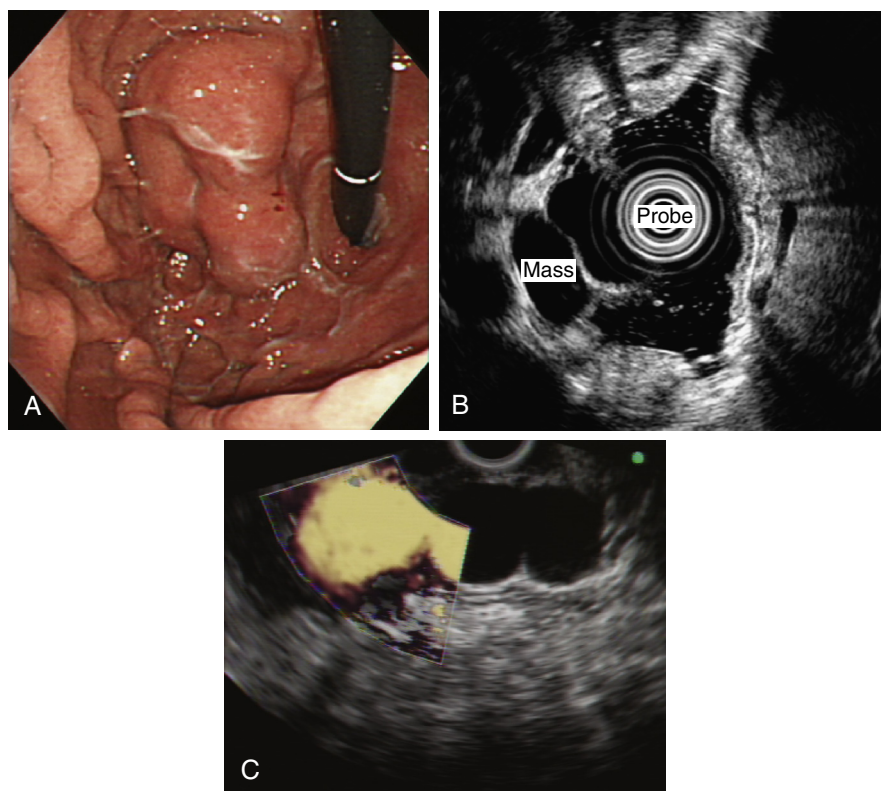


• **Fig. 11.11** Bronchogenic cyst. (A) Endoscopic view of a bulging mass lesion at the midesophagus. (B) The mass looks like a solid mass lesion on computed tomography. (C) Endoscopic ultrasound demonstrated a round, homogeneous, hypoechoic lesion in the mediastinum.

solid masses. In these cases, EUS FNA would cause serious complications, including cyst infection and mediastinitis.<sup>75</sup> Therefore antibiotic prophylaxis is needed and close attention should be paid to avoid accidental instrumentation (Video 11.2).

Duplication cysts may involve the entire GI tract, with the ileum being the most common site. The stomach is the least common site for GI duplication cysts. When they are examined

endoscopically, duplication cysts may have a slightly transparent appearance. EUS or EUS FNA (with antibiotic prophylaxis) is useful and safe for the diagnosis of duplication cysts; some of these cysts are misdiagnosed as solid masses on CT or MRI.<sup>76</sup> Duplication cysts on endosonography appear as anechoic, homogeneous lesions with regular margins arising from the third layer or extrinsic to the GI wall. The walls of duplication cysts may



**• Fig. 11.12** Gastric fundic varices. (A) Endoscopic view of a large bulging mass lesion at the gastric fundus. (B and C) Endoscopic ultrasonography confirmed large, anechoic, tubular, submucosal vessels with multiple extramural collateral vascular structures.

be seen as three- or five-layer structures because of the presence of the submucosa and muscle layer.<sup>77,78</sup> Duplication cysts are believed to have a low malignant potential, but case reports have described malignant transformation. Complications are rare and may include dysphagia, abdominal pain, bleeding, and pancreatitis when the cyst is located near the ampulla of Vater.

## Varices

### DIAGNOSTIC CHECKLIST

Origin in the third layer.  
Anechoic, tubular, serpiginous lesion.

Patients with portal hypertension may have varices. Gastric varices can be misdiagnosed endoscopically as submucosal tumors or thickened gastric folds. When varices are found incidentally during endoscopy in a patient with no relevant information, it is highly inappropriate and potentially hazardous to take a biopsy sample from such a lesion without EUS examination. On EUS, fundic varices appear as small, round to oval, and anechoic structures within the submucosa. They can be differentiated from submucosal cysts, which usually occur as solitary lesions, by their shape and easy compressibility using the ultrasound balloon. When gastric varices grow larger, they appear as anechoic, serpentine, tubular structures with smooth margins accompanied by perigastric collateral vessels (Fig. 11.12). In severe portal hypertension, cross sections of multiple fundic varices may show a "Swiss cheese" pattern.<sup>79</sup> Demonstration of flow with Doppler examination is a definite clue for diagnosis.

In portal hypertensive gastropathy, EUS findings are often normal, and endosonographic changes in intramural vessels are usually not observed. However, dilation of the azygous vein and thoracic duct and thickening of the gastric mucosa and submucosa have also been reported.<sup>80</sup> In comparative studies, EUS was inferior to endoscopy for detecting and grading esophageal varices, but it permitted detection of fundic varices earlier and more often than endoscopy in patients with portal hypertension.<sup>81</sup> EUS was used in the treatment of varices by making it possible to inject a sclerosing agent into perforating veins.<sup>82</sup> Also, there is a report about transesophageal EUS-guided treatment of gastric fundic varices. This procedure was safe and successful in 96% of cases.<sup>83</sup> Because the procedure can be performed in a better scope position with easy accessory manipulation, avoiding the thin gastric mucosa overlying the fundic varices, more frequent application of this technique is expected.

## Inflammatory Fibroid Polyps

### DIAGNOSTIC CHECKLIST

Origin in the second and/or third layer.  
Hypoechoic, relatively homogeneous lesion with indistinct margins.

Inflammatory fibroid polyp is a rare benign polypoid lesion that is usually found in the stomach, occasionally in the small bowel, and rarely in the esophagus or large bowel.<sup>84</sup> The lesion is located in the second or third sonographic layer of the gastric wall, with an intact fourth layer. The usual echoendoscopic features of inflammatory fibroid polyp are an indistinct margin and a hypoechoic and homogeneous echo pattern (Fig. 11.13). These findings

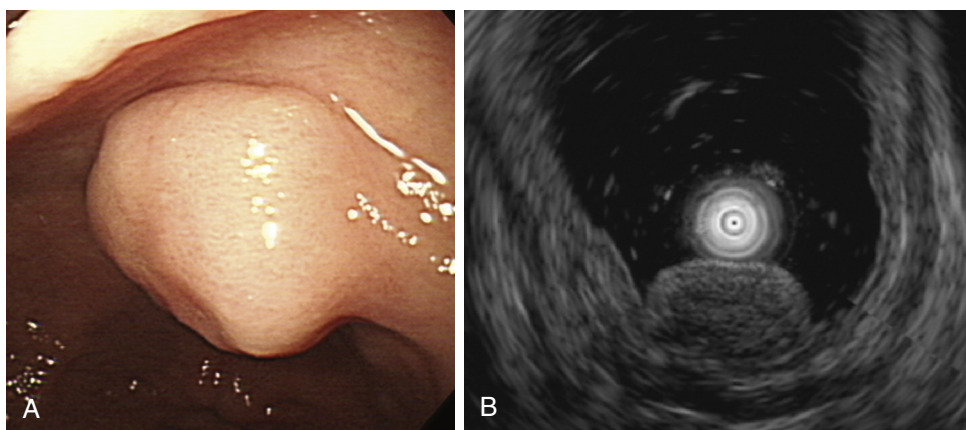


**Fig. 11.13** Inflammatory fibroid polyp. (A) Endoscopic image of a small, round, polyoid lesion at the gastric antrum. (B) Gastric endoscopic ultrasound demonstrates a homogeneous hypoechoic lesion with indistinct margins located deep in the mucosal layer.

correlate well with the histologic findings of proliferated, nonencapsulated fibrous tissue with vascular elements and eosinophilic infiltration located in the deep mucosal and submucosal layers. Sometimes the internal echo pattern is heterogeneous or hyperechoic. In that case, the inner hyperechoic area and bright echoes correspond to the presence of small blood vessels.<sup>85</sup>

The EUS patterns of leiomyomas originating from the muscularis mucosa and carcinoid tumors may be similar to those of an inflammatory fibroid polyp. However, those tumors have a distinct margin.

## Glomus Tumor

Glomus body is a contractile neuromyoarterial receptor that acts as a thermoregulator. Glomus tumor originates from modified smooth muscle cells of the glomus body. Glomus tumor of the gastrointestinal tract is a rare disease, with most found in the stomach. The majority of gastric glomus tumors are benign and found incidentally as SELs. However, some malignant gastric glomus tumors and cases of bleeding have been reported.

The glomus tumor of the stomach manifests as a circumscribed and hypoechoic mass in the third or fourth layer (Fig. 11.14). Usually it appears as an internal heterogeneous echo mixed with hyperechogenic spots.<sup>86–88</sup> A marginal halo is frequently observed. Contrast-enhanced CT reveals a homogeneous hyperdense enhancement on early and delayed phase.

## Rare Lesions

Many uncommon lesions have been reported in the endosonographic literature. The number of such lesions is too small for their appearance on EUS to be described as characteristic. Some examples are provided here.

Glandular cysts appear as small nodular to polyoid lesions in the body of the stomach. They create a uniform, relatively hyperechoic, internal echo pattern in the upper mucosa, but they do not disrupt the normal layer pattern of the gastric wall.<sup>79</sup> Lymphoma may occasionally manifest as a submucosal mass. This mass typically appears as a homogeneous, hypoechoic lesion that is contiguous with the second and third gastric wall layers, but it can also invade deeper layers. Distant metastases may also appear as submucosal masses in the GI tract. On EUS, they are seen as hypoechoic, heterogeneous masses and may involve any or all of the sonographic layers.

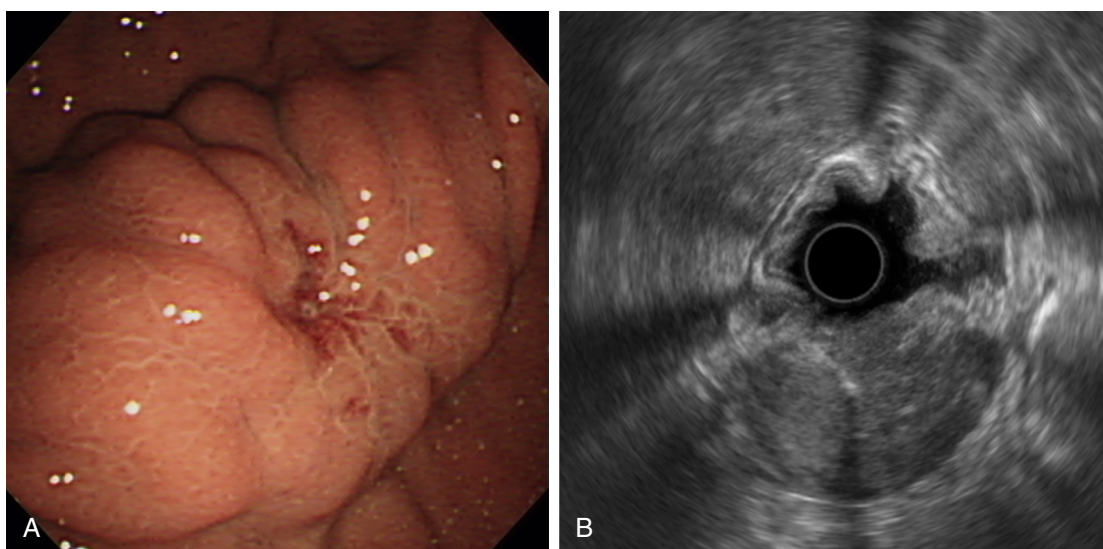
Linitis plastica can sometimes be difficult to diagnose at endoscopy, and biopsy may be unrevealing. The mucosal and submucosal

layers appear very thickened at EUS in these patients, who have poor distensibility of the GI lumen even with air insufflation. EUS FNA is diagnostic in most cases. Extrinsic malignant tumors that directly infiltrate the gut wall and manifest as submucosal lesions can be visualized easily by EUS.

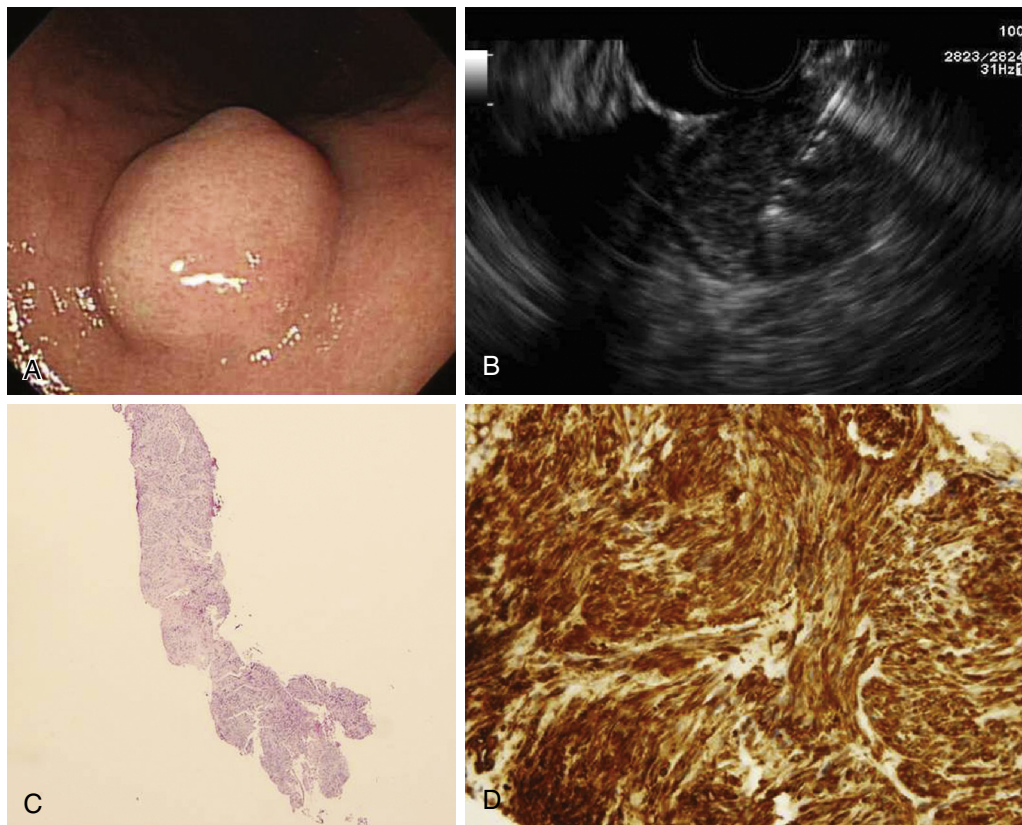
## Tissue Sampling for Histologic Assessment of Subepithelial Lesions

During the endoscopic examination of submucosal lesions, biopsy of the mucosa overlying the lesion is recommended to confirm the presence of intact epithelium. Nevertheless, when the lesion appears cystic or vascular, biopsy should not be attempted before EUS.

Some subepithelial masses arising from the lamina propria or muscularis mucosa may be diagnosed using standard endoscopic forceps biopsy. In particular, when the subepithelial mass is ulcerated, careful biopsy provides an accurate diagnosis. However, for most SELs, the results of endoscopic biopsy are inconclusive.<sup>89</sup> Trials of a bite-on-bite technique with conventional-sized forceps and jumbo biopsy forceps achieved 38% and 59.9% diagnostic yields, respectively.<sup>90,91</sup> Currently, the standard for the histologic diagnosis of SEL is EUS FNA. EUS FNA enables the procurement of tissue from subepithelial masses for cytologic examination.<sup>92,93</sup> However, the sensitivity, specificity, and accuracy of cytologic evaluation of intramural lesions are lower than those of lymph nodes or organs adjacent to the GI tract. In one study, the sensitivity of EUS FNA for mediastinal masses, mediastinal lymph nodes, celiac lymph nodes, pancreatic tumors, and submucosal tumors was 88%, 81%, 80%, 75%, and 60%, respectively.<sup>94</sup> No significant difference in diagnostic accuracy was noted according to the size of the FNA needle, but the 25-gauge needle easily punctured small mobile SELs<sup>93</sup> and the 19-gauge needle showed excellent differentiation between GIST and leiomyoma by enabling tissue procurement for immunohistochemical studies.<sup>95</sup> To overcome some of the limitations of EUS FNA, EUS-guided Tru-Cut biopsy (TCB) was introduced. In EUS TCB, according to early reports, use of a needle with a guillotine tip yielded adequate tissue with no major complications (Fig. 11.15).<sup>96</sup> In some later prospective studies, however, the diagnostic yield of EUS TCB in patients with gastric SELs was not better than that of EUS FNA, and tissue cores obtained with EUS TCB were not sufficient to examine for mitotic index in the GIST.<sup>15,97</sup> However, it is clear that EUS TCB can be complementary to EUS FNA, yielding significant additional information, although it cannot be used technically via the transduodenal route.<sup>98</sup>



• **Fig. 11.14** Glomus tumor. (A) Endoscopic image of a protruded lesion with a central depression and focal erythema covered by normal mucosa. (B) Gastric endoscopic ultrasound demonstrates a relatively hypoechoic lesion having a calcific spot connected mainly with the fourth layer of the gastric wall.



• **Fig. 11.15** Endoscopic ultrasound-guided Tru-Cut biopsy of a gastrointestinal stromal tumor in the stomach. (A) Endoscopic view reveals a round submucosal lesion at lesser curvature side of the gastric body. (B) The Tru-Cut needle is inserted into the mass with a linear echoendoscope. (C) Gross finding of acquired tissue core. (D) Immunohistochemical stains show a positive reaction of the tumor cells for CD117 and CD34.

Complications of EUS FNA and EUS TCB include infection, bleeding, and perforation, but they are very rare.

EUS FNB with the ProCore needle (Cook Endoscopy, Winston-Salem, North Carolina), Side-Port needle (Olympus, Tokyo, Japan), or SharkCore FNB needle (Medtronic, Dublin, Ireland) appears promising.<sup>89,99,100</sup> Core biopsy along with aspiration material is possible with these types of FNA needles (Fig. 11.16).

In addition, there is a suggestion that the new forward-array echoendoscope may be helpful to puncture difficult lesions including right colonic SELs.<sup>101</sup> Compared with the oblique-viewing echoendoscope, the forward-viewing echoendoscope was superior in terms of tissue sample area and procedure time.<sup>102</sup>

The average reported accuracy of EUS FNA in the diagnosis of SELs is approximately 80% (Table 11.5).<sup>14–16,55,96,103–112</sup>

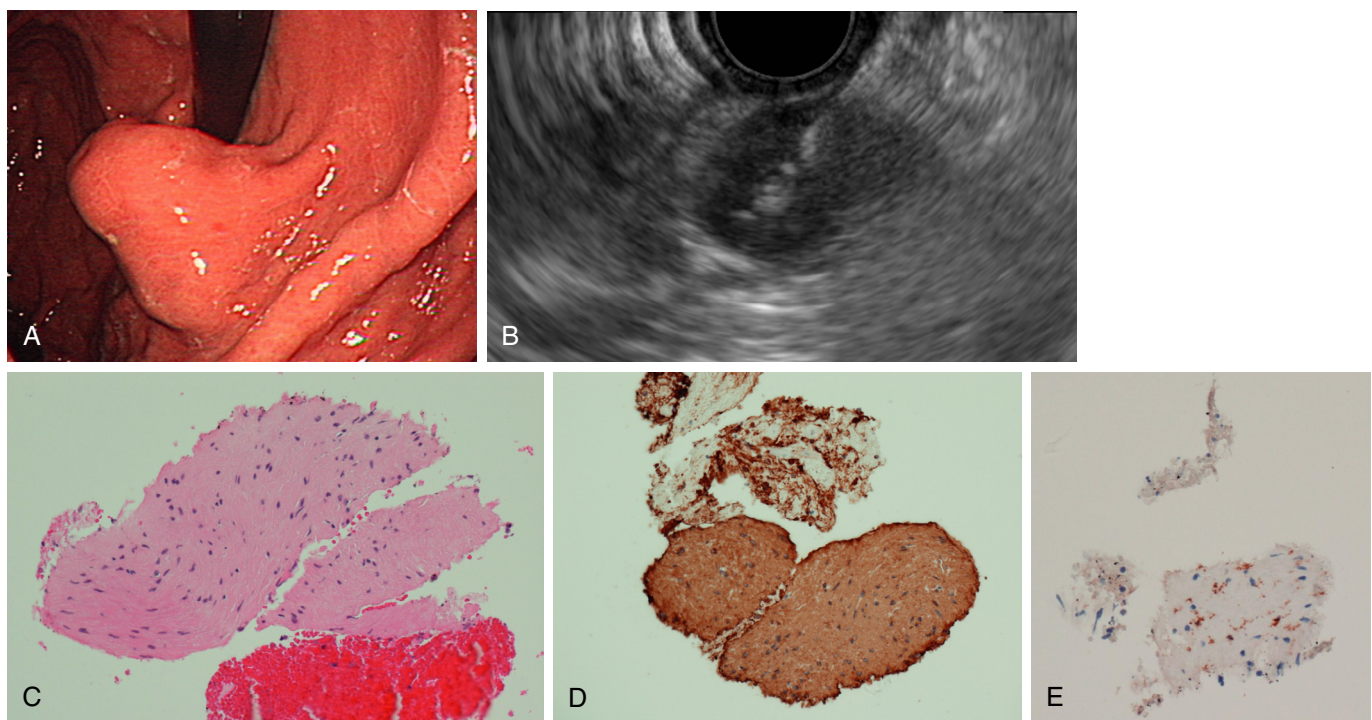


**Fig. 11.16** Endoscopic ultrasound fine-needle aspiration with a ProCore needle of a gastric leiomyoma. (A) Endoscopic view of a submucosal lesion in the gastric cardia. (B) A ProCore needle was inserted into the mass and the stylet was pulled back slowly as the needle was moved back and forth within the lesion. (C) Tissue core was obtained. (D and E) Immunohistochemical stains show a positive reaction of the tumor cells for smooth muscle actin and a negative reaction for CD117.

**TABLE 11.5 Diagnostic Accuracy of Endoscopic Ultrasound-Guided Tissue Acquisition for Gastrointestinal Subepithelial Lesions**

Authors (Year)	Number of Patients	Accuracy (%)	Diagnostic Method
Schlag C and coworkers <sup>103</sup> (2017)	20	75	EUS FNB
Lee JH and coworkers <sup>104</sup> (2016)	78	82	EUS FNB
Na HK and coworkers <sup>105</sup> (2016)	152	78 vs. 39	EUS TCB vs. EUS FNA
Kim GH and coworkers <sup>106</sup> (2014)	22	75 vs. 20	EUS FNB vs. EUS FNA
Çağlar E and coworkers <sup>107</sup> (2013)	67	98	EUS FNA
Rong and coworkers <sup>108</sup> (2012)	46	80	EUS FNA
Suzuki and coworkers <sup>109</sup> (2011)	47	75	EUS FNA
Mekky and coworkers <sup>110</sup> (2010)	69	96	EUS FNA
Hoda and coworkers <sup>111</sup> (2009)	112	84	EUS FNA
Polkowski and coworkers <sup>15</sup> (2009)	49	63	EUS TCB
Akahoshi and coworkers <sup>55</sup> (2007)	51	82	EUS FNA
Chen and coworkers <sup>16</sup> (2005)	42	98	EUS FNA
Vander Noot and coworkers <sup>112</sup> (2004)	51	82	EUS FNA
Levy and coworkers <sup>96</sup> (2003)	5	80	EUS TCB
Matsui and coworkers <sup>14</sup> (1998)	15	93	EUS FNA

EUS, Endoscopic ultrasonography; FNA, fine-needle aspiration; FNB, fine-needle biopsy; TCB, fine-needle biopsy using a Tru-Cut needle.

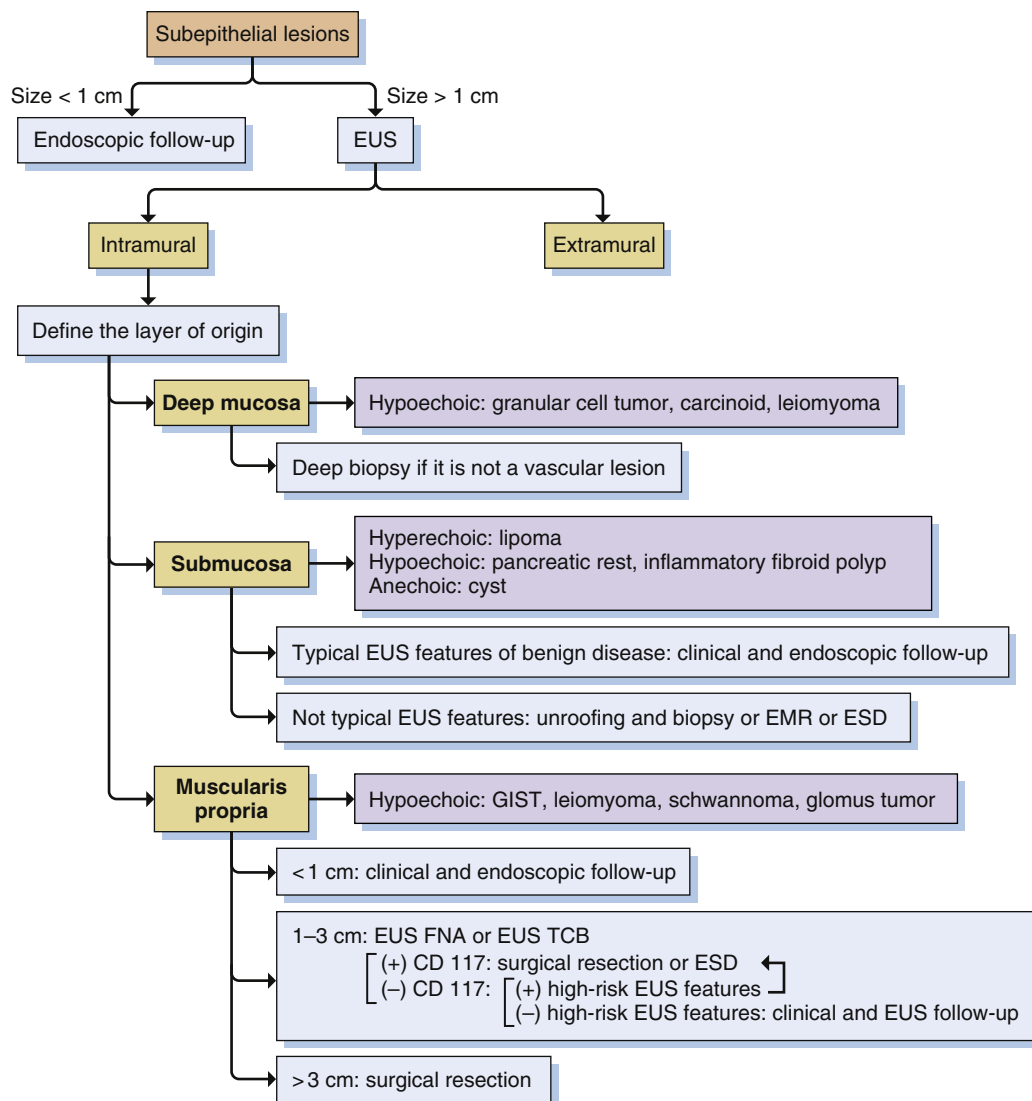


**Fig. 11.17** Algorithm for endoscopic ultrasound (EUS)-based management of different submucosal lesions based on appearance and wall layer origin. *EMR*, Endoscopic mucosal resection; *ESD*, endoscopic submucosal dissection; *FNA*, fine-needle aspiration; *FNB*, fine-needle tissue-core biopsy; *GIST*, gastrointestinal stromal tumor; *TCB*, TruCut biopsy.

EUS FNA with histologic and immunohistochemical analysis has a high reported accuracy in the differential diagnosis of mesenchymal tumors of the GI tract.<sup>49–58</sup> However, any form of needle biopsy carries the possibility of sampling error, and a negative finding does not exclude malignancy in GISTs. Because inoperable GISTs can now be treated with imatinib, a tyrosine kinase inhibitor that specifically blocks the kit receptor, EUS-guided tissue diagnosis is useful for patients with GIST who have metastasis.

Various more aggressive endoscopic techniques to acquire tissue sample from SEL were introduced, including endoscopic partial resection with unroofing, partial resection of SEL, mucosal incision, and forceps biopsy, EUS-guided single-incision with needle knife and deep forceps biopsy, bloc biopsy by submucosal endoscopy with a mucosal flap, suck-ligate-unroof biopsy, and retract-ligate-unroof biopsy.<sup>113</sup>

## Management of Subepithelial Lesions

Management of SELs can be guided by EUS findings (Fig. 11.17). Extraluminal compression by adjacent organs and benign submucosal lesions such as lipomas or simple cysts do not need further treatment or follow-up. Pancreatic rests and inflammatory fibroid polyps can be followed in situ. Suspicious superficial lesions, such as carcinoid tumors, can be diagnosed with endoscopic biopsy. Biopsy should be avoided in lesions that are suspected varices. For deeply located hypoechoic lesions, EUS FNA or EUS FNB can be performed for tissue diagnosis. If resection is planned, ESD can be used instead of surgical resection as a therapeutic tool for small mass lesions arising from the submucosal or inner circular muscularis propria layer. EUS is of value for preoperative evaluation and postoperative follow up.<sup>21</sup> Emerging techniques such as endoscopic full-thickness resection or natural orifice transmural

endoscopic surgery can also be considered, but attention should be paid to avoid tumor spillage.

Surveillance may be appropriate for SELs without definite tissue diagnosis in patients who are at high operative risk. If the lesion is a suspected GIST, changes in size and echogenicity should be monitored. If the size increases or malignant features (echogenic foci, heterogeneity, internal cystic space, irregularity of extraluminal margins, and adjacent lymphadenopathy) develop, resection should be recommended. The follow-up interval depends on the index of suspicion of the examiner and is usually 1 year. When the characteristics of the lesion do not change on two consecutive follow-up examinations with EUS, a longer follow-up interval may be justified.<sup>114</sup>

## Summary

SELs involving the GI tract are difficult to diagnose definitively by conventional imaging methods such as GI radiography, ultrasonography, CT, and MRI. Endoscopic views are limited and standard biopsy techniques have a low yield. EUS is an essential modality in the evaluation of these lesions. Any SEL that appears to be larger than 1 cm on endoscopic examination, and is not regarded as a lipoma or cyst, should be referred for EUS evaluation. With the unique ability of EUS to visualize the layers of the GI tract wall, to identify the layer of origin of the SEL, and to assess the lesion's size, extent, and sonographic characteristics, a presumptive diagnosis can be made in most cases.

Although a characteristic endosonographic appearance has been described for some SELs, EUS cannot reliably distinguish benign from malignant lesions, especially in terms of the malignant potential of GISTs. The addition of EUS FNA or EUS FNB can be helpful to obtain cytologic or histologic samples from SELs.

EUS is also helpful in the selection of patients for endoscopic resection because it can enable the examiner to determine the depth and originating wall layer of the lesion. EUS can also be used in the follow-up of SELs that are left in situ.

## EXAMINATION CHECKLIST

Transition zone: Perpendicular imaging at the edge of the lesion produces an image that shows where the normal gut wall layers are merging into the lesion.

Overlying layers: Perpendicular imaging with the transducer positioned on top of the lesion (but not touching it) demonstrates which layers overlie the lesion.

## Key References

14. Matsui M, Goto H, Niwa Y, et al. Preliminary results of fine needle aspiration biopsy histology in upper gastrointestinal submucosal tumors. *Endoscopy*. 1998;30:750–755.
15. Polkowski M, Gerke W, Jarosz D, et al. Diagnostic yield and safety of endoscopic-ultrasound guided trucut biopsy in patients with gastric submucosal tumors: a prospective study. *Endoscopy*. 2009;41:329–334.
55. Akahoshi K, Sumida Y, Matsui N, et al. Preoperative diagnosis of gastrointestinal stromal tumor by endoscopic ultrasound-guided fine needle aspiration. *World J Gastroenterol*. 2007;13:2077–2082.
57. Okubo K, Yamao K, Nakamura T, et al. Endoscopic ultrasound-guided fine-needle aspiration biopsy for the diagnosis of gastrointestinal stromal tumors in the stomach. *J Gastroenterol*. 2004;39:747–753.
58. Ando N, Goto H, Niwa Y, et al. The diagnosis of GI stromal tumors with EUS-guided fine needle aspiration with immunohistochemical analysis. *Gastrointest Endosc*. 2002;55:37–43.

## References

Access the reference list online at [ExpertConsult.com](http://ExpertConsult.com).

## References

1. Hedenbro JL, Ekelund M, Wetterberg P. Endoscopic diagnosis of submucosal gastric lesions. The results after routine endoscopy. *Surg Endosc.* 1991;5:20–23.
2. Caletti G, Zani L, Bolondi L, et al. Endoscopic ultrasonography in the diagnosis of gastric submucosal tumor. *Gastrointest Endosc.* 1989;35:413–418.
3. Yasuda K, Nakajima M, Yoshida S, et al. The diagnosis of submucosal tumors of the stomach by endoscopic ultrasonography. *Gastrointest Endosc.* 1989;35:10–15.
4. Boyce GA, Sivak Jr MV, Rosch T, et al. Evaluation of submucosal upper gastrointestinal tract lesions by endoscopic ultrasound. *Gastrointest Endosc.* 1991;37:449–454.
5. Nesje LB, Laerum OD, Svanes K, et al. Subepithelial masses of the gastrointestinal tract evaluated by endoscopic ultrasonography. *Eur J Ultrasound.* 2002;15:45–54.
6. Van Stolk RU. Subepithelial lesions. In: Van Dam J, Sivak MV, eds. *Gastrointestinal Endosonography.* 1st ed. Philadelphia: Saunders; 1999:153–165.
7. Chak A. EUS in submucosal tumors. *Gastrointest Endosc.* 2002;56(suppl):S43–S48.
8. Lim TW, Choi CW, Kang DH, et al. Endoscopic ultrasound without tissue acquisition has poor accuracy for diagnosing gastric subepithelial tumors. *Medicine (Baltimore).* 2016;95:e5246.
9. Reddymasu SC, Oropeza-Vail M, Pakseresht K, et al. Are endoscopic ultrasonography imaging characteristics reliable for the diagnosis of small upper gastrointestinal subepithelial lesions? *J Clin Gastroenterol.* 2012;46:42–45.
10. Karaca C, Turner BG, Cizginer S, et al. Accuracy of EUS in the evaluation of small gastric subepithelial lesions. *Gastrointest Endosc.* 2010;71:722–727.
11. Ji F, Wang ZW, Wang LJ, et al. Clinicopathological characteristics of gastrointestinal mesenchymal tumors and diagnostic value of endoscopic ultrasonography. *J Gastroenterol Hepatol.* 2008;23:e318–e324.
12. Kwon JG, Kim EY, Kim YS, et al. Accuracy of endoscopic ultrasonographic impression compared with pathologic diagnosis in gastrointestinal submucosal tumors. *Korean J Gastroenterol.* 2005;45:88–96.
13. Kojima T, Takahashi H, Parra-Blanco A, et al. Diagnosis of submucosal tumor of the upper GI tract by endoscopic resection. *Gastrointest Endosc.* 1999;50:516–522.
14. Matsui M, Goto H, Niwa Y, et al. Preliminary results of fine needle aspiration biopsy histology in upper gastrointestinal submucosal tumors. *Endoscopy.* 1998;30:750–755.
15. Polkowski M, Gerke W, Jarosz D, et al. Diagnostic yield and safety of endoscopic-ultrasound guided trucut biopsy in patients with gastric submucosal tumors: a prospective study. *Endoscopy.* 2009;41:329–334.
16. Chen VK, Eloubeidi MA. Endoscopic ultrasound-guided fine-needle aspiration of intramural and extraintestinal mass lesions: diagnostic accuracy, complication assessment, and impact on management. *Endoscopy.* 2005;37:984–989.
17. Shen EF, Arnott ID, Plevris J, et al. Endoscopic ultrasonography in the diagnosis and management of suspected upper gastrointestinal submucosal tumours. *Br J Surg.* 2002;89:231–235.
18. Nickl NJ, Bhutani MS, Catalano M, et al. Clinical implications of endoscopic ultrasound: the American Endosonography Club Study. *Gastrointest Endosc.* 1996;44:371–377.
19. Park YS, Park SW, Kim TI, et al. Endoscopic enucleation of upper-GI submucosal tumors by using an insulated-tip electro-surgical knife. *Gastrointest Endosc.* 2004;59:409–415.
20. Hoteya S, Iizuka T, Kikuchi D, Yahagi N. Endoscopic submucosal dissection for gastric submucosal tumor, endoscopic sub-tumoral dissection. *Dig Endoscopy.* 2009;21:266–269.
21. He G, Wang J, Chen B, et al. Feasibility of endoscopic submucosal dissection for upper gastrointestinal submucosal tumors treatment and value of endoscopic ultrasonography in pre-operation assess and post-operation follow-up: a prospective study of 224 cases in a single medical center. *Surg Endosc.* 2016;30:4206–4213.
22. Rosch T, Lorenz R, Dancygier H, et al. Endosonographic diagnosis of submucosal upper gastrointestinal tract tumors. *Scand J Gastroenterol.* 1992;27:1–8.
23. Futagami K, Hata J, Haruma K, et al. Extracorporeal ultrasound is an effective diagnostic alternative to endoscopic ultrasound for gastric submucosal tumours. *Scand J Gastroenterol.* 2001;36:1222–1226.
24. Goto O, Kambe H, Niimi K, et al. Discrepancy in diagnosis of gastric submucosal tumor among esophagogastroduodenoscopy, CT, and endoscopic ultrasonography: a retrospective analysis of 93 consecutive cases. *Abdom Imaging.* 2012;37:1074–1078.
25. Okten RS, Kacar S, Kucukay F, et al. Gastric subepithelial masses: evaluation of multidetector CT (multiplanar reconstruction and virtual gastroscopy) versus endoscopic ultrasonography. *Abdom Imaging.* 2012;37:519–530.
26. Rosch T, Kapfer B, Will U, et al. Accuracy of endoscopic ultrasonography in upper gastrointestinal submucosal lesions: a prospective multicenter study. *Scand J Gastroenterol.* 2002;37:856–862.
27. Motoo Y, Okai T, Ohta H, et al. Endoscopic ultrasonography in the diagnosis of extraluminal compressions mimicking gastric submucosal tumors. *Endoscopy.* 1994;26:239–242.
28. Zhang QL, Nian WD. Endoscopic ultrasonography diagnosis in submucosal tumor of stomach. *Endoscopy.* 1998;30(suppl):A69–A71.
29. Ra JC, Lee ES, Lee JB, et al. Diagnostic performance of stomach CT compared with endoscopic ultrasonography in diagnosing gastric subepithelial tumors. *Abdom Radiol (NY).* 2017;42:442–450.
30. Polkowski M, Butruk E. Submucosal lesions. *Gastrointest Endosc Clin N Am.* 2005;15:33–54. viii.
31. Ozta E, Oguz D, Kurt M, et al. Endosonographic evaluation of patients with suspected extraluminal compression or subepithelial lesions during upper gastrointestinal endoscopy. *Eur J Gastroenterol Hepatol.* 2011;23:586–592.
32. Miettinen M, Sabin LH, Lasota J. Gastrointestinal stromal tumors of the stomach: a clinicopathologic, immunohistochemical, and molecular genetic study of 1765 cases with long-term follow-up. *Am J Surg Pathol.* 2005;29:52–68.
33. Miettinen M, Sarlomo-Rikala M, Lasota J. Gastrointestinal stromal tumors: recent advances in understanding of their biology. *Hum Pathol.* 1999;30:1213–1220.
34. Berman J, O’Leary TJ. Gastrointestinal stromal tumor workshop. *Hum Pathol.* 2001;32:578–582.
35. Fletcher CD, Berman JJ, Corless C, et al. Diagnosis of gastrointestinal stromal tumors: a consensus approach. *Hum Pathol.* 2002;33:459–465.
36. Yoon JM, Kim GH, Park DY, et al. Endosonographic features of gastric schwannoma: a single center experience. *Clin Endosc.* 2016;49:548–554.
37. Okai T, Minamoto T, Ohtsubo K, et al. Endosonographic evaluation of c-kit-positive gastrointestinal stromal tumor. *Abdom Imaging.* 2003;28:301–307.
38. Kim GH, Park DY, Kim S, et al. Is it possible to differentiate gastric GISTs from gastric leiomyomas by EUS? *World J Gastroenterol.* 2009;15:3376–3381.
39. Jeon SW, Park YD, Chung YJ, et al. Gastrointestinal stromal tumors of the stomach: endosonographic differentiation in relation to histological risk. *J Gastroenterol Hepatol.* 2007;22:2069–2075.
40. Shah P, Gao F, Edmundowicz SA, et al. Predicting malignant potential of gastrointestinal stromal tumors using endoscopic ultrasound. *Dig Dis Sci.* 2009;54:1265–1269.

41. Onishi M, Tominaga K, Sugimori S, et al. Internal hypoechoic feature by EUS as a possible predictive marker for the enlargement potential of gastric GI stromal tumors. *Gastrointest Endosc.* 2012;75:731–738.
42. Chak A, Canto MI, Rosch T, et al. Endosonographic differentiation of benign and malignant stromal cell tumors. *Gastrointest Endosc.* 1997;45:468–473.
43. Palazzo L, Landi B, Cellier C, et al. Endosonographic features predictive of benign and malignant gastrointestinal stromal cell tumours. *Gut.* 2000;46:88–92.
44. Nickl N. Decision analysis of hypoechoic intramural tumor study results. *Gastrointest Endosc.* 2002;56(suppl):S102.
45. Kannengiesser K, Mahlke R, Petersen F, et al. Contrast-enhanced harmonic endoscopic ultrasound is able to discriminate benign submucosal lesions from gastrointestinal stromal tumors. *Scand J Gastroenterol.* 2012;47:1515–1520.
46. Ignee A, Jenssen C, Hocke M, et al. Contrast-enhanced (endoscopic) ultrasound and endoscopic ultrasound elastography in gastrointestinal stromal tumors. *Endosc Ultrasound.* 2017;6:55–60.
47. Sakamoto H, Kitano M, Matsui S, et al. Estimation of malignant potential of GI stromal tumors by contrast-enhanced harmonic EUS (with videos). *Gastrointest Endosc.* 2011;73:227–237.
48. Tsuji Y, Kusano C, Gotoda T, et al. Diagnostic potential of endoscopic ultrasonography-elastography for gastric submucosal tumors: a pilot study. *Dig Endosc.* 2016;28:173–178.
49. El Chafic AH, Loren D, Siddiqui A, et al. Comparison of FNA and fine-needle biopsy for EUS-guided sampling of suspected GI stromal tumors. *Gastrointest Endosc.* 2017. pii: S0016-5107(17)30027-5. [Epub ahead of print].
50. DeWitt J, Emerson RE, Sherman S, et al. Endoscopic ultrasound-guided Trucut biopsy of gastrointestinal mesenchymal tumor. *Surg Endosc.* 2011;25:2192–2202.
51. Watson RR, Binmoeller KF, Hamerski CM, et al. Yield and performance characteristics of endoscopic ultrasound-guided fine needle aspiration for diagnosing upper GI tract stromal tumors. *Dig Dis Sci.* 2011;56:1757–1762.
52. Fernández-Esparrach G, Sendino O, Solé M, et al. Endoscopic ultrasound-guided fine-needle aspiration and trucut biopsy in the diagnosis of gastric stromal tumors: a randomized crossover study. *Endoscopy.* 2010;42:292–299.
53. Sepe PS, Moparty B, Pitman MB, et al. EUS-guided FNA for the diagnosis of GI stromal cell tumors: sensitivity and cytologic yield. *Gastrointest Endosc.* 2009;70:254–261.
54. Chatzipantelis P, Salla C, Karoumpalis I, et al. Endoscopic ultrasound-guided fine needle aspiration biopsy in the diagnosis of gastrointestinal stromal tumors of the stomach. A study of 17 cases. *J Gastrointest Liver Dis.* 2008;17:15–20.
55. Akahoshi K, Sumida Y, Matsui N, et al. Preoperative diagnosis of gastrointestinal stromal tumor by endoscopic ultrasound-guided fine needle aspiration. *World J Gastroenterol.* 2007;13:2077–2082.
56. Mochizuki Y, Kodera Y, Fujiwara M, et al. Laparoscopic wedge resection for gastrointestinal stromal tumors of the stomach: initial experience. *Surg Today.* 2006;36:341–347.
57. Okubo K, Yamao K, Nakamura T, et al. Endoscopic ultrasound-guided fine-needle aspiration biopsy for the diagnosis of gastrointestinal stromal tumors in the stomach. *J Gastroenterol.* 2004;39:747–753.
58. Ando N, Goto H, Niwa Y, et al. The diagnosis of GI stromal tumors with EUS-guided fine needle aspiration with immunohistochemical analysis. *Gastrointest Endosc.* 2002;55:37–43.
59. Armstrong CP, King PM, Dixon JM, et al. The clinical significance of heterotopic pancreas in the gastrointestinal tract. *Br J Surg.* 1981;68:384–387.
60. Jovanovic I, Knezevic S, Micev M, et al. EUS mini probes in diagnosis of cystic dystrophy of duodenal wall in heterotopic pancreas: a case report. *World J Gastroenterol.* 2004;10:2609–2612.
61. Matsushita M, Hajiro K, Okazaki K, et al. Gastric aberrant pancreas: EUS analysis in comparison with the histology. *Gastrointest Endosc.* 1999;49:493–497.
62. Parmar JH, Lawrence R, Ridley NT. Submucous lipoma of the ileocaecal valve presenting as caecal volvulus. *Int J Clin Pract.* 2004;58:424–425.
63. Watanabe F, Honda S, Kubota H, et al. Preoperative diagnosis of ileal lipoma by endoscopic ultrasonography probe. *J Clin Gastroenterol.* 2000;31:245–247.
64. Zhou PH, Yao LQ, Zhong YS, et al. Role of endoscopic mini-probe ultrasonography in diagnosis of submucosal tumor of large intestine. *World J Gastroenterol.* 2004;10:2444–2446.
65. Garcia M, Buitrago E, Bejarano PA, et al. Large esophageal liposarcoma: a case report and review of the literature. *Arch Pathol Lab Med.* 2004;128:922–925.
66. Nakamura S, Iida M, Yao T, et al. Endoscopic features of gastric carcinoids. *Gastrointest Endosc.* 1991;37:535–538.
67. Ichikawa J, Tanabe S, Koizumi W, et al. Endoscopic mucosal resection in the management of gastric carcinoid tumors. *Endoscopy.* 2003;35:203–206.
68. Matsumoto T, Iida M, Suekane H, et al. Endoscopic ultrasonography in rectal carcinoid tumors: contribution to selection of therapy. *Gastrointest Endosc.* 1991;37:539–542.
69. Yasuda E, Tomita K, Nagura Y, et al. Endoscopic removal of granular cell tumor. *Gastrointest Endosc.* 1995;41:163–167.
70. Nakachi A, Miyazato H, Oshiro T, et al. Granular cell tumor of the rectum: a case report and review of the literature. *J Gastroenterol.* 2000;35:631–634.
71. Love MH, Glaser M, Edmunds SE, et al. Granular cell tumour of the oesophagus: endoscopic ultrasound appearances. *Australas Radiol.* 1999;43:253–255.
72. Palazzo L, Landi B, Cellier C, et al. Endosonographic features of esophageal granular cell tumors. *Endoscopy.* 1997;29:850–853.
73. Kim DU, Kim GH, Ryu DY, et al. Endosonographic features of esophageal granular cell tumors using a high-frequency catheter probe. *Scand J Gastroenterol.* 2011;46:142–147.
74. Hizawa K, Matsumoto T, Kouzuki T, et al. Cystic submucosal tumors in the gastrointestinal tract: endosonographic findings and endoscopic removal. *Endoscopy.* 2000;32:712–714.
75. Wildi SM, Hoda RS, Fickling W, et al. Diagnosis of benign cysts of the mediastinum: the role and risks of EUS and FNA. *Gastrointest Endosc.* 2003;58:362–368.
76. Fazel A, Moezardalan K, Varadarajulu S, et al. The utility and the safety of EUS-guided FNA in the evaluation of duplication cysts. *Gastrointest Endosc.* 2005;62:575–580.
77. Faigel DO, Burke A, Ginsberg GG, et al. The role of endoscopic ultrasound in the evaluation and management of foregut duplications. *Gastrointest Endosc.* 1997;45:99–103.
78. Geller A, Wang KK, DiMagno EP. Diagnosis of foregut duplication cysts by endoscopic ultrasonography. *Gastroenterology.* 1995;109:838–842.
79. Dancygier H, Lightdale CJ. Endoscopic ultrasonography of the upper gastrointestinal tract and colon. In: Stevens PD, ed. *Endosonography in Gastroenterology: Principles, Techniques, Findings.* New York: Thieme; 1999:76–89.
80. Faigel DO, Rosen HR, Sasaki A, et al. EUS in cirrhotic patients with and without prior variceal hemorrhage in comparison with noncirrhotic control subjects. *Gastrointest Endosc.* 2000;52:455–462.
81. Tio TL, Kimmings N, Rauws E, et al. Endosonography of gasteroesophageal varices: evaluation and follow-up of 76 cases. *Gastrointest Endosc.* 1995;42:145–150.
82. Lahoti S, Catalano MF, Alcocer E, et al. Obliteration of esophageal varices using EUS-guided sclerotherapy with color Doppler. *Gastrointest Endosc.* 2000;51:331–333.
83. Binmoeller KF, Weilert F, Shah JN, Kim J. EUS-guided transesophageal treatment of gastric fundal varices with combined coiling and cyanoacrylate glue injection (with videos). *Gastrointest Endosc.* 2011;74:1019–1025.

84. Matsushita M, Haji K, Okazaki K, et al. Endoscopic features of gastric inflammatory fibroid polyps. *Am J Gastroenterol*. 1996;91:1595–1598.
85. Matsushita M, Haji K, Okazaki K, et al. Gastric inflammatory fibroid polyps: endoscopic ultrasonographic analysis in comparison with the histology. *Gastrointest Endosc*. 1997;46:53–57.
86. Imamura A, Tochihara M, Natsui K, et al. Glomus tumor of the stomach: endoscopic ultrasonographic findings. *Am J Gastroenterol*. 1994;89:271–272.
87. Baek YH, Choi SR, Lee BE, Kim GH. Gastric glomus tumor: analysis of endosonographic characteristics and computed tomographic findings. *Dig Endosc*. 2013;25:80–83.
88. Tang M, Hou J, Wu D, et al. Glomus tumor in the stomach: computed tomography and endoscopic ultrasound findings. *World J Gastroenterol*. 2013;19:1327–1329.
89. Kim EY. Diagnosis of subepithelial lesion: still “tissue is the issue”. *Clin Endosc*. 2013;46:313–314.
90. Ji JS, Lee BI, Choi KY, et al. Diagnostic yield of tissue sampling using a bite-on-bite technique for incidental subepithelial lesions. *Korean J Intern Med*. 2009;24:101–105.
91. Buscaglia JM, Nagula S, Jayaraman V, et al. Diagnostic yield and safety of jumbo biopsy forceps in patients with subepithelial lesions of the upper and lower GI tract. *Gastrointest Endosc*. 2012;75:1147–1152.
92. Kim EY. Introduction: value of endoscopic ultrasound-guided fine needle aspiration. *Clin Endosc*. 2012;45:115–116.
93. Moon JS. Endoscopic ultrasound-guided fine needle aspiration in submucosal lesion. *Clin Endosc*. 2012;45:117–123.
94. Giovannini M, Seitz JF, Monges G, et al. Fine-needle aspiration cytology guided by endoscopic ultrasonography: results in 141 patients. *Endoscopy*. 1995;27:171–177.
95. Eckardt AJ, Adler A, Gomes EM, et al. Endosonographic large-bore biopsy of gastric subepithelial tumors: a prospective multicenter study. *Eur J Gastroenterol Hepatol*. 2012;24:1135–1144.
96. Levy MJ, Jondal ML, Clain J, et al. Preliminary experience with an EUS-guided Trucut biopsy needle compared with EUS-guided FNA. *Gastrointest Endosc*. 2003;57:101–106.
97. Varadarajulu S, Fraig M, Schmulewitz N, et al. Comparison of EUS-guided 19-gauge Trucut needle biopsy with EUS-guided fine-needle aspiration. *Endoscopy*. 2004;36:397–401.
98. Sáftoiu A, Vilmann P, Guldhammer Skov B, Georgescu CV. Endoscopic ultrasound (EUS)-guided Trucut biopsy adds significant information to EUS-guided fine-needle aspiration in selected patients: a prospective study. *Scand J Gastroenterol*. 2007;42:117–125.
99. Kaffes AJ, Chen RY, Tam W, et al. A prospective multicenter evaluation of a new side-port endoscopic ultrasound-fine-needle aspiration in solid upper gastrointestinal lesions. *Dig Endosc*. 2012;24:448–451.
100. DiMaio CJ, Kolb JM, Benias PC, et al. Initial experience with a novel EUS-guided core biopsy needle (SharkCore): results of a large North American multicenter study. *Endosc Int Open*. 2016;4:E974–E979.
101. Nguyen-Tang T, Shah JN, Sanchez-Yague A, Binmoeller KF. Use of the front-view forward-array echoendoscope to evaluate right colonic subepithelial lesions. *Gastrointest Endosc*. 2010;72:606–610.
102. Matsuzaki I, Miyahara R, Hirooka Y, et al. Forward-viewing versus oblique-viewing echoendoscopes in the diagnosis of upper GI subepithelial lesions with EUS-guided FNA: a prospective, randomized, crossover study. *Gastrointest Endosc*. 2015;82:287–295.
103. Schlag C, Menzel C, et al. Endoscopic ultrasound-guided tissue sampling of small subepithelial tumors of the upper gastrointestinal tract with a 22-gauge core biopsy needle. *Endosc Int Open*. 2017;5:E165–E171.
104. Lee JH, Cho CJ, Park YS, et al. EUS-guided 22-gauge fine needle biopsy for the diagnosis of gastric subepithelial tumors larger than 2 cm. *Scand J Gastroenterol*. 2016;51:486–493.
105. Na HK, Lee JH, Park YS, et al. Yields and utility of endoscopic ultrasonography-guided 19-gauge Trucut biopsy versus 22-gauge fine needle aspiration for diagnosing gastric subepithelial tumors. *Clin Endosc*. 2015;48:152–157.
106. Kim GH, Cho YK, Kim EY, et al. Comparison of 22-gauge aspiration needle with 22-gauge biopsy needle in endoscopic ultrasonography-guided subepithelial tumor sampling. *Scand J Gastroenterol*. 2014;49:347–354.
107. Çağlar E, Hatemi İ, Atasoy D, et al. Concordance of endoscopic ultrasonography-guided fine needle aspiration diagnosis with the final diagnosis in subepithelial lesions. *Clin Endosc*. 2013;46:379–383.
108. Rong L, Kida M, Yamauchi H, et al. Factors affecting the diagnostic accuracy of endoscopic ultrasonography-guided fine-needle aspiration (EUS-FNA) for upper gastrointestinal submucosal or extraluminal solid mass lesions. *Dig Endosc*. 2012;24:358–363.
109. Suzuki T, Arai M, Matsumura T, et al. Factors associated with inadequate tissue yield in EUS-FNA for gastric SMT. *ISRN Gastroenterol*. 2011;2011:619128.
110. Mekky MA, Yamao K, Sawaki A, et al. Diagnostic utility of EUS-guided FNA in patients with gastric submucosal tumors. *Gastrointest Endosc*. 2010;71:913–919.
111. Hoda KM, Rodriguez SA, Faigel DO. EUS-guided sampling of suspected GI stromal tumors. *Gastrointest Endosc*. 2009;69:1218–1223.
112. Vander Noot 3rd MR, Eloubeidi MA, Chen VK, et al. Diagnosis of gastrointestinal tract lesions by endoscopic ultrasound-guided fine-needle aspiration biopsy. *Cancer*. 2004;102:157–163.
113. Kim EY. How can we obtain tissue from a subepithelial lesion for pathologic diagnosis? *Clin Endosc*. 2017;50:6–7.
114. Hwang JH, Rulyak SD, Kimmey MB. American Gastroenterological Association Institute technical review on the management of gastric subepithelial masses. *Gastroenterology*. 2006;130:2217–2228.



**Video 11.1** Video Demonstrating the Sonographic Features of Various Subepithelial Lesions



**Video 11.2** Video Demonstrating the Difference Between a Duplication Cyst and Spindle Cell Neoplasm

# 12

## How to Perform Endoscopic Ultrasonography in the Pancreas, Bile Duct, and Liver

ROBERT H. HAWES, PAUL FOCKENS, AND SHYAM VARADARAJULU

### Pancreas

Successful pancreatic imaging requires the ability to image the entire gland. In general, the body and tail of the pancreas are imaged through the posterior wall of the stomach, and, in most cases, the transgastric approach provides images of the genu (neck) of the pancreas as well. Complete imaging of the pancreatic head, however, requires placement of the transducer in three different positions within the duodenum: the apex of the duodenal bulb (the apical view), directly opposite the papilla ("kissing the papilla"), and distal to the papilla to visualize the uncinate process. This organized, station-based approach to pancreatic imaging is critical for individuals who are just learning or who have limited experience with endoscopic ultrasonography (EUS). Although the stations are the same for radial and linear endosonography, the images produced are different, as are the techniques for maneuvering the echoendoscope. As a result, representative images and illustrations from the various stations are presented for radial and linear echoendoscopes. As the reader is learning these techniques, it is also important for him or her to refer to the corresponding videos. Obtaining complete, accurate, and high-quality images of the pancreas and biliary tree represents the most difficult task facing the endosonographer.

### Evaluation of the Body and Tail of the Pancreas

The examination of the body and tail of the pancreas begins by positioning the tip of the echoendoscope just distal to the squamocolumnar junction. From this position, the aorta is easily located and becomes the "arrow" that points the way. When the radial scope is used, the aorta is round and anechoic. With the linear scope, the aorta fills the screen as a long, anechoic structure extending across the entire monitor.

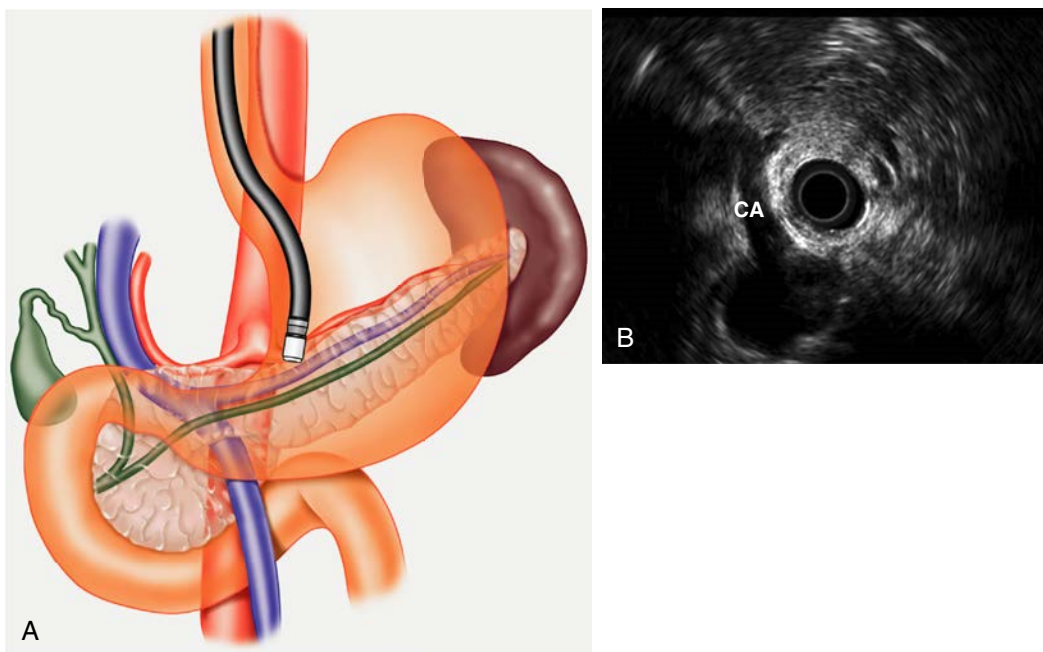
#### Radial Echoendoscopes

With the tip of the endoscope just distal to the squamocolumnar junction, the endosonographer inflates the balloon and positions the transducer in the center. The aorta is located, and with the endosonographer in a comfortable position (neither body nor scope shaft twisted or torqued), the aorta is electronically rotated

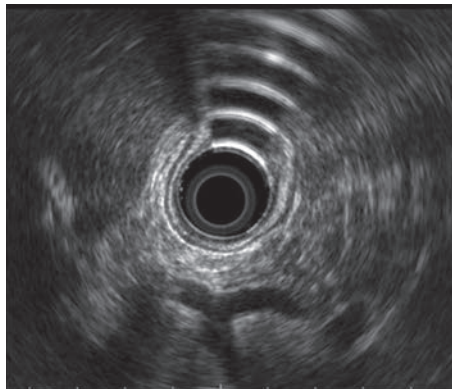
to the 6 o'clock position (Video 12.1). At this point, one usually sees a hypoechoic structure that moves from the esophageal wall and wraps partially around the aorta; this comprises the diaphragmatic crura. From here, one simply advances the echoendoscope while the aorta is kept in its cross-sectional conformation; the aorta must not be allowed to elongate. If the aorta is seen to elongate on advancement, it is an indication that the tip of the echoendoscope is being pushed laterally or is embedding in the gastric wall (often within a hiatal hernia pouch). If this occurs, the tip must be realigned and the maneuver repeated because it is important to keep the aorta in its round configuration. If this maneuver fails repeatedly, the echoendoscope should be advanced beyond the hiatal hernia and withdrawn. This maneuver helps one to visualize first the portal vein confluence (at the 6 o'clock position), and then the pancreas.

With advancement, when the crura disappear, the celiac trunk is seen to emerge from the aorta and tract toward the transducer (Fig. 12.1). In some cases with the radial scope, one first sees the splenic artery as a round, anechoic structure adjacent to the transducer. In this case, one just advances 1 to 2 cm, and the splenic artery traces into the celiac trunk. The celiac artery bifurcates into the hepatic and splenic arteries; with the radial scope, the bifurcation can look like a whale's tail (Fig. 12.2). Slight advancement of the scope beyond the celiac artery takeoff produces images of the body of the pancreas. The pancreas is seen directly below the transducer. The pancreatic parenchyma is usually slightly hypoechoic relative to surrounding tissue and has a homogeneous "salt and pepper" appearance. From this position, deep to the pancreas is an anechoic structure that looks like the head of a golf club. This is the portal vein confluence and is often referred to as the *club head* (Fig. 12.3).

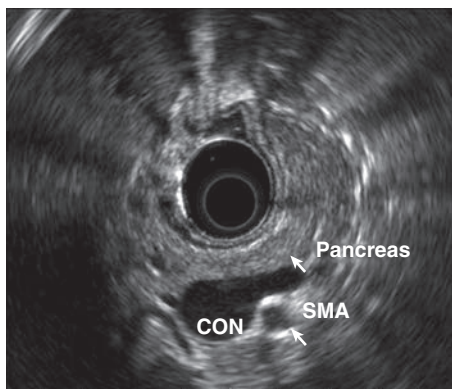
Once the club head has been identified, it becomes relatively straightforward to image the rest of the body and tail of the pancreas. Clockwise torque and withdrawal of the scope will trace the tail of the pancreas. It may also require some "right" adjustment on the left-right knob. During this maneuver, the left kidney comes into the picture as a large, oval structure with a hypoechoic, homogeneous outer "shell" (cortex) and an inhomogeneous, echo-rich central portion (medulla). The kidney roughly marks the body-tail junction of the pancreas (Fig. 12.4). On



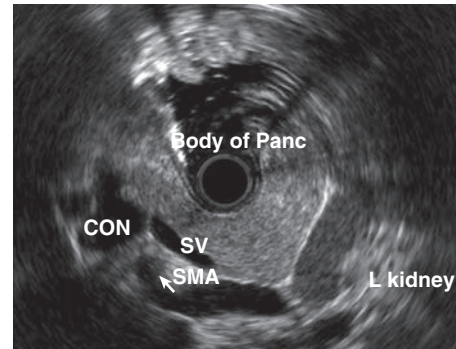
• **Fig. 12.1** Pancreatic body and tail examination: radial echoendoscope. (A) This illustration represents the starting point for imaging the pancreatic body and tail with the radial echoendoscope. The scope is advanced while the aorta is traced, starting at the gastroesophageal junction. The first branch of the aorta is the celiac artery. (B) By tracing the celiac artery (CA), the pancreatic body and tail can be found.



• **Fig. 12.2** The celiac artery bifurcates into the hepatic and splenic arteries, which on endosonography can look like a whale's tail.

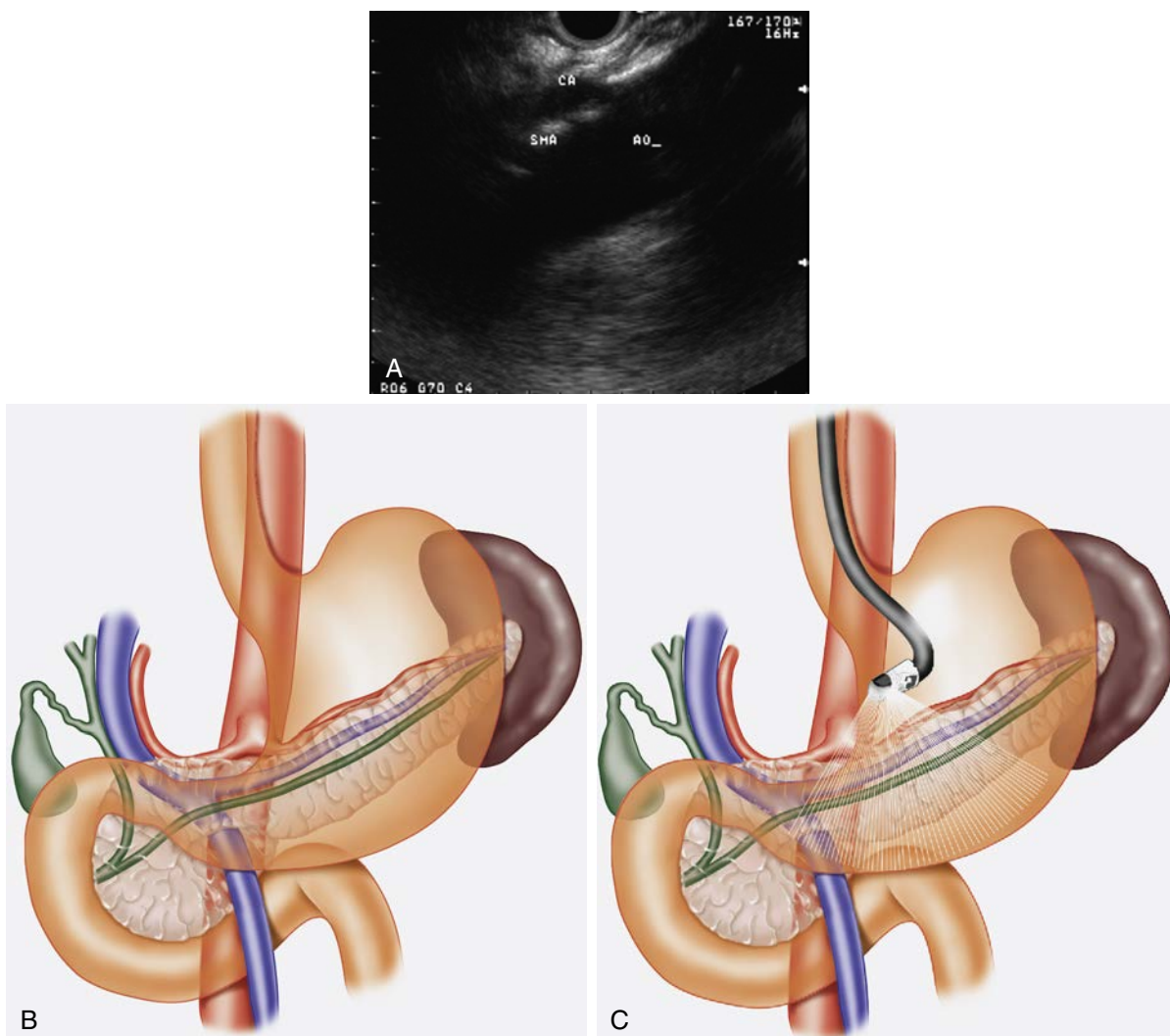


• **Fig. 12.3** The portal vein confluence (CON) is referred to as a *club head* because it looks like the head of a golf club and is located deep to the pancreas. In this view, the pancreas is located directly below the transducer and has a homogeneous “salt and pepper” pattern. SMA, Superior mesenteric artery.



• **Fig. 12.4** The left kidney has a hypoechoic outer cortex and an echo-rich medullary zone. This landmark roughly indicates the body-tail junction of the pancreas. CON, Portal vein confluence; L, left; Panc, pancreas; SMA, superior mesenteric artery; SV, superior mesenteric vein.

further withdrawal, one sees the splenic artery and vein course right below the transducer, and a homogeneous, echo-poor bean-shaped structure occupies the right side of the image. This is the spleen, and the splenic vein and artery can be seen to insert into the splenic hilum. Once this image is seen, the examination of the distal body and tail is complete. From the tail of the pancreas, one simply reverses the maneuvers by advancing the scope, torquing counterclockwise, and returning to the portal vein confluence. From here, further advancement and counterclockwise torque allow imaging of the genu (neck) of the pancreas. The pancreatic duct is seen to dive away from the transducer as it courses through the neck. During the movements mentioned earlier, some left and right tip deflection may be required to obtain an elongated view of the pancreas. Once the elongated view of the pancreas is achieved, very slow and purposeful advancement and withdrawal of the scope demonstrate the entire width of the pancreas, including the pancreatic duct.



**• Fig. 12.5** Pancreatic body and tail examination: linear echoendoscope. (A) Endoscopic ultrasonography image and (B and C) illustrations represent the starting point for imaging the pancreatic body and tail using the curvilinear echoendoscope. The transducer is advanced while the aorta is traced, starting at the gastroesophageal junction. The first branch of the aorta represents the celiac axis; by tracing along the celiac axis, the pancreatic body can be found.

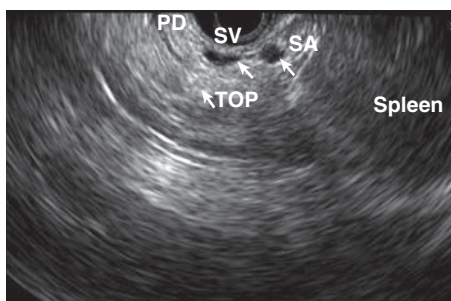
In the station approach, if one cannot see the typical landmarks that characterize the station during the course of the examination (no matter which station one is working on), one should return immediately to the starting point for that station and repeat the standard maneuvers. In the case of the pancreatic body and tail, this means returning to the gastroesophageal junction, tracing the aorta until the celiac trunk is seen, and so forth. A particular station should be examined as many times as required until the endosonographer is comfortable that the examination is complete. Sometimes, however, despite repeated attempts, one cannot achieve the imaging goals of a particular station. In this case, the endosonographer can continue the examination by going to other stations and then return later to the difficult station. Often, the return examination is successful.

### Linear Echoendoscopes

Examination of the pancreatic body and tail with the linear scope follows the same basic approach as with the radial instrument. The examination begins at the gastroesophageal junction

([Video 12.2](#)). In this case, however, the endosonographer must torque the scope shaft in a clockwise direction until the aorta is seen. Using the up-down dial, the aorta should gently slope down from right to left. Just as with the radial scope, the diaphragmatic crura are seen as a hypoechoic structure between the transducer and the aorta. This landmark is important because, as one advances the scope, the celiac trunk takes off soon after the crura disappear ([Fig. 12.5](#)).

Unlike the radial scope, with which scope advancement is a passive maneuver (because of its 360-degree image), the linear scope must be gently torqued clockwise and counter-clockwise to visualize the side of the aorta. Not uncommonly, the celiac trunk comes off the side of the aorta, and one can pass right by it if not systematically scanning back and forth. Once the celiac artery has been identified, it is traced until it bifurcates. Once the bifurcation is identified, and with 1 to 2 cm of further advancement combined with a gentle “down” on the up-down dial (“big dial away from you”), the pancreas and portal vein confluence come into view. From



• **Fig. 12.6** Clockwise torque from the portal confluence coupled with gradual scope withdrawal enables imaging of the body and tail regions of the pancreas. PD, Pancreatic duct; SA, splenic artery; SV, splenic vein; TOP, tail of pancreas.



• **Fig. 12.7** Counterclockwise rotation coupled with scope advancement enables visualization of the pancreatic genu.

here, clockwise torque and withdrawal image the pancreatic body and tail (Fig. 12.6), and counterclockwise rotation and advancement provide images of the genu (Fig. 12.7). As with a radial echoendoscope, the pancreas should be traced all the way to the tail, which is confirmed when the splenic hilum is seen. As with all aspects of linear array imaging, gentle clockwise and counterclockwise torquing is mandatory throughout the examination to obtain complete imaging. Left and right tip deflection is of minimal importance when the linear echoendoscope is used.

An alternative technique used to examine the body and tail of the pancreas when using a linear array echoendoscope is to first differentiate the left lobe of the liver from the body of the stomach. From this position, when the shaft of the echoendoscope is torqued 180 degrees clockwise, the body of the pancreas can be identified and the gland traced all the way to the tail, as described earlier (Video 12.3). A similar approach is to identify the portal vein as it enters the liver. Advancing the scope combined with clockwise torque enables one to follow the portal vein until the confluence is reached. Once the “club head” is identified, the pancreas will be between the portal vein confluence and the transducer (see Video 12.3).

### Evaluation of the Head and Uncinate Regions of the Pancreas

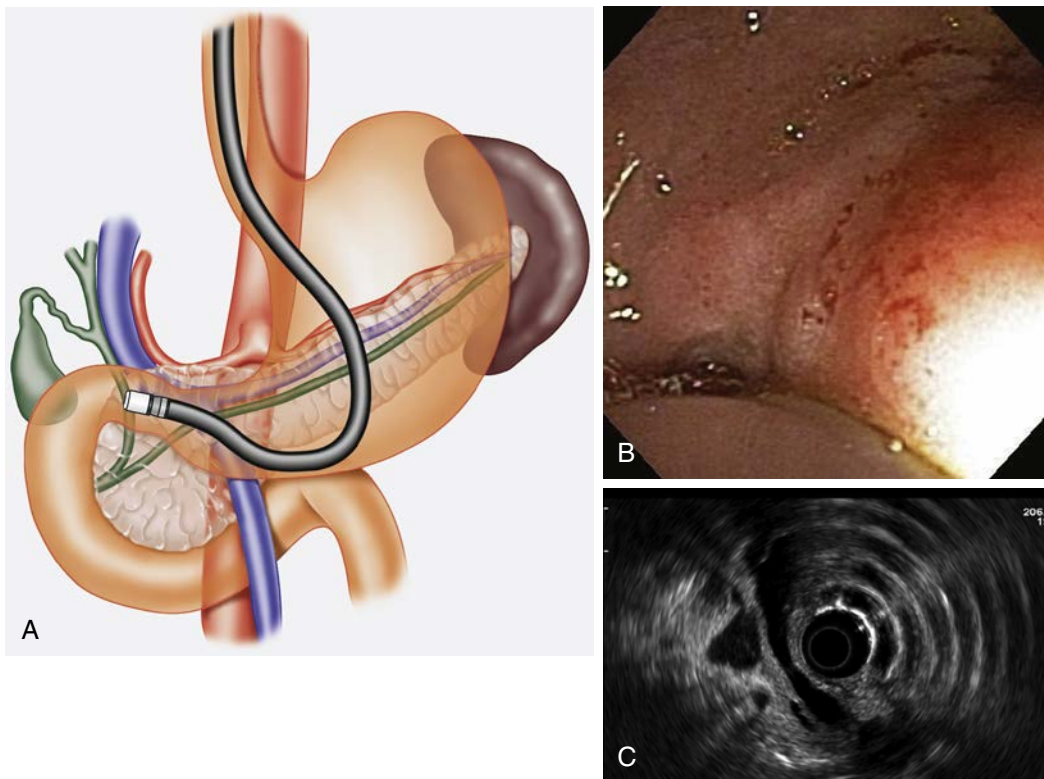
To examine the entire head of the pancreas confidently, all three positions (the apex, papilla, and distal to the papilla) should be achieved. The most efficient position is the apex of the duodenal bulb, because from this position most of the pancreatic head, distal bile duct, and portal vein can be seen together. As with other stations, positioning is the same with radial and linear scopes, but the subtle maneuvers to optimize imaging and the pictures produced are different.

### Head of the Pancreas

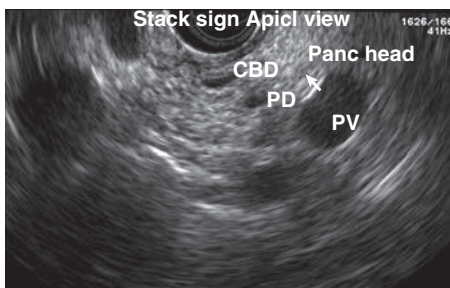
**Radial Echoendoscopes.** This position allows imaging of the entire head of the pancreas (sometimes with the exception of the uncinate process) and also includes efficient imaging of the distal common bile duct. The radial echoendoscope should be slowly advanced through the stomach and allowed to bow along the greater curve. Once the pylorus has been visualized, the tip is advanced through the pylorus, at which point air is instilled into the duodenal bulb and some gentle downward deflection is applied to the tip of the echoendoscope (Video 12.4). This maneuver allows direct endoscopic visualization of the apex of the duodenal bulb. Once the apex is visualized, the tip of the echoendoscope should be advanced until it is at the level of the apex. The balloon is then inflated until it gently occludes the lumen of the duodenum (Fig. 12.8), and any residual air is aspirated from the duodenal lumen (all done under endoscopic control). At this point, EUS imaging commences, and the endosonographer turns his or her attention to the EUS image, first looking for the liver. Once the liver has been identified, the image should be electronically rotated (*do not torque the scope*) such that the liver is positioned in the upper left-hand corner of the screen. This technique provides uniform orientation and allows the endosonographer to identify the normal and abnormal structures more easily. When the liver is in the upper left-hand corner, the head of the pancreas is at the 6 o’clock position, and the bile duct is seen as an anechoic tube lying close to the transducer and coursing from the liver down to the 6 o’clock area.

From this position, one should look for four landmarks (Fig. 12.9). The most important is the *duodenal falloff*. This is a hypoechoic line that represents the muscularis propria of the duodenal wall. It is seen to course down and away from the transducer. To the right of this line, the image is chaotic because it represents a mixture of air and fluid within the duodenal lumen. The second landmark is the *common bile duct*, a tubular anechoic structure that extends from the duodenal wall or near it toward the liver and courses closest to the transducer. This structure typically has a three-layer echo appearance. To trace the bile duct, the examiner uses counterclockwise torque and withdrawal of the scope toward the hilum and clockwise torque and advancement of the scope toward the papilla. The third landmark is the *pancreatic duct*. This may or may not be seen in the same plane of imaging as the bile duct. Often, gentle advancement of the scope combined with upward or downward tip deflection is required to see the pancreatic duct. During the entire process of imaging from the apical position, the endosonographer should be prepared to use some gentle upward or downward tip deflection to achieve complete imaging. The fourth landmark is the *portal vein*, which is seen to course in the far left of the imaging field and is the biggest tubular structure visible. One can use color Doppler imaging to identify the portal vein more easily.

Color Doppler imaging may also be required to differentiate the bile duct from the hepatic and gastroduodenal arteries. When the common bile duct, pancreatic duct, and portal vein are aligned in one view, they appear to be stacked on the top of each other. This image is known as the *stack sign*. Once the apical position is achieved, multiple small movements—which can include clockwise and counterclockwise torquing, forward advancement and withdrawal of the scope, upward and downward tip deflection, and left and right positioning of the tip—are required to define the anatomic features thoroughly from this position.



**• Fig. 12.8** Pancreatic head examination: radial echoendoscope. (A) Schema for evaluating the pancreatic head from the duodenal bulb. (B) The balloon is inflated until it occludes the apex of the duodenal bulb. (C) The liver is visualized at the left upper corner, the head of the pancreas is at the 6 o'clock position, and the bile duct will be seen as an anechoic tube closer to the transducer and coursing from the liver down to the 6 o'clock area.



**• Fig. 12.9** The stack sign. This sign is elicited during evaluation of the pancreatic head and is characterized by the common bile duct (CBD), main pancreatic duct (PD), and the portal vein (PV), which all appear “stacked” on top of each other. Also note the duodenal falloff, which represents the muscularis propria of the duodenal wall. *Apicl*, Apical; *Panc*, pancreatic.

**Linear Echoendoscopes.** Positioning the linear scope for apical imaging is the same as with the radial scope. The scope should be advanced along the greater curve and through the pylorus, where air is instilled and gentle downward tip deflection is applied. Once the apex has been identified, the tip of the linear scope is nestled into the apex of the bulb and gentle upward deflection is applied to the tip (Video 12.5). The balloon is less important with linear imaging, but some endosonographers like to inflate the balloon in the apex, as described with the radial scope. At this point, however, torquing is required, generally in a counterclockwise direction.

From this position, examination of the entire head of the pancreas (perhaps minus the uncinate process) can be achieved

(Fig. 12.10). The most recognizable structure with the linear scope in this position is the portal vein. Color Doppler imaging can be used to confirm visualization. The bile duct courses along the portal vein (closer to the transducer). The bile duct can be traced to the liver and then down to the papilla through the pancreatic head by simply torquing the scope, with little or no need for advancement or withdrawal of the instrument. The pancreatic duct runs parallel to the bile duct in the pancreatic head, but gentle torquing may be required to see it because it may not be in exactly the same plane as the bile duct (Fig. 12.11). It is critical for the endosonographer to become very comfortable with this position with the linear scope. This position provides the best imaging to assess the relationship between a pancreatic head mass and the portal vein. It is also the position of choice for performing EUS-guided fine-needle aspiration (EUS FNA) of pancreatic head masses because the mass is close to the transducer, and the back wall of the duodenum prevents the scope from pushing away from the mass when the needle is inserted (especially important if the mass is very firm).

### Papilla

**Radial Echoendoscopes.** The second position for pancreatic head imaging is from the level of the papilla. This position is best achieved by first using endoscopic visualization to localize the ampulla of Vater. Once that structure is seen, the balloon is inflated until it “kisses” the papilla (Fig. 12.12). It is best to try to orient the transducer perpendicular to the papilla and to position it so that upward tip deflection will cause the balloon to press against the papilla (Video 12.6). Once this position

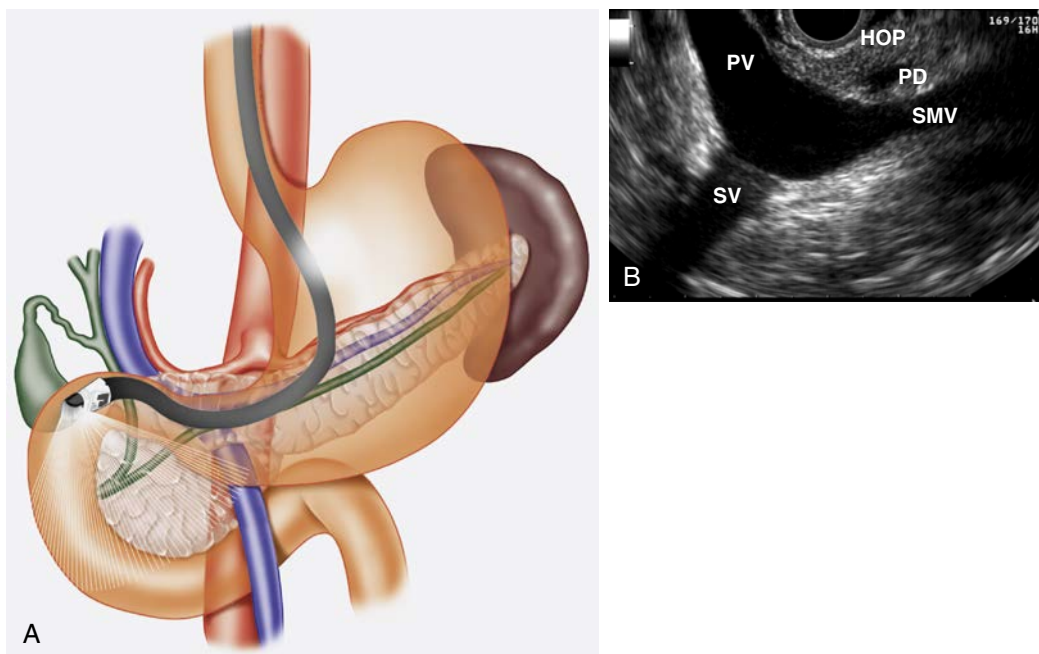


**Fig. 12.10** This is perhaps the most important station for viewing and performing fine-needle aspiration of the pancreatic head (*HOP*). (A) The transducer is placed at the level of the apex of the duodenal bulb. (B) After some manipulation of the scope tip, the neck of the pancreas can be viewed with the portal vein confluence deep to the pancreas. *PD*, Pancreatic duct; *PV*, portal vein; *SMV*, superior mesenteric vein; *SV*, splenic vein.

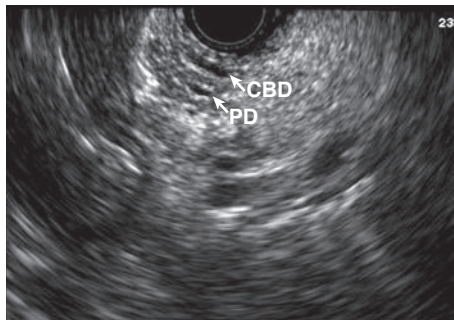


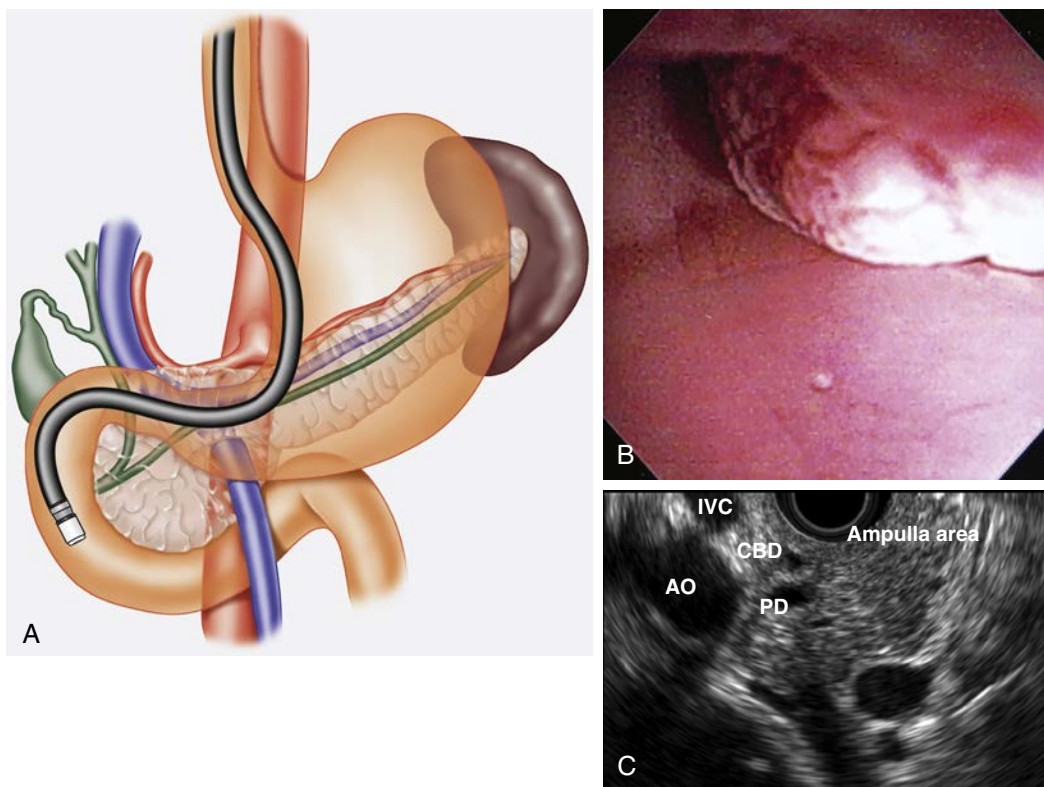
**Fig. 12.11** The pancreatic duct (*PD*) runs parallel to the common bile duct (*CBD*) in the head region of the pancreas. Gentle torquing may be required to identify and trace the ductal structures.

has been achieved, ultrasound imaging begins. The ultrasound image is rotated so that the papilla is located at the 6 o'clock position on the EUS image. From this point, the head of the pancreas is seen as a crescent-shaped structure. As the transducer is moved gently in and out, one looks to see the bile duct and pancreatic duct coursing to the duodenal wall. The pancreatic duct is deep to the bile duct relative to the position of the transducer. Because of the usual appearance of the two ducts from this position, this image is termed *snake eyes*. From this position, it is easiest to see the differentiation between the ventral and the dorsal anlage. The ventral anlage is hypoechoic and has heterogeneous echo architecture when compared with the dorsal pancreas (Fig. 12.13). The ventral anlage is triangular and occupies the left portion of the crescent-shaped pancreatic head, whereas the dorsal portion occupies the right portion. This position allows the endosonographer to see the superior mesenteric vein (closest to the pancreas) and the superior mesenteric artery (deeper and thicker wall when compared with the

superior mesenteric vein) in addition to the ventral and dorsal anlage.

This is also the position required for detailed imaging of the ampulla of Vater, either to assess an ampullary adenoma or cancer or to look for an impacted stone (in the case of gallstone pancreatitis). To image the papilla itself, the duodenum should be paralyzed with hyoscine butylbromide (Buscopan) or glucagon. Once the duodenum is paralyzed, water should be infused into the duodenum to achieve coupling of the ultrasound waves with the papilla without risking compression from the balloon. Exquisite views of the ampulla can be obtained if one can achieve perpendicular positioning of the transducer relative to the papilla, obtain adequate water coupling, and keep the duodenum motionless (Fig. 12.14). The critical anatomic landmark in staging ampullary neoplasms is the muscularis propria of the duodenal wall. If the process disrupts this layer, tumor invasion can be predicted.

**Linear Echoendoscopes.** The ampillary position is exactly the same with the linear as with the radial echoendoscope. The papilla is visualized endoscopically; then the transducer should be positioned perpendicular to the ampulla (Fig. 12.15). The orientation should be such that upward tip deflection should press the transducer against the papilla (Video 12.7). If detailed images of the papilla are required, the duodenum should be paralyzed and water infused into the duodenal lumen, just as with the radial instrument. In some circumstances, however, when either the radial or the linear echoendoscope is used, the curvature of the duodenum may be too acute to obtain perpendicular orientation between the transducer and the papilla despite maximal upward deflection of the endoscope tip. In this circumstance, imaging of the ampulla is somewhat tangential; this degrades the overall image quality and precision of interpretation. The pancreatic head appears crescent-shaped, but unlike the radial scope, with which the bile and pancreatic ducts are seen in cross section ("snake eyes"), the bile and



**• Fig. 12.12** Papilla of Vater examination: radial echoendoscope. (A) The position required for evaluating the papilla of Vater. (B) The balloon is inflated so that it “kisses” the papilla but without causing mechanical compression. (C) Gentle movement of the transducer enables visualization of the common bile duct (CBD) and the pancreatic duct (PD) coursing through the duodenal wall to the papilla. The presence of two ducts as imaged in this view is termed *snake eyes*. AO, Aorta; IVC, inferior vena cava.

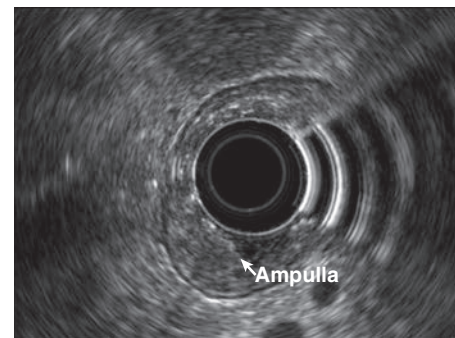


**• Fig. 12.13** The ventral anlage is hypoechoic, triangular, and heterogeneous in echo architecture. It occupies the left portion of the crescent-shaped pancreatic head as compared with the dorsal pancreas, which occupies the right portion. AO, Aorta; CBD, common bile duct; D, dorsal; PD, pancreatic duct; V, ventral.

pancreatic ducts are seen in their linear conformation, with the bile duct more superficial and the pancreatic duct deep. Imaging is carried out by slow withdrawal and continuous gentle torquing clockwise and counterclockwise until the portal vein confluence is seen. This landmark signifies the completion of this station.

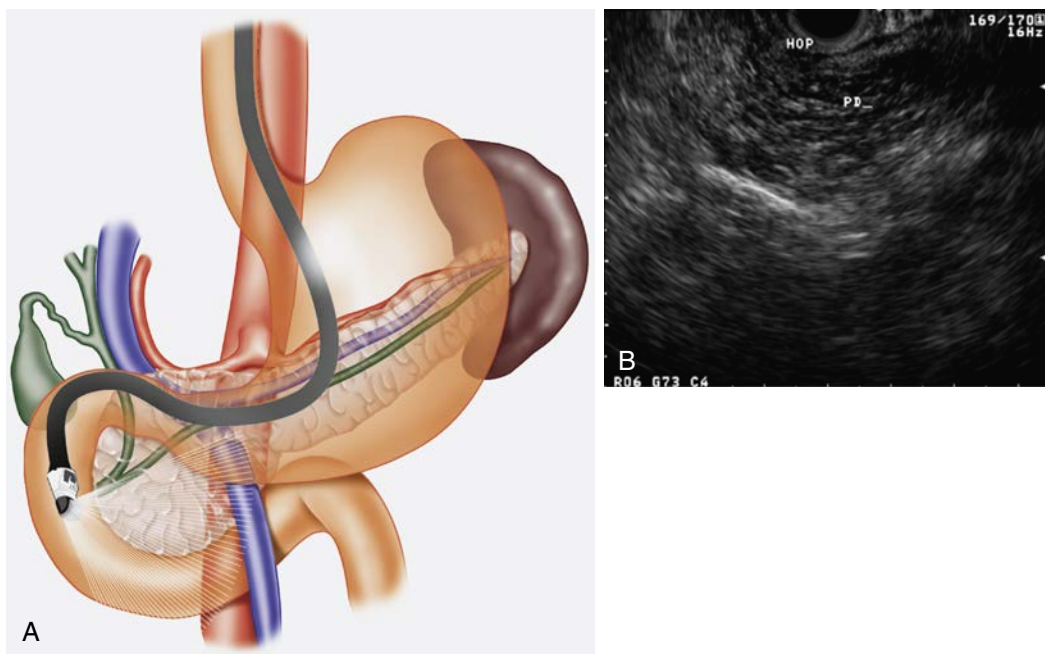
### Uncinate

**Radial Echoendoscopes.** The uncinate process can be imaged by positioning the transducer distal to the ampulla of Vater. The critical anatomic structure in this position is the aorta. The up-down dial should be turned maximally up, and the right-left control should be locked in the right position. Very gentle

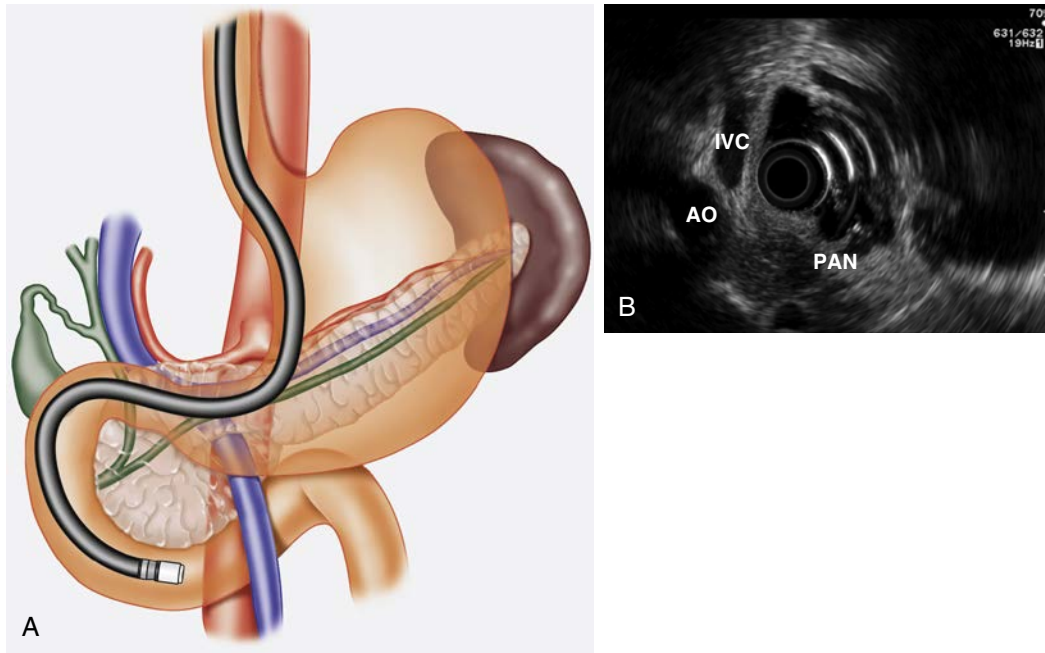


**• Fig. 12.14** The ampulla is imaged best by perpendicular positioning of the transducer relative to the papilla coupled with water insufflation and a motionless duodenum.

counterclockwise torque allows visualization of the aorta, which, if the transducer is deep enough in the duodenum, is seen initially in its longitudinal conformation. At this point electronic rotation is used to position the aorta so that it courses from top to bottom on the left side of the screen (Video 12.8). Slow withdrawal is then commenced. As the scope is withdrawn, the aorta slowly goes from linear to oval and ultimately to a cross-sectional (round) configuration. From this position, the inferior vena cava is usually visible as well and is typically superior to the aorta. At this point, if one looks to the right of the aorta, the uncinate process will emerge (Fig. 12.16). The pancreas is initially triangular but changes to a crescent shape as one withdraws to the level of the



• **Fig. 12.15** Papilla of Vater examination: linear echoendoscope. (A) The transducer is placed at a perpendicular angle to the papilla of Vater. (B) From this position, the pancreas has a crescent shape, and the bile duct and pancreatic duct can be seen to emerge from the papilla.



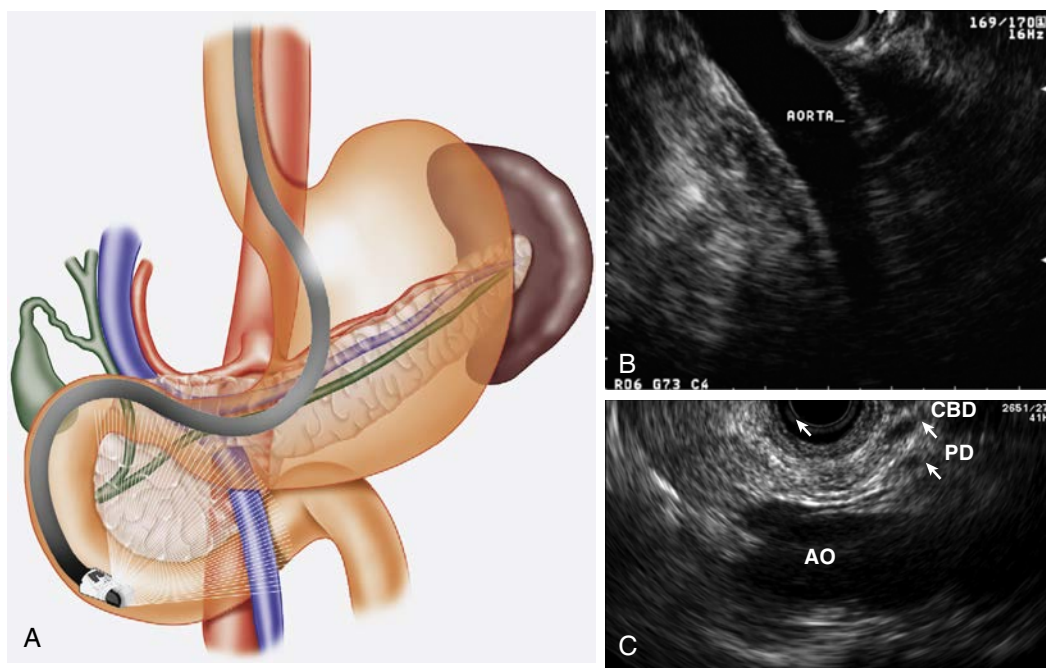
• **Fig. 12.16** Uncinate examination: radial echoendoscope. (A) This illustration reveals the echoendoscope in the second portion of the duodenum. (B) At this station, by gradual scope withdrawal, the uncinate portion of the pancreas (PAN) is visualized to the right of the aorta (AO). IVC, Inferior vena cava.

papilla. The aorta is critical for this position because if one does not see the pancreas adjacent to the aorta, one cannot be sure that the uncinate process has been visualized.

One problem that can be encountered with withdrawal from this position is that the echoendoscope can suddenly flip back into the duodenal bulb. This problem can be avoided by manipulating the echoendoscope as one would a colonoscope; instead of

slow, steady withdrawal, the echoendoscope is withdrawn a slight amount and then advanced a slight amount. If one can maintain one-to-one reaction of the echoendoscope to the manipulation of the shaft, rapid uncontrolled withdrawal can be avoided.

**Linear Echoendoscopes.** The transducer should be passed just distal to the ampulla, and the instrument shaft should be rotated clockwise or counterclockwise, as necessary, to locate the aorta.



• **Fig. 12.17** Uncinate examination: linear echoendoscope. (A) The transducer is placed distal to the papilla, and the tip of the echoendoscope is moved upward. (B) From this position, the aorta can be sought; the pancreas is viewed adjacent to it. (C) Gradual withdrawal and torquing of the echoendoscope reveal the uncinate portion of the pancreas. AO, Aorta; CBD, common bile duct; PD, pancreatic duct.

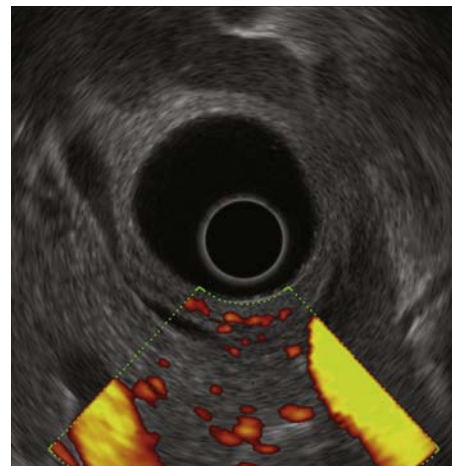
Once the aorta has been visualized, the echoendoscope should be torqued (usually clockwise) and slowly withdrawn (Video 12.9). With this maneuver, the uncinate process comes into the image adjacent to the transducer and to the right of the aorta (Fig. 12.17). The endosonographer simply withdraws the scope slowly while gently torquing back and forth.

It is not possible to read a book and translate the reading to successful imaging of the pancreas. Successful imaging has innumerable nuances, and each patient's anatomy is different. Each case presents its own unique challenges, and no endosonographer, no matter how experienced, achieves successful and complete imaging in all patients. One is always limited by the patient's individual anatomic features, and these limitations must be accepted.

## Bile Duct

EUS imaging of the bile duct is relatively straightforward, but overall it is easier and more efficiently performed with a radial scanning echoendoscope. Basically, two positions must be achieved to evaluate the extrahepatic portion of the bile duct fully. The first position, mentioned earlier, is the apical position. The second position, which is important for achieving full visualization of the bile duct, is one in which the transducer "kisses" the papilla. With a radial scanning echoendoscope, the apical position usually permits a very broad section of the bile duct to be visualized at one time.

Achieving the apical position begins with the tip of the instrument in the stomach. The echoendoscope is advanced along the greater curve of the stomach with a little downward tip deflection to enable visualization of the pylorus. Slight upward tip deflection is applied just before entering the pylorus, and, once the instrument is within the duodenal bulb, air is instilled along with slight downward tip deflection to visualize the apex of the duodenal



• **Fig. 12.18** The use of color Doppler imaging distinguishes the bile duct from the surrounding vasculature.

bulb (see Video 12.4). The tip of the scope is then positioned in the area of the apex, the balloon is inflated until it occludes the lumen, and slight clockwise torque is then applied to the instrument shaft. Ultrasound imaging then begins. The first structure to look for is the liver. The image should be rotated such that the liver is positioned in the upper left-hand portion of the screen. From this position at least a portion of the bile duct can usually be visualized, although slight advancement or withdrawal of the echoendoscope may be required. The bile duct is seen as an anechoic tubular structure coursing right, adjacent to the transducer (see Figs. 12.9 and 12.18).

The most important landmark of the apical position is the duodenal falloff. This represents the muscularis propria of the duodenum and is seen to course just adjacent to the transducer

and then to fall away directly from it in the 6 o'clock position of the screen. Once the bile duct is visualized, one should recognize that it typically has three layers. Withdrawal and counterclockwise torque of the echoendoscope allow visualization of the bile duct toward the hilum, and clockwise torque and insertion of the endoscope shaft allow visualization of the distal bile duct as it enters the papilla.

The most common mistake made with apical imaging is that the endosonographer allows the transducer to slip back into the duodenal bulb. Some gentle pressure should be kept against the shaft of the instrument to prevent this problem. It is also possible that if too much pressure is applied, the tip will slip around the apex into the second portion of the duodenum. If there is a tendency for this to occur, the balloon should be further inflated on the bulb side of the apex. Once one begins imaging from the apical position, if the bile duct is not recognized within 30 seconds, endoscopic control should be used to reposition the transducer in the apex, and ultrasound imaging should be restabilized. Three to four repositionings within the apex may sometimes be required to achieve proper imaging of the bile duct.

In some cases, a stone is impacted in the distal bile duct. In this circumstance, the only way to detect the stone may be to position the transducer directly perpendicular to the papilla (see [Video 12.6](#)). This is achieved by advancing the echoendoscope into the second portion of the duodenum and then pulling back as one would during an endoscopic retrograde cholangiopancreatography to achieve the straight scope position. The papilla should be visualized endoscopically, the duodenum paralyzed, and water instilled within the duodenal lumen. The balloon is then slightly inflated, but not enough to press firmly against the papilla. One then scans back and forth across the papilla and looks for the bile duct to emerge from the papilla (see [Fig. 12.12C](#)). One must look carefully because, if a small stone is impacted in the ampulla, only shadowing may be seen, without the intensely echogenic rim typically observed with stones in the bile duct or gallbladder. As always, complete imaging of the bile duct may require multiple attempts at each position.

The technique for imaging the bile duct with the linear echoendoscope is the same as that described for the radial instrument. The two positions remain the same: apical and opposite the papilla. Because the plane of imaging for the linear scope is more restricted than that of the radial scope, it may be difficult to obtain long views of the bile duct. The linear instrument should be positioned in the apex of the duodenal bulb, but usually counterclockwise torque is required to image the bile duct, and some left-right tip deflection may be required (see [Videos 12.5](#) and [12.7](#)). The principle remains the same; that is, withdrawal of the instrument from this position generally gives views toward the hilum, whereas advancing the echoendoscope obtains views toward the papilla (see [Fig. 12.11](#)). Use of the linear scope for biliary imaging requires much more careful tracing because one single position provides only a small section of the bile duct. Sometimes it is easier to obtain perpendicular views of the papilla with the linear scope than with the radial scope. Of course color Doppler imaging can be used to help differentiate the bile duct from surrounding vascular structures (see [Fig. 12.18](#)).

## Liver

There are basically three positions for EUS imaging of the liver. No matter how diligent the endosonographer, the extent to which the liver can be imaged depends largely on the patient's



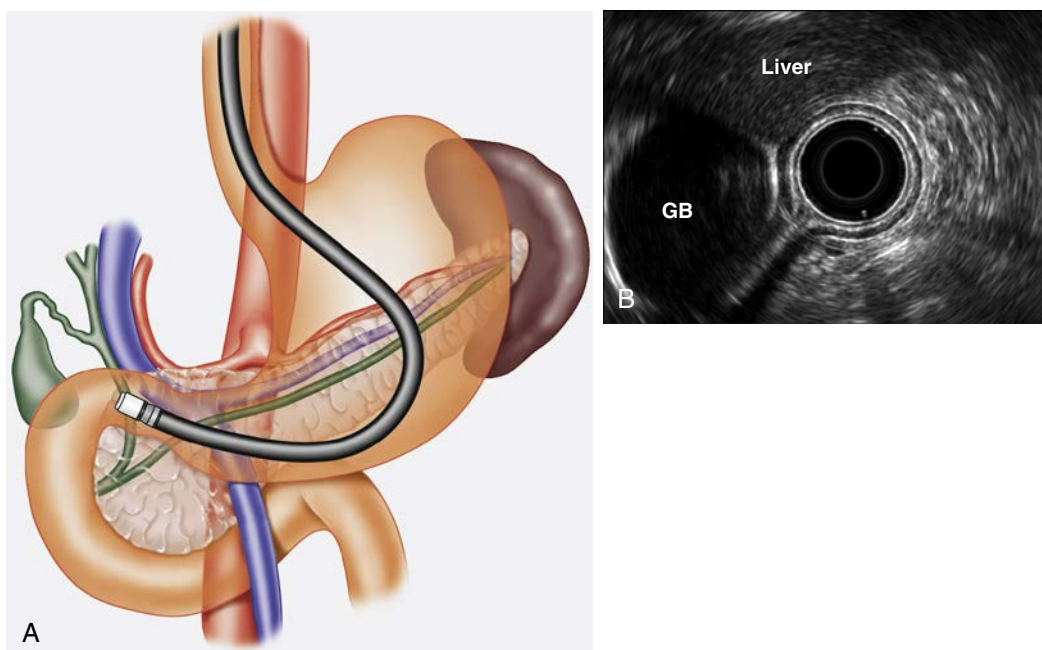
**• Fig. 12.19** The echoendoscope is “locked” in the duodenal bulb, and the tip is deflected for obtaining images of the liver and gallbladder (GB).

anatomy. In general, one should use the lowest frequency available with the instrument to maximize penetration, and the various liver imaging positions should be repeated several times before the examination is declared complete. Electronic scanning echoendoscopes, whether radial or linear, generally allow deeper penetration in liver tissue than do mechanical rotating echoendoscopes.

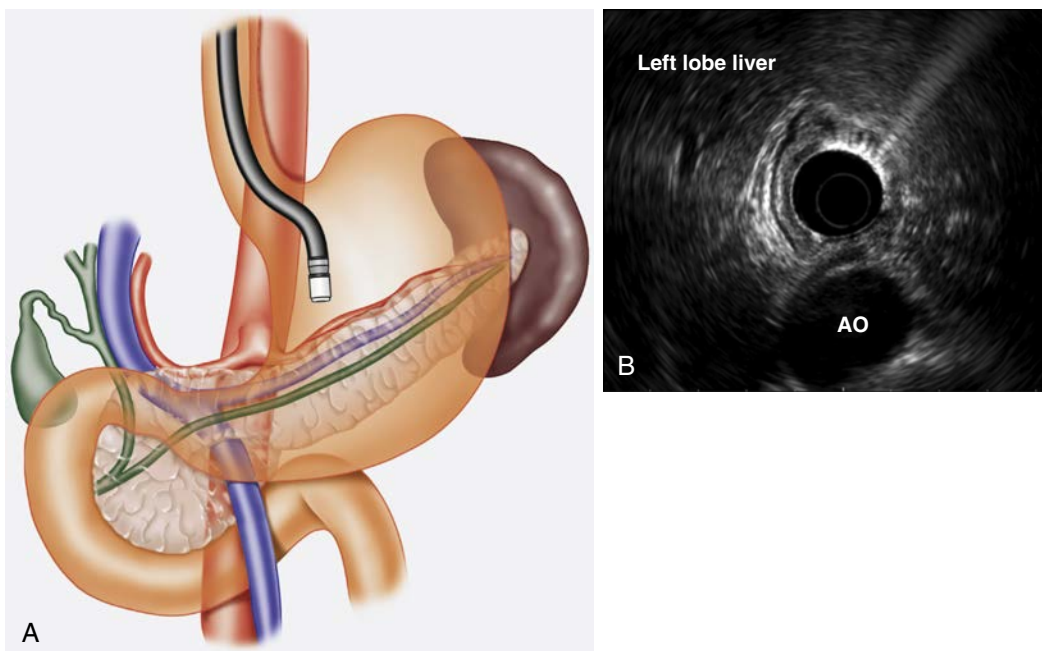
The first liver position is in the duodenal bulb (see [Figs. 12.8](#) and [12.19](#)). If one is using the radial scope, the balloon should be overinflated so that one is “locked” in the bulb ([Video 12.10](#)). From this position, the tip should be deflected so that it presses as firmly as possible against the liver. The echoendoscope is then advanced and withdrawn to its fullest extent, and at the same time clockwise and counterclockwise torquing is used. The instrument should be advanced until the liver disappears and withdrawn until firm pressure is felt against the pylorus. The duodenal bulb is also the best position for imaging the gallbladder, and the technique of balloon overinflation should be used to obtain full views of the gallbladder. Once imaging from this position has been exhausted, the balloon should be deflated and the transducer repositioned in the antrum. With the tip of the scope in the antrum and the balloon inflated ([Fig. 12.20](#)), the echoendoscope tip again should be pressed as firmly as possible against the wall of the stomach that lies next to the liver ([Video 12.11](#)). Once again, the scope should be advanced and withdrawn to its fullest extent during continuous imaging of the left lobe of the liver. The third position is from the fundus of the stomach ([Fig. 12.21](#)). Beginning at the gastroesophageal junction, the transducer is pressed against the gut wall in the direction of the left lobe of the liver ([Video 12.12](#)). From this position, the scope is slowly advanced; at the same time the endosonographer applies clockwise and counterclockwise torque to sweep across the extent of the liver. The scope should be advanced until no further imaging of the liver can be achieved.

The technique and positions are the same whether a radial or a linear instrument is used. It takes more effort with linear scopes to torque the scope shaft to accomplish as complete an examination as possible.

The anatomy of the liver is relatively simple. Branching structures with echogenic walls represent the portal venous system, whereas anechoic structures running alongside the portal venous system and without the echogenicity (and without color Doppler signal) represent branches of the biliary tree. Hepatic cysts are common and anechoic; they have a characteristic echo enhancement along the border of the cyst further from the transducer. Hepatic metastases are generally



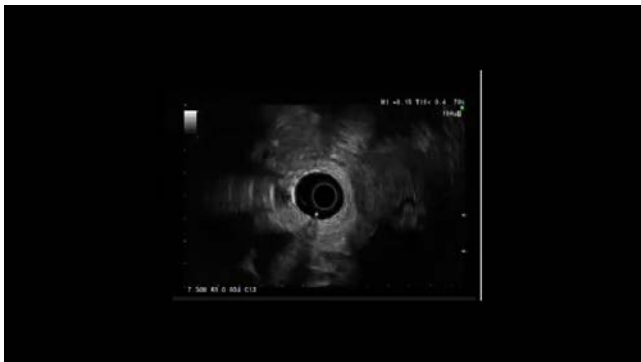
**• Fig. 12.20** Examination of the liver. (A) The echoendoscope positioned in the gastric antrum for visualizing the left lobe of the liver. (B) The echoendoscope tip should be firmly against the gastric wall to image the liver. *GB*, Gallbladder.



**• Fig. 12.21** Examination of the liver. (A) The echoendoscope in the proximal stomach. (B) The scope is pressed firmly against the gut wall to image the left lobe of the liver. *AO*, Aorta.

echo-poor, without a distinct border. Because they can be quite subtle, the endosonographer should scan slowly and carefully. Hepatic veins also lack wall echogenicity and run toward the cranial part of the liver, where they can usually be seen entering the caval vein.

Liver imaging can be a frustrating aspect of endosonography because one cannot be sure that the liver has been imaged completely. As a result, the various positions mentioned earlier should be repeated until the endosonographer is satisfied that the examination has been as complete as possible.



**Video 12.1** Evaluation of the Body and Tail of the Pancreas Using a Radial Echoendoscope



**Video 12.4** Evaluation of the Head of the Pancreas Using a Radial Echoendoscope



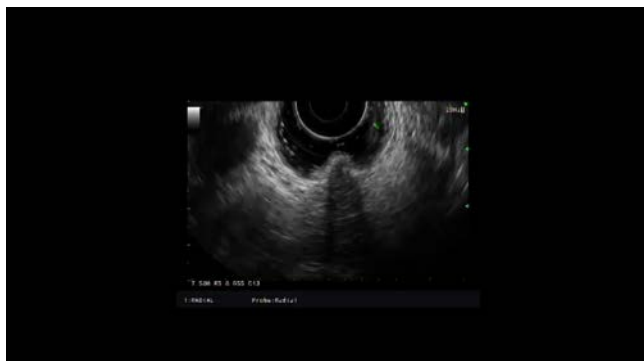
**Video 12.2** Evaluation of the Body and Tail of the Pancreas Using a Curvilinear Echoendoscope



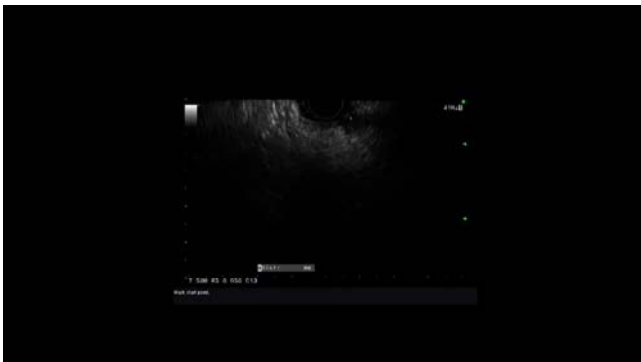
**Video 12.5** Evaluation of the Head of the Pancreas Using a Curvilinear Echoendoscope



**Video 12.3** Evaluation of the Body and Tail of the Pancreas Using a Curvilinear Echoendoscope by Adopting Alternative Techniques



**Video 12.6** Evaluation of the Papilla of Vater Using a Radial Echoendoscope



**Video 12.7** Evaluation of the Papilla of Vater Using a Curvilinear Echoendoscope



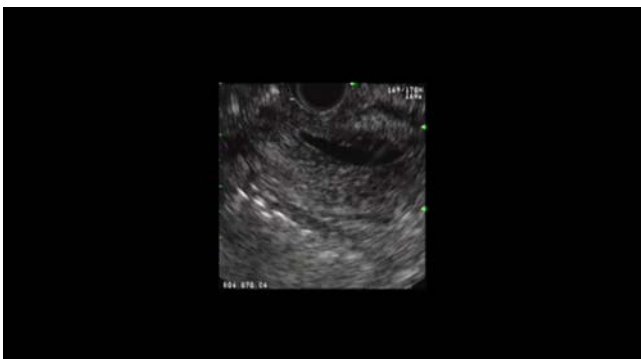
**Video 12.10** Video Demonstrating Imaging of the Liver From the Duodenal Bulb



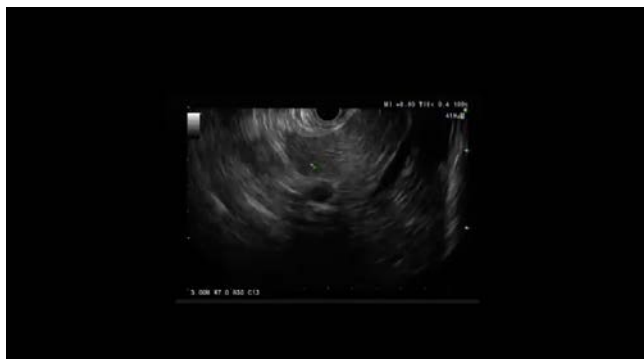
**Video 12.8** Evaluation of the Uncinate Region of the Pancreas Using a Radial Echoendoscope



**Video 12.11** Video Demonstrating Imaging of the Left Lobe of the Liver From the Gastric Antrum



**Video 12.9** Evaluation of the Uncinate Region of the Pancreas Using a Linear Echoendoscope



**Video 12.12** Video Demonstrating Imaging of the Left Lobe of the Liver From the Fundus of the Stomach

# Endoscopic Ultrasound in Inflammatory Diseases of the Pancreas

LARISSA L. FUJII-LAU, SURESH T. CHARI, THOMAS SMYRK, AND MICHAEL J. LEVY

## KEY POINTS

- Endoscopic ultrasound (EUS) imaging is subjective and often nonspecific in inflammatory diseases of the pancreas; therefore, the clinical history and presentation are important when making a final diagnosis.
- EUS-guided fine-needle aspiration (FNA) in inflammatory diseases of the pancreas is predominately used to exclude/diagnose superimposed malignant processes; the role of fine-needle biopsy (FNB) remains to be defined.
- Complementary imaging modalities such as elastography and contrast-enhanced imaging are in the experimental phase and are not recommended for routine use in the evaluation of patients with inflammatory diseases of the pancreas.

## Introduction

Some of the most common pancreatic disorders that a gastroenterologist encounters are inflammatory processes, particularly acute and chronic pancreatitis. Imaging plays a key role in the diagnosis and management of these disorders. Due to the proximity to the pancreas and high-resolution imaging, endoscopic ultrasound (EUS) provides an ideal technique for evaluating the entire pancreas. The capability to obtain aspirates for cytologic evaluation and core biopsies for histologic examination allows for definitive diagnosis of benign and malignant pancreatic processes. Its role in the management of these common inflammatory disorders is evolving and becoming further defined.

Although much less common, autoimmune pancreatitis (AIP) and benign masses of the pancreas often provide diagnostic challenges for the gastroenterologist. Therefore, novel and complementary imaging modalities that can be performed at the time of EUS, namely elastography and contrast-enhanced EUS, are increasingly being used, although with still uncertain utility. This chapter focuses on the role of EUS imaging and tissue sampling for evaluating patients with suspected inflammatory diseases of the pancreas.

## Endoscopic Ultrasound in the Nondiseased Pancreas

Endosonographically, the nondiseased pancreatic parenchyma typically has a homogenous salt and pepper appearance with a thin anechoic tubular structure that runs in the middle of the gland

corresponding to the main pancreatic duct (MPD) ([Fig. 13.1](#), [Video 13.1](#)). The outer contour of the pancreas is normally smooth without significant lobularity. The width of the pancreas in the head, body, and tail measures approximately 19 mm, 13 mm, and 12 mm respectively.<sup>1</sup> The MPD diameter measures on average 2.2 mm in the head, 1.5 mm in the body, and 1 mm in the tail of the pancreas.

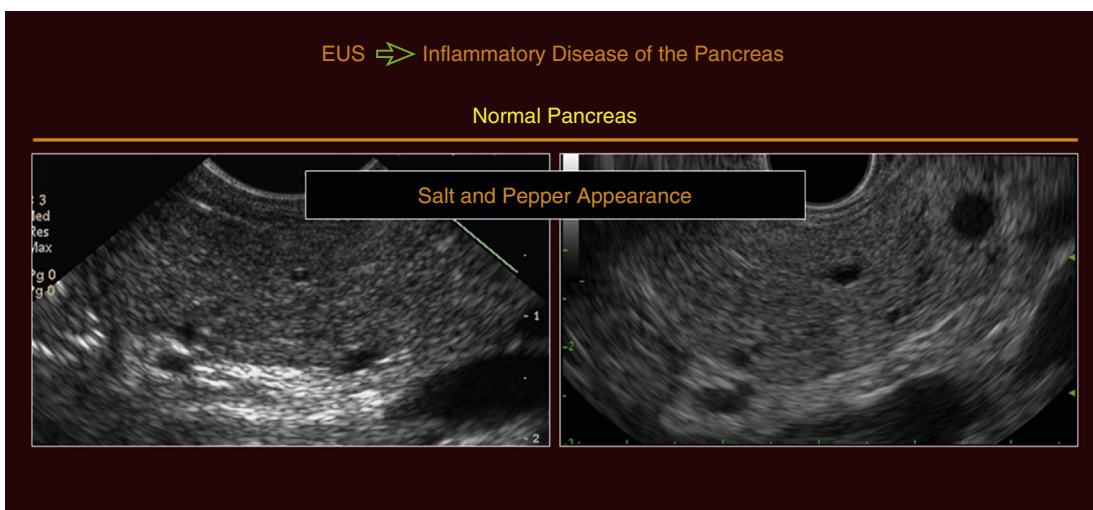
The ventral anlage appears as a focal hypoechoic area in the head of the pancreas and can be seen in up to 75% of patients on EUS.<sup>2</sup> Since the initial reports, the introduction of improved EUS processors and transducers now allows detection in nearly all patients. It is important to not mistake the ventral anlage for a pancreatic mass. Conversely, it is also important to remember that the normally appearing hypoechoic ventral anlage can mask the presence of a small neoplasia or other pathology. When occult pathology is suspected in this region, one may consider careful examination of the ventral anlage from both the bulb and second portion of the duodenum. In addition, use of the cine function and magnification can further aid careful examination.

Unfortunately, the pancreas often demonstrates an altered appearance, possessing some chronic pancreatitis-like features even in the absence of any apparent disease. In patients undergoing EUS for indications unrelated to pancreaticobiliary disease, at least one parenchymal and/or ductal abnormality can be seen in up to 28% of patients.<sup>1</sup> The likelihood of EUS imaging abnormalities increases with patient age, particularly in patients >60 years old, and male gender. The most common abnormality is hyperechoic stranding. Other studies have shown that alcohol consumption at low levels increases the likelihood of detecting hyperechoic foci, MPD dilation, and ductal wall hyperechogenicity, whereas smoking increases the finding of hyperechoic foci.<sup>3</sup> Small visible side branches <1 mm can also be seen in patients without pancreaticobiliary symptoms.<sup>4</sup>

## Chronic Pancreatitis

### Brief Overview

Chronic pancreatitis (CP) results from progressive inflammation and scarring of the pancreas. Patients may initially present with recurrent acute pancreatitis and occasionally patients presenting with their first known episode of acute pancreatitis may already have structural and functional changes secondary to chronic



• **Fig. 13.1** Endoscopic ultrasonography demonstrates the normal salt and pepper appearance in asymptomatic patients without pancreatic pathology who underwent EUS for alternate indications. (See Video 13.1.)

pancreatitis. Pain, classically located in the epigastrium with radiation to the back and worsened by eating, is the most common symptom. When more than 85% to 90% of the pancreas is affected, patients may also manifest exocrine insufficiency (with steatorrhea, weight loss, and fat-soluble vitamin deficiency) and/or endocrine insufficiency (with glucose intolerance or diabetes mellitus).<sup>5</sup>

Although the diagnosis of CP is straightforward in patients with severe disease manifested by the presence of calcifications and a dilated MPD, the diagnosis is far more challenging in early disease stages. Furthermore, whereas pancreatic calcifications most often result from CP, calcifications may be seen in other forms of pancreatic pathology including neuroendocrine tumors, intraductal papillary mucinous neoplasms, mucinous cystic neoplasia, serous cystadenoma, and some pancreatic adenocarcinomas.<sup>6</sup> The pattern and extent of calcification often provides a diagnostic clue as patients with CP often manifest MPD and parenchymal calcification, the latter of which is often actually contained within peripheral side branches. In addition, a dilated MPD may result from other important pathologies including an obstructing neoplasm or main duct intraductal papillary mucinous neoplasm (IPMN) rather than CP.

The diagnosis of CP relies on a combination of symptoms, noninvasive radiographic imaging (computed tomography [CT], magnetic resonance imaging [MRI]/magnetic resonance cholangiopancreatography [MRCP]), and/or EUS. In patients with documented CP, the most common CT findings (in decreasing order of frequency) include a dilated MPD with secondary radicals (68%), pancreatic parenchymal atrophy (54%), pancreatic calcifications (50%), fluid collections (30%), focal pancreatic enlargement (30%), biliary ductal dilation (29%), alterations in peripancreatic fat (16%), and a normal pancreas (7%).<sup>7</sup> Unfortunately, these CT findings are not specific for CP. CT is also used to help detect complications of CP and exclude other diseases associated with abdominal pain. MRI/MRCP, particularly with secretin stimulation, has improved sensitivity over CT for the detection of early CP.<sup>8</sup> Findings on MRI/MRCP include MPD dilation, side-branch abnormalities, strictures, intraductal stones, intrapancreatic cyst formation, parenchymal atrophy, and abnormal decreased signal intensity on T1-weighted images of the pancreas

with delayed and limited enhancement after contrast administration. MPD compliance with distention (normal is approximately 1 mm) and side-branch abnormalities after secretin stimulation has enhanced the ability of MRI to detect early CP.

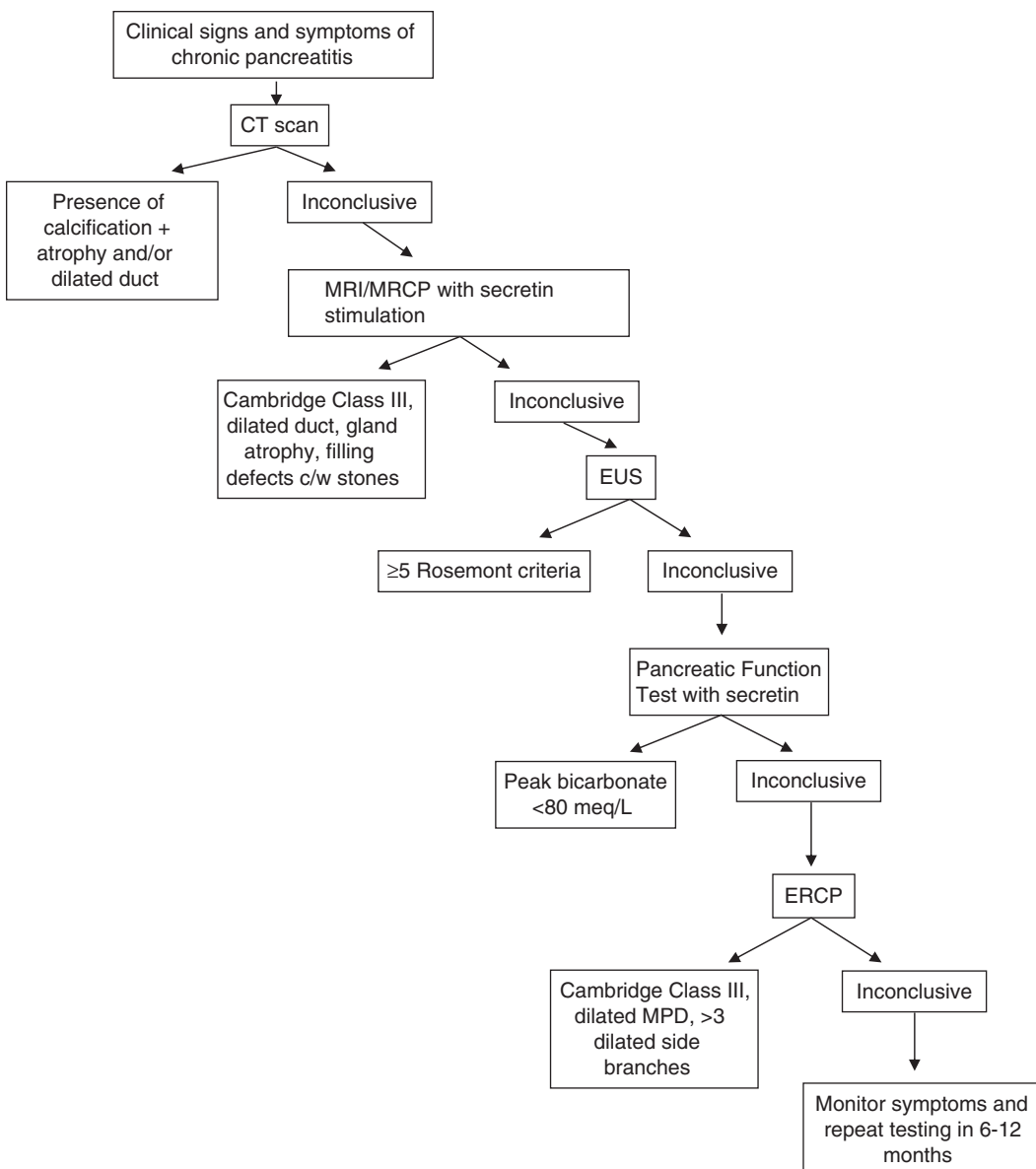
## Role of Endoscopic Ultrasound

The American Pancreatic Association (APA) recommends a step-wise approach to diagnose CP (Fig. 13.2).<sup>8</sup> In patients with compatible clinical signs and symptoms, the APA initially recommends a CT that, if nondiagnostic, should be followed by MRI/MRCP with secretin stimulation. The society recommends EUS only when the results of noninvasive imaging are nondiagnostic or inconclusive. If the EUS is inconclusive, the APA recommends pancreatic function testing with secretin administration. However, it should be noted that pancreatic function testing has a narrow role due to the limited availability, poor patient tolerance, and suboptimal diagnostic accuracy. Finally, the use of diagnostic endoscopic retrograde cholangiopancreatography (ERCP) may be considered only after the aforementioned evaluation when the diagnosis remains indeterminate. As the various clinical and imaging features of CP are often nonspecific and commonly seen in patients without pancreatic disease, it is important to interpret the findings with caution and in the appropriate clinical setting. This need is even greater when contemplating therapeutic interventions, for which EUS may have a role (Figs. 13.3 to 13.8, Videos 13.2 and 13.3).

## Endoscopic Ultrasound Imaging Characteristics

### *Endoscopic Ultrasound Criteria for Chronic Pancreatitis*

Conventional EUS criteria for the diagnosis of CP rely on the evaluation of nine features. The four parenchymal features include hyperechoic foci (distinct 1 to 2 mm hyperechoic points), hyper-echoic strands (hyperechoic irregular lines >3 mm), lobularity (2 to 5 mm lobules), and cysts (thin-walled hypoechoic structures >2 mm within the confines of the parenchyma), whereas the five ductal features include MPD dilation (>3 mm in the head, >2 mm in the body, and >1 mm in the tail of the pancreas), ductal

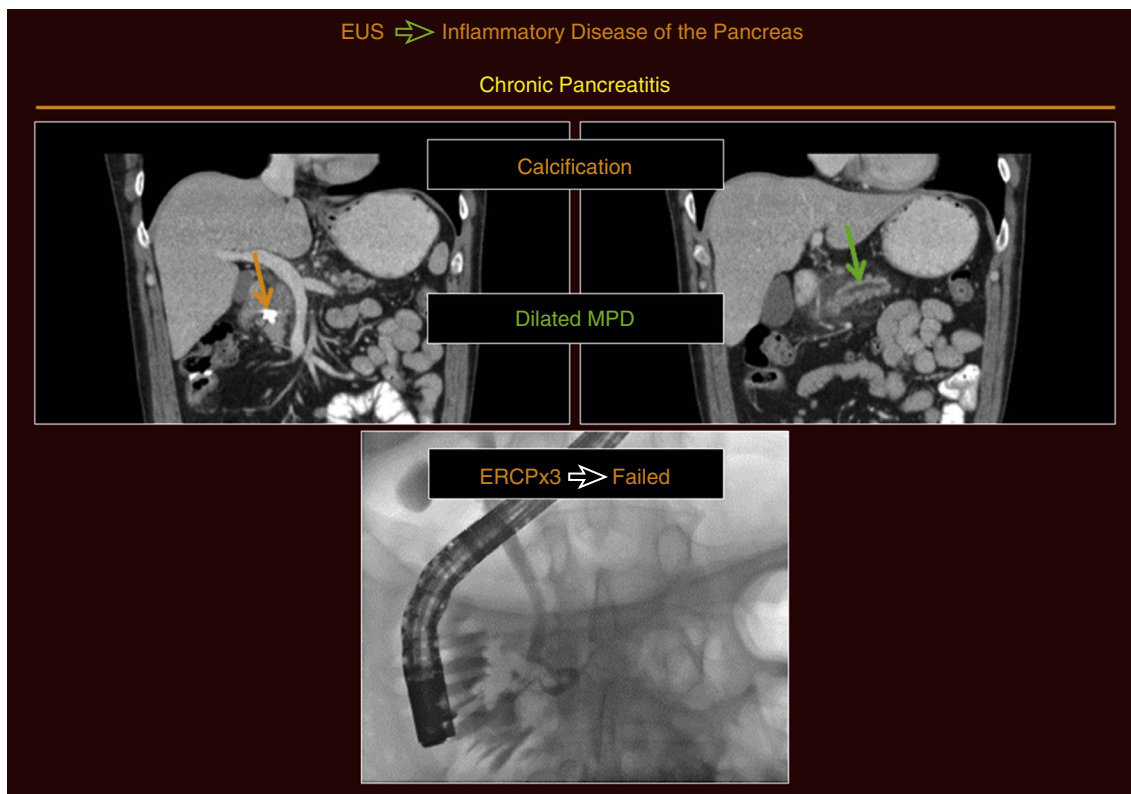


• **Fig. 13.2** Proposed algorithm for the diagnosis of chronic pancreatitis.<sup>8</sup> *CT*, Computed tomography; *ERCP*, endoscopic retrograde cholangiopancreatography; *EUS*, endoscopic ultrasound; *MPD*, main pancreatic duct; *MRCP*, magnetic resonance cholangiopancreatography; *MRI*, magnetic resonance imaging.

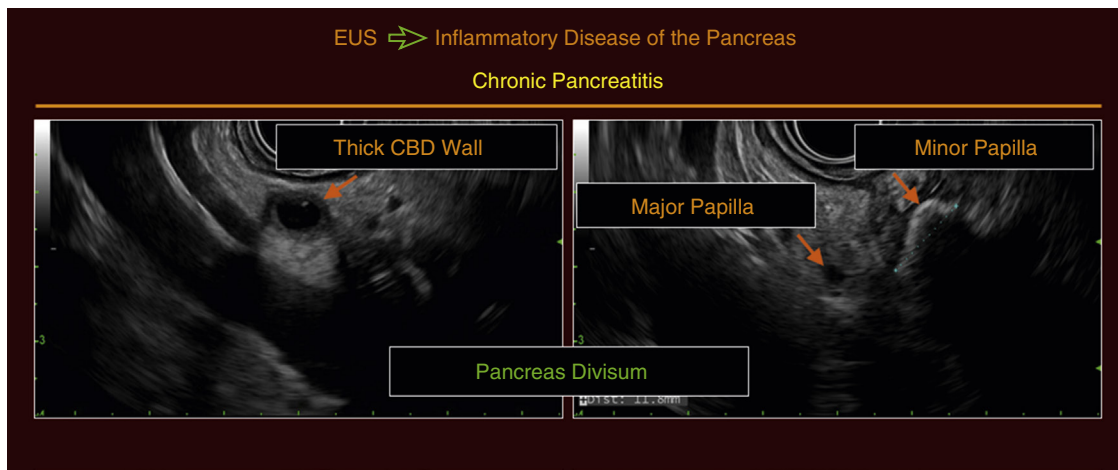
irregularity, hyperechoic duct margins, visible side branches, and intraductal stones (Figs. 13.9 to 13.12, Videos 13.4 and 13.5).<sup>8,9</sup> The ideal cutoff for the number of EUS criteria needed to diagnose CP varies among endosonographers, institutions, and study protocols. Many consider the finding of 1 to 2 criteria as indicative of a normal pancreas, 3 to 4 criteria indicate early CP, and  $\geq 5$  criteria consistent with CP.<sup>8</sup> Understandably, the higher the threshold required for diagnosis, the lower the sensitivity and higher the specificity of the criteria.

More recently, some have adopted the use of an alternate EUS-based classification system to diagnose CP (the Rosemont classification), which was developed from a consensus of internationally recognized endosonographers.<sup>10</sup> The criteria are divided into major and minor criteria based on their perceived accuracy for diagnosing CP. In addition, the three major criteria are subdivided into major A and major B features depending on their predictive diagnostic accuracy. The major criteria include: hyperechoic foci with

shadowing (major A), MPD calculi (major A), and lobularity with honeycombing (major B). The eight minor criteria include: lobularity without honeycombing, hyperechoic foci without shadowing, cysts, stranding, irregular MPD contour, dilated side branches, MPD dilation, and a hyperechoic MPD margin. Table 13.1 defines each criterion. Using these major and minor criteria, the Rosemont classification establishes a diagnosis that is “consistent with CP” if any of the following is present: 1 major A feature +  $\geq 3$  minor features, 1 major A feature + major B feature, or 2 major A features. EUS examinations “suggestive of CP” include the following: 1 major A + <3 minor features, major B and  $\geq 3$  minor features, or  $\geq 5$  minor features. Those classified as “indeterminate for CP” include: >2 minor features, <5 minor features without major features, or major B feature + <3 minor features. A “normal” result is one that has  $\leq 2$  minor features, excluding cysts, dilated MPD and side branches, hyperechoic foci without shadowing, and major features.



• **Fig. 13.3** A 48-year-old male presented with clinical and computed tomography (CT) evidence of chronic pancreatitis with a large pancreatic head duct stone and upstream ductal dilatation. Three prior efforts at endoscopic retrograde cholangiopancreatography (ERCP) failed and the patient was referred for further evaluation and stone clearance. CT revealed a large stone (orange arrow) within the main pancreatic duct within the pancreatic head with upstream ductal dilatation (green arrow). During three prior ERCPs at the referring center, there was failure to cannulate the pancreatic duct. MPD, Main pancreatic duct.



• **Fig. 13.4** A 48-year-old male presented with clinical and computed tomography evidence of chronic pancreatitis with a large pancreatic head duct stone and upstream ductal dilatation. Three prior efforts at endoscopic retrograde cholangiopancreatography failed and the patient was referred for further evaluation and stone clearance. Endoscopic ultrasound demonstrated a thickened bile duct wall suggestive of downstream obstruction (left image). Continued imaging revealed a remote location of the minor papilla, relative to the major papilla, initially establishing the diagnosis of pancreas divisum that had been missed on prior cross-sectional imaging (right image). The large stone was seen in the accessory duct. CBD, Common bile duct. (See Video 13.2.)

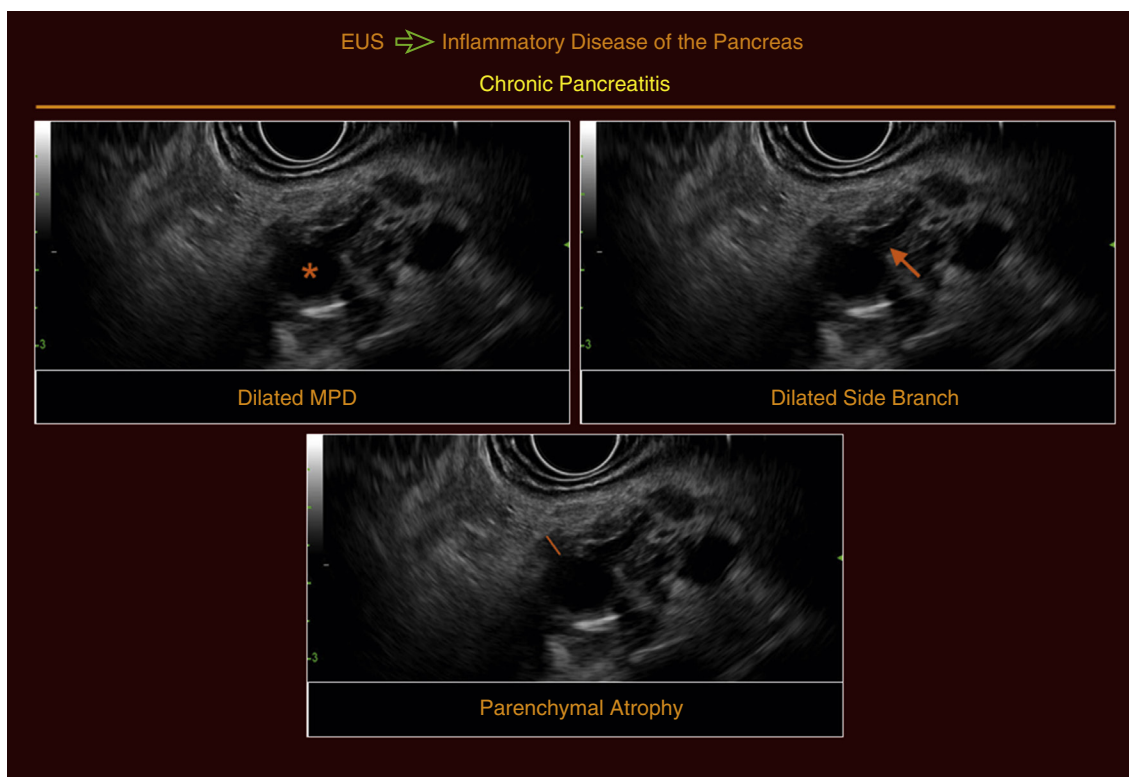


**Fig. 13.5** A 48-year-old male presented with clinical and computed tomography evidence of chronic pancreatitis with a large pancreatic head duct stone and upstream ductal dilatation. Three prior efforts at endoscopic retrograde cholangiopancreatography failed and the patient was referred for further evaluation and stone clearance. Endoscopic ultrasound demonstrated typical features of chronic pancreatitis including a dilated main pancreatic duct (MPD) (upper left), dilated side branches (upper right), and parenchymal atrophy (bottom). It is likely that some of the features were secondarily induced by the large stone and resulting obstructive changes. (See Video 13.3.)

### Comparison of Conventional and Rosemont Classification

As expected based on the definitions for each feature and multiple means in which the grouped criteria can be analyzed, the Rosemont classification is more stringent than the conventional classification and is more difficult to remember and employ in clinical practice.<sup>11</sup> Comparative studies demonstrate that when using a cutoff of 3 criteria for the conventional classification more patients are diagnosed with CP; however, when using a cutoff of 5 features there is no significant difference in the number of patients diagnosed with CP using conventional classification as compared to the Rosemont classification when combining both “consistent with” and “suggestive of” CP. The Rosemont classification of “consistent with CP” is the most stringent threshold for diagnosing CP, even more than a cutoff of 5 features in the conventional means of classification.

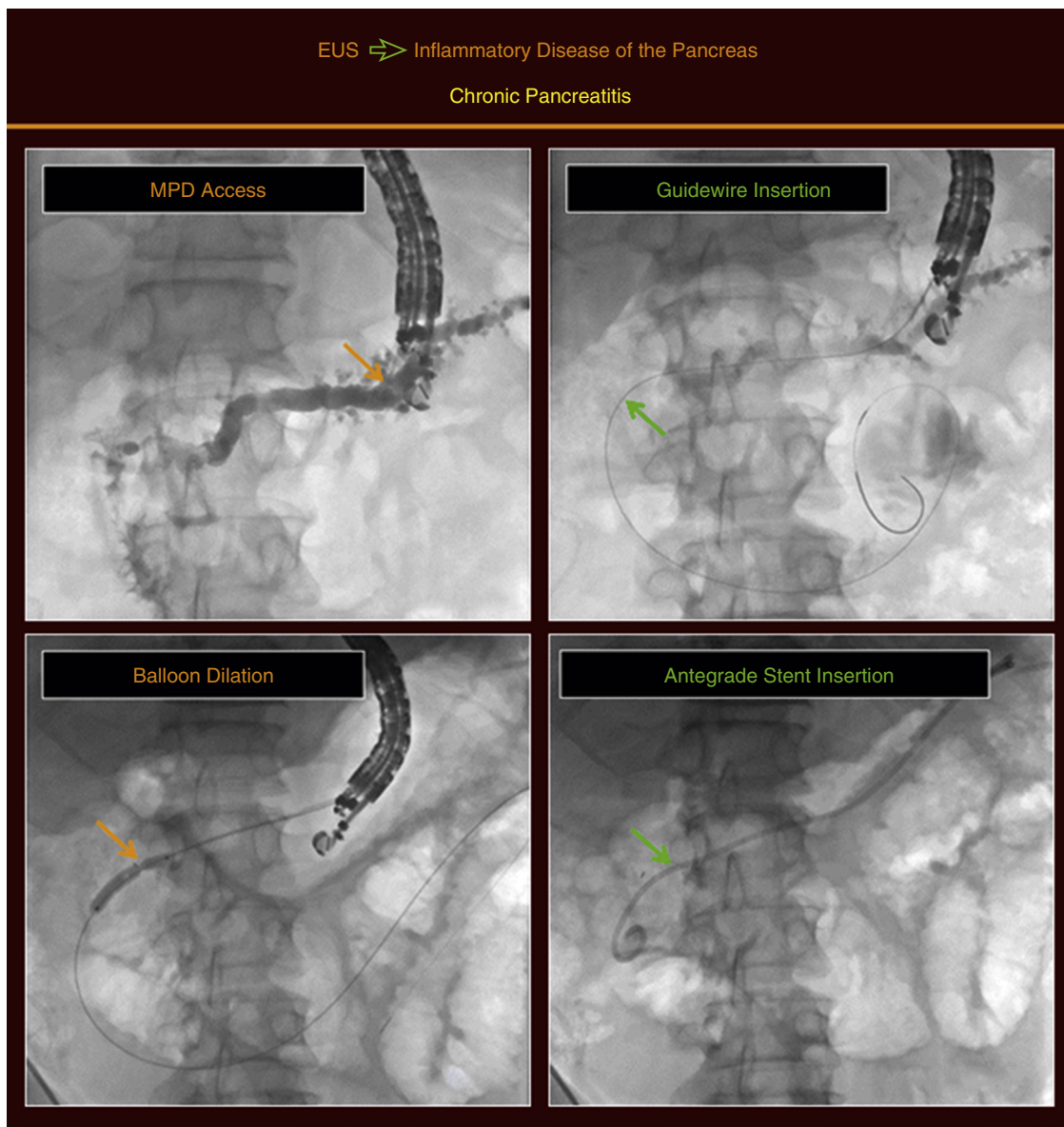
### Correlation of Endoscopic Ultrasound Findings and Surgical Histopathology

In a study assessing conventional EUS criteria in patients who later underwent pancreatic surgery, the presence of  $\geq 4$  criteria was the best predictor of histologic CP with a sensitivity, specificity, and accuracy of 90.5%, 85.7%, and 88.1%, respectively.<sup>9</sup> There was also excellent correlation between the number of EUS features and the histologic fibrosis score ( $r = 0.85$ ,  $P < .0001$ ). In particular, hyperechoic foci ( $P < .0001$ ), hyperechoic strands ( $P > .001$ ), lobularity ( $P = .04$ ), stones ( $P < .001$ ), dilated MPD ( $P < .0001$ ), irregular MPD ( $P < .0001$ ), irregular side branches ( $P < .001$ ), and hyperechoic MPD margins ( $P = .03$ ) were all significantly

associated with fibrosis on histology. A dilated or irregular MPD had the highest sensitivity, specificity, and accuracy in determining the presence of fibrosis.

Another study also demonstrated that the presence of  $\geq 4$  EUS criteria predicted the presence of CP in patients who underwent total pancreatectomy with islet autotransplantation for noncalcific CP.<sup>12</sup> However, the sensitivity, specificity, and accuracy in determining a fibrosis score  $\geq 6$  in the resected specimen was lower than the previous study at 61%, 75%, and 63%. They found a poor, but significant, correlation between EUS features and degree of fibrosis ( $r = 0.24$ ,  $P < .05$ ). None of the individual conventional features was significantly predictive of the presence of fibrosis on univariate analysis. When linear regression was performed after adjusting for age, sex, BMI, smoking, and alcohol exposure, only MPD irregularity ( $P = .02$ ) was found to be predictive of CP. As expected, in another study that used a lower cutoff for the fibrosis score on surgically resected specimens (fibrosis score  $\geq 2$ ), the presence of  $\geq 4$  EUS criteria was shown to have a higher sensitivity and specificity of 84% and 100%, respectively.<sup>13</sup>

The aforementioned study methodologies and results highlight a notable difficulty using the fibrosis score—namely, the lack of consensus regarding the appropriate threshold of this histologic criterion for diagnosing CP. Also, the use of a fibrosis score alone as a diagnostic gold standard for CP is problematic in that it may simply reflect the presence of “bland” fibrosis, which is fibrosis seen in the absence of parenchymal destruction or inflammation that is often present in asymptomatic patients without endocrine



**• Fig. 13.6** A 48-year-old male presented with clinical and computed tomography evidence of chronic pancreatitis with a large pancreatic head duct stone and upstream ductal dilatation. Three prior efforts at endoscopic retrograde cholangiopancreatography failed and the patient was referred for further evaluation and stone clearance. After failed endoscopic retrograde pancreatectomy (ERP), endoscopic ultrasound was used to guide main pancreatic duct (MPD) access (upper left), guidewire insertion (upper right), balloon dilation (bottom left), and finally antegrade stent insertion (bottom right).

or exocrine dysfunction.<sup>1</sup> Such “bland” fibrosis has been reported in the setting of alcoholism, advanced age, male gender, obesity, and cigarette smoking. This finding may be detected in patients without any evidence of CP with normal pancreatic imaging, function, and histology. However, there is some debate whether bland fibrosis indicates the presence of very early disease that is prone to progress in severity over time. This theory is unlikely to account entirely for this situation, given the unmatched finding of bland fibrosis in up to 60% versus the lifetime risk of 2% to 5% of CP in alcoholics. Whether bland fibrosis represents an early stage of CP and/or separate entity is unclear. Caution is needed when performing EUS because this clinically occult bland fibrosis may be indistinguishable from CP and can result in overdiagnosis (Figs. 13.13 and 13.14, Video 13.6).

Certain individual and grouped criteria have been found to correlate with surgical pancreatic histology. In a study evaluating 100 patients with suspected CP who underwent EUS followed within 1 year by pancreatic resection, lobularity with honeycombing, hyperechoic foci with shadowing, dilated MPD, irregular MPD, and dilated side branches were each associated with histologically diagnosed severe CP.<sup>14</sup> The highest odds ratio between EUS features and the histopathologic findings included hyperechoic foci with shadowing in the head of the pancreas and large duct diameter (odds ratio [OR] 10.9; 95% confidence interval [CI] 2.9 to 40.5), hyperechoic foci with shadowing in the head of the pancreas and calcifications (OR 8.8; 95% CI 2.6 to 28), pancreatic head cysts and pseudocysts (OR 12.9; 95% CI 3.2 to 52.3), MPD dilation in the head of the pancreas and large duct

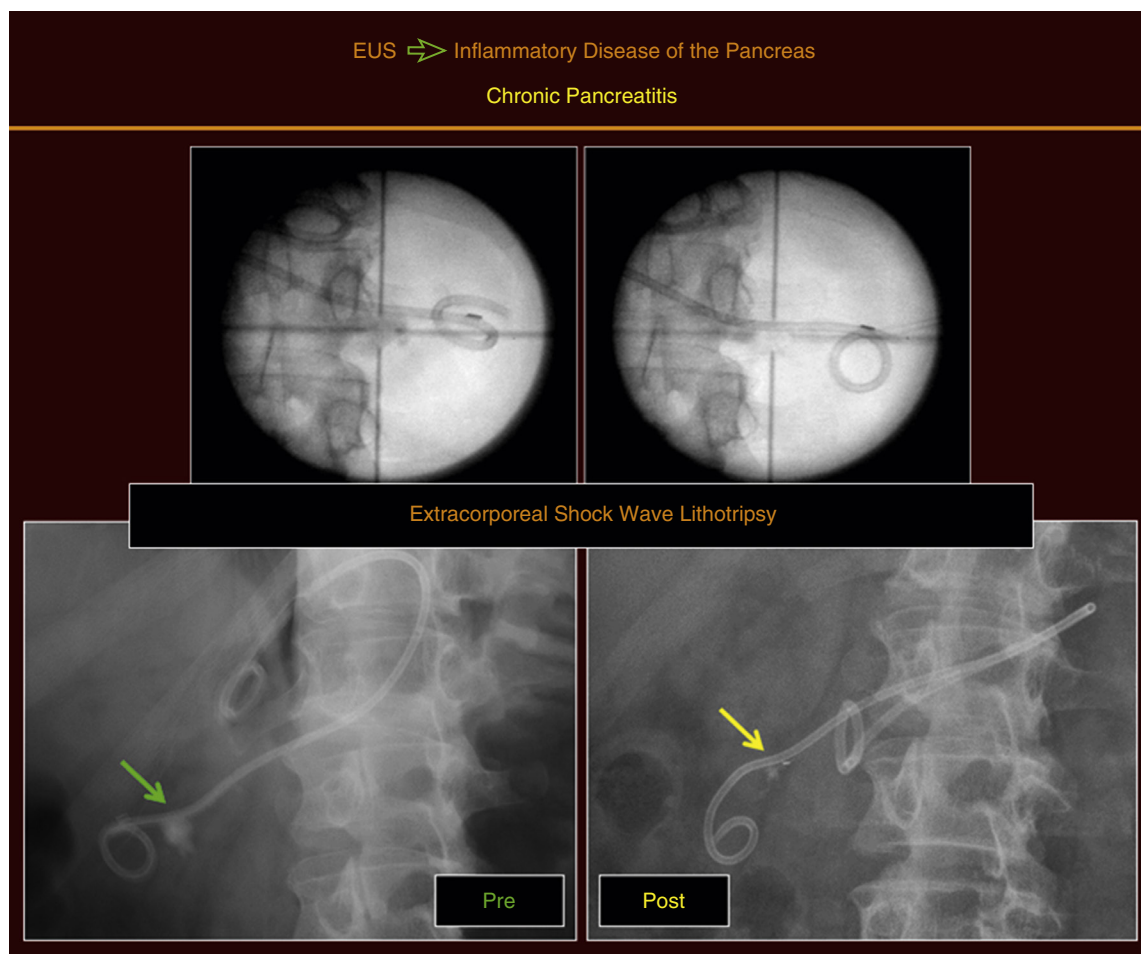


**Fig. 13.7** A 48-year-old male presented with clinical and computed tomography evidence of chronic pancreatitis with a large pancreatic head duct stone and upstream ductal dilatation. Three prior efforts at endoscopic retrograde cholangiopancreatography failed and the patient was referred for further evaluation and stone clearance. Extracorporeal shock wave lithotripsy was subsequently performed (*upper images*), which resulted in stone fracturing (*bottom images*).

distortion (OR 12.8; 95% CI 2.6 to 62.9), dilated side branches in the head of the pancreas and large duct distortion (OR 6.4; 95% CI 1.9 to 22), lobularity with honeycombing in the body or tail of the pancreas and large duct distortion (OR 6.2; 95% CI 1.3 to 30.2), and cysts in the body or tail of the pancreas and pseudocysts (OR 32; 95% CI 4.6 to 222.6). Therefore, although the standard and Rosemont classification systems rely on evaluation of the body and tail of the pancreas, this study shows that findings in the head of the pancreas may also be important in the diagnosis of CP. However, until confirmatory data are generated, we encourage caution if adopting this practice given the common presence of altered EUS morphology within the pancreatic head even among patients without any clinical evidence of pancreatic pathology.

#### Interobserver Variability

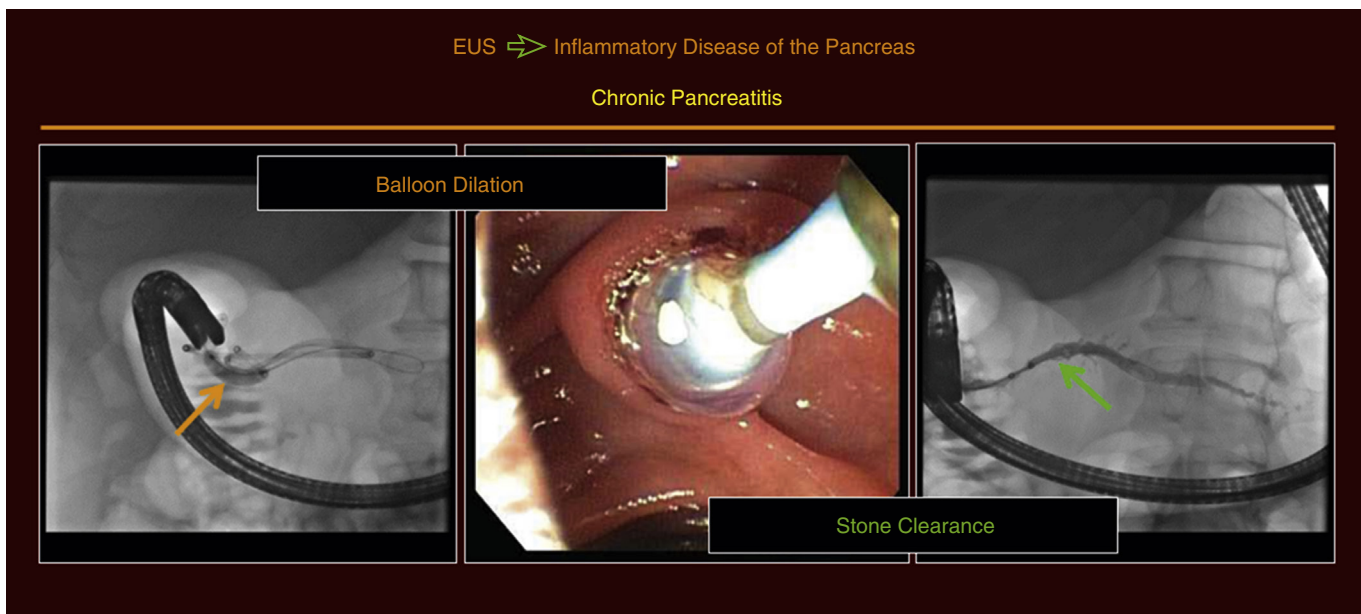
One of the major limitations when using EUS to diagnose CP is the suboptimal interobserver variability (IOA). Using conventional criteria, IOA was determined between 11 expert endosonographers who reviewed EUS videotapes from 33 patients with suspected CP and 12 controls.<sup>15</sup> The kappa was moderately good for the overall agreement on the presence of CP ( $K = 0.45$ ). In regard to individual features, only MPD dilation ( $K = 0.6$ ) and lobularity ( $K = 0.51$ ) had good agreement; the remaining seven

features had poor IOA. Another study assessed same-day back-to-back EUS examinations by two different endosonographers on 24 patients without any evidence of pancreaticobiliary disease.<sup>16</sup> Despite the lack of any clinical or imaging evidence of CP, 32% of patients had hyperechoic strands, 30% had hyperechoic ductal walls, 16% had hyperechoic foci, 14% had a dilated MPD, 9% had lobularity, and 5% had parenchymal cysts. The IOA between these two endosonographers was good for hyperechoic strands and parenchymal cysts, moderate for lobularity, dilated MPD, and hyperechoic foci, and fair for hyperechoic foci.

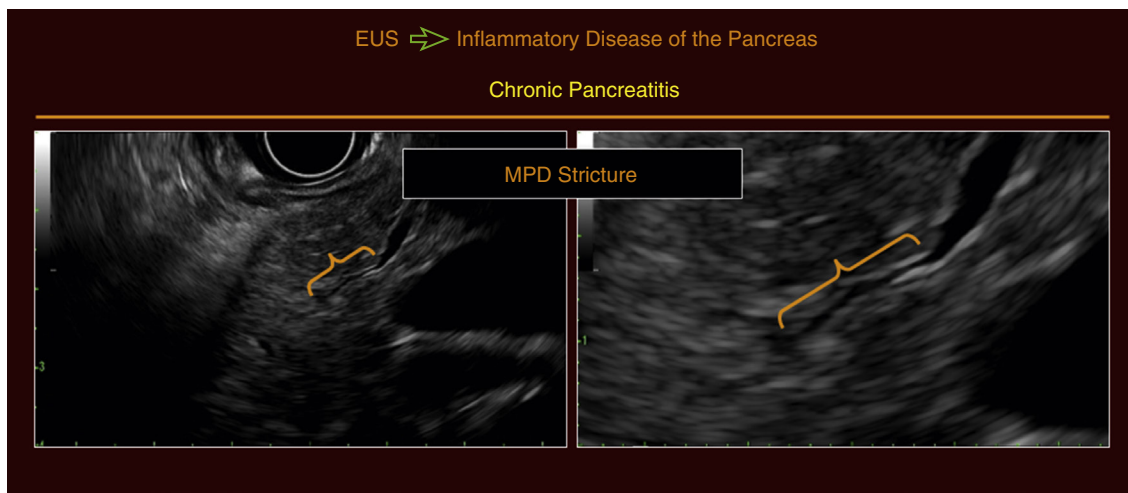
A multicenter study that compared IOA between expert endosonographers using both the conventional criteria and Rosemont classification found that there was moderate agreement ( $K = 0.54$ ; 95% CI 0.44 to 0.66) and substantial agreement ( $K = 0.65$ ; 95% CI 0.52 to 0.77), respectively.<sup>17</sup> However, there was no statistically significant difference between classification systems. Other studies have similarly shown that the Rosemont classification does not improve IOA compared to the conventional classification.<sup>18,19</sup>

#### Endoscopic Ultrasound Sampling

The main role of EUS FNA in CP is distinguishing focal (pseudotumoral) CP from pancreatic adenocarcinoma (PaC) and



• **Fig. 13.8** A 48-year-old male presented with clinical and computed tomography evidence of chronic pancreatitis with a large pancreatic head duct stone and upstream ductal dilatation. Three prior efforts at endoscopic retrograde cholangiopancreatography failed and the patient was referred for further evaluation and stone clearance. Final stone clearance was achieved at follow-up ERP.



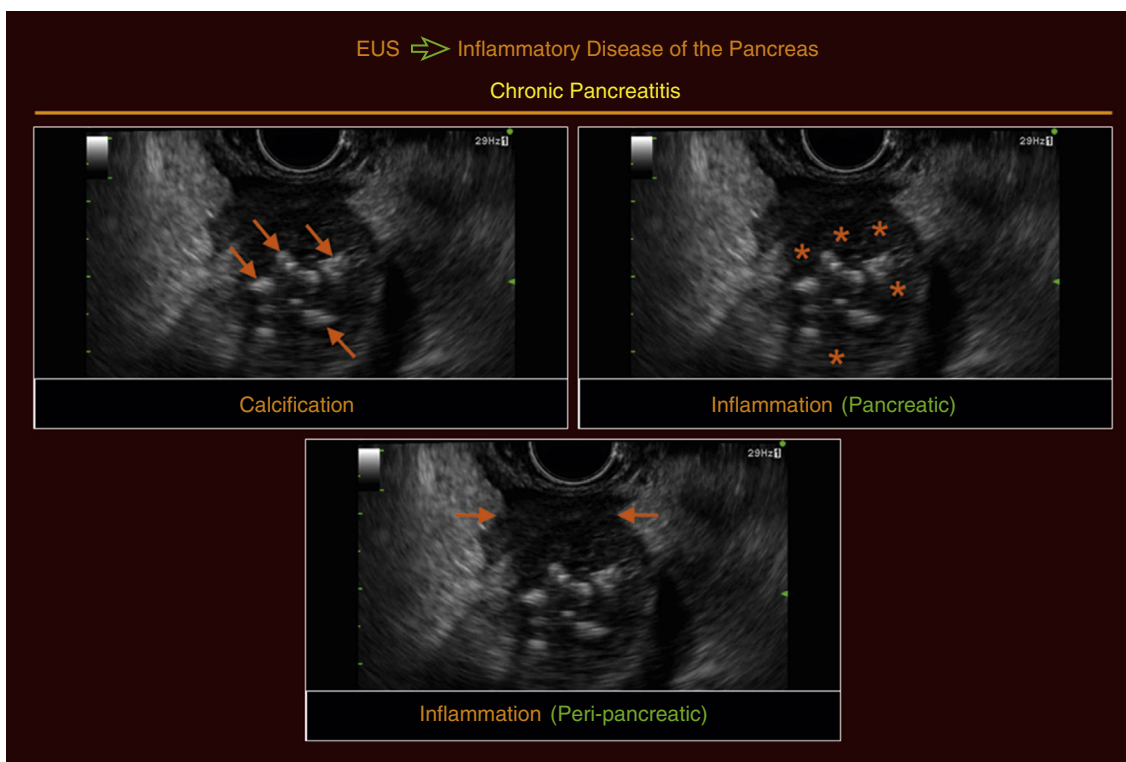
• **Fig. 13.9** Endoscopic ultrasound demonstrates a long benign stricture in a patient with chronic pancreatitis. MPD, Main pancreatic duct.

other neoplasias. PaC is found more commonly in patients with underlying CP than the general population with a cumulative risk of 1.8% (95% CI 1% to 2.6%) at 10 years and 4% (95% CI 2% to 5.9%) at 20 years.<sup>20</sup> Some have found that EUS imaging alone may be insufficient in differentiating between the two.<sup>21</sup> EUS FNA of pancreatic masses has a lower sensitivity in the presence of CP and more passes may be required to establish a diagnosis.<sup>22,23</sup> The lower diagnostic sensitivity may result from incorrectly targeted biopsies due to the inability to discern the tumor from peritumoral CP changes with EUS imaging. In addition, cytologic interpretation is more challenging when specimens contain limited malignant material along with non-tumoral CP material. For more details, see the section on Benign Pancreatic Masses.

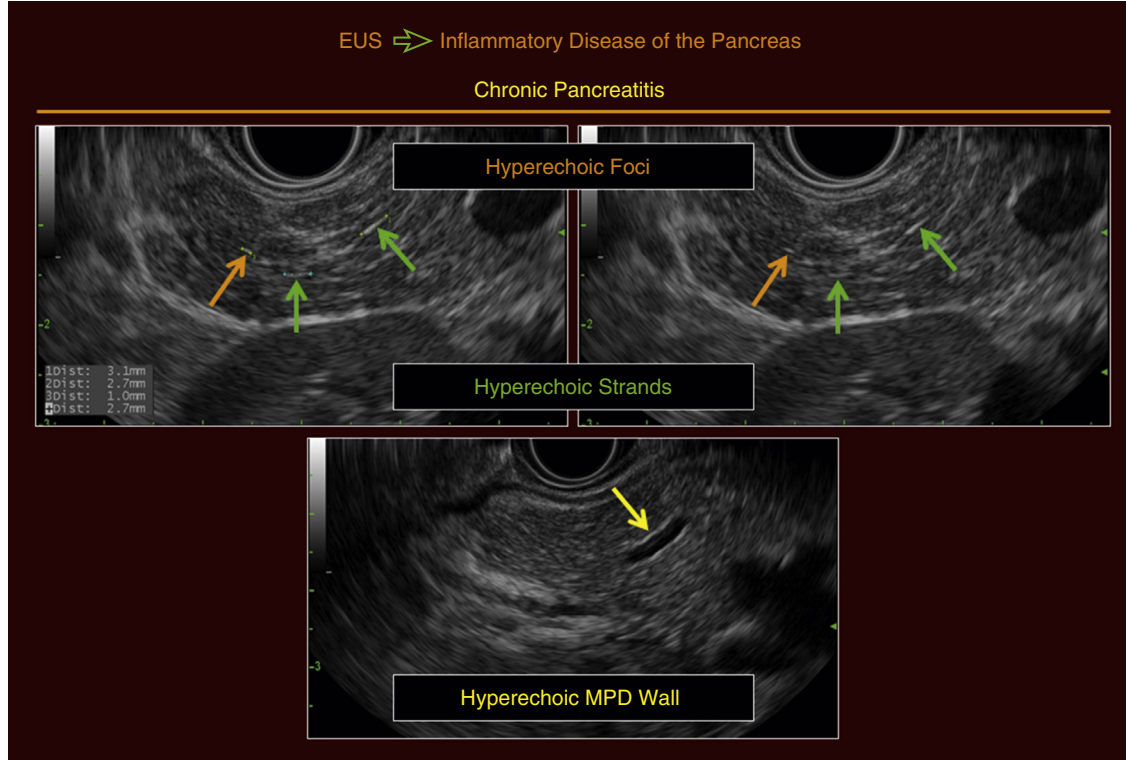
## Image-Enhancing Techniques in Endoscopic Ultrasound

### *Endoscopic Ultrasound Elastography*

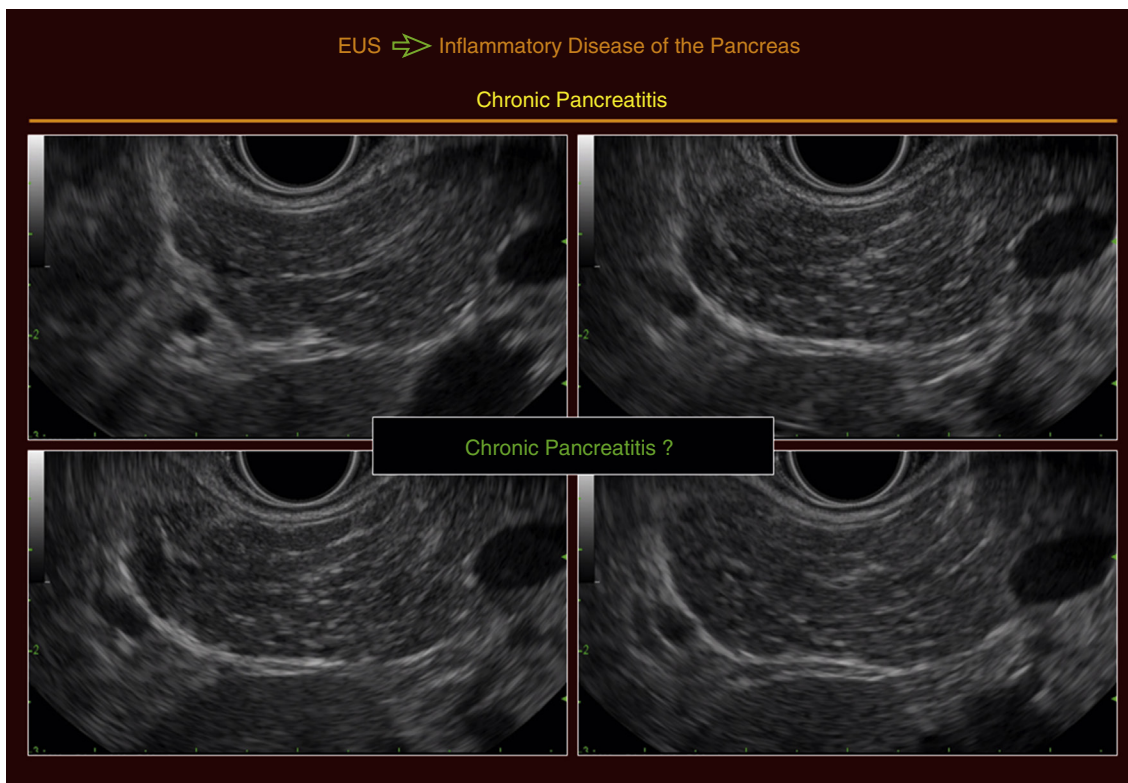
EUS elastography has been shown in several studies to enhance the EUS diagnostic accuracy of CP, with its objectivity helping to overcome the limitations of EUS interobserver variability. Elastography assesses tissue stiffness by applying slight compression and comparing images before and after compression to determine the degree of tissue displacement.<sup>24</sup> In patients with known or suspected CP, there was a negative correlation with mean value and number of Rosemont features on EUS ( $r = -0.59$ ,  $P < .001$ ).<sup>25</sup> A mean elastography value of  $90.1 \pm 19.3$ ,  $73.2 \pm 10.6$ ,  $63.7 \pm 14.2$ , and  $56.1 \pm 13.6$  was found in patients meeting the



• **Fig. 13.10** Endoscopic ultrasound in a patient with an acute exacerbation of chronic pancreatitis. In addition to the calcification (upper left), there are pancreatic (upper right) and peripancreatic (lower) inflammatory changes. (See Video 13.4.)



• **Fig. 13.11** Endoscopic ultrasound (EUS) highlights the features of chronic pancreatitis, including hyperechoic foci (orange arrows), hyperechoic strands (green arrows), and a hyperechoic main pancreatic duct wall (yellow arrow). The EUS suspicion of mild or early features of chronic pancreatitis was confirmed with core biopsies. MPD, Main pancreatic duct.



• **Fig. 13.12** Endoscopic ultrasound images are shown of a patient that was confirmed on core biopsy to have mild or early features of chronic pancreatitis. (See [Video 13.5.](#))

**TABLE 13.1** **Definition of Each Rosemont Feature**

#### Parenchymal Features

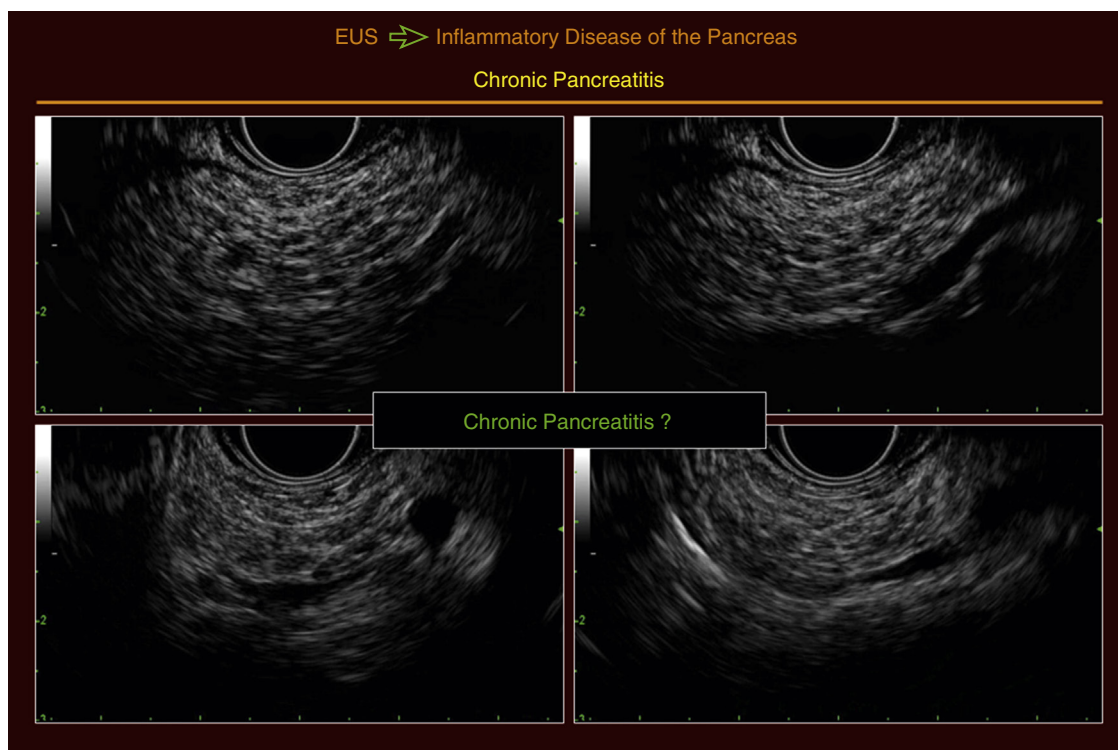
Hyperechoic foci with shadowing	≥3 echogenic structures ≥2 mm in length and width that shadow
Lobularity	Well-circumscribed, ≥5 mm structures with enhancing rim and relatively echo-poor center; ≥3 lobules in the body or tail need to be present With honeycombing: contiguous ≥3 lobules Without honeycombing: noncontiguous lobules
Hyperechoic foci without shadowing	≥3 echogenic structures ≥2 mm in length and width with no shadowing
Cysts	Anechoic, round/elliptical structures with/without septations
Stranding	≥3 hyperechoic lines ≥3 mm in length in at least 2 different directions with respect to the imaged plane

#### Ductal Features

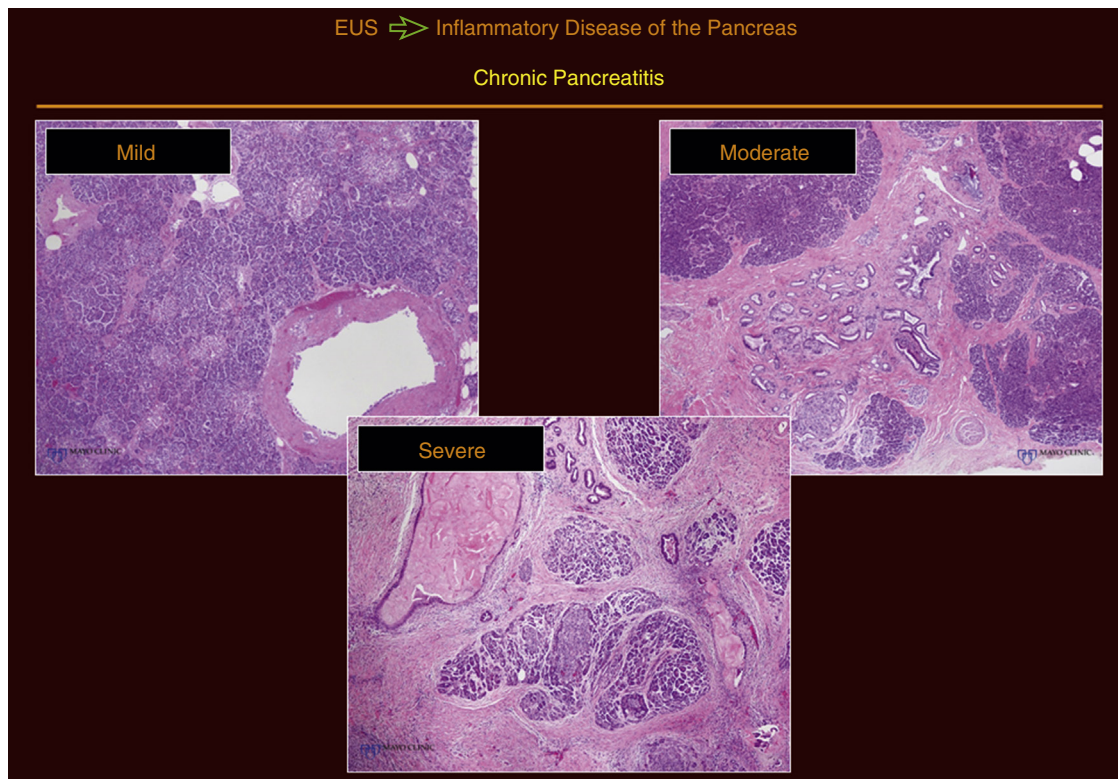
MPD calculi	Echogenic structure(s) within the MPD with acoustic shadowing
Irregular MPD contour	Uneven or irregular outline and ectatic course of the MPD; only assessed in the pancreatic body and tail
Dilated side branches	≥3 tubular anechoic structures each measuring ≥1 mm in width, budding from the MPD; only assess from the pancreatic body and tail
MPD dilation	≥3.5 mm in the body or ≥1.5 mm in the tail
Hyperechoic MPD margin	Echogenic, distinct structure greater than 50% of the entire MPD (on both the proximal and distal border) in the body and tail

MPD, Main pancreatic duct.

From Catalano MF, Sahai A, Levy M, et al. EUS-based criteria for the diagnosis of chronic pancreatitis: the Rosemont classification. *Gastrointest Endosc*. 2009;69:1251–1261.



• **Fig. 13.13** Endoscopic ultrasound (EUS) images are shown of a patient that was thought, based on EUS imaging, to have moderately severe chronic pancreatitis. However, core biopsy demonstrated a large quantity of completely normal pancreas. This patient highlights the limitations that can occur with EUS imaging. (See Video 13.6.)



• **Fig. 13.14** Pathology reveals the findings of mild (upper left), moderate (upper right), and severe (bottom) chronic pancreatitis.

Rosemont criteria for normal, indeterminate for CP, suggestive of CP, and consistent with CP categories ( $P < 0.001$  for differences between each stage), respectively. A mean strain ratio (SR; quotient B/A ratio with area A corresponding to the largest possible area of the pancreatic parenchyma and area B as the reference area corresponding to the normal surrounding gut wall) taken from an average of the head, body, and tail was found to have a direct linear correlation to the number of EUS Rosemont criteria ( $r = 0.813$ ,  $P < 0.0001$ ) with an area under the ROC curve of 0.949 (95% CI 0.916 to 0.982).<sup>26</sup>

EUS elastography has also been used to predict exocrine insufficiency in patients with CP. The 13(C)-mixed triglyceride breath test was used to diagnose exocrine insufficiency in 35 patients (30.4%) diagnosed with CP by MRI/MRCP and EUS.<sup>27</sup> A higher SR (quotient B/A ratio corresponding to the pancreatic parenchyma for area A and a soft peripancreatic reference as area B) of 4.89 (95% CI 4.36 to 5.41) was found in patients with pancreatic insufficiency than those with normal breath tests (2.99; 95% CI 2.82 to 3.16,  $P < .001$ ). In addition, patients with a SR  $>5.5$  were 92.8% likely to have pancreatic insufficiency.

## Advanced Endoscopic Ultrasound Techniques

### *Endoscopic Ultrasound-Guided Celiac Plexus Block*

Although many patients with CP suffer from abdominal pain that is occasionally severe and intractable, there are limited treatment options. Celiac plexus block (CPB) is an option in select patients and involves the injection of a local anesthetic and steroid into the celiac plexus and/or directly into celiac ganglia. CPB has historically been performed by surgeons or radiologists, but EUS-guided CPB has become the preferred approach due to the close proximity of the echoendoscope to the celiac takeoff, use of Doppler to confirm the lack of intervening structures, and continuous imaging to guide needle placement. More information regarding the indications, contraindications, risks, role, and technique may be found in Chapter 25.

## Acute Pancreatitis

### Brief Overview

Acute pancreatitis (AP) most commonly presents as acute epigastric or left upper quadrant abdominal pain that may radiate to the back, chest, or flank. The diagnosis of AP is made when at least 2 of the following criteria are met: (1) abdominal pain consistent with the disease, (2) serum amylase and/or lipase  $>3$  times the upper limit of normal, and (3) characteristic findings from abdominal imaging.<sup>28</sup> As acute biliary pancreatitis is a main cause of AP (40% to 70%), transabdominal ultrasound has a primary role in the evaluation. Routine cross-sectional imaging with CT or MRI is not recommended, but may be considered in patients who do not improve after 48 to 72 hours.

### Role of Endoscopic Ultrasound

#### *Acute Biliary Pancreatitis*

The ASGE guidelines concerning the role of endoscopy for suspected choledocholithiasis propose predictors of biliary disease as seen in Table 13.2.<sup>29</sup> The likelihood of choledocholithiasis was considered to be high (>50%) if any “very strong” predictor or both “strong” predictors were present. If no predictors were present, then the likelihood was low (<10%). An indeterminate

**TABLE 13.2 Predictors of Choledocholithiasis**

Very strong predictors	CBD stone on transabdominal ultrasound Clinical ascending cholangitis Bilirubin $>4$ mg/dL
Strong predictors	Dilated CBD on ultrasound (>6 mm in patients with gallbladder <i>in situ</i> ) Bilirubin 1.8–4 mg/dL
Moderate predictors	Abnormal liver biochemical test other than bilirubin Age $>55$ years old Clinical gallstone pancreatitis

*CBD*, Common bile duct.

From Maple JT, Ben-Menachem T, Anderson MA, et al. The role of endoscopy in the evaluation of suspected choledocholithiasis. *Gastrointest Endosc*. 2010;71:1–9.

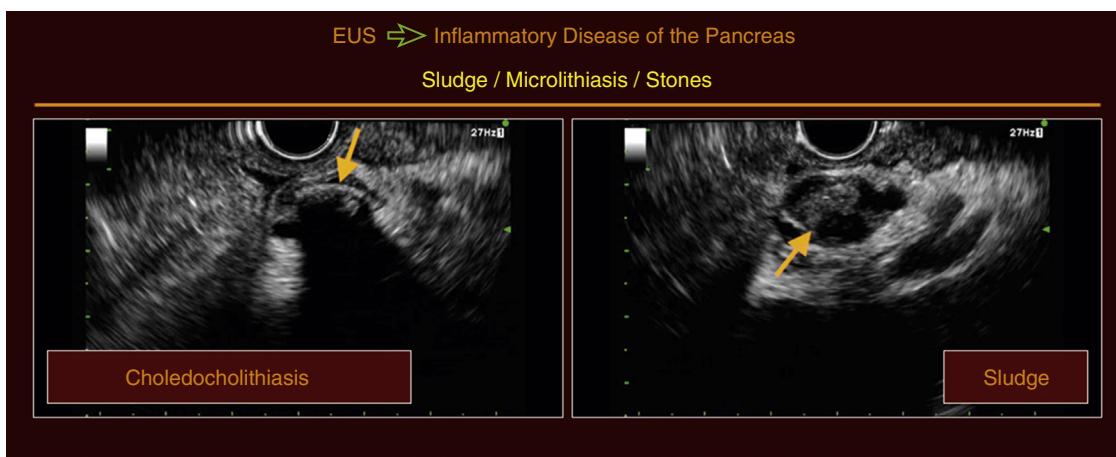
likelihood (10% to 50%) of choledocholithiasis was considered in all other patients. Based on their recommendations, patients with high likelihood should undergo ERCP prior to cholecystectomy, whereas patients with low likelihood can be taken directly to cholecystectomy. Those in the indeterminate category should have a cholangiogram performed either intraoperatively or by preoperative EUS or MRCP. Some favor EUS in this situation due to the ability to perform ERCP and stone clearance in the same setting (Fig. 13.15, Video 13.7). By adopting these criteria and performing EUS in patients with an indeterminate likelihood, unnecessary ERCP may be avoided in nearly half (44%) of patients.<sup>30</sup>

A systematic review of randomized control or clinical trials that compared ERCP and EUS for suspected acute biliary pancreatitis found that EUS had a higher success rate of completion than ERCP, largely due to the presence of duodenal/ampullary edema that impaired performance of ERCP.<sup>31</sup> It was estimated that a mean of 71.2% of unnecessary ERCPs could be avoided with the use of EUS. There were no adverse events in the EUS group, whereas 10 patients who underwent ERCP developed postspincterotomy bleeding.

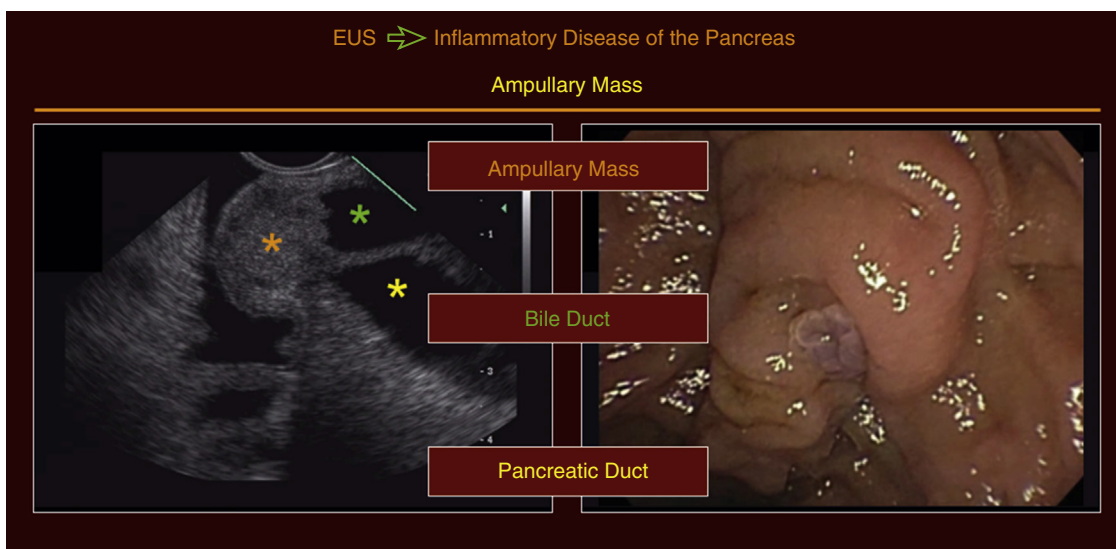
A study evaluating early EUS (within 24 hours of admission) in 41 patients with suspected acute biliary pancreatitis with a negative CT reported the detection of choledocholithiasis or bile duct sludge in 49% of patients.<sup>32</sup> EUS has also proven useful in this setting through detection of ampullary adenocarcinoma that was otherwise undetected by cross-sectional imaging (Figs. 13.16 to 13.18, Video 13.8).<sup>33</sup>

#### *Acute Idiopathic Pancreatitis*

Idiopathic pancreatitis is defined as pancreatitis without an established etiology after obtaining a thorough history (e.g., alcohol intake), laboratory testing (calcium, triglyceride), and imaging (transabdominal ultrasound, CT, and/or MRI/MRCP).<sup>28</sup> EUS has been shown to be helpful in the evaluation of idiopathic AP, but unlike suspected acute biliary pancreatitis where EUS is performed during the index hospitalization to guide management, in this setting EUS is typically performed at least 4 to 6 weeks following the episode of acute idiopathic pancreatitis to allow the acute inflammatory changes to resolve. In patients with prior negative transabdominal ultrasound, CT and/or MRI/MRCP, EUS has been shown to determine a cause in 55% to 79% of patients.<sup>34–36</sup> Biliary disease, including choledocholithiasis, gallbladder sludge, choledocholithiasis, or common



• **Fig. 13.15** In a patient with recurrent acute pancreatitis, endoscopic ultrasound imaging of the distal bile duct identified a calcified stone that produced postacoustic shadowing (left arrow). Further imaging also revealed adjacent sludge that was nonshadowing (right arrow). (See [Video 13.7](#).)

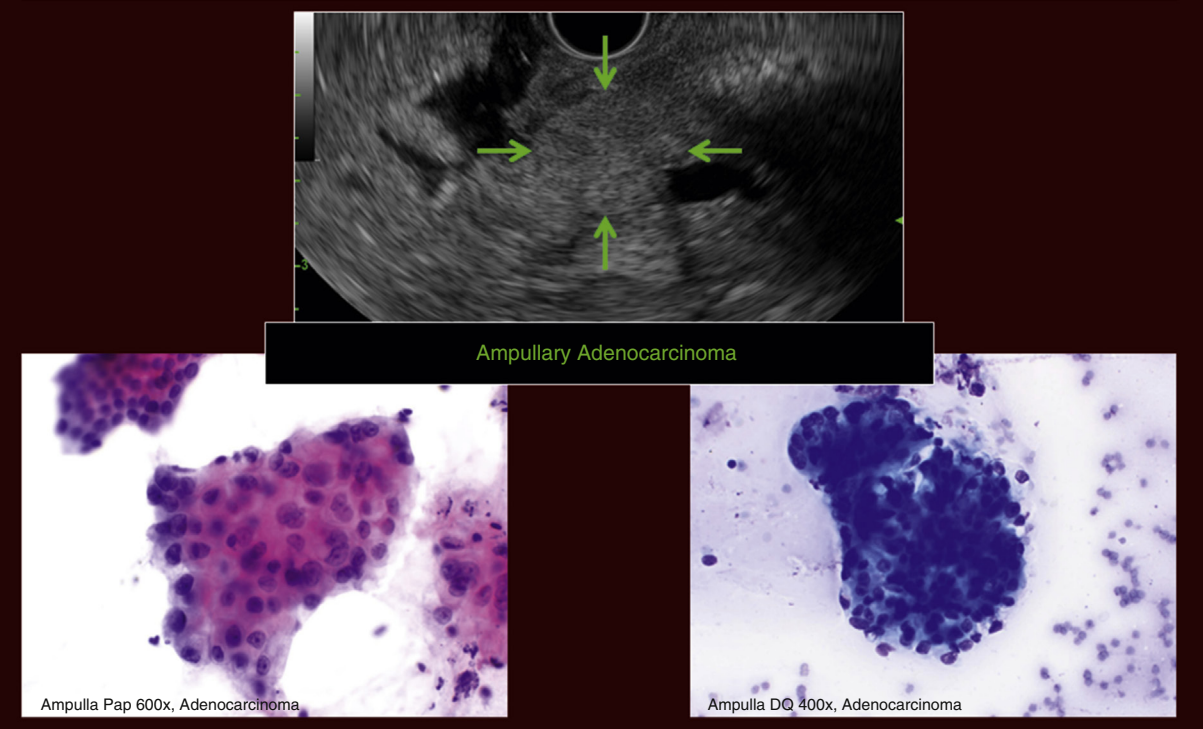


• **Fig. 13.16** In a patient with recurrent acute pancreatitis, endoscopic ultrasound revealed an ampullary mass (orange asterisk) leading to a dilated bile duct (green asterisk) and pancreatic duct (yellow asterisk). Although there was slight fullness of the papilla at duodenoscopy, there was no clear evidence of the underlying neoplasia.

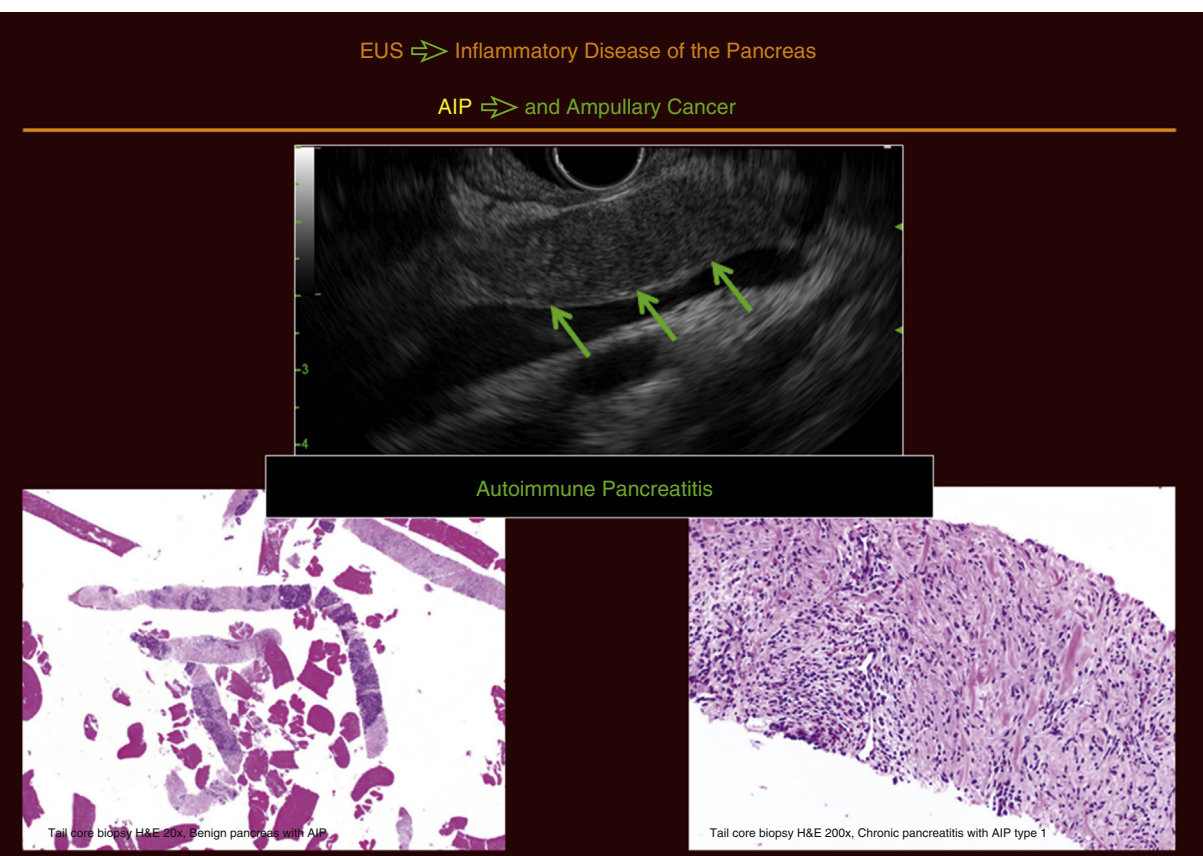
bile duct (CBD) sludge, is the most common etiology identified in patients with a positive EUS. Other findings such as CP, pancreas divisum, pancreatic cysts, tumors, and other pathology (Figs. 13.19 and 13.20) may also be detected by EUS. A suggested algorithm for the approach to acute idiopathic pancreatitis can be seen in Fig. 13.21.<sup>37</sup>

When compared to MRCP, EUS has a higher diagnostic yield (20% vs. 51%, respectively,  $P < .001$ ).<sup>38</sup> EUS was significantly more likely to detect gallbladder disease (24% vs. 4%,  $P < 0.05$ ) and CP (18% vs. 2%,  $P < 0.05$ ) than MRCP. Similarly, in another study including 38 patients with idiopathic AP who underwent both EUS and MRCP, EUS detected an etiology in 39.5% of patients compared to MRCP in 21% ( $P = .09$ ).<sup>39</sup> EUS more commonly diagnosed biliary disease, and MRCP mostly detected pancreatic duct abnormalities.

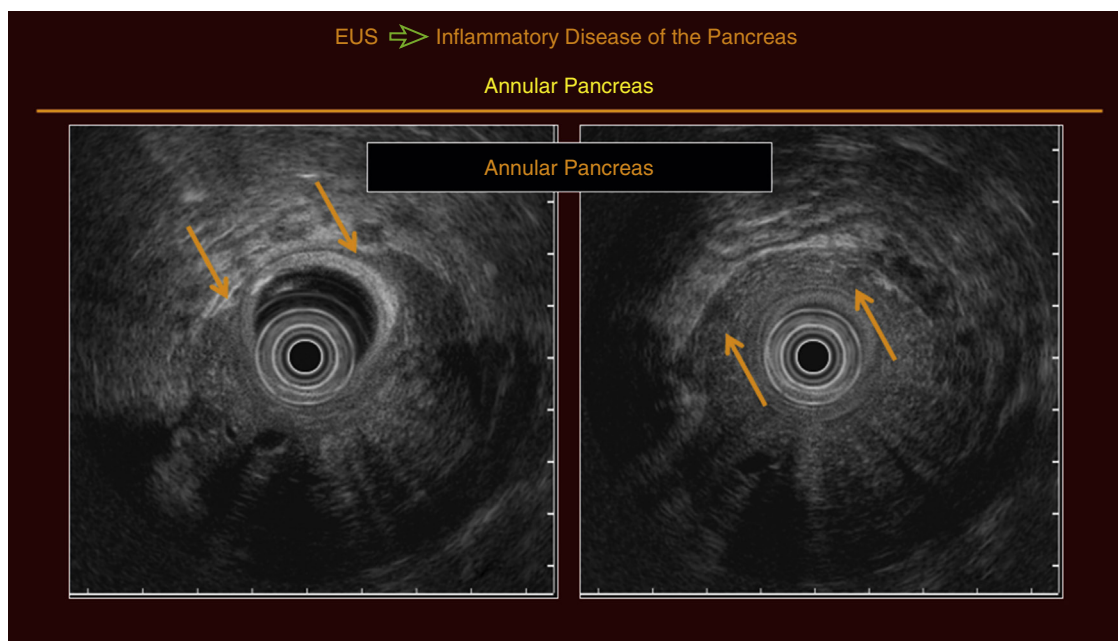
The ACG guidelines regarding the management of acute pancreatitis recommends EUS and/or MRCP in patients older than 40 years to exclude a pancreatic neoplasm (Figs. 13.22 and 13.23, Videos 13.9 and 13.10).<sup>28</sup> In a large cohort of patients from the Veterans Health Administration who had an episode of AP, the risk of PaC after an attack of AP was evaluated.<sup>40</sup> The risk of diagnosing PaC within the first (relative risk [RR] 66.01; 95% CI 47.24 to 92.23,  $P < .0001$ ) and second (RR 5.15; 95% CI 2.30 to 11.52,  $P < .0001$ ) year following an attack of AP was significantly higher in patients with prior AP as compared to those patients without prior AP. The risk of PaC in patients  $<40$  years old was zero, whereas the incidence and risk increased with age (Table 13.3). Alcohol abuse was associated with a lower risk (RR 0.37; 95% CI 0.22 to 0.62), whereas smoking and the presence of gallstone disease did not affect the risk of PaC.



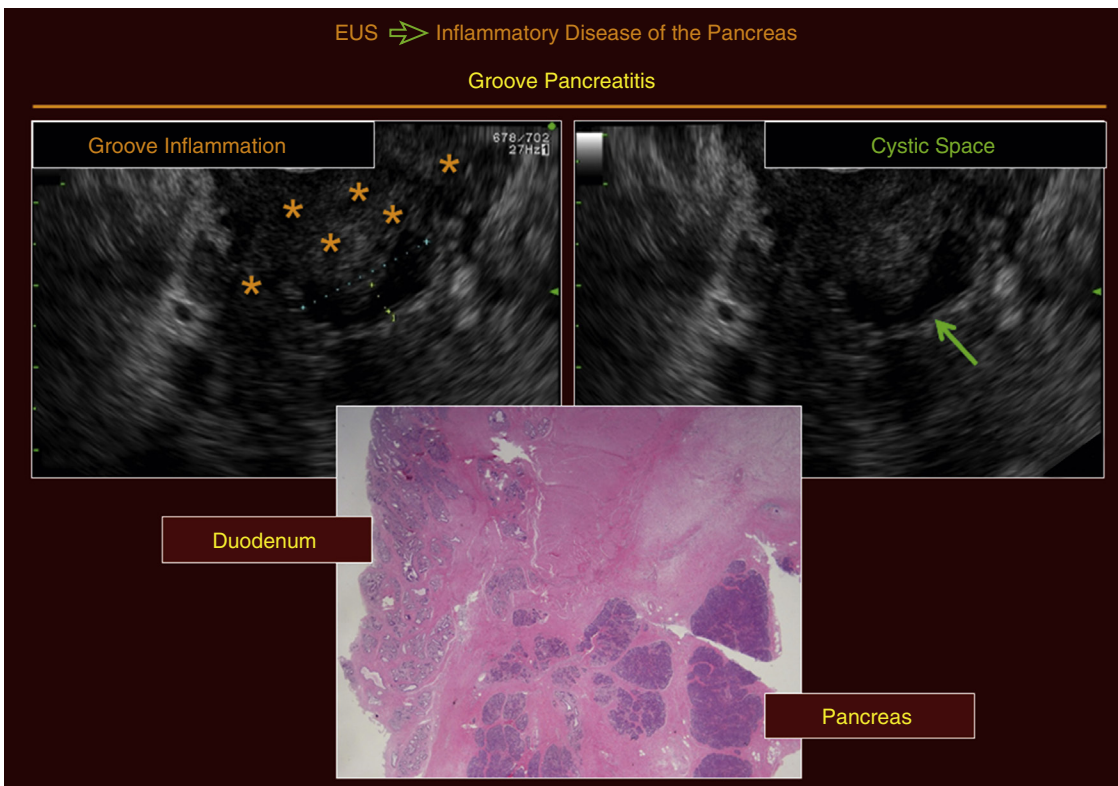
**• Fig. 13.17** A 49-year-old female presented with painless jaundice. At the referring hospital she underwent CT, MRI/MRCP, ERCP ( $\times 2$ ), and EUS ( $\times 2$ ) that were negative with no pathology seen. She was referred for second opinion. (See Video 13.8.) EUS revealed a well-circumscribed 1.5 cm isoechoic ampillary mass (arrows) that on cytology was diagnostic for an ampillary adenocarcinoma. *AIP*, Autoimmune pancreatitis.



**• Fig. 13.18** A 49-year-old female presented with painless jaundice. At the referring hospital she underwent CT, MRI/MRCP, ERCP ( $\times 2$ ), and EUS ( $\times 2$ ) that were negative with no pathology seen. She was referred for second opinion. (See Video 13.8.) Additional EUS imaging revealed changes in the pancreatic tail that were concerning for AIP (arrows), which was confirmed on EUS-guided core biopsy and surgical resection. The findings highlight the need to be familiar with the EUS appearance of neoplasia and AIP. *AIP*, Autoimmune pancreatitis.



• **Fig. 13.19** In a patient with annular pancreas, endoscopic ultrasound demonstrates the pancreatic parenchyma encircling the second portion of the duodenum (orange arrows).



• **Fig. 13.20** A patient presented with recurrent idiopathic acute pancreatitis and was found by endoscopic ultrasound to have groove pancreatitis. Surgery was ultimately required due to an unresolved disease course.

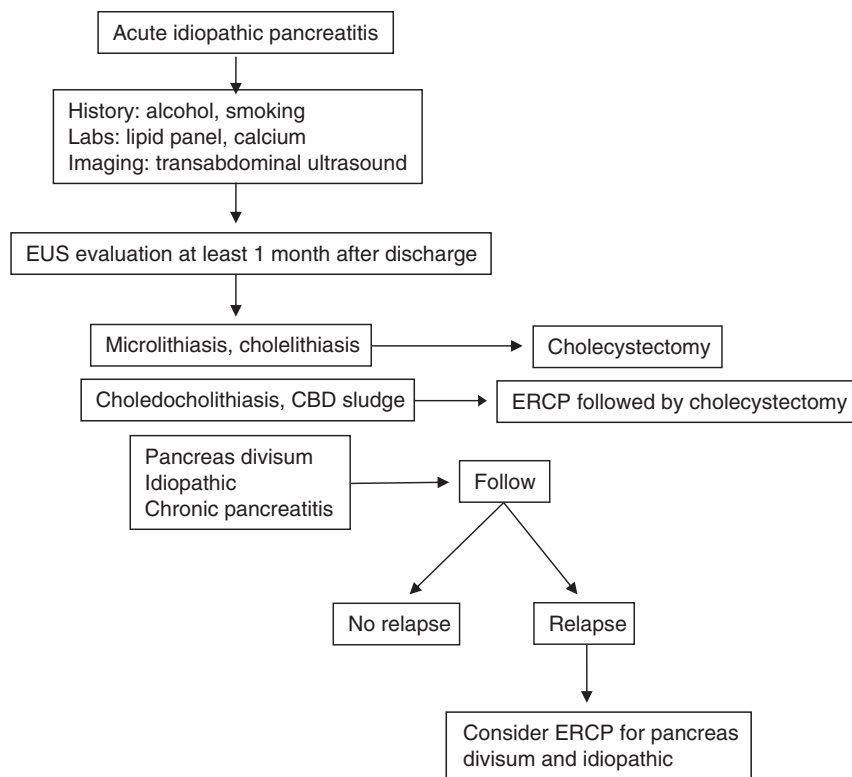


**Fig. 13.21** Proposed algorithm for the diagnostic approach to acute idiopathic pancreatitis. CBD, Common bile duct; ERCP, endoscopic retrograde cholangiopancreatography; EUS, endoscopic ultrasound. (Adapted from Wilcox CM, Seay T, Kim H, et al. Prospective endoscopic ultrasound-based approach to the evaluation of idiopathic pancreatitis: causes, response to therapy, and long-term outcome. *Am J Gastroenterol*. 2016;111:1339–1348.)

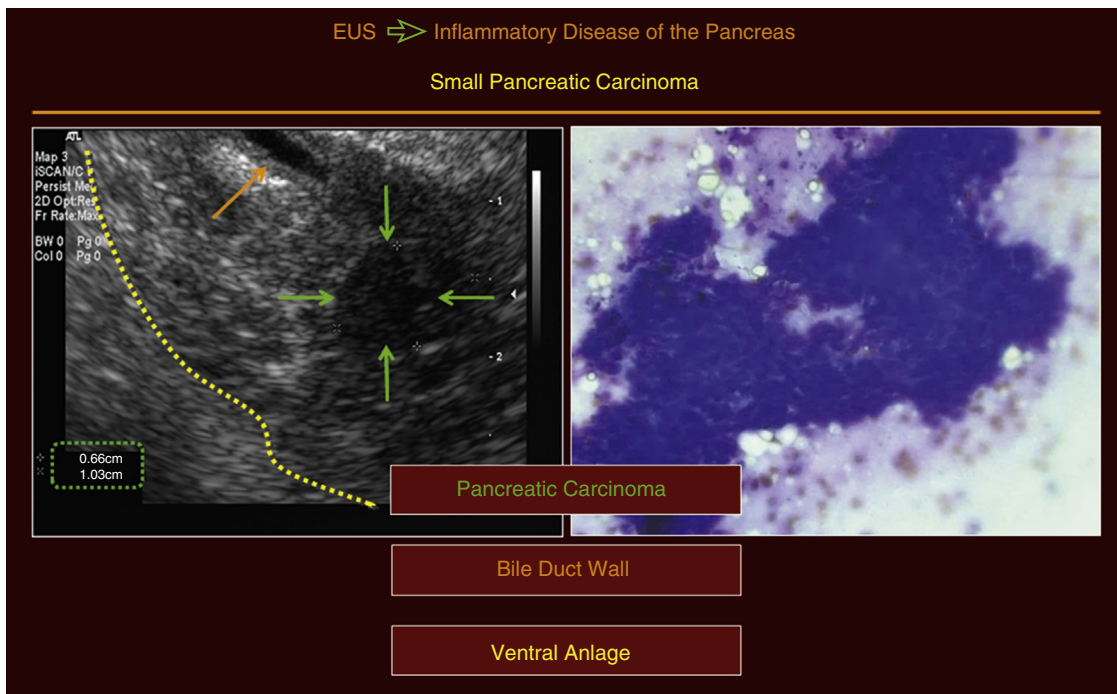


**Fig. 13.22** Endoscopic ultrasound (EUS) from a patient who presented with acute pancreatitis. Prior computed tomography and EUS revealed chronic pancreatitis and the patient was referred for further evaluation. EUS identified a small pancreatic carcinoma (green arrows) abutting the bile duct (orange arrow) that was proven at EUS-guided fine-needle aspiration (EUS FNA). The lesion was likely missed at prior examination due to the location within the ventral anlage (yellow dotted line) that can mask small lesions.

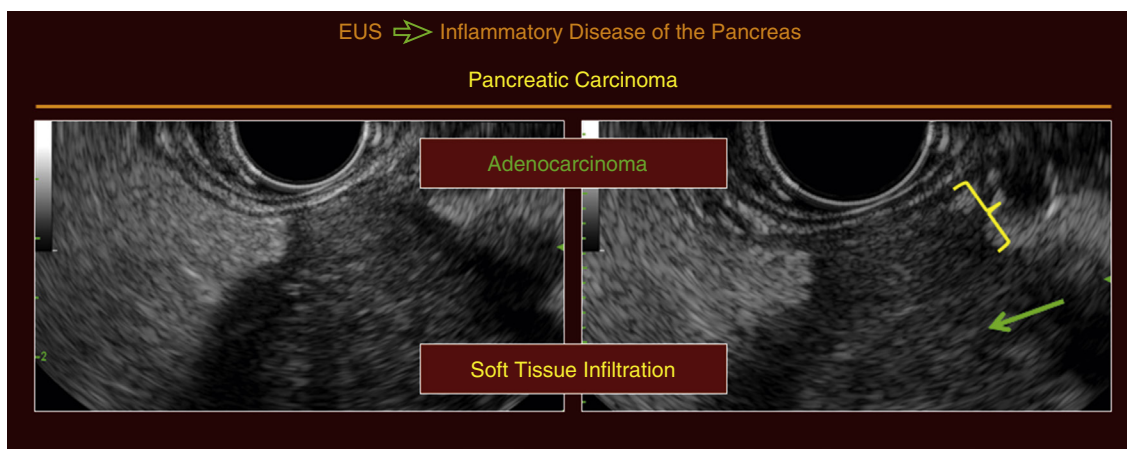


**Fig. 13.23** A 59-year-old male presented with acute pancreatitis. Prior CT ( $\times 2$ ) and endoscopic ultrasound (EUS) diagnosed acute pancreatitis and fine-needle aspiration (FNA) was negative for malignancy. The patient was referred for a second opinion. (See Videos 13.9 and 13.10.) EUS revealed a hypoechoic swollen gland without a detectable main pancreatic duct potentially indicative of acute pancreatitis or autoimmune pancreatitis. However, the finding of a focal region of soft tissue (*yellow bracket*) extension into the peripancreatic space and abutting the gastric wall raised concern for a pancreatic adenocarcinoma (*green arrow*). Both were proven at EUS FNA and subsequent surgery.

**TABLE 13.3**

**Incidence and Relative Risk of Pancreatic Cancer by Age and Prior Acute Pancreatitis**

Age	Patient With Prior AP			Patients Without Prior AP				<i>P</i> -value
	<i>N</i>	# PCA	Incidence (Per 1000 PY)	<i>N</i>	# PCA	Incidence (Per 1000 PY)	RR (95% CI)	
41–50	1470	10	7.69	121,005	13	0.11	104.78 (43.43–252.79)	<.0001
51–60	2342	28	14.28	139,977	25	0.18	79.93 (43.38–147.30)	<.0001
61–70	787	13	20.96	79,968	31	0.40	52.69 (24.95–111.27)	<.0001
>70	832	18	28.67	88,285	51	0.62	54.73 (30.26–98.98)	<.0001
Total			14.48				66 (47.23–92.22)	

AP, Acute pancreatitis; PCA, pancreatic cancer; PY, per year.

From Munigala S, Kanwal F, Xian H, et al. Increased risk of pancreatic adenocarcinoma after acute pancreatitis. *Clin Gastroenterol Hepatol*. 2014;12:1143–1150.e1.

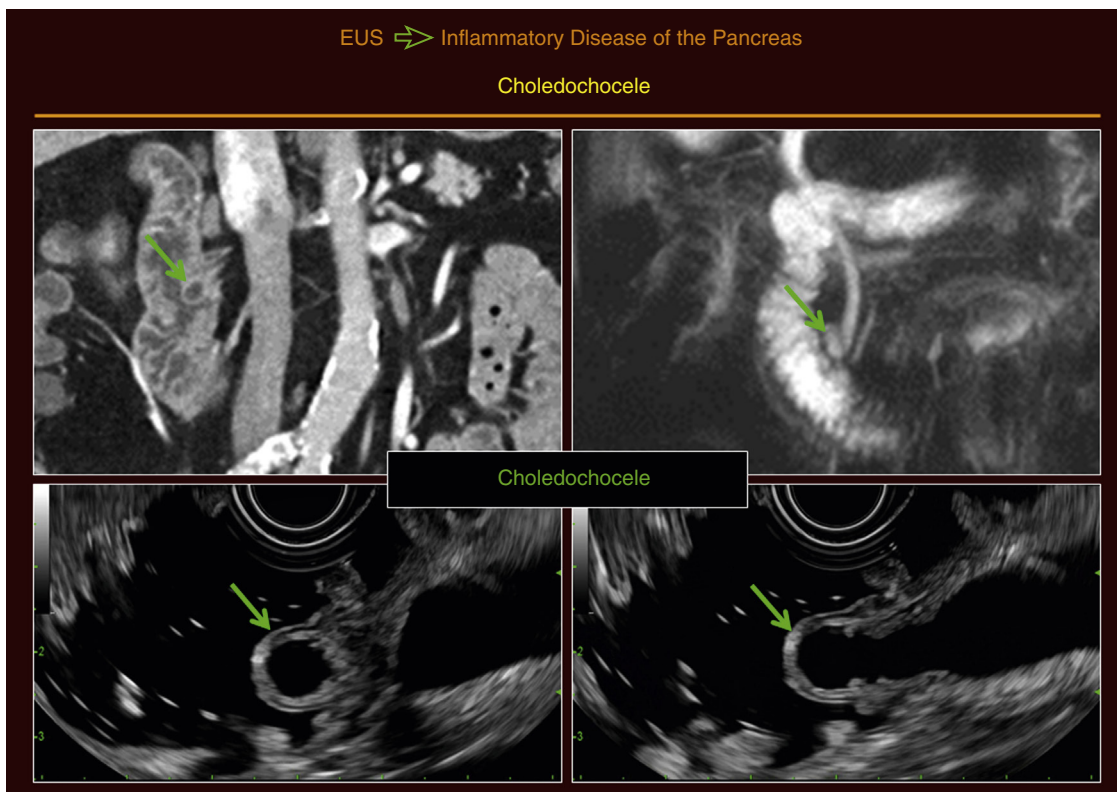
### Recurrent Acute Pancreatitis

Similar to acute idiopathic pancreatitis, when compared to secretin-stimulated MRCP and ERCP, EUS was found to have a higher diagnostic yield in patients with recurrent acute pancreatitis (RAP).<sup>41</sup> EUS detected a potential etiology in 79.5% of patients, most commonly pancreatic ductal changes such as MPD or side branch dilation in 38.6%, biliary disease and cysts <3 mm in 18.2% of patients each (Figs. 13.24 and 13.25, Videos 13.11 and 13.12), and pancreas divisum in 13.6%. MRCP was positive in 65.9% of patients, most commonly detecting pancreatic ductal changes (38.6%) and pancreas divisum (18.2%) (Figs. 13.26 to 13.28, Video 13.13). ERCP identified changes in 62.8%, with pancreatic ductal changes (30.2%) and pancreas divisum (16.3%) being the most common. Although not statistically significant, the diagnostic yield of EUS in patients with nondilated pancreatic ducts was 13.6% and 16.7% higher than MRCP and ERCP, respectively.

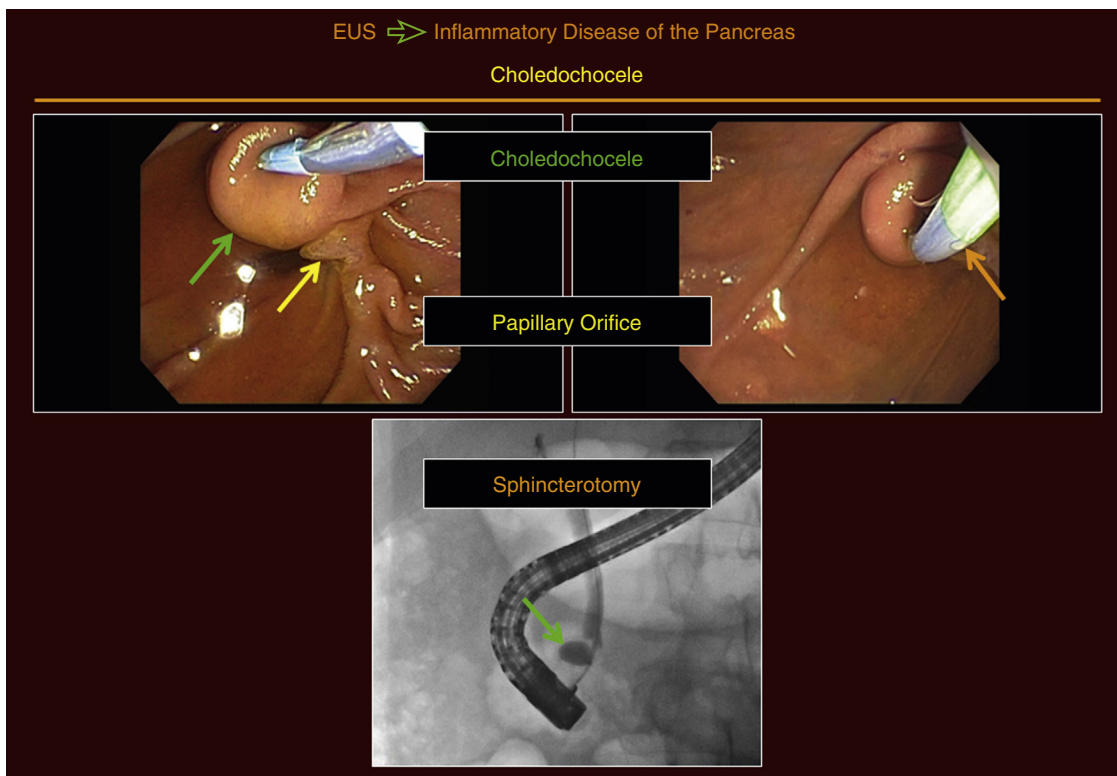
A study that compared the diagnostic yield of EUS in patients with one episode versus patients with RAP did not find a significant difference between the two groups in patients with a prior cholecystectomy (29.9% vs. 17.5%, respectively, *P* = 0.15) or gallbladder in situ (31.3% vs. 32.1%, respectively, *P* = 0.89).<sup>42</sup> In another study, EUS had similar diagnostic yields when performed after either the first attack (43.8%) or multiple attacks (45.5%).<sup>37</sup> Based on these data, many favor performing EUS after the first episode of AP instead of waiting for recurrent episodes.

### Endoscopic Ultrasound Imaging Characteristics

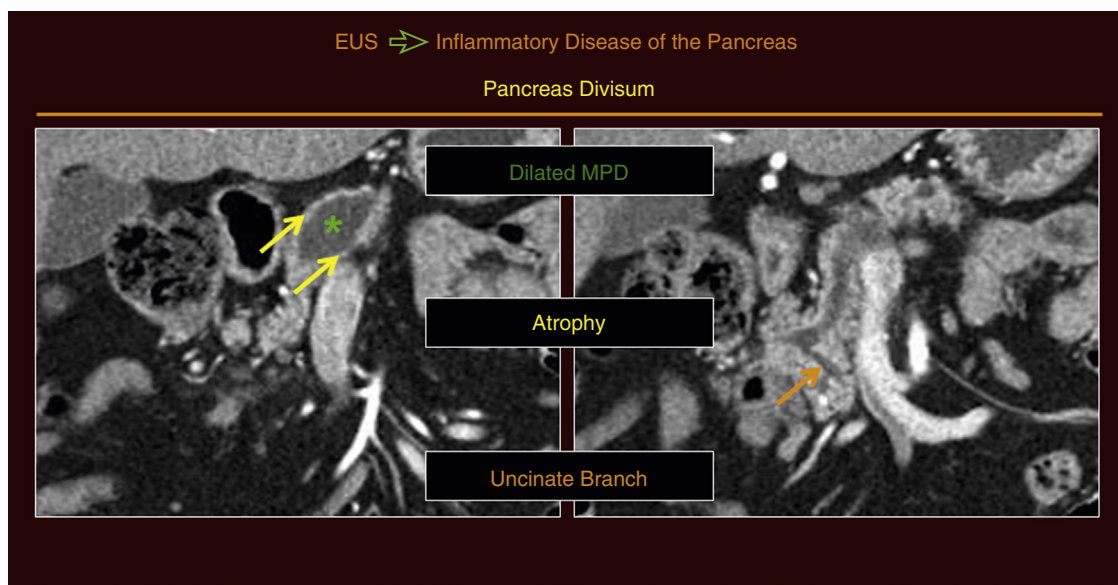
Studies have found that each of the EUS criteria seen in CP may also be seen in acute pancreatitis. However, this calls into question whether the presence of these features indicate the nonspecificity of the features and/or underlying presence of CP newly presenting with an acute flare. EUS performed in patients within 48 hours



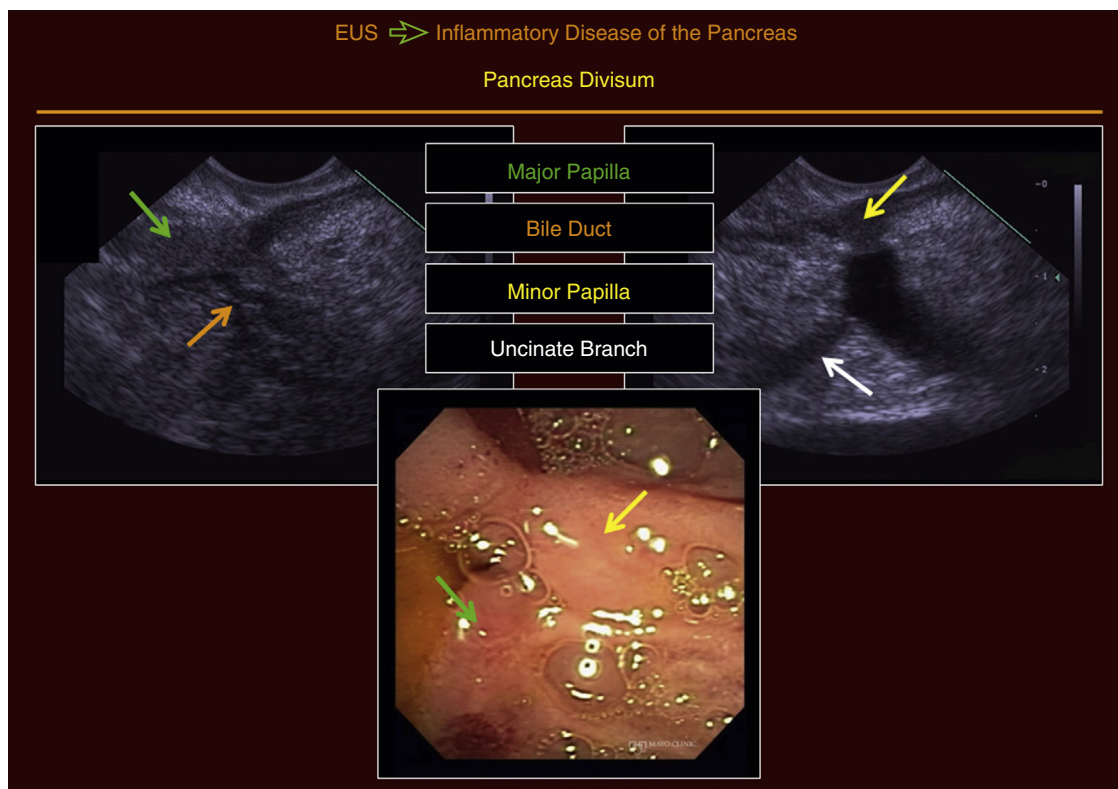
**• Fig. 13.24** A 72-year-old female presented with numerous episodes of acute pancreatitis. Computed tomography and magnetic resonance cholangiopancreatography demonstrated a cystic structure located at or near the major papilla suggestive of a choledochocele (upper left and right). Endoscopic ultrasound confirmed the presence of a cystic structure within the distal bile duct and major papilla with normal overlying wall layers compatible with a choledochocele (lower left and right). (See Videos 13.11 and 13.12.)



**• Fig. 13.25** A 72-year-old female presented with numerous episodes of acute pancreatitis. At endoscopic retrograde cholangiopancreatography, a sphincterotome was used to demonstrate the easy compressibility of the choledochocele (green arrow) and to reveal the papillary orifice (yellow arrow) and perform a therapeutic sphincterotomy (orange arrow).



• **Fig. 13.26** A 68-year-old male presented with multiple episodes of acute pancreatitis. Initial computed tomography (CT) and endoscopic ultrasound at the referring hospital revealed chronic pancreatitis with no other pathology identified. CT demonstrates a dilated main pancreatic duct (green asterisk), atrophy with only a thin margin of parenchyma remaining (yellow arrows), and the uncinate branch (orange arrow).



• **Fig. 13.27** A 68-year-old male presented with multiple episodes of acute pancreatitis. Initial computed tomography and endoscopic ultrasound (EUS) at the referring hospital revealed chronic pancreatitis with no other pathology identified. EUS demonstrates a diminutive major papilla (green arrow), and a small caliber bile duct (orange arrow). A more prominent minor papilla (yellow arrow) is seen into which the uncinate branch drains (white arrow). The findings of pancreas divisum were confirmed at EUS and subsequent endoscopic retrograde cholangiopancreatography. (See [Video 13.13](#).)

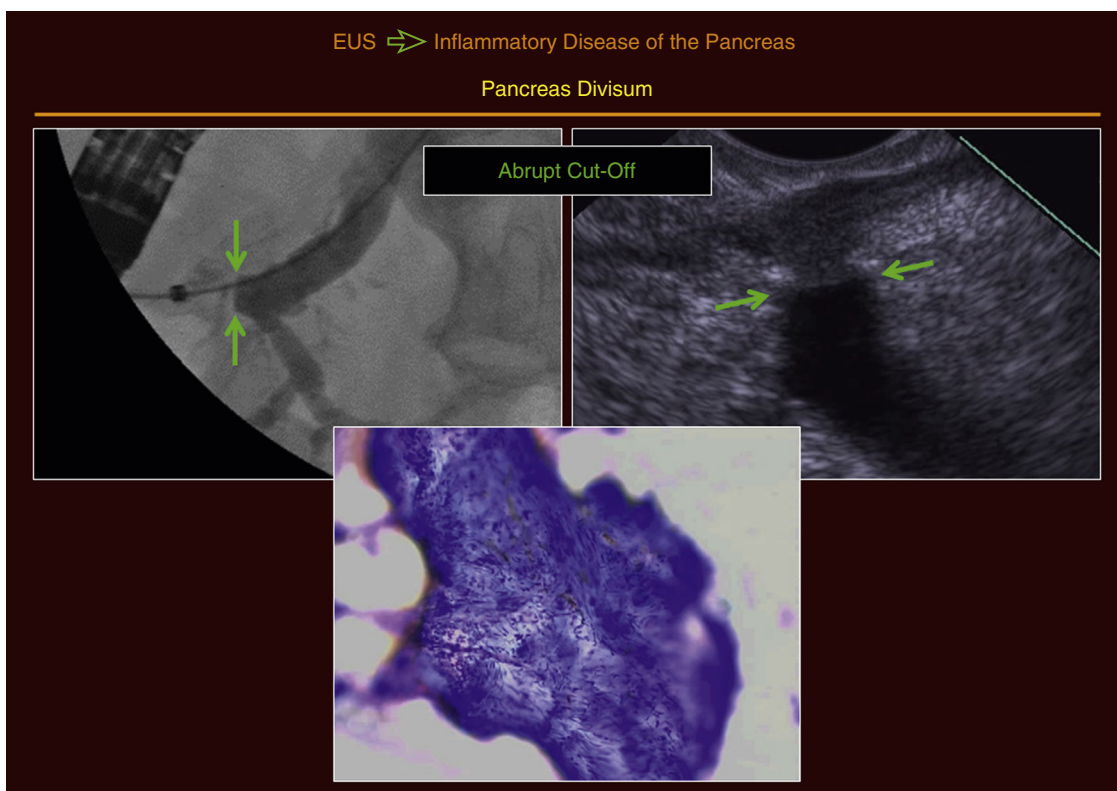


**Fig. 13.28** A 68-year-old male presented with multiple episodes of acute pancreatitis. Initial computed tomography and endoscopic ultrasound (EUS) at the referring hospital revealed chronic pancreatitis with no other pathology identified. The presence of a prominent minor papilla and abrupt duct cut-off (green arrows) raised concern for a small neoplasia. EUS-guided fine-needle aspiration was performed revealing no evidence of neoplasia, rather stromal tissue compatible with smooth muscle from the minor papilla. Following sphincterotomy and stent placement, the patient had a marked improvement in his clinical course and no evidence of an occult neoplasia during the 38-month follow-up.

of presentation of AP was compared to controls without AP.<sup>43</sup> On multivariate analysis, the presence of peripancreatic fluid (OR 13.9%; 95% CI 1.6 to 123.6), heterogeneous (OR 7.2; 95% CI 1.7 to 30.4), and hypoechoic parenchymal echogenicity (OR 10; 95% CI 3.9 to 25.8) were significantly more common in patients with AP. A geographic hyperechoic area of the pancreas was found to be predictive of severe pancreatitis (OR 2.9; 95% CI 1.1 to 8.2) that required longer hospital stays (11 days vs. 8 days without the geographic hyperechoic area present,  $P = .021$ ).

Although not commonly practiced, routine radial EUS and CT were performed on 187 patients within 72 to 96 hours after admission with acute biliary pancreatitis to determine whether EUS could predict the severity of pancreatitis.<sup>44</sup> Using a Balthazar CT score  $>6$  and/or modified Glasgow score  $>3$ , 29 patients (15.5%) had severe acute pancreatitis. There was a significant relationship between the severity of pancreatitis and the EUS findings of diffuse parenchymal edema (29.7% in mild vs. 93.1% in severe), periparenchymal plastering free fluid collections (29.7% in mild vs. 10.3% in severe), diffuse retroperitoneal free fluid accumulation (0.05% in mild vs. 79.3% in severe), and peripancreatic edema (13.2% in mild vs. 68.9% in severe; all  $P < .001$ ). The majority of patients with necrosis seen on CT had EUS features of a hypo- or anechoic gland with irregular contours that provided an accuracy of 92%, sensitivity of 85%, and specificity of 94%. In another study, the presence of peripancreatic edema, pancreas heterogeneity, CBD dilation, and ascites were found to be associated with severe AP.<sup>45</sup>

## Advanced Endoscopic Ultrasound Techniques

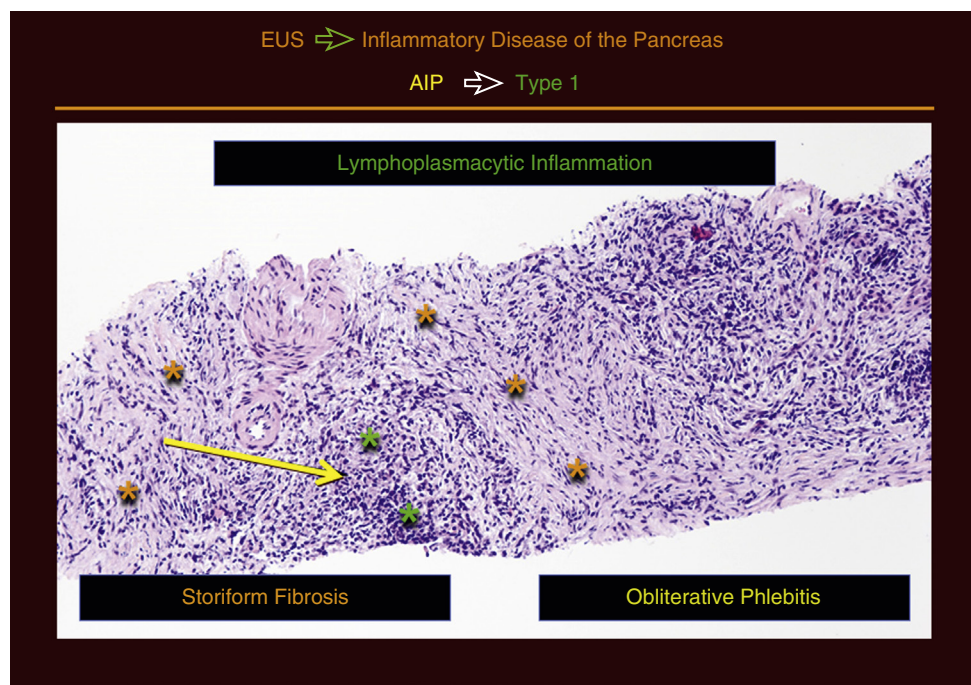
EUS has been increasingly used in the evaluation and treatment of AP-related complications such as pseudocysts and walled off pancreatic necrosis. Discussions on these topics can be found in Chapter 23.

## Autoimmune Pancreatitis

### Brief Overview

AIP has historically been considered a rare disorder, but is increasingly recognized due to an improved understanding of its diverse nature and proper means of diagnosis. AIP is a discrete form of pancreatitis characterized by lymphoplasmacytic infiltrate and fibrosis with a typical dramatic response to steroids.<sup>46</sup> The most common presentation is obstructive jaundice and/or a pancreatic mass. Less commonly, patients may present with acute pancreatitis or abdominal pain.

There are two distinct subtypes of AIP. Type 1 AIP has also been referred to as lymphoplasmacytic sclerosing pancreatitis (LPSP) or AIP without granulocyte epithelial lesions (GELs) (Fig. 13.29), and type 2 AIP has been termed idiopathic duct-centric pancreatitis (IDCP) or AIP with GELs (Fig. 13.30). The two subtypes have somewhat different clinical presentations, histopathologic features, and outcomes as outlined in Table 13.4.<sup>46,47</sup>



• **Fig. 13.29** Core biopsies from a patient with type 1 autoimmune pancreatitis (AIP) reveals the classic lymphoplasmacytic inflammation (green asterisks), storiform fibrosis (orange asterisks), and obliterative phlebitis (yellow arrow).



• **Fig. 13.30** Core biopsies from a patient with type 2 autoimmune pancreatitis (AIP) demonstrate the diagnostic feature of granulocyte epithelial lesions (green arrows).

**TABLE  
13.4****Differentiating Characteristics Between Type 1 and Type 2 AIP**

	Type 1 AIP	Type 2 AIP
<b>Also known as</b>	LPSP AIP without GELs IgG <sub>4</sub> -related pancreatitis	IDCP AIP with granulocyte epithelial lesions (GELs)
<b>Patient population</b>	Older (7th decade) Male predilection Asian & Western countries	5th decade No gender predilection Western countries
<b>Clinical presentation</b>	Obstructive jaundice—75% Abdominal pain—41% Acute pancreatitis—5%	Obstructive jaundice—47% Abdominal pain—68% Acute pancreatitis—34%
<b>Other organ involvement</b>	Common—60%	None (pancreas-specific)
<b>IBD present</b>	2%–6%	30%
<b>IgG<sub>4</sub></b>	Elevated in serum (typically $\geq 2 \times$ ULN) Stains positive in tissues ( $\geq 10$ cells per high power field)	Usually normal
<b>Diagnosis</b>	Does not require histology	Requires histology
<b>Histology</b>	Lymphoplasmacytic infiltration, storiform fibrosis	Granulocyte epithelial lesions
<b>Natural history</b>	Frequent relapses	No relapses

AIP, Autoimmune pancreatitis; GELs, granulocyte epithelial lesions; IDCP, idiopathic duct-centric pancreatitis; LPSP, lymphoplasmacytic sclerosing pancreatitis; ULN, upper limit of normal.

## Role of Endoscopic Ultrasound

Current international consensus diagnostic criteria (ICDC) for the diagnosis of AIP incorporate 5 features including imaging characteristics of the pancreatic parenchyma and duct, serology, other organ involvement, pancreatic histology, and response to steroids (Tables 13.5 and 13.6).<sup>46</sup> Imaging techniques recognized in the guidelines include CT (Figs. 13.31 and 13.32), MRI/MRCP (Fig. 13.33), and ERCP (Figs. 13.34 to 13.36). EUS is notably absent from the diagnostic algorithms.

To our knowledge, there have been no studies that directly compared EUS to other imaging modalities such as CT, MRI, or ERCP for the diagnosis of AIP. Therefore, it is unclear as to the additive value of EUS imaging to the other imaging techniques. However, a cohort of 48 patients seen at Mayo Clinic with a diagnosis of AIP using HISORt criteria (Histology, Imaging, Serology, other Organ involvement, and Response to steroid therapy)<sup>48</sup> underwent EUS with core biopsy.<sup>49,50</sup> The diagnosis of AIP was strongly suspected in 14 patients prior to EUS based on their clinical, laboratory, and imaging findings. In 22 patients, the diagnosis was considered as a part of a broader differential prior to EUS and in the remaining 12 patients the EUS appearance alone led to the initial suspicion of AIP. Therefore, this suggests that EUS imaging alone may increase the diagnostic accuracy of AIP in patients who underwent other imaging modalities without a definitive diagnosis.

## Endoscopic Ultrasound Imaging Characteristics

There are no pathognomonic EUS imaging findings of AIP. The “classic” appearance is a diffusely (sausage-shaped) pancreatic enlargement with hypoechoic, patchy, heterogeneous appearing parenchyma (Fig. 13.37).<sup>51–53</sup> In our experience, when a patient

has all of these classic features, which may be found in up to 57% of patients, there is a high probability of AIP.<sup>51,52</sup> However, patients often do not have all of the features, thereby limiting the accuracy of EUS to diagnose AIP. EUS may also identify a focal solitary mass. The usually hypoechoic lesion is most commonly located in the pancreatic head and is often associated with obstructive jaundice. The mass may appear similar to PaC with perceived involvement of adjacent vessels, resulting upstream MPD dilation, and may be associated with enlarged peripancreatic lymph nodes.<sup>51–53</sup> In areas of pancreatic involvement, the MPD may be narrowed with duct wall thickening.<sup>53</sup> Also, EUS features of the pancreatic parenchyma may overlap with those seen in CP including the presence of hyperechoic foci, hyperechoic strands, and lobularity. In a case series with patients given steroid therapy, the parenchymal enlargement, lobularity, and lobular outer margins decreased with steroid treatment while the hyperechoic foci and strands remained (Fig. 13.38).<sup>54</sup> In our experience, EUS often detects a clear line of demarcation between involved and uninvolved areas of AIP that is often not seen at CT or MRI (Fig. 13.39, Video 13.14). This transition zone should be carefully examined not only to rule out a small neoplasia, but to determine the biopsy site to help optimize the diagnostic sensitivity. Finally, EUS may demonstrate a normal appearing pancreas.

As the biliary tree is the most common extrapancreatic organ involvement in AIP, the extrahepatic duct may be abnormal on EUS. In a study of 37 patients with AIP, ultrasonographic findings of extrahepatic bile duct and gallbladder wall thickening was seen in 38%. There were 2 types of bile duct wall thickening including a “3-layer type” with a high-low-high echo appearance and a “parenchymal-echo type” with a thickened wall throughout the entire bile lumen and a parenchymal echo present within the bile duct itself.<sup>55</sup> A similar appearance to the “3-layer type” with a regular homogenous thickening with a hyper-hypo-hyperechoic

**TABLE 13.5****Idiopathic Duct-Centric Pancreatitis Level 1 and Level 2 Criteria for Type 1 Autoimmune Pancreatitis**

	Criterion	Level 1 Criteria	Level 2 Criteria
P	Parenchymal imaging	Typical: diffuse enlargement with delayed enhancement ( $\pm$ rimlike enhancement)	Indeterminate/atypical: segmental/focal enlargement with delayed enhancement
D	Ductal imaging by ERCP	Long ( $>1/3$ length of MPD) or multiple strictures without marked upstream dilation	Segmental/focal narrowing without marked upstream dilation (duct size $<5$ mm)
S	Serology	IgG4 $>2\times$ ULN value	IgG4 1–2 $\times$ ULN value
OOI	Other organ involvement	A or B (A) Histology of extrapancreatic organs Any 3 of the following: (1) Marked lymphoplasmacytic infiltration with fibrosis and without GELs (2) Storiform fibrosis (3) Obliterative phlebitis (4) Abundant ( $>10$ cells/hpf) IgG4 (+) cells (B) Typical radiologic evidence At least 1 of the following: (1) Segmental/multiple proximal (hilar or intrahepatic) or proximal and distal bile duct stricture (2) Retroperitoneal fibrosis	A or B (A) Histology of extrapancreatic organs including endoscopic biopsies of bile duct Both of the following: (1) Marked lymphoplasmacytic infiltration without GELs (2) Abundant ( $>10$ cells/hpf) IgG4 (+) cells (B) Physical or radiographic evidence At least one of the following: (1) Symmetrically enlarged salivary or lachrymal glands (2) Radiologic evidence of renal involvement described in association with AIP
H	Histology of the pancreas	LPSP on core biopsy or resection At least 3 of the following: (1) Periductal lymphoplasmacytic infiltrate without GELs (2) Obliterative phlebitis (3) Storiform fibrosis (4) Abundant ( $>10$ cells/hpf) IgG4(+) cells	LPSP on core biopsy Any 2 of the following: (1) Periductal lymphoplasmacytic infiltrate without GELs (2) Obliterative phlebitis (3) Storiform fibrosis (4) Abundant ( $>10$ cells/hpf) IgG4(+) cells
Rt	Response to steroids	Rapid (<2 week) radiologically demonstrable resolution or marked improvement in pancreatic or extrapancreatic manifestations	

Definitive type 1 AIP:  
Histology: Level 1 H  
Imaging: Any non-D level 1 or level 2 (typical) or  $\geq 2$  level 1 (+ level 2 D)  
Response to steroid: Level 1 S/OOI + Rt or level 1 D + level 2 S/OOI/H + Rt  
Probable type 1 AIP:  
Level 2 S/OOI/H + Rt

AIP, Autoimmune pancreatitis; ERCP, endoscopic retrograde cholangiopancreatography; GELs, granulocyte epithelial lesions; Ig, immunoglobulin; LPSP, lymphoplasmacytic sclerosing pancreatitis; MPD, main pancreatic duct.

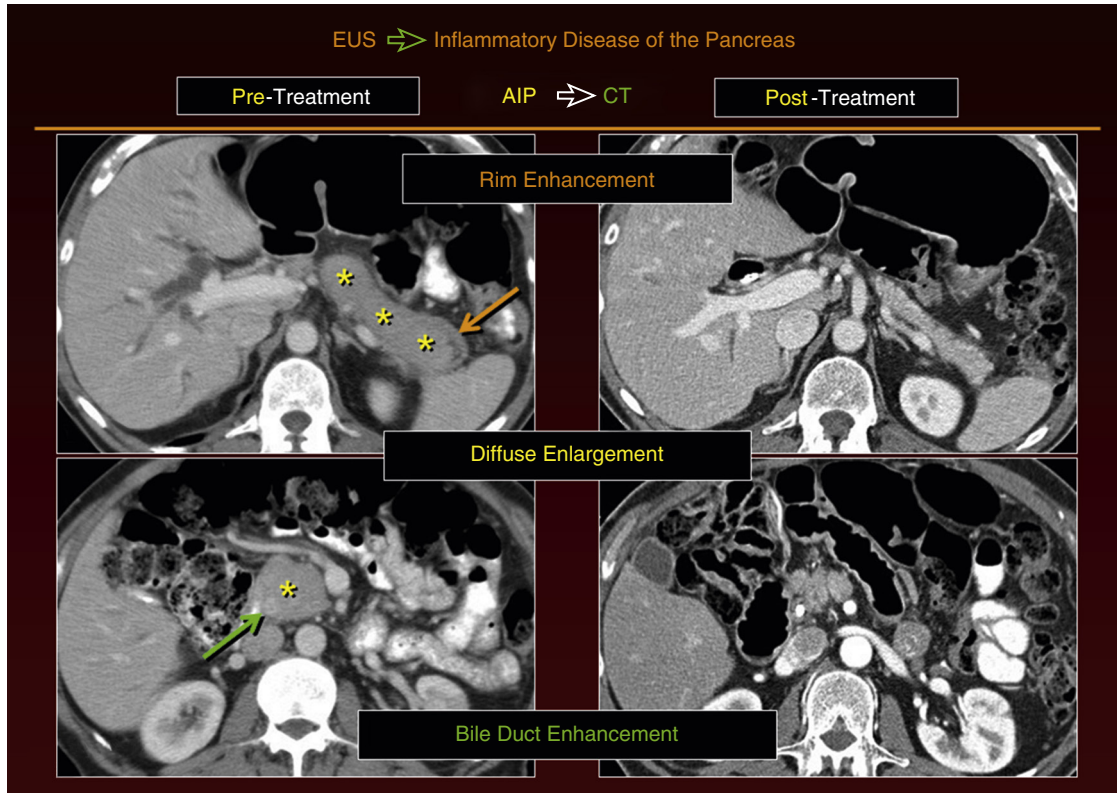
From Shimosegawa T, Chari ST, Frulloni L, et al. International consensus diagnostic criteria for autoimmune pancreatitis: guidelines of the International Association of Pancreatology. *Pancreas*. 2011;40:352–358.

**TABLE 13.6****ICDC Level 1 and Level 2 Criteria for Type 2 AIP**

	Criterion	Level 1 Criteria	Level 2 Criteria
P	Parenchymal imaging	Typical: diffuse enlargement with delayed enhancement ( $\pm$ rimlike enhancement)	Indeterminate/atypical: segmental/focal enlargement with delayed enhancement
D	Ductal imaging by ERCP	Long ( $>1/3$ length of MPD) or multiple strictures without marked upstream dilation	Segmental/focal narrowing without marked upstream dilation (duct size $<5$ mm)
OOI	Other organ involvement		Clinically diagnosed inflammatory bowel disease (IBD)
H	Histology of the pancreas	Both of the following on core biopsy or resection: (1) Granulocytic infiltration of duct wall (GEL) $\pm$ granulocytic acinar inflammation (2) Absent or scant (0–10 cells/hpf) IgG4(+) cells	Both of the following on core biopsy or resection: (1) Granulocytic and lymphoplasmacytic acinar infiltrate (2) Absent or scant (0–10 cells/hpf) IgG4(+) cells

**TABLE  
13.6****ICDC Level 1 and Level 2 Criteria for Type 2 AIP—cont'd**

Criterion	Level 1 Criteria	Level 2 Criteria
Rt	Response to steroids	Rapid (<2 week) radiologically demonstrable resolution or marked improvement in manifestations
Definitive type 2 AIP: Level 1 H or clinical IBD + level 2 H + Rt		
Probable type 2 AIP: Level 2 H/clinical IBD + Rt		
AIP, Autoimmune pancreatitis; ERCP, Endoscopic retrograde cholangiopancreatography; GEL, granulocyte epithelial lesion; Ig, immunoglobulin; MPD, main pancreatic duct.		
From Shimosegawa T, Chari ST, Frulloni L, et al. International consensus diagnostic criteria for autoimmune pancreatitis: guidelines of the International Association of Pancreatologists. <i>Pancreas</i> . 2011;40:352–358.		



• **Fig. 13.31** Typical computed tomography (CT) appearance of autoimmune pancreatitis (AIP) with rim enhancement (orange arrow), diffuse enlargement (yellow asterisk), and bile duct enhancement (green arrow). The common occurrence of pancreatic atrophy following steroid administration is shown in the pretreatment (left) versus posttreatment (right) images.

series of layers of the ductal wall (termed “sandwich pattern”) was seen on EUS in addition to bile duct dilatation in one series.<sup>52</sup> This EUS appearance is different than what is often seen with pancreaticobiliary malignancies, which may be more irregular (Fig. 13.40).

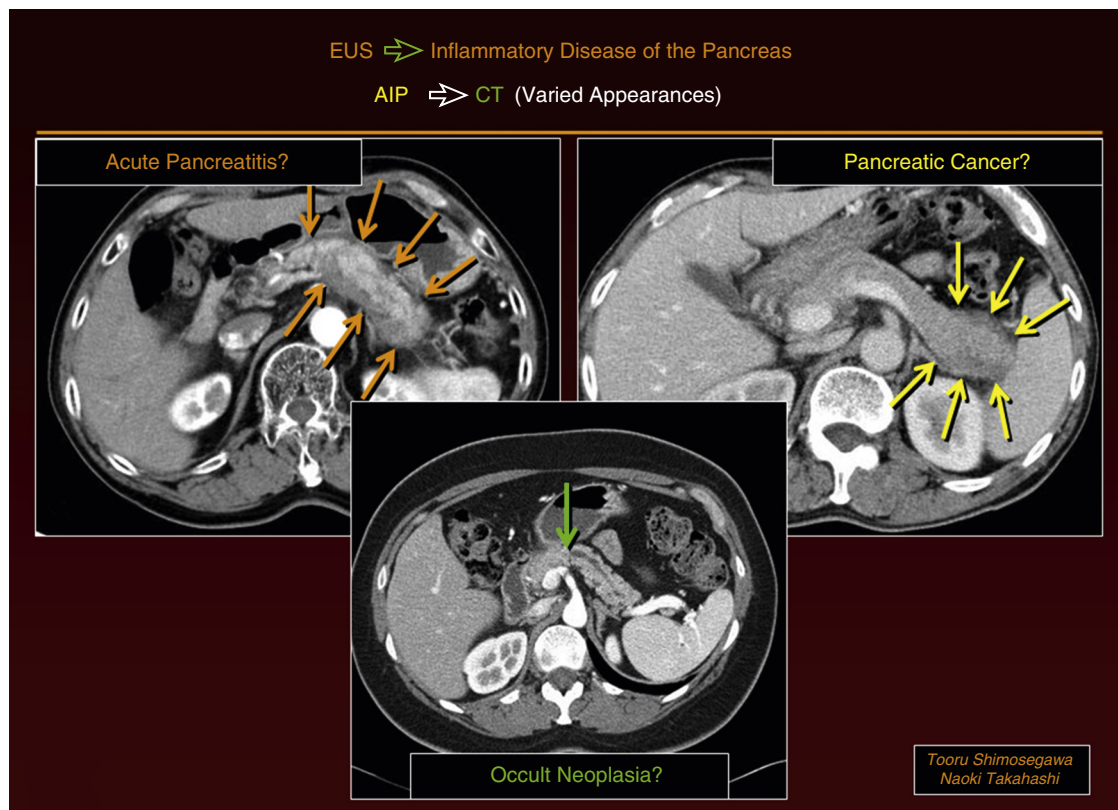
It is important to distinguish focal AIP from PaC. Hoki et al compared EUS findings in patients who were diagnosed with AIP and resected PaC.<sup>56</sup> This study found that diffuse hypoechoic areas, diffuse enlargement of the pancreas, bile duct wall thickening, and peripancreatic hypoechoic margins were more commonly seen in patients ultimately diagnosed with AIP as compared to those with pancreatic cancer. On the other hand, focal hyperechoic areas and focal enlargement were more common in patients with PaC. Although these all reach statistical significance, each

characteristic (other than peripancreatic hypoechoic margins) was seen in both diseases. In addition, lymph node enlargement was seen with similar frequencies in AIP and PaC.

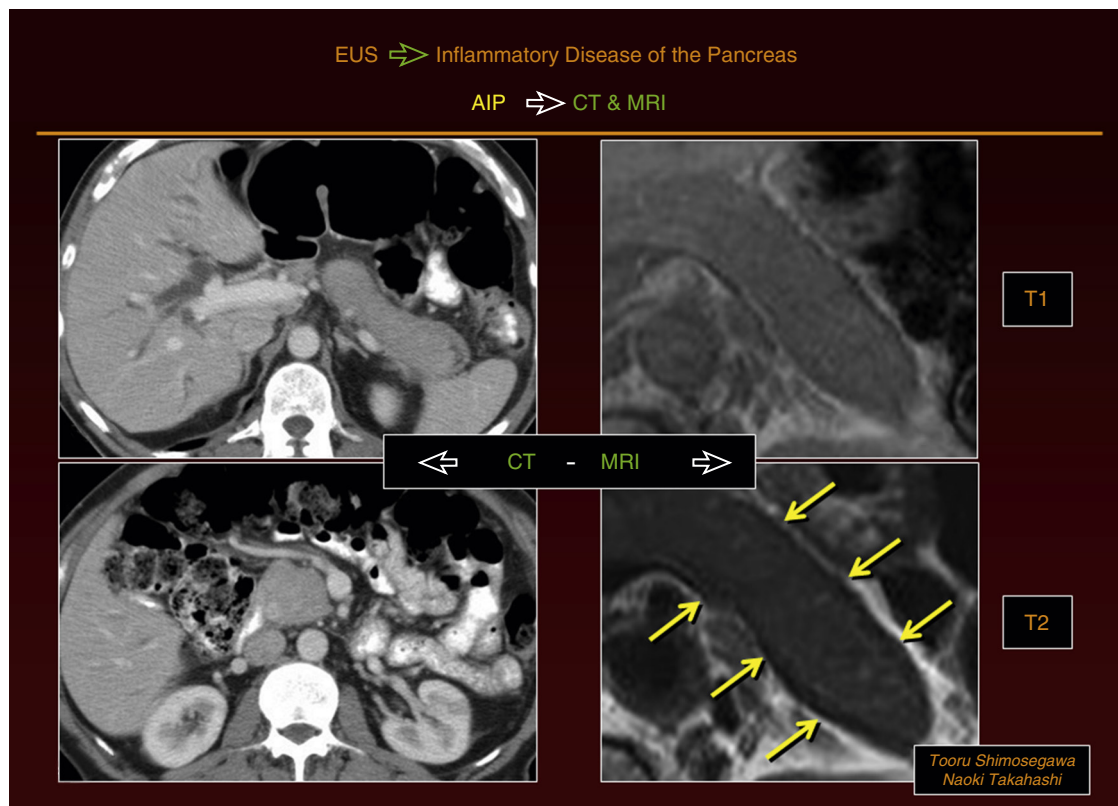
### Endoscopic Ultrasound Sampling

#### Fine-Needle Aspiration

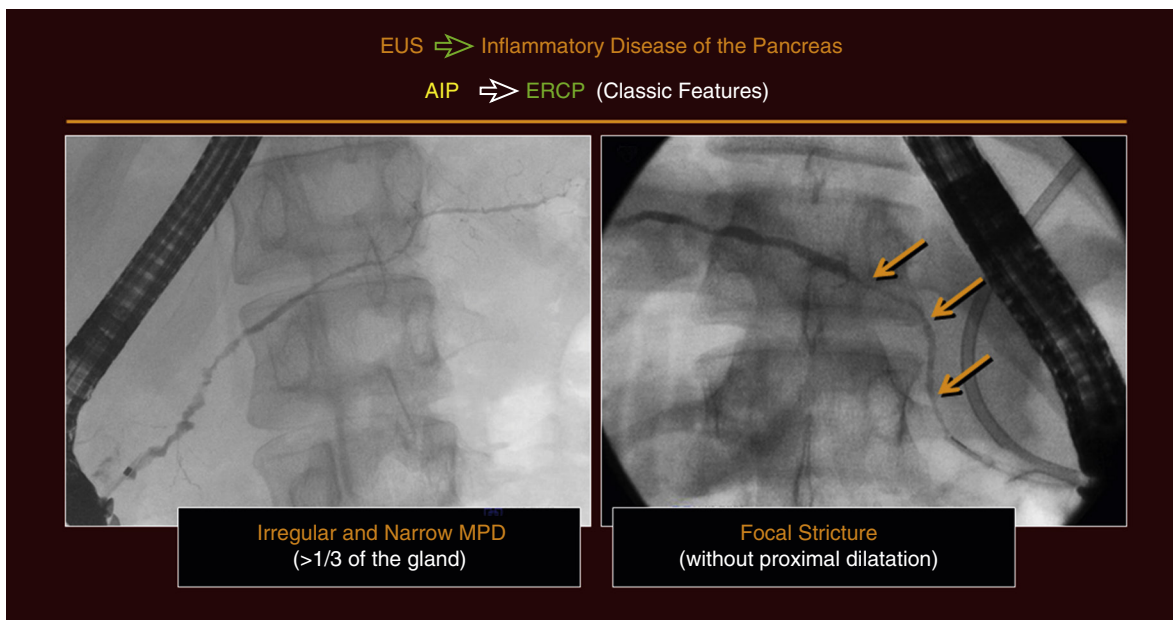
As pancreatic histology is part of all diagnostic algorithms and because EUS imaging itself has not proven to be broadly useful among endosonographers, the primary role of EUS in AIP may be to obtain tissue biopsies. Historically the most commonly performed method of tissue acquisition during EUS has been FNA, but the recent introduction of new core biopsy needles is likely to modify this practice. FNA has been shown to be superior to ERCP



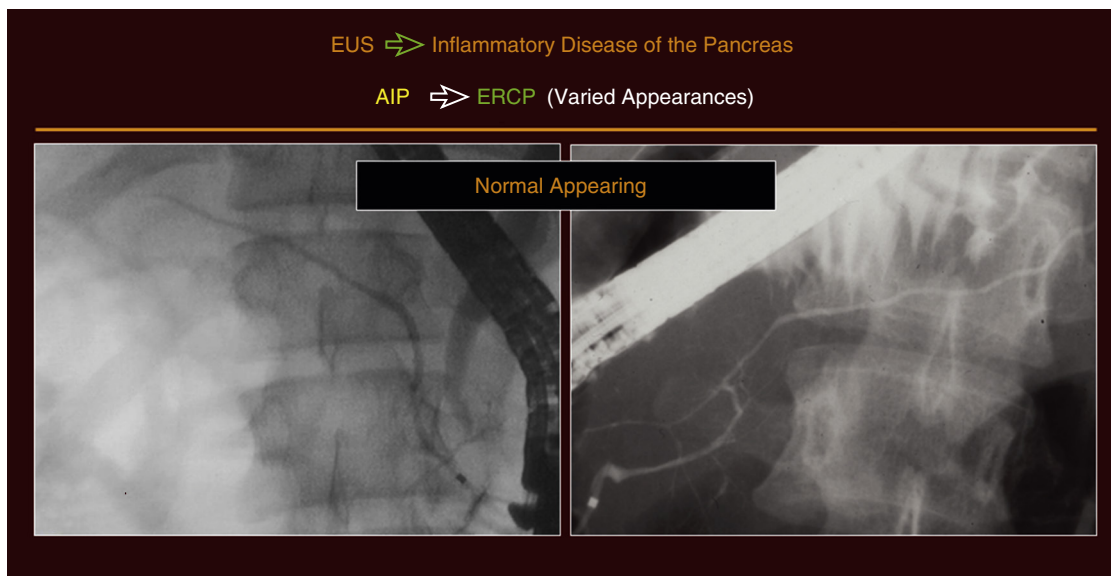
• **Fig. 13.32** Computed tomography (CT) examples of varied appearances of autoimmune pancreatitis (AIP) including acute pancreatitis (upper left arrows), focal mass (upper right arrows), and of abrupt main pancreatic duct cut-off with upstream ductal dilatation suspicious for an occult neoplasia (lower middle arrows). Each of the aforementioned patients instead had AIP as established by endoscopic ultrasound-guided core biopsies.



• **Fig. 13.33** Magnetic resonance imaging (MRI) demonstrates the delayed rim enhancement seen in autoimmune pancreatitis (arrows). CT, Computed tomography.



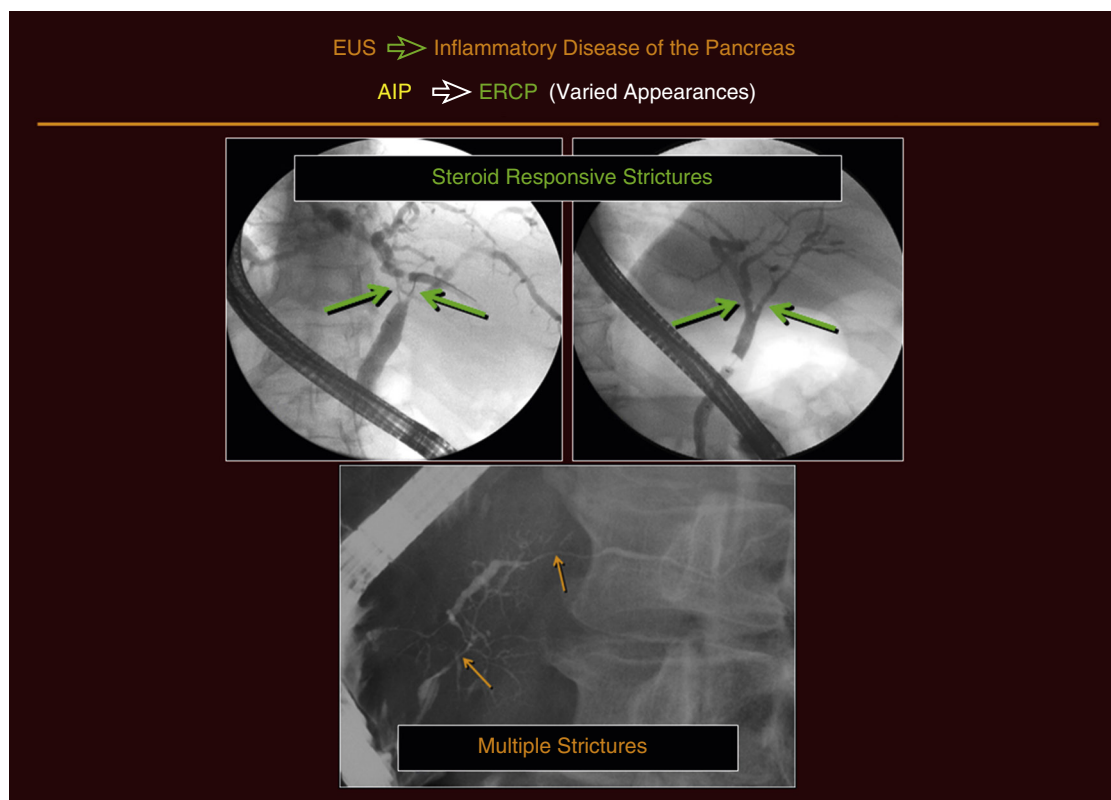
• **Fig. 13.34** ERCP demonstrating classic features of autoimmune pancreatitis (AIP) including an irregular and narrow main pancreatic duct involving at least one third of the entire duct (left) as well as the presence of a focal stricture without proximal ductal dilatation (right). *ERCP*, Endoscopic retrograde cholangiopancreatography; *MPD*, Main pancreatic duct.



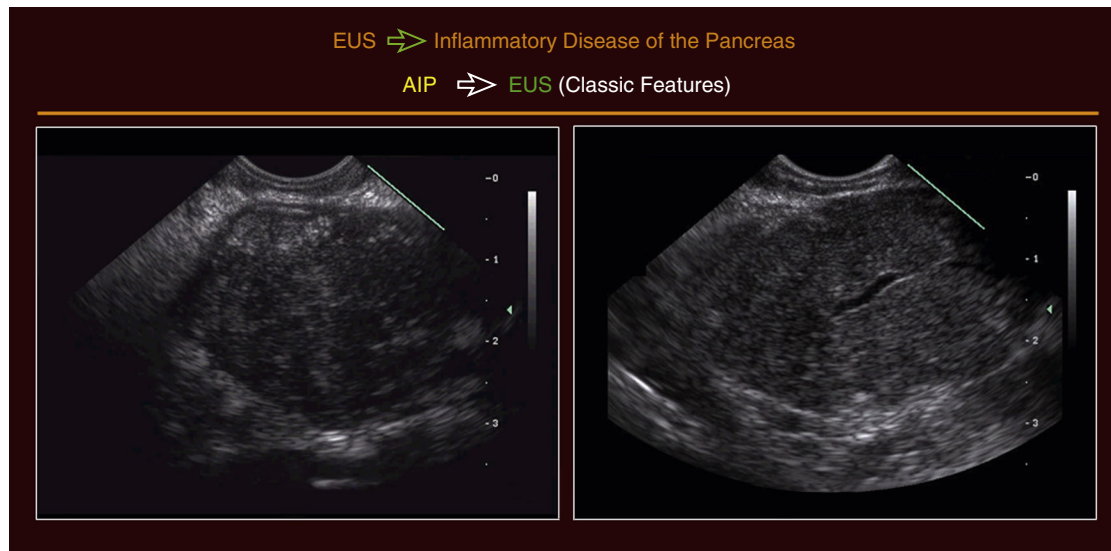
• **Fig. 13.35** The pancreatograms demonstrate a limitation of this imaging modality in two patients with biopsy proven AIP who had relatively normal pancreatography. *AIP*, Autoimmune pancreatitis; *ERCP*, endoscopic retrograde cholangiopancreatography.

with duodenal papillary biopsy for AIP.<sup>57</sup> FNA in the setting of AIP is typically performed to either sample a focal mass lesion to help exclude PaC, or from diffuse areas of glandular swelling, often in the body/tail, to establish the diagnosis of AIP. However, both AIP and PaC can present either as a focal mass or with diffuse glandular swelling. A limitation of FNA is that it usually provides a small cytologic specimen in which the tissue has lost the inherent tissue architecture. Although such cytologic specimens can easily provide a diagnosis of cancer, they are generally insufficient to diagnose AIP.

There are conflicting data as to the diagnostic utility of EUS FNA for AIP. A recent multicenter study that included 78 patients with imaging suspicion of AIP who underwent EUS FNA using a standard 22-gauge needle concluded that EUS FNA may be beneficial.<sup>58</sup> In this study, diagnostic features for type 1 AIP including  $\geq$ CD38(+) plasma cells per high power field (HPF) which was used as a marker for lymphoplasmacytic infiltrate,  $\geq$ 10 IgG4(+) cells per HPF, storiform fibrosis, and obliterative phlebitis were found in 43 (55.1%), 19 (24.4%), 49 (62.8%), and 38 (48.7%) patients, respectively. A total of 45 (57.7%) patients met the



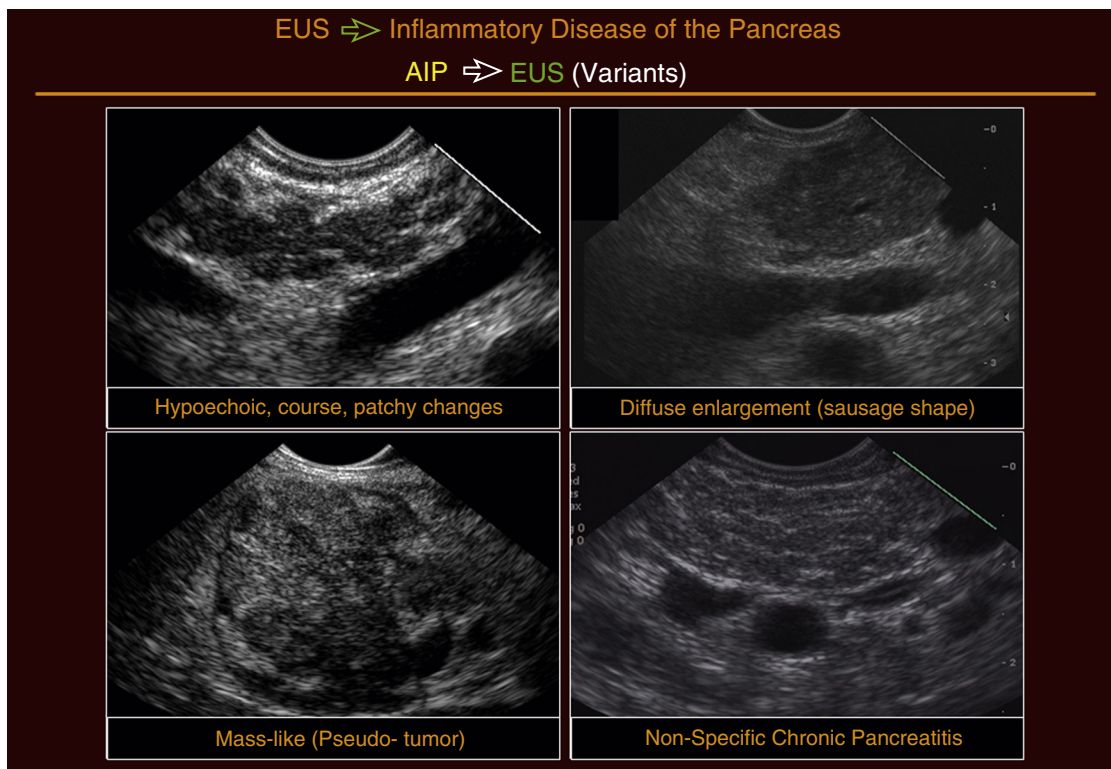
• **Fig. 13.36** In patients without classic features of autoimmune pancreatitis (AIP), there are other findings that may provide important diagnostic clues including the presence of steroid responsive strictures (green arrows) and multiple remote pancreatic duct strictures (orange arrows). *ERCP*, Endoscopic retrograde cholangiopancreatography.



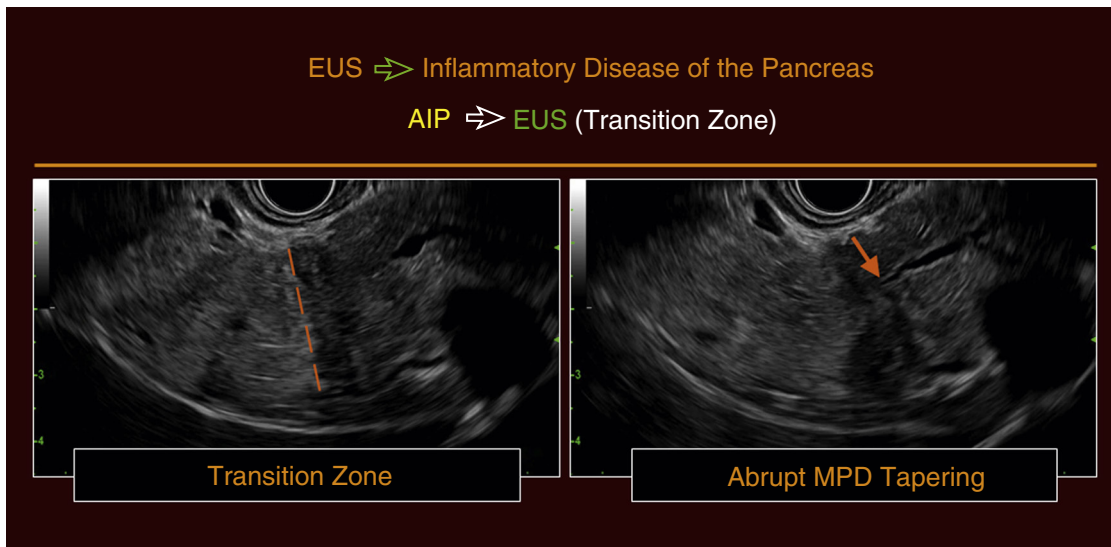
• **Fig. 13.37** EUS demonstrates the classic features of autoimmune pancreatitis (AIP) including a diffusely enlarged (*sausage-shape*) gland, parenchyma that is hypoechoic, coarse, patchy, and heterogeneous, and an irregular ectatic main pancreatic duct. *EUS*, Endoscopic ultrasound.

ICDC criteria for LPSP. In contrast, another recent multicenter study found no diagnostic utility of EUS FNA.<sup>59</sup> Lymphoplasmacytic infiltrate and abundant IgG4(+) cells were detected in 36 (72%) and 27 (54%) of patients, respectively, whereas storiform fibrosis and obliterative phlebitis were not observed. For type 2 AIP, GELs were detected in three patients. Overall, the sensitivity,

specificity, positive predictive value, and negative predictive value of EUS FNA for ICDC level 1 criteria was 7.9%, 100%, 100%, and 25.5%, respectively, and for ICDC level 2 criteria was 57.9%, 50%, 78.6%, and 27.3%, respectively. Even use of a standard 19-gauge needle for histologic review allowed diagnosis of AIP in only 43% of patients.<sup>60</sup>



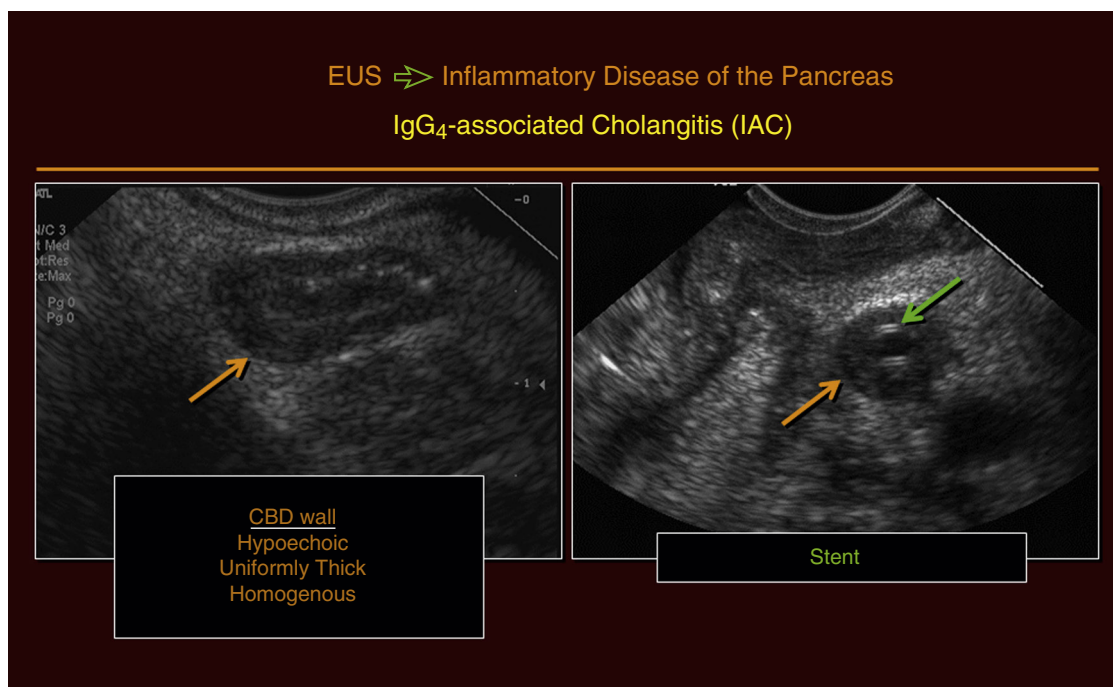
• **Fig. 13.38** In patients with autoimmune pancreatitis (AIP), endoscopic ultrasound (EUS) may also demonstrate other variants including an incomplete array of the classic findings (upper left and right), the presence of a masslike lesion or pseudo-tumor (lower left), or features of typical nonspecific chronic pancreatitis (lower right).



• **Fig. 13.39** In patients with autoimmune pancreatitis (AIP), there is often a fairly sharply demarcated transition zone that is not demonstrated on CT or MRI (dashed lines). This is a point where the gland abruptly transitions from normal appearing to the typical manifestations of AIP. It is important to carefully examine this area and to perform EUS-guided core biopsy in the appropriate region. In addition, the MPD often tapers severely in this region (arrow) heightening concern for an occult neoplasia. *EUS*, Endoscopic ultrasound; *MPD*, main pancreatic duct. (See [Video 13.14](#).)

Although many institutions use standard FNA to diagnose AIP, there are no broadly accepted consensus cytologic diagnostic criteria for AIP and most pathologists are reluctant to rely solely on FNA/cytologic specimens.<sup>61–64</sup> Due to the inability to obtain

adequate core specimens using standard FNA needles, some advocate for the use of less rigorous or incomplete pathology criteria for the cytologic diagnosis of AIP. Less stringent criteria may rely on the presence of a lymphoplasmacytic infiltrate alone without



• **Fig. 13.40** A key feature and clue to the presence of autoimmune pancreatitis, when present, is the finding of IgG<sub>4</sub>-associated cholangitis (IAC) that presents with a hypoechoic, uniformly thickened wall circumferentially, and is homogeneous in echodensity and echopattern as shown. *CBD*, Common bile duct; *Ig*, immunoglobulin.

the need for the infiltrate to be in a periductal location. Softened criteria also allow for lesser degrees of preservation of ductules, venules, or arterioles required within the specimen.<sup>61–63</sup> Although loosening the pathologic criteria requirement may allow for improved diagnostic sensitivity, it is at the expense of decreasing the specificity of FNA for AIP. This is particularly problematic for differentiating AIP from PaC, which is often associated with a lymphoplasmacytic infiltration.

Some suggest that the benefit of EUS FNA lies on its ability to exclude PaC rather than diagnose AIP.<sup>65–67</sup> However, assuming that a negative EUS FNA of a pancreas mass equates to exclusion of an underlying malignancy can be dangerous given the 10% to 40% false negative FNA rate for cancer that is reported in many centers.<sup>68–72</sup>

### **Tru-Cut Biopsy**

To overcome the limitations of FNA, larger caliber cutting biopsy needles were developed that acquire samples with preserved tissue architecture to allow histologic examination, namely the 19-gauge trucut biopsy TCB device (Quick-Core, Wilson-Cook, Winston-Salem, North Carolina).

We previously examined our experience performing EUS TCB in terms of the diagnostic sensitivity and safety among patients with a final diagnosis of AIP based on the HISORt criteria. Forty-eight patients (38 male, mean age 59.7 years) had a mean of 2.9 EUS TCB (range 1 to 7) performed. Histologic examination of the EUS TCB specimens provided a diagnosis in 35 patients (73%). The diagnostic sensitivity varied among the 5 endosonographers from 33% to 90%. Nondiagnostic cases were found to have CP ( $n = 8$ ), nonspecific histology ( $n = 2$ ), or a failed tissue acquisition ( $n = 3$ ). EUS FNA (mean 3.4 passes, range 1 to 7) was also performed and failed to establish a diagnosis in any patient using strict AIP histologic criteria. Adverse events included mild

transient abdominal pain ( $n = 3$ ) and self-limited intraprocedural bleeding ( $n = 1$ ). It is unclear if TCB and/or FNA attributed to these adverse events. No patient required hospitalization or therapeutic intervention. Of note, the serum IgG<sub>4</sub> was  $>2\times$  the upper limit of normal in only 23% of patients. None of the patients with an EUS TCB diagnosis of AIP required surgical intervention for diagnosis. Over a mean follow-up of 2.6 years, no false negative diagnoses of PaC were identified. Prior to EUS, the diagnosis of AIP was strongly suspected in 14 patients as a result of their clinical, laboratory, or imaging findings. For 22 patients, the diagnosis was considered pre-EUS as part of a broader differential. Our data suggest the potential utility of EUS imaging to the initial suspicion of AIP in 12 patients, thereby initiating pancreatic TCB and subsequent clinical evaluation of AIP. More recently, we looked at the use of EUS TCB in pediatric patients with a suspected diagnosis of AIP.<sup>73</sup> The diagnostic yield of EUS TCB in this patient population was 87%.

EUS TCB appears to be safe and may provide sufficient material to aid in the diagnosis of AIP, thereby guiding treatment and avoiding surgical intervention. Some suggest the use of EUS TCB as a “rescue” technique to obtain adequate tissue samples if EUS FNA failed.<sup>49,62</sup> The current ICDC guidelines recommend a pancreatic core biopsy in patients presenting with a focal mass and/or obstructive jaundice once cancer has been excluded and the diagnosis remains elusive.<sup>46</sup> Given the difficulty in using EUS TCB, there has been the drive to use and evaluate alternate needle types.

### **Other Endoscopic Ultrasound Fine-Needle Biopsy Techniques**

Most studies on EUS fine-needle biopsy (FNB) besides TCB such as the ProCore (Cook Medical, Bloomington, Indiana) have focused on its use in pancreatic masses rather than AIP. A recent case report used the SharkCore needle (Medtronic,

Boston, Massachusetts) which is a fork-tipped needle, to diagnose type 1 AIP.<sup>74</sup> As several new needle designs offer much promise in terms of readily obtaining core biopsies, there is sure to be a flurry of reports likely among suspected AIP and other pathologies.

## Image-Enhancing Techniques in Endoscopic Ultrasound

### Endoscopic Ultrasound Elastography

In one study on the use of elastography in AIP, five patients with focal AIP were found to have a homogenous stiff (blue) pattern in the mass and throughout the entire pancreas, which differed from pancreatic cancer or normal pancreas in which the pancreatic parenchyma was predominately of intermediate stiffness (green).<sup>75</sup>

### Contrast-Enhanced Endoscopic Ultrasound

The use of contrast-enhanced EUS has been reported in few studies, particularly when trying to differentiate between focal AIP and PCA. Contrast-enhanced EUS uses intravenously administered ultrasound contrast agents (i.e., Sonovue [sulfur hexafluoride MBs; Bracco Interventional BV, Amsterdam], Levovist [Bayer AG, Leverkusen, Germany], or Sonazoid [perfluorobutane; GE Healthcare, Little Chalfont, Buckinghamshire, UK]) to produce microbubbles that allow visualization of the vascular pattern within the pancreatic mass lesion.<sup>76</sup> In a cohort of 10 patients who received Sonovue contrast and EUS imaging in the bicolor Doppler mode, AIP was associated with hypervascularity within the masslike lesion and the surrounding pancreatic parenchyma as compared to pancreatic cancer where the mass was hypovascular in comparison to the surrounding pancreatic tissue.<sup>77</sup>

Contrast-enhanced harmonic EUS uses a dedicated contrast harmonic mode rather than Doppler imaging. The use of contrast harmonic-enhanced imaging allows for decreased artifact produced by the Doppler, including ballooning and overpainting.<sup>76</sup> In one study, 8 patients with focal AIP and 22 patients with pancreatic cancer were given Sonazoid ultrasonographic contrast and analyzed using a radial echoendoscope with the conventional tissue harmonic echo (for standard harmonic imaging) and extended pure harmonic detection (for contrast-enhanced harmonic imaging).<sup>78</sup> The ultrasonographic contrast uptake and distribution was isoenhanced homogenous in all patients with AIP compared to only one patient with pancreatic cancer. The majority of patients with pancreatic cancer had a hypoenhanced uptake in a heterogeneous pattern. Furthermore, the optimal maximum intensity gain (MIG) cutoff value to differentiate between AIP and pancreatic cancer with a 100% specificity and sensitivity using a receiver operator characteristic (ROC) curve was 12.5. The results from the aforementioned studies should be interpreted with caution and we do not regard their findings to be conclusive as to the role of image-enhancing techniques in differentiating between AIP and PaC.

## Benign Pancreatic Masses

### Brief Overview

There have been case reports/series on EUS assisting in the diagnosis of a multitude of benign pancreatic masses including but not limited to pseudopapillary neoplasms,<sup>79–81</sup> elastofibroma,<sup>82</sup>

perivascular epithelioid cell tumors,<sup>83</sup> hemangioma,<sup>84</sup> tuberculosis,<sup>85</sup> and actinomycosis.<sup>86</sup> However, the most common benign pancreatic mass is an inflammatory mass occurring in the setting of acute or CP. EUS with tissue sampling is often essential for the early and accurate diagnosis of these lesions. This section highlights the challenges in distinguishing a benign from malignant pancreatic mass and the use of different techniques that may improve the diagnostic accuracy of EUS.

### Endoscopic Ultrasound Sampling

#### Endoscopic Ultrasound Fine-Needle Aspiration

EUS FNA is a standard technique for evaluating pancreatic masses. One of the limiting factors of EUS FNA is the suboptimal false negative rate. In one study, 38 patients (9.8%) had inconclusive cytology including indeterminate, benign, atypical, or suspicious for malignancy.<sup>87</sup> Among these patients, the diagnosis was achieved in 24 (63.2%) by repeat EUS FNA, surgical or percutaneous biopsy. Five patients underwent surgical resection and were found to have benign disease. The presence of a cytopathologist for rapid on-site evaluation (ROSE) during the procedure has been shown to increase the diagnostic yield of EUS FNA.<sup>88</sup>

Molecular testing may be employed to enhance the diagnostic capability of EUS FNA specimens to help distinguish malignant from benign pancreatic masses. One study performed RNA sequencing (RNAseq) on pancreatic tissue obtained by EUS FNA using a 22-gauge needle from 15 patients with PaC and 8 patients with benign masses.<sup>89</sup> Benign masses were confirmed either by surgical resection or an extended (>1 year) benign clinical course and compatible imaging. By analysis of 85 genes that are either upregulated or downregulated in PaC, RNAseq provided a diagnostic sensitivity and specificity for malignancy of 87% (95% CI 58% to 98%) and 75% (95% CI 35% to 96%). More studies are required to determine the utility of these and other emerging forms of molecular testing of EUS FNA specimens from pancreatic masses before their use can be advocated.

#### Endoscopic Ultrasound-Guided Core Biopsy

A variety of EUS core biopsy needles of varying shapes and sizes have been introduced. Study results are often conflicting and to our knowledge none have been shown to consistently be superior over other needle types. In a meta-analysis of nine studies comparing ProCore FNB needles to standard FNA needles there was no difference in diagnostic adequacy (OR 0.26; 95% CI 0.043 to 1.53,  $P = 0.136$ ), diagnostic accuracy (OR 1.12; 95% CI 0.65 to 1.92,  $P = 0.687$ ), histologic core tissue obtained (OR 0.87; 95% CI 0.44 to 1.75,  $P = 0.7$ ), or adverse events (OR 1.1; 95% CI 0.4 to 3,  $P = 0.864$ ).<sup>90</sup> The only statistically significant finding was that FNB required fewer passes than FNA (OR -1.03; 95% CI -1.57 to -0.50,  $P < .001$ ). In contrast, one study demonstrated a lower diagnostic yield of FNB using a 22-gauge ProCore needle compared to FNA.<sup>91</sup> It would appear that the ProCore FNB is not clearly superior to standard FNA needles.

Currently, the role of EUS FNB in the diagnosis of pancreatic masses is unclear. We tend to reserve its use for select patients with prior nondiagnostic EUS FNA in which repeat EUS FNA with ROSE continues to have inadequate sampling. It remains to be seen how improvements in the available FNB needles will affect the accuracy and ease of sampling to allow them to have a bigger role in the diagnostic approach to pancreatic masses. Core biopsy needles may also prove useful as the field of molecular testing evolves.

## Image-Enhancing Techniques in Endoscopic Ultrasound

### Endoscopic Ultrasound Elastography

Both qualitative (color pattern) and quantitative (strain ratio, SR) elastography have been shown to assist with distinguishing benign from malignant pancreatic masses.<sup>92</sup> Qualitative elastography had a sensitivity and specificity of 98% (95% CI 93% to 100%) and 69% (95% CI 52% to 82%), respectively, in a meta-analysis of seven studies. Hard, stiff areas are blue, intermediate stiff areas are green, medium-soft areas are yellow, and soft areas are red.<sup>24</sup> Classically, PaC manifests as intense blue coloration, whereas benign lesions have mixed coloration of green, yellow, and less intense blue.<sup>93</sup> A predominance of green on elastography imaging essentially excludes malignancy.<sup>94</sup>

The sensitivity and specificity of quantitative elastography in distinguishing benign from malignant masses on a meta-analysis was 96% (95% CI 86% to 99%) and 76% (95% CI 58% to 87%), respectively.<sup>92</sup> Malignant masses have a higher SR than benign inflammatory masses.<sup>95–97</sup> Kim SY et al aimed to determine cutoff values for SR when differentiating between normal pancreas, CP, and PCA.<sup>95</sup> The SR (quotient B/A with area A corresponding to the largest possible area of the pancreatic parenchyma in normal pancreas and CP or the largest possible area of the mass, and area B referred to a soft peripancreatic reference area) was calculated three times in each patient and the mean value was used. The mean SR was 3.78 (SD 1.35) for normal pancreas, 8.21 (SD 5.16) for CP, and 21.80 (SD 12.23) for PCA ( $P < .001$ ). The sensitivity, specificity, and accuracy of a cutoff mean SR of 5.62 for CP was 71.6%, 75.2%, and 74.8%, respectively, whereas a cutoff mean SR of 8.86 for PCA was 95.6%, 96.3%, and 96.2%, respectively.

### Contrast-Enhanced Endoscopic Ultrasound

Several studies have shown that contrast-enhanced EUS improves the ability to differentiate CP from pancreatic malignancy.<sup>98–101</sup> EUS images in the B mode and Doppler views obtained before and after intravenous injection of 2.4 mL SonoVue (BR1, Bracco, Italy) followed by 10 mL of saline were compared to either EUS FNA and/or surgical specimens.<sup>98</sup> CP was defined as no detectable vascularization before injection and regular vascularization with no changing diameter after injection of SonoVue. PCA was defined as no visible vascularization before injection, an irregular appearance of arterial vessels over a short distance within 3 minutes after contrast injection, and the lack of venous vessels in the lesion. The specificity of the diagnosis of CP and pancreatic cancer using the previously mentioned criteria were 93.3% and 91.1%, respectively.

CP was found to be hypervascular in the early arterial phase of contrast enhancement with a dynamic enhancement pattern similar to the remainder of the pancreas, whereas PCA was

more often hypovascular with lower contrast enhancement than the normal parenchyma during low mechanical index contrast-enhanced EUS.<sup>99</sup>

One study directly compared EUS elastography (mostly red/green coding of the lesion and mostly blue coding), contrast-enhanced high mechanical index (use of Doppler imaging to show homogeneous and irregular vascularization), and low mechanical index (iso/hyperenhancement of the lesion and hypoenhancement) in the differentiation between CP and PCA, respectively.<sup>100</sup> Contrast-enhanced high mechanical index EUS was found to be the most reliable for distinguishing between the two.

## Summary

EUS has an important adjunctive role in the management of inflammatory diseases of the pancreas. EUS should be considered in the diagnostic algorithm for CP and in evaluation of idiopathic AP. EUS tissue sampling should be considered in patients with suspected AIP and has an essential role in differentiating benign from malignant pancreatic masses. More data are needed to determine if any biopsy needle is clearly superior and in what settings. Similarly, more studies are needed to understand whether complementary imaging modalities such as elastography and contrast-enhanced EUS provide any true incremental value over EUS alone in the diagnostic work-up of these inflammatory diseases of the pancreas.

## Key References

8. Conwell DL, Lee LS, Yadav D, et al. American pancreatic association practice guidelines in chronic pancreatitis: evidence-based report on diagnostic guidelines. *Pancreas*. 2014;43:1143–1162.
28. Tenner S, Baillie J, DeWitt J, et al. American College of Gastroenterology guideline: management of acute pancreatitis. *Am J Gastroenterol*. 2013;108:1400–1415; 1416.
46. Shimosegawa T, Chari ST, Frulloni L, et al. International consensus diagnostic criteria for autoimmune pancreatitis: guidelines of the International Association of Pancreatologists. *Pancreas*. 2011;40: 352–358.
52. De Lisi S, Buscarini E, Arcidiacono PG, et al. Endoscopic ultrasonography findings in autoimmune pancreatitis: be aware of the ambiguous features and look for the pivotal ones. *JOP*. 2010;11: 78–84.
53. Buscarini E, Lisi SD, Arcidiacono PG, et al. Endoscopic ultrasonography findings in autoimmune pancreatitis. *World J Gastroenterol*. 2011;17:2080–2085.

## References

Access the reference list online at [ExpertConsult.com](http://ExpertConsult.com).

## References

1. Rajan E, Clain JE, Levy MJ, et al. Age-related changes in the pancreas identified by EUS: a prospective evaluation. *Gastrointest Endosc.* 2005;61:401–406.
2. Savides TJ, Gress FG, Zaidi SA, et al. Detection of embryologic ventral pancreatic parenchyma with endoscopic ultrasound. *Gastrointest Endosc.* 1996;43:14–19.
3. Petrone MC, Arcidiacono PG, Perri F, et al. Chronic pancreatitis-like changes detected by endoscopic ultrasound in subjects without signs of pancreatic disease: do these indicate age-related changes, effects of xenobiotics, or early chronic pancreatitis? *Pancreatology.* 2010;10:597–602.
4. Wiersema MJ, Hawes RH, Lehman GA, et al. Prospective evaluation of endoscopic ultrasonography and endoscopic retrograde cholangiopancreatography in patients with chronic abdominal pain of suspected pancreatic origin. *Endoscopy.* 1993;25:555–564.
5. Majumder S, Chari ST. Chronic pancreatitis. *Lancet.* 2016;387:1957–1966.
6. Campisi A, Brancatelli G, Vullierme MP, et al. Are pancreatic calcifications specific for the diagnosis of chronic pancreatitis? A multidetector-row CT analysis. *Clin Radiol.* 2009;64:903–911.
7. Luetmer PH, Stephens DH, Ward EM. Chronic pancreatitis: reassessment with current CT. *Radiology.* 1989;171:353–357.
8. Conwell DL, Lee LS, Yadav D, et al. American pancreatic association practice guidelines in chronic pancreatitis: evidence-based report on diagnostic guidelines. *Pancreas.* 2014;43:1143–1162.
9. Varadarajulu S, Eltoum I, Tamhane A, et al. Histopathologic correlates of noncalcific chronic pancreatitis by EUS: a prospective tissue characterization study. *Gastrointest Endosc.* 2007;66:501–509.
10. Catalano MF, Sahai A, Levy M, et al. EUS-based criteria for the diagnosis of chronic pancreatitis: the rosemont classification. *Gastrointest Endosc.* 2009;69:1251–1261.
11. D’Souza SL, Anderson MA, Korsnes SJ, et al. EUS diagnostic criteria for chronic pancreatitis: a comparison of conventional versus rosemont criteria. *Dig Dis Sci.* 2015;60:3782–3787.
12. Trikudanathan G, Vega-Peralta J, Malli A, et al. Diagnostic Performance of Endoscopic Ultrasound (EUS) for Non-Calcific Chronic Pancreatitis (NCCP) based on histopathology. *Am J Gastroenterol.* 2016;111:568–574.
13. Albashir S, Bronner MP, Parsi MA, et al. Endoscopic ultrasound, secretin endoscopic pancreatic function test, and histology: correlation in chronic pancreatitis. *Am J Gastroenterol.* 2010;105:2498–2503.
14. LeBlanc JK, Chen JH, Al-Haddad M, et al. Endoscopic ultrasound and histology in chronic pancreatitis: how are they associated? *Pancreas.* 2014;43:440–444.
15. Wallace MB, Hawes RH, Durkalski V, et al. The reliability of EUS for the diagnosis of chronic pancreatitis: interobserver agreement among experienced endosonographers. *Gastrointest Endosc.* 2001;53:294–299.
16. Gardner TB, Gordon SR. Interobserver agreement for pancreatic endoscopic ultrasonography determined by same day back-to-back examinations. *J Clin Gastroenterol.* 2011;45:542–545.
17. Stevens T, Lopez R, Adler DG, et al. Multicenter comparison of the interobserver agreement of standard EUS scoring and rosemont classification scoring for diagnosis of chronic pancreatitis. *Gastrointest Endosc.* 2010;71:519–526.
18. Kalmin B, Hoffman B, Hawes R, et al. Conventional versus rosemont endoscopic ultrasound criteria for chronic pancreatitis: comparing interobserver reliability and intertest agreement. *Can J Gastroenterol.* 2011;25:261–264.
19. Del Pozo D, Poves E, Tabernero S, et al. Conventional versus rosemont endoscopic ultrasound criteria for chronic pancreatitis: interobserver agreement in same day back-to-back procedures. *Pancreatology.* 2012;12:284–287.
20. Lowenfels AB, Maisonneuve P, Cavallini G, et al. Pancreatitis and the risk of pancreatic cancer. International Pancreatitis Study Group. *N Engl J Med.* 1993;328:1433–1437.
21. Ardenghi JC, Lopes CV, Campos AD, et al. Endoscopic ultrasound and fine needle aspiration in chronic pancreatitis: differential diagnosis between pseudotumoral masses and pancreatic cancer. *JOP.* 2007;8:413–421.
22. Fritscher-Ravens A, Brand L, Knofel WT, et al. Comparison of endoscopic ultrasound-guided fine needle aspiration for focal pancreatic lesions in patients with normal parenchyma and chronic pancreatitis. *Am J Gastroenterol.* 2002;97:2768–2775.
23. Varadarajulu S, Tamhane A, Eloubeidi MA. Yield of EUS-guided FNA of pancreatic masses in the presence or the absence of chronic pancreatitis. *Gastrointest Endosc.* 2005;62:728–736; quiz 751, 753.
24. Giovannini M, Hookey LC, Bories E, et al. Endoscopic ultrasound elastography: the first step towards virtual biopsy? Preliminary results in 49 patients. *Endoscopy.* 2006;38:344–348.
25. Kuwahara T, Hirooka Y, Kawashima H, et al. Quantitative diagnosis of chronic pancreatitis using EUS elastography. *J Gastroenterol.* 2017;52:868–874.
26. Iglesias-Garcia J, Dominguez-Munoz JE, Castineira-Alvarino M, et al. Quantitative elastography associated with endoscopic ultrasound for the diagnosis of chronic pancreatitis. *Endoscopy.* 2013;45:781–788.
27. Dominguez-Munoz JE, Iglesias-Garcia J, Castineira Alvarino M, et al. EUS elastography to predict pancreatic exocrine insufficiency in patients with chronic pancreatitis. *Gastrointest Endosc.* 2015;81:136–142.
28. Tenner S, Baillie J, DeWitt J, et al. American College of Gastroenterology guideline: management of acute pancreatitis. *Am J Gastroenterol.* 2013;108:1400–1415; 1416.
29. Maple JT, Ben-Menachem T, Anderson MA, et al. The role of endoscopy in the evaluation of suspected choledocholithiasis. *Gastrointest Endosc.* 2010;71:1–9.
30. Sharma R, Menachery J, Choudhary NS, et al. Routine endoscopic ultrasound in moderate and indeterminate risk patients of suspected choledocholithiasis to avoid unwarranted ERCP: a prospective randomized blinded study. *Indian J Gastroenterol.* 2015;34:300–304.
31. De Lisi S, Leandro G, Buscarini E. Endoscopic ultrasonography versus endoscopic retrograde cholangiopancreatography in acute biliary pancreatitis: a systematic review. *Eur J Gastroenterol Hepatol.* 2011;23:367–374.
32. Park JG, Kim KB, Han JH, et al. The usefulness of early endoscopic ultrasonography in acute biliary pancreatitis with undetectable choledocholithiasis on multidetector computed tomography. *Korean J Gastroenterol.* 2016;68:202–209.
33. Zhan X, Guo X, Chen Y, et al. EUS in exploring the etiology of mild acute biliary pancreatitis with a negative finding of biliary origin by conventional radiological methods. *J Gastroenterol Hepatol.* 2011;26:1500–1503.
34. Vila JJ, Vicuna M, Irisarri R, et al. Diagnostic yield and reliability of endoscopic ultrasonography in patients with idiopathic acute pancreatitis. *Scand J Gastroenterol.* 2010;45:375–381.
35. Rana SS, Bhasin DK, Rao C, et al. Role of endoscopic ultrasound in idiopathic acute pancreatitis with negative ultrasound, computed tomography, and magnetic resonance cholangiopancreatography. *Ann Gastroenterol.* 2012;25:133–137.
36. Govil A, Agrawal MK, Agrawal D, et al. Role of endoscopic ultrasonography in patients with first episode of idiopathic acute pancreatitis. *Indian J Gastroenterol.* 2014;33:241–248.
37. Wilcox CM, Seay T, Kim H, et al. Prospective endoscopic ultrasound-based approach to the evaluation of idiopathic pancreatitis: causes, response to therapy, and long-term outcome. *Am J Gastroenterol.* 2016;111:1339–1348.

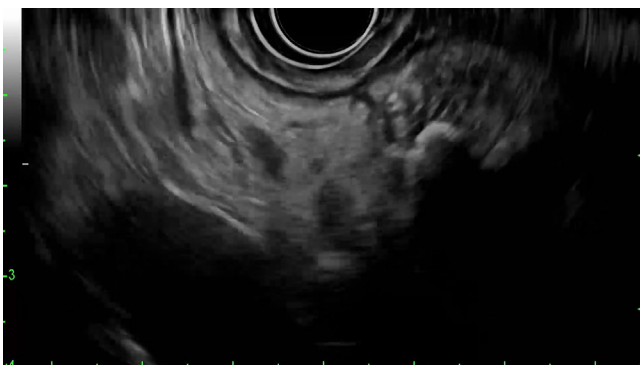
38. Ortega AR, Gomez-Rodriguez R, Romero M, et al. Prospective comparison of endoscopic ultrasonography and magnetic resonance cholangiopancreatography in the etiological diagnosis of "idiopathic" acute pancreatitis. *Pancreas*. 2011;40:289–294.
39. Thevenot A, Bourdet B, Otal P, et al. Endoscopic ultrasound and magnetic resonance cholangiopancreatography in patients with idiopathic acute pancreatitis. *Dig Dis Sci*. 2013;58: 2361–2368.
40. Munigala S, Kanwal F, Xian H, et al. Increased risk of pancreatic adenocarcinoma after acute pancreatitis. *Clin Gastroenterol Hepatol*. 2014;12:1143–1150.e1.
41. Mariani A, Arcidiacono PG, Curioni S, et al. Diagnostic yield of ERCP and secretin-enhanced MRCP and EUS in patients with acute recurrent pancreatitis of unknown aetiology. *Dig Liver Dis*. 2009;41:753–758.
42. Yusoff IF, Raymond G, Sahai AV. A prospective comparison of the yield of EUS in primary vs. recurrent idiopathic acute pancreatitis. *Gastrointest Endosc*. 2004;60:673–678.
43. Cho JH, Jeon TJ, Choi JS, et al. EUS finding of geographic hyperechoic area is an early predictor for severe acute pancreatitis. *Pancreatology*. 2012;12:495–501.
44. Alper E, Arabul M, Aslan F, et al. Radial EUS examination can be helpful in predicting the severity of acute biliary pancreatitis. *Medicine (Baltimore)*. 2016;95:e2321.
45. Sotoudehmanesh R, Hooshyar A, Kolahdoozan S, et al. Prognostic value of endoscopic ultrasound in acute pancreatitis. *Pancreatology*. 2010;10:702–706.
46. Shimosegawa T, Chari ST, Frulloni L, et al. International consensus diagnostic criteria for autoimmune pancreatitis: guidelines of the International Association of Pancreatology. *Pancreas*. 2011;40:352–358.
47. Kamisawa T, Egawa N, Nakajima H, et al. Clinical difficulties in the differentiation of autoimmune pancreatitis and pancreatic carcinoma. *Am J Gastroenterol*. 2003;98:2694–2699.
48. Chari ST, Smyrk TC, Levy MJ, et al. Diagnosis of autoimmune pancreatitis: the Mayo Clinic experience. *Clin Gastroenterol Hepatol*. 2006;4:1010–1016; quiz 934.
49. Levy MJ, Reddy RP, Wiersema MJ, et al. EUS-guided trucut biopsy in establishing autoimmune pancreatitis as the cause of obstructive jaundice. *Gastrointest Endosc*. 2005;61:467–472.
50. Levy MJ, Smyrk TC, Takahashi N, et al. Idiopathic duct-centric pancreatitis: disease description and endoscopic ultrasonography-guided trucut biopsy diagnosis. *Pancreatology*. 2011;11: 76–80.
51. Farrell JJ, Garber J, Sahani D, et al. EUS findings in patients with autoimmune pancreatitis. *Gastrointest Endosc*. 2004;60:927–936.
52. De Lisi S, Buscarini E, Arcidiacono PG, et al. Endoscopic ultrasonography findings in autoimmune pancreatitis: be aware of the ambiguous features and look for the pivotal ones. *JOP*. 2010;11:78–84.
53. Buscarini E, Lisi SD, Arcidiacono PG, et al. Endoscopic ultrasonography findings in autoimmune pancreatitis. *World J Gastroenterol*. 2011;17:2080–2085.
54. Okabe Y, Ishida Y, Kaji R, et al. Endoscopic ultrasonographic study of autoimmune pancreatitis and the effect of steroid therapy. *J Hepatobiliary Pancreat Sci*. 2012;19:266–273.
55. Koyama R, Inamura T, Okuda C, et al. Ultrasonographic imaging of bile duct lesions in autoimmune pancreatitis. *Pancreas*. 2008;37:259–264.
56. Hoki N, Mizuno N, Sawaki A, et al. Diagnosis of autoimmune pancreatitis using endoscopic ultrasonography. *J Gastroenterol*. 2009;44:154–159.
57. Jung JG, Lee JK, Lee KH, et al. Comparison of endoscopic retrograde cholangiopancreatography with papillary biopsy and endoscopic ultrasound-guided pancreatic biopsy in the diagnosis of autoimmune pancreatitis. *Pancreatology*. 2015;15: 259–264.
58. Kanno A, Masamune A, Fujishima F, et al. Diagnosis of autoimmune pancreatitis by EUS-guided FNA using a 22-gauge needle: a prospective multicenter study. *Gastrointest Endosc*. 2016;84:797–804.e1.
59. Morishima T, Kawashima H, Ohno E, et al. Prospective multicenter study on the usefulness of EUS-guided FNA biopsy for the diagnosis of autoimmune pancreatitis. *Gastrointest Endosc*. 2016;84:241–248.
60. Iwashita T, Yasuda I, Doi S, et al. Use of samples from endoscopic ultrasound-guided 19-gauge fine-needle aspiration in diagnosis of autoimmune pancreatitis. *Clin Gastroenterol Hepatol*. 2012;10:316–322.
61. Deshpande V, Mino-Kenudson M, Brugge WR, et al. Endoscopic ultrasound guided fine needle aspiration biopsy of autoimmune pancreatitis: diagnostic criteria and pitfalls. *Am J Surg Pathol*. 2005;29:1464–1471.
62. Mizuno N, Bhatia V, Hosoda W, et al. Histological diagnosis of autoimmune pancreatitis using EUS-guided trucut biopsy: a comparison study with EUS-FNA. *J Gastroenterol*. 2009;44:742–750.
63. Chari ST, Kloeppl G, Zhang L, et al. Histopathologic and clinical subtypes of autoimmune pancreatitis: the honolulu consensus document. *Pancreas*. 2010;39:549–554.
64. Kanno A, Ishida K, Hamada S, et al. Diagnosis of autoimmune pancreatitis by EUS-FNA by using a 22-gauge needle based on the International Consensus Diagnostic Criteria. *Gastrointest Endosc*. 2012;76:594–602.
65. Moon SH, Kim MH. The role of endoscopy in the diagnosis of autoimmune pancreatitis. *Gastrointest Endosc*. 2012;76:645–656.
66. Naitoh I, Nakazawa T, Hayashi K, et al. Clinical differences between mass-forming autoimmune pancreatitis and pancreatic cancer. *Scand J Gastroenterol*. 2012;47:607–613.
67. Takuma K, Kamisawa T, Gopalakrishna R, et al. Strategy to differentiate autoimmune pancreatitis from pancreas cancer. *World J Gastroenterol*. 2012;18:1015–1020.
68. Voss M, Hammel P, Molas G, et al. Value of endoscopic ultrasound guided fine needle aspiration biopsy in the diagnosis of solid pancreatic masses. *Gut*. 2000;46:244–249.
69. Eloubeidi MA, Tamhane A. EUS-guided FNA of solid pancreatic masses: a learning curve with 300 consecutive procedures. *Gastrointest Endosc*. 2005;61:700–708.
70. Mitsuhashi T, Ghafari S, Chang CY, et al. Endoscopic ultrasound-guided fine needle aspiration of the pancreas: cytmorphological evaluation with emphasis on adequacy assessment, diagnostic criteria and contamination from the gastrointestinal tract. *Cytopathology*. 2006;17:34–41.
71. Turner BG, Cizginer S, Agarwal D, et al. Diagnosis of pancreatic neoplasia with EUS and FNA: a report of accuracy. *Gastrointest Endosc*. 2010;71:91–98.
72. Chen J, Yang R, Lu Y, et al. Diagnostic accuracy of endoscopic ultrasound-guided fine-needle aspiration for solid pancreatic lesion: a systematic review. *J Cancer Res Clin Oncol*. 2012;138:1433–1441.
73. Fujii LL, Chari ST, El-Youssef M, et al. Pediatric pancreatic EUS-guided trucut biopsy for evaluation of autoimmune pancreatitis. *Gastrointest Endosc*. 2013;77:824–828.
74. Kerdsirichairat T, Saini SD, Chamberlain PR, et al. Autoimmune pancreatitis diagnosed with core biopsy obtained from a novel fork-tip EUS needle. *ACG Case Rep J*. 2017;4:e7.
75. Dietrich CF, Hirche TO, Ott M, et al. Real-time tissue elastography in the diagnosis of autoimmune pancreatitis. *Endoscopy*. 2009;41:718–720.
76. Fusaroli P, Saftoiu A, Mancino MG, et al. Techniques of image enhancement in EUS (with videos). *Gastrointest Endosc*. 2011;74:645–655.
77. Hocke M, Ignee A, Dietrich CF. Contrast-enhanced endoscopic ultrasound in the diagnosis of autoimmune pancreatitis. *Endoscopy*. 2011;43:163–165.

78. Imazu H, Kanazawa K, Mori N, et al. Novel quantitative perfusion analysis with contrast-enhanced harmonic EUS for differentiation of autoimmune pancreatitis from pancreatic carcinoma. *Scand J Gastroenterol.* 2012;47:853–860.
79. Fujii M, Saito H, Kato H, et al. Diagnosis of a solid pseudopapillary neoplasm using EUS-FNA. *Intern Med.* 2013;52:1703–1708.
80. Maimone A, Luigiano C, Baccarini P, et al. Preoperative diagnosis of a solid pseudopapillary tumour of the pancreas by endoscopic ultrasound fine needle biopsy: a retrospective case series. *Dig Liver Dis.* 2013;45:957–960.
81. Yamaguchi M, Fukuda T, Nakahara M, et al. Multicentric solid pseudopapillary neoplasms of the pancreas diagnosed by endoscopic ultrasound-guided fine needle aspiration: a case report. *Surg Case Rep.* 2015;1:110.
82. Goyal A, Jain D, Bhat I, et al. A unique case of pancreatic mass due to pancreatic elastofibromatosis. *Case Rep Gastrointest Med.* 2016;2016:2697187.
83. Collins K, Buckley T, Anderson K, et al. Perivascular epithelioid cell tumor (PEComa) of pancreas diagnosed preoperatively by endoscopic ultrasound-guided fine-needle aspiration: a case report and review of literature. *Diagn Cytopathol.* 2017;45:59–65.
84. Mondal U, Henkes N, Henkes D, et al. Cavernous hemangioma of adult pancreas: a case report and literature review. *World J Gastroenterol.* 2015;21:9793–9802.
85. Vafa H, Arvanitakis M, Matos C, et al. Pancreatic tuberculosis diagnosed by EUS: one disease, many faces. *JOP.* 2013;14:256–260.
86. Maestro S, Trujillo R, Geneux K, et al. Pancreatic actinomycosis presenting as pancreatic mass and diagnosed with endoscopic ultrasound fine needle aspiration (EUS-FNA). *Endoscopy.* 2013;45 Suppl 2 UCTN:E276–E277.
87. Sun B, Yang X, Ping B, et al. Impact of inconclusive endoscopic ultrasound-guided fine-needle aspiration results in the management and outcome of patients with solid pancreatic masses. *Dig Endosc.* 2015;27:130–136.
88. Hebert-Magee S, Bae S, Varadarajulu S, et al. The presence of a cytopathologist increases the diagnostic accuracy of endoscopic ultrasound-guided fine needle aspiration cytology for pancreatic adenocarcinoma: a meta-analysis. *Cytopathology.* 2013;24:159–171.
89. Rodriguez SA, Impey SD, Pelz C, et al. RNA sequencing distinguishes benign from malignant pancreatic lesions sampled by EUS-guided FNA. *Gastrointest Endosc.* 2016;84:252–258.
90. Bang JY, Hawes R, Varadarajulu S. A meta-analysis comparing ProCore and standard fine-needle aspiration needles for endoscopic ultrasound-guided tissue acquisition. *Endoscopy.* 2016;48:339–349.
91. Strand DS, Jeffus SK, Sauer BG, et al. EUS-guided 22-gauge fine-needle aspiration versus core biopsy needle in the evaluation of solid pancreatic neoplasms. *Diagn Cytopathol.* 2014;42:751–758.
92. Ying L, Lin X, Xie ZL, et al. Clinical utility of endoscopic ultrasound elastography for identification of malignant pancreatic masses: a meta-analysis. *J Gastroenterol Hepatol.* 2013;28:1434–1443.
93. Itokawa F, Itoi T, Sofuni A, et al. EUS elastography combined with the strain ratio of tissue elasticity for diagnosis of solid pancreatic masses. *J Gastroenterol.* 2011;46:843–853.
94. Iglesias-Garcia J, Larino-Noia J, Abdulkader I, et al. EUS elastography for the characterization of solid pancreatic masses. *Gastrointest Endosc.* 2009;70:1101–1108.
95. Kim SY, Cho JH, Kim YJ, et al. Diagnostic efficacy of quantitative endoscopic ultrasound elastography for differentiating pancreatic disease. *J Gastroenterol Hepatol.* 2016.
96. Iglesias-Garcia J, Larino-Noia J, Abdulkader I, et al. Quantitative endoscopic ultrasound elastography: an accurate method for the differentiation of solid pancreatic masses. *Gastroenterology.* 2010;139:1172–1180.
97. Dawwas MF, Taha H, Leeds JS, et al. Diagnostic accuracy of quantitative EUS elastography for discriminating malignant from benign solid pancreatic masses: a prospective, single-center study. *Gastrointest Endosc.* 2012;76:953–961.
98. Hocke M, Schulze E, Gottschalk P, et al. Contrast-enhanced endoscopic ultrasound in discrimination between focal pancreatitis and pancreatic cancer. *World J Gastroenterol.* 2006;12:246–250.
99. Gheonea DI, Streba CT, Ciurea T, et al. Quantitative low mechanical index contrast-enhanced endoscopic ultrasound for the differential diagnosis of chronic pseudotumoral pancreatitis and pancreatic cancer. *BMC Gastroenterol.* 2013;13:2.
100. Hocke M, Ignee A, Dietrich CF. Advanced endosonographic diagnostic tools for discrimination of focal chronic pancreatitis and pancreatic carcinoma—elastography, contrast enhanced high mechanical index (CEHMI) and low mechanical index (CELMI) endosonography in direct comparison. *Z Gastroenterol.* 2012;50:199–203.
101. Becker D, Strobel D, Bernatik T, et al. Echo-enhanced color- and power-doppler EUS for the discrimination between focal pancreatitis and pancreatic carcinoma. *Gastrointest Endosc.* 2001;53:784–789.



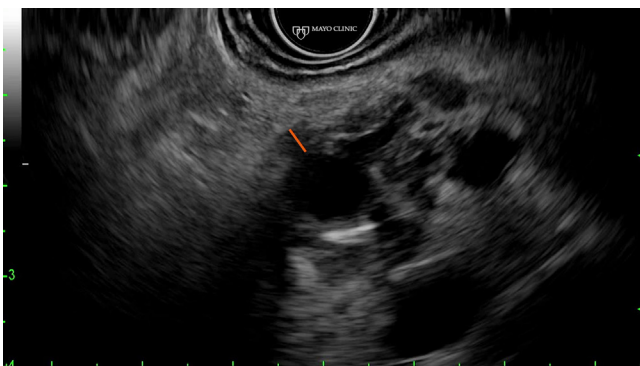
#### Video 13.1 Normal Pancreas

EUS demonstrates the typical salt and pepper appearance of the pancreas in patients without disease pathology. (See Fig. 13.25.)



#### Video 13.2 A 48-Year-Old Male Presented With Clinical and CT Evidence of Chronic Pancreatitis With a Large Pancreatic Head Duct Stone and Upstream Ductal Dilatation

Three prior efforts at ERCP failed and the patient was referred for further evaluation and stone clearance. P Div\_Major, Minor: EUS demonstrated a thickened bile duct wall indicative of downstream obstruction. EUS also revealed a remote location of the minor papilla, relative to the major papilla, initially establishing the diagnosis of pancreas divisum that had been missed on prior cross sectional imaging. The large stone was seen in the accessory duct. (See Fig. 13.27.)



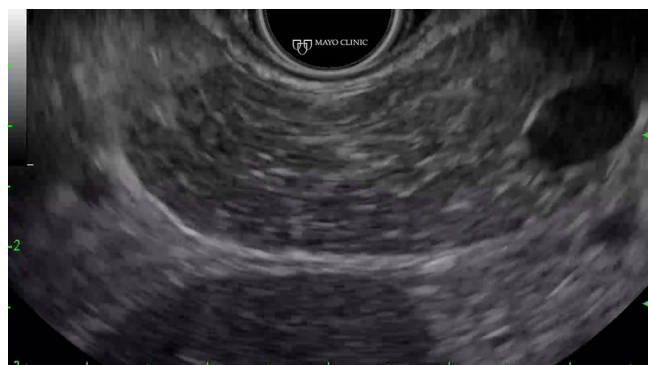
#### Video 13.3 A 48-Year-Old Male Presented With Clinical and CT Evidence of Chronic Pancreatitis With a Large Pancreatic Head Duct Stone and Upstream Ductal Dilatation

Three prior efforts at ERCP failed and the patient was referred for further evaluation and stone clearance. P Div\_MPD, SB, Atrophy: EUS demonstrated typical features of chronic pancreatitis including a dilated MPD, dilated side branches, and parenchymal atrophy. It is likely that some of the features were secondarily induced by the large stone and resulting obstructive changes. (See Fig. 13.28.)



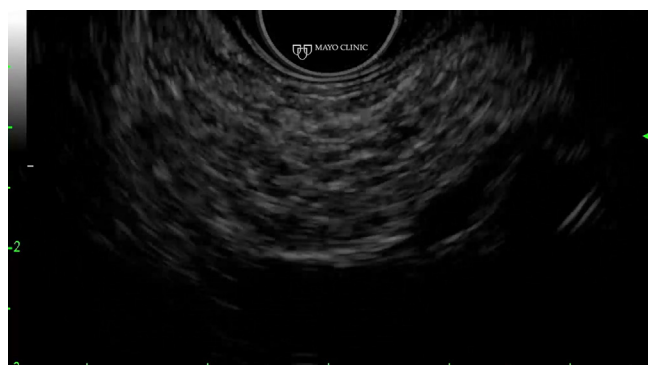
#### Video 13.4 Acute/Chronic CP

EUS in a patient with an acute exacerbation of chronic pancreatitis. In addition to the calcification, pancreatic and peripancreatic inflammatory changes are present. (See Fig. 13.33.)



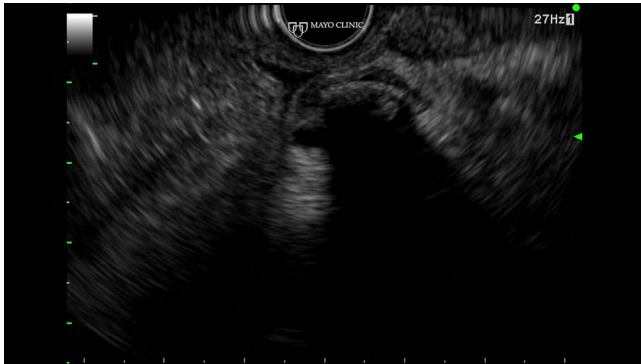
#### Video 13.5 CP (Mild)

EUS demonstrates features that were considered indicative of mild or early chronic pancreatitis. These findings were confirmed by core biopsy. (See Fig. 13.35.)



#### Video 13.6 CP (Normal)

EUS imaging demonstrates findings that were considered indicative of moderately severe chronic pancreatitis. However, core biopsy demonstrated a large quantity of completely normal pancreas. This patient highlights the limitations that can occur with EUS imaging. (See Fig. 13.36.)



### Video 13.7 Sludge, Stone

In a patient with recurrent acute pancreatitis, EUS imaging of the distal bile duct identified a calcified stone that produced postacoustic shadowing (first arrow) and adjacent sludge that was nonshadowing (second arrow). (See Fig. 13.1.)



### Video 13.8 AIP and PaC

A 49-year-old female presented with painless jaundice. At the referring hospital she underwent nondiagnostic CT, MRI/MRCP, ERCP (x2), and EUS (x2) and she was referred for second opinion. EUS revealed a well-circumscribed 1.5 cm isoechoic ampullary mass that on cytology was diagnostic for an ampullary adenocarcinoma. (See Fig. 13.29.) Additional EUS imaging revealed changes in the pancreatic tail that were concerning for AIP, which was confirmed on EUS guided core biopsy and surgical resection specimen. (See Figs. 13.21 and 13.22.)



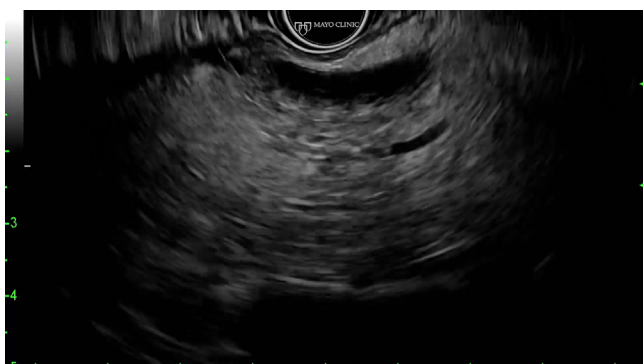
### Video 13.9 A 59-Year-Old Male Presented With Acute Pancreatitis

Prior CT (x2) and EUS with considered diagnostic for acute pancreatitis and FNA was negative for malignancy. The patient was referred for a second opinion. (See Fig. 13.10.) PaC\_Soft Tissue\_1: EUS revealed a hypoechoic swollen gland without detection of the main pancreatic duct. The finding could be suggestive of typical acute pancreatitis or autoimmune pancreatitis. However, the finding of focal extension of the process beyond the pancreas to peripancreatic soft tissue that abuts the gastric wall, and the absence of ascites, raised concern for an underlying neoplasia.



### Video 13.10 A 59-Year-Old Male Presented With Acute Pancreatitis

Prior CT (x2) and EUS with considered diagnostic for acute pancreatitis and FNA was negative for malignancy. The patient was referred for a second opinion. (See Fig. 13.10.) PaC\_Soft Tissue\_2: Additional imaging revealed this 12 x 3 mm extension that upon EUS FNA was proven to represent pancreatic adenocarcinoma.



### Video 13.11 A 72-Year-Old Female Presented With Numerous Episodes of Acute Pancreatitis

(See Figs. 13.5 and 13.6.) Choledochocoele\_Bad: Initial EUS imaging failed to detect the choledochocoele that was suspect on CT. The lesion was not identified because of poor EUS technique leading to compression of the cystic structure.



### Video 13.12 A 72-Year-Old Female Presented With Numerous Episodes of Acute Pancreatitis

(See Figs. 13.5 and 13.6.) Choledochocoele\_Good: In order to demonstrate the choledochocoele, the EUS transducer was positioned a short distance away from the major papilla to avoid compression of the cystic structure.



### Video 13.13 Pancreas Divisum

A 68-year-old male presented with recurrent acute pancreatitis. Initial CT and EUS at the referring hospital revealed only chronic pancreatitis. EUS demonstrates a prominent minor papilla from which the uncinate branch drains. Gentle counterclockwise rotation reveals an almost imperceptible major papilla and diminutive draining bile duct. The findings of pancreas divisum were confirmed at subsequent ERCP. (See Figs. 13.2–13.4.)



### Video 13.14 AIP\_Transition

In patients with AIP, there is often a fairly sharply demarcated transition zone that is not demonstrated at CT or MRI. This is a point where the gland is normal appearing on one side and demonstrated typical manifestation of AIP on the other. It is important to carefully examine this area and to perform EUS guided core biopsy in the appropriate region. In addition, the MPD often tapers severely in this region heightening concern for an occult neoplasia. (See Fig. 13.20.)

# Endoscopic Ultrasound and Pancreatic Tumors

JI YOUNG BANG AND THOMAS RÖSCH

## KEY POINTS

- Endoscopic ultrasound (EUS) is the most sensitive imaging modality for the diagnosis of pancreatic ductal adenocarcinoma, especially lesions less than 2 cm in size.
- EUS is also the most sensitive imaging modality for the detection of pancreatic neuroendocrine tumors (PNETs) and is superior to both computed tomography (CT) and magnetic resonance imaging (MRI).
- CT is the most accurate modality for the determination of tumor staging and assessment of resectability with exception of detecting portal vein invasion and small-volume ascites, where EUS may be superior. Detection of small hepatic metastases may also be more accurate with MRI and EUS.
- EUS-guided fine-needle aspiration (EUS FNA) is the gold standard for tissue acquisition in pancreatic mass lesions. Diagnostic yield can be optimized by use of the fanning technique and presence of a cytopathologist to render an on-site diagnosis. Diagnostic yield can also be maximized by the use of recently available core biopsy needles in centers without on-site cytopathology support.

## Examination Checklist for Evaluation of a Suspected Pancreatic Tumor

### Tumor

The following characteristics of all visualized masses should be noted: maximal dimensions, irregular or well-defined borders, echogenicity, associated cystic structures, and the presence of pancreatic duct dilation.

### Vascular Invasion

For tumors in the pancreatic head, their relationship to the portal vein, portosplenic confluence, superior mesenteric vessels, hepatic artery, and gastroduodenal artery should be noted. For tumors in the pancreatic body, their relationship to the celiac artery, superior mesenteric artery (SMA), portal confluence, hepatic artery, and splenic vessels should be defined. For tumors in the pancreatic tail, the splenic vessels should also be interrogated. The relationship between the tumor and the vessels should be carefully examined.

Notation may be stated as follows: intact hyperechoic tumor/vessel interface, adherent to vessel wall without irregular interface, irregular tumor/vessel interface, tumor invasion, or occlusion of the vessel. For occlusion of the portal or superior mesenteric vein (SMV), venous collaterals in the liver hilum or peridiudodenal region may be seen. For splenic vein occlusion, collaterals in the splenic hilum or gastric fundus may occur.

### Lymph Nodes

The following stations should be examined for possible metastatic disease: celiac axis, peripancreatic region (including head, body, and tail), porta hepatis, gastrohepatic ligament, aortocaval, and possibly posterior mediastinal stations. Metastatic lymph nodes will usually be round, well defined, hypoechoic, and at least 5 mm in diameter. However, not all malignant lymph nodes will have all of these features. If a suspected lymph node is identified, its characteristics and distance from the tumor should be noted. EUS FNA should be performed on suspected distant metastatic lymph nodes.

### Liver

Transgastric and limited transduodenal examination of the liver should be examined for metastatic lesions. Liver metastases from primary pancreatic cancer are usually hypoechoic and well defined. One or more than one lesion may be identified. EUS FNA of any suspected lesion should be performed when accessible.

### Ascites

This usually appears as a triangular or irregularly shaped anechoic region just outside the duodenal or gastric wall. It may be seen from peritoneal metastases or chronic venous occlusion. Omental nodules may also be visualized. EUS-guided fluid aspiration or biopsy of a nodule should be performed when possible.

### Endoscopic Ultrasound-Guided Tissue Acquisition

Tissue sampling should be performed from the most distant metastatic site first. If ascites, a distant metastatic lymph node, omental nodule, or a suspicious liver lesion is present, one of these

lesions should be sampled first. If these test negative for malignancy, either the suspected tumor or a regional lymph node may be sampled. The following information should be noted from each site biopsied: number of passes required, route of tissue acquisition, whether suction was used, and results of any onsite evaluation.

## Staging

All suspected malignant tumors of the pancreas should be identified in terms of tumor-node-metastasis (TNM) staging based on the most current American Joint Committee on Cancer (AJCC) staging classification.

## Pancreatic Ductal Adenocarcinoma

### Background

Pancreatic ductal adenocarcinoma is the fourth leading cause of cancer-related death in the United States, with 43,000 deaths per year and a dismal overall 5-year survival rate of only 8%.<sup>1</sup> Early diagnosis and management planning are therefore essential for optimal clinical outcomes in these patients, as survival is largely dependent on cancer stage, with 5-year survival rate of 29% for localized disease compared with only 3% for metastatic disease.<sup>1</sup> EUS combined with FNA is the most accurate modality available for the diagnosis of pancreatic cancer and has thus resulted in a paradigm shift in the management of these patients.

### Detection of Pancreatic Ductal Adenocarcinoma

#### Endoscopic Ultrasound Versus Computed Tomography

EUS is a very sensitive modality for detecting pancreatic cancer, with a sensitivity of 89% to 100%, specificity of 50% to 100%, and accuracy of 94% to 96%.<sup>2–6</sup> EUS has a high negative predictive value of 100%, with two studies showing that when patients with suspected pancreatic cancer had a normal EUS examination, pancreatic cancer was not diagnosed in any of them on long-term follow-up.<sup>7,8</sup> Therefore a normal-appearing pancreas on EUS examination can reliably exclude pancreatic cancer.

Pancreatic cancer is seen as a hypoattenuating mass on CT in the majority of cases, although it can be isoattenuating in 10% of patients, in which case it is more difficult to visualize.<sup>9</sup> The optimal type of CT imaging in patients with suspected pancreatic cancer is a contrast-enhanced, multiphasic (arterial phase to assess arterial involvement, pancreatic phase to visualize the mass, and portal venous phase to assess involvement of the portal vein and SMV) multidetector CT with minimal slice size of 5 mm, which has sensitivity of 70% to 100%.<sup>9–13</sup> Helical CTs appear to have lower sensitivity (63% to 77%) than multidetector CTs for detecting pancreatic tumors.<sup>2,10,14,15</sup> Also, the diagnostic sensitivity of CTs for detecting small pancreatic tumors less than 2 cm in size is only 77%.<sup>15</sup>

Studies comparing CT with EUS for the detection of pancreatic cancer have shown equivocal results. Although older studies demonstrate superiority of EUS over helical CT,<sup>6,16</sup> more recent studies show EUS to be either marginally superior<sup>2,4,11,17</sup> or only comparable to multidetector CTs.<sup>5</sup> Nevertheless, EUS appears to have a clear advantage over CT in two specific scenarios. First, studies have shown that EUS is superior to multidetector CT for

the identification of small pancreatic mass lesions less than 2 cm in size (Fig. 14.1A–C).<sup>18</sup> This is probably because small pancreatic mass lesions are more likely to be isoattenuating rather than hypoattenuating on CT and hence must be diagnosed by identifying secondary signs of pancreatic cancer, such as cutoff of the pancreatic duct, pancreatic duct dilation, atrophy of the pancreatic parenchyma, or absence of normal pancreatic contour.<sup>19</sup> Second, EUS can diagnose pancreatic cancer in patients without a distinct mass lesion on CT but with a high clinical suspicion with a sensitivity of 68% to 97%, specificity of 43% to 71%, and accuracy of 72% to 92%.<sup>20,21</sup> Therefore EUS should be performed in CT-negative patients in whom the clinical suspicion for pancreatic cancer remains high.

#### Endoscopic Ultrasound Versus Magnetic Resonance Imaging

MRI can provide detailed imaging of the pancreatic parenchyma and pancreatic duct and has a sensitivity of 78% to 100% and an accuracy of 79% to 91%<sup>10,12,13,22,23</sup> for detecting pancreatic tumors. In studies that compared EUS with MRI for the diagnosis of pancreatic cancer, EUS was at least equivalent or superior to MRI for visualizing pancreatic cancer.<sup>3,5</sup> In one study of 62 patients, MRI had the lowest accuracy for tumor detection at 62% when compared with both EUS (63%) and CT (73%).<sup>24</sup>

#### Contrast-Enhanced Endoscopic Ultrasound

Pancreatic adenocarcinoma is visualized as a hypoenhancing lesion on CE EUS, whereas chronic pancreatitis is either isoenhancing or hyperenhancing.<sup>25–27</sup> In a meta-analysis of 1139 patients, contrast-enhanced EUS was shown to have a high sensitivity for diagnosing pancreatic cancer, with a pooled sensitivity of 94% and specificity of 89%.<sup>28</sup> When compared with conventional EUS for performing FNA, although there was no significant difference in diagnostic performance between modalities, fewer passes were required to obtain a diagnostically adequate sample with contrast enhancement.<sup>29</sup> A sufficient sample was obtained with just one pass in 60% of patients compared with only 20% with conventional EUS FNA. Therefore contrast-enhanced harmonic EUS appears to have a supportive role in the EUS FNA evaluation of pancreatic mass lesions and may be useful in identifying the optimal site for FNA, especially in patients with underlying chronic pancreatitis.

#### Endoscopic Ultrasound Elastography

EUS elastography utilizes the difference in tissue elasticity to distinguish between malignant and benign lesions. EUS elastography can produce either a qualitative assessment with generation of different color hues<sup>30</sup> or a quantitative assessment with strain ratios.<sup>31</sup> Several meta-analyses have been published on this imaging technique, with a sensitivity of 95% to 98% and a specificity of 67% to 76% for diagnosing pancreatic cancer.<sup>32–35</sup>

## Assessment of Resectability and Cancer Staging

Surgical resection is the only currently available treatment with potential for cure in patients with pancreatic cancer. Even though the 5-year survival remains poor at 10% to 20% postresection,<sup>36,37</sup> survival has been shown to be significantly longer in patients undergoing margin-negative (R0) resection compared with non-surgical candidates (14 vs. 5 months,  $P < .0001$ ).<sup>36</sup> Therefore accurate and timely pancreatic cancer diagnosis and staging are paramount in order to expedite referral to surgery.

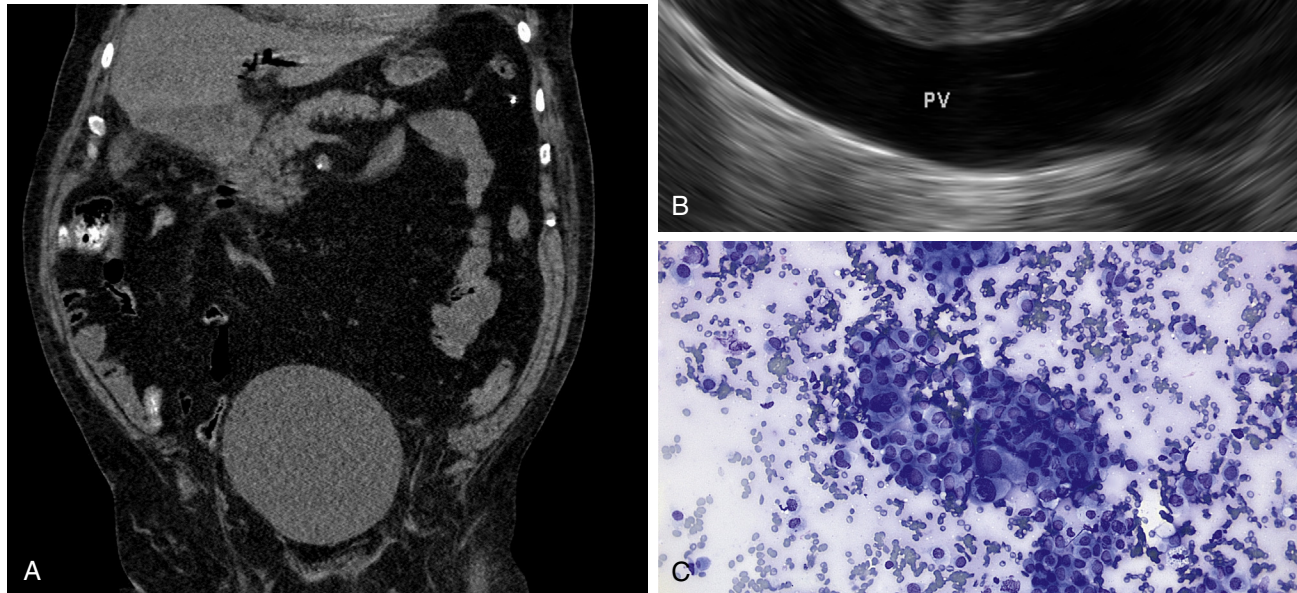


**Fig. 14.1** Computed tomography of a patient who presented with obstructive jaundice but no definitive mass on imaging (A). Linear endoscopic ultrasound imaging revealed a 2-cm pancreatic head mass (B) that on rapid onsite evaluation (ROSE) was proven to be an adenocarcinoma (C) (Diff-Quik staining 200 $\times$ ). CB, Common bile duct; PV, portal vein.

### Staging

Pancreatic cancer staging as determined by the AJCC (currently in its eighth edition) comprises the conventional TNM staging system: tumor characteristics (T), nodal involvement (N), and presence of metastatic lesions (M) (Table 14.1).<sup>38</sup> Patients with nodal involvement beyond the field of resection or metastatic disease are automatically deemed unresectable<sup>38,39</sup>; however, in patients with localized disease, resectable pancreatic cancer is defined as tumor without involvement of the surrounding major arteries, namely the celiac artery, SMA, and common hepatic artery (CHA). In addition, there is a lack of uniform consensus on the determination of suitability for resection in patients with venous involvement but without arterial involvement, with National Comprehensive Cancer Network (NCCN) and Alliance guidelines advocating surgical resection if the tumor has  $\leq 180$  degrees of contact with the portal vein or SMV.<sup>39</sup> The definitions of resectability according to the NCCN guidelines are outlined in Table 14.2.<sup>40</sup>

**Tumor Classification and Local Vascular Invasion.** Tumor size in conjunction with determination of celiac artery/SMA involvement constitute tumor classification in pancreatic ductal adenocarcinoma according to the AJCC criteria. CT is an accurate modality for assessing tumor classification and vascular involvement for the determination of resectability. The reported performance of CT in the evaluation of vascular invasion is varied, with a reported sensitivity of 56% to 85% and specificity of 82 to 100%.<sup>9,16,24,41–43</sup> In a meta-analysis of 18 studies that assessed the diagnostic performance of CT for the assessment of vascular invasion, the pooled sensitivity and specificity were 77% and 81%, respectively. However, the sensitivity and specificity were both

**TABLE 14.1** American Joint Committee on Cancer Eighth Edition for Pancreatic Cancer Staging

Tumor (T)	Lymph Nodes (N)	Metastases (M)
T1: Tumor size $\leq 2$ cm	N0: No lymph node involvement	M0: No metastasis
T2: Tumor size 2–4 cm	N1: 1–3 lymph node involvement	M1: Metastasis present
T3: Tumor size $>4$ cm	N2: $\geq 4$ lymph node involvement	
T4: Invasion of celiac artery or SMA		
Staging		
<b>Stage 1</b>	Stage 1A: T1, N0, M0	
	Stage 1B: T2, N0, M0	
<b>Stage 2</b>	Stage 2A: T3, N0, M0	
	Stage 2B: T1–3, N1, M0	
<b>Stage 3</b>	Any T, N2, M0	
	or T4, Any N, M0	
<b>Stage 4</b>	Any T, Any N, M1	

SMA, Superior mesenteric artery.

Taken from Amin MB, Edge SB, Greene FL, et al., eds. *AJCC Cancer Staging Manual*. 8th ed. New York: Springer; 2017.

**TABLE 14.2** The National Comprehensive Cancer Network Definitions of Tumor Resectability in Pancreatic Ductal Adenocarcinoma

<b>Resectable</b>	No distant metastases  Clear fat planes around celiac artery, hepatic artery, SMA  No SMV, PV distortion
<b>Borderline resectable</b>	No distant metastases  Involvement of SMV or PV but with suitable vessel proximally and distally to allow safe resection  Gastroduodenal artery encasement up to hepatic artery with short segment encasement or direct abutment of hepatic artery without extension into the celiac axis  Tumor abutment of SMA $\leq 180$ degrees of circumference of vessel wall
<b>Unresectable</b>	Distant metastases  Metastases to LNs beyond field of resection  SMA encasement $>180$ degrees  Any celiac abutment for pancreatic head tumor  Celiac encasement $>180$ degrees for pancreatic body/tail tumor  Unreconstructable SMV or PV occlusion  Invasion/encasement of aorta or IVC

IVC, Inferior vena cava; LN, lymph nodes; PV, portal vein; SMA, superior mesenteric artery; SMV, superior mesenteric vein.

Taken from Tempero MA, Malfafa MP, Behrman SW, et al. Pancreatic adenocarcinoma, version 2.2014: featured updates to the NCCN guidelines. *J Natl Compr Canc Netw*. 2014;12:1083–1093.

higher at 85% and 82%, respectively, when only five studies published from 2004 to 2008 were included. CT had a higher specificity for the assessment of arterial invasion compared with venous invasion (92% vs. 84%); however, the sensitivity was lower for arterial invasion (68% vs. 75%). Additionally, the pooled sensitivity and specificity were higher when CT with vascular reconstruction was performed: 84% and 85%, respectively, compared with 62% and 77% when vascular reconstruction was not performed.

EUS is an accurate modality for determining tumor size and yielding tissue diagnosis when used in conjunction with FNA.<sup>24</sup> Also, EUS is considered to be an accurate modality for assessing portal vein invasion due to the ease of visualization from the duodenal bulb, with a reported sensitivity of 75% and specificity of 77% (Fig. 14.2A and B).<sup>16,44</sup> In one comparative study, the overall accuracy of tumor staging was higher with EUS than with CT at 67% and 41%, respectively ( $P < .001$ ).<sup>11</sup> This was corroborated by a systematic review of 11 studies that found EUS to be more accurate than CT for tumor staging.<sup>17</sup>

**Nodal Classification.** Locoregional lymph nodes visible on EUS are located in the following stations and should be assessed when possible in all patients with suspected or FNA-proven pancreatic cancer: celiac axis, peripancreatic station, porta hepatis,

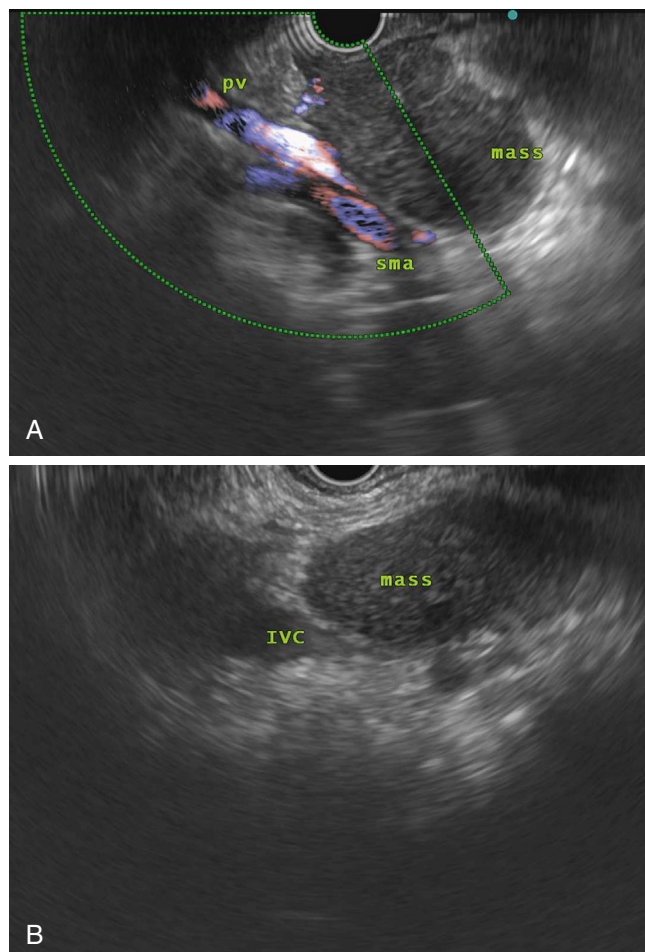
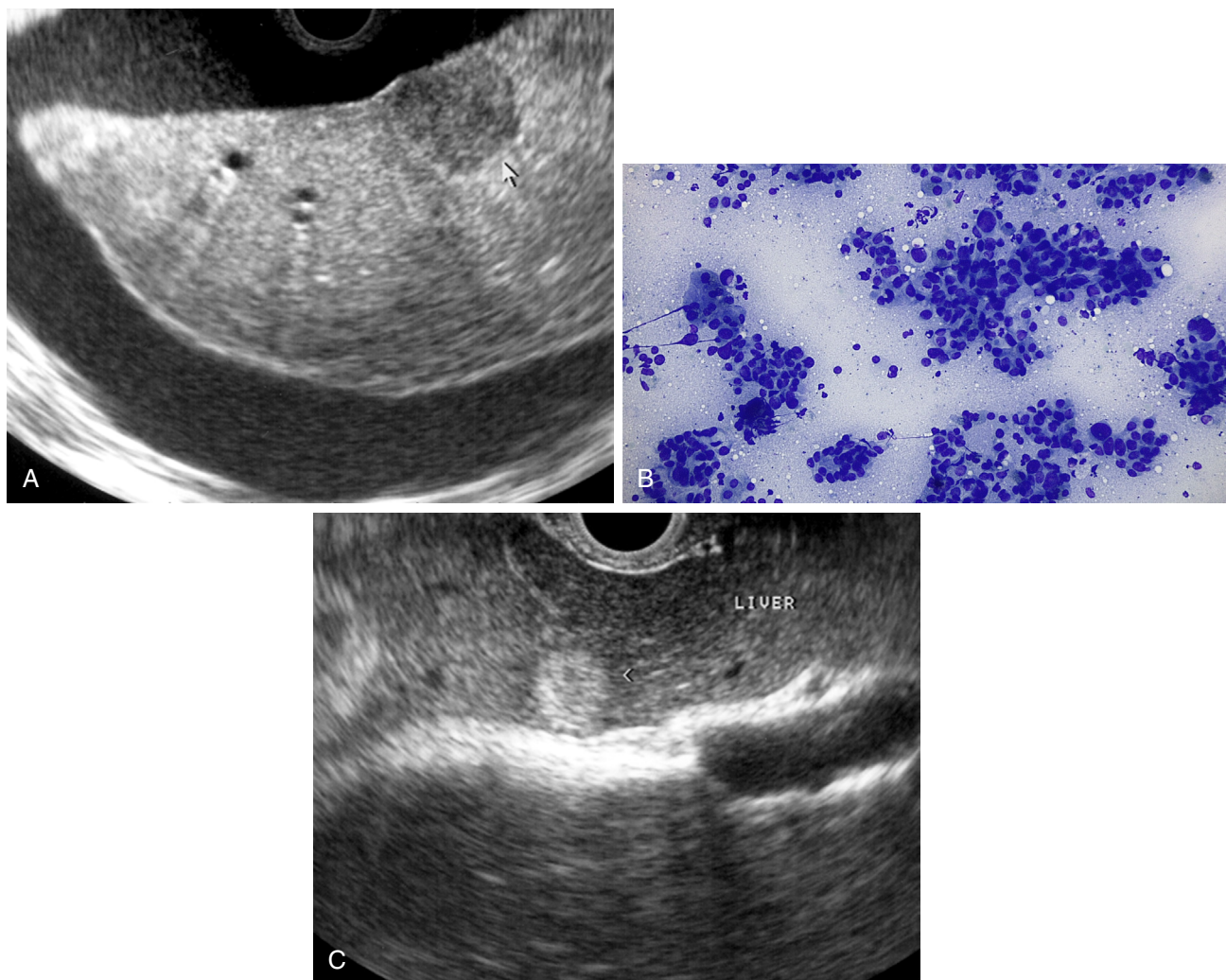


**Fig. 14.2** Linear endoscopic ultrasound imaging of the pancreatic head reveals a hypoechoic mass invading the portal vein (A). Invasion of the inferior vena cava is observed in another patient with pancreatic adenocarcinoma of the uncinate process (B). IVC, Inferior vena cava; PV, portal vein; SMA, superior mesenteric artery.

gastrohepatic ligament, and aortocaval stations. On EUS examination, metastatic lymph nodes appear round and hypoechoic; they are more than 1 cm in size and have well-defined margins.<sup>45,46</sup> When all four of these features are seen, the likelihood that the lymph node in question is malignant is 80% to 100%.<sup>45,46</sup>

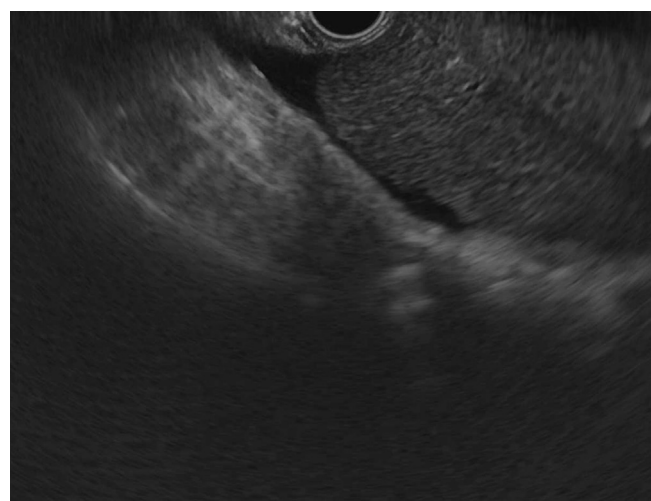
Overall, studies have shown that CT and EUS have similar operating characteristics for the assessment of lymph node involvement in pancreatic cancer, with sensitivities of 33% to 69% and 36% to 44%, respectively.<sup>11,16,24,47</sup> In one prospective observational study of 120 patients with known pancreatic cancer, accuracy for nodal staging was comparable between EUS and CT at 44% and 47%, respectively.<sup>11</sup> In a systematic review that included eight studies, the accuracy for nodal staging in five studies was found to be greater for EUS than CT.<sup>17</sup> However, three recent studies did not demonstrate any such difference between CT and EUS.

**Presence of Distant Metastases.** Owing to the inherent limitations of EUS in the assessment of structures distant to the transducer, CT was found to be superior to EUS for detecting metastatic disease, with an accuracy of 88%.<sup>24</sup> There are nevertheless two caveats to this rule. First, small hepatic metastases can be missed on CT,<sup>48</sup> and both EUS and MRI appear to have an advantage over CT in these patients (Video 14.1).<sup>49–52</sup> One must



• **Fig. 14.3** Linear endoscopic ultrasound (EUS) imaging of the left lobe of the liver demonstrates hypoechoic lesions in a patient with metastatic pancreatic cancer (A). Fine-needle aspiration using a 22-gauge needle revealed adenocarcinoma (B) (Diff-Quik staining 200 $\times$ ). Hepatic metastases can also appear as hyperechoic lesions on EUS (C).

be mindful of the fact that EUS may be limited in the assessment of the entire liver parenchyma, as the right lobe of the liver is often not well visualized on EUS (Fig. 14.3A–C). In one study of 100 patients with pancreatic cancer, the sensitivity for detecting liver metastases was significantly higher with MRI, at 85%, compared with 69% for CT ( $P = .046$ ), although no significant difference was seen between the two modalities for detection of the primary tumor.<sup>52</sup> This was supported by a smaller prospective study of 31 patients, where the sensitivity and specificity for liver metastases were higher with MRI than with CT (86.7% and 97.5% for MRI vs. 53.3% and 77.8% for CT).<sup>51</sup> Second, CT is poor at assessing peritoneal metastases, which manifest as ascites and peritoneal nodules. In particular, small-volume ascites, which may not yet be detectable on CT, can be visualized and aspirated for cytology during EUS. In one study of 85 patients with ascites present on EUS, it was not seen on CT in 82%. Subsequent EUS FNA of the ascitic fluid in 31 of these patients, resulted in a diagnosis of malignant ascites in 16% and thereby altered the treatment plan (Fig. 14.4).<sup>53</sup>



• **Fig. 14.4** Peritoneal carcinomatosis manifesting as ascites in a patient with stage IV pancreatic cancer.

**Tumor Resectability.** Studies have shown helical CTs to be accurate for determining resectability, with a positive predictive value of 45% to 87% for accurately predicting resectability and positive predictive value of 89% to 100% for assessing unresectability.<sup>54–56</sup> Contrast-enhanced multiphasic multidetector CT is the current CT imaging modality of choice for tumor staging and the assessment of local resectability. In a study of 79 patients with pancreatic ductal adenocarcinoma who underwent multidetector CT prior to surgical resection, the sensitivity, specificity, and accuracy for resectability were 100%, 71%, and 89%, respectively.<sup>57</sup>

In comparing the different diagnostic modalities for the assessment of vascular invasion and resectability, studies comparing CT with EUS have yielded variable results. In a study of 62 patients with pancreatic cancer, CT had the highest sensitivity and accuracy for determining locoregional extension (66% and 74%, respectively) and vascular invasion (67% and 83%, respectively), followed by MRI (accuracy of 68% for locoregional extension, 74% for vascular invasion) and then EUS (accuracy of 62% for locoregional extension, 76% for vascular invasion). In the assessment of tumor resectability, CT had the highest accuracy at 83%, compared with 75% for MRI and 67% for EUS.<sup>24</sup> However, in a more recent study of 86 patients, EUS was superior to CT for the evaluation of resectability at 83% compared with 60%.<sup>58</sup>

## Endoscopic Ultrasound-Guided Fine-Needle Aspiration

EUS FNA of pancreatic mass lesions has a pooled sensitivity of 85% to 89% and specificity of 96% to 98%<sup>59–62</sup>; it is the recommended first-line modality for tissue acquisition in patients with suspected pancreatic malignancy.<sup>63</sup> EUS FNA of pancreatic mass lesions is, however, considered the most challenging of all EUS FNAs; therefore the use of correct techniques, accessories, and on-site cytopathology evaluation when available are critical to maximize the diagnostic yield.

### Fine-Needle Aspiration Techniques/Accessories for Tissue Acquisition

**Needle Size.** FNA needles are available in three sizes: 19 gauge, 22 gauge, and 25 gauge. Because of the stiffness associated with traditional 19-gauge needles, especially when the echoendoscope is placed in a torqued position for transduodenal passes, 22- and 25-gauge needles are most frequently utilized for performing EUS FNA. There have been conflicting data regarding the performance of the 22- compared with the 25-gauge needle for EUS FNA of pancreatic masses. In a meta-analysis of eight comparative studies, the pooled sensitivity of the 25-gauge needle was significantly higher than that of the 22-gauge needle (93% vs. 85%), with no significant difference in the specificity (100% for the 22-gauge needle vs. 97% for the 25-gauge needle).<sup>64</sup> However, in three randomized trials, similar performance was observed between the 22-gauge and the 25-gauge needles, with no significant difference between the two needle types for diagnostic adequacy, number of passes required for diagnosis, and adverse event rates.<sup>65–67</sup> Furthermore, in a recently completed randomized trial of 352 patients with pancreatic masses, the operating characteristics of EUS FNA were comparable between the 22- and 25-gauge needles.<sup>68</sup> Therefore needle size alone does not appear to have a significant impact on the success of EUS FNA of pancreatic masses and, overall, both 22- and 25-gauge needles appear to perform equally well.

**Route of Fine-Needle Aspiration.** EUS FNA of pancreatic masses located in the body and tail is performed via the transgastric route, whereas the transduodenal route is utilized for pancreatic head and uncinate lesions. For transduodenal FNAs, the torqued echoendoscope position and acute angulation of the scope tip can result in difficulty in pushing the stiffer 22-gauge needle out of the scope. In a two-phase study of over 1000 patients, an algorithmic approach to EUS FNA was undertaken, with use of 22-gauge needles for transgastric FNAs and 25-gauge needles for transduodenal FNAs. The result was a significant reduction in the technical failure rate from 10.9% to 1.8% ( $P < 0.001$ ), with a significantly lower needle cost per procedure.<sup>69</sup>

**Fanning.** The fanning technique describes moving the FNA needle in multiple areas within the lesion during FNA rather than sampling just one area of the mass, as occurs with the standard technique. In the only randomized trial that compared the standard and fanning techniques for EUS FNA of pancreatic masses, the use of the fanning technique (four to-and-fro movements in each of the four areas sampled within the lesion) was associated with a significantly lower number of passes required for diagnosis. In addition, there was a trend toward higher diagnostic accuracy with the fanning technique at 96% versus 77%, although the difference was not statistically significant. The fanning technique should therefore be used when possible for EUS FNA of pancreatic mass lesions.

**Suction.** The current published literature on the benefit of using suction for EUS FNA of pancreatic mass lesions is both scant and equivocal. In a small randomized trial, sensitivity and accuracy were both significantly higher in the suction group,<sup>70</sup> with another second randomized trial showing just a trend toward higher sensitivity in the suction group.<sup>71</sup> However, in a recently completed four-arm randomized trial of 352 patients comparing the use of 22- and 25-gauge needles with and without suction in patients with solid pancreatic mass lesions, no significant difference in the operating characteristics of EUS FNA was seen between the four groups. However the use of suction with the 22-gauge needle was associated with increased specimen bloodiness and an increased number of passes for onsite diagnosis.<sup>68</sup>

**Stylet.** There appears to be no significant advantage to using a stylet in EUS FNA of pancreatic mass lesions, with studies showing that using a stylet is not associated with a significant improvement in diagnostic adequacy, sensitivity, specificity, or accuracy.<sup>72–75</sup> Therefore, for convenience, because the stylet is already in situ when the needle is first opened, the stylet can remain in situ for the first pass and then be discarded for subsequent passes.

### Specimen Interpretation and Processing

The availability of a cytopathologist to render an on-site diagnosis is an extremely important determinant of diagnostic accuracy in EUS FNA of pancreatic mass lesions.<sup>76</sup> In a meta-analysis of 3644 patients, the presence of an on-site cytopathologist was the only determinant of an accurate diagnosis following EUS FNA of pancreatic masses.<sup>62</sup>

However, owing to financial constraints, on-site cytopathologic evaluation is not universally available. In such cases, the aspirate can be placed in a preservative for specimen processing and off-site assessment at a later time. However, standard FNA needles may not be optimal for this purpose. In one randomized trial evaluating the 25-gauge needle for its ability to acquire diagnostic core tissue for off-site assessment (cell block), diagnostic adequacy was only 81% regardless of the number of dedicated

passes performed.<sup>77</sup> This is important to bear in mind in centers without on-site cytopathology support that rely solely on off-site evaluation of FNA samples, as the acquired sample may be nondiagnostic in up to 20% of cases.

### Challenges in Endoscopic Ultrasound-Guided Fine-Needle Aspiration of Pancreatic Mass Lesions

**Uncinate Mass Lesions.** Pancreatic masses located in the uncinate process are the most challenging lesions for EUS FNA. This is because uncinate masses usually require FNA from the second portion of the duodenum, where acute angulation of the echoendoscope can prevent easy passage of the needle into the mass. Needle passage into the mass can be aided in this situation by shortening the echoendoscope so that it is in a relatively straight position in the second portion of the duodenum; however, this position can, in turn, be unstable, causing the echoendoscope to fall back into the stomach during FNA.<sup>78</sup> Transduodenal FNAs are therefore easier with the thinner caliber and more flexible 25-gauge needles as opposed to the stiffer 22- or 19-gauge needles. The adoption of an algorithmic approach to EUS FNA—whereby 25-gauge needles are used for transduodenal FNA of the pancreatic head and uncinate masses and 22-gauge needles are used for transgastric FNA of pancreatic body and tail masses—resulted in a significant decrease in the rate of technical failure (Fig. 14.5A and B; Video 14.2).<sup>69</sup>

**Chronic Pancreatitis.** EUS FNA of pancreatic mass lesions is more challenging in patients with underlying chronic pancreatitis, in whom the mass can be more difficult to identify owing to the presence of coexisting lobulations and calcifications. Also, the interpretation of cytologic specimens can be more challenging because the inflammatory cells can mimic or obscure malignant cells.<sup>79</sup> Additionally, the aspirates are frequently acellular, resulting in an inadequate or nondiagnostic sample. Two studies have shown low sensitivity of 54% and 74% for diagnosing pancreatic cancer in the setting of chronic pancreatitis.<sup>79,80</sup> Therefore, if clinical suspicion is high—given the high rates of false-negative diagnosis in patients with pancreatic cancer and underlying chronic pancreatitis—EUS FNA should be repeated to conclusively exclude a diagnosis of malignancy (Fig. 14.6A–D).<sup>81</sup>

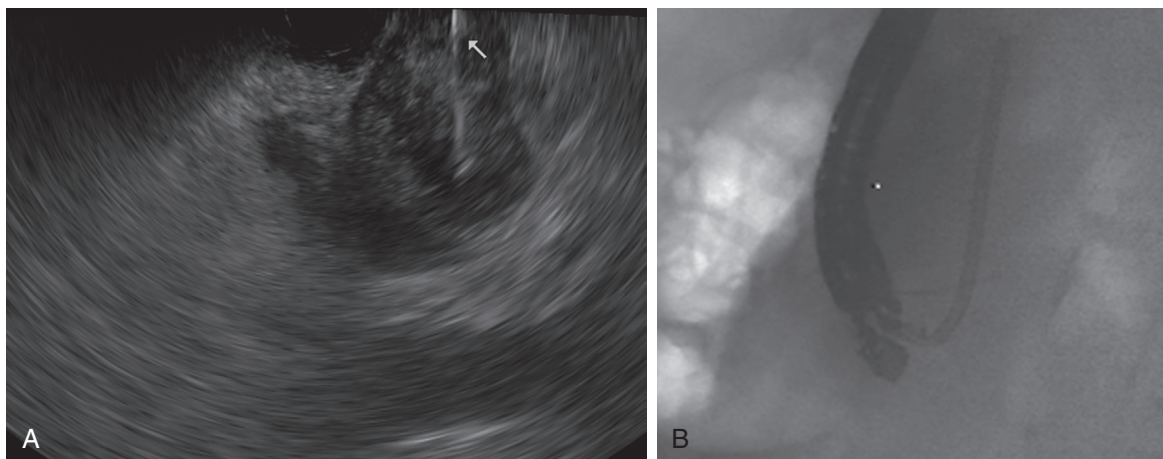
### Adverse Events of Fine-Needle Aspiration

EUS FNA of pancreatic mass lesions is generally safe. In a meta-analysis of 10,941 patients, the reported overall adverse event rate was 1%.<sup>82</sup> The type of adverse events encountered include acute pancreatitis (0.44%), abdominal pain (0.38%), bleeding (0.1%), fever (0.08%), and infection (0.02%).<sup>82</sup> The rate of tumor seeding following EUS FNA is reported at 2%, which is significantly lower than that observed with percutaneous CT-guided biopsy (16.3%;  $P < .025$ ).<sup>83</sup> Furthermore, the majority of adverse events appear to occur within 1 week of the procedure. In a prospective study of 158 patients who underwent EUS FNA of pancreatic mass lesions, adverse events occurred in 10 patients periprocedurally or immediately after the procedure, followed by adverse events in another 20 patients within 72 hours of the procedure. At 30-day follow-up, no other adverse events had been reported in the interim. The overall rate of major adverse events in this study was 2.5%.<sup>84</sup>

### Fine-Needle Biopsy

Specially designed FNB needles have been developed to obtain histologic core tissue during EUS-guided tissue sampling; these samples have several theoretical advantages over traditional FNA samples. One, due to their retained architecture, histologic core tissue specimens are easier to interpret than cytologic specimens obtained via EUS FNA. Two, histologic core tissue enables ancillary testing, especially in patients with challenging lesions such as metastatic cancers, gastrointestinal stromal cell tumors, and lymphomas.<sup>85</sup> Three, core tissue samples are more conducive to performing molecular profiling and delivering personalized anti-cancer therapy.<sup>86,87</sup>

Studies have shown varied success with FNB needles. In one meta-analysis there was no significant difference in the performance of the reverse-bevel-tip FNB needle (ProCore, Cook Endoscopy, Winston-Salem, North Carolina) as compared with standard FNA needles for EUS-guided sampling of solid lesions, including diagnostic adequacy, diagnostic accuracy, and procurement of histologic core tissue.<sup>88</sup> However, preliminary data suggest that the fork-tip (SharkCore, Medtronic Corp., Boston, Massachusetts) and Franseen (Acquire, Boston Scientific Corp., Natick, Massachusetts) needles yield better



• Fig. 14.5 Endoscopic ultrasound-guided fine-needle aspiration of a pancreatic uncinate mass (A) (arrow points to the FNA needle); note the perpendicular direction in which the lesion was sampled from the second portion of the duodenum on fluoroscopic view (B).

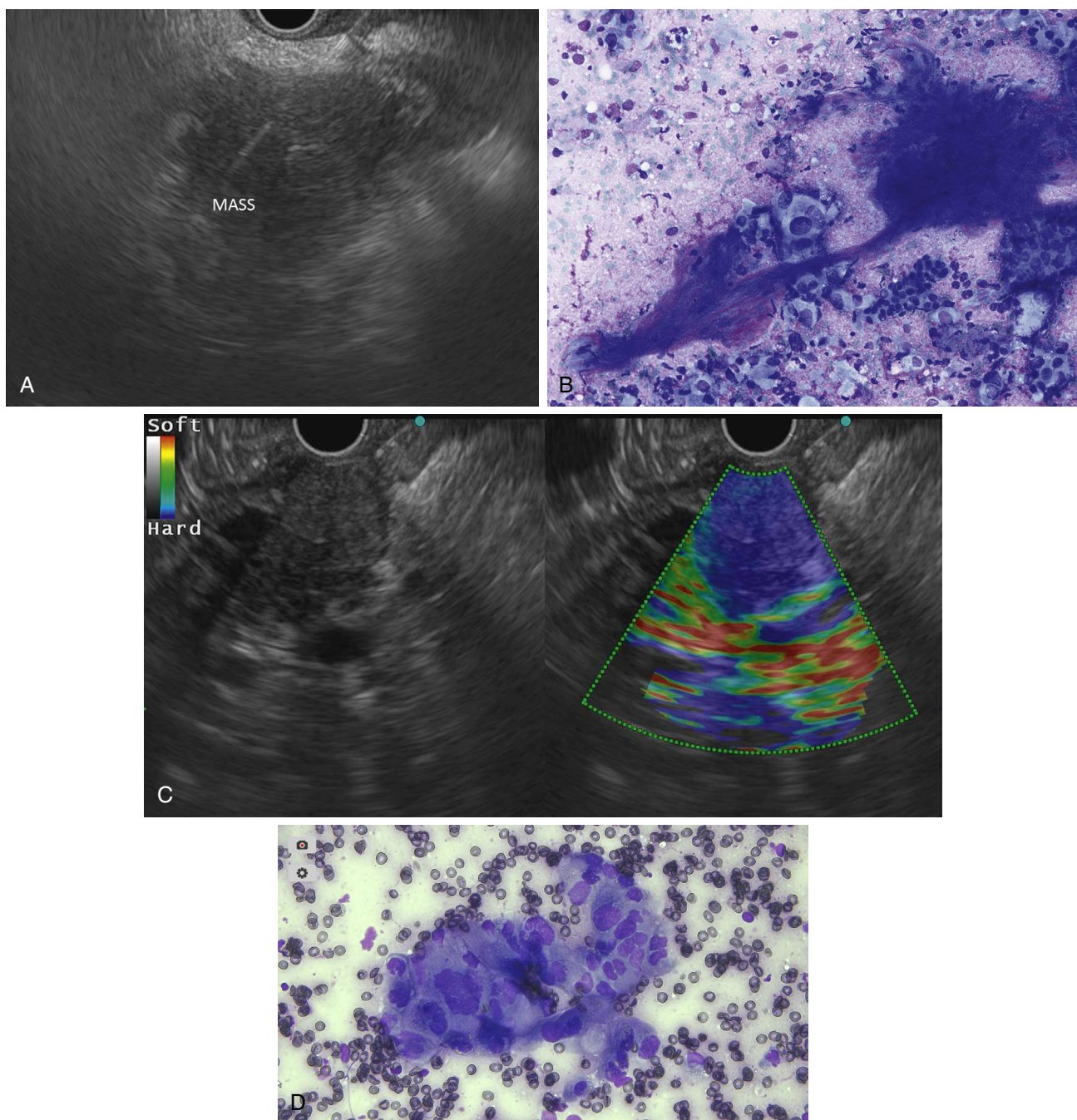
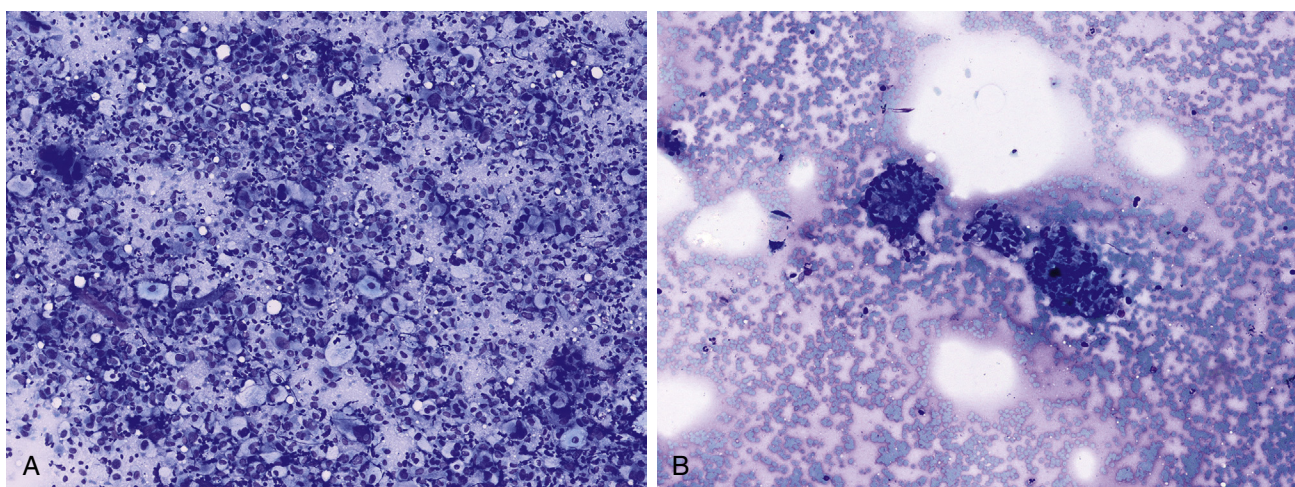


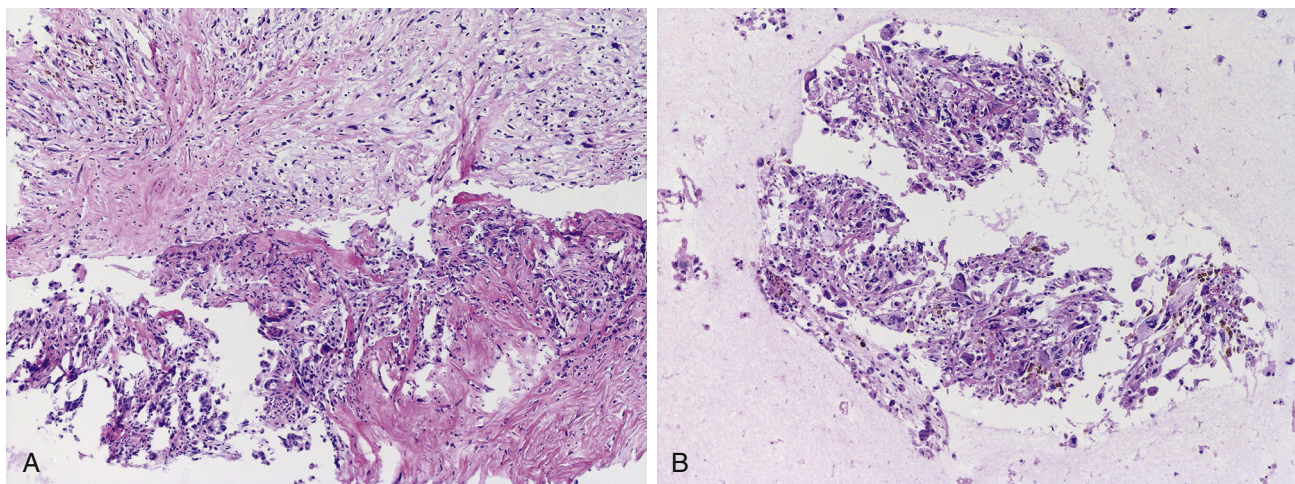
**Fig. 14.6** Endoscopic ultrasound (EUS)-guided fine-needle aspiration (FNA) of a pancreatic uncinate mass in the setting of chronic pancreatitis (A). Note the ill-defined uncinate mass, which is difficult to differentiate from the surrounding pancreatic parenchyma. Rapid onsite evaluation (ROSE) revealed ductal adenocarcinoma in the setting of desmoplastic fibrosis (B; Diff-Quik staining, 200 $\times$ ). In another patient with chronic pancreatitis, the pancreatic head mass was notable as an area of blue hue on EUS elastography (C), which was used to target for EUS FNA. ROSE revealed ductal adenocarcinoma (D; Diff-Quik staining, 400 $\times$ ).

histologic tissue. In a case-control study of 156 patients, histologic tissue was procured in a significantly higher proportion of patients using the fork-tip needle (95 vs. 59%,  $P = .001$ ), after performing a significantly lower number of passes (median 2 vs. 4 passes, 0.01).<sup>89</sup> In a series of 30 patients, the Franseen needle was able to obtain a diagnostic cell block in 96.7% of patients, which is significantly higher than that previously reported (Fig. 14.7A and B and Fig. 14.8A and B; Video 14.3).<sup>77,90</sup> Also,

successful ancillary testing was possible in all patients with gastrointestinal stromal tumors (GISTs), PNETs, and metastatic cancer.<sup>90</sup> In the first randomized trial to date comparing FNA with FNB needles (Acquire, Boston Scientific Corp.) for EUS-guided sampling of pancreatic masses, EUS FNB was associated with a significantly higher rate of diagnostic cell block (97.8 vs. 82.6%,  $P = .03$ ) and was able to procure significantly greater amount of tissue, tumor cells, and desmoplastic fibrosis.<sup>91</sup>



• **Fig. 14.7** Rapid onsite evaluation (ROSE) of a pancreatic mass biopsied using the Franseen needle reveals a cellular specimen comprising malignant cells, fibrosis, and reactive ductal epithelium (A; Diff-Quik staining, 100×). The corresponding aspirate from standard fine-needle aspiration reveals scattered malignant cells and with minimal fibrosis (B; Diff-Quik staining, 100×).



• **Fig. 14.8** Hematoxylin and eosin staining of pancreatic adenocarcinoma (100×) procured with the Franseen needle. Cores of exuberant dense desmoplastic fibrosis are seen entrapping malignant ductal epithelium and scattered benign residual acini on sections from the cell block (A). The corresponding image of a specimen from fine-needle aspiration reveals minimal tumor cells and lack of any desmoplastic fibrosis (B).

## Summary

Although multiple diagnostic modalities are available for the diagnosis and staging of pancreatic cancer, an evidence-based algorithmic approach is recommended for patient management (Fig. 14.9). Contrast-enhanced, multiphasic, multidetector CT should be performed as the initial imaging modality in patients with suspected pancreatic cancer. MRI can be performed in lieu of CT for tumor detection and staging if there is a contraindication to CT or if the expertise is locally available. If the pancreatic tumor has a characteristic appearance on CT and is clearly resectable, the patient should be referred for surgical resection after discussion in a multidisciplinary setting. Patients with unresectable/borderline resectable pancreatic cancer or unclear appearance on CT, who therefore require tissue diagnosis, should undergo EUS-guided sampling. Also, patients with high clinical suspicion for pancreatic cancer but without a definitive pancreatic mass on CT

should be referred for EUS, as the tumor could be small in size. In patients undergoing EUS, regional lymph nodes and the liver should be carefully examined for metastases, and the presence of ascites should be carefully documented. Both contrast-enhanced EUS and EUS-elastography are useful adjuncts to EUS FNA but not replacements for it.

## Pancreatic Neuroendocrine Tumor

### Background

PNET is the second most common type of pancreatic malignancy, with increasing incidence since the 1970s<sup>92</sup>; it accounts for 2% of all pancreatic neoplasms.<sup>93</sup> Although the majority of PNETs arise de novo, they can occur as part of hereditary syndromes, such as multiple endocrine neoplasia type I (MEN-1),

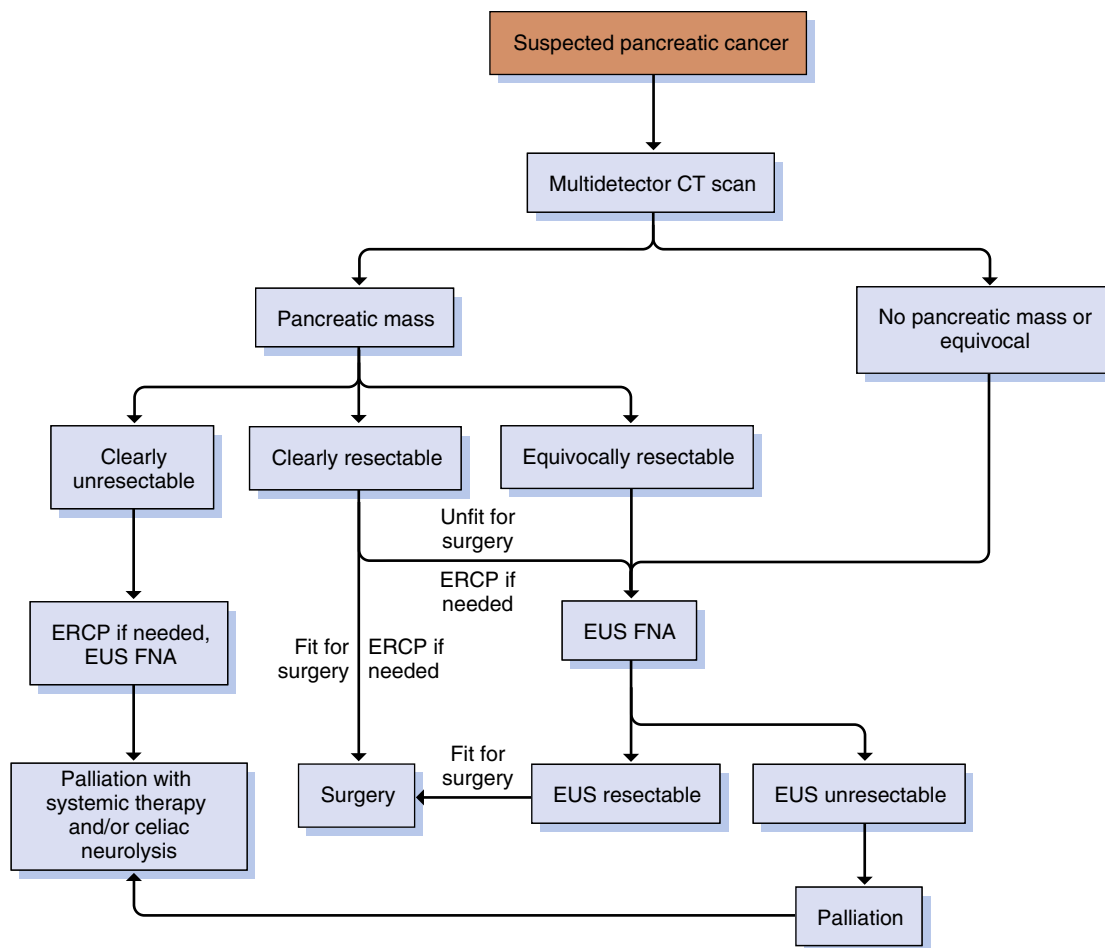


**Fig. 14.9** An evidence-based algorithmic approach to the management of pancreatic adenocarcinoma.  
CT, Computed tomography; EUS FNA, endoscopic ultrasound-guided fine-needle aspiration.

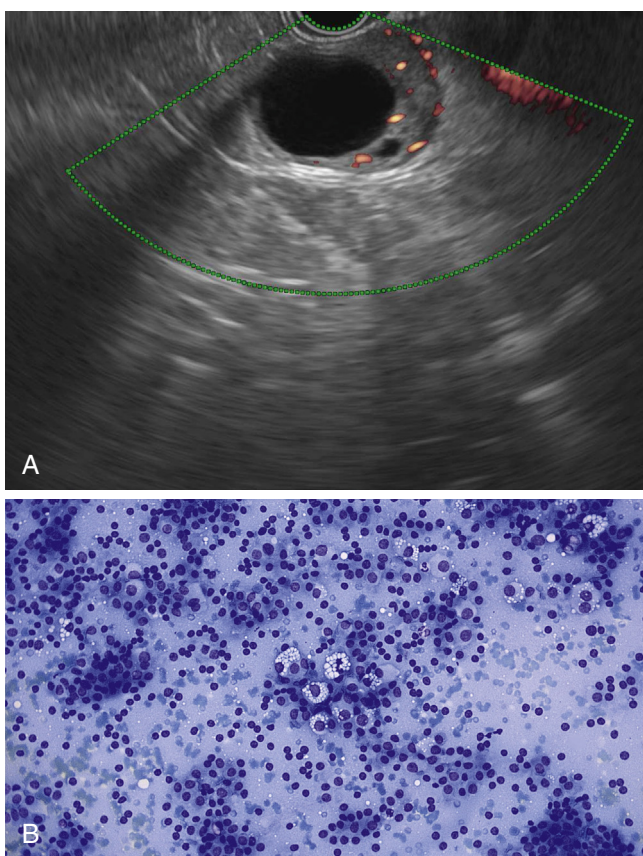
von Hippel–Lindau syndrome, neurofibromatosis type 1, and tuberous sclerosis. Some 40% to 55% of PNETs are functional due to the secretion of peptide hormones—such as insulin, glucagon, gastrin, vasoactive intestinal peptide (VIP), and somatostatin (insulinomas being the most common type)—from the pancreatic islet cells, whereas the remaining 45% to 60% are nonfunctional with absence of peptide secretion.<sup>93,94</sup> The overall 5-year survival rate is 80% for PNETs, and is highest for localized disease at 60% to 100% compared with 25% for metastatic disease.<sup>94</sup>

## Diagnosis

The diagnosis of PNETs requires tissue confirmation in all cases, along with immunohistochemical staining for the neuroendocrine markers chromogranin A and synaptophysin. Immunohistochemistry for Ki-67 index is also necessary for tumor grading according to the World Health Organization (WHO) classification. WHO tumor grade 1 is defined as Ki-67 ≤2% with a mitotic count below 2 per 10 high power fields (HPFs), grade 2 as Ki-67 3% to 20% with a mitotic count of 2 to 20 per 10 HPFs, and grade 3 (defined as neuroendocrine carcinoma) as Ki-67 greater than 20% with a mitotic count above 20 per 10 HPF.<sup>94</sup> Staging of PNETs utilizes the same AJCC TNM classification as pancreatic ductal adenocarcinoma (see Table 14.1).

## Imaging Modalities in Pancreatic Neuroendocrine Tumor

Various imaging modalities are available for the detection of PNETs, including CT, MRI, somatostatin receptor scintigraphy (SRS), positron emission tomography (PET), and EUS. Studies have shown varied sensitivities and specificities for detecting PNETs with each of these modalities. In a retrospective study of 217 patients with PNETs spanning 25 years, CT was able to detect lesions in 84% of patients, with a significant increase in sensitivity with increasing number of slices performed (76% for 1-slice vs. 89% for 64-slice CT scanners).<sup>95</sup> In a small study of 28 patients with functional PNETs, MRI had a sensitivity of 85% and specificity of 100% for tumor detection.<sup>96</sup> However, the diagnostic rate was much lower for both CT and MRI at only 40% in one study comprising MEN-type I patients<sup>97</sup> and 53.6% in a prospective study of 110 patients.<sup>98</sup> SRS utilizes a synthetic somatostatin analog to detect somatostatin receptors present in PNETs. Therefore, compared with other PNET types, SRS has the lowest sensitivity for the identification of insulinomas, with sensitivity ranging from 14% to 60% due to the low expression of somatostatin receptors in insulinomas.<sup>99–101</sup> For gastrinomas, the sensitivity of SRS is higher, at 61% to 86% for tumor detection.<sup>102,103</sup> More novel imaging modalities such as Ga-DOTATATE PET/CT appear to be accurate modalities for tumor detection, with a sensitivity of 95.5%; they are significantly more sensitive than either SPECT/CT or conventional CT/MRI.<sup>98</sup>



• **Fig. 14.10** Linear endoscopic ultrasound imaging reveals a pancreatic cyst lesion with thick walls (A). Fine-needle aspiration of the cyst wall proved the lesion to be a neuroendocrine tumor (B; Diff-Quik staining, 200x).

Hepatic metastases from PNETs are vascular and therefore are most accurately detected in the arterial phase, with one study showing the detection of maximum number of lesions (70%) on the hepatic arterial-phase MRI images.<sup>104</sup> Furthermore, MRI has the highest sensitivity for detection, followed by CT and SRS. In a prospective study of 40 patients with hepatic metastases from gastroenteropancreatic NET, MRI was the most sensitive modality (95.2% vs. 78.5% for CT and 49.3% for SRS), with a significantly higher number of lesions detected (394 lesions) than with either CT (325 lesions) or SRS (204 lesions). CT was, in turn, significantly more sensitive than SRS for the detection of liver metastases.<sup>105</sup>

#### **Endoscopic Ultrasound Versus Other Imaging Modalities**

On EUS, PNETs typically appear as vascular, hypoechoic lesions, with a smooth margin and homogeneous echogenicity.<sup>106</sup> They have a cystic component in 22% of cases and, unlike pancreatic ductal adenocarcinomas, do not result in obstruction of the main pancreatic duct in the majority of cases (91.5% cases present without pancreatic duct obstruction) (Fig. 14.10A and B; Video 14.4).<sup>107</sup> EUS appears to be the most accurate diagnostic modality for PNETs, with a sensitivity of 86% to 97% and a specificity of 95% to 98%.<sup>95,102,106,108,109</sup>

Studies consistently show the superiority of EUS over CT for the detection of PNETs.<sup>110</sup> In a large retrospective study of 217 patients comparing CT with EUS, the detection rate was significantly higher with EUS at 91.7 versus 63.3% ( $P < .001$ ); furthermore, EUS was able to detect PNETs in 91% of patients

who had negative CT scans.<sup>95</sup> In a small comparative study of 25 patients with MEN type I, EUS was significantly more sensitive than CT, with detection of PNET in 45% patients in whom the CT was negative.<sup>111</sup> This was corroborated in a meta-analysis of 17 studies that included 612 patients, which showed that EUS was able to detect PNETs in 28% of patients with negative CT scans.<sup>108</sup> Therefore, not only is EUS more sensitive for detecting PNETs, it is also able to detect lesions missed on CT.

In a study of 90 patients with MEN type I, MRI was inferior to EUS for the detection of PNETs: the results were 83% for EUS versus 74% for MRI. EUS was also superior to MRI for the detection of multiple PNETs, at 67.8 % versus 46.7%.<sup>112</sup> In another retrospective study of 61 patients with PNET diagnosed from 2007 to 2014, the sensitivity for tumor detection was significantly lower for MRI as compared with EUS, at 75.5% versus 96.7%.<sup>107</sup> Therefore EUS is more sensitive than MRI for the detection of PNETs.

#### **Endoscopic Ultrasound-Guided Tissue Acquisition**

The WHO tumor grade is a prognostic factor in patients with PNETs; therefore the ability to determine the Ki-67 index and mitotic count in an FNA sample is paramount for treatment planning. That is, in performing EUS FNA of suspected PNETs, dedicated passes must be made to obtain a cell block for immunohistochemical testing. Studies show high sensitivity and specificity of EUS FNA for the diagnosis of PNET with procured samples that allow Ki-67 staining for tumor grading; however, these studies are limited by their retrospective design and small sample sizes. The reported sensitivity and accuracy of EUS FNA in PNET were both 90% in a small case series of just 10 patients<sup>113</sup>; dual-phase helical CT had been negative in 8 of these 10 patients. This is similar to three other retrospective studies, which reported sensitivity of 82.6% to 89.2%, specificity of 85.7%, and accuracy of 83.3% to 90% (Video 14.5).<sup>107,110,114</sup>

In a retrospective study of 58 patients with PNETs, tissue procured via EUS FNA was adequate for Ki-67 staining in 82%, which, in turn, had a 77.8% concordance rate for tumor grade with surgical specimens.<sup>115</sup> In a small retrospective study of 24 patients with PNETs, Ki-67 staining for tumor grading was possible in all patients, which, in turn, correlated highly with prognosis, translating to a survival rate of 78% for G1 tumors versus 0% for G2 and G3 tumors.<sup>116</sup>

PNETs are vascular lesions; hence the FNA specimens are often more bloody, resulting in a nondiagnostic sample. Therefore strong consideration must be given to not using suction or a 19-gauge needle for tissue sampling. Also, given the need to perform ancillary testing, such as immunohistochemistry studies, it is important to perform at least two dedicated passes for cell block when a diagnosis of PNET is entertained.

#### **Endoscopic Ultrasound-Guided Ablation Therapy**

Surgical resection with lymph node clearance is the treatment modality of choice in patients with G1 and G2 PNETs; G3 PNET patients are usually not suitable candidates for curative surgical resection due to presence of widespread metastases at the time of diagnosis.<sup>94</sup> In candidates not suitable for surgery, EUS-guided radiofrequency ablation (RFA) and intratumoral alcohol injection have been performed as palliative measures, with encouraging results.

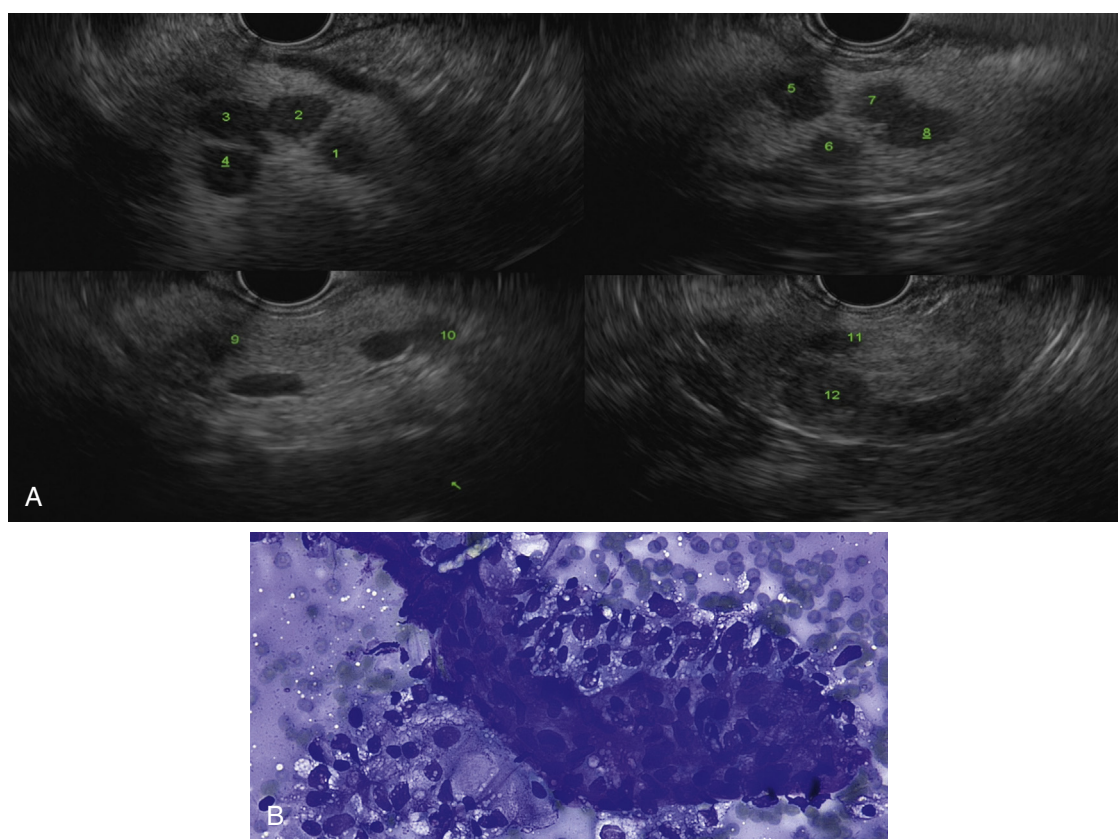


**Fig. 14.11** Linear endoscopic ultrasound image reveals multiple lesions in the pancreatic body and tail region (A) (numbers 1 to 12 denote pancreatic lesions on EUS). Fine-needle aspiration revealed the lesions to be a metastatic renal cell cancer (B; Diff-Quik staining, 400 $\times$ ).

EUS RFA involves the use of a radiofrequency probe that is inserted through a 19- or 22-gauge FNA needle. In a case series of three patients with insulinomas 14 to 22 mm in size located in the head, genu, and body of the pancreas, EUS RFA was performed successfully in all patients, with no adverse events. All patients were symptom-free at 3-, 6-, and 12-month follow-up, with normalization of fasting blood glucose, insulin, and C-peptide levels.<sup>117</sup> In another case series, EUS RFA was performed in two patients with PNET sized 15 and 40 mm located in the head of pancreas. No adverse events were noted postprocedure; however, no other information regarding clinical outcomes was available.<sup>118</sup> In a case report, EUS-guided injection of absolute alcohol was safely performed in a 1-cm PNET in the neck of the pancreas. At 6-month follow-up, the lesion was noted to have significantly decreased in size.<sup>119</sup> Larger and more definitive studies with long-term follow-up are needed to elucidate the safety and efficacy of EUS-guided ablation therapy for PNET.

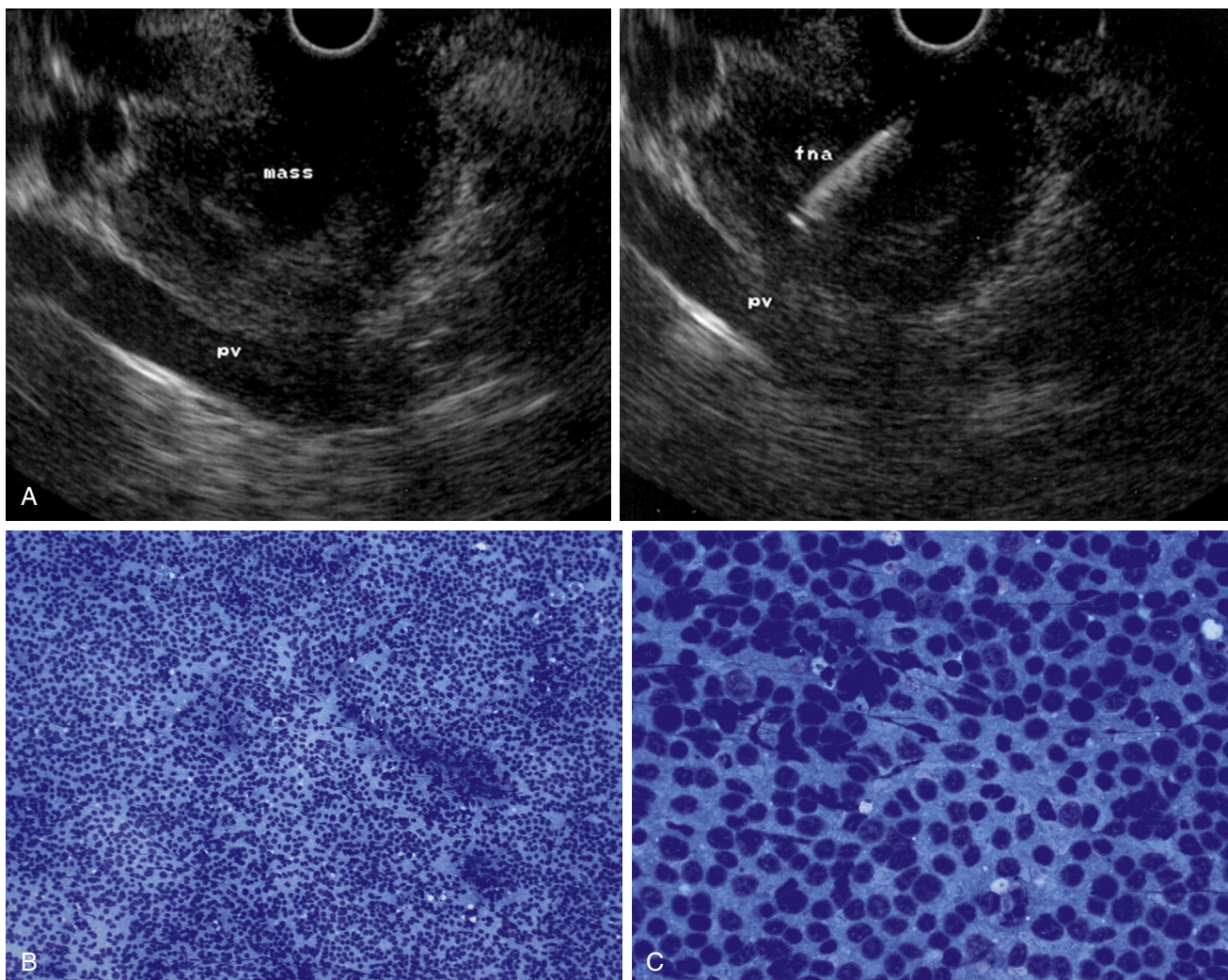
### Metastatic Lesions to the Pancreas

Metastatic lesions to the pancreas are rare, accounting for only 1.8% to 10.8% of all pancreatic tumors; they should be considered in patients with a history of malignancy, no matter how remote, as metastases to the pancreas can occur anywhere from 1 month to 29 years after initial diagnosis of the primary tumor.<sup>120–125</sup> In one retrospective study of 33 patients with pancreatic metastases from renal cell carcinoma, 31 patients had developed metastatic lesions despite previously undergoing nephrectomy.<sup>126</sup> The most common malignancies that metastasize to the pancreas include non-small cell lung cancer (5% to 38%); renal cell carcinoma (0% to

64%) and other urogenital cancers; malignant melanoma (0% to 25%); gastrointestinal cancers such as colon, gastric, gallbladder, and esophageal cancers (2% to 25%); breast cancer (0% to 18%); gynecologic cancers (0% to 18%); sarcomas; and lymphomas.<sup>120,121,123</sup> Distinguishing metastatic pancreatic lesions from primary pancreatic malignancies is important owing to significant differences in management strategies. For instance, aggressive management with surgical resection of pancreatic metastases may be effective in a selected group of patients; in one study, survival ranged from 14 to 42 months in eight patients who underwent pancreatic resection for pancreatic metastases.<sup>127</sup>

On EUS, pancreatic metastases are visualized as single or multiple lesions that are round and hypoechoic in the majority of cases with well-defined margins.<sup>124,128,129</sup> Metastatic lesions are also more likely to lack pancreatic ductal dilation as compared with primary pancreatic cancers, as was shown in a multivariate logistic regression analysis comprising 28 patients with pancreatic metastases and 60 patients with pancreatic ductal adenocarcinoma.<sup>130</sup> However, no particular features are pathognomonic for pancreatic metastases, and these lesions can also resemble primary pancreatic cancers. Therefore pancreatic metastases cannot be definitively distinguished from primary pancreatic cancer using EUS alone and must be sampled in all cases to establish a definitive diagnosis (Fig. 14.11A and B; Video 14.6).<sup>131</sup>

EUS FNA is the modality of choice for diagnosing pancreatic metastases, with sensitivity of 88% to 94%, specificity of 60% to 100%, and accuracy of 89% to 95.2%.<sup>120,122,125</sup> EUS was also able to detect pancreatic metastases in 17% of patients who had negative CT scans.<sup>120,129</sup> In performing EUS FNA of pancreatic metastases, dedicated passes for cell block must be



• **Fig. 14.12** Linear endoscopic ultrasound image revealed a 4.5-cm hypoechoic mass in the pancreatic head with adherence to the portal vein (A). Rapid onsite evaluation (ROSE) at low power (100x) reveals predominant distribution of atypical lymphocytes throughout the microscopic field (B; Diff-Quik-staining, 100x). High power (400x) demonstrates numerous large monotonous lymphocytes admixed with small, dark, round mature lymphocytes (C; Diff-Quik staining 400x). *FNA*, Fine-needle aspiration; *PV*, portal vein.

performed for immunohistochemistry testing, because metastatic lesions, especially those from lung adenocarcinoma, can appear morphologically similar to primary pancreatic ductal adenocarcinoma.<sup>120,124,126</sup>

## Pancreatic Lymphoma

Lymphoma can arise directly from the pancreatic parenchyma or can be an extension from a peripancreatic or retroperitoneal lymph node mass, making definitive diagnosis difficult. In a retrospective study of 2397 patients with pancreatic masses, 12 (0.5%) patients were diagnosed to have primary pancreatic lymphoma.<sup>132</sup> At final diagnosis, 8 of 12 patients had large B-cell lymphoma, 3 non-Hodgkin's lymphoma, and 1 small cell lymphocytic lymphoma.

At EUS, the pancreatic lymphoma usually measures more than 4 cm in size; the majority are located at the pancreatic head, and lesions appear uniformly hypoechoic (Fig. 14.12A–C). The margins are ill defined, and vascular invasion is observed in more than 40% of patients. The rest of the pancreatic parenchyma appear unremarkable, without features of chronic pancreatitis. More importantly, the main pancreatic duct is not dilated and peripancreatic

lymphadenopathy is observed in greater than 50% of patients. Rapid onsite evaluation (ROSE) typically reveals atypical lymphocytes, and flow cytometry is required to establish a definitive diagnosis.

Therefore the presence of a large heterogeneous mass lesion in the head of the pancreas without associated features of chronic pancreatitis or pancreatic ductal dilation that on ROSE reveals abundant atypical lymphocytes should prompt a diagnosis of primary pancreatic lymphoma. It is important to procure an additional specimen, as flow cytometry can establish a definitive diagnosis in the majority of patients.

## Personalized Cancer Therapy

In the near future, EUS-guided tissue acquisition will be critical not only for establishing the diagnosis but also for determining prognosis in patients with pancreatic neoplasia. Molecular profiling of tumor specimens has revealed potential targets for anticancer therapy, and desmoplastic stroma in pancreatic cancer has been shown to be an important target for improving treatment outcomes. In a recent study using digital microdissection, pancreatic cancer specimens were classified as classic or basal-like

tumors with either normal or activated stroma.<sup>133</sup> Although classic tumors with normal stroma had longer survival, patients with basal-like tumors and activated stroma had poorer outcomes. It was also observed that the classical subtype tumors showed less response to adjuvant therapy compared with basal-like tumors.<sup>133</sup> Vigorous production of desmoplastic stroma appears to inhibit chemotherapeutic drug delivery; therefore focusing on depletion of stroma may lead to an increased response to chemotherapeutic agents.<sup>134,135</sup> Also, the presence of certain KRAS mutations such as G12D in pancreatic cancer portends a poor response to gemcitabine-based chemotherapeutic regimens. The newer-generation of core biopsy needles, by virtue of their ability to yield a histologic sample, can not only establish a more definitive diagnosis but also enable molecular profiling for the delivery of personalized anticancer therapy.

## Key References

11. DeWitt J, Devvereaux B, Chriswell M, et al. Comparison of endoscopic ultrasonography and multidetector computed tomography for detecting and staging pancreatic cancer. *Ann Intern Med.* 2004;141:753–763.
16. Midwinter MJ, Beveridge CJ, Wilsdon JB, et al. Correlation between spiral computed tomography, endoscopic ultrasonography and findings at operation in pancreatic and ampullary tumours. *Br J Surg.* 1999;86:189–193.
24. Soriano A, Castells A, Ayuso C, et al. Preoperative staging and tumor resectability assessment of pancreatic cancer: prospective study comparing endoscopic ultrasonography, helical computed tomography, magnetic resonance imaging, and angiography. *Am J Gastroenterol.* 2004;99:492–501.
94. Öberg K, Knigge U, Kwekkeboom D, et al. Neuroendocrine gastro-entero-pancreatic tumors: ESMO clinical practice guidelines for diagnosis, treatment and follow-up†. *Annals of Oncology.* 2012;23: viii124–viii130.
120. Raymond SLT, Yugawa D, Chang KHF, et al. Metastatic neoplasms to the pancreas diagnosed by fine-needle aspiration/biopsy cytology: a 15-year retrospective analysis. *Diagn Cytopathol.* 2017;45:771–783.

## References

Access the reference list online at [ExpertConsult.com](http://ExpertConsult.com).

## References

1. Siegel RL, Miller KD, Jemal A. Cancer Statistics, 2017. *CA Cancer J Clin.* 2017;67:7–30.
2. Mertz HR, Sechopoulos P, Delbeke D, et al. EUS, PET, and CT scanning for evaluation of pancreatic adenocarcinoma. *Gastrointest Endosc.* 2000;52:367–371.
3. Ainsworth AP, Rafaelsen SR, Wamberg PA, et al. Is there a difference in diagnostic accuracy and clinical impact between endoscopic ultrasonography and magnetic resonance cholangio-pancreatography? *Endoscopy.* 2003;35:1029–1032.
4. Agarwal B, Abu-Hamda E, Molke KL, et al. Endoscopic ultrasound-guided fine needle aspiration and multidetector spiral CT in the diagnosis of pancreatic cancer. *Am J Gastroenterol.* 2004;99:844–850.
5. Best LM, Rawji V, Pereira SP, et al. Imaging modalities for characterising focal pancreatic lesions. *Cochrane Database Syst Rev.* 2017;4: Cd010213.
6. Muller MF, Meyenberger C, Bertschinger P, et al. Pancreatic tumors: evaluation with endoscopic US, CT, and MR imaging. *Radiology.* 1994;190:745–751.
7. Catanzaro A, Richardson S, Veloso H, et al. Long-term follow-up of patients with clinically indeterminate suspicion of pancreatic cancer and normal EUS. *Gastrointest Endosc.* 2003;58:836–840.
8. Klapman JB, Chang KJ, Lee JG, et al. Negative predictive value of endoscopic ultrasound in a large series of patients with a clinical suspicion of pancreatic cancer. *Am J Gastroenterol.* 2005;100:2658–2661.
9. Lee ES, Lee JM. Imaging diagnosis of pancreatic cancer: a state-of-the-art review. *World J Gastroenterol.* 2014;20:7864–7877.
10. Schima W, Ba-Salamah A, Kolblinger C, et al. Pancreatic adenocarcinoma. *Eur Radiol.* 2007;17:638–649.
11. DeWitt J, Devereaux B, Chriswell M, et al. Comparison of endoscopic ultrasonography and multidetector computed tomography for detecting and staging pancreatic cancer. *Ann Intern Med.* 2004;141:753–763.
12. Koelbling C, Ba-Salamah A, Goetzinger P, et al. Gadobenate dimeglumine-enhanced 3.0-T MR imaging versus multiphasic 64-detector row CT: prospective evaluation in patients suspected of having pancreatic cancer. *Radiology.* 2011;259:757–766.
13. Lee JK, Kim AY, Kim PN, et al. Prediction of vascular involvement and resectability by multidetector-row CT versus MR imaging with MR angiography in patients who underwent surgery for resection of pancreatic ductal adenocarcinoma. *Eur J Radiol.* 2010;73:310–316.
14. Irie H, Honda H, Kaneko K, et al. Comparison of helical CT and MR imaging in detecting and staging small pancreatic adenocarcinoma. *Abdom Imaging.* 1997;22:429–433.
15. Bronstein YL, Loyer EM, Kaur H, et al. Detection of small pancreatic tumors with multiphasic helical CT. *AJR Am J Roentgenol.* 2004;182:619–623.
16. Midwinter MJ, Beveridge CJ, Wilsdon JB, et al. Correlation between spiral computed tomography, endoscopic ultrasonography and findings at operation in pancreatic and ampullary tumours. *Br J Surg.* 1999;86:189–193.
17. Dewitt J, Devereaux BM, Lehman GA, et al. Comparison of endoscopic ultrasound and computed tomography for the pre-operative evaluation of pancreatic cancer: a systematic review. *Clin Gastroenterol Hepatol.* 2006;4:717–725; quiz 664.
18. Yasuda I, Iwashita T, Doi S, et al. Role of EUS in the early detection of small pancreatic cancer. *Dig Endosc.* 2011;23(suppl 1):22–25.
19. Yoon SH, Lee JM, Cho JY, et al. Small (<= 20 mm) pancreatic adenocarcinomas: analysis of enhancement patterns and secondary signs with multiphasic multidetector CT. *Radiology.* 2011;259:442–452.
20. Wang W, Shpaner A, Krishna SG, et al. Use of EUS-FNA in diagnosing pancreatic neoplasm without a definitive mass on CT. *Gastrointest Endosc.* 2013;78:73–80.
21. Krishna SG, Rao BB, Ugbarugba E, et al. Diagnostic performance of endoscopic ultrasound for detection of pancreatic malignancy following an indeterminate multidetector CT scan: a systemic review and meta-analysis. *Surg Endosc.* 2017;31:4558–4567.
22. Rieber A, Tomczak R, Nussle K, et al. MRI with mangafodipir trisodium in the detection of pancreatic tumours: comparison with helical CT. *Br J Radiol.* 2000;73:1165–1169.
23. Kauhanen SP, Komar G, Seppanen MP, et al. A prospective diagnostic accuracy study of 18F-fluorodeoxyglucose positron emission tomography/computed tomography, multidetector row computed tomography, and magnetic resonance imaging in primary diagnosis and staging of pancreatic cancer. *Ann Surg.* 2009;250:957–963.
24. Soriano A, Castells A, Ayuso C, et al. Preoperative staging and tumor resectability assessment of pancreatic cancer: prospective study comparing endoscopic ultrasonography, helical computed tomography, magnetic resonance imaging, and angiography. *Am J Gastroenterol.* 2004;99:492–501.
25. Kitano M, Kamata K, Imai H, et al. Contrast-enhanced harmonic endoscopic ultrasonography for pancreatobiliary diseases. *Dig Endosc.* 2015;27(suppl 1):60–67.
26. Saftoiu A, Vilmann P, Dietrich CF, et al. Quantitative contrast-enhanced harmonic EUS in differential diagnosis of focal pancreatic masses (with videos). *Gastrointest Endosc.* 2015;82:59–69.
27. Fusaroli P, Spada A, Mancino MG, et al. Contrast harmonic echo-endoscopic ultrasound improves accuracy in diagnosis of solid pancreatic masses. *Clin Gastroenterol Hepatol.* 2010;8:629–634.e1–e2.
28. Gong TT, Hu DM, Zhu Q. Contrast-enhanced EUS for differential diagnosis of pancreatic mass lesions: a meta-analysis. *Gastrointest Endosc.* 2012;76:301–309.
29. Sugimoto M, Takagi T, Hikichi T, et al. Conventional versus contrast-enhanced harmonic endoscopic ultrasonography-guided fine-needle aspiration for diagnosis of solid pancreatic lesions: a prospective randomized trial. *Pancreatology.* 2015;15:538–541.
30. Janssen J, Schlorer E, Greiner L. EUS elastography of the pancreas: feasibility and pattern description of the normal pancreas, chronic pancreatitis, and focal pancreatic lesions. *Gastrointest Endosc.* 2007;65:971–978.
31. Iglesias-Garcia J, Larino-Noia J, Abdulkader I, et al. Quantitative endoscopic ultrasound elastography: an accurate method for the differentiation of solid pancreatic masses. *Gastroenterology.* 2010;139:1172–1180.
32. Mei M, Ni J, Liu D, et al. EUS elastography for diagnosis of solid pancreatic masses: a meta-analysis. *Gastrointest Endosc.* 2013;77:578–589.
33. Ying L, Lin X, Xie ZL, et al. Clinical utility of endoscopic ultrasound elastography for identification of malignant pancreatic masses: a meta-analysis. *J Gastroenterol Hepatol.* 2013;28:1434–1443.
34. Li X, Xu W, Shi J, et al. Endoscopic ultrasound elastography for differentiating between pancreatic adenocarcinoma and inflammatory masses: a meta-analysis. *World J Gastroenterol.* 2013;19:6284–6291.
35. Hu DM, Gong TT, Zhu Q. Endoscopic ultrasound elastography for differential diagnosis of pancreatic masses: a meta-analysis. *Dig Dis Sci.* 2013;58:1125–1131.
36. Conlon KC, Klimstra DS, Brennan MF. Long-term survival after curative resection for pancreatic ductal adenocarcinoma. Clinicopathologic analysis of 5-year survivors. *Ann Surg.* 1996;223:273–279.
37. Wagner M, Redaelli C, Lietz M, et al. Curative resection is the single most important factor determining outcome in patients with pancreatic adenocarcinoma. *Br J Surg.* 2004;91:586–594.

38. Kamarajah SK, Burns WR, Frankel TL, et al. Validation of the American Joint Commission on Cancer (AJCC) 8th edition staging system for patients with pancreatic adenocarcinoma: a Surveillance, Epidemiology and End Results (SEER) analysis. *Ann Surg Oncol.* 2017;24:2023–2030.
39. Gilbert JW, Wolpin B, Clancy T, et al. Borderline resectable pancreatic cancer: conceptual evolution and current approach to image-based classification. *Ann Oncol.* 2017;28:2067–2076.
40. Tempero MA, Malafa MP, Behrman SW, et al. Pancreatic adenocarcinoma, version 2.2014: featured updates to the NCCN guidelines. *J Natl Compr Canc Netw.* 2014;12:1083–1093.
41. Tamburrino D, Partelli S, Crippa S, et al. Selection criteria in resectable pancreatic cancer: a biological and morphological approach. *World J Gastroenterol.* 2014;20:11210–11215.
42. Howard TJ, Chin AC, Streib EW, et al. Value of helical computed tomography, angiography, and endoscopic ultrasound in determining resectability of periampullary carcinoma. *Am J Surg.* 1997;174:237–241.
43. Tellez-Avila FI, Chavez-Tapia NC, Lopez-Arce G, et al. Vascular invasion in pancreatic cancer: predictive values for endoscopic ultrasound and computed tomography imaging. *Pancreas.* 2012;41:636–638.
44. Sugiyama M, Hagi H, Atomi Y, et al. Diagnosis of portal venous invasion by pancreatobiliary carcinoma: value of endoscopic ultrasonography. *Abdom Imaging.* 1997;22:434–438.
45. Bhutani MS, Hawes RH, Hoffman BJ. A comparison of the accuracy of echo features during endoscopic ultrasound (EUS) and EUS-guided fine-needle aspiration for diagnosis of malignant lymph node invasion. *Gastrointest Endosc.* 1997;45:474–479.
46. Catalano MF, Sivak Jr MV, Rice T, et al. Endosonographic features predictive of lymph node metastasis. *Gastrointest Endosc.* 1994;40:442–446.
47. Nawaz H, Fan CY, Kloke J, et al. Performance characteristics of endoscopic ultrasound in the staging of pancreatic cancer: a meta-analysis. *JOP.* 2013;14:484–497.
48. Smith SL, Rajan PS. Imaging of pancreatic adenocarcinoma with emphasis on multidetector CT. *Clin Radiol.* 2004;59:26–38.
49. Nguyen P, Feng JC, Chang KJ. Endoscopic ultrasound (EUS) and EUS-guided fine-needle aspiration (FNA) of liver lesions. *Gastrointest Endosc.* 1999;50:357–361.
50. tenBerge J, Hoffman BJ, Hawes RH, et al. EUS-guided fine needle aspiration of the liver: indications, yield, and safety based on an international survey of 167 cases. *Gastrointest Endosc.* 2002;55:859–862.
51. Holzapfel K, Reiser-Erkan C, Fingerle AA, et al. Comparison of diffusion-weighted MR imaging and multidetector-row CT in the detection of liver metastases in patients operated for pancreatic cancer. *Abdom Imaging.* 2011;36:179–184.
52. Motosugi U, Ichikawa T, Morisaka H, et al. Detection of pancreatic carcinoma and liver metastases with gadoteric acid-enhanced MR imaging: comparison with contrast-enhanced multi-detector row CT. *Radiology.* 2011;260:446–453.
53. Nguyen PT, Chang KJ. EUS in the detection of ascites and EUS-guided paracentesis. *Gastrointest Endosc.* 2001;54:336–339.
54. Coley SC, Strickland NH, Walker JD, et al. Spiral CT and the pre-operative assessment of pancreatic adenocarcinoma. *Clin Radiol.* 1997;52:24–30.
55. O’Malley ME, Boland GW, Wood BJ, et al. Adenocarcinoma of the head of the pancreas: determination of surgical unresectability with thin-section pancreatic-phase helical CT. *AJR Am J Roentgenol.* 1999;173:1513–1518.
56. Al-Hawary MM, Francis IR, Chari ST, et al. Pancreatic ductal adenocarcinoma radiology reporting template: consensus statement of the society of abdominal radiology and the american pancreatic association. *Gastroenterology.* 2014;146:291–304.e1.
57. Kaneko OF, Lee DM, Wong J, et al. Performance of multidetector computed tomographic angiography in determining surgical resectability of pancreatic head adenocarcinoma. *J Comput Assist Tomogr.* 2010;34:732–738.
58. Kala Z, Valek V, Hlavsa J, et al. The role of CT and endoscopic ultrasound in pre-operative staging of pancreatic cancer. *Eur J Radiol.* 2007;62:166–169.
59. Chen G, Liu S, Zhao Y, et al. Diagnostic accuracy of endoscopic ultrasound-guided fine-needle aspiration for pancreatic cancer: a meta-analysis. *Pancreatology.* 2013;13:298–304.
60. Hewitt MJ, McPhail MJ, Possamai L, et al. EUS-guided FNA for diagnosis of solid pancreatic neoplasms: a meta-analysis. *Gastrointest Endosc.* 2012;75:319–331.
61. Puli SR, Bechtold ML, Buxbaum JL, et al. How good is endoscopic ultrasound-guided fine-needle aspiration in diagnosing the correct etiology for a solid pancreatic mass?: a meta-analysis and systematic review. *Pancreas.* 2013;42:20–26.
62. Hebert-Magee S, Bae S, Varadarajulu S, et al. The presence of a cytopathologist increases the diagnostic accuracy of endoscopic ultrasound-guided fine needle aspiration cytology for pancreatic adenocarcinoma: a meta-analysis. *Cytopathology.* 2013;24:159–171.
63. Dumonceau JM, Deprez PH, Jenssen C, et al. Indications, results, and clinical impact of endoscopic ultrasound (EUS)-guided sampling in gastroenterology: European Society of Gastrointestinal Endoscopy (ESGE) Clinical Guideline—Updated January 2017. *Endoscopy.* 2017;49:695–714.
64. Madhoun MF, Wani SB, Rastogi A, et al. The diagnostic accuracy of 22-gauge and 25-gauge needles in endoscopic ultrasound-guided fine needle aspiration of solid pancreatic lesions: a meta-analysis. *Endoscopy.* 2013;45:86–92.
65. Camellini L, Carliniante G, Azzolini F, et al. A randomized clinical trial comparing 22G and 25G needles in endoscopic ultrasound-guided fine-needle aspiration of solid lesions. *Endoscopy.* 2011;43:709–715.
66. Fabbri C, Polifemo AM, Luigiano C, et al. Endoscopic ultrasound-guided fine needle aspiration with 22- and 25-gauge needles in solid pancreatic masses: a prospective comparative study with randomisation of needle sequence. *Dig Liver Dis.* 2011;43:647–652.
67. Siddiqui UD, Rossi F, Rosenthal LS, et al. EUS-guided FNA of solid pancreatic masses: a prospective, randomized trial comparing 22-gauge and 25-gauge needles. *Gastrointest Endosc.* 2009;70:1093–1097.
68. Bang JY, Hebert-Magee S, Hasan MK, et al. Randomized trial comparing the 22 and 25 gauge needles using the suction-in and no-suction (SINS) techniques for EUS-guided FNA of pancreatic masses. *United European Gastroenterology Journal.* 2016;4:A12.
69. Bang JY, Ramesh J, Trevino J, et al. Objective assessment of an algorithmic approach to EUS-guided FNA and interventions. *Gastrointest Endosc.* 2013;77:739–744.
70. Lee JK, Choi JH, Lee KH, et al. A prospective, comparative trial to optimize sampling techniques in EUS-guided FNA of solid pancreatic masses. *Gastrointest Endosc.* 2013;77:745–751.
71. Puri R, Vilmann P, Saftoiu A, et al. Randomized controlled trial of endoscopic ultrasound-guided fine-needle sampling with or without suction for better cytological diagnosis. *Scand J Gastroenterol.* 2009;44:499–504.
72. Abe Y, Kawakami H, Oba K, et al. Effect of a stylet on a histological specimen in EUS-guided fine-needle tissue acquisition by using 22-gauge needles: a multicenter, prospective, randomized, controlled trial. *Gastrointest Endosc.* 2015;82:837–844.e1.
73. Rastogi A, Wani S, Gupta N, et al. A prospective, single-blind, randomized, controlled trial of EUS-guided FNA with and without a stylet. *Gastrointest Endosc.* 2011;74:58–64.

74. Sahai AV, Paquin SC, Gariepy G. A prospective comparison of endoscopic ultrasound-guided fine needle aspiration results obtained in the same lesion, with and without the needle stylet. *Endoscopy*. 2010;42:900–903.
75. Gimeno-Garcia AZ, Paquin SC, Gariepy G, et al. Comparison of endoscopic ultrasonography-guided fine-needle aspiration cytology results with and without the stylet in 3364 cases. *Dig Endosc*. 2013;25:303–307.
76. Klapman JB, Logrono R, Dye CE, et al. Clinical impact of on-site cytopathology interpretation on endoscopic ultrasound-guided fine needle aspiration. *Am J Gastroenterol*. 2003;98:1289–1294.
77. Varadarajulu S, Bang JY, Holt BA, et al. The 25-gauge EUS-FNA needle: Good for on-site but poor for off-site evaluation? Results of a randomized trial. *Gastrointest Endosc*. 2014;80:1056–1063.
78. Ramesh J, Varadarajulu S. How can we get the best results with endoscopic ultrasound-guided fine needle aspiration? *Clin Endosc*. 2012;45:132–137.
79. Varadarajulu S, Tamhane A, Eloubeidi MA. Yield of EUS-guided FNA of pancreatic masses in the presence or the absence of chronic pancreatitis. *Gastrointest Endosc*. 2005;62:728–736; quiz 751, 753.
80. Fritscher-Ravens A, Brand L, Knofel WT, et al. Comparison of endoscopic ultrasound-guided fine needle aspiration for focal pancreatic lesions in patients with normal parenchyma and chronic pancreatitis. *Am J Gastroenterol*. 2002;97:2768–2775.
81. Eloubeidi MA, Varadarajulu S, Desai S, et al. Value of repeat endoscopic ultrasound-guided fine needle aspiration for suspected pancreatic cancer. *J Gastroenterol Hepatol*. 2008;23: 567–570.
82. Wang KX, Ben QW, Jin ZD, et al. Assessment of morbidity and mortality associated with EUS-guided FNA: a systematic review. *Gastrointest Endosc*. 2011;73:283–290.
83. Micames C, Jowell PS, White R, et al. Lower frequency of peritoneal carcinomatosis in patients with pancreatic cancer diagnosed by EUS-guided FNA vs. percutaneous FNA. *Gastrointest Endosc*. 2003;58:690–695.
84. Eloubeidi MA, Chen VK, Eltoum IA, et al. Endoscopic ultrasound-guided fine needle aspiration biopsy of patients with suspected pancreatic cancer: diagnostic accuracy and acute and 30-day complications. *Am J Gastroenterol*. 2003;98:2663–2668.
85. Ribeiro A, Vazquez-Sequeiros E, Wiersma LM, et al. EUS-guided fine-needle aspiration combined with flow cytometry and immunocytochemistry in the diagnosis of lymphoma. *Gastrointest Endosc*. 2001;53:485–491.
86. Wakatsuki T, Irisawa A, Terashima M, et al. ATP assay-guided chemosensitivity testing for gemcitabine with biopsy specimens obtained from unresectable pancreatic cancer using endoscopic ultrasonography-guided fine-needle aspiration. *Int J Clin Oncol*. 2011;16:387–394.
87. Brais RJ, Davies SE, O'Donovan M, et al. Direct histological processing of EUS biopsies enables rapid molecular biomarker analysis for interventional pancreatic cancer trials. *Pancreatology*. 2012;12:8–15.
88. Bang JY, Hawes R, Varadarajulu S. A meta-analysis comparing ProCore and standard fine-needle aspiration needles for endoscopic ultrasound-guided tissue acquisition. *Endoscopy*. 2016;48:339–349.
89. Kandel P, Tranesh G, Nassar A, et al. EUS-guided fine needle biopsy sampling using a novel fork-tip needle: a case-control study. *Gastrointest Endosc*. 2016;84:1034–1039.
90. Bang JY, Hebert-Magee S, Hasan MK, et al. Endoscopic ultrasonography-guided biopsy using a franseen needle design: initial assessment. *Dig Endosc*. 2017;29:338–346.
91. Bang JY, Hebert-Magee S, Hasan MK, et al. Randomized trial comparing the 22G franseen biopsy and 22G aspiration needles for EUS-guided sampling of solid pancreatic mass lesions; 2017.
92. Yao JC, Hassan M, Phan A, et al. One hundred years after “carcinoid”: epidemiology of and prognostic factors for neuroendocrine tumors in 35,825 cases in the United States. *J Clin Oncol*. 2008;26:3063–3072.
93. Salaria SN, Shi C. Pancreatic neuroendocrine tumors. *Surg Pathol Clin*. 2016;9:595–617.
94. Öberg K, Knigge U, Kwekkeboom D, et al. Neuroendocrine gastro-entero-pancreatic tumors: ESMO clinical practice guidelines for diagnosis, treatment and follow-up†. *Annals of Oncology*. 2012;23:vii124–vii130.
95. Khashab MA, Yong E, Lennon AM, et al. EUS is still superior to multidetector computerized tomography for detection of pancreatic neuroendocrine tumors. *Gastrointest Endosc*. 2011;73:691–696.
96. Thoeni RF, Mueller-Lisse UG, Chan R, et al. Detection of small, functional islet cell tumors in the pancreas: selection of MR imaging sequences for optimal sensitivity. *Radiology*. 2000;214:483–490.
97. van Asselt SJ, Brouwers AH, van Dullemen HM, et al. EUS is superior for detection of pancreatic lesions compared with standard imaging in patients with multiple endocrine neoplasia type 1. *Gastrointest Endosc*. 2015;81:159–167.e2.
98. Sadowski SM, Neychev V, Millo C, et al. Prospective study of 68Ga-DOTATATE positron emission tomography/computed tomography for detecting gastro-entero-pancreatic neuroendocrine tumors and unknown primary sites. *J Clin Oncol*. 2016;34:588–596.
99. Kimura N, Pilichowska M, Date F, et al. Immunohistochemical expression of somatostatin type 2A receptor in neuroendocrine tumors. *Clin Cancer Res*. 1999;5:3483–3487.
100. De Angelis C, Carucci P, Repici A, et al. Endosonography in decision making and management of gastrointestinal endocrine tumors. *Eur J Ultrasound*. 1999;10:139–150.
101. Proye C, Malvaux P, Pattou F, et al. Noninvasive imaging of insulinomas and gastrinomas with endoscopic ultrasonography and somatostatin receptor scintigraphy. *Surgery*. 1998;124:1134–1143; discussion 1143–1144.
102. Zimmer T, Stolzel U, Bader M, et al. Endoscopic ultrasonography and somatostatin receptor scintigraphy in the preoperative localisation of insulinomas and gastrinomas. *Gut*. 1996;39: 562–568.
103. Termanini B, Gibril F, Reynolds JC, et al. Value of somatostatin receptor scintigraphy: a prospective study in gastrinoma of its effect on clinical management. *Gastroenterology*. 1997;112: 335–347.
104. Dromain C, de Baere T, Baudin E, et al. MR imaging of hepatic metastases caused by neuroendocrine tumors: comparing four techniques. *AJR Am J Roentgenol*. 2003;180:121–128.
105. Dromain C, de Baere T, Lumbroso J, et al. Detection of liver metastases from endocrine tumors: a prospective comparison of somatostatin receptor scintigraphy, computed tomography, and magnetic resonance imaging. *J Clin Oncol*. 2005;23:70–78.
106. Anderson MA, Carpenter S, Thompson NW, et al. Endoscopic ultrasound is highly accurate and directs management in patients with neuroendocrine tumors of the pancreas. *Am J Gastroenterol*. 2000;95:2271–2277.
107. Fujimori N, Osoegawa T, Lee L, et al. Efficacy of endoscopic ultrasonography and endoscopic ultrasonography-guided fine-needle aspiration for the diagnosis and grading of pancreatic neuroendocrine tumors. *Scand J Gastroenterol*. 2016;51: 245–252.
108. James PD, Tsolakis AV, Zhang M, et al. Incremental benefit of preoperative EUS for the detection of pancreatic neuroendocrine tumors: a meta-analysis. *Gastrointest Endosc*. 2015;81:848–856.e1.
109. Puli SR, Kalva N, Bechtold ML, et al. Diagnostic accuracy of endoscopic ultrasound in pancreatic neuroendocrine tumors: a systematic review and meta analysis. *World J Gastroenterol*. 2013;19:3678–3684.

110. Ardengh JC, de Paulo GA, Ferrari AP. EUS-guided FNA in the diagnosis of pancreatic neuroendocrine tumors before surgery. *Gastrointest Endosc.* 2004;60:378–384.
111. Hellman P, Hennings J, Akerstrom G, et al. Endoscopic ultrasonography for evaluation of pancreatic tumours in multiple endocrine neoplasia type 1. *Br J Surg.* 2005;92:1508–1512.
112. Barbe C, Murat A, Dupas B, et al. Magnetic resonance imaging versus endoscopic ultrasonography for the detection of pancreatic tumours in multiple endocrine neoplasia type 1. *Dig Liver Dis.* 2012;44:228–234.
113. Gines A, Vazquez-Sequeiros E, Soria MT, et al. Usefulness of EUS-guided fine needle aspiration (EUS-FNA) in the diagnosis of functioning neuroendocrine tumors. *Gastrointest Endosc.* 2002;56:291–296.
114. Ridtidid W, Halawi H, DeWitt JM, et al. Cystic pancreatic neuroendocrine tumors: outcomes of preoperative endosonography-guided fine needle aspiration, and recurrence during long-term follow-up. *Endoscopy.* 2015;47:617–625.
115. Hasegawa T, Yamao K, Hijioka S, et al. Evaluation of Ki-67 index in EUS-FNA specimens for the assessment of malignancy risk in pancreatic neuroendocrine tumors. *Endoscopy.* 2014;46:32–38.
116. Diaz Del Arco C, Esteban Lopez-Jamar JM, Ortega Medina L, et al. Fine-needle aspiration biopsy of pancreatic neuroendocrine tumors: correlation between Ki-67 index in cytological samples and clinical behavior. *Diagn Cytopathol.* 2017;45:29–35.
117. Lakhtakia S, Ramchandani M, Galasso D, et al. EUS-guided radiofrequency ablation for management of pancreatic insulinoma by using a novel needle electrode (with videos). *Gastrointest Endosc.* 2016;83:234–239.
118. Pai M, Habib N, Senturk H, et al. Endoscopic ultrasound guided radiofrequency ablation, for pancreatic cystic neoplasms and neuroendocrine tumors. *World J Gastrointest Surg.* 2015;7:52–59.
119. Teoh AY, Chong CC, Chan AW, et al. EUS-guided alcohol injection of pancreatic neuroendocrine tumor. *Gastrointest Endosc.* 2015;82:167.
120. Raymond SLT, Yugawa D, Chang KHF, et al. Metastatic neoplasms to the pancreas diagnosed by fine-needle aspiration/biopsy cytology: a 15-year retrospective analysis. *Diagn Cytopathol.* 2017;45:771–783.
121. Layfield LJ, Hirschowitz SL, Adler DG. Metastatic disease to the pancreas documented by endoscopic ultrasound guided fine-needle aspiration: a seven-year experience. *Diagn Cytopathol.* 2012;40:228–233.
122. Atiq M, Bhutani MS, Ross WA, et al. Role of endoscopic ultrasound in evaluation of metastatic lesions to the pancreas: a tertiary cancer center experience. *Pancreas.* 2013;42:516–523.
123. El II H, LeBlanc JK, Sherman S, et al. Endoscopic ultrasound-guided biopsy of pancreatic metastases: a large single-center experience. *Pancreas.* 2013;42:524–530.
124. Sekulic M, Amin K, Mettler T, et al. Pancreatic involvement by metastasizing neoplasms as determined by endoscopic ultrasound-guided fine needle aspiration: a clinicopathologic characterization. *Diagn Cytopathol.* 2017;45:418–425.
125. Alomari AK, Ustun B, Aslanian HR, et al. Endoscopic ultrasound-guided fine-needle aspiration diagnosis of secondary tumors involving the pancreas: an institution's experience. *Cytjournal.* 2016;13:1.
126. Pannala R, Hallberg-Wallace KM, Smith AL, et al. Endoscopic ultrasound-guided fine needle aspiration cytology of metastatic renal cell carcinoma to the pancreas: a multi-center experience. *Cytjournal.* 2016;13:24.
127. Sperti C, Pasquali C, Liessi G, et al. Pancreatic resection for metastatic tumors to the pancreas. *J Surg Oncol.* 2003;83:161–166; discussion 166.
128. Palazzo L, Borotto E, Cellier C, et al. Endosonographic features of pancreatic metastases. *Gastrointest Endosc.* 1996;44:433–436.
129. DeWitt J, Jowell P, Leblanc J, et al. EUS-guided FNA of pancreatic metastases: a multicenter experience. *Gastrointest Endosc.* 2005;61:689–696.
130. Hijioka S, Hara K, Mizuno N, et al. Diagnostic performance and factors influencing the accuracy of EUS-FNA of pancreatic neuroendocrine neoplasms. *J Gastroenterol.* 2016;51:923–930.
131. Fritscher-Ravens A, Sriram PV, Krause C, et al. Detection of pancreatic metastases by EUS-guided fine-needle aspiration. *Gastrointest Endosc.* 2001;53:65–70.
132. Ramesh J, Hebert-Magee S, Kim H, et al. Frequency of occurrence and characteristics of primary pancreatic lymphoma during endoscopic ultrasound guided fine needle aspiration: a retrospective study. *Dig Liver Dis.* 2014;46:470–473.
133. Moffitt RA, Marayati R, Flate EL, et al. Virtual microdissection identifies distinct tumor- and stroma-specific subtypes of pancreatic ductal adenocarcinoma. *Nat Genet.* 2015;47:1168–1178.
134. Sato N, Cheng XB, Kohi S, et al. Targeting hyaluronan for the treatment of pancreatic ductal adenocarcinoma. *Acta Pharm Sin B.* 2016;6:101–105.
135. Jacobetz MA, Chan DS, Neesse A, et al. Hyaluronan impairs vascular function and drug delivery in a mouse model of pancreatic cancer. *Gut.* 2013;62:112–120.

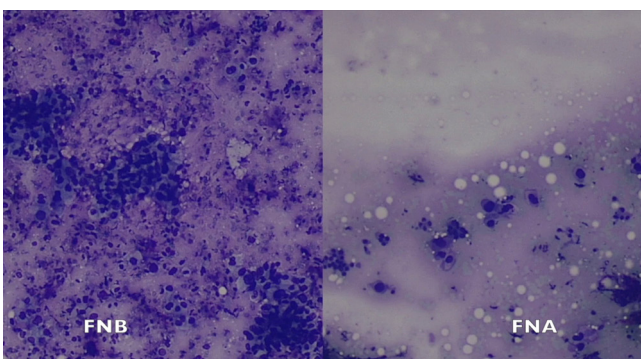


**Video 14.1** Endoscopic Ultrasound-Guided Fine-Needle Aspiration of a Hypoechoic Mass in the Left Lobe of the Liver Reveals Metastatic Pancreatic Adenocarcinoma

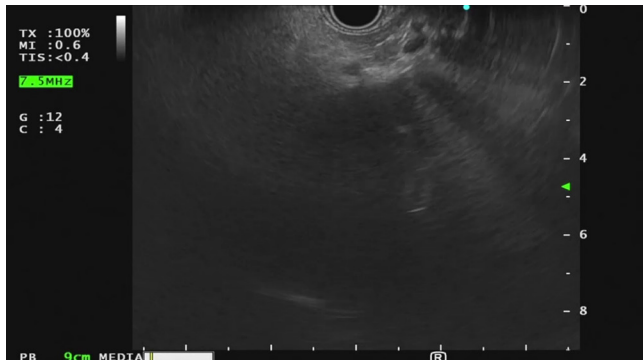


**Video 14.2** Endoscopic Ultrasound-Guided Fine-Needle Aspiration of a Pancreatic Uncinate Mass Using a 25-Gauge Needle

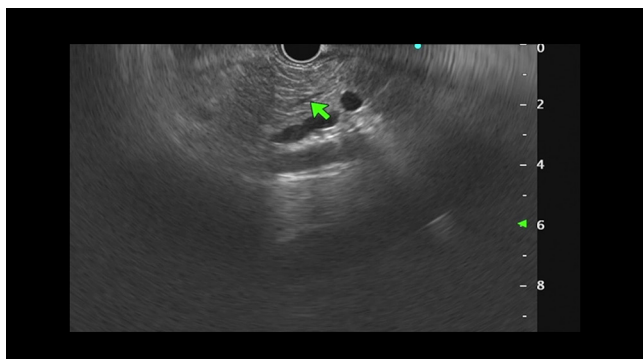
The fluoroscopic image reveals technical challenges associated with sampling of pancreatic uncinate masses.



**Video 14.3** Endoscopic Ultrasound-Guided Sampling of a Pancreatic Mass Obtained With Fine-Needle Aspiration (FNA) Using a Standard-Bevel FNA Needle and a Franseen Fine-Needle Biopsy Needle  
Note the difference in cellularity, both at rapid onsite evaluation (ROSE) and in the cell block.



**Video 14.4** Endoscopic Ultrasound-Guided Fine-Needle Aspiration of a Pancreatic Cyst Mass Revealing a Neuroendocrine Tumor



**Video 14.5** Endoscopic Ultrasound-Guided Fine-Needle Aspiration of a 6-cm Pancreatic Neck Mass Revealing a Neuroendocrine Tumor

Note the well-circumscribed lesion with surrounding normal pancreas and nondilated main pancreatic duct.



**Video 14.6** Endoscopic Ultrasound-Guided Fine-Needle Aspiration of Multiple Hypoechoic Lesions in the Pancreatic Body and Tail Regions Reveal Metastatic Renal Cell Cancer

# 15

## Endoscopic Ultrasonography in the Evaluation of Pancreatic Cysts

ROBERT MORAN AND ANNE MARIE LENNON

### KEY POINTS

- The differential diagnosis of pancreatic cystic lesions is wide: the majority of these lesions are benign, but detection of mucinous neoplasms (IPMN and MCN) is important because these cysts may be malignant or have malignant potential.
- The diagnostic accuracy of EUS based on morphology alone is limited.
- A combination of EUS features, fluid cytology, carcinoembryonic level, mucin staining, and molecular markers is used to differentiate pancreatic cysts.
- FNA of cystic lesions under antibiotic cover is safe, with low rates of bleeding, infection, and pancreatitis.
- Accurate diagnosis and management of pancreatic cystic lesions require careful evaluation of the clinical setting, other imaging modalities, and multidisciplinary collaboration.

### Introduction

Pancreatic cysts, once thought to be rare, are now detected more frequently as a result of the increased use of high-resolution imaging. Between 2% and 13% of patients undergoing computed tomography (CT)<sup>1</sup> or magnetic resonance imaging (MRI)<sup>2</sup> with no symptoms or history of pancreatic disease are found to have pancreatic cysts. These lesions represent a broad spectrum of pathologic changes from benign cysts to premalignant and malignant cysts. Pancreatic cysts thus represent an important and increasing disease burden and pose a difficult diagnostic and management problem: that is, how to accurately predict which lesions contain malignancy and require resection versus those that can be followed safely by interval imaging or require no further follow-up.

Despite advances in CT and MRI, the ability of cross-sectional modalities to identify the exact nature of a cyst remains limited.<sup>3</sup> Endoscopic ultrasonography (EUS) is ideally suited for the imaging of pancreatic lesions because of its high resolution and ability to sample cystic lesions. This chapter discusses the different types of pancreatic cysts, their endosonographic features, and the role of fine-needle aspiration (FNA) for cytologic and tumor marker analysis. A diagnostic approach to patients with pancreatic cysts is also described.

### Types of Pancreatic Cysts

There are many different types of pancreatic cysts, including cysts with no or very low malignant potential, those that have the ability to develop high-grade dysplasia (HGD) or invasive carcinoma (IC), and cysts that harbor IC (Table 15.1). Pseudocysts are common in general practice but account for less than 10% of resected pancreatic cysts. In modern surgical series, the most commonly resected pancreatic cysts are intraductal papillary mucinous neoplasms (IPMNs), mucinous cystic neoplasms (MCNs), and serous cystadenomas (SCAs), which account for 50%, 16%, and 12% of resected cysts, respectively.<sup>4</sup> Solid neoplasms can also undergo cystic degeneration, with cystic pancreatic neuroendocrine tumors (PanNETs), solid pseudopapillary neoplasms (SPNs), and cystic pancreatic ductal adenocarcinomas accounting for between 1% and 9% of resected cysts. The clinical presentation, endoscopic features, and management of these cysts are discussed below.

### Diagnostic Approach

#### Clinical History and Imaging

Taking a good clinical history is important. Key questions are whether there is a history of pancreatitis, jaundice, or recent onset of diabetes; is there any pancreatic type of abdominal or back pain, anorexia, or weight loss? The presence of any of these features is worrisome for the presence of HGD/IC, and these patients should undergo a very careful EUS and be evaluated by a multidisciplinary team.<sup>5</sup> Is there a personal or family history of related cancers to suggest multiple endocrine neoplasia (MEN) 1, von Hippel–Lindau (VHL) syndrome, or any history to suggest an increased risk of pancreatic adenocarcinoma, hereditary non-polyposis colorectal cancer (HNPCC), Peutz–Jeghers syndrome, *BRCA1/BRCA2* mutation, or familial atypical multiple mole melanoma (FAMMM)?<sup>6</sup>

**Grant Support:** Supported by the Lustgarten Foundation for Pancreatic Cancer Research, the Sol Goldman Center for Pancreatic Cancer Research, the Virginia and D. K. Ludwig Fund for Cancer Research, Susan Wojcicki and Dennis Troper, the Michael Rolfe Foundation, and grant P50 CA62924 from the National Institutes of Health. Dr. Lennon is supported by the Benjamin Baker Scholarship.

**Disclosures:** Dr. Lennon is a consultant for Novo Nordisk and Olympus. Dr. Moran has no disclosures.

Most patients have already undergone cross-sectional imaging before they are referred for EUS, but if not, an MRI or pancreatic protocol CT scan is helpful. From this scan and the clinical features, a diagnosis may be apparent. It may also be clear that the patient requires surgical resection. EUS is indicated when the diagnosis is unclear or where the patient has worrisome symptoms. A pragmatic algorithm for the differential diagnosis and management of pancreatic cysts is shown in Fig. 15.1.

**TABLE 15.1** Classification of Pancreatic Cysts

No or Very Low Malignant Potential	Malignant Potential	Malignant
Pseudocyst	IPMN	Pancreatic ductal adenocarcinoma
Serous cystadenoma	MCN	Neuroendocrine tumor
Lymphoepithelial cyst		Solid pseudopapillary neoplasm
Retention cyst		Pancreatoblastoma
Congenital cyst		Acinar cell cystadenocarcinoma
Lymphangioma		

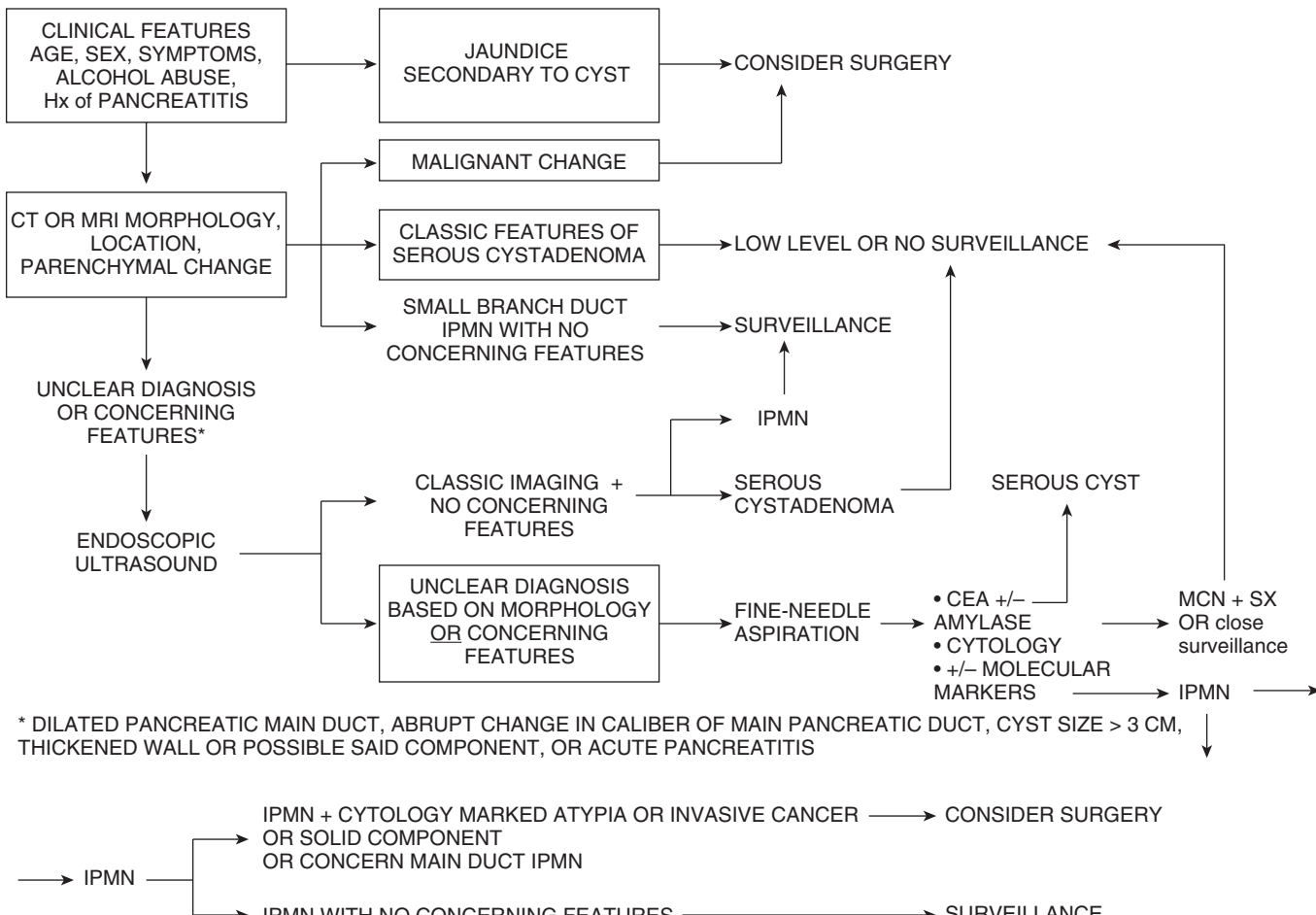
IPMN, Intraductal papillary mucinous neoplasm; MCN, mucinous cystic neoplasm.

## Endoscopic Ultrasound

The EUS approach to examining the pancreas is described in detail in Chapter 12, and FNA techniques are described in Chapter 20. The general EUS approach to pancreatic cysts is described in this section; the appearances of specific cysts are described later.

When a cystic lesion has been identified, it is important to note the number of cysts; their exact location and size; and whether the cyst is within, adjacent to, or outside of the pancreas. This information may influence management (Table 15.2). If the lesion is clearly a pseudocyst, it is assessed for the need and suitability for EUS-guided drainage. The cyst itself should be examined to determine the wall thickness and the presence of a mural nodule or associated mass (see “Examination Checklist”). The size of the individual cysts (microcystic, macrocystic [ $>1$  cm], or a mixture of both), the presence and thickness of any septations (Fig. 15.2), and the presence of echo-dense mucus or debris within the cyst should be documented. The size of the main pancreatic duct (MPD) in the head, body, and tail, whether it communicates with the cyst, the presence of mucin or a mural nodule within the pancreatic duct, or any focal dilation should be noted.

There are several features on EUS that are worrisome for malignant transformation of the cyst. These include the presence of a thick wall or septum, an associated solid mass, or a mural nodule (Fig. 15.3). The presence of focal dilation



• **Fig. 15.1** Endoscopic ultrasonography-based algorithmic approach to the management of pancreatic cystic lesions.

of the MPD, a pancreatic duct measuring  $\geq 10$  mm, or an MPD measuring between 5 and 9 mm with a mural nodule are concerning, and are associated with an increased risk of malignant transformation.<sup>7</sup> One of the EUS features that is most difficult to differentiate in predicting malignant potential is a mural nodule versus a “mucin ball.” Several features that can be used and are quite helpful in differentiating these two lesions are listed in Fig. 15.4 and shown in Video 15.1. Mucin typically has a round, hyperechoic, well-demarcated outer edge with a hypoechoic center. When these features are present on EUS it is associated with mucin in 90% of cases.<sup>8</sup> In addition, mucin can be shown to move within the cyst either by moving the patient’s position or by targeting the lesion during endoscopic ultrasonography-guided fine-needle aspiration (EUS FNA), which is then shown to move with

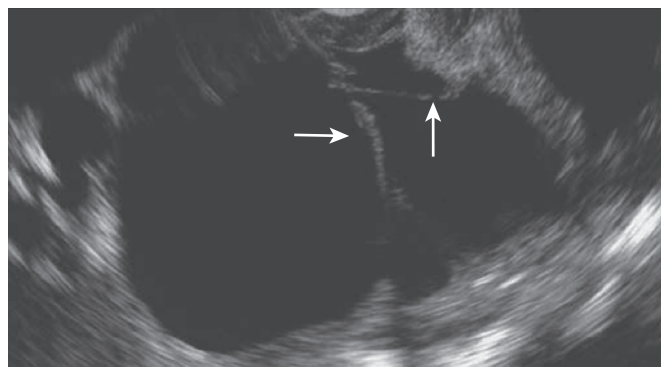
the needle (see Video 15.1). One of the key questions when a mural nodule is found is whether there is a difference between a 2-mm and a 20-mm mural nodule. One Japanese group tried to answer this question by classifying mural nodules into four types; type I has 1- to 2-mm fine papillary protrusions; type II has a larger polypoid nodule; type III has a larger, protruding component with a thickened wall; and type IV is a papillary nodule associated with an ill-defined hypoechoic area within the parenchyma.<sup>9</sup> This group found that mural nodules increased in size with a mean diameter of 5, 6, 11, and 20 mm for types I to IV, respectively. Furthermore types III or IV were associated with IC in almost 90% of the patients.<sup>10</sup> The take-home message is that large mural nodules or those associated with an ill-defined mass are highly concerning for the presence of HGD or IC. One technique that can be very

**TABLE 15.2** Features of Cystic Pancreatic Lesions

	SCA	MCN	IPMN	SPN	Pseudocyst	Cystic Neuroendocrine Tumor
<b>Location</b>	Any location	Body/tail	Arise from main PD or side branch Head > body/tail	Any location	Any location	Any location
<b>Malignant potential</b>	Extremely low	Moderate	Moderate. High when main PD involved	Yes	None	High when tumor $>2$ cm or if a high mitotic rate (Ki-67)
<b>EUS features</b>	Multiple small cysts; often microcystic “honeycomb”; central fibrosis or calcification (“central scar”)  Macrocytic and solid variants also possible	Macrocytic, septations, nodularity or papillary projections. Peripheral calcifications seen in 10%–25%	Dilated main PD or dilated side branch  Can have mural nodule or mass	Mixed solid-cystic; hemorrhagic center	Unilocular, variable size and wall thickness; echogenic material; features of acute/chronic pancreatitis	Round, well-demarcated hypoechoic solid lesion with anechoic area of cystic degeneration
<b>Communication with PD</b>	No	Rare	Yes	No	Sometimes	No
<b>Cytology</b>	Bland glycogen-positive cuboidal cells	Columnar/cuboidal, mucin-positive cells; may show mild, moderate, marked atypia or invasive adenocarcinoma	Columnar/cuboidal mucin-positive cells; may show mild, moderate, marked atypia or invasive adenocarcinoma	Heterogeneous; eosinophilic, papillary cells, PAS-positive deposits, vimentin positivity	Macrophages, inflammatory cells, debris	Stains positive for the following immunohistochemical markers: chromogranin A, synaptophysin, CDX, CD56, and neuron-specific enolase
<b>Cyst fluid</b>	Low viscosity	High viscosity	High viscosity	Low viscosity, bloody and necrotic	Low viscosity, blood-stained or turbid	Low viscosity; may be blood-stained
<b>Amylase</b>	Variable	Variable	Variable	Variable	High	Variable
<b>CEA</b>	Low	Usually high	Usually high	Unknown	Low	Low
<b>Molecular marker analysis</b>	VHL mutation and LOH in Chr 3	KRAS mutation	KRAS and GNAS mutations	CTNNB1 mutation	No mutations	Not applicable

CEA, Carcinoembryonic antigen; Chr, chromosome; EUS, endoscopic ultrasonography; IPMN, intraductal papillary mucinous neoplasia; LOH, loss of heterozygosity; MCN, mucinous cystic neoplasm; PAS, periodic acid-Schiff; PD, pancreatic duct; SCA, serous cystadenoma; SPN, solid pseudopapillary neoplasm; VHL, von Hippel-Lindau.

helpful is contrast-enhanced EUS (CE EUS). Microbubbles are injected into a peripheral vein, which circulate through the pancreas 30 to 40 seconds later. The technique works on the hypothesis that a malignant tumor has a different vascular pattern than either normal pancreatic tissue or mucin. CE EUS may demonstrate vascularity in mural nodules and is useful for differentiating a mural nodule from a mucin ball.<sup>10,11</sup> A prospective study found that CE EUS correctly identified 75% of mural nodules with HGD or IC.<sup>12</sup> Tissue harmonic

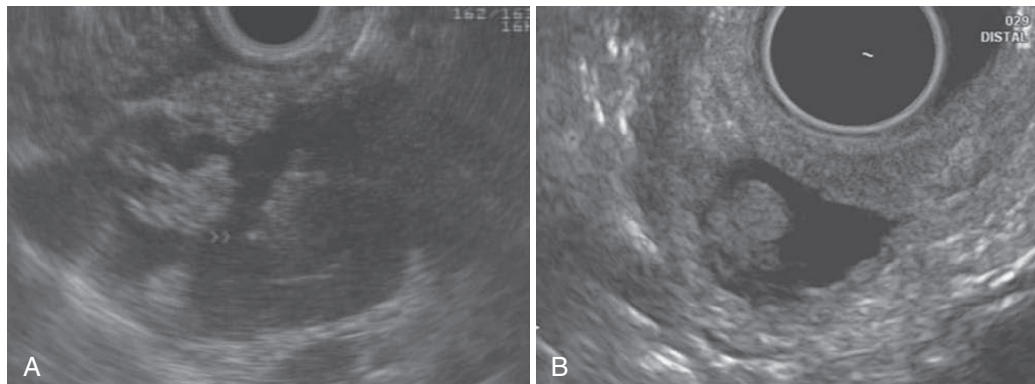


• **Fig. 15.2** Pseudocyst. Thin-walled internal septations (arrows) in a patient with a long-standing pseudocyst.

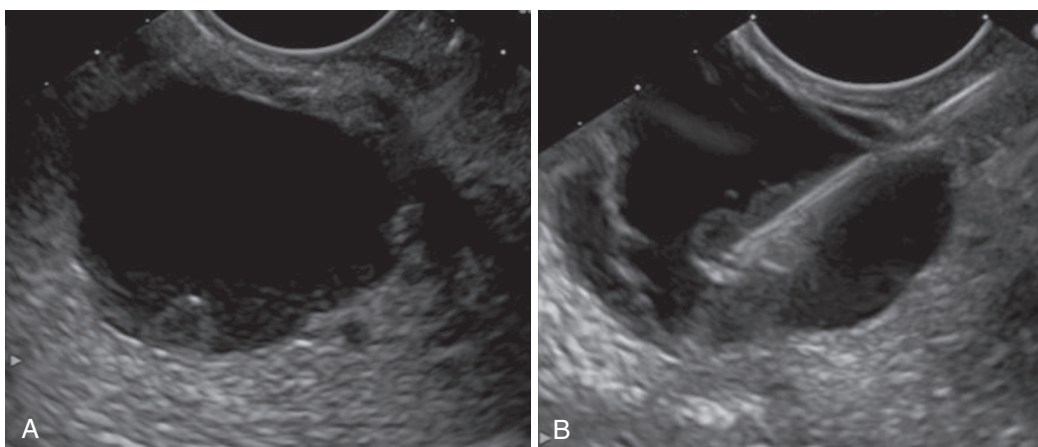
echo (THE) imaging is a further development in EUS. Preliminary studies appear promising and show superior image visualization of mural nodules compared with normal B-mode imaging.<sup>13</sup> Further information about CE EUS can be found in [Chapter 5](#). Finally, it is important to inspect the entire parenchyma and not just the cyst, particularly in individuals with IPMNs, who can develop concomitant pancreatic adenocarcinoma in a region separate from the cyst.<sup>14</sup>

### Confocal Laser Endomicroscopy

Confocal laser endomicroscopy (CLE) is a novel imaging technique in which a low-power laser illuminates and scans a single plane of tissue and generates a real-time optical image or biopsy of the tissue ([Fig. 15.5](#); [Video 15.2](#)).<sup>15</sup> A needle-based CLE (nCLE) has been developed that can be passed through a 19-gauge EUS FNA needle and enable imaging of the epithelium to several hundred microns. There have been two multicenter studies, one of which was retrospective (INSPECT) and one prospective (CONTACT), that have evaluated the role of nCLE in differentiating SCAs from other types of cysts. The result was that nCLE had excellent (100%) specificity and moderate (59% to 69%) specificity for differentiating SCAs from other types of cysts.<sup>16,17</sup> A multicenter prospective study (DETECT) found that nCLE again had excellent specificity (100%) and good sensitivity (80%) for



• **Fig. 15.3** Main duct intraductal papillary mucinous neoplasia (MD-IPMN). (A) The main pancreatic duct is markedly dilated, and hyperechoic nodules can be seen arising from the duct wall. (B) Mural nodule arising from the pancreatic duct wall in a patient with a MD-IPMN.



• **Fig. 15.4** (A) Mucin. There is a lesion in the six o'clock position adjacent to the wall. It is well defined, with a hyperechoic wall and hypoechoic center. These features are suggestive of mucin. (B) On endoscopic ultrasonography-guided fine-needle aspiration, the lesion was shown to move, confirming that it was mucin and not a mural nodule. (Copyright AM Lennon.)

discriminating mucin-producing cysts (IPMNs and MCNs) from other types of cysts.<sup>18</sup> The initial results are promising; however, there are significant limitations in the studies published to date. These include that consecutive patients were not always enrolled, many small cysts were excluded, and, most importantly, that the nCLE diagnosis was confirmed by surgical pathology in only 7% to 23% of the cases, with the diagnosis being made by an expert group using imaging and the analysis of cyst fluid. As shown in the next section, the analysis of cyst fluid has limited accuracy. Larger, prospective studies in consecutive patients that compare the results of nCLE with surgical pathology are required to fully evaluate the potential and role of this technology.

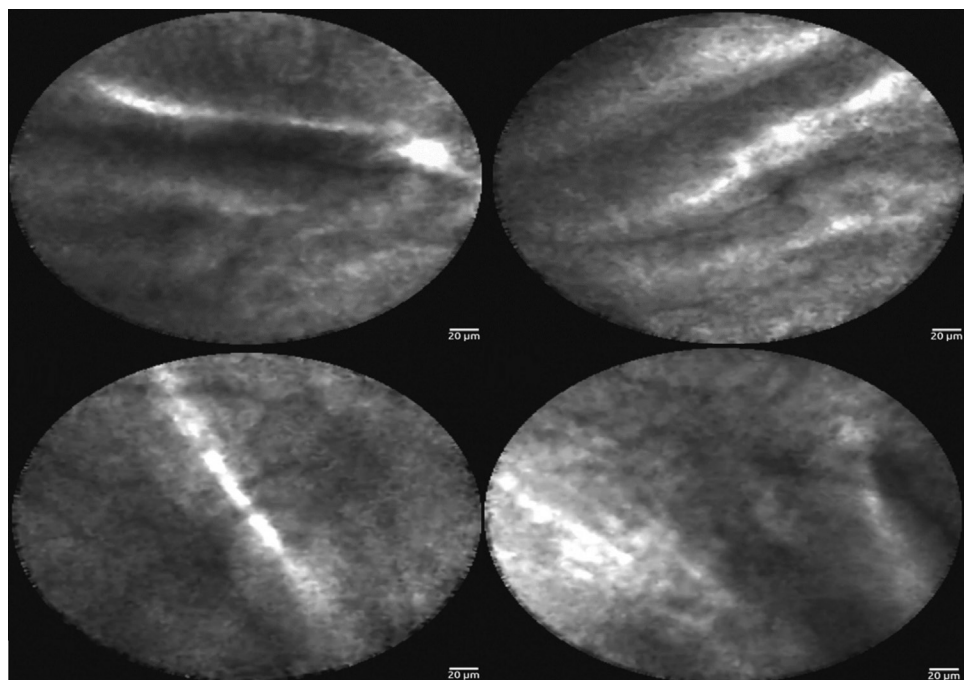
### Endoscopic Ultrasound-Guided Fine-Needle Aspiration

EUS morphology alone is imperfect at identifying the exact type of pancreatic cyst. A large prospective multicenter study<sup>19</sup> found that the accuracy of EUS imaging features for diagnosing mucin-producing cysts was only 51%, although a more recent study from the Netherlands reported a sensitivity of 78%.<sup>20</sup> Slightly worrying in the Dutch study, however, was the sensitivity for detecting malignancy in pancreatic cysts, which was only 25% for EUS. Other retrospective studies have shown a higher accuracy for the detection of malignant/potentially malignant lesions with a reported sensitivity of 91%.<sup>21</sup> However, despite its high resolution, EUS alone clearly has limitations.

EUS FNA is often performed in patients with pancreatic cysts in the Western countries, as it provides additional information that can be helpful in confirming the type of cyst or detecting the presence of HGD or IC. There is no specific type or size of needle that should be used; the choice is determined by the size of the cyst, its location, and the presence of vessels around the cyst. If possible, a single pass is made into the cyst to minimize the risk of complication and the fluid in that cyst locale is fully aspirated (Fig. 15.6). Aspirating the cyst locale to dryness may decrease the

risk of infection, although the evidence for this is slim. Lesions that have a vascular component, such as cystic PanNETs, often yield bloody samples if large-bore needles are used; in such instances, a smaller-gauge needle (e.g., 22 or 25 gauge) may be helpful. Microcystic SCAs are particularly challenging to FNA. It is often difficult or impossible to obtain sufficient fluid for analysis from small cysts. In these cases, a 19-gauge needle can sometimes be used to obtain a core biopsy of the cyst. New core biopsy needles have been developed that can be helpful with lesions such as microcystic SCA (discussed in detail in Chapter 21). These needles have been shown to be helpful in solid pancreatic lesions; however, there are as yet no data for pancreatic cysts. One helpful technique is to target the wall of the cyst with a gentle to-and-fro motion to try to aspirate cells from the wall itself rather than simply aspirating fluid from the center of the cyst. This has been shown to increase the cytologic diagnostic yield for mucin-producing and malignant cysts.<sup>22</sup>

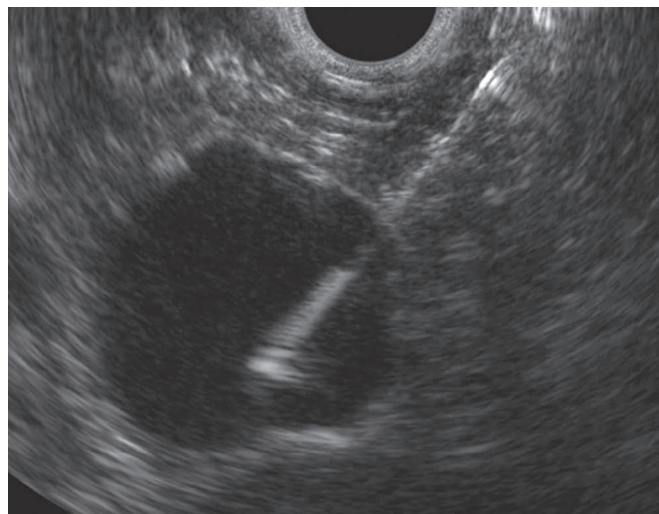
A 25-gauge through-the-needle cytologic brush was developed for the EUS-guided assessment of PCLs. Although studies have shown that use of a cytologic brush was associated with a higher yield of epithelial cells and that this brush appears to be superior in providing diagnostic cells<sup>23</sup> and intracellular mucin<sup>24</sup> compared with direct cyst fluid aspirate, other studies found no difference in the diagnostic yield between aspiration and brushing (55%).<sup>8</sup> In addition, adverse events of up to 18% were reported, with major complications occurring in up to 8% to 10%, including one fatality.<sup>23,24</sup> We therefore do not recommend routine use of this device. A new through-the-needle microbiopsy forceps (Moray microforceps; US Endoscopy, Mentor, Ohio) has been developed that is placed within a 19-gauge EUS FNA needle. The needle is inserted into the cyst and the biopsy forceps advanced under endoscopic guidance into the cyst. The forceps are opened and advanced to the wall, and a biopsy obtained (Video 15.3). This approach offers the potential of obtaining a larger biopsy sample than is possible with regular FNA. There are a small number of promising preliminary case reports. Several prospective multicenter studies are ongoing; we await the results of these to determine the potential



• Fig. 15.5 Confocal laser endomicroscopy (CLE). The four images demonstrate the classical papillary projections associated with intraductal papillary mucinous neoplasia as seen on CLE. (Copyright AM Lennon.)

of this device, its adverse event profile, and its potential role in the evaluation of pancreatic cystic lesions.

The risk of adverse events from EUS FNA is slightly higher in pancreatic cystic lesions compared with FNA of a solid lesion.<sup>12</sup> In a systematic review of almost 1000 patients who underwent EUS FNA of a PCL, the overall complication rate was 2.75%.<sup>12</sup> The most common complication was pancreatitis, which occurred in 1.1% of patients, followed by pain (0.77%), bleeding (0.33%), fever (0.33%), and infection (0.22%).<sup>12</sup> Pancreatitis is usually



• **Fig. 15.6** Endoscopic ultrasound fine-needle aspiration. A 19-gauge, 22-gauge, or 25-gauge needle can be used. In this case, a 22-gauge needle was sufficient to aspirate the lesion completely. Aspiration should continue until the lesion collapses.

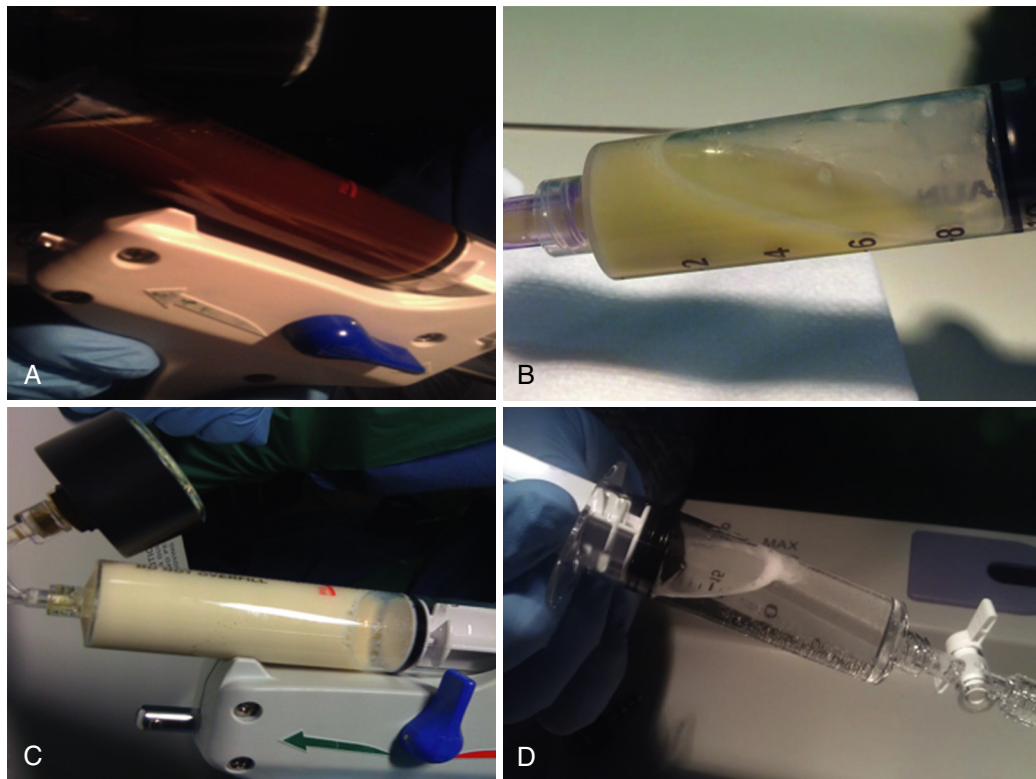
mild; however, severe cases and one death have been reported.<sup>12</sup> Interestingly, in contrast to EUS FNA of solid lesions, the overall risk of adverse events was lower, at 2.33%, in prospective studies compared with 5.07% in retrospective studies.<sup>12</sup>

Antibiotic prophylaxis is recommended, usually with intravenous ciprofloxacin, before the procedure. The American Society of Gastrointestinal Endoscopy (ASGE) suggests that 3 to 5 days of oral ciprofloxacin may be continued, although the evidence base to support this recommendation is not strong.<sup>25</sup> A retrospective study evaluated the risk of malignant seeding of IPMNs in patients who underwent EUS FNA. One concern about performing EUS FNA in pancreatic cystic lesions, which may harbor HGD or IC, is the potential risk of peritoneal seeding from FNA. This risk was evaluated in a retrospective study of 243 patients, 175 of whom had undergone EUS FNA and 68 of whom had undergone resection with no preoperative tissue sampling. There was no statistically significant difference in the rate of peritoneal seeding, which occurred in 2.3% of the EUS FNA group and 4.4% of the no-sampling group ( $P = .403$ ).<sup>26</sup>

## Analysis of Cyst Fluid

### Appearance of the Aspirate and the String Test

Evaluation of the appearance of aspirated cyst fluid can give some limited information about the underlying type of cyst. Fluid from pseudocysts can have a brown, bloody, or purulent exudate due to the presence of neutrophils (Fig. 15.7). Lymphoepithelial cysts have a distinctive white, opaque fluid. Fluid from mucin-producing cysts is typically clear. Mucin-producing cysts typically produce viscous fluid, which may be difficult to aspirate. The “string test” is a simple clinical tool that relies on the viscosity of fluid to differentiate mucin-producing from non-mucin producing cysts. Following EUS FNA,



• **Fig. 15.7** Cyst fluid. (A) Hemorrhagic and (B) turbid fluid from a pseudocyst. (C) Opaque fluid from a lymphoepithelial cyst. (D) Clear fluid from a mucinous cyst.

a drop of fluid is placed between two gloved fingers, which are then slowly spread apart. The fluid can also be evaluated by watching it drip from the EUS FNA needle. A positive test is one in which a string of cyst fluid measuring 1 cm in length is formed and lasts for 1 second or more before disruption. One study that evaluated the string test found that it had performance characteristics similar to cyst fluid carcinoembryonic antigen (CEA), with the combination of the string test and cyst fluid CEA having improved performance characteristics as compared with each of these tests individually.<sup>27</sup>

## Cytology

The specificity of cytology in most studies is excellent and approaches 100%, but the sensitivity varies considerably in reported series. This finding reflects the difficulty of interpreting these lesions, especially when the cellularity of samples is low. Brandwein<sup>28</sup> and Brugge et al.<sup>17</sup> reported sensitivities of 55% and 59%, respectively, for differentiating benign from malignant or potentially malignant PCLs. In contrast, studies by Hernandez<sup>29</sup> and Frossard et al.<sup>30</sup> demonstrate sensitivities of 89% and 97%, respectively. The sensitivity of cytology can be affected by several factors. Sampling error may occur in both microcystic and mucinous lesions in which cellular atypia is patchy, which may lead to false-negative results. Moreover, the presence of blood or benign epithelial cells from the gastric or duodenal mucosa can make interpretation difficult or lead to false-positive results. The presence of on-site evaluation for adequacy of samples obtained by EUS FNA can improve results, although results are equally good whether this is performed by a cytotechnologist or a cytopathologist.<sup>31</sup> The experience of the operator and/or institution does appear to be important, with a recent study showing a trend toward increased accuracy with greater experience.<sup>31</sup> Pancreatic ductal fluid can also be analyzed with cytology, with sensitivity varying from 21%<sup>32</sup> to 75%<sup>33</sup> depending on the study.

## Protein Markers

### Carcinoembryonic Antigen

CEA is found in high levels in mucin-producing cysts, whereas levels are low in pseudocysts and SCAs (see Table 15.2). The sensitivity and specificity of CEA vary depending on the study and the CEA threshold used. The cutoff used by most endoscopists to differentiate a mucin-producing from a non-mucin producing cyst is greater than 192 ng/mL. This was based on a prospective multicenter trial that found this value to be associated with an accuracy of 79% for differentiating mucin-producing cysts from other cyst types, which was significantly better than the accuracy of EUS morphology alone (51%) or cytology (59%).<sup>17</sup> However, other studies have found a lower accuracy. A systematic review and meta-analysis of 18 papers found that CEA had a pooled sensitivity of 63% (95% confidence interval [CI] 59 to 67) and specificity of 93% (95% CI 90 to 95) for identifying mucin-producing cysts.<sup>34</sup> To complicate matters, other studies have suggested an alternative cutoff that varies from 100 to 800 ng/mL.<sup>19,30,35,36</sup> Among the reasons for this are that CEA assays are standardized for serum and not cyst fluid and different assays exist, making comparisons among various studies or centers difficult. A pooled analysis of 12 studies<sup>24</sup> found that a CEA concentration greater than 800 ng/mL strongly suggested a mucin-producing lesion (sensitivity, 48%; specificity, 98%). Conversely, a low level of CEA in cyst fluid of less than 5 ng/mL is strongly suggestive of a non-mucin producing PCL, such as a SCA (sensitivity, 50%; specificity, 95%). Another problem with

CEA is that laboratories require anywhere from 0.25 to 1 mL of fluid. A study from the Netherlands found that sufficient fluid for CEA analysis was obtained in just under 60% of patients.<sup>20</sup> An important point is that, in large studies, an elevated level of CEA in cyst fluid has not been shown to be associated with an increased risk of HGD or IC; therefore it should not be used as a marker of malignant transformation.<sup>37</sup> Despite these limitations, a very high or low cyst fluid CEA is helpful in either identifying or excluding a mucin-producing cyst.

### Cyst Fluid Amylase

Cyst fluid amylase requires approximately 0.5 mL of fluid for analysis in most laboratories and should be sent if a pseudocyst is within the differential diagnosis. A level of less than 250 U/mL virtually excludes a pseudocyst (sensitivity, 44%; specificity, 98%).<sup>30</sup> The levels of cyst fluid amylase vary in both MCN and IPMN and cannot be used to differentiate between these two entities.<sup>38</sup>

### Other Markers

A number of protein biomarkers in cyst fluid have been examined, including CA 72-4, CA 125, CA 19-9, and CA 15-3; however, they have been found to have a lower accuracy than CEA and are therefore not used.<sup>39</sup>

## Molecular Markers

The entire coding regions of IPMNs, MCNs, SCAs, and SPNs were identified in 2011.<sup>40</sup> This landmark study found that several PCLs had a unique genetic profile (see Table 15.1). Almost all SPNs have a mutation in the *CTNNB1* gene.<sup>41</sup> SCAs have mutations in the *VHL* gene or loss of heterozygosity (LOH) in chromosome (Chr) 3, where the *VHL* gene is located. IPMNs and MCNs can both have mutations in a range of genes including *KRAS*, and *RNF43*, whereas a mutation in *GNAS* is found almost exclusively in IPMNs.<sup>41</sup> Using SafeSeqSequencing, which is the most sensitive technique available, 91% of IPMNs had a mutation in either *GNAS* or *KRAS*, 100% of SPNs had a mutation in *CTNNB1*, and 67% of SCAs had either a mutation in *VHL* or LOH of Chr 3. Overall, use of the molecular markers discriminated IPMNs, MCNs, SCAs, and SPNs with 76% to 100% sensitivity and 75% to 100% specificity.<sup>41</sup> Other studies have also shown the added benefit of molecular markers.<sup>42</sup>

## When to Perform Endoscopic Ultrasound-Guided Fine-Needle Aspiration and What to Send It for

We perform EUS FNA when the diagnosis is unclear and the result could alter management. For example, in Fig. 15.8, the EUS image is classic for a SCA. In this case, we would not perform EUS FNA as we are confident of the diagnosis, and EUS FNA is unlikely to alter management. In contrast, in Fig. 15.9, the type of cyst is unclear. Here EUS FNA and the analysis of cyst fluid would be very useful. Similarly, in Fig. 15.10, there is a large solid mass lesion, which is highly concerning for IC. Unless neoadjuvant chemotherapy is being considered, EUS FNA is not required because no matter what the result, this patient would be referred for surgical resection. In contrast, in Fig. 15.4, there is a slight irregularity of the wall, which may represent a small mural nodule. In this case we would consider performing EUS FNA, first, to confirm that we were indeed dealing with an IPMN and, second, if the cytology returned showing marked atypia (the cytologic equivalent of HGD), to consider surgical resection.

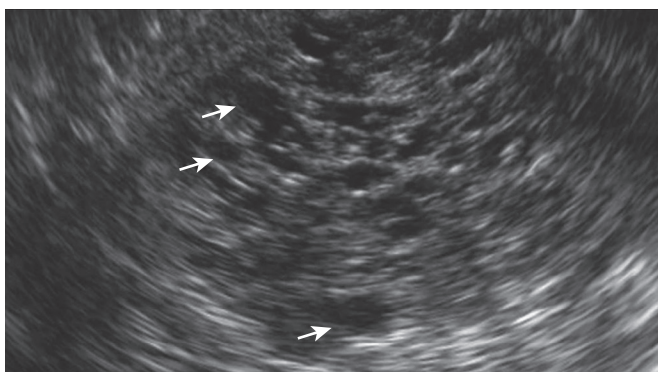


**Fig. 15.8** Serous cystadenoma. Typical appearance of a 2.5-cm microcystic serous cystadenoma. It has multiple small (arrows) anechoic cystic areas and a “honeycomb” appearance. This lesion does not show the central area of fibrosis or calcification that is sometimes present.

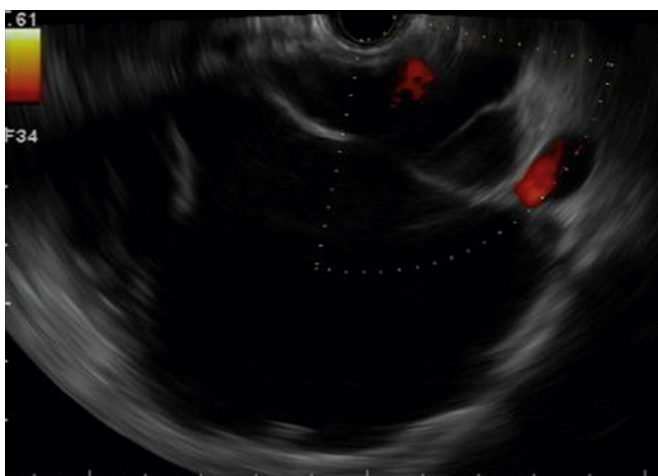


**Fig. 15.9** Macrocytic (oligocystic) serous cystadenoma. There is a 9-cm anechoic well-circumscribed cyst in the tail of the pancreas with thin septations. It was associated with low carcinoembryonic antigen and amylase levels; however, the patient was symptomatic and the cyst was therefore removed. Surgical pathology confirmed a serous cystadenoma. (Copyright AM Lennon.)

When we perform EUS FNA, we currently send cyst fluid for CEA analysis, as a very high or low CEA, respectively, is helpful for identifying or excluding a mucin-producing cyst. In cases where a pseudocyst is in the differential diagnosis, we include cyst fluid amylase, as a level of less than 250 U/mL virtually excludes a pseudocyst. If the cyst is clearly not a pseudocyst, we do not send for an amylase level. Although there is a low yield from cytology, we do send for this if we are concerned about the presence of HGD or IC, as it is easy to do and requires very little sample.

It is likely that this format will change in the next 2 to 3 years. There are increasing data supporting the use of molecular markers, in particular KRAS and GNAS. We currently send for molecular markers in cases in where the diagnosis is unclear based on CEA and cytology. One very important factor to consider when sending molecular markers, is what technique is being used at the center to where the sample is being sent. Some centers use Sanger sequencing, which can detect a mutation only if it is present in less than 20% of alleles, which could result in a false-negative result. The most sensitive test currently available is SafeSeqSequencing, which can detect a mutant allele present in 0.01%,<sup>41</sup> followed by next-generation sequencing, which can detect a mutation if it is present in 4% or more of alleles.<sup>42</sup> GNAS mutations have been shown to

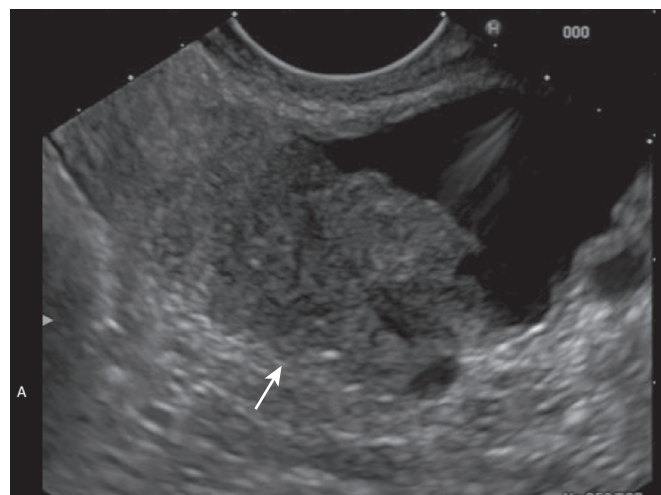


**Fig. 15.10** Branch duct intraductal papillary mucinous neoplasia (IPMN) with a solid component. IPMNs have malignant potential. This patient had a cyst that communicated with the main pancreatic duct, which was associated with a high level of carcinoembryonic antigen in the cyst fluid, consistent with a branch duct IPMN. As we scan through the cyst, the wall becomes thickened with an irregular edge (arrow). These features are consistent with a type IV mural nodule and are worrisome for malignant transformation of a branch duct IPMN. (Copyright AM Lennon.)

be present at levels as low as 0.8%,<sup>43</sup> highlighting the importance of evaluating molecular markers with a highly sensitive technique.

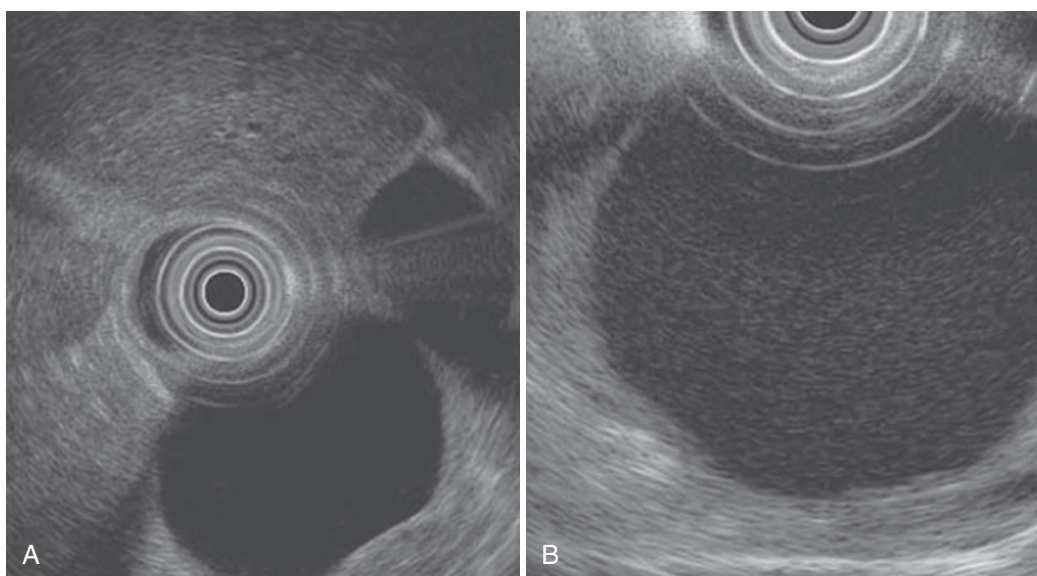
There are very few case reports examining the role of through-the-needle biopsy forceps. If large prospective multicenter studies show that this technique can obtain an adequate pathologic sample to confirm a diagnosis of SCA or to provide additional data on mural nodules that would alter patient outcome, this may increase the use of cytology/pathology. nCLE is also interesting. However, for all three of these technologies, additional well-designed multicenter studies comparing the results with surgical pathology and showing an added benefit over currently available tests are required.

## Type of Pancreatic Cysts

There are many different types of pancreatic cysts. An excellent overview of rare pancreatic cysts—such as benign epithelial cysts, lymphangiomas, hemangiomas, acinar cell cystadenomas/adenocarcinomas, pancreaticoblastomas, and others—can be found in Sakorafas et al.,<sup>44</sup> with the most commonly seen pancreatic cysts.

## Pseudocysts

Pseudocysts are the most common type of pancreatic cyst seen; they almost always occur in the setting of an episode of acute pancreatitis or in patients with chronic pancreatitis. Knowledge of the clinical presentation is therefore essential in aiding accurate differentiation of pseudocysts from cystic neoplasms. Pseudocysts lack a true epithelial lining, as their walls consist of inflammatory and fibrous tissue. These walls are thin in early pseudocysts, but they may become thicker as they mature. Pseudocysts can be any size and are usually unilocular and anechoic (Video 15.4; Fig. 15.11). This appearance may change owing to the presence of necrotic debris or infection, thus mimicking a cystic neoplasm (Figs. 15.12 and 15.13). Septations are rare but do occur, and pseudocysts often demonstrate direct communication with the MPD. It is often helpful to look for features of acute or chronic pancreatitis



**• Fig. 15.11** Pseudocysts. (A) Radial endoscopic ultrasound in a patient with a recent episode of pancreatitis reveals a 3-cm, thin-walled, anechoic cystic lesion in close contact with the gastric wall. (B) Similar findings in another patient with chronic abdominal pain who presented with chronic pancreatitis and a pseudocyst.



**• Fig. 15.12** Atypical appearance of a pseudocyst. The patient presented with chronic abdominal pain and weight loss. The endoscopic ultrasound appearance is suspicious for a mucinous neoplasm, but fine-needle aspiration revealed old blood-stained fluid with inflammatory cells, low carcinoembryonic antigen levels, and an amylase concentration greater than 66,000 U/mL. Because of ongoing concerns, the lesion was resected and a pseudocyst was confirmed.



**• Fig. 15.13** Infected pseudocyst in a patient with severe acute pancreatitis and fever. The irregular hyperechoic material seen within the cyst raises suspicion of a cystic neoplasm, but it is not murally based. Fine-needle aspiration cytology revealed only macrophages and debris; the amylase concentration was greater than 6000 U/mL.

elsewhere in the gland, which would support the diagnosis of a pseudocyst. Other features that should be noted are the distance between the intestinal wall and the cyst lumen and the presence of interposed (by Doppler examination) collateral vessels as evidence of segmental portal hypertension secondary to portal or splenic vein thrombosis. These features are important if endoscopic drainage of the pseudocyst is to be performed. Reactive, inflammatory-looking lymph nodes may also be seen adjacent to the pseudocyst.

Because pseudocysts lack an epithelial lining, no epithelial cells should be present in FNA samples unless there is contamination of the needle with gastric or duodenal epithelium during puncture. Aspirated fluid is of low viscosity; it is often dark, turbid, or even bloody (see Fig. 15.7) and contains inflammatory cells such

as macrophages and histiocytes. Raised amylase ( $>5000$  U/mL) concentrations are present, but levels of other tumor markers should be low, although increased CEA levels have been reported when infection is present. A low amylase level, of less than 250 U/mL, virtually excludes a pseudocyst.<sup>39</sup> Pseudocysts are benign and do not require intervention unless they are infected or symptomatic. A detailed discussion of the management of pseudocysts is provided in Chapter 23.

### Serous Cystadenoma

SCAs occur more commonly, although not exclusively, in women. They are usually unifocal, or single cysts, which can occur anywhere

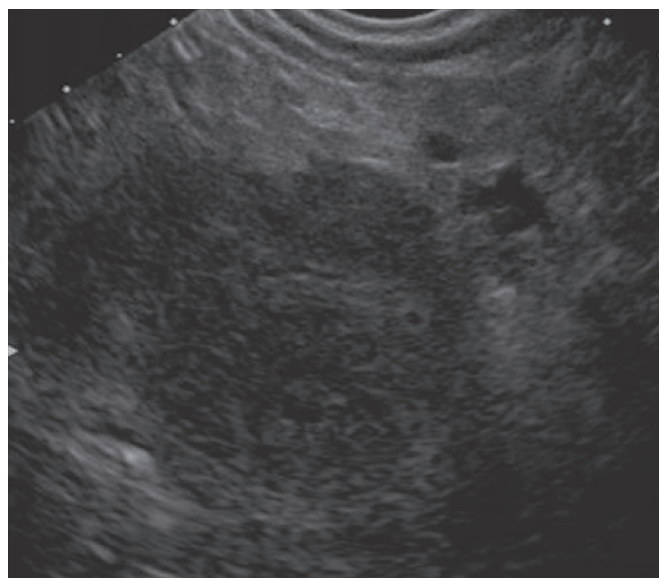
in the pancreas and do not communicate with the MPD.<sup>45–47</sup> They carry an exceptionally small (0.1%) risk of transformation into cystadenocarcinomas.<sup>48</sup> Thus differentiating these very low-risk cysts from other types of neoplastic cysts is extremely important for appropriate clinical management. A microcystic (individual locules measuring <1 cm) appearance is found in 45% to 58% of SCAs (see Fig. 15.8; Video 15.5); 32% to 35% have a macrocystic (individual locules measuring >1 cm; see Fig. 15.9) and 18% to 28% a mixed macrocystic or microcystic appearance.<sup>47</sup> Finally, 5% to 6% present as solid lesions due to the coalescence of multiple tiny (1- to 2-mm) cysts (Fig. 15.14).<sup>46</sup> Macrocytic SCAs can be difficult to differentiate from MCNs and branch duct IPMNs (BD-IPMN), whereas solid SCAs can occasionally be mistaken for PanNETs. Central fibrosis or calcification is a classic appearance in SCA, but it occurs in fewer than 20% of cases. The appearance of focal nodularity or thickening of the cyst wall, intracystic mucin, or floating debris is unusual and suggests that the lesion may be a mucin-producing tumor. SCAs can occasionally cause dilatation of the pancreatic duct or appear to communicate with the MPD, although these appearances are rare.<sup>46,48</sup>

The morphologic characteristics of SCAs are often diagnostic (see Video 15.5). Nevertheless, cytologic examination may improve the diagnostic accuracy of EUS, particularly in the absence of the classic microcystic appearance. The cytologic appearance is of serous fluid containing small cuboidal cells that stain for glycogen but not mucin. The fluid classically is clear (Video 15.6) and has a very low CEA concentration, with a level less than 5 ng/mL virtually excluding a mucin-producing cyst and lending support to the diagnosis of SCA.<sup>39</sup> However obtaining adequate amounts of cyst fluid for CEA analysis can be difficult due to the small size of the cysts. Amylase levels are variable and can be high.

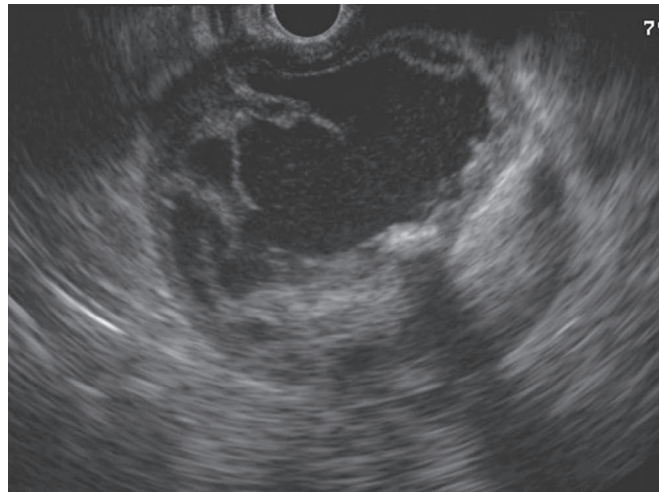
SCAs have a tiny risk of malignant transformation, with the largest series in over 2500 patients found a risk of serous cystadenocarcinoma of 0.1%.<sup>47</sup> Given their benign nature, SCAs should be resected only if they are clearly causing symptoms or where the diagnosis is unclear and imaging is concerning for the presence of HGD or IC. Given the very low risk of malignant transformation, some groups have suggested that cases in which the diagnosis is certain do not require further follow-up, while others have recommended surveillance. It is important to have a detailed discussion with patients about the pros and cons of both approaches. Given the lack of evidence, both approaches appear reasonable.

## Mucinous Cystic Neoplasm

MCNs are single cysts, which occur most often in young or middle-aged women and are found in the body or tail of the pancreas in over 90% of cases. They are extremely rare in men, who account for only 2% of cases.<sup>49,50</sup> They are differentiated from IPMNs by the presence of ovarian stroma that contains both estrogen and progesterone receptors. On EUS they appear as macrocystic lesions (Video 15.7; Fig. 15.15). Peripheral calcification, which is found in 15% of patients, is highly suggestive of MCN but may also be seen in SPN. MCNs classically do not communicate with the MPD, a feature used to differentiate them from BD-IPMN. However, a multicenter study found that 18% of patients with MCN who had undergone endoscopic retrograde cholangiopancreatography (ERCP) were found to have a communication with the MPD.<sup>49</sup> MCNs are almost always single cysts. The presence of other cystic lesions elsewhere in the pancreas or a dilated pancreatic duct is unusual; if present, a diagnosis of IPMN should be considered. The presence of an irregular or thickened cyst wall; a



• **Fig. 15.14** Solid-appearing serous cystadenoma seen as a 4-cm hypoechoic lesion in the body of the pancreas. Endoscopic ultrasound-guided fine-needle aspiration was performed. No cyst fluid was obtained and cytology was nondiagnostic. The lesion was confirmed as a serous cystadenoma at surgery. (Copyright AM Lennon.)



• **Fig. 15.15** Mucinous cystadenoma. This 5-cm anechoic lesion was well circumscribed and contained a slightly thickened (4-mm) septation. Endoscopic ultrasound-guided fine-needle aspiration was performed, confirming a high level of carcinoembryonic fluid within the cyst. Cytology revealed mucin. A mucinous cystadenoma was confirmed on surgical pathology.

solid region within the cyst; an adjacent solid mass (see Figs. 15.15 and 15.16); or a strictured, obstructed, or displaced pancreatic duct suggests malignant transformation (Video 15.8). FNA can be useful in confirming the diagnosis. The fluid is usually clear (see Fig. 15.7D). Cytology demonstrates viscous fluid containing mucin and columnar epithelial cells. The presence of columnar cells is not pathognomonic because these cells are also found in IPMNs. The presence of columnar epithelial cells from the stomach or duodenum can further complicate the cytologic interpretation; hence care should be taken to avoid contamination of the cyst fluid by using a stylet during initial puncture. As discussed earlier, cyst fluid amylase levels vary and are not useful for differentiating MCNs from IPMNs.<sup>38</sup>



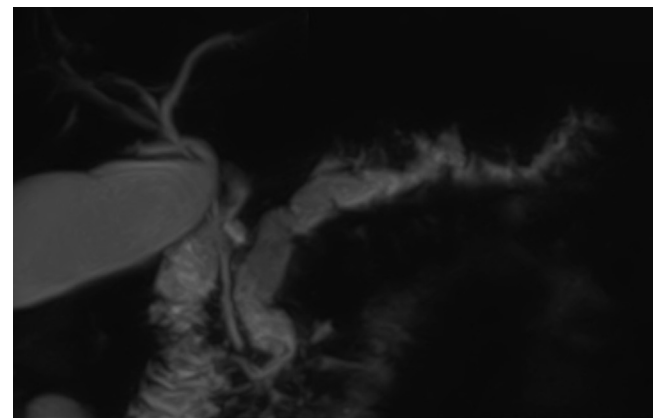
• **Fig. 15.16** Mucinous cystadenoma. The cyst wall is irregular and markedly thickened. (Copyright AM Lennon.)

Unlike SCAs, MCNs have a risk of malignant transformation. There are no long-term studies examining the natural history of MCNs; thus the estimate of the risk of malignant transformation into pancreatic adenocarcinoma is based on retrospective surgical series. A wide range of HGD or IC is reported in the literature, varying between 0% and 34%.<sup>51</sup> Many of the higher estimates come from older studies, with recent series reporting a risk of IC of between 4% and 13%.<sup>49,52</sup>

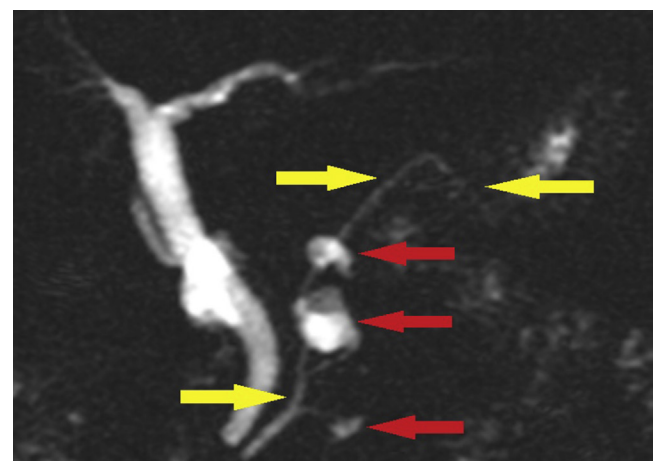
There is debate about whether MCNs can be watched or should all undergo surgical resection.<sup>53–56</sup> There is agreement that MCNs that are clearly causing symptoms, such as acute pancreatitis, have imaging features concerning for malignant transformation—such as a solid component or cytology showing marked atypia or IC—should undergo surgical resection. However authors, guidelines, and surgeons differ as to the management of presumed MCNs that measure less than 3 cm and have no concerning features. Some authors argue that all MCNs should be resected.<sup>53</sup> This is based on the fact that (1) they occur in young women, who would otherwise require 30 to 40 years of surveillance, (2) they are single cysts, which, in contrast to IPMNs, do not recur, and (3) they are located in the body or tail of the pancreas, which is technically easier to surgically resect than to perform a Whipple procedure. However others argue that it is not always possible to differentiate MCNs from IPMNs preoperatively, that more recent data suggest that the risk of malignant transformation of MCNs is less than that of BD-IPMNs and that although these lesions are associated with a low mortality, a distal pancreatectomy has a morbidity of about 25%, including a 15% to 20% risk of diabetes.<sup>54,55</sup> In caring for a patient with a presumed MCN, it is important discuss these two differing views and the pros and cons of each approach as well as to ensure that the patient is reviewed by a multidisciplinary pancreatic cyst group.<sup>5</sup> Once a patient undergoes surgical resection for an MCN in the absence of IC, no further follow up is required.

## Intraductal Papillary Mucinous Neoplasia

IPMNs now account for almost 50% of surgically resected pancreatic cysts.<sup>4</sup> Unlike MCNs and SCAs, IPMNs are equally common in men and women. They can occur at any age but most frequently present in the sixth decade. IPMNs can occur throughout the pancreas but have a slight preponderance in the head of the pancreas. In up to 40% of cases, multiple cysts occur.<sup>57</sup>



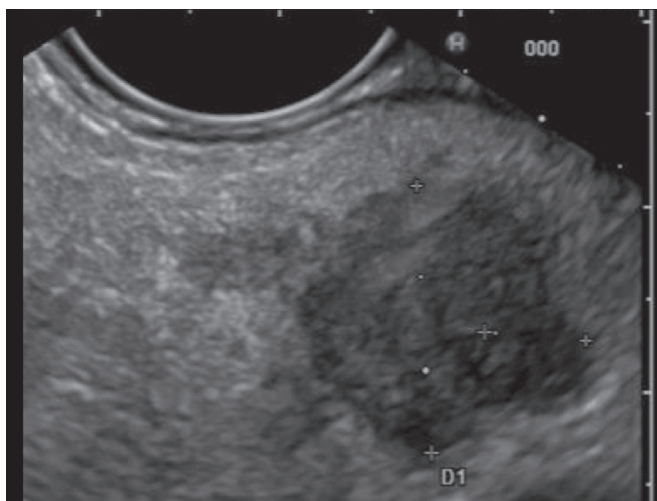
• **Fig. 15.17** Main duct intraductal papillary mucinous neoplasia (MD-IPMN). On magnetic resonance cholangiopancreatography there was pronounced dilation of the main pancreatic duct in the head and body of the pancreas, measuring up to 13 mm in the head. The main pancreatic duct in the tail is of normal size. The patient underwent a Whipple resection, which revealed a MD-IPMN with high-grade dysplasia. (Copyright AM Lennon.)



• **Fig. 15.18** Branch duct intraductal papillary mucinous neoplasia (BD-IPMN). This is a magnetic resonance cholangiopancreatography image of a patient with multifocal BD-IPMN. Multiple small cysts that communicate with the main pancreatic duct are depicted by the red arrows. The main pancreatic duct (yellow arrows) is not dilated. (Copyright AM Lennon.)

IPMNs are classified as involving the MPD (MD-IPMN; **Fig. 15.17**), the BD-IPMN (**Fig. 15.18**), or both, in which case it is termed a mixed type of IPMN. Involvement of the MPD is defined as a focal or diffuse dilation of the MPD measuring more than 5 mm.<sup>53</sup> This differentiation is very important as it determines the risk of malignant transformation and the management of these patients.

Endoscopic appearances include the presence of focal or diffuse dilation of the MPD and/or the presence of dilated side branches. Communication between side and main duct branches is a characteristic feature of BD-IPMN or mixed-IPMN (**Video 15.9**), although this is not always seen because it can be obstructed by mucin. Filling defects can be seen in the MPD as well as in cysts and can result from either a mural nodule (see **Fig. 15.3**) or mucous plugs (see **Fig. 15.4**; **Video 15.1**). Differentiating these lesions can be difficult and is discussed in detail in the earlier section on EUS imaging. IPMNs have malignant potential and can be associated with a solid mass arising from the pancreatic cyst



• **Fig. 15.19** Adenocarcinoma arising apart from an intraductal papillary mucinous neoplasm (IPMN). This patient had undergone resection of a high-grade IPMN in the head of the pancreas 4 years previously. All the margins were clear. There is an irregular hypoechoic area separate from the cyst. Endoscopic ultrasound-guided fine-needle aspiration of this area was performed, confirming adenocarcinoma. (Copyright AM Lennon.)

that appears as a hypoechoic irregular mass (see Fig. 15.10; Video 15.10). In addition, there is increasing evidence that patients with IPMNs are at increased risk of developing an IC, known as a concomitant pancreatic ductal adenocarcinoma, in an area entirely separate from the cyst (Fig. 15.19).<sup>14,57-62</sup> It is therefore very important to inspect not only the cyst but also the entire pancreatic parenchyma. The ampulla of Vater should be inspected, as a gaping “fish mouth” papilla extruding mucus is occasionally seen. The presence of features such as a focal hypoechoic mass or mural nodules (see Figs. 15.3 and 15.10) is suggestive of malignancy. When there is concern for MD-IPMN, it is important to exclude other causes of main duct dilation such as chronic pancreatitis, a small pancreatic adenocarcinoma, or an ampullary mass. It is important to visualize the ampulla endoscopically to exclude an ampullary lesion. The MPD should be traced to the ampulla to ensure that there is no small obstructing lesion, and features of chronic pancreatitis should be sought. In cases where the diagnosis remains unclear, EUS FNA of the MPD can be performed and samples sent for CEA, cytology looking for mucin, and molecular markers if required. If the diagnosis is still uncertain and it could alter management (i.e., a decision to operate or not), ERCP with pancreatectomy can be considered. This is rarely required.

EUS FNA allows samples to be obtained for cyst fluid CEA, amylase, and cytology. The fluid is usually clear (see Fig. 15.7D). IPMNs, like MCNs, are mucin-producing cysts and are associated with an elevated CEA in cyst fluid. Cyst fluid amylase should be sent for if there is a question as to whether the cyst is an IPMN or a pseudocyst. With this exception, cyst fluid amylase levels are not routinely performed as they are not helpful in differentiating an MCN from an IPMN. Cytology should be performed, however, as the presence of markedly atypical cytology is one of the criteria for considering surgical resection.<sup>53</sup> The presence of mucin is helpful in confirming the diagnosis of either MCN or IPMN.

Four epithelial subtypes have been identified based on the cell morphology and expression patterns of glycoproteins containing

**TABLE 15.3** Comparison of Pancreatic Cyst Guidelines

	2012 Fukuoka Guidelines	2013 European Guidelines	2015 AGA Guidelines
<b>Process</b>	Multidisciplinary experts	Multidisciplinary experts	AGA committee
<b>Cyst type</b>	Mucin-producing cysts (IPMNs, MCNs)	Neoplastic cysts (IPMNs, MCNs, SPNs, SCNs)	Asymptomatic neoplastic cysts
<b>Target</b>	High-grade dysplasia or PDAC	High-grade dysplasia or PDAC	PDAC
<b>Methods</b>	Scientific review	Scientific review, grading	Technical review, GRADE
<b>Key decisions</b>	Surgery EUS FNA	Surgery No routine EUS FNA	Surgery EUS FNA
	Surveillance schedule	Surveillance schedule	Surveillance schedule Stopping surveillance

AGA, American Gastroenterological Society; EUS FNA, endoscopic ultrasound-guided fine-needle aspiration; IPMNs, intraductal papillary mucinous neoplasias; MCNs, mucinous cystic neoplasms; PDAC, pancreatic ductal adenocarcinoma; SCN, serous cyst neoplasm; SPNs, solid pseudopapillary neoplasms.

mucin (MUC)—gastric, intestinal, pancreaticobiliary, and oncocytic. The epithelial subtype has been correlated with the degree of dysplasia, with gastric-type cysts being more likely at low risk for dysplasia (accounting for 91% of all low-risk cysts), whereas pancreaticobiliary and intestinal types were more likely to be at high risk for dysplasia (accounting for 79% of all high-risk cysts).<sup>63,64</sup> However, epithelial subtype can currently be determined only on gross resection specimens, although the development of the through-the-needle biopsy forceps may alter this. The potential of these markers was shown in a study by Maker et al., who found higher levels of MUC2 and MUC4 in cysts with HGD or IC.<sup>64</sup> These results are interesting, but there is not yet sufficient evidence for them to be used in routine clinical practice.

The risk of malignant transformation, and hence the management of IPMNs, is determined by whether or not there is involvement of the MPD. MD-IPMNs or mixed IPMNs pose a significantly higher risk than BD-IPMNs, with the majority of surgical series reporting a risk of HGD or IC of between 45% and 60%.<sup>53</sup> In contrast, only 16% to 24% of patients with BD-IPMNs who undergo surgical resection are found to have HG or IC.

There are several different guidelines, including the International Consensus Guidelines (ICGs), the European Guidelines (EGs), and the American Gastroenterological Society (AGA) guidelines (Table 15.3). The EGs and ICGs were developed by a multidisciplinary group of pancreatic cyst experts and are

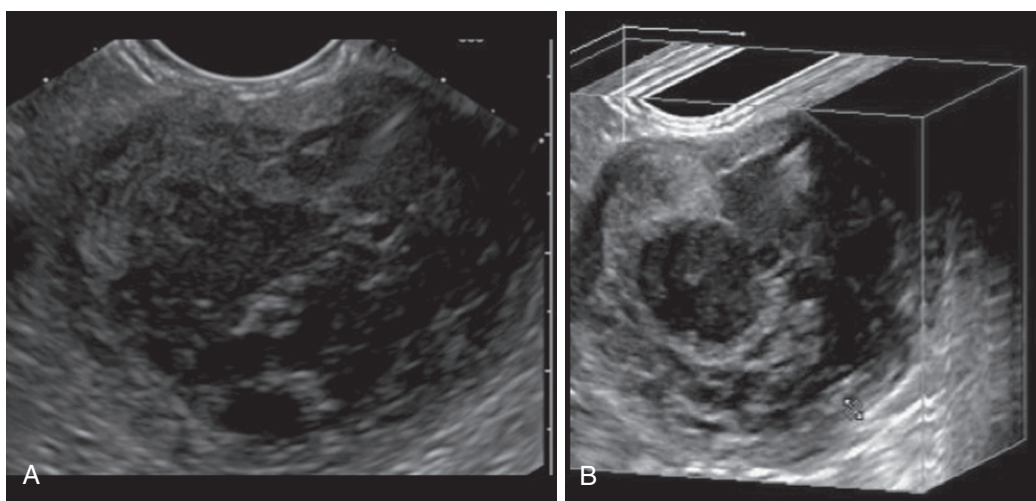


**Fig. 15.20** Solid pseudopapillary neoplasm. (A) This is the classic appearance of a solid pseudopapillary neoplasm. It is well defined, with both cystic and solid areas. (B) This is a three-dimensional image of the cyst; the hemorrhagic center is clearly seen. (Copyright AM Lennon.)

very similar with respect to the management of IPMNs and the indications for consideration of surgical resection. In contrast, the AGA guidelines were developed by the AGA committee using the Grading of Recommendations, Assessment, Development and Evaluations (GRADE) criteria. The aim of the EGs and ICGs is to detect HGD or IC; in contrast, the aim of the AGA guidelines is to identify IC. The AGA guidelines have generated considerable controversy.<sup>65–67</sup> We currently follow the revised ICGs for the management of mucin-producing cysts.<sup>53</sup> These recommend surgery for fit patients with IPMNs associated with jaundice or an enhancing solid component. Patients who have a recent history of pancreatitis, a nonenhancing mural nodule, MPD dilation measuring between 5 and 9 mm, or where there was an abrupt change in the caliber of the MPD should undergo EUS. If there are features suspicious for malignancy on EUS (i.e., mural nodule, marked cytological atypia), surgical resection should be considered. Previous guidelines had recommended surgical resection for all IPMNs greater than 3 cm; however, the most recent guidelines acknowledge the growing body of evidence that size alone is a weak predictor of malignancy. Surgery should be considered in young, fit patients with BD-IPMN with cysts larger than 3 cm; however, surveillance can be considered in older patients with cysts larger than 3 cm without suspicious features. Patients whose cysts have no suspicious features can undergo surveillance alone, with the interval determined by the size of the largest cysts. MRI and EUS are the most commonly used modalities. In our institution we typically use MRI for the surveillance of small cysts, reserving EUS for larger cysts or if we feel the cyst is at higher risk for malignant transformation.

One key difference between IPMNs and other types of pancreatic cysts is that IPMNs can recur in the remnant pancreas following surgery (see Fig. 15.19), with a recent study reporting that 15% of patients develop lesions requiring surgical intervention. Thus all patients who undergo surgical resection of an IPMN, even if no cysts are apparent within the remnant pancreas, require surveillance. The intervals at which they are followed are determined by the pathologic grade of the resected specimen and by the size of cysts within the remnant pancreas.<sup>53</sup>

## Solid Pseudopapillary Neoplasm

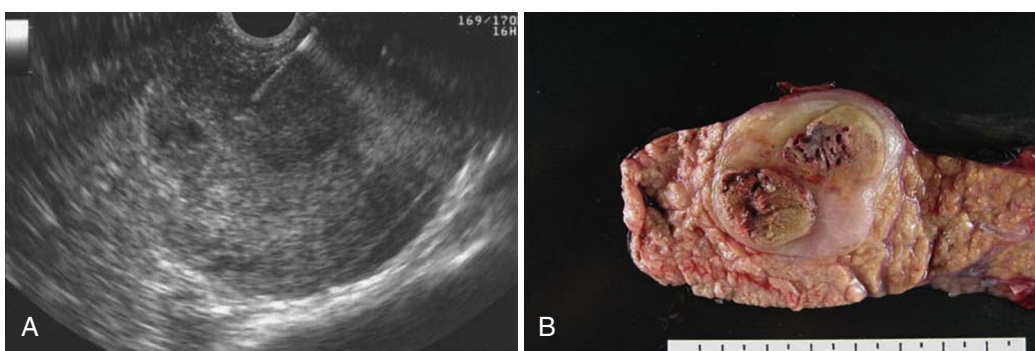
Although the SPN was once thought to be rare, this distinctive lesion is now better recognized and accounts for 5% of resected cystic pancreatic tumors.<sup>4</sup> SPNs usually occur in women, who make up 90% of cases. They can present over a wide age range but are typically found in patients in their mid-20s.<sup>68</sup> Patients often have vague, nonspecific symptoms, with jaundice and pancreatitis being very rare presentations. With the increased use of cross-sectional imaging, SPNs are increasingly being detected incidentally, with almost 40% of patients presenting in this manner.

SPNs are almost always single cysts and can be found in the head, body, or tail of the pancreas. They are usually well circumscribed. The hallmark of this lesion is central hemorrhagic cystic degeneration, creating the classic solid, cystic appearance (see Fig. 15.20; Video 15.11); however, some can have a mainly solid appearance (Fig. 15.21). A small number of case series have evaluated the role of EUS and EUS FNA and have found it helpful if other imaging is nondiagnostic.<sup>69</sup> Lesions are usually well demarcated and may appear solid or mixed solid and cystic with or without septations. Peripheral calcification can occur and can also be seen in patients with MCNs. The hemorrhagic degeneration often results in a bloody, necrotic FNA sample that can provide a clue to the diagnosis, although the histologic features are usually characteristic.

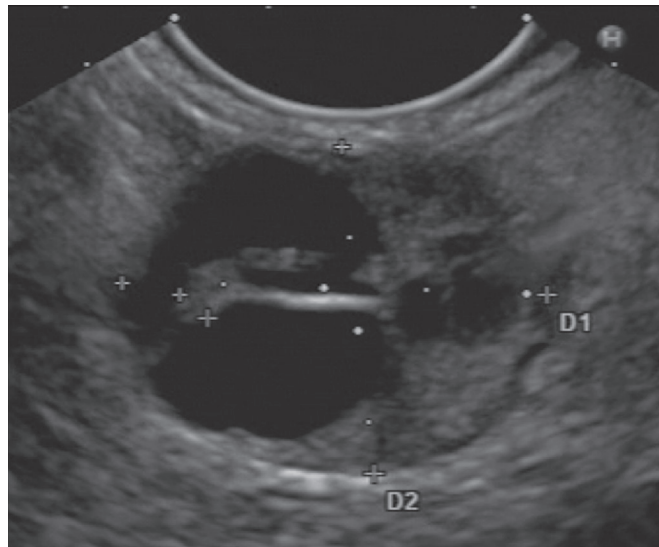
SPNs have clear malignant potential, with either lymph node involvement or distant metastases found in almost 8% of patients.<sup>68</sup> Surgical resection is therefore recommended for all patients with SPNs. Patients who have undergone resection of a SPN should be followed for 5 years, as 5% will develop a recurrence.<sup>68</sup>

## Cystic Neuroendocrine Tumors

Most PanNETs are solid, but a small number can present with cystic degeneration (Figs. 15.22 and 15.23). They can occur anywhere in the pancreas and are usually single unless they are associated with a syndrome such as MEN or VHL syndrome. They



• **Fig. 15.21** Solid pseudopapillary neoplasm. (A) Endoscopic ultrasound image of a pancreatic cyst lesion in the body of the gland revealing both solid and cystic components. Fine-needle aspiration proved this to be a solid cystic pseudopapillary neoplasm. (B) The corresponding surgical specimen from distal pancreatectomy.

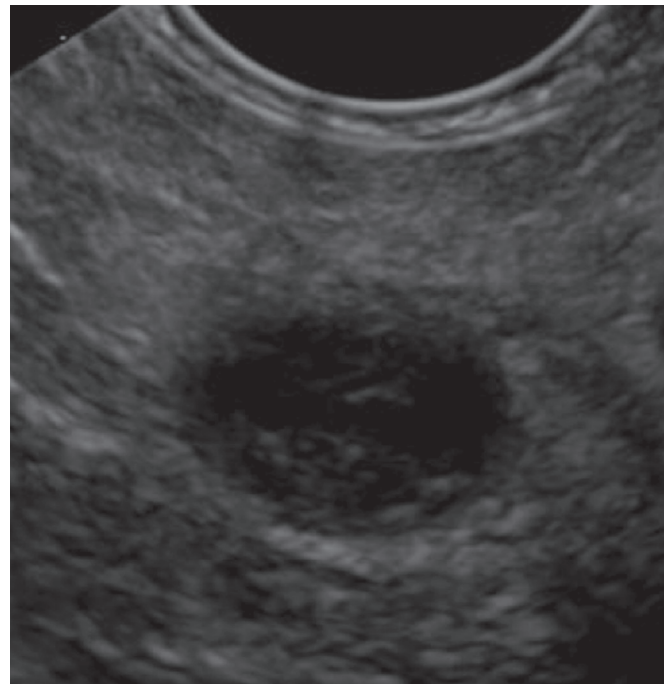


• **Fig. 15.22** Pancreatic neuroendocrine tumor. This cyst has a thin separation; however, the wall is markedly thickened between the one and six o'clock positions. The solid component was targeted with endoscopic ultrasound-guided fine-needle aspiration and the diagnosis confirmed a pancreatic neuroendocrine tumor. (Copyright AM Lennon.)

are usually well-defined lesions and do not communicate with the MPD. Although they can appear as mainly cystic lesions, the majority usually have a thickened wall or solid component. The remaining parenchyma and pancreatic duct are normal. EUS FNA is helpful in confirming a diagnosis, which can usually be made on cytology. Neither cyst fluid CEA nor amylase is helpful in identifying these cysts.

### Cystic Ductal Adenocarcinoma

Ductal adenocarcinoma of the pancreas may occasionally show cystic degeneration, which can confuse the clinical picture. These cysts differ from the others already described. They are ill-defined, and often have irregular, thickened walls with solid components (Fig. 15.24; Video 15.12). The diagnosis can be confirmed with EUS FNA, which should target the solid component. The evaluation and management of pancreatic ductal adenocarcinoma is discussed in depth in Chapter 14.



• **Fig. 15.23** Pancreatic neuroendocrine tumor. This is a mainly cystic lesion; a small, irregular, solid component can be seen in the six o'clock position. (Copyright AM Lennon.)

## Future Developments

### Analysis of Molecular Markers in Pancreatic Juice

EUS, CEA, and cytology are not without limitations in the evaluation of pancreatic cysts (Table 15.4). One interesting development in this area is the analysis of pancreatic juice, which is collected by aspirating it from under the major papilla following secretin stimulation. As discussed previously, *GNAS* mutations appear to be unique to IPMNs and have been detected in both pancreatic tissue and pancreatic cyst fluid. In a further development of this, Kanda et al.<sup>70</sup> were able to identify *GNAS* mutations in pancreatic juice from patients with IPMNs. Similar to the prior studies, no *GNAS* mutation was found in patients with other types of cysts. The use of pancreatic juice could potentially be particularly helpful

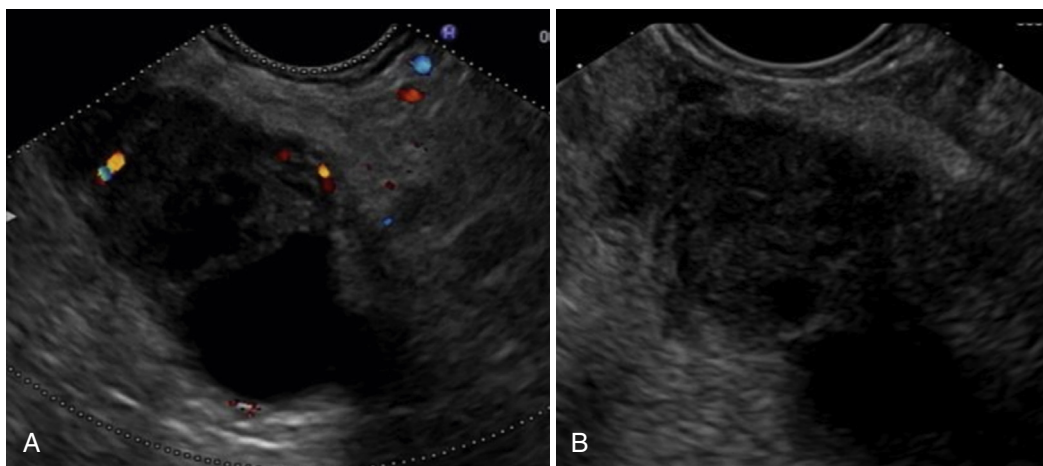


**Fig. 15.24** Cystic pancreatic ductal adenocarcinoma. (A) There is a cyst with a possible solid component between the 9 and 12 o'clock positions. (B) On further scanning, an irregular hypoechoic mass with an irregular edge becomes clear. Fine-needle aspiration (FNA) of the cyst fluid showed a low level of carcinoembryonic antigen and no mucin on cytology. FNA of the solid component confirmed an adenocarcinoma. (Copyright AM Lennon.)

**TABLE 15.4** Important Limitations of Endoscopic Ultrasound in the Evaluation of Pancreatic Cystic Lesions

Procedure Aspect	Limitation
Technical	Attenuation of imaging in large (>6 cm) lesions
EUS imaging	Considerable overlap of morphologic features of lesions
FNA	Aspiration of viscous fluid with 22- or 25-gauge needles Small volumes obtained in microcystic lesions that may not be sufficient for CEA/ amylase Limited accuracy of cytology: contamination with columnar gastroduodenal epithelium; sampling error: dysplasia and malignant change may be patchy in mucinous lesions
Amylase level	Levels may be variable in lesions that communicate with the main pancreatic duct
CEA level	May be raised in infected pseudocysts and lymphoepithelial cysts; very high or undetectable levels are helpful but levels in between are not
Other tumor markers (e.g., CA19-9, CA72-4)	Unproven value; investigational role
DNA analysis (KRAS, GNAS, VHL)	Emerging technology, negates the need to obtain large volumes of fluid as analysis can be run on 0.2 mL; markers appear to be promising in differentiating benign from premalignant cysts

CEA, Carcinoembryonic antigen; EUS, Endoscopic ultrasound; FNA, fine-needle aspiration; VHL, von Hippel–Lindau.

in patients with very small pancreatic cysts where it is impossible to obtain sufficient pancreatic cyst fluid for analysis. Although *GNAS* and *KRAS* mutations are useful for differentiating the type of pancreatic cyst present, both occur in cystic neoplasms with low- and intermediate-grade dysplasia and thus cannot be used as markers of the degree of dysplasia in a lesion. In contrast, *TP53* mutations are found in IPMNs and MCNs with HGD or IC. The same group identified *TP53* mutations in pancreatic juice in patients with IPMNs and either HGD or IC, with only a tiny number of patients with intermediate-grade dysplasia and none with low-grade dysplasia were found to have any mutations.<sup>22</sup> Although exciting, these results now need to be validated in large prospective trials prior to being incorporated into clinical practice.

### Cyst Ablation

Pancreatic surgery is associated with significant morbidity and, in the case of pancreaticoduodenectomy, a mortality rate of 1% to 2% in high-volume centers.<sup>4</sup> This has stimulated research into alternative methods of treating cysts. Several studies have examined whether EUS-guided alcohol or alcohol and paclitaxel injection into pancreatic cystic tumors can be used to ablate the epithelium and thus obviate the need for surgery.<sup>71–76</sup> The results have been varied, with cyst resolution reported in 33% to 79% of the cases.<sup>35–40</sup> One of the questions with this type of therapy is how effective it is in ablating all the epithelial lining rather than just decreasing the size of the cyst. In patients who have undergone surgical resection after cyst ablation, the reported success rates range from 0% to 100%. Pilot data from the CHARM study reported no difference in the successful ablation of pancreatic cysts in patients treated with paclitaxel and gemcitabine combined with alcohol versus paclitaxel and gemcitabine alone, suggesting that the ablation of cysts with paclitaxel and gemcitabine alone may be sufficient.<sup>77</sup> Radiofrequency ablation (RFA) is an alternative to alcohol or paclitaxel. A multicenter study in patients with both PanNET and pancreatic cysts found that cyst size decreased in 75% of patients, with complete resolution on imaging in 25%.<sup>41</sup> These are interesting results that now require larger clinical trials in patients who

undergo surgical resection so as to determine the exact amount of epithelial ablation of the cyst and also to determine the side-effect profile of the intervention.

### EXAMINATION CHECKLIST

Localize and describe cyst

- Site and size
- Wall thickness
- Distance from lumen, interposed vessels
- Focal irregularity, papillary projections, or mural nodules and the size of these lesion(s)
- Associated mass lesion
- Central or peripheral calcification
- Presence and size of septation(s)
- Debris or echogenic material in cyst
- Communication and diameter of the pancreatic duct

Examine the remaining pancreatic parenchyma looking in particular for a mass lesion not associated with the cyst.

Perform EUS-guided fine-needle aspiration (FNA) of all solid lesions.

Perform EUS-guided FNA of cyst fluid under antibiotic cover.

Evacuate cyst contents if possible.

Send cyst fluid for carcinoembryonic antigen level and cytologic evaluation.

### Key References

4. Valsangkar NP, Morales-Oyarvide V, Thayer SP, et al. 851 resected cystic tumors of the pancreas: a 33-year experience at the Massachusetts General Hospital. *Surgery*. 2012;152:S4–S12.
12. Wang KX, Ben QW, Jin ZD, et al. Assessment of morbidity and mortality associated with EUS-guided FNA: a systematic review. *Gastrointest Endosc*. 2011;73:283–290.
19. Brugge WR, Lewandrowski K, Lee-Lewandrowski E, et al. Diagnosis of pancreatic cystic neoplasms: a report of the cooperative pancreatic cyst study. *Gastroenterology*. 2004;126:1330–1336.
41. Springer S, Wang Y, Dal Molin M, et al. A combination of molecular markers and clinical features improve the classification of pancreatic cysts. *Gastroenterology*. 2015;149:1501–1510.
53. Tanaka M, Fernandez-Del Castillo C, Adsay V, et al. International consensus guidelines 2012 for the management of IPMN and MCN of the pancreas. *Pancreatology*. 2012;12:183–197.

### References

Access the reference list online at [ExpertConsult.com](http://ExpertConsult.com).

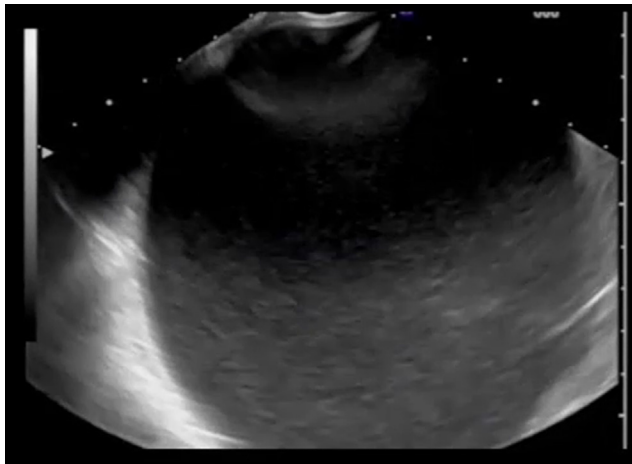
## References

1. Laffan TA, Horton KM, Klein AP, et al. Prevalence of unsuspected pancreatic cysts on MDCT. *AJR Am J Roentgenol.* 2008;191:802–807.
2. Lee KS, Sekhar A, Rofsky NM, et al. Prevalence of incidental pancreatic cysts in the adult population on MR imaging. *Am J Gastroenterol.* 2010;105:2079–2084.
3. Jones MJ, Buchanan AS, Neal CP, et al. Imaging of indeterminate pancreatic cystic lesions: a systematic review. *Pancreatology.* 2013;13:436–442.
4. Valsangkar NP, Morales-Oyarvide V, Thayer SP, et al. 851 resected cystic tumors of the pancreas: a 33-year experience at the Massachusetts General Hospital. *Surgery.* 2012;152:S4–S12.
5. Lennon AM, Manos LL, Hruban RH, et al. Role of a multidisciplinary clinic in the management of patients with pancreatic cysts: a single-center cohort study. *Ann Surg Oncol.* 2014;21:3668–3674.
6. Shin EJ, Canto MI. Pancreatic cancer screening. *Gastroenterol Clin North Am.* 2012;41:143–157.
7. Anand N, Sampath K, Wu BU. Cyst features and risk of malignancy in intraductal papillary mucinous neoplasms of the pancreas: a meta-analysis. *Clin Gastroenterol Hepatol.* 2013;11:913–921. quiz e59–e60.
8. Thomas T, Bebb J, Mannath J, et al. EUS-guided pancreatic cyst brushing: a comparative study in a tertiary referral centre. *JOP.* 2010;11:163–169.
9. Ohno E, Hirooka Y, Itoh A, et al. Intraductal papillary mucinous neoplasms of the pancreas: differentiation of malignant and benign tumors by endoscopic ultrasound findings of mural nodules. *Ann Surg.* 2009;249:628–634.
10. Deleted in review.
11. Kurihara N, Kawamoto H, Kobayashi Y, et al. Vascular patterns in nodules of intraductal papillary mucinous neoplasms depicted under contrast-enhanced ultrasonography are helpful for evaluating malignant potential. *Eur J Radiol.* 2012;81:66–70.
12. Wang KX, Ben QW, Jin ZD, et al. Assessment of morbidity and mortality associated with EUS-guided FNA: a systematic review. *Gastrointest Endosc.* 2011;73:283–290.
13. Matsumoto K, Katanuma A, Maguchi H, et al. Performance of novel tissue harmonic echo imaging using endoscopic ultrasound for pancreatic diseases. *Endosc Int Open.* 2016;4:E42–50.
14. Law JK, Wolfgang CL, Weiss MJ, et al. Concomitant pancreatic adenocarcinoma in a patient with branch-duct intraductal papillary mucinous neoplasm. *World J Gastroenterol.* 2014;20:9200–9204.
15. Neumann H, Kiesslich R, Wallace MB, et al. Confocal laser endomicroscopy: technical advances and clinical applications. *Gastroenterology.* 2010;139:388–392, 392 e1–2.
16. Konda VJ, Meining A, Jamil LH, et al. A pilot study of in vivo identification of pancreatic cystic neoplasms with needle-based confocal laser endomicroscopy under endosonographic guidance. *Endoscopy.* 2013;45:1006–1013.
17. Napoleon B, Lemaistre AI, Pujol B, et al. A novel approach to the diagnosis of pancreatic serous cystadenoma: needle-based confocal laser endomicroscopy. *Endoscopy.* 2015;47:26–32.
18. Nakai Y, Iwashita T, Park DH, et al. Diagnosis of pancreatic cysts: EUS-guided, through-the-needle confocal laser-induced endomicroscopy and cystoscopy trial: DETECT study. *Gastrointest Endosc.* 2015;81:1204–1214.
19. Brugge WR, Lewandrowski K, Lee-Lewandrowski E, et al. Diagnosis of pancreatic cystic neoplasms: a report of the cooperative pancreatic cyst study. *Gastroenterology.* 2004;126:1330–1336.
20. de Jong K, van Hooft JE, Nio CY, et al. Accuracy of preoperative workup in a prospective series of surgically resected cystic pancreatic lesions. *Scand J Gastroenterol.* 2012;47:1056–1063.
21. Sedlack R, Affi A, Vazquez-Sequeiros E, et al. Utility of EUS in the evaluation of cystic pancreatic lesions. *Gastrointest Endosc.* 2002;56:543–547.
22. Hong SK, Loren DE, Rogart JN, et al. Targeted cyst wall puncture and aspiration during EUS-FNA increases the diagnostic yield of premalignant and malignant pancreatic cysts. *Gastrointest Endosc.* 2012;75:775–782.
23. Sendino O, Fernandez-Esparrach G, Sole M, et al. Endoscopic ultrasonography-guided brushing increases cellular diagnosis of pancreatic cysts: a prospective study. *Dig Liver Dis.* 2010;42:877–881.
24. Al-Haddad M, Gill KR, Raimondo M, et al. Safety and efficacy of cytology brushings versus standard fine-needle aspiration in evaluating cystic pancreatic lesions: a controlled study. *Endoscopy.* 2010;42:127–132.
25. ASGE Standards Of Practice C, Banerjee S, Shen B, et al. Antibiotic prophylaxis for GI endoscopy. *Gastrointest Endosc.* 2008;67:791–798.
26. Yoon WJ, Daglilar ES, Fernandez-del Castillo C, et al. Peritoneal seeding in intraductal papillary mucinous neoplasm of the pancreas patients who underwent endoscopic ultrasound-guided fine-needle aspiration: the PIPE Study. *Endoscopy.* 2014;46:382–387.
27. Bick BL, Enders FT, Levy MJ, et al. The string sign for diagnosis of mucinous pancreatic cysts. *Endoscopy.* 2015;47:626–631.
28. Brandwein SL, Farrell JJ, Centeno BA, et al. Detection and tumor staging of malignancy in cystic, intraductal, and solid tumors of the pancreas by EUS. *Gastrointest Endosc.* 2001;53:722–727.
29. Hernandez LV, Mishra G, Forsmark C, et al. Role of endoscopic ultrasound (EUS) and EUS-guided fine needle aspiration in the diagnosis and treatment of cystic lesions of the pancreas. *Pancreas.* 2002;25:222–228.
30. Frossard JL, Amouyal P, Amouyal G, et al. Performance of endosonography-guided fine needle aspiration and biopsy in the diagnosis of pancreatic cystic lesions. *Am J Gastroenterol.* 2003;98:1516–1524.
31. Olson MT, Ali SZ. Cytotechnologist on-site evaluation of pancreas fine needle aspiration adequacy: comparison with cytopathologists and correlation with the final interpretation. *Acta Cytol.* 2012;56:340–346.
32. Maire F, Couvelard A, Hammel P, et al. Intraductal papillary mucinous tumors of the pancreas: the preoperative value of cytologic and histopathologic diagnosis. *Gastrointest Endosc.* 2003;58:701–706.
33. Lai R, Stanley MW, Bardales R, et al. Endoscopic ultrasound-guided pancreatic duct aspiration: diagnostic yield and safety. *Endoscopy.* 2002;34:715–720.
34. Thornton GD, McPhail MJ, Nayagam S, et al. Endoscopic ultrasound guided fine needle aspiration for the diagnosis of pancreatic cystic neoplasms: a meta-analysis. *Pancreatology.* 2013;13:48–57.
35. Cizginer S, Turner BG, Bilge AR, et al. Cyst fluid carcinoembryonic antigen is an accurate diagnostic marker of pancreatic mucinous cysts. *Pancreas.* 2011;40:1024–1028.
36. Hammel P, Voitot H, Vilgrain V, et al. Diagnostic value of CA 72-4 and carcinoembryonic antigen determination in the fluid of pancreatic cystic lesions. *Eur J Gastroenterol Hepatol.* 1998;10:345–348.
37. Park WG, Mascarenhas R, Palaez-Luna M, et al. Diagnostic performance of cyst fluid carcinoembryonic antigen and amylase in histologically confirmed pancreatic cysts. *Pancreas.* 2011;40:42–45.
38. Al-Rashdan A, Schmidt CM, Al-Haddad M, et al. Fluid analysis prior to surgical resection of suspected mucinous pancreatic cysts. A single centre experience. *J Gastrointest Oncol.* 2011;2:208–214.
39. van der Waaij LA, van Dullemen HM, Porte RJ. Cyst fluid analysis in the differential diagnosis of pancreatic cystic lesions: a pooled analysis. *Gastrointest Endosc.* 2005;62:383–389.
40. Wu J, Jiao Y, Dal Molin M, et al. Whole-exome sequencing of neoplastic cysts of the pancreas reveals recurrent mutations in components of ubiquitin-dependent pathways. *Proc Natl Acad Sci U S A.* 2011;108:21188–21193.
41. Springer S, Wang Y, Dal Molin M, et al. A combination of molecular markers and clinical features improve the classification of pancreatic cysts. *Gastroenterology.* 2015;149:1501–1510.

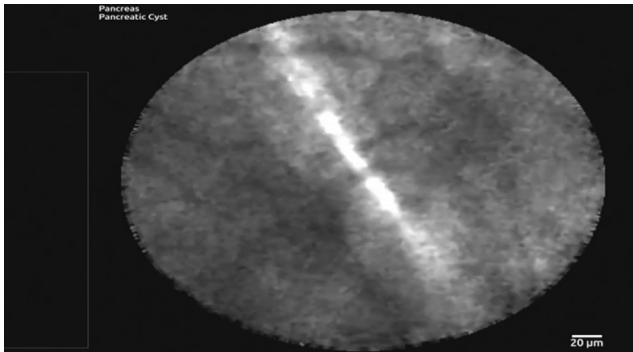
42. Singhi AD, Zeh HJ, Brand RE, et al. American gastroenterological association guidelines are inaccurate in detecting pancreatic cysts with advanced neoplasia: a clinicopathologic study of 225 patients with supporting molecular data. *Gastrointest Endosc.* 2016;83:1107–1117. e2.
43. Wu J, Matthaei H, Maitra A, et al. Recurrent GNAS mutations define an unexpected pathway for pancreatic cyst development. *Sci Transl Med.* 2011;3:92ra66.
44. Sakorafas GH, Smyrniotis V, Reid-Lombardo KM, et al. Primary pancreatic cystic neoplasms of the pancreas revisited. Part IV: rare cystic neoplasms. *Surg Oncol.* 2012;21:153–163.
45. Khashab MA, Shin EJ, Amateau S, et al. Tumor size and location correlate with behavior of pancreatic serous cystic neoplasms. *Am J Gastroenterol.* 2011;106:1521–1526.
46. Kimura W, Moriya T, Hanada K, et al. Multicenter study of serous cystic neoplasm of the Japan pancreas society. *Pancreas.* 2012;41:380–387.
47. Jais B, Rebours V, Malleo G, et al. Pancreatic serous cystadenoma related mortality is nil. Results of a multinational study under the auspices of the International Association of Pancreatology and the European Pancreatic Club. *Gut.* 2015. [Epub ahead of print].
48. Jais B, Rebours V, Malleo G, et al. Serous cystic neoplasm of the pancreas: a multinational study of 2622 patients under the auspices of the International Association of Pancreatology and European Pancreatic Club (European Study Group on Cystic Tumors of the Pancreas). *Gut.* 2016;65:305–312.
49. Yamao K, Yanagisawa A, Takahashi K, et al. Clinicopathological features and prognosis of mucinous cystic neoplasm with ovarian-type stroma: a multi-institutional study of the Japan pancreas society. *Pancreas.* 2011;40:67–71.
50. Reddy RP, Smyrk TC, Zapia M, et al. Pancreatic mucinous cystic neoplasm defined by ovarian stroma: demographics, clinical features, and prevalence of cancer. *Clin Gastroenterol Hepatol.* 2004;2:1026–1031.
51. Nilsson LN, Keane MG, Shamali A, et al. Nature and management of pancreatic mucinous cystic neoplasm (MCN): a systematic review of the literature. *Pancreatology.* 2016;16:1028–1036.
52. Baker ML, Seeley ES, Pai R, et al. Invasive mucinous cystic neoplasms of the pancreas. *Exp Mol Pathol.* 2012;93:345–349.
53. Tanaka M, Fernandez-Del Castillo C, Adsay V, et al. International consensus guidelines 2012 for the management of IPMN and MCN of the pancreas. *Pancreatology.* 2012;12:183–197.
54. Del Chiaro M, Verbeke C, Salvia R, et al. European experts consensus statement on cystic tumours of the pancreas. *Dig Liver Dis.* 2013;45:703–711.
55. Vege SS, Ziring B, Jain R, et al. American gastroenterological association institute guideline on the diagnosis and management of asymptomatic neoplastic pancreatic cysts. *Gastroenterology.* 2015;148:819–822.
56. Khalid A, Brugge W. ACG practice guidelines for the diagnosis and management of neoplastic pancreatic cysts. *Am J Gastroenterol.* 2007;102:2339–2349.
57. Ohtsuka T, Kono H, Tanabe R, et al. Follow-up study after resection of intraductal papillary mucinous neoplasm of the pancreas; special references to the multifocal lesions and development of ductal carcinoma in the remnant pancreas. *Am J Surg.* 2012;204:44–48.
58. Mori Y, Ohtsuka T, Tsutsumi K, et al. Multifocal pancreatic ductal adenocarcinomas concomitant with intraductal papillary mucinous neoplasms of the pancreas detected by intraoperative pancreatic juice cytology. A case report. *JOP.* 2010;11:389–392.
59. Uehara H, Nakaizumi A, Ishikawa O, et al. Development of ductal carcinoma of the pancreas during follow-up of branch duct intraductal papillary mucinous neoplasm of the pancreas. *Gut.* 2008;57:1561–1565.
60. Kanno A, Satoh K, Hirota M, et al. Prediction of invasive carcinoma in branch type intraductal papillary mucinous neoplasms of the pancreas. *J Gastroenterol.* 2010;45:952–959.
61. Singanayagam A, Manalan K, Sridhar S, et al. Evaluation of screening methods for identification of patients with chronic rheumatological disease requiring tuberculosis chemoprophylaxis prior to commencement of TNF-alpha antagonist therapy. *Thorax.* 2013;68:955–961.
62. Ingkakul T, Sadakari Y, Ienaga J, et al. Predictors of the presence of concomitant invasive ductal carcinoma in intraductal papillary mucinous neoplasm of the pancreas. *Ann Surg.* 2010;251:70–75.
63. Furukawa T, Kloppel G, Volkman Adsay N, et al. Classification of types of intraductal papillary-mucinous neoplasm of the pancreas: a consensus study. *Virchows Arch.* 2005;447:794–799.
64. Maker AV, Katai N, Gonem M, et al. Pancreatic cyst fluid and serum mucin levels predict dysplasia in intraductal papillary mucinous neoplasms of the pancreas. *Ann Surg Oncol.* 2011;18:199–206.
65. Lennon AM, Ahuja N, Wolfgang CL. AGA guidelines for the management of pancreatic cysts. *Gastroenterology.* 2015;149:825.
66. Canto MI, Hruban RH. Managing pancreatic cysts: less is more? *Gastroenterology.* 2015;148:688–691.
67. Fernandez-Del Castillo C, Tanaka M. Management of pancreatic cysts: the evidence is not here yet. *Gastroenterology.* 2015;148:685–687.
68. Law JK, Ahmed A, Singh VK, et al. A systematic review of solid-pseudopapillary neoplasms: are these rare lesions? *Pancreas.* 2014;43:331–337.
69. Law JK, Stoita A, Wever W, et al. Endoscopic ultrasound-guided fine needle aspiration improves the pre-operative diagnostic yield of solid-pseudopapillary neoplasm of the pancreas: an international multicenter case series (with video). *Surg Endosc.* 2014;28:2592–2598.
70. Kanda M, Knight S, Topazian MD, et al. Mutant GNAS detected in duodenal collections of secretin-stimulated pancreatic juice indicates the presence or emergence of pancreatic cysts. *Gut.* 2013;62:1024–1033.
71. Gan SI, Thompson CC, Lauwers GY, et al. Ethanol lavage of pancreatic cystic lesions: initial pilot study. *Gastrointest Endosc.* 2005;61:746–752.
72. Oh HC, Seo DW, Lee TY, et al. New treatment for cystic tumors of the pancreas: EUS-guided ethanol lavage with paclitaxel injection. *Gastrointest Endosc.* 2008;67:636–642.
73. Oh HC, Seo DW, Kim SC, et al. Septated cystic tumors of the pancreas: is it possible to treat them by endoscopic ultrasonography-guided intervention? *Scand J Gastroenterol.* 2009;44:242–247.
74. DeWitt J, McGreevy K, Schmidt CM, et al. EUS-guided ethanol versus saline solution lavage for pancreatic cysts: a randomized, double-blind study. *Gastrointest Endosc.* 2009;70:710–723.
75. Oh HC, Seo DW, Song TJ, et al. Endoscopic ultrasonography-guided ethanol lavage with paclitaxel injection treats patients with pancreatic cysts. *Gastroenterology.* 2011;140:172–179.
76. DiMaio CJ, DeWitt JM, Brugge WR. Ablation of pancreatic cystic lesions: the use of multiple endoscopic ultrasound-guided ethanol lavage sessions. *Pancreas.* 2011;40:664–668.
77. Moyer MT, Dye CE, Sharzehi S, et al. Is alcohol required for effective pancreatic cyst ablation? The prospective randomized CHARM trial pilot study. *Endosc Int Open.* 2016;4:E603–E607.



**Video 15.1** Video Demonstrating the Classic Appearance of Mucin Within a Cyst



**Video 15.4** Video Demonstrating a Pseudocyst



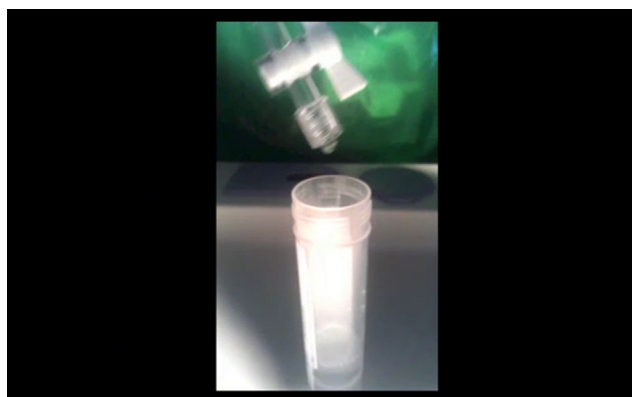
**Video 15.2** Video of a Confocal Laser Endomicroscopy Examination of a Mucinous Cyst



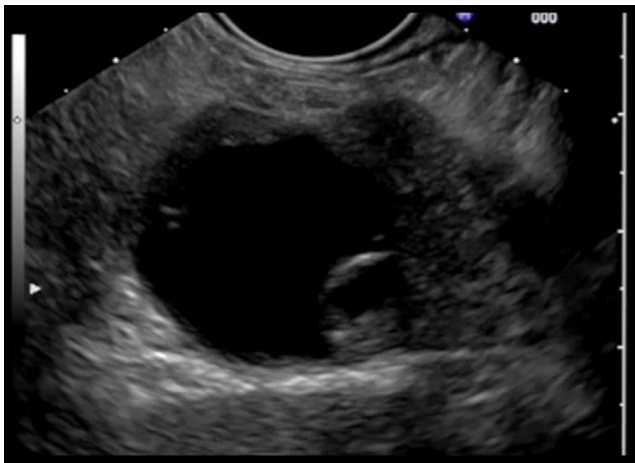
**Video 15.5** Video Demonstrating an Endoscopic Ultrasound Examination of a Cyst Lesion in the Pancreas With Numerous Small Septations Consistent With Serous Cystadenoma



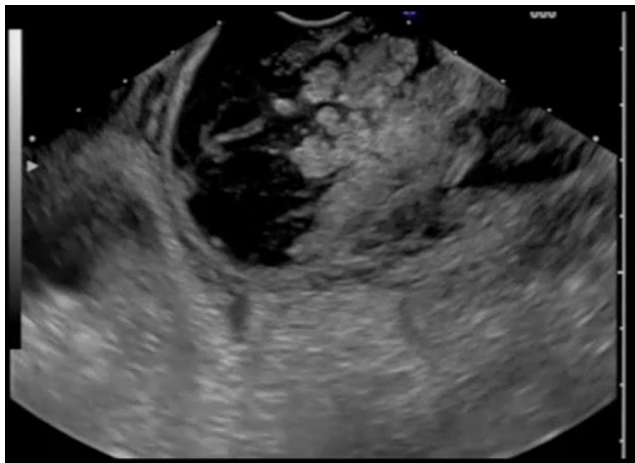
**Video 15.3** Video of a Through-the-Scope Needle Biopsy Forceps Sampling the Distal Wall of an Indeterminate Pancreatic Cyst



**Video 15.6** Video Demonstrating Clear, Thin Fluid Found in a Serous Cystadenoma



**Video 15.7** Mucinous Cystic Neoplasm



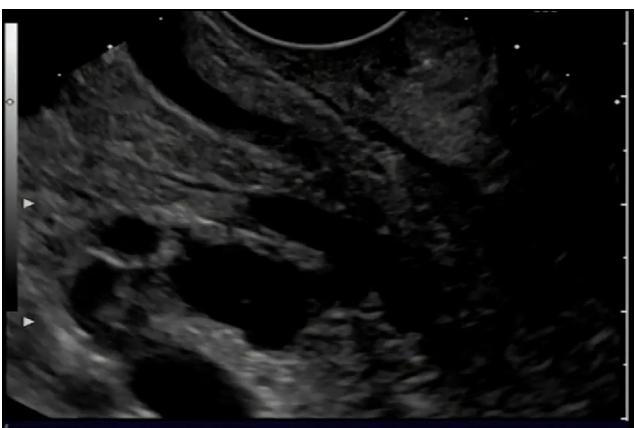
**Video 15.10** Video of a Pancreatic Adenocarcinoma Arising Within an Intraductal Papillary Mucinous Neoplasm



**Video 15.8** Video Demonstrating an Irregular or Thickened Cyst Wall, a Solid Region Within the Cyst, an Adjacent Solid Mass or a Structured, Obstructed, or Displaced Pancreatic Duct  
These features are concerning and may be associated with malignant transformation.



**Video 15.11** Video of a Solid Pseudopapillary Neoplasm



**Video 15.9** Video Demonstrating Endoscopic Ultrasound Evaluation of the Pancreas  
A multiloculated cyst in the head of the pancreas is seen to be communicating with the main pancreatic duct. The main pancreatic duct is also mildly dilated, raising concern for mixed intraductal papillary mucinous neoplasia.



**Video 15.12** Video Demonstrating a Solid Component Within a Pancreatic Cyst Lesion  
Endoscopic ultrasound-guided fine-needle aspiration of the solid component revealed an adenocarcinoma.

# 16

## Endoscopic Ultrasound in Bile Duct, Gallbladder, and Ampullary Lesions

MOHAMMAD AL-HADDAD

### KEY POINTS

- In patients with low to moderate clinical probability of common bile duct (CBD) stones, endoscopic ultrasound (EUS) or magnetic resonance cholangiopancreatography (MRCP) is recommended before endoscopic retrograde cholangiopancreatography (ERCP) is performed.
- In patients with acute pancreatitis of unknown origin or right upper quadrant pain with normal transabdominal ultrasound, EUS should be considered.
- In patients with a CBD stricture of unknown origin, EUS should be performed and, if inconclusive, ERCP should follow with tissue sampling and consideration of cholangiography with or without intraductal ultrasonography (IDUS).
- Gallbladder polyps larger than 5 mm in size may be investigated with EUS to determine the malignancy potential and the subsequent therapeutic approach.
- Ampullary tumors can be staged with EUS and IDUS. EUS is best to differentiate between early (adenoma, T1) and advanced (T2 to T4) tumors and guide therapy.

### GENERAL EXAMINATION CHECKLIST FOR BILIARY STONES AND TUMORS AND AMPULLARY LESIONS

- Extrahepatic ducts (dilation, stones, strictures)
- Intrahepatic ducts (dilation)
- Left and right liver lobes (masses)
- Gallbladder
- Ampulla (including IDUS in the case of T1 ampullary lesions)
- Pancreatic main and accessory ducts
- Lymph nodes
- Ascites
- Portal hypertension

### Endoscopic Ultrasound and Biliary Stones

#### Bile Duct Stones

Endoscopic retrograde cholangiopancreatography (ERCP) has long been considered the best diagnostic method for common bile duct (CBD) stones. Moreover, ERCP allows stone removal during the same endoscopic session when combined with endoscopic

sphincterotomy (ES). Nevertheless, it remains an invasive procedure and carries a substantial risk of complications,<sup>1</sup> although when performed by experienced endoscopists, the complications and mortality rates can be reduced to under 5% and 0.1%, respectively.<sup>2</sup> Furthermore, because it can be difficult to differentiate small stones from aerobilia, a substantial proportion of ERCP procedures are completed with ES, in order to confirm the diagnosis of choledocholithiasis. ES has a complication rate of 5% to 10%,<sup>3</sup> with a current mortality being less than 1%.<sup>3</sup> Long-term complications, such as stenosis and nonobstructive cholangitis, are rare occurring in approximately 10% or fewer of patients.<sup>4,5</sup>

As such, ERCP is no longer acceptable as a diagnostic tool for CBD stones albeit it remains the therapeutic modality of choice. Transabdominal ultrasonography (TUS) is a widely available, noninvasive imaging modality that should be part of the initial evaluation of any patient with clinical and/or laboratory suspicion of CBD stones. However, although TUS is very sensitive and specific for cholelithiasis, its sensitivity for the diagnosis of choledocholithiasis remains limited, even in heavily calcified CBD stones. The location and orientation of the bile duct, along with adjacent duodenal air, make imaging of the distal bile duct difficult, and abdominal fat attenuates ultrasound waves, making this technique less effective in obese patients.

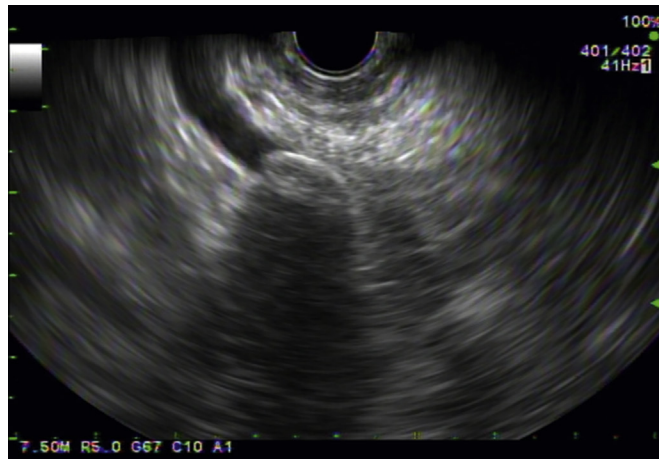
Other imaging modalities such as multidetector computed tomography (CT), endoscopic ultrasonography (EUS), and magnetic resonance cholangiopancreatography (MRCP) have been effectively employed for the diagnosis of CBD stones. The sensitivity, specificity, and accuracy of helical CT range from 85% to 88%, 88% to 97%, and 86% to 94%, respectively. Nevertheless, the sensitivity of CT for detecting stones under 5 mm in size remains significantly lower than those measuring 5 mm or more.<sup>6</sup> In one comparative study with MRCP and EUS, helical CT was inferior to either,<sup>7</sup> although multiplanar reconstructions with multidetector CT can improve its specificity.<sup>8,9</sup> Therefore EUS and MRCP remain the most accurate minimally invasive methods for diagnosing CBD stones.

#### Endoscopic Ultrasound Technique for Detecting Choledocholithiasis

EUS provides excellent sonographic visualization of the extrahepatic biliary tree. Bile duct stones are shown as echo-dense structures (Figs. 16.1 and 16.2) within the ampulla or CBD, sometimes freely moving within the duct, with or without acoustic



• **Fig. 16.1** Linear endoscopic ultrasound image (7.5 MHz) of common bile duct stone (+) in a patient presenting with right upper quadrant pain and elevated transaminases.



• **Fig. 16.2** Linear endoscopic ultrasound image (7.5 MHz) of a shadowing 9 mm common bile duct stone without significant upstream ductal dilation.

shadowing or thickening of the bile duct wall ([Videos 16.1A and B](#)). The accuracy of EUS was found to be higher than that of ERCP for the detection of small CBD stones<sup>10</sup> ([Fig. 16.3](#)), with a negative predictive value (NPV) exceeding 95% and specificity in ruling out the presence of CBD stones of 95% or higher in the majority of published studies ([Table 16.1](#)). Additionally, EUS detects bile duct sludge as well as microlithiasis ([Video 16.2](#)), often missed by the other imaging techniques.<sup>11</sup>

In most EUS literature, EUS radial echoendoscopes were used for assessment of choledocholithiasis. Nevertheless, the accuracy of linear EUS appeared to be comparable to that of the radial exam, as indicated in some series comparing EUS with ERCP plus ES, or choledochotomy with choledochoscopy (see [Table 16.1](#)).<sup>12–20</sup> The advantages of radial echoendoscopes reside in their ability to visualize the bile duct in a long section (along its main axis) without having to torque the scope. Nevertheless, it can miss hilar stones due to the distance. A linear echoendoscope, on the other hand, provides cross-sectional or tangential views of the bile duct but requires continuous torque to visualize the entire

duct: clockwise to interrogate the bile duct from the hilum to the papilla and counterclockwise to interrogate the duct in the opposite direction (see [Videos 16.1 and 16.3](#)).

The ability of either echoendoscope to visualize intrahepatic stones remains low due to the distance from the tip of the scope and the presence of several intervening structures. In addition, stones impacted at the level of the papilla can be missed unless full visualization of the duct at its insertion into the duodenal wall is possible. This ampullary view can be difficult to obtain in some cases from the duodenal bulb, where deep insertion into the second part of the duodenum followed by slow withdrawal with the tip of the scope in full upward deflection could help bring the ampulla to view and stabilize the scope within the duodenal sweep. It is also recommended to instill water in the second part of the duodenum, particularly when the radial scope is being utilized to improve acoustic coupling of the periampullary area.

#### ***The Use of Endoscopic Ultrasound, Magnetic Resonance Cholangiopancreatography, and Endoscopic Retrograde Cholangiopancreatography in the Management of Choledocholithiasis***

MRCP is a noninvasive, radiation-free imaging modality and is more accurate than CT for the diagnosis of choledocholithiasis ([Table 16.2](#)).<sup>7,21–38</sup> The disadvantages of this technique include the limited spatial resolution, the difficulty of diagnosing CBD stones in the periampullary region, lack of availability in some areas, need for operator's experience to interpret findings, and the high cost.<sup>39</sup> Moreover, MRCP is contraindicated in patients with metallic hardware such as pacemakers or cerebral aneurysm clips and is difficult to conduct in claustrophobic patients; EUS offers higher spatial resolution than MRCP (0.1 vs. 1 to 1.5 mm), and its sensitivity for detecting choledocholithiasis does not vary with the stone size like MRCP.<sup>40</sup> Thus, it is not surprising that stones missed by MRCP were always smaller than 10 mm,<sup>41,42</sup> and that the sensitivity of MRCP decreased to approximately 65% for diagnosing stones smaller than 5 mm.<sup>7,40</sup> Nevertheless, improvements in imaging may in the future permit the detection of even smaller stones. In a recent systematic review, the sensitivity of MRCP in detecting CBD stones was 90% with a specificity of 95%.<sup>43</sup>

The diagnostic performance of EUS has been evaluated in two meta-analyses covering 3532 and 2673 patients.<sup>44,45</sup> The pooled sensitivity and specificity of EUS were 89% to 94% and 94% to 95%, respectively. The evidence for the use of MRCP for the diagnosis of CBD stones has been examined in a systematic review of 10 studies and was shown to provide a high sensitivity (range 80% to 100%) and specificity (range 83% to 98%).<sup>46</sup> In comparative studies of the two technologies, EUS was found to be either superior<sup>47,48</sup> or equivalent<sup>47,49–51</sup> to MRCP for the diagnosis of choledocholithiasis. One meta-analysis<sup>52</sup> and two systematic reviews<sup>53,54</sup> comparing EUS and MRCP for depicting CBD stones showed a high diagnostic performance for both modalities. Although no statistically significant differences were found between the two modalities, there was a trend towards higher sensitivity and specificity for EUS compared to MRCP. This was especially obvious in the case of small stones causing acute biliary pancreatitis. Nevertheless, the choice between these two techniques should depend on other factors such as resource availability, operator experience, and cost.

The use of noninvasive imaging modalities resulted in a considerable reduction in the number of inappropriate ERCP with bile duct cannulation.<sup>10,55–58</sup> One meta-analysis comparing an EUS-guided ERCP strategy with an ERCP-only strategy found that the

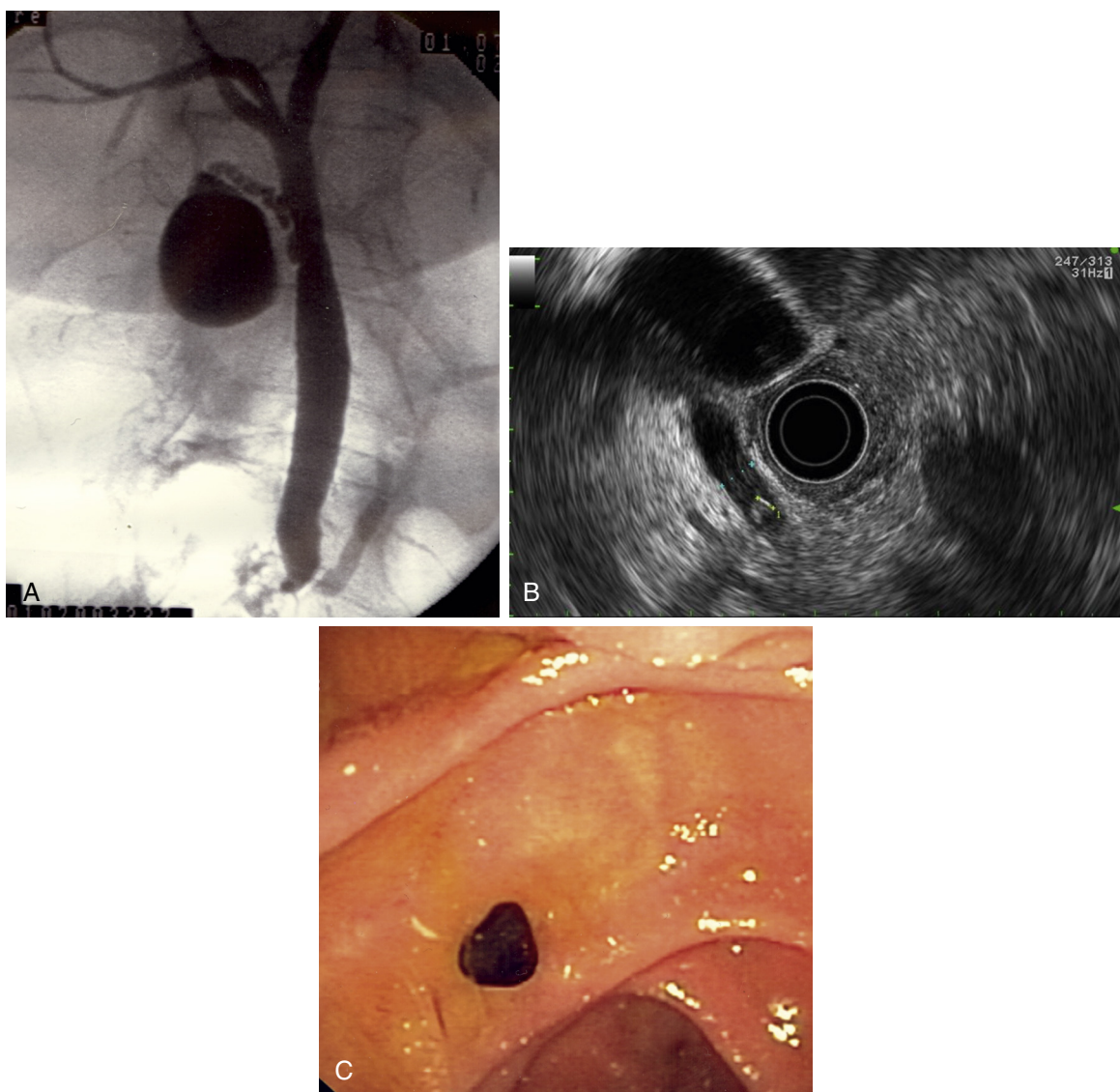


**Fig. 16.3** (A) Fluoroscopy image of a common bile duct without any filling defects at endoscopic retrograde cholangiopancreatography. (B) Small stone identified on endoscopic ultrasound (radial echoendoscope, 6 MHz). (C) Stone confirmed by biliary sphincterotomy and after balloon sweeping of the common bile duct.

use of EUS significantly reduced the risk of overall complications (relative risk 0.35) by safely avoiding ERCP in 67% of patients.<sup>58</sup> Whether or not an EUS or MRCP would be necessary prior to ERCP depends on the pretest probability of having a stone in the CBD. Patients suspected of having choledocholithiasis on clinical and laboratory criteria and/or ultrasound (US) can be grouped into risk groups, ranging from low to intermediate to high risk.<sup>59–61</sup> Patients in the high-risk group include those with CBD stones on transabdominal US, clinical ascending cholangitis, and bilirubin greater than 4 mg/dL.<sup>59</sup> When considering all published studies, the proportion of high-risk patients who actually have CBD stones was less than 80% (66% to 78%),<sup>55,62–64</sup> whereas fewer than 40% of patients classified as being at intermediate (also called moderate) risk had choledocholithiasis (19% to 44%).<sup>63,65–69</sup> Most experts agree that ERCP could be performed as a first-line approach in patients at high risk of CBD stones,<sup>10,63,68</sup> although it may be impossible to avoid unnecessary ERCP procedures altogether.<sup>70</sup> EUS as a first-line approach in patients in the high-risk

category could still be performed if available to exclude a stone or to evaluate other causes of biliary symptoms.<sup>55,71,72</sup> Moreover, EUS confirming CBD stones would justify the use of aggressive techniques, such as precut papillotomy, if needed. However, there is still no general agreement in regard to the routine utilization of EUS in such cases.<sup>73</sup> Practically, the best approach is probably to perform EUS followed by ERCP (with or without ES) when a stone is found during the same endoscopic session.<sup>74,75</sup>

Intermediate risk patients include those who present with symptoms compatible with biliary origin, along with liver test abnormalities or dilated CBD on TUS. The consensus in this group of patients is to consider EUS (or MRCP) as the first-line diagnostic approach (after TUS).<sup>56–58,76,77</sup> This approach was evaluated in the context of laparoscopic cholecystectomy in a series of 300 patients.<sup>66</sup> Choledocholithiasis was found on preoperative EUS in 19% of the intermediate risk, and on ERCP in 78% of the high risk. For low-risk patients, who typically have no biliary symptoms or liver test abnormalities, and have no CBD dilatation

**TABLE  
16.1****Performance of Endoscopic Ultrasound in the Diagnosis of Common Bile Duct Stones**

Reference (Year)	Level of Evidence <sup>a</sup>	No. of Patients Included	Frequency of CBD Stones (%)	Endoscopic Ultrasound Performance Characteristics				
				Sensitivity (%)	Specificity (%)	PPV (%)	NPV (%)	Accuracy (%)
Kohut et al. <sup>12</sup> (2002)	1	134	68	93	93	98	87	94
Meroni et al. <sup>17</sup> (2004)	1	47	15	71	90	55	95	
Liu et al. <sup>90</sup> (2000)	2	139	35	98	98	100	96	99
Prat et al. <sup>18</sup> (2001)	2	123	27	100	100	100	100	100
Berdah et al. <sup>66</sup> (2001)	2	68	20	96	97	93	100	98
Buscarini et al. <sup>55</sup> (2003)	2	463	52	98	99	99	98	97
Kohut et al. <sup>16</sup> (2003)	2	55	9	75	99	100	98	98
Aube et al. <sup>47</sup> (2005)	2	45	34	94	97	94	97	96
Ney et al. <sup>19</sup> (2005)	2	68	32	96	99	100	97	98
Lachter et al. <sup>13</sup> (2000)	3	50	66	96	75	89	93	94
Materne et al. <sup>50</sup> (2000)	3	50	26	97	88	94	93	94
Scheiman et al. <sup>20</sup> (2001)	3	28	18	80	95	80	96	—
Ainsworth et al. <sup>49</sup> (2004)	3	163	33	90	99	98	94	93
Kondo et al. <sup>7</sup> (2005)	3	30	86	98	50	92	100	93
Dittrick et al. <sup>72</sup> (2005)	3	30	37	100	84	56	100	—
Jeon et al. <sup>64</sup> (2016)	3	200	83	98	80	95	89	94
Netinatsunton et al. <sup>61</sup> (2016)	3	141	59	98	80	98	80	

<sup>a</sup>Level 1: Technique compared with ERC + systematic ES with a very short interval between the technique and ERCP; Level 2: Technique compared with ERCP + ES if positive, and clinical and biological follow-up of at least 6 months if negative; Level 3: Technique compared with ERC or with intraoperative cholangiography.

CBD, Common bile duct; ERC, endoscopic retrograde cholangiography; ERCP, endoscopic retrograde cholangiopancreatography; ES, endoscopic sphincterotomy.

on TUS, no further examination is necessary in this case. We suggest an algorithm to investigate patients with suspected choledocholithiasis based on their risk stratification (Fig. 16.4).

The utilization of EUS was associated with potential financial advantages as a first-line strategy in cost-effectiveness studies. In a prospective study of 485 patients suspected of having CBD stones where EUS was always performed regardless of the risk classification, the mean cost for patients managed by the EUS-based strategy was significantly lower than that for patients who had ERCP.<sup>55</sup> In another study, the EUS-guided ERCP strategy resulted in 14% reduction in ERCP procedures, and was associated with significant cost savings.<sup>78</sup> Other studies have found that EUS was the most cost-effective strategy in the intermediate-risk group, whereas in patients with a probability of CBD stones above 50% (high-risk group), the most cost-effective approach was an ERCP first approach.<sup>49,63,70,79</sup> In patients with acute biliary pancreatitis, an economic evaluation also concluded that EUS was

the strategy associated with lower costs, and fewer procedures and complications. This was especially obvious in patients with severe acute pancreatitis.<sup>80</sup> Finally, a randomized study comparing EUS and ERCP during the same endoscopic session versus EUS and ERCP in two separate sessions for the management of choledocholithiasis<sup>75</sup> showed that the average procedure time and days of hospitalization were significantly reduced in the first group, resulting in significant reductions in total costs.

Two adjunct ultrasound-based technologies have been studied in the last 2 decades: extraductal catheter probe EUS (EDUS) and intraductal ultrasonography (IDUS). The use of EDUS has been evaluated in two studies and appears to be accurate in detecting CBD stones and is nearly as accurate as linear array EUS for that purpose.<sup>14,81</sup> In the earlier published prospective study, EDUS with a radial scanning catheter probe was performed before ERCP and ES in patients with suspected CBD stones.<sup>81</sup> EDUS detected 33 of 34 bile duct stones. In eight patients, the stones were missed

**TABLE 16.2 Performance of Magnetic Resonance Cholangiopancreatography in the Diagnosis of Common Bile Duct Stones**

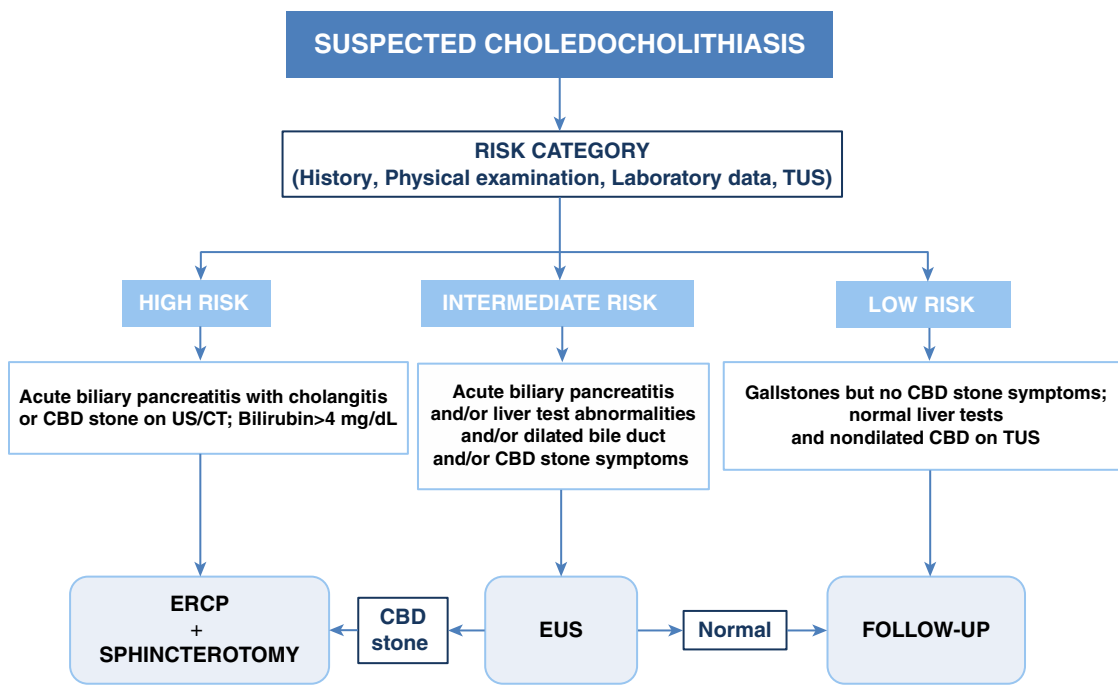
Reference (Year)	Level of Evidence <sup>a</sup>	Number of Patients	Sensitivity (%)	Specificity (%)	PPV (%)	NPV (%)	Accuracy (%)
Gautier et al. <sup>31</sup> (2004)	2	99	96	99	—	—	—
Aube et al. <sup>47</sup> (2005)	2	45	88	97	93	93	—
Topal et al. <sup>22</sup> (2003)	2	315	95	100	100	98	—
Mofidi et al. <sup>21</sup> (2008)	2	49	100	96	—	—	—
Scaffidi et al. <sup>23</sup> (2009)	2	120	88	72	87	72	83
Cervi et al. <sup>32</sup> (2000)	3	60	100	94	—	—	—
Demartines et al. <sup>33</sup> (2000)	3	70	100	96	93	100	—
Stiris et al. <sup>34</sup> (2000)	3	50	88	94	97	81	—
Materne et al. <sup>50</sup> (2000)	3	50	91	94	88	95	92
Scheiman et al. <sup>20</sup> (2001)	3	28	40	96	66	88	—
Kim et al. <sup>35</sup> (2002)	3	121	95	95	—	—	95
Taylor et al. <sup>36</sup> (2002)	3	146	98	89	84	99	—
Griffin et al. <sup>25</sup> (2003)	3	115	84	96	91	93	92
Ainsworth et al. <sup>49</sup> (2004)	3	163	87	97	95	93	—
Kondo et al. <sup>7</sup> (2005)	3	30	88	75	96	50	86
Ausch et al. <sup>24</sup> (2005)	3	773	94	98	80	99	—
Hallal et al. <sup>27</sup> (2005)	3	29	100	91	50	100	92
Makary et al. <sup>67</sup> (2005)	3	64	94	98	94	98	—
Moon et al. <sup>28</sup> (2005)	3	32	80	83	89	71	81
De Waele et al. <sup>26</sup> (2007)	3	104	83	98	91	95	94
Norero et al. <sup>30</sup> (2008)	3	125	97	74	89	90	90
Richard et al. <sup>29</sup> (2013)	3	70	27	83	36	77	69
Badger et al. <sup>37</sup> (2016)	3	527	90	86	97	60	—

<sup>a</sup>Level 1: Technique compared with ERC + systematic ES with a very short interval between the technique and ERCP; Level 2: Technique compared with ERCP + ES if positive, and clinical and biological follow-up of at least 6 months if negative; Level 3: Technique compared with ERC or with intraoperative cholangiography.

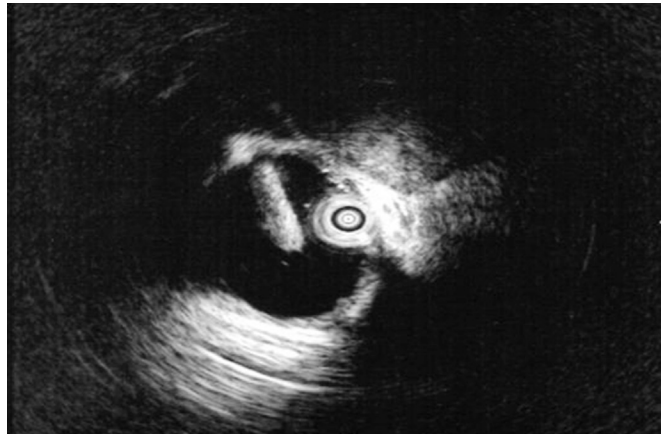
CBD, Common bile duct; ERC, endoscopic retrograde cholangiography; ERCP, endoscopic retrograde cholangiopancreatography; ES, endoscopic sphincterotomy.

on ERCP but seen after ES. The same authors conducted a subsequent prospective trial to compare the diagnostic potential of EDUS with that of conventional EUS,<sup>14</sup> where EDUS was found to be nearly as accurate as linear array EUS. IDUS has also been proposed to assess for CBD stones (Fig. 16.5). In a prospective study of patients with suspected CBD stones who underwent ERCP, 20 MHz IDUS exam was performed in those with equivocal cholangiograms or cholangiographic evidence of stones.<sup>82</sup> Interestingly, no stones were found in 36% of patients with a positive finding on ERCP, which is likely due to the presence of aerobilia. In 35% of patients with a negative ERCP, sludge or stones were found on IDUS and were confirmed on ES. Another study demonstrated that the addition of IDUS to confirm complete stone clearance after ES decreased the recurrence rate of CBD stones (13%

in the non-IDUS group compared to 3% in the IDUS group).<sup>83</sup> In one prospective trial, the sensitivity of MRCP, ERCP, and IDUS for the diagnosis of choledocholithiasis was 80%, 90%, and 95%, respectively. The accuracy of IDUS plus ERCP was superior to that of ERCP alone in this study.<sup>84</sup> IDUS could be particularly helpful in nonopaque stones, as recently demonstrated in a study including patients with various calcium density CBD stones,<sup>85</sup> where IDUS identified all 148 patients with duct stones (100%) as opposed to ERCP which missed three stones in the same group of patients. However, IDUS cannot be proposed as a routine procedure because of the morbidity associated with ERCP. It can be utilized prior to ES in patients in whom CBD stones have been found on EUS or MRCP, but not on ERCP, or following ES to confirm complete stone clearance.



• **Fig. 16.4** An algorithm for the management of patients with suspected choledocholithiasis. CT, Computed tomography; CBD, common bile duct; ERCP, endoscopic retrograde cholangiopancreatography; EUS, endoscopic ultrasound; TUS, transabdominal ultrasonography; US, ultrasound.



• **Fig. 16.5** Two-dimensional intraductal ultrasonography showing a shadowing common bile duct stone.

## Summary

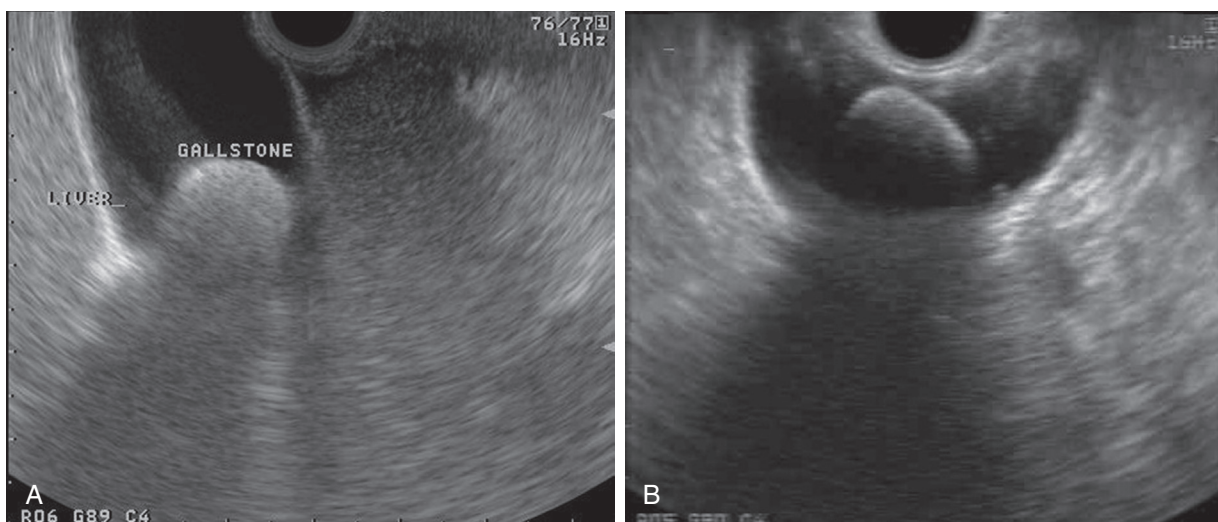
EUS is the ideal alternative to cholangiography for the evaluation of choledocholithiasis, selecting only those patients with confirmed CBD stones for ERCP. MRCP can be utilized as an alternative when there are contraindications to sedation, or when EUS is not available. ERCP should be avoided, if biliary EUS proved normal,<sup>10,56–58</sup> unless symptoms persist or recur during follow-up. Ideally, EUS and ERCP should be combined in a single endoscopic session whenever possible to reduce risks of repeated sedation and minimize cost. When this approach is not feasible, high-risk patients could be managed with ERCP at first.

## Gallstones

Transabdominal ultrasound (TUS) is an excellent modality for the diagnosis of cholelithiasis, with exceedingly high sensitivity

and specificity, but its performance is limited in smaller size stones and large body habitus. Because of its value in diagnosing small CBD stones, EUS has also been evaluated for detecting cholelithiasis (Figs. 16.6 and 16.7; Video 16.4). EUS can influence the management of patients with biliary pain and normal initial imaging with TUS or CT.<sup>86,87</sup> For example, Thorboll et al.<sup>87</sup> studied patients with a normal TUS, but with suspected gallstones based on clinical grounds and detected cholelithiasis in 18/35 patients (52%).

Idiopathic acute pancreatitis (IAP) can be the result of biliary sludge or microlithiasis undetected by other imaging techniques (Fig. 16.8). Although the reported incidence of occult gallstones in IAP varies (ranging from 10% to 73%),<sup>88,89</sup> this remains the most common cause of pancreatitis in patients with intact gallbladder. In one study, gallstones were found by EUS in 14 of 18 patients with negative findings on TUS.<sup>90</sup> In a larger series,<sup>11</sup> 168 patients with IAP were referred for EUS which identified gallbladder sludge or very small stones in 40% of patients, with or without associated CBD stones, that had been missed by other examinations. Overall, EUS was able to detect a cause for the acute pancreatitis in 80% of patients. Yusoff et al. reported that EUS established a presumptive diagnosis in 31% of 201 patients with a single episode of IAP,<sup>91</sup> the most frequent causes in those with *in situ* gallbladders being chronic pancreatitis and biliary sludge. A systematic review evaluating the role of EUS in idiopathic pancreatitis showed a high diagnostic yield, especially in patients with a single idiopathic episode, and in patients with recurrent episodes and gallbladder *in situ*.<sup>92</sup> Moreover, a cost analysis identified EUS as the most cost-effective initial test in the evaluation of IAP when compared with other strategies including ERCP with manometry and bile aspiration, and laparoscopic cholecystectomy.<sup>93</sup> Therefore an EUS-based strategy appears to be the best approach to evaluate patients with IAP because of the high diagnostic accuracy of EUS, not only for gallbladder sludge and stones, but also for pancreatic diseases, and its minimally



• **Fig. 16.6** (A) A shadowing gallbladder stone incidentally noted during linear (7.5 MHz) endoscopic ultrasound (EUS) exam. (B) A solitary shadowing gallbladder stone (linear EUS image; 7.5 MHz) with significant acoustic void beyond the stone due to its echodensity. This was incidentally noted during assessment of an esophageal subepithelial lesion. ([A] Figure courtesy of Dr. John DeWitt.)



• **Fig. 16.7** Linear endoscopic ultrasound image (7.5 MHz) of multiple small calcified gallstones. (Figure courtesy of Dr. John DeWitt.)

invasive nature. In patients with multiple unexplained attacks, particularly in those postcholecystectomy, ERCP and sphincter of Oddi manometry should be considered after negative EUS results.

## Summary

EUS is the most effective method for confirming the presence or absence of CBD stones. Its utility in avoiding unnecessary ERCP has been validated in patients at low or moderate risk of CBD stones. MRCP can probably be used as an alternative to EUS if available and there are no contraindications. EUS remains the preferred diagnostic test in the setting of acute pancreatitis where biliary stones can be very small and can be missed on MRCP. For patients at high risk of CBD stones, ERCP ± ES (in case CBD stones were found on cholangiography) can be considered as the first-line approach; however, if EUS is available and can be



• **Fig. 16.8** Linear endoscopic ultrasound image (7.5 MHz) of extensive gallbladder sludge. (Figure courtesy of Dr. John DeWitt.)

performed during the same endoscopic session with ERCP, then that would be optimal. EUS is now a well-established modality after TUS for the diagnosis of gallbladder stones and sludge in patients with unexplained right-upper-quadrant pain, and also in those with an acute pancreatitis of unknown origin.

## DIAGNOSTIC CHECKLIST

### CBD or Gallstone

- Hyperechoic mobile structure with or without acoustic shadowing

### Associated Signs

- Dilation of extrahepatic ducts and/or cystic duct
- Thickening of the gallbladder and/or bile duct wall
- Thickening of the ampulla
- Pericholecystic fluid

## Endoscopic Ultrasound in Bile Duct Strictures

Benign and malignant bile duct strictures remain a diagnostic challenge for the gastroenterologist. TUS and CT imaging can reliably demonstrate dilated bile ducts, but are often inadequate in assessing underlying cause of dilation. ERCP is highly accurate for the confirmation of obstructive jaundice, but little additional information could be obtained for tumor staging, as only indirect tumor signs, such as stenosis, supra-stenotic dilation, or both, can be visualized, and the tumor itself is generally not well seen. MRCP, on the other hand, can demonstrate a small tumor or focal narrowing in the bile duct, but appears to add little to ERCP for the diagnosis of malignancy except for detecting contiguous tumor invasion or metastasis.<sup>94</sup> However, MRCP could be superior in investigating the anatomic extent of the lesion compared to ERCP because it displays the biliary tree proximal to the obstruction.<sup>95</sup>

Intraductal tissue sampling is commonly used at the time of ERCP. Brushing has a low sensitivity for the diagnosis of bile duct tumors of 27% to 56%,<sup>96–100</sup> owing to their desmoplastic nature or submucosal spread of the tumor, and is often negative for extrinsic tumors (pancreatic cancer, gallbladder cancer, metastatic lymph nodes). New ancillary cytology-based techniques have been developed over the last decade to improve the sensitivity of routine cytology. Such techniques include fluorescence in situ hybridization (FISH) analysis, which detects chromosomal polysomy using fluorescent probes, and digital image analysis (DIA) technique to assess for the presence of aneuploidy.<sup>101–104</sup> FISH plays an increasing role in the diagnosis of malignancy from ERCP-obtained

samples, whereby in one study it was shown to increase the sensitivity of brush cytology from 21% to 58%,<sup>105</sup> and increased sensitivity to 72% when combined with brush cytology results.<sup>106</sup> Recently, PCR-based DNA mutation profiling has been studied in biliary brushings and was shown to augment the sensitivity of cytology and FISH from 32% for cytology alone to 73% when all three modalities were combined.<sup>107</sup>

Additional means of tissue sampling include direct forceps biopsies during ERCP, which has a higher sensitivity than brush cytology alone, with sensitivity ranging from 44% to 89% in cholangiocarcinoma and 33% to 71% in pancreatic cancer.<sup>108–110</sup> Nevertheless, this technique is limited by its low NPY. This has led to the development of new methods to abrade the tumor surface in order to improve cytologic yield including a combination of stricture dilation, endoscopic needle aspiration, and biliary brush cytology.<sup>111–114</sup> Currently, bile duct biopsy under direct cholangioscopy presents the most promising method of biliary sampling using the single operator cholangioscopy system (SOC), with a sensitivity up to 90% based on direct biopsies as will be discussed later in this section.<sup>115–120</sup>

## Endoscopic Ultrasound-Fine-Needle Aspiration Considerations in Biliary Strictures and Tumors

EUS has proved to be a useful tool in assessing biliary obstruction, as it readily visualizes the entire CBD. Therefore it can be helpful in the differential diagnosis of bile duct strictures and neoplasia, and local tumor staging (Fig. 16.9).<sup>121</sup> The ability to acquire tissue by

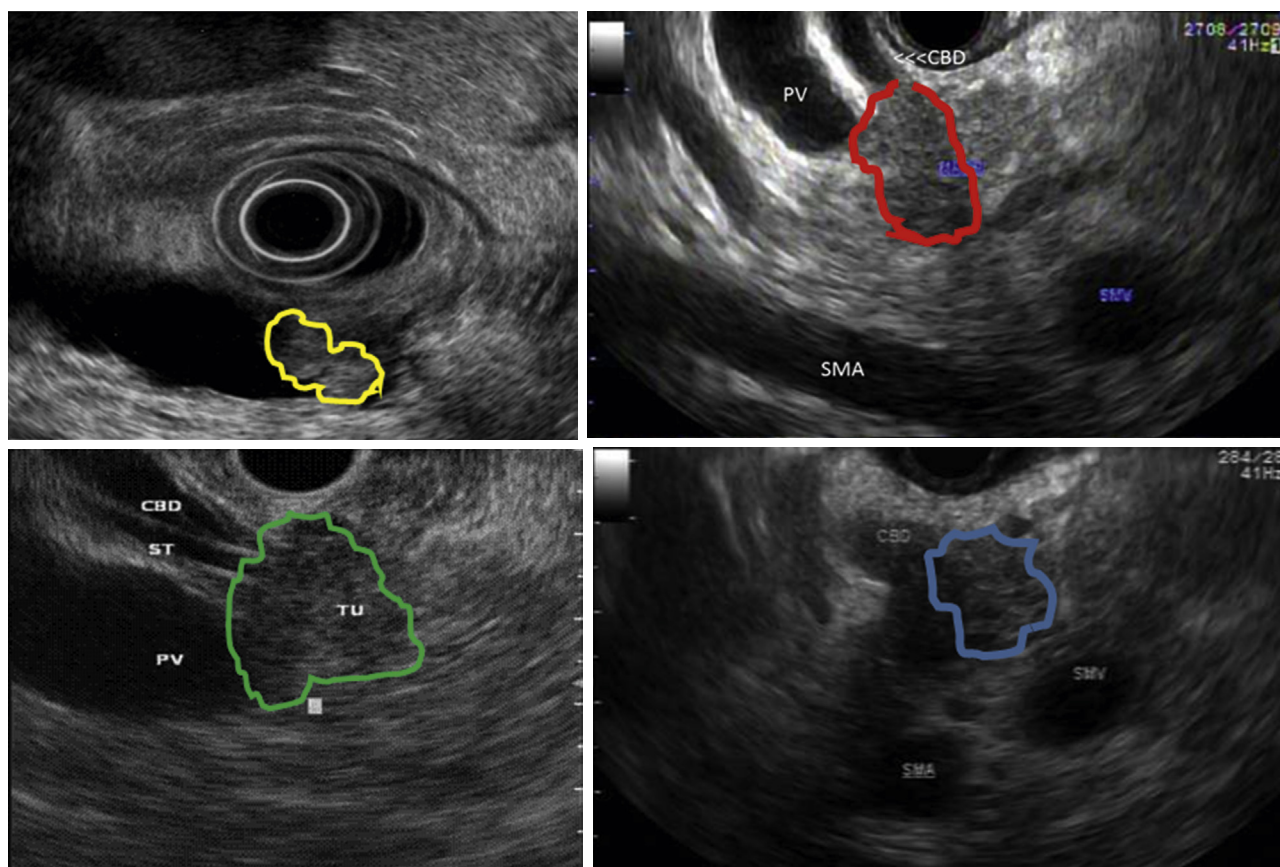


**Fig. 16.9** Linear and radial endoscopic ultrasound images (7.5 MHz) of four distinct cholangiocarcinoma lesions in patients presenting with jaundice and bile duct stricture without a definite mass on computed tomography scan or magnetic resonance cholangiopancreatography. The masses are outlined in various colors. CBD, Common bile duct; PV, portal vein; SMA, superior mesenteric artery; SMV, superior mesenteric vein; ST, stent; TU, tumor.

EUS-guided fine-needle aspiration (FNA) significantly improves the diagnostic yield when evaluating biliary strictures, and is associated with a minimal risk of complications (Fig. 16.10). In a recent meta-analysis of 20 studies involving 957 patients, EUS FNA had a pooled sensitivity and specificity for diagnosis of malignant biliary stricture of 80% and 97%, respectively.<sup>122</sup> As the distal CBD is located immediately under the echoendoscope transducer when examined from the duodenal bulb, EUS performs extremely well for evaluating distal biliary strictures (Video 16.5). EUS FNA is highly accurate in diagnosing malignancy in distal biliary strictures, particularly in patients with masses within the pancreatic head.<sup>123–132</sup> In this setting, the overall EUS FNA sensitivity and specificity rates range from 81% to 91% and from 71% to 100%, respectively. However, its sensitivity for proximal biliary strictures drops and has ranged between 25% and 89% (Tables 16.3 and 16.4).<sup>123,125,129–131,133–146</sup> Nevertheless, the reported accuracies are lower for cholangiocarcinomas, mainly due to the inclusion of the hilar cholangiocarcinomas (Klastkin tumors) and the difficulty visualizing and sampling such tumors via EUS due to distance from the probe. Moreover, proximal biliary lesions tend to often be small and diffusely infiltrating, unlike the distal biliary ones that frequently present as focal solid masses (Fig. 16.11). Cytologic diagnosis is an important adjunct to EUS and helps direct patient management and avoid unnecessary surgery (see Fig. 16.10). Limited experience with a forward-viewing linear echoendoscope (Olympus Medical Center Valley, Pennsylvania) suggests improved imaging of hilar strictures and easier EUS FNA technique.<sup>147,148</sup>

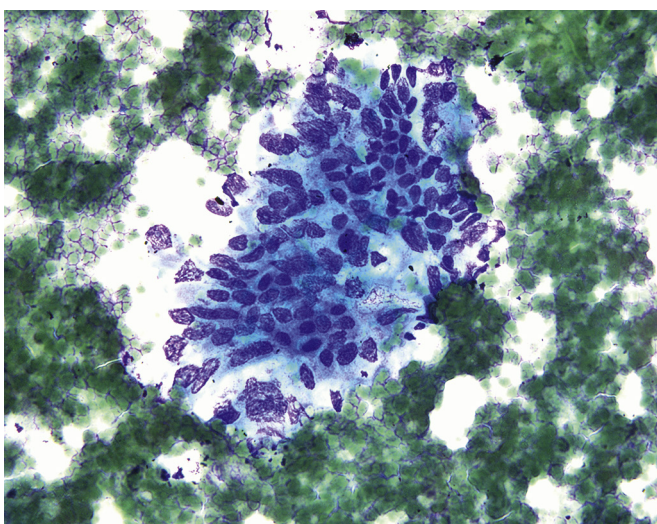
**Technique:** Visualizing and sampling biliary strictures during EUS can pose a challenge to the endosonographer (see Fig. 16.9). Bile duct lesions are best visualized and sampled from the duodenum. Distal CBD lesions can sometimes be missed if the exam is only performed from the duodenal bulb. Therefore scope advancement to the second part of the duodenum followed by slow withdrawal through the duodenal sweep while maintaining full upward deflection is recommended to localize small distal and periampullary lesions. During FNA, maintaining a close apposition of the echoendoscope to the duodenal wall is essential to help stabilize the scope and minimize the amount of tissue the needle

has to traverse. This position creates an angulation in the tip of the scope, and therefore 25-gauge needles are recommended due to ease of advancement through the scope. Additionally, 25-gauge needles have been shown to be equivalent to 22-gauge needles in their diagnostic accuracy,<sup>149–151</sup> and may result in less bleeding during FNA, particularly when close to vascular structures like the portal vein and hepatic artery. If the clinical suspicion of a malignancy is high but no mass can be seen on EUS, targeting the stricture area with FNA under fluoroscopic guidance after CBD stenting might help improve tissue yield (Video 16.6).

**Presence of biliary stents:** A biliary stent was in place at the time of EUS in a significant proportion of patients undergoing assessment of biliary strictures (see Table 16.4). The presence of an indwelling biliary stent can impair EUS imaging due to stent-induced artifacts and sludge build up in its lumen (Video 16.7). However, impaired imaging is probably of little impact on mass visualization and FNA as demonstrated by two studies.<sup>152,153</sup> It is conceivable, though, that a stent may hinder the detection of a very small bile duct mass or prevent the detection of a very distal lesion in the bile duct in the setting of a metallic stent. Imaging can be optimized by examination of various locations, by limiting the amount of air insufflated that may pass through the stent into the duct, or by removing the stent prior to EUS whenever possible. The presence of a stent can facilitate detection of a biliary mass as the stent often courses through the lesion aiding detection, particularly with plastic stents (Fig. 16.12).

**Cytopathologic considerations:** Cytologic specimens from FNA of biliary strictures (manifesting as biliary thickening on EUS) or small solid lesions tend to be of low cellularity and highly contaminated by duodenal and pancreatic epithelium. Even when cellularity is adequate, other factors can limit the interpretation even by highly experienced cytopathologists. Dysplasia can be very difficult to discern or be misinterpreted, especially in the setting of reactive inflammation or due to the presence of a biliary stent. Using the same argument, well-differentiated carcinomas can be difficult to characterize from reactive atypia. Such limitations often lead to many FNA samples being interpreted as atypical or suspicious without positively confirming malignancy. A multimodality tissue sampling approach, as described earlier in this section, is essential to provide a solid tissue diagnosis in this group of patients.

**Tumor seeding:** The perceived risk and implications of tumor seeding following EUS FNA for cholangiocarcinoma continues to be a source of debate. Tumor seeding by disseminating tumor cells across the needle track has been reported following EUS<sup>154–156</sup> and imaging-guided FNA of various sites.<sup>157–162</sup> The risk of clinically apparent tumor seeding following FNA is estimated to be approximately 1/10,000 or less.<sup>163,164</sup> However, the reported rates likely underestimate the true occurrence of seeding due to the high mortality and short survival of patients with pancreateobiliary malignancies. Additionally, deposits along the small needle track are practically indistinguishable from local tumor recurrence that occurs with time and therefore it can be difficult to prove the origin of the deposits with certainty. This hypothesis is supported in a study that evaluated the rates of peritoneal carcinomatosis in matched pancreatic adenocarcinoma cohorts diagnosed by either EUS or percutaneously guided FNA.<sup>165</sup> Peritoneal carcinomatosis developed in one and seven patients (2% vs. 16%;  $P < .025$ ) in the EUS FNA versus percutaneous FNA group, respectively. The findings indicate a potential difference in tumor seeding risk between biopsy approaches and potentially greater frequency of tumor seeding than historically appreciated. Similarly, a meta-analysis of eight studies identified tumor seeding in 3% of patients following hepatocellular carcinoma biopsy.<sup>166</sup>



• **Fig. 16.10** Cytology photomicrograph from a cholangiocarcinoma sampled by endoscopic ultrasound fine-needle aspiration after negative biliary brushings on endoscopic retrograde cholangiopancreatography. Glandular epithelium with nuclear enlargement, pleomorphism, and scant cytoplasm was diagnostic of malignancy (Diff Quick,  $\times 40$ ).

**TABLE  
16.3****Operating Characteristics of Endoscopic Ultrasound-Fine-Needle Aspiration in Biliary Strictures**

Reference (Year)	Number of Strictures	Number of Strictures		Overall Performance in All Strictures					Sensitivity in Hilar Strictures (%)
		Confirmed	Hilar Biliary Malignant <sup>a</sup>	Sensitivity (%)	Specificity (%)	PPV (%)	NPV (%)	Accuracy (%)	
Fritscher-Ravens et al. <sup>135</sup> (2000)	10	10	10	80	—	100	—	—	80
Rosch et al. <sup>38</sup> (2002)	43	26	3	79	62	76	66	—	—
Lee et al. <sup>136</sup> (2004)	42	24	1	47	100	100	50	—	—
Eloubeidi et al. <sup>139</sup> (2004)	28	21	15	86	100	100	57	88	67
Fritscher-Ravens et al. <sup>140</sup> (2004)	44	32	44	89	100	100	67	91	89
Rosch et al. <sup>138</sup> (2004)	50	28	11	75	100	100	58	70	25
Byrne et al. <sup>133</sup> (2004)	35	11	3	45	100	100	—	—	—
Meara et al. <sup>137</sup> (2006)	46	30	—	87	100	—	—	—	—
DeWitt et al. <sup>134</sup> (2006)	24	23	24	77	100	100	29	79	77
Saifuku et al. <sup>144</sup> (2010)	34	17	0	94	82	84	93	88	—
Mohamadnejad et al. <sup>131</sup> (2011)	81	81	30	73	100	—	—	—	59
Ohshima et al. <sup>142</sup> (2011)	22	18	2	100	100	100	100	100	—
Nayar et al. <sup>143</sup> (2011)	32	24	32	52	100	100	54	68	52
Tummala et al. <sup>141</sup> (2013)	342	248	—	92	—	—	81	92	—
Weilert et al. <sup>132</sup> (2014)	68	65	—	94	100	100	50	94	—
Tellez-Ávila et al. <sup>145</sup> (2014)	39	28	39	79	100	100	42	82	—

<sup>a</sup>Based on surgical pathology, unequivocal cytology, or prolonged clinical follow-up.

The clinical ramifications of needle track seeding were demonstrated in another study including 191 patients with hilar cholangiocarcinoma who underwent primary tumor FNA as part of liver transplant evaluation.<sup>167</sup> A total of 16 patients underwent transperitoneal FNA (13 percutaneous, 3 EUS). During intraoperative staging, peritoneal deposits were discovered in only 14/175 (8%) patients who did not undergo FNA versus 5/6 (83%), with a positive preoperative FNA ( $P = .01$ ). On the other hand, El Chafic et al. reported no difference in progression-free or overall survival between patients with cholangiocarcinoma who underwent preoperative FNA and those who did not in patients undergoing curative intent resections.<sup>168</sup> Although the presence of peritoneal metastasis can be explained by the disease stage and other factors not well assessed by the studies published so far, FNA of biliary masses has been since adopted as a contraindication to liver transplantation by many centers.

### The Performance of Intraductal Ultrasonography in Biliary Strictures

With the advent of high-frequency (20 MHz) mini-probes over a guidewire, IDUS has emerged as a feasible and promising imaging technique in the diagnosis of biliary strictures. Mini-probes can be easily inserted through the papilla without the need for

sphincterotomy in most cases<sup>169,170</sup> and are capable of performing linear and radial imaging simultaneously in two or three dimensions in one scanning operation. Despite the limited penetration depth, a precise image of an intraductal lesion is often possible, allowing assessment of invasion or compression of adjacent structures. IDUS should be performed prior to drainage in order to avoid inflammatory artifacts, and therefore is best performed by ERCP experts during the same procedure. Literature demonstrates that IDUS can be advanced through biliary strictures in 86% to 100% of cases allowing a complete exam of the stricture,<sup>111,170–175</sup> mostly without previous dilation. Most failures were due to tight strictures of the hilum or intrahepatic ducts that the guidewire could not traverse.<sup>170,174</sup> As with EUS, three layers are seen in the bile duct wall with IDUS. The first hyperechoic layer corresponds to the mucosa in addition to a border echo; the second hypoechoic layer is the smooth muscle fiber with fibroelastic tissue; and the third hyperechoic layer is the thin and loose connective tissue with a border echo. The criteria for malignancy in a stricture were described as disruption of the normal three-layer sonographic pattern of the bile duct wall (outer echogenic, middle hypoechoic, inner echogenic), a hypoechoic infiltrating lesion with irregular margins, heterogeneous echo-poor areas invading surrounding tissue, and continuation of the main hypoechoic mass into adjacent structures (Fig. 16.13). Findings considered

**TABLE 16.4****Performance Characteristics of Fine-Needle Aspiration in Biliary Strictures Based on Location of Stricture**

Study	Design	Overall Sample Size	Primary Stricture/Tumor Site and Number Per Site	Diagnostic Sensitivity of Malignancy on FNA (Including Suspicious Interpretation)	Stent Presence at Time of EUS
Rosch et al. <sup>138</sup> (2004)	Prospective	50	Hilar CBD 4 8	3/11 (27%)	~
Eloubeidi et al. <sup>139</sup> (2004)	Prospective	28	Proximal Distal 15 13	18/21 (86%)	27/28 (96%)
Lee et al. <sup>136</sup> (2004)	Retrospective	42	CHD CBD 1 39	11/24 (47%)	40/42 (95%)
Byrne et al. <sup>133</sup> (2004)	Retrospective	35	CHD CBD 3 32	9/14 (64%)	
Fritscher-Ravens et al. <sup>140</sup> (2004)	Prospective	44	Hilar 44	32/36 (89%)	44/44 (100%)
DeWitt et al. <sup>134</sup> (2006)	Retrospective	24	Proximal 24	17/24 (71%)	
Saifuku et al. <sup>144</sup> (2010)	Retrospective	34	Distal 34	16/17 (94%)	
Mohamadnejad et al. <sup>131</sup> (2011)	Retrospective	81	Proximal Distal 30 51	54/74 (73%)	64/74 (86%) <sup>a</sup>
Nayar et al. <sup>143</sup> (2011)	Retrospective	32	Proximal 32	24/32 (75%)	
Weilert et al. <sup>132</sup> (2014)	Prospective	15	Proximal Distal 7 8	11/15 (73%) <sup>b</sup>	8/51 (16%) <sup>c</sup>

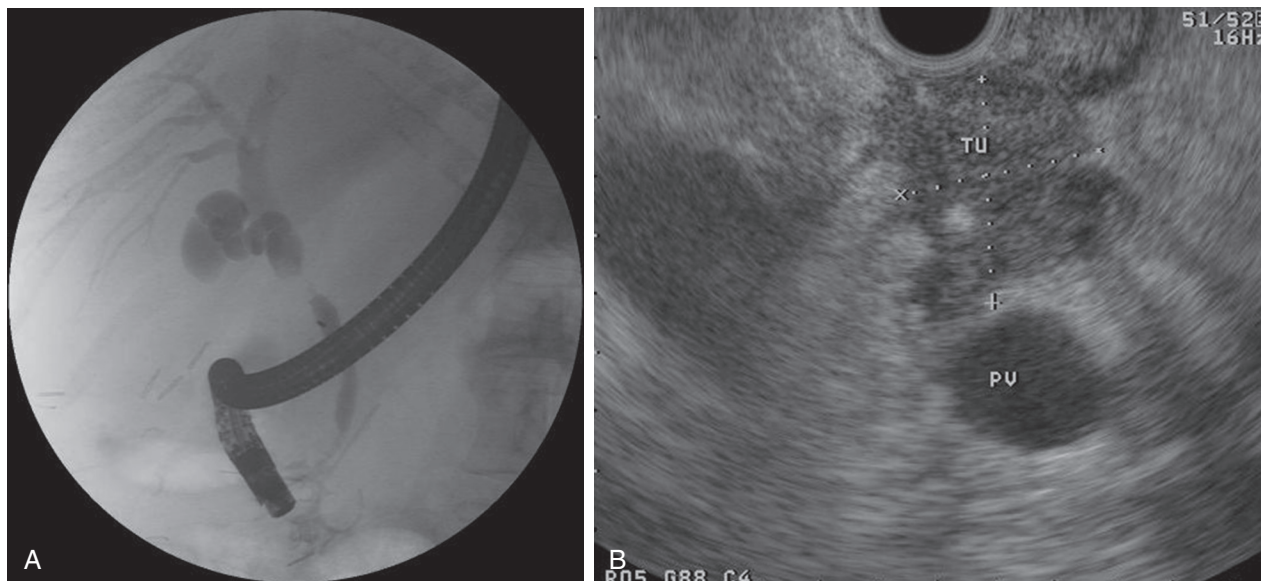
<sup>a</sup>The diagnostic sensitivity of EUS FNA was 45 of 64 (70%) vs. 9 of 10 (90%) for patients with and without a stent, respectively.

<sup>b</sup>This increased to 13/15 (87%) when additional were from FNA of nonprimary sites (lymph node, liver lesion).

<sup>c</sup>Patients with pancreatic masses included in the general cohort ( $n = 34$ ) in addition to the patients with biliary strictures.

Proximal tumors are those designated as hilar or occurring in the common hepatic duct. Distal tumors are those designated as distal or occurring in the common bile duct.

CBD, Common bile duct; CHD, common hepatic duct; EUS, endoscopic ultrasound; FNA, fine-needle aspiration.



• **Fig. 16.11** (A) ERC image of a patient with mid bile duct stricture presenting with jaundice and proximal common bile duct dilation on magnetic resonance cholangiopancreatography. (B) Corresponding linear endoscopic ultrasound images of the patient in 11a confirming an irregular 19 mm bile duct mass without encasement of the portal vein. Fine-needle aspiration confirmed adenocarcinoma. PV, Portal vein; TU, tumor. (Figures courtesy of Dr. John DeWitt.)

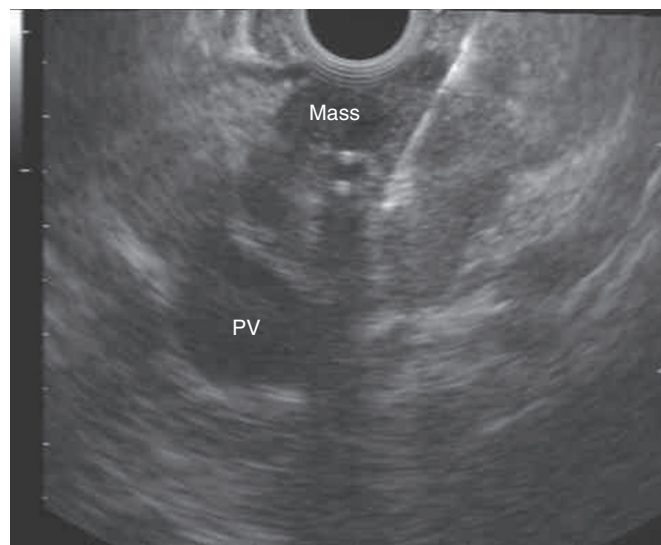


**Fig. 16.12** A linear exam of a hilar cholangiocarcinoma being aspirated. A plastic biliary stent is seen in the lumen of the duct which could help localize the lesions on endoscopic ultrasound. PV, Portal vein. (Figure courtesy of Dr. John DeWitt.)

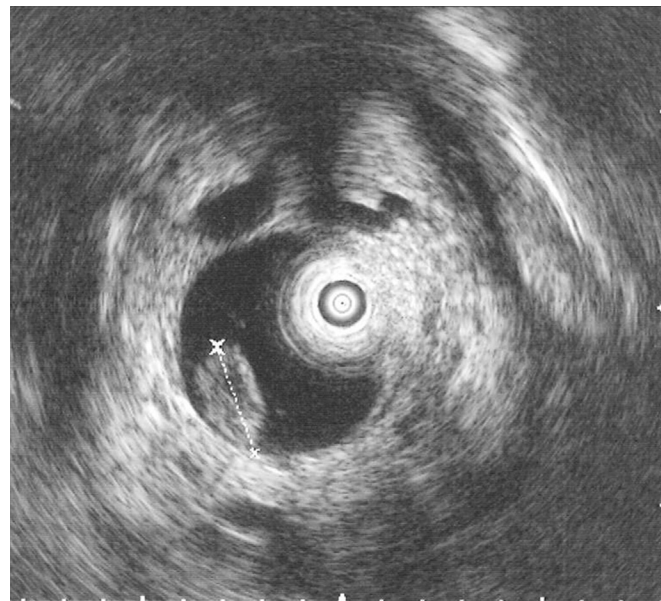


**Fig. 16.13** Two-dimensional intraductal ultrasonography image of a small solid mass (white crosses) protruding in the lumen of the common bile duct consistent with early stage cholangiocarcinoma.

diagnostic of a benign stricture include preservation of the normal three-layer sonographic wall pattern, homogeneous echo patterns, smooth margins, hyperechoic lesions, and the absence of a mass lesion. Additional criteria proposed include interruption of the bile duct wall, presence of any sessile morphology of a tumor, and tumor size greater than 10 mm.<sup>176</sup> The accuracy of IDUS in differentiating benign from malignant strictures ranges from 76% to 92% in series of patients with various causes of biliary strictures.<sup>111,170,171,173,175-177</sup> The vast majority of patients without the above-mentioned criteria and with negative samplings do not have a malignant lesion with 95% accuracy and 100% NPV.<sup>176</sup> The presence of two of the criteria, even with negative biopsies, is highly suspicious of malignancy. An additional negative predictive

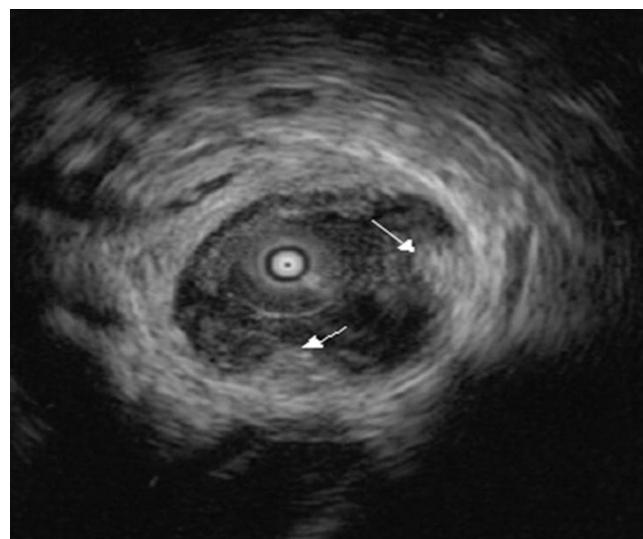
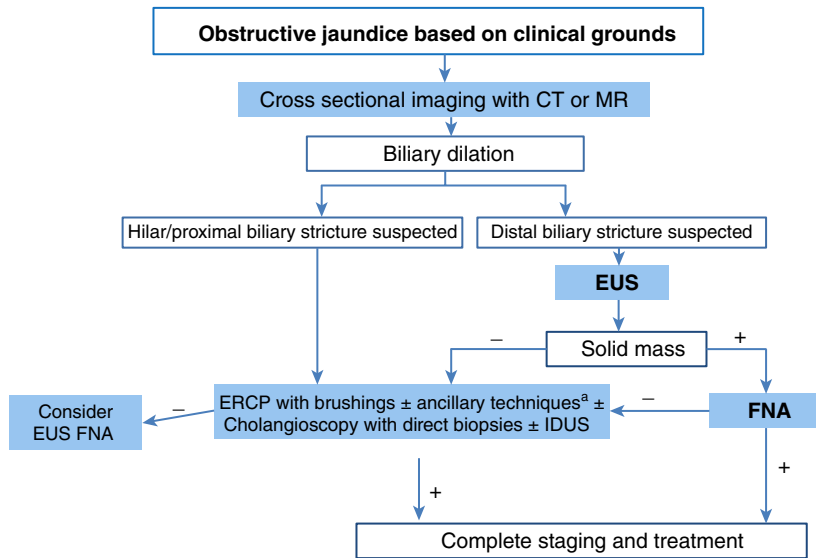


**Fig. 16.14** Two-dimensional intraductal ultrasonography image showing biliary papillomatosis with intrahepatic polypoid spread (arrows).

criterion added by Krishna et al. was wall thickness of  $\leq 7$  mm, which was associated with NPV of 100% in the absence of extrinsic compression.<sup>172</sup> When recently compared to CT and EUS in a large surgical cohort, the combination of ERCP and IDUS provided a statistically superior accuracy in diagnosing malignant biliary strictures.<sup>178</sup> Additionally, IDUS is very effective in confirming an extrinsic compression by a vascular structure or by a stone impacted in the cystic duct and compressing the CBD (Mirizzi's syndrome).<sup>111,176,179</sup> Biliary papillomatosis, frequently misdiagnosed with other imaging such as EUS, ERCP, and magnetic resonance imaging (MRI), appears on IDUS as normal biliary ducts with alternating areas covered by polypoid lesions protruding into the lumen (Fig. 16.14).<sup>180</sup> In 30 patients with cholangiocarcinoma studied by IDUS, biliary papillomatosis was shown in three (10%) and confirmed by biopsy or surgery.<sup>179</sup> The clinical impact of this diagnosis can be important, as young patients with biliary papillomatosis without advanced cholangiocarcinoma should be treated with pancreaticoduodenectomy in combination with partial hepatectomy or liver transplantation.<sup>180</sup> In primary sclerosing cholangitis (PSC) presenting with dominant strictures, IDUS has been traditionally considered no more accurate than other imaging modalities in the diagnosis of cholangiocarcinoma.<sup>181</sup> However, recent studies show encouraging results.<sup>102,182</sup> In a prospective study, 40 patients with PSC underwent ERCP with IDUS which was associated with a sensitivity, specificity, accuracy, positive predictive value (PPV), and NPV of 88%, 91%, 90%, 70%, and 97%, respectively, for predicting malignancy.<sup>182</sup>

### Cholangioscopy in Biliary Strictures

As the design, maneuverability, and optical resolution of cholangioscopes continue to improve,<sup>183</sup> peroral cholangioscopy is emerging as an important adjunct to ERCP in the assessment of biliary strictures, particularly the proximal ones. Direct visualization and targeted biopsy of bile duct lesions should be performed whenever possible during cholangioscopy. When compared with ERCP brush cytology, peroral cholangioscopy was 100% sensitive and 89% specific for biliary strictures and increased the diagnostic accuracy to more than 90% in earlier literature.<sup>184</sup> In a Japanese multicenter trial, the accuracy



• **Fig. 16.15** An algorithm for the management of jaundiced patients suspected to have cholangiocarcinoma. *CT*, Computed tomography; *ERCP*, endoscopic retrograde cholangiopancreatography; *EUS*, endoscopic ultrasound; *FNA*, fine-needle aspiration; *IDUS*, intraductal ultrasonography; *MR*, magnetic resonance.

of endoscopic retrograde cholangiography (ERC) alone, ERC with cholangioscopy, and ERC with cholangioscopy + biopsy for the diagnosis of bile duct malignancy were 74%, 84%, and 93%, respectively.<sup>119</sup> More recently, Nguyen et al. reported on the utilization of EUS FNA before considering cholangioscopy in brushing-negative biliary strictures.<sup>185</sup> The need for cholangioscopy was avoided in 60% of patients where EUS FNA provided tissue diagnosis, resulting in reduction of complications by 2.5% and in cost savings.<sup>185</sup> However, in patients with proximal biliary strictures, the performance of EUS-FNA remains suboptimal. Siddiqui et al. demonstrated that cholangioscopy provided a definitive diagnosis in 77% of patients where ERCP-guided cytology brushing and EUS FNA were both inconclusive.<sup>186</sup> Finally, a recent cost utility analysis demonstrated that SOC with targeted biopsies provided a more cost-effective strategy compared to ERCP with brushings and FISH in patients with PSC strictures.<sup>187</sup> Based on the above, we recommend an EUS FNA approach first in distal biliary strictures, reserving cholangioscopy to mid and proximal biliary strictures with complementary EUS FNA.

A new digital cholangioscope is increasingly available and provides high-definition endoscopic images and allows direct tissue sampling. Navaneethan et al.<sup>115</sup> reported on the use of this system in 98 patients in a multicenter trial. Superior views of the ductal lumen and mucosa were obtained in all 44 patients with indeterminate biliary strictures. Among the 44 patients who underwent SOC-guided biopsies, the specimen was adequate for histologic evaluation in 43 (98%). The sensitivity and specificity of SOC visual impression for diagnosis of malignancy was 90% and 96%, respectively. The sensitivity and specificity of SOC-guided biopsies for diagnosis of malignancy was 85% and 100%. Similar results were recently reported by Tanaka et al. from Japan.<sup>188</sup> Cholangioscopy-related complications were reported to be as high as 7%<sup>189</sup>; however, more recent data from the digital SOC indicate an overall adverse event rate of 3% that were mainly postprocedural pancreatitis and cholangitis.<sup>115</sup>

## Multimodality Approach to Bile Duct Strictures

Because the performance of different diagnostic tests remains suboptimal, the decision concerning the use of the various imaging and tissue sampling modalities remains critical and often involves a combination of studies. In a prospective study of 142 patients with cholestasis and common hepatic duct dilatation of unclear etiology showed that a diagnostic algorithm with MRCP followed by EUS was highly sensitive and specific (90% and 98%, respectively) for the early diagnosis of extrahepatic bile duct carcinoma.<sup>190</sup> The respective limitations and risks of EUS (+/-FNA) and ERCP + IDUS should be considered as well prior to the assessment of any biliary stricture. If the stricture is localized at the level of the CBD, EUS should be proposed after noninvasive imaging modalities, due to its excellent performance in distal biliary lesions and its ability to sample tissue (Fig. 16.15). Needle track seeding should not be a concern while sampling distal biliary masses in surgically fit patients with highly suspected malignancy because the resection field encompasses the needle track. In patients with more proximal strictures, EUS and EUS FNA have several limitations and digital SOC, IDUS, and other ERCP-based tissue sampling techniques should be considered instead.<sup>115,120</sup> In view of its low NPV in proximal strictures, EUS FNA should be reserved for negative or nondiagnostic ERCP brush cytology or cholangioscopy results and only if high probability of malignancy exists. Nevertheless, some authors propose the systematic addition of EUS FNA to ERCP brushings to optimize the diagnostic yield.<sup>191</sup>

In summary, we propose the following for the management of the bile duct strictures (see Fig. 16.15).

- *For CBD strictures:* EUS plus FNA first, followed by ERCP and brush cytology/forceps biopsy/cholangioscopy and IDUS if needed.

- For common hepatic duct and hilar strictures: MRI plus ERCP with cholangioscopy. If cholangioscopy is not available, brush cytology/forceps biopsy under fluoroscopy (with FISH) should be considered in addition to IDUS if available. EUS FNA can be considered when a strong clinical suspicion for malignancy persists after a negative ERCP-based workup.

### Staging of Cholangiocarcinoma

When a bile duct carcinoma is diagnosed, the aim of the staging is to primarily determine candidacy for surgical resection, which offers the only practical chance of cure. Histologically, tumor invasion is limited to the mucosa or fibromuscular layer of the extrahepatic bile duct in early cancers, regardless of lymph node metastasis. Pathologically, bile duct carcinomas are generally staged according to the modified version of the tumor, node, and metastases (TNM) staging system: T1, where tumor is limited to the CBD wall; T2, tumor invasion beyond the CBD wall; and T3, tumor invasion of adjacent structures such as the pancreas, duodenum, and portal vein.

In a prospective study comparing EUS and IDUS in biliary strictures, the accuracy of IDUS in T staging (78%) was higher than that of EUS (54%).<sup>127</sup> EUS accuracy was inferior mainly in hilar or common hepatic duct strictures due to the limited field of examination. N staging accuracy was comparable in both modalities, but other authors found that the depth of penetration of the standard 20-MHz catheter probe was not adequate for the evaluation of lymph nodes associated with advanced malignant strictures.<sup>111</sup> In a large surgical series,<sup>192</sup> the sensitivity, specificity, and accuracy of IDUS for biliary strictures were 93%, 89%, and 91%, respectively. In the subgroup analysis of malignancy prediction, IDUS showed best performance in cholangiocarcinoma (sensitivity of 98%) followed by pancreatic carcinoma (94%), gallbladder cancer (89%), and ampullary cancer (81%).<sup>192</sup>

From a practical perspective, the main question for the staging of biliary tumors is resectability, which relies on vascular, longitudinal, and tumor spread to adjacent organs like the pancreas. Conventional cross-sectional imaging such as MRI and CT can be useful to identify nonresectable patients, such as those with a Bismuth type IV Klatskin tumor and those with metastatic disease. New generation multidetector CT scanners and MRI provide high-resolution imaging to identify lateral spread of the tumor to vessels; however, the extent of longitudinal spread of tumor along the bile duct remains very difficult to assess. The accurate assessment of microscopic involvement of the bile duct wall remains challenging as well, resulting in understaging of the resection margins in some patients. Cholangiography and peroral cholangioscopy with biopsy can be limited in determining the extent of longitudinal and depth of spread.<sup>193,194</sup> IDUS has a reported sensitivity as high as 85% for cholangiocarcinoma staging when asymmetric wall thickening was considered as a criterion of longitudinal tumor spread on the proximal and distal sides of the lesion compared with cholangiography (47% and 43%, respectively).<sup>174,195</sup> However, prior drainage of the biliary tract causes inflammatory thickening of the duct wall and limits the performance of IDUS.<sup>196</sup> Therefore IDUS must be carried out at the same time as the index ERCP for optimal results. Additionally, IDUS can be very accurate in defining portal vein and right hepatic artery involvement (Fig. 16.16), which are the two most frequently involved vessels. In addition, invasion of the adjacent pancreatic parenchyma by a bile duct tumor should

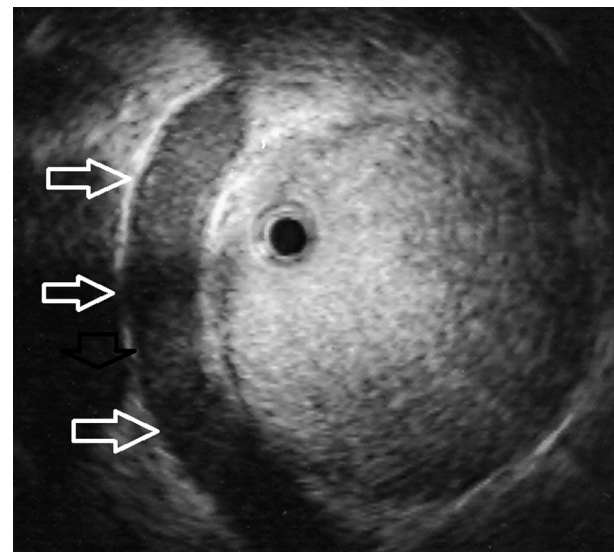


**Fig. 16.16** Two-dimensional intraductal ultrasonography obtained for staging of cholangiocarcinoma. It shows no infiltration of the right hepatic artery (arrows).

be determined preoperatively, and in this case, pancreaticoduodenectomy in combination with bile duct resection is recommended. Controlled series comparing the performance of each imaging modality (CT, MRCP, EUS, and IDUS) in staging of bile duct tumors are lacking. A clinical approach in patients with Klatskin tumors should be to start with MRI and MRCP. In patients with resectable tumors, ERCP plus IDUS, if available, should be the second step, carried out to assist in surgical planning. For bile duct tumors, EUS remains the most effective approach. ERCP plus IDUS could be utilized when the upper part of the tumor cannot be seen with EUS, or when doubt remains concerning spread to the portal vein. Finally, EUS and IDUS are useful tools in determining the nature of a biliary stenosis and for the staging of cholangiocarcinoma. As a result of their respective limitations (hilum imaging for EUS, and need for biliary access and drainage with IDUS), their use depends on the presence of local expertise, clinical presentation, and results of conventional imaging.

### DIAGNOSTIC CHECKLIST

#### Cholangiocarcinoma

- Hypoechoic thickening of the wall with or without a mass
- Polyoid intraluminal tumor
- Involvement of vessels, pancreas, liver, ampulla, or duodenum
- Bile duct dilation
- Presence of adenopathy

#### Papillomatosis

- Polyoid intraluminal tumor alternating with normal bile duct wall

#### Mirizzi Syndrome

- Compression of CBD by intracystic stone
- Regular thickening of bile duct wall

#### Other Benign Stenoses

- Regular or symmetric thickening without wall disruption

## Endoscopic Ultrasound in Gallbladder Disease (Excluding Stones)

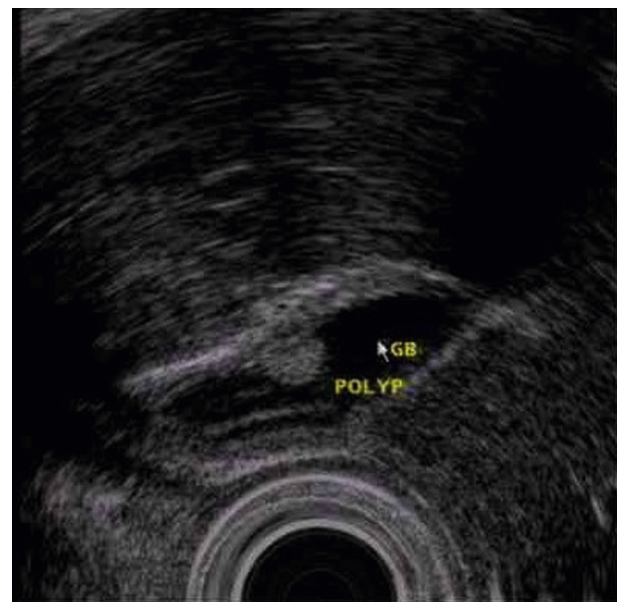
### Gallbladder Polyps

The widespread use of US has led to the identification of an increasing number of polypoid lesions of the gallbladder which can be present in up to 5% of the population.<sup>197</sup> Cholesterol, inflammatory and fibrous polyps have no malignant potential, and surgical intervention is not required as long as the patient is asymptomatic. In contrast, adenomatous polyps must be resected as the adenoma-carcinoma sequence is well characterized in the biliary epithelium of the gallbladder. Given that gallbladder carcinoma carries one of the most dismal prognoses among malignancies of the digestive system, management of adenomatous gallbladder polyps is crucial.

The incidental finding of a gallbladder polyp on TUS, CT, or MRI in an asymptomatic patient often leads to a clinical dilemma. The presence of a solitary lesion, measuring greater than 10 mm in diameter, of sessile appearance, irregular contour, and hypoechoogenicity on TUS are findings suggestive of a neoplastic polyp<sup>198</sup> and cholecystectomy is recommended.<sup>199</sup> However, polyps smaller than 5 mm in diameter with echogenic and pedunculated appearance usually represent cholesterol and inflammatory polyps,<sup>200</sup> where only imaging follow-up is recommended. This approach, however, has been debated because a significant proportion of polyps exceeding 10 mm in size can be nonneoplastic. Therefore offering cholecystectomy for gallbladder polyps larger than 10 mm will result in resection of otherwise benign polyps with low neoplastic potential.<sup>201</sup> On the other hand, 19% to 29% of polyps between 5 and 10 mm of size were found to be adenomas in some studies,<sup>198,200</sup> with a few malignancies reported in this size range.<sup>202</sup> Therefore a highly accurate diagnostic study is necessary to determine the best therapeutic approach. TUS is well suited as a first line test due to its safety and availability; however, its sensitivity for diagnosing gallbladder polyps was only 50% in a large surgical series.<sup>203</sup> Owing to its high resolution, EUS is better positioned to provide more accurate imaging than TUS for gallbladder lesions.<sup>198,200,204,205</sup>

The gallbladder wall can readily be seen with EUS as a two-layered structure. The inner hypoechoic layer represents the mucosa, muscular layer, and subserosal fibrous layer. The outer hyperechoic layer represents the subserosal fat layer and serosa. On EUS, gallbladder polyps are fixed structures protruding into the gallbladder lumen without acoustic shadowing. EUS was superior to TUS in diagnosing the nature of gallbladder polyps in earlier studies where 87% of polyps were correctly diagnosed by EUS, compared with only 52% by TUS. The sensitivity, specificity, PPV, and NPV of EUS in the diagnosis of carcinoma were 92%, 88%, 76%, and 97%, respectively.<sup>204</sup> However, a recent comparative study showed that high-resolution TUS provided comparable results to EUS with sensitivity and specificity for carcinoma of 83% and 44% using HRUS, and 86% and 22% using EUS.<sup>206</sup>

Two series proposed a scoring system that relied on EUS findings in order to ascertain the risk of neoplasia.<sup>200,207</sup> In a retrospective analysis of EUS findings in 70 patients operated on for polypoid gallbladder lesions smaller than 20 mm, Sadamoto et al.<sup>207</sup> analyzed the morphologic characteristics of gallbladder polyps by multivariate stepwise logistic regression. Internal echo pattern and size were positively associated with neoplasia, whereas hyperechoic spots were negatively associated with neoplasia. All neoplastic polyps, including the smaller ones, were shown to have a relatively heterogeneous internal echo pattern on EUS. In



• **Fig. 16.17** Radial endoscopic ultrasound image of a small gallbladder polyp (arrow).

contrast, large cholesterol polyps (more than 10 mm in diameter) had a homogeneous internal echo pattern. In this study, the sensitivity, specificity, and accuracy with an EUS-based scoring system developed from the above criteria were 78%, 83%, and 83%, respectively.<sup>207</sup> Another scoring system based on five EUS variables has been proposed to predict the malignancy of gallbladder polyps.<sup>200</sup> This system is based on layer structure, echo pattern, margin, stalk, and number of polyps. According to this study, size was the most significant predictor of neoplasia in polyps. All polyps with a diameter of 5 mm or less were nonneoplastic, whereas 94% of polyps larger than 15 mm were neoplastic. When the size of a gallbladder polyp exceeded 15 mm, the risk of neoplasia increased significantly compared with that of polyps measuring 5 to 10 or 10 to 15 mm in diameter. It is clear from the above studies that polyp size remains a simple but strong predictor of neoplasia in gallbladder polyps. Although the presence of hypoechoic foci was the best individual predictive factor for neoplastic polyps in a more recent series,<sup>208</sup> polyps exceeding 15 mm in size were strongly associated with malignancy (odds ratio [OR] of 22). In another study, EUS was always superior to TUS in accurately identifying neoplastic polyps of all sizes; however, EUS accuracy was only 44% among polyps smaller than 10 mm, in comparison with 89% for those greater than 10 mm.<sup>209</sup> Finally, the advent of adjunct technologies has helped improve the ability of EUS to detect malignant gallbladder polyps. Choi et al. reported on the use of contrast-enhanced harmonic (CEH) EUS for this indication.<sup>205</sup> The presence of an irregular vessel pattern in malignant polyps resulted in an improved sensitivity and specificity of CEH-EUS compared to conventional EUS (94% and 93% vs. 90% and 91%, respectively). In another smaller series, Park et al.<sup>210</sup> found that CEH-EUS also helped differentiate cholesterol polyps from gallbladder adenomas. In view of this performance, EUS can be proposed also as a surveillance tool for polyps not meeting resection criteria; however, longitudinal studies are lacking in this field.

A systematic surgical approach for gallbladder polyps more than 1 cm in size remains a safe and widely practiced approach. It could be proposed to apply EUS for polyps that measure between 5 and 10 mm (Fig. 16.17). In cases where EUS identifies suspicious

features, surgery should be strongly considered. In other cases, EUS would be a reference examination for polyps that exhibit growth or changes in echo patterns and shape on TUS follow-up.<sup>211</sup>

## Gallbladder Tumors

The wide replacement of open cholecystectomy by the laparoscopic approach highlighted the significance of accurate preoperative diagnosis of gallbladder cancer due to increased risk of abdominal wall cancer recurrence after laparoscopic cholecystectomy of carcinomas.<sup>212,213</sup> Recent advances in TUS and CT have made it possible to diagnose gallbladder carcinoma at an earlier stage. However, these modalities can stage only advanced lesions. As EUS can be helpful in differentiating benign from malignant polyps, it can also help to guide the optimal surgical approach: laparoscopy for benign polyps or early cancer, and open surgery for advanced cancer.

Gallbladder cancer is staged according to the American Joint Committee on Cancer (AJCC) TNM staging classification system (Table 16.5). The accuracy of EUS in gallbladder cancer staging depends on the criteria chosen. The integrity of the wall layers at the base of a gallbladder polyp remains the determinant criterion for deep invasion (Fig. 16.18). Fujita et al.<sup>214</sup> classified the tumors based on depth of invasion in a retrospective EUS study with good interobserver correlation. After correlation of EUS and histopathology, the authors proposed that solid echogenic pattern and fine nodular surface indicate stage *Tis*, whereas irregularity of the outer hyperechoic layer of the gallbladder by a mass lesion correlates to *T2* stage where the tumor invades the adipose layer of the subserosa. In another retrospective study of 41 patients with gallbladder cancer,<sup>215</sup> a strong correlation between EUS and histopathologic tumor stage was found. EUS images were classified according to the shape of the tumor and the adjacent gallbladder wall structure as follows: type A, pedunculated mass with preserved adjacent wall structure; type B, sessile and/or broad-based mass with a preserved outer hyperechoic layer of the gallbladder wall; type C, sessile and/or broad-based mass with a narrowed outer hyperechoic layer; and type D, sessile and/or broad-based mass with a disrupted outer hyperechoic layer (Fig. 16.19). On histopathology, type A corresponded to *Tis*, type B to *T1*, type C to *T2*, and type D to *T3* to *T4* stages with corresponding accuracies of 100%, 76%, 85%, and 93% for the four types, respectively. The best staging performance was found in *Tis* and *T3* to *T4* tumors.

FNA of gallbladder masses has been attempted and found to be accurate in diagnosing primary and metastatic malignant tumors, with sensitivity ranging from 80% to 100% (Table 16.6).<sup>137,216–221</sup> The incidence of complications from direct puncture of the gallbladder appears to be low from the small published series, but biliary peritonitis and acute cholecystitis<sup>219</sup> have been reported following FNA of masses and during sampling of bile for crystals to evaluate for causes of acute pancreatitis.<sup>222</sup> To minimize this risk, 25-gauge needles should be used for this indication and the least number of passes be performed, ideally in the presence of on-site cytopathology review (Fig. 16.20; Video 16.8).

From a management perspective, an extended cholecystectomy with systematic lymph node dissection and resection of the liver bed should be applied to all *T3* and *T4* tumors, whereas laparoscopic cholecystectomy is likely sufficient for *Tis* tumors. The preoperative differentiation of *T1* and *T2* tumors is more difficult on EUS and the appropriate surgical approach in this group of patients remains controversial.<sup>223</sup> When a hypoechoic area within

**TABLE 16.5** TNM Staging of Gallbladder Cancer

### Primary Tumor (T)

TX	Primary tumor cannot be assessed
T0	No evidence of primary tumor
Tis	Carcinoma in situ
T1	Tumor invades lamina propria or muscular layer
T1a	Tumor invades lamina propria
T1b	Tumor invades muscular layer
T2	Tumor invades perimuscular connective tissue on the peritoneal side, without involvement of the serosa (visceral peritoneum) <i>Or</i> tumor invades perimuscular connective tissue on the hepatic side with no extension into the liver
T2a	Tumor invades perimuscular connective tissue on the peritoneal side, without involvement of the serosa (visceral peritoneum)
T2b	Tumor invades perimuscular connective tissue on the hepatic side, with no extension into the liver
T3	Tumor perforates the serosa (visceral peritoneum) and/or directly invades the liver and/or one other adjacent organ or structure, such as the stomach, duodenum, colon, pancreas, omentum, or extrahepatic bile ducts
T4	Tumor invades main portal vein or hepatic artery or invades two or more extrahepatic organs or structures

### Regional Lymph Nodes (N)

NX	Regional lymph nodes cannot be assessed
N0	No regional lymph node metastasis
N1	Metastases to one to three regional lymph nodes <sup>a</sup>
N2	Metastases to four or more regional lymph nodes

### Distant Metastasis (M)

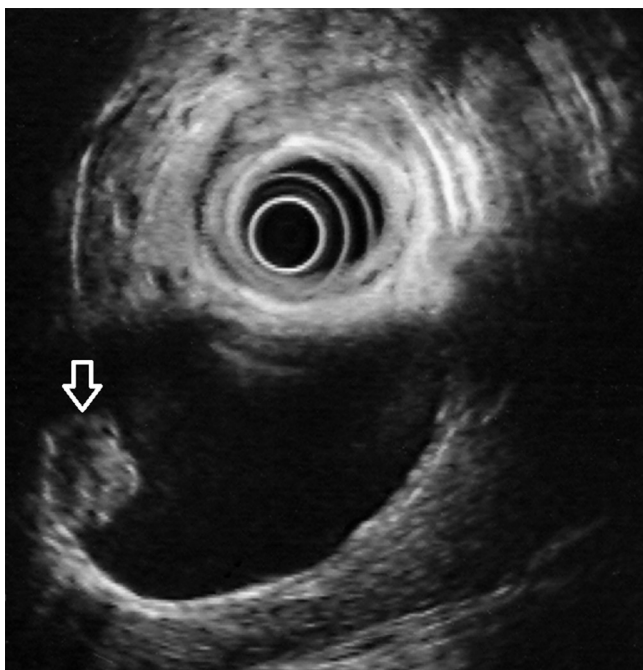
M0	No distant metastasis
M1	Distant metastasis

<sup>a</sup>Including lymph nodes along the cystic duct, common bile duct, hepatic artery, and/or portal vein.

the deeper part of the tumor was found on EUS, the differentiation between *T1* and *T2* tumors was possible, and indicated subserosal invasion.<sup>224</sup> However, this finding is only valuable in polypoid gallbladder tumors.

## Summary

The value of EUS FNA for the diagnosis and staging of gallbladder tumors remains questionable. This approach appears to be safe for obtaining diagnostic samples from gallbladder masses for cytologic examination.<sup>137,218,220</sup> It could also be used for confirming lymph node involvement, as the existence of malignant lymph nodes indicates stage III disease irrespective of *T* staging (see Table 16.5). Nevertheless, due to the limited NPV of FNA, surgery should be pursued in all patients with suspicious gallbladder lesions despite a negative cytology.



• **Fig. 16.18** Radial endoscopic ultrasound image of an adenomatous gallbladder polyp measuring 15 mm in diameter (arrow).



• **Fig. 16.19** Linear endoscopic ultrasound image (7.5 MHz) of a large gallbladder mass in a 55-year-old female patient presenting with weight loss, right upper quadrant pain, and elevated liver enzymes. Substantial thickening of the gallbladder wall with complete loss of the wall layers, along with invasion of the adjacent liver parenchyma were the basis of T3 staging in this case. The lumen of the gallbladder is significantly restricted with sludge seen in it.

Due to the small and retrospective nature of EUS series in the staging of gallbladder cancer, the utility of EUS for the routine staging of this disease remains unclear. Nevertheless, EUS appears to be effective in the detection of early tumors and allows the appropriate classification of more advanced cases (T3, T4, and N1 disease), where open cholecystectomy with radical resection should be performed. In all other cases, open cholecystectomy with adaptation of the extent of resection during surgery should be pursued on a case-by-case basis.

## Other Gallbladder Disorders Presenting With Wall Thickening

Localized or diffuse thickening of the gallbladder wall can be associated with a myriad of disorders (Table 16.7). When diffuse thickening and perivesicular fluid are present, differentiation of acute cholecystitis from other conditions such as ascites, portal hypertension, viral hepatitis, and hypoalbuminemia can be difficult.<sup>225</sup> Therefore it is important to rely on the clinical presentation and findings of other imaging studies in these cases.

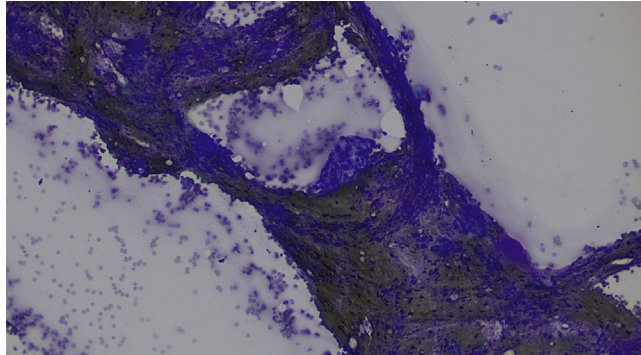
Other conditions with diffuse or localized gallbladder wall thickening can be difficult to differentiate from neoplastic disease. Chronic cholecystitis is a common condition where gallstones are seen in association with a hyperechoic wall with a preserved layer structure. The wall is usually uniformly involved, but localized thickening is possible.<sup>226</sup> Adenomyomatosis of the gallbladder is generally considered a benign condition associated with diffuse thickening of its wall along with the presence of small cysts, which usually represent intramural diverticula (dilated Rokitansky-Aschoff sinuses). Ultrasonographically, layers are preserved despite a thickened wall but sometimes can be associated with hyperechoic echoes (comet-tail artifact).<sup>198</sup> According to the extent and site of involvement, adenomyomatosis can be classified into localized, generalized, and segmental types. The diagnosis is generally straightforward on TUS and cancer mimicking adenomyomatosis is extremely rare.<sup>227</sup> Nevertheless, some cases can be difficult to diagnose, especially the localized type, and segmental adenomyomatosis has been linked to gallbladder carcinoma, especially in elderly patients.<sup>228</sup> Xanthogranulomatous cholecystitis (XGC) is an uncommon form of chronic inflammation of the gallbladder, the clinical presentation of which is similar to that of cholecystitis. In a large 15-year series of cholecystectomy, XGC was present in 1.5% of patients<sup>229</sup> and was associated with lithiasis in 85% of patients. XGC may simulate gallbladder cancer (see Table 16.7), and EUS can sometimes visualize hyperechoic nodules in the gallbladder wall, probably representing xanthogranulomas.<sup>230</sup>

Overall, the role of EUS in the diagnosis of gallbladder wall thickening remains poorly defined. Mizuguchi et al.<sup>231</sup> compared EUS, conventional US, CT, and MRI in the differential diagnosis of gallbladder wall thickening. The multiple-layer pattern was demonstrated more effectively by EUS than by other imaging modalities. Loss of multiple-layer patterns of the gallbladder wall demonstrated by EUS was the most specific finding in diagnosing gallbladder cancer. It is nevertheless not pathognomonic, as this finding can also be seen in XGC.<sup>230</sup> In a series by Kim et al., EUS characteristics were reviewed in 134 patients with gallbladder wall thickening including 11 cancers who subsequently underwent cholecystectomy. Wall thickening greater than 10 mm and hypoechoic internal echogenicity were associated with neoplastic wall thickening on multivariate analysis.<sup>232</sup> More recently, the utility of harmonic EUS and contrast enhanced harmonic EUS was evaluated in 36 patients with thickened gallbladder wall.<sup>233</sup> The overall sensitivity, specificity, and accuracy for diagnosing malignant gallbladder (GB) wall thickening of H-EUS and CH-EUS were 83% versus 90%, 65% versus 98% ( $P < .001$ ), and 73% versus 94% ( $P < .001$ ), respectively, indicating an additive role contrast enhancement provides for this indication. EUS can also help define gallbladder involvement in other less common conditions such as sclerosing cholangitis,<sup>234</sup> portal venous obstruction resulting in internal gallbladder varices,<sup>235</sup> and diffuse uniform wall thickening in patients with anomalous arrangement of the pancreaticobiliary

**TABLE 16.6 Performance Characteristics of Endoscopic Ultrasound-Fine-Needle Aspiration for the Diagnosis of Gallbladder Masses**

Reference (Year)	No. of Patients	Sensitivity	Specificity	Complications	Comments
Imazu et al. <sup>233</sup> (2014)	36	83% for harmonic EUS; 90% for contrast enhanced harmonic	65% for harmonic EUS; 98% for contrast enhanced harmonic	No complications	No FNA performed, solely based on imaging features
Kim et al. <sup>219</sup> (2012)	13	84.6%	100%	Cholecystitis in 1 patient	Regional adenopathy sampled in 18 patients
Hijioka et al. <sup>217</sup> (2012)	24	96%	100%	No complications	ERC had a diagnostic sensitivity of 47%
Hijioka et al. <sup>216</sup> (2010)	15	89%	100%	No complications	<ul style="list-style-type: none"> <li>Final diagnosis: Xanthogranulomatous cholecystitis in 5 and adenocarcinoma in 10</li> <li>FNA helped appropriately classify XGC in 5 out of 6 suspected cases</li> <li>22-G needles were used in all patients</li> </ul>
Meara et al. <sup>137</sup> (2006)	7	80%	100%	Not specified	22-G needles were used in all patients
Varadarajulu et al. <sup>220</sup> (2005)	6	100%	100%	No complications	
Jacobson et al. <sup>218</sup> (2003)	6	100%	100%	No complications	<ul style="list-style-type: none"> <li>One case of XGC included</li> <li>Suspicious cytology was considered confirmatory</li> <li>22-G needles were used in all patients</li> </ul>

EUS, Endoscopic ultrasound; FNA, fine-needle aspiration; XGC, xanthogranulomatous cholecystitis.



- Fig. 16.20** Cytology image from a gallbladder mass aspirated under endoscopic ultrasound guidance. Features diagnostic of adenocarcinoma include nuclear enlargement, pleomorphism, and increased nuclear cytoplasmic ratio (Diff Quick,  $\times 200$ ).

duct.<sup>236</sup> Finally, the diffuse papillomatosis of the biliary tract may also involve the gallbladder, presenting as a thickening with a protruding mass<sup>237</sup> combined with biliary ducts polyps. FNA appears to be safe as an adjunct to EUS imaging alone and could provide adequate tissue to confirm the diagnosis.<sup>238</sup>

## Summary

In conclusion, the utility of EUS for the diagnosis of gallbladder disease remains less defined than its role in bile duct tumors and stones. TUS, CT, or MRI are generally sufficient to determine

the diagnosis and guide the treatment. EUS could have a niche role in the preoperative assessment of patients with small gallbladder polyps, especially those 5 to 10 mm in size or those greater than 10 mm in poor operative candidates. It may also be helpful before surgery in patients with suspected gallbladder cancer or in those with large polyps suspected to be malignant. Finally, in cases of uncertainty on TUS, EUS could be useful in differentiating benign from malignant gallbladder lesions in the presence of diffuse wall thickening.

## Ampullary Tumors

Tumors of the ampulla of Vater originate from the pancreaticobiliary-duodenal junction, guarded by the sphincter of Oddi. The pancreatic duct and CBD join in the ampulla of Vater and form a distal common channel in about 85% of individuals. The normal ampulla starts about 2 mm outside the duodenal wall and penetrates the muscularis propria somewhat more distally, forming an intraduodenal segment of variable length. A wide variety of tumors arise from the ampulla of Vater, including benign tubular and tubulovillous adenomas, carcinomas, and several other rare pathologic types, such as lipomas, fibromas, neurofibromas, leiomyomas, lymphangiomas, hemangiomas, and various neuroendocrine tumors. Adenomas can occur sporadically and in the setting of polyposis syndromes. They are considered premalignant and the adenoma–carcinoma sequence has been assumed to be behind the pathogenesis of ampullary cancer similar to other locations within the GI tract. Benign adenomas are increasingly detected

**TABLE 16.7****Characteristics and Etiologies of Gallbladder Wall Thickening on EUS**

Disorder	EUS Characteristics	
	Thickening	Others Signs
Acute cholecystitis	Localized or diffuse, layers preserved	Pericholecystic fluid
Chronic cholecystitis	High echogenicity	
Gallbladder carcinoma	Localized, layers inconsistently preserved	Polyp or mass
Adenomyomatosis	Localized or diffuse, layers preserved	Anechoic areas (cysts), hyperechoic echoes, comet tail artifact
Xanthogranulomatous cholecystitis	Localized or diffuse, layers inconsistently preserved	Hyperechoic nodules in the gallbladder wall
Portal hypertension, viral hepatitis, ascites or hypoalbuminemia	Diffuse, layers preserved	Extraluminal ascites
Extrahepatic portal venous obstruction	Localized, layers preserved	Varices inside the gallbladder wall
Primary sclerosing cholangitis	Diffuse, layers preserved	Irregular thickening
Diffuse papillomatosis	Localized or diffuse, layers inconsistently preserved	
Anomalous arrangement of the pancreaticobiliary duct	Diffuse, layers preserved	Predominant thickening of the hypoechoic layer

EUS, Endoscopic ultrasound.

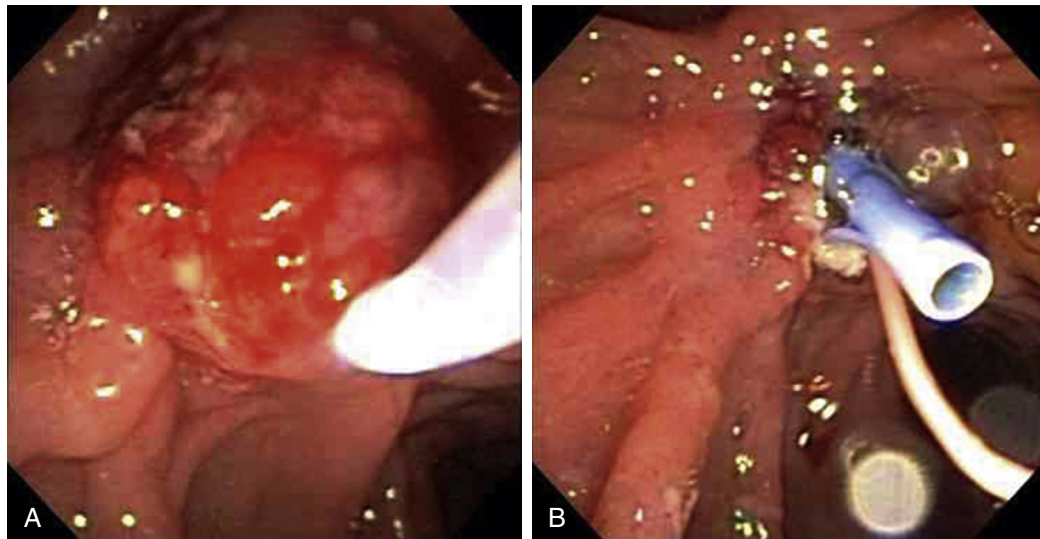


**Fig. 16.21** (A) Endoscopic image of an ampillary adenoma confirmed on mucosal biopsies obtained on previous endoscopy. The patient was referred for endoscopic ampullectomy after endoscopic ultrasound assessment. A snare is noted encircling the lesion. (B) Endoscopic image of the adenoma after endoscopic resection is completed. Note the biliary stent (blue) and pancreatic stent (orange).

during routine upper endoscopy performed for unrelated reasons, and now represent an important proportion of endoscopically treated ampillary tumors (Fig. 16.21).<sup>239</sup> Moreover, endoscopic and EUS surveillance programs are recommended for patients with familial adenomatosis polyposis syndrome (FAP),<sup>240</sup> where the major papilla is a common site of extracolonic adenomas or malignancy in these patients. Tumors can also be discovered in symptomatic patients presenting with jaundice, abdominal pain, weight loss, pancreatitis, or anemia.

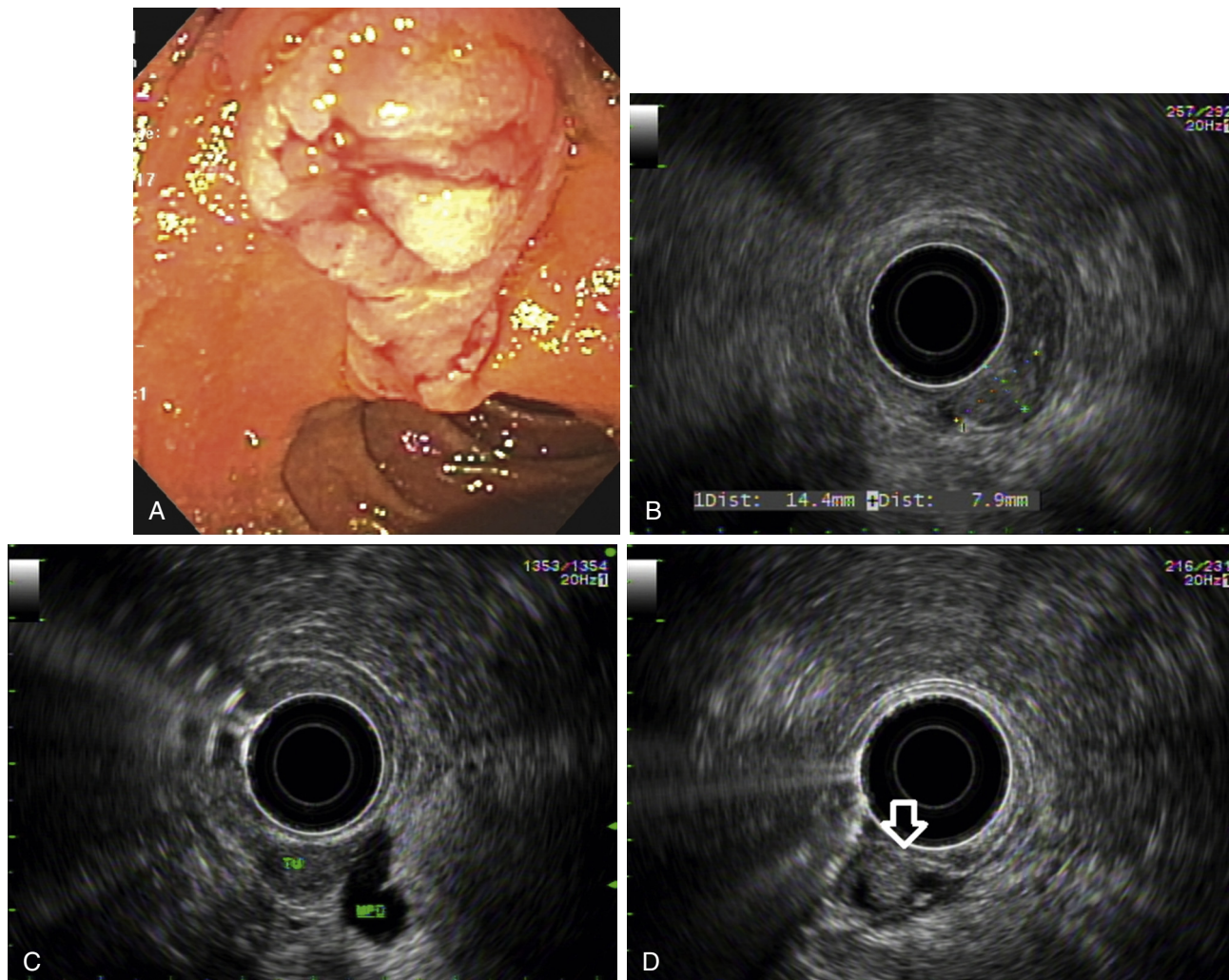
Carcinoma of the ampulla (papillary carcinoma) spreads by extension to contiguous organs and by invasion of lymphatic and/or blood vessels. Most ampillary cancers develop from the mucosa

of the ampulla and infiltrate the Oddi sphincter going through it. They gradually invade the muscularis propria and the serosa of the duodenum, and grow beyond the serosa towards the pancreas. Nevertheless, compared with pancreatic cancer, ampillary neoplasia carries a much better prognosis due to onset of symptoms at an earlier tumor stage.<sup>241</sup> Diagnosis of an ampillary tumor is not always easy endoscopically due to variable appearance ranging from polypoid to ulcerative morphology. Confirming the diagnosis with pathology can also be difficult in ampillary cancers. Mucosal biopsies can be falsely negative owing to intramural extension of the tumor, whereby ES is necessary to expose the endoampillary growth and allow adequate sampling of the tumor. In addition,

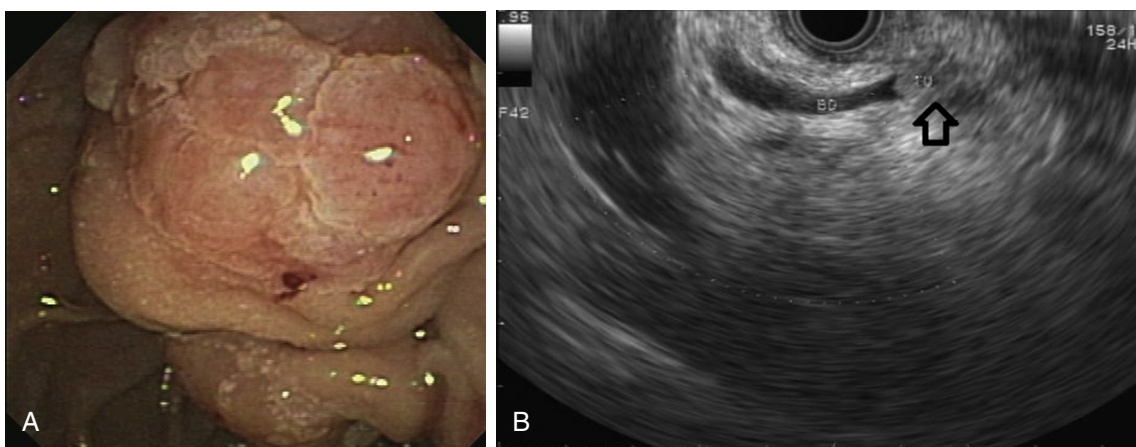


• **Fig. 16.22** A T3 ampullary mass seen in this linear endoscopic ultrasound image. The mass infiltrates the muscularis propria (MP) and invades pancreatic parenchyma. CBD, Common bile duct.

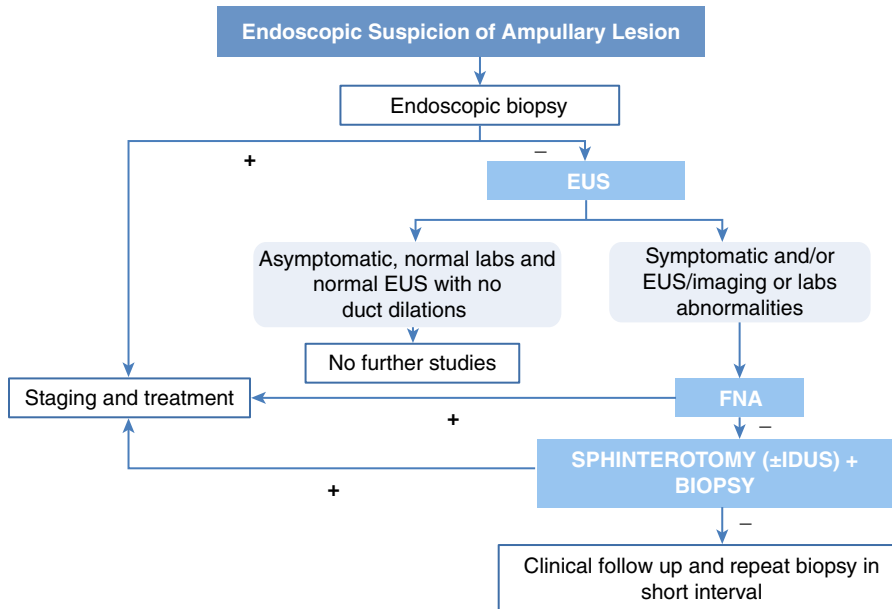
the differential diagnosis between inflammatory changes and an adenoma with low-grade dysplasia can be difficult for the pathologist, and repeated biopsies may be necessary. Finally, standard forceps biopsies may not reliably represent the tumor due to focality of carcinoma within adenomatous lesions leading to an under-detection of malignancy in up to 26% of patients.<sup>242</sup> In view of these limitations, the differentiating a variant of a normal ampulla from an inflamed one, or from a real tumor can be difficult. EUS has been proposed to aid in the diagnosis of a suspected ampillary lesion when faced with a protruding ampulla without mucosal abnormalities. Will et al.<sup>243</sup> reported a series of 133 patients with a variety of ampillary and peri-ampillary lesions found on duodenoscopy. The sensitivity and specificity of EUS in the detection of malignant lesions were 93% and 75%, respectively, using histopathology as the reference standard. This low specificity was also demonstrated by other series where the only specific signs confirming an ampillary mass were infiltration of the duodenal muscularis propria (Fig. 16.22), or the presence of endoluminal growth in the CBD (Figs. 16.23 and 16.24; Video 16.9), or the main pancreatic duct (Video 16.10).<sup>244</sup> The other criteria including echogenicity, enlargement of the ampulla, and CBD or main duct dilation were not specific and were seen in nonneoplastic



• **Fig. 16.23** (A) Endoscopic view of ampillary adenocarcinoma in a patient presenting with a dilated bile duct and elevated transaminases. (B) Partial submucosal infiltration was noted on radial endoscopic ultrasound (EUS) interrogation of the mass. (C) A moderately dilated main pancreatic duct (MPD) on radial EUS exam. (D) Intraductal extension of the tumor noted in the distal part of the dilated bile duct (arrow).



• Fig. 16.24 (A) Ampullary adenocarcinoma (endoscopic view) in a patient presenting with painless jaundice. (B) Intraductal extension of the tumor into the bile duct (arrow). No pancreatic parenchymal invasion noted.



• Fig. 16.25 An algorithm for the management of patients with suspected ampullary lesions. EUS, Endoscopic ultrasound; FNA, fine-needle aspiration; IDUS, intraductal ultrasonography.

pathologies or even in normal ampullae. The sensitivity of EUS in the detection of an ampullary tumor remains high in symptomatic patients presenting with jaundice, for example, but is lower in asymptomatic ones. For example, it is not uncommon in patients with FAP to harbor ampullary tumors without EUS abnormalities. This emphasizes the fact that despite the high sensitivity of EUS for the diagnosis of ampullary tumors, its NPV remains limited and sometimes only a mucosal biopsy can reliably confirm the diagnosis. On the other hand, mucosal biopsies can be inconclusive due to intramural spread of the tumor, whereby the tumor is covered by either ulcerated or inflamed mucosa. Multiple mucosal samples from various parts of the lesion, and repeat sampling from the same area “bite-on-bite” technique can increase the diagnostic yield of mucosal biopsies. The other challenge resides in the fact that even when a representative sample of the tumor is obtained, malignant epithelium tends to be fragmented on biopsies making it difficult to determine the degree of dysplasia in an adenomatous lesion or degree of invasiveness of an adenocarcinoma when no or limited submucosa is present in the biopsy. Given these limitations, FNA can be safely used as an alternative to confirm the

diagnosis and to avoid the risks associated with ES to expose an underlying tumor.<sup>245,246</sup> One major limitation of FNA cytology is to fully characterize the spectrum of cytopathological changes from reactive atypia to high-grade dysplasia to invasive adenocarcinoma, which requires histological assessment not provided by routine cytologic samples.<sup>247</sup> Core biopsy needles have been increasingly used in sampling malignant pancreatic lesions, but their role in ampullary cancers is less clear in the literature. Therefore in patients with a suspicion of ampullary obstruction (based on clinical, biochemical, or imaging criteria) but with inconclusive biopsies and negative EUS, ES with repeated biopsies is needed. On the other hand, asymptomatic patients with a suspicion of an ampullary tumor on endoscopy but with inconclusive biopsies and unremarkable EUS should undergo clinical follow-up (Fig. 16.25).

Ampullary tumors are staged according to the AJCC classification (Table 16.8).<sup>248</sup> Nevertheless, this classification has limitations, as T1 encompasses early cancers invading the mucosa as well as those invading the duodenal submucosa. An alternative more selective staging system was developed to address those

limitations, where T1 tumors are divided into d0 tumors limited to the sphincter of Oddi layer and d1 tumors that invade the duodenal submucosa. The biological behavior of d0 and d1 is significantly different in terms of the risk of lymph node metastasis,<sup>249–252</sup> which varies from 0% for d0 to 30% for d1 tumors.<sup>253–255</sup> The presence of metastatic lymph nodes correlates with the T stage for more advanced tumors: 55% in T2 and 78% in T3 to T4 lesions.<sup>255</sup> Following this staging strictly makes d0 tumors the only true early cancer where endoscopic ampullectomy can be offered as the standard of care. Various imaging modalities, such as TUS, CT, angiography, ERCP, MRCP, and EUS, have been used to stage ampullary tumors and evaluate resectability. These tumors often grow around the ampulla, far from the mesenteric and portal vessels, with rapid symptom development such as jaundice and pancreatitis. It is therefore rare to see a large tumor originating from the ampulla and invading the vessels. The resectability of those tumors is therefore easier to determine than for pancreatic and biliary adenocarcinomas. T staging remains of

**TABLE 16.8** TNM Staging for Ampullary Carcinoma

<b>Primary Tumor (T)</b>	
TX	Primary tumor cannot be assessed
T0	No evidence of primary tumor
Tis	Carcinoma in situ
T1	Tumor limited to the ampulla of Vater or sphincter of Oddi or tumor invades beyond the sphincter of Oddi (perisphincteric invasion) and/or into duodenal submucosa
T1a	Tumor limited to the ampulla of Vater or sphincter of Oddi
T1b	Tumor invades beyond the sphincter of Oddi (perisphincteric invasion) and/or into duodenal submucosa
T2	Tumor invades into the muscularis propria of the duodenum
T3	Tumor directly invades the pancreas (up to 0.5 cm) or tumor extends more than 0.5 cm into the pancreas, or extends into the peripancreatic or periduodenal tissue or duodenal serosa without involvement of the celiac axis or superior mesenteric artery
T3a	Tumor directly invades the pancreas (up to 0.5 cm)
T3b	Tumor extends more than 0.5 cm into the pancreas, or extends into the peripancreatic or periduodenal tissue or duodenal serosa without involvement of the celiac axis or superior mesenteric artery
T4	Tumor involves the celiac axis, superior mesenteric artery, and/or common hepatic artery, irrespective of size
<b>Regional Lymph Nodes (N)</b>	
NX	Regional lymph nodes cannot be assessed
NO	No regional lymph node metastasis
N1	Metastases to one to three regional lymph nodes
N2	Metastases to four or more regional lymph nodes
<b>Distant Metastasis (M)</b>	
M0	No distant metastasis
M1	Distant metastasis

ultimate importance, as it determines prognosis and guides the choice of treatment between a surgical or endoscopic resection.

EUS remains the most reliable modality for local preoperative staging of these lesions. Earlier series that demonstrated the superiority of EUS to CT, and US, for T and N staging of ampullary tumors, have been confirmed in more recent studies comparing EUS with conventional or helical CT for staging as well as for resectability.<sup>256–263</sup> In a meta-analysis of 14 studies involving 422 patients,<sup>264</sup> the pooled sensitivity and specificity of EUS to diagnose T1-stage tumors were 77% and 78%, respectively, compared to sensitivity of 84% and specificity of 74% for T4 tumors. In the same analysis, the sensitivity, specificity, positive likelihood ratio, negative likelihood ratio of EUS for nodal status were 70%, 74%, 2.49%, 0.46%, respectively. Ridtitid et al. recently reported on 119 patients with ampullary neoplasms, of whom surgical pathology was available in 102. The sensitivity and specificity of EUS were 80% and 93%, which was comparable to that of ERCP (83% and 93%, respectively). The overall accuracy of EUS for local staging was 90%, leading to complete endoscopic resection in 91% of patients.<sup>247</sup> A common limitation of EUS in general is its tendency to understage true T3 or overstage true T2 ampullary carcinomas, which accounts for most of the errors in the EUS T-stage assessment. One can speculate that this lack of accuracy in staging observed in most mucosal GI cancers could stem from desmoplastic peritumoral reaction, which cannot easily be differentiated from foci of invasive carcinoma. From a practical standpoint, differentiation of T2 and T3 lesions is of little value, as the same surgical treatment is recommended for both T stages (Figs. 16.26 and 16.27). What is more important clinically is the accuracy of EUS in determining whether or not endoscopic resection can be used to achieve complete resection with tumor-free margins. The accuracy of EUS in confirming that the T stage is higher than T1 is around 90% (Table 16.9) and its ability to predict intraductal extension of the tumor is accurate in studies using surgical resection as the reference standard.<sup>247,259</sup> However, EUS is limited in its ability to show infiltration of the duodenal submucosa, as the sphincter of Oddi is not well recognized with the 6 to 12 MHz EUS probes, even though the infiltration of the third hyperechoic layer of the duodenum sometimes enables the diagnosis of a d1 tumor (Fig. 16.28). On the other hand, EUS also has relatively limited accuracy in the detection of lymph node metastases (53% to 87%), with a NPV of less

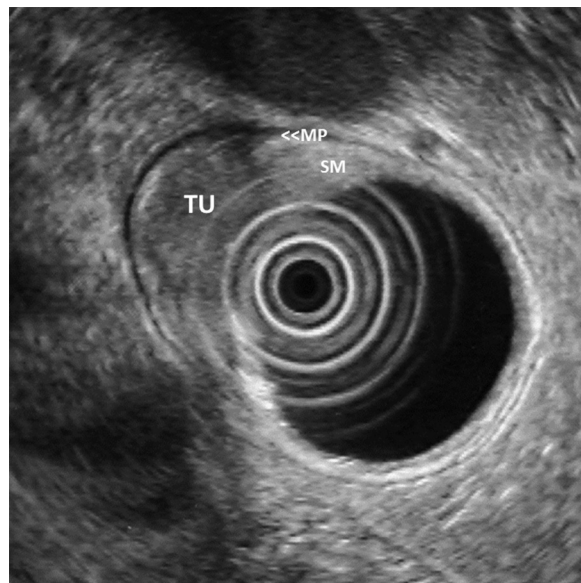


• **Fig. 16.26** Radial endoscopic ultrasound image (6 MHz) of a large ampullary mass infiltrating the duodenal wall (D2) and the head of the pancreas (HOP).

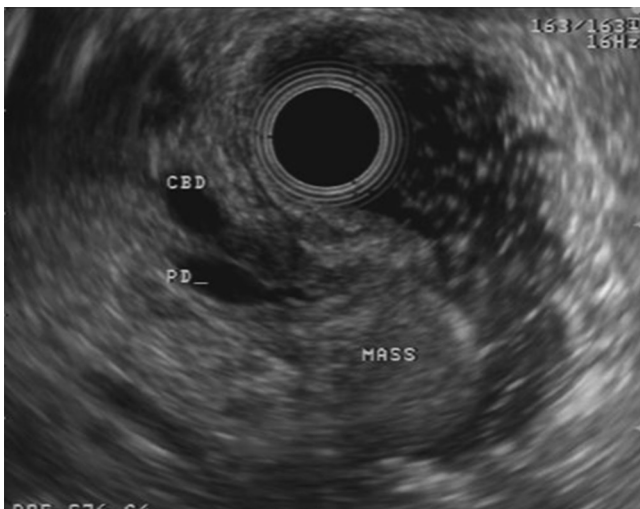
than 75%.<sup>249,250,256,258,260,265–271</sup> In addition, MRI has been found to be not statistically superior to EUS for nodal staging,<sup>137</sup> whereas CT was less sensitive and specific.<sup>256,258</sup> As EUS-guided FNA is highly accurate in sampling tissue from periduodenal adenopathy, use of this technique might increase the diagnostic accuracy of pre-operative EUS, although supportive data is limited.

## Role of Intraductal Ultrasonography in Ampullary Tumors

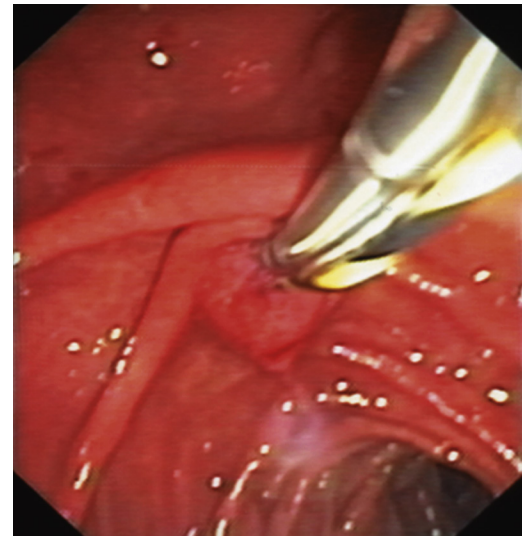
EUS can therefore be considered highly accurate in predicting the unresectability of ampullary carcinoma and determining the T stage. Nevertheless, EUS is limited by its inability to accurately demarcate the sphincter of Oddi, and its NPV for the presence of metastatic lymph nodes remains low. Therefore two complementary examinations, duodenoscopy and IDUS, may be useful. On duodenoscopy, ulceration above the roof of the ampulla indicates a locally invasive lesion extending to the duodenal submucosa.<sup>272</sup> To improve staging performance, IDUS has been proposed as a more accurate ultrasonographic imaging tool for the staging of ampullary neoplasms. Intraductal catheter probes (Fig. 16.29) employ a higher frequency (20 MHz) resulting in enhanced resolution compared with the 7.5 or 12 MHz used for conventional



• **Fig. 16.28** Radial endoscopic ultrasound image (6 MHz) of a uT1sm ampullary tumor (TU) with disruption of the submucosa (SM). The muscularis propria (MP) is intact with no invasion.



• **Fig. 16.27** Large polypoid ampullary mass protruding into the duodenal lumen best seen on this radial endoscopic ultrasound exam after filling the duodenal lumen with water. CBD, Common bile duct.



• **Fig. 16.29** Endoscopic image of an intraductal ultrasonography probe being advanced over a guidewire for staging of an ampullary tumor.

**TABLE 16.9 Performance of Endoscopic Ultrasound in the Staging of the Ampullary Tumors**

Reference (Year)	No. of Patients	Technique	Sensitivity (%)	Specificity (%)	PPV (%)	NPV (%)	Accuracy (%)
Ito et al. <sup>259</sup> (2007)	40	EUS/IDUS <sup>a</sup>	95	62	69	93	78
Artifon et al. <sup>256</sup> (2009)	27	EUS	100	—	93	—	93
Chen et al. <sup>258</sup> (2009)	31	EUS	96	57	89	80	88
Manta et al. <sup>271</sup> (2010)	24	EUS	88	100	100	89	94
Wee et al. <sup>270</sup> (2012)	79	EUS	69	88	66	88	—
Riditidit et al. <sup>274</sup> (2015)	119	EUS	80	93	—	—	90

<sup>a</sup>IDUS was combined with EUS in all cases.

EUS, Endoscopic ultrasound; IDUS, intraductal ultrasonography.

EUS. However, the use of such probes has some restrictions: the ultrasonic probe should be inserted into the tumor via ERCP, and the depth of penetration of ultrasound waves is limited due to the higher frequency, resulting in suboptimal N staging. The ability to delineate the sphincter of Oddi and the duodenal submucosa allows superior T staging, particularly of early tumors that could be triaged to endoscopic therapy. In addition, IDUS provides accurate assessment of intraductal extension of tumors, further refining the selection process of endoscopic or surgical resection. Heinzow et al. demonstrated a superior diagnostic accuracy of malignancy for IDUS in combination with ERCP compared to CT scan or EUS alone.<sup>178</sup>

EUS and IDUS, if available, should be performed to stage ampullary tumors before any invasive treatment is pursued, particularly prior to ES or biliary stent insertion. Such interventions may compromise endosonographic interpretation by introducing air and creating artifacts. In one series, the presence of a transpapillary endobiliary stent resulted in a reduction of EUS T-stage accuracy from 84% to 72%,<sup>249</sup> which was most likely due to the understaging of T2 and T3 carcinomas. Moreover, the bile duct wall thickness, measured by an intraductal ultrasonographic probe, was more than doubled in patients with an endobiliary drainage catheter in place for as little as 14 days,<sup>196</sup> and could be interpreted as intraductal spread. Finally, economic studies assessing the value of pretherapeutic staging of ampullary tumors are scarce. Only one series has shown that use of EUS in the selection of patients for local resection may be a cost-effective approach in the management of ampullary tumors.<sup>273</sup>

## Multimodality Approach in the Management of Ampullary Tumors

Considering all three imaging modalities—duodenoscopy, EUS, and IDUS—a multimodality approach is proposed to ascertain whether an ampullary tumor may be treated adequately by endoscopic ampullectomy versus surgical resection:

- Duodenoscopy:* Large infiltrating tumors with ulcerations seen above the roof of the ampulla usually indicate submucosal infiltration; and pancreaticoduodenectomy should be considered in this case.
- EUS:* Any tumors staged above uT1 due to submucosal or muscularis propria invasion and all tumors with intraductal infiltration should be selected for pancreaticoduodenectomy. In surgically unfit patients, endoscopic ampullectomy can be attempted in lesions confined to the submucosa.
- IDUS:* Any uT1 tumors confirmed to have no submucosal infiltration or intraductal spread should be considered for endoscopic ampullectomy with curative intent.

Traditionally, pancreaticoduodenectomy has been the only potentially curative treatment offered for patients with benign ampullary tumors or early cancer alike.<sup>274</sup> Surgical ampullectomy was infrequently done, owing to its morbidity and the inability to rule out the presence of metastatic lymph nodes due to limited resection. In the last 2 decades, evolving endoscopic techniques for ampullectomy have made curative treatment of benign adenomas (see Fig. 16.21) or early cancers possible in the majority of patients.<sup>239,275,276</sup> Endoscopic ampullectomy is associated with a lower morbidity rate (6% to 36%)<sup>239,275–280</sup> than local surgical excision<sup>275,281</sup>; nevertheless, careful patient selection is required to triage patients to the appropriate resection approach. Despite its favorable outcomes, endoscopic ampullectomy is limited by its inability to assess for lymph node metastasis, which is estimated to be present in up to 30% of patients with T1 disease.<sup>252</sup> Additionally, neoplastic tissue extending inside the pancreatic or bile ducts is inadequately removed using this approach. These limitations

highlight the importance of pretreatment staging, not only to assess the resectability of the tumor but also to determine which tumors may be resected endoscopically versus surgically.

Due to the predisposition of ampullary tumors to recur after endoscopic ampullectomy (13%, range: 0% to 30%),<sup>239,273,277,278,282–294</sup> EUS is needed, in combination with endoscopy and biopsy, in the follow-up of patients with ampullary adenomas treated endoscopically, especially to detect intraductal recurrence. Lesions with high-grade dysplasia or adenocarcinoma, and those with incomplete endoscopic resection, were more likely to recur after endoscopic therapy.<sup>239</sup> Pancreaticoduodenectomy should be considered in all surgically fit patients presenting with local recurrence.<sup>239,295</sup>

## Summary

EUS can be helpful in the diagnosis of ampullary tumors, especially lesions with intramural spread and negative mucosal biopsies. Its role in directing the management of ampullary cancer resides in its ability to accurately stage advanced tumors where surgical resection should be performed. For benign and early cancers of the ampulla, accurate staging could be achieved using a combination of endoscopic, EUS, IDUS, and cross-sectional imaging. In such cases, endoscopic resection appears to be adequate and provides good long-term results.

## DIAGNOSTIC CHECKLIST

### Ampullary Tumors

- Hypoechoic or hyperechoic thickening of the ampulla
- Polypoid intraductal tumor
- Involvement of vessels, pancreas, or duodenum
- Bile or pancreatic duct dilation
- Bile or pancreatic duct intraductal growth
- Presence of peri-duodenal adenopathy

### Benign Changes

- Hypoechoic or hyperechoic thickening of the ampulla
- Duodenal wall layers preserved
- No intraductal polypoid infiltration
- No bile or pancreatic duct dilation observed

## Key References

37. Badger WR, Borgert AJ, Kallies KJ, et al. Utility of MRCP in clinical decision making of suspected choledocholithiasis: an institutional analysis and literature review. *Am J Surg.* 2017;214:251–255.
54. De Castro VL, Moura EG, Chaves DM, et al. Endoscopic ultrasound versus magnetic resonance cholangiopancreatography in suspected choledocholithiasis: a systematic review. *Endosc Ultrasound.* 2016;5:118–128.
60. He H, Tan C, Wu J, et al. Accuracy of ASGE high-risk criteria in evaluation of patients with suspected common bile duct stones. *Gastrointest Endosc.* 2017;86:525–532.
114. Sakuma Y, Kodama Y, Sogabe Y, et al. Diagnostic performance of a new endoscopic scraper for malignant biliary strictures: a multicenter prospective study. *Gastrointest Endosc.* 2017;85:371–379.
248. Amin MB, Edge S, Greene F, et al., eds. *American Joint Committee on Cancer Staging Manual.* 8th ed. Switzerland: Springer International Publishing AG; 2017.

## References

Access the reference list online at [ExpertConsult.com](http://ExpertConsult.com).

## References

1. Andriulli A, Loperfido S, Napolitano G, et al. Incidence rates of post-ERCP complications: a systematic survey of prospective studies. *Am J Gastroenterol.* 2007;102:1781–1788.
2. Cotton PB, Garrow DA, Gallagher J, et al. Risk factors for complications after ERCP: a multivariate analysis of 11,497 procedures over 12 years. *Gastrointest Endosc.* 2009;70:80–88.
3. Barthet M, Lesavre N, Desjeux A, et al. Complications of endoscopic sphincterotomy: results from a single tertiary referral center. *Endoscopy.* 2002;34:991–997.
4. Folkers MT, Disario JA, Adler DG. Long-term complications of endoscopic biliary sphincterotomy for choledocholithiasis: a North-American perspective. *Am J Gastroenterol.* 2009;104:2868–2869.
5. Sugiyama M, Atomi Y. Risk factors predictive of late complications after endoscopic sphincterotomy for bile duct stones: long-term (more than 10 years) follow-up study. *Am J Gastroenterol.* 2002;97:2763–2767.
6. Tseng CW, Chen CC, Chen TS, et al. Can computed tomography with coronal reconstruction improve the diagnosis of choledocholithiasis? *J Gastroenterol Hepatol.* 2008;23:1586–1589.
7. Kondo S, Isayama H, Akahane M, et al. Detection of common bile duct stones: comparison between endoscopic ultrasonography, magnetic resonance cholangiography, and helical-computed-tomographic cholangiography. *Eur J Radiol.* 2005;54:271–275.
8. Anderson SW, Rho E, Soto JA. Detection of biliary duct narrowing and choledocholithiasis: accuracy of portal venous phase multidetector CT. *Radiology.* 2008;247:418–427.
9. Okada M, Fukada J, Toya K, et al. The value of drip infusion cholangiography using multidetector-row helical CT in patients with choledocholithiasis. *Eur Radiol.* 2005;15:2140–2145.
10. Napoleon B, Dumortier J, Keriven-Souquet O, et al. Do normal findings at biliary endoscopic ultrasonography obviate the need for endoscopic retrograde cholangiography in patients with suspicion of common bile duct stone? A prospective follow-up study of 238 patients. *Endoscopy.* 2003;35:411–415.
11. Frossard JL, Sosa-Valencia L, Amouyal G, et al. Usefulness of endoscopic ultrasonography in patients with “idiopathic” acute pancreatitis. *Am J Med.* 2000;109:196–200.
12. Kohut M, Nowakowska-Dulawa E, Marek T, et al. Accuracy of linear endoscopic ultrasonography in the evaluation of patients with suspected common bile duct stones. *Endoscopy.* 2002;34:299–303.
13. Lachter J, Rubin A, Shiller M, et al. Linear EUS for bile duct stones. *Gastrointest Endosc.* 2000;51:51–54.
14. Wehrmann T, Martchenko K, Riphäus A. Catheter probe extraductal ultrasonography vs. conventional endoscopic ultrasonography for detection of bile duct stones. *Endoscopy.* 2009;41:133–137.
15. Katanuma A, Maguchi H, Osanai M, et al. The difference in the capability of delineation between convex and radial arrayed echoendoscope for pancreas and biliary tract; case reports from the standpoint of both convex and radial arrayed echoendoscope. *Dig Endosc.* 2011;23(suppl 1):2–8.
16. Kohut M, Nowak A, Nowakowska-Dulawa E, et al. Endosonography with linear array instead of endoscopic retrograde cholangiography as the diagnostic tool in patients with moderate suspicion of common bile duct stones. *World J Gastroenterol.* 2003;9:612–614.
17. Meroni E, Bisagni P, Bona S, et al. Pre-operative endoscopic ultrasonography can optimise the management of patients undergoing laparoscopic cholecystectomy with abnormal liver function tests as the sole risk factor for choledocholithiasis: a prospective study. *Dig Liver Dis.* 2004;36:73–77.
18. Prat F, Edery J, Meduri B, et al. Early EUS of the bile duct before endoscopic sphincterotomy for acute biliary pancreatitis. *Gastrointest Endosc.* 2001;54:724–729.
19. Ney MV, Maluf-Filho F, Sakai P, et al. Echo-endoscopy versus endoscopic retrograde cholangiography for the diagnosis of choledocholithiasis: the influence of the size of the stone and diameter of the common bile duct. *Arg Gastroenterol.* 2005;42:239–243.
20. Scheiman JM, Carlos RC, Barnett JL, et al. Can endoscopic ultrasound or magnetic resonance cholangiopancreatography replace ERCP in patients with suspected biliary disease? A prospective trial and cost analysis. *Am J Gastroenterol.* 2001;96:2900–2904.
21. Mofidi R, Lee AC, Madhavan KK, et al. The selective use of magnetic resonance cholangiopancreatography in the imaging of the axial biliary tree in patients with acute gallstone pancreatitis. *Pancreatology.* 2008;8:55–60.
22. Topal B, Van de Moortel M, Fieuws S, et al. The value of magnetic resonance cholangiopancreatography in predicting common bile duct stones in patients with gallstone disease. *Br J Surg.* 2003;90:42–47.
23. Scaffidi MG, Luigiano C, Consolo P, et al. Magnetic resonance cholangio-pancreatography versus endoscopic retrograde cholangio-pancreatography in the diagnosis of common bile duct stones: a prospective comparative study. *Minerva Med.* 2009;100:341–348.
24. Ausch C, Hochwarter G, Taher M, et al. Improving the safety of laparoscopic cholecystectomy: the routine use of preoperative magnetic resonance cholangiography. *Surg Endosc.* 2005;19:574–580.
25. Griffin N, Wastle ML, Dunn WK, et al. Magnetic resonance cholangiopancreatography versus endoscopic retrograde cholangiopancreatography in the diagnosis of choledocholithiasis. *Eur J Gastroenterol Hepatol.* 2003;15:809–813.
26. De Waele E, Op de Beeck B, De Waele B, et al. Magnetic resonance cholangiopancreatography in the preoperative assessment of patients with biliary pancreatitis. *Pancreatology.* 2007;7:347–351.
27. Hallal AH, Amortegui JD, Jeroukhimov IM, et al. Magnetic resonance cholangiopancreatography accurately detects common bile duct stones in resolving gallstone pancreatitis. *J Am Coll Surg.* 2005;200:869–875.
28. Moon JH, Cho YD, Cha SW, et al. The detection of bile duct stones in suspected biliary pancreatitis: comparison of MRCP, ERCP, and intraductal US. *Am J Gastroenterol.* 2005;100:1051–1057.
29. Richard F, Boustany M, Britt LD. Accuracy of magnetic resonance cholangiopancreatography for diagnosing stones in the common bile duct in patients with abnormal intraoperative cholangiograms. *Am J Surg.* 2013;205:371–373.
30. Norero E, Norero B, Huete A, et al. Accuracy of magnetic resonance cholangiopancreatography for the diagnosis of common bile duct stones. *Rev Med Chil.* 2008;136:600–605.
31. Gautier G, Pilleul F, Crombe-Ternamian A, et al. Contribution of magnetic resonance cholangiopancreatography to the management of patients with suspected common bile duct stones. *Gastroenterol Clin Biol.* 2004;28:129–134.
32. Cervi C, Aube C, Tuech JJ, et al. Nuclear magnetic resonance cholangiography in biliary disease. Prospective study in 60 patients. *Ann Chir.* 2000;125:428–434.
33. Demartines N, Eisner L, Schnabel K, et al. Evaluation of magnetic resonance cholangiography in the management of bile duct stones. *Arch Surg.* 2000;135:148–152.
34. Stirris MG, Tennoe B, Aadland E, et al. MR cholangiopancreatography and endoscopic retrograde cholangiopancreatography in patients with suspected common bile duct stones. *Acta Radiol.* 2000;41:269–272.
35. Kim JH, Kim MJ, Park SI, et al. MR cholangiography in symptomatic gallstones: diagnostic accuracy according to clinical risk group. *Radiology.* 2002;224:410–416.

36. Taylor AC, Little AF, Hennessy OF, et al. Prospective assessment of magnetic resonance cholangiopancreatography for noninvasive imaging of the biliary tree. *Gastrointest Endosc.* 2002;55:17–22.
37. Badger WR, Borgert AJ, Kallies KJ, et al. Utility of MRCP in clinical decision making of suspected choledocholithiasis: an institutional analysis and literature review. *Am J Surg.* 2017;214: 251–255.
38. Rosch T, Meining A, Fruhmorgen S, et al. A prospective comparison of the diagnostic accuracy of ERCP, MRCP, CT, and EUS in biliary strictures. *Gastrointest Endosc.* 2002;55:870–876.
39. MacEneaney P, Mitchell MT, McDermott R. Update on magnetic resonance cholangiopancreatography. *Gastroenterol Clin North Am.* 2002;31:731–746.
40. Savides TJ. EUS-guided ERCP for patients with intermediate probability for choledocholithiasis: is it time for all of us to start doing this? *Gastrointest Endosc.* 2008;67:669–672.
41. Mendlar MH, Bouillet P, Sautereau D, et al. Value of MR cholangiography in the diagnosis of obstructive diseases of the biliary tree: a study of 58 cases. *Am J Gastroenterol.* 1998;93:2482–2490.
42. Zidi SH, Prat F, Le Guen O, et al. Use of magnetic resonance cholangiography in the diagnosis of choledocholithiasis: prospective comparison with a reference imaging method. *Gut.* 1999;44:118–122.
43. Chen W, Mo JJ, Lin L, et al. Diagnostic value of magnetic resonance cholangiopancreatography in choledocholithiasis. *World J Gastroenterol.* 2015;21:3351–3360.
44. Garrow D, Miller S, Sinha D, et al. Endoscopic ultrasound: a meta-analysis of test performance in suspected biliary obstruction. *Clin Gastroenterol Hepatol.* 2007;5:616–623.
45. Tse F, Liu L, Barkun AN, et al. EUS: a meta-analysis of test performance in suspected choledocholithiasis. *Gastrointest Endosc.* 2008;67:235–244.
46. Al Samarae A, Khan U, Almashta Z, et al. Preoperative diagnosis of choledocholithiasis: the role of MRCP. *Br J Hosp Med (Lond).* 2009;70:339–343.
47. Aube C, Delorme B, Yzet T, et al. MR cholangiopancreatography versus endoscopic sonography in suspected common bile duct lithiasis: a prospective, comparative study. *AJR Am J Roentgenol.* 2005;184:55–62.
48. Frossard JL, Hadengue A, Amouyal G, et al. Choledocholithiasis: a prospective study of spontaneous common bile duct stone migration. *Gastrointest Endosc.* 2000;51:175–179.
49. Ainsworth AP, Rafalsen SR, Wamberg PA, et al. Cost-effectiveness of endoscopic ultrasonography, magnetic resonance cholangiopancreatography and endoscopic retrograde cholangiopancreatography in patients suspected of pancreaticobiliary disease. *Scand J Gastroenterol.* 2004;39:579–583.
50. Materne R, Van Beers BE, Gigot JF, et al. Extrahepatic biliary obstruction: magnetic resonance imaging compared with endoscopic ultrasonography. *Endoscopy.* 2000;32:3–9.
51. Montariol T, Msika S, Charlier A, et al. Diagnosis of asymptomatic common bile duct stones: preoperative endoscopic ultrasonography versus intraoperative cholangiography—a multicenter, prospective controlled study. French Associations for Surgical Research. *Surgery.* 1998;124:6–13.
52. Ledro-Cano D. Suspected choledocholithiasis: endoscopic ultrasound or magnetic resonance cholangio-pancreatography? A systematic review. *Eur J Gastroenterol Hepatol.* 2007;19:1007–1011.
53. Verma D, Kapadia A, Eisen GM, et al. EUS vs MRCP for detection of choledocholithiasis. *Gastrointest Endosc.* 2006;64: 248–254.
54. De Castro VL, Moura EG, Chaves DM, et al. Endoscopic ultrasound versus magnetic resonance cholangiopancreatography in suspected choledocholithiasis: a systematic review. *Endosc Ultrasound.* 2016;5:118–128.
55. Buscarini E, Tansini P, Vallisa D, et al. EUS for suspected choledocholithiasis: do benefits outweigh costs? A prospective, controlled study. *Gastrointest Endosc.* 2003;57:510–518.
56. Karakan T, Cindoruk M, Alagozlu H, et al. EUS versus endoscopic retrograde cholangiography for patients with intermediate probability of bile duct stones: a prospective randomized trial. *Gastrointest Endosc.* 2009;69:244–252.
57. Lee YT, Chan FK, Leung WK, et al. Comparison of EUS and ERCP in the investigation with suspected biliary obstruction caused by choledocholithiasis: a randomized study. *Gastrointest Endosc.* 2008;67:660–668.
58. Petrov MS, Savides TJ. Systematic review of endoscopic ultrasonography versus endoscopic retrograde cholangiopancreatography for suspected choledocholithiasis. *Br J Surg.* 2009;96:967–974.
59. Committee ASOP, Maple JT, Ben-Menachem T, et al. The role of endoscopy in the evaluation of suspected choledocholithiasis. *Gastrointest Endosc.* 2010;71:1–9.
60. He H, Tan C, Wu J, et al. Accuracy of ASGE high-risk criteria in evaluation of patients with suspected common bile duct stones. *Gastrointest Endosc.* 2017;86:525–532.
61. Netinatsunton N, Attasaranya S, Sottisuporn J, et al. Comparing cost-effectiveness between endoscopic ultrasound and endoscopic retrograde cholangiopancreatography in diagnosis of common bile duct stone in patients with predefined risks: a study from a developing country. *Endosc Ultrasound.* 2016;5:165–172.
62. Abboud PA, Malet PF, Berlin JA, et al. Predictors of common bile duct stones prior to cholecystectomy: a meta-analysis. *Gastrointest Endosc.* 1996;44:450–455.
63. Canto MI, Chak A, Stellato T, et al. Endoscopic ultrasonography versus cholangiography for the diagnosis of choledocholithiasis. *Gastrointest Endosc.* 1998;47:439–448.
64. Jeon TJ, Cho JH, Kim YS, et al. Diagnostic value of endoscopic ultrasonography in symptomatic patients with high and intermediate probabilities of common bile duct stones and a negative computed tomography scan. *Gut Liver.* 2017;11: 290–297.
65. Amouyal P, Amouyal G, Levy P, et al. Diagnosis of choledocholithiasis by endoscopic ultrasonography. *Gastroenterology.* 1994;106:1062–1067.
66. Berdah SV, Orsoni P, Bege T, et al. Follow-up of selective endoscopic ultrasonography and/or endoscopic retrograde cholangiography prior to laparoscopic cholecystectomy: a prospective study of 300 patients. *Endoscopy.* 2001;33:216–220.
67. Makary MA, Duncan MD, Harmon JW, et al. The role of magnetic resonance cholangiography in the management of patients with gallstone pancreatitis. *Ann Surg.* 2005;241:119–124.
68. Palazzo L, Girollet PP, Salmeron M, et al. Value of endoscopic ultrasonography in the diagnosis of common bile duct stones: comparison with surgical exploration and ERCP. *Gastrointest Endosc.* 1995;42:225–231.
69. Prat F, Amouyal G, Amouyal P, et al. Prospective controlled study of endoscopic ultrasonography and endoscopic retrograde cholangiography in patients with suspected common-bileduct lithiasis. *Lancet.* 1996;347:75–79.
70. Sahai AV, Mauldin PD, Marsi V, et al. Bile duct stones and laparoscopic cholecystectomy: a decision analysis to assess the roles of intraoperative cholangiography, EUS, and ERCP. *Gastrointest Endosc.* 1999;49:334–343.
71. Bret PM, Reinhold C. Magnetic resonance cholangiopancreatography. *Endoscopy.* 1997;29:472–486.
72. Dittrick G, Lamont JP, Kuhn JA, et al. Usefulness of endoscopic ultrasound in patients at high risk of choledocholithiasis. *Proc (Bayl Univ Med Cent).* 2005;18:211–213.
73. Das A, Chak A. Endoscopic ultrasonography. *Endoscopy.* 2004;36:17–22.
74. Benjaminov F, Stein A, Lichtman G, et al. Consecutive versus separate sessions of endoscopic ultrasound (EUS) and endoscopic retrograde cholangiopancreatography (ERCP) for symptomatic choledocholithiasis. *Surg Endosc.* 2013;27: 2117–2121.

75. Fabbri C, Polifemo AM, Luigiano C, et al. Single session versus separate session endoscopic ultrasonography plus endoscopic retrograde cholangiography in patients with low to moderate risk for choledocholithiasis. *J Gastroenterol Hepatol.* 2009;24: 1107–1112.
76. Polkowski M, Regula J, Tilszer A, et al. Endoscopic ultrasound versus endoscopic retrograde cholangiography for patients with intermediate probability of bile duct stones: a randomized trial comparing two management strategies. *Endoscopy.* 2007;39:296–303.
77. Kim KM, Lee JK, Bahng S, et al. Role of endoscopic ultrasonography in patients with intermediate probability of choledocholithiasis but a negative CT scan. *J Clin Gastroenterol.* 2013;47:449–456.
78. Alhayat N, Lalor E, Bain V, et al. The clinical impact and cost implication of endoscopic ultrasound on use of endoscopic retrograde cholangiopancreatography in a Canadian university hospital. *Can J Gastroenterol.* 2008;22:138–142.
79. Arguedas MR, Dupont AW, Wilcox CM. Where do ERCP, endoscopic ultrasound, magnetic resonance cholangiopancreatography, and intraoperative cholangiography fit in the management of acute biliary pancreatitis? A decision analysis model. *Am J Gastroenterol.* 2001;96:2892–2899.
80. Romagnuolo J, Currie G. Noninvasive vs. selective invasive biliary imaging for acute biliary pancreatitis: an economic evaluation by using decision tree analysis. *Gastrointest Endosc.* 2005;61:86–97.
81. Seifert H, Wehrmann T, Hilgers R, et al. Catheter probe extra-ductal EUS reliably detects distal common bile duct abnormalities. *Gastrointest Endosc.* 2004;60:61–67.
82. Catanzaro A, Pfau P, Isenberg GA, et al. Clinical utility of intraductal US for evaluation of choledocholithiasis. *Gastrointest Endosc.* 2003;57:648–652.
83. Tsuchiya S, Tsuyuguchi T, Sakai Y, et al. Clinical utility of intraductal US to decrease early recurrence rate of common bile duct stones after endoscopic papillotomy. *J Gastroenterol Hepatol.* 2008;23:1590–1595.
84. Sotoudehmanesh R, Kolahdoozan S, Asgari AA, et al. Role of endoscopic ultrasonography in prevention of unnecessary endoscopic retrograde cholangiopancreatography: a prospective study of 150 patients. *J Ultrasound Med.* 2007;26:455–460.
85. Lu J, Guo CY, Xu XF, et al. Efficacy of intraductal ultrasonography in the diagnosis of non-opaque choledocholith. *World J Gastroenterol.* 2012;18:275–278.
86. Mirbagheri SA, Mohamadnejad M, Nasiri J, et al. Prospective evaluation of endoscopic ultrasonography in the diagnosis of biliary microlithiasis in patients with normal transabdominal ultrasonography. *J Gastrointest Surg.* 2005;9:961–964.
87. Thorboll J, Vilsmann P, Jacobsen B, et al. Endoscopic ultrasonography in detection of cholelithiasis in patients with biliary pain and negative transabdominal ultrasonography. *Scand J Gastroenterol.* 2004;39:267–269.
88. Kaw M, Brodmerkel Jr GJ. ERCP, biliary crystal analysis, and sphincter of Oddi manometry in idiopathic recurrent pancreatitis. *Gastrointest Endosc.* 2002;55:157–162.
89. Lee SP, Hayashi A, Kim YS. Biliary sludge: curiosity or culprit? *Hepatology.* 1994;20:523–525.
90. Liu CL, Lo CM, Chan JK, et al. EUS for detection of occult cholelithiasis in patients with idiopathic pancreatitis. *Gastrointest Endosc.* 2000;51:28–32.
91. Yusoff IF, Raymond G, Sahai AV. A prospective comparison of the yield of EUS in primary vs. recurrent idiopathic acute pancreatitis. *Gastrointest Endosc.* 2004;60:673–678.
92. Wilcox CM, Varadarajulu S, Eloubeidi M. Role of endoscopic evaluation in idiopathic pancreatitis: a systematic review. *Gastrointest Endosc.* 2006;63:1037–1045.
93. Wilcox CM, Kilgore M. Cost minimization analysis comparing diagnostic strategies in unexplained pancreatitis. *Pancreas.* 2009;38:117–121.
94. Park MS, Kim TK, Kim KW, et al. Differentiation of extrahepatic bile duct cholangiocarcinoma from benign stricture: findings at MRCP versus ERCP. *Radiology.* 2004;233:234–240.
95. Zidi SH, Prat F, Le Guen O, et al. Performance characteristics of magnetic resonance cholangiography in the staging of malignant hilar strictures. *Gut.* 2000;46:103–106.
96. Stewart CJ, Mills PR, Carter R, et al. Brush cytology in the assessment of pancreaticobiliary strictures: a review of 406 cases. *J Clin Pathol.* 2001;54:449–455.
97. Cote GA, Sherman S. Biliary stricture and negative cytology: what next? *Clin Gastroenterol Hepatol.* 2011;9:739–743.
98. Glasbrenner B, Ardan M, Boeck W, et al. Prospective evaluation of brush cytology of biliary strictures during endoscopic retrograde cholangiopancreatography. *Endoscopy.* 1999;31:712–717.
99. Kipp BR, Stadheim LM, Halling SA, et al. A comparison of routine cytology and fluorescence in situ hybridization for the detection of malignant bile duct strictures. *Am J Gastroenterol.* 2004;99:1675–1681.
100. Lee JG, Leung JW, Baillie J, et al. Benign, dysplastic, or malignant—making sense of endoscopic bile duct brush cytology: results in 149 consecutive patients. *Am J Gastroenterol.* 1995;90:722–726.
101. Fritchler EG, Kipp BR, Halling KC, et al. A multivariable model using advanced cytologic methods for the evaluation of indeterminate pancreaticobiliary strictures. *Gastroenterology.* 2009;136:2180–2186.
102. Levy MJ, Baron TH, Clayton AC, et al. Prospective evaluation of advanced molecular markers and imaging techniques in patients with indeterminate bile duct strictures. *Am J Gastroenterol.* 2008;103:1263–1273.
103. Chaiteerakij R, Barr Fritchler EG, Angsuwatcharakon P, et al. Fluorescence in situ hybridization compared with conventional cytology for the diagnosis of malignant biliary tract strictures in Asian patients. *Gastrointest Endosc.* 2016;83:1228–1235.
104. Levy MJ, Oberg TN, Campion MB, et al. Comparison of methods to detect neoplasia in patients undergoing endoscopic ultrasound-guided fine-needle aspiration. *Gastroenterology.* 2012;142:1112–1121. e2.
105. Gonda TA, Glick MP, Sethi A, et al. Polysomy and p16 deletion by fluorescence in situ hybridization in the diagnosis of indeterminate biliary strictures. *Gastrointest Endosc.* 2012;75:74–79.
106. Smoczyński M, Jabłonska A, Matyśkiewicz A, et al. Routine brush cytology and fluorescence in situ hybridization for assessment of pancreaticobiliary strictures. *Gastrointest Endosc.* 2012;75:65–73.
107. Gonda TA, Viterbo D, Gausman V, et al. Mutation profile and fluorescence in situ hybridization analyses increase detection of malignancies in biliary strictures. *Clin Gastroenterol Hepatol.* 2017;15:913–919.
108. de Bellis M, Sherman S, Fogel EL, et al. Tissue sampling at ERCP in suspected malignant biliary strictures (Part 2). *Gastrointest Endosc.* 2002;56:720–730.
109. De Bellis M, Sherman S, Fogel EL, et al. Tissue sampling at ERCP in suspected malignant biliary strictures (Part 1). *Gastrointest Endosc.* 2002;56:552–561.
110. Higashizawa T, Tamada K, Tomiyama T, et al. Biliary guidewire facilitates bile duct biopsy and endoscopic drainage. *J Gastroenterol Hepatol.* 2002;17:332–336.
111. Farrell RJ, Jain AK, Brandwein SL, et al. The combination of stricture dilation, endoscopic needle aspiration, and biliary brushings significantly improves diagnostic yield from malignant bile duct strictures. *Gastrointest Endosc.* 2001;54:587–594.
112. de Bellis M, Fogel EL, Sherman S, et al. Influence of stricture dilation and repeat brushing on the cancer detection rate of brush cytology in the evaluation of malignant biliary obstruction. *Gastrointest Endosc.* 2003;58:176–182.
113. Curcio G, Traina M, Moccia F, et al. Intraductal aspiration: a promising new tissue-sampling technique for the diagnosis of suspected malignant biliary strictures. *Gastrointest Endosc.* 2012;75:798–804.

114. Sakuma Y, Kodama Y, Sogabe Y, et al. Diagnostic performance of a new endoscopic scraper for malignant biliary strictures: a multicenter prospective study. *Gastrointest Endosc.* 2017;85:371–379.
115. Navaneethan U, Hasan MK, Kommaraju K, et al. Digital, single-operator cholangiopancreatostomy in the diagnosis and management of pancreatobiliary disorders: a multicenter clinical experience (with video). *Gastrointest Endosc.* 2016;84:649–655.
116. Chen YK, Parsi MA, Binmoeller KF, et al. Single-operator cholangioscopy in patients requiring evaluation of bile duct disease or therapy of biliary stones (with videos). *Gastrointest Endosc.* 2011;74:805–814.
117. Chen YK, Pleskow DK. SpyGlass single-operator peroral cholangiopancreatostomy system for the diagnosis and therapy of bile-duct disorders: a clinical feasibility study (with video). *Gastrointest Endosc.* 2007;65:832–841.
118. Draganov PV, Chauhan S, Wagh MS, et al. Diagnostic accuracy of conventional and cholangioscopy-guided sampling of indeterminate biliary lesions at the time of ERCP: a prospective, long-term follow-up study. *Gastrointest Endosc.* 2012;75:347–353.
119. Osanai M, Itoi T, Igarashi Y, et al. Peroral video cholangioscopy to evaluate indeterminate bile duct lesions and preoperative mucosal cancerous extension: a prospective multicenter study. *Endoscopy.* 2013;45:635–642.
120. Parsi MA, Jang S, Sanaka M, et al. Diagnostic and therapeutic cholangiopancreatostomy: performance of a new digital cholangioscope. *Gastrointest Endosc.* 2014;79:936–942.
121. Songur Y, Temucin G, Sahin B. Endoscopic ultrasonography in the evaluation of dilated common bile duct. *J Clin Gastroenterol.* 2001;33:302–305.
122. Sadeghi A, Mohamadnejad M, Islami F, et al. Diagnostic yield of EUS-guided FNA for malignant biliary stricture: a systematic review and meta-analysis. *Gastrointest Endosc.* 2016;83:290–298. e1.
123. Agarwal B, Abu-Hamda E, Molke KL, et al. Endoscopic ultrasound-guided fine needle aspiration and multidetector spiral CT in the diagnosis of pancreatic cancer. *Am J Gastroenterol.* 2004;99:844–850.
124. Gress F, Gottlieb K, Sherman S, et al. Endoscopic ultrasonography-guided fine-needle aspiration biopsy of suspected pancreatic cancer. *Ann Intern Med.* 2001;134:459–464.
125. Harewood GC, Wiersema MJ. Endosonography-guided fine needle aspiration biopsy in the evaluation of pancreatic masses. *Am J Gastroenterol.* 2002;97:1386–1391.
126. Hollerbach S, Klamann A, Topalidis T, et al. Endoscopic ultrasonography (EUS) and fine-needle aspiration (FNA) cytology for diagnosis of chronic pancreatitis. *Endoscopy.* 2001;33:824–831.
127. Menzel J, Poremba C, Dietl KH, et al. Preoperative diagnosis of bile duct strictures—comparison of intraductal ultrasonography with conventional endosonography. *Scand J Gastroenterol.* 2000;35:77–82.
128. Palazzo L, Roseau G, Gayet B, et al. Endoscopic ultrasonography in the diagnosis and staging of pancreatic adenocarcinoma. Results of a prospective study with comparison to ultrasonography and CT scan. *Endoscopy.* 1993;25:143–150.
129. Raut CP, Grau AM, Staerkel GA, et al. Diagnostic accuracy of endoscopic ultrasound-guided fine-needle aspiration in patients with presumed pancreatic cancer. *J Gastrointest Surg.* 2003;7:118–126. discussion 127–128.
130. Varadarajulu S, Tamhane A, Eloubeidi MA. Yield of EUS-guided FNA of pancreatic masses in the presence or the absence of chronic pancreatitis. *Gastrointest Endosc.* 2005;62:728–736. quiz 751, 753.
131. Mohamadnejad M, DeWitt JM, Sherman S, et al. Role of EUS for preoperative evaluation of cholangiocarcinoma: a large single-center experience. *Gastrointest Endosc.* 2011;73:71–78.
132. Weilert F, Bhat YM, Binmoeller KF, et al. EUS-FNA is superior to ERCP-based tissue sampling in suspected malignant biliary obstruction: results of a prospective, single-blind, comparative study. *Gastrointest Endosc.* 2014;80:97–104.
133. Byrne MF, Gerke H, Mitchell RM, et al. Yield of endoscopic ultrasound-guided fine-needle aspiration of bile duct lesions. *Endoscopy.* 2004;36:715–719.
134. DeWitt J, Misra VL, Leblanc JK, et al. EUS-guided FNA of proximal biliary strictures after negative ERCP brush cytology results. *Gastrointest Endosc.* 2006;64:325–333.
135. Fritscher-Ravens A, Broering DC, Sriram PV, et al. EUS-guided fine-needle aspiration cytodiagnosis of hilar cholangiocarcinoma: a case series. *Gastrointest Endosc.* 2000;52:534–540.
136. Lee JH, Salem R, Aslanian H, et al. Endoscopic ultrasound and fine-needle aspiration of unexplained bile duct strictures. *Am J Gastroenterol.* 2004;99:1069–1073.
137. Meara RS, Jhala D, Eloubeidi MA, et al. Endoscopic ultrasound-guided FNA biopsy of bile duct and gallbladder: analysis of 53 cases. *Cytopathology.* 2006;17:42–49.
138. Rosch T, Hofrichter K, Frimberger E, et al. ERCP or EUS for tissue diagnosis of biliary strictures? A prospective comparative study. *Gastrointest Endosc.* 2004;60:390–396.
139. Eloubeidi MA, Chen VK, Jhala NC, et al. Endoscopic ultrasound-guided fine needle aspiration biopsy of suspected cholangiocarcinoma. *Clin Gastroenterol Hepatol.* 2004;2:209–213.
140. Fritscher-Ravens A, Broering DC, Knoefel WT, et al. EUS-guided fine-needle aspiration of suspected hilar cholangiocarcinoma in potentially operable patients with negative brush cytology. *Am J Gastroenterol.* 2004;99:45–51.
141. Tummala P, Munigala S, Eloubeidi MA, et al. Patients with obstructive jaundice and biliary stricture+/-mass lesion on imaging: prevalence of malignancy and potential role of EUS-FNA. *J Clin Gastroenterol.* 2013;47:532–537.
142. Ohshima Y, Yasuda I, Kawakami H, et al. EUS-FNA for suspected malignant biliary strictures after negative endoscopic transpapillary brush cytology and forceps biopsy. *J Gastroenterol.* 2011;46:921–928.
143. Nayar MK, Manas DM, Wadehra V, et al. Role of EUS/EUS-guided FNA in the management of proximal biliary strictures. *Hepatogastroenterology.* 2011;58:1862–1865.
144. Saifuku Y, Yamagata M, Koike T, et al. Endoscopic ultrasonography can diagnose distal biliary strictures without a mass on computed tomography. *World J Gastroenterol.* 2010;16:237–244.
145. Tellez-Avila FI, Bernal-Mendez AR, Guerrero-Vazquez CG, et al. Diagnostic yield of EUS-guided tissue acquisition as a first-line approach in patients with suspected hilar cholangiocarcinoma. *Am J Gastroenterol.* 2014;109:1294–1296.
146. Horwhat JD, Paulson EK, McGrath K, et al. A randomized comparison of EUS-guided FNA versus CT or US-guided FNA for the evaluation of pancreatic mass lesions. *Gastrointest Endosc.* 2006;63:966–975.
147. Larghi A, Lecca PG, Ardito F, et al. Evaluation of hilar biliary strictures by using a newly developed forward-viewing therapeutic echoendoscope: preliminary results of an ongoing experience. *Gastrointest Endosc.* 2009;69:356–360.
148. Lee S, See DW, Choi JH, et al. Evaluation of the feasibility and efficacy of forward-viewing endoscopic ultrasound. *Gut Liver.* 2015;9:679–684.
149. Siddiqui UD, Rossi F, Rosenthal LS, et al. EUS-guided FNA of solid pancreatic masses: a prospective, randomized trial comparing 22-gauge and 25-gauge needles. *Gastrointest Endosc.* 2009;70:1093–1097.
150. Lee JK, Lee KT, Choi ER, et al. A prospective, randomized trial comparing 25-gauge and 22-gauge needles for endoscopic ultrasound-guided fine needle aspiration of pancreatic masses. *Scand J Gastroenterol.* 2013;48:752–757.

151. Madhoun MF, Wani SB, Rastogi A, et al. The diagnostic accuracy of 22-gauge and 25-gauge needles in endoscopic ultrasound-guided fine needle aspiration of solid pancreatic lesions: a meta-analysis. *Endoscopy*. 2013;45:86–92.
152. Ranney N, Phadnis M, Trevino J, et al. Impact of biliary stents on EUS-guided FNA of pancreatic mass lesions. *Gastrointest Endosc*. 2012;76:76–83.
153. Fisher JM, Gordon SR, Gardner TB. The impact of prior biliary stenting on the accuracy and complication rate of endoscopic ultrasound fine-needle aspiration for diagnosing pancreatic adenocarcinoma. *Pancreas*. 2011;40:21–24.
154. Paquin SC, Gariepy G, Lepanto L, et al. A first report of tumor seeding because of EUS-guided FNA of a pancreatic adenocarcinoma. *Gastrointest Endosc*. 2005;61:610–611.
155. Shah JN, Fraker D, Guerry D, et al. Melanoma seeding of an EUS-guided fine needle track. *Gastrointest Endosc*. 2004;59:923–924.
156. Doi S, Yasuda I, Iwashita T, et al. Needle tract implantation on the esophageal wall after EUS-guided FNA of metastatic mediastinal lymphadenopathy. *Gastrointest Endosc*. 2008;67:988–990.
157. Ito Y, Asahi S, Matsuzuka F, et al. Needle tract implantation of follicular neoplasm after fine-needle aspiration biopsy: report of a case. *Thyroid*. 2006;16:1059–1062.
158. Suzuki K, Takamochi K, Funai K, et al. Needle tract implantation clearly visualized by computed tomography following needle biopsy of malignant mesothelioma. *Eur J Cardiothorac Surg*. 2006;29:1051.
159. Fowler N, Asatianni E, Cheson B. Needle tract seeding after bone marrow biopsy in non-Hodgkin lymphoma. *Leuk Lymphoma*. 2008;49:156–158.
160. Chang S, Kim SH, Lim HK, et al. Needle tract implantation after percutaneous interventional procedures in hepatocellular carcinomas: lessons learned from a 10-year experience. *Korean J Radiol*. 2008;9:268–274.
161. Rowe LR, Mulvihill SJ, Emerson L, et al. Subcutaneous tumor seeding following needle core biopsy of hepatocellular carcinoma. *Diagn Cytopathol*. 2007;35:717–721.
162. Liu Y-W, Chen C-L, Chen Y-S, et al. Needle tract implantation of hepatocellular carcinoma after fine needle biopsy. *Dig Dis Sci*. 2007;52:228–231.
163. Lundstedt C, Stridbeck H, Andersson R, et al. Tumor seeding occurring after fine-needle biopsy of abdominal malignancies. *Acta Radiologica*. 1991;32:518–520.
164. Smith EH. Complications of percutaneous abdominal fine-needle biopsy. *Radiology*. 1991;178:253–258.
165. Micames C, Jowell PS, White R, et al. Lower frequency of peritoneal carcinomatosis in patients with pancreatic cancer diagnosed by EUS-guided FNA vs. percutaneous FNA. *Gastrointest Endosc*. 2003;58:690–695.
166. Silva MA, Hegab B, Hyde C, et al. Needle track seeding following biopsy of liver lesions in the diagnosis of hepatocellular cancer: a systematic review and meta-analysis. *Gut*. 2008;57:1592–1596.
167. Heimbach JK, Sanchez W, Rosen CB, et al. Trans-peritoneal fine needle aspiration biopsy of hilar cholangiocarcinoma is associated with disease dissemination. *HPB*. 2011;13:356–360.
168. El Chafti AH, Dewitt J, Leblanc JK, et al. Impact of preoperative endoscopic ultrasound-guided fine needle aspiration on postoperative recurrence and survival in cholangiocarcinoma patients. *Endoscopy*. 2013;45:883–889.
169. Farrell RJ, Agarwal B, Brandwein SL, et al. Intraductal US is a useful adjunct to ERCP for distinguishing malignant from benign biliary strictures. *Gastrointest Endosc*. 2002;56:681–687.
170. Vazquez-Sequeiros E, Baron TH, Clain JE, et al. Evaluation of indeterminate bile duct strictures by intraductal US. *Gastrointest Endosc*. 2002;56:372–379.
171. Domagk D, Wessling J, Reimer P, et al. Endoscopic retrograde cholangiopancreatography, intraductal ultrasonography, and magnetic resonance cholangiopancreatography in bile duct strictures: a prospective comparison of imaging diagnostics with histopathological correlation. *Am J Gastroenterol*. 2004;99:1684–1689.
172. Krishna NB, Saripalli S, Safdar R, et al. Intraductal US in evaluation of biliary strictures without a mass lesion on CT scan or magnetic resonance imaging: significance of focal wall thickening and extrinsic compression at the stricture site. *Gastrointest Endosc*. 2007;66:90–96.
173. Stavropoulos S, Larghi A, Verna E, et al. Intraductal ultrasound for the evaluation of patients with biliary strictures and no abdominal mass on computed tomography. *Endoscopy*. 2005;37:715–721.
174. Tamada K, Nagai H, Yasuda Y, et al. Transpapillary intraductal US prior to biliary drainage in the assessment of longitudinal spread of extrahepatic bile duct carcinoma. *Gastrointest Endosc*. 2001;53:300–307.
175. Varadarajulu S, Eloubeidi MA, Wilcox CM. Prospective evaluation of indeterminate ERCP findings by intraductal ultrasound. *J Gastroenterol Hepatol*. 2007;22:2086–2092.
176. Tamada K, Tomiyama T, Wada S, et al. Endoscopic transpapillary bile duct biopsy with the combination of intraductal ultrasonography in the diagnosis of biliary strictures. *Gut*. 2002;50:326–331.
177. Tamada K, Ueno N, Tomiyama T, et al. Characterization of biliary strictures using intraductal ultrasonography: comparison with percutaneous cholangioscopic biopsy. *Gastrointest Endosc*. 1998;47:341–349.
178. Heinzel HS, Kammerer S, Rammes C, et al. Comparative analysis of ERCP, IDUS, EUS and CT in predicting malignant bile duct strictures. *World J Gastroenterol*. 2014;20:10495–10503.
179. Wehrmann T, Riphaus A, Martchenko K, et al. Intraductal ultrasonography in the diagnosis of Mirizzi syndrome. *Endoscopy*. 2006;38:717–722.
180. Dumortier J, Scoazec JY, Valette PJ, et al. Successful liver transplantation for diffuse biliary papillomatosis. *J Hepatol*. 2001;35:542–543.
181. Tamada K, Tomiyama T, Oohashi A, et al. Bile duct wall thickness measured by intraductal US in patients who have not undergone previous biliary drainage. *Gastrointest Endosc*. 1999;49:199–203.
182. Tischendorf JJ, Meier PN, Schneider A, et al. Transpapillary intraductal ultrasound in the evaluation of dominant bile duct stenoses in patients with primary sclerosing cholangitis. *Scand J Gastroenterol*. 2007;42:1011–1017.
183. Itoi T, Reddy DN, Sofuni A, et al. Clinical evaluation of a prototype multi-bending peroral direct cholangioscope. *Dig Endosc*. 2014;26:100–107.
184. Fukuda Y, Tsuyuguchi T, Sakai Y, et al. Diagnostic utility of peroral cholangioscopy for various bile-duct lesions. *Gastrointest Endosc*. 2005;62:374–382.
185. Nguyen NQ, Schoeman MN, Ruszkiewicz A. Clinical utility of EUS before cholangioscopy in the evaluation of difficult biliary strictures. *Gastrointest Endosc*. 2013;78:868–874.
186. Siddiqui AA, Mehendiratta V, Jackson W, et al. Identification of cholangiocarcinoma by using the Spyglass Spyscope system for peroral cholangioscopy and biopsy collection. *Clin Gastroenterol Hepatol*. 2012;10:466–471. quiz e48.
187. Njei B, McCarty TR, Varadarajulu S, et al. Cost utility of ERCP-based modalities for the diagnosis of cholangiocarcinoma in primary sclerosing cholangitis. *Gastrointest Endosc*. 2017;85:773–781.e10.
188. Tanaka R, Itoi T, Honjo M, et al. New digital cholangiopancreatostomy for diagnosis and therapy of pancreaticobiliary diseases (with videos). *J Hepatobiliary Pancreat Sci*. 2016;23:220–226.

189. Sethi A, Chen YK, Austin GL, et al. ERCP with cholangiopancreatoscopy may be associated with higher rates of complications than ERCP alone: a single-center experience. *Gastrointest Endosc.* 2011;73:251–256.
190. Sai JK, Suyama M, Kubokawa Y, et al. Early detection of extrahepatic bile-duct carcinomas in the nonicteric stage by using MRCP followed by EUS. *Gastrointest Endosc.* 2009;70:29–36.
191. Mishra G, Conway JD. Endoscopic ultrasound in the evaluation of radiologic abnormalities of the liver and biliary tree. *Curr Gastroenterol Rep.* 2009;11:150–154.
192. Meister T, Heinzel HS, Woestmeyer C, et al. Intraductal ultrasound substantiates diagnostics of bile duct strictures of uncertain etiology. *World J Gastroenterol.* 2013;19:874–881.
193. Nimura Y. Staging cholangiocarcinoma by cholangioscopy. *HPB (Oxford).* 2008;10:113–115.
194. Sato M, Inoue H, Ogawa S, et al. Limitations of percutaneous transhepatic cholangioscopy for the diagnosis of the intramural extension of bile duct carcinoma. *Endoscopy.* 1998;30:281–288.
195. Inui K, Miyoshi H. Cholangiocarcinoma and intraductal sonography. *Gastrointest Endosc Clin N Am.* 2005;15:143–155. x.
196. Tamada K, Tomiyama T, Ichiyama M, et al. Influence of biliary drainage catheter on bile duct wall thickness as measured by intraductal ultrasonography. *Gastrointest Endosc.* 1998;47:28–32.
197. Myers RP, Shaffer EA, Beck PL. Gallbladder polyps: epidemiology, natural history and management. *Can J Gastroenterol.* 2002;16:187–194.
198. Sugiyama M, Atomi Y, Yamato T. Endoscopic ultrasonography for differential diagnosis of polypoid gall bladder lesions: analysis in surgical and follow up series. *Gut.* 2000;46:250–254.
199. Kim JS, Lee JK, Kim Y, et al. US characteristics for the prediction of neoplasm in gallbladder polyps 10 mm or larger. *Eur Radiol.* 2016;26:1134–1140.
200. Choi WB, Lee SK, Kim MH, et al. A new strategy to predict the neoplastic polyps of the gallbladder based on scoring system using EUS. *Gastrointest Endosc.* 2000;52:372–379.
201. Corwin MT, Siewert B, Sheiman RG, et al. Incidentally detected gallbladder polyps: is follow-up necessary?—Long-term clinical and US analysis of 346 patients. *Radiology.* 2011;258:277–282.
202. Wiles R, Varadpande M, Muly S, et al. Growth rate and malignant potential of small gallbladder polyps—systematic review of evidence. *Surgeon.* 2014;12:221–226.
203. French DG, Allen PD, Ellsmere JC. The diagnostic accuracy of transabdominal ultrasonography needs to be considered when managing gallbladder polyps. *Surg Endosc.* 2013;27:4021–4025.
204. Azuma T, Yoshikawa T, Araida T, et al. Differential diagnosis of polypoid lesions of the gallbladder by endoscopic ultrasonography. *Am J Surg.* 2001;181:65–70.
205. Choi JH, Seo DW, Park DH, et al. Utility of contrast-enhanced harmonic EUS in the diagnosis of malignant gallbladder polyps (with videos). *Gastrointest Endosc.* 2013;78:484–493.
206. Lee JS, Kim JH, Kim YJ, et al. Diagnostic accuracy of transabdominal high-resolution US for staging gallbladder cancer and differential diagnosis of neoplastic polyps compared with EUS. *Eur Radiol.* 2017;27:3097–3103.
207. Sadamoto Y, Oda S, Tanaka M, et al. A useful approach to the differential diagnosis of small polypoid lesions of the gallbladder, utilizing an endoscopic ultrasound scoring system. *Endoscopy.* 2002;34:959–965.
208. Cho JH, Park JY, Kim YJ, et al. Hypoechoic foci on EUS are simple and strong predictive factors for neoplastic gallbladder polyps. *Gastrointest Endosc.* 2009;69:1244–1250.
209. Cheon YK, Cho WY, Lee TH, et al. Endoscopic ultrasonography does not differentiate neoplastic from non-neoplastic small gallbladder polyps. *World J Gastroenterol.* 2009;15:2361–2366.
210. Park CH, Chung MJ, Oh TG, et al. Differential diagnosis between gallbladder adenomas and cholesterol polyps on contrast-enhanced harmonic endoscopic ultrasonography. *Surg Endosc.* 2013;27:1414–1421.
211. Kimura K, Fujita N, Noda Y, et al. Differential diagnosis of large-sized pedunculated polypoid lesions of the gallbladder by endoscopic ultrasonography: a prospective study. *J Gastroenterol.* 2001;36:619–622.
212. Nasiri S, Gafuri A, Karamnejad M, et al. Four port-site recurrences of gall bladder cancer after laparoscopic cholecystectomy. *ANZ J Surg.* 2009;79:75–76.
213. Hu JB, Sun XN, Xu J, et al. Port site and distant metastases of gallbladder cancer after laparoscopic cholecystectomy diagnosed by positron emission tomography. *World J Gastroenterol.* 2008;14:6428–6431.
214. Fujita N, Noda Y, Kobayashi G, et al. Diagnosis of the depth of invasion of gallbladder carcinoma by EUS. *Gastrointest Endosc.* 1999;50:659–663.
215. Sadamoto Y, Kubo H, Harada N, et al. Preoperative diagnosis and staging of gallbladder carcinoma by EUS. *Gastrointest Endosc.* 2003;58:536–541.
216. Hijioka S, Hara K, Mizuno N, et al. Diagnostic yield of endoscopic retrograde cholangiography and of EUS-guided fine needle aspiration sampling in gallbladder carcinomas. *J Hepatobiliary Pancreat Sci.* 2012;19:650–655.
217. Hijioka S, Mekky MA, Bhatia V, et al. Can EUS-guided FNA distinguish between gallbladder cancer and xanthogranulomatous cholecystitis? *Gastrointest Endosc.* 2010;72:622–627.
218. Jacobson BC, Pitman MB, Brugge WR. EUS-guided FNA for the diagnosis of gallbladder masses. *Gastrointest Endosc.* 2003;57:251–254.
219. Kim HJ, Lee SK, Jang JW, et al. Diagnostic role of endoscopic ultrasonography-guided fine needle aspiration of gallbladder lesions. *Hepatogastroenterology.* 2012;59:1691–1695.
220. Varadarajulu S, Eloubeidi MA. Endoscopic ultrasound-guided fine-needle aspiration in the evaluation of gallbladder masses. *Endoscopy.* 2005;37:751–754.
221. Antonini F, Acito L, Sisti S, et al. Metastatic melanoma of the gallbladder diagnosed by EUS-guided FNA. *Gastrointest Endosc.* 2016;84:1072–1073.
222. Jacobson BC, Waxman I, Parmar K, et al. Endoscopic ultrasound-guided gallbladder bile aspiration in idiopathic pancreatitis carries a significant risk of bile peritonitis. *Pancreatology.* 2002;2:26–29.
223. Downing SR, Cadogan KA, Ortega G, et al. Early-stage gallbladder cancer in the surveillance, epidemiology, and end results database: effect of extended surgical resection. *Arch Surg.* 2011;146:734–738.
224. Fujimoto T, Kato Y, Kitamura T, et al. Case report: hypoechoic area as an ultrasound finding suggesting subserosal invasion in polypoid carcinoma of the gall bladder. *Br J Radiol.* 2001;74:455–457.
225. Kim MY, Baik SK, Choi YJ, et al. Endoscopic sonographic evaluation of the thickened gallbladder wall in patients with acute hepatitis. *J Clin Ultrasound.* 2003;31:245–249.
226. Sato M, Ishida H, Konno K, et al. Segmental chronic cholecystitis: sonographic findings and clinical manifestations. *Abdom Imaging.* 2002;27:43–46.
227. Ishizuka D, Shirai Y, Tsukada K, et al. Gallbladder cancer with intratumoral anechoic foci: a mimic of adenomyomatosis. *Hepatogastroenterology.* 1998;45:927–929.
228. Nabatame N, Shirai Y, Nishimura A, et al. High risk of gallbladder carcinoma in elderly patients with segmental adenomyomatosis of the gallbladder. *J Exp Clin Cancer Res.* 2004;23:593–598.
229. Guzman-Valdivia G. Xanthogranulomatous cholecystitis: 15 years' experience. *World J Surg.* 2004;28:254–257.
230. Muguruma N, Okamura S, Okahisa T, et al. Endoscopic sonography in the diagnosis of xanthogranulomatous cholecystitis. *J Clin Ultrasound.* 1999;27:347–350.
231. Mizuguchi M, Kudo S, Fukahori T, et al. Endoscopic ultrasonography for demonstrating loss of multiple-layer pattern of the thickened gallbladder wall in the preoperative diagnosis of gallbladder cancer. *Eur Radiol.* 1997;7:1323–1327.

232. Kim HJ, Park JH, Park DI, et al. Clinical usefulness of endoscopic ultrasonography in the differential diagnosis of gallbladder wall thickening. *Dig Dis Sci.* 2012;57:508–515.
233. Imazu H, Mori N, Kanazawa K, et al. Contrast-enhanced harmonic endoscopic ultrasonography in the differential diagnosis of gallbladder wall thickening. *Dig Dis Sci.* 2014;59:1909–1916.
234. Eaton JE, Thackeray EW, Lindor KD. Likelihood of malignancy in gallbladder polyps and outcomes following cholecystectomy in primary sclerosing cholangitis. *Am J Gastroenterol.* 2012;107:431–439.
235. Palazzo L, Hochain P, Helmer C, et al. Biliary varices on endoscopic ultrasonography: clinical presentation and outcome. *Endoscopy.* 2000;32:520–524.
236. Tanno S, Obara T, Maguchi H, et al. Thickened inner hypoechoic layer of the gallbladder wall in the diagnosis of anomalous pancreaticobiliary ductal union with endosonography. *Gastrointest Endosc.* 1997;46:520–526.
237. Kawakatsu M, Vilgrain V, Zins M, et al. Radiologic features of papillary adenoma and papillomatosis of the biliary tract. *Abdom Imaging.* 1997;22:87–90.
238. Ogura T, Kurisu Y, Masuda D, et al. Can endoscopic ultrasound-guided fine needle aspiration offer clinical benefit for thick-walled gallbladders? *Dig Dis Sci.* 2014;59:1917–1924.
239. Laleman W, Verreth A, Topal B, et al. Endoscopic resection of ampullary lesions: a single-center 8-year retrospective cohort study of 91 patients with long-term follow-up. *Surg Endosc.* 2013;27:3865–3876.
240. Gluck N, Strul H, Rozner G, et al. Endoscopy and EUS are key for effective surveillance and management of duodenal adenomas in familial adenomatous polyposis. *Gastrointest Endosc.* 2015;81:960–966.
241. Sommerville CA, Limongelli P, Pai M, et al. Survival analysis after pancreatic resection for ampullary and pancreatic head carcinoma: an analysis of clinicopathological factors. *J Surg Oncol.* 2009;100:651–656.
242. Kim HN, Kim KM, Shin JU, et al. Prediction of carcinoma after resection in subjects with ampullary adenomas on endoscopic biopsy. *J Clin Gastroenterol.* 2013;47:346–351.
243. Will U, Bosseckert H, Meyer F. Correlation of endoscopic ultrasonography (EUS) for differential diagnostics between inflammatory and neoplastic lesions of the papilla of Vater and the peripapillary region with results of histologic investigation. *Ultraschall Med.* 2008;29:275–280.
244. Keriven O, Napoléon B, Souquet JC, et al. Patterns of the ampulla of Vater at endoscopic ultrasonography (abstract). *Gastrointest Endosc.* 1993;39:A290.
245. Pang JC, Minter RM, Kwon RS, et al. The role of cytology in the preoperative assessment and management of patients with pancreaticobiliary tract neoplasms. *J Gastrointest Surg.* 2013;17:501–510.
246. Defrain C, Chang CY, Srikureja W, et al. Cytologic features and diagnostic pitfalls of primary ampullary tumors by endoscopic ultrasound-guided fine-needle aspiration biopsy. *Cancer.* 2005;105:289–297.
247. Ridditid W, Schmidt SE, Al-Haddad MA, et al. Performance characteristics of EUS for locoregional evaluation of ampullary lesions. *Gastrointest Endosc.* 2015;81:380–388.
248. Amin MB, Edge S, Greene F, et al., eds. *American Joint Committee on Cancer Staging Manual.* 8th ed. Switzerland: Springer International Publishing AG; 2017.
249. Cannon ME, Carpenter SL, Elta GH, et al. EUS compared with CT, magnetic resonance imaging, and angiography and the influence of biliary stenting on staging accuracy of ampullary neoplasms. *Gastrointest Endosc.* 1999;50:27–33.
250. Tio TL, Sie LH, Kallimanis G, et al. Staging of ampullary and pancreatic carcinoma: comparison between endosonography and surgery. *Gastrointest Endosc.* 1996;44:706–713.
251. Yoshida T, Matsumoto T, Shibata K, et al. Patterns of lymph node metastasis in carcinoma of the ampulla of Vater. *Hepatogastroenterology.* 2000;47:880–883.
252. Winter JM, Cameron JL, Olino K, et al. Clinicopathologic analysis of ampullary neoplasms in 450 patients: implications for surgical strategy and long-term prognosis. *J Gastrointest Surg.* 2010;14:379–387.
253. Nakao A, Harada A, Nonami T, et al. Prognosis of cancer of the duodenal papilla of Vater in relation to clinicopathological tumor extension. *Hepatogastroenterology.* 1994;41:73–78.
254. Shirai Y, Tsukada K, Ohtani T, et al. Carcinoma of the ampulla of Vater: histopathologic analysis of tumor spread in Whipple pancreatoduodenectomy specimens. *World J Surg.* 1995;19:102–106. discussion 106–107.
255. Yamaguchi K, Enjoji M. Carcinoma of the ampulla of vater. A clinicopathologic study and pathologic staging of 109 cases of carcinoma and 5 cases of adenoma. *Cancer.* 1987;59:506–515.
256. Artifon EL, Couto Jr D, Sakai P, et al. Prospective evaluation of EUS versus CT scan for staging of ampullary cancer. *Gastrointest Endosc.* 2009;70:290–296.
257. Buscail L, Pages P, Berthelemy P, et al. Role of EUS in the management of pancreatic and ampullary carcinoma: a prospective study assessing resectability and prognosis. *Gastrointest Endosc.* 1999;50:34–40.
258. Chen CH, Yang CC, Yeh YH, et al. Reappraisal of endosonography of ampullary tumors: correlation with transabdominal sonography, CT, and MRI. *J Clin Ultrasound.* 2009;37:18–25.
259. Ito K, Fujita N, Noda Y, et al. Preoperative evaluation of ampullary neoplasm with EUS and transpapillary intraductal US: a prospective and histopathologically controlled study. *Gastrointest Endosc.* 2007;66:740–747.
260. Maluf-Filho F, Sakai P, Cunha JE, et al. Radial endoscopic ultrasound and spiral computed tomography in the diagnosis and staging of periampullary tumors. *Pancreatology.* 2004;4:122–128.
261. Midwinter MJ, Beveridge CJ, Wilksdon JB, et al. Correlation between spiral computed tomography, endoscopic ultrasonography and findings at operation in pancreatic and ampullary tumours. *Br J Surg.* 1999;86:189–193.
262. Rivadeneira DE, Pochapin M, Grobmyer SR, et al. Comparison of linear array endoscopic ultrasound and helical computed tomography for the staging of periampullary malignancies. *Ann Surg Oncol.* 2003;10:890–897.
263. Rejeski JJ, Kundu S, Hauser M, et al. Characteristic endoscopic ultrasound findings of ampullary lesions that predict the need for surgical excision or endoscopic ampullectomy. *Endosc Ultrasound.* 2016;5:184–188.
264. Trikudanathan G, Njei B, Attam R, et al. Staging accuracy of ampullary tumors by endoscopic ultrasound: meta-analysis and systematic review. *Dig Endosc.* 2014;26:617–626.
265. Itoh A, Goto H, Naitoh Y, et al. Intraductal ultrasonography in diagnosing tumor extension of cancer of the papilla of Vater. *Gastrointest Endosc.* 1997;45:251–260.
266. Menzel J, Hoepffner N, Sulkowski U, et al. Polypoid tumors of the major duodenal papilla: preoperative staging with intraductal US, EUS, and CT—a prospective, histopathologically controlled study. *Gastrointest Endosc.* 1999;49:349–357.
267. Mukai H, Nakajima M, Yasuda K, et al. Evaluation of endoscopic ultrasonography in the pre-operative staging of carcinoma of the ampulla of Vater and common bile duct. *Gastrointest Endosc.* 1992;38:676–683.
268. Roberts KJ, McCulloch N, Sutcliffe R, et al. Endoscopic ultrasound assessment of lesions of the ampulla of Vater is of particular value in low-grade dysplasia. *HPB (Oxford).* 2013;15:18–23.
269. Rosch T, Braig C, Gain T, et al. Staging of pancreatic and ampullary carcinoma by endoscopic ultrasonography. Comparison with conventional sonography, computed tomography, and angiography. *Gastroenterology.* 1992;102:188–199.

270. Wee E, Lakhtakia S, Gupta R, et al. The diagnostic accuracy and strength of agreement between endoscopic ultrasound and histopathology in the staging of ampullary tumors. *Indian J Gastroenterol.* 2012;31:324–332.
271. Manta R, Conigliaro R, Castellani D, et al. Linear endoscopic ultrasonography vs magnetic resonance imaging in ampullary tumors. *World J Gastroenterol.* 2010;16:5592–5597.
272. Napoleon B, Pialat J, Saurin JC, et al. Adenomas and adenocarcinomas of the ampulla of Vater: endoscopic therapy. *Gastroenterol Clin Biol.* 2004;28:385–392.
273. Vogt M, Jakobs R, Benz C, et al. Endoscopic therapy of adenomas of the papilla of Vater. A retrospective analysis with long-term follow-up. *Dig Liver Dis.* 2000;32:339–345.
274. Brown KM, Tompkins AJ, Yong S, et al. Pancreaticoduodenectomy is curative in the majority of patients with node-negative ampullary cancer. *Arch Surg.* 2005;140:529–532. discussion 532–533.
275. Ceppa EP, Burbridge RA, Rialon KL, et al. Endoscopic versus surgical ampullectomy: an algorithm to treat disease of the ampulla of Vater. *Ann Surg.* 2013;257:315–322.
276. Napoleon B, Gincul R, Ponchon T, et al. Endoscopic papillectomy for early ampullary tumors: long-term results from a large multicenter prospective study. *Endoscopy.* 2014;46:127–134.
277. Catalano MF, Linder JD, Chak A, et al. Endoscopic management of adenoma of the major duodenal papilla. *Gastrointest Endosc.* 2004;59:225–232.
278. Desilets DJ, Dy RM, Ku PM, et al. Endoscopic management of tumors of the major duodenal papilla: refined techniques to improve outcome and avoid complications. *Gastrointest Endosc.* 2001;54:202–208.
279. Ponchon T, Berger F, Chavaillon A, et al. Contribution of endoscopy to diagnosis and treatment of tumors of the ampulla of Vater. *Cancer.* 1989;64:161–167.
280. Patel R, Davitte J, Varadarajulu S, et al. Endoscopic resection of ampullary adenomas: complications and outcomes. *Dig Dis Sci.* 2011;56:3235–3240.
281. Clary BM, Tyler DS, Dematos P, et al. Local ampullary resection with careful intraoperative frozen section evaluation for presumed benign ampullary neoplasms. *Surgery.* 2000;127:628–633.
282. Binmoeller KF, Boaventura S, Ramsperger K, et al. Endoscopic snare excision of benign adenomas of the papilla of Vater. *Gastrointest Endosc.* 1993;39:127–131.
283. Norton ID, Gostout CJ, Baron TH, et al. Safety and outcome of endoscopic snare excision of the major duodenal papilla. *Gastrointest Endosc.* 2002;56:239–243.
284. Saurin JC, Chavaillon A, Napoleon B, et al. Long-term follow-up of patients with endoscopic treatment of sporadic adenomas of the papilla of vater. *Endoscopy.* 2003;35:402–406.
285. Zadorova Z, Dvofak M, Hajer J. Endoscopic therapy of benign tumors of the papilla of Vater. *Endoscopy.* 2001;33:345–347.
286. Cheng CL, Sherman S, Fogel EL, et al. Endoscopic snare papillectomy for tumors of the duodenal papillae. *Gastrointest Endosc.* 2004;60:757–764.
287. Han J, Lee SK, Park DH, et al. Treatment outcome after endoscopic papillectomy of tumors of the major duodenal papilla. *Korean J Gastroenterol.* 2005;46:110–119.
288. Irani S, Arai A, Ayub K, et al. Papillectomy for ampullary neoplasm: results of a single referral center over a 10-year period. *Gastrointest Endosc.* 2009;70:923–932.
289. Jung MK, Cho CM, Park SY, et al. Endoscopic resection of ampullary neoplasms: a single-center experience. *Surg Endosc.* 2009;23:2568–2574.
290. Katsinelos P, Paroutoglou G, Kountouras J, et al. Safety and long-term follow-up of endoscopic snare excision of ampullary adenomas. *Surg Endosc.* 2006;20:608–613.
291. Martin JA, Haber GB. Ampullary adenoma: clinical manifestations, diagnosis, and treatment. *Gastrointest Endosc Clin N Am.* 2003;13:649–669.
292. Moon JH, Cha SW, Cho YD, et al. Wire-guided endoscopic snare papillectomy for tumors of the major duodenal papilla. *Gastrointest Endosc.* 2005;61:461–466.
293. Yamao T, Isomoto H, Kohno S, et al. Endoscopic snare papillectomy with biliary and pancreatic stent placement for tumors of the major duodenal papilla. *Surg Endosc.* 2010;24:119–124.
294. Ma T, Jang EJ, Zukerberg LR, et al. Recurrences are common after endoscopic ampullectomy for adenoma in the familial adenomatous polyposis (FAP) syndrome. *Surg Endosc.* 2014;28:2349–2356.
295. Boix J, Lorenzo-Zuniga V, Moreno de Vega V, et al. Endoscopic resection of ampullary tumors: 12-year review of 21 cases. *Surg Endosc.* 2009;23:45–49.



**Video 16.1A** Linear Endoscopic Ultrasound Exam (7.5 MHz) of the Bile Duct Demonstrating a 15-mm Shadowing Stone in the Distal Bile Duct With Upstream Common Bile Duct Dilation

The patient presented with jaundice and intermittent right upper quadrant pain.

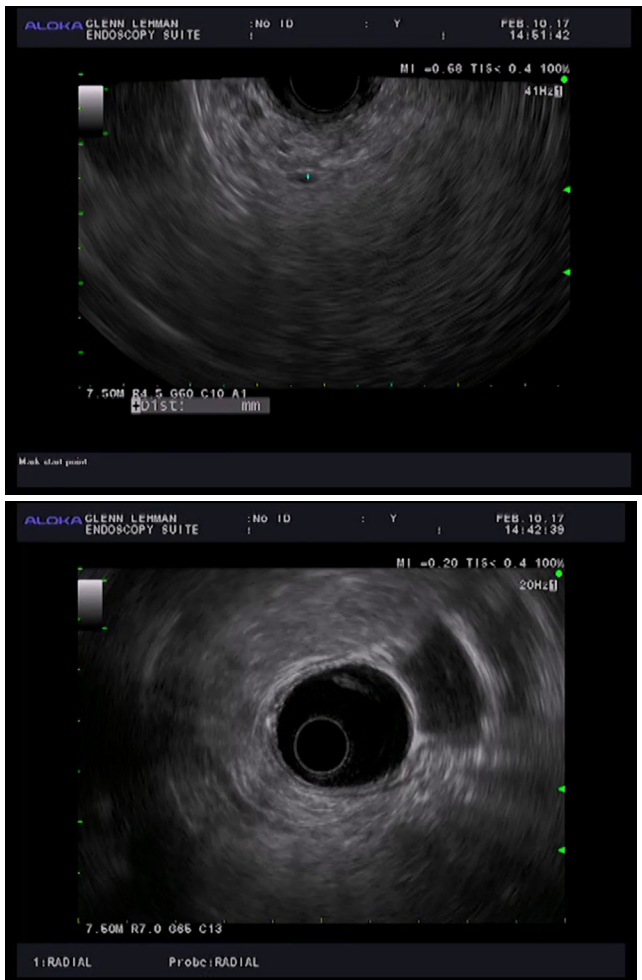


**Video 16.1B** The Same Stone Interrogated With a Radial Echoendoscope



**Video 16.2** Interrogation of the Head of the Pancreas, Distal Bile Duct, and Pancreatic Duct Using a Radial Echoendoscope in a Patient Presenting With Right Upper Quadrant Pain and Elevated Transaminases

A free-floating nonshadowing echogenic structure, likely sludge but could be a noncalcified stone, is noted in the common bile duct.



**Videos 16.3A and B** These Videos Demonstrate the Technique of Interrogating the Bile Duct From the First Part of the Duodenum Using a Linear (A) and Radial (B) Echoendoscope

The nondilated bile duct is seen coursing through the pancreatic head until it enters the duodenal wall.



**Video 16.4** Linear Echoendoscope Examination of the Gallbladder  
Several irregular calcified gallstones are seen in the gallbladder lumen. The patient was asymptomatic from biliary standpoint.



**Video 16.5** Interrogation of the Bile Duct Using a Linear Echoendoscope in a Patient Presenting With Obstructive Jaundice

A solid distal bile duct mass is noted, in association with loss of the characteristic layers of the bile duct wall in that location. A bile duct stent appears as a hyperechoic structure in the lumen of the bile duct. The bile duct wall upstream from the stricture appears thickened.



**Video 16.7** Linear Endoscopic Ultrasound (EUS) Examination of a Bile Duct Mass in a Patient Who Presented With Painless Jaundice and Underwent Endoscopic Retrograde Cholangiopancreatography Where a Fully Covered Metallic Stent Was Placed Ahead of the EUS Procedure

Despite artifacts from the stent, the bile duct mass was clearly visualized on EUS and staging confirmed no vascular invasion. Fine-needle aspiration cytology confirmed adenocarcinoma.



**Video 16.6** Examination of the Head of the Pancreas Along With the Common Bile Duct Showed a Dilated Bile Duct Upstream From a Mass

Endoscopic retrograde cholangiopancreatography was completed prior to endoscopic ultrasound (EUS) with plastic stent placement across a distal bile duct stricture. On EUS, a segment of loss of interface between the mass and portal vein indicates tumor invasion. The site of fine-needle aspiration is confirmed to be within the stricture on fluoroscopy. Final cytology review confirmed adenocarcinoma. (Courtesy of Dr. Shyam Varadarajulu.)



**Video 16.8** Linear Endoscopic Ultrasound Exam of a Large Gallbladder Mass

Substantial thickening of the gallbladder wall seen with complete loss of the wall layers, along with invasion of the adjacent liver parenchyma, were the basis of T3 staging in this case. The lumen of the gallbladder is significantly restricted with stones and sludge seen in it. Fine-needle aspiration was performed using a 25-gauge needle and cytology was diagnostic of adenocarcinoma.



**Video 16.9** Radial Echoendoscope Examination of the Head of the Pancreas Along With the Main Pancreatic and Common Bile Ducts in a Patient With Ampullary Tumor Presenting With Dilated Ducts on Computed Tomography

The tumor invades the submucosa and extends into the very distal portion of the bile duct.



**Video 16.10** The Bile Duct Has Been Previously Stented and Appears Decompressed

On the contrary, the pancreatic duct (PD) remains significantly dilated. The ampullary mass invades the duodenal wall and distal bile and PDs.

# How to Perform Anorectal Endoscopic Ultrasonography

PAUL FOCKENS, ROBERT H. HAWES, AND SHYAM VARADARAJULU

## The Perianal Area

Examination of the perianal area is simplicity itself. No special patient preparation is required. The patient is told that any discomfort will be similar to having a finger in the anus and that the procedure will likely be less uncomfortable than digital rectal examination by a doctor. To the patient, the rigid probe is potentially a frightening piece of equipment, so it is worth mentioning that only the distal few centimeters will enter the anus (as opposed to rectal endosonography, in which insertion is obviously deeper). Some endosonographers place all patients in the left lateral position, whereas others prefer female patients to be in the prone position for examination. Placing women in the left lateral position can potentially distort anterior perineal anatomic features, with the result that the asymmetric images obtained will be difficult to interpret, especially with respect to perineal scarring.<sup>1</sup>

Appropriate equipment is essential for successful anal endoscopic ultrasonography (EUS). The standard (most commonly described in the literature) is the Brüel-Kjaer mechanical radial rigid probe. In the early days of EUS, when the principal instrument was the mechanical radial echoendoscope, examiners attempted to use this scope for anal EUS examination. However, the near-field imaging was poor, and the anal sphincters were often obscured by the ringdown artifact. Consequently, Olympus designed and marketed a rigid rectal probe compatible with its mechanical radial processor. However, with the introduction of electronic radial echoendoscopes, a flexible instrument is now available that can deliver high-quality images of anal anatomy and has rendered the dedicated rigid probe obsolete.

The rigid probe is prepared as necessary for the transducer being used. Some systems, for example, require the transducer head to be filled with degassed water to achieve acoustic coupling. This is accomplished by injection using a syringe through a side port. The probe must be maneuvered during filling so that all air is expelled through a pinhole located at the tip of the cone.

Whether or not water filling is required, the rigid probe tip is lubricated with ultrasound jelly and then is covered with a condom, which is itself lubricated to facilitate insertion. The probe is then inserted into the anus, and image acquisition is started by the operator. The probe is inserted so that its tip lies just in the distal rectum. The probe is then withdrawn gently to examine the anal sphincters. As for all ultrasound examinations, the clinical findings are generally based on the image displayed on the

monitor screen in real time (with the exception of three-dimensional acquisition, in which case the examination in its entirety can be replayed later). However, still images are usually required, and it is convenient to obtain these at three levels: the proximal, middle, and distal anal canal. These three anatomic levels are imaged at standard magnification, and the examination is then repeated at a higher magnification so that six images are obtained, three at each magnification. The probe is oriented so that anterior (i.e., the 12-o'clock position) is uppermost and is then withdrawn. The examination is normally very quick, perhaps only a minute or so for the experienced operator who is familiar with normal and abnormal anatomy, especially when the sphincters are normal. The technique for imaging does not vary whether a rigid probe or an electronic radial flexible probe is used.

## The Rectum

EUS of the rectum is mainly performed to examine suspicious rectal polyps or to stage rectal cancer. From country to country, huge differences exist in the use of EUS for this indication. Patients should be prepared with an enema or complete bowel preparation to evacuate all stool from the area to be investigated. For the start of the examination, the patient is usually placed in the left lateral position. The position may be changed during the examination. For noncircumferential masses or laterally spreading polyps, the patient should be positioned so that the mass or polyp is in the dependent position to allow easy submersion in water. This is also an easy way to determine which wall of the rectum is involved (anterior, posterior, left, or right). Sedation is not usually necessary because the rectosigmoid junction is not passed with the instrument.

The examination is usually begun with a therapeutic endoscope with a built-in washing function. This equipment allows inspection of the mass and provides an opportunity to clear any residual stool that could degrade imaging. It also allows filling of the rectum to indicate position of the patient that will optimize water filling.

There is no standard advice for the equipment to be used. For staging of tumors located very distally in the rectum, rigid radial scanning probes are often used. An alternative is a radial scanning echoendoscope, as used in the upper gastrointestinal tract. The advantage of echoendoscopes is that they can be advanced higher up into the rectum with help of the (oblique-viewing) optics.

Linear echoendoscopes can also be used, with the advantage of enabling the examiner to perform EUS fine-needle aspiration (FNA) biopsy of extrarectal abnormalities such as lymph nodes or suspected tumor recurrences after surgery. The linear probes sometimes offer a further advantage because the tumor and mural layers can be followed in the same image. This sometimes makes it easier to determine the exact involvement of the deeper layers. Finally, mini-probes can be used in patients with superficial lesions. With 12-MHz mini-probes, a penetration depth of 2 cm is generally possible.

Using a balloon around the tip of the rigid probe or echoendoscope removes the air and allows for good acoustic coupling between probe and tumor. Filling of the rectum with water is sometimes helpful, especially in the case of smaller lesions that would otherwise be compressed with a balloon. Complete filling of the rectum with water is usually not possible and should not be attempted because it is much easier to change the patient's position. When the bowel has been prepared with an enema, care should be taken not to fill the colon extensively with water, because this may mobilize stool located in the proximal colon.

Usually, the instrument is positioned proximal to the tumor, the balloon is slowly inflated, and the lumen is filled with water (Video 17.1). From this position, the transducer should be positioned in the center of the colon to achieve perpendicular imaging of the rectal wall layers (Fig. 17.1). One should then look for the perirectal anatomic features. The universal landmark is the urinary bladder. Once the bladder has been identified, the image should be mechanically rotated so the bladder is located at the 12-o'clock position (Fig. 17.2). The instrument should be withdrawn slowly, with the transducer kept in the middle of the colon. The left-right and up-down dials should be used to adjust the transducer to maintain its position in the middle of the colon. The examiner must *not* torque the instrument because this will cause tangential imaging and potentially lead to inaccurate assessment of the depth of tumor penetration. When withdrawing the probe in the male, the seminal vesicles will be seen as echo-poor, elongated structures at the 12-o'clock position (see Fig. 17.2). Further withdrawal will bring the prostate into view. The prostate is seen as a hypoechoic, bean-shaped structure at the 12-o'clock position (Fig. 17.3). In female patients, withdrawal of the scope from the bladder first

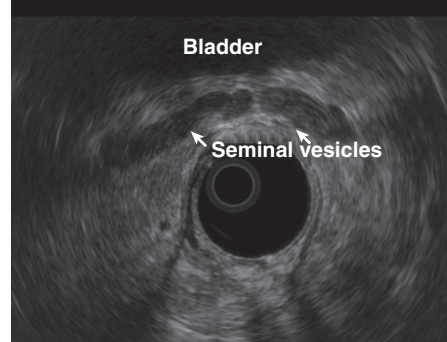
reveals the uterus (Fig. 17.4A), which is a rounded, hypoechoic structure at the 12-o'clock position. Then the vagina is seen as an elongated oval, hypoechoic structure with a characteristic hyper-echoic band in the center that represents air (see Fig. 17.4B). It is important to recognize perirectal structures because invasion into any of them represents T4 disease. In addition, one must distinguish these structures, especially the seminal vesicles, from lymph nodes.

Once the tumor is seen with EUS, the lesion is examined extensively, and all layers of the colon wall are followed underneath the tumor. Houston's valves and the rectosigmoid junction make it almost impossible to maintain a perpendicular view of the rectal wall at all times with a radial instrument scan. Adaptation of the plane of scanning with the controls of the echoendoscope is important to prevent overstaging by nonperpendicular imaging.

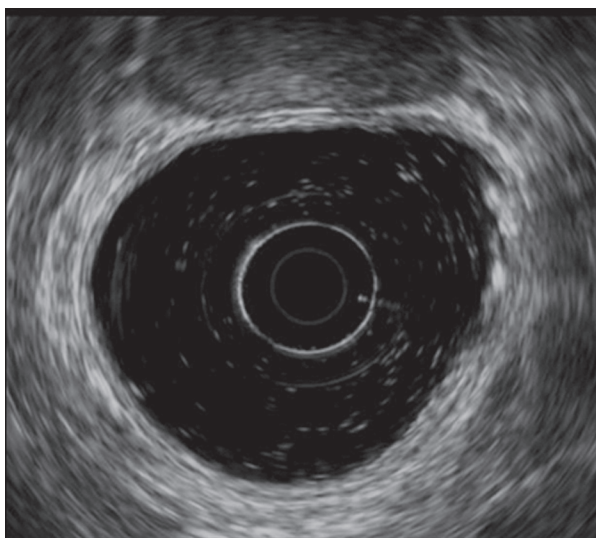
After imaging of the tumor, the echoendoscope is advanced to the rectosigmoid junction to look for suspicious perirectal lymph nodes. Although it may be possible to advance the echoendoscope higher up, this maneuver is generally not advised. Images of the lesion and all other findings should be made; there are no standard positions at which images should be captured in every examination.

In cases of small mucosal or submucosal lesions of the rectum, the practitioner may find it easier to use a dual-channel endoscope and a mini-probe. This equipment allows simultaneous water instillation, endoscopic visualization of the lesion, and ultrasound imaging.

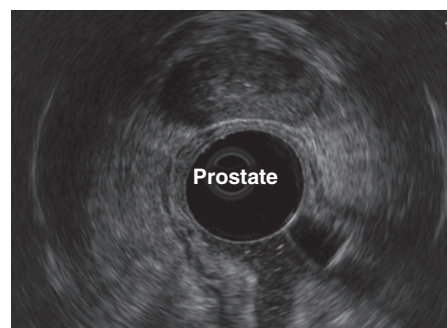
Transrectal EUS FNA is feasible and safe. Antibiotic administration is recommended before the needle is passed. Indications



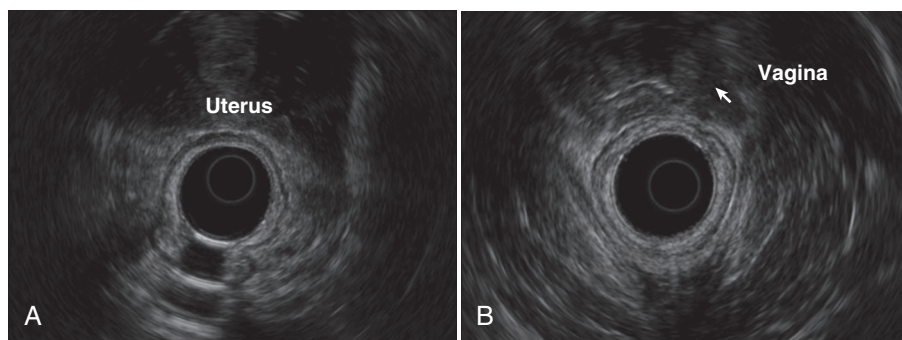
• **Fig. 17.2** The anechoic structure at the 12-o'clock position represents the urinary bladder. In men, the echo-poor elongated structures seen below the urinary bladder represent the seminal vesicles.



• **Fig. 17.1** Rectal wall layers as imaged using a radial echoendoscope.



• **Fig. 17.3** The prostate. On gradual withdrawal of the echoendoscope, a hypoechoic, bean-shaped structure is seen in men, which represents the prostate.



• **Fig. 17.4** The uterus and vagina. In the female patient, withdrawal from the bladder first reveals the uterus (A), which is a rounded, hypoechoic structure at 12 o'clock, and then the vagina (B), which is seen as an elongated oval, hypoechoic structure with a characteristic hyperechoic band in the center that represents air.

for transrectal EUS FNA include suspicious lymph nodes associated with known primary rectal cancer when the lymph nodes are not “protected” by the primary tumor (tumor lies between the transducer and the lymph node) and perirectal masses of unknown origin.

### Key Reference

1. Frudinger A, Bartram CI, Halligan S, et al. Examination techniques for endosonography of the anal canal. *Abdom Imaging*. 1998;23: 301–303.



**Video 17.1** Demonstrating the Technique for Examination of the Rectum Using a Radial Echoendoscope

# 18

## Endoscopic Ultrasonography in Rectal Cancer

FERGA C. GLEESON

### KEY POINTS

- The importance of nodal status guiding therapeutic decision-making is increasingly recognized for rectal cancer.
- Endoscopic ultrasonography (EUS) fine-needle aspiration (FNA) is recognized as being an essential component of locoregional clinical staging.
- Although EUS still has insufficient accuracy for T-staging, EUS FNA can accurately predict patients who have evidence of iliac vessel node disease by upstaging 7% of patients presenting for evaluation, in addition to establishing the presence of perirectal space nodal disease.
- Staging with EUS following neoadjuvant therapy should be approached with caution.
- The benefit of EUS FNA is in the postoperative surveillance period, due to its ability to biopsy the extramural perirectal space to establish local disease recurrence.

An estimated 40,000 new cases of primary de novo rectal cancer occur per annum in the United States.<sup>1</sup> Based on current data, the prognosis for such patients is directly related to several factors, with the most important being the extent of primary tumor invasion (T stage), the number of lymph nodes involved (N stage), involvement of the circumferential resection margin (CRM), and the presence of distant metastases (M stage). Contemporary staging and therapy are dependent on presurgical diagnostic imaging modalities, including endoscopic ultrasonography (EUS), magnetic resonance imaging (MRI), or computed tomography (CT), which will influence the indication for neoadjuvant therapy and the decision-making process concerning the most appropriate surgical approach.

The diagnostic accuracy of lower gastrointestinal (GI) EUS assessments of rectal cancer staging has recently been questioned and criticized because clinical practice and current literature do not appear to support the early very positive literature reports. A German multicenter prospective quality assurance study ( $n = 7000$  patients, from 2000 to 2008) compared radial EUS examination to surgical pathology T-stage biopsies, in the absence of neoadjuvant therapy.<sup>2</sup> The T-stage concordance was 65% but improved with increasing procedure volumes. The frequency of both understaging and overstaging was 18% and 17%, respectively. In addition, further scrutiny from a United States center

revealed that EUS non-fine-needle aspiration (FNA) lymph node evaluation (from 1993 to 2007) did not reliably identify patients with nodal disease. The evidence to support this statement was based on a 29% lymph node morphology false-positive rate, and 23% of patients were understaged when using surgical pathology as the gold standard.<sup>3</sup> It is recognized that neither study included the important utility of EUS FNA, with a view to enhanced disease staging and subsequent appropriate triage of care.

The objective of this chapter is to provide a comprehensive overview using practical up-to-date evidence to collectively enhance and consolidate our knowledge and skill mix. We discuss the incremental benefit of EUS and alternative imaging modalities for the assessment of primary de novo rectal cancer, evaluation following neoadjuvant therapy, and postoperative disease surveillance utility. The final section presents innovative interventions for lower GI EUS.

### Relevant Anorectal Anatomy and the American Joint Committee on Cancer 2010 Staging System for Rectal Cancer

#### Anorectal Anatomy

The rectum extends from the upper end of the anal canal to the rectosigmoid junction and is approximately 12 cm in length.<sup>4</sup> It is subdivided into proximal, middle, and distal thirds, depending on the distance of the most distal aspect of the tumor from the anal verge. The surgical anal canal extends from the anorectal junction until the anal verge and measures between 2.5 and 4 cm in length.<sup>5</sup> The anatomic anal canal corresponds to the distal two-thirds of the surgical anal canal and is separated from the proximal one-third by the dentate line. Above the dentate line, the anal canal is lined with columnar epithelium, whereas it is lined with squamous epithelium distal to the dentate line. The anal transitional zone corresponds to an approximately 10-mm area between the columnar and squamous epithelial zones where the mucosa is of variable histology.<sup>6</sup>

The rectal wall is composed of mucosa, submucosa, and muscularis propria. The mucosa and submucosa complex appears as a three-layered wall structure on EUS. The mucosa is composed of two wall layers: an inner hyperechoic layer (the interface between

the mucosa and the ultrasound probe) and an outer hypoechoic wall layer. This is accompanied by the third wall layer, which is hyperechoic, representing the submucosa. The muscularis propria of the rectum, or fourth wall layer, is composed of an outer longitudinal and inner circular smooth muscle layer. The inner circular smooth muscle becomes thickened distally and continues as the internal anal sphincter. The outer longitudinal muscle fuses with fibers from the levator ani.<sup>5</sup> The outermost layer of the sphincter complex is formed by striated muscles: the levator ani and puborectalis muscles superiorly and the inferior part of the external anal sphincter inferiorly.

The rectum is surrounded by mesorectal fat containing lymph nodes, superior hemorrhoidal vessels, and fibrous tissue collectively known as the *mesorectum*. The mesorectum is continuous with the fat of the sigmoid mesocolon superiorly and is usually thicker along the posterior rectum in its intraperitoneal portion; on occasion it is absent anteriorly. It is bound circumferentially by the mesorectal fascia. This fascia extends inferiorly and coalesces with the Denonvilliers fascia in men, and anterior to it are the seminal vesicles and the prostate gland. Conversely, in women the anterior mesorectal fascia coalesces with rectovaginal fascia, anterior to which is the vagina. The mesorectal fascia forms an important barrier to the radial spread of upper and middle third rectal tumors and forms the plane of dissection used in total mesorectal excision (TME).

Nodal drainage of the rectum occurs initially to the perirectal lymph nodes within the mesorectum.<sup>7</sup> The majority of such nodes follow the rectal blood supply and are located superiorly and posteriorly. Common nodal spread is along the superior rectal artery into the apical mesorectum and the inferior mesenteric artery into the sigmoid mesocolon. The middle rectal artery arises from the internal iliac artery directly, and the inferior rectal artery arises from the internal pudendal artery, which is a branch of the anterior division of the internal iliac artery. The inferior and middle rectal arteries anastomose at the anorectal junction, and although uncommon, distal rectal cancers can spread to the nodes along the internal pudendal and internal iliac arteries.

### Rectal Cancer Tumor-Node-Metastasis Staging

The tumor-node-metastasis (TNM) system advocated by the American Joint Committee on Cancer (AJCC) and the International Union Against Cancer (UICC) have become the worldwide standard for staging colorectal cancer.<sup>8,9</sup> The TNM system classifies the extent of the tumor (T stage) by the depth of tumor invasion into and through the rectal wall. Nodal substations classified as regional lymph nodes for rectal cancer are perirectal, sigmoid mesenteric, inferior mesenteric, lateral sacral, presacral, sacral promontory, internal pudendal, internal iliac, superior rectal, middle rectal, and inferior rectal. The involvement of lymph nodes outside these groups, such as in the external or common iliac substations, is considered to be distant metastases (M stage; Table 18.1).

Other tumor characteristics that are important to consider for imaging purposes include the proximal and distal tumor margins, the extent of tumor annularity, the presence of ulceration, anal sphincter complex invasion, and the relationship of the distal tumor margin to the middle valve of Houston. The valve of Houston is thought to be a surrogate marker for the anterior peritoneal reflection, and the location of a tumor proximal or distal to the anterior peritoneal reflection has important surgical planning implications.

**TABLE 18.1** The 2010 American Joint Committee on Cancer Staging System for Primary Rectal Cancer

#### Primary Tumor (T)

TX	Primary tumor cannot be assessed
T0	No evidence of primary tumor
Tis	Carcinoma in situ: intraepithelial or invasion of lamina propria <sup>a</sup>
T1	Tumor invades submucosa
T2	Tumor invades muscularis propria
T3	Tumor invades through the muscularis propria into peri-colorectal tissues
T4a	Tumor penetrates to the surface of the visceral peritoneum <sup>b</sup>
T4b	Tumor directly invades or is adherent to other organs or structures <sup>b,c</sup>

#### Regional Lymph Nodes (N)<sup>d</sup>

NX	Regional lymph nodes cannot be assessed
N0	No regional nodal metastasis
N1	Metastasis in 1–3 regional lymph nodes
N1a	Metastasis in 1 regional lymph node
N1b	Metastasis in 2–3 regional lymph nodes
N1c	Tumor deposit(s) in the subserosa, mesentery, or non-peritonealized pericolic or perirectal tissues without regional nodal metastasis
N2	Metastasis in 4 or more regional lymph nodes
N2a	Metastasis in 4–6 regional lymph nodes
N2b	Metastasis in 7 or more regional lymph nodes

#### Distant Metastasis (M)

M0	No distant metastasis
M1	Distant metastasis
M1a	Metastasis confined to one organ or site (i.e., liver, lung, ovary, nonregional node)
M1b	Metastases in more than one organ/site or the peritoneum

<sup>a</sup>Tis include cancer cells confined within the glandular basement membrane (intraepithelial) or mucosal lamina propria (intramucosal) with no extension through the muscularis mucosa into the submucosa.

<sup>b</sup>Direct invasion in T4 includes invasion of other organs or other segments of the colorectum as a result of direct extension through the serosa, as confirmed on microscopic examination (e.g., invasion of the sigmoid colon by a carcinoma of the cecum), for cancers in a retroperitoneal or subperitoneal location or direct invasion of other organs or structures by virtue of extension beyond the muscularis propria (i.e., respectively, a tumor on the posterior wall of the descending colon invading the left kidney or lateral abdominal wall or a mid or distal rectal cancer with invasion of prostate, seminal vesicles, cervix, or vagina).

<sup>c</sup>Tumor that is adherent to other organs or structures, grossly, is classified as T4b. However, if no tumor is present in the adhesion, microscopically, the classification should be T1-4a, depending on the anatomic depth of wall invasion. The V and L classifications should be used to identify the presence or absence of vascular or lymphatic invasion, whereas the perineural (PN) site-specific factor should be used for perineural invasion.

<sup>d</sup>A satellite peritumoral nodule in the peri-colorectal adipose tissue of a primary carcinoma without histologic evidence of residual lymph node in the nodule may represent discontinuous spread, venous invasion with extravascular spread (V1/2), or a totally replaced lymph node (N1/2). Replaced nodes should be counted separately as positive nodes in the N category, whereas discontinuous spread or venous invasion should be classified and counted in the site-specific factor category tumor deposits (TD). (From Edge S, Byrd DR, Compton CC, Fritz AG, Greene FL, Trotti A, eds. AJCC Cancer Staging Manual. 7th ed. New York, NY: Springer; 2010:157.)

## Rectal Endoscopic Ultrasonography in the Setting of De Novo Rectal Cancer

The introduction of transrectal EUS has improved the ability to delineate the histologic layers of the rectal wall and as a result has improved treatment allocation by achieving a more accurate determination of the depth of tumor invasion.<sup>10–13</sup> It has emerged as an important imaging modality for the pretreatment staging of rectal cancer, with superior T-staging accuracy compared to CT.<sup>14–17</sup> The technique of rectal EUS has been previously described (Chapter 17) and may be performed with either a radial or, more recently and frequently, a curvilinear echoendoscope.<sup>18</sup>

### T-Staging Considerations

Rectal cancer usually appears as a hypoechoic lesion that disrupts the normal five-layer sonographic structure of the rectal wall. It is important to document where the distal border of the tumor is in relation to the seminal vesicles in males and the cervix in females, in order to clarify the lesion location in relation to the anterior peritoneal reflection. This is then compared with the endoscopic estimate of the distal tumor border. In published studies, the accuracy of EUS T-staging ranges from 80% to 95%, compared with 65% to 75% for CT and 75% to 85% for MRI (Fig. 18.1).<sup>19–21</sup> With respect to T stage, one particular problem is the overstaging of T2 tumors

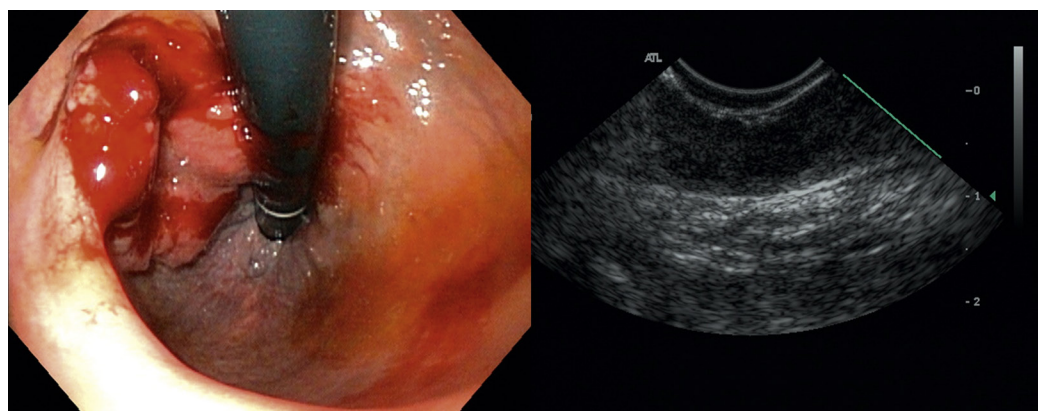
due to the difficulty in differentiating peritumoral inflammation secondary to a desmoplastic reaction from tumor fibrosis (Fig. 18.2).<sup>22</sup>

A T3 tumor must extend through the entire thickness of the muscularis propria into the perirectal fat, obliterating the sharp fat–muscle interface with features of pseudopodia (Video 18.1). It is thought that all T3 rectal tumors are not equal, with minimally invasive disease carrying a more favorable prognosis.<sup>23</sup> Therefore by discriminating minimally invasive from advanced T3 disease (invasion  $\leq 2$  or  $>3$  mm beyond the muscularis propria), preoperative EUS may provide important prognostic information. However, the challenge is that overstaging is noted to be more common in minimally invasive T3 (50%) when compared with advanced T3 disease.<sup>24</sup> A maximum tumor thickness measured in a T3 cancer is also an independent prognostic factor for local and overall recurrence.<sup>25</sup> A maximum tumor thickness cutoff measurement  $\geq 19$  mm has been proposed to be useful when classifying patients preoperatively and to select patients for primary surgery or neoadjuvant therapy.

Conversely, understaging may be caused by a failure to detect microscopic cancer infiltration, owing to the limits of EUS resolution. Resolution is improved by increasing ultrasound frequency but at the expense of a reduction in the depth of penetration, such that it may be impossible to visualize the leading edge of a tumor. This may limit the detection of invasion of adjacent organs. Important variables that influence the accuracy of tumor staging include operator experience and the location of the tumor within the rectum, with reduced accuracy for more distal tumors.<sup>22,26–28</sup>



• **Fig. 18.1** A superficial primary rectal cancer (T1N0) on the distal valve of Houston in an 84-year-old male, managed conservatively by a snare resection.



• **Fig. 18.2** An ulcerated friable distal primary rectal cancer (T2N0) in a 62-year-old female who proceeded directly to an abdominoperineal resection. The tumor invaded the muscularis propria (hypoechoic fourth endoscopic ultrasonography layer) but did not penetrate through it (T3) or extend beyond the five echo layers into the surrounding perirectal tissue.

**TABLE 18.2** Endoscopic Ultrasonography Accuracy When Differentiating T Stages Suggests That Endoscopic Ultrasonography Sensitivity Is Greatest for Advanced Disease Rather Than for Early Disease

T Stage	Sensitivity (%)	Specificity (%)
T1	87.8	98.3
T2	80.5	95.6
T3	96.4	90.6
T4	95.4	98.3

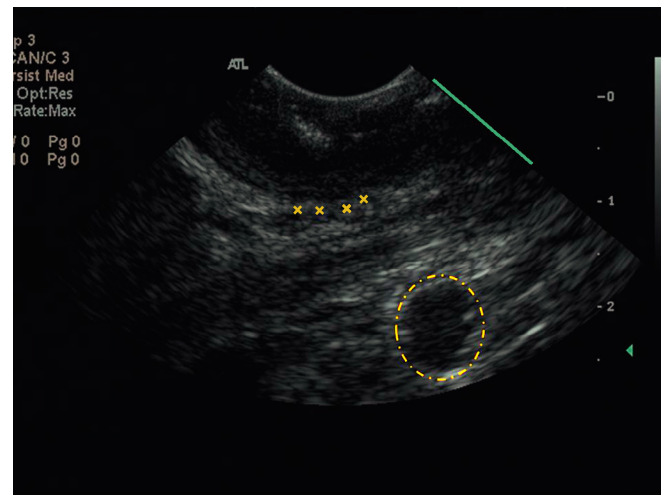
A meta-analysis of 42 studies ( $n = 5039$  patients, from 1980 to 2008) that reviewed the EUS accuracy when differentiating T stages suggested that EUS sensitivity is greatest for advanced disease compared with early disease (Table 18.2).<sup>29</sup>

### N-Staging Considerations

Conventional EUS nodal echo features that accurately predict nodal metastasis have been identified in patients with esophageal cancer.<sup>30</sup> These ultrasound features include lymph node short axis size, echogenicity, shape, and border. Features proposed to correlate with malignancy include an enlarged node ( $\geq 1$  cm in short axis), hypoechoic appearance, round shape, and smooth border (Fig. 18.3; Table 18.3). However, these conventional EUS nodal criteria have proven inaccurate for staging many nonesophageal cancers.<sup>30–32</sup> No single criterion is predictive of malignancy in patients with lung, esophageal, and pancreatic cancer. If all four abnormal morphologic features are present, the accuracy for malignant invasion is 80%. However, all four features of malignant involvement are present in only 25% of malignant lymph nodes (Table 18.4).

Although EUS FNA is the most accurate modality for locoregional staging of cancer, the N-staging accuracy is only 70% to 75% and was recently reported to be as low as 42%.<sup>33,34</sup> It was previously assumed that EUS was incapable of detecting benign perirectal lymph nodes.<sup>18</sup> Therefore in patients with rectal cancer, the visualization of lymph nodes was considered to be an accurate surrogate marker of nodal metastasis, thereby obviating the need for FNA. A meta-analysis (35 studies,  $n = 2732$  patients, from 1966 to 2008) that reviewed the literature regarding N stage EUS accuracy suggested that the sensitivity and specificity of EUS is moderate and that further refinements in diagnostic criteria are needed to improve the diagnostic accuracy.<sup>35</sup> It is important to note that all of these studies were non-FNA, primarily radial EUS examinations.

Prior transrectal ultrasound studies identified a nodal size of  $\geq 7$  mm as an optimal size cutoff for predicting nodal metastases in rectal cancer, with an accuracy of 83% when compared with surgical pathology.<sup>36</sup> A dedicated FNA study based on a perception that metastatic locoregional nodes are only minimally different in morphologic appearance when compared with benign nodes noted that the number of conventional malignant echo features per lymph node did not accurately differentiate benign from malignant nodes, unless all four features were present.<sup>37</sup> The accuracy of conventional criteria to include short axis  $\geq 10$  mm, hypoechoic appearance, round shape, and smooth border for detecting malignant lymphadenopathy was 61%, 65%, 51%,



• **Fig. 18.3** A T3N1 lesion in a 54-year-old male who proceeded to neoadjuvant therapy followed by surgery (xxxx = tumor breaching through the fourth muscularis layer and making the lesion a T3 lesion). The highlighted node is perilesional and therefore not amenable to fine-needle aspiration. It has a hypoechoic appearance and short axis greater than 5 mm but is oval in shape with an irregular border.

**TABLE 18.3** Endoscopic Ultrasonography Morphologic Features of Benign and Malignant Lymph Nodes

Endoscopic Ultrasonography Features	Benign Features	Malignant Features
Echogenicity	Hyperechoic	Hypoechoic
Shape	Irregular	Round
Border	Irregular	Smooth
Size (short axis)	<10 mm	$\geq 10$ mm

**TABLE 18.4** Performance Characteristics Relative to the Number of Conventional Endoscopic Ultrasonography Malignant Nodal Features

	Two or More Features	Three or More Features	Four Features
Sensitivity (%)	77	68	23
Specificity (%)	29	52	100
PPV (%)	53	60	100
NPV (%)	55	61	55
Accuracy (%)	54	61	61

NPV, Negative predictive value; PPV, positive predictive value.

and 51%, respectively. A lymph node short-axis length  $\geq 5$  mm or hypoechoic appearance was the only conventional feature predictive of malignant infiltration. An optimum short- and long-axis length of 6 and 9 mm yielded the best power distinction for malignancy. Using surgical histopathology specimens, Knight and colleagues assessed the performance characteristics for overall sensitivity, specificity, and positive and negative predictive

values of FNA in the setting of primary or metastatic colorectal carcinoma, reflecting values of 89%, 79%, 89%, and 79%, respectively.<sup>38</sup>

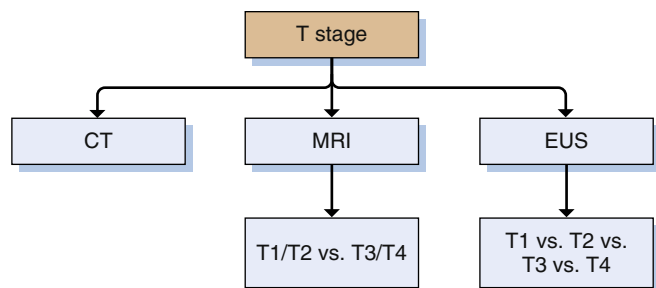
The preoperative FNA identification of extramesenteric lymph node metastases upstages 7% of primary rectal cancers undergoing an EUS evaluation. For example, external iliac lymph node infiltration is outside the standard operative field for TME. This location, if recognized at EUS, may impact medical and surgical planning by altering the standard radiation fields or may alter surgical planning to extend the TME resection to include an extensive lymph node dissection.<sup>39</sup> Significant clinical, endoscopic, and sonographic features associated with such metastases include serum carcinoembryonic antigen (CEA) level, tumor length  $\geq 4$  cm, tumor annularity  $\geq 50\%$ , sessile morphology, and lymph node size.

The recent findings indicate that FNA should be used when verifying nodal status and when making critical decisions regarding the use of neoadjuvant therapy rather than relying on nodal appearance alone. Failure to use FNA risks stage-inappropriate therapy and, in turn, inappropriate patient outcomes. A note of caution is that luminal fluid cytology may be positive for malignancy in 48% of luminal cancers, including rectal cancer, but is not affected by performing FNA.<sup>40</sup> This translocated cell contamination, along with endosonographer technique and cytologic misinterpretation, are risk factors for false-positive EUS FNA cytology.<sup>41</sup>

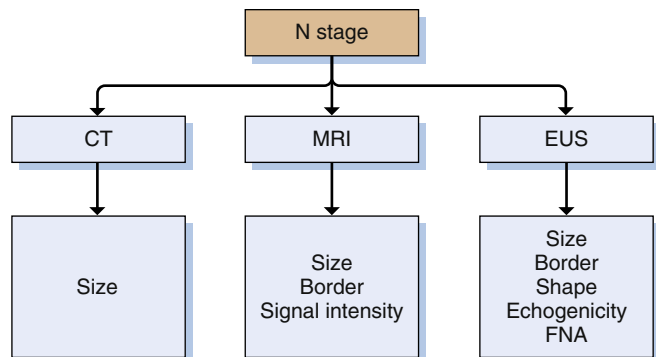
EUS FNA of solid lesions in the lower GI tract is considered to be a low-risk procedure for infectious complications and does not warrant prophylactic administration of antibiotics for the prevention of bacterial endocarditis.<sup>42</sup> Until adverse event data become available, perirectal cystic structures should not be sampled, as abscess formation requiring percutaneous drainage has occurred despite the administration of prophylactic antibiotics.<sup>43</sup>

## Magnetic Resonance Imaging Assessment Versus Endoscopic Ultrasonography

The use of MRI for the local staging of rectal cancer, particularly with an endorectal coil technique, has been described.<sup>44–46</sup> It offers several theoretic advantages over EUS, as it reveals a larger field of view and permits the study of stenotic tumors.<sup>26,47,48</sup> Recently the identification of the anterior peritoneal reflection, an important landmark to assist the surgical team, has been identified in 74% of patients.<sup>49</sup> This important landmark cannot be reliably identified by EUS and is a partial explanation as to why MRI is gaining popularity in clinical practice. Furthermore, there is an increasing demand to establish the impact neoadjuvant therapy has on tumor volume and downstaging of disease. Objectively this is best obtained by a standard MRI scanner protocol rather than EUS for precise comparative purposes.<sup>50</sup> A meta-analysis of 90 articles (from 1995 to 2002) compared the use of MRI, radial EUS without FNA, and CT for staging with histopathology correlation as the gold standard. The study came to the following conclusions: (1) for T1/T2 lesions, EUS and MRI had similar sensitivity but specificity was higher for EUS (86% vs. 69%); and (2) for T3 tumors, the sensitivity of EUS was significantly higher than that of MRI or CT (Fig. 18.4).<sup>51</sup> A more recent prospective study comparing radial EUS with MRI revealed that MRI was unable to visualize any T1 tumors, whereas EUS understaged all T4 tumors.<sup>52</sup> Furthermore, the presence of luminal stenosis and polypoid morphology was inversely associated with the accuracy of either EUS or MRI.



• Fig. 18.4 Imaging options to potentially assess T stage. CT, Computed tomography; EUS, endoscopic ultrasonography; MRI, magnetic resonance imaging.



• Fig. 18.5 Imaging options to potentially assess N stage. CT, Computed tomography; EUS, endoscopic ultrasonography; FNA, fine-needle aspiration; MRI, magnetic resonance imaging.

MRI may also be used to evaluate mesorectal nodal involvement, as lymph nodes are characterized by imaging features rather than by size criteria alone. The most reliable MRI criteria for lymph node metastasis are an irregular contour and inhomogeneous signal when correlated with histologic findings, and it may also identify nodal metastasis beyond the boundaries of the mesorectum.<sup>53,54</sup> Many studies have evaluated the prediction of lymph node involvement (Fig. 18.5). A meta-analysis from 2004 revealed that the sensitivity and specificity of MRI were 66% and 76%, respectively, compared with 67% and 78% for radial EUS without FNA and 55% and 74% for CT.<sup>46,51</sup> In another meta-analysis there was similarly no significant difference in N-staging between MRI and EUS, although EUS had a slight advantage, mostly based upon specificity.<sup>55</sup> The 2016 St. Gallen European Organization for Research and Treatment of Cancer Gastrointestinal Cancer Consensus Conference reinforces the principle that optimal pretherapeutic imaging is a key to any stage-based treatment decision. The panel recommended MRI routinely or MRI plus EUS as mandatory image-based staging modalities, in particular for early T1 lesions. The complementary imaging of EUS in addition to MRI was considered to be most important, due to the superior near field resolution of EUS.<sup>56</sup>

## Computed Tomography and Positron Emission Tomography-Computed Tomography Evaluation Versus Endoscopic Ultrasonography

Traditionally the role of CT was to identify metastatic disease, as its resolution was considered to be inadequate to make a distinction between the various rectal wall layers.<sup>57,58</sup> More recently,

however, multislice CT has been used for the assessment of mesorectal fascia involvement, especially when a lesion is located proximal to and including the midrectum; however, the accuracy of an involved margin in a distal rectal cancer is suboptimal.<sup>59,60</sup> The optimum CT lymph node size to predict nodal metastasis with the best negative predictive value was 7 mm.<sup>61</sup> However, an abdominal CT in addition to EUS is considered to be the most cost-effective staging strategy for nonmetastatic proximal rectal cancer, but this may change with the increasing use of pelvic MRI.<sup>62</sup>

Positron emission tomography (PET)-CT provides additional information to conventional staging in primary rectal cancer and may be used selectively in more advanced stages and where indeterminate findings exist with conventional staging.<sup>63</sup> Contrast-enhanced PET-CT is superior to nonenhanced PET-CT for the precise definition of regional nodal status and is considered to enhance the staging/therapy in one-third of patients.<sup>64,65</sup> Some authorities suggest that the standardized uptake values ( $SUV_{max}$ ) following neoadjuvant therapy predict downstaging and a complete pathologic response.<sup>66,67</sup> However, no EUS FNA versus PET-CT comparative study has been reported to date.

## Endoscopic Ultrasonography Evaluation Following Neoadjuvant Therapy

Tumor response to neoadjuvant therapy is a strong predictor of disease-free survival. However, the accuracy of EUS for staging rectal cancer following such therapy is markedly decreased due to the effects of postradiation edema, inflammation, necrosis, and fibrosis.<sup>68,69</sup> EUS has not been extensively studied in this scenario, but it has been suggested that its routine use for staging purposes following such therapy should be discouraged.<sup>70</sup> The T-stage accuracy following neoadjuvant therapy is 50%.<sup>71–76</sup> As outcome is most accurately estimated by final pathologic stage, restaging tumors following such therapy is limited, and clinical correlation is most important to dictate operative and postoperative management modalities. However, the use of nonperitumoral lymph node FNA in this setting may establish the presence of residual nodal malignancy, which may offer useful information for further management decisions.

## Endoscopic Ultrasonography for Recurrent Rectal Cancer Following Radical and Local Surgery

A positive CRM, serosal involvement, lymphovascular invasion, extramural venous invasion, and poor histologic differentiation are important independent predictive factors for the development of local recurrence (LR).<sup>77</sup> The combination of neoadjuvant therapy and TME has significantly reduced the incidence of LR (<10%), the incidence of which is greatest within the first 2 years following surgery.<sup>78,79</sup> Early detection of a recurrent local tumor may result in earlier treatment and improved survival. As LR often occurs in the extraluminal region, follow-up with forward-viewing endoscopy may fail to detect LR at a sufficiently early stage. EUS may not be able to visually distinguish recurrence from postoperative change due to fibrosis or inflammation, and images may be obscured by artifacts from surgically placed clips or sutures. However, FNA of the residual rectal wall or perirectal space (91% sensitivity, 93% specificity) may offer a diagnosis that

is superior to clinical evaluation or EUS imaging alone. There is no clear strategy for the early detection of LR. Two prospective studies have demonstrated that EUS was superior to CT for LR detection in rectal cancer.<sup>80,81</sup> The sensitivity of EUS was higher (100%) in both studies compared with CT (82% to 85%). EUS was also more sensitive than digital rectal examination, CT, and CEA levels to detect LR in asymptomatic patients.<sup>82</sup> The optimal interval for EUS surveillance following surgical intervention is unknown. However, performing EUS every 6 months for the first 2 years after low anterior resection may be a reasonable surveillance modality for recurrent rectal cancer.<sup>83</sup>

Local excision is an alternative management approach for early rectal cancers and for patients unfit for radical surgery. It is, however, associated with a high LR rate. Mucosal scar biopsy and EUS FNA of either a lymph node or the deep rectal wall are methods to establish LR.<sup>84</sup> In addition, EUS FNA with or without Tru-Cut biopsy (TCB) may be useful in the diagnostic evaluation of patients with extraluminal perirectal lesions to determine a therapeutic plan (Figs. 18.6 and 18.7).<sup>85</sup>

Rectal implantation cysts occurring at an anastomotic site following a low anterior resection for rectal cancer need to be distinguished from locally recurrent rectal cancer. EUS may reveal cystic lesions at the anastomotic site with heterogeneous wall thickness, and FNA may reveal mucin containing some inflammatory cells in the absence of malignant cells.<sup>86</sup> EUS FNA and TCB are sensitive for the diagnosis of malignancy in pelvic masses but carry a 7% complication rate if cystic pelvic masses are sampled, and this should therefore be discouraged.<sup>87,88</sup>

## Endoscopic Ultrasonography for Rectal Wall Metastases

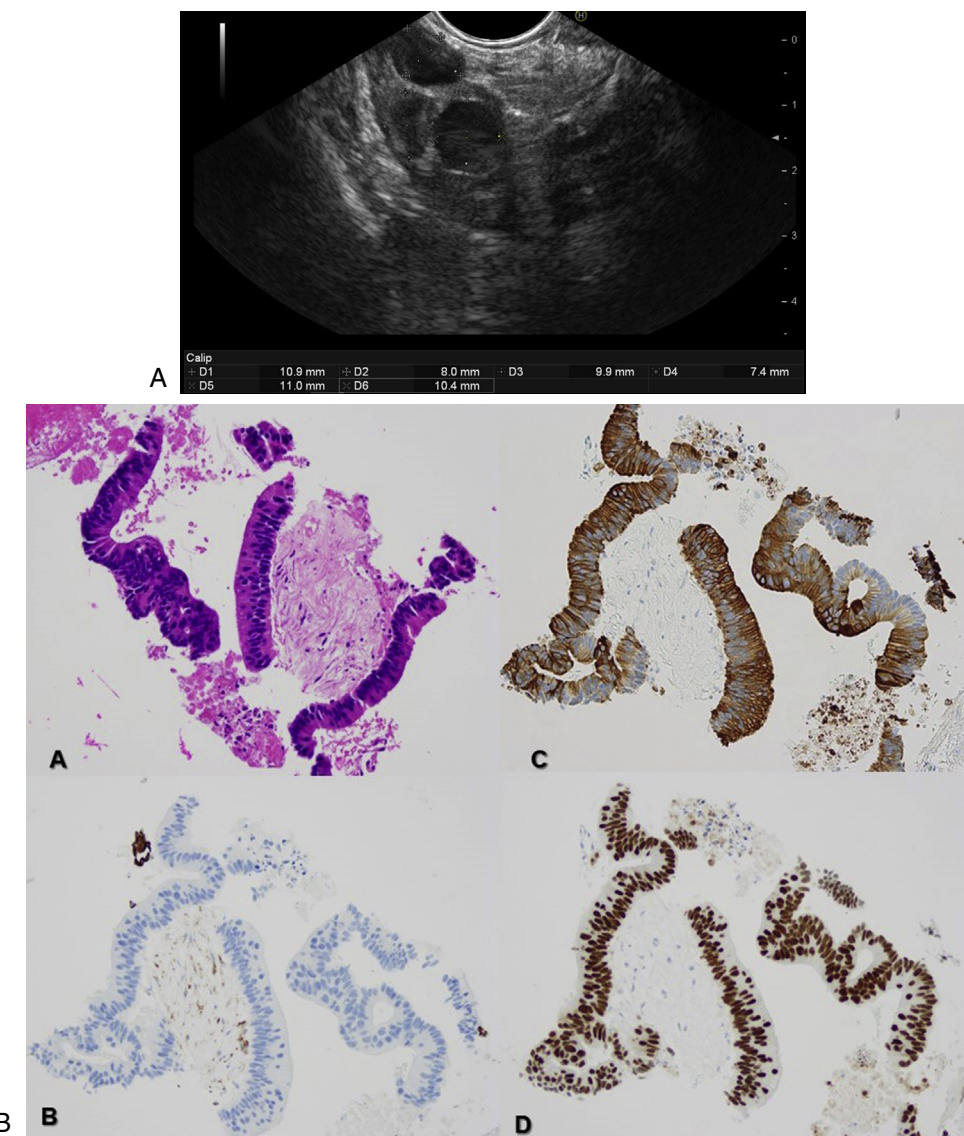
Distant primary cancers, in general, rarely metastasize to the GI wall. Such findings are estimated to be 1 of 3847 (0.03%) upper endoscopies and only 1 of 1871 (0.05%) colonoscopies.<sup>89</sup> The EUS appearance without FNA of secondary rectal linitis plastica is that of circumferential wall thickening affecting predominantly the submucosal and muscularis propria layers, similar to that of primary gastric linitis plastica (Fig. 18.8).<sup>90</sup> The role of FNA to aid the diagnosis secondary to prostate cancer has also been reported.<sup>91</sup> This appearance is in contrast to similar processes such as rectal endometriotic implants that are either hypoechoic or heterogeneous deposits involving the fourth and fifth layer with intact mucosal layers. It is also in contrast to local rectal cancer recurrence that is usually in an extraluminal location.<sup>92,93</sup> EUS FNA with or without TCB may confirm the diagnosis and identify the primary malignancy, which to date has included cancers originating from the bladder, breast, stomach, and cutaneous melanoma.<sup>94</sup>

## Innovative Interventions and Adverse Event Profile for Lower Gastrointestinal Endoscopic Ultrasonography

EUS-guided drainage and stenting provides another option for the management of postoperative pelvic fluid collections.<sup>95</sup> EUS-guided drainage of abdominopelvic abscesses unrelated to diverticular disease may be another future therapeutic indication.<sup>96</sup> EUS fine-needle injection with ethanol for persistent malignant pelvic lymph nodes following therapy in nonsurgical candidates has also been reported, in addition to EUS-guided coil and glue



• **Fig. 18.6** Posttransanal excision scar 18 months following local therapy. Endoscopic ultrasonography detected an enlarged hypoechoic nonperilesional lymph node that was positive for malignancy.



• **Fig. 18.7** (A) A 5 cm solid cystic left ovarian mass 1 year following a right hemicolectomy for a 3 cm T3N1 moderately differentiated ileocecal valve adenocarcinoma. (B) The endoscopic ultrasonography FNB core biopsy immunohistochemistry reflected an intestinal phenotype consistent with a colorectal adenocarcinoma metastasis—(A) Hematoxylin and eosin immunostain, (B) CK7 immunostain negative, (C) CK20 immunostain positive, and (D) CDX2 immunostain positive.

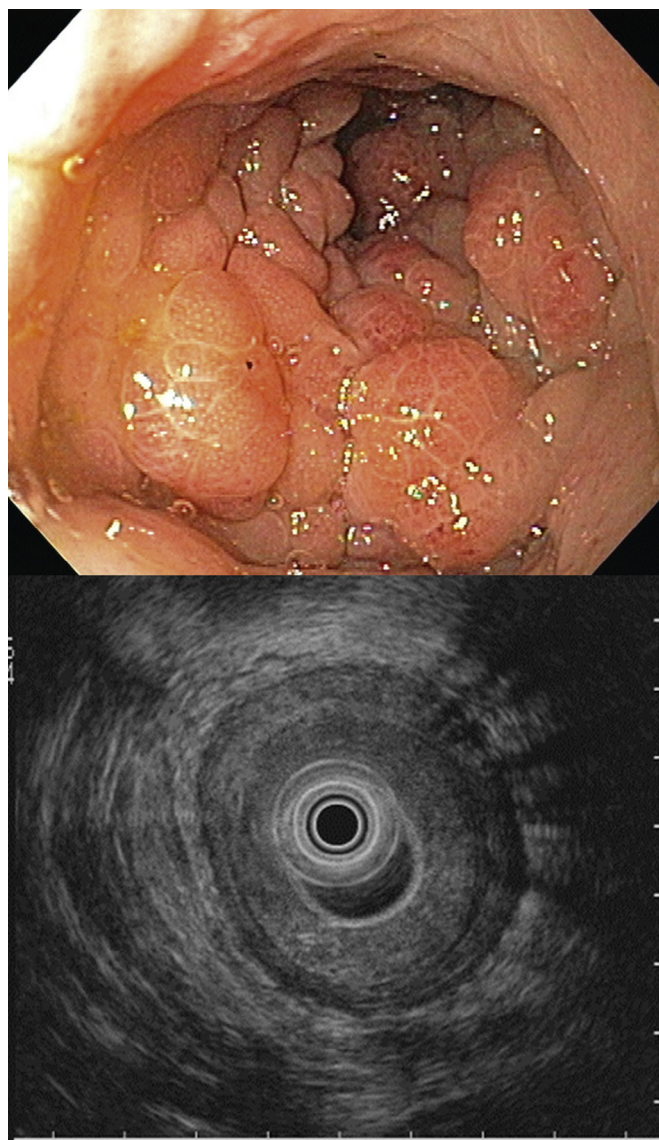


**Fig. 18.8** Circumferential cobblestone mucosal appearance with a corresponding hypoechoic wall thickness in a patient with a history of transitional cell cancer of the bladder, 2 years previously.

placement for bleeding rectal varices.<sup>97,98</sup> The incidence and factors associated with adverse events following lower GI EUS FNA were prospectively studied over an 8-year period evaluating a cohort of greater than 500 patients. The adverse events were graded utilizing Common Terminology Criteria. Adverse events developed in 20.5% patients and were classified as grade 1, 2, 3, or 4 in 6.8%, 8.2%, 4.6%, and 1.0% of patients, respectively. The most common events were postprocedural bleeding and pain, and were associated with the presence of preprocedural rectal pain (odds ratio [OR]: 3.83, 95% confidence interval [CI]: 2.35 to

6.25), FNA from a site other than a lymph node or gut wall (OR: 2.26, 95% CI: 1.10 to 4.70), and malignant FNA cytology (OR: 1.80, 95% CI: 1.10 to 2.97).<sup>99</sup>

## Translational Medicine

EUS has the potential to move from a diagnostic test to one that could also facilitate the personalization of cancer-directed therapy. The determination of a particular tumor's genetic architecture yields significant information on cancer pathogenesis signaling pathways. The performance of targeted next-generation DNA sequencing multigene mutation panel testing of malignant cells from EUS FNA cytology smears has a role in the evolution of precision medicine.<sup>100,101</sup> It can identify pathogenic alteration-mutation frequency and distribution with encouraging accuracy, and may have theranostic potential for individualized patient care.

## Conclusion

As the increasing importance of nodal status in therapeutic decision-making is recognized for rectal cancer, EUS FNA has emerged as an essential component of locoregional clinical staging. Although EUS still has insufficient accuracy for T-staging, EUS FNA can accurately predict patients who have evidence of iliac vessel node disease by upstaging 7% of patients presenting for evaluation and establishing the presence of perirectal space nodal disease. Staging with EUS following neoadjuvant therapy should be approached with caution but overall may be of greater benefit in the postoperative surveillance period because of the possibility to biopsy the extramural perirectal space to establish local disease recurrence.

## Key References

5. Wexner SD, Jorge JM. Anatomy and embryology of the anus, rectum, and colon. In: Corman ML, ed. *Colon and Rectal Surgery*. Philadelphia, PA: Lippincott-Raven; 1998:1–26.
18. Wiersema MJ, Harewood GC. Endoscopic ultrasound for rectal cancer. *Gastroenterol Clin North Am*. 2002;31:1093–1105.
22. Kauer WK, Prantl L, Dittler HJ, Siewert JR. The value of endosonographic rectal carcinoma staging in routine diagnostics: a 10-year analysis. *Surg Endosc*. 2004;18(7):1075–1078.
30. Catalano MF, Sivak MV, Rice T, et al. Endosonographic features predictive of lymph node metastasis. *Gastrointest Endosc*. 1994;40:442–446.
51. Bipat S, Glas AS, Slors FJ, et al. Rectal cancer: local staging and assessment of lymph node involvement with endoluminal US, CT, and MR imaging, a meta-analysis. *Radiology*. 2004;232:773–783.

## References

Access the reference list online at [ExpertConsult.com](http://ExpertConsult.com).

## References

1. <http://www.cancer.gov/cancertopics/types/colon-and-rectal>.
2. Marusch F, Ptak H, Sahm M, et al. Endorectal ultrasound in rectal carcinoma—do the literature results really correspond to the realities of routine clinical care? *Endoscopy*. 2011;43(5):425–431.
3. Shapiro R, Ali UA, Lavery IC, Kiran RP. Endorectal ultrasound does not reliably identify patients with uT3 rectal cancer who can avoid neoadjuvant chemoradiotherapy. *Int J Colorectal Dis*. 2013;28:993–1000.
4. Nelson H, Petrelli N, Carlin A, et al. Guidelines 2000 for colon and rectal cancer surgery. *J Natl Cancer Inst*. 2001;93:583–596.
5. Wexner SD, Jorge JMN. Anatomy and embryology of the anus, rectum, and colon. In: Corman ML, ed. *Colon and Rectal Surgery*. Philadelphia: Lippincott-Raven; 1998:1–26.
6. Kaiser AM, Ortega AE. Anorectal anatomy. *Surg Clin North Am*. 2002;82(6):1125–1138.
7. Canessa CE, Badia F, Fierro S, et al. Anatomic study of the lymph nodes of the mesorectum. *Dis Colon Rectum*. 2001;44:1333–1336.
8. Greene FL, Page DL, Fleming ID, et al., eds. *AJCC Cancer Staging Manual*. 7th ed. New York, NY: Springer; 2010.
9. Sabin LH, Wittekind C, eds. *TNM: Classification of Malignant Tumours*. 6th ed. New York, NY: Wiley-Liss; 2002.
10. Fedyaev EB, Volkova EA, Kuznetsova EE. Transrectal and transvaginal ultrasonography in the preoperative staging of rectal carcinoma. *Eur J Radiol*. 1995;20(1):35–38.
11. Dershaw DD, Enker WE, Cohen AM, Sigurdson ER. Transrectal ultrasonography of rectal carcinoma. *Cancer*. 1990;66(11):2336–2340.
12. Cohen JL, Grotz RL, Welch JP, Deckers PJ. Intrarectal sonography. A new technique for the assessment of rectal tumors. *Am Surg*. 1991;57(7):459–462.
13. Hawes RH. New staging techniques. Endoscopic ultrasound. *Cancer*. 1993;71(suppl 12):4207–4213.
14. Schwartz DA, Harewood GC, Wiersema MJ. EUS for rectal disease. *Gastrointest Endosc*. 2002;56(1):100–109.
15. Kwok H, Bissett IP, Hill GL. Preoperative staging of rectal cancer. *Int J Colorectal Dis*. 2000;15(1):9–20.
16. Rifkin MD, Ehrlich SM, Marks G. Staging of rectal carcinoma: prospective comparison of endorectal US and CT. *Radiology*. 1989;170(2):319–322.
17. Holdsworth PJ, Johnston D, Chalmers AG, et al. Endoluminal ultrasound and computed tomography in the staging of rectal cancer. *Br J Surg*. 1988;75(10):1019–1022.
18. Wiersema MJ, Harewood GC. Endoscopic ultrasound for rectal cancer. *Gastroenterol Clin North Am*. 2002;31:1093–1105.
19. Golifieri R, Giampalma E, Leo P, et al. Comparison of magnetic resonance (0, 5 T), computed tomography, and endorectal ultrasonography in the preoperative staging of neoplasms of the rectum-sigma. Correlation with surgical and anatomopathologic findings. *Radiol Med*. 1993;85(6):773–783.
20. Kim NK, Kim MJ, Yun SH, et al. Comparative study of transrectal ultrasonography, pelvic computerized tomography, and magnetic resonance imaging in preoperative staging of rectal cancer. *Dis Colon Rectum*. 1999;42(6):770–775.
21. Halefoglu AM, Yildirim S, Avlanmis O, et al. Endorectal ultrasonography versus phased-array magnetic resonance imaging for preoperative staging of rectal cancer. *World J Gastroenterol*. 2008;14(22):3504–3510.
22. Kauer WK, Prantl L, Dittler HJ, Siewert JR. The value of endoscopic rectal carcinoma staging in routine diagnostics: a 10-year analysis. *Surg Endosc*. 2004;18(7):1075–1078.
23. Harewood GC, Kumar KS, Clain JE, et al. Clinical implications of quantification of mesorectal tumor invasion by endoscopic ultrasound: all T3 rectal cancers are not equal. *Gastroenterol Hepatol*. 2004;19(7):750–755.
24. Jürgensen C, Teubner A, Habeck JO, et al. Staging of rectal cancer by EUS: depth of infiltration in T3 cancers is important. *Gastrointest Endosc*. 2011;73(2):325–328.
25. Esclapez P, Garcia-Granero E, Flor B, et al. Prognostic heterogeneity of endosonographic T3 rectal cancer. *Dis Colon Rectum*. 2009;52(4):685–691.
26. Orrom WJ, Wong WD, Rothenberger DA, et al. Endorectal ultrasound in the preoperative staging of rectal tumors. A learning experience. *Dis Colon Rectum*. 1990;33(8):654–659.
27. Solomon MJ, McLeod RS, Cohen EK, et al. Reliability and validity studies of endoluminal ultrasonography for anorectal disorders. *Dis Colon Rectum*. 1994;37(6):546–551.
28. Sailer M, Leppert R, Bussen D, et al. Influence of tumor position on accuracy of endorectal ultrasound staging. *Dis Colon Rectum*. 1997;40(10):1180–1186.
29. Puli SR, Bechtold ML, Reddy JB, et al. How good is endoscopic ultrasound in differentiating various T stages of rectal cancer? Meta-analysis and systematic review. *Ann Surg Oncol*. 2009;16(2):254–265.
30. Catalano MF, Sivak MV, Rice T, et al. Endosonographic features predictive of lymph node metastasis. *Gastrointest Endosc*. 1994;40:442–446.
31. Murata Y, Muroi M, Yoshida M, et al. Endoscopic ultrasonography in the diagnosis of esophageal carcinoma. *Surg Endosc*. 1987;1:11–16.
32. Tio TL, Coene PP, Luiken GJ, et al. Endosonography in the clinical staging of esophagogastric carcinoma. *Gastrointest Endosc*. 1990;36(suppl 2):S2–S10.
33. Rosen LS, Bilchik AJ, Beart Jr RW, et al. New approaches to assessing and treating early-stage colon and rectal cancer: summary statement from 2007 Santa Monica Conference. *Clin Cancer Res*. 2007;13:6853s–6856s.
34. Tsendsuren T, Jun SM, Mian XH. Usefulness of endoscopic ultrasonography in preoperative TNM staging of gastric cancer. *World J Gastroenterol*. 2006;12:43–47.
35. Puli SR, Reddy JB, Bechtold ML, et al. Accuracy of endoscopic ultrasound to diagnose nodal invasion by rectal cancers: a meta-analysis and systematic review. *Ann Surg Oncol*. 2009;16(5):1255–1265.
36. Heneghan JP, Salem RR, Lange RC, et al. Transrectal sonography in staging rectal carcinoma: the role of gray-scale, color-flow, and Doppler imaging analysis. *AJR Am J Roentgenol*. 1997;169:1247–1252.
37. Gleeson FC, Clain JE, Papachristou GI, et al. Prospective assessment of EUS criteria for lymphadenopathy associated with rectal cancer. *Gastrointest Endosc*. 2009;69(4):896–903.
38. Knight CS, Eloubeidi MA, Crowe R, et al. Utility of endoscopic ultrasound-guided fine-needle aspiration in the diagnosis and staging of colorectal carcinoma. *Diagn Cytopathol*. 2013;41:1031–1037.
39. Gleeson FC, Clain JE, Rajan E, et al. EUS-FNA assessment of extramesenteric lymph node status in primary rectal cancer. *Gastrointest Endosc*. 2011;74(4):897–905.
40. Levy MJ, Gleeson FC, Campion MB, et al. Prospective cytological assessment of gastrointestinal luminal fluid acquired during EUS: a potential source of false-positive FNA and needle tract seeding. *Am J Gastroenterol*. 2010;105(6):1311–1318.
41. Gleeson FC, Kipp BR, Caudill JL, et al. False positive endoscopic ultrasound fine needle aspiration cytology: incidence and risk factors. *Gut*. 2010;59(5):586–593.
42. Levy MJ, Norton ID, Clain JE, et al. Prospective study of bacteremia and complications With EUS FNA of rectal and perirectal lesions. *Clin Gastroenterol Hepatol*. 2007;5(6):684–689.
43. Mohamadnejad M, Al-Haddad MA, Sherman S, et al. Utility of EUS-guided biopsy of extramural pelvic masses. *Gastrointest Endosc*. 2012;75(1):146–151.

44. Brown G, Richards CJ, Bourne MW, et al. Morphologic predictors of lymph node status in rectal cancer with use of high-spatial-resolution MR imaging with histopathologic comparison. *Radiology*. 2003;227:371–377.
45. Gualdi GF, Casciani E, Guadaluaxara A, et al. Local staging of rectal cancer with transrectal ultrasound and endorectal magnetic resonance imaging: comparison with histologic findings. *Dis Colon Rectum*. 2000;43:338–345.
46. Bianchi P, Ceriani C, Palmisano A, et al. A prospective comparison of endorectal ultrasound and pelvic magnetic resonance in the preoperative staging of rectal cancer. *Ann Ital Chir*. 2006;77(1):41–46.
47. Hulsmans FJ, Tio TL, Fockens P, et al. Assessment of tumor infiltration depth in rectal cancer with transrectal sonography: caution is necessary. [see comment] *Radiology*. 1994;190(3):715–720.
48. Hildebrandt U, Feifel G. Preoperative staging of rectal cancer by intrarectal ultrasound. *Dis Colon Rectum*. 1985;28(1):42–46.
49. Gollub MJ, Maas M, Weiser M, et al. Recognition of the anterior peritoneal reflection at rectal MRI. *AJR Am J Roentgenol*. 2013;200(1):97–101.
50. Blazic IM, Campbell NM, Gollub MJ. MRI for evaluation of treatment response in rectal cancer. *Br J Radiol*. 2016;89(1064):20150964.
51. Bipat S, Glas AS, Slors FJ, et al. Rectal cancer: local staging and assessment of lymph node involvement with endoluminal US, CT, and MR imaging, a meta-analysis. *Radiology*. 2004;232:773–783.
52. Fernández-Esparrach G, Ayuso-Colella JR, Sendino O, et al. EUS and magnetic resonance imaging in the staging of rectal cancer: a prospective and comparative study. *Gastrointest Endosc*. 2011;74(2):347–354.
53. Brown G, Richards CJ, Bourne MW. Morphologic predictors of lymph node status in rectal cancer with use of high-spatial-resolution MR imaging with histopathologic comparison. *Radiology*. 2003;227(2):371–377.
54. Brown G, Kirkham A, Williams GT, et al. High-resolution MRI of the anatomy important in total mesorectal excision of the rectum. *AJR Am J Roentgenol*. 2004;182(2):431–439.
55. Lahaye MJ, Engelen SM, Kessels AG, et al. USPIO-enhanced MR imaging for nodal staging in patients with primary rectal cancer: predictive criteria. *Radiology*. 2008;246(3):804–811.
56. Lutz MP, Zalberg JR, Glynn-Jones R, et al. Second St. Gallen European Organisation for Research and Treatment of Cancer Gastrointestinal Cancer Conference: consensus recommendations on controversial issues in the primary treatment of rectal cancer. *Eur J Cancer*. 2016;63:11–24.
57. Heriot AG, Grundy A, Kumar D. Preoperative staging of rectal carcinoma. *Br J Surg*. 1999;86:17–28.
58. Kim NK, Kim MJ, Yun SH, et al. Comparative study of transrectal ultrasonography, pelvic computerized tomography, and magnetic resonance imaging in preoperative staging of rectal cancer. *Dis Colon Rectum*. 1999;42:770–775.
59. Wolberink SV, Beets-Tan RG, de Haas-Kock DF, et al. Multislice CT as a primary screening tool for the prediction of an involved mesorectal fascia and distant metastases in primary rectal cancer: a multicenter study. *Dis Colon Rectum*. 2009;52(5):928–934.
60. Vliegen R, Dresen R, Beets G, et al. The accuracy of Multi-detector row CT for the assessment of tumor invasion of the mesorectal fascia in primary rectal cancer. *Abdom Imaging*. 2008;33(5):604–610.
61. Pomerri F, Maretto I, Pucciarelli S, et al. Prediction of rectal lymph node metastasis by pelvic computed tomography measurement. *Eur J Surg Oncol*. 2009;35(2):168–173.
62. Harewood GC, Wiersema MJ. Cost-effectiveness of endoscopic ultrasonography in the evaluation of proximal rectal cancer. *Am J Gastroenterol*. 2002;97(4):874–882.
63. Eglinton T, Luck A, Bartholomeusz D, et al. Positron-emission tomography/computed tomography (PET/CT) in the initial staging of primary rectal cancer. *Colorectal Dis*. 2010;12(7):667–673.
64. Davey K, Heriot AG, Mackay J, et al. The impact of 18-fluorodeoxyglucose positron emission tomography-computed tomography on the staging and management of primary rectal cancer. *Dis Colon Rectum*. 2008;51(7):997–1003.
65. Tateishi U, Maeda T, Morimoto T, et al. Non-enhanced CT versus contrast-enhanced CT in integrated PET/CT studies for nodal staging of rectal cancer. *Eur J Nucl Med Mol Imaging*. 2007;34(10):1627–1634.
66. Kim JW, Kim HC, Park JW, et al. Predictive value of (18) FDG PET-CT for tumour response in patients with locally advanced rectal cancer treated by preoperative chemoradiotherapy. *Int J Colorectal Dis*. 2013;28:1217–1224.
67. Bampo C, Alessi A, Fantini S, et al. Is the standardized uptake value of FDG-PET/CT predictive of pathological complete response in locally advanced rectal cancer treated with capecitabine-based neoadjuvant chemoradiation? *Oncology*. 2013;84(4):191–199.
68. Siddiqui AA, Fayiga Y, Huerta S. The role of endoscopic ultrasound in the evaluation of rectal cancer. *Int Semin Surg Oncol*. 2006;3:36.
69. Williamson PR, Hellinger MD, Larach SW, Ferrara A. Endorectal ultrasound of T3 and T4 rectal cancers after preoperative chemoradiation. *Dis Colon Rectum*. 1996;39(1):45–49.
70. Marone P, de Bellis M, Avallone A, et al. Accuracy of endorectal ultrasound in staging and restaging patients with locally advanced rectal cancer undergoing neoadjuvant chemoradiation. *Clin Res Hepatol Gastroenterol*. 2011;35(10):666–670.
71. Vanagunas A, Lin DE, Stryker SJ. Accuracy of endoscopic ultrasound for restaging rectal cancer following neoadjuvant chemoradiation therapy. *Am J Gastroenterol*. 2004;99(1):109–112.
72. Romagnuolo J, Parent J, Vuong T, et al. Predicting residual rectal adenocarcinoma in the surgical specimen after preoperative brachytherapy with endoscopic ultrasound. *Can J Gastroenterol*. 2004;18(7):435–440.
73. Rau B, Hunerbein M, Barth C, et al. Accuracy of endorectal ultrasound after preoperative radiochemotherapy in locally advanced rectal cancer. *Surg Endosc*. 1999;13:980–984.
74. Maor Y, Nadler M, Barshack I, et al. Endoscopic ultrasound staging of rectal cancer: diagnostic value before and following chemoradiation. *J Gastroenterol Hepatol*. 2006;21(2):454.
75. Napoleon B, Pujol B, Berger F, et al. Accuracy of endosonography in the staging of rectal cancer treated by radiotherapy. *Br J Surg*. 1991;78:785–788.
76. Ramirez JM, Mortensen NJ, Takeuchi N, Humphreys MM. Endoluminal ultrasonography in the follow-up of patients with rectal cancer. *Br J Surg*. 1994;81:692–694.
77. Dresen RC, Peters EE, Rutten HJ, et al. Local recurrence in rectal cancer can be predicted by histopathological factors. *Eur J Surg Oncol*. 2009;35(10):1071–1077.
78. Law WL, Chu KW. Anterior resection for rectal cancer with mesorectal excision: a prospective evaluation of 622 patients. *Ann Surg*. 2004;240(2):260–268.
79. Jörgren F, Johansson R, Damberg L, Lindmark G. Risk factors of rectal cancer local recurrence: population-based survey and validation of the Swedish Rectal Cancer Registry. *Colorectal Dis*. 2010;12(10):977–986.
80. Novell F, Pascual S, Viella P, Trias M. Endorectal ultrasonography in the follow-up of rectal cancer. Is it a better way to detect early local recurrence? *Int J Colorectal Dis*. 1997;12:78–81.

81. Lohnert M, Dohrmann P, Stoffregen C, Hamelmann H. Value of endorectal sonography in the follow-up of patients treated surgically for rectum carcinoma. *Zentralbl Chir.* 1991;116:461–464.
82. Mellgren A, Sirivongs P, Rothenberger DA, et al. Is local excision adequate therapy for early rectal cancer? *Dis Colon Rectum.* 2000;43:1064–1071.
83. Rex DK, Kahi CJ, Levin B, et al. Guidelines for colonoscopy surveillance after cancer resection: a consensus update by the American Cancer Society and the US Multi-Society Task Force on Colorectal Cancer. *Gastroenterology.* 2006;130(6):1865–1871.
84. Gleeson FC, Larson DW, Dozois EJ, et al. Recurrence detection following transanal excision facilitated by EUS-FNA. *Hepato-gastroenterology.* 2012;59(116):1102–1107.
85. Boo SJ, Byeon JS, Park do H, et al. EUS-guided fine needle aspiration and trucut needle biopsy for examination of rectal and perirectal lesions. *Scand J Gastroenterol.* 2011;46(12):1510–1518.
86. Honda K, Akahoshi K, Matsui N, et al. Role of EUS and EUS-guided FNA in the diagnosis of rectal implantation cyst at an anastomosis site after a previous low anterior resection for a rectal cancer without evidence of cancer recurrence. *Gastrointest Endosc.* 2008;68(4):782–785.
87. Mohamadnejad M, Al-Haddad MA, Sherman S, et al. Utility of EUS-guided biopsy of extramural pelvic masses. *Gastrointest Endosc.* 2012;75(1):146–151.
88. Puri R, Eloubeidi MA, Sud R, et al. Endoscopic ultrasound-guided drainage of pelvic abscess without fluoroscopy guidance. *J Gastroenterol Hepatol.* 2010;25(8):1416–1419.
89. Wei SC, Su WC, Chang MC, et al. Incidence, endoscopic morphology and distribution of metastatic lesions in the gastrointestinal tract. *J Gastroenterol Hepatol.* 2007;22(6):827–831.
90. Dumontier I, Roseau G, Palazzo L, et al. Endoscopic ultrasonography in rectal linitis plastica. *Gastrointest Endosc.* 1997;46(6):532–536.
91. Bhutani MS. EUS and EUS-guided fine-needle aspiration for the diagnosis of rectal linitis plastica secondary to prostate carcinoma. *Gastrointest Endosc.* 1999;50(1):117–119.
92. Pishvaian AC, Ahlawat SK, Garvin D, Haddad NG. Role of EUS and EUS-guided FNA in the diagnosis of symptomatic rectosigmoid endometriosis. *Gastrointest Endosc.* 2006;63(2):331–335.
93. Mascagni D, Corbellini L, Urciuoli P, Di Matteo G. Endoluminal ultrasound for early detection of local recurrence of rectal cancer. *Br J Surg.* 1989;76(11):1176–1180.
94. Gleeson FC, Clain JE, Rajan E, et al. Secondary linitis plastica of the rectum: EUS features and tissue diagnosis (with video). *Gastrointest Endosc.* 2008;68(3):591–596.
95. Ulla-Rocha JL, Vilar-Cao Z, Sardina-Ferreiro R. EUS-guided drainage and stent placement for postoperative intra-abdominal and pelvic fluid collections in oncological surgery. *Therap Adv Gastroenterol.* 2012;5(2):95–102.
96. Ramesh J, Bang JY, Trevino J, Varadarajulu S. Comparison of outcomes between EUS-guided trans-colonic and trans-rectal drainage of abdominopelvic abscesses. *J Gastroenterol Hepatol.* 2013;28(4):620–625.
97. DeWitt J, Mohamadnejad M. EUS-guided alcohol ablation of metastatic pelvic lymph nodes after endoscopic resection of polypoid rectal cancer: the need for long-term surveillance. *Gastrointest Endosc.* 2011;74(2):446–447.
98. Weilert F, Shah JN, Marson FP, Binmoeller KF. EUS-guided coil and glue for bleeding rectal varix. *Gastrointest Endosc.* 2012;76(4):915–916.
99. Levy MJ, Abu Dayyeh BK, Fujii LL, et al. Prospective evaluation of adverse events following lower gastrointestinal tract EUS FNA. *Am J Gastroenterol.* 2014;109(5):676–685.
100. Gleeson FC, Kipp BR, Voss JS, et al. Endoscopic ultrasound fine-needle aspiration cytology mutation profiling using targeted next-generation sequencing: personalized care for rectal cancer. *Am J Clin Pathol.* 2015;143(6):879–888.
101. Gleeson FC, Kipp BR, Voss JS, et al. Frequency of mitogen-activated protein kinase and phosphoinositide 3-kinase signaling pathway pathogenic alterations in EUS-FNA sampled malignant lymph nodes in rectal cancer with theranostic potential. *Gastrointest Endosc.* 2015;82(3):550–556.e1.



**Video 18.1** Staging of Rectal Cancer as T3NI by Endoscopic Ultra-sonography

# 19

## Evaluation of the Anal Sphincter by Anal Endosonography

STEVE HALLIGAN

### KEY POINTS

- Anal endosonography (AES) is simple to perform and visualizes the anal sphincter complex—notably the external and internal anal sphincters.
- AES is able to image sphincter tears and defects.
- AES can also characterize sphincter morphology and determine muscular quality.
- AES is the single most important investigation in patients with anal incontinence.

### Introduction

First described in 1989,<sup>1</sup> anal endosonography (AES) was the first technique to visualize the anal sphincter complex with enough spatial resolution to resolve the individual components of the sphincter mechanism. Despite the advent of magnetic resonance imaging (MRI), including endoanal receiver coils, AES generally remains the technique with the highest spatial resolution, and is also quick and easy to perform. The introduction of AES precipitated a significant reappraisal of the causes of anal incontinence (and its treatment), which had hitherto been thought to be mainly the result of pelvic neuropathy.<sup>2</sup> When incontinent patients were studied with AES, it rapidly became clear that occult anal sphincter disruption was present in many cases. Patients with disrupted sphincters can be scheduled for surgical procedures that aim to restore integrity to the sphincter ring, whereas patients whose sphincters are intact, or whose muscles are thought to be of poor quality, can be directed toward conservative measures or alternative surgical approaches.

At present, AES has replaced physiologic testing as the pivotal examination in the clinical decision-making process for these patients, although both are usually performed. Although AES is probably most useful to characterize obstetric injury, it has also facilitated the characterization of other causes of fecal incontinence. For example, with AES, the examiner can identify neurogenic incontinence by way of specific patterns of sphincter atrophy and can identify occult and unintended sphincter damage following anal surgical procedures.

### Equipment and Examination Technique

Although it is possible to perform AES using an echoendoscope, the best results by far are obtained using a dedicated anal

ultrasound probe. The anus is a very superficial structure, and an echoendoscope is cumbersome and expensive when compared with a probe designed specifically for the purpose. AES first employed a 7.5-MHz transducer that had been designed initially for rectal cancer staging and prostatic imaging. The transducer was covered by a rubber balloon, then inserted through the anus into the rectum, the balloon inflated with degassed water, and the transducer rotated mechanically to produce 360-degree images of the rectal wall. Professor Clive Bartram of St. Mark's Hospital, London, realized that by simply replacing the soft rubber balloon with a rigid plastic cone, the rotating transducer could be withdrawn into the anus safely.<sup>1</sup> This maneuver was previously impossible because the balloon would be torn when compressed by the anus against the rotating metal transducer.

Modern probes encapsulate a fixed transducer within a permanent hard cover and are of higher frequency (Fig. 19.1). Some also possess three-dimensional (3D) capacity, achieved either by withdrawing the probe during image acquisition (e.g., EUP-R54AW-19/33, Hitachi Medical Systems, Wellingborough, UK) or by incorporating a transducer that moves along the Z-axis of the probe, inside the exterior capsule, while the head is held stationary within the anal canal (e.g., 2052 transducer, BK Medical, Herlev, Denmark).

As noted earlier, anal imaging is best achieved using a dedicated rigid probe. However, an echoendoscope can be used if a dedicated probe is unavailable. When such systems were first introduced in the late 1980s, the only instrument available was the mechanical radial system (GF-UM3 and EU-M3, Olympus, Tokyo). Initially, attempts were made to utilize this instrument to evaluate the anal sphincter but this was problematic because the optimal focal zone for the UM3 was 1 to 2 cm from the transducer (i.e., beyond the sphincter muscles). The only way to bring the sphincters into this focal zone was to inflate the balloon surrounding the transducer but doing so distorts and compresses the sphincters and is very uncomfortable, and image interpretation is unreliable. In the early 1990s, units that wished to perform anal sphincter examinations had to purchase dedicated systems (as mentioned previously). In response, Olympus began to market rigid mechanical radial probes in 2000 (RU-75M-R1 and RU-12M-R1) intended to examine the sphincters and rectum and which were compatible with their existing radial endoscopic ultrasound processors. These rigid probes are still marketed today and are compatible with the EU-ME2 and EU-ME2 Premier Plus Ultrasound processors. With time, mechanical radial technology yielded

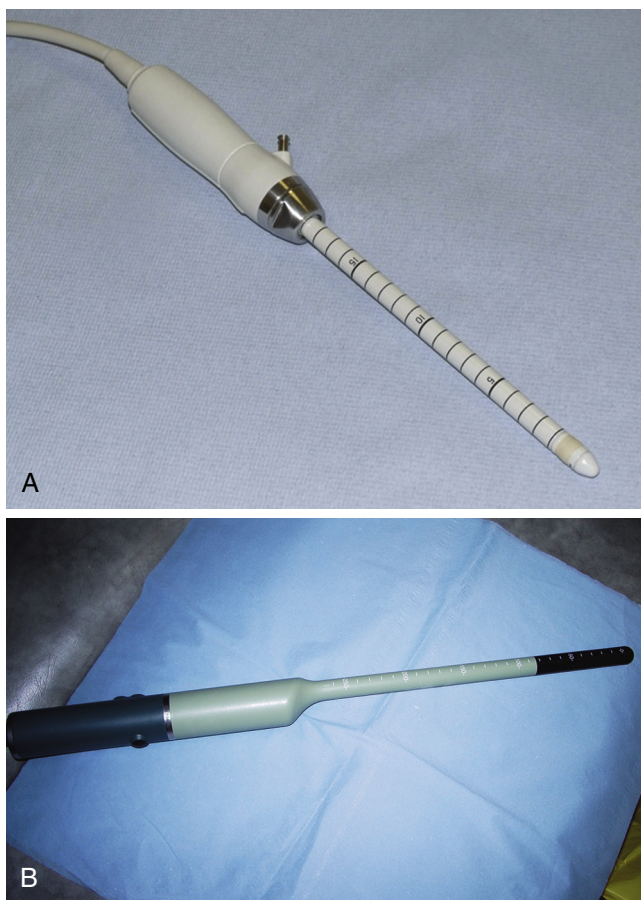


**Fig. 19.1** Probes for ultrasound examination of the anal sphincter complex. (A) Hitachi EUP-R54AW-19/33 electronic radial probe. (B) B and K medical 1846 probe. ([A] Courtesy of Hitachi Medical Systems, Wellingborough, UK. [B] Courtesy of BK Medical, Herlev, Denmark.)

to electronic array systems. The advantage of electronic radial technology is its variable focal length combined with very good resolution. Though not tested in comparative studies, many practitioners feel that the current electronic radial systems are adequate for anal sphincter evaluation.

The examination is simple, well tolerated by the patient, and very rapid when performed by an experienced operator. No special patient preparation is required. The patient is told that discomfort, if any, will be similar to having a small finger in the anus, and the procedure will likely be much less uncomfortable than digital rectal examination by a doctor. To the patient, the probe is potentially quite a frightening piece of equipment, so it is worth mentioning that only the distal few centimeters will enter the anus (as opposed to rectal endosonography, in which insertion is obviously deeper).

Men are examined in the left lateral patient position, but the prone patient position is preferable for examining women. Placing women in the left lateral position can occasionally distort anterior perineal anatomy and can induce an asymmetrical image, which makes it difficult to distinguish perineal scarring from normal anatomic features.<sup>3</sup> In the past, it was necessary to fill the transducer head with degassed water to achieve acoustic coupling, accomplished by injection using a syringe through a side port and then maneuvering the probe so that all air was expelled through a pinhole located at the tip of the cone. However, modern probes merely require the tip to be lubricated with ultrasound jelly and then covered with a condom, which is itself lubricated to facilitate

insertion. The probe tip is then inserted into the anus, and image acquisition commenced. The aim is to insert the probe so that the transducer lies just into the distal rectum. The probe is then withdrawn gently and slowly to examine the anal sphincters.

As for all ultrasound examinations, clinical findings are generally based on the image displayed on the monitor screen in real time (with the exception of 3D acquisition, in which case the examination in its entirety can be replayed later). However, still images are usually required for archival purposes, and the author finds it is convenient to obtain these still images at three levels: the proximal, middle, and distal anal canal (see later). These three anatomic levels are imaged at standard magnification, and the examination is then repeated at a higher magnification, for a total of six images, three at each magnification. The probe is oriented so that anterior (i.e., the 12 o'clock position) is uppermost, which mimics the standard used for axial medical imaging. The examination is normally very quick, perhaps only a minute or so for the experienced operator who is familiar with normal and abnormal anatomy, and especially if the sphincters are normal.

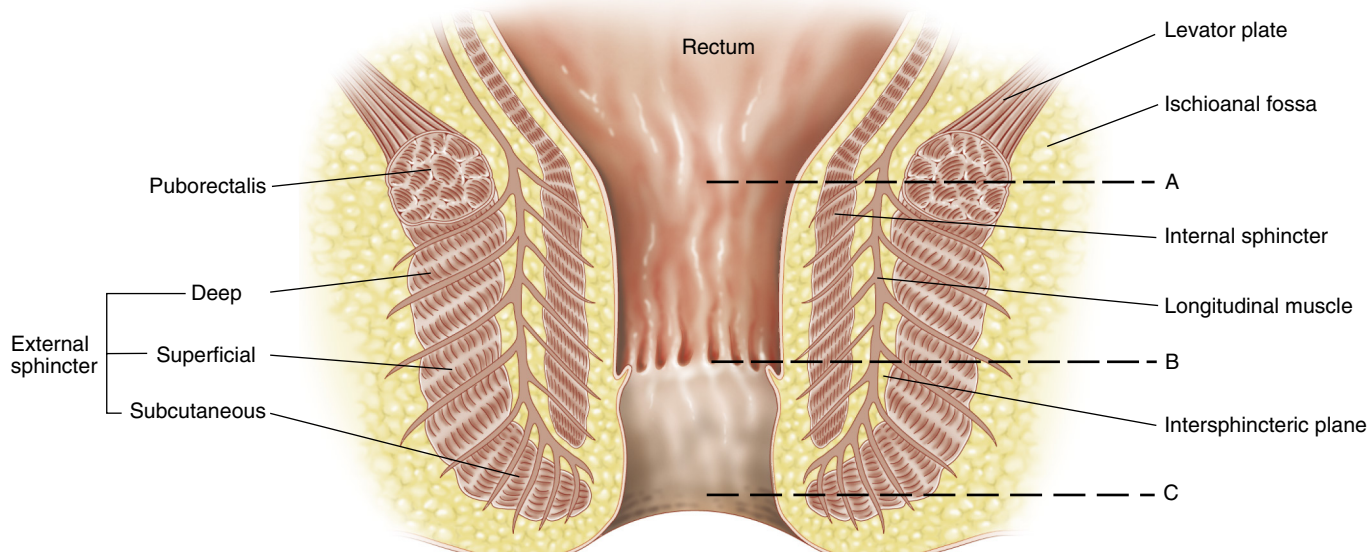
## Anal Sphincter Anatomy

Clearly a sound understanding of basic anal anatomy is a prerequisite for accurate interpretation of endosonographic findings. There are two anal sphincters: the external anal sphincter (EAS) is composed of striated muscle, whereas the internal anal sphincter (IAS) is smooth muscle. These form two cylindrical layers, with the IAS innermost (Fig. 19.2).

The EAS arises from the striated muscles of the pelvic floor and is composed of three cylindrical bundles lying on top of one another (deep, superficial, and subcutaneous) that are difficult to distinguish in practice. The deep portion is fused with the puborectalis (or pubococcygeus) muscle, which itself merges with the levator plate of the pelvic floor. The EAS extends approximately 1 cm distal to the IAS, where it forms the subcutaneous part of the EAS muscle. Anteriorly the EAS is closely related to several surrounding structures, such as the superficial transverse muscle of the perineum and the perineal body. Posteriorly it is continuous with the anococcygeal ligament, a structure that is often more prominent in men and should not be mistaken for a posterior sphincter defect. The EAS is much shorter anteriorly (in the craniocaudal direction; i.e., longitudinal) in women than in men, and this feature should not be confused with a sphincter defect.

The IAS is the distal termination and condensation of the circular smooth muscle of the gut tube. It extends from the anorectal junction to approximately 1 to 1.5 cm below the dentate line (see Fig. 19.2). The longitudinal muscle of the gut tube also terminates in the anal canal, but it is less apparent than the IAS. The longitudinal muscle interdigitates between the EAS and the IAS and terminates in the subcutaneous EAS and subcutaneous anus. Its exact sphincteric action, if any, is much less clear than that of the EAS and IAS, and it is thought that its main purpose is to brace the anus and thus prevent anal eversion during defecation.<sup>4</sup> Lying between the EAS and the longitudinal muscle is a potential plane, the intersphincteric space, which may contain fat. The components of the anal sphincter are surrounded by the ischioanal space (often referred to by surgeons as the ischiorectal fossa), which contains fat predominantly.

Directly anterior to the anal sphincter is the central perineal tendon or perineal body. In men, this lies posterior to the bulbospongiosus and corpus cavernosum and their related muscles,



• Fig. 19.2 Coronal diagrammatic representation of important anal canal structures. Scan levels indicated correspond to Fig. 19.3.

whereas in women, it lies within the anovaginal septum. Many structures insert fibers into the perineal body, such as the EAS, the deep and superficial transverse muscles of the perineum, the bulbocavernous muscle, and the puborectalis muscle. These structures should not be confused with sphincter defects. For example, normal variants of anal sphincter anatomy have been identified, such as differing relationships between the superficial transverse perineal muscle and the EAS.<sup>5</sup>

The distal anal canal is lined with stratified squamous epithelium, richly supplied by sensory receptors. These receptors are most concentrated at the dentate line, which demarcates the junction with proximal columnar epithelium. The anal subepithelial tissues are relatively thick, and this lining and its underlining vascular spaces—the anal cushions—also play a role in maintaining continence.

## Normal Endosonographic Findings

Because the anus and surrounding sphincter muscles are cylindrical, a 360-degree field of view is optimal, and the axial plane is also the most relevant surgically when considering sphincter defects. As stated earlier, it is convenient to obtain baseline images at three levels at a minimum: the proximal, middle, and distal anal canal.

The proximal anal canal is primarily identified by the puborectalis and transverse perineal muscles (Fig. 19.3A). The puborectalis slings around the anorectal junction and can be distinguished from the EAS, with which it blends imperceptibly, because its anterior ends splay outward as they travel toward their fusion with the pubic arch (see Fig. 19.3A). The IAS is visible as a continuous hypoechoic ring and is generally the easiest structure to differentiate from other adjacent anal canal components because it is normally very hyporeflective. The subepithelial tissues, EAS, and longitudinal muscle all normally show varying degrees of hyperreflectivity, and their margins can often be difficult to define precisely, although direct comparisons with endoanal MRI have helped tremendously.<sup>6</sup> Increases in transducer frequency that improve spatial resolution have also helped clarify sonographic anatomy,<sup>7</sup> as has 3D imaging.<sup>8</sup>

In their seminal early studies, Sultan et al.<sup>9</sup> carefully imaged cadaveric specimens following sequential histologic dissection of anal layers and thereby validated the sonographic appearances. These investigators found that the echogenicity of normal muscle changed as its orientation was altered with respect to the transducer. Thus normal variant striated muscle slips may appear hypoechoic, depending on their orientation to the transducer, and should not be confused with sphincter tears or scars.

If the probe is withdrawn just a centimeter or so from the proximal anal canal position, the anterior ends of the normal puborectalis muscle will converge anteriorly as they segue imperceptibly into the EAS. The mid-anal canal is thus defined where the EAS forms a complete ring anteriorly (see Fig. 19.3B). The IAS is also normally thickest and best seen at this level. At this level, the intersphincteric plane and longitudinal muscle may also be resolved as two distinct layers, with the longitudinal muscle forming distinct bundles of smooth muscle fibers.

Withdrawing the probe slightly more will move the field of view into the subcutaneous EAS (see Fig. 19.3C). This lies below the termination of the IAS, which is either not visualized or only partially visualized if its termination is irregular (a common normal variant). It is usually impossible to visualize the longitudinal muscle reliably at this level because it has thinned out as it interdigitates into the EAS, and it is mainly composed of fibroelastic tissue rather than the smooth muscle found more proximally.

Correct interpretation of AES is possible only if the operator has a firm grasp of normal sonographic anatomy. Pathology is defined by either muscular discontinuity (i.e., from sphincter tears or lacerations, secondary to a variety of causes) or abnormal muscular quality (which is usually caused by neuromuscular atrophy or degeneration). To appreciate muscular quality correctly, it is important to realize that normal sonographic appearances are contingent on both age and sex. Frudinger et al.<sup>7</sup> examined 150 nulliparous women with high-frequency AES to define normal age-related differences in sphincter morphology and found a highly significant positive correlation between IAS thickness and increasing age. In contrast, EAS thickness showed a highly significant negative correlation with increasing age.<sup>7</sup> Some evidence also

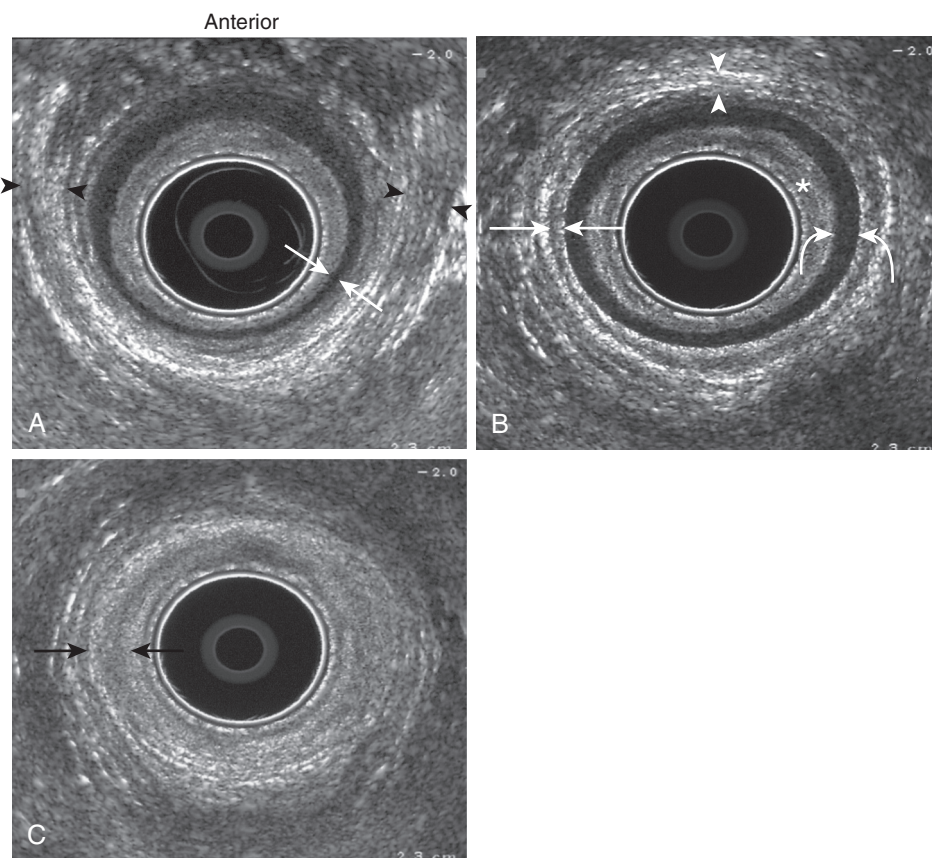


**Fig. 19.3** Normal endosonographic anatomy of the anal canal in a woman. This scan was obtained using a 10-MHz 360-degree probe. (A) Proximal anal canal level. At this level, the anterior ends of puborectalis muscle are well seen bilaterally (*between arrowheads*) as the muscle fibers course forward toward the pubis. The hyporeflective internal anal sphincter is also clearly seen (*between arrows*). (B) Midanal canal level. At this level, the external sphincter (superficial part) forms a complete ring around the anal canal, notably anteriorly (*between arrowheads*). The internal sphincter is also at its thickest (*between curved arrows*). The intersphincteric plane and longitudinal muscle (*between arrows*) lie between the external and internal sphincters. The subepithelial tissues (*asterisk*) lie medial to the internal sphincter. (C) Distal anal canal level. At this level, the predominant muscle is the subcutaneous external sphincter (*between arrows*) because the scan plane is caudal to the termination of the internal sphincter.

suggested that IAS reflectivity increased with age. No significant correlation was noted between age and thickness of subepithelial tissues, the longitudinal muscle, or the puborectalis muscle.<sup>7</sup>

On average, the IAS measures 2 to 3 mm thick in normal adults (measured at either the 3 or 9 o'clock position at mid-anal canal level). A thin IAS has more significance in an older person with symptoms (see later sections). In addition, although the IAS can be measured easily because it contrasts with adjacent structures, other muscles may be more difficult to measure and are subject to greater interobserver variation. Gold et al.<sup>10</sup> measured anal canal structures in 51 consecutive referrals: intraobserver agreement was superior to interobserver agreement and the 95% limits of agreement for EAS measurements spanned 5 mm versus 1.5 mm for IAS measurements.<sup>10</sup> Interobserver agreement for diagnosis of sphincter disruption and IAS echogenicity was very good, suggesting that AES has generalizable diagnostic utility ( $\kappa = 0.80$  and 0.74, respectively).<sup>10</sup>

Clear sonographic differences exist between men and women with respect to the dimensions of anal canal structures and their sonographic appearances. Most importantly, the anterior complete ring of the EAS is shorter in women in the craniocaudal (longitudinal) direction. This difference has been widely appreciated

for some time: Williams et al.<sup>8</sup> used 3D AES to show that craniocaudal EAS length was approximately 17 mm in women versus 30 mm in men. A short anterior EAS in a woman should not be misinterpreted as a sphincter defect. In addition, in men the various muscular components generally show a more striated appearance (Fig. 19.4).

## Anal Sphincter Function

Most clinical referrals for AES are in response to patients complaining of anal incontinence, either to gas alone or to both gas and feces. It is therefore important to have some basic understanding of normal anal sphincter function.

The anal sphincter is the most complex sphincter in the human body. Continence is maintained by a multifaceted interrelationship between anal and pelvic floor musculature, integrating somatic and autonomic nervous pathways, the effects of which must be temporarily overcome during the act of defecation. The IAS is innervated by sympathetic presacral nerve fibers and is not under conscious control. It is primarily responsible for closing the anal canal at rest, at which time it is in a state of continuous involuntary contraction. Despite being striated muscle,

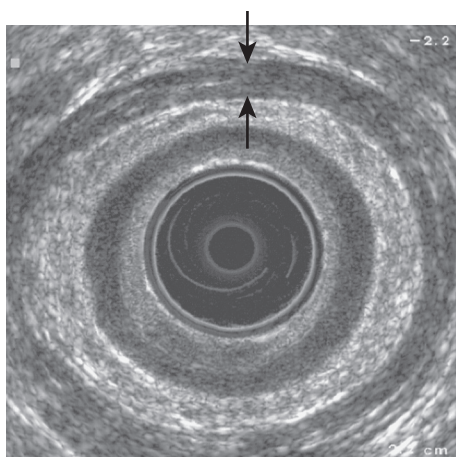


**Fig. 19.4** Anal endosonography at the midanal canal in an asymptomatic man. Note the generally more striated appearance when compared with Fig. 19.3. The external sphincter (between arrows), in particular, is relatively hyporeflective.

the puborectalis and EAS also display some resting tone and can contract rapidly without conscious control in response to any sudden increase in intraabdominal pressure, to prevent anal incontinence. The EAS is innervated by the pudendal nerves (S2, S3, and S4).

Defecation is initiated by colonic smooth muscle contractions—for example, those provoked by waking and eating. These contractions propel stool from the sigmoid colon into the normally empty rectum and stimulate rectal sensory nerves that produce an urge to defecate. These nerves are also able to determine the nature of rectal content (i.e., solid, liquid, or gas). The sensation of a full rectum and the ability to discriminate among gaseous, liquid, and solid content are important components of continence, in addition to sphincter integrity. Sensation is retained after rectal excision, a finding suggesting that some sensory receptors reside in the pelvic floor itself.<sup>11</sup> Rectal filling causes reflex IAS relaxation (via the rectoanal inhibitory reflex), rectal contraction, and contraction of the puborectalis and the EAS, both of which are heavily modulated by conscious control. Stool within the anal canal contacts sensory receptors concentrated at the dentate line and greatly intensifies the urge to defecate, which is resisted by vigorous striated muscle contraction until circumstances for defecation are appropriate. When this is so, pelvic floor relaxation and increased intraabdominal pressure create a positive pressure gradient from rectum to anus and evacuation ensues.

The normal function and contribution of the EAS and IAS to anal continence can be used to predict which muscles are abnormal in incontinent patients. For example, IAS abnormality generally results in passive incontinence (i.e., the patient is unaware that leakage is about to occur), whereas EAS abnormality more frequently manifests as urge incontinence (i.e., the patient is unable consciously to defer defecation).<sup>12</sup>

## Anorectal Physiologic Testing

Sphincter integrity and function can also be determined by anorectal physiologic testing, which evaluates nervous integrity, conduction, and muscular performance. Few physiologic tests are absolutely diagnostic, and most need to be considered together with symptoms, clinical findings, and imaging. For example, low pressures could be due to sphincter defects or

neurologic deficit, and conversely, it is possible to have a sphincter defect and normal pressures. However, anorectal physiology provides valuable complementary information and continues to be requested in combination with AES, and endosonographers should be aware of their implications. Normal values vary among laboratories.

## Manometry

Manometry determines rectal and anal pressures more precisely than simple digital examination. Complexity varies, from simple balloons connected to a pressure transducer to multichannel probes capable of measuring pressures at several sites simultaneously and displaying pressures in 3D, and even ambulatory systems recording over several hours. The pressure recorded rises when a rectal catheter is withdrawn into the anus, and falls again when it reaches the anal margin. This high-pressure zone defines the functional anal canal length (as opposed to anatomic length, which is usually shorter). The pressure zone is frequently diminished in incontinent patients. A static anal probe measures resting pressure, which predominantly reflects IAS function; reduced resting pressure broadly reflects IAS disease. In contrast, the squeeze pressure is the incremental rise over resting pressure elicited when the patient is asked to contract their anus voluntarily, and broadly reflects EAS function. Squeeze pressure is frequently reduced when incontinence results from EAS laceration, as occurs following obstetric injury. Dual-sphincter disease is implicated when both resting and squeeze pressures are abnormal, and neither finding is absolutely specific in an individual patient.

## Pudendal Nerve Latency

Pudendal nerve terminal motor latency can be determined from the time taken for a digitally delivered pudendal nerve stimulus to elicit anal sphincter contraction. A common system employs a disposable glove with a stimulating electrode at its fingertip, coupled with a pressure sensor at its base.<sup>13</sup> The nerve is stimulated near the ischial spine and has both sensory and motor components. Slow conduction is thought to predominantly result from stretch-induced injury (e.g., following childbirth<sup>2,14</sup> or chronic straining<sup>15</sup>) and can even be demonstrated transiently in normal individuals when asked to strain excessively. The clinical relevance of pudendal neuropathy remains unclear, especially because the degree of neuropathy, pelvic floor descent, and anal sensation should be directly related, but studies cannot demonstrate this.<sup>16</sup> Nevertheless, patients with abnormal latencies but intact sphincters usually have their incontinence attributed to neuropathic sphincter degeneration, and sphincter repair is less successful if underlying neuropathy is present.<sup>17</sup>

## Electromyography

A needle electrode inserted into the EAS can determine both its activity and muscular quality. Sphincter denervation is followed by reinnervation via neighboring healthy axons, which can be quantified electromyographically because the recorded action potentials become polyphasic. Until the advent of AES, electromyography was the only reliable way to diagnose sphincter tears directly (as opposed to indirectly via reduced pressures, for which there are multiple causes); the needle was inserted into the suspected defect, which was confirmed if no muscular potentials could be recorded subsequently (also possible if the needle tip missed

normal muscle because of incorrect placement—easily done when insertion is blind!). Sphincter defects were mapped out by “blind” needle passes made circumferentially around the anus. Electromyography is painful because local anesthetic interferes with recording so isn’t used. Fortunately, AES is superior for detecting sphincter defects when the two modalities are compared directly.<sup>18</sup>

## Sonographic Findings in Anal Incontinence

As mentioned earlier, most clinical referrals for AES are to investigate anal incontinence. Anal incontinence has a variety of causes, many of which relate to the integrity and quality of the sphincter mechanism. AES has assumed a central role in the diagnostic workup for assessment of this problem because AES reliably identifies those patients who have a sphincter tear, selects individuals likely to benefit from surgery that aims to restore integrity to the sphincter ring, and prevents unnecessary surgery in others. Physical examination cannot detect anal sphincter defects reliably, and although anal canal pressures can help determine whether sphincter function is abnormal, they cannot indicate precisely whether the cause is loss of sphincter integrity or neuropathy.

Anal incontinence is common, especially in women, and its prevalence increases with age. Two percent of the general population older than 45 years have anal incontinence,<sup>19</sup> with prevalence rising to 7% of persons more than 65 years old.<sup>20</sup> In retirement homes or hospitals, approximately one-third of individuals have anal incontinence.<sup>19</sup> Prevalence is likely to be even higher because of underreporting. Anal incontinence has considerable economic impact. A 1988 study estimated that more than \$400 million annually was spent on incontinence appliances in the United States alone, and anal incontinence was the second most common cause of placement in a nursing home.<sup>21</sup> Several clinical grading systems for anal incontinence have been developed.

## Obstetric Injury

Childbirth is a common cause of anal incontinence, either directly, from anal sphincter laceration, or indirectly, from damage to sphincter innervation. Obstetric anal sphincter injury is often termed “OASIS.” Until the advent of AES, it was assumed that neuropathy resulting from damage to sphincter innervation was the primary cause of obstetric-related incontinence because impaired pudendal nerve conduction can be demonstrated after vaginal delivery, presumably from stretch-induced injury.<sup>2</sup> Anal sphincter laceration was thought to be a relatively rare event because it was identified clinically in only 1 out of 200 vaginal deliveries.<sup>22</sup> However, AES revealed that anal sphincter tears were far more common than assumed. An early sonographic study of 11 women with a diagnosis of neurogenic fecal incontinence revealed that four had also sustained unsuspected anal sphincter tears.<sup>23</sup> A further study of 62 women whose incontinence was related to childbirth found EAS tears in 56 (90%).<sup>24</sup>

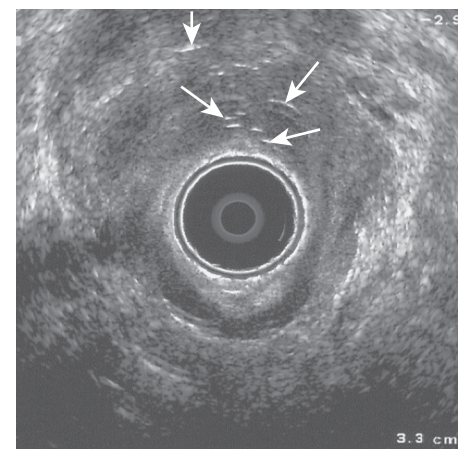
In a landmark study, Sultan et al.<sup>25</sup> used AES to study 202 consecutive unselected women before and after vaginal delivery, finding anal sphincter tears in 28 of 79 (35%) of primiparous subjects and in 21 of 48 (44%) of multiparous subjects. Furthermore, endosonographic evidence of sphincter laceration was associated with symptoms of anal incontinence 6 weeks following delivery and correlated positively with impaired physiology—namely reduced anal resting and squeeze pressures. No primiparous woman had a sphincter defect before childbirth, and no subject undergoing cesarean section developed a new defect.

These findings confirmed that sphincter injury was caused by vaginal delivery, especially forceps extraction. Moreover, the study confirmed that clinical examination of the perineum immediately after vaginal delivery missed most sphincter tears.

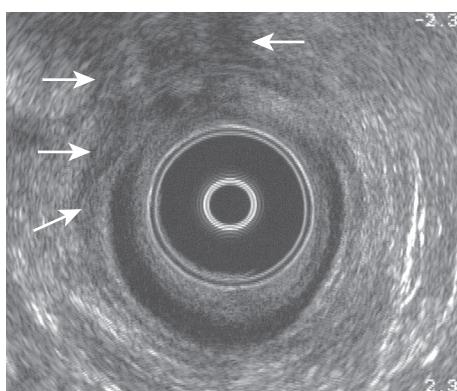
Anal incontinence occurs immediately after delivery if trauma is substantial, but many women present years later, presumably because the cumulative effects of multiple deliveries, progressive neuropathy, aging, and menopause overcome their compensatory mechanisms. Many women are also too embarrassed to complain, or they or their doctors believe that the condition is incurable. The accuracy of endosonography has been validated both histologically<sup>9</sup> and intraoperatively,<sup>18</sup> and approaches 95%.<sup>23,26,27</sup> For example, a study of 44 patients found that all 23 EAS defects and 21 of 22 IAS defects visualized on preoperative AES were confirmed subsequently by surgery.<sup>26</sup>

The sphincters are cylindrical structures, so discontinuity is diagnostic of a sphincter tear. A break in the hypoechoic IAS ring indicates an IAS defect, whereas EAS defects are defined by discontinuity of the more heterogeneous EAS, located peripheral to the intersphincteric plane and the longitudinal muscle. In severe disruptions, the entire sphincter mechanism is completely absent anteriorly, with a cloacal defect between the vagina and anal canal (Fig. 19.5). Obstetric injury is practically always anterior, because this is where the vagina lies. Because the EAS and IAS are in very close proximity, it is usual for obstetric injury to involve both sphincters. Isolated EAS injury is relatively uncommon, and isolated IAS injury is rarely the result of obstetric injury alone.

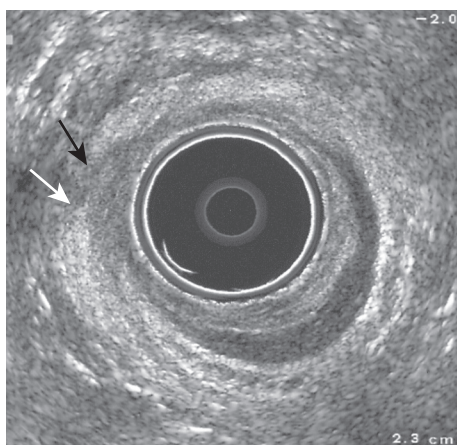
Scar tissue forms between the sphincter ends and creates a sonographic “defect” (Figs. 19.6 to 19.8). It is unclear how symptoms relate to the sonographic extent of the injury. For example, a study of 330 women found that although women with an EAS tear had lower basal squeeze pressures than those with no tear, beyond this no consistent relationship between the morphology of the tear (in terms of both its longitudinal and circumferential extent) and either symptoms or impaired anal pressures was observed.<sup>28</sup> Women may first present several years after the initial injury (see Fig. 19.8), and some patients with large defects may be entirely asymptomatic initially (see Fig. 19.6). Supporting this finding, a prospective study found that some women with clear evidence of sphincter disruption on AES were entirely asymptomatic following delivery,<sup>29</sup> and a study of 124 consecutive women



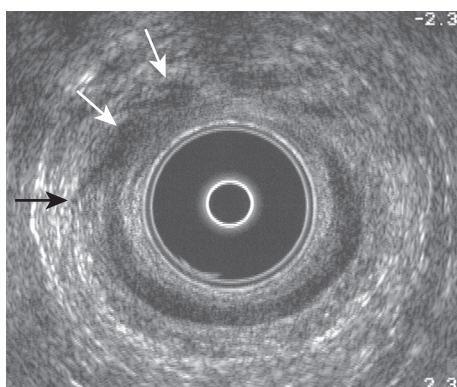
**• Fig. 19.5** Obstetric injury. Anterior cloacal defect in a woman following vaginal delivery of a 5-kg baby. Note there is no external or internal sphincter anteriorly, and air within the defect (arrows) extends right to the probe surface.



**• Fig. 19.6** Typical anterior obstetric injury affecting both the external and internal anal sphincters. This 29-year-old woman was completely asymptomatic and was examined as part of a research study. The primary repair following delivery has opposed the external sphincter to some degree, but a sonographic defect remains (arrows).



**• Fig. 19.7** Typical anterior obstetric injury affecting both the external and internal sphincters. The sphincters have been reasonably well approximated (arrows) by primary repair, but the patient complained of anal incontinence immediately following childbirth.

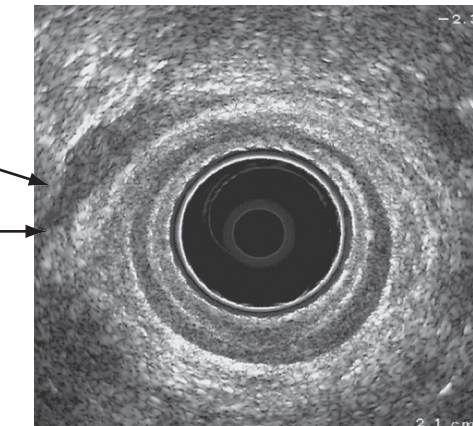


**• Fig. 19.8** Typical anterior obstetric injury affecting both the external and internal anal sphincters. This 55-year-old woman had symptoms of anal incontinence that developed several years after vaginal delivery. Although it would be easy to ascribe this deterioration to progressive neuropathy, endosonography clearly reveals a sonographic defect centered on the right anterior quadrant (arrows).

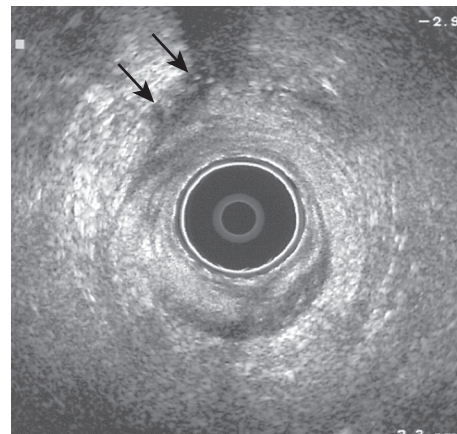
with late-onset anal incontinence after vaginal delivery found that 71% had sonographic sphincter defects that were believed to be the cause of symptoms despite the temporal separation between childbirth and symptoms.<sup>30</sup>

Perineal tears that do not involve the sphincter muscles directly are much less likely to be associated with immediate symptoms (Fig. 19.9). A prospective study of 55 nulliparous women using 3D AES found postpartum trauma in 29%. However, those women whose damage was limited to the puboanalis or transverse perineal muscles did not have symptoms or reduced anal pressures.<sup>31</sup> It is also believed that anal sphincter morphology may change postpartum without any direct tearing of the perineum or sphincters. In particular, both two-dimensional (2D) and 3D studies have found that the anterior EAS may shorten following vaginal delivery without any sonographic evidence of a tear (i.e., stretching of the sphincter during delivery alters its shape permanently but without frank tearing).<sup>32,33</sup> At the other extreme, AES may be used to examine women who have an anovaginal fistula following delivery because gas within the fistula is highly reflective and allows delineation of the tract and its relationship with the sphincter mechanism (Fig. 19.10).

Following clinical diagnosis of a sphincter tear, “primary repair” is performed immediately after childbirth to close the perineum, usually under local anesthesia (or topped-up epidural)



**• Fig. 19.9** Perineal scar. Endosonography following vaginal delivery reveals a right anterior quadrant perineal scar (arrows) in this asymptomatic woman.

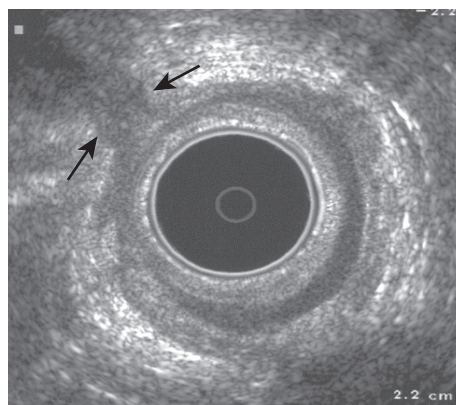


**• Fig. 19.10** Anterior anovaginal fistula (arrows) in a woman following prolonged vaginal delivery.

unless there is very significant disruption. The competence with which primary repair is performed varies enormously and AES is pivotal to both diagnose a tear, the extent of injury, and the extent and competency of primary repair. It is clear that many women suffer anal incontinence following primary repair, despite recognition of the tear and attempted repair. A study of 156 such women found that 40% of respondents were anally incontinent, which was associated with a persistent sphincter defect on AES.<sup>34</sup> Another study found that 44 of 56 (79%) women who had undergone primary sphincter repair for a clinically recognized EAS tear following vaginal delivery had persistent sphincter defects on AES and were more symptomatic than those whose repair showed no substantial sonographic defect.<sup>35</sup> These findings were confirmed by other workers, suggesting that primary repair was incomplete in many women.<sup>36</sup>

Thus, although primary sphincter repair aims to restore integrity to the sphincter ring, it seems this is not achieved in many cases (Fig. 19.11). This could be because the perineum is very edematous and bruised immediately following vaginal delivery, factors that may conspire against anatomical clarity and successful repair, or inadequate training for obstetricians and/or midwives to recognize and repair sphincter injuries. A study of 48 women 2 to 7 days following primary repair found that 90% had sonographic defects. Many of these defects were confined to the proximal anal canal, suggesting that the initial repair had been incomplete.<sup>37</sup> The investigators concluded that inadequate repair was due to surgical inexperience rather than the extent of damage, because junior doctors or midwives had undertaken many of the procedures. Recent data have also found that sphincter injuries may also be diagnosed clinically when none are present on AES, again reflecting clinical inexperience.<sup>38</sup> A Cochrane review found some evidence that AES used routinely prior to primary repair might reduce subsequent anal incontinence by identifying tears and ensuring that primary repair was adequate.<sup>39</sup> AES used routinely following vaginal delivery could identify women with clinically occult sphincter tears whose sphincter may be at further risk from subsequent deliveries,<sup>40</sup> which is known to increase the risk of cumulative damage.<sup>41,42</sup>

Endosonography has also been used to investigate whether routinely collected obstetric variables predict subsequent sphincter disruption. A study of 159 women found no correlation between sonographic tears and head circumference, baby weight, episiotomy, or the duration of active pushing.<sup>43</sup> However, forceps



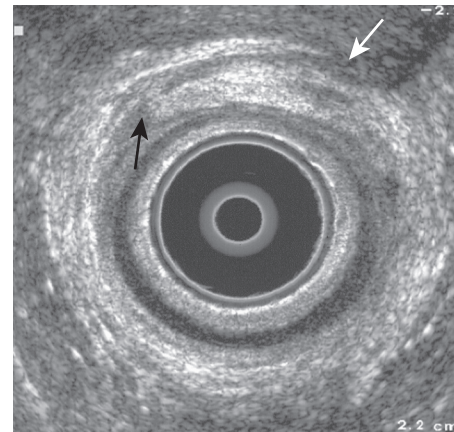
• Fig. 19.11 Anal endosonography following primary repair of a clinically recognized third-degree tear following vaginal delivery. A persistent external sphincter defect is visible (arrows).

delivery was strongly associated with sphincter tears,<sup>43</sup> an association recognized by other workers.<sup>25,44</sup> Other investigators identified a link between sphincter tears and a second stage of labor prolonged by epidural anesthesia, which increased the risk of disruption by an odds ratio of 2:1.<sup>44</sup> Where access to AES is limited, it may be possible to identify women who harbor sphincter tears by administering a simple incontinence questionnaire following delivery. Frudinger et al.<sup>29</sup> found that such an approach was able to identify 60% of women who sustained EAS tears following vaginal delivery.

If symptoms remain following primary repair and there is sonographic evidence of a sphincter defect, then women may be offered formal sphincter repair. An increasingly common option is to perform an anterior overlap repair, in which the disrupted EAS ends are mobilized, overlapped (thus tightening the anal canal), and then sutured together. Symptoms improve in approximately 85% of women immediately afterward, but this improvement is not sustained, and the percentage drops to approximately 50% at 5 years.<sup>45</sup> The cause of this deterioration is unclear, but concomitant progressive neuropathy is implicated, possibly resulting from pudendal damage or perhaps sphincter denervation and ischemia during the surgical procedure. However, repeated attempts at secondary sphincter repair are possible and can improve symptoms, even after many previous attempts, and delayed sphincter repair is also possible, with good symptomatic outcome.<sup>46,47</sup> An alternative is to simply oppose the sphincter ends, an “end-to-end” repair. Although a Cochrane review found this inferior to overlap repair at 1-year follow-up, the two approaches were equivalent at 3 years.<sup>48</sup>

Endosonography has also assumed a role in the assessment of such secondary repairs. For example, the sonographic integrity of the repair correlates with symptoms and improved physiologic status.<sup>49</sup> Endosonography following a good anterior sphincter repair reveals sphincter ends that are well overlapped (Fig. 19.12), whereas poor repairs are detected by persistent sphincter defects (Fig. 19.13). Only the EAS is repaired, because attempts at IAS repair have not proved worthwhile. Residual IAS defects in the presence of a good EAS repair may underpin persistent symptoms—especially those of passive incontinence.

AES revolutionized the management of women with OASIS, but it is fair to say that some controversy persists regarding the exact incidence of EAS tears. For example, although the



• Fig. 19.12 Good sonographic appearances following anterior overlapping sphincter repair. The external sphincter ends are well overlapped (between arrows), and there is no residual defect.

landmark study by Sultan et al.<sup>25</sup> found an incidence of 35% in primiparous women, Varma et al.<sup>50</sup> suggested that the true incidence was closer to 9%, and other investigators suggested 17%.<sup>51</sup> In an attempt to resolve this uncertainty, a meta-analysis of 717 vaginal deliveries found a 27% incidence of sphincter defects in nulliparous women, and 30% of these were symptomatic. The investigators concluded that the probability that postpartum anal incontinence was caused by sphincter disruption was on the order of 80%.<sup>52</sup>

### Idiopathic Internal Anal Sphincter Degeneration and External Anal Sphincter Atrophy

Not all anal incontinence is caused by sphincter disruption. Many incontinent patients have intact sphincters, but the functional quality of their sphincter muscle is impaired by neuromuscular degeneration. Vaizey et al.<sup>53</sup> reported 52 anally incontinent patients whose EAS and IAS were intact on endosonography, but whose IAS was thinned and hyperreflective. Resting pressures, reflecting IAS function, were significantly lowered while squeeze pressures and pudendal nerve latencies were normal. The investigators concluded that discrete and isolated primary degeneration of the IAS was likely responsible for anal incontinence in these patients. Because the IAS normally thickens with age,<sup>7</sup> IAS thinning is relatively easy to diagnose using AES, and the diagnosis should be considered in any older patient whose IAS measures 1 mm or less in thickness (Fig. 19.14). A rare cause of isolated IAS thinning is systemic sclerosis (scleroderma).<sup>54</sup>

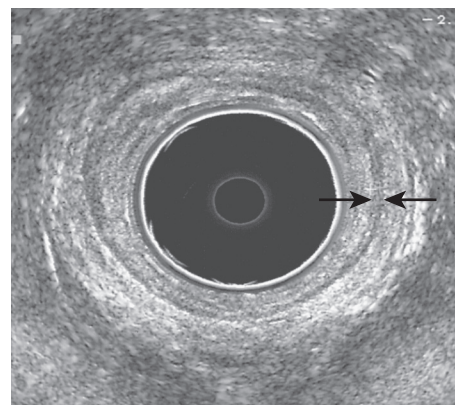
The EAS may also degenerate—a process termed *atrophy*. This phenomenon was first recognized using endoanal MRI because the striated fibers of the EAS contrast strongly against ischioanal fat, and it is therefore easier to appreciate muscular bulk than on AES.<sup>55</sup> Although the mechanisms are unclear, one possibility being long-standing pudendal neuropathy, EAS atrophy is important because it adversely affects the outcome of sphincter repair. Briel et al.<sup>55</sup> found that surgical procedures for concomitant EAS defects in this group were unsuccessful presumably because the functional quality of the EAS was compromised by atrophy. Using both endoanal MRI and AES, Williams et al.<sup>56</sup> were able to define the sonographic features of EAS atrophy, finding it patchy and poorly defined. In particular, the lateral edge of the EAS was

indistinct, and the muscle was thinner than normal.<sup>56</sup> IAS degeneration and EAS atrophy may be combined in the same patient, and these are probably the sonographic features of what has long been termed *neurogenic* fecal incontinence (Fig. 19.15). Indeed, atrophy of both sphincters and concomitant tears can be found in the same patient.

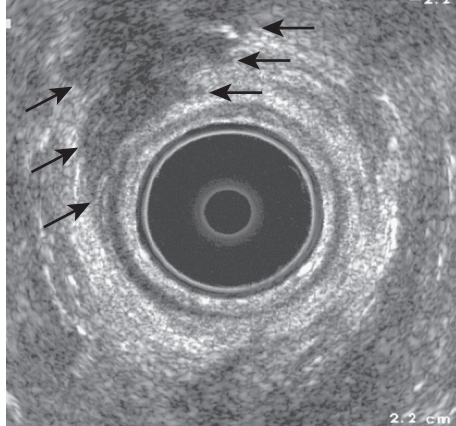
Although endoanal MRI is likely superior to AES for diagnosis of EAS atrophy, investigators found that both modalities are equivalent for diagnosis of sphincter tears. AES is particularly adept for diagnosis of IAS degeneration because this muscle is normally well visualized during endosonography and is thinned in these patients, whereas it is normally thicker in older people, an observation that facilitates the distinction between normal and abnormal.<sup>57</sup> EAS atrophy is more difficult to diagnose reliably with AES, not only because the sphincter is relatively difficult to define, but also because the normal EAS tends to thin with age.<sup>7</sup>

### Iatrogenic Sphincter Injury and Anal Trauma

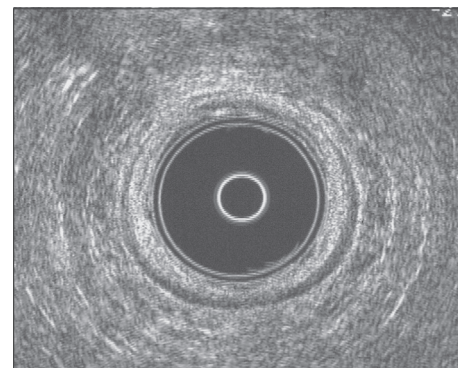
Unfortunately, iatrogenic damage is a relatively common cause of anal incontinence. A study of 50 patients following a variety of anal surgical procedures found subsequent sphincter defects



• Fig. 19.14 Anal endosonography in a 69-year-old woman with passive anal incontinence. The internal sphincter (between arrows) is intact but barely visible and measured 0.7 mm at its thickest. The findings suggest idiopathic degeneration of the internal anal sphincter.



• Fig. 19.13 Poor sonographic appearances in a woman who remained symptomatic following a formal sphincter repair. A large persistent defect is visible (arrows).



• Fig. 19.15 Anal endosonography in a 50-year-old woman complaining of anal incontinence. Both sphincters are intact but are very poorly seen. The lateral margins of the external anal sphincter (EAS) are indistinct, suggesting EAS atrophy, and the internal anal sphincter is very thin, suggesting degeneration.

in 46%.<sup>58</sup> Although some procedures purposely seek to divide the sphincter mechanism, most obviously IAS sphincterotomy, other procedures should not normally cause sphincter damage. An association between unintentional sphincter division and hemorrhoidectomy is now well recognized (Fig. 19.16). A study of 16 patients undergoing hemorrhoidectomy found subsequent sphincter defects in 50%.<sup>59</sup> Quadrantic IAS division is relatively common in symptomatic patients, but occasionally the incision is unintentionally deep enough to divide the longitudinal muscle and the EAS as well.

The IAS may also be damaged in patients who have undergone procedures that require anal dilatation. In these cases, the appearances tend to be those of generalized IAS fragmentation around its circumference (Fig. 19.17). Anal stretch (the Lord procedure) for anal fissure is a common cause of such disruption, as is manual rectal evacuation for intractable constipation, if it is not performed carefully.<sup>60</sup> Transanal stapling instruments, such as those used for low anterior resection, may also unintentionally incorporate the IAS, causing defects and subsequent passive incontinence.<sup>61,62</sup> Whereas the IAS is divided purposefully during lateral sphincterotomy, the intent is usually to divide only the most caudal one third of its length. However, prospective

sonographic studies of IAS morphology following sphincterotomy have revealed that division is often more extensive than intended, notably in women, probably because their anatomic anal canal is shorter than in men.<sup>63</sup> Such studies have increased physician awareness of overextensive IAS division, and many operators are now very cautious. The result is that sonographic studies have revealed that some patients whose anal fissure persisted after sphincterotomy may not actually have had any muscle divided during the procedure.<sup>64</sup>

A current role is also emerging for AES in the treatment of anal incontinence, although this work is largely preliminary. For example, AES is necessary to monitor injection of bulking material, such as silicone, into the anal sphincter so that implants are placed correctly.<sup>65–67</sup> More recent work has used AES to deliver autologous myoblasts into EAS defects, with the hope that the engineered cells will integrate into their surroundings and restore functionality to the damaged striated muscle.<sup>68,69</sup>

## Sonographic Findings in Other Anal Disorders

Although the main role for AES is management of anal incontinence, AES has other useful applications. The most prominent of these is probably for imaging fistula-in-ano. Surgeons operating on these patients need to know the relationship between the fistula tract and anal sphincter complex because treatment often involves cutting down onto the fistula and laying it open, so that infection can drain and heal subsequently. This practically always necessitates a degree of unavoidable sphincter division, the extent of which may be predicted by AES.

Early attempts to use AES for preoperative assessment of fistula-in-ano were relatively disappointing, and assessment was no better than that achieved by digital examination by an experienced colorectal surgeon.<sup>70</sup> However, later studies using higher frequency probes were more optimistic. A study of 108 fistulas in 104 patients found that AES correctly classified the primary fistula tract in 81% of cases, as opposed to 61% for digital examination by an experienced surgeon.<sup>71</sup> Endosonography was particularly accurate for predicting the site of the internal anal opening, being correct in 91% of cases<sup>71</sup>—the internal opening is inevitably close to the transducer surface and is therefore visualized with high spatial resolution. However, AES has specific disadvantages. Most importantly, insufficient depth penetration, especially with high-frequency transducers, limits detection of tracts and abscesses relatively distant from the probe. Unfortunately, these lesions usually underpin recurrent disease.<sup>72</sup> Moreover, AES cannot reliably distinguish infection from fibrosis, because both appear hypoechoic on ultrasound. This inability causes particular difficulties in patients with recurrent disease where active tracts and fibrotic scars are frequently combined. Attempts have been made to clarify the course of patent tracts by injecting hydrogen peroxide or ultrasound contrast agents into the external opening during examination.<sup>73,74</sup>

Another disadvantage of AES is its inability to image in the surgically important (for fistulas) coronal plane, making it very difficult to distinguish supralevator from infralevator extensions. Some investigators have attempted to overcome this via 3D probes (Fig. 19.18).<sup>75,76</sup> However, there is little doubt that MRI is a superior technique overall, and therefore the major role of

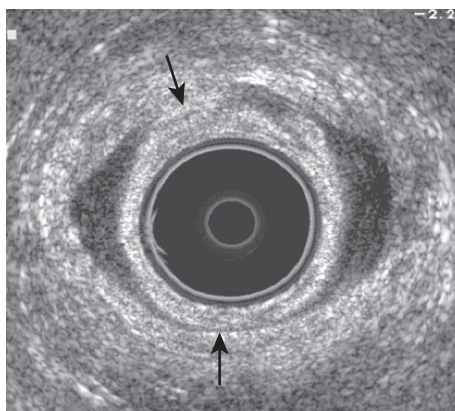


**Fig. 19.16** Endosonography in a man who became incontinent following hemorrhoidectomy. The scan reveals extensive internal sphincter division, with large anterior and posterior defects (arrows).

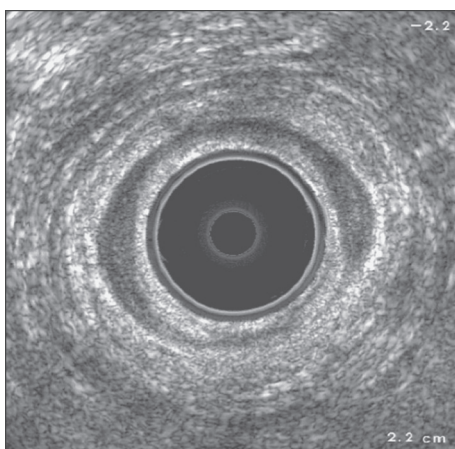


**Fig. 19.17** Internal anal sphincter fragmentation. Endosonography reveals internal sphincter fragmentation in this woman who had anal dilation for an anal fissure and who now complains of anal incontinence.

AES in fistula disease is probably to assess the degree of sphincter disruption in those patients who become anally incontinent following fistula repair operations. AES also has a particular role in those patients who may have a small intersphincteric abscess that could be difficult to resolve using standard body or phased array surface coil MRI (Fig. 19.19). AES also assumes a pivotal role where MRI is unavailable.

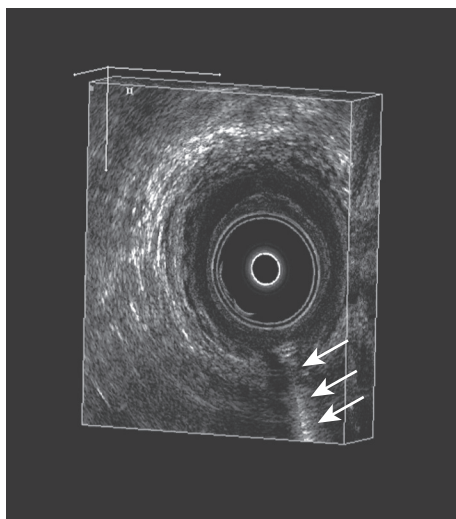
Endosonography has revealed sphincter abnormalities in patients who are severely constipated, although the significance of these abnormalities remains largely uncertain. For example, patients with solitary rectal ulcer syndrome are known to have an abnormally thickened IAS (Fig. 19.20),<sup>77</sup> and this finding has been correlated with the presence of high-grade prolapse of rectal mucosa.<sup>78</sup> IAS hypertrophy has also been demonstrated by AES in children with intractable constipation.<sup>79</sup> A study of 144 constipated children found that this finding correlated with duration and severity of symptoms, size of megarectum, and amplitude of rectal contraction.<sup>80</sup> The investigators suggested that IAS thickening was caused by hypertrophy as a result of chronic stimulation owing to the presence of feces in the rectum.<sup>80</sup> Endosonography may also be useful when it is necessary to determine the correct anatomic position of the

neoanus with respect to any residual musculature in children with imperforate anus and, unlike MRI, can easily be performed perioperatively.<sup>81–83</sup>

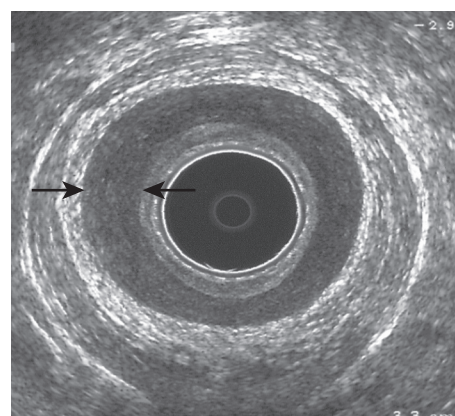
Endosonography may also be used to stage anal tumors locally because it can determine the depth of penetration into surrounding tissues (Fig. 19.21),<sup>84</sup> but because of depth limitations, MRI will be most useful where available. Investigators have found AES poor for detecting local recurrence; all 14 recurrences in a series of 82 patients were detected by visual inspection and digital examination alone.<sup>85</sup>

## Recent Developments

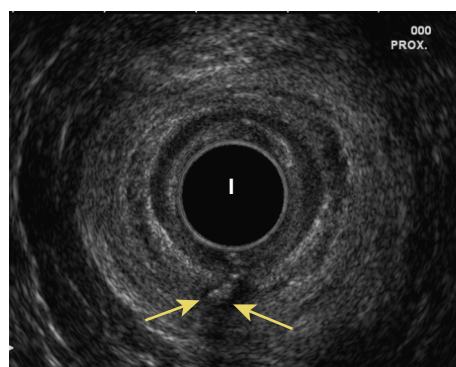
The last few years have seen many publications describing results from 3D AES (e.g., describing the longitudinal extent of internal sphincter division following sphincterotomy for anal fissure).<sup>86</sup> The author believes that 3D acquisition is not substantially superior to standard 2D imaging when the latter is used by experienced practitioners; the author uses only 2D imaging for his clinical work. The major advantage of 3D would seem to be practical—because a volume of data is acquired that encompasses the entire anal sphincter complex, a complete examination can be acquired and reviewed subsequently, whereas only selected “slices” are acquired during standard examinations.



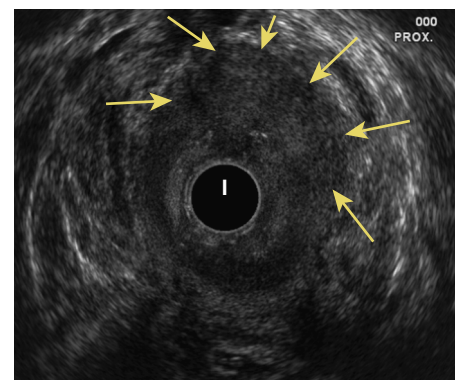
**• Fig. 19.18** Three-dimensional anal endosonography following hydrogen peroxide injection through the external opening of a fistula-in-ano. Echogenic gas is present within an intersphincteric tract (arrows).



**• Fig. 19.20** Male patient with solitary rectal ulcer syndrome. The internal sphincter (between arrows) measured 7.5 mm, far greater than normal.



**• Fig. 19.19** Endosonography clearly reveals a posterior intersphincteric abscess (arrows) in this patient with anal pain. The digital rectal examination had been normal.



**• Fig. 19.21** Anal squamous tumor. Endosonography in a man with a primary anal squamous tumor reveals a large left anterior quadrant mass (arrows) that has breached the anal sphincter complex to reach the surrounding tissues.

Transperineal ultrasound has also attracted significant recent attention, presumably because it does not require the purchase of dedicated anal ultrasound probes; a standard linear transducer is applied to the perineum and used to image the sphincter complex and pelvic floor. Although cited as “less invasive,”<sup>87</sup> the author would argue there is no substantial difference between rubbing an ultrasound probe over a patient’s perineum versus inserting a small-diameter probe a couple of centimeters into their anus. However, the ability to use a standard ultrasound probe is a distinct advantage if the technique is accurate, although there is some evidence that it is not as accurate as AES.<sup>88</sup> Clearly, the anatomical display is very different from endoanal imaging. An alternative approach is to image the “undisturbed” anal sphincter via transvaginal ultrasound, but this may also be inferior to AES.<sup>88</sup> It is also appreciated increasingly that women who sustain obstetric anal sphincter damage may also sustain deeper trauma, notably levator avulsion, which some investigators have studied using transperineal ultrasound.<sup>89</sup> MRI is also used for this diagnosis but at the time of writing it is unclear what the implications of such injuries are.

## Key References

2. Snooks SJ, Setchell M, Swash M, Henry MM. Injury to the innervation of the pelvic floor sphincter musculature in childbirth. *Lancet*. 1984;2:546–550.
7. Frudinger A, Halligan S, Bartram CI, et al. Female anal sphincter: age-related differences in asymptomatic volunteers with high-frequency endoanal US. *Radiology*. 2002;224:417–423.
10. Gold DM, Halligan S, Kmiot WA, Bartram CI. Intraobserver and interobserver agreement in anal endosonography. *Br J Surg*. 1999;86:371–375.
25. Sultan AH, Kamm MA, Hudson CN, et al. Anal sphincter disruption during vaginal delivery. *N Engl J Med*. 1993;329:1905–1911.
88. Ros C, Martínez-Franco E, Wozniak MM, et al. Postpartum 2D and 3D ultrasound evaluation of the anal sphincter complex in women with obstetric anal sphincter injuries. *Ultrasound Obstet Gynecol*. 2017;49:508–514.

## References

Access the reference list online at [ExpertConsult.com](http://ExpertConsult.com).

## References

1. Law PJ, Bartram CI. Anal endosonography: technique and normal anatomy. *Gastrointest Radiol.* 1989;14:349–353.
2. Snooks SJ, Setchell M, Swash M, Henry MM. Injury to the innervation of the pelvic floor sphincter musculature in childbirth. *Lancet.* 1984;2:546–550.
3. Frudinger A, Bartram CI, Halligan S, Kamm M. Examination techniques for endosonography of the anal canal. *Abdom Imaging.* 1998;23:301–303.
4. Lunniss PJ, Phillips RK. Anatomy and function of the anal longitudinal muscle. *Br J Surg.* 1992;79:882–884.
5. Stoker J, Rocci E, Zwamborn AW, et al. Endoluminal MR imaging of the rectum and anus: technique, applications, and pitfalls. *Radiographics.* 1999;19:383–398.
6. Williams AB, Bartram CI, Halligan S, et al. Endosonographic anatomy of the normal anal canal compared with endocoil magnetic resonance imaging. *Dis Colon Rectum.* 2002;45:176–183.
7. Frudinger A, Halligan S, Bartram CI, et al. Female anal sphincter: age-related differences in asymptomatic volunteers with high-frequency endoanal US. *Radiology.* 2002;224:417–423.
8. Williams AB, Bartram CI, Halligan S, et al. Multiplanar anal endosonography: normal anal canal anatomy. *Colorectal Dis.* 2001;3:169–174.
9. Sultan AH, Nicholls RJ, Kamm MA, et al. Anal endosonography and correlation with in vitro and in vivo anatomy. *Br J Surg.* 1993;80:508–511.
10. Gold DM, Halligan S, Kmiot WA, Bartram CI. Intraobserver and interobserver agreement in anal endosonography. *Br J Surg.* 1999;86:371–375.
11. Lane RH, Parks AG. Function of the anal sphincters following colo-anal anastomosis. *Br J Surg.* 1977;64:596–599.
12. Engel AG, Kamm MA. Relationship of symptoms in faecal incontinence to specific sphincter abnormalities. *Int J Colorectal Dis.* 1995;10:152–155.
13. Rogers J, Henry MM, Misiewicz JJ. Disposable pudendal nerve stimulator: evaluation of the standard instrument and new device. *Gut.* 1988;29:1131–1133.
14. Kiff ES, Swash M. Slowed conduction in the pudendal nerves in idiopathic (neurogenic) faecal incontinence. *Br J Surg.* 1984;71:614–616.
15. Parks AG, Porter NH, Hardcastle JD. The syndrome of the descending perineum. *Proc R Soc Med.* 1966;59:477–482.
16. Jorge JMN, Wexner SD, Ehrenpreis ED, et al. Does perineal descent correlate with pudendal neuropathy? *Dis Colon Rectum.* 1993;36:475–483.
17. Gilliland R, Altomare DF, Moreira H, et al. Pudendal neuropathy is predictive of failure following anterior overlapping sphincteroplasty. *Dis Colon Rectum.* 1998;41:1516–1522.
18. Sultan AH, Kamm MA, Talbot IC, et al. Anal endosonography for identifying external sphincter defects confirmed histologically. *Br J Surg.* 1994;81:463–465.
19. Denis P, Bercoff E, Bizien MF. Etude de la prevalence de l'incontinence anale chez l'adulte. *Gastroenterol Clin Biol.* 1992;16:344–350.
20. Talley NJ, O'Keefe EA, Zinsmeister AR, Melton JL. Prevalence of gastrointestinal symptoms in the elderly: a population based study. *Gastroenterology.* 1992;102:895–901.
21. Lahr CJ. Evaluation and treatment of incontinence. *Pract Gastroenterol.* 1988;12:27–35.
22. Sultan AH, Kamm MA, Hudson CN, Bartram CI. Third degree obstetric tears: risk factors and outcome of primary repair. *BMJ.* 1994;308:887–891.
23. Law PJ, Kamm MA, Bartram CI. Anal endosonography in the investigation of faecal incontinence. *Br J Surg.* 1991;78:312–314.
24. Burnett SJD, Spence-Jones C, Speakman CTM, et al. Unsuspected sphincter damage following childbirth revealed by anal endosonography. *Br J Radiol.* 1991;64:225–227.
25. Sultan AH, Kamm MA, Hudson CN, et al. Anal sphincter disruption during vaginal delivery. *N Engl J Med.* 1993;329:1905–1911.
26. Deen KI, Kumar D, Williams JG, et al. Anal sphincter defects: correlation between endoanal ultrasound and surgery. *Ann Surg.* 1993;218:201–205.
27. Sentovich SM, Wong WD, Blatchford GJ. Accuracy and reliability of transanal ultrasound for anterior anal sphincter injury. *Dis Colon Rectum.* 1998;41:1000–1004.
28. Voyvodic F, Rieger NA, Skinner S, et al. Endosonographic imaging of anal sphincter injury: does the size of the tear correlate with the degree of dysfunction? *Dis Colon Rectum.* 2003;46:735–741.
29. Frudinger A, Halligan S, Bartram CI, et al. Assessment of the predictive value of a bowel symptom questionnaire in identifying perianal and anal sphincter trauma after vaginal delivery. *Dis Colon Rectum.* 2003;46:742–747.
30. Oberwalder M, Dinnewitzer A, Baig MK, et al. The association between late-onset fecal incontinence and obstetric anal sphincter defects. *Arch Surg.* 2004;139:429–432.
31. Williams AB, Bartram CI, Halligan S, et al. Anal sphincter damage after vaginal delivery using three-dimensional endosonography. *Obstet Gynaecol.* 2001;97:770–775.
32. Frudinger A, Halligan S, Bartram CI, et al. Changes in anal anatomy following vaginal delivery revealed by anal endosonography. *Br J Obstet Gynaecol.* 1999;106:233–237.
33. Williams AB, Bartram CI, Halligan S, et al. Alteration of anal sphincter morphology following vaginal delivery revealed by multiplanar anal endosonography. *BJOG.* 2002;109:942–946.
34. Poen AC, Felt-Bersma RJ, Strijers RL, et al. Third-degree obstetric perineal tear: long-term clinical and functional results after primary repair. *Br J Surg.* 1998;85:1433–1438.
35. Davis K, Kumar D, Stanton SL, et al. Symptoms and anal sphincter morphology following primary repair of third-degree tears. *Br J Surg.* 2003;90:1573–1579.
36. Savoye-Collet C, Savoye G, Koning E, et al. Endosonography in the evaluation of anal function after primary repair of a third-degree obstetric tear. *Scand J Gastroenterol.* 2003;38:1149–1153.
37. Starck M, Bohe M, Valentin L. Results of endosonographic imaging of the anal sphincter 2–7 days after primary repair of third- or fourth-degree obstetric sphincter tears. *Ultrasound Obstet Gynecol.* 2003;22:609–615.
38. Sioutis D, Thakar R, Sultan AH. Overdiagnosis and rising rates of Obstetric Anal Sphincter Injuries (OASIS). Time for reappraisal. *Ultrasound Obstet Gynecol.* 2017;50:642–647.
39. Walsh KA, Grivell RM. Use of endoanal ultrasound for reducing the risk of complications related to anal sphincter injury after vaginal birth. *Cochrane Database Syst Rev.* 2015;(10):CD010826.
40. Faltin DL, Boulvain M, Irion O, et al. Diagnosis of anal sphincter tears by postpartum endosonography to predict fecal incontinence. *Obstet Gynecol.* 2000;95:643–647.
41. Fines M, Donnelly V, Behan M, et al. Effect of second vaginal delivery on anorectal physiology and faecal continence: a prospective study. *Lancet.* 1999;354:983–986.
42. Faltin DL, Sangalli MR, Roche B, et al. Does a second delivery increase the risk of anal incontinence? *BJOG.* 2001;108:684–688.
43. Varma A, Gunn J, Lindow SW, Duthie GS. Do routinely measured delivery variables predict anal sphincter outcome? *Dis Colon Rectum.* 1999;42:1261–1264.
44. Donnelly V, Fynes M, Campbell D, et al. Obstetric events leading to anal sphincter damage. *Obstet Gynecol.* 1998;92:955–961.
45. Malouf AJ, Norton CS, Engel AF, et al. Long-term results of overlapping anterior anal-sphincter repair for obstetric trauma. *Lancet.* 2000;355:260–265.
46. Pinedo G, Vaizey CJ, Nicholls RJ, et al. Results of repeat anal sphincter repair. *Br J Surg.* 1999;86:66–69.

47. Giordano P, Renzi A, Efron J, et al. Previous sphincter repair does not affect the outcome of repeat repair. *Dis Colon Rectum.* 2002;45:635–640.
48. Fernando RJ, Sultan AH, Kettle C, Thakar R. Methods of repair for obstetric anal sphincter injury. *Cochrane Database Syst Rev.* 2013;CD002866. <https://doi.org/10.1002/14651858.CD002866>.
49. Felt-Bersma RJ, Cuesta MA, Koorevaar M. Anal sphincter repair improves anorectal function and endosonographic image: a prospective clinical study. *Dis Colon Rectum.* 1996;39:878–885.
50. Varma A, Gunn J, Gardiner A, et al. Obstetric anal sphincter injury: prospective evaluation of incidence. *Dis Colon Rectum.* 1999;42:1537–1543.
51. Abramowitz L, Sobhani I, Ganansia R, et al. Are sphincter defects the cause of anal incontinence after vaginal delivery? Results of a prospective study. *Dis Colon Rectum.* 2000;43:590–596; discussion 596–598.
52. Oberwalder M, Connor J, Wexner SD. Meta-analysis to determine the incidence of obstetric anal sphincter damage. *Br J Surg.* 2003;90:1333–1337.
53. Vaizey CJ, Kamm MA, Bartram CI. Primary degeneration of the internal anal sphincter as a cause of passive faecal incontinence. *Lancet.* 1997;349:612–615.
54. Engel AF, Kamm MA, Talbot IC. Progressive systemic sclerosis of the internal anal sphincter leading to passive faecal incontinence. *Gut.* 1994;35:857–859.
55. Briel JW, Stoker J, Rocci E, et al. External anal sphincter atrophy on endoanal magnetic resonance imaging adversely affects continence after sphincteroplasty. *Br J Surg.* 1999;86:1322–1327.
56. Williams AB, Bartram CI, Modhwadia D, et al. Endocoil magnetic resonance imaging quantification of external anal sphincter atrophy. *Br J Surg.* 2001;88:853–859.
57. Malouf AJ, Williams AB, Halligan S, et al. Prospective assessment of accuracy of endoanal MR imaging and endosonography in patients with fecal incontinence. *AJR Am J Roentgenol.* 2000;175:741–745.
58. Felt-Bersma RJ, van Baren R, Koorevaar M, et al. Unsuspected sphincter defects shown by anal endosonography after anorectal surgery: a prospective study. *Dis Colon Rectum.* 1995;38:249–253.
59. Abbasakoor F, Nelson M, Beynon J, et al. Anal endosonography in patients with anorectal symptoms after haemorrhoidectomy. *Br J Surg.* 1998;85:1522–1524.
60. Gattuso JM, Kamm MA, Halligan SM, Bartram CI. The anal sphincter in idiopathic megarectum: effects of manual disimpaction under general anaesthetic. *Dis Colon Rectum.* 1996;39:435–439.
61. Ho YH, Tsang C, Tang CL, et al. Anal sphincter injuries from stapling instruments introduced transanally: randomized, controlled study with endoanal ultrasound and anorectal manometry. *Dis Colon Rectum.* 2000;43:169–173.
62. Farouk R, Duthie GS, Lee PW, Monson JR. Endosonographic evidence of injury to the internal anal sphincter after low anterior resection: long-term follow-up. *Dis Colon Rectum.* 1998;41:888–891.
63. Sultan AH, Kamm MA, Nicholls RJ, Bartram CI. Prospective study of the extent of internal anal sphincter division during lateral sphincterotomy. *Dis Colon Rectum.* 1994;37:1031–1033.
64. Garcia-Granero E, Sanahuja A, Garcia-Armengol J, et al. Anal endosonographic evaluation after closed lateral subcutaneous sphincterotomy. *Dis Colon Rectum.* 1998;41:598–601.
65. Tjandra JJ, Lim JF, Hiscock R, Rajendra P. Injectable silicone biomaterial for fecal incontinence caused by internal anal sphincter dysfunction is effective. *Dis Colon Rectum.* 2004;47:2138–2146.
66. Maeda Y, Vaizey CJ, Kamm MA. Long-term results of perianal silicone injection for faecal incontinence. *Colorectal Dis.* 2007;9:357–361.
67. Guerra F, La Torre M, Giuliani G, et al. Long term evaluation of bulking agents for the treatment of fecal incontinence: clinical outcomes and ultrasound evidence. *Tech Coloproct.* 2015;19: 23–27.
68. Frudinger A, Kölle D, Schwaiger W, et al. Muscle-derived cell injection to treat anal incontinence due to obstetric trauma: pilot study with 1 year follow-up. *Gut.* 2010;59:55–61.
69. Frudinger A, Pfeifer J, Paedé J, et al. Autologous skeletal muscle-derived cell injection for anal incontinence due to obstetric trauma: a five-year follow-up of an initial study of ten patients. *Colorectal Dis.* 2015;17:794–801.
70. Choen S, Burnett S, Bartram CI, Nicholls RJ. Comparison between anal endosonography and digital examination in the evaluation of anal fistulae. *Br J Surg.* 1991;78:445–447.
71. Buchanan GN, Halligan S, Bartram CI, et al. Clinical examination, endosonography, and magnetic resonance imaging for pre-operative assessment of fistula-in-ano: comparison to an outcome based reference standard. *Radiology.* 2004;233:674–681.
72. Buchanan G, Halligan S, Williams A, et al. Effect of MRI on clinical outcome of recurrent fistula-in-ano. *Lancet.* 2002;360:1661–1662.
73. Kruskal JB, Kane RA, Morrin MM. Peroxide-enhanced anal endosonography: technique, image interpretation, and clinical applications. *Radiographics.* 2001;21:173–189.
74. Buchanan GN, Bartram CI, Williams AB, et al. Value of hydrogen peroxide enhancement of three-dimensional endoanal ultrasound in fistula-in-ano. *Dis Colon Rectum.* 2005;48:141–147.
75. West RL, Zimmerman DD, Dwarkasing S, et al. Prospective comparison of hydrogen peroxide-enhanced three-dimensional endoanal ultrasonography and endoanal magnetic resonance imaging of perianal fistulas. *Dis Colon Rectum.* 2003;46:1407–1415.
76. Ding JH, Bi LX, Zhao K, et al. Impact of three-dimensional endoanal ultrasound on the outcome of anal fistula surgery: a prospective cohort study. *Colorectal Dis.* 2015;17:1104–1112.
77. Halligan S, Sultan A, Rottenberg G, Bartram CI. Endosonography of the anal sphincters in solitary rectal ulcer syndrome. *Int J Colorectal Dis.* 1995;10:79–82.
78. Marshall M, Halligan S, Fotheringham T, et al. Predictive value of internal anal sphincter thickness for diagnosis of rectal intussusception in patients with solitary rectal ulcer syndrome. *Br J Surg.* 2002;89:1281–1285.
79. Hosie GP, Spitz L. Idiopathic constipation in childhood is associated with thickening of the internal anal sphincter. *J Pediatr Surg.* 1997;32:1041–1043; discussion 1043–1044.
80. Keshtgar AS, Ward HC, Clayden GS, Sanei A. Thickening of the internal anal sphincter in idiopathic constipation in children. *Pediatr Surg Int.* 2004;20:817–823.
81. Jones NM, Humphreys MS, Goodman TR, et al. The value of anal endosonography compared with magnetic resonance imaging following the repair of anorectal malformations. *Pediatr Radiol.* 2003;33:183–185.
82. Yamataka A, Yoshida R, Kobayashi H, et al. Intraoperative endosonography enhances laparoscopy-assisted colon pull-through for high imperforate anus. *J Pediatr Surg.* 2002;37:1657–1660.
83. Stensrud KJ, Emblem R, Bjørnland K. Anal endosonography and bowel function in patients undergoing different types of endorectal pull-through procedures for Hirschsprung disease. *J Pediatr Surg.* 2015;50:1341–1346.
84. Tarantino D, Bernstein MA. Endoanal ultrasound in the staging and management of squamous-cell carcinoma of the anal canal: potential implications of a new ultrasound staging system. *Dis Colon Rectum.* 2002;45:16–22.
85. Lund JA, Sundstrom SH, Haaverstad R, et al. Endoanal ultrasound is of little value in follow-up of anal carcinomas. *Dis Colon Rectum.* 2004;47:839–842.

86. Murad-Regadas SM, Fernandes GO, Regadas FS, et al. How much of the internal sphincter may be divided during lateral sphincterotomy for chronic anal fissure in women? Morphologic and functional evaluation after sphincterotomy. *Dis Colon Rectum.* 2013;56:645–651.
87. Alberquerque A, Pereira E. Current applications of transperineal ultrasound in gastroenterology. *World J Radiol.* 2016;8:370–377.
88. Ros C, Martínez-Franco E, Wozniak MM, et al. Postpartum 2D and 3D ultrasound evaluation of the anal sphincter complex in women with obstetric anal sphincter injuries. *Ultrasound Obstet Gynecol.* 2017;49:508–514.
89. Valsky DV, Cohen SM, Lipschuetz M, et al. Third- or fourth-degree intrapartum anal sphincter tears are associated with levator ani avulsion in primiparas. *J Ultrasound Med.* 2016;35:709–715.

# How to Perform Endoscopic Ultrasonography-Guided Fine-Needle Aspiration

SARTO C. PAQUIN AND ANAND V. SAHAI

## KEY POINTS

- The needle should be kept in the visual plane at all times.
- Excessive force should never be used to pass the needle sheath past an acute bend in the endoscope tip.
- Use of the stylet does not increase the yield of endoscopic ultrasonography-fine-needle aspiration and is more cumbersome to use.
- Twenty-five-gauge needles provide better diagnostic yield when sampling pancreatic lesions compared with 22-G needles.
- When aspirating a cyst, the endosonographer should fully aspirate all fluid, make only one pass, use antibiotics, and not try to perform aspiration cytology from the cyst wall.

## Introduction

Fine-needle aspiration (FNA) provides some of the most clinically powerful information that endoscopic ultrasonography (EUS) has to offer—pathological confirmation of the presence (or absence) of malignancy and/or metastasis to secondary sites (“histological staging”). Like any procedure, proficiency requires adequate experience, but EUS FNA is not a universally difficult technique to master. Some cases are more technically demanding than others. Sampling a 5-mm pancreatic nodule buried deep in the uncinate process is certainly more challenging than sampling a 4-cm subcarinal lymph node. Interestingly, some of the easiest cases provide information that can have a tremendous impact on patient management (e.g., such as prevention of surgery by documentation of mediastinal node involvement in a patient with non–small cell lung cancer).

EUS FNA can be broken down into a series of steps. Proper execution of each step will make EUS FNA easier and probably increase the yield for malignancy. Experts have varying opinions of the best way to perform EUS FNA; however, objective data are constantly emerging to help clarify which procedural variables improve results and which have no clear impact.

This chapter will provide a detailed description of a generic EUS FNA technique that can be applied to the great majority of

lesions, to obtain specimens for cytologic analysis and/or to prepare a cell block. Special consideration will also be given to issues that provide particular challenges.

Cytologic specimens are adequate for diagnostic purposes in the great majority of cases. They can be used to confirm or exclude epithelial malignancies, allow for immunochemical staining (e.g., to diagnose neuroendocrine tumors and small cell lung cancer, to look for specific tumor receptors), and permit flow cytometry, which can help diagnose or exclude monoclonal lymphoid processes. Cytologic specimens may also be sufficient to identify granulomas, which may help diagnose diseases such as sarcoidosis. However, in some cases, true histologic specimens may be required, and core specimens should be sought using larger gauge or specialized needles. The techniques required to obtain a “core” biopsy specimen for true histologic analysis are addressed elsewhere.

## Indications and Contraindications

Indications for EUS FNA for tissue acquisition have broadened over time. Tissue sampling is performed most often to confirm suspected cancer,<sup>1</sup> although it may also be useful in benign conditions such as diagnosing sarcoidosis or infections (e.g., tuberculosis, fungal disease). Table 20.1 summarizes the common sites for performing EUS FNA.

Contraindications to EUS FNA are limited. Before performing EUS FNA, the endosonographer must be certain that there is a reasonable chance that tissue sampling will be clinically useful.

As a general rule, FNA should be avoided in patients with significant coagulopathy (international normalized ratio [INR] >1.5, platelets <100,000, recent use of thienopyridines [e.g., clopidogrel], etc.).<sup>2</sup> However, the use of aspirin or nonsteroidal anti-inflammatory drugs (NSAIDs) is not a problem. Patients receiving anticoagulant therapy such as warfarin or novel oral anticoagulants (NOACs) such as dabigatran should discontinue their medication prior to the procedure (3 to 5 days for warfarin, 48 hours for NOACs). If the patient is at high risk for thromboembolic events, bridge therapy with low molecular weight heparin should be considered. Patients receiving antiplatelet therapy such as clopidogrel should also withhold them for 7 to 10 days prior to the procedure if they carry a low thromboembolic risk.

**TABLE 20.1** Common Sites for Performing Endoscopic Ultrasonography-Fine-Needle Aspiration

Pancreas
Bile duct
Digestive wall lesions <sup>a</sup>
Suspicious wall thickening
Subepithelial lesions
Adrenal glands
Liver
Retroperitoneal masses
Lymph nodes
Posterior mediastinum
Suspicious lymph nodes
Pulmonary masses <sup>b</sup>

<sup>a</sup>Digestive wall lesions include the esophagus, stomach, duodenum, and rectum.

<sup>b</sup>Pulmonary masses must abut the posterior mediastinum to be visualized under endoscopic ultrasonography.

**TABLE 20.2** Contraindications for Performing Endoscopic Ultrasonography-Fine-Needle Aspiration

Contraindication for endoscopic examination
Cardiac or respiratory instability
Suspected perforated viscus
Nonfasting patient or undecompressed upper GI obstruction
Coagulation disorder
Anticoagulants
Antiplatelet therapy <sup>a</sup>
Inaccessible lesion
Lesion not visualized
Large vessel or duct interposition
Metastatic lesion with primary mass interposition
EUS FNA results will not alter subsequent management

<sup>a</sup>Aspirin or nonsteroidal anti-inflammatory drug use are not contraindicated.

EUS FNA, Endoscopic ultrasonography-fine-needle aspiration; GI, gastrointestinal.

Some high-risk patients may not safely discontinue their treatment. In these situations, where the risk of stopping anticoagulation is potentially greater than the risk of FNA-induced bleeding (e.g., FNA of a large mediastinal node in a patient anticoagulated for massive pulmonary embolus), it may be reasonable to attempt EUS FNA without stopping anticoagulants, while using a small-gauge (25-G) needle and minimizing the number of passes (e.g., with onsite cytology).

Finally, certain anatomical challenges may also contraindicate EUS FNA, such as a large vessel or duct interposing itself between the targeted lesion and the ultrasound probe. Lymph nodes may not be accessible if the primary mass is preventing direct node sampling, carrying the risk of false-positive results. Table 20.2 provides an overview to EUS FNA contraindications.

## Steps for Endoscopic Ultrasonography-Fine-Needle Aspiration

1. Verify the indication.
2. Localize the lesion and position the echoendoscope.
3. Choose the correct needle.
4. Insert the EUS FNA needle into the echoendoscope.
5. Position the lesion in the needle path.

6. Puncture the lesion and move the needle within the lesion.
7. Withdraw the needle and process the aspirate.
8. Prepare the needle for subsequent passes.
9. Evolving trends in EUS FNA:
  - a. Use of the stylet
  - b. Use of suction
  - c. Sampling techniques
10. FNA particularities according to site:
  - a. Esophagus
  - b. Stomach
  - c. Duodenal bulb
  - d. Duodenal sweep (D2)

### Verify the Indication

Before performing EUS FNA, the indication should be clear and the endoscopy suite and team adequately prepared. Like any test, EUS FNA does not need to “change management” to be useful. However, before considering EUS FNA in a given patient, it should be clear that the information obtained has a reasonable chance of being clinically useful (to those managing the patient and/or to the patient). If the endosonographer is not in charge of the patient’s management, his or her opinion as to the value of the information need not affect the decision to perform EUS FNA, unless there is compelling evidence that the risks of the procedure will likely far outweigh the possible benefits. If there is any doubt, these issues should be addressed with the referring physician before the procedure (or even *during* the procedure) if necessary.

EUS FNA should be avoided if it will clearly not influence management or treatment, if there is a risk of tumor seeding that could worsen clinical outcomes, or if there is an excessive risk of puncture-related complications (e.g., bleeding, infection, trauma to surrounding structures).

When faced with the possibility of performing FNA on multiple sites, one should focus on the lesion likely to provide the most relevant information first. For instance, in the setting of a pancreatic head mass with suspicious liver nodules, FNA of the liver lesions may provide a positive cytological diagnosis and confirm that the patient is not a surgical candidate.

### Localize the Lesion and Position the Echoendoscope

Whenever possible, the echoendoscope should be straight. This makes needle movement easier, and reduces the risks of damage to the accessory channel during insertion of the needle into the scope.

In our experience, most pancreatic lesions (including pancreatic head/uncinate lesion) can also be sampled with the scope in a straight position. To do so, the scope should be passed into the second duodenum and then withdrawn into a “short” position. By withdrawing the scope toward the duodenal bulb, most pancreatic head lesions can be accessed and punctured. However, when withdrawn too far, this position will become unstable and the scope will slip into the stomach. Lesions near the pancreatic genu are often difficult to biopsy with this withdrawal technique, because they often become visible just at the moment that the position becomes unstable.

For these lesions (and any other lesions that cannot be accessed with the scope in a straight position), it is necessary to assume a “long” position, with the scope in the bulb or prepyloric region. This position will also provide a mechanical advantage when trying to puncture indurated lesions in the pancreatic head region.

**TABLE 20.3** Randomized Trials Comparing 22 Versus 25 Needle Gauges in Pancreatic and Nonpancreatic Lesions

Author, Year	No. Patients	Lesion	Accuracy % (22 G)	Accuracy % (25 G)
Siddiqui UD, 2009	131	Pancreatic	88	96
Camellini L, 2011	127	All	78	78
Fabbri C, 2011	50	Pancreatic	86	94
Lee JK, 2013	188	Pancreatic	89	88
Vilmann P, 2013	135	All	89	90
Carrara S, 2016	144	All	68	81

### Choose the Correct Needle

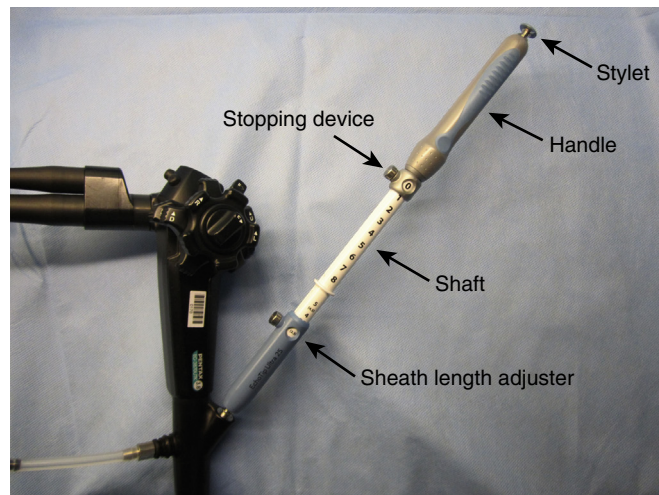
At the time of this writing, there are three needle sizes available for EUS FNA that can be used to obtain material for cytology: 19 G, 22 G, and 25 G. These needle sizes are also available in models featuring a beveled side-hole near the tip, or multiple prongs, which may help collect more material into the needle.<sup>3,4</sup>

There is increasing evidence that smaller needles offer at least similar results in diagnostic yield compared with larger needles, while at the same time being easier to manipulate.<sup>5–10</sup> Large-diameter needles tend to be harder to maneuver (particularly the 19-G needle), are more traumatic, and may provide bloodier samples—which may actually reduce their effectiveness when compared with smaller diameter needles. Traditionally, 22-G needles were used for solid lesions, mainly because it was the first size that was commercially available. However, 25-G needles eventually came to market, and some hypothesized that a 25-G needle would be better (easier to penetrate hard lesions and more maneuverable, providing less bloody aspirates)—particularly for challenging pancreatic head lesions.<sup>9,11–14</sup>

The first retrospective comparisons of the 22-G and 25-G needles showed the 25-G needle to be more sensitive for cancer in pancreatic masses,<sup>11,12</sup> but subsequent, prospective studies failed to show statistically significant advantages.<sup>9,13</sup> However, a recent meta-analysis showed that, for pancreatic masses, the sensitivity of the 22-G needle is clearly inferior to that of the 25-G needle (85% [95% confidence interval (CI): 82 to 88%] vs. 93% [95% CI: 91% to 96%],  $P = .0003$ ).<sup>10</sup> Given that the 25-G needle is more flexible, and hence easier to manipulate, it appears reasonable to favor the 25-G needle for all cases of solid lesion EUS-guided FNA when the objective is to obtain material for cytology. Table 20.3 summarizes the available data from randomized trials comparing needle sizes.

### Insert the Endoscopic Ultrasonography-Fine-Needle Aspiration Needle Into the Echoendoscope

Whether or not the needle system is inserted into the biopsy channel before or after the echoendoscope is in position for FNA is a matter of personal preference. However, it should be noted that once the echoendoscope is in position, it might be difficult or impossible to pass the needle system completely into position if the echoendoscope is not sufficiently straight. In this situation,



• Fig. 20.1 The needle system is firmly Luer locked to the operating channel of the echoendoscope.

the sheath may become stuck in the bending portion of the instrument near the tip. One should *never* use excessive force to push the sheath past an excessive bend at this location, because the needle sheath may perforate the inner sheath of the biopsy channel. Instead, the echoendoscope should be withdrawn into a straight configuration before attempting to reinsert the needle system completely.

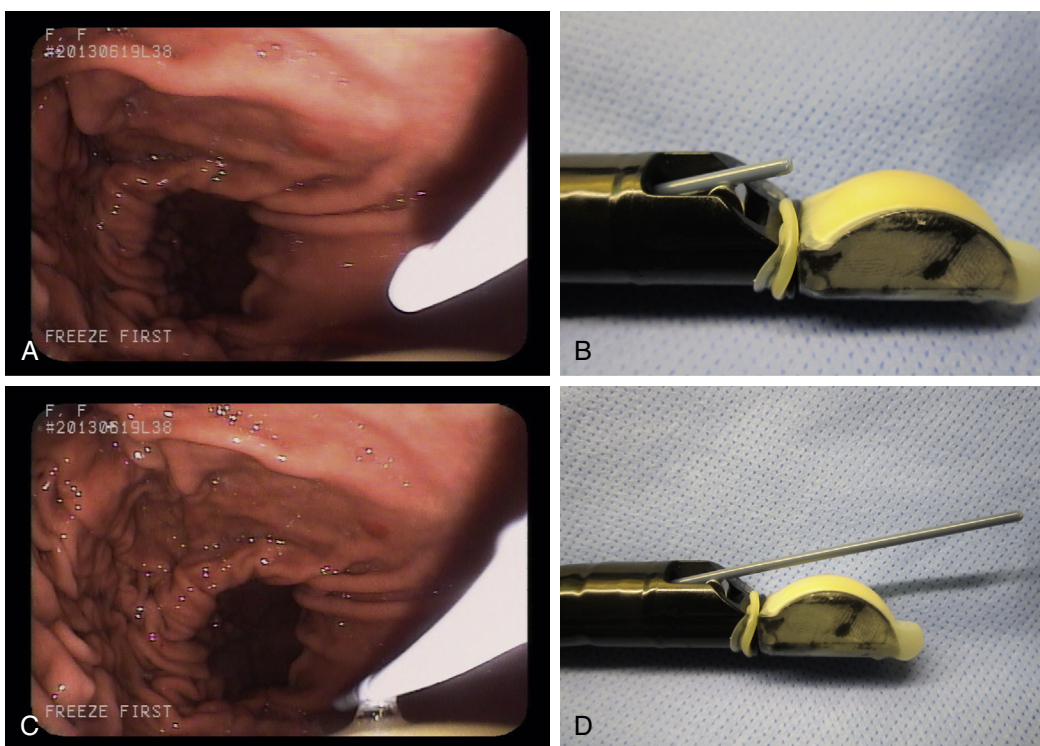
For lesions to be accessed from the second duodenum, the needle should be inserted into the scope only *after* the scope has been placed into the second duodenum. In other words, the duodenal sweep should not be negotiated with the needle and/or sheath protruding from the biopsy channel, because there is a risk of duodenal laceration during this maneuver. The scope should be positioned in a “short scope” fashion prior to attempting needle insertion.

The rubber cap covering the operating channel must be removed prior to inserting the needle system. Once the needle is fully inserted into the echoendoscope, the base of the needle should be Luer locked to the operating channel (Fig. 20.1).

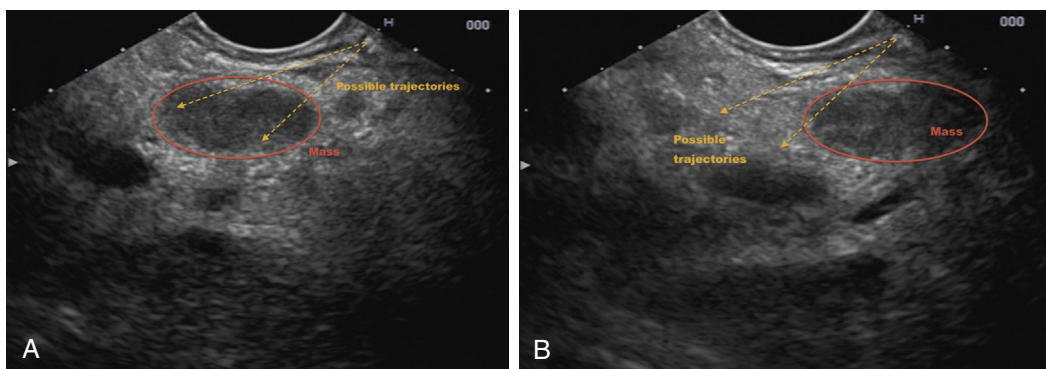
In some cases, a lesion that is clearly visible before the needle deployment may become difficult to see once the needle assembly is in place. The needle/sheath may produce artifact or may slightly reduce complete coupling between the ultrasound probe and the gut wall, producing air artifact. Slight repositioning of the echoendoscope, application of suction, or reinsertion of the needle assembly may help correct the problem.

### Position the Lesion in the Needle Path

Optimal positioning of the echoendoscope with respect to the lesion should make EUS FNA easier, safer, and more effective. The needle sheath should be adjusted so that it protrudes just beyond the elevator. Most commercially available needles are manufactured with a sheath length adjuster. This device is located near the bottom of the needle shaft and allows the endosonographer to determine the proper length of sheath to exit the echoendoscope into the gut lumen (see Fig. 20.1). In order to minimize ultrasound artifacts caused by the shaft and to maximize elevator deflection capabilities, the needle sheath should be kept at a short distance from the operating channel exit. However, to avoid traumatizing the inner lining of the operating channel during needle



• Fig. 20.2 Adjusting needle sheath length. (A and B) Correct distance. (C and D) Excessively long distance.



• Fig. 20.3 Correct positioning of a perigastric lymph node prior to fine-needle aspiration. (A) The lesion is within the natural path of the needle and elevator path. (B) Incorrect positioning.

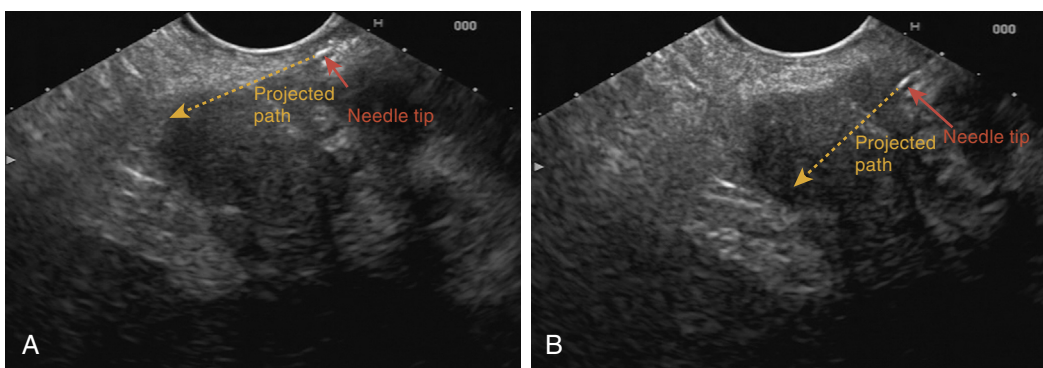
deployment, one must be certain that the needle sheath terminates outside the operating channel (Fig. 20.2).

After needle sheath adjustment is performed, the screw must be tightly wound to avoid inadvertently advancing the sheath during needle thrusting, which could result in gut wall trauma. Needle sheath adjustment is usually performed when the needle is first used, and rarely requires further manipulation during the subsequent passes.

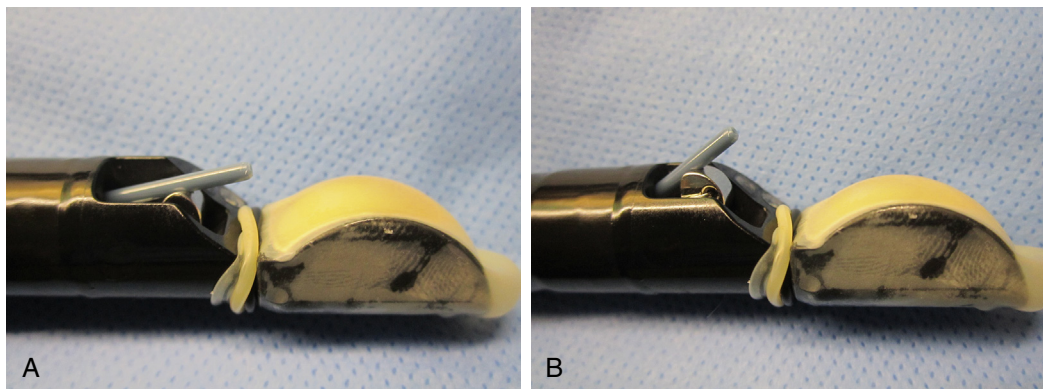
Once the lesion is identified, it should be positioned as much as possible within the natural path of the needle (i.e., the path taken by the needle when no elevator is applied; Fig. 20.3). This varies depending on the instrument used. If this is not possible, it should be positioned within the range of deflection offered by the elevator (Fig. 20.4). The elevator can be used to *increase* the angle formed between the echoendoscope shaft and the needle. It cannot *reduce* this angle (Fig. 20.5). Once adequate elevator adjustment is attained, it is best to lock the

up-down control, so that the thumb can then be used to move the elevator, if needed.

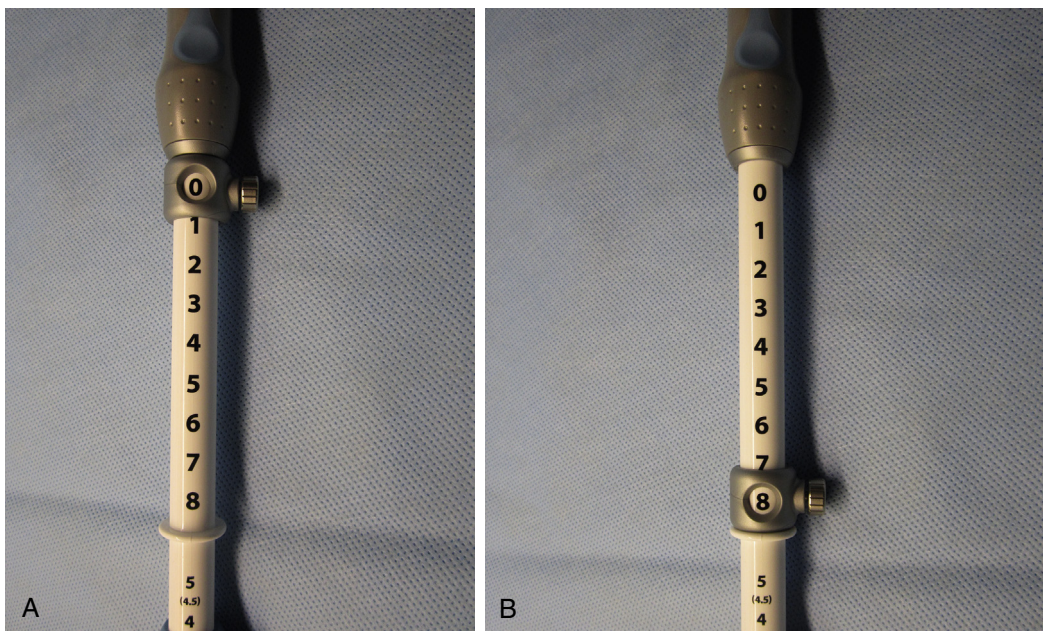
A stopping device locks the needle inside the sheath, avoiding accidental injury or scope trauma during manipulation and insertion of the needle into the echoendoscope. Prior to puncturing the lesion, the stopping device must be unscrewed to allow needle deployment. The stopping device can be set so as to limit the maximum distance that the needle can travel (Fig. 20.6). This can be helpful in situations where inserting the needle beyond the limits of the target lesion would be dangerous (e.g., the target lies directly over a vascular structure). To ensure maximum control, the fixed component of the needle handle should be grasped between the palm and the last two or three fingers of the right hand. The movable portion should be held between the thumb and index finger. This allows fine or vigorous needle movements to be performed, but with control. Any method that does not allow such control should be avoided (Fig. 20.7).



• **Fig. 20.4** Using the elevator to provide adequate needle trajectory. (A) The needle is in its natural state with the elevator in neutral position, resulting in inadequate positioning. (B) Elevator use deflects the needle trajectory into a correct path.



• **Fig. 20.5** Elevator range of movement. (A) No elevator use. (B) Maximal deflection of elevator.

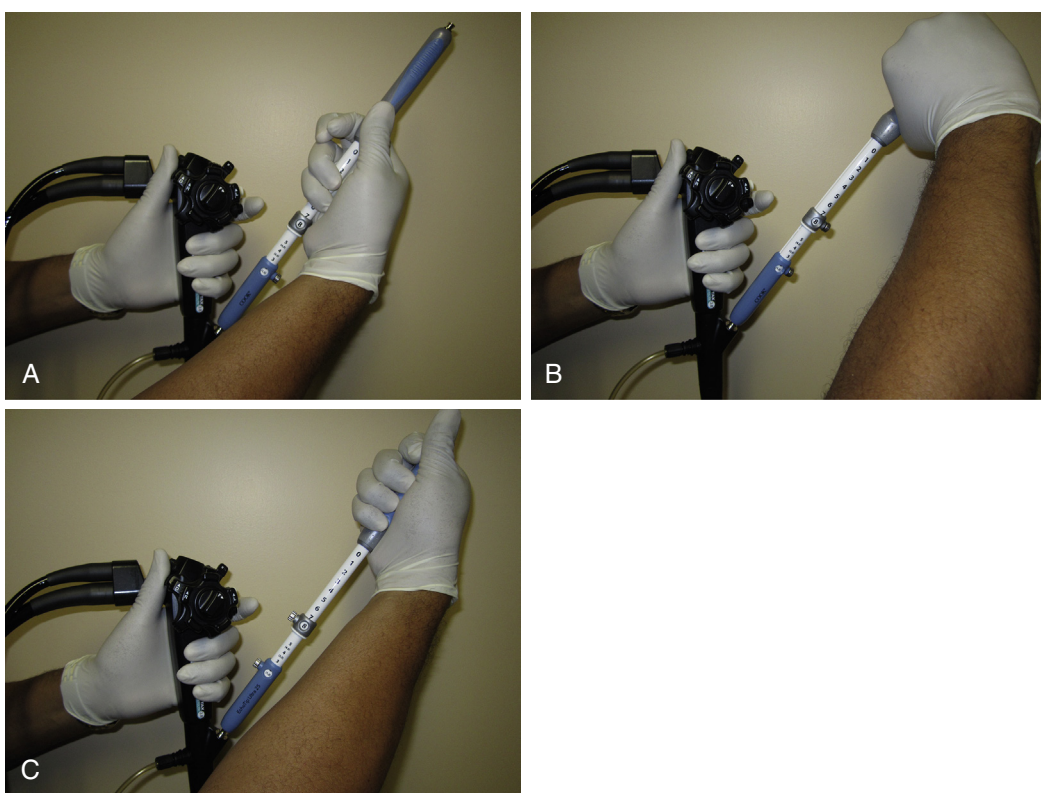


• **Fig. 20.6** Stopper adjustment. (A) Stopper on. (B) Stopper off.

As discussed earlier, movement of the FNA needle is easier if it is straight. Any bend in the needle induced by excessively tipping up and/or torquing the echoendoscope, or by applying pressure with the elevator will increase resistance during needle deployment, and may cause the needle to bend in an axis that will

make it disappear from the ultrasound field of view. This situation is encountered most often when the EUS probe is placed in the duodenal bulb or the second duodenum.

In order to minimize risks of puncturing other vital structures, one should try to limit the distance the needle must travel to reach



• **Fig. 20.7** Holding the needle. (A) Correct positioning. (B) Incorrect method. (C) Another incorrect method.

the target. Undrained, obstructed ducts should not be punctured because this may provoke cholangitis or pancreatitis.

Should a structure such as a bile duct or blood vessel be punctured, it is logical to assume that the risk of leakage is lower if the needle enters perpendicular to the vessel/duct as opposed to passing tangentially and causing a linear laceration. Therefore contact with all vessels should be avoided, but particularly when passing the needle laterally to a vessel. Scanning the FNA path with power Doppler prior to needle insertion is a good way to exclude any unsuspected significant blood vessels in the targeted path.

### Puncture the Lesion and Move the Needle Within the Lesion

Once the needle assembly and lesion are in adequate position, tissue sampling may begin. The needle should always be seen under real-time ultrasound guidance during tissue sampling to avoid traumatizing other structures. The goal is to insert the needle into the lesion, making repetitive back-and-forth thrusting movements into the lesion to shear off cells and collect them within the needle lumen. This requires that the needle be kept in the ultrasound-imaging plane and that thrusting movements be deliberate, always keeping an eye on the distal tip of the needle. Care should be taken to ensure that the needle does not exit the confines of the lesion during sampling. This will avoid contamination of the specimen with unwanted surrounding tissues.

Once the lesion is ready for puncture, sweeping the projected needle path with power Doppler to detect blood vessels can be performed. Before beginning to advance the needle, firm upward tip deflection should be applied using the up/down dial. This tends to bring the lesion closer to the echoendoscope and to reduce the

tendency of the needle to push the ultrasound probe away from the gut wall, which can reduce the ultrasound image quality by allowing air to seep in between the probe and the gut wall. It also provides a mechanical advantage when trying to puncture an indurated lesion. Firm upward tip deflection also increases tension on the gut wall, thereby facilitating the puncture of mobile and thick walls such as the stomach body.

The needle should first be advanced approximately 1 cm out of the sheath, just enough to localize the tip in the ultrasound field. Once the tip has been identified, the elevator can be used to adjust the needle trajectory if needed. The needle can then be advanced into the lesion under ultrasound guidance.

If, for some reason, the needle tip can no longer be seen once the lesion has been punctured, all forward movement of the needle should be stopped. *Continuing to advance the needle in the hope that the tip will become visible is a mistake and can result in inadvertent puncture of structures deep or lateral to the target lesion.* Instead, the first reflex should be to slowly withdraw the needle. This will help localize the tip without risking puncture of deep structures. If this is ineffective, slow left and right movement of the shoulders can help bring the needle into the ultrasound imaging plane.

If both these techniques fail, the needle should be withdrawn completely from the lesion into the sheath. If it is possible that the scope position could have caused the needle to be bent, the needle assembly should be removed from the echoendoscope and the needle straightened as needed (discussed later). The puncture can then be attempted again. This situation may be frequently encountered when the scope is torqued, especially in the duodenal bulb or sweep.

Once the needle is in the lesion and the tip clearly seen, the needle is moved back and forth several times within the lesion, with

adequate force to produce cell shearing. Should needle thrusting reduce visibility by separating the transducer from the gut wall, slight forward pressure applied to the echoendoscope shaft will push the probe back against the wall. Constant gut lumen suctioning with the echoendoscope during needle deployment can also reduce any air seepage risk between the probe and gut wall.

If the elevator deflection tip was used to adjust the needle angle, it may be helpful to return the elevator to the relaxed position once the needle is inside the lesion. This will allow the needle to move more freely.

### Withdraw the Needle and Process the Aspirate

After completing a pass, the needle should be completely withdrawn into the sheath. The locking device should be returned to its original upmost position and secured with the screw. In order to confirm complete needle withdrawal, the "0" numeral should be clearly seen within the locking device (see Fig. 20.6A).

To avoid clotting in the needle, the aspirate should be expressed from the needle as quickly as possible. We expel all samples onto a glass slide using a 10-cc air-filled syringe. The sample is then smeared using a second slide. This produces two slides per pass. If a cell block is required, a different sample is expelled with an air-filled syringe into a receptacle containing 20 cc of 50% alcohol.

If the needle is blocked, the aspirate can be forced out by inserting the stylet. Once the clot has been expressed onto a slide or container, the syringe should be used to express any remaining material from the needle.

### Prepare the Needle for Subsequent Passes

The same needle can be used for several passes and need not be changed unless it malfunctions or the needle tip becomes too dull. If previous aspirates were bloody, it may be helpful to rinse the lumen with normal saline before the next pass.

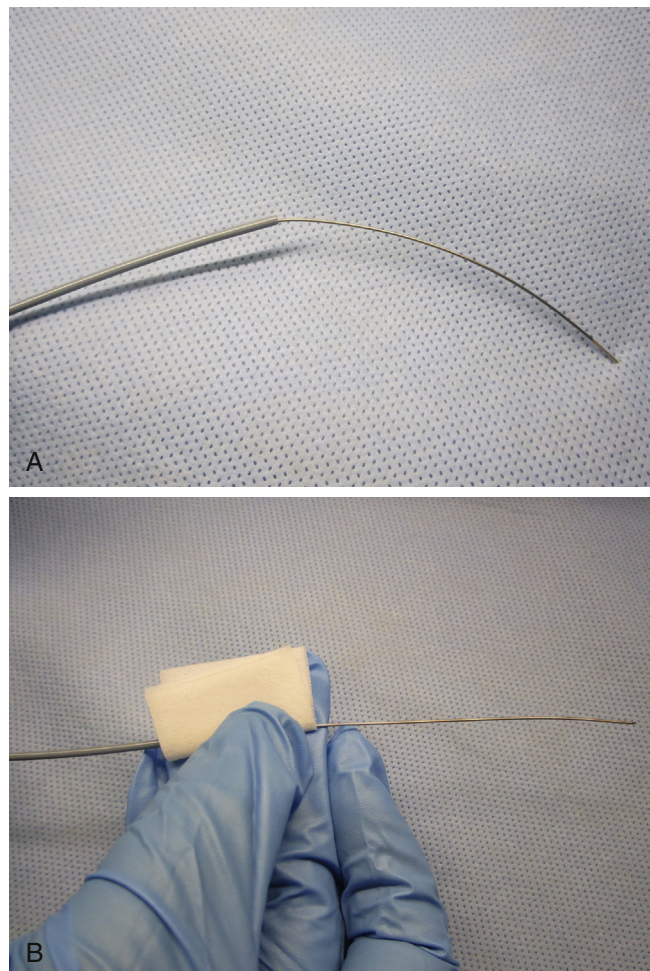
If the needle is bent, it must be straightened; otherwise it will deflect out of the ultrasound beam on subsequent passes. To straighten the needle, push it completely out of the sheath; then use your fingers to straighten it manually (Fig. 20.8). An alcohol swab can then be used to clean the outer surface of the needle.

If a cytologist is available, passes should be performed until adequate material or a diagnosis is obtained. If not, the available data suggest that approximately 3 to 5 passes should be sufficient to obtain a diagnosis (if cancer is indeed present).<sup>15–19</sup> There is no absolute limit to the number of passes that can be performed with the same needle. However, it should be changed if it malfunctions, becomes too difficult to reinsert the stylet and so on.

## Evolving Trends in Endoscopic Ultrasonography-Fine-Needle Aspiration

### Use of the Stylet

All commercially available EUS FNA systems include a removable stylet. It was believed that the stylet helped prevent clogging of the needle by gut wall tissue, which could limit the ability to aspirate cells from the target lesion. This is a logical assumption, but there are no data clearly demonstrating that the use of a stylet increases the yield of EUS FNA. Manipulation of the stylet increases the time and energy required to perform EUS FNA, increases the risks of needle stick injury, and likely increases the costs of EUS FNA needle systems. In some circumstances, the stylet may actually make EUS FNA impossible. For example, it



• **Fig. 20.8** Straightening the needle. (A) Bent needle. (B) Straightening the needle.

may be impossible to advance or to remove the stylet once the target has been punctured. This tends to occur only if the echoendoscope is bent (particularly when sampling from the bulb or duodenal sweep) and a large (19-G) needle is being used.

There are now five randomized published trials,<sup>20–24</sup> and several retrospective series<sup>25,26</sup> comparing the results of EUS FNA with and without the stylet. These studies are universally in agreement—the stylet does not increase the yield of EUS FNA.<sup>27</sup> Some studies also showed that stylet use is correlated with a significant increase in sample bloodiness.<sup>21,22</sup> Table 20.4 summarizes the results of the randomized trials comparing the results of EUS-FNA with and without the stylet.

EUS FNA without the stylet is also technically much simpler and faster, because the stylet withdrawal and reinsertion maneuvers are eliminated. Therefore it is currently recommended to *not* use the stylet for EUS FNA. However, the stylet may be used to unblock the needle during expulsion of the aspirate if needed. The stylet may also be useful in certain select indications, such as preventing a mucosal plug when aspirating cyst fluid, or delivering fiducial markers in solid lesions.

### Use of Suction

There is emerging evidence concerning the use of suction to obtain adequate material. Although some experts recommend the use of suction, others state that it may actually hinder adequate cytological analysis by causing aspirates to become

**TABLE 20.4** Randomized Trials Comparing Endoscopic Ultrasonography-Fine-Needle Aspiration With and Without the Stylet

Author, Year	No. Patients	Sample Adequacy (Stylet vs. No Stylet)	Bloodiness (Stylet vs. No Stylet)
Sahai AV, 2010	111	75% vs. 87%	75% vs. 52% <sup>a</sup>
Rastogi A, 2011	101	57% vs. 62%	50% vs. 59% <sup>a</sup>
Wani S, 2012	100	79% vs. 77%	54% vs. 56%
Nijhawan S, 2014	115	89% vs. 89%	66% vs. 69%
Abe Y, 2015	107	55% vs. 56%	P = ns

<sup>a</sup>P < .05

ns, Nonsignificant.

**TABLE 20.5** Randomized Trials Comparing Endoscopic Ultrasonography-Fine-Needle Aspiration With and Without Suction

Author, Year	No. Patients	Lesion Site	Diagnostic Yield % (Suction vs. No Suction)	Bloodiness % (Suction vs. No Suction)
Wallace MB, 2001	43	Lymph node	ns	No suction better <sup>a</sup>
Puri R, 2009	52	All	86% vs. 67% <sup>a</sup>	77% vs. 86%
Lee JK, 2013	81	Pancreatic masses	73% vs. 59% <sup>a</sup>	No suction better <sup>a</sup>

<sup>a</sup>P < .05

ns, Nonsignificant.

diluted with blood. To our knowledge, there are three published randomized trials evaluating suction use when performing FNA of lymph nodes and pancreatic masses (Table 20.5).<sup>17,28,29</sup> These studies showed that applying suction while sampling solid pancreatic lesions produces significantly better specimens. However, the use of suction when sampling lymph nodes does not increase sensitivity, and produces bloodier passes. Therefore for pancreatic lesions, endosonographers may consider applying 5 to 10 cc of suction for a few seconds for all passes or applying continuous suction for the second pass, if the first pass (performed with no suction) appears to have produced insufficient material. Current European Society of Gastrointestinal Endoscopy (ESGE) technical guidelines recommend the application of continuous suction for EUS FNA of solid masses, but no suction for lymph nodes.<sup>30</sup>

Traditionally, suction is applied with an empty syringe. More recently, methods involving application of suction using slow withdrawal of the stylet (“slow-pull” or “capillary” technique) or a water-filled syringe (“wet” technique) have gained some notoriety.

**Capillary (“Slow-Pull”) Technique.** This technique involves slowly removing the stylet after puncturing a lesion, with back-and-forth movement of the needle inside the lesion during stylet

withdrawal (Video 20.1). There is conflicting evidence that this may improve cytological diagnosis<sup>31–33</sup> or whether it actually provides any actual suction,<sup>34</sup> and there are currently no randomized trials evaluating this technique to FNA with no suction. Moreover, this technique requires that the lesion be punctured with the stylet in the needle, which is more cumbersome than using no stylet.

**Wet Technique.** This technique consists of removing the stylet and flushing the needle with saline prior to sampling the lesion. A syringe with residual saline is Luer locked on the proximal part on the needle device. Maximal suction is applied once the needle is passed into the lesion and during the whole FNA sequence (Video 20.2). The specimen is then expressed by flushing the material with the stylet or a syringe.<sup>35,36</sup>

A recent randomized-controlled trial using a 22-G needle comparing standard air-dry specimen expression versus wet technique showed significantly better specimen cell-block adequacy (86% vs. 75%, P < .035).<sup>35</sup> Further studies are needed to better evaluate this technique.

## Sampling Techniques

**Sampling Different Areas of the Same Lesion: “Fanning” or “Multiple Pass” Techniques.** In order to gather as much material as possible, several areas within the lesion should be sampled before processing it on the slide.<sup>37</sup>

To sample different areas of the same lesion during the same pass, a “fanning” technique may be possible if the lesion is sufficiently soft (Video 20.3). Fanning is obtained by manipulation of the elevator and/or up/down tip deflection to guide the needle into different regions of the target lesion or to orient the needle into the long axis of an oval or oblong lesion—without withdrawing the needle from the lesion.<sup>38</sup>

However, if the lesion is too hard, adequate fanning may be impossible. In this case, the “multiple pass” technique may be used (Video 20.4). This involves sampling widely through the lesion many times, before removing the needle from the scope. The needle is moved through the entire diameter of the lesion for 5 to 10 strokes; the needle is withdrawn from the lesion (but not from the intestinal wall if possible) and moved to a different region of the lesion. Approximately five regions per lesion are sampled before processing the sample. The multipass technique differs from the “fanning” technique in that the latter involves trying to sample different regions without removing the needle completely from the lesion (Fig. 20.9).<sup>39</sup>

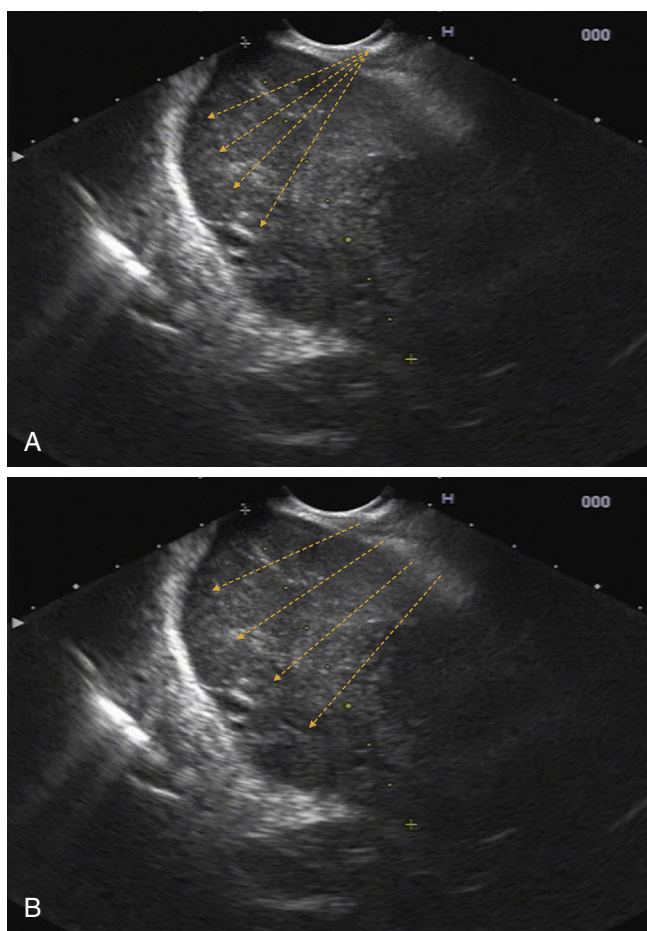
Some authors favor a “door knocking” movement. The stopper is set at an appropriate distance, and then the handle is moved rapidly back and forth so that it “knocks” on the stopper. There is however no evidence that this technique improves results.<sup>40</sup>

## Fine-Needle Aspiration Particularities According to Site

The site in the gut from which EUS FNA is performed may make the technique easier or more difficult. The following describes common pitfalls and solutions based on EUS FNA site.

### Esophagus

This region is commonly the easiest area from which to perform EUS FNA. Most lesions accessed through this site are mediastinal lymph nodes or masses. The echoendoscope is virtually always in a straight position, and the tubular anatomy of the esophagus will naturally prevent the scope from bending.



• **Fig. 20.9** Fine-needle aspiration sampling of multiple sites. (A) The fanning technique. (B) The multiple-pass technique.

## Stomach

The stomach probably has the thickest wall of all the sites from which EUS FNA is commonly performed. It is also very compliant, meaning that it will tend to recoil during needle advancement. This can make traversing the gastric wall difficult and targeting perigastric lesions problematic, particularly if they are small and/or mobile (e.g., gastro-hepatic ligament lymph nodes). If this problem arises, it may be helpful to divide the EUS FNA maneuver into two stages. First, focus on traversing the gastric wall. To facilitate wall puncture, collapse the stomach by sucking out the air. The wall will be more stable if the echoendoscope is withdrawn into position (from the antrum), rather than if it is pushed into position from the region of the gastroesophageal junction. A strong tip up maneuver will also help hold the echoendoscope close to the wall. Successful gastric puncture may require an unusually quick, strong, yet controlled jab. If present, the safety stopper on the needle may be used to prevent inadvertently advancing the needle too far. Once the needle has successfully been passed through the gastric wall into the perigastric space, focus on the second stage, which is puncturing the target lesion.

## Duodenal Bulb

When positioning the echoendoscope in the duodenal bulb, it naturally assumes a “long-scope” position. Although this position may offer a mechanical advantage to more forcefully puncture

an indurated lesion, the bending in the scope may render needle insertion into the scope difficult. To avoid this situation, insert the needle into the scope while it is still in the stomach antrum. Once the needle is loaded in the scope, intubate the pylorus and reposition yourself in the bulb.

Accessing hilar lesions from the bulb usually requires a large amount of counterclockwise torquing. When excessive torquing is applied, this will create a bend in the needle. As you deploy the needle out of the sheath, it may deflect out of the ultrasound plane and may not be visible. Removing the needle from the scope and correcting any bend should be attempted at this point. If the problem recurs, deploy the needle a few millimeters out of the sheath into the gut lumen when facing the lesion. Gently rotating *counterclockwise* will usually make the needle tip appear. After realizing how much left rotation was needed to identify the needle, withdraw the needle back into its sheath. Reposition yourself at the level of the lesion. Rotate away from the lesion by torquing *clockwise*. Deploy the needle for a few millimeters and counterrotate *counterclockwise*. If a sufficient amount of “extra” rotation was applied, the needle should be in front of the lesion. Remember that, ideally, the needle should be visualized at *all times* during FNA. It should also be remembered that it may be easier to access hilar lesions from the stomach, because the echoendoscope will be in a straight configuration, and little torque is needed.

## Duodenal Sweep (D2)

Similar difficulties can be encountered when performing FNA from the duodenal sweep. Needle scope insertion can be problematic. To avoid this, withdraw the scope completely into a “short-scope” position while remaining in the sweep. This should remove any bend in the scope and make initial needle insertion easy. One may still encounter some resistance a few centimeters before being able to Luer lock the needle. At this point, remove any locks applied to the dials of the echoendoscope and generate a large amount of tip deflection down using the up/down dial. This should remove any resistance to scope needle insertion. Once properly Luer locked to the scope shaft, you can reposition yourself as wanted into the duodenal sweep. The authors find that this technique can enable needle insertion of any caliber, including the 19-G needle in most situations.

Needle bending can also occur in this location based on the amount of torquing needed to visualize the lesion. The same technique described for duodenal bulb lesions can be applied.

## Special Issues

### Sampling of Multiple Lesions

When there are several potential biopsy sites or lesions in an individual patient (e.g., pancreatic mass, celiac node, liver lesion, mediastinal node), sampling should be performed starting with the lesion that, if positive, will confirm the most advanced stage. If the first lesion is negative, the lesion offering the next highest stage should be sampled. If a metastatic lesion is confirmed, the primary lesion need not necessarily be biopsied, unless there is a compelling reason to do so. If the previously noted sequence of biopsy sites is employed (i.e., from distant lesions toward the primary lesion), then several lesions can be sampled using a single EUS FNA needle. If not, a new needle should be used for each lesion, to avoid the risk of creating false-positive results and/or seeding distant sites.

## Endoscopic Ultrasonography-Fine-Needle Aspiration of Cystic Lesions

Cystic lesions may be punctured for cyst fluid analysis, sampling of the cyst wall, and/or treatment. The primary concerns relate to the risk of infection and bleeding. Bleeding is alarming, but rarely serious, because it is usually contained by the cyst cavity. Infections, however, can lead to serious morbidity and mortality. Therefore perhaps more than with other lesions, cysts should not be punctured unless it is clear that the information obtained will likely be useful to someone. Prophylactic antibiotics are indicated prior to FNA of a cystic lesion.<sup>41</sup>

Unless there is clear evidence of a mass component, it is the authors' opinion that sampling of the wall is rarely productive and only increases the risk of bleeding. Likewise, cyst fluid cytology is almost always negative. Therefore for cysts *without* a significant mass component, the primary goal should be to aspirate sufficient fluid to perform tumor marker analysis. Conversely, if there is a significant mass component, it is reasonable to perform EUS FNA of the mass alone and avoid the risks of cyst puncture. Biochemistry laboratory personnel should be consulted to determine the minimum quantity of cyst fluid that will be required to perform the desired analyses.

For larger diameter lesions (>1 to 2 cm), the authors prefer using a 19-G needle instead of a smaller gauge needle, to allow for more rapid and complete cyst fluid aspiration (especially if the fluid is viscous). As indicated earlier, the use of the stylet is reasonable in this setting to avoid clogging the needle with a mucosal plug that will hinder aspiration. Once the needle is in the cyst cavity, the stylet can be withdrawn and suction may begin. Always use a *new* needle to puncture a cyst and, if possible, perform only one pass. If more than one pass is required, change to a new needle.

Many experts believe that the risk of infection is lower if the cyst is drained completely; so this is probably a reasonable goal. However, in the case of a multiloculated cyst, it may be safer to focus on draining only a single, superficial loculation—one that appears to contain sufficient fluid for marker analysis.

Once the cyst has been punctured, try to place the tip in the center of the cavity before aspirating. During aspiration and as the cyst collapses, the needle should be repositioned as needed to stay away from the wall or any debris that may clog the needle lumen. If the needle clogs before the cyst has collapsed completely, one may halt suction and try to reposition the needle gently, *without removing it from the cyst*. When the cyst is almost completely collapsed, drainage frequently stops and it often becomes difficult to locate the needle tip. Attempts to reposition the needle to get "every last drop" should be avoided, because this may lead to bleeding. Once adequate fluid has been obtained for analysis, the remaining fluid can be drained by repeatedly filling a syringe or by connecting the aspiration port of the needle to wall suction. After cyst drainage, the cyst should be observed for a short time to look for early recurrence or bleeding.

### Mobile Lesions

Lesions that are not fixed, such as retroperitoneal nodes, can be difficult to puncture because they tend to bounce off the needle tip. This may be compounded if the lesion is not directly adjacent to the gut wall, is small, or if there is excessive respiratory movement. To effectively puncture these lesions, it may be helpful

first to focus on traversing the gut wall with the needle. Once the needle tip is in the extraluminal space, one can then focus on puncturing the lesion.

To puncture the lesion, advance the needle tip so that it is abutting the lesion wall. Coordination with respiratory movement may be required. To enter the lesion, use a rapid single thrust to stab the lesion effectively. It may be necessary to actually pass the needle completely through the lesion. If this occurs, the lesion will be immobilized and the needle tip can then slowly be withdrawn until it is within the confines of the lesion.

### Indurated Lesions

Occasionally it may be difficult to penetrate a lesion because it is indurated. If a lesion is difficult to penetrate, one must first verify that the needle is functioning correctly. The needle tip may have become dull (e.g., due to multiple previous passes), or may not be exiting the sheath effectively.

If the needle is functioning properly, the lesion can be punctured by using more forceful stabbing maneuvers. However, this should be a last resort, because it is difficult to stab forcefully *and* to simultaneously control the depth of penetration. Instead, firm upward tip deflection should be applied, the needle tip should be placed against the leading edge of the lesion, and firm, progressively increasing pressure should be applied to the needle. If this fails, it may be helpful to apply force by actually advancing the echoendoscope (assuming that the echoendoscope is in a position that ensures that pressure can be applied in the same axis as the needle).

### Tumor Seeding

Although very rare, tumor seeding has been described with EUS FNA.<sup>42–48</sup> In the presence of a potentially resectable malignant lesion, EUS FNA should be reconsidered if the biopsy tract will not be included in the surgical specimen (e.g., FNA through the gastric wall in the case of a pancreatic body lesion). Instead, if at all possible, an attempt should be made to perform biopsies through a part of the gut wall that will be removed should the patient go to surgery (e.g., lesions of the pancreatic genu should be biopsied through the duodenum if possible).

To avoid seeding extraluminal sites, such as nodes, EUS FNA should never be performed through an area of the gut wall that is overtly or possibly infiltrated by malignancy or dysplasia.

### Conclusion

EUS FNA is a powerful clinical tool. It can be technically challenging, but often straightforward if the lesion can be located, is sufficiently large, and can be brought in to the needle path with the echoendoscope in a fairly straight position. Many additions to the basic EUS FNA technique have been described, but none appear to clearly improve the yield other than (1) moving the needle effectively, (2) sampling many different areas of the lesion, and (3) using a smaller (25-G) needle. The stylet should not be used, because all the data show that it does not improve results, but increases procedural complexity. Suction may provide a role in acquiring better pancreatic samples, but is not useful for softer lesions (e.g., lymph nodes). Quality comparative trials will be required before modifications to the basic FNA technique that have been described in this chapter can be recommended.

## Key References

10. Madhoun MF, Wani SB, Rastogi A, et al. The diagnostic accuracy of 22-gauge and 25-gauge needles in endoscopic ultrasound-guided fine needle aspiration of solid pancreatic lesions: a meta-analysis. *Endoscopy*. 2013;45:86–92.
27. Kim JH, Park SW, Kim MK, et al. Meta-analysis for cyto-pathological outcomes in endoscopic ultrasonography-guided fine-needle aspiration with and without the stylet. *Dig Dis Sci*. 2016;61(8):2175–2184.
28. Puri R, Vilman P, Säfoui A, et al. Randomized controlled trial of endoscopic ultrasound-guided fine-needle sampling with or without suction for better cytological diagnosis. *Scand J Gastroenterol*. 2009;44(4):499–504.
35. Attam R, Arain MA, Bloechl SJ, et al. “Wet suction technique (WEST)”: a novel way to enhance the quality of EUS-FNA aspirate. Results of a prospective, single-blind, randomized, controlled trial using a 22-gauge needle for EUS-FNA of solid lesions. *Gastrointest Endosc*. 2015;81(6):1401–1407.
38. Bang JY, Magee SH, Ramesh J, et al. Randomized trial comparing fanning with standard technique for endoscopic ultrasound-guided fine-needle aspiration of solid pancreatic mass lesions. *Endoscopy*. 2013;45(6):445–450.

## References

Access the reference list online at [ExpertConsult.com](http://ExpertConsult.com).

## References

1. Dumonceau JM, Polkowski M, Larghi A, et al. Indications, results, and clinical impact of endoscopic ultrasound (EUS)-guided sampling in gastroenterology: European Society of Gastrointestinal Endoscopy (ESGE) clinical guideline. *Endoscopy*. 2011;43:1–16.
2. ASGE Standards of Practice Committee Anderson MA, Ben-Menachem T, Gan SI, et al. Management of antithrombotic agents for endoscopic procedures. *Gastrointest Endosc*. 2009;70(6):1060–1070.
3. Sterlacci W, Sioulas AD, Veits L, et al. 22-gauge core vs 22-gauge aspiration needle for endoscopic ultrasound-guided sampling of abdominal masses. *World J Gastroenterol*. 2016;22(39):8820–8830.
4. Schulman AR, Thompson CC, Odze R, et al. Optimizing EUS-guided liver biopsy sampling: comprehensive assessment of needle types and tissue acquisition techniques. *Gastrointest Endosc*. 2017;85(2):419–426.
5. Lee JK, Lee KT, Choi ER, et al. A prospective, randomized trial comparing 25-gauge and 22-gauge needles for endoscopic ultrasound-guided fine needle aspiration of pancreatic masses. *Scand J Gastroenterol*. 2013;48(6):752–757.
6. Affolter KE, Schmidt RL, Matynia AP, et al. Needle size has only a limited effect on outcomes in EUS-guided fine needle aspiration: a systematic review and meta-analysis. *Dig Dis Sci*. 2013;58(4):1026–1034.
7. Camellini L, Carlinfante G, Azzolini F, et al. A randomized clinical trial comparing 22G and 25G needles in endoscopic ultrasound-guided fine-needle aspiration of solid lesions. *Endoscopy*. 2011;43:709–715.
8. Fabbri C, Polifemo AM, Luigiano C, et al. Endoscopic ultrasound-guided fine needle aspiration with 22- and 25-gauge needles in solid pancreatic masses: a prospective comparative study with randomisation of needle sequence. *Dig Liver Dis*. 2011;43:647–652.
9. Siddiqui UD, Rossi F, Rosenthal LS, et al. EUS-guided FNA of solid pancreatic masses: a prospective, randomized trial comparing 22-gauge and 25-gauge needles. *Gastrointest Endosc*. 2009;70:1093–1097.
10. Madhoun MF, Wani SB, Rastogi A, et al. The diagnostic accuracy of 22-gauge and 25-gauge needles in endoscopic ultrasound-guided fine needle aspiration of solid pancreatic lesions: a meta-analysis. *Endoscopy*. 2013;45:86–92.
11. Yusuf TE, Ho S, Pavay DA, et al. Retrospective analysis of the utility of endoscopic ultrasound-guided fine-needle aspiration (EUS-FNA) in pancreatic masses, using a 22-gauge or 25-gauge needle system: a multicenter experience. *Endoscopy*. 2009;41(5):445–448.
12. Nguyen TT, Lee CE, Whang CS, et al. A Comparison of the diagnostic yield and specimen adequacy between 22 and 25 gauge needles for Endoscopic Ultrasound Guided Fine-Needle Aspiration (EUS-FNA) of Solid Pancreatic Lesions (SPL): is bigger better? *Gastrointest Endosc*. 2008;67(5):AB100.
13. Lee JH, Stewart J, Ross WA, et al. Blinded prospective comparison of the performance of 22-gauge and 25-gauge needles in endoscopic ultrasound-guided fine needle aspiration of the pancreas and peri-pancreatic lesions. *Dig Dis Sci*. 2009;54(10):2274–2281.
14. Paquin SC, Gariepy G, Sahai AV. A prospective, randomized, controlled trial of EUS-FNA with and without a stylet: no stylet is better. *Gastrointest Endosc*. 2007;65(5):AB198.
15. Rong L, Kida M, Yamauchi H, et al. Factors affecting the diagnostic accuracy of endoscopic ultrasonography-guided fine-needle aspiration (EUS-FNA) for upper gastrointestinal submucosal or extraluminal solid mass lesions. *Dig Endosc*. 2012;24(5):358–363.
16. Suzuki R, Irisawa A, Bhutani MS, et al. Prospective evaluation of the optimal number of 25-gauge needle passes for endoscopic ultrasound-guided fine-needle aspiration biopsy of solid pancreatic lesions in the absence of an onsite cytopathologist. *Dig Endosc*. 2012;24(6):452–456.
17. Wallace MB, Kennedy T, Durkalski V, et al. Randomized controlled trial of EUS-guided fine needle aspiration techniques for the detection of malignant lymphadenopathy. *Gastrointest Endosc*. 2001;54(4):441–447.
18. LeBlanc JK, Ciaccia D, Al-Assi MT, et al. Optimal number of EUS-guided fine needle passes needed to obtain a correct diagnosis. *Gastrointest Endosc*. 2004;59(4):475–481.
19. Savides TJ. Tricks for improving EUS-FNA accuracy and maximizing cellular yield. *Gastrointest Endosc*. 2009;69(suppl 2):S130–S133.
20. Abe Y, Kawakami H, Oba K, et al. Effect of a stylet on a histological specimen in EUS-guided fine-needle tissue acquisition by using 22-gauge needles: a multicenter, prospective, randomized, controlled trial. *Gastrointest Endosc*. 2015;82:837–844.
21. Rastogi A, Wani S, Gupta N, et al. A prospective, single-blind, randomized, controlled trial of EUS-guided FNA with and without a stylet. *Gastrointest Endosc*. 2011;74:58–64.
22. Sahai AV, Paquin SC, Gariepy G. A prospective comparison of endoscopic ultrasound-guided fine needle aspiration results obtained in the same lesion, with and without the needle stylet. *Endoscopy*. 2010;42:900–903.
23. Nijhawan S, Singh B, Kumar A, et al. Randomized controlled trial of comparison of the adequacy, and diagnostic yield of endoscopic ultrasound guided fine needle aspiration with and without a stylet in Indian patients: a prospective single blind study. *J Dig Endosc*. 2014;5:149–153.
24. Wani S, Early D, Kunkel J, et al. Diagnostic yield of malignancy during EUS-guided FNA of solid lesions with and without a stylet: a prospective, single blind, randomized, controlled trial. *Gastrointest Endosc*. 2012;76(2):328–335.
25. Wani S, Gupta N, Gaddam S, et al. A comparative study of endoscopic ultrasound guided fine needle aspiration with and without a stylet. *Dig Dis Sci*. 2011;56:2409–2414.
26. Gimeno-Garcia AZ, Paquin SC, Gariepy G, et al. Comparison of endoscopic ultrasonography-guided fine-needle aspiration cytology results with and without the stylet in 3364 cases. *Dig Endosc*. 2013;25:303–307.
27. Kim JH, Park SW, Kim MK, et al. Meta-analysis for cytological outcomes in endoscopic ultrasonography-guided fine-needle aspiration with and without the stylet. *Dig Dis Sci*. 2016;61(8):2175–2184.
28. Puri R, Vilimann P, Säfstoia A, et al. Randomized controlled trial of endoscopic ultrasound-guided fine-needle sampling with or without suction for better cytological diagnosis. *Scand J Gastroenterol*. 2009;44(4):499–504.
29. Lee JK, Choi JH, Lee KH, et al. A prospective, comparative trial to optimize sampling techniques in EUS-guided FNA of solid pancreatic masses. *Gastrointest Endosc*. 2013;77(5):745–751.
30. Polkowski M, Larghi A, Weynand B, et al. Learning, techniques, and complications of endoscopic ultrasound (EUS)-guided sampling in gastroenterology: European Society of Gastrointestinal Endoscopy (ESGE) technical guideline. *Endoscopy*. 2012;44:190–206.
31. Kin T, Katanuma A, Yane K, et al. Diagnostic ability of EUS-FNA for pancreatic solid lesions with conventional 22-gauge needle using the slow pull technique: a prospective study. *Scand J Gastroenterol*. 2015;50(7):900–907.
32. Chen JY, Ding QY, Lv Y, et al. Slow-pull and different conventional suction techniques in endoscopic ultrasound-guided fine-needle aspiration of pancreatic solid lesions using 22-gauge needles. *World J Gastroenterol*. 2016;22(39):8790–8797.

33. Nakai Y, Isayama H, Chang KJ, et al. Slow pull versus suction in endoscopic ultrasound-guided fine-needle aspiration of pancreatic solid masses. *Dig Dis Sci.* 2014;59(7):1578–1585.
34. Katanuma A, Itoi T, Baron TH, et al. Bench-top testing of suction forces generated through endoscopic ultrasound-guided aspiration needles. *J Hepatobiliary Pancreat Sci.* 2015;22(5):379–385.
35. Attam R, Arain MA, Bloechl SJ, et al. “Wet suction technique (WEST)”: a novel way to enhance the quality of EUS-FNA aspirate. Results of a prospective, single-blind, randomized, controlled trial using a 22-gauge needle for EUS-FNA of solid lesions. *Gastrointest Endosc.* 2015;81(6):1401–1407.
36. Villa NA, Berzosa M, Wallace MB, et al. Endoscopic ultrasound-guided fine needle aspiration: the wet suction technique. *Endosc Ultrasound.* 2016;5(1):17–20.
37. Varadarajulu S, Fockens P, Hawes RH. Best practices in endoscopic ultrasound-guided fine-needle aspiration. *Clin Gastroenterol Hepatol.* 2012;10(7):697–703.
38. Bang JY, Magee SH, Ramesh J, et al. Randomized trial comparing fanning with standard technique for endoscopic ultrasound-guided fine-needle aspiration of solid pancreatic mass lesions. *Endoscopy.* 2013;45(6):445–450.
39. Wyse JM, Paquin SC, Joseph L, et al. EUS-FNA without the stylet: the yield is comparable to that with the stylet and sampling of multiple sites during the same pass may improve sample quality and yield. *Gastrointest Endosc.* 2009;69(5):AB330–AB331.
40. Mukai S, Itoi T, Ashida R, et al. Multicenter, prospective, cross-over trial comparing the door-knocking method with the conventional method for EUS-FNA of solid pancreatic masses (with videos). *Gastrointest Endosc.* 2016;83(6):1210–1217.
41. ASGE Guideline: Antibiotic Prophylaxis for GI Endoscopy. *Gastrointest Endosc.* 2008;67:791–798.
42. Hirooka Y, Goto H, Itoh A, et al. Case of intraductal papillary mucinous tumor in which endosonography-guided fine-needle aspiration biopsy caused dissemination [letter]. *J Gastroenterol Hepatol.* 2003;18:1323–1324.
43. Shah JN, Fraker D, Guerry D, et al. Melanoma seeding of an EUS-guided fine needle track. *Gastrointest Endosc.* 2004;59:923–924.
44. Paquin SC, Gariépy G, Lepanto L, et al. A first report of tumor seeding because of EUS-guided FNA of a pancreatic adenocarcinoma. *Gastrointest Endosc.* 2005;61(4):610–611.
45. Doi S, Yasuda I, Iwashita T, et al. Needle tract implantation on the esophageal wall after EUS-guided FNA of metastatic mediastinal lymphadenopathy. *Gastrointest Endosc.* 2008;67(6):988–990.
46. Chong A, Venugopal K, Segarajasingam D, et al. Tumor seeding after EUS-guided FNA of pancreatic tail neoplasia. *Gastrointest Endosc.* 2011;74(4):933–935.
47. Katanuma A, Maguchi H, Hashigo S, et al. Tumor seeding after endoscopic ultrasound-guided fine-needle aspiration of cancer in the body of the pancreas. *Endoscopy.* 2012;44 suppl 2 UCTN: E160–E161.
48. Tomonari A, Katanuma A, Matsumori T, et al. Resected tumor seeding in stomach wall due to endoscopic ultrasonography-guided fine needle aspiration of pancreatic adenocarcinoma. *World J Gastroenterol.* 2015;21(27):8458–8461.



**Video 20.1** Capillary Technique



**Video 20.3** Fanning Technique



**Video 20.2** Wet Suction Technique



**Video 20.4** Multiple Pass Technique

# Techniques for Endoscopic Ultrasound-Guided Fine-Needle Biopsy

MIHAI RIMBAŞ AND ALBERTO LARGHI

## KEY POINTS

- Although endoscopic ultrasound-guided fine-needle aspiration (EUS FNA) is very accurate, it cannot fully characterize certain neoplasms, and lack of cytology expertise may result in a limited perceived utility of endoscopic ultrasound.
- Standard 19-G and 22-G fine-needle aspiration needles with or without high negative pressure have proven to be reliable in obtaining high-quality histologic samples in various indications.
- The novel 19-G and 22-G ProCore needles have demonstrated a high yield in obtaining histologic samples, whereas 25-G ProCore seems unsuitable for histology.
- Data on the newly developed 20-G ProCore, SharkCore, and Acquire needles are limited, but appear very promising.
- In perspective, endoscopic ultrasound-guided fine-needle biopsy (EUS FNB) is expected to refine differential diagnostic capabilities, favor widespread EUS utilization, and pave the road to targeted therapies and monitoring of treatment response.

## Introduction

In the last decade, different techniques and specifically designed needles to acquire samples for histological evaluation have been developed.<sup>1</sup> These efforts have been made in an attempt to overcome some of the limitations of endoscopic ultrasound-guided fine-needle aspiration (EUS FNA)—in particular, the need for rapid on-site evaluation (ROSE) of the collected specimens to be able to reach a diagnostic accuracy greater than 90%.<sup>2–5</sup> However, the limited availability of ROSE throughout the world associated with the lack of cytology expertise outside high volume tertiary care centers<sup>6</sup> has resulted in a limited perceived utility of EUS and has created a barrier to the dissemination of the procedure in the community and in many countries.<sup>7</sup>

Recently in centers where ROSE is not available it has been recommended to perform EUS-guided fine-needle biopsy (EUS FNB) to acquire samples for histologic evaluation.<sup>8</sup> This should result in a greater chance to be accurate due to the easier interpretation by the pathologists, with the additional advantage of providing tissue samples to perform ancillary tests. The latter is particularly important in view of the increasing

interest in evaluating core tissue samples for molecular markers that may serve as prognostic predictors and targets for individualized chemotherapy in patients with cancer.<sup>9,10</sup> If this will occur, diagnostic EUS will be transformed into a more therapeutic procedure performed not only to provide a diagnosis, but also to offer the best possible therapy for each individual patient.<sup>11,12</sup>

A Tru-Cut biopsy needle dedicated for EUS-guided fine-needle biopsy (EUS FNB), the Quick-Core (Cook Medical, Bloomington, Indiana) needle, was developed but without meaningful advantages over EUS FNA.<sup>13–16</sup> Among the newly available needles specifically designed to perform FNB, the 25-G ProCore (Cook Medical) has been found to be able to gather tissue core samples in only about 40% of the cases.<sup>17,18</sup> Moreover, no overall clear advantages of the 22-G ProCore (Cook Medical) over standard 22-G FNA needles have been demonstrated.<sup>19</sup> Finally, very promising results have been initially reported for the 19-G ProCore, but these were not followed by additional experiences.<sup>20–21</sup> Many studies, on the other hand, have described a high accuracy of standard 19-G needles in acquiring tissue core biopsy samples for various indications.<sup>22–30</sup> The 19-G needle, however, is not easy to use from the duodenum and is in general avoided by nonexpert endosonographers because of the fear of complications. Based on these premises, other needles for EUS FNB have been developed, the 20-G ProCore (Cook Medical), the 22- and 25-G SharkCore (Medtronic PLC, Dublin, Ireland), and the 22- and 25-G Acquire (Boston Scientific Corp., Marlborough, Massachusetts). Preliminary data on these smaller needles for both pancreatic and nonpancreatic lesions are very encouraging.<sup>31–35</sup>

This chapter will review the EUS FNB techniques developed so far, their clinical results, their limitations, as well as their future perspectives.

## Endoscopic Ultrasound-Guided Tru-Cut Biopsy

The first needle specifically developed for EUS FNB is the Quick-Core (Cook Medical), a 19-G Tru-Cut biopsy needle that is capable of collecting an 18-mm-long tissue specimen sufficient for histologic examination.<sup>36</sup> This endoscopic ultrasound-guided Tru-Cut biopsy (EUS TCB) device has an outer catheter sheath,

an internal 19-G cutting sheath, an 18-mm-long specimen tray, a 5-mm-long stylet tip (Fig. 21.1), and a built-in spring-loaded mechanism that makes automated acquisition of biopsy specimens possible. However, various studies have proven that it has no meaningful advantages over EUS FNA<sup>13–16</sup> and its use has been mostly abandoned.

## Endoscopic Ultrasound-Guided Fine-Needle Biopsy Using a Standard 22-Gauge Needle

### Background

In 2000, Voss and colleagues,<sup>37</sup> in an attempt to overcome some of the limitations of EUS FNA, described their experience in obtaining tissue specimens from pancreatic masses using a standard 22-G FNA needle in association with high negative suction pressure by using a 30-ml syringe. They were able to gather tissue core specimens in 81% of the patients, with a diagnostic accuracy of 74%. Subsequently other groups reported their experience in using a standard 22-G FNA needle with or without high negative suction pressure to obtain samples for histologic evaluation.<sup>38–45</sup> In particular, Larghi et al.<sup>38</sup> used the Alliance II system to obtain a high steady and continuous negative suction. They named their procedure EUS-guided fine-needle tissue acquisition (EUS FNTA) to distinguish it from standard EUS FNA.



**Fig. 21.1** Nonhandle portion of the Tru-Cut needle demonstrating the following: outer “catheter sheath,” internal 19-G “cutting sheath” that shaves off the tissue specimen; an 18-mm-long “specimen tray,” which accommodates the tissue core; and a 5-mm-long “stylet tip.” (Adapted with permission from Levy MJ, Wiersema MJ. EUS-guided Trucut biopsy. Gastrointest Endosc 2005;62:417–26.)

### Design and Technique

The EUS FNTA technique with high negative pressure developed by Larghi et al.<sup>38</sup> is performed by using the Alliance II inflation system (Boston Scientific Corp.). Once the needle is advanced into the target lesion under real-time EUS imaging, the stylet is withdrawn and the Alliance II system is attached to the proximal end of the standard 22-G FNA needle. The Alliance II system is then turned into the suction mode, and a high negative continuous pressure corresponding to the 35-mL or the 60-mL syringe is applied. The lock of the syringe is then opened to steadily and continuously apply high negative suction pressure during the to-and-fro movements of the needle inside the target lesion.

### Results

Results of studies evaluating the possibility of acquiring a tissue biopsy sample for histologic examination using a standard 22-G needle are summarized in Table 21.1. Variable yields and diagnostic accuracies have been found in the different studies, possibly related to the different techniques used and how the samples were

**TABLE 21.1** Studies Evaluating the Possibility of Acquiring a Tissue Biopsy Sample for Histologic Examination Using a Standard 22-Gauge Fine-Needle Aspiration Needle

Author (Year)	No. of Patients	Patient Population	Yield of Core Tissue (%)	Diagnostic Accuracy (%)
Voss (2000) <sup>37,a</sup>	99	Pancreatic masses	81	68
Larghi (2005) <sup>38,b,c</sup>	27	Solid masses	96	76.9
Iglesias-Garcia (2007) <sup>39</sup>	62	Pancreatic masses	83.9	88.7
Möller (2009) <sup>40</sup>	192	Pancreatic masses	86.5	71.4
Gerke (2010) <sup>41,c</sup>	120	Solid masses and lymph nodes	27.8	77.8 <sup>d</sup>
Noda (2010) <sup>42</sup>	32	Solid masses and lymph nodes	NA	93.9
Imai (2011) <sup>43</sup>	21	Autoimmune pancreatitis	100	0
Imai (2011) <sup>43</sup>	64	Pancreatic cancer	NA	92
Kanno (2012) <sup>44</sup>	25	Autoimmune pancreatitis	80	84
Seicean (2016) <sup>45</sup>	118	Pancreatic masses	94	89

<sup>a</sup>Using high negative suction pressure with a 30-mL syringe.

<sup>b</sup>Using high negative suction pressure obtained using the Alliance II inflation system.

<sup>c</sup>Results obtained with a single needle pass for tissue acquisition performed at the end of a standard fine-needle aspiration.

<sup>d</sup>Diagnostic accuracy calculated based on both histologic and cytologic specimens.

handled. More recently, most of the studies evaluating the capability of standard 22-G needles to acquire tissue specimens for histologic examination and to reach a definitive diagnosis have been conducted in comparison with the 22-G ProCore (Cook Medical) needles, and their results will be presented in a paragraph that follows. Briefly, standard FNA needles demonstrated a diagnostic adequacy of 75%, a diagnostic accuracy of 86%, and a rate of histologic core specimen acquisition of 78%.<sup>19</sup>

## Endoscopic Ultrasound Fine-Needle Biopsy Using a Standard 19-Gauge Needle

### Background

Between 2005 and 2006, two Japanese investigators first reported their experience in using a standard 19-G needle to gather core biopsy specimens for histologic examination in patients with solid pancreatic masses and with mediastinal and/or intraabdominal lymphadenopathy of unknown origin.<sup>22,23</sup> They reported overall diagnostic accuracies of 69% and 98%, respectively. This discrepancy in the overall reported accuracy was due to the high rate of failure (five out of eight patients, 62.5%) when the sampling procedure was performed from the duodenum, as required for patients with pancreatic head and uncinate process masses.<sup>22</sup>

Inspired by these very promising results and in an attempt to overcome the limitations of using a standard 19-G needle through the duodenum, we modified the technique described by Itoi et al.<sup>22</sup> and by Yasuda et al.<sup>23</sup> by removing the stylet before insertion of the needle into the working channel of the EUS scope in order to increase needle flexibility and improve its performance.<sup>25</sup> This technique, which we continued to name

EUS FNTA to distinguish it from EUS FNA, was tested in different patient populations and in some specific cases, in which a histologic sample could be more useful to reach a definitive diagnosis.<sup>26,46-48</sup>

### Endoscopic Ultrasound-Guided Fine-Needle Biopsy Technique

The EUS FNTA technique is performed by using a disposable standard 19-G needle. The needle is prepared before insertion into the working channel of the echoendoscope by removing the stylet and attaching to its proximal end a 10-mL syringe already preloaded with 10 mL of negative pressure (Video 21.1). The needle is then advanced under EUS guidance a few millimeters inside the target lesion. After opening the lock of the syringe to apply negative pressure, two or three to-and-fro motions inside the lesion using the fanning technique<sup>49</sup> are made, which together account for one needle pass. The needle is removed after closing the lock of the syringe, and the collected specimens are placed directly in formalin by flushing the needle with saline and sent for histologic examination.

### Results

The results of all studies in which a standard 19-G FNA needle has been used to gather samples for histologic analysis, independent of the technique utilized, are summarized in Table 21.2,<sup>22-30,46-48,50-52</sup> and representative cases of histologic samples obtained with a standard 19-G FNA needle are presented in Fig. 21.2. As shown in Table 21.2, apart from the study by Itoi et al.,<sup>22</sup> in which a high technical failure rate was found when the procedure was performed through the duodenum, and the study by Eckardt et al.<sup>50</sup>

**TABLE 21.2** Studies Evaluating the Possibility of Acquiring a Tissue Biopsy Sample for Histologic Examination Using a Standard 19-Gauge Fine-Needle Aspiration Needle

Author (Year)	No. of Patients	Patient Population	Technical Success (%)	Yield (%)	Diagnostic Accuracy (%)
Itoi (2005) <sup>22,a</sup>	16	Pancreatic masses	81	68.8	68.8
Yasuda (2006) <sup>23</sup>	104	Mediastinal and/or abdominal lymphadenopathy	100	100	98.1; 88 accuracy in subclassification of lymphoma
Iwashita (2008) <sup>24</sup>	41	Mediastinal lymphadenopathy suspicious for sarcoidosis	100	95.1	95.1
Larghi (2011) <sup>25,b,c</sup>	120	Heterogeneous patient population	99.2	96.7	93.2;
Larghi (2012) <sup>26,c</sup>	30	Pancreatic masses suspicious for non-functional neuroendocrine neoplasia	100	93.3	93.3
Iwashita (2012) <sup>27</sup>	44	Pancreatic masses suggestive of autoimmune pancreatitis	100	93	43.2
Yasuda (2012) <sup>28</sup>	152	Mediastinal and/or abdominal lesions suspicious for lymphoma	97	97	93.4; 95 accuracy in subclassification of lymphoma (142 patients)
Varadarajulu (2012) <sup>30</sup>	38	Pancreatic masses/subepithelial lesions	100	94.7	94.7
Stavropoulos (2012) <sup>29,d</sup>	22	Patients with abnormal liver tests undergoing endoscopic ultrasound to rule out biliary obstruction	100	91	91

Continued

**TABLE 21.2 Studies Evaluating the Possibility of Acquiring a Tissue Biopsy Sample for Histologic Examination Using a Standard 19-Gauge Fine-Needle Aspiration Needle—cont'd**

Author (Year)	No. of Patients	Patient Population	Technical Success (%)	Yield (%)	Diagnostic Accuracy (%)
Eckardt (2012) <sup>50</sup>	46	Gastric subepithelial lesions	NA	59	52
Larghi (2014) <sup>46,e,c</sup>	121	GI Subepithelial lesions	99.2	93.4	93.4
Diehl (2015) <sup>51</sup>	110	Abnormal liver tests or hepatic disease	100	98	98
Iwashita (2015) <sup>52</sup>	111	Patients with solid lesions	99	79 <sup>f</sup>	95 <sup>g</sup>

<sup>a</sup>All failures occurred when sampling was performed from the duodenum.

<sup>b</sup>Consecutive patients with subepithelial lesions, esophagogastric wall thickening, mediastinal and abdominal masses/lymphadenopathy of unknown origin, pancreatic body or tail lesions after a negative FNA were included in the study.

<sup>c</sup>The endoscopic ultrasound-guided fine-needle tissue acquisition technique was used.

<sup>d</sup>Adequate specimen defined as a length of 15 mm with the presence of at least 6 portal tracts.

<sup>e</sup>All procedures were performed using the forward-viewing endoscopic ultrasound scope.

<sup>f</sup>Reported as percentage of all passes.

<sup>g</sup>Only diagnostic accuracy for malignancy is reported.

involving patients with GI subepithelial lesions, the overall technical success and yield for a tissue core in all the published studies were above 90%. Moreover, the overall diagnostic accuracy was also found to be higher than 90%, with the only exception being the study by Iwashita and colleagues,<sup>27</sup> in which only patients with a pancreatic mass suspicious for autoimmune pancreatitis (AIP) were evaluated. In the latter study, despite specimens for histologic analysis being obtained in 93% of the patients, a definitive histologic diagnosis of AIP based on lymphoplasmacytic infiltration around pancreatic ducts, obliterative phlebitis, and/or positive IgG4 immunostaining could be possible in only 43% of the cases. This low diagnostic yield can be attributed to the patchy distribution of the specific histologic changes of AIP,<sup>53</sup> thus rendering the amount of tissue obtained with EUS-guided biopsy insufficient to establish a definitive diagnosis. On the other hand, in all patients with available tissue, a malignant etiology could be excluded, which is extremely important in order to safely start empirical therapy for AIP with steroids.<sup>27</sup>

In another study involving patients with suspected nonfunctional neuroendocrine tumors, comparison between the ki-67 index determination on biopsy specimens and on surgical specimens using a cutoff of greater than 5% to define G2 tumors found an agreement in all patients.<sup>26</sup> Moreover, in patients with GI stromal tumors, Ricci et al.<sup>54</sup> were able to perform genetic analysis for diagnostic and prognostic purposes, allowing optimization of chemotherapy for initially unresectable cases, where neoadjuvant therapy may be an option.<sup>55,56</sup>

## Endoscopic Ultrasound-Guided Fine-Needle Biopsy Using ProCore Needles

### Introduction

Although the Quick-Core needle failed to reach widespread use due to the technical difficulty associated with its utilization and the relative lack of advantages over standard FNA needles, the same manufacturer developed a new needle with a different design, the ProCore needle.<sup>20</sup> To meet most of the needs of EUS-guided FNB, three needle sizes have been initially

developed: 19 G, 22 G, and 25 G (Fig. 21.3). Moreover, more recently a 20-G needle with a different design has become available (Fig. 21.4).

### Design and Technique

All ProCore needles are 1.705 m long, made of stainless steel with a nitinol stylet that runs through the cannula of the needle and matches the bevel tip. In all there is a lateral opening of varying length depending on the needle size (Table 21.3, Fig. 21.3), which presents a reverse bevel to hook and cut the tissue, entrapping it into the needle. The EchoTip ProCore 20 G has a Menghini bevel and lateral core trap technology designed for receiving tissue into the needle (see Fig. 21.4). The coiled sheath facilitates needle flexibility, and the ReCoil stylet system aids stylet management, minimizing the risk of contamination.

In the first published study,<sup>20</sup> which involved five European centers, each participating center used a different sampling technique. At multivariate analysis, the only variable associated with obtainment of an optimal sample for histologic analysis able to make a correct final diagnosis was evaluation of the sample by an experienced pathologist.<sup>20</sup> In a subsequent study from the same European group,<sup>57</sup> a standardized sample acquisition protocol was developed as follows: (1) the needle was advanced into the target lesion under EUS guidance; (2) once inside the lesion, the stylet was removed and negative suction pressure was applied using a 10-mL syringe for 30 seconds; (3) three to-and-fro movements within the lesion were made; (4) suction was then released by closing the lock of the syringe; and (5) the needle was finally removed. Tissue samples were recovered in formalin or cytolyte by flushing the needle with saline.<sup>57</sup>

A different sampling technique, the slow pull technique, has been proposed for tissue acquisition performed using the 25-G ProCore needle.<sup>17</sup> With this technique, once the needle is inside the lesion, the negative suction pressure is obtained by slowly and continuously pulling out the stylet from the needle while 10 to 20 to-and-fro movements are performed (Video 21.2). Preliminary results<sup>58</sup> have reported this technique to result in a significantly higher yield as compared with the suction method used in both the European ProCore studies.<sup>20,57</sup>

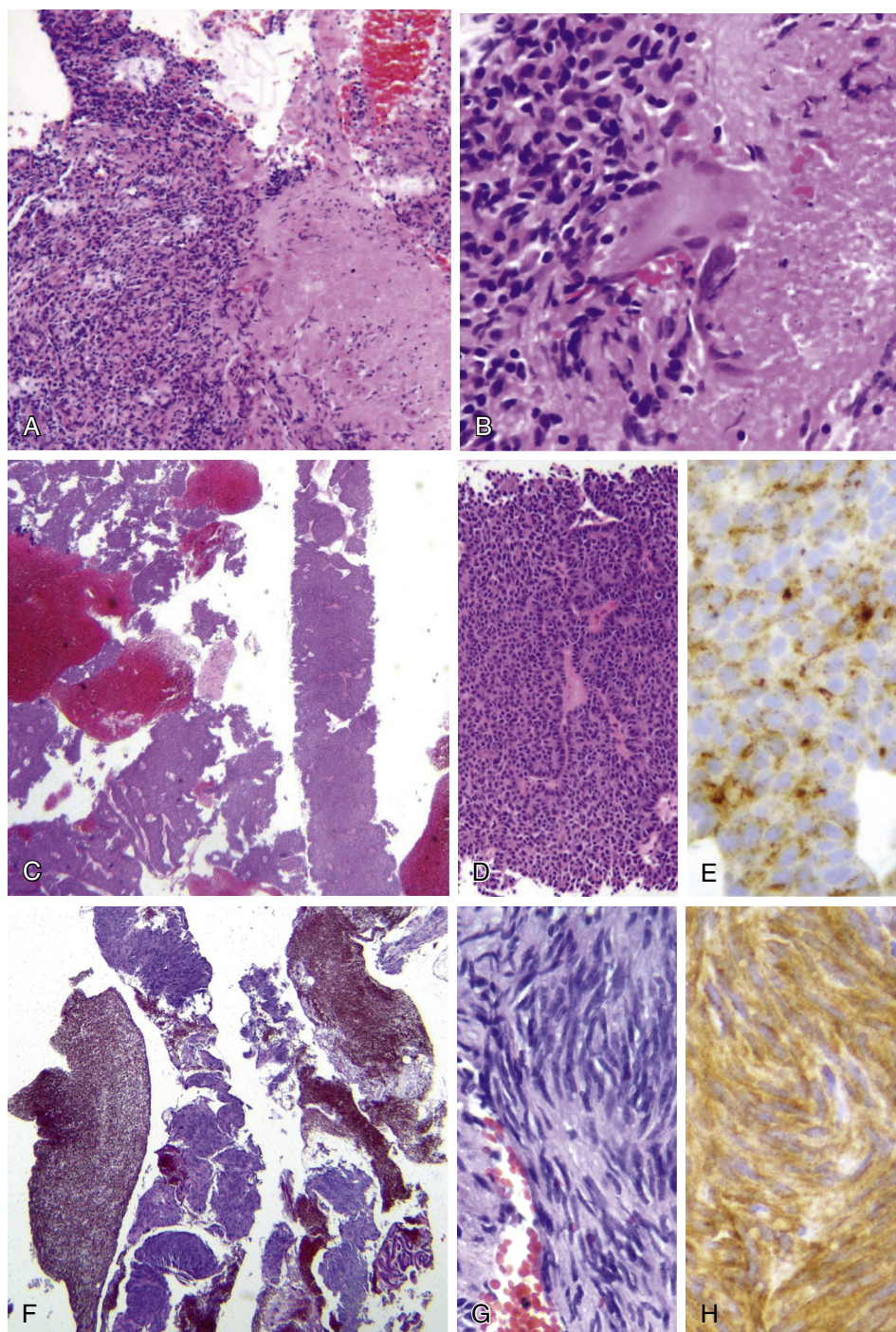


**Fig. 21.2** Representative cases of specimens obtained by EUS FNTA. (A, B) Mediastinal lymph node: (A) abundant tissue fragments, at higher magnification (B) showing caseous material and multinucleated giant cells consistent with a tubercular granuloma, as also later confirmed by polymerase chain reaction (PCR) methods; H&E. (C–E) Body-tail of the pancreas: (C, D) multiple large tissue fragments of a well-differentiated, nonfunctioning, neuroendocrine tumor, with a typical trabecular structure, low-grade histology void of necrosis and mitotic figures (D), and chromogranin A expression at immunohistochemistry (E); (C, D) H&E; (E) immunoperoxidase. (F–H) Perigastric lesion: (F), abundant, large fragments of neoplastic tissue with solid structure, in the absence of necrosis, composed of regular, fused cells with mild atypia (G) intensely immunoreactive for c-Kit (H), consistent with gastrointestinal stromal tumor; (F, G) H&E, (H) immunoperoxidase. (From Larghi A, Verna EC, Ricci R, et al. EUS-guided fine-needle tissue acquisition by using a 19-gauge needle in a selected patient population: a prospective study. *Gastrointest Endosc* 2011;74:504–10.)



• **Fig. 21.3** Novel 19-G, 22-G, and 25-G ProCore needles with reverse bevel technology for acquisition of tissue samples. (Permission for use granted by Cook Medical, Bloomington, Indiana.)



• **Fig. 21.4** The tip of the ProCore 20-G needle with the Menghini bevel and lateral core trap technology designed for receiving tissue into the needle. (Permission for use granted by Cook Medical, Bloomington, Indiana.)

## Results

The performance of the 19-G ProCore needle in the diagnosis of intraintestinal and extraintestinal lesions was evaluated in a multicenter study by Iglesias-Garcia et al.<sup>20</sup> and in a single center study by the same author.<sup>21</sup> A diagnostic accuracy of 89.5% and 95.4%, respectively, were found. Interestingly, in the former study the only factor that positively correlated with a significant increase in the potential of making a definitive histologic diagnosis was the involvement of an expert pathologist.<sup>20</sup>

A study evaluating the interobserver agreement in grading the quality of specimens obtained with the 19-G ProCore needle among five expert pathologists from the five participating centers was performed.<sup>59</sup> Overall, an excellent interobserver agreement in the assessment of the histologic material was found among the involved pathologists, and this was particularly high (91.2%) with regard to sample adequacy, with a Fleiss  $\kappa$  that was 0.73 (95% confidence interval [CI] 0.61–0.81).<sup>59</sup>

The same study group subsequently evaluated the performance of the 22-G ProCore needle in a cohort of 61 patients with pancreatic masses, which in 57% of the cases were located in the pancreatic head or uncinate, thus requiring a transduodenal approach.<sup>57</sup> Only one needle pass was performed in the protocol described previously, resulting in tissue specimens that were retrieved for histologic examination in 55 patients (90%), with an overall accuracy of 88.5%.

After this experience, different studies have evaluated the performance of the 22-G ProCore needle compared with the standard 22-G (Table 21.4). On this topic a meta-analysis including nine studies (total 576 patients) has recently been published.<sup>19</sup> No significant differences in diagnostic adequacy (75.2% vs. 89.0%, odds ratio [OR] 0.39,  $P = .23$ ), diagnostic accuracy (85.8% vs. 86.2%, OR 0.88,  $P = .53$ ), or rate of histologic core specimen acquisition (77.7% vs. 76.5%, OR 0.94,  $P = .85$ ) between the ProCore and standard FNA needles were found. The mean number of passes required for diagnosis, however, was significantly lower when using the ProCore needle (standardized mean difference, 1.2,  $P < .001$ ).

Iwashita and colleagues<sup>17</sup> reported the first experience in using the 25-G ProCore needle for the evaluation of 50 consecutive patients with solid pancreatic lesions. They applied the slow pull technique described previously, and the obtained material was expressed onto a glass slide by reinsertion of the stylet, any visible core being lifted off and placed in formalin, while smears for on-site cytopathologic

**TABLE 21.3** Main Characteristics of the Different Available EchoTip ProCore Needles

	ECHO-HD-25-C	ECHO-HD-22-C	ECHO-HD-3-20-C	ECHO-HD-19-C
Needle outer diameter	0.56 mm	0.71 mm	0.91 mm	1.07 mm
Needle inner diameter	0.37 mm	0.51 mm	0.76 mm	0.94 mm
Needle length	1.705 m	1.705 m	1.705 m	1.705 m
Needle bevel	Lancet	Lancet	Menghini	Lancet
Stylet tip design	Recessed ball	Recessed ball	Recessed ball	Recessed ball
Bevel length	2 mm	2 mm	2.9 mm	4 mm
Distance of the needle tip from the bevel	3 mm	3.9 mm	3.8 mm	5 mm
Sheath size	5.2 Fr	5.2 Fr	7.95 Fr	4.8 Fr
Needle material	Stainless steel	Stainless steel	Stainless steel	Stainless steel
Stylet material	Nitinol	Nitinol	Nitinol	Nitinol

**TABLE 21.4** Studies Evaluating the Performances of a 22-Gauge ProCore Needle as Compared to a Standard 22-Gauge Fine-Needle Aspiration Needle

Author (Year)	Study Design	No. of Patients	Target Organ	Number of Needle Passes (SD)		Histologic Tissue Specimens		Overall Diagnostic Accuracy	
				ProCore	Fine-Needle Aspiration	ProCore	Fine-Needle Aspiration	ProCore	FNA
Bang (2012) <sup>60</sup>	Randomized	56	Pancreas	1.28 (0.54)	1.61 (0.88)	14/18 (77.8)	8/12 (66.7)	NR	NR
Hucl (2013) <sup>61</sup>	Prospective	145	Pancreas/LFN	1.23 (0.47)	2.47 (0.93)	125/145 (86.2)	127/145 (87.6)	75.9	77.2
Witt (2013) <sup>62</sup>	Retrospective	36	Pancreas/LFN, mediastinal, gastric, pelvic	2.11	2.94	8/11 (72.7)	10/13 (76.9)	94.4	99.4
Vanbiervliet (2014) <sup>63</sup>	Randomized	80	Pancreas	NR	NR	56/80 (70)	70/80 (87.6)	90	92.5
Kim (2014) <sup>64</sup>	Randomized	22	Subepithelial lesions	1.28 (0.54)	1.61 (0.88)	NR	NR	77.8	66.7
Lee (2014) <sup>65</sup>	Randomized	116	Pancreas	NR	NR	48/58 (82.8)	45/58 (77.6)	68.3	94.8
Strand (2014) <sup>66</sup>	Prospective	32	Pancreas	1.4 (0.7)	2.1 (1.6)	19/27 (70.4)	7/9 (77.8)	NR	NR
Berzosa (2015) <sup>67</sup>	Retrospective	61	Pancreas	1.7	3.5	NR	NR	68.9	75.4
Mavrogenis (2015) <sup>68</sup>	Prospective	28	Pancreas/LFN	NR	NR	22/28 (78.6)	24/28 (85.7%)	85.7	85.7
Aadam (2016) <sup>69</sup>	Randomized	140	Pancreas/LFN, gastric, pelvic	2.8 (1.0)	3.0 (1.0)	NR	NR	90.1	67.1 <sup>a</sup>
Sterlacci (2016) <sup>70</sup>	Prospective	56	Pancreas/LFN, gastric, pelvic	1.5 (0.6)	1.6 (1.0)	NR	NR	96.1	88.9

<sup>a</sup> $P = .002$ .

LFN, Lymphnodes; NR, not reported.

evaluation were made from the residual material. The authors found an impressively high sensitivity (83%) for cytologic diagnosis on the first pass, which increased to 91% and 96% at the second and third pass, respectively. Interestingly, the presence of a histologic core was found in only 12% of cases after the first needle pass and in 32% of the patients at the subsequent two to four passes. This latter finding is similar to our experience with a core for histologic examination found in 40.5% of patients.<sup>18</sup> In our opinion, these results indicate that the 25-G ProCore needle is a proficient needle to gather diagnostic cytologic specimens, probably even more efficient than a standard 25-G FNA needle, but cannot be used when a tissue core biopsy specimen is required to make the diagnosis.

Finally, regarding the 20-G ProCore, a multicenter prospective randomized study, the ASPRO study, comparing the 20 G for EUS FNB with the standard 25 G for EUS FNA, is ongoing (ClinicalTrials.gov: NCT02167074). Representative cases of histologic samples obtained with the 20-G ProCore needle are presented in Fig. 21.5.

## Endoscopic Ultrasound-Guided Fine-Needle Biopsy Using the Sharkcore and the Acquire Needles

### Design and Technique

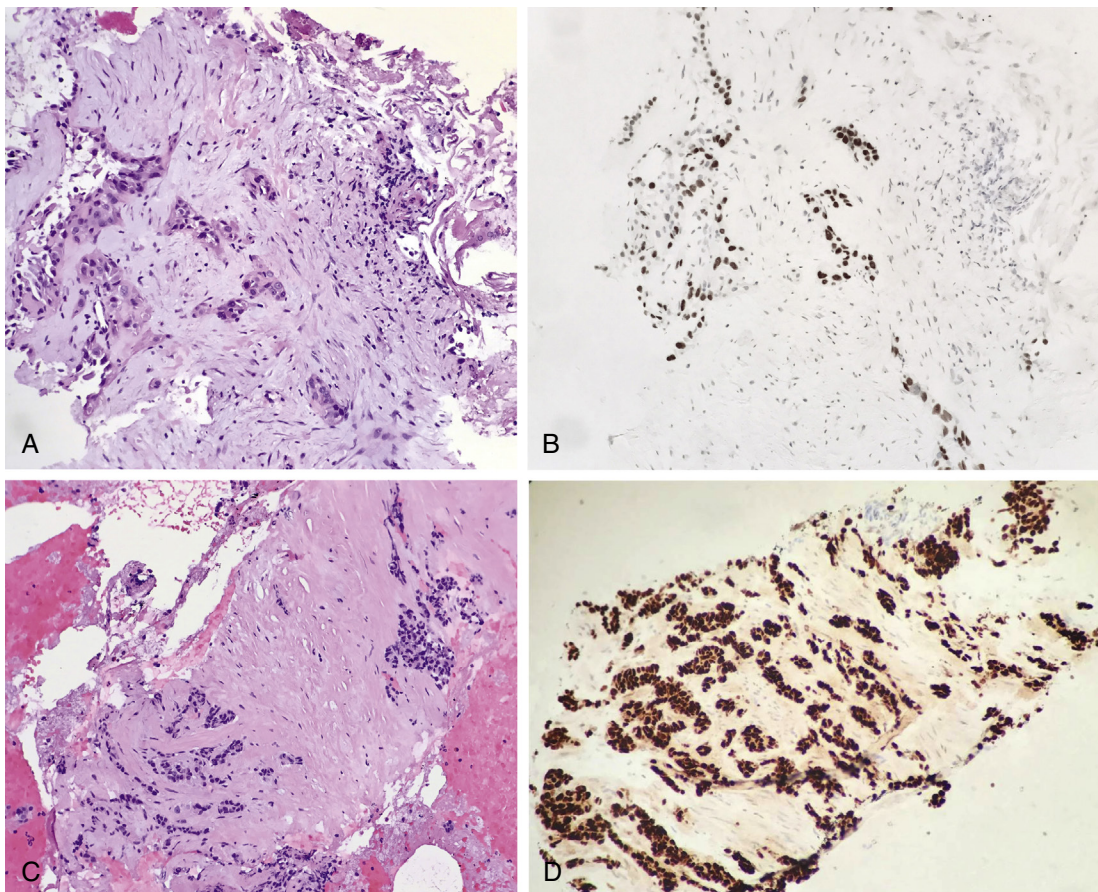
The SharkCore 22-G and 25-G needles are both made of stainless steel, with a nitinol stylet. These devices feature a newly

designed multifaceted opposing bevel with two protruding sharp points (the “fork-tip”) and six cutting-edge surfaces, designed to promote tissue capture with maintenance of its architecture (Fig. 21.6; Video 21.3). The biopsy is usually performed using the slow pull technique.

The Acquire needle has an outer diameter of 0.72 mm and an adjustable working length of 137.5 to 141.5 cm. The needle tip design is a crown-tip with three symmetrical surfaces that represent three cutting edges (Fig. 21.7; Video 21.4). The biopsy is usually performed using the “wet suction” technique, in which after removal of the stylet, the inner channel of the needle is filled up with saline and a 10- or 20-mL syringe is attached to the Luer lock of the needle, ready to apply negative aspiration pressure as soon as the needle is advanced into the lesion.<sup>71</sup>

### Results

For the SharkCore needle, preliminary data from a small prospective<sup>31</sup> and few retrospective studies<sup>32–34,72</sup> for both pancreatic and nonpancreatic lesions are encouraging. In a retrospective case-control study of 39 patients who underwent sampling using all the available SharkCore needles,<sup>32</sup> 95% of the specimens obtained using the SharkCore needles were of sufficient size for histologic evaluation, compared with 59% for EUS FNA ( $P = .01$ ). In addition, the median number of passes required to achieve a diagnostic sample was significantly lower in the SharkCore group compared with the EUS FNA group



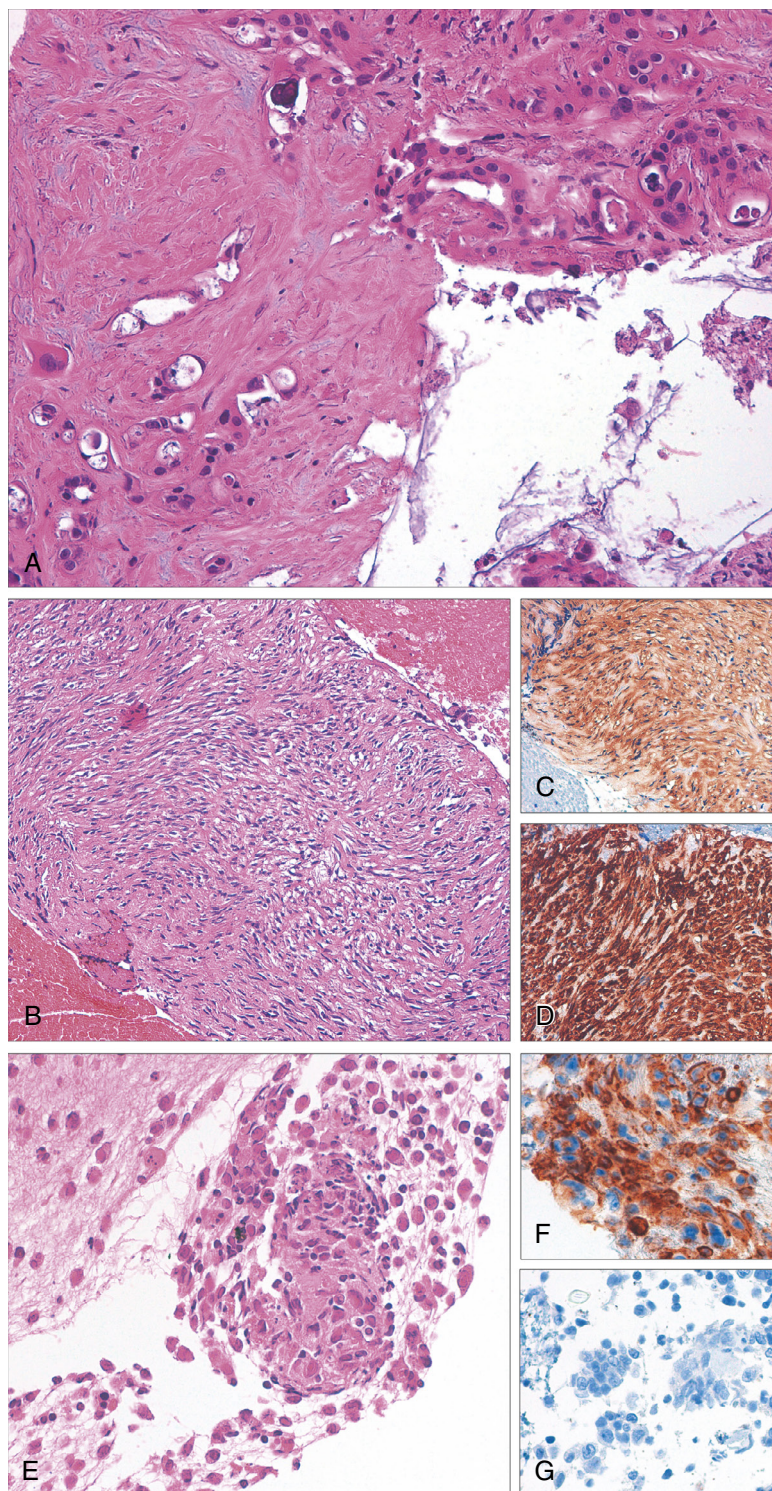
**• Fig. 21.5** Representative histological samples obtained with the ProCore 20-G needle. Pancreatic body mass: (A) a core of fibrous tissue infiltrated by irregular aggregates and small nests of epithelial cells with moderate nuclear pleomorphism, intercellular bridges, and glassy eosinophilic cytoplasm, diffusely positive to p63 (B), documenting squamous differentiation. Pancreatic tail mass: (C) A core of fibrous tissue showing invasion by strands and cords of small- to medium-sized cells with moderate nuclear pleomorphism, (D) positive for GATA 3 antibody diagnostic for breast cancer metastasis.



**• Fig. 21.6** The tip design of the newly developed SharkCore needle, with its multifaceted opposing bevel incorporating six cutting-edge surfaces, intended to promote tissue capture. (All rights reserved. Used with permission of Medtronic.)



**• Fig. 21.7** The 22-G Acquire endoscopic ultrasound-guided fine-needle biopsy needle with its crown shaped tip revealing the three planes for tissue acquisition. (Reproduced with the permission from Boston Scientific Corp.)



• **Fig. 21.8** Representative histologic samples obtained with the 22-G SharkCore. (A) Pancreatic head mass: Tissue core biopsy characterized by desmoplastic stroma with atypical glands, invasion of single cells, and mucin production diagnostic for ductal adenocarcinoma. (B–D) Subepithelial lesion of the gastric fundus; (B) large biopsy specimen characterized by proliferation of monomorphic spindle cells, positive at immunohistochemistry for CD117 (C) and DOG1 (D), results diagnostic for gastrointestinal stromal tumors. (E–G). Pancreatic tail lesion with abundant tissue fragments, at higher magnification showing aggregates of large atypical cells (E) positive for leukocyte common antigen (LCA) (F) and negative for CK CAM5.2 (G), diagnostic for non-Hodgkin anaplastic large cell lymphoma.

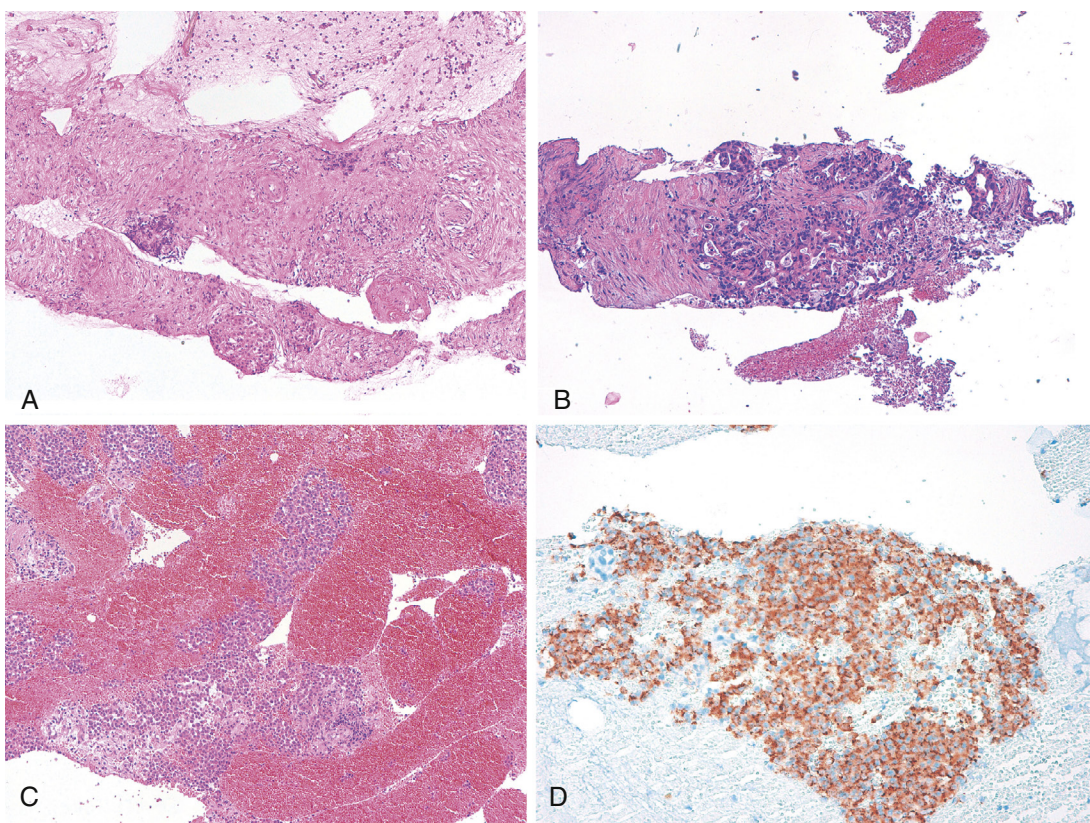


**Fig. 21.9** Representative histologic samples obtained with the 22-G Acquire. (A) abundant tissue fragments showing large areas of fibrosis with focal residual endocrine islets suggestive of chronic pancreatitis; (B) infiltration of ductal adenocarcinoma characterized by irregular glands with cribriform architecture, and marked nuclear pleomorphism; (C) groups of monomorphic epithelioid cells positive for chromogranin A at immunohistochemistry (D) diagnostic for a well-differentiated neuroendocrine neoplasm.

(2 passes vs. 4 passes,  $P = .001$ ). In a multicenter retrospective study by DiMaio et al. on 224 patients,<sup>33</sup> 250 lesions were biopsied using the 22-G or the 25-G SharkCore needles. A pathologic diagnosis was obtained in 130/147 (88%) specimens with a median number of two passes. Ten patients (10/226, 4%) experienced adverse events: four acute pancreatitis, five pain, and one cholangitis. In a single-center study the performance of the 22-G or 25-G SharkCore needles was compared with that of the ProCore 20-G, 22-G, and 25-G needles.<sup>34</sup> Higher sensitivity (71.1% vs. 90.1%;  $P = .0006$ ) and overall accuracy (74% vs. 92%;  $P = .0006$ ) for the SharkCore in discriminating malignant from benign solid pancreatic masses were found. Moreover, the proportion of samples classified as adequate for histologic analysis was 87% for the ProCore versus 99% for the SharkCore.

So far only one study has evaluated the performance of the Acquire needle in 30 patients with solid mass lesions throughout the GI tract.<sup>35</sup> Diagnostic adequacy for ROSE was 96.6%, and histologic diagnosis was established in 96.7% of patients. Median tissue area was  $2.9 \text{ mm}^2$  (IQR =  $0.68\text{--}8.71 \text{ mm}^2$ ) and the presence of tumor cells in the retrieved tissue was 73.9% (IQR =  $44\text{--}97.6$ ). Rates of technical success and adverse events were 96.7% and 3.3%, respectively.

Representative histologic samples obtained with the SharkCore and the Acquire are shown in Figs. 21.8 and 21.9.

## Conclusions and Future Perspective

In the last decade in an attempt to overcome some of the limitations of EUS FNA, alternative endoscopic techniques and dedicated needles to obtain core tissue biopsy specimens for histologic examination under EUS guidance have been developed and tested with varying success. These efforts are leading to a shift in this field from cytology to histology, which is easier to interpret, thus potentially contributing to the widespread diffusion of EUS utilization in the community and in countries where cytology expertise may be difficult to be developed. Moreover, in the era of individualized medicine, this shift will likely pave the road to targeted therapies and better approaches to the treatment of most gastrointestinal malignancies, as tissue samples for histologic examination are more adequate to perform predictive molecular markers or cell culture with chemosensitivity testing to guide individualized therapies. This will transform diagnostic EUS into a more therapeutic procedure that not only gives a diagnostic answer but also offers the possibility to deliver the best treatment for individual patients. Based on these premises, leading companies have developed their own EUS FNB needle in order to fulfill the evolving patients' and physicians' needs. These newly developed needles have shown promising results in preliminary studies. Regardless of the needle type, a close collaboration between endosonographers and pathologists remains of paramount importance to succeed and should be strongly encouraged.

## Key References

20. Iglesias-Garcia J, Poley JW, Larghi A, et al. Feasibility and yield of a new EUS histology needle: results from a multicenter, pooled, cohort study. *Gastrointest Endosc.* 2011;73:1189–1196.
22. Itoi T, Itokawa F, Sofuni A, et al. Puncture of solid pancreatic tumors guided by endoscopic ultrasonography: a pilot study series comparing Trucut and 19-gauge and 22-gauge aspiration needles. *Endoscopy.* 2005;37:362–366.
23. Yasuda I, Tsurumi H, Omar S, et al. Endoscopic ultrasound-guided fine needle aspiration biopsy for lymphadenopathy of unknown origin. *Endoscopy.* 2006;38:919–924.
26. Larghi A, Capurso G, Carnuccio A, et al. Ki-67 grading of non-functioning pancreatic neuroendocrine tumors on histologic samples obtained by EUS-guided fine-needle tissue acquisition: a prospective study. *Gastrointest Endosc.* 2012;76:570–577.
57. Larghi A, Iglesias-Garcia J, Poley JW, et al. Feasibility and yield of a novel 22-gauge histology EUS needle in patients with pancreatic masses: a multicenter prospective cohort study. *Surg Endosc.* 2013;27:3733–3738.

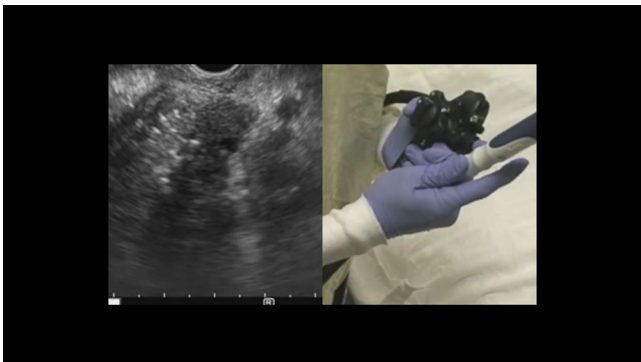
## References

Access the reference list online at [ExpertConsult.com](#).

## References

1. Wani S, Muthusamy VR, Komanduri S. EUS-guided tissue acquisition: an evidence-based approach (with videos). *Gastrointest Endosc.* 2014;80:939–959.
2. Eloubeidi MA, Tamhane A, Jhala N, et al. Agreement between rapid onsite and final cytologic interpretations of EUS-guided FNA specimens: implications for the endosonographer and patient management. *Am J Gastroenterol.* 2006;101:2841–2847.
3. Iglesias-Garcia J, Dominguez-Munoz JE, Abdulkader I, et al. Influence of on-site cytopathology evaluation on the diagnostic accuracy of endoscopic ultrasound-guided fine needle aspiration (EUS-FNA) of solid pancreatic masses. *Am J Gastroenterol.* 2011;106:1705–1710.
4. Hébert-Magee S, Bae S, Varadarajulu S, et al. The presence of a cytopathologist increases the diagnostic accuracy of endoscopic ultrasound-guided fine needle aspiration cytology for pancreatic adenocarcinoma: a meta-analysis. *Cytopathology.* 2013;24:159–171.
5. Matynia AP, Schmidt RL, Barraza G, et al. Impact of rapid on-site evaluation on the adequacy of endoscopic-ultrasound guided fine-needle aspiration of solid pancreatic lesions: a systematic review and meta-analysis. *J Gastroenterol Hepatol.* 2014;29:697–705.
6. Jhala NC, Jhala DN, Chhieng DC, et al. Endoscopic ultrasound-guided fine-needle aspiration. A cytopathologist's perspective. *Am J Clin Pathol.* 2003;120:351–367.
7. Kaltatzakis E, Panos M, Sadik R, et al. Clinicians' attitudes towards endoscopic ultrasound: a survey of four European countries. *Scand J Gastroenterol.* 2009;44:100–107.
8. Varadarajulu S, Hawes RH. The changing paradigm in EUS-guided tissue acquisition. *Gastrointest Endosc Clin N Am.* 2014;24:1–7.
9. Braat H, Bruno M, Kuipers EJ, et al. Pancreatic cancer: promise for personalised medicine? *Cancer Lett.* 2012;318:1–8.
10. Brais RJ, Davies SE, O'Donovan M, et al. Direct histological processing of EUS biopsies enables rapid molecular biomarker analysis for interventional pancreatic cancer trials. *Pancreatology.* 2012;12:8–15.
11. Kim EY. Fine-needle biopsy: should this be the first choice in endoscopic ultrasound-guided tissue acquisition? *Clin Endosc.* 2014;47(5):425–428.
12. Panic N, Larghi A. Techniques for endoscopic ultrasound-guided fine-needle biopsy. *Gastrointest Endosc Clin N Am.* 2014;24:83–107.
13. Varadarajulu S, Fraig M, Schmulewitz N, et al. Comparison of EUS guided 19-gauge Trucut needle biopsy with EUS-guided fine-needle aspiration. *Endoscopy.* 2004;36:397–401.
14. Shah SM, Ribeiro A, Levi J, et al. EUS-guided fine needle aspiration with and without trucut biopsy of pancreatic masses. *JOP.* 2008;9:422–430.
15. Thomas T, Kaye PV, Ragunath K, et al. Efficacy, safety, and predictive factors for a positive yield of EUS-guided trucut biopsy: a large tertiary referral center experience. *Am J Gastroenterol.* 2009;104:584–591.
16. DeWitt J, Cho CM, Lin J, et al. Comparison of EUS-guided tissue acquisition using two different 19-gauge core biopsy needles: a multicenter, prospective, randomized, and blinded study. *Endosc Int Open.* 2015;3:E471–E478.
17. Iwashita T, Nakai Y, Samarasena JB, et al. High single-pass diagnostic yield of a new 25-gauge core biopsy needle for EUS-guided FNA biopsy in solid pancreatic lesions. *Gastrointest Endosc.* 2013;77:909–915.
18. Attili F, Petrone G, Abdulkader I, et al. Accuracy and interobserver agreement of the Procore™ 25 gauge needle for endoscopic ultrasound-guided tissue core biopsy. *Dig Liver Dis.* 2015;47:943–949.
19. Bang JY, Hawes R, Varadarajulu S. A meta-analysis comparing ProCore and standard fine-needle aspiration needles for endoscopic ultrasound-guided tissue acquisition. *Endoscopy.* 2016;48:339–349.
20. Iglesias-Garcia J, Poley JW, Larghi A, et al. Feasibility and yield of a new EUS histology needle: results from a multicenter, pooled, cohort study. *Gastrointest Endosc.* 2011;73:1189–1196.
21. Iglesias-Garcia J, Abdulkader I, Larriño-Noia J, Domínguez-Muñoz JE. Evaluation of the adequacy and diagnostic accuracy of the histology samples obtained with a newly designed 19-gauge EUS histology needle. *Rev Esp Enferm Dig.* 2014;106:6–14.
22. Itoi T, Itokawa F, Sofuni A, et al. Puncture of solid pancreatic tumors guided by endoscopic ultrasonography: a pilot study series comparing Trucut and 19-gauge and 22-gauge aspiration needles. *Endoscopy.* 2005;37:362–366.
23. Yasuda I, Tsurumi H, Omar S, et al. Endoscopic ultrasound-guided fine needle aspiration biopsy for lymphadenopathy of unknown origin. *Endoscopy.* 2006;38:919–924.
24. Iwashita T, Yasuda I, Doi S, et al. The yield of endoscopic ultrasound-guided fine needle aspiration for histological diagnosis in patients suspected of stage I sarcoidosis. *Endoscopy.* 2008;40:400–405.
25. Larghi A, Verna EC, Ricci R, et al. EUS-guided fine-needle tissue acquisition by using a 19-gauge needle in a selected patient population: a prospective study. *Gastrointest Endosc.* 2011;74:504–510.
26. Larghi A, Capurso G, Carnuccio A, et al. Ki-67 grading of non-functioning pancreatic neuroendocrine tumors on histologic samples obtained by EUS-guided fine-needle tissue acquisition: a prospective study. *Gastrointest Endosc.* 2012;76:570–577.
27. Iwashita T, Yasuda I, Doi S, et al. Use of samples from endoscopic ultrasound-guided 19-gauge fine-needle aspiration in diagnosis of autoimmune pancreatitis. *Clin Gastroenterol Hepatol.* 2012;10:316–322.
28. Yasuda I, Goto N, Tsurumi H, et al. Endoscopic ultrasound-guided fine needle aspiration biopsy for diagnosis of lymphoproliferative disorders: feasibility of immunohistological, flow cytometric, and cytogenetic assessments. *Am J Gastroenterol.* 2012;107:397–404.
29. Stavropoulos SN, Im GY, Jlayer Z, et al. High yield of same-session EUS-guided liver biopsy by 19-gauge FNA needle in patients undergoing EUS to exclude biliary obstruction. *Gastrointest Endosc.* 2012;75:310–318.
30. Varadarajulu S, Bang JY, Hebert-Magee S. Assessment of the technical performance of the flexible 19-gauge EUS-FNA needle. *Gastrointest Endosc.* 2012;76:336–343.
31. Adler DG, Witt B, Chadwick B, et al. Pathologic evaluation of a new endoscopic ultrasound needle designed to obtain core tissue samples: a pilot study. *Endosc Ultrasound.* 2016;5:178–183.
32. Kandel P, Tranesh G, Nassar A, et al. EUS-guided fine needle biopsy sampling using a novel fork-tip needle: a case-control study. *Gastrointest Endosc.* 84:1034–1039.
33. DiMaio CJ, Kolb JM, Benias PC, et al. Initial experience with a novel EUS-guided core biopsy needle (SharkCore): results of a large North American multicenter study. *Endosc Int Open.* 2016;4: E974–E979.
34. Nayar MK, Paranandi B, Dawwas MF, et al. Comparison of the diagnostic performance of 2 core biopsy needles for EUS-guided tissue acquisition from solid pancreatic lesions. *Gastrointest Endosc.* 2016. pii: S0016-5107(16)30554-5. <https://doi.org/10.1016/j.gie.2016.08.048>. [Epub ahead of print] PubMed PMID: 27633157.
35. Bang JY, Hebert-Magee S, Hasan MK, et al. Endoscopic ultrasound-guided biopsy using a Franseen needle design: initial assessment. *Dig Endosc.* 2017;29:338–346.
36. Levy MJ, Wiersema MJ. EUS-guided Trucut biopsy. *Gastrointest Endosc.* 2005;62:417–426.

37. Voss M, Hammel P, Molas G, et al. Value of endoscopic ultrasound guided fine needle aspiration biopsy in the diagnosis of solid pancreatic masses. *Gut*. 2000;46:244–249.
38. Larghi A, Noffsinger A, Dye CE, et al. EUS-guided fine needle tissue acquisition by using high negative pressure suction for the evaluation of solid masses: a pilot study. *Gastrointest Endosc*. 2005;62:768–774.
39. Iglesias-Garcia J, Dominguez-Munoz E, Lozano-Leon A, et al. Impact of endoscopic ultrasound-guided fine needle biopsy for diagnosis of pancreatic masses. *World J Gastroenterol*. 2007;13:289–293.
40. Möller K, Papapnikolaou IS, Toermer T, et al. EUS-guided FNA of solid pancreatic masses: high yield of 2 passes with combined histologic-cytologic analysis. *Gastrointest Endosc*. 2009;70:60–69.
41. Gerke H, Rizk MK, Vanderheyden AD, et al. Randomized study comparing endoscopic ultrasound-guided Trucut biopsy and fine needle aspiration with high suction. *Cytopathology*. 2010;21:44–51.
42. Noda Y, Fujita N, Kobayashi G, et al. Diagnostic efficacy of the cellblock method in comparison with smear cytology of tissue samples obtained by endoscopic ultrasound-guided fine-needle aspiration. *J Gastroenterol*. 2010;45:868–875.
43. Imai K, Matsubayashi H, Fukutomi A, et al. Endoscopic ultrasonography-guided fine needle aspiration biopsy using 22-gauge needle in diagnosis of autoimmune pancreatitis. *Dig Liver Dis*. 2011;43:869–874.
44. Kanno A, Ishida K, Hamada S, et al. Diagnosis of autoimmune pancreatitis by EUS-FNA by using a 22-gauge needle based on the International Consensus Diagnostic Criteria. *Gastrointest Endosc*. 2012;76:594–602.
45. Seicean A, Gheorghiu M, Zaharia T, et al. Performance of the standard 22G needle for endoscopic ultrasound-guided tissue core biopsy in pancreatic cancer. *J Gastrointest Liver Dis*. 2016;25:213–218.
46. Larghi A, Fuccio L, Chiarello G, et al. Fine-needle tissue acquisition from subepithelial lesions using a forward-viewing linear echoendoscope. *Endoscopy*. 2014;46:39–45.
47. Larghi A, Lococo F, Ricci R, et al. Pleural tuberculosis diagnosed by EUS-guided fine-needle tissue acquisition. *Gastrointest Endosc*. 2010;72:1307–1309.
48. Larghi A, Lugli F, Sharma V, et al. Pancreatic metastases from a bronchopulmonary carcinoid diagnosed by endoscopic ultrasonography-guided fine-needle tissue acquisition. *Pancreas*. 2012;41:502–504.
49. Bang JY, Magee SH, Ramesh J, et al. Randomized trial comparing fanning with standard technique for endoscopic ultrasound-guided fine-needle aspiration of solid pancreatic mass lesions. *Endoscopy*. 2013;45:445–450.
50. Eckardt AJ, Adler A, Gomes EM, et al. Endosonographic large-bore biopsy of gastric subepithelial tumors: a prospective multicenter study. *Eur J Gastroenterol Hepatol*. 2012;24:1135–1144.
51. Diehl DL, Johal AS, Khara HS, et al. Endoscopic ultrasound-guided liver biopsy: a multicenter experience. *Endosc Int Open*. 2015;3:E210–E215.
52. Iwashita T, Yasuda I, Mukai T, et al. Macroscopic on-site quality evaluation of biopsy specimens to improve the diagnostic accuracy during EUS-guided FNA using a 19-gauge needle for solid lesions: a single-center prospective pilot study (MOSE study). *Gastrointest Endosc*. 2015;81:177–185.
53. Zamboni G, Lüttges J, Capelli P, et al. Histopathological features of diagnostic and clinical relevance in autoimmune pancreatitis: a study on 53 resection specimens and 9 biopsy specimens. *Virchows Arch*. 2004;445:552–563.
54. Ricci R, Chiarello G, Attili F, et al. Endoscopic ultrasound-guided fine needle tissue acquisition biopsy samples do not allow a reliable proliferation assessment of gastrointestinal stromal tumours. *Dig Liver Dis*. 2015;47:291–295.
55. Corless CL, Barnett CM, Heinrich MC. Gastrointestinal stromal tumours: origin and molecular oncology. *Nat Rev Cancer*. 2011;11:865–878.
56. Eisenberg BL, Smith KD. Adjuvant and neoadjuvant therapy for primary GIST. *Cancer Chemother Pharmacol*. 2011;67(Suppl 1): S3–S8.
57. Larghi A, Iglesias-Garcia J, Poley JW, et al. Feasibility and yield of a novel 22-gauge histology EUS needle in patients with pancreatic masses: a multicenter prospective cohort study. *Surg Endosc*. 2013;27:3733–3738.
58. Iwashita T, Nakai Y, Samarasena JB, et al. Endoscopic ultrasound-guided fine needle aspiration and biopsy (EUS-FNAB) using a novel 25-gauge core biopsy needle: optimizing the yield of both cytology and histology. *Gastrointest Endosc*. 2012;75:AB183.
59. Petrone MC, Poley JW, Bonzini M, et al. Interobserver agreement among pathologists regarding core tissue specimens obtained with a new endoscopic ultrasound histology needle; a prospective multicentre study in 50 cases. *Histopathology*. 2013;62:602–608.
60. Bang JY, Hebert-Magee S, Trevino J, et al. Randomized trial comparing the 22-gauge aspiration and 22-gauge biopsy needles for EUS-guided sampling of solid pancreatic mass lesions. *Gastrointest Endosc*. 2012;76:321–327.
61. Hucl T, Wee E, Anuradha S, et al. Feasibility and efficiency of a new 22G core needle: a prospective comparison study. *Endoscopy*. 2013;45:792–798.
62. Witt BL, Adler DG, Hilden K, et al. A comparative needle study: EUS-FNA procedures using the HD ProCore and EchoTip 22-gauge needle types. *Diagn Cytopathol*. 2013;41:1069–1074.
63. Vanbiervliet G, Napoléon B, Paul MCS, et al. Core needle versus standard needle for endoscopic ultrasound-guided biopsy of solid pancreatic masses: a randomized crossover study. *Endoscopy*. 2014;46:1063–1070.
64. Kim GH, Cho YK, Kim EY, et al. Comparison of 22-gauge aspiration needle with 22-gauge biopsy needle in endoscopic ultrasonography-guided subepithelial tumor sampling. *Scand J Gastroenterol*. 2014;49:347–354.
65. Lee YN, Moon JH, Kim HK, et al. Core biopsy needle versus standard aspiration needle for endoscopic ultrasound-guided sampling of solid pancreatic masses: a randomized parallel-group study. *Endoscopy*. 2014;46:1056–1062.
66. Strand DS, Jeffus SK, Sauer BG, et al. EUS-guided 22-gauge fine-needle aspiration versus core biopsy needle in the evaluation of solid pancreatic neoplasms. *Diagn Cytopathol*. 2014;42:751–758.
67. Berzosa M, Villa N, El-Serag HB, et al. Comparison of endoscopic ultrasound guided 22-gauge core needle with standard 25-gauge fine-needle aspiration for diagnosing solid pancreatic lesions. *Endosc Ultrasound*. 2015;4:28–33.
68. Mavrogenis G, Weynand B, Sibille A, et al. 25-gauge histology needle versus 22-gauge cytology needle in endoscopic ultrasonography-guided sampling of pancreatic lesions and lymphadenopathy. *Endosc Int Open*. 2015;3:E63–E68.
69. Aadam AA, Wani S, Amick A, et al. A randomized controlled cross-over trial and cost analysis comparing endoscopic ultrasound fine needle aspiration and fine needle biopsy. *Endosc Int Open*. 2016;04:E497–E505.
70. Sterlacci W, Sioulas AD, Veits L, et al. 22-gauge core vs 22-gauge aspiration needle for endoscopic ultrasound-guided sampling of abdominal masses. *World J Gastroenterol*. 2016;22:8820–8830.
71. Attam R, Arain MA, Bloechl SJ, et al. “Wet suction technique (WEST)”: a novel way to enhance the quality of EUS-FNA aspirate. Results of a prospective, single-blind, randomized, controlled trial using a 22-gauge needle for EUS-FNA of solid lesions. *Gastrointest Endosc*. 2015;81(6):1401–1407.
72. Rodrigues-Pinto E, Jalaj S, Grimm IS, Baron TH. Impact of EUS-guided fine-needle biopsy sampling with a new core needle on the need for onsite cytopathologic assessment: a preliminary study. *Gastrointest Endosc*. 2016;84:1040–1046.



**Video 21.1** Technique of Endoscopic Ultrasound-Guided Fine-Needle Tissue Acquisition Using a Standard 19-G Needle



**Video 21.3** Technique of Endoscopic Ultrasound-Guided Fine-Needle Biopsy Using the SharkCore Needle



**Video 21.2** Technique of Endoscopic Ultrasound-Guided FNB Using a 25-G ProCore Needle in Conjunction With the Stylet-Pull Technique



**Video 21.4** Technique of Endoscopic Ultrasound-Guided Fine-Needle Biopsy Using the Acquire Needle

# Cytology Primer for Endosonographers

DARSHANA JHALA AND NIRAG JHALA

## KEY POINTS

- Communication between the endosonographer and the cytopathologist is the key to a successful endoscopic ultrasonography-guided fine-needle aspiration (EUS FNA) service.
- A cytopathology service should be involved early in the planning process for establishing an EUS FNA service.
- Using an algorithmic approach to diagnosing a patient will facilitate a correct diagnosis.

Conceptual breakthroughs, based on developed theories, and discoveries in science bring accolades. Advances in the biotechnology field are signs of the dominance of creative imagination expressed through technology over abstract conceptual thinking. Despite such subtle differences in the concepts put forth, most clinicians involved in patient care agree that advances in the biomedical sciences have significantly broadened horizons and have redefined patient management.

The field of endoscopic ultrasonography (EUS)-guided fine-needle aspiration (FNA) should be viewed as no different. It could be said that the keystone events in the development of modern endosonography were the conceptualization and production of flexible endoscopes for human use in the late 1950s.<sup>1</sup> In the 1980s, ultrasound probes were attached to endoscopes, and Doppler imaging capability was introduced. These improvements allowed better visualization of lesions and an understanding of vascular flow. These powerful scopes could characterize lesions not only of the luminal gastrointestinal tract, but also of the gastrointestinal tract wall, the peri-luminal lymph nodes (intrathoracic and intraabdominal), the pancreas, the liver (mostly the left side), the left kidney, the spleen, and the adrenal glands. The list continues to grow.<sup>2–6</sup> EUS imaging alone, however, may not be sufficient to differentiate neoplastic from nonneoplastic and a benign from malignant lesion.<sup>7</sup> Further advances in technology made since the early 1990s permit the performance of FNA under EUS guidance.<sup>8,9</sup> The ability to obtain cytologic material safely under real-time visualization makes this a powerful modality that offers an opportunity for prompt and accurate diagnosis and staging.

The outcome of the EUS FNA diagnosis depends on effective collaboration between the cytopathologist and endoscopist. The best results are achieved by those clinicians who really believe in cytology for their own patients and who work in close cooperation with cytologists. Thus an understanding of relevant issues by both endosonographers and cytopathologists involved in obtaining and interpreting cytologic specimens optimizes the diagnostic

yield.<sup>3,10</sup> When such visions are synchronized, the diagnostic performance of EUS FNA far exceeds expectations.<sup>11</sup> As predicted earlier,<sup>2</sup> this technique has now become a standard of care at many institutions and continues to replace other modalities for tissue diagnoses, staging, and adequate management of patients.

The objective of this chapter is to help both endosonographers and cytopathologists learn the technical aspects of cytology procedures and to understand the basic principles of interpretive cytopathology diagnosis. Thus the chapter reviews pertinent technical aspects that may influence cytology interpretation and affect outcome. It also discusses the algorithmic approach and salient cytologic features of benign and malignant lesions commonly sampled by EUS FNA.

## Technical Aspects of Endoscopic Ultrasonography That Improve Diagnostic Yield

Fundamental to the success of EUS FNA is the procurement of adequate cells to provide the most effective diagnosis and potential for additional management. This requires careful planning and understanding of factors that can affect cellularity of the target lesion.

### Preliminary Planning

Ideally, an interested pathologist should be involved in the development of the EUS FNA service from the earliest stages of the planning process. This includes such crucial factors as the location of the endosonography suite, the type of instrument and needle used, the personnel involved, the scheduling of FNA, the type of preparation, the transport medium, the need for immediate cytologic evaluation (ICE) or rapid onsite specimen evaluation (ROSE) for determination of adequacy and diagnosis, the need for performing ancillary studies, and the role of the procedure in the patient management algorithm (Table 22.1). Further planning should also involve ordering of supplies, stocking and provision of the FNA cart or cabinet, or maintenance of a permanent small space for supplies in the endoscopy suite area.

The type of tissue specimen preparation (direct smear, liquid-based cytologic preparation, cell block, core biopsy, or a combination) depends on institutional practice, staffing issues, and the physical distance between the pathologist and the endoscopy suite, in addition to the relative sensitivity, specificity, and diagnostic accuracy of the various choices. If needed, based on physical location and personnel availability, one should strongly consider use of real-time telepathology system for ICE or ROSE. Developing adequate skills for accurate interpretation of EUS samples

not only depends on an experienced cytopathologist but may also require additional specific experience in interpreting these samples in a high volume service. Experience indicates that cytopathologists who are specifically interested in gastrointestinal diseases tend to be more effective in providing accurate diagnoses.<sup>12</sup>

**TABLE 22.1** Factors to Consider in Preliminary Planning for Cytology Services

Factor	Details
Type of biopsy	Needle core or cytology (fine needle)
Size of needle	25 G, 22 G, 19 G, or other
Fixation or processing for cores	Formalin, other
Type of preparation of cells for FNA	Direct smears, transport media (proprietary, culture media [RPMI-1640], formalin, other)
Type of smear	Air-dried, alcohol-fixed, or both
Personnel	GI suite staff, laboratory staff, training
Immediate cytologic assessment	Cytopathologist, cytotechnologist, advanced trainee, not performed
Database archives for cytology information	Diagnosis, number of passes, pathologist, type of smears prepared, cell block available, special studies

FNA, Fine-needle aspiration; GI, gastrointestinal.

For the pathologist and laboratory staff, a comprehensive understanding of their direct role in the EUS procedure and the patient care algorithm ensures appropriate support. Diagnostic strategies depend on whether the procedure is a screening test, a diagnostic test in a patient who may not undergo further diagnostic workup, or a test to procure material for performance of ancillary studies to enhance patient management decisions.

A further preliminary planning step is consideration of database archives of cytology and diagnostic data. In combination with the EUS characteristics of lesions and other clinical information, these data can provide valuable feedback regarding diagnostic accuracy, individual practitioner competency, utility of ICE, and other quality assurance measures.

Professional staff should be properly trained and should understand the limitations of their expertise and of the technique. In the United States, both the technical and the interpretive services in the cytology laboratory are regulated at state and federal levels by the provisions of the Clinical Laboratory Improvement Amendments, the Laboratory Accreditation Program of the College of American Pathologists (CAP), and others. Such mandatory and voluntary standards ensure high-quality laboratories.

The following sections discuss technical factors that may improve diagnostic yield for EUS biopsy procedures, including needle type and size, suction or “capillary” aspiration, number of passes, and direction of passes. These factors are listed in Table 22.2.

## Fine-Needle Aspirates

Fine-needle aspirates are used widely for EUS, computed tomography (CT), and other image-guided biopsy techniques, as well as for percutaneous biopsies of palpable masses. The material

**TABLE 22.2** Technical Aspects That May Positively Influence Diagnostic Yield

Technical Feature	Advantage	Disadvantage
Preliminary planning	Optimal laboratory support	None
Endoscopist skill	More likely to procure adequate specimen	None
Pathologist skill	Few if any false-positive or “atypical” diagnoses	None
Core biopsy	Histologic diagnosis	Possible more tissue injury
	Tissue for special stains	No capacity for on-site evaluation for adequacy
	Does not require on-site laboratory personnel for specimen processing or evaluation	
Aspiration biopsy	More cells	Few disadvantages
		Risk of inadequate sample for some lesions or sites
Smaller needle size	Less tissue injury	Relatively fewer cells
Suction	Retrieves more cells	Increases bleeding in tissue
		May compromise some cell features
More passes	More cells	Injury to tissue
Cytopathologist in room	Specimens adequate for diagnosis	Time and cost
Air-dried and alcohol-fixed smears	Complementary stains yield optimal nuclear and cytologic detail	Increased technical effort required
Cell block	Tissue available for special stains	Not a stand-alone preparation; best in combination with smears

contained within a fine-needle aspirate is usually smeared onto slides, and the resulting monolayer of cells is immediately fixed or dried and stained. Material obtained from a fine needle is generally dispersed as single and small groups of cells, rather than intact tissue cores. As the preparation is not sectioned, the cells represented on an aspirate smear are intact. Thus cells round up or splay out, depending on how they are treated in further processing steps. The monolayer smears prepared from fine-needle aspirates are very important to decipher details of the nucleus and cytoplasm that is superior to many other modalities.

Recently new developments have allowed acquisition of core biopsies utilizing endoscopy ultrasound-guided route. These samples have the advantage of providing tissue architecture.

## Choice of Needles

Fine needles are defined as needles that have 22 G or smaller bore. Varying sizes of EUS instruments and needles are available on the market, and the choice of needle may also influence cytology findings. The cutting edge of the needle plays a role in obtaining samples; for example, a beveled edge requires less force in comparison with circular edges. Similarly, needle sizes also have an impact on the procurement of tissue samples. In current practice, EUS needles range from 19 G to 25 G.<sup>13–15</sup> Contrary to intuitive thinking that larger size is always better for FNA samples, sometimes the smaller-bore needle provides better sampling.

Several prospective studies and meta-analysis of published literature have been attempted to determine the impact on cell yield and diagnostic performance of samples obtained by the various EUS FNA needle types.<sup>14–18</sup> Some of these investigators suggested that needle aspirates from 25-G needles provide less hypocellular or acellular and bloody specimens, have better diagnostic performance, and perhaps induce less tissue injury in comparison with samples from a 22-G needle.<sup>14,15,19</sup> Other investigators, however, could not independently confirm this finding and found either no or minimal difference between 22-G and 25-G needles with regard to the ability to render a diagnosis.<sup>13,17,20</sup>

FNA samples are also increasingly used for ancillary studies. In a study designed to determine the optimum needle size and number of passes to obtain material for RNA quantitation, the number of cells obtained from needles of varying sizes was counted. With 10 needle excursions into a tumor, 32,000 cells were obtained with a 25-G needle.<sup>21</sup> Although large numbers of cells are important for some tests, such as RNA extraction, it is generally accepted that diagnoses can be made on smears containing fewer than 100 cells. Investigators have suggested that a larger needle (e.g., 22 G) may be useful for lesions associated with less risk of complication or that require large numbers of cells for classification. Unraveling of underlying molecular targets that may affect diagnosis, prognosis, or therapeutic predictions are increasingly being characterized. This has resulted in increased utilization of small tissue samples in performance of molecular tests such as fluorescence in situ hybridization (FISH) analysis, pyrosequencing, and newer platforms to generate genetic profiles utilizing techniques such as next-generation sequencing (NGS).<sup>22–24</sup> As a unique technique, the authors have also destained Diff-Quik-stained smears and performed FISH analysis to detect specific chromosomal translocations in lymphomas to improve diagnostic performance.<sup>25</sup> This method has the clear advantage of making a morphologic determination and then using the same cells for detection of characteristic chromosomal translocations to clinch the diagnosis.

Given the tradeoff between more cells and more complications with larger fine needles, the choice of needle size should be based on

the site and type of lesion to be aspirated. Indications for a smaller needle (e.g., 25 G) include patients with coagulopathy, organs in which leakage of fluid or air may occur, organs in which tissue trauma may increase complications (e.g., pancreas), and vascular organs or lesions. A smaller needle size decreases potential complications such as bleeding into the tissue and hemodilution or obscuring of the cytology sample by excessive blood. Smaller needles also cause less tissue damage and thus possibly less risk of pancreatitis.

## Needle Core Biopsy Versus Fine-Needle Aspiration

Unlike many cytopathologists, for several reasons some clinicians and surgical pathologists believe that a tissue core yields unequivocally better diagnostic material. This belief perhaps stems from the concept that tissue cores will result in adequate samples with fewer needle passes, they do not involve on-site specimen assessment, they provide architecture, and ancillary studies can be performed on these samples.<sup>11,26–28</sup> It is also true that needle core biopsies (14 G to 19 G) have been used for a long time to obtain tissue samples. Sections made from these core biopsies are thin, 3- to 5-μm slices of the tissue that, when stained and viewed microscopically, show cells or portions of cells within their intact tissue stroma. Most histopathologists are very familiar with this method of tissue-based assessment and therefore promote the use of core needle biopsy samples.

Conversely, however, one should also be aware that analysis of tissue core may not always provide adequate diagnostic clues. Tru-Cut biopsy also induces greater tissue injury than a fine-needle biopsy and is considered more invasive. Such considerations should deter clinicians from using large-bore Tru-Cut needles routinely. It is also true that needle core biopsies can pose greater challenges for diagnosing well-differentiated carcinomas of the pancreas in comparison with FNA samples. In preliminary analyses, the success of FNA sampling using EUS guidance led to a sharp decline in performance of percutaneous needle core biopsies and CT-guided FNA. Such a change dramatically altered practice management decisions for pancreatic neoplasms.

A possible explanation for the failure of core needles to sample the lesion may be the attributes of the lesion itself, given that a larger needle may deflect from the surface of a firm or rubbery lesion. In addition, a Tru-Cut biopsy represents a single pass into the tissue and is not able to sample the lesion widely without further passes into the tissue. The use of larger needles increases the risk of bleeding and complications, although these risks remain very low. In addition, technical limitations of the currently available EUS-guided Tru-Cut biopsy equipment limit the anatomic regions that can be sampled for biopsy successfully.

The use of EUS-guided Tru-Cut biopsies has recently demonstrated a significant promise in review of lymphadenopathy as well as from other solid organs. Tru-Cut biopsy is useful not only to establish the diagnosis of lymphoma but also to characterize cellular architecture, which is more important in disorders such as follicular center cell lymphomas. Tru-Cut biopsy also may be more useful in cases in which flow cytometry results can provide false-negative results, such as large B-cell lymphomas.<sup>25</sup> EUS-guided Tru-Cut biopsy may also be helpful in establishing the difficult diagnosis of Hodgkin lymphoma, in which morphology is varied and often challenging to identify. Needle core biopsies are also very useful for lesions rich in stroma such as gastrointestinal tract stromal tumors. Epithelial rich lesions such as most carcinomas are amenable to aspirations.

Recently, newer biopsy needles have been introduced to procure samples with minimal fragmentation, thereby retaining

architecture. Histologically, an ideal core has uninterrupted structure or architecture, whereby cell groups maintain their interface with extracellular matrix or stroma. Architecture can be crucial to the definitive diagnosis and/or staging. Three needles are being utilized more frequently in today's practice which include reverse bevel needles (Procore, Cook Endoscopy, Winston Salem, North Carolina), fork-tip needles (Shark Core, Medtronic Corp., Boston, Massachusetts), and Franseen tip needles (Acquire, Boston Scientific, Marlborough, Massachusetts). Initial assessment of Procore needles; 25-G, 22-G, 19-G fork-tip needles (Shark Core, Medtronic Corp., Boston, Massachusetts); and the 22-G Franseen tip needle (Acquire, Boston Scientific, Marlborough, Massachusetts) has demonstrated a strong promise in tissue acquisition studies. Their performance from pathologist review perspectives, however, has not been adequately assessed.

The decision to obtain cores instead of, or in addition to, aspirates rests on certain factors, including the available equipment and personnel, the training and expertise of the pathologists and staff, and the endoscopist's preference. Each type of biopsy has advantages and disadvantages that must be considered for individual lesions or patients. Overall, FNA is considered a more sensitive diagnostic method, and it can be complemented by core biopsy or cell block.

## To Apply or Not to Apply Suction

For many fine-needle biopsies, suction is applied to the needle to attempt to increase cell yield. This is the origin of the term *fine-needle aspirate*, which is often used more generally for any fine-needle biopsy. The purpose of suction is not to draw cells into the needle, but rather to "hole" the tissue against the cutting edge of the needle. Suction should be turned off before the needle is withdrawn.

In another technique, the cells are obtained without applying suction. The lumen is filled with cells by the direct cutting action of the needle through the tissue or capillary action. A study of 670 superficial and deep lesions sampled by biopsy with a fine needle without suction showed that diagnostic material was obtained in more than 90% of the cases.<sup>29</sup> Specific to EUS FNA, a study by Wallace and colleagues<sup>30</sup> found no difference in suction versus no suction in terms of overall diagnostic yield for lymph nodes, but these investigators noted excess blood in the specimens to which suction was applied. Another study demonstrated that EUS-guided fine-needle sampling with suction increased the number of slides ( $17.8 \pm 7.1$  slides) needed to be prepared, as compared with a significantly ( $P < .0001$ ) reduced number of slides to be prepared for samples in which no suction was applied.<sup>31</sup>

In general, applying suction to the needle increases cellular yield but potentially increases artifact and blood, especially in vascular organs and lesions. Suction is commonly used because the increased cellular yield of specimens often outweighs the disadvantages. Some clinicians attempt up to three passes without suction and add further passes with suction if the cellular yield is low. Although no suction improves analysis, the choice to use or not to use suction should be dictated by the type of lesion.<sup>32</sup>

When a large amount of blood is aspirated and the specimen clots, a less desirable but useful salvage of material is to gently microdissect the clot or fragment the clot with a scalpel blade or needle tip. The fragments are then lifted from the slide and are placed in formalin for subsequent cell block preparation. Forceful smearing of the clot to disperse the cells may cause significant crush artifact and may render the cells uninterruptible.

## Number of Passes

A pass usually comprises 10 or more needle excursions or movements of the needle to-and-fro once the needle is within the lesion. The number of passes needed to obtain diagnostic material depends on multiple factors, including experience of the endosonographer, location of the lesion, type of lesion, cellularity of the lesion, and risk of complications. Many investigators suggest that after a certain number of passes, the procedure reaches a state of diminishing returns for obtaining diagnostic cellularity.

The landmark study was performed earlier where the issues of number of passes and specimen adequacy rates were more carefully investigated in 204 cases. In our early analysis of more than 204 cases, diagnostic cellularity was obtained after five passes in more than 90% of cases. It also emerged in this study that the rate of diminishing returns was reached earlier for lymph nodes and later for the pancreas. For solid pancreatic lesions, adequate cellularity was achieved with fewer numbers of passes when the lesion was smaller ( $\leq 25$  mm) compared with larger lesions.<sup>33</sup> This study also demonstrated that after five passes, lymph nodes offered little benefit in obtaining diagnostic cells. It was also evident that for lymph nodes, a mean of only three passes was needed for obtaining diagnostic cellularity. LeBlanc and colleagues determined that at least seven passes were needed in pancreatic lesions to obtain a sensitivity and specificity of 83% and 100%, respectively, although only five passes were needed in lymph node aspirates for a respective sensitivity and specificity of 77% and 100%.<sup>34</sup> In recent years, better technique and experience and fellowships in advanced endoscopies have led to a reduction in the number of passes needed to procure adequate diagnostic cellularity.

A well-known advantage of real-time image-guided biopsies, especially EUS, is the ability to direct the needle to a small point of interest. Selection of the exact site of biopsy may influence the cytologic yield. Biopsy of the necrotic center of a tumor may be nondiagnostic, whereas the edge may contain viable tumor cells. Conversely, biopsy of the edge of a pancreatic carcinoma may show only chronic pancreatitis, a common reactive change in the surrounding pancreatic tissue.

Depending on the anatomic site, directing the needle to specific portions of the lesion may be advantageous. Metastatic tumor in lymph nodes may be histologically more apparent in the subcapsular sinus, but in lymph node aspirates evaluated by EUS FNA, aspiration of the edge of the node did not increase the likelihood of a correct diagnosis. Nonetheless, because EUS allows visualization of the lesion, biopsy of a necrotic area can be avoided, and as discussed later, on-site evaluation of the specimen can provide guidance to another location if the first site is necrotic.

A main advantage of the FNA technique is the wide sampling of a lesion by maneuvering the needle in different directions with each back-and-forth movement. Small redirections of the needle to make a fan shape will result in sampling of new areas of the lesion each time. Utilization of the fanning technique, as described in Chapter 20, in comparison to the standard multiple pass technique to obtain cells helps reduce the number of passes and improves diagnostic cellularity rates.<sup>35</sup> Repeated needle excursions in the same direction, along the same needle tract, result in biopsy of the blood or fluid that can fill the area with blood.

## Immediate Cytologic Evaluation

One way to ensure adequate material from an FNA procedure is the use of ICE (Video 22.1). The goal of ICE is to provide

real-time feedback about the content and quality of the smears, to reduce the number of nondiagnostic or atypical biopsies, and to maximize the efficiency of the procedure. We, as well as other investigators, have demonstrated that ICE yields increased highly reliable preliminary diagnosis and will also help triage the specimen for performing ancillary studies.<sup>36</sup> Other investigators have demonstrated that specimen adequacy is more than 90% when a cytopathologist is present in the endoscopy suite for ICE.<sup>33</sup> Such high specimen adequacy rates drop when cytopathologists are not present in the endoscopy suite for ICE.<sup>37</sup> In a direct comparison of EUS FNA procedures performed by the same endoscopist at two institutions, with and without a pathologist present during the procedure, ICE was more likely to result in a definitive diagnosis and less likely to involve an inadequate specimen.<sup>37</sup> Most false-negative EUS results are caused by inadequate sampling, which may necessitate a second procedure. It is also true that the most effective way to reduce a sampling error is ICE.

A retrospective analysis was conducted of changes noted after the transition from CT-guided FNA to EUS-guided FNA sampling from the pancreas. Cytopathologists were present to provide ICE in an endoscopy suite, whereas this practice was not in place for samples obtained under CT guidance. The results demonstrated that EUS FNA provided more definitive diagnoses and fewer unsatisfactory or equivocal diagnoses. The investigators were also able to procure additional samples for ancillary studies. Such efforts at other institutions have also seen greater than 90% specimen adequacy rates and reductions in equivocal diagnosis. When ICE is performed, selected air-dried slides are stained in the endoscopy suite or an adjacent room and are reviewed immediately by the pathologist, so that feedback can be given to the endoscopist regarding the adequacy of the pass. If diagnostic material is present, additional passes are not made, and the procedure is stopped. If the smears are nondiagnostic, further passes are made. If there are no cells or only necrosis, the needle can be redirected for the next pass, and the procedure can be continued until adequate material for diagnosis is obtained.

In addition to minimizing the number of passes needed to obtain diagnostic material, another advantage of ICE is the triage of specimens for special studies. Such a practice may allow for the procurement of samples for ancillary studies such as lymphoma workup or for cell block when the initial smears show a tumor that may need classification by immunohistochemistry, *in situ* hybridization, or other studies for better patient management. Thus obtaining additional directed passes is encouraged for creating an adequate cell block.

Although ICE clearly improves diagnostic yield, this practice is variable throughout the world. The use of ICE is influenced by the physical location of the laboratory and gastrointestinal suite, personnel, and cost issues. Reluctance of a pathologist to attend EUS FNA procedures may relate to lack of time and inadequate reimbursement for the time investment required.

Unfortunately, however, lack of will on the part of consumers of these services has not helped change the conventional stance on reimbursements in the United States. Instead, the reimbursement rates are increasingly becoming more cost prohibitive. All institutions and regions of any country are different, and they need to develop their own cost-effective strategies for the sake of providing optimal health care for their patients.

In an attempt to minimize the impact of the lack of ICE, different investigators, with variable success, have investigated alternatives. These alternatives include assessment of cellularity by visual inspection, performance of smears and evaluation

by endosonography personnel, and the use of services of advanced cytotechnologists following adequate training<sup>38,39</sup> or advanced trainees in cytopathology. In this context, the use of dynamic telecytology for adequacy assessment was also investigated.<sup>40-42</sup>

Regardless of whether ICE is used or not, an adequate sample is the foundation of the diagnosis. The needle must be placed into the lesion; the technical aspects of the sampling must be optimized to obtain cells for evaluation; and the smears must be free of crush, drying, staining, or other artifact, and obscuring blood, inflammation, or necrosis.

## Factors Associated With Improved Cytologic Preparation

The material from EUS-guided biopsy can be prepared in many different ways, each of which has advantages and disadvantages. Some preparations are complementary, and two or three types are often prepared from the same biopsy specimen. The following sections define preparation of air-dried and alcohol-fixed smears, cell block, and the stains used for highlighting various cell features.

### Cytology Smears and Cell Block

A smear slide is the standard method of preparing cells obtained from a fine-needle biopsy for viewing. As in a blood smear, the biopsy material is dispersed or “smeared” onto a glass slide, stained, and viewed as individual cells. For EUS FNA, after the needle is removed from the endoscope, the tip is placed near the frosted end of a labeled slide, and a single small drop is expressed onto the slide by slowly advancing the stylet into the needle. Dropping the material from a distance, squirting, or spraying it onto the slide can result in drying of the specimen and unwanted artifact. A second slide is then drawn over the drop of material, to pull the material into a monolayer. The technique requires practice. If the smear is too thick, the cells are obscured by one another or by background cells; if too much pressure is applied, the cells are artificially disrupted from their normal microarchitecture or are lysed. Imperfect smears may reduce the diagnostic yield. Another technique is called the “butterfly technique,” where a drop is placed in the center of the slide and two slides are placed at right angles such that the material spreads between two slides by capillary action. One slide is then air-dried and the counterpart is immediately fixed in alcohol for additional stains. No pressure is applied. This technique requires less technical expertise without compromising the quality of diagnosis.

Should one acquire tissue core biopsies, then one should firmly touch the core tissue to transfer cells on the slides. Firmly applying pressure to the core may result in squashing the tissue which may or may not provide optimal information.

In contrast to smears, a cell block is a preparation in which the cells are placed into a liquid medium or fixative, transported to the laboratory, spun into a pellet, formalin fixed, paraffin embedded, and selected for standard hematoxylin and eosin (H&E) staining. This routine formalin fixation and paraffin embedding is not optimal for preserving cytologic detail. A cell block is often made from leftover material rinsed from the needle. Its value as an adjunct to diagnosis can improve if an additional directed pass is obtained at the end of the procedure. This technique is highly recommended, especially for lesions that may require special stains.

## Air-Dried or Alcohol-Fixed Smears

Generally, smears prepared from FNA material are either air-dried or alcohol-fixed. Air-dried smears are stained rapidly (using a modified Romanowsky stain [e.g., Diff-Quik]) and are typically used for ICE. Some institutions use H&E or rapid Papanicolaou (Pap) stains for ICE.

Diff-Quik-stained, air-dried smear preparations highlight intracytoplasmic material and extracellular substances. Alcohol fixation causes cells to shrink and round up, but it preserves nuclear features and is followed by Pap or H&E staining. The Pap stain highlights nuclear detail and chromatin quality, in addition to demonstrating the keratinization of squamous cells. The cytoplasm appears more transparent in Pap-stained slides. Slides can be fixed in preparation for a Pap stain by immersing or spraying them with alcohol. The Pap and Diff-Quik stains are complementary, and optimal cytologic detail is provided when both alcohol-fixed and air-dried smears are prepared from the FNA.

## Transport Media and Liquid-Based Preparations

Samples are frequently collected in transport media for subsequent preparations. Although many media are available, Hank's balanced salt solution is preferred. This medium allows for the preparation of cytopsins and cell blocks, and should one require lymphoma consideration later, this medium can also be used for flow cytometric analysis. For consideration of any lymphoma workup, many institutions also collect their samples in RPMI 1640. This is also a useful medium to collect for cytogenetic analysis, as well as gene rearrangement studies.

Liquid-based cytology is now firmly embedded in clinical practices. Oftentimes when ICE/ROSE is not possible, these samples can be placed in the transport medium for cytologic interpretation. Several studies have suggested that this can obviate the need for ICE/ROSE. It is also becoming more evident that for pancreatic cysts utilizing this approach is more beneficial, which is increasingly being investigated. Currently two methods have been approved by the Food and Drug Administration: ThinPrep (Cytoc Co, Marlborough, Massachusetts) and SurePath (TriPath Inc., Burlington, North Carolina). There are slight differences between the two methods but both offer advantages of monolayer cell dispersion, elimination of obscuring mucus and blood, and consistent cell preparation without artifacts of preparation, as noted with smear preparations.

These techniques, however, increase the cost of preparation and cannot be used for ICE. Because the preparations may disaggregate cells (loss of architecture) and alter some cytologic details, they offer challenges to interpretation. Some of the proprietary liquid fixatives contain methanol, a coagulative fixative (rather than a protein cross-linking fixative such as formalin), which may lead to suboptimal fixation for immunohistochemistry. Liquid-based cytology preparations do not fare as well as direct smear preparations. However, liquid-based cytology offers a viable alternative when ICE is not a consideration. Samples from pancreas prepared using liquid-based cytology preparations demonstrated smaller cell clusters, smaller cell size in comparison with air-dried smears, better nuclear characteristics, and diminished or absent mucin. Furthermore, these samples could not be used at a later time for flow cytometry analysis. Such considerations should be taken into account during selection of transport media and preparations. A detailed model of an optimized EUS FNA procedure is shown in Table 22.3.

## Cytology Interpretation

Evaluation of the biopsy begins the moment material is expressed from the needle onto a slide or into a fixative. An adequate aspirate, or one that is likely to yield a diagnosis, is cellular, so that when placed on the slides and smeared out, a finely granular quality is apparent. In contrast, in a hypocellular or purely bloody smear, the thin sheen of material is smooth. When the material is placed in fixative, visible particulate matter or cloudiness is usually present. Mucus, pus, and necrosis may also be grossly apparent.

### Adequacy

Once under the microscope, the smear is first assessed for adequacy. For an aspirate to be interpretable, it must be free of technical artifacts and must contain cells for evaluation. A global assessment of cellularity as a measure of adequacy, however, may be misleading in FNA, because the number of cells relates to the lesion. For example, aspiration of neuroendocrine tumors usually yields highly cellular smears, whereas aspiration of a gastrointestinal stromal tumor (GIST) may yield few cells but both may be equally adequate for diagnosis.

For diagnostic nongynecologic cytology specimens, a sample is adequate when it explains the clinical situation or target lesion. The aspirator must be certain that the lesion has been sampled, and the pathologist must be able to interpret the slides. The concept of the "triple test" is also applicable to EUS FNA. The clinical, imaging, and FNA findings should agree and correlate on whether the lesion is benign or malignant. Some lesions have characteristic morphologic features, and therefore a cell number criterion for such tumors is not a requirement.

## Diagnostic Evaluation of the Slide

Whether on-site or in the laboratory, the cytotechnologist or pathologist begins the slide evaluation by assessing the cell types, cell arrangement, and cellular features on the smear. Central to a cytology diagnosis is the appearance of the nuclear and cytoplasmic features of individual cells; these are quite distinct, depending on the lesion sampled. No single feature is diagnostic of malignancy, but rather the composite picture of cell type, microarchitecture, and nuclear and cytoplasmic characteristics determines the diagnosis. It is useful to know the common pathologic diagnoses as well as the characteristic of the normal tissue in the region sampled (Table 22.4 and Fig. 22.1).

As in histologic sections, order and aesthetics reign in cytologic preparations of benign tissue. The appearance and composition of a benign aspirate reflect the various cell populations in normal tissue. Epithelial cells are round to oval, have moderate to abundant cytoplasm, and are cohesive. Benign epithelial cells show evidence of differentiation. Squamous cells acquire keratin as they mature, whereas their nuclei become progressively smaller and darker (pyknotic). A benign superficial squamous cell exfoliated from the esophagus has a large, polyhedral shape, with a small, uniformly dark, nucleus described as an "ink dot" (Fig. 22.2). The cytoplasm is orange-pink to blue, depending on the degree of keratin accumulation. Benign, mature squamous cells appear single, unless they are from the deeper layers of the epithelium, in which case they may remain together as large sheets of cells with less keratinization of the cytoplasm. Benign glandular epithelium from the stomach (Fig. 22.3), intestine, and pancreas also demonstrates an orderly arrangement of differentiated cells with organ-specific variations. In smears, duodenal epithelium consists of folded or draped sheets of columnar

cells, with interspersed goblet cells appearing as clear spaces among the absorptive cells (Fig. 22.4). Glandular cells are polarized, with the nucleus present at one end of each cell in the sheet of epithelium. The cytoplasm may be filled with a single mucin droplet (the goblet cell), smaller more finely divided vacuoles, or other secretory products such as zymogen granules. Classically, benign columnar epithelium has a honeycomb pattern. Changing the microscope plane to focus reveals the hexagonal borders of the apical cytoplasm and polarized, orderly nuclei at the base of the honeycomb sheet. In contrast, benign stromal or mesenchymal cells have elongated nuclei and usually abundant cytoplasm. Occasionally, small vascular structures are visible in smears of benign tissue.

The cells represented in an aspirate of normal tissue are proportionate to their mixture in the organ. For example, benign pancreatic tissue is composed mostly of acini, with relatively few ductal structures (Fig. 22.5) and islets usually represented on FNA smears. A benign reactive lymph node (Fig. 22.6) contains a polymorphic mixture of cell types, with large and small lymphocytes, macrophages, and sometimes identifiable germinal centers, whereas lymphoid malignancy is usually monomorphic. In contrast to the order inherent in benign tissue, malignant cells deviate

in their organization and demonstrate predictable unpredictability in architecture.

Normal epithelial cells exhibit cohesion, whereas malignant epithelial cells are loosely aggregated or single cells. The degree of dyshesion is relative and is an important criterion in the overall assessment of malignancy. In contrast to epithelial cells, some tissue types are normally dyshesive. Unlike carcinomas, which reveal cohesive cell clusters and many single cells, FNA from noncarcinoïd tumors and melanoma are usually noted as single cells. An overzealous smearing technique may artificially separate epithelial cells and may lead to overestimation of dyshesion.

Malignant cells also exhibit disorganization of their normal arrangement of polarity. The loss of polarity is a particular diagnostic feature in lesions arising in columnar epithelium. An important EUS FNA example is the diagnosis of atypia or malignancy in mucinous neoplasms. Once the low-power assessment of the general characteristic of the smear has been evaluated for cell types, overall organization, cohesion, and detailed analysis of the nucleus and cytoplasm allow for the characterization of a cell as benign or malignant. Specific nuclear features determine malignancy, whereas cytoplasmic features and microarchitecture demonstrate differentiation of the cell.

**TABLE 22.3**

### Optimized Endoscopic Ultrasonography Fine-Needle Aspiration Model Technique

Stage	Description
Preparation	When the procedure is scheduled, arrangements are made for the cytology technician and pathologist to be at the site. Clinical findings are discussed with the pathologist at the start of the procedure. The locations of the lesions or other details must be known, based on previous imaging studies. Conscious sedation is provided to the patient with intravenous meperidine and midazolam.
Needle preparation	The stylet is removed completely from a 22-G EUS FNA needle, and the needle is flushed with heparin. Air is then flushed through the needle to expel the excess heparin. The stylet is replaced, and the needle is ready for use. The needle may also be straightened manually between passes if necessary.
Radial EUS	A radial echoendoscope is first used for an overview of appropriate anatomic landmarks. The location of lesions is noted.
Linear array EUS FNA	The radial echoendoscope is replaced with a linear array echoendoscope. The scope is advanced to the distance at which the lesion of interest was identified with radial endosonography. The lesion is visualized, and color Doppler is used if there is concern about intervening blood vessels. The EUS FNA needle is inserted and fastened to the biopsy channel of the echoendoscope, and then it is advanced just slightly beyond the scope into the gut lumen. At this point, the stylet is retracted approximately 1 cm. The needle is passed into the lesion. The stylet is replaced into the needle to expel any tissue from normal structures and then is removed completely, and a suction syringe is attached. Sampling is performed with and without suction. The needle is moved into various locations throughout the lesion ("fanning the lesion") to improve sampling. After approximately 20 back-and-forth movements, the suction is turned off, the needle is retracted back into the catheter, and the entire assembly is removed.
Expressing material on slide	A dedicated cytology technician holds the end of the catheter over a labeled glass slide. The needle is advanced approximately 1 cm from the catheter by the endoscopy technician, and a stylet is slowly advanced back into the needle. This produces a controlled passage of drops of material out from the tip. The cytology technician alternately places drops onto a slide and into transport medium. Finally, the needle is flushed with a few milliliters of saline and then air to expel any remaining material into the liquid medium.
Preparing and staining cytologic material	Slides are prepared depending on the amount of material. As rapidly as possible, the drops of aspirated material are spread downward onto the slides by using another clean glass slide. Half of the slides are air-dried, and the remaining slides are immediately immersed in 95% ethyl alcohol for later Papanicolaou staining. The air-dried slides are stained with Diff-Quik stain for immediate cytologic evaluation by the pathologist (see later in the chapter). When the procedure is finished, an additional dedicated pass may be placed in transport medium (e.g., Hank's balanced salt solution) and transported to the laboratory, and a cell block is prepared. The material in cell suspension is centrifuged into a pellet, to which thrombin is added. The pellet is resuspended, and the resulting clot is removed, wrapped in lens paper, placed in a tissue cassette, fixed in formalin, and routinely processed for paraffin embedding and H&E or immunostaining. If indicated, material for flow cytometric immunophenotyping or other studies is removed from the medium, and the cell block is prepared. The alcohol-fixed slides are stained with a standard Papanicolaou stain.
Immediate cytologic evaluation	A pathologist, advanced trainee, or experienced cytotechnologist examines air-dried Diff-Quik-stained slides prepared at the site and provides assessment of specimen adequacy. Based on this report, the endoscopist may continue with the same technique or may change needle position to procure more tissue. Immediate cytologic evaluation also helps triage the specimen or obtain additional passes for special studies.

EUS, Endoscopic ultrasonography; FNA, fine-needle aspiration; H&E, hematoxylin and eosin.

## Endoscopic Ultrasonography Fine-Needle Aspiration of Specific Sites

The usefulness of EUS FNA in various organ systems and the associated pitfalls in diagnostic interpretation are discussed in the following sections.

### Pancreas

EUS is, in itself, a highly effective modality for detecting, staging, and determining respectability of pancreatic carcinomas. FNA was documented to be as accurate as frozen section diagnosis and

is less invasive, faster, and more cost effective for the diagnosis of both resectable as well as nonresectable pancreatic carcinomas. Investigators also showed that EUS FNA is better than percutaneous FNA for obtaining an accurate preoperative diagnosis. The objectives of EUS FNA of lesions of the pancreas are to obtain the initial diagnosis of a clinically suspicious malignant neoplasm, to obviate the need for surgery for the purpose of obtaining tissue for diagnosis, and to obtain tissue confirmation of the diagnosis before surgical resection with curative intent or initiating adjuvant chemotherapy. As a result, this modality has now found its rightful place as a preferred technique for obtaining tissue diagnosis and confirmation by the members of the National Comprehensive Cancer Network.

### Global Approach to Diagnosis

Authors have developed an algorithmic approach also known as “Jhala algorithm” for diagnosis of pancreatic lesions (Fig. 22.7). This algorithm-based approach to the diagnosis of pancreatic FNA may result in a better diagnostic workup and determine the need for additional ancillary studies to confirm and support the diagnosis (see Fig. 22.7). This is utilized by cytopathologists in various countries with success. What treating clinicians want to know from a cytologist is whether a given lesion is benign or malignant. This determination and the associated differential diagnosis generally rest on the imaging characteristics of the lesion (solid vs. cystic pancreatic lesion).

Table 22.5 demonstrates more common lesions that should be considered in the differential diagnosis of solid pancreatic lesions. When a solid pancreatic mass in an older patient is noted, the major differential diagnosis remains pancreatic adenocarcinoma versus chronic pancreatitis.

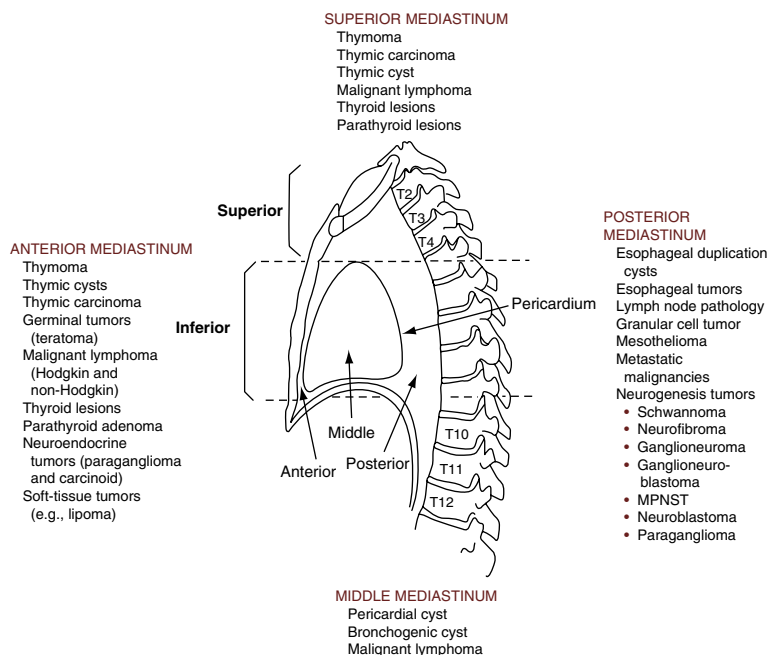
### Pancreatic Adenocarcinoma and Chronic Pancreatitis

Distinguishing chronic pancreatitis from pancreatic carcinoma is not a diagnostic challenge when cellular features are characteristic. This is more challenging for cytopathologists when a well-differentiated pancreatic adenocarcinoma is aspirated. Diagnostic

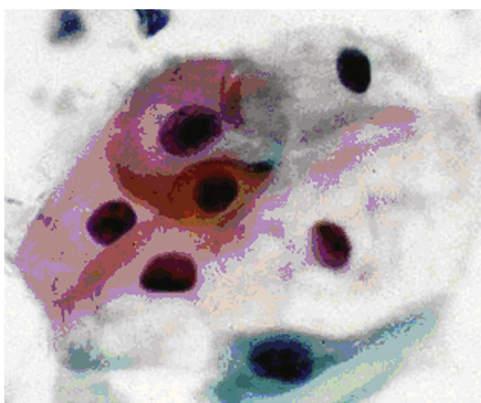
**TABLE 22.4 Some Common Endoscopic Ultrasonography Cytologic Diagnoses in Specific Sites**

Site	Cytologic Diagnoses
Lung	Adenocarcinoma, squamous carcinoma, small cell carcinoma, granuloma or infection
Esophagus	Squamous carcinoma, adenocarcinoma, granular cell tumors, leiomyoma or other spindle cell tumors (GIST or neurofibroma)
Stomach	Carcinoma, carcinoid, GIST, MALT lymphoma
Pancreas	Ductal adenocarcinoma, chronic pancreatitis, autoimmune pancreatitis, pancreatic endocrine neoplasm, metastatic carcinoma, intraductal papillary mucinous neoplasm, mucinous cystic neoplasm, solid pseudopapillary tumor
Rectum and perirectal lymph nodes	Metastatic adenocarcinoma or squamous carcinoma, GIST
Liver	Metastatic carcinoma, melanoma, sarcoma, lymphoma, primary hepatocellular tumors

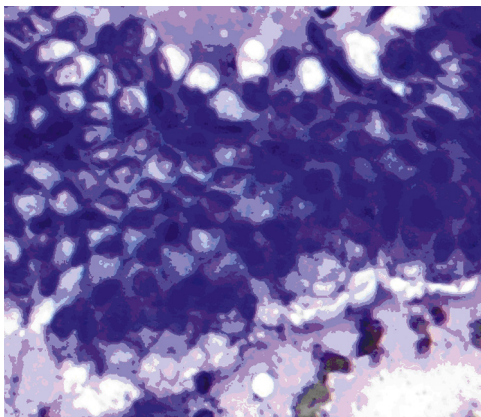
GIST, Gastrointestinal stromal tumor; MALT, mucosa-associated lymphoid tissue.



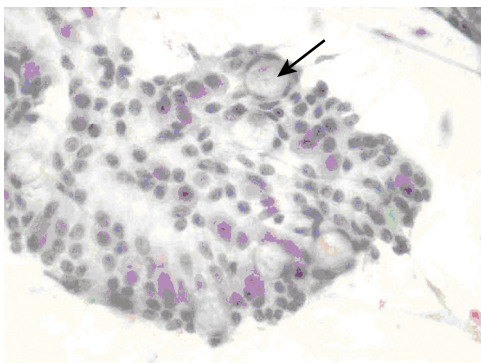
• Fig. 22.1 Common lesions of the mediastinum. MPNST, Malignant peripheral nerve sheath tumor.



• **Fig. 22.2** Sample from the esophageal squamous mucosa showing polygonal cells with abundant hard cytoplasm with hyperchromatic nuclei. Squamous cells also show maturation, as evidenced by keratinization.

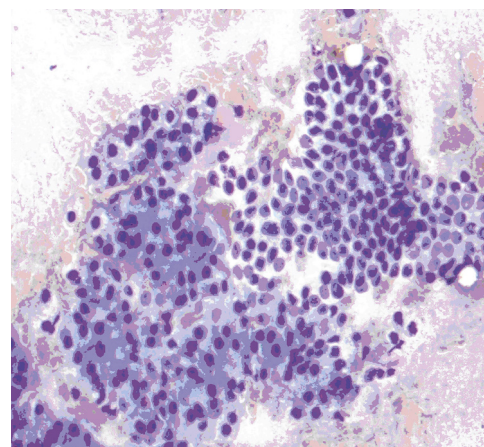


• **Fig. 22.3** Smears from the gastric mucosa reveal foveolar cells with cohesive cell groups with minimal overlapping. The cells show a columnar shape with nuclei lined at the base. They also show a round, regular nuclear membrane and inconspicuous nucleoli, if any (Diff-Quik stain; magnification  $\times 20$ ).

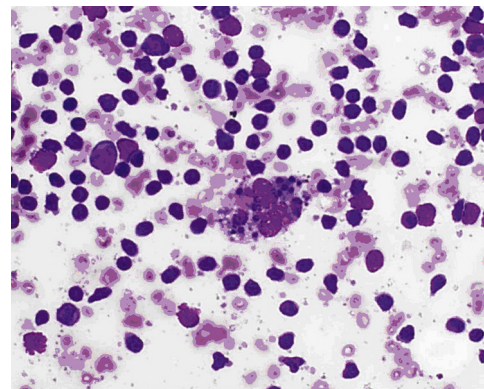


• **Fig. 22.4** Smear reveals a cohesive two-dimensional group of epithelial cells with a honeycomb appearance. The group also reveals interspersed goblet cells (arrow) consistent with surface duodenal mucosal cells (Papanicolaou stain; magnification  $\times 40$ ).

criteria for pancreatic adenocarcinoma have been described in the literature, and they include the following: increased cellularity, the predominance of a single cell type; three-dimensional groups (overlapping cells), a “drunken honeycomb” appearance (Fig. 22.8), swirling of cells in well-differentiated carcinomas, the presence of many pleomorphic single cells (Fig. 22.9), tall cells with large nuclei

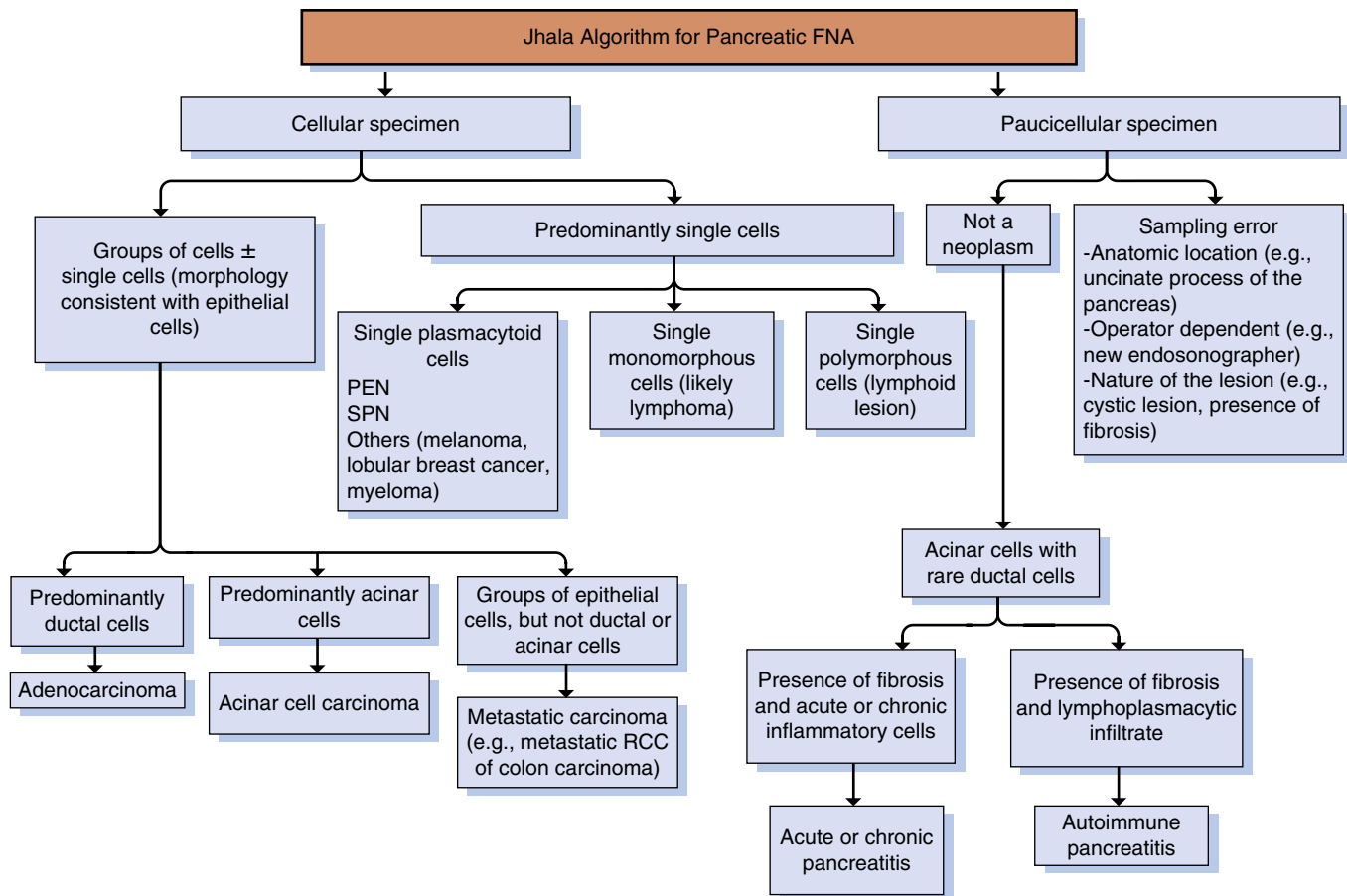


• **Fig. 22.5** Smear from endoscopic ultrasonography fine-needle aspiration of pancreas reveals many acini and ductal cells. Acinar cells show moderate granular and two-toned amphophilic cytoplasm. The nuclei are centrally placed with a round, regular nuclear membrane. In comparison, the smear also reveals ductal epithelial cells. These cells show a cohesive two-dimensional honeycomb group of ductal epithelial cells. These cells reveal clear, well-demarcated cytoplasm (Diff-Quik stain; magnification  $\times 20$ ).



• **Fig. 22.6** Endoscopic ultrasonography fine-needle aspiration from a reactive mediastinal lymph node reveals many lymphocytes of varying sizes. Tingible body macrophages are also noted (Diff-Quik stain; magnification  $\times 20$ ).

(tombstones), foam cells, intranuclear cytoplasmic inclusions, and cells with an increased nuclear-to-cytoplasmic (N/C) ratio, irregular nuclear membrane, coarse and clumped chromatin, macronucleoli, and abnormal mitoses. The presence of abortive glands in a background of tumor-associated necrosis is another feature that may help suggest carcinoma over reactive ductal epithelium.<sup>43</sup> Carcinomas may also show tumor diathesis, mucus production, occasional signet ring cells with mucus vacuoles, bizarre cells, and squamoid cells. Cytologic features of pancreatic carcinoma vary by histologic subtype, including the presence of keratinization in adenosquamous carcinomas and many giant cells in giant cell tumors of the pancreas. In contrast, reactive ductal epithelial cells show many tight cohesive two-dimensional groups of ductal cells with minimal, if any, overlapping. Reactive cells show moderate cytoplasm, well-defined borders, nuclei with a round and regular nuclear membrane, and inconspicuous nucleoli. In some instances, however, nuclear enlargement may be more conspicuous, there may be more single cells, and occasional cytologic atypia may be noted. Chronic pancreatitis may also be characterized by dense fibrous connective tissue and few chronic inflammatory cells (Fig. 22.10).

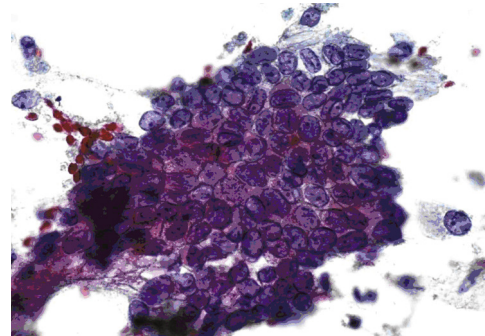


• Fig. 22.7 Morphology-based practical algorithm approach to pancreatic fine-needle aspiration (FNA). PEN, Pancreatic endocrine neoplasm; RCC, renal cell carcinoma; SPN, solid pseudopapillary neoplasm.

**TABLE 22.5** Differential Diagnosis of Common Solid Pancreatic Lesions

Benign	Malignant
Chronic pancreatitis	Pancreatic carcinoma
Autoimmune pancreatitis	Acinar cell carcinoma
Pancreatic endocrine neoplasm	Pancreatic endocrine neoplasm (well-differentiated endocrine carcinoma)
Acute pancreatitis	Metastatic malignancies
Infections	Non-Hodgkin lymphoma

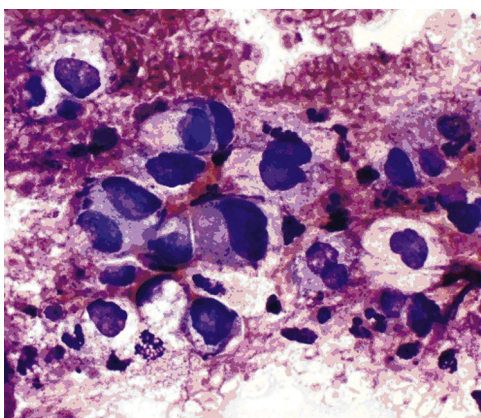
**Pitfalls.** A polymorphous cell population as opposed to predominance of cells of one type is a major consideration when evaluating specimens for pancreatic adenocarcinoma. With EUS FNA, the pancreatic mass is approached from the gastrointestinal tract. The approach to the lesion in the pancreas using EUS varies with its topographic location. In addition, in EUS FNA, as with percutaneous FNA, the needle passes through a background of chronic pancreatitis before it reaches the target lesion. This may cause additional cells to be noted on the slide preparations and may give the false impression of a polymorphous cell population. The approaches taken by the endoscopist to lesions in different locations in the pancreas and the cells that may be observed by a cytopathologist are listed in Table 22.6. Cytopathologists are very familiar with recognizing the morphology



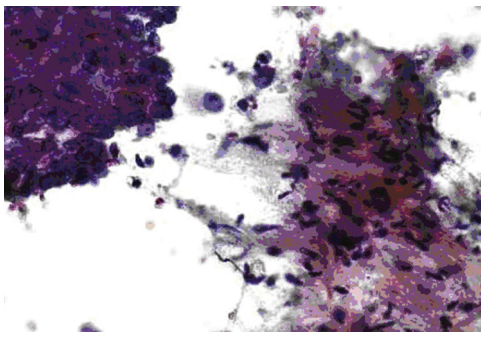
• Fig. 22.8 Smear from a well-differentiated adenocarcinoma of the pancreas reveals a tightly cohesive group of epithelial cells. Cells show mild overlapping with loss of cell polarity. Nuclei show coarse chromatin clumping, nuclear membrane irregularity, and conspicuous nucleus (Papanicolaou stain; magnification  $\times 20$ ).

of common epithelial cells of the gastrointestinal tract. One of the major pitfalls is the Brunner gland, which cytopathologists remain very unfamiliar with recognizing. We recently described morphologic features for this not so uncommon epithelial type.

Increased cellularity is one of the criteria used to distinguish well-differentiated adenocarcinoma from chronic pancreatitis. The cellularity of a sample is influenced by several factors, including operator technique and the anatomic location of the tumor. Trained operators usually obtain cellular samples from EUS FNA. Some of the possible reasons for the increased cellularity of the



• **Fig. 22.9** Pancreatic carcinoma. Smear from a poorly differentiated pancreatic carcinoma reveals many single cells with marked cytologic atypia, including enlarged nuclei, marked nuclear membrane irregularity, and background necrosis (Papanicolaou stain; magnification  $\times 40$ ).



• **Fig. 22.10** Smear from chronic pancreatitis. The smear reveals reactive ductal cells with tight cohesive groups, few inflammatory cells, and dense fibrous connective tissue (Papanicolaou stain; magnification  $\times 40$ ).

**TABLE 22.6** Transluminal Approach to Pancreas and Gastrointestinal Mucosal Cells

EUS Approach	Lesion in the Pancreas	Contaminating Gastrointestinal Mucosal Cells
Transgastric	Body and tail, occasionally uncinate process	Foveolar cells, parietal cells, chief cells, smooth muscle cells
Transduodenal	Head and uncinate process	Villi, Brunner glands <sup>a</sup> , and smooth muscle

<sup>a</sup>Lastra R, Jhala D, Ahmad N, et al. Brunner gland: a major pitfall in assessing endoscopic ultrasound guided fine needle aspiration of the pancreas. *Path Case Rev.* 2015;20:182–185.

samples obtained with EUS FNA include the proximity to the lesion and the better visualization of the lesions. The use of cellularularity as a criterion in the differentiation of chronic pancreatitis and well-differentiated adenocarcinoma should therefore be used with caution, especially when the samples have been obtained using EUS FNA.

**Causes of False-Negative Diagnosis.** False-negative diagnoses may result from technical difficulties, sampling error, or interpretive errors. For a cytopathologist, offering a diagnosis based on hypocellular samples is a common cause of false diagnosis.

A sampling error may result from the technical difficulty associated with reaching the tumor, such as when a tumor is located in the uncinate process. It also is possible that the marked desmoplasia of pancreatic adenocarcinoma may result in an inadequate specimen or an inconclusive diagnosis (atypical or suspicious for malignancy), both of which require further investigations or repeat FNA.

Interpretative causes of false-negative diagnosis may include a tumor with mixed cellularity, in which a component of chronic pancreatitis is also noted along with few tumor cells. It is also challenging to make a diagnosis of well-differentiated adenocarcinoma of the pancreas because of subtle morphologic changes.

**Ancillary Studies Supporting Diagnosis of Carcinoma (Table 22.7).** Powerful technologies continue to help identify biomarkers to refine our diagnostic practices. The list of such markers is ever increasing. Investigators have demonstrated that a lack of SMAD4 and clusterin in suspicious cells supports the diagnosis of carcinoma. In addition, mesothelin, p53, and MUC4 expression in suspicious cells further aids in supporting the diagnosis of carcinoma.<sup>44</sup> In an ever-expanding field, other markers such as S100P, XIAP, fascin, and multiprobe FISH have also been investigated.<sup>45–47</sup> In the authors' analysis, an abnormal pattern is consistently noted when a set of four FISH probes was used. Recently, the Papanicolaou society charged a group of investigators with vast experience in this area to review the literature and offer their recommendations based on input from investigators across the globe. This finding shows great promise as an adjunct to morphology in the diagnosis of pancreatic carcinoma on limited samples.<sup>21</sup>

**Causes of False-Positive Diagnosis.** Chronic pancreatitis and autoimmune pancreatitis are the most common reasons for a false-positive diagnosis of malignancy. Some of the cytologic features that may mimic malignancy in chronic pancreatitis are occasional atypical cells, which include enlarged cells, enlarged nuclei with degenerative vacuoles, single cells, and occasional mitosis. Chronic pancreatitis may also be characterized by areas with necrosis, especially in patients with development of early pseudocysts.

Aspirations from autoimmune pancreatitis often show marked stromal reaction with embedded small clusters of epithelial cells. These cells may show features of reactive atypia. However, autoimmune pancreatitis should be suspected if the patient has a history of autoimmune disease, a characteristic EUS image, and an associated increase in lymphoplasmacytic infiltrates. When in doubt, serum or tissue estimations of immunoglobulin G<sub>4</sub> (IgG<sub>4</sub>) may further aid in suggesting this diagnosis. This value becomes more informative when elevated IgG<sub>4</sub> levels are interpreted in context of total IgG levels.

The cytologic features of primary pancreatic carcinomas are similar to the features of many other adenocarcinomas that can metastasize to the pancreas. Thus, it is crucial for endosonographers to provide adequate clinical information about any history of prior malignant diseases. It also may happen that a history of prior malignancy is obtained after the EUS FNA sample is procured. In some cases, it becomes important to determine the primary site of origin. Several immunohistochemical stains can reliably suggest possible primary tumor sites. Therefore some investigators suggested an additional dedicated pass, to make a cell block to aid in performing immunohistochemical stains if and when required.

**TABLE 22.7****Utilization of Ancillary Studies in Supporting Diagnosis of Pancreatic Adenocarcinoma**

Marker	Use	Finding	How to Use the Test
SMAD4	Supporting diagnosis Selecting therapy	Lack of staining by immunohistochemistry Mutational analysis	Supports diagnosis of carcinoma on suspicious cytology cases May help select aggressive therapy
Mesothelin	Supporting diagnosis	Positive staining of carcinoma cells	Expression of mesothelin supports diagnosis of adenocarcinoma Has been utilized for vaccine therapy
Multiprobe FISH	Supports diagnosis of adenocarcinoma	Abnormalities in CEP3, CEP7, CEP17, and/or abnormalities of locus-specific probe for 9p21	Helps confirm diagnosis of carcinoma in conjunction with cytology
k-ras	Supports diagnosis of carcinoma	Mutation in hot spot area is associated with adenocarcinoma	Supports diagnosis of adenocarcinoma
Hot spot profiling of genes—next-generation sequencing platform	Helps identify targetable mutations	Select panel of genes	Helps select therapy for targetable mutations
micro RNAs	Support diagnosis of adenocarcinoma	Detection of micro RNA including miR-21 and 155	Supports diagnosis of adenocarcinoma—More studies are needed

*FISH*, Fluorescence in situ hybridization.

### Pancreatic Neuroendocrine Tumors

Pancreatic neuroendocrine tumors (PNETs) more frequently manifest in the body or tail of the pancreas. They are usually well-demarcated solid lesions, although they may infrequently manifest as cystic lesions as well. Cytologic characteristics of these tumors include moderate to highly cellular smears.<sup>48</sup> These smears predominantly have single cells with occasional loose cellular aggregates, as well as rosette formation (Fig. 22.11A).<sup>49</sup> Neoplastic cells are plasmacytoid without perinuclear huff, small cytoplasmic vacuoles, and the cytoplasm may show neurosecretory granules (see Fig. 22.11B).<sup>50</sup> Nuclei show a round, regular nuclear membrane and usually do not reveal conspicuous nucleoli, although exceptions have been noted. Cells may also show marked anisonucleosis. Cytologic features usually cannot distinguish benign from malignant neoplasms. However, increased proliferative activity and necrosis have been associated with malignant lesions.

### Major Differential Diagnosis

**Solid Pseudopapillary Neoplasm of the Pancreas.** These tumors are usually noted in the body or tail of the pancreas of young females. A multiinstitutional study noted that solid pseudopapillary neoplasms (SPNs) of the pancreas are not infrequently diagnosed as pancreatic neuroendocrine neoplasms (PENs) on EUS FNA samples.<sup>51</sup> In a recent study, Hooper and colleagues noted that when adequate samples were procured by endosonographers, one of the most significant errors in their hands was tumor misclassification, which was most often SPN of the pancreas.<sup>52</sup> Some of the factors that may lead to such misclassification are a result of overlapping morphologic spectrum shared by PNET and SPN. Both tumors may show moderate cellularity, dyscohesive cells, low N/C ratio, and plasmacytoid cells. Some of the features that suggest SPN over PEN include pseudopapillary groups, cytoplasmic hyaline globules, and a chromatic matrix material and nuclei with “coffee bean” appearance (Fig. 22.12). We have recently identified that in cases where the morphologic differential diagnosis is

between PNET and SPN, detection of large cytoplasmic vacuoles would favor SPNs.<sup>50</sup> Other observers now independently validate this finding.

Cytologic features, however, are not always confirmatory. In such instances, a limited panel of immunohistochemical stains is needed to distinguish PEN from SPN. There are many immunohistochemical stains that have been utilized to characterize immunophenotypic pattern for SPN.<sup>53</sup> Positive staining with chromogranin, synaptophysin, and CD56 stains support a diagnosis of PEN. Infrequently, SPN may also stain for chromogranin. Most SPNs will stain for CD56 and about one-third of cases with synaptophysin. We have identified that FNA samples are extremely limited in quantity; a judicious staining with chromogranin, CD10 and E-cadherin, and/or β-catenin will reliably separate SPN from PNET.<sup>54</sup>

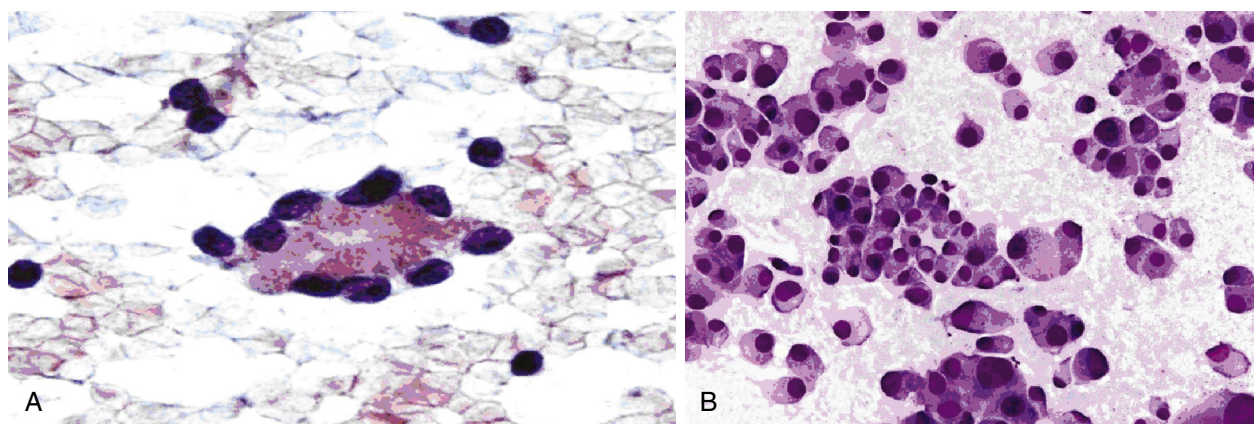
Other tumors that may mimic PNET such as acinar cell carcinoma and pancreaticoblastoma are out of the scope of this chapter.

### Cystic Pancreatic Lesions

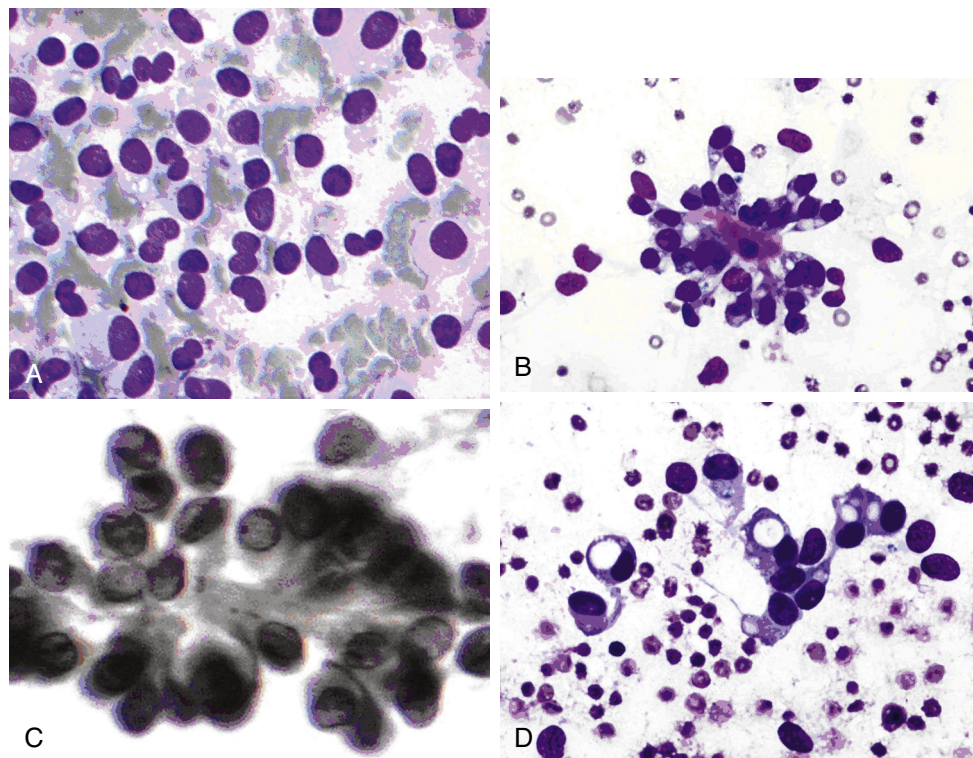
Guidelines for performing FNA for cystic lesions and associated morphologic findings are changing, and as a result, not all cysts should be aspirated. As a result, the role of the cytopathologist is also constantly evolving.

The diagnosis of cystic lesions requires a coordinated multispecialty team approach. Cytologists are largely faced with the assessment of five major cystic lesions of the pancreas that have characteristic demographic, EUS, and cytologic features. However, taken individually, clinical features, EUS findings, and cytologic features do not provide adequate sensitivity.

It is known that cysts that are lined by mucinous epithelium (intraductal papillary mucinous neoplasm [IPMN] and mucinous cystic neoplasia) can progress to adenocarcinoma of the pancreas. As a result it is important to detect them early and identify dysplasia occurring in these cysts early for early interventions (Fig. 22.13).



• **Fig. 22.11** Pancreatic endocrine neoplasms. (A) Smears from pancreatic endocrine neoplasms usually show moderate cellularity with rosette formation and many single cells with peripherally placed nuclei (Papanicolaou stain; magnification  $\times 40$ ). (B) The nuclei reveal evenly dispersed chromatin without conspicuous nucleoli. They also reveal coarse neurosecretory granules (Diff-Quik stain; magnification  $\times 20$ ).



• **Fig. 22.12** (A–D) Fine-needle aspirates from a solid pseudopapillary neoplasm of the pancreas show wispy nondescript cytoplasm with nuclei lined away from the stroma. These cells also show (A) a preserved nuclear-to-cytoplasmic ratio, plasmacytoid cells and an eosinophilic cytoplasmic globule (Diff-Quik stain; magnification  $\times 20$ ), (B) a characteristic metachromatic matrix (Diff-Quik stain; magnification  $\times 20$ ), (C) nuclei with a "coffee bean" appearance (Papanicolaou stain; magnification  $\times 40$ ), and (D) large cytoplasmic vacuoles (Diff-Quik stain; magnification  $\times 40$ ).

**Intraductal Papillary Mucinous Neoplasia.** Our understanding has substantially improved because this tumor was first characterized as a separate entity. These tumors can occur within the main duct (main duct IPMN) or within smaller branches of the pancreatic ducts (side branch IPMN or branch duct IPMN). In essence both forms of IPMN develop cysts lined by mucin-secreting epithelium and will communicate with the pancreatic duct. Main duct IPMNs generally are noted in male patients and more often are noted near the head of the pancreas. Pancreatic ducts in such cases are generally dilated, and mucin is often noted to ooze out from the ampulla in the second portion of the duodenum. In contrast, branch duct IPMNs do communicate with

the main pancreatic ducts but do not result in dilatation of the main pancreatic duct. These lesions are often multicentric, and their risk of developing into carcinoma is lower than that of main duct IPMNs. IPMNs, regardless of whether they are main duct or branch duct, are lined by different types of mucin-secreting epithelia (intestinal, pancreaticobiliary, foveolar, and oncocytic), and their risk of progression to carcinoma also varies. International consensus guidelines have been developed to manage patients with IPMN.<sup>55</sup>

When such lesions are aspirated, they characteristically have large papillary epithelial groups with a fibrovascular core lying in pools of mucin (Fig. 22.14). The neoplastic cells are columnar or

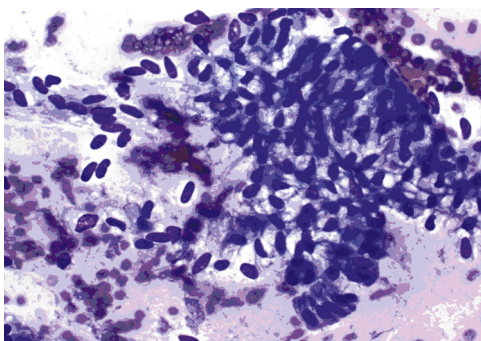


**Fig. 22.13** Endoscopic ultrasonography fine-needle aspiration of the pancreas from a mucinous cyst adenoma reveals cuboidal neoplastic epithelial cells. These cells are in close proximity to the spindled cells representing the ovarian stroma (Papanicolaou stain; magnification  $\times 40$ ).

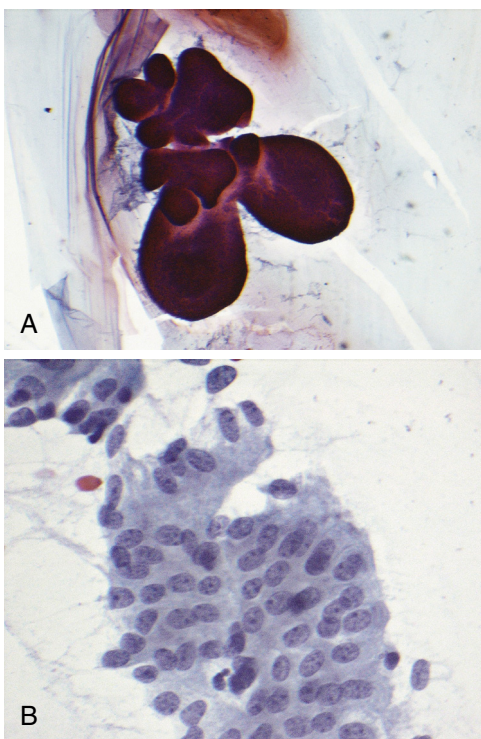


**Fig. 22.14** Intraductal papillary mucinous neoplasm. (A) Smear from intraductal papillary mucinous neoplasia reveals pool of mucin with a large papillary epithelial group (Papanicolaou stain; magnification  $\times 10$ ). (B) Higher magnification reveals columnar cells with a preserved nuclear-to-cytoplasmic ratio. The nuclei show a round, regular nuclear membrane with inconspicuous nucleoli (Papanicolaou stain; magnification  $\times 40$ ).

cuboidal and show loss of cell polarity. A few single cells may also be seen. Individual cells may demonstrate a wide range of morphologic changes, depending upon the type of epithelium that lines the cyst. It is recognized that sensitivity of cytology is low in distinguishing mucinous from nonmucinous cysts of the pancreas. It is, however, quite clear that cytologic characteristics do help in determining the degree of dysplasia and malignant transformation within neoplastic cysts.<sup>56,57</sup>

**Causes of False Diagnosis.** These tumors are lined by various cell types, including gastric foveolar epithelium, colonic epithelium, pancreaticobiliary epithelium, and oncocytic cells with granular eosinophilic cytoplasm. This poses significant challenges

of interpretation when there is contamination in samples when a needle traverses either the stomach or the duodenum. Intestinal-type IPMN will be very difficult to characterize when a needle traverses through the duodenum. Similarly, it will be difficult to distinguish neoplastic foveolar cells when the needle traverses through the stomach. A close interaction between endosonographers and cytopathologists is of paramount importance to accurately determine the site of lesion as well as which route is used to obtain cells from the pancreas (transduodenal vs. transgastric).

It is also important to note the type of mucin. Thick mucin that develops a ferning pattern when air-dried is an important clue to being neoplastic mucin as opposed to mucin noted when the gastric mucosa is aspirated.

**Mucinous Cystic Neoplasm.** These tumors almost exclusively arise in female patients. They also are noted in young patients and are predominantly located in the tail of the pancreas. These tumors do not communicate with the main pancreatic duct. When cells are obtained from the center of the cyst, they reveal only cyst contents as suggested by cell debris, macrophages, and crystals. When the wall is aspirated, these tumors may show cuboidal or columnar mucin-secreting epithelial cells with a preserved N/C ratio. Smears from these tumors reveal elongated stromal cells in close approximation to bland cuboidal or columnar epithelial cells (see Fig. 22.14). The stromal cells most likely represent ovarian stroma. When these cysts have dysplastic or malignant components, the cells begin to show atypia. Features of atypia include many single cells and hyperchromatic and enlarged nuclei with cell pleomorphism. The nuclei begin to look wrinkled and also may reveal prominent nucleoli.

#### Causes of False Diagnosis

**Paucicellular Aspirates.** Aspiration from these cysts frequently reveals paucicellular aspirates. In this setting, a definitive diagnosis of neoplastic mucinous cyst cannot be made with certainty. Mucinous cystic neoplasms also frequently reveal sloughed mucosa. Aspiration from such areas may reveal only acellular debris or necrotic debris with inflammatory cells reminiscent of pseudocysts.

**Lining Cells.** When aspirate reveals goblet cells, it becomes a challenge to differentiate these cells from duodenal cells. Knowledge of the point of needle entry is very useful in this setting to avoid false-negative interpretation.

#### Ancillary Studies That Can Help Distinguish Neoplastic Mucinous From Nonmucinous Cysts of the Pancreas (Table 22.8)

**Biochemical Estimations.** One of the major challenges facing clinical teams is to distinguish between a neoplastic mucinous cyst and a nonmucinous cyst (e.g., pseudocyst). Determining the fluid viscosity is a simple method of distinguishing between the two types of cysts. Fluid viscosity of greater than 1.6 is generally associated with a neoplastic mucinous cyst.<sup>58</sup> Over a period of time, biochemical estimation of carcinoembryonic antigen (CEA) in combination with estimation of amylase levels has emerged as a powerful adjunct to distinguish a neoplastic mucinous cyst from a nonneoplastic cyst. This concept was developed and popularized by robust studies conducted by the cooperative pancreatic cyst study group led by Brugge and colleagues.<sup>7</sup> In this initial study, a CEA level more than 192 ng/dL was associated with a neoplastic mucinous cyst. Later, based on analysis of pooled data from multiple studies it was suggested that a CEA level greater than 800 ng/dL provides a specificity of 98% for a mucinous cyst.<sup>59</sup> A more recent follow-up study on more than 800 patients suggests

**TABLE 22.8** Ancillary Studies That Differentiate Mucinous From Nonmucinous Neoplastic Cysts

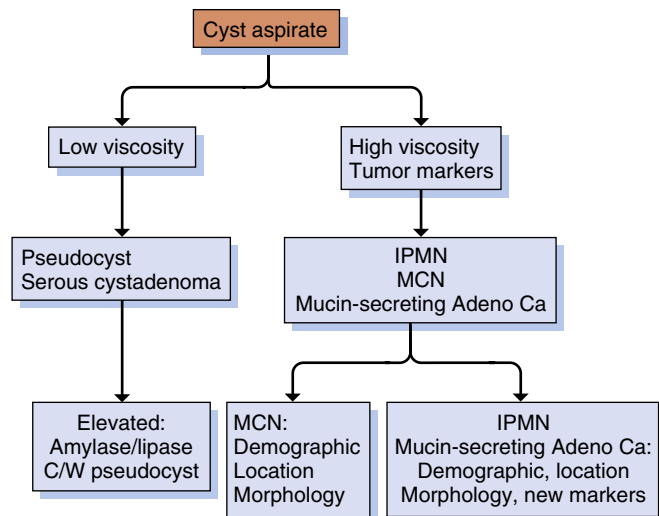
	IPMN	MCN	SCA
Viscosity (thick or thin mucin)	High	High	Low
CEA	High	High	Low
Amylase	Variable	Variable	Low
k-ras mutation	Present	Present	Not seen
GNAS mutation codon 201	Present	Negative	Negative
VHL gene	Negative	Negative	Present

CEA, Carcinoembryonic antigen; IPMN, intraductal papillary mucinous neoplasia; MCN, mucinous cystic neoplasm; SCA, serous cystadenoma.

that CEA cyst fluid levels of 110 ng/dL or above will also provide similar sensitivity and specificity.<sup>60</sup> In our own data evaluating a large number of cases, we have noticed that a lower cutoff value of 75 ng/dL will offer similar results. This brings up a very crucial point for endosonographers that while evaluating cyst fluids from pancreatic cysts, they should utilize cutoff values based on validation of CEA results in their own practice settings. The CEA as well as amylase levels change based on the type of sample, preparation, as well as platform utilized to assess this analyte. It is also interesting to note that cyst fluid amylase levels in thousands should be viewed in conjunction with CEA levels. A very low CEA level in conjunction with amylase levels in thousands is supportive of a pseudocyst. In comparison, higher CEA levels along with higher amylase levels will be associated with a neoplastic mucinous cyst. Occasionally, lymphoepithelial cysts as well as pseudocysts may be associated with spurious elevations in cyst fluid CEA levels.

**Molecular Analysis of Cyst Fluid.** The algorithmic approach highlighted in Fig. 22.15 is useful for distinguishing common cystic pancreatic lesions. A few studies also demonstrated how molecular analysis of the cysts can help improve the diagnosis of cystic lesions. This analysis used determinations of DNA quality and quantity, loss of heterozygosity of k-ras mutation and its amplification, and mutations in seven other loci.<sup>61,62</sup> Based on a set formula, the cysts are categorized into neoplastic versus nonneoplastic cysts. It has now become clear that instead of performing an extensive assessment of loss of heterozygosity for multiple loci, utilizing an approach to determine the quality of DNA and determining the mutational status of k-ras is adequate.

**Newer Markers.** The use of high-throughput technologies has produced novel findings that are specifically associated with IPMN. Recent studies show that mutation in codon 201 of the GNAS gene is specifically noted in IPMN but not with any other types of cysts, including mucinous cystadenomas. It is also noted by these observers that GNAS mutations were present in 66% of IPMNs and that either k-ras or GNAS mutations could be identified in 96% of these cases.<sup>63</sup> Mutation in GNAS is also more frequently noted in intestinal type IPMN. This mutation, however, cannot reliably distinguish the degree of dysplasia noted in these neoplastic cysts.<sup>64</sup> By these studies it becomes clear that mutation in codon 201 of the GNAS gene along with k-ras can reliably distinguish IPMN from other cysts of the pancreas.



• **Fig. 22.15** Algorithmic approach to the diagnosis of cystic pancreatic lesions. Ca, Carcinoma; C/W, consistent with; IPMN, intraductal papillary mucinous neoplasia; MCN, mucinous cystic neoplasm.

## Lymph Nodes

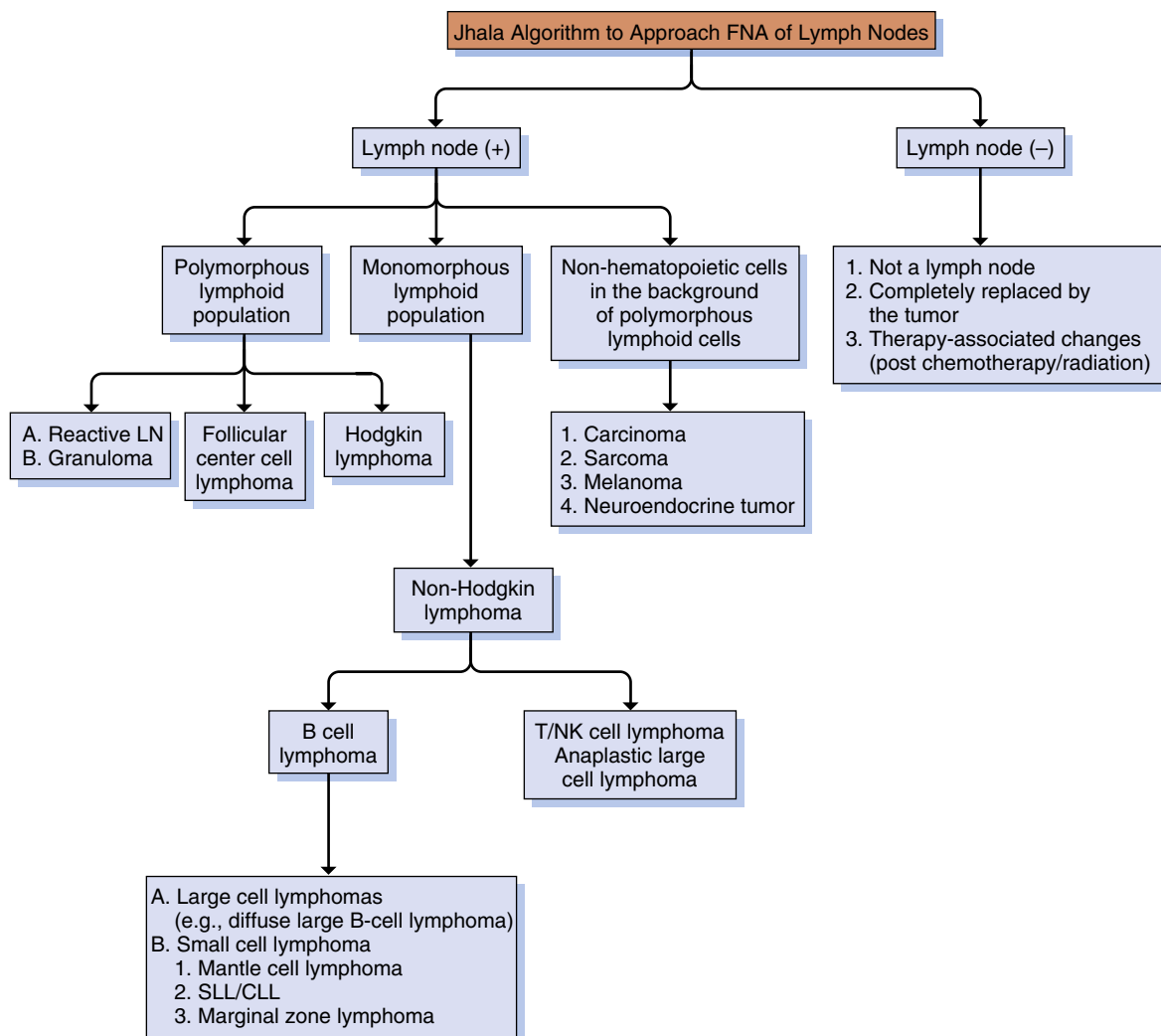
EUS FNA for mediastinal and intraabdominal lymphadenopathy has emerged as a very rapid, cost-effective, and reliable modality to stage malignancies as well as to detect primary or secondary hematopoietic malignancies.<sup>25,65–69</sup> Most of the studies evaluated the use of EUS FNA for staging of malignancies, including those from the lung, gastrointestinal tract, and pancreas. Determination of nodal metastasis by EUS FNA results in a change in preoperative staging that prevents unnecessary surgeries and a change in management strategies for patients with primary malignant neoplasms of the lung, gastrointestinal tract, and pancreas. EUS FNA of deep-seated lymphadenopathy can also be used to provide a diagnosis of primary lesions, including granulomas, infections, and lymphomas (non-Hodgkin and Hodgkin lymphoma).

### Sample Collection

If the clinical information or the rapid interpretation of on-site cytology suggests malignant non-Hodgkin lymphoma, the endoscopist should provide an additional sample for flow cytometric, gene rearrangement, or cytogenetic examination. Generally these cells should be collected in RPMI 1640 solution for flow cytometric analysis or molecular genetic analysis. Experience suggests that simple Hank's balanced salt solution can also be used as a transport medium to perform flow cytometric evaluation. If the sample has not been collected for flow cytometry, a sample collected for cell block can be stained with immunohistochemical stains for appropriate phenotyping. It is also equally important to understand that transport media do affect further management. A saline-rich medium might affect extraction of DNA and may give false-negative diagnosis. Sample collected in popular transport media used for liquid-based preparations such as Thin Prep can also be used to perform molecular testing. Optimization of sample collection especially for staging of lung cancer is therefore critical. Gene rearrangement studies can also be performed on such samples.

### Algorithmic Approach to Interpretation of Lymph Node Aspirates

Using a stepwise methodical approach for lymph node aspirations leads to improved accuracy<sup>66</sup> (Fig. 22.16). Earlier reports



• **Fig. 22.16** An algorithmic approach to the interpretation of lymph node aspirates. *FNA*, Fine-needle aspiration; *LN*, lymph node; *NK*, natural killer; *SLL/CLL*, small lymphocytic lymphoma/chronic lymphocytic lymphoma.

suggested that FNA was not always useful to test diagnoses of malignant non-Hodgkin lymphoma. This, however, is proved incorrect by several observers. The power of EUS-guided tissue sampling is increasing exponentially. Use of aspirates combined with Tru-Cut biopsies can improve the diagnosis of difficult lesions such as Hodgkin lymphoma.

### How to Confirm Lymph Nodes

Lymphoid tissue demonstrates cellular aspirates with many single dyscohesive cells composed of polymorphous lymphoid cells of varying sizes. These cells may have germinal centers with debris containing (tingible body) macrophages. Diff-Quik stain also highlights the presence of cytoplasmic fragments such as lymph glandular bodies (see Fig. 22.6).

### Differential Diagnosis

When a range of small, medium, and large lymphocytes is noted in a lymph node aspirate in elderly patients from unexplained lymphadenopathy, one must be aware of conditions such as follicular center cell lymphoma and other small lymphocytic lymphomas. A similar pleomorphic cell type with plasma cells and eosinophils should raise suspicion for Hodgkin lymphoma. In

such instances, additional samples should be obtained for flow cytometry, cytogenetics, or cell block analysis. Cell block analysis is more useful especially for the diagnosis of Hodgkin lymphoma, in which additional immunohistochemical stains rather than flow cytometry will provide a definitive answer.

Similarly, if lymph node aspirates reveal many polygonal cells that also have reniform nuclei with inconspicuous nucleoli, granuloma should be suspected. Granulomas show aggregates of epithelioid histiocytes (Fig. 22.17), with occasional multinucleated giant cells. In such instances, additional studies should be undertaken to determine possible causes.

### Monomorphous Lymphoid Population

When a lymph node aspirate reveals a sea of monomorphic lymphoid population (small, intermediate, or large), the strong possibility of lymphoma should be considered, and additional samples should be obtained for ancillary studies.

**Pitfalls.** Diffuse large B-cell non-Hodgkin lymphomas have fragile cytoplasm and therefore frequently reveal large nuclei stripped of their cytoplasm. These cells also reveal prominent nucleoli that raise the suspicion of a differential diagnosis of

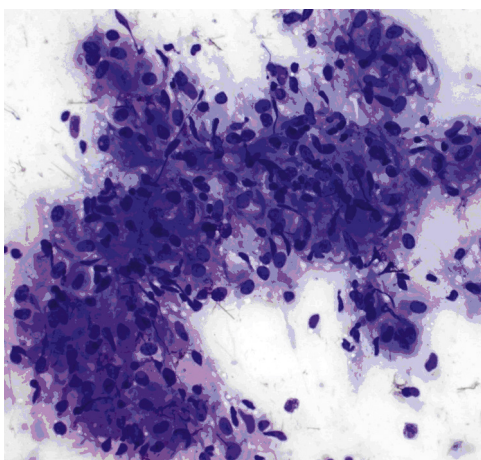


**Fig. 22.17** Endoscopic ultrasonography fine-needle aspiration of mediastinal lymph node. The aspirate reveals aggregates of epithelioid histiocytes characteristic of granulomas (Diff-Quik stain; magnification  $\times 40$ ).

melanoma. The cytoplasm with B-cell markers may be sheared while passing through the narrow capillary bore of a flow cytometer. Thus it is not uncommon to see that flow cytometry may have a false-negative result.<sup>25</sup> Immunohistochemical stains performed on cell block or gene rearrangement studies may aid in confirming this difficult diagnosis.

Small lymphocytic lymphomas fall on the other end of the spectrum. The smears may contain only small, mature lymphocytes. These lesions cannot be distinguished from mature lymphocytes or lymphocyte-predominant Hodgkin lymphoma, or other lymphomas with small lymphoid morphology such as mantle cell or marginal zone lymphomas. Therefore in a patient with multiple groups of lymph node enlargement, it is advisable to obtain an additional sample for ancillary studies.

#### **Nonhematopoietic Cells in Background of Lymphoid Cells**

When nonhematopoietic cells are noted in lymph node aspirates, the diagnosis is metastatic malignancy unless proved otherwise. These metastases can be from carcinoma, melanoma, or neuroendocrine tumors. The characteristic morphologic features of each entity can distinguish these tumors.

**Pitfalls.** Although generally it is not difficult to distinguish metastatic malignancies, the diagnosis of small cell carcinomas may pose diagnostic challenges. Tumor cells in small cell carcinomas demonstrate an increased N/C ratio, nuclei that are hyperchromatic, and possibly also nuclear molding. These cells are fragile and reveal a stretching of DNA material. They also show frequent apoptosis and absent or inconspicuous nucleoli. Although these features are easily recognizable, poorly prepared smears from lymph nodes may also reveal a shearing of cells from overzealous spread. They may show loose aggregates of cells that reveal a low N/C ratio, hyperchromatic nuclei, and inconspicuous nucleoli. In such cases, the pattern of chromatin architecture may help differentiate the two. Small cell carcinomas reveal a fine, evenly distributed chromatin pattern, whereas lymphocytes may have margination of the chromatin pattern.

One must also not overinterpret benign gastrointestinal tract epithelium noted in a background of lymph node aspirates as diagnostic of metastatic malignancy. When these aspirates are evaluated carefully, up to 60% may show some form of gastrointestinal contamination.

#### **Nonhematopoietic Cells Without the Background of Lymphoid Cells**

Rarely, a lesion deemed as a lymph node on EUS imaging turns out to be a tumor nodule. This possibility should be suspected when multiple passes reveal only neoplastic cells, and no lymphoid component is noted. Tumor cells generally fall into one of four categories: (1) carcinoma, in which cells show cohesive groups with single cells; (2) melanoma, in which the cells are mostly single, with mild to moderate cytoplasm that may or may not have pigment (nuclei also reveal intranuclear cytoplasmic inclusions and prominent nucleoli; this tumor not infrequently has double mirror image nuclei); (3) carcinoid tumors, which are well-differentiated neuroendocrine carcinomas that reveal many single plasmacytoid cells with anisonucleosis (the cytoplasm may show neurosecretory granules, and occasionally these tumors also have a spindled appearance giving rise to a biphasic pattern of cells; these tumors may also form rosettes); and (4) sarcoma. In rare instances, patients treated with either chemotherapy or radiation therapy show transformational changes in lymph nodes; in such cases, they may only show mucinous or myxoid change with few inflammatory cells.<sup>2</sup>

In recent years, EUS FNA samples are increasingly being utilized to characterize underlying molecular background of cells to guide therapies. Increasingly medical oncology teams request such assays, including analysis for EGFr, KRAS, BRAF, EMALK44, and ROS1 mutations, increasing the power of small samples.<sup>70</sup> These targets are increasingly recognized, and we should be prepared to look beyond morphology for managing these patients. Many platforms are utilized to detect such molecular alterations. New guidelines for managing lung cancer diagnosis now may require high throughput and very sensitive technologies such as platforms, including NGS of cells to help identify mutations that are not easily identified by standard technologies.

#### **Spleen**

FNA of the spleen has proven useful for the detection of malignant non-Hodgkin lymphoma, metastatic carcinoma, sarcoidosis, infectious conditions, and extramedullary hematopoiesis.<sup>71–73</sup> Percutaneous FNA of the spleen is highly specific (100%) and yields an overall accuracy of 84.9% to 88% for needle aspirates. Eloubeidi and colleagues noted that the diagnostic accuracy of splenic FNA can be increased by obtaining samples for flow cytometry.<sup>71</sup> Some investigators suggested, however, that a potential risk for increased bleeding contributes to the lack of use of FNA of the spleen in the United States. Preliminary experience suggested that judicious use of EUS FNA may permit the detection of unsuspected neoplasms, the determination of a preoperative diagnosis of splenic lesions, or both. However, further studies are needed to determine the safety and efficacy of this modality in the detection of splenic lesions.

#### **Gastrointestinal Tract**

For cytologic diagnosis, endoscopic brushing is a useful modality for the detection of surface lesions.<sup>1</sup> However, this modality is not useful for the diagnosis of submucosal lesions. EUS with FNA offers the advantages of direct visualization of the mucosal surface and accuracy in determining the extent and size of the submucosal lesion.<sup>74</sup> Therefore EUS permits preoperative determination of the depth of tumor invasion, or T-staging, as well as determination

of the N status, and thus provides valuable information concerning the TNM staging of gastrointestinal tract malignancies.<sup>18,74</sup> EUS also has been used to determine the extent of involvement and response to therapy of mucosa-associated lymphoid tissue (MALT) lymphomas of the stomach. Specifically, EUS FNA has shown value in the following areas for cytologic diagnosis.

### Detection of Foregut Cysts

One of the major differential diagnoses for a patient with a posterior mediastinal lesion, which may manifest with dysphagia, is a foregut duplication cyst.<sup>75</sup> This category includes esophageal reduplication and bronchogenic cysts.<sup>76</sup> These cysts may be differentiated based on the presence of complete muscle wall, the type of lining epithelium, and results of imaging studies. An esophageal reduplication cyst is a rare developmental anomaly that clinically and radiologically can mimic a neoplasm.

The cytologic features of the cysts show degenerated cell debris and hemosiderin-laden macrophages (Fig. 22.18). In addition, these aspirates may also contain detached ciliated cell fragments, which can be demonstrated by both light and electron microscopy. The presence of numerous squamous cells supports the diagnosis of an esophageal reduplication cyst. The presence of numerous goblet cells with an absence of squamous cells supports the diagnosis of a bronchogenic cyst. Cytologic features alone are not pathognomonic for the diagnosis of a foregut cyst, but can be used to rule out malignant neoplasm and can help support the diagnosis of foregut cyst when cytology is used in conjunction with imaging studies, including EUS findings.<sup>76</sup>

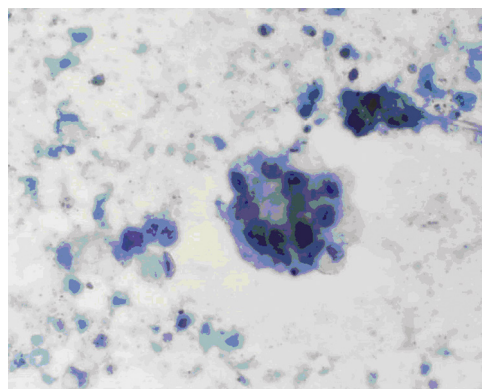
### Gastrointestinal Stromal Tumors

GISTs usually are submucosal and cannot be detected by brush sampling or forceps biopsy. EUS with its associated capabilities such as Doppler as well as FNA capability helps determine the site, size, and extent of the lesion. Underlying molecular typing to detect these tumors characterizes molecular changes that could be utilized to predict therapeutic response.<sup>77–80</sup> FNA samples from GISTs show hypercellular groups of spindled cells (Fig. 22.19A) and, rarely, epithelioid cells. The spindled cells also show blunted nuclei and may have nuclear angulations. The major pitfall associated with EUS FNA of GISTs is the aspiration of muscle cells from the wall of the gastrointestinal tract or smooth muscle tumors. Because the definitive differentiation of GISTs from other spindle cell lesions influences subsequent therapy, every attempt should be made to distinguish among these lesions. A panel of immunohistochemical stains, including primary antibodies against *c-kit* (CD117; see Fig. 22.19B), CD34, smooth muscle antigen, muscle-specific actin, DOG1, and S-100, may be used to distinguish GISTs from muscle cells, smooth muscle tumors, and rare tumors, such as solitary fibrous tumors of the gastrointestinal tract. Additional *c-kit* mutational analysis is being investigated to determine utility of EUS FNA as a predictive tool in management for GIST tumors.

## Hepatobiliary Tree

### Liver

CT and ultrasound scans have been used to detect and guide the collection of FNA samples from hepatic masses. Several studies explored the usefulness of EUS in the diagnosis of hepatic lesions, as well as the ability of EUS to promote early intervention.<sup>81–83</sup> Investigators reported that EUS is able to identify hepatic lesions when a previous CT scan failed to detect a lesion. FNA is used

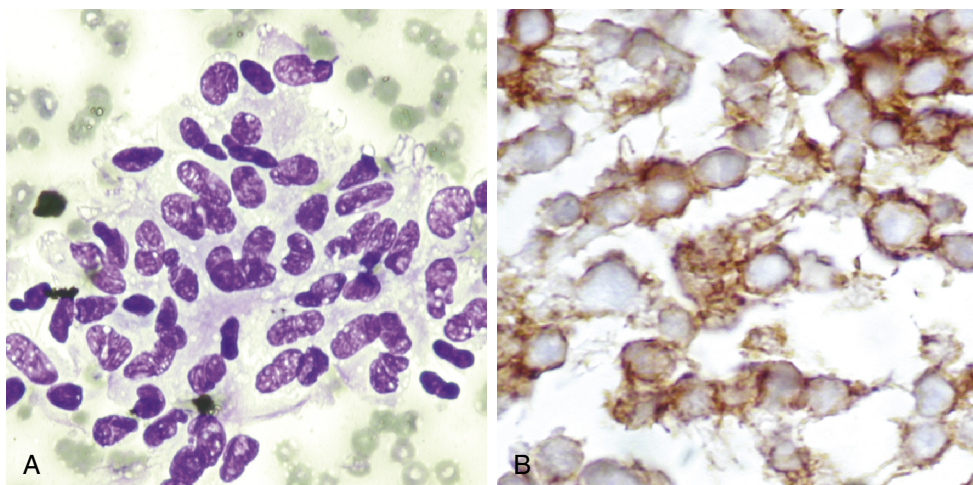


• **Fig. 22.18** Endoscopic ultrasonography fine-needle aspiration of an esophageal duplication cyst. The aspirate reveals macrophages, giant cells, and cell debris consistent with the cyst content (Papanicolaou stain; magnification  $\times 40$ ).

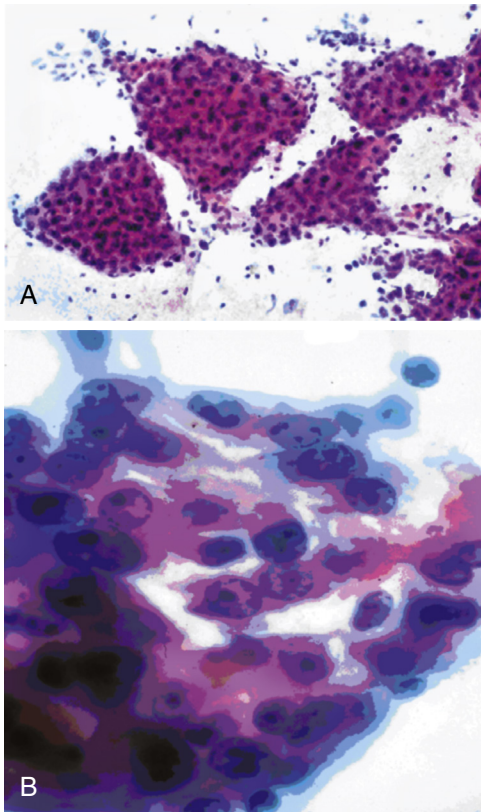
generally to confirm the diagnosis of metastatic tumors or to diagnose primary tumors such as hepatocellular carcinoma and cholangiocarcinoma. Aspirates from hepatocellular carcinomas generally show adequately cellular samples. The neoplastic hepatocytes may be in groups or single cells. Two patterns of morphologic features are characteristic: (1) groups of hepatocytes with overlapping cells that are lined by sinusoids (basket pattern; Fig. 22.20A), and (2) overlapping cell groups with vessels transgressing these neoplastic cells. Neoplastic hepatocytes may have a range of morphologic features based on their cellular differentiation and histologic subtype. It may be difficult to distinguish well-differentiated hepatocellular carcinomas from hepatocellular adenoma, focal nodular hyperplasia, or macroregenerative nodules. In such instances, an altered architectural pattern highlighted on reticulin stain on cell block examination may prove to be a valuable adjunct.<sup>84</sup> Moderately or more poorly differentiated tumors may show many single atypical hepatocytes, the presence of bile, or single nuclei stripped of their cytoplasm. These cells also may have clear cytoplasmic vacuoles representing steatosis. Malignant cells show an increased N/C ratio, nuclear membrane irregularity, abnormal mitoses, and prominent nucleoli (see Fig. 22.20B). Similarly, EUS FNA has also been useful in the diagnosis of biliary and gallbladder carcinomas.<sup>85,86</sup> This optimistic outlook should be weighed against cautionary notes of potential needle seeding, as well as the impact on the future role of transplantation for patients with cholangiocarcinomas. Potential for such seeding and outcomes have also been highlighted, and hence additional studies are needed to further characterize the challenges and opportunities for this procedure.<sup>87</sup>

### Adrenal Glands

EUS can detect adrenal gland lesions and can effectively obtain FNA samples from left-sided and some right-sided lesions.<sup>88</sup> This modality is useful for detecting metastatic malignant neoplasms to the adrenal gland, especially from the lung.<sup>89,90</sup> Samples from normal adrenal glands reveal single cells or small aggregates. The cells usually are uniform; however, anisocytosis sometimes can be noted. The nuclei generally have regular nuclear membranes. Some cells may reveal conspicuous nucleoli. The cytoplasm may be eosinophilic, foamy, or rich in lipids. Because the cytoplasm frequently is disrupted, naked nuclei are often identified, with lipid vacuoles noted in the background.



• **Fig. 22.19** (A and B) Endoscopic ultrasonography fine-needle aspiration of a gastric submucosal tumor reveals a paucicellular aspirate with many spindled cells suggestive of gastrointestinal tract stromal tumor (GIST). These cells also were stained by CD117 (*c-kit*), which confirmed the diagnosis of GIST tumor (A, Diff-Quik stain; magnification  $\times 40$ ; B, immunohistochemical stain; magnification  $\times 40$ ).



• **Fig. 22.20** Hepatocellular carcinoma. (A) Aspirate from hepatocellular carcinoma shows increased cellularity and reveals groups of hepatocytes with sinusoids around the periphery (basketing pattern; Papanicolaou stain; magnification  $\times 20$ ). (B) Individual tumor cells either show no or very little cytoplasm with increased nuclear-to-cytoplasmic ratio. Nuclei reveal irregular nuclear membranes and have prominent nucleoli (Papanicolaou stain; magnification  $\times 40$ ).

## Summary

EUS is a powerful modality that has forever changed practice patterns related to deep-seated malignant neoplasms. Advances in this technology and rapid evolution of molecular technology platforms and understanding will continue to challenge conventional wisdom in the coming years. Effective use of this technique for patient management, however, requires that cytopathologists form an integral part of the patient management team. Although the diagnostic criteria for a majority of lesions are not affected, endosonographers as well as cytopathologists should be aware of the benefits, limitations, and pitfalls of evaluating samples obtained by EUS-guided FNA.

## Key References

2. Jhala NC, Jhala DN, Chhieng DC, et al. Endoscopic ultrasound-guided fine-needle aspiration. A cytopathologist's perspective. *Am J Clin Pathol*. 2003;120(3):351–367.
3. Varadarajulu S, Hasan MK, Bang JY, et al. Endoscopic ultrasound-guided tissue acquisition. *Dig Endosc*. 2014;26(suppl 1):62–69.
14. Sakamoto H, Kitano M, Komaki T, et al. Prospective comparative study of the EUS guided 25-gauge FNA needle with the 19-gauge Trucut needle and 22-gauge FNA needle in patients with solid pancreatic masses. *J Gastroenterol Hepatol*. 2009;24(3):384–390.
15. Siddiqui UD, Rossi F, Rosenthal LS, et al. EUS-guided FNA of solid pancreatic masses: a prospective, randomized trial comparing 22-gauge and 25-gauge needles. *Gastrointest Endosc*. 2009;70(6):1093–1097.
25. Nunez AL, Jhala NC, Carroll AJ, et al. Endoscopic ultrasound and endobronchial ultrasound-guided fine-needle aspiration of deep-seated lymphadenopathy: analysis of 1338 cases. *Cytojournal*. 2012;9:14.

## References

Access the reference list online at [ExpertConsult.com](http://ExpertConsult.com).

## References

1. Jhala N, Jhala D. Gastrointestinal tract cytology: advancing horizons. *Adv Anat Pathol.* 2003;10(5):261–277.
2. Jhala NC, Jhala DN, Chhieng DC, et al. Endoscopic ultrasound-guided fine-needle aspiration. A cytopathologist's perspective. *Am J Clin Pathol.* 2003;120(3):351–367.
3. Varadarajulu S, Hasan MK, Bang JY, et al. Endoscopic ultrasound-guided tissue acquisition. *Dig Endosc.* 2014;26(suppl 1):62–69.
4. Eltoum IA, Alston EA, Roberson J. Trends in pancreatic pathology practice before and after implementation of endoscopic ultrasound-guided fine-needle aspiration: an example of disruptive innovation effect? *Arch Pathol Lab Med.* 2012;136(4):447–453.
5. Yamao K, Sawaki A, Mizuno N, et al. Endoscopic ultrasound-guided fine-needle aspiration biopsy (EUS-FNAB): past, present, and future. *J Gastroenterol.* 2005;40(11):1013–1023.
6. Vazquez-Sequeiros E, Levy MJ, Van Domselaar M, et al. Diagnostic yield and safety of endoscopic ultrasound guided fine needle aspiration of central mediastinal lung masses. *Diagn Ther Endosc.* 2013;2013:150492.
7. Brugge WR, Lewandrowski K, Lee-Lewandrowski E, et al. Diagnosis of pancreatic cystic neoplasms: a report of the cooperative pancreatic cyst study. *Gastroenterology.* 2004;126(5):1330–1336.
8. Vilmann P, Jacobsen GK, Henriksen FW, Hancke S. Endoscopic ultrasonography with guided fine needle aspiration biopsy in pancreatic disease. *Gastrointest Endosc.* 1992;38(2):172–173.
9. Wiersema MJ, Hawes RH, Tao LC, et al. Endoscopic ultrasonography as an adjunct to fine needle aspiration cytology of the upper and lower gastrointestinal tract. *Gastrointest Endosc.* 1992;38(1):35–39.
10. Varadarajulu S, Jhala NC. Cytopathology: a dying art or something that a gastroenterologist should know? *Gastrointest Endosc.* 2012;76(2):397–399.
11. Varadarajulu S, Fockens P, Hawes RH. Best practices in endoscopic ultrasound-guided fine-needle aspiration. *Clin Gastroenterol Hepatol.* 2012;10(7):697–703.
12. Eltoum IA, Chhieng DC, Jhala D, et al. Cumulative sum procedure in evaluation of EUS-guided FNA cytology: the learning curve and diagnostic performance beyond sensitivity and specificity. *Cytopathology.* 2007;18(3):143–150.
13. Kida M, Araki M, Miyazawa S, et al. Comparison of diagnostic accuracy of endoscopic ultrasound-guided fine-needle aspiration with 22- and 25-gauge needles in the same patients. *J Interv Gastroenterol.* 2011;1(3):102–107.
14. Sakamoto H, Kitano M, Komaki T, et al. Prospective comparative study of the EUS guided 25-gauge FNA needle with the 19-gauge Trucut needle and 22-gauge FNA needle in patients with solid pancreatic masses. *J Gastroenterol Hepatol.* 2009;24(3):384–390.
15. Siddiqui UD, Rossi F, Rosenthal LS, et al. EUS-guided FNA of solid pancreatic masses: a prospective, randomized trial comparing 22-gauge and 25-gauge needles. *Gastrointest Endosc.* 2009;70(6):1093–1097.
16. Bang JY, Hebert-Magee S, Trevino J, et al. Randomized trial comparing the 22-gauge aspiration and 22-gauge biopsy needles for EUS-guided sampling of solid pancreatic mass lesions. *Gastrointest Endosc.* 2012;76(2):321–327.
17. Affolter KE, Schmidt RL, Matynia AP, et al. Needle size has only a limited effect on outcomes in EUS-guided fine needle aspiration: a systematic review and meta-analysis. *Dig Dis Sci.* 2013;58(4):1026–1034.
18. Knight CS, Eloubeidi MA, Crowe R, et al. Utility of endoscopic ultrasound-guided fine-needle aspiration in the diagnosis and staging of colorectal carcinoma. *Diagn Cytopathol.* 2011;41(12):1031–1037.
19. Madhoun MF, Wani SB, Rastogi A, et al. The diagnostic accuracy of 22-gauge and 25-gauge needles in endoscopic ultrasound-guided fine needle aspiration of solid pancreatic lesions: a meta-analysis. *Endoscopy.* 2013;45(2):86–92.
20. Lee JH, Stewart J, Ross WA, et al. Blinded prospective comparison of the performance of 22-gauge and 25-gauge needles in endoscopic ultrasound-guided fine needle aspiration of the pancreas and peri-pancreatic lesions. *Dig Dis Sci.* 2009;54(10):2274–2281.
21. Layfield LJ, Ehya H, Filie AC, et al. Papanicolaou Society of Cytopathology. Utilization of ancillary studies in the cytologic diagnosis of biliary and pancreatic lesions: the Papanicolaou Society of Cytopathology guidelines for hepatobiliary cytology. *Diagn Cytopathol.* 2014;42(4):351–362.
22. Stigt JA, 't Hart NA, Knol AJ, et al. Pyrosequencing analysis of EGFR and KRAS mutations in EUS and EBUS-derived cytologic samples of adenocarcinomas of the lung. *J Thorac Oncol.* 2013;8(8):1012–1018.
23. Kanagal-Shamanna R, Portier BP, Singh RR, et al. Next-generation sequencing-based multi-gene mutation profiling of solid tumors using fine needle aspiration samples: promises and challenges for routine clinical diagnostics. *Modern Pathol.* 2013;27(2):314–327.
24. Deftereos G, Finkelstein SD, Jackson SA, et al. The value of mutational profiling of the cytocentrifugation supernatant fluid from fine-needle aspiration of pancreatic solid mass lesions. *Modern Pathol.* 2014;27:594–601.
25. Nunez AL, Jhala NC, Carroll AJ, et al. Endoscopic ultrasound and endobronchial ultrasound-guided fine-needle aspiration of deep-seated lymphadenopathy: analysis of 1338 cases. *Cytjournal.* 2012;9:14.
26. Storch I, Jordi M, Thurer R, et al. Advantage of EUS Trucut biopsy combined with fine-needle aspiration without immediate on-site cytopathologic examination. *Gastrointest Endosc.* 2006;64(4):505–511.
27. Varadarajulu S, Bang JY, Hebert-Magee S. Assessment of the technical performance of the flexible 19-gauge EUS-FNA needle. *Gastrointest Endosc.* 2012;76(2):336–343.
28. Bang JY, Ramesh J, Trevino J, et al. Objective assessment of an algorithmic approach to EUS-guided FNA and interventions. *Gastrointest Endosc.* 2013;77(5):739–744.
29. Kate MS, Kamal MM, Bobhate SK, Kher AV. Evaluation of fine needle capillary sampling in superficial and deep-seated lesions. An analysis of 670 cases. *Acta Cytol.* 1998;42(3):679–684.
30. Wallace MB, Kennedy T, Durkalski V, et al. Randomized controlled trial of EUS-guided fine needle aspiration techniques for the detection of malignant lymphadenopathy. *Gastrointest Endosc.* 2001;54(4):441–447.
31. Puri R, Vilman P, Saftoiu A, et al. Randomized controlled trial of endoscopic ultrasound-guided fine-needle sampling with or without suction for better cytological diagnosis. *Scand J Gastroenterol.* 2009;44(4):499–504.
32. Weston BR, Bhutani MS. Optimizing diagnostic yield for EUS-guided sampling of solid pancreatic lesions: a technical review. *Gastroenterol Hepatol.* 2013;9(6):352–363.
33. Jhala NC, Jhala D, Eltoum I, et al. Endoscopic ultrasound-guided fine-needle aspiration biopsy: a powerful tool to obtain samples from small lesions. *Cancer.* 2004;102(4):239–246.
34. LeBlanc JK, Ciaccia D, Al-Assi MT, et al. Optimal number of EUS-guided fine needle passes needed to obtain a correct diagnosis. *Gastrointest Endosc.* 2004;59(4):475–481.
35. Bang JY, Magee SH, Ramesh J, et al. Randomized trial comparing fanning with standard technique for endoscopic ultrasound-guided fine-needle aspiration of solid pancreatic mass lesions. *Endoscopy.* 2013;45(6):445–450.
36. Jhala NC, Eltoum IA, Eloubeidi MA, et al. Providing on-site diagnosis of malignancy on endoscopic-ultrasound-guided fine-needle aspirates: should it be done? *Ann Diagn Pathol.* 2007;11(3):176–181.
37. Klapman JB, Logrono R, Dye CE, Waxman I. Clinical impact of on-site cytopathology interpretation on endoscopic ultrasound-guided fine needle aspiration. *Am J Gastroenterol.* 2003;98(6):1289–1294.

38. Petrone MC, Arcidiacono PG, Carrara S, et al. Does cytotechnician training influence the accuracy of EUS-guided fine-needle aspiration of pancreatic masses? *Dig Liv Dis.* 2012;44(4):311–314.
39. Burlingame OO, Kesse KO, Silverman SG, Cibas ES. On-site adequacy evaluations performed by cytotechnologists: correlation with final interpretations of 5241 image-guided fine-needle aspiration biopsies. *Cancer Cytopathol.* 2012;120(3):177–184.
40. Collins BT. Telepathology in cytopathology: challenges and opportunities. *Acta Cytol.* 2013;57(3):221–232.
41. Marotti JD, Johncox V, Ng D, et al. Implementation of telecytology for immediate assessment of endoscopic ultrasound-guided fine-needle aspirations compared to conventional on-site evaluation: analysis of 240 consecutive cases. *Acta Cytol.* 2012;56(5):548–553.
42. Goyal A, Jhala N, Gupta P. TeleCyP (Telecytopathology): real-time fine-needle aspiration interpretation. *Acta Cytol.* 2012;56(6):669–677.
43. Eloubeidi MA, Jhala D, Chhieng DC, et al. Yield of endoscopic ultrasound-guided fine-needle aspiration biopsy in patients with suspected pancreatic carcinoma. *Cancer.* 2003;99(5):285–292.
44. Jhala N, Jhala D, Vickers SM, et al. Biomarkers in diagnosis of pancreatic carcinoma in fine-needle aspirates. *Am J Clin Pathol.* 2006;126(4):572–579.
45. Kosarac O, Takei H, Zhai QJ, et al. S100P and XIAP expression in pancreatic ductal adenocarcinoma: potential novel biomarkers as a diagnostic adjunct to fine needle aspiration cytology. *Acta Cytol.* 2011;55(2):142–148.
46. Dim DC, Jiang F, Qiu Q, et al. The usefulness of S100P, mesothelin, fascin, prostate stem cell antigen, and 14-3-3 sigma in diagnosing pancreatic adenocarcinoma in cytological specimens obtained by endoscopic ultrasound guided fine-needle aspiration. *Diagn Cytopathol.* 2014;42:193–199.
47. Reicher S, Boyar FZ, Albitar M, et al. Fluorescence in situ hybridization and K-ras analyses improve diagnostic yield of endoscopic ultrasound-guided fine-needle aspiration of solid pancreatic masses. *Pancreas.* 2011;40(7):1057–1062.
48. Gu M, Ghafari S, Lin F, Ramzy I. Cytological diagnosis of endocrine tumors of the pancreas by endoscopic ultrasound-guided fine-needle aspiration biopsy. *Diagn Cytopathol.* 2005;32(4):204–210.
49. Jhala D, Eloubeidi M, Chhieng DC, et al. Fine needle aspiration biopsy of the islet cell tumor of the pancreas: a comparison between computerized axial tomography and endoscopic ultrasound guided fine needle aspiration biopsy. *Ann Diagn Pathol.* 2002;2:106–112.
50. Jhala N, Siegal GP, Jhala D. Large, clear cytoplasmic vacuolation: an under-recognized cytologic clue to distinguish solid pseudopapillary neoplasms of the pancreas from pancreatic endocrine neoplasms on fine-needle aspiration. *Cancer.* 2008;114(4):249–254.
51. Bardales RH, Centeno B, Mallory JS, et al. Endoscopic ultrasound-guided fine-needle aspiration cytology diagnosis of solid-pseudopapillary tumor of the pancreas: a rare neoplasm of elusive origin but characteristic cytomorphologic features. *Am J Clin Pathol.* 2004;121(5):654–662.
52. Hooper K, Mukhtar F, Li S, Eltoum IA. Diagnostic error assessment and associated harm of endoscopic ultrasound-guided fine-needle aspiration of neuroendocrine neoplasms of the pancreas. *Cancer Cytopathol.* 2013;121:653–660.
53. Liu X, Rauch TM, Siegal GP, Jhala N. Solid-pseudopapillary neoplasm of the pancreas: three cases with a literature review. *Appl Immunohistochem Mol Morphol.* 2006;14(4):445–453.
54. Burford H, Baloch Z, Liu X, et al. E-cadherin/beta-catenin and CD10: a limited immunohistochemical panel to distinguish pancreatic endocrine neoplasm from solid pseudopapillary neoplasm of the pancreas on endoscopic ultrasound-guided fine-needle aspirates of the pancreas. *Am J Clin Pathol.* 2009;132(6):831–839.
55. Tanaka M, Fernandez-del Castillo C, Adsay V, et al. International Consensus Guidelines 2012 for the management of IPMN and MCN of the pancreas. *Pancreatology.* 2012;12(3):183–197.
56. Pitman MB, Centeno BA, Daglilar ES, et al. Cytological criteria of high-grade epithelial atypia in the cyst fluid of pancreatic intraductal papillary mucinous neoplasms. *Cancer Cytopathol.* 2014;122(1):40–47.
57. Genevay M, Mino-Kenudson M, Yaeger K, et al. Cytology adds value to imaging studies for risk assessment of malignancy in pancreatic mucinous cysts. *Ann Surg.* 2011;254(6):977–983.
58. Bhutani MS, Gupta V, Guha S, et al. Pancreatic cyst fluid analysis—a review. *J Gastrointest Liver Dis.* 2011;20(2):175–180.
59. van der Waaij LA, van Dullemen HM, Porte RJ. Cyst fluid analysis in the differential diagnosis of pancreatic cystic lesions: a pooled analysis. *Gastrointest Endosc.* 2005;62(3):383–389.
60. Cizginer S, Turner BG, Bilge AR, et al. Cyst fluid carcinoembryonic antigen is an accurate diagnostic marker of pancreatic mucinous cysts. *Pancreas.* 2011;40(7):1024–1028.
61. Sreenarasimhaiah J, Lara LF, Jazrawi SF, et al. A comparative analysis of pancreas cyst fluid CEA and histology with DNA mutational analysis in the detection of mucin producing or malignant cysts. *JOP.* 2009;10(2):163–168.
62. Sawhney MS, Devarajan S, O'Farrel P, et al. Comparison of carcinoembryonic antigen and molecular analysis in pancreatic cyst fluid. *Gastrointest Endosc.* 2009;69(6):1106–1110.
63. Wu J, Mattheei H, Maitra A, et al. Recurrent GNAS mutations define an unexpected pathway for pancreatic cyst development. *Sci Transl Med.* 2011;3(92):92ra66.
64. Dal Molin M, Mattheei H, Wu J, et al. Clinicopathological correlates of activating GNAS mutations in intraductal papillary mucinous neoplasm (IPMN) of the pancreas. *Ann Surg Oncol.* 2013;20:3802–3808.
65. Pugh JL, Jhala NC, Eloubeidi MA, et al. Diagnosis of deep-seated lymphoma and leukemia by endoscopic ultrasound-guided fine-needle aspiration biopsy. *Am J Clin Pathol.* 2006;125(5):703–709.
66. Bakdounes K, Jhala N, Jhala D. Diagnostic usefulness and challenges in the diagnosis of mesothelioma by endoscopic ultrasound guided fine needle aspiration. *Diagn Cytopathol.* 2008;36(7):503–507.
67. Srinivasan R, Bhutani MS, Thosani N, et al. Clinical impact of EUS-FNA of mediastinal lymph nodes in patients with known or suspected lung cancer or mediastinal lymph nodes of unknown etiology. *J Gastrointest Liver Dis.* 2012;21(2):145–152.
68. Coe A, Conway J, Evans J, et al. The yield of EUS-FNA in undiagnosed upper abdominal adenopathy is very high. *J Clin Ultrasound.* 2013;41(4):210–213.
69. Eloubeidi MA, Desmond R, Desai S, et al. Impact of staging transesophageal EUS on treatment and survival in patients with non-small-cell lung cancer. *Gastrointest Endosc.* 2008;67(2):193–198.
70. Fischer AH, Benedict CC, Amrikachi M. Five top stories in cytopathology. *Arch Pathol Lab Med.* 2013;137(7):894–906.
71. Eloubeidi MA, Varadarajulu S, Eltoum I, et al. Transgastric endoscopic ultrasound-guided fine-needle aspiration biopsy and flow cytometry of suspected lymphoma of the spleen. *Endoscopy.* 2006;38(6):617–620.
72. Handa U, Tiwari A, Singhal N, et al. Utility of ultrasound-guided fine-needle aspiration in splenic lesions. *Diagn Cytopathol.* 2013;41(12):1038–1042.
73. Iwashita T, Yasuda I, Tsurumi H, et al. Endoscopic ultrasound-guided fine needle aspiration biopsy for splenic tumor: a case series. *Endoscopy.* 2009;41(2):179–182.
74. Bhutani MS. Endoscopic ultrasound in the diagnosis, staging and management of colorectal tumors. *Gastroenterol Clin North Am.* 2008;37(1):215–227, viii.
75. Faigel DO, Burke A, Ginsberg GG, et al. The role of endoscopic ultrasound in the evaluation and management of foregut duplications. *Gastrointest Endosc.* 1997;45(1):99–103.

76. Napolitano V, Pezzullo AM, Zeppa P, et al. Foregut duplication of the stomach diagnosed by endoscopic ultrasound guided fine-needle aspiration cytology: case report and literature review. *World J Surg Oncol.* 2013;11:33.
77. Ito H, Inoue H, Ryozawa S, et al. Fine-needle aspiration biopsy and endoscopic ultrasound for pretreatment pathological diagnosis of gastric gastrointestinal stromal tumors. *Gastroenterol Res and Pract.* 2012;2012:139083.
78. Gomes AL, Bardales RH, Milanezi F, et al. Molecular analysis of c-Kit and PDGFRA in GISTs diagnosed by EUS. *Am J Clin Pathol.* 2007;127(1):89–96.
79. Gu M, Ghafari S, Nguyen PT, Lin F. Cytologic diagnosis of gastrointestinal stromal tumors of the stomach by endoscopic ultrasound-guided fine-needle aspiration biopsy: cytomorphic and immunohistochemical study of 12 cases. *Diagn Cytopathol.* 2001;25(6):343–350.
80. Saftoiu A. Endoscopic ultrasound-guided fine needle aspiration biopsy for the molecular diagnosis of gastrointestinal stromal tumors: shifting treatment options. *J Gastrointest Liver Dis.* 2008;17(2):131–133.
81. Crowe DR, Eloubeidi MA, Chhieng DC, et al. Fine-needle aspiration biopsy of hepatic lesions: computerized tomographic-guided versus endoscopic ultrasound-guided FNA. *Cancer.* 2006;108(3):180–185.
82. Crowe A, Knight CS, Jhala D, et al. Diagnosis of metastatic fibrolamellar hepatocellular carcinoma by endoscopic ultrasound-guided fine needle aspiration. *Cytojournal.* 2011;8:2.
83. tenBerge J, Hoffman BJ, Hawes RH, et al. EUS-guided fine needle aspiration of the liver: indications, yield, and safety based on an international survey of 167 cases. *Gastrointest Endosc.* 2002;55(7):859–862.
84. Wee A, Sampatanukul P, Jhala N. Focal liver lesions suspicious for hepatocellular carcinoma. In Geisinger K, Pitman M, eds. *Cytobiology of Focal Liver Lesions.* Cambridge University Press. 2014;100–139.
85. Meara RS, Jhala D, Eloubeidi MA, et al. Endoscopic ultrasound-guided FNA biopsy of bile duct and gallbladder: analysis of 53 cases. *Cytopathology.* 2006;17(1):42–49.
86. Ohshima Y, Yasuda I, Kawakami H, et al. EUS-FNA for suspected malignant biliary strictures after negative endoscopic transpapillary brush cytology and forceps biopsy. *J Gastroenterol.* 2011;46(7):921–928.
87. Levy MJ, Heimbach JK, Gores GJ. Endoscopic ultrasound staging of cholangiocarcinoma. *Curr Opin Gastroenterol.* 2012;28(3):244–252.
88. Jhala NC, Jhala D, Eloubeidi MA, et al. Endoscopic ultrasound-guided fine-needle aspiration biopsy of the adrenal glands: analysis of 24 patients. *Cancer.* 2004;102(5):308–314.
89. Uemura S, Yasuda I, Kato T, et al. Preoperative routine evaluation of bilateral adrenal glands by endoscopic ultrasound and fine-needle aspiration in patients with potentially resectable lung cancer. *Endoscopy.* 2013;45(3):195–201.
90. Bodtger U, Vilmann P, Clementsen P, et al. Clinical impact of endoscopic ultrasound-fine needle aspiration of left adrenal masses in established or suspected lung cancer. *J Thorac Oncol.* 2009;4(12):1485–1489.



**Video 22.1** Video of On-Site Processing of Specimen Procured by Endoscopic Ultrasonography-Guided Fine-Needle Aspiration

# Endoscopic Ultrasound-Guided Drainage of Pancreatic Fluid Collections

JI YOUNG BANG AND SHYAM VARADARAJULU

## KEY POINTS

- Recognition of different types of pancreatic fluid collections is crucial for appropriate management.
- Endoscopic-ultrasonography (EUS)-guided drainage is the treatment of choice in the management of pancreatic pseudocysts, with clinical outcomes comparable to surgical cystogastrostomy.
- The endoscopic management of walled-off necrosis (WON) is more complex and is tailored to the size and location of the fluid collection. An algorithmic step-up approach, consisting of the creation of multiple transmural tracts, percutaneous drain insertion, and endoscopic necrosectomy, may be required to achieve successful clinical outcomes.
- Identification of disconnected pancreatic duct syndrome (DPDS) is crucial in patients with WON, as they require plastic transmural stents to remain in situ indefinitely to minimize the risk of recurrence.

## Definitions

Pancreatic fluid collections (PFCs) can be broadly divided into four main types: (1) acute peripancreatic fluid collection, (2) pancreatic pseudocyst, (3) acute necrotic collection, and (4) WON, with the classification depending on the presence of a mature wall and the degree of solid, necrotic debris.<sup>1</sup>

Acute peri-PFC and pancreatic pseudocysts both result from acute interstitial edematous pancreatitis and therefore contain no necrotic material. Acute PFCs usually develop less than 4 weeks from the onset of acute pancreatitis and can be differentiated from pancreatic pseudocysts by the absence of a mature outer wall. In contrast, pancreatic pseudocysts are characterized by the presence of a mature wall, which usually requires 3 to 4 weeks to develop from the inciting event (Fig. 23.1A and B).

Acute necrotic fluid collections and WON occur as a result of acute necrotizing pancreatitis and therefore are characterized by the presence of solid, necrotic debris of varying quantity. Similar to the difference between acute peri-PFC and pancreatic pseudocysts, acute necrotic fluid collections are present early on in the course of acute necrotizing pancreatitis (Fig. 23.2A and B), whereas WON develops after sufficient time has passed for a mature wall to form around the necrotic collection (usually >4 weeks after the onset of acute pancreatitis) (Fig. 23.3A and B and Table 23.1).<sup>2</sup>

Computed tomography (CT) with contrast enhancement is the most commonly performed imaging modality to diagnose PFCs; however, studies have shown superiority of magnetic resonance imaging (MRI) over CT for quantification of necrotic debris.<sup>3,4</sup> The differentiation between necrotic and nonnecrotic PFCs is, in turn, critical owing to the difference in clinical outcomes, with significantly higher treatment success rates, lower adverse events rates, fewer reinterventions, and shorter duration of hospitalization observed following endoscopic drainage of pseudocysts compared to WON.<sup>5</sup> Therefore pseudocysts and WON must be recognized as separate disease entities warranting different management strategies. Furthermore, PFCs can arise in peripancreatic regions with extension into the retroperitoneal space, such as the paracolic gutters, which can pose additional management challenges. In this chapter, we outline the various EUS-guided treatment strategies that can be adopted to maximize treatment success.

## Indications for Intervention

The general consensus is that interventions should be avoided in acute peripancreatic or necrotic collections and should ideally be delayed until a mature wall has developed around the fluid collection.<sup>6,7</sup> Also, patients with asymptomatic PFCs do not require drainage, regardless of the PFC size. However, intervention is required in patients with either symptomatic or infected PFCs, which can result in abdominal pain, failure to thrive, persistent organ failure despite maximum supportive therapy, sepsis, gastric/intestinal outlet obstruction, and biliary obstruction.

## Types of Interventions

### Surgical Drainage

#### Pseudocysts

Surgical interventions in pancreatic pseudocysts primarily consist of either open or laparoscopic cystogastrostomy or cystoenterostomy. However, as pseudocysts are primarily fluid-filled and lack necrotic debris (unlike WON), the larger transmural conduit that can be created via surgical cystogastrostomy is not required. In a randomized trial comparing surgical cystogastrostomy with EUS-guided cystogastrostomy for the drainage of pancreatic pseudocysts, high treatment success was achieved with both modalities (95% in endoscopy vs. 100% in surgery group); however, endoscopic drainage was associated with a significantly shorter hospital

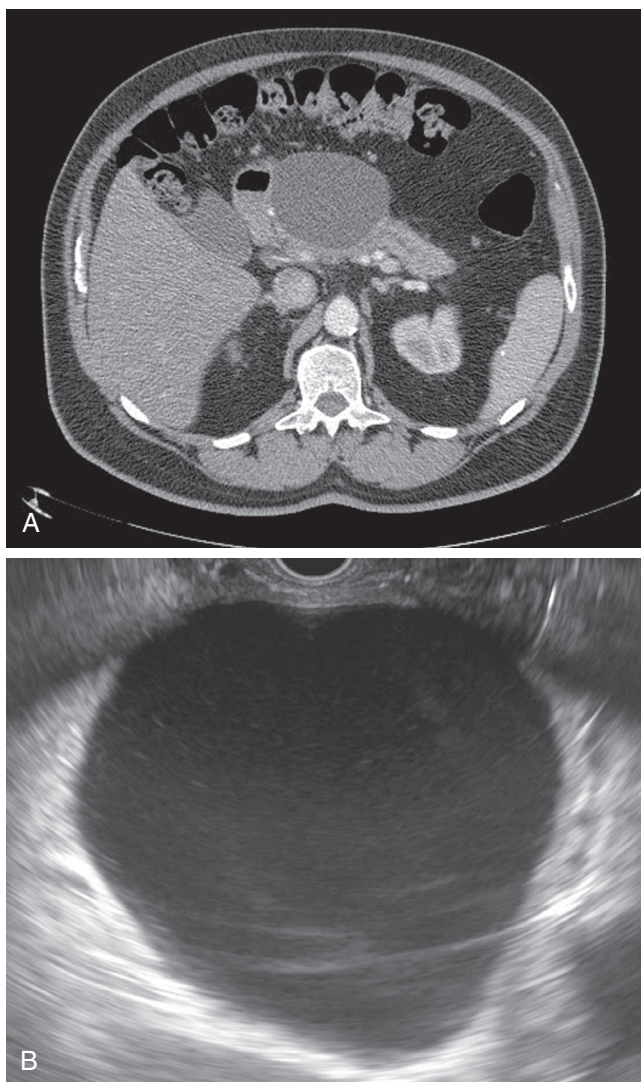


**Fig. 23.1** (A) Axial computed tomography image of a pseudocyst. A definitive wall can be seen surrounding a fluid collection with no solid debris. (B) Pseudocyst on endoscopic ultrasonography: anechoic fluid collection with a definitive wall can be seen.

stay, better physical and mental health, and lower costs.<sup>8</sup> Therefore EUS-guided drainage is the modality of choice in the management of uncomplicated pseudocysts.

## Walled-Off Necrosis

There has been a paradigm shift in the surgical management of WON in recent times, from invasive to minimally invasive surgical techniques. Open surgical necrosectomy is now no longer recommended due to the high morbidity (40% to 55%) and mortality (15% to 20%) associated with this technique.<sup>9,10</sup> Minimally invasive surgical drainage options currently include cystogastrostomy with laparoscopic transabdominal necrosectomy and videoscopic-assisted retroperitoneal debridement (VARD).<sup>11</sup> In a randomized trial (PAncreatitis, Necrosectomy versus sTEp up appRoach [PANTER] trial: Minimally invasive step-up approach versus maximal necrosectomy in patients with acute necrotizing pancreatitis) comparing the step-up minimally invasive surgical approach (consisting of percutaneous drain placement followed by minimally invasive surgical drainage) to open necrosectomy, the

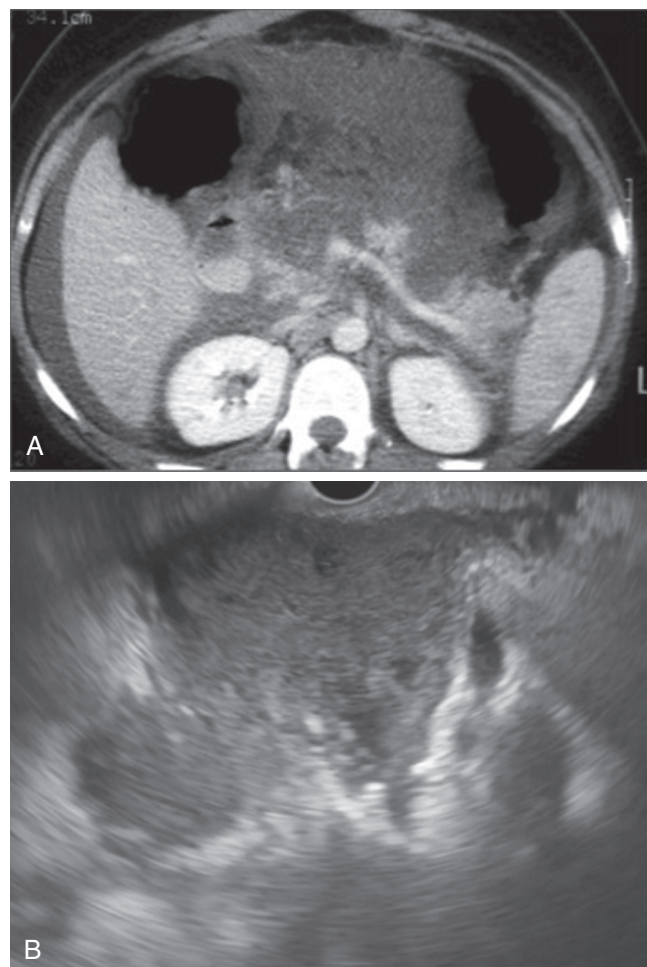


**Fig. 23.2** (A) Axial computed tomography image of an acute necrotic collection. (B) Acute necrotic collection on endoscopic ultrasonography: this is characterized as an ill-defined fluid collection lacking a definitive wall.

latter technique was associated with a significantly higher rate of major adverse events.<sup>10</sup> Additionally, according to the results from a recent randomized trial (TESION trial: Transluminal endoscopic step-up approach vs. minimally invasive surgical step-up approach in patients with infected necrotizing pancreatitis), when compared to the step-up endoscopic approach (transmural drainage followed by endoscopic necrosectomy), the step-up minimally invasive surgical technique (percutaneous drain insertion followed by minimally invasive surgical necrosectomy) resulted in similar rates of major adverse events. However, endoscopic therapy was associated with shorter duration of hospitalization, lower costs, and lower rates of pancreatic fistula formation.<sup>12</sup> Therefore when the requisite expertise is available, endoscopic drainage (with or without necrosectomy) should be undertaken as the first-line therapy in the management of WON.

## Percutaneous Drainage

Percutaneous drain insertion under radiologic guidance is increasingly performed as the initial treatment modality in the step-up surgical approach to the management of WON, and as adjunctive therapy in patients with collections not amenable to endoscopic drainage.<sup>13</sup> One of the main advantages of this modality is that no further necrosectomy may be required in a significant proportion (up to 55%) of WON patients following

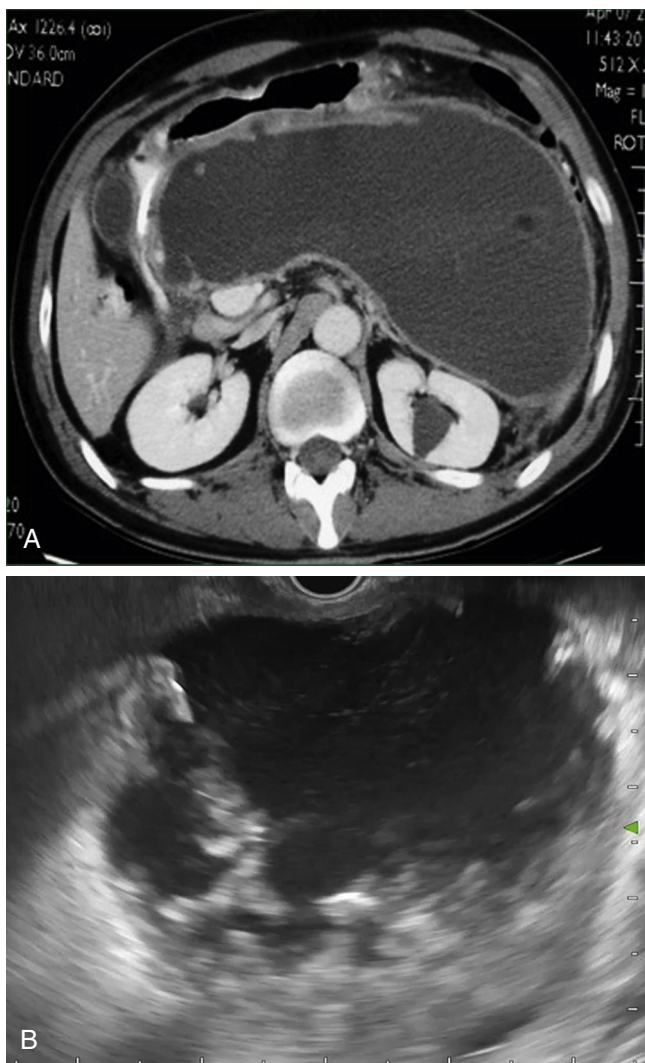


**Fig. 23.3** (A) Axial computed tomography image of walled-off pancreatic necrosis (WON): a well-defined collection containing solid debris surrounded by an outer wall is seen. (B) WON on endoscopic ultrasonography: solid debris can be seen within the WON as hyperechoic structures.

percutaneous drainage<sup>14</sup>; in those requiring further interventions, the percutaneous tract can be dilated to provide a conduit for sinus tract necrosectomy or VARD. However, as yet, no clear guidelines exist regarding the timing of drainage, the size of drain required, or the optimal duration of insertion, and there have been no studies comparing percutaneous drainage alone with endoscopic drainage. Also, adverse event rates associated with percutaneous drainage can range from 22% to 50%, and consist of bleeding, colonic perforation, and pancreaticocutaneous or pancreaticoenteric fistula formation.<sup>14–16</sup> In our practice, we request insertion of a large bore percutaneous drain (16 Fr) for large WON >12 cm in size with extension into the paracolic gutters, so it can be used in conjunction with EUS-guided transmural drainage as a part of the “dual-modality” technique (see section on dual-modality).

### Endoscopic-Ultrasonography-Guided Drainage

Since the first description of the single-step technique in 1998, EUS-guided drainage is now the standard of care technique for endoscopic drainage of PFCs.<sup>17,18</sup> The treatment success following

**TABLE 23.1** Summary of Pancreatic Fluid Collection Types

Pancreatic Fluid Collection Types	Etiology	Time for Development (Weeks)	Presence of a Mature Wall	Necrotic Debris
Acute peripancreatic fluid collection	Interstitial pancreatitis	<4	No	No
Pseudocyst	Interstitial pancreatitis	≥4	Yes	No
Acute necrotic collection	Necrotizing pancreatitis	<4	No	Yes
Walled-off necrosis	Necrotizing pancreatitis	≥4	Yes	Yes

Adapted from Holt BA, Varadarajulu S. The endoscopic management of pancreatic pseudocysts (with videos). Gastrointest Endosc 2015;81:804–12.

EUS-guided drainage of pancreatic pseudocysts is high at 73% to 100%, in contrast to the suboptimal treatment success rates of 60% to 70% observed with WON.<sup>19</sup> In the following section, various EUS-guided drainage techniques will be described, with the aim of optimizing clinical outcomes and minimizing adverse events.

### Preprocedure Checklist

Prior to EUS-guided drainage of PFCs, the following steps should be undertaken:

- History and physical examination, with a review of vital signs and laboratory values to determine the indication for drainage, the presence of systemic inflammatory response syndrome (SIRS), sepsis, and organ failure.
- Review of the most recent cross-sectional imaging to assess for the presence of solid debris and confirmation of the presence of a mature wall.
- Optimization of coagulation parameters (international normalized ratio [INR] ≤ 1.5, platelet count > 50,000/mm<sup>3</sup>).
- Optimization of nutritional status with enteral feeding via nasojejunal or percutaneous gastrojejunal tube if unable to tolerate adequate oral diet.
- Administration of broad-spectrum intravenous antibiotics prior to instrumentation. Intravenous ciprofloxacin or piperacillin/tazobactam are the preferred antibiotics of choice and should be continued for 5 days postdrainage.
- Multidisciplinary care in consultation with pancreatic surgeons and interventional radiologists.

### Cautions Prior to Endoscopic Ultrasonography-Guided Pancreatic Fluid Collection Drainage

Prior to drainage of any PFC, a careful EUS examination should be performed as EUS has been shown to alter the management in up to 37.5% of patients referred for endoscopic drainage, due to several reasons.<sup>20</sup> First, the suitability for endoscopic drainage

as determined by the presence of a mature wall around the PFC that is adherent to the gastric or duodenal wall can be confirmed on EUS, especially if less than 3 to 4 weeks have passed since the inciting event. If the wall is still immature without adequate adherence, endoscopic drainage should be postponed ([Video 23.1](#)). Second, the presence of malignancy can be excluded as the etiology of the PFC on EUS, which has been shown to occur in 1.25% of patients referred for endoscopic drainage ([Video 23.2](#)).<sup>21</sup> Finally, other types of cysts can mimic PFCs, such as duplication cysts and mucinous cysts (mucinous cystic neoplasms and intraductal papillary mucinous neoplasm). In one study, 5% of patients originally diagnosed with pancreatic pseudocysts on CT were found to have mucinous cystic neoplasms on EUS ([Video 23.3](#)).<sup>22</sup>

### Procedure Techniques

EUS-guided drainage of PFCs should be performed in a thoughtful and systematic manner, adopting variations in endoscopic techniques according to the type, size, and location of the PFC, and the subsequent response to treatment. This approach, in conjunction with collaborative management with pancreatic surgeons and interventional radiologists, is especially important in the management of WON, where treatment success can be suboptimal at only 60% to 70%.<sup>23</sup>

**Single-Gate Technique.** The single-gate technique consists of the creation of a single transmural tract through which plastic or metal stents are placed for PFC drainage. This is a multistep process when plastic stents are being deployed ([Video 23.4](#)), but can be a single-step process when using lumen-apposing metal stents (LAMS) with an electrocautery-enhanced delivery system (Hot AXIOS, Boston Scientific Corporation, Marlborough, Massachusetts) ([Video 23.5](#)).

#### Plastic Stent Insertion.

##### Accessories.

- Therapeutic linear array echoendoscope with a 3.7-mm working channel
- Fluoroscopy
- 19-Gauge fine-needle aspiration (FNA) needle
- Syringe for aspiration of PFC contents for Gram stain and culture
- 0.025- or 0.035-inch guidewire
- Two types of dilators: (1) a 4.5-Fr tapered tip endoscopic retrograde cholangiopancreatography (ERCP) cannula, or needle-knife catheter, or cystotome catheter; AND (2) a graded balloon dilator
- Two or more 7 Fr diameter 4 cm length double pigtail plastic stents

##### Technique.

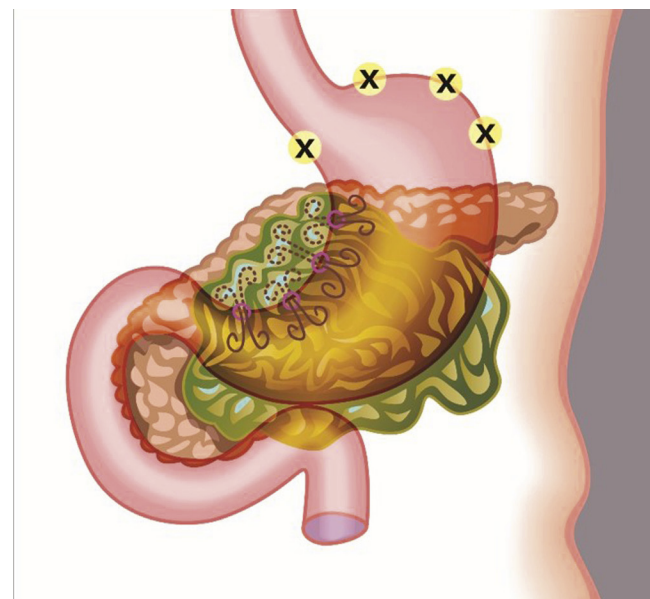
###### 1. PFC puncture and guidewire insertion

After excluding the presence of vasculature in the path of the needle by using color Doppler ultrasound, a 19-gauge FNA needle is used to puncture the PFC under EUS guidance ([Fig. 23.4](#)). A sample of the PFC fluid is aspirated at this time and sent for Gram stain and culture if there is a clinical suspicion of infection. In patients with WON, where endoscopic necrosectomy may be required in the future, the creation of transmural tracts should be avoided in the cardia and fundus, if possible, as these sites make future access to the necrotic cavity difficult or impossible ([Fig. 23.5](#); [Video 23.6](#)).

A 0.025- or 0.035-inch guidewire is then introduced through the needle and allowed to coil several times within the PFC cavity under fluoroscopic guidance ([Fig. 23.6](#)).



• **Fig. 23.4** Endoscopic ultrasonography image of a fine-needle aspiration needle puncturing the pancreatic fluid collections.



• **Fig. 23.5** Diagram to show the sites to avoid (cardia, fundus) during endoscopic ultrasonography-guided drainage of walled-off pancreatic necrosis.

###### 2. Transmural tract creation and dilation

The transmural tract is sequentially dilated under both endosonographic and fluoroscopic guidance. Various over-the-wire devices can be used for the first stage of dilation, including a 4.5-Fr ERCP cannula, needle knife catheter, or cystotome. In order to minimize the risk of bleeding and perforation, the over-the-wire device must penetrate the wall of the PFC perpendicularly; however, this can be particularly challenging with the use of a needle knife as the tip may not follow the direction of the inserted guidewire ([Video 23.7](#)). Once within the PFC cavity, the catheter device should be withdrawn into the echoendoscope and reinserted into the PFC several times to mature the tract in preparation for balloon dilation.

The second stage of tract dilation is performed under both endosonographic and fluoroscopic guidance using an 8- to 15-mm

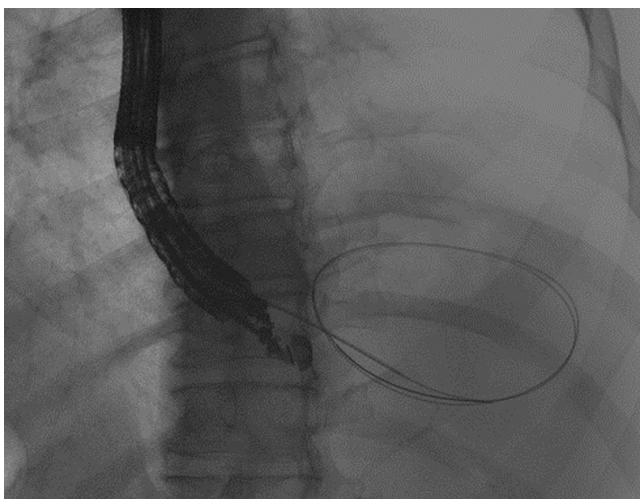


**Fig. 23.6** A soft-tip guidewire is inserted into the pancreatic fluid collections through the fine-needle aspiration needle and looped several times within the pancreatic fluid collections.

over-the-wire biliary balloon dilator. In our practice, smaller dilation is performed for PFCs <6 cm in size or for transduodenal tract dilation. Also, the dilating balloon should be visualized endosonographically at all times to ensure adequate apposition of the PFC to the gastrointestinal wall, thereby minimizing the risk of leak and perforation (Fig. 23.7A and B).

### 3. Plastic stents

Plastic stents 7 Fr in diameter and 3 to 5 cm in length are utilized, with a mark made in the center of the stent to prevent accidental deployment of the proximal end inside the PFC lumen. The 7-Fr stents are preferred to the larger diameter 10-Fr stents due to the ease of deployment of the smaller stent through the smaller working channel of a therapeutic echoendoscope. The stents are deployed with the aid of a push catheter so the distal pigtail is within the PFC and the proximal pigtail is in the gastrointestinal tract. In patients with WON undergoing single-gate drainage, usually two or three plastic stents are deployed in an attempt to create a larger diameter tract to facilitate better drainage of necrotic contents (Fig. 23.8A and B). Once the first stent is deployed, subsequent stent placement can be performed by accessing the PFC using a standard cannula and a guidewire.

**Double-Wire Technique.** The double-wire technique comprises the insertion of two guidewires into the transmural tract, rather than one, following balloon dilation. This technique should be adopted in patients with transmural tracts created in the gastric cardia or fundus, where recannulation of the tract with a catheter for second guidewire insertion is extremely challenging following deployment of the first plastic stent.

After balloon dilation of the transmural tract per standard technique, a 10-Fr plastic catheter is inserted into the PFC cavity, over the single guidewire that is already in place. This is then followed by insertion of a second guidewire into the PFC cavity, through the lumen of the 10-Fr catheter. The catheter is then removed, allowing the insertion of two plastic stents into the transmural tract, one after the other. An important technical issue to note is that due to the size of the echoendoscope working channel (3.7 mm), a 10-Fr plastic stent cannot be passed through the working channel with two guidewires in place (Fig. 23.9A–C; Video 23.8).

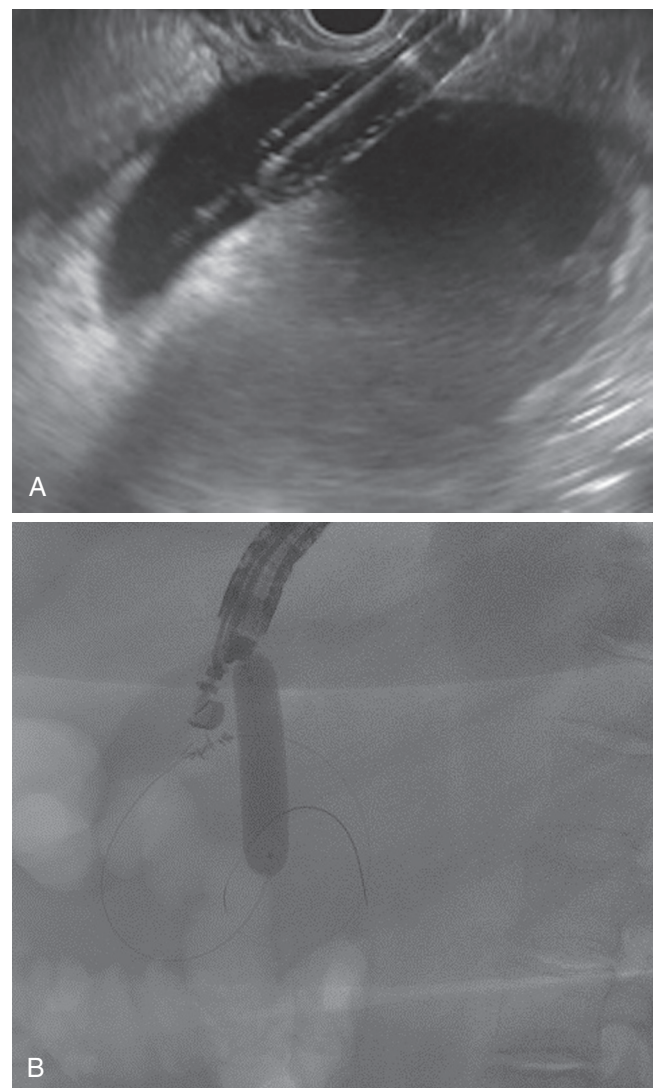


**Fig. 23.7** Balloon dilation of the transmural tract visualized on endoscopic ultrasonography (A) and fluoroscopy (B).

**Metal Stent Insertion.** Metal stents are commonly used for PFC drainage despite the paucity of data. In a recent systematic review, no significant difference was observed in the rates of treatment success, adverse events, or recurrence between metal and plastic stents, regardless of the PFC type.<sup>19</sup>

Novel LAMS specifically designed for PFC drainage have recently been developed (AXIOS, Boston Scientific Corporation; NAGI and SPAXUS, Taewoong Medical, Goyang-Si, Gyeonggi-do, South Korea). These are fully covered stents with a wide lumen (8 to 16 mm diameter) to expedite the drainage of PFC contents and also possess bilateral flanges at both ends to minimize stent migration. In a case-control study of 60 patients with pseudocysts and WON, no significant difference in clinical outcomes was observed between plastic stents and LAMS (Hot AXIOS, Boston Scientific Corporation); however, LAMS placement was associated with a significantly shorter procedure duration (8.5 vs. 25 min;  $P < .001$ ), but was more costly (Fig. 23.10A–C).<sup>24</sup> A randomized trial comparing these two stent types in WON patients is currently underway (NCT02685865).

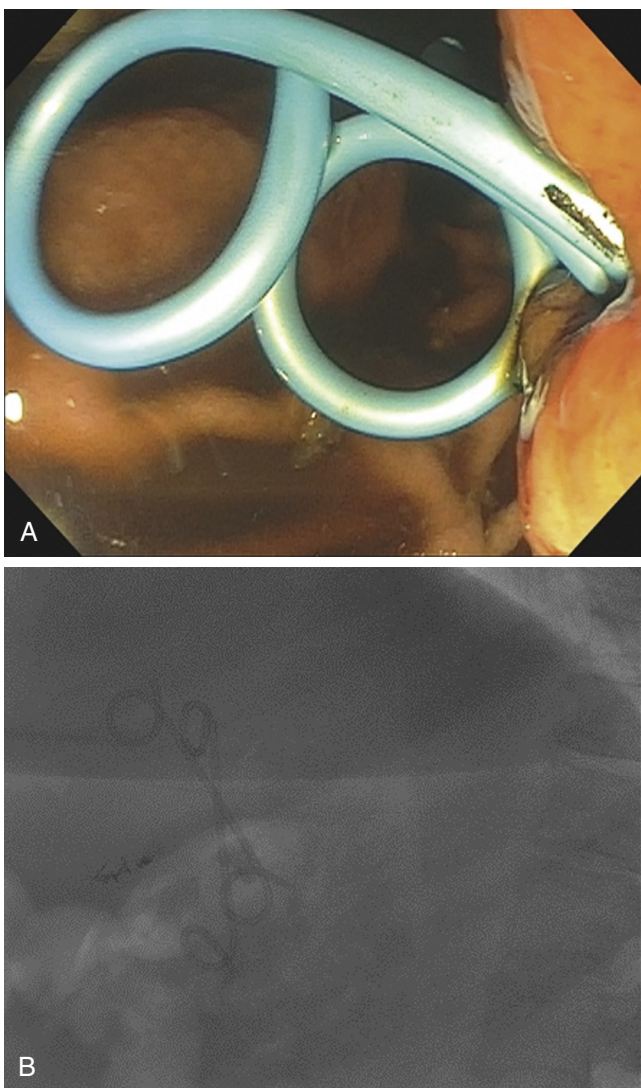


**Fig. 23.8** Two double pigtail stents inserted into the transmural tract as seen on endoscopic view (A) and fluoroscopy (B).

#### Accessories.

- Therapeutic linear array echoendoscope with a  $\geq 3.7$  mm working channel
- Fluoroscopy
- 19-Gauge FNA needle
- Syringe for aspiration of PFC contents for Gram stain and culture
- 0.025- or 0.035-inch guidewire
- Two types of dilators: (1) a 4.5-Fr tapered tip ERCP cannula or needle-knife catheter or cystotome catheter; and (2) a graded balloon dilator
- LAMS with or without an electrocautery-enhanced delivery system

**Technique.** LAMS can be equipped with or without an electrocautery-enhanced delivery system. In the following section, the steps in the management of LAMS using both delivery systems will be described.

LAMS with nonelectrocautery-enhanced delivery system ([Video 23.9](#)):

1. The PFC is punctured under endosonographic guidance using a 19-G FNA needle, followed by the insertion of a 0.025- or

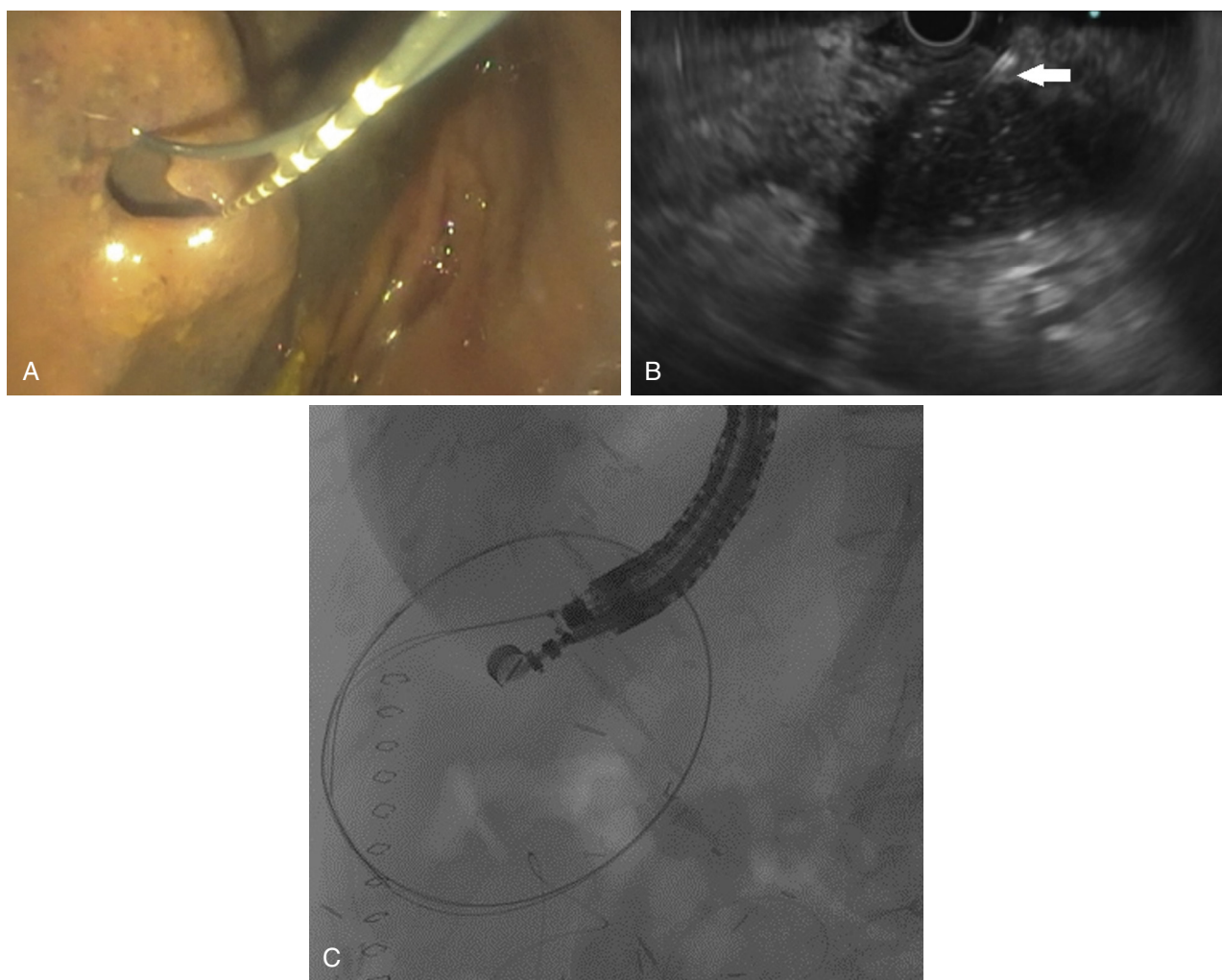
0.035-inch guidewire through the needle, which is looped several times inside the PFC.

2. The transmural tract is sequentially dilated over the guidewire using first an ERCP cannula/needle knife catheter/cystotome, followed by a 4- to 6-mm dilating balloon.
  3. LAMS on a delivery system is inserted over the guidewire into the PFC. The distal flange is deployed first under endosonographic guidance, followed by deployment of the proximal flange under either endosonographic or endoscopic view.
  4. The delivery system and guidewire are removed from the patient.
- LAMS with an electrocautery-enhanced delivery system ([Video 23.5](#)):
1. The PFC is directly punctured using the electrocautery-enhanced tip of the stent delivery system under endosonographic guidance, without the need for a guidewire.
  2. The delivery system is advanced into the PFC.
  3. The distal flange is deployed first under endosonographic guidance, followed by deployment of the proximal flange under either endosonographic or endoscopic view.
  4. The delivery system and guidewire are removed from the patient.

**Multi-Gate Technique.** The multi-gate technique, defined as the creation of more than one transmural tract for PFC drainage, is rarely needed in patients with pseudocysts because the single-gate technique is sufficient to achieve treatment success in >95% of cases.<sup>25</sup> However, the multi-gate technique is necessary in patients with WON  $\geq 12$  cm in size or those with WON  $< 12$  cm that fail to respond to the single-gate technique.<sup>23</sup> The multi-gate technique can be successfully performed using just plastic stents ([Fig. 23.11A and B](#); [Video 23.10](#)) or metal stents ([Fig. 23.12](#); [Video 23.11](#)) or a combination of both plastic and metal stents (see section on Disconnected Pancreatic Duct Syndrome). When creating multiple transmural tracts, we recommend starting with tract creation from the distal stomach or duodenum and proceeding to the proximal stomach, to avoid accidental stent dislodgement during multiple tract creation. Also, it is important not to aspirate vigorously once the initial tract is created, so that the PFC cavity does not collapse completely, thereby precluding subsequent access to the PFC.

**Irrigation of Walled-Off Pancreatic Necrosis Cavity.** In patients with WON, the PFC cavity is aggressively irrigated with sterile water mixed with 120 mg gentamicin following initial stent insertion, in order to expedite the drainage of fluid and necrotic contents. Irrigation can be performed either through the transmural tract using a 5.5-Fr ERCP cannula or through the percutaneous drain if present. Irrigation is continued until the fluid extruding from the transmural tract is clear with minimal solid debris ([Video 23.12](#)). In patients with percutaneous drains, irrigation of the WON cavity is continued postprocedure using 150 to 250 mL of sterile water mixed with 120 mg gentamicin, every 6 hours for at least 48 hours and until no fluid can be aspirated from the percutaneous drain.

**Dual Modality Technique.** The dual modality technique consists of a combination of endoscopic transmural drainage with insertion of a percutaneous drain.<sup>26</sup> This technique is performed in patients with very large WON or when the WON is inaccessible by endoscopic transmural drainage (e.g., extension into the paracolic gutter). As described in the previous section, irrigation of the WON via the percutaneous



• **Fig. 23.9** Two separate wires can be seen on endoscopic view (A), endoscopic ultrasonography (B), and fluoroscopy (C) when using the double-wire technique.

drain is continued for at least 48 hours and until no output is seen from the percutaneous drain following irrigation. It is very important to ensure that large bore drains (>15 Fr) are placed to facilitate better lavage of the necrotic cavity (Video 23.13).

#### **Endoscopic Necrosectomy**

Of the patients with WON, 35% to 49% do not require necrosectomy following drainage.<sup>10,12</sup> Therefore endoscopic necrosectomy should be reserved for patients who fail to respond to EUS-guided drainage using the multi-gate or dual modality technique, manifested by ongoing symptoms, SIRS, sepsis, and/or organ failure. The WON cavity can be accessed from either the transluminal route (direct endoscopic necrosectomy) or from the percutaneous route (sinus tract necrosectomy)—this decision being largely determined by the proximity of the tracts to the WON. Although no dedicated tools have been specifically designed for endoscopic necrosectomy, a combination of forceps, snares, nets, and pentapod devices are commonly used (Video 23.14). Necrosectomy should be continued until all solid necrotic debris has been removed, which is indicated by

the visualization of red granulation tissue that lines the inside of the WON cavity.<sup>27</sup> At the end of each necrosectomy session, it is our practice to irrigate the WON cavity using sterile water/gentamicin solution, followed by hydrogen peroxide solution. Irrigation using hydrogen peroxide should be reserved as the last step at the end of necrosectomy, as it causes a thin film of bubbles to coat the WON cavity, which can significantly impede visualization. An algorithmic approach to PFC management is shown in Fig. 23.13.

#### **Adverse Events**

The reported rates of adverse events following endoscopic drainage of PFCs vary widely, ranging from 0% to 44%, and include infection, bleeding, perforation, and stent migration.<sup>19</sup> In one study from a tertiary referral center, reported adverse events following EUS-guided drainage of 148 patients with pseudocysts or WON included infection in 2.7%, bleeding in 0.67%, perforation in 1.3%, and stent migration in 0.67%.<sup>28</sup> The risk of perforation during PFC drainage can be minimized by ensuring the presence of a mature wall that is adherent to the gastric or the duodenal wall. The risk of perforation is also

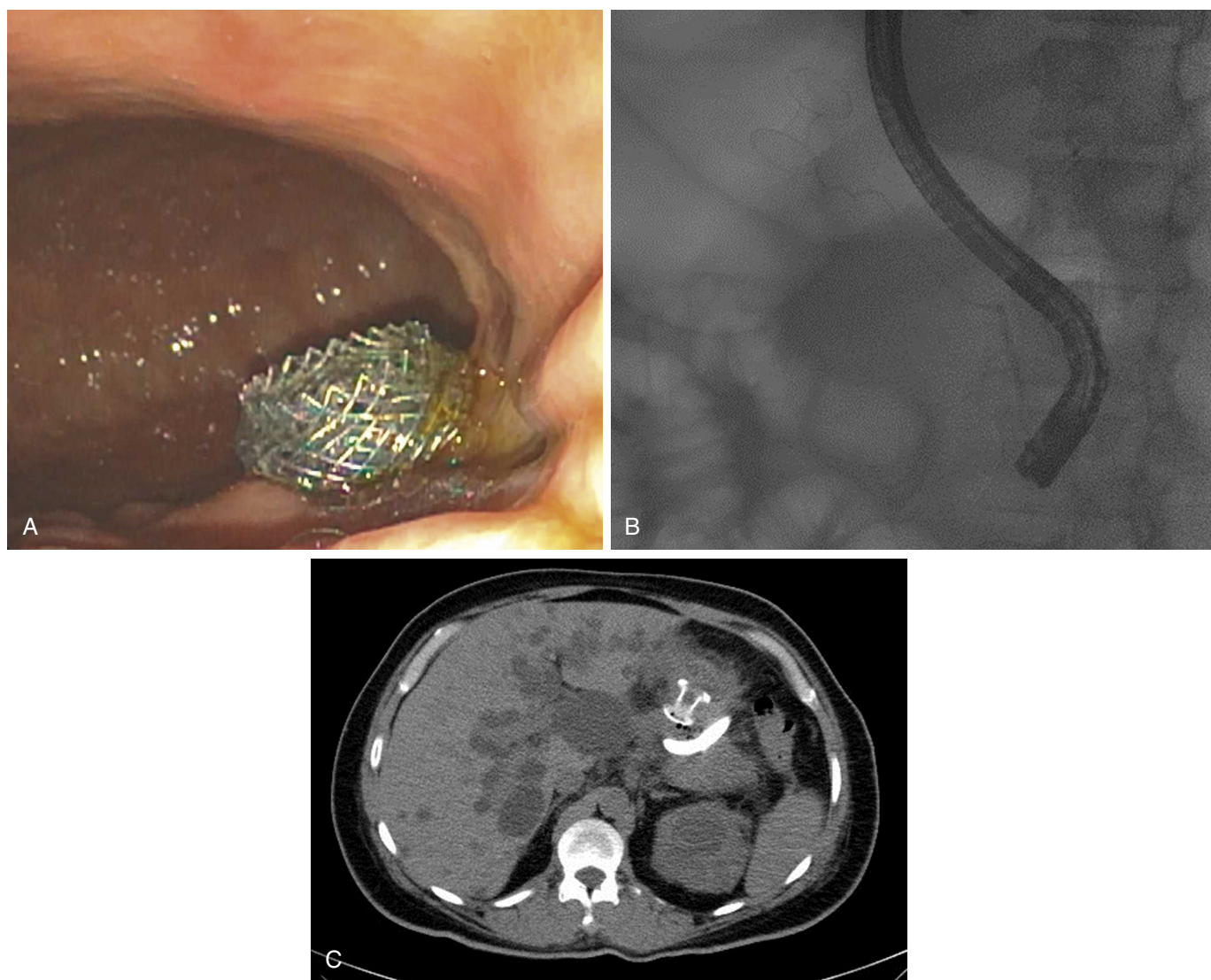


**Fig. 23.10** Single AXIOS stent inserted into the transmural tract as seen on endoscopic view (A), fluoroscopy (B), and computed tomography (C).

significant when performing drainage of PFCs located in the uncinate process via the transgastric route, due to the migration of the PFC away from the gastric wall following tract dilation as the PFC cavity collapses. Therefore PFCs located in the uncinate process should be drained via the transduodenal route ([Video 23.15](#)).

The risk of bleeding can be minimized by ensuring the correction of coagulation abnormalities prior to drainage, and careful examination of the PFC using a color Doppler prior to puncture, to check for intervening vasculature that can course through the inside or over the surface of the PFC ([Video 23.16](#)). Bleeding during PFC drainage can usually be managed using endoscopic techniques ([Video 23.17](#)); however, severe bleeding requires interventional radiology or surgical intervention.

Stent migration can occur either internally into the PFC cavity or externally out of the PFC cavity, rarely resulting in bowel obstruction in the latter scenario.<sup>28,29</sup> A preliminary

audit of the data from the ongoing randomized trial comparing plastic stents with LAMS (NCT02685865), revealed a significantly higher rate of stent-related adverse events in the LAMS group (50 vs. 0%;  $P = .019$ ), which were mostly bleeding.<sup>30</sup> We hypothesize that on resolution of the PFC following transmural drainage, unlike with plastic stents, the distal flange of LAMS remains anchored within the PFC, which can then irritate the local vasculature leading to bleeding. LAMS should therefore be removed 3 to 4 weeks following insertion, to minimize the risk of adverse events.

#### Follow-Up

Patients with pancreatic pseudocysts are followed up with a repeat CT scan at 6 weeks postplastic stent insertion and at 3 to 4 weeks post-LAMS insertion. If the pseudocyst has resolved (<2 cm in size) and the patient is asymptomatic, all stents are removed (with the exception of patients with DPDS—see next section).

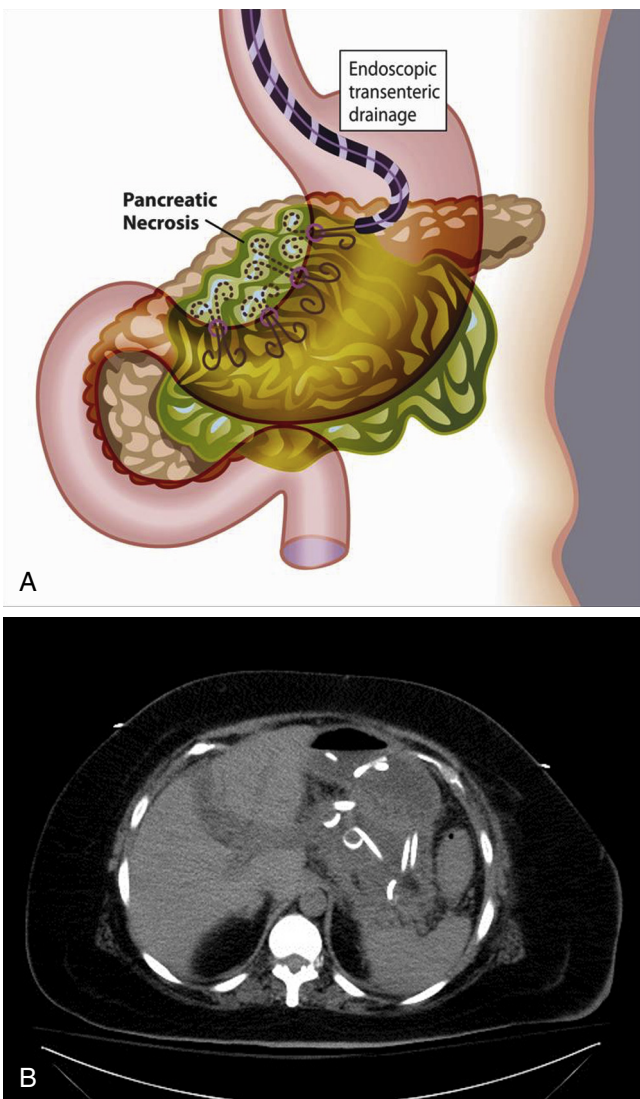


**Fig. 23.11** (A) A diagram depicting the multi-gate technique with creation of multiple transmural tracts. (B) Axial computed tomography image following multi-gate technique using plastic stents.

In patients with WON, an initial follow-up CT scan is performed at 72 hours postinitial drainage to assess treatment response. In patients with inadequate treatment response, additional transmural drainage or endoscopic necrosectomy are required, as outlined in the treatment algorithm (see Fig. 23.13). As with pseudocysts, WON patients with complete clinical and radiologic response should undergo plastic stent removal at 6 weeks, and LAMS removal at 3 to 4 weeks.

## Disconnected Pancreatic Duct Syndrome

DPDS occurs in up to 50% of patients with necrotizing pancreatitis and is defined as the complete disruption of the main pancreatic duct with resultant disconnection of the viable upstream distal pancreatic gland from the main pancreatic duct downstream.<sup>31</sup> DPDS has important clinical and management implications as it can lead to nonresolving WON, pancreatic ascites, and pancreaticocutaneous fistula.<sup>32,33</sup> In a recent study of 361



**Fig. 23.12** Axial computed tomography image following multi-gate technique using lumen-apposing metal stents.

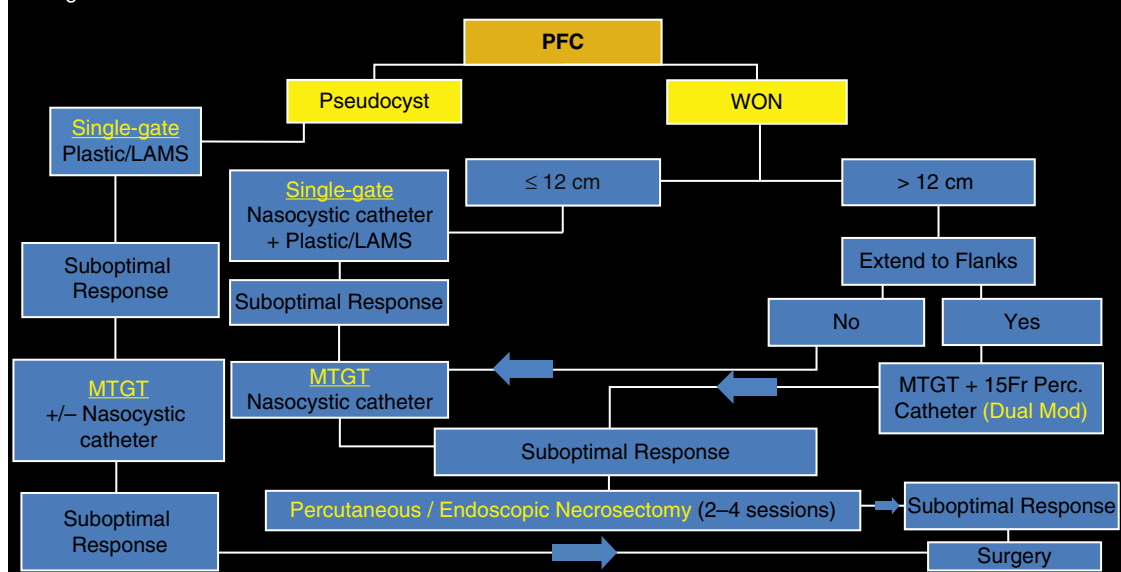
patients with PFCs, when compared to those without DPDS, a significantly higher proportion of patients with DPDS required the multi-gate or dual-modality drainage techniques, endoscopic necrosectomy, rescue surgical interventions, and longer hospitalization.<sup>31</sup> Therefore recognition of this disease entity using magnetic resonance cholangiopancreatography (MRCP) with secretin, EUS, and/or ERCP is crucial so that patients with WON can be managed appropriately (Fig. 23.14A–C). DPDS is characterized on EUS by the presence of a well-defined fluid collection along the course of the main pancreatic duct, with the upstream pancreatic parenchyma and duct terminating into the fluid collection.<sup>34</sup> In a recent study, EUS accurately diagnosed DPDS in 100% of patients, when correlated with findings on CT, pancreatography, and/or surgical pathology (Video 23.18).<sup>34</sup>

Unlike disruption (rather than disconnection) in the pancreatic duct, which can be bridged during ERCP with pancreatic stenting, a disconnected pancreatic duct cannot be bridged endoscopically. Therefore patients with concomitant WON and DPDS require placement of permanent transmural plastic stents in order to provide a conduit for continued drainage of the disconnected upstream pancreatic gland. This has been shown to significantly decrease the rate of WON recurrence in several studies and can obviate the need for surgical resection of the disconnected upstream pancreatic segment.<sup>31,35</sup> Recently, we have developed the “modified multi-gate technique,” where LAMS is inserted into one transmural tract to allow rapid drainage of the WON contents, and plastic stents are inserted into a separate transmural tract in patients with suspected DPDS. On subsequent follow-up, only the LAMS is removed leaving the plastic stents *in situ* indefinitely to drain the disconnected gland (Video 23.19).

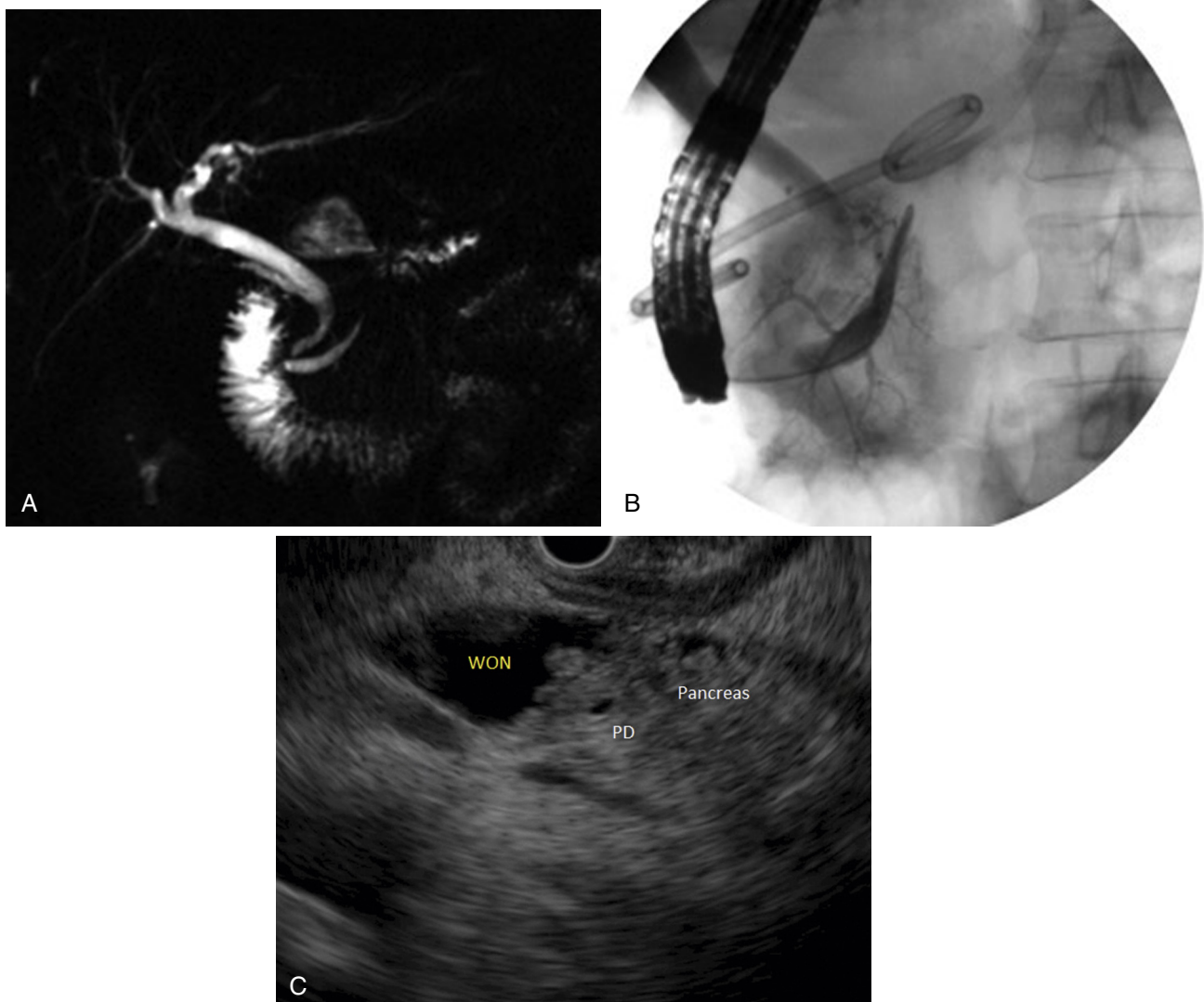
## Summary

EUS-guided drainage of PFCs is highly effective in the management of pancreatic pseudocysts and is therefore the current standard of care. However, the management of WON requires a multidisciplinary approach in conjunction with pancreatic surgeons and interventional radiologists in order to achieve optimal outcomes. When treating patients with WON, a step-up approach should be adopted, starting with EUS-guided drainage and/or percutaneous drain placement, followed by necrosectomy if required. Finally, establishing the presence of DPDS is critical to determine the need for permanent transmural stents to minimize disease recurrence.

**Endoscopic Step-up Approach**



• **Fig. 23.13** Flow diagram showing an algorithmic approach to the management of pseudocysts and walled-off pancreatic necrosis. *LAMS*, Lumen-apposing metal stents; *PFC*, pancreatic fluid collections; *WON*, walled-off pancreatic necrosis.



• **Fig. 23.14** Disconnected pancreatic duct syndrome is visualized on magnetic resonance cholangio-pancreatography (A), pancreatectogram (B), and endoscopic ultrasonography (C). *PD*, Pancreatic duct; *WON*, walled-off pancreatic necrosis.

## Key References

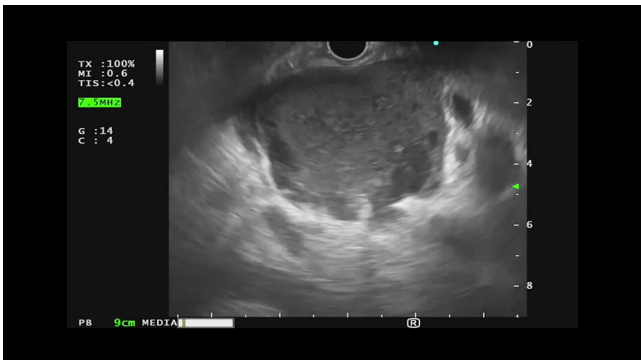
10. van Santvoort HC, Besselink MG, Bakker OJ, et al. A step-up approach or open necrosectomy for necrotizing pancreatitis. *N Engl J Med.* 2010;362:1491–1502.
12. van Brunshot S, van Grinsven J, van Santvoort HC, et al. Endoscopic or surgical step-up approach for infected necrotising pancreatitis: a multicentre randomised trial. *Lancet.* 2018;391:51–58.
19. Bang JY, Hawes R, Bartolucci A, et al. Efficacy of metal and plastic stents for transmural drainage of pancreatic fluid collections: a systematic review. *Dig Endosc.* 2015;27:486–498.
31. Bang JY, Wilcox CM, Navaneethan U, et al. Impact of disconnected pancreatic duct syndrome on the endoscopic management of pancreatic fluid collections. *Ann Surg.* 2018;267:561–568.
34. Bang JY, Navaneethan U, Hasan MK, et al. EUS correlates of disconnected pancreatic duct syndrome in walled-off necrosis. *Endosc Int Open.* 2016;4:E883–E889.

## References

Access the reference list online at [ExpertConsult.com](http://ExpertConsult.com).

## References

1. Banks PA, Bollen TL, Dervenis C, et al. Classification of acute pancreatitis—2012: revision of the Atlanta classification and definitions by international consensus. *Gut*. 2013;62:102–111.
2. Holt BA, Varadarajulu S. The endoscopic management of pancreatic pseudocysts (with videos). *Gastrointest Endosc*. 2015;81:804–812.
3. Hirota M, Kimura Y, Ishiko T, et al. Visualization of the heterogeneous internal structure of so-called “pancreatic necrosis” by magnetic resonance imaging in acute necrotizing pancreatitis. *Pancreas*. 2002;25:63–67.
4. Morgan DE, Baron TH, Smith JK, et al. Pancreatic fluid collections prior to intervention: evaluation with MR imaging compared with CT and US. *Radiology*. 1997;203:773–778.
5. Varadarajulu S, Bang JY, Phadnis MA, et al. Endoscopic transmural drainage of peripancreatic fluid collections: outcomes and predictors of treatment success in 211 consecutive patients. *J Gastrointest Surg*. 2011;15:2080–2088.
6. IAP/APA evidence-based guidelines for the management of acute pancreatitis. *Pancreatology*. 2013;13:e1–e15.
7. Tenner S, Baillie J, DeWitt J, et al. American college of gastroenterology guideline: management of acute pancreatitis. *Am J Gastroenterol*. 2013;108:1400–1415, 1416.
8. Varadarajulu S, Bang JY, Sutton BS, et al. Equal efficacy of endoscopic and surgical cystogastrostomy for pancreatic pseudocyst drainage in a randomized trial. *Gastroenterology*. 2013;145: 583–590. e1.
9. Harrison S, Kakade M, Varadarajulu S, et al. Characteristics and outcomes of patients undergoing debridement of pancreatic necrosis. *J Gastrointest Surg*. 2010;14:245–251.
10. van Santvoort HC, Besselink MG, Bakker OJ, et al. A step-up approach or open necrosectomy for necrotizing pancreatitis. *N Engl J Med*. 2010;362:1491–1502.
11. van Brunschot S, Bakker OJ, Besselink MG, et al. Treatment of necrotizing pancreatitis. *Clin Gastroenterol Hepatol*. 2012;10:1190–1201.
12. van Brunshot S, van Grinsven J, van Santvoort HC, et al. Endoscopic or surgical step-up approach for infected necrotizing pancreatitis: a multicentre randomised trial. *Lancet*. 2018; 391:51–58.
13. van Grinsven J, van Santvoort HC, Boermeester MA, et al. Timing of catheter drainage in infected necrotizing pancreatitis. *Nat Rev Gastroenterol Hepatol*. 2016;13:306–312.
14. van Baal MC, van Santvoort HC, Bollen TL, et al. Systematic review of percutaneous catheter drainage as primary treatment for necrotizing pancreatitis. *Br J Surg*. 2011;98:18–27.
15. Adams DB, Anderson MC. Percutaneous catheter drainage compared with internal drainage in the management of pancreatic pseudocyst. *Ann Surg*. 1992;215:571–576. discussion 576–578.
16. Bradley 3rd EL, Howard TJ, van Sonnenberg E, et al. Intervention in necrotizing pancreatitis: an evidence-based review of surgical and percutaneous alternatives. *J Gastrointest Surg*. 2008;12:634–639.
17. Giovannini M, Bernardini D, Seitz JF. Cystogastrotomy entirely performed under endosonography guidance for pancreatic pseudocyst: results in six patients. *Gastrointest Endosc*. 1998;48:200–203.
18. Vilmann P, Hancke S, Pless T, et al. One-step endosonography-guided drainage of a pancreatic pseudocyst: a new technique of stent delivery through the echo endoscope. *Endoscopy*. 1998;30:730–733.
19. Bang JY, Hawes R, Bartolucci A, et al. Efficacy of metal and plastic stents for transmural drainage of pancreatic fluid collections: a systematic review. *Dig Endosc*. 2015;27:486–498.
20. Fockens P, Johnson TG, van Dullemen HM, et al. Endosonographic imaging of pancreatic pseudocysts before endoscopic transmural drainage. *Gastrointest Endosc*. 1997;46:412–416.
21. Holt BA, Varadarajulu S. EUS-guided drainage: beware of the pancreatic fluid collection (with videos). *Gastrointest Endosc*. 2014;80:1199–1202.
22. Varadarajulu S, Wilcox CM, Tamhane A, et al. Role of EUS in drainage of peripancreatic fluid collections not amenable for endoscopic transmural drainage. *Gastrointest Endosc*. 2007;66:1107–1119.
23. Bang JY, Holt BA, Hawes RH, et al. Outcomes after implementing a tailored endoscopic step-up approach to walled-off necrosis in acute pancreatitis. *Br J Surg*. 2014;101:1729–1738.
24. Bang JY, Hasan MK, Navaneethan U, et al. Lumen-apposing metal stents for drainage of pancreatic fluid collections: when and for whom? *Dig Endosc*. 2017;29:83–90.
25. Bang JY, Wilcox CM, Trevino JM, et al. Relationship between stent characteristics and treatment outcomes in endoscopic transmural drainage of uncomplicated pancreatic pseudocysts. *Surg Endosc*. 2014;28:2877–2883.
26. Gluck M, Ross A, Irani S, et al. Dual modality drainage for symptomatic walled-off pancreatic necrosis reduces length of hospitalization, radiological procedures, and number of endoscopies compared to standard percutaneous drainage. *J Gastrointest Surg*. 2012;16:248–256. discussion 256–257.
27. Rana SS, Bhasin DK, Sharma RK, et al. Do the morphological features of walled off pancreatic necrosis on endoscopic ultrasound determine the outcome of endoscopic transmural drainage? *Endosc Ultrasound*. 2014;3:118–122.
28. Varadarajulu S, Christein JD, Wilcox CM. Frequency of complications during EUS-guided drainage of pancreatic fluid collections in 148 consecutive patients. *J Gastroenterol Hepatol*. 2011;26:1504–1508.
29. Varadarajulu S, Wilcox CM. Endoscopic placement of permanent indwelling transmural stents in disconnected pancreatic duct syndrome: does benefit outweigh the risks? *Gastrointest Endosc*. 2011;74:1408–1412.
30. Bang JY, Hasan M, Navaneethan U, et al. Lumen-apposing metal stents (LAMS) for pancreatic fluid collection (PFC) drainage: may not be business as usual. *Gut*. 2017;66:2054–2056.
31. Bang JY, Wilcox CM, Navaneethan U, et al. Impact of disconnected pancreatic duct syndrome on the endoscopic management of pancreatic fluid collections. *Ann Surg*. 2018;267:561–568.
32. Nadkarni NA, Kotwal V, Sarr MG, et al. Disconnected pancreatic duct syndrome: endoscopic stent or surgeon’s knife? *Pancreas*. 2015;44:16–22.
33. Tann M, Maglinte D, Howard TJ, et al. Disconnected pancreatic duct syndrome: imaging findings and therapeutic implications in 26 surgically corrected patients. *J Comput Assist Tomogr*. 2003;27:577–582.
34. Bang JY, Navaneethan U, Hasan MK, et al. EUS correlates of disconnected pancreatic duct syndrome in walled-off necrosis. *Endosc Int Open*. 2016;4:E883–E889.
35. Arvanitakis M, Delhayre M, Bali MA, et al. Pancreatic-fluid collections: a randomized controlled trial regarding stent removal after endoscopic transmural drainage. *Gastrointest Endosc*. 2007;65:609–619.



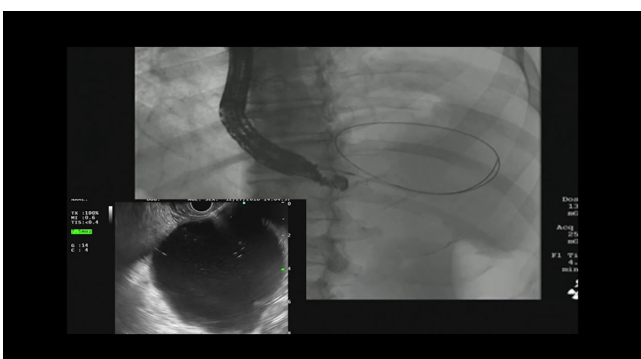
**Video 23.1** Video Showing Features of Acute Necrotic Collection on Endoscopic Ultrasonography



**Video 23.2** Video Showing Pancreatic Cancer Resulting in a Pseudo-Pseudocyst



**Video 23.3** Video Showing a Duplication Cyst, Which May Mimic a Pancreatic Fluid Collection



**Video 23.4** Video Showing the Single-Gate Technique of Pancreatic Fluid Collections Drainage Using Plastic Stents



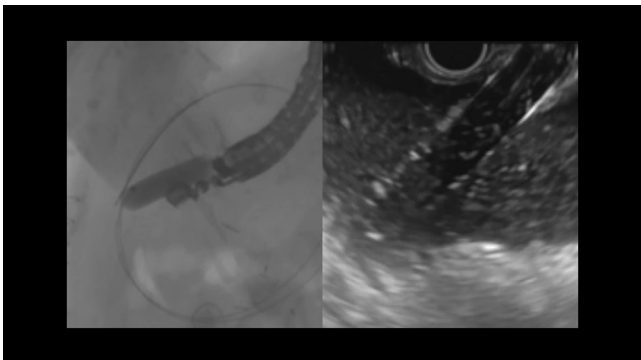
**Video 23.5** Video Showing the Single-Gate Technique of Pancreatic Fluid Collections Drainage Using Lumen-Apposing Metal Stents With an Electrocautery-Enhanced Delivery System



**Video 23.6** Video Demonstrating the Challenges of Performing Endoscopic Necrosectomy From the Gastric Cardia



**Video 23.7** Video Showing Endoscopic Ultrasonography-Guided Drainage of Pancreatic Fluid Collections Using a Needle Knife Catheter to Create the Transmural Tract



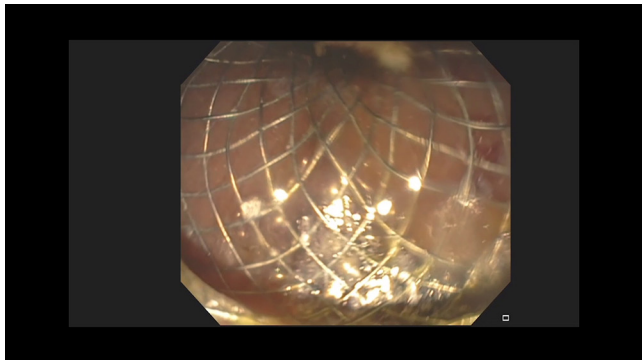
**Video 23.8** Video Showing the Double-Wire Technique of Endoscopic Ultrasonography-Guided Pancreatic Fluid Collections Drainage



**Video 23.11** Video Showing the Multi-Gate Technique of Walled-Off Pancreatic Necrosis Drainage Using Lumen-Apposing Metal Stents



**Video 23.9** Video Showing the Single-Gate Technique of Pancreatic Fluid Collections Drainage Using Lumen-Apposing Metal Stents



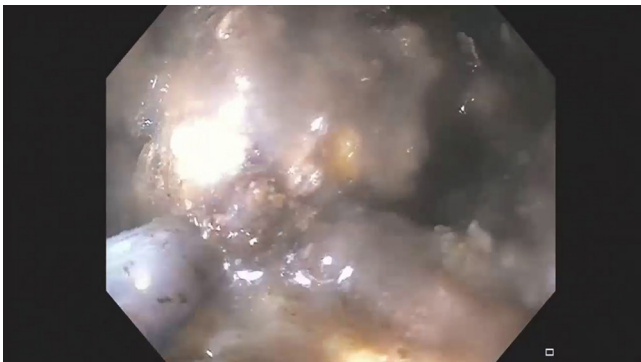
**Video 23.12** Video Showing Irrigation of the Walled-Off Pancreatic Necrosis Cavity Via the Transmural Tract



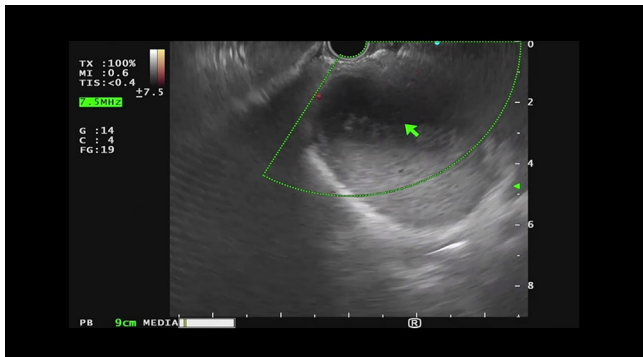
**Video 23.10** Video Showing the Multi-Gate Technique of Walled-Off Pancreatic Necrosis Drainage Using Plastic Stents



**Video 23.13** Video Showing the Dual Modality Technique of Walled-Off Pancreatic Necrosis Drainage



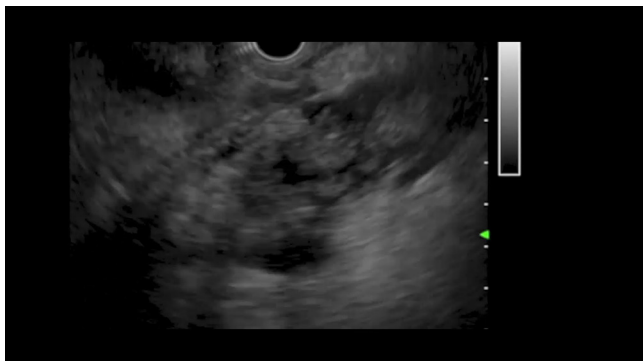
**Video 23.14** Video Showing the Technique of Endoscopic Necrosectomy, Followed by Irrigation of the Walled-Off Pancreatic Necrosis Cavity Using Sterile Water Mixed With Gentamicin and Hydrogen Peroxide



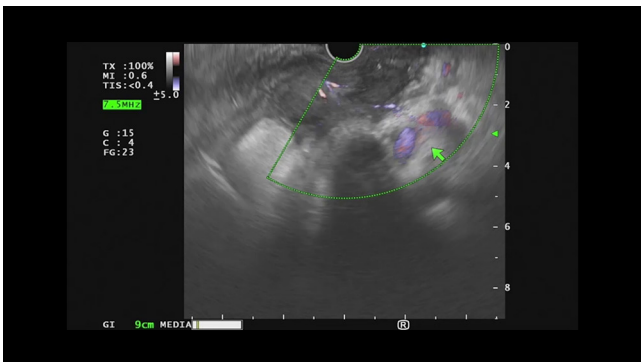
**Video 23.17** Video Showing Endoscopic Management of Bleeding During Pancreatic Fluid Collection Drainage



**Video 23.15** Video Showing Perforation During Drainage of an Uncinate Pancreatic Fluid Collection From the Gastric Cardia



**Video 23.18** Endoscopic Ultrasonography Features of Disconnected Pancreatic Duct Syndrome



**Video 23.16** Video Showing Blood Vessels Located Within Pancreatic Fluid Collections



**Video 23.19** Video Showing the Modified Multi-Gate Technique of Endoscopic Ultrasonography-Guided Walled-Off Pancreatic Necrosis Drainage in Patients With Disconnected Pancreatic Duct Syndrome

# Endoscopic Ultrasonography-Guided Drainage of the Biliary-Pancreatic Ductal Systems and Gallbladder

ANTHONY YUEN BUN TEOH, KAZUO HARA, MOUEN KHASHAB, DONGWOOK OH,  
AND DO HYUN PARK

## KEY POINTS

- Endoscopic ultrasonography-guided biliary drainage (EUS-BD) is gaining popularity as the procedure of choice over percutaneous methods in patients with failed biliary cannulation in endoscopic retrograde cholangiopancreatography.
- The different approaches in EUS-BD are associated with different outcomes and the choice should be tailored to individual patient needs according to an algorithm.
- EUS-guided pancreatic duct drainage is a safe and feasible option for pancreatic ductal drainage in patients with symptomatic obstructed pancreatic duct.
- EUS-guided transmural gallbladder drainage is becoming the choice of procedure over percutaneous methods to drain the gallbladder in patients suffering from acute cholecystitis and who are unfit for cholecystectomy.
- Advanced techniques and dedicated devices are required for the above procedures to achieve superior efficacy and good safety profile of the procedures.

## Introduction

Endoscopic retrograde cholangiopancreatography (ERCP) is currently an indispensable tool for achieving endoscopic biliary and pancreatic duct drainage. Successful deep cannulation of the biliary tree can be achieved in ≥90% of ERCPs performed by the experienced endoscopist.<sup>1</sup> Failure of cannulation could occur in patients with unusual anatomy or obstructing tumors, or when the papilla is inaccessible due to surgically altered anatomy. In patients with failed ERCP, biliary drainage could be achieved by percutaneous or surgical means, whereas pancreatic duct drainage could only be achieved by surgery. Percutaneous biliary drainage is associated with technical success rates of 77% to 100% and adverse events rates of 6% to 31%.<sup>2,3</sup> However, it is often less preferred by patients as the external drainage tube causes inconvenience and tube-related problems. Surgical biliary drainage is associated with lower rates of recurrent biliary obstruction, but the invasive nature of the procedure causes more adverse events resulting in a longer hospital stay.

Recently, endoscopic ultrasonography (EUS)-guided biliary and pancreatic duct drainage has gained popularity as an alternative approach to achieve bile or pancreatic duct drainage. The approach could achieve internal biliary and pancreatic duct drainage, with multiple options of access routes depending upon the anatomy and level of obstruction at the same session of a failed ERCP. This chapter will provide an overview on the various approaches, techniques and accessories, advantages and disadvantages, the reported outcomes, and the adverse events of these techniques.

## Endoscopic Ultrasonography-Guided Biliary Drainage

### Nomenclature

EUS-guided biliary interventions comprise of a group of procedures where the echoendoscope is used for bile duct access, drainage, and stone extraction.<sup>4,5</sup> The types of procedures are shown in Fig. 24.1. EUS-rendezvous ERCP (EUS-Rv biliary) is a type of access procedure, where the role of EUS is to provide bile duct access and insertion of a guidewire to guide subsequent cannulation during ERCP. EUS-guided biliary drainage (EUS-BD) procedures are divided into transluminal and antegrade procedures depending on whether a neo-transluminal fistula is created for drainage (transluminal), or if drainage is done in an antegrade fashion from the intrahepatic ducts toward the distal bile duct in the native biliary system (antegrade). Transluminal drainage could be further classified by the anatomical site of drainage into choledochoduodenostomy (CDS) and hepatico-gastrostomy (HGS). A CDS involves EUS-guided creation of a transmural fistula between the first part of the duodenum and the distal bile duct followed by placement of a stent. EUS-HGS involves EUS-guided creation of a transmural fistula between the left intrahepatic ducts and the stomach followed by placement of a stent. Antegrade procedures could be further classified by the location of the distal end of the stent into trans-anastomotic, suprapapillary, and trans-papillary procedures. It involves EUS-guided transhepatic puncturing of

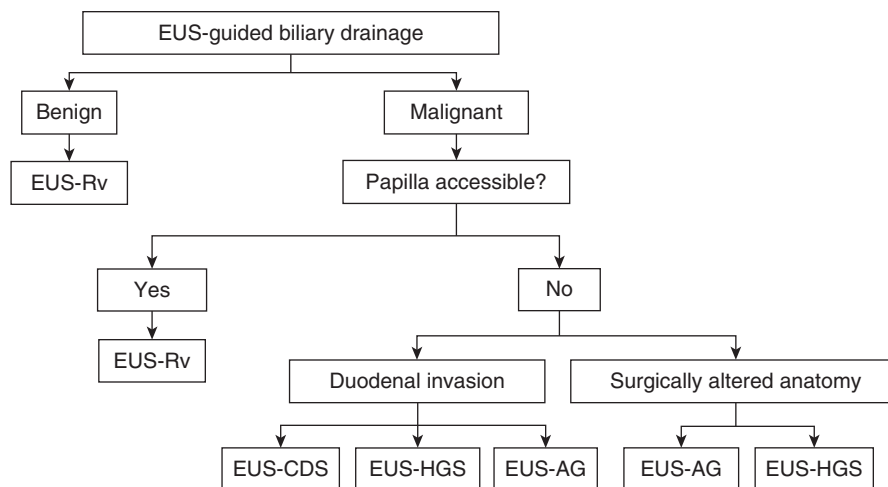


**Fig. 24.1** Nomenclature of endoscopic ultrasonography-guided biliary drainage. *EUS-AG*, Endoscopic ultrasonography-guided antegrade; *EUS-CDS*, endoscopic ultrasonography-choledochoduodenostomy; *EUS-HGS*, endoscopic ultrasonography-hepatico-gastrostomy; *EUS-Rv*, endoscopic ultrasonography-guided rendezvous.

the intrahepatic ducts, followed by antegrade placement of a stent. EUS-guided antegrade stone extraction is used for stone extraction when the papilla is not accessible, often in patients with prior gastric bypass and a long afferent limb. It involves EUS-guided antegrade advancement of stones across the ampulla using a balloon catheter. The use of a standard nomenclature is important, as individual procedures differ markedly in efficacy and risk profiles, and their outcomes should not be analyzed together.

## Indications of Endoscopic Ultrasonography-Guided Biliary Drainage

The current indications of EUS-BD are listed in *Table 24.1*. The most common indication of EUS-BD is failed deep cannulation of the bile duct or an inaccessible papilla.<sup>6</sup> The decision to perform EUS-BD in the event of failed ERCP should depend on the institution's success rates in achieving biliary cannulation with advanced ERCP techniques and the availability of endosonographers experienced in EUS-BD. In the event of difficult cannulation, advanced ERCP techniques should achieve cannulation in 73.4% to 100% of the patients.<sup>6</sup> Thus the use of EUS-BD as a salvage for failed ERCP should be uncommon.<sup>7</sup>

## Outcomes of the Endoscopic Ultrasonography-Guided Biliary Drainage Procedures

### Endoscopic Ultrasonography-Rendezvous Endoscopic Retrograde Cholangiopancreatography (Biliary)

EUS-Rv is favored by many endoscopists over the transluminal techniques as it avoids the formation of a permanent bilio-enteric fistula and the need to dilate the fistulous tract, which may lead to an increased risk of adverse events. However, the EUS-Rv approach may not be conceivable if the guidewire cannot be advanced through the site of obstruction and papilla, often due to severe ductal dilation, angulation, or a tight biliary/anastomotic stricture. The outcomes of studies with more than 20 patients that received EUS-Rv are shown in *Table 24.2*.<sup>8–18</sup> The results from comparative studies are limited and mostly included a small number of patients.

**TABLE 24.1**

### Indications of Endoscopic Ultrasonography-Guided Biliary, Pancreatic and Gallbladder Drainage

#### Indications of EUS-Guided Biliary Drainage

1. Failed deep biliary cannulation
  - Tortuous common channel
  - Tumor obstruction
2. Inaccessible papilla
  - Altered GI anatomy
  - Malignant duodenal obstruction
  - Prior duodenal metallic stenting
3. Unavailable or refusal of percutaneous drainage/surgical procedures

#### Indications of EUS-Guided Pancreatic Duct Drainage

Patients with painful obstructive pancreatitis

- Inability to access/cannulate the papilla by endoscopic retrograde pancreatography
- Surgically altered anatomy not accessible to deep enteroscopy
- Disconnected pancreatic duct syndrome

#### Indications of EUS-Guided Gallbladder Drainage

1. High-risk surgical candidate suffering from acute cholecystitis
2. Failure to wean from long-term cholecystostomy

*EUS*, Endoscopic ultrasonography; *GI*, gastrointestinal.

A retrospective study compared EUS-Rv with precut sphincterotomy after failed cannulation for benign and malignant conditions.<sup>11</sup> Patients with failed cannulation after precut sphincterotomy received a second ERCP 72 hours later. Both methods were comparable in the overall rates of cannulation, but the EUS-Rv group had higher cannulation rates in the first session. There were no differences in the rate of adverse events, but the groups differed in risk profiles, with more patients suffering from pancreatitis and bleeding in the precut group, and more periductal contrast leak in the EUS-Rv group. In another study, two ERCP cohorts comprising

**TABLE 24.2** Outcomes of Endoscopic Ultrasonography-Rendezvous Endoscopic Retrograde Cholangiopancreatography (Biliary)

Author	Year	Patients	Technical Success	Extrahepatic	Transhepatic	Adverse Events
Kahaleh et al. <sup>8</sup>	2006	23	65%	4/5	11/18	17%
Shah et al. <sup>9</sup>	2012	50	75%	—	—	12%
Iwashita et al. <sup>10</sup>	2012	40	73%	25/31	4/9	13%
Dhir et al. <sup>11</sup>	2012	58	98%	57/58	0	3%
Vila et al. <sup>12</sup>	2012	60	68%	—	—	22%
Park et al. <sup>13</sup>	2013	20	80%	3/6	13/14	0%
Dhir et al. <sup>14</sup>	2013	35	97%	18/18	16/17	23%
Iwashita et al. <sup>15</sup>	2016	20	80%	13/15	3/4	15%
Tang et al. <sup>16</sup>	2016	25	80%	20/24	1/1	—
Lee et al. <sup>17</sup>	2017	50	94%	5/5	42/45	—
Bill et al. <sup>18</sup>	2016	20	76%	—	—	28%

**TABLE 24.3** Outcomes of Endoscopic Ultrasonography-Guided Antegrade Stenting

Author	Year	Patients	Technical Success	Adverse Events
Park et al. <sup>13</sup>	2013	14	60%	14%
Ogura et al. <sup>20</sup>	2014	12	100%	8.3%
Dhir et al. <sup>22</sup>	2014	25	92%	32%
Iwashita et al. <sup>21</sup>	2017	20	95%	20%

more than 1000 patients in each group were compared.<sup>17</sup> EUS-BD methods were employed in the event of failed cannulation in one group. The failure rate when both precut and EUS-BD methods were available was significantly lower than the group with only ERCP available (1% vs. 3.6%,  $P < .001$ ). The success rate of EUS-BD was also significantly higher than for precut sphincterotomy (95.1% vs. 75.3%,  $P < .001$ ), mainly due to superiority in patients with malignant obstruction (93.5% vs. 64%,  $P < .001$ ). Khashab et al. also compared patients that underwent EUS-BD with the rendezvous technique (13 patients) versus the transluminal technique (20 patients).<sup>19</sup> There were no differences in technical and clinical success, procedural time, length of hospital stay, and adverse events. A study then compared EUS-Rv with percutaneous biliary drainage in patients with malignant distal biliary obstruction.<sup>18</sup> A lower success rate in obtaining biliary drainage was observed in the EUS-Rv group (76% vs. 100%,  $P = .002$ ). However, the length of hospital stay was shorter ( $P = .02$ ) and the need for repeated biliary interventions was lower ( $P = .001$ ) in the EUS-Rv group.

#### Endoscopic Ultrasonography-Guided Antegrade Stenting

The outcomes of EUS-guided antegrade stenting (EUS-AG) are less well reported than other EUS-BD procedures.

EUS-AG is usually chosen in patients where the papilla is not accessible and the guidewire is successful in traversing the stricture. The studies that reported the individual outcomes for EUS-AG are shown in Table 24.3.<sup>13,20–22</sup> Overall, EUS-AG seems to be associated with high technical success rates and an acceptable risk of adverse events. However, EUS-AG also suffers from difficulties of guidewire manipulation as in EUS-Rv, thus some endoscopist may prefer transluminal techniques over EUS-AG.

#### Endoscopic Ultrasonography-Guided Choledochoduodenostomy and Hepatogastrostomy

EUS-CDS and HGS are both transmural techniques that achieve biliary drainage. However, there are several important differences between the two procedures. In making a CDS, a fistula is created between the common bile duct and the duodenum. The common bile duct is located directly behind the first part of the duodenum and is relatively fixed with minimal respiratory influence. Thus the risk of the organs separating after creation of the fistula is low, and the risk of stent migration is uncommon. In EUS-HGS, needle puncture through the thicker gastric wall and a few centimeters of hepatic parenchyma with greater tissue resistance is required. This makes puncture and stent deployment more challenging. Furthermore, the stomach is regularly undergoing peristalsis and the liver moves during respiration. The stent placed is more prone to the risk of migration resulting in bilomas or free perforation. These complications may be fatal, and attention to technical details is therefore paramount.<sup>12</sup> In the event of misdeployment, salvage stent placement may be impossible. In addition, because HGS involves transhepatic puncturing of the bile ducts, the procedure is susceptible to similar risks as seen during percutaneous transhepatic puncturing of the ducts. These procedural characteristics are responsible for the differences in results seen in both procedures.

The outcomes of studies with more than 20 patients are shown in Table 24.4.<sup>12,22–36</sup> The overall clinical success rates of both procedures in expert hands were 63.2% to 100%.

**TABLE 24.4****Outcomes of Studies Comparing Endoscopic Ultrasonography-Choledochoduodenostomy and Hepatoco-Gastrostomy**

Author	Year	Patients	Type of Procedure	Clinical Success (%)	30-Day Adverse Events (%)	Mean Duration of Stent Patency (Days)
Park et al. <sup>23</sup>	2011	57	CDS 26 HGS 31	96.5	20	152 132
Villa et al. <sup>12</sup>	2012	65	CDS 26 HGS 34	63.2	22.6	—
Dhir et al. <sup>22</sup>	2014	45	—	93.7	22.9	—
Kawakubo et al. <sup>24</sup>	2014	64	CDS 44 HGS 20	95	19	—
Song et al. <sup>26</sup>	2014	27	CDS 17 HGS 10	96.3	18.5	—
Dhir et al. <sup>27</sup>	2015	104	CDS 68	98.3	8.65	—
Poincloux et al. <sup>28</sup>	2015	92	CDS 26 HGS 66	92.1	11.9	174
Ogura et al. <sup>20, a</sup>	2014	51	All HGS	100	—	202
Umeda et al. <sup>30</sup>	2015	23	All HGS	100	4.3	120
Cho et al. <sup>32</sup>	2016	54	CDS 33 HGS 21	100	16.6	329 166
Kunda et al. <sup>33</sup>	2016	57	All CDS	94.7	7	—
Khashab et al. <sup>19</sup>	2013	20	CDS 15 HGS 5	97	12	—
Khashab et al. <sup>31</sup>	2016	121	CDS 60 HGS 61	85.5 82.1	19.7 13	—
Kawakubo et al. <sup>35</sup>	2016	26	All CDS	96.2	26.9	—
Ogura et al. <sup>36</sup>	2016	39	CDS 13 HGS 26	100	0	37 133

<sup>a</sup>The study included patients with duodenal obstruction.

CDS, Choledochoduodenostomy; HGS, hepatico-gastrostomy.

The rate of adverse events was between 4.3% and 26.9%. The mean duration of stent patency was 37 to 329 days. The cause of stent dysfunction was mainly due to stones or sludge.<sup>37,38</sup> The difference in outcomes of EUS-CDS and HGS are procedure specific.

In comparing EUS-CDS and HGS, the results from a few comparative studies are available. In a randomized trial, 49 patients with unresectable distal malignant biliary obstruction and failed ERCP received EUS-CDS or EUS-HGS.<sup>39</sup> The technical success rates were comparable among the procedures (91% vs. 96%, respectively,  $P = .61$ ). Clinical success was lower in the EUS-CDS group but did not reach statistical significance (77% vs. 91%, respectively,  $P = .23$ ). HGS was associated with a higher risk of adverse events but it did not reach statistical significance (12.5% vs. 20%, respectively,  $P = .729$ ).

In another study, a total of 121 patients underwent EUS-BD (CDS 60, HGS 61).<sup>31</sup> The technical and clinical success rates were comparable among the two procedures ( $P = .75$  and  $P = .64$ , respectively). Adverse events were more common in the EUS-HGS group

(19.67% vs. 13.3%;  $P = .37$ ). Both plastic stenting (odds ratio [OR] 4.95; 95% confidence interval [CI]: 1.41 to 17.38;  $P = .01$ ) and the use of noncoaxial electrocautery (OR 3.95; 95% CI: 1.16 to 13.40;  $P = .03$ ) were independently associated with adverse events. The length of hospital stay was significantly shorter in the CDS group (5.6 days vs. 12.7 days;  $P < .001$ ). The 1-year stent patency probability was greater in the EUS-CDS group (OR 0.98; 95% CI: 0.76 to 0.96 vs. OR 0.60; 95% CI: 0.35 to 0.78) but overall patency was not significantly different. Park et al. also studied predictors of adverse events in 57 patients who underwent EUS-CDS or HGS.<sup>23</sup> Similar to the above studies, Park's study showed no difference in technical success, clinical success, or rates of adverse events between two groups. However, the use of noncoaxial electrocautery (needle knife) was independently associated with the occurrence of adverse events (OR 12.4;  $P = .01$ ).

Ogura et al. then compared EUS-CDS and HGS in patients with concomitant duodenal and biliary obstruction in a randomized study.<sup>36</sup> No difference in technical success, clinical success, and adverse events rates were observed. However, EUS-CDS was

associated with a significantly shorter duration of stent patency in an obstructed duodenum (43 days vs. 133 days;  $P = .05$ ).

Khan et al. conducted a systematic review and meta-analysis of studies reporting on the outcomes of EUS-BD.<sup>40</sup> Seven studies were included, and overall there was no difference in technical success between EUS-CDS and HGS (OR 1.32;  $P = .56$ ). Six studies described postprocedure adverse events based on the method of drainage. EUS-CDS appeared to be significantly safer to HGS with a pooled OR of 0.40 ( $P = .02$ ).

In view of the above results, it could be concluded that both EUS-CDS and HGS are effective and safe techniques for the treatment of distal biliary obstruction after failed ERCP. However, EUS-CDS appears to be associated with a shorter hospital stay, improved stent patency, and fewer adverse events. In addition, metallic stents should be placed whenever feasible and noncoaxial electrocautery should be avoided when possible. In the presence of duodenal obstruction, EUS-HGS may be the preferred procedure as it is associated with a longer stent patency, whereas a CDS may be prone to restenosis due to tumor ingrowth or overgrowth.

### **Comparison of Endoscopic Ultrasonography-Guided Biliary Drainage With Percutaneous Transhepatic Biliary Drainage**

Three randomized studies (one available in abstract only) have compared EUS-BD and percutaneous transhepatic biliary drainage (PTBD; Table 24.5).<sup>41–43</sup> All have shown equivalent success rates. The adverse events rate and the need for reinterventions

in two studies were significantly lower in the EUS-BD group. A meta-analysis then included nine comparative studies and 483 patients.<sup>44</sup> There was no difference in technical success between two procedures (OR = 1.78; 95% CI: 0.69 to 4.59); however, EUS-BD was associated with better clinical success (OR = 0.45; 95% CI: 0.23 to 0.89), fewer postprocedure adverse events (OR = 0.23; 95% CI: 0.12 to 0.47), and lower rate of reintervention (OR = 0.13; 95% CI: 0.07 to 0.24). There was no difference in length of hospital stay after the procedures. Thus EUS-BD should be preferred over PTBD in the event of failed ERCP.

### **Pros and Cons of Each Procedure**

The pros and cons of each procedure are shown in Table 24.6. The considerations on planning the appropriate procedure include the difficulty of needle puncture, wire manipulation, dilation of the fistula tract, and stent placement. EUS-Rv is mainly an access procedure and usually does not involve fistula dilation. The risk of the procedure is mainly a result of the difficult ERCP, and there is limited added risk from the EUS intervention. However, the procedure is associated with several potential disadvantages. First, rendezvous completion is successful in 65% to 80% of the cases in most series and requires an accessible papilla, which may not be possible in patients with surgical upper gastrointestinal (GI) anatomy or gastric outlet obstruction (GOO).<sup>9</sup> A second shortcoming is the need to exchange the echoendoscope for a duodenoscope, during which time there may be inadvertent displacement of the

**TABLE 24.5 Comparison of Endoscopic Ultrasonography-Guided Biliary Drainage With Percutaneous Transhepatic Biliary Drainage**

Author	Year	Patients	Technical Success (%)	Clinical Success (%)	Adverse Events (%)	Reinterventions (%)	
Artifon et al. <sup>41</sup>	2012	EUS 13	100	100	15.3	<i>P</i> value = NS	
		PTBD 12	100	100	25		
Lee et al. <sup>42</sup>	2016	EUS 34	94.1	87.5	8.8	<i>P</i> value = 0.022	25
		PTBD 32	96.9	87.1	31.2		54.8
Giovannini et al. <sup>43</sup>	2015	EUS 20	95	95	35	NA	—
		PTBD 20	85	85	60		

EUS, Endoscopic ultrasonography; NA, not applicable; NS, not significant; PTBD, percutaneous transhepatic biliary drainage.

**TABLE 24.6 The Pros and Cons of Each Type of Endoscopic Ultrasonography-Guided Biliary Drainage Procedure**

	Needle Puncture	Guidewire Manipulation	Tract Dilation	Ease of Stent Insertion	Stent Patency
EUS-Rv	Several options depending on the site obstruction and ductal dilation	Requires manipulation across the stricture and papilla	Usually not required	Similar to ERCP	Similar to ERCP
EUS-AG	Requires dilation of the intrahepatic ducts	Requires manipulation across the stricture and papilla	Required	Relatively straight forward	Similar to ERCP
EUS-CDS	Not possible in patients with duodenal invasion	Requires deep insertion into the intrahepatic ducts	Required	Similar to ERCP	6–12 months
EUS-HGS	Requires dilation of the intrahepatic ducts	Requires deep insertion into the intrahepatic ducts	Required	Technically demanding	3–4 months

EUS-AG, Endoscopic ultrasonography-guided antegrade; EUS-CDS, endoscopic ultrasonography-choledochoduodenostomy; EUS-HGS, endoscopic ultrasonography-hepatico-gastrostomy; EUS-Rv, endoscopic ultrasonography-guided rendezvous.

guidewire. A third limitation is the prolonged procedural times as a result of guidewire manipulation through the site of obstruction and ampulla, the need to exchange the echoendoscope for a duodenoscope, and the subsequent retrograde biliary interventions. A final shortcoming of EUS-Rv is the risk of acute pancreatitis due to manipulation of the papilla.

EUS-AG requires a dilated intrahepatic duct for needle puncture. The guidewire then needs to be negotiated across the site of obstruction for stent placement. Therefore it is susceptible to problems of guidewire manipulation as in the EUS-Rv procedure. However, if the guidewire is successful in traversing the stricture, the placement of the stent is relatively straightforward and is associated with a low risk of adverse events. There is a potential of bile leak from the access site, but the risk is low if drainage from the stent is adequate.

EUS-CDS and HGS are both transmural techniques and there are several advantages. These techniques are associated with no risk of pancreatitis as the papilla is not manipulated. The risk of tumor in-growth into the stent is also low as the stent placed does not traverse the tumor. Ductal puncture and access is usually easy in the presence of a dilated duct. However, the creation of the fistula tract requires multiple exchanges of instruments, and this may risk bile leak during the procedure. Furthermore, the integrity of the anastomosis is entirely dependent on the stent placed. Thus selection of an appropriate stent is paramount. Potential adverse events from transmural procedures are higher and include pneumoperitoneum, bleeding, cholangitis, stent dislocation, free perforation, bile leak, and bile peritonitis. Rarer complications include hemobilia, acute cholecystitis, duodenal double puncture, mediastinitis, and mortality.

## Algorithm for Drainage and Choice of Procedure

The optimal algorithm for EUS-BD is still in evolution. It is unclear whether one type of EUS-BD procedure is preferred for a particular indication. The choice of procedure would need to balance on the technical and clinical success rates, stent patency, and risk profile of each procedure. Such an algorithm also should be individualized for each institution based on the technical expertise available. Our current approach is shown in Fig. 24.2. The cause of failed ERCP should be examined. For benign causes, EUS-Rv ERCP should be attempted first. Transmural drainage should only be used with strong justification. For unresectable malignancies, transpapillary or antegrade procedures should be attempted first, depending on disease and anatomical considerations. When guidewire manipulation across the stricture is not possible, then

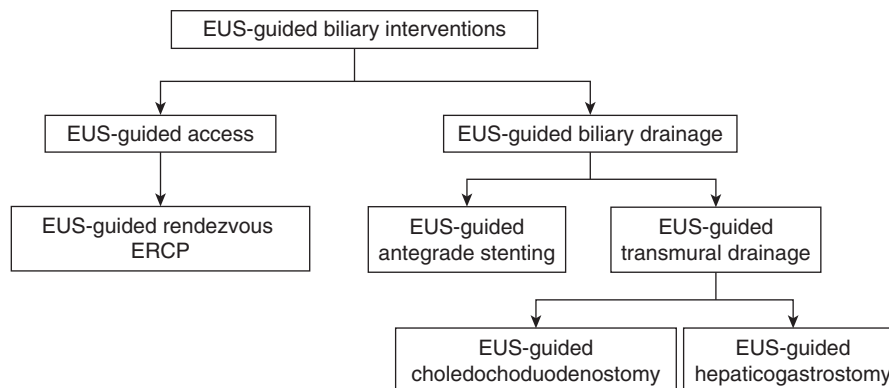
transluminal approaches should be employed. In expert hands, both transpapillary and transluminal procedures appear to have similar efficacies and risks. Hence, transluminal procedures may be used more frequently. Park et al. proposed an algorithm based on accessibility of the papilla in patients with failed ERCP.<sup>13</sup> A rendezvous procedure was performed first if the papilla was accessible. An antegrade procedure was then performed if the papilla was not accessible. Transluminal procedures were then performed if tumor invasion was present in the duodenum. Tyberg et al. categorized their patients based on cross-sectional imaging.<sup>45</sup> If the intrahepatic ducts were dilated, an antegrade procedure was the first choice. If the ducts were not dilated, then a rendezvous procedure was performed. When these procedures failed, transluminal drainage was performed.

## Endoscopic Ultrasonography-Guided Pancreatic Duct Drainage

Endoscopic retrograde pancreatography (ERP) is the conventional method for treating pancreatic ductal obstruction caused by strictures, stones, or congenital anomalies. The procedure may not be technically possible in about 3% to 10% of patients due to surgically altered anatomy, tight strictures, complete ductal obstructions, or disrupted ducts.<sup>46</sup> Surgical interventions may be required for failed ERP.<sup>47</sup> Recently, EUS-guided pancreatic duct drainage (EUS-PD) has been described as a rescue method for the management of patients in whom ERP is unsuccessful.<sup>46</sup> However, EUS-PD seems to be one of the most technically demanding EUS-guided interventions, and it is associated with up to 43% risk of adverse events.<sup>48–50</sup> Therefore it has only been performed by highly skilled endoscopists in tertiary centers with extensive experience in therapeutic ERP and EUS procedures.

## Indications for Endoscopic Ultrasonography-Guided Pancreatic Duct Drainage

There are no guidelines as to when EUS-PD should be considered. Based on the previous literature and our experience, the potential indications for EUS-PD are summarized in Table 24.1. Indications should be decided cautiously by taking into account the condition of the patient, the endoscopist's experience, and the facilities available. Only experienced endoscopists trained in EUS and ERP should attempt this procedure.



• **Fig. 24.2** Algorithm for endoscopic ultrasonography (EUS)-guided biliary drainage. *ERCP*, Endoscopic retrograde cholangiopancreatography.

## Nomenclature

EUS-PD can be classified into the EUS-guided rendezvous technique and EUS-guided transmural drainage (Fig. 24.3).<sup>51</sup> In the rendezvous technique (EUS-Rv pancreatic), EUS is used for pancreatic duct access and guidewire insertion to facilitate cannulation and stent placement in subsequent ERCP. When the papilla or anastomosis is inaccessible or unable to be traversed with the guidewire, EUS-guided transmural drainage can be performed. EUS-guided transmural PD can be divided into EUS-antegrade pancreatic duct drainage (EUS-AG PD) or EUS-guided pancreatico-gastrostomy (EUS-PG). Both procedures involve creation of a transmural fistula and transgastric placement of stents. In EUS-AG PD, antegrade placement of the stent traverses the papilla or surgical anastomosis. In EUS-PG, a pancreatico-gastrostomy is created with stent placement without traversing the papilla or anastomosis.

## Outcomes of Endoscopic Ultrasonography-Guided Pancreatic Duct Drainage Procedures

EUS-PD is a challenging procedure. There have been few reports on the outcomes of EUS-Rv technique.<sup>52–62</sup> The technical success

rate of this procedure ranged from 25% to 100%. The outcomes of EUS-transmural PD in studies with more than 20 patients are shown in Table 24.7. In recent systematic reviews of EUS-guided transmural PD, the overall technical success rate was 70% to 100%.<sup>63–66</sup> The possible reasons for low technical success rates are (1) small diameter of pancreatic ducts; (2) hard sclerotic pancreatic parenchyma; (3) difficult guidewire manipulation in a tortuous main pancreatic duct (MPD); and (4) a lack of dedicated devices.<sup>5</sup>

Overall, complete resolution of pain was achieved in 69.6% to 100% in both types of EUS-PD.<sup>66,67</sup> However, 20% to 25% of patients develop recurrence of symptoms after endoscopic therapy, requiring multiple interventions or surgery.<sup>68</sup> In the EUS-Rv technique, adverse event rates ranged from 0% to 25% and included pancreatitis, peripancreatic abscess, and pancreatic fluid leakage,<sup>63</sup> whereas for EUS-guided transmural PD, the adverse event rates ranged from 0% to 67% and included abdominal pain, pancreatitis, bleeding, perforation, shaving of the guidewire coating, peripancreatic abscess, pseudocyst, and stent migration.<sup>65,66</sup> Adverse event rates were higher for EUS-guided transmural drainage and may be due to the need for fistula tract dilation and risk of pancreatic fluid leakage. Stent dysfunction, including stent occlusion and migration, has been reported in 25% to 55% of the patients.<sup>47,67,69</sup> A higher rate of stent occlusion is seen in EUS-PD

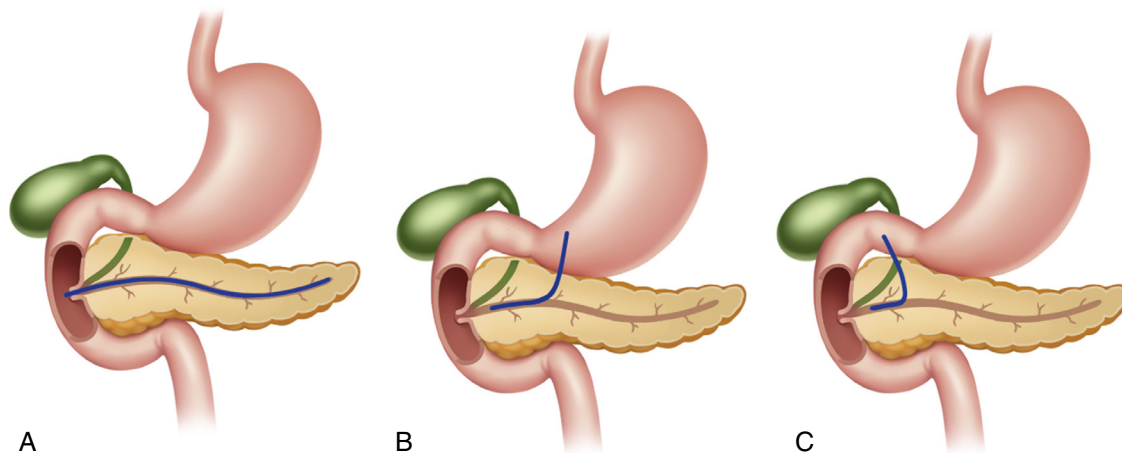


**Fig. 24.3** Schematic illustration of endoscopic ultrasonography (EUS)-guided techniques for pancreatic duct drainage. (A) EUS-guided rendezvous technique. (B) EUS-guided transmural drainage via the stomach, pancreaticogastrostomy. (C) EUS-guided transmural drainage via the duodenum, pancreaticoduodenostomy. (Modified from Tyberg A, Sharaiha RZ, Kedia P, et al. EUS-guided pancreatic drainage for pancreatic strictures after failed ERCP: a multicenter international collaborative study. Gastrointest Endosc 2017;85:164–169.)

**TABLE  
24.7**

### Outcomes of Endoscopic Ultrasonography-Guided Transmural Pancreatic Duct Drainage

Author	Year	Patients	Puncture Route	Type of Stent	Technical Success (%)	Clinical Success (%)	Early Adverse Events (%)	Late Adverse Events (%)	Reintervention Rate (%)
Tessier et al. <sup>69</sup>	2007	36	TG/TB	PS	92	70	5%	None	55
Oh et al. <sup>119</sup>	2016	25	TG/TB/TE	SEMS	100	100	5%	None	48
Tyberg et al. <sup>121</sup>	2017	80	TG/TB	PS	81 <sup>a</sup>	81	20%	11%	N/A
Chen et al. <sup>122</sup>	2017	40	N/A	PS	92.5 <sup>b</sup>	87.5	35%	None	N/A

<sup>a</sup>80 cases including 20 cases of rendezvous technique.

<sup>b</sup>40 cases including 3 cases of rendezvous technique.

N/A, Not available; PS, plastic stent; SEMS, self-expandable metallic stents; TB, transbulbar; TE, transenteric; TG, transgastric.

and may be due to the small caliber of plastic stents.<sup>67</sup> Stent migration is related to the limited intraductal length of the stents and the intragastric location, which may be subjected to strong expulsive contractions.<sup>46</sup>

### Algorithm for Endoscopic Ultrasonography-Guided Pancreatic Duct Drainage Procedures

Similar to EUS-BD, the algorithm for EUS-PD is in evolution. The choice of procedure would need to be balanced on the technical and clinical success rates, the stent patency, and the risk profile of each procedure. In general, the EUS-Rv PD should be attempted before transmural PD. There are two major reasons for this strategy. First, the rendezvous technique can achieve ideal drainage from the ampulla or pancreaticodigestive anastomosis for subsequent treatment for pancreatic duct or anastomotic stricture. Second, EUS transmural PD requires dilation of the needle tract and carries the potential of serious adverse events. Thus the procedure should be performed as salvage when the guidewire cannot traverse the papilla or stenosis.

### Endoscopic Ultrasonography-Guided Gallbladder Drainage

The gold standard of treatment for acute cholecystitis is laparoscopic cholecystectomy.<sup>70–74</sup> However, the procedure is associated with a risk of postoperative complications in 13% to 20%, and a conversion rate to open surgery in 17% to 25% of patients. In patients that are unfit for cholecystectomy, percutaneous cholecystostomy (PTC) is recommended for drainage of the gallbladder.<sup>75,76</sup> However, in elderly patients, the procedure may be associated with a mortality rate of 16% and a morbidity rate of 47%.<sup>77</sup> Furthermore, care of the external tube is frequently cumbersome for these elderly patients. In order to avoid problems associated with an external tube, endoscopic transpapillary gallbladder drainage (ETGBD) has been reported.<sup>78–82</sup> For successful transpapillary gallbladder drainage, the cystic duct needs to be cannulated and any stones obstructing the Hartman's pouch must be dislodged. Thus the clinical success rates of the procedure were between 62% and 89%. In addition, the stent needs to be periodically changed, and the procedure does not deal with the gallstones in the gallbladder posing a risk to recurrent cholecystitis.

Recently, EUS-guided transmural gallbladder drainage (EGBD) has been described.<sup>83–99</sup> The technique uses the EUS-guided creation of a cholecysto-gastric or duodenal fistula and placement of a stent for gallbladder drainage. The technique is an attractive alternative to PTC or ETGBD as it avoids the need to

cannulate the cystic duct and obstructed stones, the need for the periodical exchange of stents, and lacks an external tube. Furthermore, the large diameter stents allow for access to the gallbladder for complete clearance of stones, and this may potentially reduce the risk of recurrent cholecystitis.<sup>100</sup>

### Indications for Endoscopic Ultrasonography-Guided Transmural Gallbladder Drainage

As mentioned previously, laparoscopic cholecystectomy may be associated with a high risk of mortality and morbidity in patients with multiple comorbidities, and PTC should be considered in these patients. Thus EGBD is an alternative to percutaneous drainage in patients that are at high risk for cholecystectomy indicated for gallbladder drainage (see Table 24.1). In addition, EGBD is indicated in patients on long-term cholecystostomy drainage who desire to convert to internal drainage.<sup>90</sup> Of note, EGBD should not be performed in patients where laparoscopic cholecystectomy may be considered, as the presence of a cholecysto-gastric or duodenal fistula may complicate future surgery and increase the chance of conversion to open cholecystectomy.

### Outcomes of Endoscopic Ultrasonography-Guided Transmural Gallbladder Drainage

Studies that reported the outcomes of EGBD for treatment of acute cholecystitis in over 20 patients are shown in Table 24.8. Comparative studies are discussed in the section below. In the majority of these studies, the gallbladder was drained by an EUS-specific stent with antimigratory properties. A technical success of 90% to 98.7% and a clinical success of 89% to 98.4% were reported. Adverse events rates were between 4.8% and 22% and included bleeding, recurrent cholecystitis, stent migration, and occlusion. Stone clearance from the gallbladder could be achieved in 88% of the patients in one study, requiring a mean number of 1.25 sessions of per-oral cholecystoscopy.<sup>100</sup>

### Comparison Between Endoscopic Ultrasonography-Guided Transmural Gallbladder Drainage and Percutaneous Cholecystostomy

A number of studies have compared the outcomes between EGBD and PTC. Three comparative studies compared EGBD to PTC in patients suffering from acute cholecystitis that are at high-risk for surgery.<sup>94–96</sup> All studies reported comparable technical

**TABLE 24.8** The Outcomes of Endoscopic Ultrasonography-Guided Transmural Gallbladder Drainage for Treatment of Acute Cholecystitis

Author	Year	Patients	Technical Success (%)	Clinical Success (%)	Adverse Events (%)	Reinterventions (%)	FU Time (Days)
Choi et al. <sup>89</sup>	2014	63	98.4	98.4	4.8	3.6	275
Walter et al. <sup>91</sup>	2016	30	90	96	13	—	298
Kahaleh et al. <sup>93</sup>	2016	35	91.4	89	22	—	91.5
Dollhopf et al. <sup>99</sup>	2017	75	98.7	95.9	10.7	—	201

FU, Follow-up.

and clinical success rates between the two procedures. Teoh et al. reported significantly lower 1-year adverse events rates ( $P < .001$ ) and readmission rates ( $P < .001$ ) in the EGBD group. The majority of these were due to tube-related problems in the PTC group. Recurrent acute cholecystitis was also lower although this did not reach statistical significance ( $P = .12$ ), whereas the other two studies reported a similar 30-day adverse events rate but a lower reintervention rate in the EGBD group. Irani et al. also reported lower postprocedural pain scores in the EGBD group.<sup>96</sup>

In contrast, one study compared EGBD to PTC in patients with acute cholecystitis secondary to malignant cystic duct obstruction.<sup>97</sup> No difference in success rates and adverse events were observed, but the EGBD group was associated with a shorter hospital stay.

## Techniques Used in Endoscopic Ultrasonography-Guided Drainage Procedures

### Procedural Considerations and Equipment

The usual steps of any drainage procedure include needle puncture of the target organ, guidewire insertion, fistula tract dilation, and stent insertion. The standard preparation of patients and equipment required for the procedure are listed below. The toolbox for instruments and accessories commonly used is shown in Table 24.9.

#### Patient Preparation

Patients should be checked for blood type and screen and any coagulopathy should be corrected. Patients should temporarily discontinue anticoagulants and antiplatelet agents prior to the procedure. The patient should be fasted for 4 to 6 hours before the procedure. Prophylactic antibiotics should be given. The procedure should be performed with the patient in the supine or prone position. Carbon dioxide insufflation should be employed to reduce the risk of pneumoperitoneum.<sup>101</sup> The procedures could be done under conscious sedation, but monitored anesthesia or general anesthesia is preferred.

**TABLE 24.9** **Toolbox of Instruments and Accessories Used in Endoscopic Ultrasonography-Guided Drainage Procedures**

Categories	Tools
Needles	Principle needle: 19-gauge fine-needle aspiration needle (nitinol) Rarely: 22-gauge fine-needle aspiration needle
Guidewires	0.025- or 0.035-inch curved tip guidewires 0.035-inch curved tip hydrophilic guidewire 0.018- or 0.021-inch guidewire (used with 22-gauge needle)
Tract dilation	Tapered dilating catheter Screw-type stent retriever Wire-guided needle knife 6 Fr or 8.5 Fr cystotome 4 mm hydrostatic balloon
Stents	Plastic stent or covered self-expandable metal stent

#### Echoendoscope

EUS-guided drainage procedures should be performed using a linear array therapeutic echoendoscope with a 3.8-mm working channel. Forward viewing therapeutic echoendoscope could be used if a transduodenal puncture for EUS-Rv or CDS is planned. This type of echoendoscope offers a larger degree of angulation for needle puncture and guidewire manipulation, and may reduce the risk of double penetration of the duodenum mucosa.<sup>37,102</sup>

#### Needles and Guidewires

A 19-gauge needle should be used for duct puncture. The use of needles made with nitinol may improve the maneuverability of the echoendoscope in the duodenum.<sup>103,104</sup> Access needles with a blunted tip after removal of the stylet are also available.<sup>105</sup> These needles are designed to reduce the chance of wire sheering by the needle during needle manipulation. However, manipulation of these needles is difficult in the duodenum. Furthermore, readjustment of the needle position after removal of the stylet is difficult. A 0.025- or 0.035-inch guidewire should be used to negotiate the bile ducts. Curved tip hydrophilic guidewires may improve the steerability of the wire. In patients with smaller ducts or ducts located at an acute angle, a 22-gauge needle could be used but only a 0.018- or 0.021-inch guidewire would pass through the needle. These wires are soft and difficult to manipulate and will need to be handled with care.

#### Tract Dilation

Dilation of the needle tract could be achieved by the use of mechanical or cautery devices.

Mechanical dilation of the tract could be achieved by a tapered dilating catheter, hydrostatic balloons, or occasionally a screw-type stent retriever.<sup>106,107</sup> Cautery devices include needle-knife sphincterotome or a 6-Fr or 8.5-Fr coaxial cystotome. The use of mechanical dilation may in principle reduce the risk of damaging the surrounding structures. However, it is sometimes difficult to insert these instruments into the tract for dilation. Hence the use of cautery is frequently required. When using cautery, a coaxial cystotome is the preferred instrument, because the use of a needle-knife has been shown to be a risk factor for developing adverse events.<sup>23</sup> This may be a result of the different path of insertion of the needle on the sphincterotome to the guidewire. To date, there have been no comparative trials to clarify the relative value of available devices. The selection of devices depends on personal experience and availability. Multiple devices are often serially employed for fistula tract dilation.

#### Stents

When performing EUS-Rv or EUS-AG, the consideration for stents is generally similar to that of ERCP, whereas for transmural drainage procedures, because the integrity of the anastomosis is dependent on the properties of the stent, the choice of stent should be made cautiously. When EUS-guided biliary drainage was first developed, plastic stents were commonly used. However, the risk of bile or pancreatic leak after plastic stent placement may be higher when compared to metal stents.<sup>108</sup> Thus the use of fully or partially covered metallic stents (self-expandable metallic stents [SEMS]) is usually favored in EUS-BD and EGBD, whereas for EUS-PD, plastic stents are usually used as the diameter of the PD is too small to accommodate biliary SEMS. When inserting metal stents in EUS drainage procedures, there are several considerations. Fully covered SEMS (FCSEMS) are prone to migration. This may be catastrophic when it is used for transmural drainage procedures, as migration of the stent

will cause dehiscence of the anastomosis and free perforation or leakage. This problem is generally overcome by using a very long FCSEMS, partially covered SEMS, or SEMS with antimigratory design for better anchorage. One can also insert a double pigtail stent into the CSEMS as anchorage. Furthermore, after EUS-guided drainage, the target organ will collapse and the stent may impinge onto the walls of the organ causing erosion, bleeding, or stent obstruction.

In view of these considerations, several EUS-specific stents have been developed. They can be broadly classified into lumen-apposing stents (LAS) or tubular stents.<sup>32,86,109–112</sup> For the LAS, there are several design characteristics common to the devices (Fig. 24.4). These stents are very short in length ranging between 1 and 3 cm. The ends of the stents are flanged to generate some lumen-apposing force and improve the antimigratory properties of the stent.<sup>112</sup> However, the forces generated by different stent designs are markedly different, and choosing the right stent for the clinical situation is important. Regarding tubular stents, they may be uncovered at one side to provide anchorage and be fully covered at the other end to bridge the anastomosis from the target organ to the lumen. Other types of tubular stents have antimigratory flaps to reduce the risk of migration.

Cautery-equipped stent delivery systems also have become available.<sup>111</sup> The cautery at the tip of the sheath allows a single-step puncture of the target organ and delivery of the stent, thereby avoiding the need for multiple device exchanges during the procedure (see Fig. 24.4). The system may thus reduce the chances of bile leak or wire dislodgement. The system has been used in CDS and EGBD. Dedicated stents for each procedure will be discussed in the respective sections.

## Technique of Endoscopic Ultrasonography-Rendezvous (Biliary)

### Considerations

The main aim of EUS-Rv is to insert and pass a guidewire across any stenosis through the papilla to guide cannulation by ERCP. Manipulation of the guidewire is the most difficult part of the procedure. For successful guidewire manipulation, endoscopist-controlled wire guidance may be helpful as compared to assistant-controlled wire guidance, similar to wire-guided biliary cannulation.<sup>113</sup> Selection of an appropriate site for puncture has a tremendous influence on the

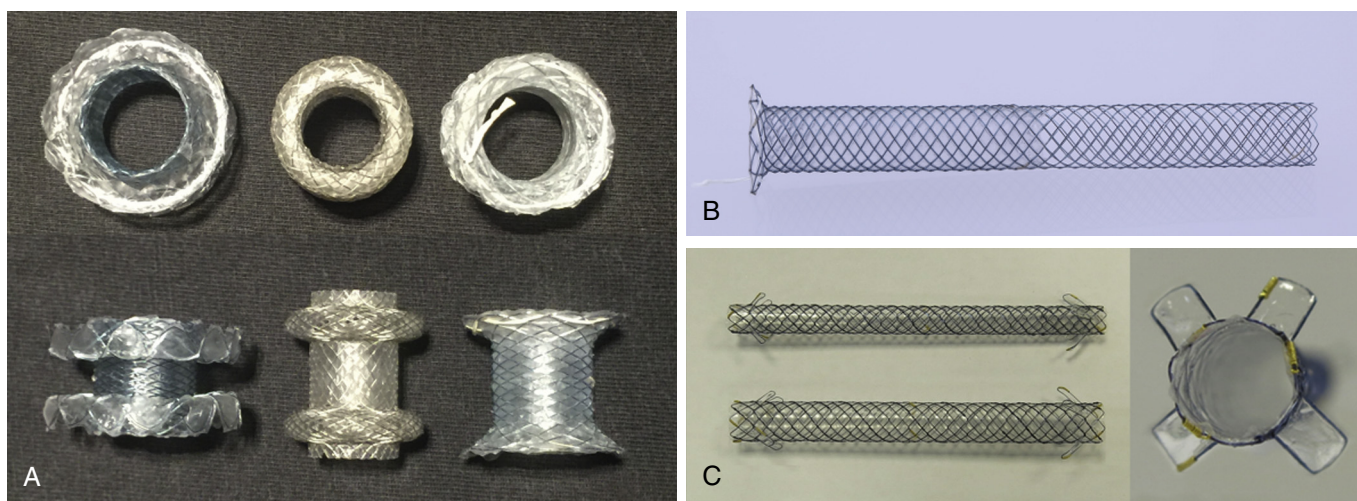
direction of the guidewire and affects the ease of wire manipulation. The use of a short-wire system also has been described to improve the ease of wire manipulation.<sup>114</sup>

### Site of Needle Puncture

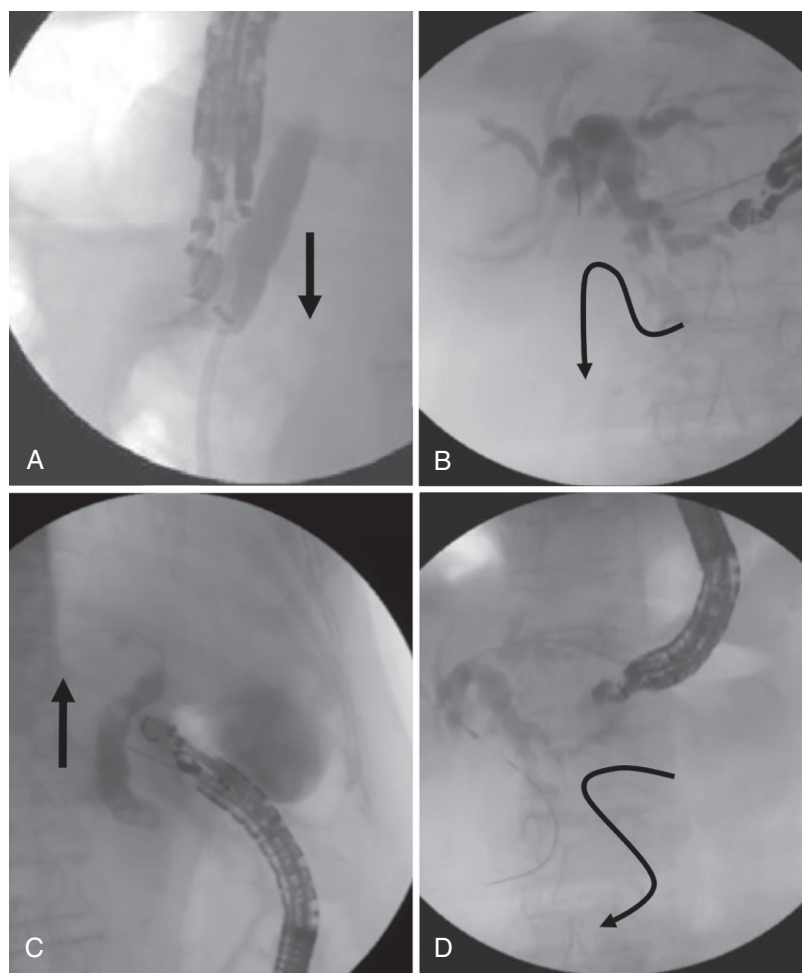
For EUS-Rv, the bile duct could be punctured at the second part of the duodenum, the first part of the duodenum, or the left intrahepatic duct (Fig. 24.5).<sup>15</sup> In the second part of the duodenum, the linear echoendoscope is in a short-scope position. The direction of needle puncture is toward the papilla, and the pathway of the guidewire would be in line with the direction of the needle. Thus wire manipulation would be easiest in this position, but the scope position is unstable. In the first part of the duodenum, the common bile duct is directly behind the duodenum, and needle puncture is easy. However, the echoendoscope is frequently in a long-scope position, and the direction of the needle would be toward the liver hilum. Thus the guidewire would have a tendency to pass toward the hilum instead of the papilla. Regarding the left intrahepatic ducts, one prerequisite is that adequate duct dilation must be present. The authors prefer to puncture close to the junction between segment 2 and 3 ducts as it improves the ease of guidewire manipulation toward the papilla and avoids unnecessary entry into intrahepatic side branches.

### The Procedure (Fig. 24.6 and Video 24.1)

- The bile duct is punctured from one of the positions as described previously.
- Bile is aspirated to confirm puncture of the bile duct and prevent bile leak before injection of the contrast medium.
- Contrast is injected to perform a full cholangiogram.
- A guidewire is inserted through the needle into the bile duct to negotiate across any stenosis and pass through the papilla.
- Once the guidewire has passed through the papilla, the insertion of an excess of guidewire is continued and made to loop in the duodenum.
- The echoendoscope is then changed to a duodenoscope. The guidewire is then retrieved by a snare or forceps. Slippage of the wire can occur during retrieval, and care must be taken to avoid accidentally retracting the guidewire back into the papilla.
- Once the guidewire is retrieved into the duodenoscope, the procedure can continue similar to an ERCP procedure.



• **Fig. 24.4** Endoscopic ultrasonography specific stents. (A) Lumen-apposing stents. (B) Half-covered self-expandable metallic stents. (C) Fully covered self-expandable metal stent with antimigratory flaps.



• **Fig. 24.5** Possible sites of puncture for endoscopic ultrasonography-guided rendezvous biliary and the direction of passage of the guidewire. (A) Puncture at the D2 with the direction of guidewire toward the papilla. (B) Puncture at segment 3 ducts with the direction of guidewire following a tortuous pathway. (C) Puncture at D1 with the guidewire pointing toward the liver hilum. (D) Puncture at segment 2 ducts with the guidewire following a tortuous pathway toward the papilla.

### Troubleshooting

The most difficult part to EUS-Rv (biliary) is manipulation of the guidewire. The use of a curve-tipped 0.025-inch guidewire or hydrophilic guidewire may improve the ease of guidewire manipulation. The use of a forward viewing echoendoscope allows additional angulation to guide the direction of the needle when puncturing from the first part of duodenum. Occasionally, the guidewire may become stuck in the EUS-fine-needle aspiration (FNA) needle. In such a situation, gentle withdrawal of the EUS-FNA needle into the liver parenchyma may allow the easy manipulation of a guidewire.<sup>115</sup> If shearing of the guidewire occurs, the needle and wire may need to be removed together to avoid leaving a part of the guidewire in the patient.

### Technique of Endoscopic Ultrasonography-Guided Antegrade Biliary

#### Considerations

In EUS-AG biliary, the aim is to insert and pass a guidewire across any stenosis through the papilla or surgical anastomosis to place a stent directly with the echoendoscope. Again, the main difficulty is guidewire manipulation across any stenotic site.

### The Procedure (Fig. 24.7 and Video 24.2)

- The authors usually puncture from the left intrahepatic duct at the junction between the segment 2 and 3 ducts due to a similar rationale as in EUS-Rv to improve the ease of guidewire manipulation.
- Bile is aspirated to confirm the puncture of the bile duct and to prevent bile leak before the injection of contrast medium.
- Contrast is injected to perform a full cholangiogram.
- A guidewire is inserted through the needle into the intrahepatic bile duct.
- The guidewire is passed across any stenosis to exit through the papilla or surgical anastomosis.
- The needle is then removed and the needle tract is dilated with a 6-Fr cystotome or 4-mm biliary balloon.
- A partially covered or uncovered SEMS is then inserted on the guidewire across the stenotic segment.
- There is no need to close the puncture site in the stomach as it will usually seal off by itself. The risk of bile leak from the liver is also low, provided that adequate drainage has been provided by the antegrade stent. In case of doubt, a nasobiliary drain could be inserted to bridge the needle tract and the stomach. The drain can be removed a few days later.

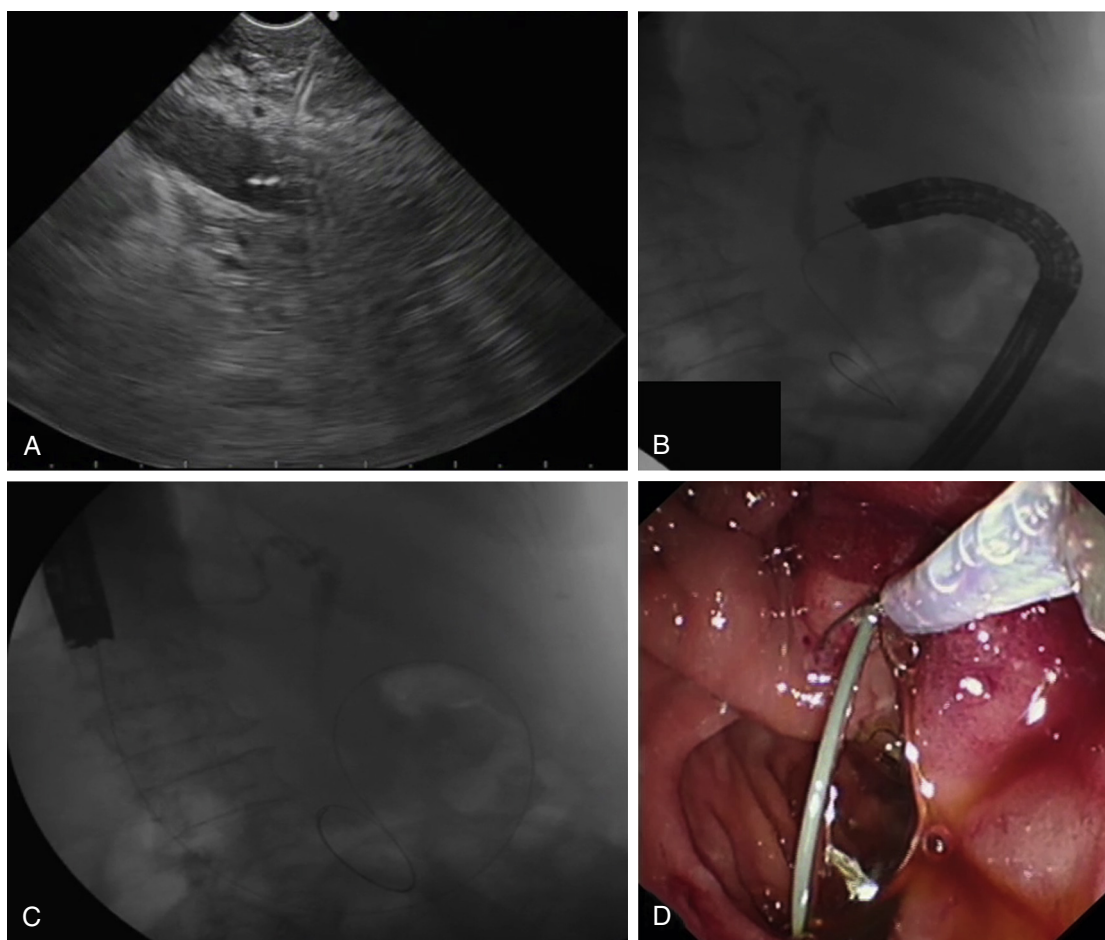


**Fig. 24.6** The endoscopic ultrasonography-guided rendezvous biliary procedure. (A) The common bile duct was punctured with a forward viewing echoendoscope at the first part of the duodenum. (B) The guidewire was passed into the bile duct, through the papilla, and looped in the duodenum. (C) The echoendoscope is changed for a duodenoscope. (D) The wire is retrieved with a snare with the duodenoscope.

### Troubleshooting

The difficulty in EUS-AG is similar to EUS-Rv and involves guidewire manipulation across the papilla.

### Technique of Endoscopic Ultrasonography-Choledochoduodenostomy

#### Considerations

EUS-CDS may not be possible when there is tumor infiltration to the first part of the duodenum. The site of biliary obstruction must be at the distal common bile duct.

#### The Procedure (Fig. 24.8 and Video 24.3)

- The extrahepatic common bile duct is visualized from the duodenal bulb and punctured.
- The direction of the needle should be toward to the hepatic hilum.
- Bile is aspirated to confirm puncture of the bile duct and to prevent bile leak before injecting the contrast medium.
- Contrast is injected to perform a full cholangiogram.
- A guidewire is inserted through the needle into the intrahepatic bile duct.
- The needle is then exchanged for a dilation device to dilate the needle tract while maintaining the intraductal position of the guidewire.

- A metal stent is then placed through the needle tract and deployed below the hilum, landing in the duodenum.
- If a cautery-equipped stent delivery device is available, a single-step direct puncture of the common bile duct with delivery of the stent is possible.<sup>33</sup>

### Troubleshooting

As the bile duct is relatively fixed in position and located directly behind the first part of the duodenum, the risk of stent migration is low. Troubleshooting is uncommon.

### Technique of Endoscopic Ultrasonography-Hepatico-Gastrostomy

#### Considerations

The left intrahepatic segment can be easily seen and accessed from the stomach even when only minimally dilated (3 to 4 mm). In general, the authors prefer to puncture the segment 3 ducts, because puncturing the segment 2 ducts may risk the needle tract traversing the lower mediastinum resulting in mediastinitis. Furthermore, puncturing the segment 2 ducts may result in the stent landing in the lower esophagus. The most worrisome adverse event in HGS is stent migration into the peritoneal cavity. Thus it is important to leave more than 3 cm of the SEMS in the gastric

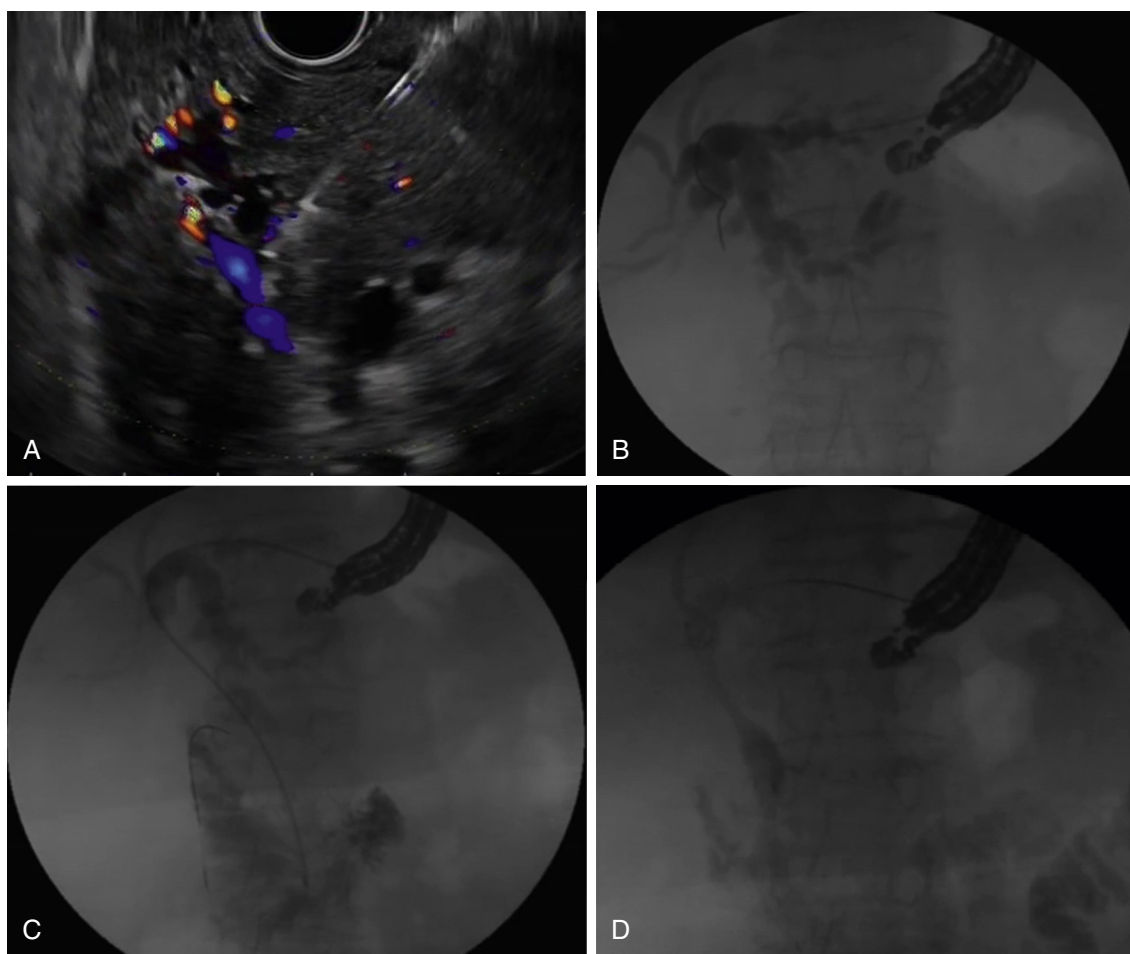


**Fig. 24.7** The endoscopic ultrasonography-guided antegrade biliary procedure. (A) The segment 2 intrahepatic duct was punctured with a 19-G needle. (B) A 0.025-inch guidewire was passed towards the common hepatic duct stricture. (C) The guidewire negotiated the stricture after the introduction of a 6-Fr cystotome and passed to the duodenum to locate the landing site of the stent. (D) Complete deployment of an uncovered metal stent.

lumen to account for both metal stent foreshortening and movement of the stomach away from the liver during respiration.

#### The Procedure (Fig. 24.9 and Video 24.4)

- The site of puncture is identified by EUS. The angle of entry to the biliary system is an important aspect of the procedure with the aim of advancing the guidewire toward the hepatic confluence.
- Bile is aspirated to confirm puncture of the bile duct and prevent bile leak before injecting the contrast medium.
- Contrast is injected to perform a full cholangiogram.
- A guidewire is inserted through the needle into the intrahepatic bile duct.
- The needle is then exchanged for a dilation device to dilate the needle tract while maintaining the intraductal position of the guidewire.
- A fully covered or partially covered SEMS is then inserted and deployed. Care must be taken to maintain the position of the stent during deployment of the gastric side of the stent to prevent intraperitoneal deployment. After opening the liver side of the stent, the authors prefer to deploy the gastric side of the stent inside the channel of the echoendoscope. The stent is then pushed out from the channel with simultaneous retraction of the endoscope. These movements are repeated until the stent is completely deployed.

- A cholangiogram is then performed through the stent to check for potential sites of leakage, particularly when partially covered stents are used.

#### Troubleshooting

The most feared situation during HGS is deployment of the proximal part of the stent intraperitoneally. In such a situation, it is important to have the guidewire left in situ to allow insertion of an additional stent in a stent-on-stent manner to bridge the stomach to the HGS stent. If guidewire access is lost, then the stomach opening should be closed and a single attempt to puncture the intraperitoneal stent could be performed by an experienced endosonographer. If successful, then insertion of a bridging stent may be possible to salvage the mis-deployed stent. Otherwise, the patient may need to undergo surgical removal of the stent and surgical biliary drainage.

#### Technique of Endoscopic Ultrasonography-Guided Pancreatic Duct Drainage

##### Considerations

The choice of the technique for EUS-PD is largely based on the aim of the procedure. The optimal point of MPD access depends on the site of ductal obstruction and the method of drainage.<sup>66</sup>

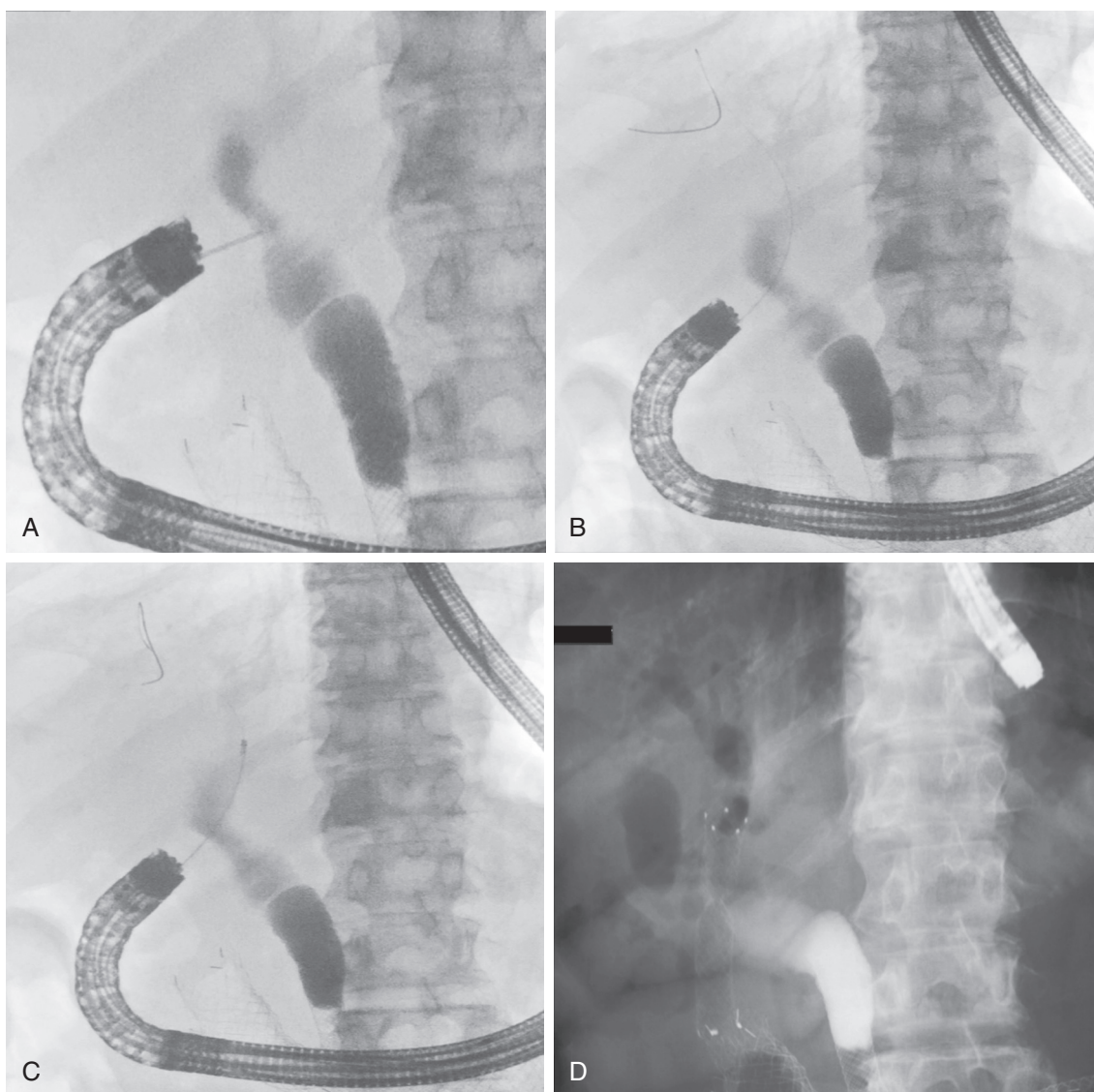


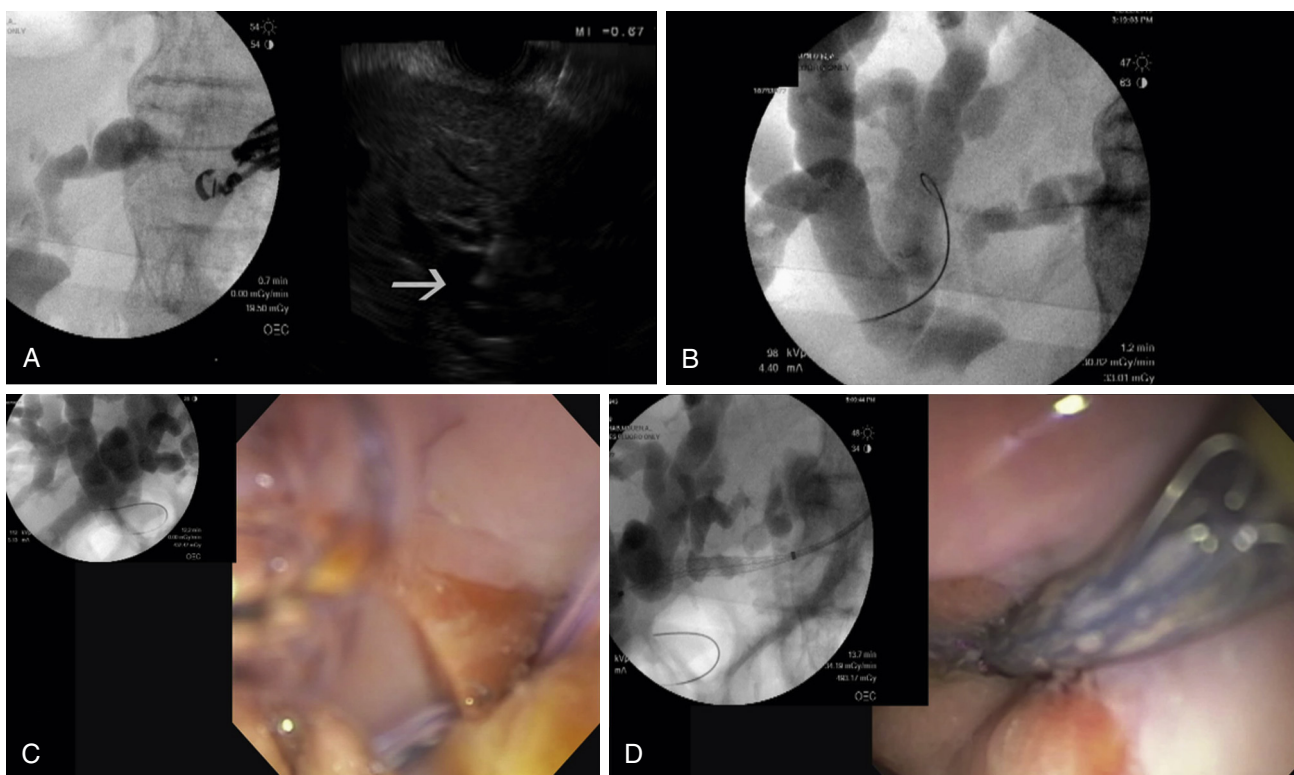
**Fig. 24.8** The endoscopic ultrasonography-choledochoduodenostomy procedure. (A) The common bile duct punctured from the first part of the duodenum with a 19-gauge needle with contrast injection. (B) The guidewire passed into the intrahepatic bile duct. (C) The needle tract is dilated with a needle knife. (D) Complete deployment of the metal stent.

The optimal access site also should be selected based on the shortest distance between the bowel lumen and the MPD without intervening vessels. The transgastric approach is the most preferred access point. A large MPD diameter may be easier for puncture, but successful MPD access and drainage has been reported in ducts as small as 3 mm in expert hands.<sup>47</sup> The optimal site of puncture for EUS-Rv PD is at the neck of the pancreas for easier guidewire manipulation compared with the body or tail of the pancreas. The optimal site of MPD puncture in EUS-guided transmural stenting is at the body or body-tail junction of the pancreas to allow for placement of an appropriate length of the stent in MPD. In addition, the fistula tract needs to be dilated after wire insertion to facilitate the passage of other accessories and/or for dilation of anastomotic strictures.<sup>64</sup> The pancreatic parenchyma is often very hard, and the use of cautery dilators is frequently required.

Appropriate stent selection is also important. Currently, plastic stents are usually used for EUS-PD. Straight type, single pigtail,

or double pigtail plastic stents can be used for drainage. However, stent-related adverse events, such as stent migration, failure in stent placement, pancreatic duct leak, and stent occlusion have been reported.<sup>47,67,69</sup> Recently, a newly designed 7-Fr single pigtail plastic stent has been developed for EUS-PD.<sup>116</sup> The stent has a tapered tip, four internal flanges (two in the distal end and two at the proximal end), and a single external flange. Placement of the dedicated pancreatic duct stent appears feasible (technical success 100%) and effective during a mean follow-up of 7.4 months.

On the other hand, FCSEMS have not been used for EUS-PD with transmural stenting. Biliary SEMS are often too large in diameter; the stents are prone to migration and they may block the side branches of the PD. However, FCSEMS may provide longer stent patency as seen in benign and malignant biliary strictures.<sup>117,118</sup> Recently, the effectiveness and safety of a dedicated FCSEMS for EUS-PD in patients with failed ERP have been reported.<sup>119</sup> The FCSEMS was modified with proximal and distal anchoring flaps for EUS-PD (see Fig. 24.2). There were no FCSEMS-related



• **Fig. 24.9** The endoscopic ultrasonography-hepatico-gastrostomy procedure. (A) The segment 3 intrahepatic duct was punctured with a 19-gauge needle. (B) A guidewire passed to the common hepatic duct. (C) The needle tract dilated with a needle knife. (D) Insertion of a partially covered self-expandable metallic stent.

adverse events, including migration, during stent placement. Whether the use of FCSEMS designed for EUS-PD provides additional benefit over plastic stents remains to be seen.

### The Procedure

#### EUS-Rv pancreatic (Fig. 24.10)

- Locate the optimal site for duct puncture and puncture the pancreatic duct with a 19-gauge needle.
- Inject contrast to obtain a pancreatogram.
- A 0.025-inch guidewire is advanced and manipulated across the papilla into the duodenum or anastomosis site into the jejunum.
- The echoendoscope is then withdrawn leaving the guidewire in place. A duodenoscope is inserted by the side of the guidewire. In patients with surgically altered anatomy, ERP is performed with a pediatric colonoscope or an enteroscope.<sup>52</sup>
- Cannulation is attempted first by the side of the guidewire coming out of the papilla or anastomosis orifice. If this does not succeed, the guidewire is grasped with a snare or biopsy forceps and is withdrawn into the working channel for retrograde introduction of a catheter over the wire.<sup>120</sup>
- The stent can then be introduced in the standard fashion. EUS-guided transmural PD (Fig. 24.11)
- In contrast to the rendezvous procedure, transmural drainage is completed with echoendoscope alone. In this procedure, the steps from duct puncture to advancing the guidewire into the MPD are identical to those for the rendezvous procedure.

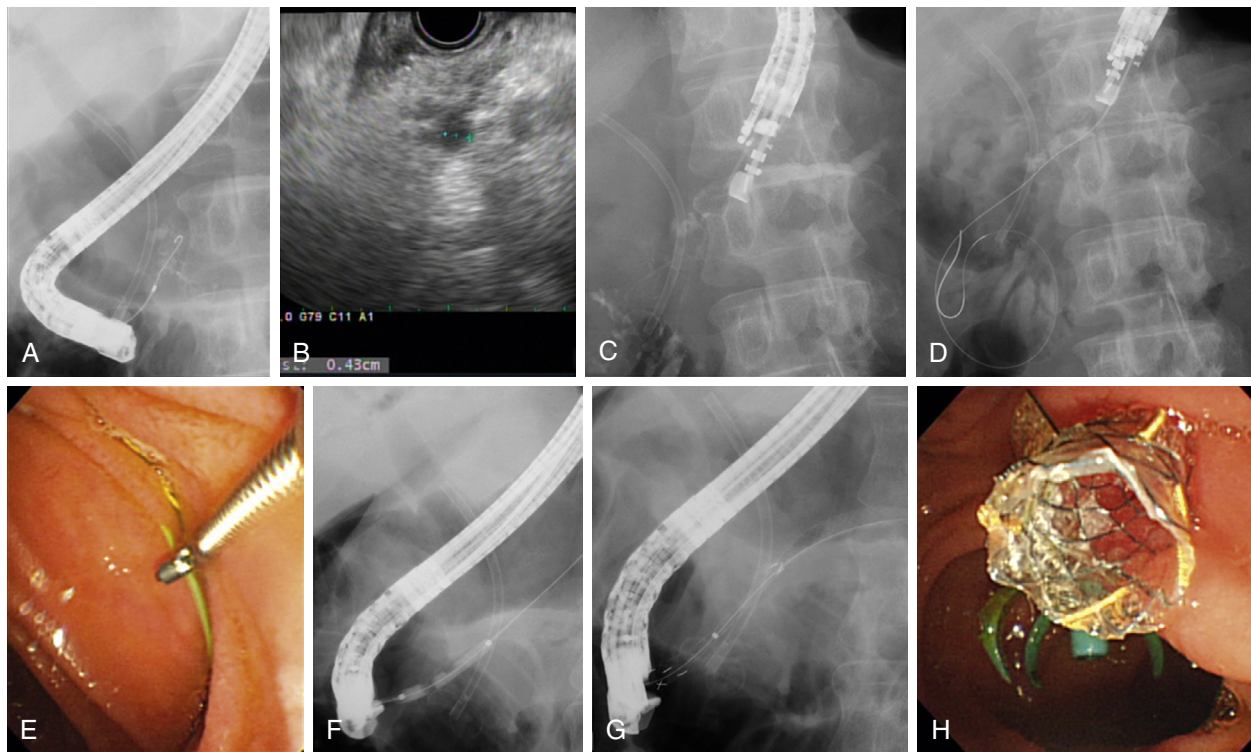
- After the guidewire has entered the MPD, the needle is exchanged for a dilator for fistula tract dilation. This is one of the most challenging steps in EUS-guided transmural drainage due to misalignment of the needle-guidewire angle and/or the fibrotic nature of the pancreatic parenchyma in chronic pancreatitis.<sup>58</sup> Cautery devices, including the needle knife or 6-Fr cystotome, are usually required.
- After tract dilation, the plastic stent is inserted.

### Troubleshooting

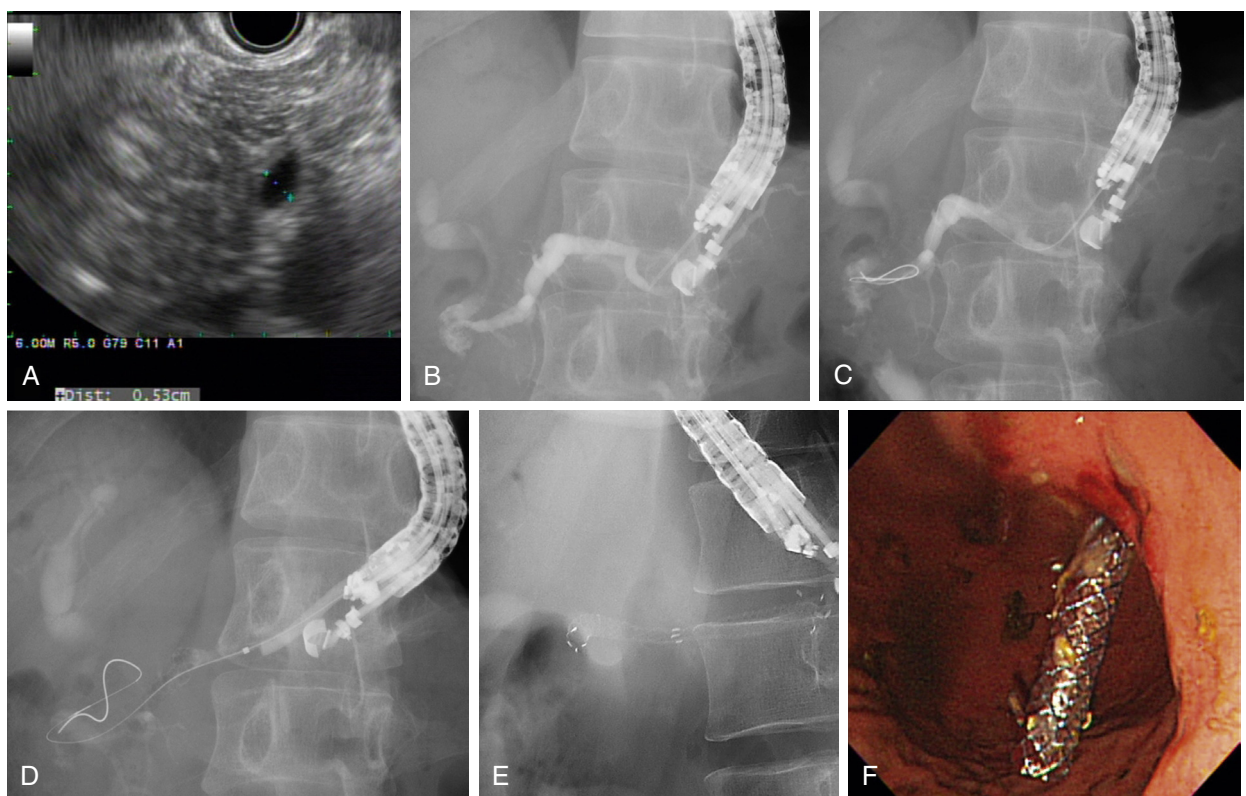
The most common problems encountered during EUS-PD are wire manipulation and difficulty in dilating the fistula tract. The technical problems could be overcome adopting the methods described above.

## Technique of Endoscopic Ultrasonography-Guided Transmural Gallbladder Drainage Considerations

In contrast to the liver and pancreas, the gallbladder is a freely mobile organ. The position is variable and a prerequisite for successful and safe EGBD is the presence of a distended gallbladder. The integrity of any anastomosis created by EUS is highly dependent on the stent placed. Hence fully covered LAS with higher lumen-apposing force or short tubular stents with antimigratory properties is preferred. The authors prefer to drain the gallbladder from the duodenum as this lowers the risk of food impaction into the gallbladder. No difference in



**• Fig. 24.10** The endoscopic ultrasonography (EUS)-guided rendezvous pancreatic technique in a patient with failed endoscopic retrograde pancreatography due to a tight main pancreatic duct (MPD). (A) A pancreateogram showing the failure of guidewire advancement due to a tight MPD stricture. (B) EUS revealing a dilated MPD. (C) The echoendoscope was positioned to puncture the MPD and a pancreateogram was obtained. (D) A 0.025-inch guidewire was inserted into the MPD and passed in an antegrade fashion across the major papilla. (E) The echoendoscope was exchanged for a side-viewing duodenoscope. A guidewire was captured with biopsy forceps. (F) MPD stricture was dilated with a 4-mm balloon catheter. (G) A fully covered self-expandable metal stent was placed across the stricture. (H) Endoscopic imaging revealed a well-placed stent.



**• Fig. 24.11** Endoscopic ultrasonography (EUS)-guided transmural pancreatic duct drainage in patients with surgically altered anatomy. (A) An EUS image revealing the dilated main pancreatic duct (MPD). (B) A 19-gauge needle was punctured into the dilated MPD and a pancreateogram was obtained. (C) A 0.025-inch guidewire was inserted into the MPD. (D) The fistula tract was dilated with a needle knife followed by a 4-mm balloon catheter. (E) A fully covered self-expandable metal stent was placed over the wire across the pancreatogastrostomy. (F) A well-placed stent was confirmed endoscopically.

outcome was noted when drainage is performed in the antrum or the duodenum.<sup>94</sup>

### The Procedure (Fig. 24.12 and Video 24.5)

- The gallbladder is initially identified from the first part of the duodenum.
- It is then punctured with a 19-G needle, and a 0.035- or 0.025-inch guidewire is inserted and coiled within the gallbladder.
- The needle is then exchanged for a cautery dilator for tract dilation. This is followed by exchange with a 4-mm balloon.
- After dilation, a fully covered metallic stent is inserted.
- If a cautery-equipped stent delivery device is available, single-step direct puncture of the gallbladder with delivery of the stent is possible.

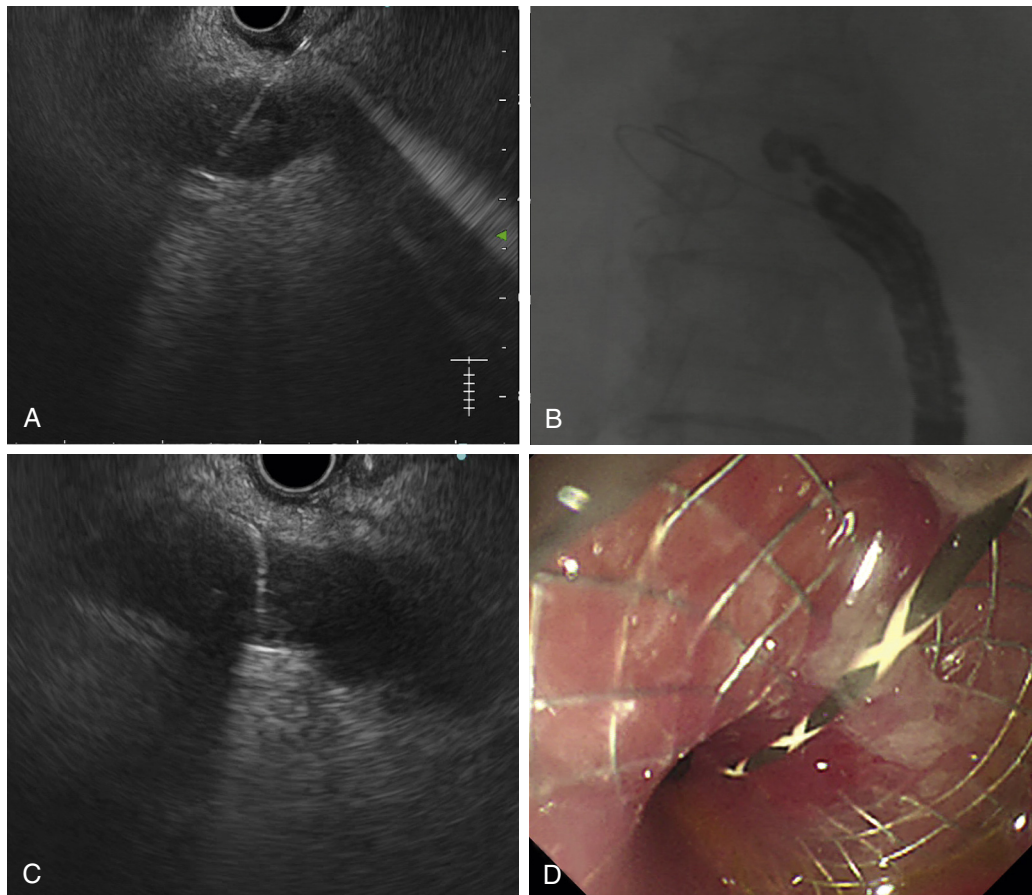
### Troubleshooting

The gallbladder is a nonadherent organ. If problems are encountered during stent deployment, it may result in bile leak and free perforation of the duodenum. Problems with stent deployment may occur if the gallbladder is not adequately distended, particularly in patients where a PTC is already inserted and the gallbladder is contracted. Occasionally, the LAS is completely deployed in the gallbladder. In such a situation, it is paramount that the guidewire to the gallbladder is left in situ to allow the insertion of an additional stent in a stent-on-stent fashion. If guidewire access is completely lost, then the duodenal opening must be closed and a PTC drainage catheter must be placed. Food impaction may

sometimes occur when stents are deployed via the antrum. Early stent removal may be required in such patients, and the gastric opening needs to be closed endoscopically.

### Future Perspectives

Evidence is accumulating in support of EUS-BD as the procedure of choice in patients with failed ERCP. Future studies are required to assess whether one type of EUS-BD procedure is preferred for a particular indication. Studies assessing the potential of EUS-BD to replace ERCP in malignant biliary obstruction are underway. In addition, the learning curve of EUS-BD needs to be better quantified. For EUS-PD, studies comparing the outcomes of EUS-PD versus ERP are lacking. Also, how the rendezvous technique compares to transmural stenting is unknown. For EGBD, accumulating evidence in support of EGBD over PTC for patients that are unfit for surgery is present. A randomized trial comparing EGBD versus PTC in patients that are unfit for cholecystectomy is being conducted and it may provide more evidence in support of the procedure. More studies are required to assess the optimal timing of stent placement, the time interval between stent exchanges, and the total duration of stent placement in EUS-guided transmural drainage. Furthermore, new devices that could allow one-step duct puncture and stent placement are required to reduce the complexity of the procedures. These new devices could, in turn, improve the technical success rates and reduce the chances of adverse events occurring during the procedures.



• **Fig. 24.12** The endoscopic ultrasonography-guided transmural gallbladder drainage procedure. (A) The gallbladder punctured with a 19-gauge needle from the first part of the duodenum. (B) A guidewire inserted and looped in the gallbladder. (C) The opening of the distal flange of a lumen-apposing stent. (D) The opening of the proximal flange of a lumen-apposing stent.

## Key References

5. Dhir V, Isayama H, Itoi T, et al. Endoscopic ultrasonography-guided biliary and pancreatic duct interventions. *Dig Endosc.* 2017;29:472–485.
42. Lee TH, Choi JH, Park do H, et al. Similar efficacies of endoscopic ultrasound-guided transmural and percutaneous drainage for malignant distal biliary obstruction. *Clin Gastroenterol Hepatol.* 2016;14:1011–1019. e3.
94. Teoh AY, Serna C, Penas I, et al. Endoscopic ultrasound-guided gallbladder drainage reduces adverse events compared with percutaneous cholecystostomy in patients who are unfit for cholecystectomy. *Endoscopy.* 2017;49:130–138.
121. Tyberg A, Sharaiha RZ, Kedia P, et al. EUS-guided pancreatic drainage for pancreatic strictures after failed ERCP: a multicenter international collaborative study. *Gastrointest Endosc.* 2017;85:164–169.
122. Chen YI, Levy MJ, Moreels TG, et al. An international multicenter study comparing EUS-guided pancreatic duct drainage with enteroscopy-assisted endoscopic retrograde pancreatography after Whipple surgery. *Gastrointest Endosc.* 2017;85:170–177.

## References

Access the reference list online at [ExpertConsult.com](#).

## References

1. Baron TH, Petersen BT, Mergener K, et al. Quality indicators for endoscopic retrograde cholangiopancreatography. *Am J Gastroenterol.* 2006;101:892–897.
2. van Delden OM, Lameris JS. Percutaneous drainage and stenting for palliation of malignant bile duct obstruction. *Eur Radiol.* 2008;18:448–456.
3. Zhao XQ, Dong JH, Jiang K, et al. Comparison of percutaneous transhepatic biliary drainage and endoscopic biliary drainage in the management of malignant biliary tract obstruction: a meta-analysis. *Dig Endosc.* 2015;27:137–145.
4. Itoi T, Sofuni A, Itokawa F, et al. Endoscopic ultrasonography-guided biliary drainage. *J Hepatobiliary Pancreat Sci.* 2010;17:611–616.
5. Dhir V, Isayama H, Itoi T, et al. Endoscopic ultrasonography-guided biliary and pancreatic duct interventions. *Dig Endosc.* 2017;29:472–485.
6. Liao WC, Angsuwatcharakorn P, Isayama H, et al. International consensus recommendations for difficult biliary access. *Gastrointest Endosc.* 2017;85:295–304.
7. Holt BA, Hawes R, Hasan M, et al. Biliary drainage: role of EUS guidance. *Gastrointest Endosc.* 2016;83:160–165.
8. Kahaleh M, Hernandez AJ, Tokar J, et al. Interventional EUS-guided cholangiography: evaluation of a technique in evolution. *Gastrointest Endosc.* 2006;64:52–59.
9. Shah JN, Marson F, Weilert F, et al. Single-operator, single-session EUS-guided anterograde cholangiopancreatography in failed ERCP or inaccessible papilla. *Gastrointest Endosc.* 2012;75:56–64.
10. Iwashita T, Lee JG, Shinoura S, et al. Endoscopic ultrasound-guided rendezvous for biliary access after failed cannulation. *Endoscopy.* 2012;44:60–65.
11. Dhir V, Bhandari S, Bapat M, et al. Comparison of EUS-guided rendezvous and precut papillotomy techniques for biliary access (with videos). *Gastrointest Endosc.* 2012;75:354–349.
12. Villa JJ, Perez-Miranda M, Vazquez-Sequeiros E, et al. Initial experience with EUS-guided cholangiopancreatography for biliary and pancreatic duct drainage: a Spanish national survey. *Gastrointest Endosc.* 2012;76:1133–1141.
13. Park DH, Jeong SU, Lee BU, et al. Prospective evaluation of a treatment algorithm with enhanced guidewire manipulation protocol for EUS-guided biliary drainage after failed ERCP (with video). *Gastrointest Endosc.* 2013;78:91–101.
14. Dhir V, Bhandari S, Bapat M, et al. Comparison of transhepatic and extrahepatic routes for EUS-guided rendezvous procedure for distal CBD obstruction. *United European Gastroenterol J.* 2013;1:103–108.
15. Iwashita T, Yasuda I, Mukai T, et al. EUS-guided rendezvous for difficult biliary cannulation using a standardized algorithm: a multicenter prospective pilot study (with videos). *Gastrointest Endosc.* 2016;83:394–400.
16. Tang Z, Igbinomwanhia E, Elhanafi S, et al. Endoscopic ultrasound guided rendezvous drainage of biliary obstruction using a new flexible 19-gauge fine needle aspiration needle. *Diagn Ther Endosc.* 2016;2016:3125962.
17. Lee A, Aditi A, Bhat YM, et al. Endoscopic ultrasound-guided biliary access versus precut papillotomy in patients with failed biliary cannulation: a retrospective study. *Endoscopy.* 2017;49:146–153.
18. Bill JG, Darcy M, Fujii-Lau LL, et al. A comparison between endoscopic ultrasound-guided rendezvous and percutaneous biliary drainage after failed ERCP for malignant distal biliary obstruction. *Endosc Int Open.* 2016;4:E980–E985.
19. Khashab MA, Valeshabad AK, Modayil R, et al. EUS-guided biliary drainage by using a standardized approach for malignant biliary obstruction: rendezvous versus direct transluminal techniques (with videos). *Gastrointest Endosc.* 2013;78:734–741.
20. Ogura T, Masuda D, Imoto A, et al. EUS-guided hepaticogastrostomy combined with fine-gauge antegrade stenting: a pilot study. *Endoscopy.* 2014;46:416–421.
21. Iwashita T, Yasuda I, Mukai T, et al. Endoscopic ultrasound-guided antegrade biliary stenting for unresectable malignant biliary obstruction in patients with surgically altered anatomy: Single-center prospective pilot study. *Dig Endosc.* 2017;29:362–368.
22. Dhir V, Artifon EL, Gupta K, et al. Multicenter study on endoscopic ultrasound-guided expandable biliary metal stent placement: choice of access route, direction of stent insertion, and drainage route. *Dig Endosc.* 2014;26:430–435.
23. Park DH, Jang JW, Lee SS, et al. EUS-guided biliary drainage with transluminal stenting after failed ERCP: predictors of adverse events and long-term results. *Gastrointest Endosc.* 2011;74:1276–1284.
24. Kawakubo K, Isayama H, Kato H, et al. Multicenter retrospective study of endoscopic ultrasound-guided biliary drainage for malignant biliary obstruction in Japan. *J Hepatobiliary Pancreat Sci.* 2014;21:328–334.
25. Gupta K, Perez-Miranda M, Kahaleh M, et al. Endoscopic ultrasound-assisted bile duct access and drainage: multicenter, long-term analysis of approach, outcomes, and complications of a technique in evolution. *J Clin Gastroenterol.* 2014;48:80–87.
26. Song TJ, Lee SS, Park DH, et al. Preliminary report on a new hybrid metal stent for EUS-guided biliary drainage (with videos). *Gastrointest Endosc.* 2014;80:707–711.
27. Dhir V, Itoi T, Khashab MA, et al. Multicenter comparative evaluation of endoscopic placement of expandable metal stents for malignant distal common bile duct obstruction by ERCP or EUS-guided approach. *Gastrointest Endosc.* 2015;81:913–923.
28. Poincloux L, Rouquette O, Buc E, et al. Endoscopic ultrasound-guided biliary drainage after failed ERCP: cumulative experience of 101 procedures at a single center. *Endoscopy.* 2015;47:794–801.
29. Ogura T, Yamamoto K, Sano T, et al. Stent length is impact factor associated with stent patency in endoscopic ultrasound-guided hepaticogastrostomy. *J Gastroenterol Hepatol.* 2015;30:1748–1752.
30. Umeda J, Itoi T, Tsuchiya T, et al. A newly designed plastic stent for EUS-guided hepaticogastrostomy: a prospective preliminary feasibility study (with videos). *Gastrointest Endosc.* 2015;82:390–396. e2.
31. Khashab MA, Messallam AA, Penas I, et al. International multicenter comparative trial of transluminal EUS-guided biliary drainage via hepatogastrostomy vs. choledochoduodenostomy approaches. *Endosc Int Open.* 2016;4:E175–181.
32. Cho DH, Lee SS, Oh D, et al. Long-term outcomes of a newly developed hybrid metal stent for EUS-guided biliary drainage (with videos). *Gastrointest Endosc.* 2017;85:1067–1075.
33. Kunda R, Perez-Miranda M, Will U, et al. EUS-guided choledochoduodenostomy for malignant distal biliary obstruction using a lumen-apposing fully covered metal stent after failed ERCP. *Surg Endosc.* 2016;30:5002–5008.
34. Khashab MA, Van der Merwe S, Kunda R, et al. Prospective international multicenter study on endoscopic ultrasound-guided biliary drainage for patients with malignant distal biliary obstruction after failed endoscopic retrograde cholangiopancreatography. *Endosc Int Open.* 2016;4:E487–E496.
35. Kawakubo K, Kawakami H, Kuwatani M, et al. Endoscopic ultrasound-guided choledochoduodenostomy vs. transpapillary stenting for distal biliary obstruction. *Endoscopy.* 2016;48:164–169.
36. Ogura T, Chiba Y, Masuda D, et al. Comparison of the clinical impact of endoscopic ultrasound-guided choledochoduodenostomy and hepaticogastrostomy for bile duct obstruction with duodenal obstruction. *Endoscopy.* 2016;48:156–163.
37. Hara K, Yamao K, Hijikata S, et al. Prospective clinical study of endoscopic ultrasound-guided choledochoduodenostomy with direct metallic stent placement using a forward-viewing echoendoscope. *Endoscopy.* 2013;45:392–396.

38. Hara K, Yamao K, Niwa Y, et al. Prospective clinical study of EUS-guided choledochoduodenostomy for malignant lower biliary tract obstruction. *Am J Gastroenterol.* 2011;106:1239–1245.
39. Artifon EL, Marson FP, Gaidhane M, et al. Hepaticogastrostomy or choledochoduodenostomy for distal malignant biliary obstruction after failed ERCP: is there any difference? *Gastrointest Endosc.* 2015;81:950–959.
40. Khan MA, Akbar A, Baron TH, et al. Endoscopic ultrasound-guided biliary drainage: a systematic review and meta-analysis. *Dig Dis Sci.* 2016;61:684–703.
41. Artifon EL, Aparicio D, Paione JB, et al. Biliary drainage in patients with unresectable, malignant obstruction where ERCP fails: endoscopic ultrasonography-guided choledochoduodenostomy versus percutaneous drainage. *J Clin Gastroenterol.* 2012;46:768–774.
42. Lee TH, Choi JH, Park do H, et al. Similar efficacies of endoscopic ultrasound-guided transmural and percutaneous drainage for malignant distal biliary obstruction. *Clin Gastroenterol Hepatol.* 2016;14:1011–1019. e3.
43. Giovannini M, Bories B, Bertrand N, et al. Multicenter randomized phase II study: percutaneous biliary drainage vs EUS guided biliary drainage: results of the intermediate analysis [abstract]. *Gastrointest Endosc.* 2015;81:AB174.
44. Sharaiha RZ, Khan MA, Kamal F, et al. Efficacy and safety of EUS-guided biliary drainage in comparison with percutaneous biliary drainage when ERCP fails: a systematic review and meta-analysis. *Gastrointest Endosc.* 2017;85:904–914.
45. Tyberg A, Desai AP, Kumta NA, et al. EUS-guided biliary drainage after failed ERCP: a novel algorithm individualized based on patient anatomy. *Gastrointest Endosc.* 2016;84:941–946.
46. Widmer J, Sharaiha RZ, Kahaleh M. Endoscopic ultrasonography-guided drainage of the pancreatic duct. *Gastrointest Endosc Clin N Am.* 2013;23:847–861.
47. Fujii LL, Topazian MD, Abu Dayyeh BK, et al. EUS-guided pancreatic duct intervention: outcomes of a single tertiary-care referral center experience. *Gastrointest Endosc.* 2013;78:854–864. e1.
48. Giovannini M. EUS-guided pancreatic duct drainage: ready for prime time? *Gastrointest Endosc.* 2013;78:865–867.
49. Itoi T, Yasuda I, Kurihara T, et al. Technique of endoscopic ultrasonography-guided pancreatic duct intervention (with video). *J Hepatobiliary Pancreat Sci.* 2014;21:E4–E9.
50. Prachayakul V, Aswakul P. Endoscopic ultrasound-guided interventions in special situations. *World J Gastrointest Endosc.* 2016;8:104–112.
51. Kahaleh M, Hernandez AJ, Tokar J, et al. EUS-guided pancreaticogastrostomy: analysis of its efficacy to drain inaccessible pancreatic ducts. *Gastrointest Endosc.* 2007;65:224–230.
52. Mallery S, Matlock J, Freeman ML. EUS-guided rendezvous drainage of obstructed biliary and pancreatic ducts: Report of 6 cases. *Gastrointest Endosc.* 2004;59:100–107.
53. Barkay O, Sherman S, McHenry L, et al. Therapeutic EUS-assisted endoscopic retrograde pancreatography after failed pancreatic duct cannulation at ERCP. *Gastrointest Endosc.* 2010;71:1166–1173.
54. Will U, Meyer F, Manger T, et al. Endoscopic ultrasound-assisted rendezvous maneuver to achieve pancreatic duct drainage in obstructive chronic pancreatitis. *Endoscopy.* 2005;37:171–173.
55. Papachristou GI, Gleeson FC, Petersen BT, et al. Pancreatic endoscopic ultrasound-assisted rendezvous procedure to facilitate drainage of nondilated pancreatic ducts. *Endoscopy.* 2007;39(Suppl 1):E324–E325.
56. Itoi T, Kikuyama M, Ishii K, et al. EUS-guided rendezvous with single-balloon enteroscopy for treatment of stenotic pancreaticojejunal anastomosis in post-Whipple patients (with video). *Gastrointest Endosc.* 2011;73:398–401.
57. Kikuyama M, Itoi T, Ota Y, et al. Therapeutic endoscopy for stenotic pancreaticodigestive tract anastomosis after pancreateoduodenectomy (with videos). *Gastrointest Endosc.* 2011;73:376–382.
58. Kurihara T, Itoi T, Sofuni A, et al. Endoscopic ultrasonography-guided pancreatic duct drainage after failed endoscopic retrograde cholangiopancreatography in patients with malignant and benign pancreatic duct obstructions. *Dig Endosc.* 2013;25(Suppl 2):109–116.
59. Bataille L, Deprez P. A new application for therapeutic EUS: main pancreatic duct drainage with a “pancreatic rendezvous technique”. *Gastrointest Endosc.* 2002;55:740–743.
60. Keenan J, Mallery S, Freeman ML. EUS rendezvous for pancreatic stent placement during endoscopic snare ampullectomy. *Gastrointest Endosc.* 2007;66:850–853.
61. Saftoiu A, Dumitrescu D, Stoica M, et al. EUS-assisted rendezvous stenting of the pancreatic duct for chronic calcifying pancreatitis with multiple pseudocysts. *Pancreatology.* 2007;7:74–79.
62. Cooper ST, Malick J, McGrath K, et al. EUS-guided rendezvous for the treatment of pancreaticopleural fistula in a patient with chronic pancreatitis and pancreas pseudodivisum. *Gastrointest Endosc.* 2010;71:652–654.
63. Itoi T, Kasuya K, Sofuni A, et al. Endoscopic ultrasonography-guided pancreatic duct access: techniques and literature review of pancreatography, transmural drainage and rendezvous techniques. *Dig Endosc.* 2013;25:241–252.
64. Chapman CG, Waxman I, Siddiqui UD. Endoscopic ultrasound (EUS)-guided pancreatic duct drainage: the basics of when and how to perform EUS-guided pancreatic duct interventions. *Clin Endosc.* 2016;49:161–167.
65. Jirapinyo P, Lee LS. Endoscopic ultrasound-guided pancreaticobiliary endoscopy in surgically altered anatomy. *Clin Endosc.* 2016;49:515–529.
66. Fujii-Lau LL, Levy MJ. Endoscopic ultrasound-guided pancreatic duct drainage. *J Hepatobiliary Pancreat Sci.* 2015;22:51–57.
67. Ergun M, Aouattah T, Gillain C, et al. Endoscopic ultrasound-guided transluminal drainage of pancreatic duct obstruction: long-term outcome. *Endoscopy.* 2011;43:518–525.
68. Gines A, Varadarajulu S, Napoleon B, et al. EUS 2008 Working Group document: evaluation of EUS-guided pancreatic-duct drainage (with video). *Gastrointest Endosc.* 2009;69:S43–S48.
69. Tessier G, Bories E, Arvanitakis M, et al. EUS-guided pancreaticogastrostomy and pancreatobulbstomy for the treatment of pain in patients with pancreatic ductal dilatation inaccessible for transpapillary endoscopic therapy. *Gastrointest Endosc.* 2007;65:233–241.
70. Kolla SB, Aggarwal S, Kumar A, et al. Early versus delayed laparoscopic cholecystectomy for acute cholecystitis: a prospective randomized trial. *Surg Endosc.* 2004;18:1323–1327.
71. Lai PB, Kwong KH, Leung KL, et al. Randomized trial of early versus delayed laparoscopic cholecystectomy for acute cholecystitis. *Br J Surg.* 1998;85:764–767.
72. Lo CM, Liu CL, Fan ST, et al. Prospective randomized study of early versus delayed laparoscopic cholecystectomy for acute cholecystitis. *Ann Surg.* 1998;227:461–467.
73. Johansson M, Thune A, Nelvin L, et al. Randomized clinical trial of open versus laparoscopic cholecystectomy in the treatment of acute cholecystitis. *Br J Surg.* 2005;92:44–49.
74. Teoh AY, Chong CN, Wong J, et al. Routine early laparoscopic cholecystectomy for acute cholecystitis after conclusion of a randomized controlled trial. *Br J Surg.* 2007;94:1128–1132.
75. Tsuyuguchi T, Itoi T, Takada T, et al. TG13 indications and techniques for gallbladder drainage in acute cholecystitis (with videos). *J Hepatobiliary Pancreat Sci.* 2013;20:81–88.
76. McKay A, Abulfaraj M, Lipschitz J. Short- and long-term outcomes following percutaneous cholecystostomy for acute cholecystitis in high-risk patients. *Surg Endosc.* 2012;26:1343–1351.

77. Melloul E, Denys A, Demartines N, et al. Percutaneous drainage versus emergency cholecystectomy for the treatment of acute cholecystitis in critically ill patients: does it matter? *World J Surg.* 2011;35:826–833.
78. Toyota N, Takada T, Amano H, et al. Endoscopic naso-gallbladder drainage in the treatment of acute cholecystitis: alleviates inflammation and fixes operator's aim during early laparoscopic cholecystectomy. *J Hepatobiliary Pancreat Surg.* 2006;13:80–85.
79. Kjaer DW, Kruse A, Funch-Jensen P. Endoscopic gallbladder drainage of patients with acute cholecystitis. *Endoscopy.* 2007;39:304–308.
80. Itoi T, Sofuni A, Itokawa F, et al. Endoscopic transpapillary gallbladder drainage in patients with acute cholecystitis in whom percutaneous transhepatic approach is contraindicated or anatomically impossible (with video). *Gastrointest Endosc.* 2008;68:455–460.
81. Itoi T, Kawakami H, Katanuma A, et al. Endoscopic nasogastric tube or stent placement in acute cholecystitis: a preliminary prospective randomized trial in Japan (with videos). *Gastrointest Endosc.* 2015;81:111–118.
82. Itoi T, Takada T, Hwang TL, et al. Percutaneous and endoscopic gallbladder drainage for the acute cholecystitis: International multicenter comparative study by a propensity score-matched analysis. *J Hepatobiliary Pancreat Sci.* 2017;24:362–368.
83. Lee SS, Park DH, Hwang CY, et al. EUS-guided transmural cholecystostomy as rescue management for acute cholecystitis in elderly or high-risk patients: a prospective feasibility study. *Gastrointest Endosc.* 2007;66:1008–1012.
84. Jang JW, Lee SS, Park DH, et al. Feasibility and safety of EUS-guided transgastric/transduodenal gallbladder drainage with single-step placement of a modified covered self-expandable metal stent in patients unsuitable for cholecystectomy. *Gastrointest Endosc.* 2011;74:176–181.
85. Jang JW, Lee SS, Song TJ, et al. Endoscopic ultrasound-guided transmural and percutaneous transhepatic gallbladder drainage are comparable for acute cholecystitis. *Gastroenterology.* 2012;142:805–811.
86. Itoi T, Binmoeller KF, Shah J, et al. Clinical evaluation of a novel lumen-apposing metal stent for endosonography-guided pancreatic pseudocyst and gallbladder drainage (with videos). *Gastrointest Endosc.* 2012;75:870–876.
87. de la Serna-Higuera C, Perez-Miranda M, Gil-Simon P, et al. EUS-guided transtestic gallbladder drainage with a new fistula-forming, lumen-apposing metal stent. *Gastrointest Endosc.* 2013;77:303–308.
88. Moon JH, Choi HJ, Kim DC, et al. A newly designed fully covered metal stent for lumen apposition in EUS-guided drainage and access: a feasibility study (with videos). *Gastrointest Endosc.* 2014;79:990–995.
89. Choi JH, Lee SS, Choi JH, et al. Long-term outcomes after endoscopic ultrasonography-guided gallbladder drainage for acute cholecystitis. *Endoscopy.* 2014;46:656–661.
90. Law R, Grimm IS, Stavas JM, et al. Conversion of Percutaneous Cholecystostomy to Internal Transmural Gallbladder Drainage Using an Endoscopic Ultrasound-Guided, Lumen-Apposing Metal Stent. *Clin Gastroenterol Hepatol.* 2016;14:476–480.
91. Walter D, Teoh AY, Itoi T, et al. EUS-guided gall bladder drainage with a lumen-apposing metal stent: a prospective long-term evaluation. *Gut.* 2016;65:6–8.
92. Ge N, Sun S, Sun S, et al. Endoscopic ultrasound-assisted transmural cholecystoduodenostomy or cholecystogastrostomy as a bridge for per-oral cholecystoscopy therapy using double-flanged fully covered metal stent. *BMC Gastroenterol.* 2016;16:9.
93. Kahaleh M, Perez-Miranda M, Artifon EL, et al. International collaborative study on EUS-guided gallbladder drainage: Are we ready for prime time? *Dig Liver Dis.* 2016;48:1054–1057.
94. Teoh AY, Serna C, Penas I, et al. Endoscopic ultrasound-guided gallbladder drainage reduces adverse events compared with percutaneous cholecystostomy in patients who are unfit for cholecystectomy. *Endoscopy.* 2017;49:130–138.
95. Tyberg A, Saumoy M, Sequeiros EV, et al. EUS-guided Versus Percutaneous Gallbladder Drainage: Isn't It Time to Convert? *J Clin Gastroenterol.* 2018;52:79–84.
96. Irani S, Ngamruengphong S, Teoh A, et al. Similar Efficacies of Endoscopic Ultrasound Gallbladder Drainage With a Lumen-Apposing Metal Stent Versus Percutaneous Transhepatic Gallbladder Drainage for Acute Cholecystitis. *Clin Gastroenterol Hepatol.* 2017;15:738–745.
97. Choi JH, Kim HW, Lee JC, et al. Percutaneous transhepatic versus EUS-guided gallbladder drainage for malignant cystic duct obstruction. *Gastrointest Endosc.* 2017;85:357–364.
98. Kamata K, Takenaka M, Kitano M, et al. Endoscopic ultrasound-guided gallbladder drainage for acute cholecystitis: Long-term outcomes after removal of a self-expandable metal stent. *World J Gastroenterol.* 2017;23:661–667.
99. Dollhopf M, Larghi A, Will U, et al. EUS-Guided Gallbladder Drainage in Patients with Acute Cholecystitis and High Surgical Risk Using an Electrocautery-Enhanced Lumen-Apposing Metal Stent Device. *Gastrointest Endosc.* 2017;86:636–643.
100. Chan SM, Teoh AY, Yip HC, et al. Feasibility of per-oral cholecystoscopy and advanced gallbladder interventions after EUS-guided gallbladder stenting (with video). *Gastrointest Endosc.* 2017;85:1225–1232.
101. Dellen ES, Hawk JS, Grimm IS, et al. The use of carbon dioxide for insufflation during GI endoscopy: a systematic review. *Gastrointest Endosc.* 2009;69:843–849.
102. Kida M, Araki M, Miyazawa S, et al. Fine needle aspiration using forward-viewing endoscopic ultrasonography. *Endoscopy.* 2011;43:796–801.
103. Varadarajulu S, Bang JY, Hebert-Magee S. Assessment of the technical performance of the flexible 19-gauge EUS-FNA needle. *Gastrointest Endosc.* 2012;76:336–343.
104. Kumbhari V, Penas I, Tieu AH, et al. Interventional EUS Using a Flexible 19-Gauge Needle: An International Multicenter Experience in 162 Patients. *Dig Dis Sci.* 2016;61:3552–3559.
105. Romagnuolo J. Endoscopic choledochoenterostomy using a new blunt-ended endoscopic ultrasound-guided access device. *Endoscopy.* 2011;43(Suppl 2). UCTN: E356–7.
106. Ogura T, Sano T, Onda S, et al. Endoscopic ultrasound-guided biliary drainage with a novel fine-gauge balloon catheter: one-step placement technique. *Endoscopy.* 2015;47(Suppl 1). UCTN: E245–6.
107. Prachayakul V, Aswakul P. Feasibility and safety of using Soehendra stent retriever as a new technique for biliary access in endoscopic ultrasound-guided biliary drainage. *World J Gastroenterol.* 2015;21:2725–2730.
108. Hanada K, Iiboshi T, Ishii Y. Endoscopic ultrasound-guided choledochoduodenostomy for palliative biliary drainage in cases with inoperable pancreas head carcinoma. *Dig Endosc.* 2009;21(Suppl 1):S75–S78.
109. Lee TH, Choi JH, Lee SS, et al. A pilot proof-of-concept study of a modified device for one-step endoscopic ultrasound-guided biliary drainage in a new experimental biliary dilatation animal model. *World J Gastroenterol.* 2014;20:5859–5866.
110. Park do H, Lee TH, Paik WH, et al. Feasibility and safety of a novel dedicated device for one-step EUS-guided biliary drainage: A randomized trial. *J Gastroenterol Hepatol.* 2015;30:1461–1466.
111. Teoh AY, Binmoeller KF, Lau JY. Single-step EUS-guided puncture and delivery of a lumen-apposing stent for gallbladder drainage using a novel cautery-tipped stent delivery system. *Gastrointest Endosc.* 2014;80:1171.
112. Teoh AY, Ng EK, Chan SM, et al. Ex vivo comparison of the lumen-apposing properties of EUS-specific stents (with video). *Gastrointest Endosc.* 2016;84:62–68.

113. Buxbaum J, Leonor P, Tung J, et al. Randomized Trial of Endoscopist-Controlled vs. Assistant-Controlled Wire-Guided Cannulation of the Bile Duct. *Am J Gastroenterol.* 2016;111:1841–1847.
114. Dhir V, Kwek BE, Bhandari S, et al. EUS-guided biliary rendezvous using a short hydrophilic guidewire. *J Interv Gastroenterol.* 2011;1:153–159.
115. Ogura T, Masuda D, Takeuchi T, et al. Liver impaction technique to prevent shearing of the guidewire during endoscopic ultrasound-guided hepaticogastrostomy. *Endoscopy.* 2015;47:E583–e584.
116. Itoi T, Sofuni A, Tsuchiya T, et al. Initial evaluation of a new plastic pancreatic duct stent for endoscopic ultrasonography-guided placement. *Endoscopy.* 2015;47:462–465.
117. Park DH, Kim MH, Choi JS, et al. Covered versus uncovered wallstent for malignant extrahepatic biliary obstruction: a cohort comparative analysis. *Clin Gastroenterol Hepatol.* 2006;4:790–796.
118. Park DH, Lee SS, Lee TH, et al. Anchoring flap versus flared end, fully covered self-expandable metal stents to prevent migration in patients with benign biliary strictures: a multicenter, prospective, comparative pilot study (with videos). *Gastrointest Endosc.* 2011;73:64–70.
119. Oh D, Park do H, Cho MK, et al. Feasibility and safety of a fully covered self-expandable metal stent with antimigration properties for EUS-guided pancreatic duct drainage: early and midterm outcomes (with video). *Gastrointest Endosc.* 2016;83:366–373. e2.
120. Brauer BC, Chen YK, Fukami N, et al. Single-operator EUS-guided cholangiopancreatography for difficult pancreaticobiliary access (with video). *Gastrointest Endosc.* 2009;70:471–479.
121. Tyberg A, Sharaiha RZ, Kedia P, et al. EUS-guided pancreatic drainage for pancreatic strictures after failed ERCP: a multicenter international collaborative study. *Gastrointest Endosc.* 2017;85:164–169.
122. Chen YI, Levy MJ, Moreels TG, et al. An international multicenter study comparing EUS-guided pancreatic duct drainage with enteroscopy-assisted endoscopic retrograde pancreatography after Whipple surgery. *Gastrointest Endosc.* 2017;85:170–177.



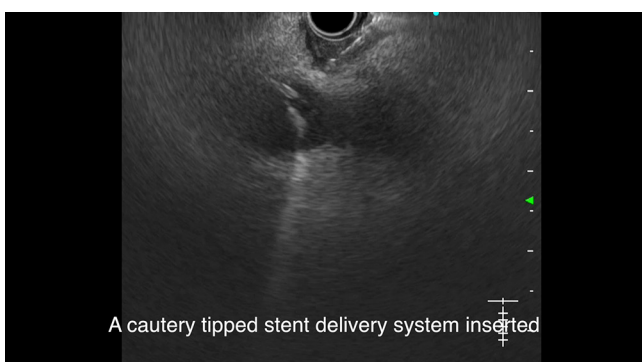
**Video 24.1** The Endoscopic Ultrasonography-Guided Rendezvous Biliary Procedure



**Video 24.4** The Endoscopic Ultrasonography-Hepatico-Gastrostomy Procedure



**Video 24.2** The Endoscopic Ultrasonography-Guided Antegrade Biliary Procedure



**Video 24.5** The Endoscopic Ultrasonography-Guided Transmural Gallbladder Drainage Procedure



**Video 24.3** The Endoscopic Ultrasonography-Choledochoduodenostomy Procedure

# 25

## Endoscopic Ultrasonography-Guided Ablation Therapy and Celiac Plexus Interventions

ABDURRAHMAN KADAYIFCI, OMER BASAR, AND WILLIAM R. BRUGGE

### KEY POINTS

- Endoscopic ultrasonography (EUS)-guided ablative therapy consists of the injection of cytotoxic agents into cystic cavities or ganglia to eliminate premalignant epithelium or to produce neurolysis.
- Celiac plexus block or neurolysis is the most common EUS-guided intervention in current practice. Significant pain control is achieved with the injection of ethanol in the setting of pancreatic cancer. More modest results are seen in patients with abdominal pain arising from chronic pancreatitis.
- More advanced techniques include the use of radiofrequency ablation and brachytherapy in selected cases unfit for surgery or for palliative control of locally advanced cancers. Although preliminary data are promising, most of these procedures are still under clinical investigation.
- Although many of these EUS-based techniques are designed to be used to ablate or control pancreatic malignancies, some may facilitate the delivery of radiation therapy by placement of radiopaque markers into the tumor.

Endoscopic ultrasonography (EUS) today is not only an essential diagnostic tool for the diagnosis of gastrointestinal diseases but has also become a significant part of our therapeutic armamentarium. Using fine-needle aspiration (FNA) accessories, interventional EUS is often based on fine-needle injection (FNI) therapy. Developments in interventional EUS have also highlighted a broad range of therapies beyond FNI, including tissue ablation and cancer therapeutics. In this chapter, the current clinical and experimental applications of interventional EUS for ablation therapy and celiac plexus neurolysis are reviewed and described with technical details.

### Endoscopic Ultrasound-Guided Radiotherapy (Table 25.1)

#### Radiofrequency Ablation

The principle of radiofrequency ablation (RFA) is the induction of thermal injury to the target tissue through the use of

electromagnetic energy. In monopolar RFA, the patient is part of a closed-loop circuit that includes a radiofrequency (RF) generator, an electrode needle, and a large dispersive electrode (ground pad). Cells experiencing the thermal damage undergo coagulative necrosis over the course of several days.

The procedural technique used for RFA is based on the EUS guidance of a needle catheter into the target lesion. In RFA of liver and pancreatic lesions, this procedure requires placement of the needle across the gastric or duodenal walls. Once the needle has been successfully placed into the tissue mass, the RF current is delivered. During heating of tissue, ultrasound monitoring demonstrates a hyperechoic “cloud” surrounding the tip of the needle. EUS-guided delivery of ablative energy to localized malignant tumors has become increasingly possible through the introduction of commercial devices. In recent clinical studies, the Habib EUS-RFA probe (Habib catheter, Emcision Ltd., London) was used to apply EUS-guided RFA to the pancreas. The Habib catheter is a monopolar RFA probe with a working length of 190 cm, 3.6-Fr (1.2-mm) diameter, and 1-Fr (0.33-mm) wire, compatible with 19- and 22-G FNA needles (Figs. 25.1 and 25.2). It is designed to achieve more limited injury to tissue as compared with other RFA devices.

#### Procedural Technique (Video 25.1)

The echoendoscope is inserted through the esophagus to the stomach and duodenum. After the pancreatic lesion has been located, a 19- or 22-G FNA needle is inserted through the working channel of the echoendoscope into the target lesion. The stylet is then removed from the FNA needle and the monopolar Habib catheter gently advanced through the lumen of the FNA needle. The RFA probe is connected to an electrosurgical RF generator, for which the wattage and exposure time have not yet been standardized. However, in pilot studies, RF energy with the Habib catheter was applied for 90 to 120 seconds at the 5- to 25-W setting. The ablation was repeated two to six times in each session in previous clinical studies.<sup>1,2</sup>

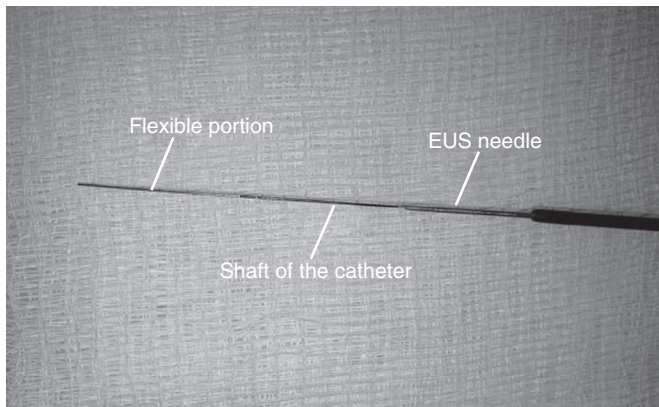
#### Clinical Outcomes

EUS RFA of pancreatic cystic neoplasms (PCNs), neuroendocrine tumors (NETs), and pancreatic ductal adenocarcinomas (PDACs)

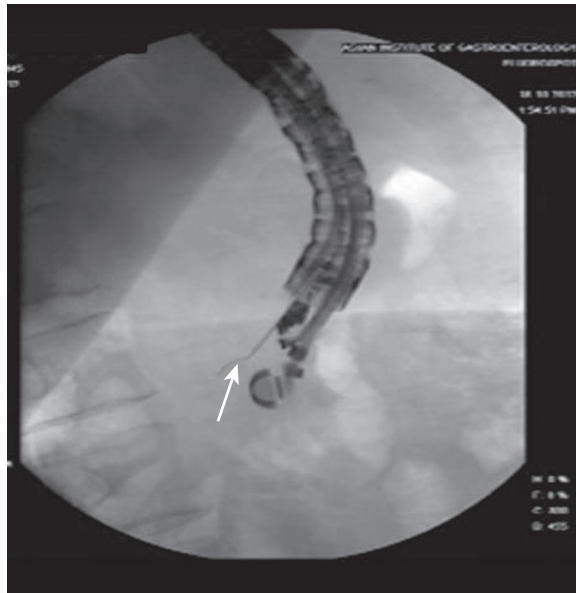
**TABLE 25.1****Endoscopic Ultrasonography-Guided Radiotherapy for Tumor Ablation**

	Radiofrequency Ablation	Cryotherapy (Cool-Tipped RFA)	Brachytherapy	Fiducial Placements
Device used	Needle prongs	Dedicated catheter	FNA needle	19-G or 22-G EUS FNA needle
Mechanism of action	Heat-induced necrosis	Heat-induced necrosis	DNA damage	Tattoo the tissue for RT
Target lesion	Pancreatic cancer, cystic lesions, neuroendocrine tumors, celiac ganglion	Pancreatic cancer	Pancreatic cancer	Any GI tumors that can be accessed by EUS
Human studies	Yes	Yes	Yes	Yes
Availability	Clinical trials	Clinical trials	Clinical trials	Wide

EUS, Endoscopic ultrasonography; FNA, fine-needle aspiration; NET, neuroendocrine tumor; RFA, radiofrequency ablation; RT, radiotherapy.



• **Fig. 25.1** The tip of the endoscopic ultrasonography (EUS) Habib radiofrequency ablation catheter.



• **Fig. 25.2** Fluoroscopy showing the tip (arrow) of the Habib endoscopic ultrasonography radiofrequency ablation catheter.

was first described in humans using the Habib EUS RFA catheter in two different studies.<sup>1,2</sup> The PDAC study<sup>1</sup> included seven patients with the lesions located in the head of pancreas in five and in the body of pancreas in two. RF was applied at 5 to 15 W

over 90 seconds and the procedure was completed in all patients. The postprocedure imaging after 3 to 6 months showed a decrease in the size of the lesion in two patients, whereas the lesions were unchanged in the remaining patients. The procedure was well tolerated by all patients and no adverse event was encountered except for mild pancreatitis in one. In a study<sup>2</sup> that included eight patients with neoplastic lesion (six with PCNs and two with NETs) in the head of pancreas who were treated by EUS-RFA, postprocedure imaging after 3 to 6 months revealed complete resolution of the cysts in two patients and a 48.4% reduction in size in three; only one patient had to undergo a second treatment session. Cross-sectional imaging in the two patients with NETs demonstrated a change in vascularity and central necrosis after EUS-RFA. No episodes of pancreatitis, perforation, or bleeding were reported, suggesting that the procedure is technically easy and safe.

In a recent study, an 18-G endoscopic RFA electrode was used for ablation of unresectable pancreatic cancer in six patients (four with lesions in the head and two with lesions in the body).<sup>3</sup> RF was applied at 20 to 50 W ablation power for 10 seconds and was repeated to sufficiently cover the tumor mass. The procedure was performed successfully in all patients and only two experienced mild abdominal pain. In another study, a prototype 19-G internally cooled needle electrode was used for ablation in three patients with symptomatic pancreatic insulinoma at a power of 50 W.<sup>4</sup> All patients had rapid symptom relief with biochemical improvement and remained symptom-free at 11 to 12 months' follow-up. No procedure-related adverse event was reported.

Jin et al. administered EUS-RFA to the celiac ganglion for pain control in a patient with pancreatic cancer.<sup>5</sup> In this procedure, the celiac ganglion was punctured with a 19-G needle (Video 25.2). Then an RF probe, the Habib RF DUO 13, was advanced via the lumen of the needle to the center of the celiac ganglion; thereafter the needle was partially withdrawn to disengage contact with the active part of the probe. Ablation parameters were set at 10 W for 120 seconds and 15 W for 120 seconds. With the application of RFA, the center of the celiac ganglion gradually became hyperechoic. After the procedure, the patient's visual analog scale (VAS) pain score decreased significantly and no opioid analgesics were needed.<sup>5</sup>

A commercial cool-tipped cryotherapy device was designed and tested for pancreatic ablation (Fig. 25.3).<sup>6</sup> A flexible bipolar ablation probe combining RF and cryotechnology was used to induce foci of complete pancreatic ablation. The heated tip of the probe was cooled with simultaneous cryogenic carbon dioxide (650 psi). In the first human clinical trial, the flexible bipolar ablation probe



• **Fig. 25.3** Cool-tipped radiofrequency catheter designed for endoscopic ultrasonography.

was successfully applied under EUS guidance in 16 of 22 (72.8%) patients with advanced pancreatic carcinoma.<sup>7</sup> Technical failure in six patients was due to excessive resistance to probe passage via the gastrointestinal wall and tumor. The median postablation survival time was 6 months.

These studies demonstrate that EUS-RFA is technically feasible and may be beneficial for selected pancreatic premalignant and malignant lesions. Although no major adverse events were observed, more prospective studies are needed to demonstrate the safety and overall survival benefit before widespread use can be recommended in clinical practice.

## Brachytherapy

Brachytherapy in the form of small seeds can be used for the local control of malignant disease. Solid gastrointestinal malignant tumors often respond to the local administration of radiation therapy, and the risk of recurrence is reduced.<sup>8</sup> Traditionally radiation therapy was provided intraoperatively, but precise targeting is difficult. Computed tomography (CT)-guided placement of radiation seeds adjacent to malignant gastrointestinal tumors is reportedly safe and somewhat effective.<sup>9</sup> EUS-guided brachytherapy was first attempted in a pilot study of 15 patients with unresectable stage III and stage IV pancreatic adenocarcinoma.<sup>10</sup> Through an 18-G EUS needle, multiple small radioactive seeds were placed into the pancreatic tissue to provide interstitial brachytherapy. Although the tumor response to brachytherapy was modest (33% of the tumors were stabilized), there was a transient clinical benefit in patients (30%), who experienced a reduction in abdominal pain. Similar results were also confirmed with iodine-125 seeds in 22 patients with unresectable pancreatic carcinoma.<sup>11</sup> In another study, the long-term outcome of EUS-guided brachytherapy was prospectively evaluated in 100 cases of unresectable pancreatic cancer.<sup>12</sup> Gemcitabine chemotherapy was combined with RFA in 85 patients 1 week after brachytherapy. The mean follow-up time was 7.8 ± 6.1 months. The estimated median disease progression-free survival and overall survival were 4.5 months and 7.0 months, respectively. VAS scores dropped significantly 1 week postimplantation and were maintained at significantly lower levels until the third month. Patients who underwent postimplantation chemotherapy had a longer median survival of 7.8 months versus 4 months for patients who did not receive chemotherapy. The outcome of the study suggested that EUS-guided iodine-125

seed implantation plus chemotherapy is an effective technique to prolong patient survival in pancreatic cancer. The effectiveness and safety of EUS-guided <sup>125</sup>I seed brachytherapy was investigated in malignant left-sided liver tumors that were difficult to access by image-guided interventions.<sup>13</sup> After localization of the tumor using a linear EUS scope, a transgastric puncture was performed with a 19-G injection needle and iodine seeds were placed directly into the lesion. Complete treatment response was achieved in 12 of 13 patients in 6 months; two patients needed a retreatment due to incomplete response. In the same study, anhydrous ethanol injections were undertaken in 10 patients with malignant left-sided liver tumors, and a complete response was achieved in 3 patients. EUS-guided <sup>125</sup>I seed brachytherapy was found to be safe and highly effective for malignant liver tumors and superior to EUS-guided ethanol injection. For left-sided liver tumors, especially when located in proximity to the lesser curvature of the stomach, transgastric EUS can exclude interference by intestinal gas and provide safe access to the liver for any EUS-guided intervention.<sup>13</sup>

## Endoscopic Ultrasonography-Guided Fiducial Placement

Advances in radiation therapy have provided the opportunity for the real-time delivery of radiation using three-dimensional mapping guided by radiopaque markers. Respiration-dependent movement of the target lesions often results in inappropriate radiation exposure to surrounding tissue. Marking of focal malignancy allows the precise targeting by focused beams of radiation despite respiratory movements.

Although CT scanning is capable of guiding the placement of fiducials in and adjacent to pancreatic tumors, EUS guidance is likely more precise.<sup>14</sup> These small radiopaque markers are placed into the periphery of a malignant lesion to facilitate better targeting by radiation therapy.

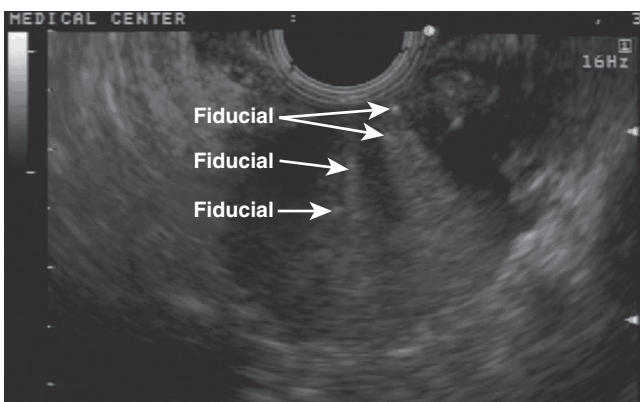
### Procedural Technique

After identifying the tumor and excluding the presence of intervening vasculature, EUS-guided fiducial placement is undertaken using 19-G or 22-G FNA needles ([Videos 25.3 and 25.4](#)). Commercially available sterilized gold fiducial markers are preloaded into the needle by retracting the stylet and manually backloading the fiducials into the tip of the needle. The tip of the needle is then sealed with bone wax to prevent accidental dislodgment of the fiducials. After identifying a target lesion, the tumor is punctured and the fiducial is deployed by advancing the stylet or guidewire forward. Resistance can be encountered during the deployment of fiducials if the tip of the echoendoscope is deflected. This resistance can be overcome by removing the stylet and applying hydrostatic pressure from a syringe containing sterile water attached to the needle to deposit the markers into the tumor. Depending on the size of the tumor, three to six fiducials should be deployed into the tumor to provide for ample separation of fiducials in distance, angulation, and plane. Both fluoroscopic and ultrasonographic visualization may be used to enable correct positioning of the fiducials within the tumor mass ([Figs. 25.4 and 25.5](#)). Dedicated preloaded fiducial devices are now commercially available (see [Video 25.4](#)).

The safety and effectiveness of EUS-guided fiducial placement in pancreatic malignancies have been shown in multiple studies, including large series, with high technical and clinical success rates (85% to 90%) and only a few minor adverse



• **Fig. 25.4** Fluoroscopy demonstrating the placement of fiducials within a pancreatic mass.



• **Fig. 25.5** Endoscopic ultrasonography image demonstrating fiducial placement within a pancreatic mass.

events.<sup>14–16</sup> Recent studies have shown that fiducials can potentially be deployed into any malignant tumor that can be accessed by EUS.<sup>16–19</sup> Also, the technique has been adopted to facilitate intraoperative localization of small neuroendocrine tumors in patients undergoing enucleation or other resection procedures (Fig. 25.6).<sup>20</sup> EUS-guided tattooing of pancreatic tumors with a marking solution before surgery has been attempted in six patients in a pilot study.<sup>21</sup> The tattoo mark was easily detected during surgery and localized in a small area in five patients with no adverse events.

### Celiac Ganglion Irradiation

EUS-guided direct celiac ganglion irradiation with iodine-125 seeds was applied in 23 patients with unresectable pancreatic carcinoma for the palliation of pain in a recent study.<sup>22</sup> The mean number of seeds implanted in the celiac ganglion per patient was four. Although there was no difference in pain relief and analgesic consumption immediately after the procedure, 6 of the 12 patients (26%) reported an exacerbation of symptoms. However, the VAS score and mean analgesic consumption reduced significantly 2 weeks later. No procedure-related deaths or major adverse events were reported. This study demonstrated that EUS-guided direct celiac ganglion irradiation is feasible, but further studies are needed to prove its efficacy.

## Endoscopic Ultrasound-Guided Injection Therapies

**Ethanol or chemotherapy injection for solid tumors.** EUS-guided ethanol injection therapy was first applied to pancreatic insulinoma.<sup>23</sup> The resolution of tumor and hypoglycemic symptoms were reported in two case series.<sup>24,25</sup> In a single-center study, five patients with pancreatic insulinoma were treated with EUS-FNI without any significant adverse effect.<sup>24</sup> Patients did not report any hypoglycemia-related symptoms after the procedure during a median 13-month follow-up period. Similar results were also reported in four patients with pancreatic insulinoma in a recent study.<sup>25</sup> These reports demonstrated that EUS-FNI using alcohol may be an alternative treatment option for patients with pancreatic insulinoma who are not candidates for surgery. A gastrointestinal stromal cell tumor, adrenal metastasis from lung cancer, left hepatic metastatic carcinoma, and two metastatic pelvic lymph nodes in a patient with rectal cancer were treated by EUS-guided ethanol injection without any procedure-related complications.<sup>16</sup>

EUS-guided intrahepatic arterial chemotherapy (5-fluoracil or 5-fluorodeoxyuridine) has been compared with interventional radiology-guided injection in a randomized trial of 25 patients with colorectal cancer and liver metastasis.<sup>26</sup> Although the overall treatment response and survival were comparable between the two groups, the median duration of hospitalization and rate of adverse events were significantly lower in EUS-FNI cohort. The study suggested that EUS-guided intraarterial chemotherapy administration is feasible and safe in a subset of patients with metastatic liver disease.

EUS-FNI of intratumoral gemcitabine was administered as one-time induction therapy prior to conventional multimodality therapy in 36 patients with locally advanced or metastatic pancreatic cancer.<sup>27</sup> The primary endpoint of the study was toxicity. There were no procedure-related adverse events. Four patients (20%) with stage III unresectable tumor were downstaged and underwent a R0 resection. The study demonstrated the feasibility, safety, and effectiveness of intratumoral EUS-FNI using gemcitabine for pancreatic cancer.

In summary, although important advances have been made in recent years for the treatment of abdominal malignancies by EUS-guided injection (Table 25.2), prospective trials evaluating procedural indications and adverse events are needed before the treatment can be recommended for routine clinical use.

**Novel antitumoral agents for pancreatic and esophageal cancers.** The possibility of providing local control of pancreatic cancer by EUS-FNI using various biologic agents remains a major challenge. The original report of injection therapy into pancreatic malignancy used a sensitized culture of lymphocytes and established the feasibility and safety of the therapy in a phase I clinical trial.<sup>28</sup> A total of eight patients with unresectable pancreatic adenocarcinoma underwent EUS-FNI with escalating doses of lymphocyte cytoimplants (3, 6, or 9 billion cells). The median survival was 13.2 months, with two partial responders and one minor response. Low-grade fever was encountered in seven of the eight patients and was symptomatically treated. Although the study demonstrated safety, no large-scale trials have been performed.

The technique of EUS-guided FNI has also been applied to deliver antitumor viral therapy.<sup>29</sup> ONYX-015 (dl1520) is an E1B 55-kDa gene-deleted replication-selective adenovirus that preferentially replicates in malignant cells and causes cell death. Twenty-one patients with locally advanced adenocarcinoma of the pancreas or metastatic disease underwent eight sessions of

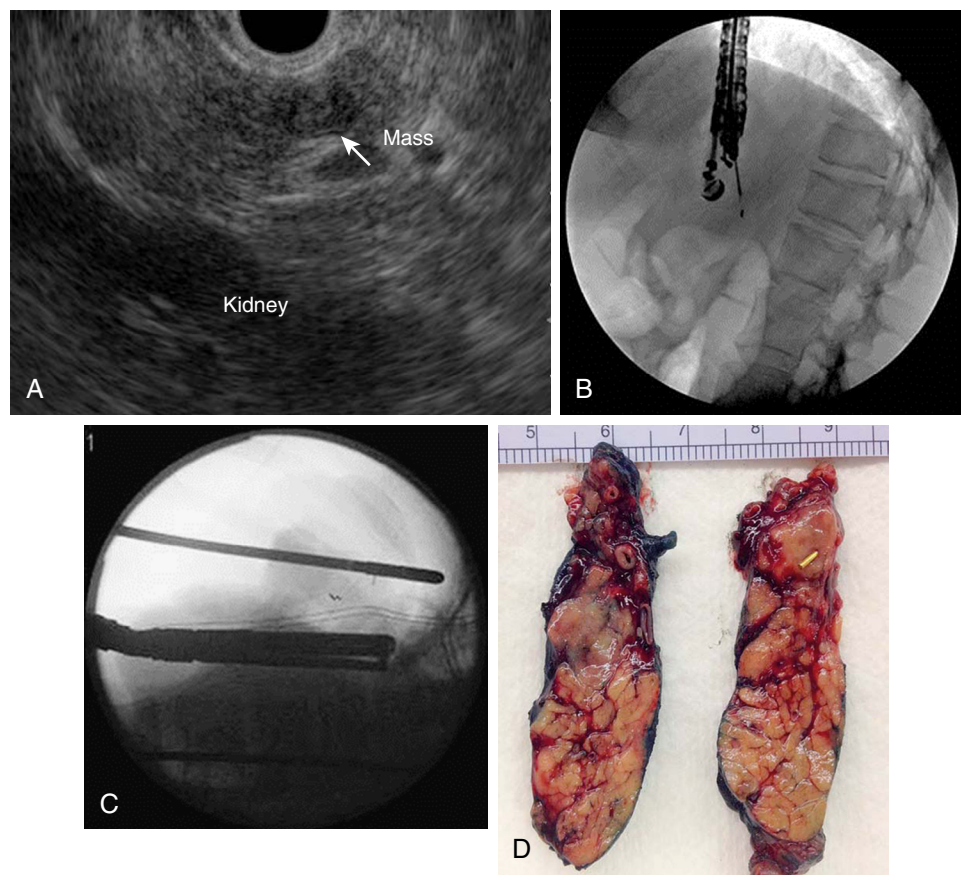


**Fig. 25.6** (A) At endoscopic ultrasonography (EUS), a small neuroendocrine tumor is identified in the body of the pancreas. (B) Using EUS guidance, fiducial is deployed within the tumor as observed on fluoroscopy. (C) The fiducial is identified intraoperatively using cross-table fluoroscopy. (D) The fiducial is seen within the substance of the tumor in the resected specimen.

**TABLE 25.2** Endoscopic Ultrasonography-Guided Fine-Needle Injection of Gastrointestinal Tumors

Authors (Year)	Agent	Patients ( <i>n</i> )	Target	Results	Complications
Levy et al. (2012) <sup>24</sup>	Ethanol	5	Pancreatic insulinoma	Complete symptom resolution	None
Qin et al. (2014) <sup>25</sup>	Ethanol	4	Pancreatic insulinoma	Complete symptom resolution	None
Artifon et al. (2013) <sup>26</sup>	5-Fluoracil or 5-fluorodeoxyuridine	25	Liver metastases	Shorter hospitalization and fewer complications than interventional radiology	Minimal
Levy et al. (2016) <sup>27</sup>	Gemcitabine	36	Pancreatic adenoca	20% of stage III patients were downstaged and underwent R0 resection	None
Chang et al. (2000) <sup>28</sup>	Lymphocyte cytoimplants	8	Pancreatic adenoca	2 partial, 1 minor response	Low-grade fever
Hecht et al. (2003) <sup>29</sup>	ONYX-015 + gemcitabine	21	Pancreatic adenoca	2 partial, 2 minor response, 6 stable, 11 progressive	Sepsis in 2 patients
Irisawa et al. (2007) <sup>30</sup>	Dendritic cells	7	Pancreatic adenoca	No difference of survival	None
Hirooka et al. (2009) <sup>31</sup>	Dendritic cells + gemcitabine	5	Pancreatic adenoca	1 partial response, 2 stable, survival better	None
Hecht et al. (2012) <sup>32</sup>	TNFerade + chemoradio	50	Pancreatic adenoca	Locoregional control and downstaging at higher dose	Mild toxicity
Herman et al. (2013) <sup>33</sup>	TNFerade + chemoradio	187	Pancreatic adenoca	No survival benefit	Minimal
Chang et al. (2012) <sup>34</sup>	TNFerade + chemoradio	24	Esophageal cancer	Longer survival	Frequent adverse events, thromboembolism in higher doses

Adenoca, Adenocarcinoma.

EUS-FNI of ONYX-015 over 8 weeks. The final four treatments were administered in conjunction with intravenous gemcitabine ( $1000 \text{ mg/m}^2$ ). After combination therapy, 2 patients had partial regressions of the injected tumor, 2 had minor responses, 6 had stable disease, and 11 had progressive disease.

Dendritic cells (DCs) are potent antigen-presenting cells that can stimulate a T-cell-dependent immune response. They have been used in experimental studies as a vaccine therapy against various cancers. In a pilot study, seven patients with advanced pancreatic cancer and refractory to gemcitabine therapy received intratumoral injection of immature DCs by EUS FNI.<sup>30</sup> DCs were administrated on days 1, 8, and 15 of every 28-day cycle as often as possible. All injections were well tolerated without clinical toxicity, but the median survival was only 9.9 months, which is comparable with the outcomes of patients treated with chemotherapy only. EUS FNI DC therapy was combined with gemcitabine in five patients with advanced pancreatic cancer.<sup>31</sup> Of these, three patients demonstrated a significant treatment response with a partial response in one patient and prolonged disease stability in two patients. The median survival time was 15.9 months. No serious treatment-related adverse events were observed during the study period. It is likely that combination therapy may have a role in the treatment of pancreatic cancer with a synergistic effect of immunotherapy and chemotherapy.

TNFerade is a second-generation replication-deficient adenovirus vector that expresses the human TNF (tumor necrosis factor) alpha gene, which is regulated by a chemoradiation-inducible promoter. It has the potential to maximize local antitumor activity and minimize systemic toxicity. In a multicenter study, TNFerade was applied to 50 locally advanced pancreatic cancers by EUS-FNI ( $n = 27$ ) or percutaneous injection ( $n = 23$ ) in escalating doses for 5 weeks and in combination with 5-fluorouracil and radiation.<sup>32</sup> Compared with the lower-dose cohorts ( $n = 30$ ), the higher-dose group ( $n = 11$ ) had better locoregional control, longer disease progression-free survival, stable or decreasing CA 19-9 levels, higher surgical resection rates (45%), and an improved overall median survival time. At the higher dose, four of five patients whose tumors became surgically resectable achieved pathologically negative margins and three survived more than 24 months. The method of TNFerade biologic administration, by either EUS or the percutaneous route, did not influence overall outcome. The long-term results showed that toxicities potentially related to TNFerade were mild and well tolerated. However, in a phase III trial involving 187 patients with locally advanced pancreatic cancer who were treated with TNFerade, no difference in survival was observed as compared with patients receiving standard-of-care treatment.<sup>33</sup> TNFerade by EUS FNI or direct endoscopic injection was combined with standard chemoradiotherapy before surgery in 24 patients with locally advanced but resectable esophageal cancer in a phase I multicenter study.<sup>34</sup> The combination therapy was associated with longer survival but frequent adverse events, including fatigue, fever, nausea, vomiting, esophagitis, and chills. In addition, thromboembolic events developed in five of eight patients receiving the higher doses ( $4 \times 10^{11}$  particle units) of TNFerade.

Although some of these results appear promising, there are no randomized controlled trials to confirm the true clinical benefit of these novel EUS-FNI treatments for intraabdominal tumors (see Table 25.2). Safety may be a concern when administering higher doses of TNFerade. Based on current data, these treatments should be offered only under research protocols or for selective patients who are unsuitable for surgery.

## Endoscopic Ultrasonography-Guided Pancreatic Cyst Ablation

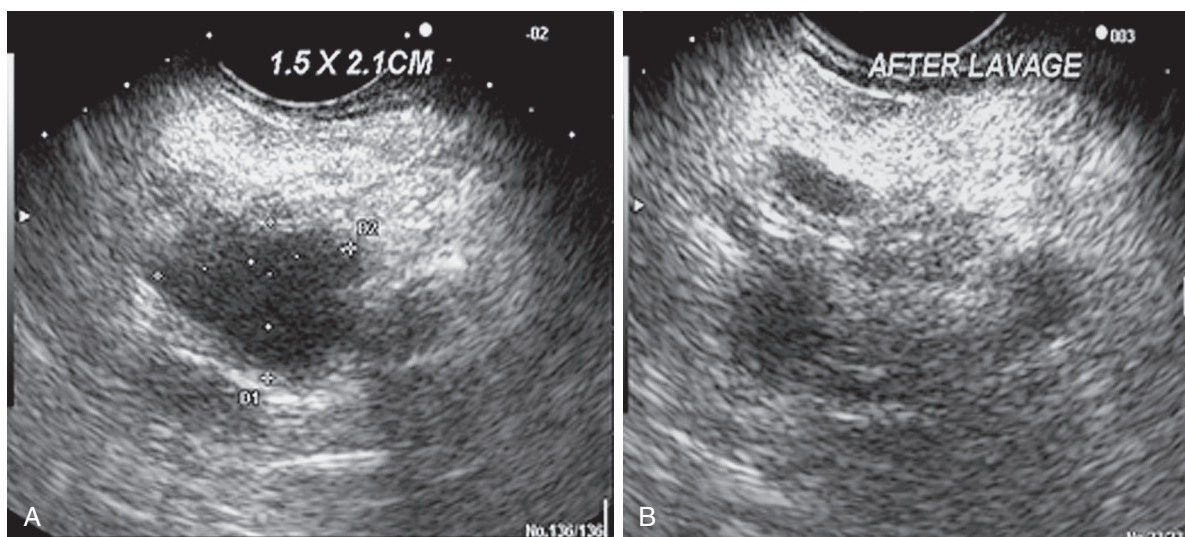
The behavior of pancreatic cystic neoplasms (PCNs) may range from staying benign to progressing to low-grade dysplasia or frank malignancy. Therefore their management can be challenging, because surgery or long-term follow-up may be needed for most patients. Safe and effective minimally invasive treatment options are required as an alternative to surgical treatment approaches. EUS-guided pancreatic cyst ablation is based on the principle that injection of a cytotoxic agent into a pancreatic cyst lesion will result in ablation of the cyst's epithelium. The close contact between the injected agent and the epithelium results in both immediate and delayed tissue necrosis. The cytotoxic agent remains within the cyst cavity without extravasation into the parenchyma.

### Procedural Technique (Video 25.5)

EUS-guided ethanol lavage of pancreatic cystic lesions employs techniques based on FNA of the pancreas (Fig. 25.7). After prophylactic antibiotics are administered, a linear echoendoscope positioned in the duodenum, gastric body, or fundus provides access to pancreatic head, body, or tail, respectively, and guides the use of FNA. The injection of ablative agents into a cyst lesion requires the complete or partial evacuation of the cyst's fluid contents. Although it may be difficult to aspirate the highly viscous fluid of mucinous cysts, it is necessary to provide room for the injected ablative agent. This principle of cyst injection therapy, coupled with a dead space of approximately 0.8 mL in the aspiration needle, limits target cysts to be more than 10 mm in diameter. Once the needle is in place within the lumen of the cyst, the ablative agent is injected under ultrasound guidance. Swirls of aerated liquid are readily observed on sonography and the distribution can be easily determined during the procedure. Unilocular cysts with a diameter of 1 to 2 cm are easily treated in one or two sessions. Larger and more complex lesions may require multiple treatment sessions.<sup>35</sup> The endpoint of ethanol lavage is elimination of the cyst as evidenced by cross-sectional imaging.

### Clinical Outcomes (Table 25.3)

EUS-guided ethanol injection into pancreatic cyst lesions was originally described using a range of low ethanol concentrations.<sup>36</sup> In the initial studies, the safety of cyst injection therapy was established first using saline solution, followed by highly dilute ethanol. There was no evidence of clinical pancreatitis with injection of ethanol using concentrations up to 80%. Small numbers of lavaged cystic lesions were resected, and evidence of epithelial ablation with pancreatitis was noted.<sup>36</sup> In a multicenter, randomized trial, ethanol lavage was found to provide greater rates of complete ablation compared with saline lavage.<sup>37</sup> The overall rate of complete pancreatic cyst ablation as observed by CT was 33.3%. The histology of four resected cysts demonstrated epithelial ablation ranging from 0% (saline solution alone) to 50% to 100% (one or two ethanol lavages). Twelve patients with pancreatic cysts that had previously resolved after ethanol lavage were followed to determine long-term results. The median follow-up was 26 months (range 13 to 39) after initial resolution, and no evidence of cyst recurrence was observed in any patient.<sup>38</sup> The effectiveness of two EUS-guided ethanol lavage sessions for suspected branch duct intraductal papillary mucinous neoplasms was evaluated in 13 patients.<sup>35</sup> Complete resolution of the cyst lesion was not seen



• **Fig. 25.7** (A) A  $1.5 \times 2.1$  cm cystic lesion in the head of the pancreas is consistent with branch duct-intraductal papillary mucinous neoplasia. (B) The cyst was lavaged with ethanol after fluid aspirated by fine-needle biopsy.

**TABLE  
25.3**

**Endoscopic Ultrasonography-Guided Ablation of Pancreatic Cystic Lesions**

Authors (Year)	Agent	Target	Results	Complications
Gan et al. (2005) <sup>36</sup>	5%-80% ethanol (diluted with saline)	Pancreatic cystic lesions	Resolution of cystic lesion in 8 of 23 patients; resected patients had ablated epithelium	None
DeWitt et al. (2009) <sup>37</sup>	80% ethanol compared with saline	Pancreatic cystic lesions	Resolution of cystic lesion in 12 of 36 patients	Abdominal pain; rare pancreatitis
Oh et al. (2009) <sup>41</sup>	80%-90% ethanol and paclitaxel	Septated pancreatic cystic lesions	Resolution in 6 of 10 patients	Episode of mild pancreatitis in one patient
DiMaio et al. (2011) <sup>35</sup>	80% ethanol	Two sessions for BD IPMN	Resolution in 38% (5/13) after second session	Minor abdominal pain in a patient
Oh et al. (2011) <sup>39</sup>	80%-90% ethanol and paclitaxel	Pancreatic cystic lesions	Resolution of cystic lesion in 29 of 52 patients	Mild pancreatitis in 1 and splenic vein obliteration in 1 patient
Dewitt et al. (2014) <sup>40</sup>	80% ethanol and paclitaxel	Pancreatic cystic lesions	Complete resolution in 10, and partial resolution in 5 of 20 patients at median 27-month follow-up	Moderately severe in 4 patients (3 pancreatitis, 1 peritonitis)
Moyer et al. (2016) <sup>42</sup>	Lavage by 80% ethanol or saline then paclitaxel plus gemcitabine	Mucinous pancreatic cysts	Complete ablation at 12 months: 67% in saline and 75% in ethanol arm	1 pancreatitis in ethanol arm

BD IPMN, Branch duct intraductal papillary mucinous neoplasm.

on follow-up imaging in any patient after the first session but was observed in 5 (38%) of 13 patients after the second treatment.

Ethanol lavage has been coupled with paclitaxel injection in a large series with a variety of pancreatic cyst lesions.<sup>39</sup> The combination of ethanol and paclitaxel injection resulted in resolution of the cysts, as determined by CT imaging, in 29 of 47 (62%) patients at a median follow-up of 21.7 months (Fig. 25.8). On univariate analysis, cyst diameter at EUS and original cyst volume predicted resolution. However, the high viscosity of paclitaxel makes injection difficult. In contrast, ethanol can be easily injected and aspirated from the cyst and at times reduces the cyst fluid viscosity, thus aiding in cyst evacuation. A recent study involving

20 patients reported 50% complete and 25% partial response with the same combination regimen at a median follow-up of 27 months. This study also showed a significant alteration in cyst fluid genetics following ablation.<sup>40</sup> The combination of ethanol and paclitaxel is also capable of ablating septated cystic lesions, a much more difficult target for EUS injection therapy.<sup>1</sup> Complete resolution was achieved in 6 of 10 patients and partial resolution in 2 patients with septated cysts. Presumably, the surface area of a septated cyst is quite large, and it is difficult to be certain that the cytotoxic injectant stays in contact with all of the epithelium.

A recent randomized pilot study compared EUS-FNI of paclitaxel and gemcitabine combination after the lavage of mucinous



• **Fig. 25.8** Pancreatic cyst lavage. Computed tomography scanning before (A) and after (B) ethanol paclitaxel (Taxol) lavage of a pancreatic cyst (arrows).

pancreatic cysts with either 80% ethanol or normal saline in 10 patients.<sup>42</sup> The complete ablation rates at 12 months were 67% in saline and 75% in ethanol arm. One patient in the ethanol arm developed acute pancreatitis. The authors proposed that alcohol may not be required for cyst ablation.

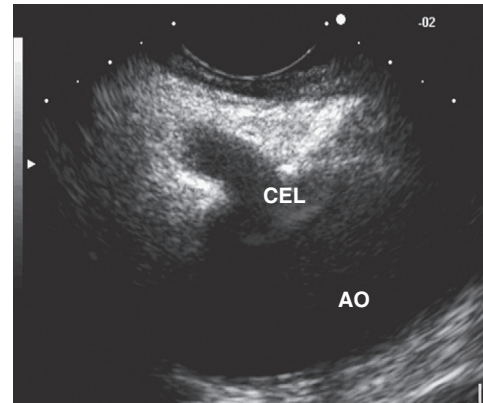
These preliminary studies demonstrate the feasibility and safety of EUS-guided alcohol and paclitaxel injection for ablation of PCNs. These agents inhibit or slow the growth of the cyst and complete ablation may be possible in some cases. While the results at short-term follow-up (2 years) are encouraging, their long-term efficacy is unclear. Also, most studies did not include a control group. Given these limitations, the practice of cyst ablation should be limited to a select cohort of patients such as those at high risk for surgery and its routine use in clinical practice should be restricted until more definitive data are available.

### Endoscopic Ultrasonography-Guided Celiac Plexus Injections

The principle of celiac injection therapy is based on the ability of EUS to guide injection of cytotoxic agents into the retrogastric space containing the celiac ganglia (Fig. 25.9). Presumably, the injected agent, such as ethanol, comes into contact with the ganglia and disrupts the ascending sympathetic ganglia. Histologically, there is evidence of neuronal vacuolization in nerves injected with



• **Fig. 25.9** Illustration of an endoscopic ultrasonography-guided celiac ganglia injection.

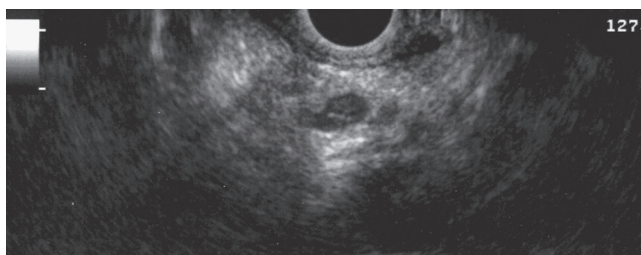


• **Fig. 25.10** Celiac plexus neurolysis being undertaken at the space around the celiac artery (CEL). Note the needle at the base of the celiac artery. AO, Aorta.

ethanol.<sup>43</sup> Because the efferent nerves from the pancreas travel with the sympathetic chain, interruption of the celiac ganglia should result in a decreased sense of pain. In the setting of pancreatic cancer, there is evidence of sensory nerve hyperplasia, and this may be the basis for the often observed chronic abdominal pain.

### Procedural Technique (Video 25.6)

The technique for EUS-guided celiac plexus neurolysis (EUS CPN) and block is identical; the only difference is in the substances injected. With a curvilinear array echoendoscope, the region of the celiac plexus is visualized from the lesser curve of the stomach by following the aorta to the origin of the main celiac artery (Fig. 25.10). With careful inspection, it is often possible, by using slight rotational movements, even to visualize the celiac ganglia directly (Fig. 25.11).



• **Fig. 25.11** Endoscopic ultrasonography imaging of a focal round, hypoechoic celiac ganglion.

A 22- or 19-G EUS FNA needle is usually used, but in some countries a dedicated 20-G spray needle with multiple side holes is available and allows solutions to disperse over a greater area. The needle tip is placed slightly anterior and cephalad to the origin of the celiac artery or directly into the ganglia if these can be identified as discrete structures. Aspiration is first performed to ensure that vascular puncture has not occurred. Bupivacaine is injected first, followed by alcohol (or triamcinolone for block). One of two strategies can be used: injection of the entire solution into the area cephalad of the celiac trunk or injection into the right and left sides of the celiac artery. Patients should be observed for 2 to 4 hours with careful monitoring of pulse, blood pressure, temperature, and pain scores.

#### Clinical Outcomes

The safety and efficacy of EUS CPN to alleviate refractory pain due to pancreatic cancer has been demonstrated in multiple large prospective clinical studies.<sup>16,44</sup> The pooled analysis of eight studies revealed a pain-relief proportion of 80.1% (74% to 85%) by EUS CPN (Table 25.4).<sup>44</sup>

The effect of early EUS CPN was investigated in 96 patients with newly diagnosed, painful, inoperable pancreatic cancer in a randomized, double-blind, controlled trial.<sup>45</sup> Pain relief was greater in the EUS-treated group at 1 month and significantly greater at 3 months. Morphine consumption tended to be lower at 3 months in the neurolysis group. However, there was no difference in quality of life or survival between the groups. Similar to this study, large trials have failed to demonstrate a significant improvement in survival time in patients with pancreatic cancer despite the high rates of symptom response to injection therapy.

A large retrospective study has demonstrated that bilateral EUS CPN was more effective than central injection in terms of pain reduction.<sup>46</sup> More than 70.4% of patients reported a decrease in pain levels at 7 days, compared with 45.9% of patients receiving a single injection. However, another recent study did not find a statistically significant difference in the median percent pain reduction at 4 weeks between the bilateral (60%) and central (50%) techniques.<sup>47</sup>

Injection therapy in patients with pain associated with chronic pancreatitis has not been as successful as reported for pain control in pancreatic cancer.<sup>44</sup> The overall rate of treatment response has been approximately 60%, and responses have been transient.<sup>44</sup> Ganglion blockade using local anesthetics rather than permanent chemical neurolysis has generally been the approach for pain control in chronic pancreatitis. LeBlanc and colleagues, in a prospective trial, determined that the average duration of effect of a ganglion block was 1 month, and that one injection of bupivacaine and triamcinolone yielded the same effect as two injections.<sup>48</sup> Many investigators believe that short-term relief of pain

may not be a clinically important effect in the long-term care of patients with chronic pancreatitis.

To improve the efficacy of EUS CPN, EUS-guided broad plexus neurolysis (EUS BPN) extending over the territory of the superior mesenteric artery (SMA) was investigated and compared with standard EUS CPN in 67 patients with advanced abdominal cancer.<sup>49</sup> EUS BPN patients exhibited significantly greater pain reduction at days 7 and 30 without incurring serious complications. This study suggests that broad neurolysis over the SMA may provide superior analgesia, but no further data have been published to confirm these promising observations. The same group reported that EUS celiac ganglia neurolysis (CGN) in conjunction with EUS BPN, when the celiac ganglia are visible, yielded significantly better pain relief at 1 and 4 weeks.<sup>50</sup>

#### Direct Ganglia Injection

Developments have focused on the ability of EUS to target the celiac ganglia specifically with injection therapy (Video 25.7). In a retrospective study, 33 patients underwent celiac injections for unresectable pancreatic cancer or for chronic pancreatitis using bupivacaine (0.25%) and alcohol (99%) for neurolysis or methylprednisolone (Depo-Medrol, 80 mg/2 mL) for nerve blockade.<sup>51</sup> Nearly all patients with cancer (94%) reported pain relief. In contrast, patients with chronic pancreatitis experienced lower response rates (80% response rate with alcohol injection and 38% response rate with steroids). Direct celiac ganglia neurolysis after EUS visualization was reported in a large series of patients with pancreatic cancer.<sup>52</sup> Of the 64 patients enrolled in the study, 40 patients (62.5%) with visible celiac ganglia (range 1 to 4) underwent EUS ganglia neurolysis with 98% alcohol. The 24 patients with unidentified ganglia underwent bilateral injections at the celiac vessel trunk. The response rate, which was defined as at least a 2-point drop in pain as measured by the VAS in the first week, was 65% in the direct injection group and only 25% in the alternate cohort. This translated to a five-fold higher chance of treatment response for those patients with visible ganglia compared to those without visible ganglia and multivariate model showed that visualization of the ganglia was the best predictor of treatment response. A recent multicenter, randomized, trial confirmed the superiority of direct CGN over CPN in 68 patients with cancer pain.<sup>53</sup> The visualization of ganglia was possible in 88% of patients and the treatment response rate was 73.5% versus 45.5% on the 7th day of the procedure. Although these studies demonstrate significantly better short-term pain relief with the direct ganglia injection approach, the long-term efficacy data is lacking and the procedural technique is yet to be standardized.

Overall EUS CPN was safe in most of the clinical studies, and major adverse effects such as bleeding, abscess, abdominal ischemia, and injury to adrenal artery were reported rarely.<sup>16</sup> The most common complication of CPN was postprocedural hypotension, at a rate of 3.2%.<sup>54</sup> Occasionally patients complained of severe abdominal pain and diarrhea after injection.<sup>54</sup> In a recent study, a change in heart rate of more than 15 beats per minute was observed in 25 of 51 patients (49%) during EUS CPN. The patients with an increase in intraprocedural heart rate experienced significant improvement in pain and quality-of-life components compared with patients without a significant change.<sup>55</sup> However, there was no significant difference in postprocedural opioid use or survival between groups.

**TABLE  
25.4****Selected Clinical Trials of Endoscopic Ultrasonography-Guided Celiac Injection Therapy**

Authors (Year)	Patients ( <i>n</i> )	Diagnosis	Technique	Pain Score Change
Puli et al. (2009) <sup>44</sup> (meta-analysis)	283	Pancreatic cancer	CPN	80% improved (pooled data)
Puli et al. (2009) <sup>44</sup> (meta-analysis)	376	Chronic pancreatitis	CPN	59% improved (pooled data)
Wyse et al. (2011) <sup>45</sup>	48	Pancreatic cancer	Early CPN	Significant decrease in mean pain score
Sahai et al. (2009) <sup>46</sup>	160	Pancreatic cancer	Central or bilateral CPN or block	Pain reduction: 70% for bilateral and 45% for central injection at first week
Tellez-Avila et al. (2013) <sup>47</sup>	53	Pancreatic cancer	Central or bilateral CPN	Pain reduction: 60% for bilateral and 50% for central injection at 4 weeks
LeBlanc et al. (2009) <sup>48</sup>	50	Chronic pancreatitis	1 or 2 injections for block	65% for 1 injection and 59% for 2 injections at 4 weeks
Sakamoto et al. (2010) <sup>49</sup>	77	Pancreatic cancer	CPN or BPN	Significantly better pain reduction in BPN cohort
Levy et al. (2008) <sup>51</sup>	33	Pancreatic cancer and chronic pancreatitis	Direct ganglia injection	94% improved (cancer); 50% improved (chronic pancreatitis)
Ascunce et al. (2011) <sup>52</sup>	64	Pancreatic cancer	Direct ganglia injection or bilateral neurolysis	65% improved at direct ganglia, 25% in bilateral at first week
Doi et al. (2013) <sup>53</sup>	68	Pancreatic cancer	Direct ganglia or celiac plexus neurolysis	73% for ganglia and 45% for celiac plexus at first week

BPN, Broad plexus neurolysis; CPN, celiac plexus neurolysis.

## Summary

EUS-guided FNI therapy is based on the accurate placement of ablative or hemostatic agents into various gastrointestinal lesions or tissues. Its technical success has been very high in almost all studies, but clinical outcomes have varied according to the targeted lesion and the agent being utilized. Celiac plexus neurolysis is the most common injection therapy being practiced; its clinical efficacy is modest. Ablation of solid and cystic pancreatic lesions by injecting ethanol, paclitaxel, or various biologic agents has been reported in case series, and are still under evaluation in clinical trials. The role of EUS-guided RFA and other novel therapies remains investigational.

## Key References

- Pai M, Yang J, Zhang X, et al. PWE-055 endoscopic ultrasound guided radiofrequency ablation (EUS-RFA) for pancreatic ductal adenocarcinoma. *Gut*. 2013;62:A153.
- Pai M, Habib N, Senturk H, et al. Endoscopic ultrasound guided radiofrequency ablation for pancreatic cystic neoplasms and neuroendocrine tumors. *World J Gastrointest Surg*. 2015;7:52–59.
- Fabbri C, Luigiano C, Lisotti A, et al. Endoscopic ultrasound-guided treatments. Are we getting evidence based-a systematic review. *World J Gastroenterol*. 2014;20:8424–8448.
- Qin SY, Lu XP, Jiang HX. EUS-guided ethanol ablation of insulinomas: case series and literature review. *Medicine (Baltimore)*. 2014;93:1–5.
- Puli SR, Reddy JB, Bechtold ML, et al. EUS-guided celiac plexus neurolysis for pain due to chronic pancreatitis or pancreatic cancer pain: a meta-analysis and systematic review. *Dig Dis Sci*. 2009;54:2330–2337.

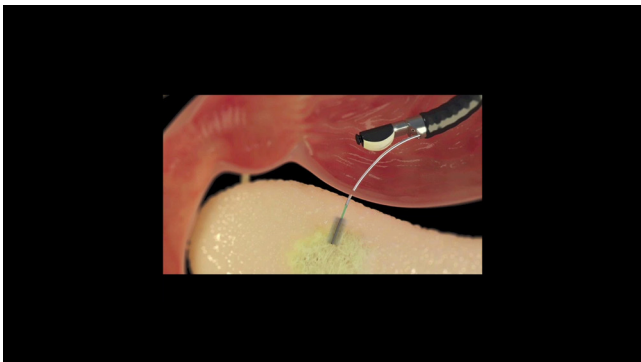
## References

Access the reference list online at [ExpertConsult.com](http://ExpertConsult.com)

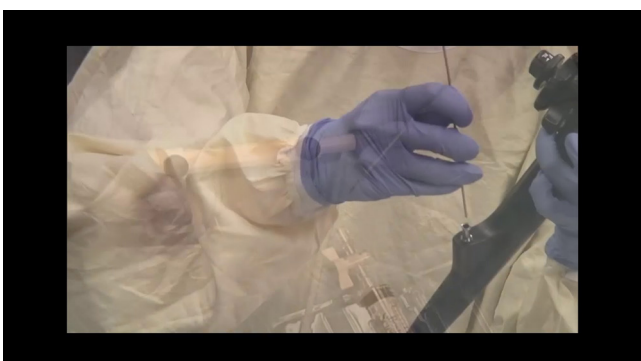
## References

1. Pai M, Yang J, Zhang X, et al. PWE-055 endoscopic ultrasound guided radiofrequency ablation (EUS-RFA) for pancreatic ductal adenocarcinoma. *Gut*. 2013;62:A153.
2. Pai M, Habib N, Senturk H, et al. Endoscopic ultrasound guided radiofrequency ablation for pancreatic cystic neoplasms and neuroendocrine tumors. *World J Gastrointest Surg*. 2015;7:52–59.
3. Song TJ, Seo DW, Lakhtakia S, et al. Initial experience of EUS-guided radiofrequency ablation of unresectable pancreatic cancer. *Gastrointest Endosc*. 2016;83:440–443.
4. Lakhtakia S, Ramchandani M, Galasso D, et al. EUS-guided radiofrequency ablation for management of pancreatic insulinoma by using a novel needle electrode. *Gastrointest Endosc*. 2016;83:234–239.
5. Jin ZD, Wang L, Li Z. Endoscopic ultrasound-guided celiac ganglion radiofrequency ablation for pain control in pancreatic carcinoma. *Dig Endosc*. 2015;27:163–164.
6. Carrara S, Arcidiacono PG, Albarello L, et al. Endoscopic ultrasound-guided application of a new hybrid cryotherm probe in porcine pancreas: a preliminary study. *Endoscopy*. 2008;40:321–326.
7. Arcidiacono PG, Carrara S, Reni M, et al. Feasibility and safety of EUS-guided cryothermal ablation in patients with locally advanced pancreatic cancer. *Gastrointest Endosc*. 2012;76:1142–1151.
8. Skandalajah AR, Lynch AC, Mackay JR, et al. The role of intraoperative radiotherapy in solid tumors. *Ann Surg Oncol*. 2009;16:735–744.
9. Calvo FA, Meirino RM, Orecchia R. Intraoperative radiation therapy part 2. Clinical results. *Crit Rev Oncol Hematol*. 2006;59:116–127.
10. Sun S, Xu H, Xin J, et al. Endoscopic ultrasound-guided interstitial brachytherapy of unresectable pancreatic cancer: results of a pilot trial. *Endoscopy*. 2006;38:399–403.
11. Jin Z, Du Y, Li Z, et al. Endoscopic ultrasonography-guided interstitial implantation of iodine 125-seeds combined with chemotherapy in the treatment of unresectable pancreatic carcinoma: a prospective pilot study. *Endoscopy*. 2008;40:314–320.
12. Jin Z, Du Y, Li Z. Su1575 long-term effect of gemcitabine-combined endoscopic ultrasonography-guided brachytherapy in pancreatic cancer. *Gastrointest Endosc*. 2013;77:AB373.
13. Jiang TA, Deng Z, Tian G, et al. Efficacy and safety of endoscopic ultrasonography-guided interventional treatment for refractory malignant left-side liver tumors: a case series of 26 patients. *Sci Rep*. 2016;6:36098.
14. Pishvaian AC, Collins B, Gagnon G, et al. EUS-guided fiducial placement for CyberKnife radiotherapy of mediastinal and abdominal malignancies. *Gastrointest Endosc*. 2006;64:412–417.
15. Park WG, Yan BM, Schellenberg D, et al. EUS-guided gold fiducial insertion for image-guided radiation therapy of pancreatic cancer: 50 successful cases without fluoroscopy. *Gastrointest Endosc*. 2010;71:513–518.
16. Fabbri C, Luigiano C, Lisotti A, et al. Endoscopic ultrasound-guided treatments. Are we getting evidence based-a systematic review. *World J Gastroenterol*. 2014;20:8424–8448.
17. Yang J, Abdel-Wahab M, Ribeiro A. EUS-guided fiducial placement after radical prostatectomy before targeted radiation therapy for prostate cancer recurrence. *Gastrointest Endosc*. 2011;73:1302–1305.
18. Chandran S, Vaughan R, Efthymiou M, et al. A pilot study of EUS-guided fiducial insertion for the multidisciplinary management of gastric cancer. *Endosc Int Open*. 2014;2:153–159.
19. Machiels M, van Hooft J, Jin P, et al. Endoscopy/EUS-guided fiducial marker placement in patients with esophageal cancer: a comparative analysis of 3 types of markers. *Gastrointest Endosc*. 2015;82(4):641–649.
20. Law JK, Singh VK, Khashab MA, et al. Endoscopic ultrasound (EUS)-guided fiducial placement allows localization of small neuroendocrine tumors during parenchymal-sparing pancreatic surgery. *Surg Endosc*. 2013;27:3921–3926.
21. Okuzono T, Kanno Y, Nakahori M, et al. Preoperative endoscopic ultrasonography-guided tattooing of the pancreas with a minuscule amount of marking solution using a newly designed injector. *Dig Endosc*. 2016;28:744–748.
22. Wang KX, Jin ZD, Du YQ, et al. EUS-guided celiac ganglion irradiation with iodine-125 seeds for pain control in pancreatic carcinoma: a prospective pilot study. *Gastrointest Endosc*. 2012;76:945–952.
23. Jurgensen C, Schuppan D, Neser F, et al. EUS-guided alcohol ablation of an insulinoma. *Gastrointest Endosc*. 2006;63:1059–1062.
24. Levy MJ, Thompson GB, Topazian MD, et al. EUS-guided ethanol ablation of insulinomas: a new treatment option. *Gastrointest Endosc*. 2012;75:200–206.
25. Qin SY, Lu XP, Jiang HX. EUS-guided ethanol ablation of insulinomas: case series and literature review. *Medicine (Baltimore)*. 2014;93:1–5.
26. Artifon EL, Cunha MAB, Da Silveira EB, et al. 349 EUS-guided or interventional radiology to hepatic intra-arterial chemotherapy: a prospective trial. *Gastrointest Endosc*. 2013;77:AB142–AB143.
27. Levy MJ, Alberts SR, Bamlet WR, et al. EUS guided fine-needle injection of gemcitabine for locally advanced and metastatic pancreatic cancer. *Gastrointest Endosc*. 2017;86:161–169.
28. Chang KJ, Nguyen PT, Thompson JA, et al. Phase I clinical trial of allogeneic mixed lymphocyte culture (cytoimplant) delivered by endoscopic ultrasound-guided fine-needle injection in patients with advanced pancreatic carcinoma. *Cancer*. 2000;88:1325–1335.
29. Hecht JR, Bedford R, Abbruzzese JL, et al. A phase I/II trial of intratumoral endoscopic ultrasound injection of ONYX-015 with intravenous gemcitabine in unresectable pancreatic carcinoma. *Clin Cancer Res*. 2003;9:555–561.
30. Irisawa A, Takagi T, Kanazawa M, et al. Endoscopic ultrasound-guided fine-needle injection of immature dendritic cells into advanced pancreatic cancer refractory to gemcitabine: a pilot study. *Pancreas*. 2007;35:189–190.
31. Hirooka Y, Itoh A, Kawashima H, et al. A combination therapy of gemcitabine with immunotherapy for patients with inoperable locally advanced pancreatic cancer. *Pancreas*. 2009;38:e69–e74.
32. Hecht JR, Farrell JJ, Senzer N, et al. EUS or percutaneously guided intratumoral TNFerade biologic with 5-fluorouracil and radiotherapy for first-line treatment of locally advanced pancreatic cancer: a phase I/II study. *Gastrointest Endosc*. 2012;75:332–338.
33. Herman JM, Wild AT, Wang H, et al. Randomized phase III multi-institutional study of TNFerade biologic with fluorouracil and radiotherapy for locally advanced pancreatic cancer: final results. *J Clin Oncol*. 2013;31:886–894.
34. Chang KJ, Reid T, Senzer N, et al. Phase I evaluation of TNFerade biologic plus chemoradiotherapy before esophagectomy for locally advanced resectable esophageal cancer. *Gastrointest Endosc*. 2012;75:1139–1146.
35. DiMaio CJ, DeWitt JM, Brugge WR. Ablation of pancreatic cystic lesions: the use of multiple endoscopic ultrasound-guided ethanol lavage sessions. *Pancreas*. 2011;40:664–668.
36. Gan SI, Thompson CC, Lauwers GY, et al. Ethanol lavage of pancreatic cystic lesions: initial pilot study. *Gastrointest Endosc*. 2005;61:746–752.
37. DeWitt J, McGreevy K, Schmidt CM, Brugge WR. EUS-guided ethanol versus saline solution lavage for pancreatic cysts: a randomized, double-blind study. *Gastrointest Endosc*. 2009;70:710–723.

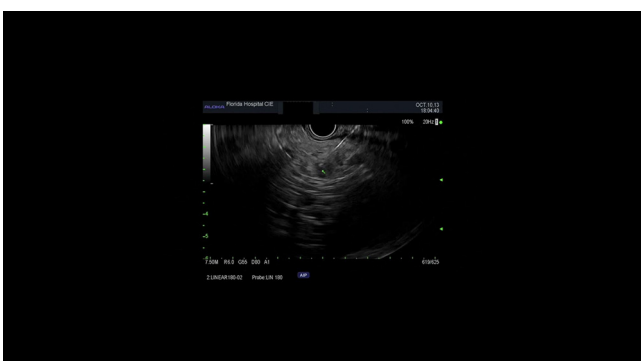
38. DeWitt J, DiMaio CJ, Brugge WR. Long-term follow-up of pancreatic cysts that resolve radiologically after EUS-guided ethanol ablation. *Gastrointest Endosc.* 2010;72:862–866.
39. Oh HC, Seo DW, Song TJ, et al. Endoscopic ultrasonography-guided ethanol lavage with paclitaxel injection treats patients with pancreatic cysts. *Gastroenterology.* 2011;140:172–179.
40. DeWitt JM, Al-Haddad M, Sherman S, et al. Alterations in cyst fluid genetics following endoscopic ultrasound-guided pancreatic cyst ablation with ethanol and paclitaxel. *Endoscopy.* 2014;46:457–464.
41. Oh HC, Seo DW, Kim SC, et al. Septated cystic tumors of the pancreas: is it possible to treat them by endoscopic ultrasonography-guided intervention? *Scand J Gastroenterol.* 2009;44:242–247.
42. Moyer MT, Dye CE, Sharzehi S, et al. Is alcohol required for effective pancreatic cyst ablation? The prospective randomized CHARM trial pilot study. *Endosc Int Open.* 2016;4:603–607.
43. Vranken JH, Zuurmond WW, Van Kemenade FJ, Dzoljic M. Neurohistopathologic findings after a neurolytic celiac plexus block with alcohol in patients with pancreatic cancer pain. *Acta Anaesthesiol Scand.* 2002;46:827–830.
44. Puli SR, Reddy JB, Bechtold ML, et al. EUS-guided celiac plexus neurolysis for pain due to chronic pancreatitis or pancreatic cancer pain: a meta-analysis and systematic review. *Dig Dis Sci.* 2009;54:2330–2337.
45. Wyse JM, Carone M, Paquin SC, et al. Randomized, double-blind, controlled trial of early endoscopic ultrasound-guided celiac plexus neurolysis to prevent pain progression in patients with newly diagnosed, painful, inoperable pancreatic cancer. *J Clin Oncol.* 2011;29:3541–3546.
46. Sahai AV, Lemelin V, Lam E, Paquin SC. Central versus bilateral endoscopic ultrasound-guided celiac plexus block or neurolysis: a comparative study of short-term effectiveness. *Am J Gastroenterol.* 2009;104:326–329.
47. Tellez-Avila FI, Romano-Munive AF, Herrera-Esquivel Jde J, Ramirez-Luna MA. Central is as effective as bilateral endoscopic ultrasound-guided celiac plexus neurolysis in patients with unresectable pancreatic cancer. *Endoscopic Ultrasound.* 2013;2:153–156.
48. LeBlanc JK, DeWitt J, Johnson C, et al. A prospective randomized trial of 1 versus 2 injections during EUS-guided celiac plexus block for chronic pancreatitis pain. *Gastrointest Endosc.* 2009;69:835–842.
49. Sakamoto H, Kitano M, Kamata K, et al. EUS-guided broad plexus neurolysis over the superior mesenteric artery using a 25-gauge needle. *Am J Gastroenterol.* 2010;105:2599–2606.
50. Minaga K, Kitano M, Sakamoto H, et al. Predictors of pain response in patients undergoing endoscopic ultrasound-guided neurolysis for abdominal pain caused by pancreatic cancer. *Therap Adv Gastroenterol.* 2016;9:483–494.
51. Levy MJ, Topazian MD, Wiersema MJ, et al. Initial evaluation of the efficacy and safety of endoscopic ultrasound-guided direct ganglia neurolysis and block. *Am J Gastroenterol.* 2008;103:98–103.
52. Ascunc G, Ribeiro A, Reis I, et al. EUS visualization and direct celiac ganglia neurolysis predicts better pain relief in patients with pancreatic malignancy (with video). *Gastrointest Endosc.* 2011;73:267–274.
53. Doi S, Yasuda I, Kawakami H, et al. Endoscopic ultrasound-guided celiac ganglia neurolysis vs. celiac plexus neurolysis: a randomized multicenter trial. *Endoscopy.* 2013;45:362–369.
54. O'Toole TM, Schmulewitz N. Complication rates of EUS-guided celiac plexus blockade and neurolysis: results of a large case series. *Endoscopy.* 2009;41:593–597.
55. Bang JY, Hasan MK, Sutton B, et al. Intraprocedural increase in heart rate during EUS-guided celiac plexus neurolysis: clinically relevant or just a physiologic change? *Gastrointest Endosc.* 2016;84:773–779.



**Video 25.1** Animation Demonstrating the Technique of Endoscopic Ultrasonography-Guided Radiofrequency Ablation in Pancreatic Cancer Using the Habib Catheter



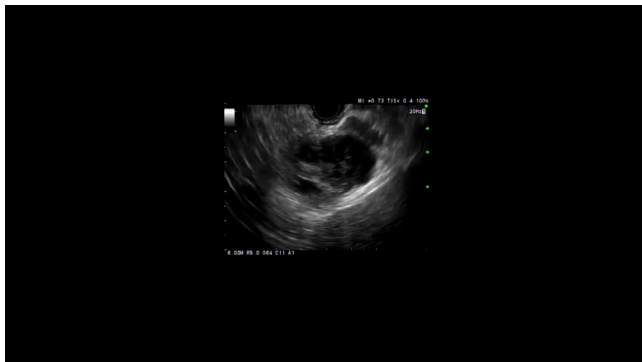
**Video 25.2** Endoscopic Ultrasonography-Guided Radiofrequency Ablation of the Celiac Ganglia Using the Habib Catheter



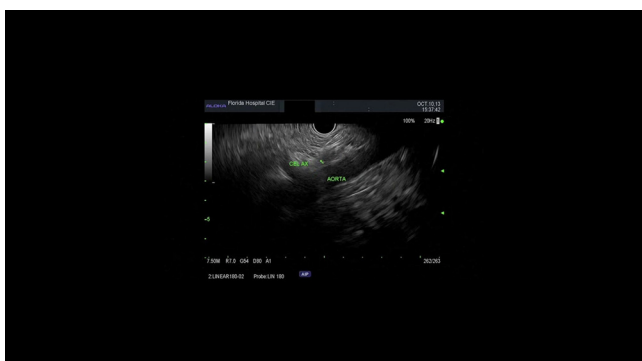
**Video 25.3** Technique of Endoscopic Ultrasonography-Guided Placement of Fiducials



**Video 25.4** Technique of Endoscopic Ultrasonography-Guided Placement of Fiducials Using a Dedicated Shark-Core Platform



**Video 25.5** Technique of Endoscopic Ultrasonography-Guided Pancreatic Cyst Ablation



**Video 25.6** Technique of Endoscopic Ultrasonography-Guided Celiac Plexus Neurolysis



**Video 25.7** Endoscopic Ultrasonography-Guided Celiac Ganglion Neurolysis

# 26

## Endoscopic Ultrasonography-Guided Anastomosis, Drainage of Abdominopelvic Fluid Collections, and Vascular Interventions

TAKAO ITOI AND SHYAM VARADARAJULU

### KEY POINTS

- An anastomosis can be established between the stomach and the jejunum under the guidance of endoscopic ultrasonography (EUS) in patients with gastric outlet obstruction. A lumen-apposing metal stent (LAMS) can either be deployed directly or with balloon assistance using fluoroscopic and sonographic guidance. Although experience is limited, the preliminary data appear promising.
- EUS facilitates transmural drainage of postoperative abdominal and pelvic fluid collections adjacent to the stomach, duodenum, rectum, or colonic lumen and within the reach of an echoendoscope. Both procedures are safe, with a treatment success rate greater than 90%. Adverse events are mild and can be managed conservatively in most patients.
- Essentials for such procedures include a fluoroscopy unit, therapeutic echoendoscope, accessories such as 19-G needles, endoscopic retrograde cholangiopancreatography cannula or needle-knife catheters, guidewires, balloon dilators, LAMS, double-pigtail plastic stents, and biliary drainage catheters.
- EUS-guided hemostasis in gastric varices can be attained with coil embolization and/or glue injection. The technique appears to be clinically effective, with promising treatment outcomes.

The use of the linear array echoendoscope has expanded the realm of therapeutic interventions to include drainage of obstructive biliary ductal system, peripancreatic fluid collections and pelvic abscesses, placement of coils or injection of sclerotic agents in varices, and more recently the creation of an anastomosis between the stomach and small bowel for palliation of gastric outlet obstruction (GOO). In this chapter, the technique and outcomes of endoscopic EUS-guided anastomosis, drainage of abdominal fluid collections and pelvic abscesses, and its role in the obliteration of gastric varices are reviewed.

### Endoscopic Ultrasonography-Guided Anastomosis

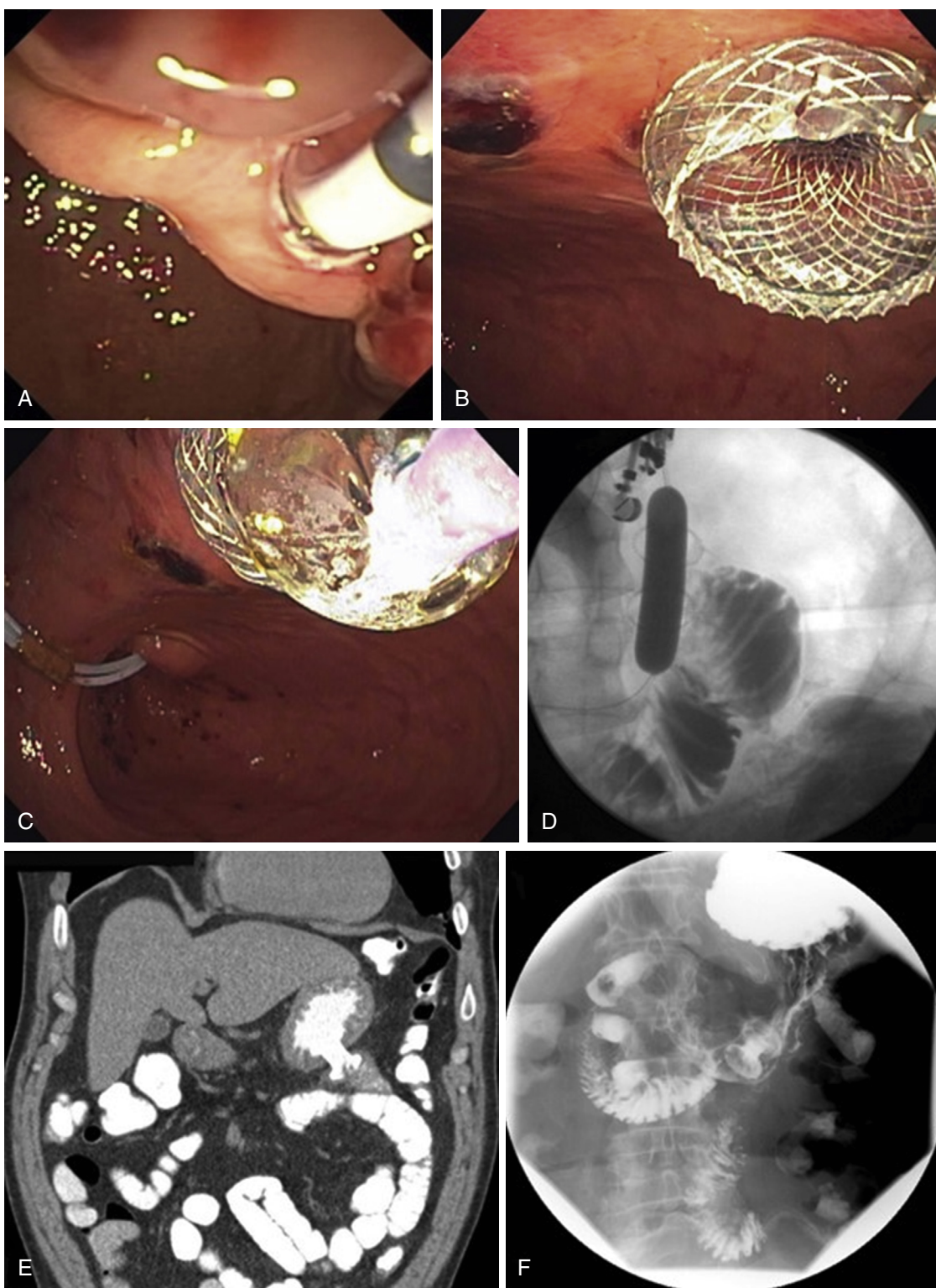
Options for the treatment of GOO include open or laparoscopic gastrojejunostomy and the endoscopic placement of self-expanding metal stents (SEMS) across the luminal obstruction. Recently there have been reports of successful creation of gastroenteric anastomoses performed under endosonographic guidance.<sup>1–3</sup> The procedure has the potential to offer long-lasting luminal patency without the risk of stent obstruction by tumor ingrowth, and it also avoids the morbidity of a surgical procedure.

### Procedural Technique

EUS-guided gastroenterostomy (EUS-GE) can be performed by adopting one of three techniques: direct EUS-GE, assisted EUS GE, and EUS-guided balloon-occluded gastrojejunostomy bypass (EPASS).

#### *Direct Endoscopic Ultrasonography-Guided Gastroenterostomy Technique*

- A 19-G needle is inserted transgastrically into the small-bowel loop to distend the duodenum and jejunum by infusing saline under EUS visualization.
- An enterogram is then obtained by injecting a radiocontrast agent and a 0.025/0.035-inch guidewire is passed through the 19-G needle into the small bowel.
- The GE tract is dilated using a 40 mm long and 4 mm wide over-the-wire dilating balloon followed by the placement of a 15- by 10-mm lumen-apposing metal stent (LAMS) (Fig. 26.1A–F; Video 26.1). It may sometimes be necessary to create a tract using a needle-knife catheter prior to performing balloon dilation. Alternatively, the electrocautery-enhanced delivery system can be used to puncture the small bowel directly for LAMS deployment.
- The lumen of the LAMS may be dilated, if required, using a radial expansion balloon to create a wider opening.



• **Fig. 26.1** Placement of lumen-apposing stent during endoscopic ultrasonography-guided gastrojejunostomy. (A) Endoscopic image of fistula tract dilation by using a 4-mm balloon. (B) Endoscopic image of the proximal end of the stent deployed in the stomach. (C) Endoscopic image of balloon dilation of the stent. (D) Fluoroscopic image of balloon dilation of the stent. (E) Coronal computed tomography image demonstrating contrast material flowing through the stent into the distal small bowel. (F) Image from a small-bowel series demonstrating contrast material flowing through the stent into the distal small bowel. (Courtesy of Dr. Mouen Khashab.)

### Assisted Endoscopic Ultrasonography-Guided Gastroenterostomy Technique

The assisted EUS-GE technique involves the passage of a retrieval/dilating balloon or ultraslim endoscope across the stricture to the duodenal-jejunal flexure to assist in the placement of a LAMS.<sup>4,5</sup> The balloon serves as an anatomic marker for the creation of the anastomosis (Video 26.2).

1. The retrieval or dilating balloon catheter is passed over a guidewire into the small bowel and then inflated with fluid (water mixed with contrast) while it is being positioned in the duodenum or jejunum.
2. The echoendoscope is then passed alongside the balloon catheter into the stomach and the fluid-filled balloon is localized by sonography.
3. The balloon is punctured using a 19-G needle. Bursting of the balloon indicates correct positioning of the needle tip within the small-bowel lumen.
4. A guidewire is advanced through the needle and a LAMS is subsequently deployed. It may be necessary to dilate the transmural tract if a nonelectrocautery-based LAMS is being deployed.

When an ultraslim endoscope-assisted EUS-GE is performed, the small-caliber endoscope is passed perorally or through an existing gastrostomy site into the stomach and then beyond the stricture. Saline is injected through the ultraslim scope to distend the bowel lumen. The echoendoscope is then advanced into the stomach (alongside the ultraslim scope in cases where the ultraslim scope is introduced perorally). A guidewire is advanced through the needle and coiled within the bowel lumen. A biopsy forceps is then passed through the ultraslim scope to grasp the guidewire, thus providing traction in an internal rendezvous maneuver. A fistulous tract is then created for LAMS deployment. There are reports of using a nasobiliary catheter for saline and contrast injection into the duodenum-jejunum so as to facilitate fluoroscopic and sonographic visualization.<sup>3</sup>

### Endoscopic Ultrasonography-Guided Balloon-Occluded Gastrojejunostomy Bypass Technique

1. A standard upper endoscope is advanced to the third portion of the duodenum and a guidewire is advanced as far as possible into the jejunum (Fig. 26.2A and B; Video 26.3).
2. The endoscope is removed, leaving the guidewire in place. An overtube is helpful to facilitate passage of the preinflated balloon catheter to avoid looping in the fornix of the stomach as it passes through the pyloric-duodenal stenosis.
3. A double-balloon tube (Tokyo Medical University type, Create Medic Co., Ltd., Yokohama, Japan) is inserted perorally over the guidewire and the two balloons are placed in the duodenum and jejunum in an area adjacent to the stomach.
4. Both balloons are filled with saline and contrast material to anchor the small intestine in place. A sufficient quantity of saline with contrast material is introduced into the space between the two balloons to distend the small bowel lumen.
5. An echoendoscope is advanced to the stomach to identify the distended duodenum or jejunum.
6. EUS-guided balloon-occluded gastrojejunostomy bypass (EPASS) can then be undertaken by one of two techniques, namely the “free style” or “standard” technique. The former is performed using a direct electrocautery-enhanced tip delivery system insertion without needle puncture, whereas the latter involves placement of the LAMS over a guidewire, as described previously.

### Technical and Treatment Outcomes

Three case series have reported an overall technical success rate of approximately 90% regardless of the technique adopted (Table 26.1). In the EPASS procedure, the success rate of the free-style technique was higher than that of the standard technique (100% vs. 82%).<sup>2</sup> Treatment success was observed in almost all cases where the LAMS was successfully placed. Although there was no mortality, adverse events such as peritonitis or bleeding were encountered in several patients, although none were life-threatening. One failed case of balloon-assisted EUS-GE required conversion to a laparoscopic gastrojejunostomy. In two cases of stent maldeployment using the EPASS procedure, both patients responded well to conservative treatment measures.

### Technical Limitations

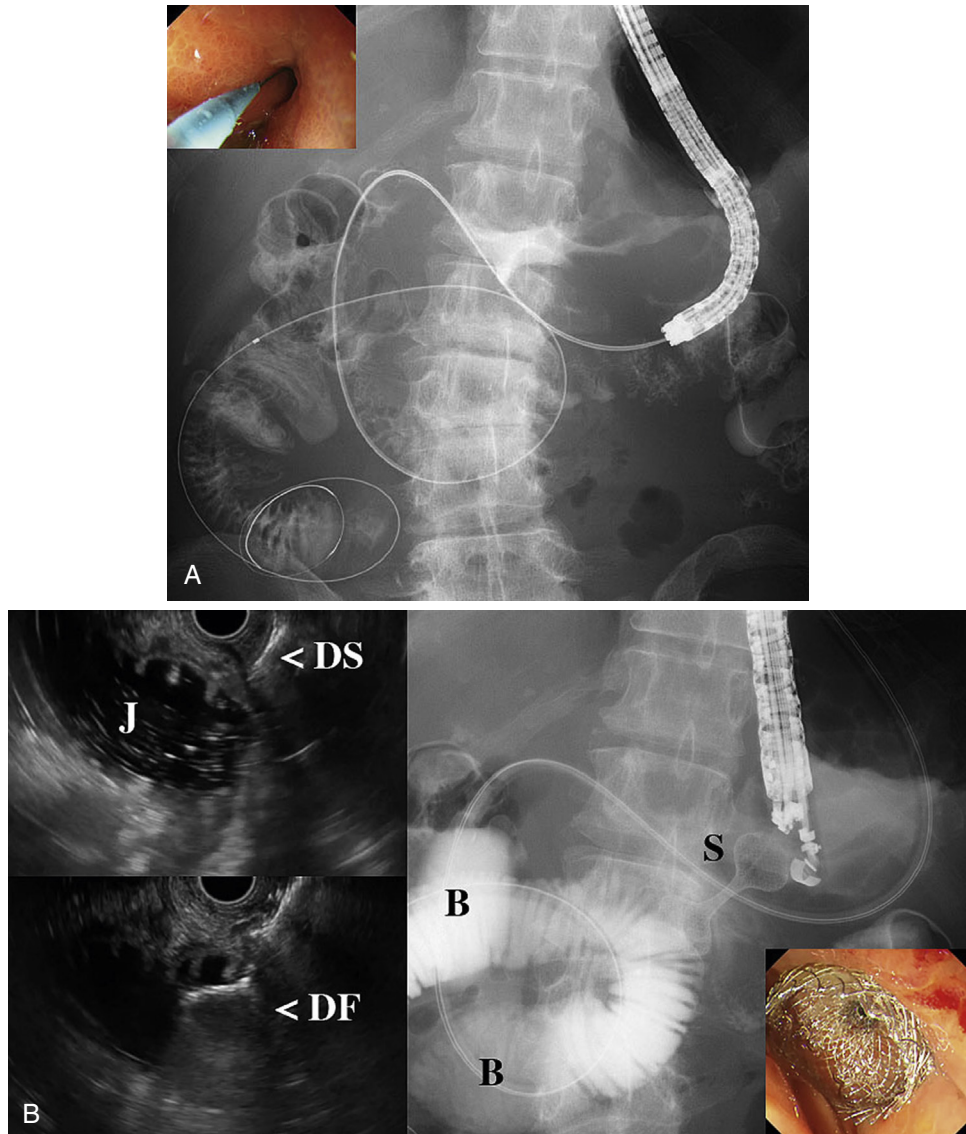
Limitations of the EUS-guided gastroenteric anastomosis include the following: (1) If the most proximal enteric lumen is located farther from stomach, EUS-guided anastomosis may not be appropriate unless alternate lumen-apposing devices such as T-tags are used and (2) the procedure cannot be performed safely when LAMS are not available due to the lack of adhesion between the stomach and the enteric tract.

### Endoscopic Ultrasonography-Guided Drainage of Abdominopelvic Fluid Collections

Abdominal and/or pelvic abscesses can occur postoperatively after pancreatic, liver, and bariatric surgery or in patients with medical conditions such as Crohn disease, diverticulitis, ischemic colitis, sexually transmitted diseases, or septic emboli from endocarditis. Management of postoperative fluid collections (POFCs) and pelvic abscesses can be technically challenging due to the need for navigation around multiple vital organs, including the bony pelvis, bowel loops, bladder, reproductive organs in females, prostate in men, rectum, and other neurovascular structures. Undrained POFCs have a high morbidity and mortality. Historically these collections have necessitated surgery, ultrasound-guided transrectal or transvaginal intervention, or were drained percutaneously under computed tomography (CT) guidance. Recent advances in the field of interventional EUS have opened a new avenue for the management of POFCs<sup>4–10</sup> and pelvic abscesses.<sup>11–18</sup>

### Procedural Technique

In cases of abdominopelvic abscess drainage, all patients should undergo dedicated CT or magnetic resonance imaging (MRI) of the abdomen and pelvis to define the anatomy and location of the fluid collection/abscess. If the POFC/pelvic abscess is multiloculated, measures less than 4 cm in size, has immature walls (without a definitive rim), is located at the level of the dentate line or greater than 2 cm from the EUS transducer, it should be managed by alternative techniques. Commonly it is recommended that patients be administered prophylactic antibiotics prior to the procedure. In case of POFC drainage, the overall procedural technique is similar to that of conventional EUS-guided drainage of peripancreatic fluid collections. In cases of pelvic abscess drainage, patients should undergo local preparation with an enema to optimize visualization and minimize contamination. Laboratory



• **Fig. 26.2** (A) Fluoroscopic image reveals a standard upper endoscope being advanced to the third portion of the duodenum and a guidewire is advanced as far as possible into the jejunum (*left upper corner*: endoscopic imaging of catheter and guidewire). (B) Fluoroscopic image shows both balloons are filled with saline and contrast material to anchor the small intestine in place. A sufficient quantity of saline with contrast material is introduced into the space between the two balloons to distend the small bowel lumen. An echoendoscopic image showed the distended jejunum (*left upper*) and deployment of distal flange (*left lower*). Fluoroscopic image shows the proximal flange deployed under endoscopic guidance (*right lower corner*). *B*, Balloon; *DF*, distal flange; *DS*, delivery system; *J*, distended jejunum; *S*, stent.

**TABLE 26.1** Outcome of Endoscopic Ultrasonography-Guided Gastroenterostomy Using Lumen-Apposing Metal Stents for Gastric Outlet Obstruction in Series With 10 or More Patients

Author (Year)	No. of Cases	Technique	Type of Balloon	Study Design	Single/Multicenter	Technical Success	Clinical Success <sup>a</sup>	Adverse Event	Convert to Surgery
Khashab et al. (2015) <sup>1</sup>	10	D, 1/B, 9	RB, 4/DB, 5	R	Multicenter	90%	90%	None	1 <sup>b</sup>
Itoi et al. (2016) <sup>2</sup>	20	EPASS 1-step, 9; 2-step, 11	Double balloon enteric tube	P	Single	1-step, 100%; 2-step, 82%	90%	Pneumoperitoneum 1	None
Tyberg et al. (2016) <sup>3</sup>	26	D, 3/NOTES, 2/B, 13/ USS, 5/NBD, 2	NA	R	Multicenter	92%	85%	Peritonitis 1 Bleeding 1, Pain 1	1 <sup>b</sup>

<sup>a</sup>Intention-to-treat analysis.

<sup>b</sup>Possibly the same case.

*B*, Balloon-assisted EUS-gastroenterostomy; *D*, direct EUS-gastrojejunostomy; *DB*, dilating balloon; *EPASS*, EUS-guided double balloon-occluded gastrojejunostomy bypass; *EUS*, endoscopic ultrasonography; *LAMS*, lumen-apposing metal stent; *NA*, not applicable; *NBD*, nasobiliary drain; *NOTES*, natural orifice transluminal endoscopic surgery; *P*, prospective; *R*, retrospective; *RB*, retrieval balloon; *USS*, ultraslim endoscope.

parameters must be checked to ensure that patients are not coagulopathic or thrombocytopenic. It is essential that the procedure take place in a unit equipped with fluoroscopy to guide stent and drain placements within the abscess cavity. Also, patients should either void prior to the procedure or have an indwelling Foley catheter to ensure that a distended bladder does not impair visualization of a small fluid collection or that it is not mistaken for an abscess.

The following procedural steps are undertaken in sequence:

1. First, POFC or the abscess must be located using a curved linear array echoendoscope. Once located, intervening vasculature must be excluded using color Doppler. Under EUS guidance, a 19-G fine-needle aspiration (FNA) needle is used to puncture the POFC or abscess cavity (Fig. 26.3A–E; Videos 26.4 and 26.5). The stylet is removed and the needle flushed with saline and aspirated to evacuate as much pus as possible. A sample of purulent material may be sent for gram staining and culture. A standard 0.035-inch guidewire or a stiff-type 0.025-in guidewire is then passed through the needle and coiled within the fluid collection. The needle is then exchanged over the guidewire for a 5-Fr endoscopic retrograde cholangiopancreatography (ERCP) cannula, needle-knife catheter, or cystotome to dilate the tract between gastrointestinal tract and the fluid collection. The tract is then further dilated using an 8-mm over-the-wire biliary balloon dilator.
2. Once the tract has been dilated, one or two 7-Fr/10-Fr 4-cm double-pigtail transmural stents are deployed. The decision to place one or more stents is based on the viscosity of the abscess contents: one if the fluid flowed smoothly and more if the contents were thicker.
3. In patients with POFC/pelvic abscesses that measure 8 cm or more in size and in those that do not drain well despite placement of transmural stents, an additional transluminal drainage catheter is deployed. The POFC or abscess cavity is accessed with a 5-Fr ERCP cannula to pass another 0.035-inch or 0.025-inch guidewire. A 10-Fr single-pigtail drain is then deployed over the guidewire. In case of a POFC, this drain will exit via the nose or anus when pelvic abscesses are drained. This drain is then flushed with 30 to 50 mL of normal saline every 4 hours until the aspirate is clear. Alternatively, drainage can be undertaken using LAMS with an indwelling nasocystic drain for irrigation of the fluid collection.<sup>19</sup>
4. A follow-up CT should be obtained at 48 hours to assess treatment response. If there is a greater than 50% reduction in size of the fluid collection, the drainage catheter (if left in situ) is removed and the patient can be discharged (Fig. 26.4A and B).
5. The transmural stents can continue to assist with drainage and be removed in 2 weeks by endoscopy as long as a repeat CT shows complete resolution of the fluid collection.

## Technical and Treatment Outcomes

**POFC drainage.** Seven studies (Table 26.2) have evaluated the effectiveness of EUS for the treatment of POFCs.<sup>4–10</sup> The first report by these authors described EUS-guided transgastric POFC drainage after distal pancreatectomy.<sup>4</sup> The procedure was technically successful in all patients and the treatment was effective in 90% over a 30-month period. One patient with a refractory fluid collection had persistent symptoms requiring reoperation. A majority of POFCs are encountered after pancreatic surgery and most resolve after EUS-guided drainage, with low rates of procedure-related adverse events. In a retrospective study that compared EUS

(n = 13) with percutaneous techniques (n = 32), there was no statistically significant difference in technical success (100% vs. 91%), treatment success (100% vs. 84%), recurrence (31% vs. 25%), adverse events (0% vs. 6%), or mortality (8% vs. 6%) between the EUS-guided and percutaneous drainage groups, respectively.

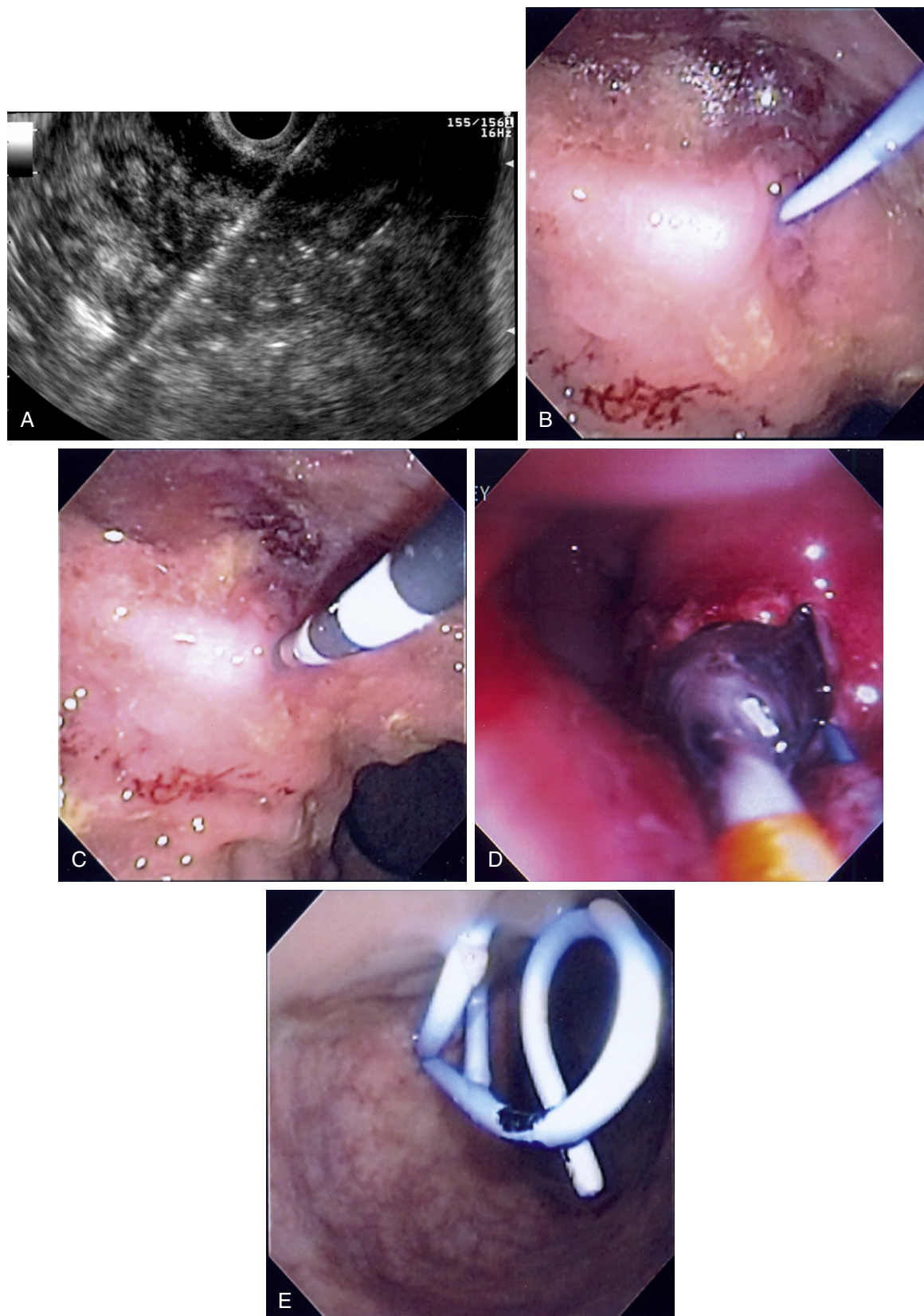
**Pelvic abscess drainage.** A total of eight studies (Table 26.3) have evaluated the effectiveness of EUS for the treatment of pelvic abscesses.<sup>11–18</sup> The overall treatment success ranged between 75% and 100%, with low rates of adverse events. In the first report, by Giovannini and colleagues, an 8.5- or 10-Fr transrectal stent was deployed for a period of 3 to 6 months, yielding a successful clinical outcome in 8 of 12 patients (75%). Treatment failures were more common in patients with large abscess that measured more than 8 cm in size. The limitation with transrectal stents is their potential to clog easily, particularly by fecal matter or pus; when left in place long-term, they can cause perirectal pain or migrate spontaneously. In the second study, this limitation was overcome by placement of a transrectal drainage catheter in four patients.<sup>12</sup> Although the technical and treatment outcomes were successful, there was the potential for accidental dislodgement of the drainage catheter. Additionally, the need for periodic flushing and aspiration of the drainage catheter mandated a prolonged hospital stay (median, 4 days) for most patients. Therefore a combined technique that included EUS-guided placement of a transrectal drainage catheter and stent for drainage of the pelvic abscess was adopted.<sup>13</sup> The short-term (36 to 48 hours) drainage catheter provided access for continued evacuation of the abscess, whereas the medium-term (2 weeks) stent facilitated maintenance of a patent transmural tract for eventual abscess resolution. This combined therapy demonstrated favorable outcomes for resolution of the abscess in all patients and shortened the postprocedure length of stay to a median of 2 days.

The effectiveness of the above combined approach was then prospectively validated in a cohort of 25 patients with long-term follow-up.<sup>14</sup> The etiology of the abscesses was postsurgical in 68% of patients; perforated diverticulitis or appendicitis in 20%; and ischemic colitis, infective endocarditis, or trauma in the remaining 12%. Two of 25 patients had previously failed treatment using percutaneous catheter placements. The mean size of the abscesses was 68.5 mm (range, 40 to 96 mm). The authors placed transrectal stents in all patients and an additional drainage catheter in 10 patients whose abscesses measured 8 cm or more in size. The procedures were technically successful in all patients with a treatment success rate of 96%; no complications were encountered. Seventy-six percent of the abscesses were drained via the transrectal route and others via the left colon. In this study, 2 of 25 patients who were critically ill in the intensive care unit underwent EUS-guided drainage at bedside. The mean and median procedural durations were 23 and 14 minutes, respectively. The median duration of postprocedure hospital stay was only 2 days.

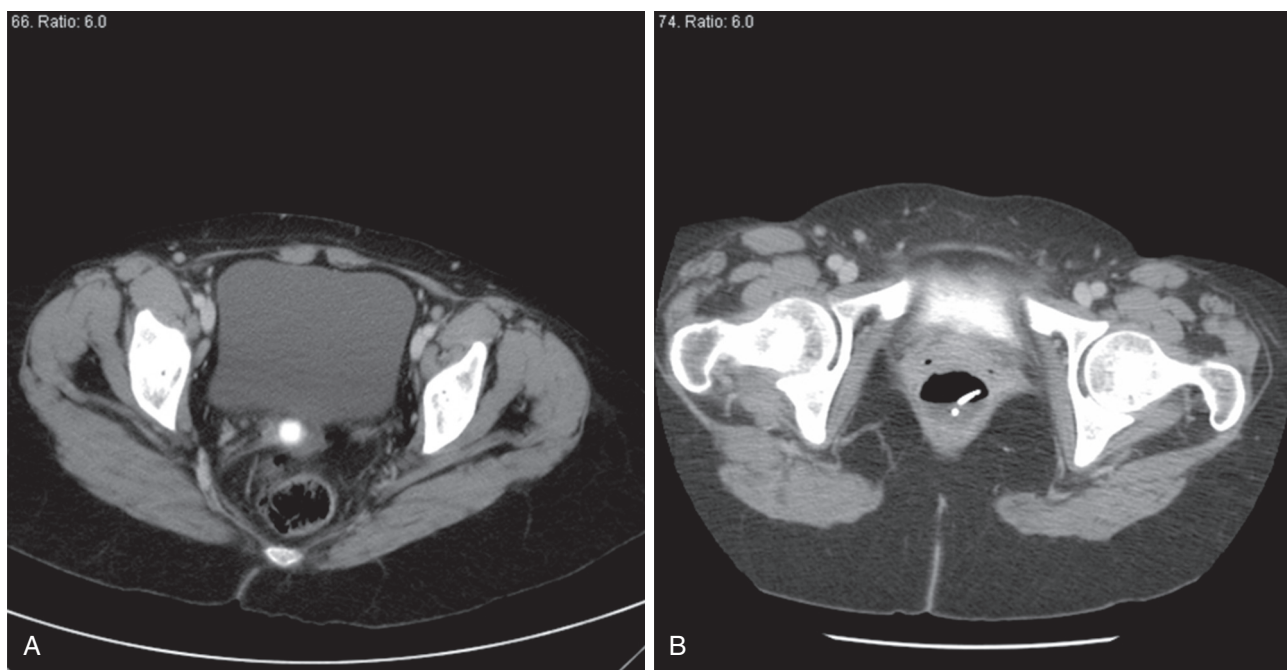
Two studies that compared transcolonic with transrectal drainage routes revealed no difference in rates of technical success, treatment success, or adverse events between cohorts.<sup>16,17</sup> However, one of these studies<sup>16</sup> observed that when evaluated by etiology, treatment success for diverticular abscess was significantly lower compared with others (25% vs. 97%, P = .002).

## Technical Limitations

Some limitations of the EUS-guided technique include the following: (1) transmural stenting may not be possible if an abscess is located greater than 2 cm from the gastrointestinal lumen and



• **Fig. 26.3** (A) A 19-G needle is passed into the pelvic abscess under endoscopic ultrasonography guidance. (B) A 0.035-in guidewire is coiled within the abscess cavity. (C) The transmural tract is dilated using a taper-tip endoscopic retrograde cholangiopancreatography cannula. (D) The transmural tract is then sequentially dilated using an 8-mm balloon dilator. (E) Two double-pigtail plastic stents are deployed within the abscess cavity.



• **Fig. 26.4** (A) A computed tomography (CT) image of the pelvic cavity demonstrating an abscess that measures 80 by 60 mm. (B) After endoscopic ultrasonography-guided drainage, a follow-up CT at 36 hours demonstrates near complete resolution of the abscess.

**TABLE 26.2 Outcome of Endoscopic Ultrasonography-Postoperative Fluid Collection Drainage in Series Involving Seven or More Patients**

Author (Year)	No. of POFc	Location	Mean/Median Size of Abscess (mm)	Technique	Technical Success	Clinical Success	Adverse Event	Recurrence	Required Surgery
Varadarajulu et al. (2007) <sup>4</sup>	10	Perigastric 10	91.4	Stenting (7-Fr/10-Fr PS)	100%	90%	10% (stent migration 1)	None	1
Varadarajulu et al. (2011) <sup>5</sup>	20	Periesophageal 3 Perigastric 17	78.5 × 56.5	Stenting (7-Fr PS)	100%	100%	None	3	None
Ulla-Rocha et al. (2012) <sup>6</sup>	7	Perigastric 4 Perirectal 3	60.6 × 49.9	Stenting (8-Fr PS)	100%	100%	None	NA	None
Gupta et al. (2012) <sup>7</sup>	49	Perigastric 42 Peroduodenal 3 Perijejunal 3 Periesophageal 1	80 ± 4	Stenting (7-Fr/8-Fr PS) and/or Nasocystic drain)	96%	80%	14.6% (bleeding 4, stent migration 2, pulmonary embolism 1)	18	7%
Kwon et al. (2013) <sup>8</sup>	12	Perigastric 12	89	Stenting (8-Fr/10-Fr PS)	100%	100%	None	None	None
Tilara et al. (2014) <sup>9</sup>	31	Perigastric 30 Peroduodenal 1	85 × 60	Stenting (7-Fr/10-Fr PS)	100%	93%	6% (bleeding 1, aspiration pneumonia 1)	NA	None
Téllez-Ávila et al. (2015) <sup>10</sup>	16	Perigastric 14 Peroduodenal 2	65	Aspiration/dilation/stenting	100%	100%	None	4	3

NA, Not applicable; POFc, postoperative fluid collection; PS, plastic stent.

**TABLE 26.3** Outcome of Endoscopic Ultrasonography-Guided Pelvic Abscess Drainage in Series Involving Four or More Patients

Author (Year)	No. of Cases	Location	Mean/Median Size of Abscess (mm)	Technique	Technical Success	Clinical Success	Adverse Event	Required Surgery
Giovannini et al. (2003) <sup>11</sup>	12	Perisigmoid, 12	48.9 by 43.4	Aspiration or Stenting (8.5-Fr/10-Fr PS)	100%	75%	25% (abdominal pain 1, fever 2)	None
Varadarajulu and Drelichman (2007) <sup>12</sup>	4	Pelvic	68 by 72	Drainage catheter	100%	75%	None	None
Trevino et al. (2008) <sup>13</sup>	4	Pelvic	93 by 61	Drainage catheter/stenting	100%	100%	None	None
Varadarajulu and Drelichman (2009) <sup>14</sup>	25	Pelvic	68.5 by 52.4	Drainage catheter/stenting	100%	96%	None	None
Puri et al. (2010) <sup>15</sup>	14	Pelvic	73 by 66	Aspiration/Dilation/Stenting	100%	93%	None	1
Ramesh et al. (2013) <sup>16</sup>	38	Transcolonic 11, Transrectal 27	65 (TC)/70 (TR)	Dilation and stenting (one or two 7-FR PS)	100%	70%/96% (TC/TR)	None	4
Puri et al. (2014) <sup>17</sup>	30	Prostatic 4, Perisigmoid 7, Perirectal 19	25 (P)/47(TR)/54(TC)	Aspiration/dilation/stenting	100%	71%/88% (TC/TR)	None	2
Hadithi and Bruno (2014) <sup>18</sup>	8	Perisigmoid 2 Perirectal 6	73 by 43	Dilation and stenting (one or two 7-FR PS)	100%	100%	None	None

PS, Plastic stent; TC, transcolonic; TR, transrectal.

(2) with the current limited maneuverability of the curvilinear-array echoendoscopes, accessing abscesses that are located more proximally in the colon is not feasible.

## Endoscopic Ultrasonography-Guided Vascular Interventions

EUS-guided vascular treatment has been introduced as a novel technique of emergent or elective hemostasis in the gastric varices.<sup>20–26</sup> Cyanoacrylate (CYA) glues have been traditionally applied for the treatment of these. More recently, intravariceal stainless steel coils are being deployed before glue injection. It is believed that intravariceal deployment of a coil before glue injection may minimize the risk of glue embolization. In addition to gastric varices, coil and/or glue have been successfully applied for the treatment of ectopic and rectal varices.<sup>25,27</sup>

### Procedural Technique

The following procedural steps are undertaken in sequence (Video 26.6):

- First, if required, the gastric fundus is filled with water to aid visualization of the varices.
- An echoendoscope is positioned either in the distal esophagus in an antegrade fashion (transesophageal-transcrural approach) or in the gastric fundus (transgastric approach).
- A coil size is selected based on the short-axis diameter of the varix to be treated.



• **Fig. 26.5** The presence of a coil and glue within the varix as seen at endoscopic ultrasonography.

- The varix is punctured with a saline solution–primed 19- or 22-G FNA needle (depending on the size of coil to be delivered). Intravariceal position can be confirmed by either blood aspiration or the injection of saline solution, which will produce a flow of bubbles.
- The coil is loaded into the needle and advanced by using the stylet or the stiff end of a guidewire.
- Coil deployment within the varix is visualized as a curvilinear echogenic pattern at EUS (Fig. 26.5).

**TABLE 26.4** Outcome of Endoscopic Ultrasonography-Guided Vascular Therapy for Gastric Varices Involving Three or More Patients

Author (Year)	No. of Cases	Technique	Echoendoscope	Route	Size of Needle	Type of Glue/Coil	Single/Multicenter	Technical Success	Rebleeding	Adverse Event
Romero-Castro et al. (2007) <sup>20</sup>	5	CYA injection	OVCLA	TG	22 G	N-Butyl-2-cyanoacrylate	Single	90%	None	None
Romero-Castro et al. (2010) <sup>21</sup>	4	Coil embolization	OVCLA	TG	19 G	8- to 15-mm diameter, 50- to 150-mm length	Single	75%	None	None
Binmoeller et al. (2011) <sup>22</sup>	30	CYA injection + coil embolization	FVCLA/OVCLA	TE	19 G	2-Octyl-cyanoacrylate/12- to 20-mm diameter	Single	100%	16.6%	None
Gonzalez et al. (2012) <sup>23</sup>	3	CYA/PD injection	OVCLA	TG	19 G	N-Butyl-2-cyanoacrylate	Single	100%	None	None
Romero-Castro et al. (2013) <sup>24</sup>	30	CYA injection (19) vs. coil embolization (11)	OVCLA	TG	Injection, 22 G; coil, 19 G	N-Butyl-2-cyanoacrylate/8- to 20-mm diameter, 50- to 150-mm length	Multicenter	97.4% vs. 90.9%	NA	None
Fujii-Lau et al. (2016) <sup>25</sup>	6	CYA injection + coil embolization (3) and coil embolization (3)	OVCLA	NA	Injection, 22 G; coil, 22 G	2-Octyl-cyanoacrylate/6- to 10-mm diameter, 70- to 140-mm length	Single	100%	None/33% (esophageal varices)	None
Bhat et al. (2016) <sup>26</sup>	152	CYA injection and coil embolization	FVCLA/OVCLA	TG/TE	19G or 22G	2-Octyl-cyanoacrylate/10- to 20-mm diameter, 70- to 140-mm length	Single	99%	16% (early/late:12/8)	Pain 4, PE 1, bleeding 1

CYA, Cyanoacrylate; FVCLA, forward-view curved linear array echoendoscope; G, gauge; OVCLA, oblique-view curved linear array echoendoscope; PD, polidocanol; PE, pulmonary embolism; TE, transesophageal; TG, transgastric.

7. Coil deployment is immediately followed by the injection of 1 mL of undiluted acrylate glue over 45 to 60 seconds. The glue produces intense echogenicity and shadowing as it fills the varix lumen.
8. The needle is flushed with 1 mL of saline solution to clear glue in the “dead space” and is then withdrawn into the sheath. After the injection of glue, the sheath is advanced 2 to 3 cm beyond the echoendoscope’s tip and the scope is withdrawn to avoid any contact of CYA with the echoendoscope’s working channel.
9. Several minutes are allowed for complete glue polymerization. Varix obliteration is confirmed with color-flow Doppler. Alternatively, the treated varix can be blunt “palpated” with a closed forceps under endoscopic guidance. An obliterated varix will be hard on palpation.

### Technical and Treatment Outcomes

Seven case series have been published evaluating the technical and treatment outcomes of EUS-guided vascular therapy (Table 26.4).<sup>20–26</sup> Glue alone, coil embolization alone, or

glue in combination with coil embolization were used. Except for two case series in which a forward-view echoendoscope was used,<sup>22,26</sup> the oblique-view curved linear array echoendoscope was used. The procedures can be performed using either a 19- or 22-G needle. Two types of glue, N-butyl-2-CYA or 2-octyl-CYA, were used in the clinical studies. They appear to have similar efficacy for achieving hemostasis and preventing recurrent bleeding. Although the gastric varices can be accessed via the esophagus or the stomach, the transesophageal route enables injection in a straight scope position and is unencumbered by the presence of gastric contents. In addition, by avoiding puncture across the gastric mucosa, often thinned out by large varices, “backbleeding” into the gastric lumen after needle removal can be prevented. Regardless of the route of access, technical success was almost 100% in all series. A comparative study revealed that there was no significant difference in treatment success rates between glue injection and coil embolization (97.4% vs. 90.9%), respectively.<sup>24</sup> One large case series reported procedure-related adverse events in 7%, including one case of pulmonary embolization, and early or late posttreatment bleeding in 16% of patients.<sup>26</sup>

## Technical Limitations

Limitations of the EUS-guided vascular technique include the following: (1) limited access to the varices via either approach due to difficult echoendoscope positioning or patient anatomy and (2) local complications such as bleeding and embolic incidents induced by injection therapy.

## Key References

16. Ramesh J, Bang JY, Trevino JM, et al. Comparison of outcomes between endoscopic ultrasound-guided transcolonic and transrectal drainage of abdominopelvic abscesses. *J Gastroenterol Hepatol*. 2013;28:620–625.
17. Puri R, Choudhary NS, Kotecha H, et al. Endoscopic ultrasound-guided pelvic and prostatic abscess drainage: experience in 30 patients. *Indian J Gastroenterol*. 2014;33:410–413.
24. Romero-Castro R, Ellrichmann M, Ortiz-Moyano C, et al. EUS-guided coil versus cyanoacrylate therapy for the treatment of gastric varices: a multicenter study (with videos). *Gastrointest Endosc*. 2013;78:711–721.
25. Fujii-Lau LL, Law R, Wong Kee Song LM, et al. Endoscopic ultrasound (EUS)-guided coil injection therapy of esophagogastric and ectopic varices. *Surg Endosc*. 2016;30:1396–1404.
26. Bhat YM, Weilert F, Fredrick RT, et al. EUS-guided treatment of gastric fundal varices with combined injection of coils and cyanoacrylate glue: a large U.S. experience over 6 years (with video). *Gastrointest Endosc*. 2016;83:1164–1172.

## References

Access the reference list online at [ExpertConsult.com](http://ExpertConsult.com).



## References

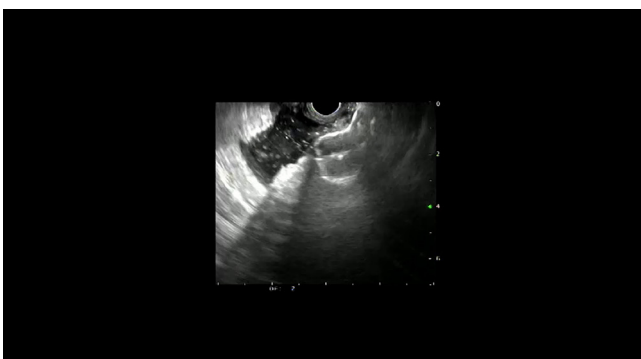
1. Khashab MA, Kumbhari V, Grimm IS, et al. EUS-guided gastroenterostomy: the first U.S. clinical experience (with video). *Gastrointest Endosc.* 2015;82:932–938.
2. Itoi T, Ishii K, Ikeuchi N, et al. Prospective evaluation of endoscopic ultrasonography-guided double-balloon-occluded gastrojejunostomy bypass (EPASS) for malignant gastric outlet obstruction. *Gut.* 2016;65:193–195.
3. Tyberg A, Perez-Miranda M, Sanchez-Ocaña R, et al. Endoscopic ultrasound-guided gastrojejunostomy with a lumen-apposing metal stent: a multicenter, international experience. *Endosc Int Open.* 2016;4:E276–E281.
4. Varadarajulu S, Trevino JM, Christein JD. EUS for the management of peripancreatic fluid collections after distal pancreatectomy. *Gastrointest Endosc.* 2009;70:1260–1265.
5. Varadarajulu S, Wilcox CM, Christein JD. EUS-guided therapy for management of peripancreatic fluid collections after distal pancreatectomy in 20 consecutive patients. *Gastrointest Endosc.* 2011;74:418–423.
6. Ulla-Rocha JL, Vilar-Cao Z, Sardina-Ferreiro R. EUS-guided drainage and stent placement for postoperative intra-abdominal and pelvic fluid collections in oncological surgery. *Therap Adv Gastroenterol.* 2012;5:95–102.
7. Gupta T, Lemmers A, Tan D, et al. EUS-guided transmural drainage of postoperative collections. *Gastrointest Endosc.* 2012;76:1259–1265.
8. Kwon YM, Gerdes H, Schattner MA, et al. Management of peripancreatic fluid collections following partial pancreatectomy: a comparison of percutaneous versus EUS-guided drainage. *Surg Endosc.* 2013;7:2422–2427.
9. Tilara A, Gerdes H, Allen P, et al. Endoscopic ultrasound-guided transmural drainage of postoperative pancreatic collections. *J Am Coll Surg.* 2014;218:33–40.
10. Téllez-Ávila F, Carmona-Aguilera GJ, Valdovinos-Andraca F, et al. Postoperative abdominal collections drainage: Percutaneous versus guided by endoscopic ultrasound. *Dig Endosc.* 2015;27:762–726.
11. Giovannini M, Bories E, Mourtadier V, et al. Drainage of deep pelvic abscesses using therapeutic echo endoscopy. *Endoscopy.* 2003;35:511–514.
12. Varadarajulu S, Drelichman ER. EUS-guided drainage of pelvic abscess. *Gastrointest Endosc.* 2007;66:372–376.
13. Trevino J, Drelichman ER, Varadarajulu S. Modified technique for EUS-guided drainage of pelvic abscess. *Gastrointest Endosc.* 2008;68:1215–1219.
14. Varadarajulu S, Drelichman ER. Effectiveness of EUS in drainage of pelvic abscesses in 25 consecutive patients. *Gastrointest Endosc.* 2009;70:1121–1127.
15. Puri R, Eloubeidi MA, Sud R, et al. Endoscopic ultrasound-guided drainage of pelvic abscess without fluoroscopy guidance. *J Gastroenterol Hepatol.* 2010;25:1416–1419.
16. Ramesh J, Bang JY, Trevino JM, et al. Comparison of outcomes between endoscopic ultrasound-guided transcolonic and transrectal drainage of abdominopelvic abscesses. *J Gastroenterol Hepatol.* 2013;28:620–625.
17. Puri R, Choudhary NS, Koticha H, et al. Endoscopic ultrasound-guided pelvic and prostatic abscess drainage: experience in 30 patients. *Indian J Gastroenterol.* 2014;33:410–413.
18. Hadithi M, Bruno MJ. Endoscopic ultrasound-guided drainage of pelvic abscess: a case series of 8 patients. *World J Gastrointest Endosc.* 2014;6:373–378.
19. Itoi T, Binmoeller, Shah J, et al. Clinical evaluation of a novel lumen-apposing metal stent for endosonography-guided pancreatic pseudocyst and gallbladder drainage (with video). *Gastrointest Endosc.* 2012;75:870–876.
20. Romero-Castro R, Pellicer-Bautista FJ, Jimenez-Saenz M, et al. EUS-guided injection of cyanoacrylate in perforating feeding veins in gastric varices: results in 5 cases. *Gastrointest Endosc.* 2007;66:402–407.
21. Romero-Castro R, Pellicer-Bautista FJ, Giovannini M, et al. Endoscopic ultrasound (EUS)-guided coil embolization therapy in gastric varices. *Endoscopy.* 2010;42:E35–E36.
22. Binmoeller KF, Weilert F, Shah JN, et al. EUS-guided transesophageal treatment of gastric fundal varices with combined coiling and cyanoacrylate glue injection (with videos). *Gastrointest Endosc.* 2011;74:1019–1025.
23. Gonzalez JM, Giacino C, Pioche M, et al. Endoscopic ultrasound-guided vascular therapy: is it safe and effective? *Endoscopy.* 2012;44:539–542.
24. Romero-Castro R, Ellrichmann M, Ortiz-Moyano C, et al. EUS-guided coil versus cyanoacrylate therapy for the treatment of gastric varices: a multicenter study (with videos). *Gastrointest Endosc.* 2013;78:711–721.
25. Fujii-Lau LL, Law R, Wong Kee Song LM, et al. Endoscopic ultrasound (EUS)-guided coil injection therapy of esophagogastric and ectopic varices. *Surg Endosc.* 2016;30:1396–1404.
26. Bhat YM, Weilert F, Fredrick RT, et al. EUS-guided treatment of gastric fundal varices with combined injection of coils and cyanoacrylate glue: a large U.S. experience over 6 years (with video). *Gastrointest Endosc.* 2016;83:1164–1172.
27. Weilert F, Shah JN, Marson FP, et al. EUS-guided coil and glue for bleeding rectal varix. *Gastrointest Endosc.* 2012;76:915–916.



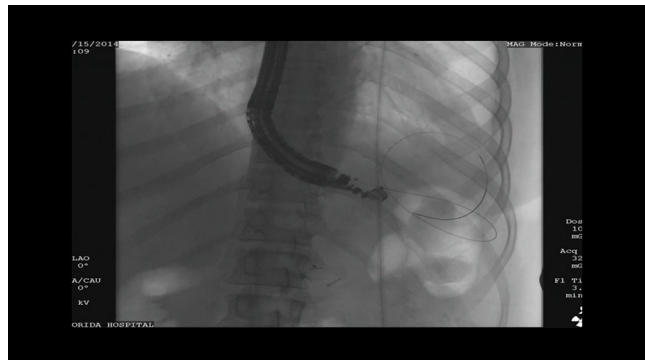
**Video 26.1** The Technique of Direct Endoscopic Ultrasonography-Guided Gastroenteric Anastomosis



**Video 26.2** The Technique of Balloon Assisted Endoscopic Ultrasonography-Gastroenteric Anastomosis



**Video 26.3** Endoscopic Ultrasonography-Guided Balloon-Occluded Gastrojejunostomy Bypass Technique



**Videos 26.4** Endoscopic Ultrasonography-Guided Drainage of a Peripancreatic Fluid Collection After a Distal Pancrectomy



**Video 26.5** Endoscopic Ultrasonography-Guided Drainage of a Pelvic Abscess



**Video 26.6** Endoscopic Ultrasonography-Guided Variceal Obliteration by Placement of Coils

# Index

## A

Abdominopelvic fluid collections,  
EUS-guided drainage of, 332–337  
procedural technique, 332–334  
  prophylactic antibiotics, 332–334  
  steps, 334, 335f–337f  
technical and treatment outcomes, 334  
technical limitations, 334–337

Aberrant pancreas, 116–118, 118f  
  definition, 116–117  
  diagnostic checklist, 116b  
ectopic pancreas, 116–117  
heterotopic pancreas, 116–117  
pancreatic rest, 116–117

Abscesses, 107–108

Absorption, 4

Accessories, 21  
  fine-needle aspiration needles, 21–22, 22t, 23f  
  fine-needle biopsy needles, 22–28, 24f–25f, 24t

ACGME-accredited gastroenterology fellowship programs, 32–33

ACGME/NAS, 33

Acoustic impedance, 3

Acquire needle, 267–270, 268f, 270f

Acute necrotic fluid collections, 291, 292f

Acute pancreatitis, 151–159, 206–207  
  acute biliary pancreatitis, 151, 151t, 152f–153f  
  acute idiopathic pancreatitis, 151–152, 154f–156f  
  advanced endoscopic ultrasound techniques, 159  
  EUS, 151–156  
  overview, 151  
  recurrent acute pancreatitis, 156, 157f–159f

Acute peri-PFC, 291

Adenomas, 218–219  
  benign, 218–219

Adenomatous polyps, 215

Adrenal glands, 63–64, 63f  
  EUS FNA of, 289

Adverse effects, risks, 44–46  
  bleeding, 45  
  esophageal cancer, 44  
  esophagus intubation, 44

EUS and EUS FNA, 45

infection, 45

pancreatitis, 45

perforation, 44–45

therapeutic endoscopic ultrasound, 45–46

AES. *See* Anal endosonography (AES)

Air-dried smear, 277

AJCC. *See* American Joint Committee on Cancer (AJCC)

Alcohol-fixed smear, 277

Alliance II system, in EUS FNTA, 262

American College of Gastroenterology (ACG), 36

American Joint Committee on Cancer (AJCC), 36, 172

  ampullary tumors, 221–222, 222t

  gallbladder cancer, 216, 216t

  pancreatic cancer, 173, 173t

  rectal cancer, 230, 230t

American Society for Gastrointestinal Endoscopy (ASGE), 41  
  advanced endoscopy fellowships training, 31

  privileges

    credentialing, EUS, 33–36

    recredentialing, EUS, 33–36

    renewal, EUS, 33–36

  quality metrics, EUS, 36

  simulators, 36

  training, 30–31

American Thoracic Society (ATS), 61

Ampullary lesions, examination checklist for, 201b

Ampullary tumors

  adenomas, 218–219

  AJCC classification, 221–222, 222t

  algorithm management, 219–221, 221f

  benign adenomas, 218–219

  biliary stent and pancreatic stent, 218–219, 219f

  diagnosis of, 219–221

  diagnostic checklist for, 224b

  with dilated bile duct and elevated

    transaminases, 219–221, 220f

  imaging modalities, 221–222

  intraductal extension, of tumor, 219–221, 221f

  intraductal ultrasonography (IDUS), 223–224, 223f

  large polypoid ampullary mass, 222–223, 223f

  mucosal biopsies, 218–219, 219f

  multimodality approach, 219f, 224

    duodenoscopy, 224

    EUS, 224

    IDUS, 224

Ampullary tumors (*Continued*)

  muscularis propria (MP), 219–221, 220f

  painless jaundice, 219–221, 221f

  pancreatic parenchyma, 219–221, 220f

  papillary carcinoma, 219–221

  radial endoscopic ultrasound image

  large ampullary mass infiltrating,

    222–223, 222f

  uT1sm ampullary tumor (TU), with

    disruption of submucosa (SM),

    222–223, 223f

  staging, 222–223, 223t

  T3 ampullary mass, 219–221, 220f

  TNM staging for, 221–222, 222t

Anal endosonography (AES), 237

  anal incontinence, treatment of, 246

  applications, 246

  disadvantage of, 246–247

  fecal incontinence, 237

  in fistula disease, 246–247

  fistula-in-ano, 246

  interpretation of, 239–240

  intersphincteric abscess, 246–247

  midanal canal, 239–240, 241f

  obstetric injury, 237

  sphincter defects, 241–242

  vaginal delivery, 244

Anal sphincter

  anal incontinence, sonographic findings in,

    242–246

  external anal sphincter atrophy, 245

  iatrogenic sphincter injury and anal

    trauma, 245–246

  idiopathic internal anal sphincter

    degeneration, 245

  obstetric injury, 242–245

  prevalence, 242

  anatomy of, 238–239, 239f

  anorectal physiologic testing, 241–242

    electromyography, 241–242

    manometry, 241

    pudendal nerve latency, 241

  equipment and examination technique,

    237–238

  anatomic levels, 238

  placing women and men, 238

  probes for, 237, 238f

  transducer, 237

  function of, 240–241

  normal endosonographic findings,

    239–240

- Anal sphincter (*Continued*)  
 anal endosonography (AES), 239–240, 241f  
 distal anal canal, 239, 240f  
 mid-anal canal, 239, 240f–241f  
 probe withdrawing, 239  
 proximal anal canal, 239, 240f  
 other anal disorders, sonographic findings  
   in, 246–247  
   abscesses, 246  
   fistula-in-ano, 246  
   solitary rectal ulcer syndrome, 247, 247f  
   tumors, 247, 247f  
   recent developments, 247–248
- Anal squamous tumor, 247, 247f
- Anal stretch, for anal fissure, 246
- Anal subepithelial tissues, 239
- Anal trauma, 245–246
- Anastomosis, EUS-guided, 330–332  
 procedural technique  
   assisted EUS-GE technique, 332  
   EUS-guided balloon-occluded  
     gastrojejunostomy bypass (EPASS), 332, 333f  
   EUS-guided gastroenterostomy (EUS-GE), 330, 331f  
 technical and treatment outcomes, 332, 333t  
 technical limitations, 332
- Ancillary cytology-based techniques, 208
- Anorectal anatomy, rectal cancer, 229–230
- Anorectal EUS  
 perianal area, 226  
 rectum  
   antibiotic administration, 227–228  
   examination, 226  
   linear echoendoscopes, 226–227  
   prostate, 227, 227f  
   rectal wall layers, 227, 227f  
   urinary bladder, 227, 227f  
   uterus and vagina, 227, 228f
- Anorectal physiologic testing, 241–242  
 electromyography, 241–242  
 manometry, 241  
 pudendal nerve latency, 241
- Antibiotic prophylaxis, 190
- Anticoagulant therapy, 250
- Antiplatelet therapy, 250
- Antithrombotic drugs  
 ASGE, 41  
 BSG, 41  
 continuation, 43  
 endoscopic polypectomy, 42  
 endoscopic procedures, 41  
 EUS FNA, 41  
 EUS-guided therapy, 41  
 guidelines, 42  
 hemorrhage, 42  
 periprocedural management, 41  
 resuming antithrombotic therapy, 43  
 sphincterotomy, 42
- Aortic arch (AO), 61, 62f
- Aortopulmonary window, 62, 63f
- Area under receiver operating characteristic (AUROC), 49–50
- Artificial neural network (ANN) model, 50
- Ascites, 171  
 peritoneal carcinomatosis manifesting, 174–175, 175f
- ASGE. *See* American Society for Gastrointestinal Endoscopy (ASGE)
- Aspirates  
 fine-needle, 273–274  
 adequacy, 277  
 of lymph nodes, 286–287, 287f  
 paucicellular, 285  
 processing of, 254f, 256
- Aspirin, 250
- Assisted EUS-GE technique, 332
- Atrophy, 245
- ATS. *See* American Thoracic Society (ATS)
- Attenuation coefficient, 4
- Autoimmune pancreatitis, 53, 159–169  
 contrast-enhanced endoscopic ultrasound, 169  
 endoscopic ultrasound elastography, 169  
 endoscopic ultrasound sampling, 163–169  
 EUS, 161, 162t–163t, 163f–166f  
 EUS fine-needle biopsy (FNB), 168–169  
 FNA, 163–168  
 image-enhancing techniques, 169  
 imaging characteristics, 161–163, 166f–168f  
 overview, 159, 160f, 161t  
 tru-cut biopsy, 168
- Autoimmune pancreatitis (AIP), 263–264
- Axial resolution, 6, 6f
- AXIOS Stent, 26
- Azygous vein, 61, 62f
- B**
- Balloon dilation, for single-gate technique, 294–295, 295f
- Balloon inflation method  
 esophagus, 59  
 stomach EUS, 110, 110f
- Barrett esophagus, 60
- Beacon needle, 21–22
- Benign adenomas, 218–219
- Benign pancreatic masses, 169–170  
 contrast-enhanced endoscopic ultrasound, 170  
 endoscopic ultrasound elastography, 170  
 endoscopic ultrasound-guided core biopsy, 169  
 endoscopic ultrasound sampling, 169  
 EUS FNA, 169  
 image-enhancing techniques, 170  
 overview, 169
- Benign posterior mediastinal lymph nodes, 100, 101f, 104–105  
 granulomatous lymph nodes, 104  
 histoplasmosis, 105  
 other infections, 105  
 reactive lymph nodes, 104  
 sarcoid, 104, 105f, 105t  
 tuberculosis, 105, 105f, 105t
- Benign posterior mediastinal masses, 107–108  
 abscesses, 107–108  
 mediastinal cysts, 107, 107f  
 mediastinal pseudocysts, 107–108
- Bile duct, 137–138  
 color Doppler imaging, 137, 137f  
 duodenal falloff, 137–138  
 duodenal lumen, 138  
 stone, 138
- Bile duct strictures  
 benign, 208  
 cholangiocarcinoma, staging of, 214, 214f  
 cholangioscopy, 212–213  
 EUS FNA, 208–210, 211f  
 biliary stents, 209, 212f  
 cholangiocarcinoma lesions, 208–209, 208f  
 clinical ramifications, of needle track seeding, 210  
 cytology photomicrograph, 208–209, 209f  
 cytopathological considerations, 209  
 operating characteristics, 208–209, 210t  
 performance characteristics, 208–209, 211t  
 sensitivity and specificity rates, 208–209  
 technique, 208f, 209  
 tumor seeding, 209
- Intraductal ultrasonography (IDUS), 210–212  
 accuracy of, 210–212  
 algorithm management, 210–212, 213f  
 biliary papillomatosis, 210–212  
 cholangiocarcinoma, 210–212, 212f  
 vs. ERCP, 210–212  
 layers, 210–212  
 primary sclerosing cholangitis (PSC), 210–212
- malignant, 208
- multimodality approach, 213–214, 213f  
 for CBD strictures, 213  
 for common hepatic duct and hilar strictures, 214
- Biliary-pancreatic ductal systems, EUS-guided  
 drainage of, 307–310  
 algorithm for, 309  
 considerations, 314–316  
 indications for, 303t, 307  
 nomenclature, 308, 308f  
 outcomes of, 308–309, 308t  
 procedure, 316, 317f  
 troubleshooting, 316
- Biliary papillomatosis, 210–212
- Biliary sludge, 206–207
- Biliary stones  
 bile duct stones, 201  
 choledocholithiasis, 201–205  
 algorithm management, 203–204, 206f  
 diagnosis of, 202  
 echo-dense structures, 201–202, 202f  
 endoscopic retrograde cholangiopancreatography (ERCP), 202–203

- Biliary stones (*Continued*)  
 extraductal catheter probe EUS (EDUS), 204–205  
 intermediate risk patients, 203–204  
 intraductal ultrasonography (IDUS), 204–205  
 linear echoendoscope, 202  
 magnetic resonance  
   cholangiopancreatography (MRCP), 205t  
 noninvasive imaging modalities, 202–203  
 radial echoendoscopes, 202  
 examination checklist for, 201b
- Biopsy**  
 EUS-guided fine-needle, 261–271.e3  
 forceps, 332
- Bleeding**, risks of, 45
- Body-tail junction**, pancreas, 129–130, 130f
- Brachytherapy**, EUS-guided, 322
- Branch duct intraductal papillary mucinous neoplasia (BD-IPMN)**, 195, 195f
- Branch duct intraductal papillary mucinous neoplasia (IPMN)**, 191, 192f
- British Society of Gastroenterology (BSG)**, 41
- Bruel-Kjaer mechanical radial rigid probe**, 226
- BSG**. *See* British Society of Gastroenterology (BSG)
- Bulk modulus**, 2–3, 3t
- Butterfly technique**, 276
- C**
- CA** 15-3, 191  
 CA 19-9, 191  
 CA 72-4, 191  
 CA 125, 191  
**Capillary (“slow-pull”) technique**, EUS FNA of, 257  
**Carbon dioxide insufflation**, 310  
**Carcinoembryonic antigen (CEA)**  
 protein markers, 187t, 191  
 with string test, 190–191  
**Carcinoid tumor**, 118, 119f  
**Cautery devices**, 310  
**CE EUS**. *See* Contrast-enhanced endoscopic ultrasound (CE EUS)  
**Celiac artery**, pancreas body and tail, 129, 130f  
**Celiac ganglion irradiation**, 323  
**Celiac plexus**  
 block/neurolysis, 327f  
 injections, 327–328, 327f  
   clinical outcomes, 328, 329t  
   clinical trials of, 329t  
   procedural technique, 327–328, 327f–328f  
   interventions, 320–329.e3  
**Celiac trunk**, 129, 130f  
**Cell block**, cytology, 276  
**Chemotherapeutic drug delivery**  
 desmoplastic stroma, 183–184
- Cholangiocarcinoma**  
 diagnostic checklist for, 214b  
 staging of, 214, 214f  
**Cholangioscopy**, bile duct strictures, 212–213
- Choledocholithiasis**  
 biliary stones, 201–205  
   algorithm management, 203–204, 206f  
   diagnosis of, 202  
   echo-dense structures, 201–202, 202f  
   endoscopic retrograde  
    cholangiopancreatography (ERCP), 202–203  
   extraductal catheter probe EUS (EDUS), 204–205  
   intermediate risk patients, 203–204  
   intraductal ultrasonography (IDUS), 204–205  
   linear echoendoscope, 202  
   magnetic resonance  
    cholangiopancreatography (MRCP), 205t  
   noninvasive imaging modalities, 202–203  
   radial echoendoscopes, 202
- Cholelithiasis**, transabdominal ultrasonography (TUS), 206
- Chronic cholecystitis**, 217
- Chronic pancreatitis**, 140–151, 172, 177, 178f  
 advanced endoscopic ultrasound techniques, 151  
 celiac plexus block (CPB), 151  
 computed tomography (CT), 141  
 conventional and rosemont classification, 144  
 criteria, EUS, 141–142, 147f–149f, 149t  
 endoscopic retrograde  
   cholangiopancreatography (ERCP), 141  
 EUS, 141, 142f–147f  
 EUS elastography, 147–151  
 fibrosis, 144–145  
 findings and surgical histopathology, 144–146, 150f  
 imaging characteristics, 141–146  
 interobserver variability (IOA), 146  
 magnetic resonance  
   cholangiopancreatography (MRCP), 141  
   magnetic resonance imaging (MRI), 141  
 MPD, 141  
 overview, 140–141  
 pancreatic adenocarcinoma (PaC), 146–147  
 sampling, EUS, 146–147  
 smears, 279–280, 282f  
**Chronic pseudotumoral pancreatitis**, 48f, 50
- Ciprofloxacin**, 190
- Clinical Laboratory Improvement Amendments of 1988 (CLIA 1988)**, 273
- Club head**, pancreas body and tail, 129, 130f
- Cognitive education**, 30
- Coil deployment**, 337
- College of American Pathologists (CAP)**, 273
- Color Doppler imaging**, bile duct, 137, 137f
- Common bile duct (CBD) stones**, 201  
 balloon sweeping, 203f, 224.e9  
 diagnosis of, 201, 204t  
 diagnostic checklist for, 207b  
 endoscopic retrograde  
   cholangiopancreatography (ERCP), 202–203  
 extraductal catheter probe EUS (EDUS), 204–205  
 fluoroscopy image of, 203f, 224.e9  
 imaging modalities, 201  
 intraductal ultrasonography (IDUS), 204–205  
 magnetic resonance  
   cholangiopancreatography (MRCP), 202  
 periampillary region, 202  
 stone confirmation by biliary sphincterotomy, 203f, 224.e9  
 transabdominal ultrasonography (TUS), 201  
 two-dimensional intraductal ultrasonography, 204–205, 206f
- Competence assessments**, 33  
 formative assessment, 33  
 summative assessment, 33
- Compressibility**, 2–3  
 ultrasound and, 2–3
- Computed tomography (CT)**, 36, 39, 60, 100, 179
- CBD stones**, 201  
*vs.* endoscopic ultrasonography, 230t, 233–234  
*vs.* EUS  
 obstructive jaundice, 172, 173f  
 suspected pancreatic cancer, 172, 173f
- pancreatic fluid collections (PFCs)**, 291
- pelvic abscess drainage guided with**, 332
- peritoneal metastases**, 174–175
- tumor classification and vascular involvement**, 173–174
- Confocal laser endomicroscopy (CLE)**, 25–26, 26f  
 for pancreatic cysts, 185, 189f
- Contraindications**, 40
- Contrast-enhanced endoscopic ultrasound (CE EUS)**  
 pancreatic cysts, 186–188  
 pancreatic ductal adenocarcinoma, 172  
 vascularity, 186–188
- Contrast-enhanced endoscopic ultrasound elastography**  
 clinical applications, 52–56  
 contrast-enhanced transabdominal ultrasound, 57
- Doppler signal enhancement**, 52
- dynamic contrast harmonic imaging (dCHI)**, 52
- future techniques**, 56–57
- gastrointestinal stromal tumor (GISTs)**, 56, 56f
- mechanical index (MI) techniques**, 52

Contrast-enhanced endoscopic ultrasound elastography (*Continued*)  
other applications, 56, 56f  
pancreatic diseases, 53–56  
peak negative pressure (PNP), 52  
phospholipid-stabilized microbubbles, 52  
real-time polymerase chain reaction (RT-PCR), 56  
sulfur hexafluoride, 52  
technical details, 52  
time-intensity curves (TIC analysis), 52  
transabdominal ultrasound, 52  
ultrasound contrast agents (UCAs), 52  
vascular endothelial growth factor (VEGF), 56

Contrast-enhanced harmonic (CEH) EUS, 12–14, 13f, 215

Contrast-enhanced power Doppler, 53, 53f–54f

Core biopsy needles, 219–221

Cryotherapy (cool-tipped RFA), 321t, 322f

CT-guided biopsy, 40

Cumulative sum analysis (CUSUM), 32, 32f

CUSUM. *See* Cumulative sum analysis (CUSUM)

Cyanoacrylate (CYA) glues, 337

Cyst ablation, 199–200

Cyst fluid  
analysis of, 188–192  
aspirate appearance and string test, 190–191, 190f  
cytology, 191  
EUS FNA, 191–192, 192f  
molecular markers, 191  
protein markers, 191  
molecular analysis of, 286, 286f

Cyst fluid amylase, 191

Cystic lesions, EUS FNA of, 259

Cystic pancreatic ductal adenocarcinoma, 185, 198, 199f

Cystic pancreatic lesions  
EUS FNA of, 283–286, 285f  
ancillary studies, 285–286, 286t  
false diagnosis, 285  
intraductal papillary mucinous neoplasia (IPMN), 284–285, 285f  
molecular analysis of cyst fluid, 286, 286f  
mucinous cystic neoplasm, 285, 285f  
newer markers, 286

Cystic pancreatic neuroendocrine tumors (PanNETs), 197–198, 198f

Cystogastrostomy  
EUS-guided, 291–292  
surgical, 291–292

Cysts, 121f, 121f, 120–122. *See* Pancreatic cysts

Cytology, 272–290.e4  
cyst fluid analysis, 191  
EUS FNA of specific sites, 279–289  
adrenal glands, 289  
gastrointestinal tract, 288–289

Cytology (*Continued*)  
hepatobiliary tree, 289  
pancreas, 279–286  
spleen, 288  
factors, with improved cytologic preparation, 276–278  
air-dried/alcohol-fixed smears, 277  
diagnostic evaluation of slide, 277–278  
interpretation, 277  
smears and cell block, 276  
transport media and liquid-based preparations, 277  
technical aspects improve diagnostic yield, 272–276  
choice of needles, 274  
fine-needle aspirates, 273–274  
immediate cytologic evaluation, 275–276  
needle core biopsy *vs.* fine-needle aspiration, 274–275  
number of passes, 275  
preliminary planning, 272–273, 273t  
suction, to apply or not, 275

## D

Dabigatran, 250  
Deeper sedation, 41  
Defecation, 241  
Dendritic cells (DCs), 325  
Denonvilliers fascia, 230  
De novo rectal cancer, 231–233  
N-staging considerations  
benign and malignant lymph nodes, 232, 232t  
performance characteristics, 232, 232t  
preoperative FNA identification, 233  
T3N1 lesion, 54-year-old male, 232, 232f

T-staging considerations, 231–232, 231f, 232t  
Density, 2–3, 3t  
Diagnostic imaging

EBUS TBNA diagnosis and staging, 72–74, 73f  
combined nodal staging, 75, 75f  
endoscopic ultrasonography, 75, 76t  
intrapulmonary tumors (T) staging, 72, 74f  
nodal staging (N), 73–74, 74f  
procedure, 72, 73f  
surgical staging, 75, 76t  
EUS FNA for diagnosis and staging of, 65–70, 66t  
distant metastases (M1) staging, 70, 71f–72f  
endoscopic ultrasonography, diagnostic reach of, 67–69  
endoscopic ultrasonography *vs.*, 69, 70f–71f  
intrapulmonary tumors (T) staging, 66, 67f  
left paratracheal lymph node, 67–69, 68f  
lower paratracheal lymph node, 67–69, 68f

Diagnostic imaging (*Continued*)  
mediastinal nodal (N) staging, 66–67  
mediastinal (N) staging, 69–70  
procedure, 65, 66f  
video-assisted thoracoscopy (VATS), 67–69  
indications, 39  
Diff-Quik-stained smears, 274  
Digital microdissection, 183–184  
Direct ganglia injection, 328  
Disconnected pancreatic duct syndrome (DPDS), 299, 300f  
Distal anal canal, 239  
Distant metastases  
metastatic pancreatic cancer, 174–175, 175f  
M1 staging, 70, 71f–72f  
peritoneal carcinomatosis, 174–175, 175f  
Doppler effect, 7–8, 8f  
color Doppler, 8  
continuous-wave Doppler, 7–8  
Doppler shift, 7  
power Doppler, 8  
Drainage. *See* EUS-guided drainage  
Dual modality technique, for EUS-guided drainage, 296–297  
Dual-sphincter disease, 241  
Duodenal bulb  
EUS FNA particularities, 258  
Duodenal falloff, bile duct, 137–138  
Duodenal sweep, EUS FNA particularities, 258  
Duplex scanning, 8  
Dynamic contrast harmonic imaging (dCHI), 52  
Dysplasia, 209

**E**

Early esophageal cancer, 87–88, 88f  
endoscopic evaluation, 88, 88t  
high-frequency probes, 88  
EBUS. *See* Endobronchial ultrasound (EBUS)  
EBUS Assessment Tool (EBUSAT), 73–74  
EBUS TBNA. *See* Endobronchial ultrasound-guided transbronchial needle aspiration (EBUS TBNA)  
Echoendoscopes  
AES using, 237  
anorectal EUS, 226–227  
balloon catheter, 332  
EUS-guided drainage, 310  
pancreas  
linear, 131–132  
radial, 129–131  
EchoTip ProCore 20 G, 264  
characteristics of, 264, 266t  
EchoTipUltra Celiac Plexus Neurolysis Needle, 25, 25f  
Elastography, EUS, 11–12, 13f, 19, 20f  
Electromyography, of anal sphincter, 241–242  
Electronic radial echoendoscope, 59  
Elevation resolution, 6

Endobronchial EUS (EBUS)  
posterior mediastinal lesions, 102  
Endobronchial ultrasound (EBUS), 40, 102  
Endobronchial ultrasound-guided  
transbronchial needle aspiration (EBUS TBNA)  
diagnosis and staging, 72–74, 73f  
combined nodal staging, 75, 75f  
endoscopic ultrasonography, 75, 76t  
intrapulmonary tumors (T) staging, 72, 74f  
nodal staging (N), 73–74, 74f  
procedure, 72, 73f  
surgical staging, 75, 76t  
Endoscope-based confocal laser  
endomicroscopy (eCLE), 25–26  
Endoscopic evaluation, 88, 88t  
Endoscopic mucosal resection (EMR), 110–111  
Endoscopic necrosectomy, for EUS-guided drainage, 297, 300f  
Endoscopic retrograde cholangiography (ERC), 212–213  
Endoscopic retrograde  
cholangiopancreatography (ERCP), 15, 201, 206, 302–304  
cholangioscopy, 212–213  
intraductal tissue sampling, 208  
obstructive jaundice, 208  
tissue sampling, 208  
tumor staging, 208  
Endoscopic retrograde pancreaticography (ERP), 307  
Endoscopic sphincterotomy (ES), 201  
Endoscopic submucosal dissection (ESD), 112  
Endoscopic ultrasonography-guided  
fine-needle aspiration (EUS FNA)  
accessories, for tissue acquisition, 176  
fanning, 176  
needle size, 176  
route of, 176  
stylet, 176  
suction, 176  
accuracy, 102–103, 102t  
adenocarcinoma, 174–175, 175f  
of adrenal glands, 289  
adverse events of, 177  
anatomical challenges, 251  
anticoagulant therapy, 250  
antiplatelet therapy, 250  
bile duct strictures, 208–210, 211f  
biliary stents, 209, 212f  
cholangiocarcinoma lesions, 208–209, 208f  
clinical ramifications, of needle track seeding, 210  
cytology photomicrograph, 208–209, 209f  
cytopathological considerations, 209  
operating characteristics, 208–209, 210t  
performance characteristics, 208–209, 211t

Endoscopic ultrasonography-guided  
fine-needle aspiration (EUS FNA)  
*(Continued)*  
sensitivity and specificity rates, 208–209  
technique, 208f, 209  
tumor seeding, 209  
bridge therapy, 250  
challenges in  
chronic pancreatitis, 177, 178f  
uncinate mass lesions, 177, 177f  
cholangioscopy, 212–213  
common sites for, 250, 251t  
compared with other modalities, 103  
contraindications, 250–251, 251t  
cytological specimens, 250  
diagnosing, 102–103, 102t  
diagnosis and staging, 65–70, 66t  
distant metastases (M1) staging, 70, 71f–72f  
endoscopic ultrasonography, diagnostic reach of, 67–69  
endoscopic ultrasonography *vs.*, 69, 70f–71f  
intrapulmonary tumors (T) staging, 66, 67f  
left paratracheal lymph node, 67–69, 68f  
lower paratracheal lymph node, 67–69, 68f  
mediastinal nodal (N) staging, 66–67  
mediastinal (N) staging, 69–70  
procedure, 65, 66f  
video-assisted thoracoscopy (VATS), 67–69  
endobronchial ultrasound (EBUS), 102  
evolving trends in, 256–257  
sampling techniques, 257, 258f  
stylet use, 256, 257t  
suction use, 256–257, 257t  
fine-needle biopsy, 178f  
ancillary testing, 177–178  
fork-tip needle, 177–178  
Franseen needle, 177–178, 179f  
hematoxylin and eosin staining, 177–178, 179f  
*vs.* reverse-bevel-tip FNB needle, 177–178  
ROSE, of pancreatic mass, 177–178, 179f  
of gastrointestinal tract, 288–289  
detection of foregut cysts, 289, 289f  
gastrointestinal stromal tumors (GIST), 289, 290f  
of hepatobilary tree, 289  
liver, 289, 290f  
indications for, 250  
liver, 171  
lymph nodes, 171  
of lymph nodes, 286–288  
algorithmic approach to interpretation, 286–287, 287f  
confirm, 287  
differential diagnosis, 287, 288f

Endoscopic ultrasonography-guided  
fine-needle aspiration (EUS FNA)  
*(Continued)*  
monomorphic lymphoid population, 287–288  
nonhematopoietic cells in background of lymphoid cells, 288  
nonhematopoietic cells without the background of lymphoid cells, 288  
sample collection, 286  
malignant mediastinal lymph node, 100, 101f  
needle for  
correct, 252, 252t  
holding of, 253, 255f  
insertion into echoendoscope, 252, 252f  
preparation for subsequent passes, 256, 256f  
stopping device, 253, 254f  
stylet, 256, 257t  
withdrawal and aspirate processing, 254f, 256  
of pancreas, 279–286  
chronic pancreatitis, 279–282  
cystic pancreatic lesions, 283–286  
global approach to diagnosis, 279, 281f, 281t  
pancreatic adenocarcinoma, 279–282  
pancreatic neuroendocrine tumors (PNETs), 283  
pancreatic cysts, 186–188  
adverse events, 190  
antibiotic prophylaxis, 190  
branch duct intraductal papillary mucinous neoplasia (IPMN), 191, 192f  
19-gauge, 189, 190f  
22-gauge, 189, 190f  
25-gauge, 189–190, 190f  
macrocystic (oligocystic) serous cystadenoma, 191, 192f  
serous cystadenomas (SCAs), 191, 192f  
string test, 190–191  
pancreatic mass lesions, 172  
pancreatic metastases, 182–183  
particularities according to site, 257–258  
duodenal bulb, 258  
duodenal sweep (D2), 258  
esophagus, 257  
stomach, 258  
pleural effusions, 107–108  
posterior mediastinal lesions, 101–102  
preliminary planning of, 272–273, 273t  
rectal cancer, 236  
lower gastrointestinal (GI) endoscopic ultrasound (EUS), 233  
N-staging accuracy, 232  
risks, 103  
special issues of, 258–259  
cystic lesions, 259  
indurated lesions, 259

Endoscopic ultrasonography-guided fine-needle aspiration (EUS FNA) (*Continued*)  
 mobile lesions, 259  
 multiple lesions, 258  
 tumor seeding, 259  
 of spleen, 288  
 steps for, 251–258  
     correct needle, 252, 252t  
     evolving trends in, 256–257  
     indication, verify, 251  
     insertion into echoendoscope, 252, 252f  
     lesion, localize, 251  
     particularities according to site, 257–258  
     position the lesion, in needle path, 252–255, 253f–255f  
     preparation for subsequent passes, 256, 256f  
     puncture the lesion, 255–256  
     withdrawal and aspirate processing, 254f, 256  
 subsequent thoracic surgery rates, 105–106  
 technique, 101–102, 102f  
 transesophageal cytology, 101, 101t  
 triple test, 277  
 tumors, 208–210  
 Endoscopic ultrasound elastography, 48, 48f–49f, 51, 51f–52f, 172  
 Endoscopic ultrasound, gastric cancer  
     M staging, 93–95  
     staging limitations, 95  
     T staging, 92–95, 93t–94t  
 Endoscopic ultrasound-guided fiducial placement, 25, 25f  
 Endoscopic ultrasound-guided lumen-apposing stents, 26–28, 26f–27f, 28t  
 Enlarged posterior mediastinal lymph nodes  
     benign posterior mediastinal lymph nodes, 100, 101f  
     diagnosis, 103  
     endobronchial ultrasound, 102  
 EUS evaluation, 100–103  
 EUS FNA  
     accuracy, 102–103  
     biopsy, 103  
     malignant posterior mediastinal lymph nodes, 100, 101f  
     posterior mediastinal lesions, 101–102  
     transesophageal EUS FNA cytology, 101, 101t  
 Equipment  
     accessories, 21  
     fine-needle aspiration needles, 21–22, 22t, 23f  
     fine-needle biopsy needles, 22–28, 24f–25f, 24t  
     confocal laser endomicroscopy (CLE), 25–26, 26f  
     echoendoscopes  
         linear scopes, 16, 18f  
         radial scopes, 15, 16t, 17f  
     elastography, EUS, 19, 20f

Equipment (*Continued*)  
     endoscopic retrograde  
         cholangiopancreatography (ERCP), 15  
     endoscopic ultrasound-guided fiducial placement, 25, 25f  
     endoscopic ultrasound-guided  
         lumen-apposing stents, 26–28, 26f–27f, 28t  
         miniprobes, 19–21, 21f, 21t  
         optical biopsies, 15  
         processors, 17–19, 19f–20f  
         radiofrequency ablation (RFA), 15, 26, 26f  
         rectal probes, 21  
     ERCP. *See* Endoscopic retrograde  
         cholangiopancreatography (ERCP)  
 Erlangen Active Simulator for Interventional  
     Endoscopy (EASIE-R), 36  
 Esophageal cancer, 79–89  
     background, 79  
     computed tomography (CT), 81  
     cost-effectiveness, EUS, 89  
     early esophageal cancer, 87–88, 88f  
         endoscopic evaluation, 88, 88t  
         high-frequency probes, 88  
     endoscopic ultrasound examination  
         technique, 82–85  
         high-frequency probe (HFP), 82  
         miniprobe ultrasound, 82  
         M staging, 84t–85t, 85, 86f  
         N staging, 84–85, 84t–85t, 86f  
         obstructing tumors, 82, 83f  
         patient preparation, 82  
         scope selection, 82  
         T staging, 82–83, 84t–85t, 86f  
     esophagogastric junction cancers, 81t  
     fine-needle aspiration (FNA), 81, 85–87, 87f  
     fluorodeoxyglucose (FDG), 81  
     gastrointestinal (GI) tract, 80  
     learning curve, 89  
     management pathways, 79–81  
     mucosa, 79–80  
     National Comprehensive Cancer Network (NCCN) guidelines, 81  
     neoadjuvant chemoradiotherapy, 80–81  
     neoadjuvant therapy, restaging after, 88–89  
     patient management, EUS, 89  
     preoperative chemoradiotherapy, 80–81  
     procedural volume, 89  
     squamous cell carcinoma (SCC), 79  
     stage-dependent treatment protocols, 81  
     staging, 79, 80t  
         M staging, 79  
         newly diagnosed esophageal cancer, 81–82  
         N staging, 79  
         T staging, 79  
     submucosa, 79–80  
     survival, EUS, 89  
 Esophagus, 59–60  
     balloon inflation, 59  
     bare catheter, 59  
     Barrett esophagus, 60

Esophagus (*Continued*)  
     electronic radial echoendoscope, 59  
     EUS FNA particularities, 257  
     maneuver sprays, 59  
     radial scanning echoendoscope, 59  
     single-/dual-channel forward-viewing  
         endoscope, 59  
     tangential imaging, 60, 60f  
     transparent/low-compliance condom, 59–60, 60f  
     ultrasound catheter, 59  
 Ethanol lavage, paclitaxel injection with, 326  
 European Society of Gastrointestinal  
     Endoscopy (ESGE), 256–257  
 EUS Assessment Tool (EUSAT), 66–67  
 EUS-BD. *See* EUS-guided biliary drainage (EUS-BD)  
 EUS FNA. *See* Endoscopic ultrasonography-guided fine-needle aspiration (EUS FNA)  
 EUS FNB. *See* EUS-guided fine-needle biopsy (EUS FNB)  
 EUS-guided ablation therapy, 320–329.e3, 181–182  
     brachytherapy, 322  
     celiac ganglion irradiation, 323  
     celiac plexus injections, 327–328  
     direct ganglia injection, 328  
     fiducial placements, 322–323  
     injection therapies, 323–325  
     of pancreatic cyst, 325  
     radiofrequency ablation, 320–322  
 EUS-guided anastomosis, 330–332  
     procedural technique  
         assisted EUS-GE technique, 332  
         EUS-guided balloon-occluded  
             gastrojejunostomy bypass (EPASS), 332, 333f  
         EUS-guided gastroenterostomy (EUS-GE), 330, 331f  
     technical and treatment outcomes, 332, 333t  
         pelvic abscess drainage, 334, 337t  
         POFCs drainage, 332, 334, 336t  
         technical limitations, 332  
 EUS-guided antegrade stenting (EUS-AG), 304, 304t, 307, 312–313  
     considerations, 312  
     procedure, 312, 314f  
     troubleshooting, 313  
 EUS-guided balloon-occluded  
     gastrojejunostomy bypass (EPASS), 332, 333f  
 EUS-guided biliary drainage (EUS-BD)  
     algorithm for, 307, 307f  
     indications of, 303, 303t  
     nomenclature of, 302–303, 303f  
     outcomes of  
         EUS-guided antegrade stenting (EUS-AG), 304, 304t  
         EUS-guided choledochoduodenostomy (EUS-CDS), 304–306, 305t

EUS-guided biliary drainage (EUS-BD) (*Continued*)  
 EUS-guided hepaticogastrostomy (EUS-HGS), 304–306, 305t  
 EUS-rendezvous ERCP (EUS-Rv biliary), 303–304, 304t  
*vs.* percutaneous transhepatic biliary drainage (PTBD), 306, 306t  
 procedures, 303–306  
 choices of, 307  
 pros and cons of, 306–307, 306t  
 EUS-guided celiac plexus neurolysis (EUS CPN), 328, 329t  
 EUS-guided choledochoduodenostomy (EUS-CDS), 302–307, 305t, 313  
 considerations, 313  
 procedure, 313, 315f  
 troubleshooting, 313  
 EUS-guided drainage  
 of abdominopelvic abscesses, 234–236  
 of abdominopelvic fluid collections, 332–337  
 procedural technique, 332–334  
 technical and treatment outcomes, 334  
 technical limitations, 334–337  
 of biliary-pancreatic ductal systems, 307–310  
 algorithm for, 309  
 considerations, 314–316  
 indications for, 303t, 307  
 nomenclature, 308, 308f  
 outcomes of, 308–309, 308t  
 procedure, 316, 317f  
 troubleshooting, 316  
 EUS-guided antegrade stenting (EUS-AG), 312–313  
 considerations, 312  
 procedure, 312, 314f  
 troubleshooting, 313  
 EUS-guided choledochoduodenostomy (EUS-CDS), 313  
 considerations, 313  
 procedure, 313, 315f  
 troubleshooting, 313  
 EUS-guided hepaticogastrostomy (EUS-HGS), 313–314  
 considerations, 313–314  
 procedure, 314, 316f  
 troubleshooting, 314  
 EUS-rendezvous ERCP (EUS-Rv biliary), 311–312  
 considerations, 311  
 procedure, 311, 313f  
 site of needle puncture, 311, 312f  
 troubleshooting, 312  
 of gallbladder, 309  
 considerations, 316–318  
 indications of, 303, 303t, 309  
 outcomes of, 309, 309t  
*vs.* percutaneous cholecystostomy, 309–310  
 procedure, 318, 318f  
 troubleshooting, 318

EUS-guided drainage (*Continued*)  
 of pancreatic fluid collections (PFCs), 291–301.e2  
 definitions, 291, 292f–293f  
 disconnected pancreatic duct syndrome (DPDS), 299, 300f  
 indications for intervention, 291  
 types of interventions, 291–292  
 walled-off necrosis (WON), 292–299  
 procedural considerations and equipment, 310–311, 310t  
 echoendoscope, 310  
 needles and guidewires, 310  
 patient preparation, 310  
 stents, 310–311, 311f  
 of walled-off necrosis (WON), 292–299  
 adverse events, 297–298  
 axial computed tomography image of, 291, 293f  
 cautions, 293–294  
 endoscopic necrosectomy, 297, 300f  
 EUS in, 291, 293f  
 follow-up, 298–299  
 percutaneous drainage, 292–293  
 preprocedure checklist, 293  
 procedure techniques, 294–297  
 EUS-guided fiducial placement, 322–323  
 EUS-guided fine-needle biopsy (EUS FNB), 261–271.e3  
 Acquire needle, 267–270, 268f, 270f  
 Sharkcore needle, 267–270, 268f–269f  
 Tru-Cut biopsy needle, 261–262, 262f  
 using ProCore needles  
 design and technique, 264, 266t  
 19-G, 22-G, and 25-G, 264, 266f  
 results of, 266–267, 267t  
 tip of, 20-G needle, 264, 266f  
 using standard 19-G needle  
 background, 263  
 results of, 263–264, 263t–264t, 265f  
 technique, 263  
 using standard 22-G needle  
 background, 262  
 design and technique, 262  
 results of, 262–263, 262t  
 EUS guided-fine-needle injection (EUS-FNI), 320  
 antitumor viral therapy, 323–325  
 dendritic cells (DCs), 325  
 of gastrointestinal tumors, 323, 324t  
 intraabdominal tumors, treatments for, 324t, 325  
 of intratumoral gemcitabine, 323  
 of paclitaxel and gemcitabine, 326–327  
 TNFerade, 325  
 using alcohol, 323  
 EUS-guided fine-needle tissue acquisition (EUS FNTA), 262–263  
 specimen cases, 263–264, 265f  
 EUS-guided gastroenterostomy (EUS-GE), 330, 331f

EUS-guided hepaticogastrostomy (EUS-HGS), 302–307, 305t, 313–314  
 considerations, 313–314  
 procedure, 314, 316f  
 troubleshooting, 314  
 EUS-guided pancreatic cyst ablation, 325  
 EUS-guided radiofrequency ablation (RFA), 181  
 pancreatic neuroendocrine tumor (PNET), 182  
 use, of radiofrequency probe, 182  
 EUS-guided transhepatic puncturing, of intrahepatic ducts, 302–303  
 EUS-guided Tru-Cut biopsy (EUS TCB)  
 nonhandle portion of, 261–262, 262f  
 EUS-guided vascular interventions, 337–339  
 procedural technique, 337–338, 337f  
 technical and treatment outcomes, 338, 338t  
 technical limitations, 339  
 EUS-rendezvous ERCP (EUS-Rv biliary), 302–303, 311–312  
 cannulation, 303–304  
 considerations, 311  
 outcomes of, 303–304, 304t  
 procedure, 311, 313f  
 risk of, 306–307  
 site of needle puncture, 311, 312f  
 troubleshooting, 312  
 EUS service  
 accessories for, 21  
 balloons for, 19–21  
 delivering, 17, 26  
 processors, 17–19, 19f–20f, 26  
 EUS tissue acquisition, 181  
 Examination technique, EUS, 82–85  
 high-frequency probe (HFP), 82  
 miniprobe ultrasound, 82  
 M staging, 84t–85t, 85, 86f  
 N staging, 84–85, 84t–85t, 86f  
 obstructing tumors, 82, 83f  
 patient preparation, 82  
 scope selection, 82  
 T staging, 82–83, 84t–85t, 86f  
 External anal sphincter (EAS), 238–239, 239f, 245, 245f  
 abnormality, 241  
 atrophy, 245  
 needle electrode, 241–242  
 obstetric injury, 242  
 pudendal nerves, 240–241  
 squeeze pressure, 241  
 Extraluminal compression, 114, 114f  
 Extrathoracic malignancy, 104, 104f  
**F**  
 False diagnosis  
 lining cells, 285  
 paucicellular aspirates, 285

False-negative diagnosis, of pancreatic adenocarcinoma/chronic pancreatitis, 282  
 False-positive diagnosis, of pancreatic adenocarcinoma/chronic pancreatitis, 282  
 Fanning technique, 176  
     utilization of, 275  
 FDG PET-active hilar nodes, 74  
 Fiducial placements, EUS-guided, 322–323  
     procedural technique, 322–323, 323f–324f  
 Fine-needle aspiration (FNA), 15, 85–87, 87f, 176, 250, 273–275, 320  
     advantage of, 275  
     adverse events of, 177  
     esophageal cancer, 85–87, 87f  
     EUS-Rv (biliary), 312  
     fanning, 176  
     metastatic renal cell cancer, 182, 182f  
     vs. needle core biopsy, 274–275  
     needle size, 176  
     optimized endoscopic ultrasonography, 277, 278t  
     pancreatic fluid collections, 294, 294f  
     route of, 176  
     stylet, 176  
     suction, 176  
 Fine-needle biopsy (FNB) needles, 22–25, 178f  
     Acquire, 267–270, 268f, 270f  
     ancillary testing, 177–178  
     fork-tip needle, 177–178  
     Franseen needle, 177–178, 179f  
     hematoxylin and eosin staining, 177–178, 179f  
     ProCore, 264–267, 266f  
     Quick-Core, 261–262  
     vs. reverse-bevel-tip FNB needle, 177–178  
     ROSE, of pancreatic mass, 177–178, 179f  
     Sharkcore, 267–270, 268f–269f  
     Tru-Cut, 261–262, 262f  
 Fluorescence in situ hybridization (FISH)  
     chromosomal polysomy, 208  
     chromosomal translocations, 274  
 Fluorodeoxyglucose (FDG), 65, 81  
 FNA. *See* Fine-needle aspiration (FNA)  
 FNA-induced bleeding, 251  
 Fork tip needles, 274–275  
 Formative assessment, 33  
 Franseen tip needles, 274–275  
 Frequency, of ultrasound wave, 2  
 Fujifilm echoendoscopes, 16  
 Fujifilm equipment, 16  
     linear scopes, 16  
     miniprobes, 19–21, 21t  
     processors, 17  
     radial scopes, 15  
 Fusion imaging, 57

**G**  
 Ga-DOTATATE PET/CT, 180  
 Gallbladder  
     disease  
         polyps, 215–216, 215f  
         tumors, 216, 216t, 217f–218f, 218t  
         with wall thickening, 217–218, 219t  
 EUS-guided drainage of, 309  
     considerations, 316–318  
     indications of, 303, 303t, 309  
     outcomes of, 309, 309t  
     vs. percutaneous cholecystostomy, 309–310  
     procedure, 318, 318f  
     troubleshooting, 318  
     polyps, 215–216, 215f  
     tumors, 216, 216t, 217f–218f, 218t  
 Gallstones  
     chronic cholecystitis, 217  
     diagnostic checklist for, 207b  
     idiopathic acute pancreatitis (IAP), 206–207  
     multiple unexplained attacks, 206–207  
     shadowing gall bladder stone, 206, 207f  
     solitary shadowing gall bladder stone, 206, 207f  
 Gastric adenocarcinoma, 51, 51f, 56, 56f  
 Gastric antrum, 110–111, 111f  
 Gastric cancer, 89–96  
     accuracy of endoscopic ultrasound  
         M staging, 93–95  
         staging limitations, 95  
         T staging, 92–95, 93t–94t  
     background, 89–90  
     ESD, 92  
     esophagogastric junction (EGJ), 90  
     EUS, 90  
     EUS with other imaging modalities, 95–96  
     examination checklist, 96  
     *Helicobacter pylori* infection, 89–90  
     management pathways, 92  
     metastatic disease, 92  
     staging, 90–92, 91f, 91t  
         M staging, 92, 92f  
         N staging, 92  
         T staging, 91, 92f  
     staging laparoscopy patient selection, 96  
     submucosal involvement, 92  
     superficial cancers, 92  
     surgery, 92  
     survival after neoadjuvant chemotherapy, 96  
         work-up, 90, 90f  
 Gastric outlet obstruction (GOO), 330  
 Gastrinomas, 180  
 Gastroesophageal (GE) junction, 61f  
 Gastrointestinal (GI) cancers, 39  
 Gastrointestinal stromal tumor (GIST), 56, 56f, 106, 114–116, 277  
     asymptomatic mesenchymal tumors, 116  
     CD34, 114–115  
     CD117, 114–115

Gastrointestinal stromal tumor (GIST)  
     *(Continued)*  
     contrast-enhanced harmonic EUS (CEH EUS), 116  
     EUS FNA, 116  
     EUS FNB, 116  
     gastric schwannomas, 115  
     immunohistochemical staining techniques, 114–115  
     leiomyomas, 114–115  
     leiomyosarcomas, 114–115  
     pacemaker cells, 114–115  
     schwannomas, 115–116  
     SELs, 114–115  
 Gastrointestinal (GI) tract, 80  
     EUS FNA of, 288–289  
         detection of foregut cysts, 289, 289f  
         gastrointestinal stromal tumors (GIST), 289, 290f  
     Gemcitabine, 199–200  
     Glomus tumor, 123, 124f  
     GNAS gene, 286  
     GNAS mutations, pancreatic juice, 198–199  
     22-G needles, 252  
     25-G needles, 252  
     Granular cell tumor, 120, 120f  
     Granulomatous lymph nodes, 104

**H**  
 Habib, 26  
 Helical CTs, 172  
     CBD stones, 201  
     *Helicobacter pylori* infection, 89–90  
 Hematoxylin and eosin (H&E) staining, 276  
 Hemorrhoidectomy, 245–246, 246f  
 Hepatic metastases, from PNETs, 181  
 Hepatic veins, 138–139  
 Hepatobiliary tree  
     EUS FNA of, 289  
     liver, 289, 290f  
 HGD/IC, 185  
 HIFU. *See* High-intensity focused ultrasound (HIFU)  
 High-frequency probes, 88  
 High-intensity focused ultrasound (HIFU), 14, 14f  
 High-quality imaging, 110  
 Histoplasmosis, 105  
 Hitachi-Aloka ProSound F75/EU-ME2, 17–19  
 Hitachi Ultrasound platform, 17  
 Hit and run approach, 73–74

**I**  
 Iatrogenic sphincter injury, 245–246  
 Idiopathic acute pancreatitis (IAP), 206–207  
 Idiopathic internal anal sphincter degeneration, 245, 245f  
 Imaging artifacts, 8–11  
     acoustic shadowing, 9–10, 11f  
     reflection (mirror image), 9, 10f  
     reverberation, 8–9, 9f

- I**
- Imaging artifacts (*Continued*)
    - side lobe artifacts, 11, 12f
    - tangential scanning, 10, 12f
    - through transmission, 10, 11f
  - Imaging modalities
    - vs. EUS, 181, 181f
    - in pancreatic neuroendocrine tumor (PNET), 180–181
  - Imaging principles, 6–7
    - A-mode scanning, 6–7, 8f
    - B-mode imaging, 7
    - resolution, 6
      - axial resolution, 6, 6f
      - elevation resolution, 6
      - lateral resolution, 6, 7f
  - Immediate cytologic evaluation (ICE), 272
    - advantage of, 276
    - endoscopy suite for, 275–276
    - liquid-based cytology, 277
    - specimen adequacy, 275–276
  - Incontinence, anal, 237, 242–246
    - external anal sphincter atrophy, 245
    - iatrogenic sphincter injury and anal trauma, 245–246
    - idiopathic internal anal sphincter degeneration, 245
    - obstetric injury, 242–245
    - prevalence, 242
  - Indications, 39–40
    - contraindications, 40
    - diagnostic imaging, 39
    - therapy, 40
    - tissue acquisition, 40
    - tumor staging, 39–40
  - Indurated lesions, EUS FNA of, 259
  - Infection, risks of, 45
  - Inflammatory diseases, pancreas, 140–170.e4
  - Inflammatory fibroid polyps, 122–123, 123f
  - Injection therapies, endoscopic
    - ultrasonography-guided, 323–325
    - dendritic cells (DCs), 325
    - ethanol/chemotherapy injection, solid tumors, 323
    - novel antitumoral agents for, 323
    - TNFerade, 325
  - Instrumentation, 5–6, 5f
    - processors, 5–6
      - signal processor, 5–6
      - system gain compensation, 5
      - time gain compensation, 5
      - transmit/receive, 5
    - transducers, 5
  - Interactions, ultrasound, 3–4
    - absorption, 4
    - reflection, 3, 3f
    - refraction, 3–4, 4f
    - scattering, 4, 4f
  - Internal anal sphincter (IAS), 238–239, 239f
    - abnormality, 241
    - fragmentation, 246, 246f
    - hypertrophy, 246–247
    - lateral sphincterotomy, 246
  - Internal anal sphincter (IAS) (*Continued*)
    - obstetric injury, 242
    - rectal filling, 241
    - resting pressure, 241
    - sympathetic presacral nerve fibers, 240–241
    - thickening, 247
  - Intraabdominal lesions microvascularity, 56
  - Intraductal papillary mucinous neoplasia (IPMN), 185–188, 195–197
    - adenocarcinoma, 195–196, 196f
    - branch duct intraductal papillary mucinous neoplasia (BD-IPMN), 195, 195f
    - cyst fluid amylase, 191
    - endoscopic appearances, 195–196
    - epithelial subtypes, 196
    - EUS FNA, 190, 196
    - filling defects, 195–196
    - guidelines, 196–197
    - main duct intraductal papillary mucinous neoplasia (MD-IPMN), 195–196
    - malignant potential, 195–196
    - malignant transformation, risk of, 196
    - mutations, 191
  - Intraductal papillary mucinous neoplasia (IPMN), 284–285, 285f
  - Intraductal tissue sampling, 208
  - Intraductal ultrasonography (IDUS), 204–205
    - ampullary tumors, 223–224, 223f
    - bile duct strictures, 210–212, 214
      - accuracy of, 210–212
      - algorithm management, 210–212, 213f
      - biliary papillomatosis, 210–212
      - cholangiocarcinoma, 210–212, 212f
      - vs. ERCP, 210–212
      - layers, 210–212
      - primary sclerosing cholangitis (PSC), 210–212
    - Intrahepatic arterial chemotherapy, EUS-guided, 323
    - Intrapulmonary tumors (T) staging, 66, 67f, 72, 74f
    - Intratumoral alcohol injection, 181
    - Irradiation, celiac ganglion, 323
  - J**
  - Jhala algorithm, 279, 281f
  - K**
  - KRAS mutations, 183–184, 198–199
  - L**
  - Laparoscopic ultrasound (LUS), 57
  - Lateral resolution, 6, 7f
  - Learning curve, esophageal cancer, 89
  - Left adrenal gland (LAG), 65
  - Left atrium, 61, 61f
  - Leiomyoma, 115
    - stromal tumors, 106
  - Linear array echoendoscope, 61–63
  - Linear echoendoscopes
    - celiac trunk, 129, 130f
    - pancreas, 131–132
  - Linear scopes, 16, 18f
  - Lining cells, 285
  - Lipoma, 118, 119f
    - diagnostic checklist, 118b
    - resection, 118
  - Liquid-based preparations, for cytologic specimens, 277
  - Liver, 138–139, 139f
    - anatomy, 138–139
    - duodenal bulb, 138
    - EUS FNA, 171
    - hepatic veins, 138–139
    - hepatobiliary tree, 289, 290f
    - imaging, 139
  - Local excision, for rectal cancers, 234
  - Locoregional lymph nodes, 174
  - Lower gastrointestinal (GI) endoscopic ultrasound (EUS), 229, 233
    - rectal cancer
      - adverse event profile, 234–236
      - innovative interventions, 234–236
  - Low mechanical index contrast-enhanced endoscopic ultrasound, 54f–56f, 56
  - Lumen-apposing metal stent (LAMS), 330, 331f
  - Lung cancer, 103–104
  - Lymph nodes, 251
    - EUS FNA, 171
    - EUS FNA of, 286–288
      - algorithmic approach to interpretation, 286–287, 287f
      - confirm, 287
      - differential diagnosis, 287, 288f
      - monomorphic lymphoid population, 287–288
      - nonhematopoietic cells in background of lymphoid cells, 288
      - nonhematopoietic cells without the background of lymphoid cells, 288
      - sample collection, 286
      - metastatic tumor in, 275
  - Lymphoepithelial cysts, 190–191
  - Lymphoma, 104
    - pancreatic, 183, 183f
  - M**
  - Macrocytic (oligocystic) serous cystadenoma, 191, 192f
  - Magnetic resonance cholangiopancreatography (MRCP)
    - CBD stones, 201
    - choledocholithiasis, 202–205
    - metallic hardware, 202
    - small tumor/focal narrowing, 208
  - Magnetic resonance imaging (MRI), 36, 39, 101, 179
    - anal sphincter, 237
      - anal endosonography (AES), 245
    - vs. EUS
      - pancreatic ductal adenocarcinoma, 172
      - liver metastases, 174–175
      - pancreatic cysts, 186

Magnetic resonance imaging (MRI)  
*(Continued)*  
pancreatic fluid collections (PFCs), 291  
pancreatic neuroendocrine tumor (PNET),  
181

Main duct intraductal papillary mucinous neoplasia (MD-IPMN), 186–188, 188f, 194, 195f

Main pancreatic duct (MPD), 186

Malignant gastrointestinal stromal tumor, 51, 52f

Malignant lymph nodes, 171

Malignant neuroendocrine tumor, 53, 54f–55f

Malignant posterior mediastinal lymph nodes, 100, 101f, 102t, 103–104

lymphoma, 104

metastatic disease, 103–104

extrathoracic malignancy, 104, 104f

lung cancer, 103–104

mesothelioma, 104, 104f

thoracic tumors, 103–104

Malignant posterior mediastinal masses, 106–108, 106f

gastrointestinal stromal tumors, 106

leiomyoma stromal tumors, 106

mesothelioma, 106–107

neurogenic tumors, 106

Management pathways

- esophageal cancer, 79–81
- gastric cancer, 92

Maneuver sprays, 59

Manometry, of anal sphincter, 241

Mediastinal cysts, 107, 107f

Mediastinal lymph nodes, 73

Mediastinal masses, 106–108

Mediastinal nodal (N) staging, 66–67, 69–70

Mediastinum, 60–64

- adrenal gland, 63–64, 63f
- American Thoracic Society (ATS), 61
- anatomic structures, 61
- aortic arch (AO), 61, 62f
- aortopulmonary window, 62, 63f
- azygous vein, 61, 62f
- computed tomography (CT), 60
- gastroesophageal (GE) junction, 61f
- left atrium, 61, 61f
- linear array echoendoscope, 61–63
- lymph nodes, 61
- radial echoendoscope, 60–61
- splenic vein, 63–64
- subcarinal region, 61, 62f
- trachea, 61, 62f

Medications

- patient preparation, 41–43
- antithrombotic drugs, 41–43, 42t
- daily medications, 41
- prophylactic antibiotics, 43, 44t
- resuming antithrombotic therapy, 42t, 43

Mesorectal fascia, 230

Mesorectum, 230

Mesothelioma, 104, 104f, 106–107

Metal stent insertion, for EUS-guided drainage, 295–296

accessories, 296

technique, 296

Metastatic disease, 103–104

- extrathoracic malignancy, 104, 104f
- lung cancer, 103–104
- mesothelioma, 104, 104f
- thoracic tumors, 103–104

Metastatic lesions, pancreas, 182–183, 182f

Metastatic lymph nodes, 174

Metastatic tumor, in lymph nodes, 275

Microbubbles, 186–188

Microlithiasis, 206–207

Miniprobes, 19–21, 21f, 21t, 45

Mirizzi syndrome

- diagnostic checklist for, 214b

Mobile lesions, EUS FNA of, 259

Molecular markers

- for cyst fluid, 186t, 191
- in pancreatic juice, 198–199, 199t

Molecular profiling, of tumor specimens, 183–184

Moray, 22–25

Motionless duodenum, ampulla, 134, 135f

M staging

- esophageal cancer, 79, 84t–85t, 85, 86f
- gastric cancer, 92–95, 92f

Mucin, 186–188, 188f

Mucinous cystic neoplasm, 285, 285f

Mucinous cystic neoplasm (MCN), 185, 194–195

- cyst fluid amylase, 191
- main duct intraductal papillary mucinous neoplasia (MD-IPMN), 194, 195f
- mucinous cystadenoma, 194, 194f–195f
- mutations, 191

Mucin-producing cysts, 190–191

Mucosa

- esophageal cancer, 79–80
- inner hyperechoic layer, 229–230
- outer hypoechoic wall layer, 229–230

Multidetector computed tomography (MDCT), 112–113

Multi-gate technique, for EUS-guided drainage, 296, 299f

Multiple lesions, EUS FNA of, 258

Multiple reflections, 4

Mural nodule, 188f

- CE EUS vascularity, 186–188
- vs. mucin ball, 186–188
- type I, 186–188
- type II, 186–188
- type III, 186–188
- type IV, 186–188

**N**

NAS. *See* Next Accreditation System (NAS)

National Comprehensive Cancer Network (NCCN)

- pancreatic ductal adenocarcinoma, 173, 174t

Natural orifice transluminal endoscopic surgery (NOTES), 57

Nediastinal pseudocysts, 107–108

Needle-based confocal laser endomicroscopy (nCLE), 76, 192

- diagnosis, 188–189
- with surgical pathology, 188–189

Needle core biopsy *vs.* fine-needle aspiration, 274–275

Needle-knife catheter, 330

Needles

- bending, 258
- choice of, 274
- for EUS FNA
- correct, 252, 252t
- insertion into echoendoscope, 252, 252f
- preparation for subsequent passes, 256, 256f
- withdrawal and aspirate processing, 254f, 256

lesion position, 252f

- adequate needle trajectory, 253, 254f
- correct positioning, 253, 253f
- elevator range of movement, 253, 254f
- holding, 253, 255f
- sheath adjustment, 252–253, 253f
- stopper adjustment, 253, 254f

preparation of

- holding the needle, 253, 255f
- stopping device, 253, 254f
- styret, 256, 257t
- puncture the lesion, 255–256

Noadjuvant therapy

- rectal cancer, 234
- restaging after
- esophageal cancer, 88–89

Neoplastic hepatocytes, 289

Neuroendocrine tumors, 53

Neurogenic tumors, 106

New techniques, EUS, 47–57.e5

- contrast-enhanced endoscopic ultrasound
- elastography, 52–57
- fusion imaging, 57
- real-time endoscopic ultrasound
- elastography, 47–52

Next Accreditation System (NAS), 32–33

Nodal classification, 174

Nodal drainage of, rectum, 230

Nondiseased pancreas

- ductal wall hyperechogenicity, 140
- main pancreatic duct (MPD), 140, 141f
- pancreas, 140
- small visible side branches, 140
- ventral anlage, 140

Nonobstructive cholangitis, 201

Non-small cell lung cancer (NSCLC), 40

- competency, 76
- EBUS TBNA diagnosis and staging, 72–74, 73f
- combined nodal staging, 75, 75f
- endoscopic ultrasonography, 75, 76t

Non–small cell lung cancer (NSCLC)  
*(Continued)*  
 intrapulmonary tumors (T) staging, 72, 74f  
 nodal staging (N), 73–74, 74f  
 procedure, 72, 73f  
 surgical staging, 75, 76t  
 EUS and EBUS, 72, 72f  
 EUS and EBUS in staging algorithms, 75–76, 77f  
 EUS FNA for diagnosis and staging of, 65–70, 66t  
 distant metastases (M1) staging, 70, 71f–72f  
 endoscopic ultrasonography, diagnostic reach of, 67–69  
 endoscopic ultrasonography *vs.*, 69, 70f–71f  
 intrapulmonary tumors (T) staging, 66, 67f  
 left paratracheal lymph node, 67–69, 68f  
 lower paratracheal lymph node, 67–69, 68f  
 mediastinal nodal (N) staging, 66–67  
 mediastinal (N) staging, 69–70  
 procedure, 65, 66f  
 video-assisted thoracoscopy (VATS), 67–69  
 future perspectives, 76  
 training, 76  
 Nonspecular reflection, 4  
 Nonsteroidal antiinflammatory drugs (NSAIDs), 250  
 Novel oral anticoagulants (NOACs), 250  
 NSCLC. *See* Non–small cell lung cancer (NSCLC)  
 N staging, 73–74, 74f  
 esophageal cancer, 79, 84–85, 84t–85t, 86f  
 gastric cancer, 92

**O**  
 Obstetric injury, anal incontinence  
 anterior anovaginal fistula, 243, 243f  
 cause of, 242  
 external and internal anal sphincters, 242, 243f  
 forceps delivery, 244  
 good sonographic appearances, 244, 244f  
 occurrence, 242  
 perineal scar, 243, 243f  
 poor sonographic appearances, 244, 245f  
 primary repair, 243–244, 244f  
 symptoms, 244  
 scar tissue, 242–243  
 Obstructive jaundice, 172, 173f  
 Olympus equipment, 16t  
 balloons, 19–21  
 EUS processors, 17–19, 19f–20f  
 linear scopes, 16, 18f  
 miniprobes, 19–21, 21f, 21t  
 radial scopes, 15, 16t, 17f  
 rectal probes, 21

Omental nodules, 171  
 ONYX-015 (dl1520), 323–325  
 Optical biopsy, 15

**P**  
 Paclitaxel, 199–200  
 Pancreas  
 acute pancreatitis, 151–159  
 acute biliary pancreatitis, 151, 151t, 152f–153f  
 acute idiopathic pancreatitis, 151–152, 154f–156f  
 advanced endoscopic ultrasound techniques, 159  
 EUS, 151–156  
 overview, 151  
 recurrent acute pancreatitis, 156, 157f–159f  
 autoimmune pancreatitis, 159–169  
 contrast-enhanced endoscopic ultrasound, 169  
 endoscopic ultrasound elastography, 169  
 endoscopic ultrasound sampling, 163–169  
 EUS, 161, 162t–163t, 163f–166f  
 EUS fine-needle biopsy (FNB), 168–169  
 FNA, 163–168  
 image-enhancing techniques, 169  
 imaging characteristics, 161–163, 166f–168f  
 overview, 159, 160f, 161t  
 tru-cut biopsy, 168  
 benign pancreatic masses, 169–170  
 contrast-enhanced endoscopic ultrasound, 170  
 endoscopic ultrasound elastography, 170  
 endoscopic ultrasound-guided core biopsy, 169  
 endoscopic ultrasound sampling, 169  
 EUS FNA, 169  
 image-enhancing techniques, 170  
 overview, 169  
 body and tail, 129–132  
 body-tail junction, 129–130, 130f  
 celiac artery, 129, 130f  
 clockwise torque, 129–132, 132f  
 club head, 129, 130f  
 counterclockwise rotation, 131–132, 132f  
 pancreatic duct, 129–130  
 radial echoendoscopes, 129–131, 130f  
 chronic pancreatitis, 140–151  
 advanced endoscopic ultrasound techniques, 151  
 celiac plexus block (CPB), 151  
 computed tomography (CT), 141  
 conventional and rosemont classification, 144  
 criteria, EUS, 141–142, 147f–149f, 149t  
 endoscopic retrograde cholangiopancreatography (ERCP), 141  
 Pancreas (*Continued*)  
 EUS, 141, 142f–147f  
 EUS elastography, 147–151  
 fibrosis, 144–145  
 findings and surgical histopathology, 144–146, 150f  
 image-enhancing techniques, 147–151  
 imaging characteristics, 141–146  
 interobserver variability (IOA), 146  
 magnetic resonance cholangiopancreatography (MRCP), 141  
 magnetic resonance imaging (MRI), 141  
 MPD, 141  
 overview, 140–141  
 pancreatic adenocarcinoma (PaC), 146–147  
 sampling, EUS, 146–147  
 EUS FNA of, 279–286  
 chronic pancreatitis, 279–282  
 cystic pancreatic lesions, 283–286  
 global approach to diagnosis, 279, 281f, 281t  
 pancreatic adenocarcinoma, 279–282  
 pancreatic neuroendocrine tumors (PNETs), 283  
 transluminal approach, 281, 282t  
 head regions, 132–137  
 color Doppler imaging, 132  
 common bile duct, 132  
 duodenal bulb, 132, 133f  
 duodenal falloff, 132, 133f  
 linear echoendoscopes, 133, 134f  
 pancreatic duct, 132  
 papilla, 133–135, 135f  
 portal vein, 132  
 radial echoendoscopes, 132  
 stack sign, 132, 133f  
 uncinate, 135–137  
 inflammatory disease, EUS, 140–170.e4  
 metastatic lesions, 182–183, 182f  
 nondiseased pancreas, 140  
 ductal wall hyperechogenicity, 140  
 main pancreatic duct (MPD), 140, 141f  
 pancreas, 140  
 small visible side branches, 140  
 ventral anlage, 140  
 Pancreatic adenocarcinoma, 49f, 50–51, 51f, 53–55, 53f, 55f  
 Pancreatic carcinoma  
 diagnosis of, 283t  
 smears, 279–280, 282f  
 Pancreatic cystic neoplasms (PCNs), 325  
 Pancreatic cyst lesions, EUS-guided ablation of, 325–327, 326t  
 Pancreatic cysts, 185  
 ablation for, 325  
 clinical outcomes, 325–327, 326t  
 endoscopic ultrasonography-guided, 327f  
 procedural technique, 325–328, 326f

Pancreatic cysts (*Continued*)

- classification of, 185, 186t
- cyst fluid analysis, 190–192
- aspirate appearance and string test, 190–191, 190f
- cytology, 191
- EUS FNA, 191–192, 192f
- molecular markers, 191
- protein markers, 191
- diagnostic approach, 185–190
  - clinical history and imaging, 185–186, 186f
  - confocal laser endomicroscopy (CLE), 188–189, 189f
  - endoscopic ultrasound, 186–188, 187t, 188f
  - EUS FNA, 189–190, 190f
  - features of, lesions, 186, 187t
  - pragmatic algorithm for, 186, 186f
- examination checklist for, 200b
- future developments, 198–200
  - cyst ablation, 199–200
  - molecular markers analysis, in pancreatic juice, 198–199
- types of, 185, 192
  - cystic pancreatic ductal adenocarcinoma, 185, 198
  - cystic pancreatic neuroendocrine tumors (PanNETs), 185, 197–198
  - intraductal papillary mucinous neoplasia (IMPN), 185–188, 195–197
  - mucinous cystic neoplasm (MCN), 185, 194–195
  - pseudocysts, 185, 192–193
  - serous cystadenomas (SCAs), 185, 193–194
  - solid pseudopapillary neoplasm (SPN), 185, 197
- Pancreatic duct, 129–130
- Pancreatic ductal adenocarcinoma, 172–179
  - background, 172
  - detection of, 172
    - contrast-enhanced endoscopic ultrasound (CE EUS), 172
    - endoscopic ultrasound elastography, 172
    - EUS vs. computed tomography, 172, 173f
    - EUS vs. magnetic resonance imaging, 172
  - EUS FNA of, 176–178
    - accessories, for tissue acquisition, 176
    - challenges in, 177, 177f
    - specimen interpretation and processing, 176–177
  - evidence-based algorithmic approach, 179, 180f
  - resectability, assessment of, 172–176
  - staging, 172–176
    - distant metastases, 174–175, 175f
    - local vascular invasion, 173–174, 174f
    - nodal classification, 174
    - tumor classification, 173–174
    - tumor resectability, 176

## Pancreatic fluid collections (PFCs)

- intervention, indications for, 291
- intervention, types of, 291–292
- types, 291
- walled-off pancreatic necrosis (WON), 292–299
  - EUS-guided drainage, 293–299
  - percutaneous drainage, 292–293

## Pancreatic juice, 198–199, 199t

## Pancreatic lesions, 251

## Pancreatic lymphoma, 183, 183f

- Pancreatic neuroendocrine tumor (PNET), 179–182
  - background, 179–180
  - diagnosis, 173t, 180–181
    - EUS tissue acquisition, 181
    - EUS vs. imaging modalities, 181, 181f
    - imaging modalities, 180–181
  - EUS FNA of, 284f
  - pancreatic neuroendocrine neoplasms (PENs), 283
  - solid pseudopapillary neoplasms (SPNs), 283

## EUS-guided ablation therapy, 181–182

## Pancreatic protocol CT scan, 186

## Pancreatic pseudocysts

- amylase level, 193
- appearance, 192–193
- aspirated fluid, 193
- atypical appearance of, 192–193, 193f
- chronic abdominal pain and weight loss, 192–193, 193f
- chronic pancreatitis, 192–193, 193f
- endoscopic drainage, 192–193
- endoscopic ultrasound (EUS)-guided drainage of, 291–292
  - axial computed tomography image, 291, 292f
  - surgical cystogastrostomy, 291–292
- fluid from, 190–191
- with MPD, 192–193
- pancreatitis, 192–193, 193f
- septations, 192–193
- size of, 192–193
- thin-walled internal septations, 186, 188f

## Pancreatic tumors

- EUS-guided tattooing of, 322–323
- pancreatic ductal adenocarcinoma, 172–179
  - background, 172
  - cancer staging, 172–176
  - detection of, 172, 173f
  - EUS FNA of, 176–178
  - resectability, assessment of, 172–176
- pancreatic neuroendocrine tumor (PNET), 179–182
  - background, 179–180
  - diagnosis, 180–181
  - EUS-guided ablation therapy, 181–182
  - suspected pancreatic tumor, 171–172
    - ascites, 171

Pancreatic tumors (*Continued*)

- liver, 171
- lymph nodes, 171
- staging, 172
- tissue acquisition, 171–172
- tumor, 171
- vascular invasion, 171

## Pancreatitis, 190

- acute, 206–207
- idiopathic acute pancreatitis (IAP), 206–207
- risks of, 45

## Papilla, 133–135, 135f

- pancreas head and uncinate regions, 133–135, 135f
- linear echoendoscopes, 134–135
- motionless duodenum, ampulla, 134, 135f
- radial echoendoscopes, 133–134
- snake eyes, 133–134
- vater examination, 134–135, 135f
- ventral anlage, 133–134, 135f
- water insufflation, ampulla, 134, 135f

## Papillary carcinoma, 219–221

## Papillomatosis, diagnostic checklist for, 214b

## Pap stain, 277

## Para-aortal nodes, 67–69

## Patient management, esophageal cancer, 89

## Patient preparation, 40–43

- factors, 41b
- general measures, 40–41
- laboratory studies, 41
- medications, 41–43
  - antithrombotic drugs, 41–43, 42t
  - daily medications, 41
  - prophylactic antibiotics, 43, 44t
- resuming antithrombotic therapy, 42t, 43

## monitored anesthesia care (MAC), 41

## routine preoperative testing, 41

## upper gastrointestinal (UGI), EUS, 41

## Paucicellular aspirates, 285

PCNs. *See* Pancreatic cystic neoplasms (PCNs)

## Peak negative pressure (PNP), 52

## Pelvic abscess, EUS-guided drainage of, 334, 337t

## Pentax equipment, 16t

- confocal laser endomicroscopy (CLE), 25–26
- EUS elastography (EUS-E), 19
- linear scopes, 16
- processors, 17, 19f
- radial scopes, 15

## Pentax HiVision Preirus, 19

## Pentax linear echoendoscopes, 16

## Percutaneous drainage, of walled-off pancreatic necrosis, 292–293

## Percutaneous transhepatic biliary drainage (PTBD), 302, 306, 306t

## Perforation, risks of, 44–45

## Period, of ultrasound waves, 2, 3f

## Peritoneal carcinomatosis, 174–175, 175f

## Personalized cancer therapy, 183–184

PFCs. *See* Pancreatic fluid collections (PFCs)

Physics, of ultrasound, 2–5

bulk modulus, 2–3

compressibility, 2–3

density, 2–3

frequency, 2

intensity, 4–5

velocity, 2

wavelength, 2

Piezoelectric ceramics, 5

Plastic stent insertion, for EUS-guided drainage

accessories, 294

double-wire technique, 295, 297f

PFC puncture and guidewire insertion, 294, 294f

tract dilation, 294–295, 295f

transmural tract creation, 294

two double pigtail stents, 295, 296f

Pleural effusions, 107–108

Pleural effusions, EUS FNA, 107–108

PNET. *See* Pancreatic neuroendocrine tumor (PNET)

Pneumoperitoneum, 310

Portal vein, 132

Positron emission tomography (PET), 39, 65, 101

*vs.* endoscopic ultrasonography, 230t, 233–234

Posterior mediastinal lesions, 100–108.e4

EUS FNA

diagnosing accuracy, 102–103, 102t

risks, 103

technique, 101–102

Posterior mediastinal lymph nodes

benign posterior mediastinal lymph nodes, 100, 101f

biopsy, 103

diagnosis, 103

endobronchial ultrasound (EBUS), 102

EUS FNA. *See* Endoscopic ultrasonography

fine-needle aspiration (EUS FNA)

evaluation, 103

malignant posterior mediastinal lymph nodes. *See* Malignant posterior mediastinal lymph nodes

Postoperative fluid collections (POFCs), 332, 334, 336t

Preoperative chemoradiotherapy, esophageal cancer, 80–81

Primary gastric non-hodgkin lymphoma, 96–98

accuracy EUS, staging, 97

diffuse large B-cell lymphoma (DLBCL), 96

limitations, EUS, 98

mucosa-associated lymphoid tissue (MALT) lymphoma, 96–97

endoscopic ultrasound, 97

staging, 97

non-Hodgkin lymphoma (NHL), 96

therapy and in follow-up, predicting response, 97–98

Primary sclerosing cholangitis

(PSC), 210–212

probe-based confocal laser endomicroscopy (pCLE), 25–26

Procedural volume, esophageal cancer, 89

Processors, 5–6, 5f

signal processor, 5–6

system gain compensation, 5

time gain compensation, 5

transmit/receive, 5

ProCore needles

assessment of, 274–275

design and technique, 264, 266t

19-G, 22-G, and 25-G, 264, 266f

results of, 266–267, 267t

tip of, 20-G needle, 264, 266f

Prophylactic antibiotics, 43, 332–334

American Heart Association (AHA), 43

Bacteremia, 43

drainage of pancreatic fluid

collections, 43

EUS and EUS FNA, 43

EUS-guided celiac plexus block, 43

EUS-guided ductal access procedures, 43

Proposed quality indicators, 37t

Protein markers

cyst fluid analysis, 191

CA 15-3, 191

CA 19-9, 191

CA 72-4, 191

CA 125, 191

carcinoembryonic antigen (CEA), 187t, 191

cyst fluid amylase, 191

Pseudocysts. *See* Pancreatic pseudocysts

Pseudotumoral chronic pancreatitis, 53–55, 53f–54f

PTBD. *See* Percutaneous transhepatic biliary drainage (PTBD)

Pudendal nerve latency, of anal sphincter, 241

Pulmonary ligamentum, 67–69

Pulsatility index (PI), 53

## R

Radial echoendoscopes, 60–61

advantages of, 202

pancreas, 129–131

Radial expansion balloon, 330

Radial scanning echoendoscope, 59

Radial scopes, 15, 16t, 17f

Radiofrequency ablation (RFA), 26, 26f, 51–52, 199–200, 320–322

clinical outcomes, 320–322

cool-tipped radiofrequency catheter, 321–322, 322f

18-G endoscopic RFA electrode, 321

Habib RF DUO 13, 321

gemcitabine chemotherapy with, 322

Habib catheter, 320, 321f

procedural technique, 320

Radiofrequency (RF) signal, 5–6

Radiotherapy, endoscopic ultrasonography-guided, 320–323, 321t

Rapid on-site evaluation (ROSE), 261, 272

Rare lesions, 123

Reactive lymph nodes, 104

Real-time endoscopic ultrasound

elastography

benign mediastinal lymph node, 47, 48f

breast and prostate cancer, 47

chronic pseudotumoral pancreatitis, 48f

clinical applications, 48–51

combined autocorrelation method, 47

complex algorithm, 47

esophageal tumors, 51

European Federation Societies in

Ultrasound in Medicine and Biology (EFSUMB), 47

EUS elastography, 48

focal liver lesions, 47

future techniques, 51–52

gastric tumors, 51

gastrointestinal stromal tumors (GISTs), 51

lymph nodes, 47, 49–50

area under receiver operating

characteristic (AUROC), 49

negative predictive value (NPV), 49

positive predictive value (PPV), 49

sensitivity, 49t

specificity, 49t

malignant mediastinal lymph node, 48, 48f

malignant tumors, 47

other applications, 51

pancreatic adenocarcinoma, 49f

pancreatic masses, 50–51, 50t

technical details, 47–48

thyroid masses, 47

tissue elasticity values, 48

Real-time polymerase chain reaction (RT-PCR), 56

ReCoil stylet system, 264

Rectal cancer

American Joint Committee on Cancer (AJCC), 230, 230t

anorectal anatomy, 229–230

EUS

*vs.* computed tomography (CT), 230t, 233–234

*vs.* magnetic resonance imaging (MRI), 233, 233f

*vs.* positron emission tomography (PET)-CT, 230t, 233–234

for rectal wall metastases, 234, 236f

recurrent rectal cancer, 234, 235f

lower gastrointestinal (GI) endoscopic ultrasound (EUS), 229

adverse event profile, 234–236

innovative interventions, 234–236

neoadjuvant therapy, 234

prognosis, 229

setting of de novo rectal cancer, 231–233

N-staging considerations, 232–233, 232f, 232t

- Rectal cancer (*Continued*)  
 T-staging considerations, 231–232, 231f, 232t  
 translational medicine, 236  
 tumor-node-metastasis (TNM) system, 230, 230t
- Rectal implantation cysts, 234
- Rectal probes, 21
- Rectal wall  
 composition, 229–230  
 metastases, 234, 236f
- Rectum  
 anorectal EUS  
 antibiotic administration, 227–228  
 examination, 226  
 linear echoendoscopes, 226–227  
 prostate, 227, 227f  
 rectal wall layers, 227, 227f  
 urinary bladder, 227, 227f  
 uterus and vagina, 227, 228f
- mesorectal fat, 230
- mesorectum, 230
- muscularis propria, 229–230
- nodal drainage of, 230
- Reflection, 3, 3f
- Refraction, 3–4, 4f
- Regions of interest (ROIs), 50–51
- Resectability, of pancreatic tumors, 173–174
- Resistivity index (RI), 53
- Resolution, ultrasound, 6  
 axial resolution, 6, 6f  
 elevation resolution, 6  
 lateral resolution, 6, 7f
- Reverse bevel needles, 274–275
- RFA. *See* Radiofrequency ablation (RFA)
- Ring artifact, 8–9
- Risks and adverse effects, 44–46  
 bleeding, 45  
 esophageal cancer, 44  
 esophagus intubation, 44  
 EUS and EUS FNA, 45  
 infection, 45  
 pancreatitis, 45  
 perforation, 44–45  
 therapeutic endoscopic ultrasound, 45–46
- RNA extraction, 274
- Routine preoperative testing, patient preparation, 41
- RT-PCR. *See* Real-time polymerase chain reaction (RT-PCR)
- S**
- SafeSeqSequencing, 191
- Saline, 332
- Sampling error, 191
- Sarcoid, 104, 105f, 105t
- Scattering, 4, 4f
- Self-expanding metal stents (SEMS), 330
- Sensory receptors, 239
- Serous cystadenomas (SCAs), 185, 189, 191, 192f, 193–194  
 malignant transformation, risk of, 194  
 morphologic characteristics, 194  
 mutations, 191  
 needle-based CLE (nCLE), 188–189  
 solid-appearing serous cystadenoma, 193–194, 194f
- Sharkcore needle, 267–270, 269f  
 tip design of, 267, 268f
- Simbionix GI-Mentor II EUS training module, 36
- Single-/dual-channel forward-viewing endoscope, 59
- Single-gate technique, for EUS-guided drainage  
 metal stent insertion, 295–296  
 accessories, 296  
 technique, 296
- plastic stent insertion  
 accessories, 294  
 double-wire technique, 295, 297f
- PFC puncture and guidewire insertion, 294, 294f  
 tract dilation, 294–295, 295f  
 transmural tract creation, 294  
 two double pigtail stents, 295, 296f
- Single operator cholangioscopy (SOC), 208
- Slide, diagnostic evaluation of  
 common pathologic diagnoses, 277, 279t  
 esophageal squamous mucosa, 277–278, 280f
- EUS FNA, from reactive mediastinal lymph node, 278, 280f  
 lesions, of mediastinum, 277, 279f
- Smears  
 air-dried/alcohol-fixed, 277  
 chronic pancreatitis, 279–280, 282f  
 cytology, 276  
 pancreatic carcinoma, 279–280, 282f  
 slide, diagnostic evaluation of  
 cohesive two-dimensional group of epithelial cells with honeycomb appearance, 277–278, 280f
- endoscopic ultrasonography fine-needle aspiration of pancreas, 278, 280f  
 gastric mucosa reveal foveolar cells with cohesive cell groups, 277–278, 280f
- well-differentiated adenocarcinoma, 279–280, 281f
- Snake eyes, 133–134
- Solid pseudopapillary neoplasm (SPN), 185, 197, 283  
 classic appearance of, 197, 197f  
 malignant potential, 197  
 mutation, 191  
 pancreatic cyst lesion, 197, 198f  
 surgical specimen from distal pancreatectomy, 197, 198f
- three-dimensional image of cyst, 197, 197f
- Solitary rectal ulcer syndrome, 247, 247f
- Somatostatin receptor scintigraphy (SRS), 180–181
- Sound Speed Correction technologies, 17
- Spatial pulse length (SPL), 6
- Sphincter defects, 241–242
- Sphincter denervation, 241–242
- SPL. *See* Spatial pulse length (SPL)
- Splenic vein, 63–64
- Split-screen capability, 36
- Squamous cell carcinoma (SCC), esophageal cancer, 79
- Staging, 65–70, 66t  
 accurate staging, 39  
 ampullary tumors, 222–223, 223t  
 cholangiocarcinoma, 214, 214f  
 combined nodal staging, 75, 75f  
 distant metastases (M1) staging, 70, 71f–72f  
 EBUS TBNA diagnosis, 72–74, 73f  
 combined nodal staging, 75, 75f  
 endoscopic ultrasonography, 75, 76f  
 intrapulmonary tumors (T) staging, 72, 74f  
 nodal staging (N), 73–74, 74f  
 procedure, 72, 73f  
 surgical staging, 75, 76t
- esophageal cancer, 79, 80t  
 M staging, 79, 84t–85t, 85, 86f  
 N staging, 79, 84–85, 84t–85t, 86f  
 T staging, 79, 82–83, 84t–85t, 86f
- EUS FNA diagnosis, 65–70, 66t  
 distant metastases (M1) staging, 70, 71f–72f  
 endoscopic ultrasonography, diagnostic reach of, 67–69  
 endoscopic ultrasonography *vs.*, 69, 70f–71f  
 intrapulmonary tumors (T) staging, 66, 67f  
 left paratracheal lymph node, 67–69, 68f  
 lower paratracheal lymph node, 67–69, 68f  
 mediastinal nodal (N) staging, 66–67  
 mediastinal (N) staging, 69–70  
 procedure, 65, 66f  
 video-assisted thoracoscopy (VATS), 67–69
- gastric cancer, 90–92, 91f, 91t  
 laparoscopy patient selection, 96
- M staging, 92, 92f
- N staging, 92
- T staging, 91, 92f
- intrapulmonary tumors (T) staging, 66, 67f, 72, 74f
- mediastinal nodal (N) staging, 66–67, 69–70
- nodal staging (N), 73–74, 74f
- N-staging, 39
- overstaging, 39
- rectal cancer, 231–233  
 N-staging considerations, 232–233, 232f, 232t
- T-staging considerations, 231–232, 231f, 232t
- surgical staging, 75, 76t

- Staging (Continued)**
- suspected pancreatic tumor, 172
  - T-staging, 39
  - tumor, 39–40
  - Standard 19-G needle, EUS FNB of background, 263
    - results of, 263–264, 263t–264t, 265f
    - technique, 263
  - Standard 22-G needle, EUS FNB of background, 262
    - design and technique, 262
    - results of, 262–263, 262t
  - Stenosis, 201
  - Stent migration, 298
  - Stereotactic body radiotherapy (SBRT), 25
  - Stomach, 109–111.e1
    - EUS FNA particularities, 258
  - Stones
    - bile duct, 201
      - algorithm management, 203–204, 206f
      - choledocholithiasis, 201–205
      - diagnosis of, 202
      - echo-dense structures, 201–202, 202f
      - endoscopic retrograde cholangiopancreatography (ERCP), 202–203
      - examination checklist for, 201b
      - extraductal catheter probe EUS (EDUS), 204–205
      - intermediate risk patients, 203–204
      - intraductal ultrasonography (IDUS), 204–205
      - linear echoendoscope, 202
      - magnetic resonance cholangiopancreatography (MRCP), 205t
      - noninvasive imaging modalities, 202–203
      - radial echoendoscopes, 202
    - gallstones
      - diagnostic checklist for, 207b
      - idiopathic acute pancreatitis (IAP), 206–207
      - multiple unexplained attacks, 206–207
      - shadowing gall bladder stone, 206, 207f
      - solitary shadowing gall bladder stone, 206, 207f
    - Stopping device, for needles, 253, 254f
    - String test, for cyst fluid, 190–191, 190f
    - Stylets, 256, 257t
      - for EUS FNA, 176
    - Subcarinal region, 61, 62f
    - Subepithelial lesions (SEL)
      - aberrant pancreas. *See* Aberrant pancreas
      - accuracy comparison, EUS, 112–113
      - adjacent structures, 114
      - carcinoïd tumor, 118, 119f
      - cysts, 120–122, 121f
      - diagnostic information, 112
      - endoscopic submucosal dissection (ESD), 112
      - enlarged mediastinal lymph nodes, 114
      - Subepithelial lesions (SEL) (*Continued*)
        - evaluation, 114
        - examination checklist, 114b
        - extraluminal compression, 114, 114f
        - gastrointestinal stromal tumors (GISTs), 114–116
        - glomus tumor, 123, 124f
        - granular cell tumor, 120, 120f
        - histologic assessment, tissue sampling for, 123–126, 124f, 125t
        - inflammatory fibroid polyps, 122–123, 123f
        - leiomyomas, 115
        - lipoma, 118, 119f
        - management, 126–127, 126f
        - multidetector computed tomography (MDCT), 112–113
        - rare lesions, 123
        - submucosal lesion, 112
        - tissue sampling, 123–126
        - varices, 122, 122f
      - Submucosal involvement, gastric cancer, 92
      - Submucosal lesion, 112
      - Subsequent thoracic surgery rates, 105–106
      - Suction, EUS FNA, 176, 275
      - Summative assessment, 33
      - Super CCD chip technology, 17
      - SurePath, 277
      - Surgical biliary drainage, 302
      - Surgical cystogastrostomy, 291–292
      - Surgical resection
        - with lymph node clearance, 181
        - pancreatic cancer, 172
      - Surgical staging, 75, 76t
      - Survival, esophageal cancer, 89
      - Survival, gastric cancer, 96
      - Suspected pancreatic tumor
        - examination checklist for, 171–172
        - ascites, 171
        - liver, 171
        - lymph nodes, 171
        - staging, 172
        - tissue acquisition, 171–172
        - tumor, 171–172
        - vascular invasion, 171
    - T
      - TaeWoong Medical, 26
      - Tangential imaging, 60, 60f
      - TEESAT. *See* The EUS and ERCP Skills Assessment Tool (TEESAT)
        - (TEESAT), 33, 34f–35f
      - The EUS and ERCP Skills Assessment Tool (TEESAT), 33, 34f–35f
      - Therapeutic endoscopic ultrasound, risks of, 45–46
      - Therapy, indications, 40
      - Thickened gastric folds
        - evaluation, 98–99, 98t
        - endoscopic ultrasound-based work-up, 99
        - large gastric folds, 98–99
        - lititis plastica, 98
        - Ménétier disease, 98
    - ThinPrep, 277
    - Thoracic tumors, 103–104
    - Time-intensity curves (TIC) analysis, 52, 54–55
    - Tissue
      - physical properties of, 3t
      - ultrasound interactions in, 3–4
    - Tissue acquisition, 176
      - indications, 40
    - Tissue harmonic echo (THE)
      - pancreatic cysts, 186–188
    - Tissue sampling, 123–126, 250
      - ascites, 171–172
      - direct forceps biopsies, 208
    - Tissue specimen preparation, type of, 272–273
    - TNM staging classification system
      - ampullary tumors, 221–222, 222t
      - gallbladder cancer, 216, 216t
    - Total mesorectal excision (TME), 230
    - TP53 mutations, 198–199
    - Trachea, 61, 62f
    - Training
      - cognitive and technical aspects, EUS, 30–31
      - competence, 31–32
      - competency assessment guidelines, 31, 31t
      - competency-based medical education (CBME), 32–33
      - cumulative sum analysis (CUSUM), 31–32, 32f
      - current status, 31
      - endoscopic ultrasound, 30–31
      - end points, 30t
      - The EUS and ERCP Skills Assessment Tool (TEESAT), 33, 34f–35f
      - EUS-guided fine-needle aspiration (EUS FNA), 29
      - EUS-guided fine-needle biopsy (FNB), 29
      - EUS-guided tissue acquisition (EUS TA), 29
        - learning curves, 31–32
        - pancreaticobiliary EUS, 32
        - privileges credentialing, 33–36
        - privileges recredentialing, 33–36
        - privileges renewal, 33–36
        - quality metrics, EUS, 36, 37t
        - simulators, 36
      - TNM staging, 30
    - Transabdominal ultrasonography (TUS), 40, 57
      - CBD stones, 201
      - cholelithiasis, 206
    - Transanal stapling instruments, 246
    - Transducers, 5
    - Transduodenal FNAs, 177
    - Translational medicine, 236
    - Transluminal drainage, 302–303, 307
    - Transparent/low-compliance condom, 59–60, 60f
    - Transperineal ultrasound, 248
    - Transport media, for cytologic specimens, 277

Transrectal EUS FNA, 227–228

Triple test, 277

Tru-cut biopsy (TCB), 234, 261–262, 262f, 274

#### T staging

  accurate staging, 39

  computed tomography (CT), 39

  endobronchial ultrasound (EBUS), 40

  esophageal cancer, 79, 82–83, 84t–85t, 86f

  gastric cancer, 91–95, 92f, 93t–94t

  indications, 39–40

  magnetic resonance imaging (MRI), 39

  non–small cell lung cancer (NSCLC), 40

  positron emission tomography (PET), 39

Tuberculosis, 105, 105f, 105t

Tumor necrosis factor (TNF) erade, 325

Tumor-node-metastasis (TNM) system, 66–67  
  rectal cancer, 230, 230t

#### Tumors

  EUS-guided fine-needle aspiration (EUS FNA), 208–210

  examination checklist for, 201b

  in pancreatic tail, 171

  resectability, 176

  seeding, EUS FNA of, 259

#### U

Ultraslim endoscope-assisted EUS-GE, 332

#### Ultrasound

  catheter, 59

  contrast-enhanced harmonic imaging, 12–14, 13f

  Doppler, 7–8

  elastography, 11–12, 13f

  high-intensity focused ultrasound (HIFU), 14, 14f

  imaging

    artifacts, 8–11

#### Ultrasound (*Continued*)

  principles of, 6–7

  instrumentation, 5–6, 5f

  processors, 5–6

  transducers, 5

  interactions in tissue, 3–4

  absorption, 4

  reflection, 3, 3f

  refraction, 3–4, 4f

  scattering, 4, 4f

  physics of, 2–5

    bulk modulus, 2–3

    compressibility, 2–3

    density, 2–3

    frequency, 2

    intensity, 4–5

    velocity, 2

    wavelength, 2

  Ultrasound contrast agents (UCAs), 12–14, 52

#### Uncinate

  linear echoendoscopes, 136–137, 137f

  mass lesions, 177, 177f

  radial echoendoscopes, 135–136, 136f

Union for International Cancer Control (UICC), 36

#### V

Valve of Houston, 230

Varices, 122, 122f

Vascular endothelial growth factor (VEGF), 56

Vascular invasion, suspected pancreatic tumor, 171

Vascularity index, 53

Vater examination, 134–135, 135f

Velocity, 2

Ventral anlage, 133–134, 135f

Video-assisted thoracoscopy (VATS), 67–69

VIVA Combo generator, 26

#### W

Walled-off pancreatic necrosis, for

  EUS-guided drainage

  adverse events, 297–298

  axial computed tomography image of, 291, 293f

  cautions, 293–294

  cavity, 296

  endoscopic necrosectomy, 297, 300f

  EUS in, 291, 293f

  follow-up, 298–299

  percutaneous drainage, 292–293

  preprocedure checklist, 293

  procedure techniques

    dual modality technique, 296–297

    irrigation of walled-off pancreatic necrosis cavity, 296

    metal stent insertion, 295–296, 298f

    multi-gate technique, 296, 299f

    single-gate technique, 294–296, 294f–296f

Warfarin, 250

Water-filled method, 110, 110f

Water insufflation, ampulla, 134, 135f

Wavelength, 2

Wet technique, EUS FNA of, 257

Work-up, gastric cancer, 90, 90f

#### X

Xanthogranulomatous cholecystitis (XGC), 217

#### Z

ZONE Sonography, 17